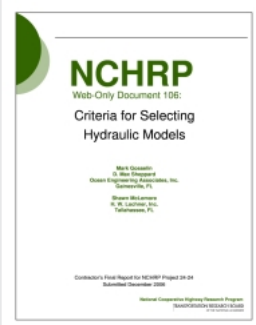

Criteria for Selecting Hydraulic Models

DETAILS

0 pages | null | PAPERBACK
ISBN 978-0-309-43086-9 | DOI 10.17226/17622

AUTHORS

ACKNOWLEDGMENT

This work was sponsored by the American Association of State Highway and Transportation Officials (AASHTO), in cooperation with the Federal Highway Administration, and was conducted in the National Cooperative Highway Research Program (NCHRP), which is administered by the Transportation Research Board (TRB) of the National Academies.

THE NATIONAL ACADEMIES

Advisers to the Nation on Science, Engineering, and Medicine

The **National Academy of Sciences** is a private, nonprofit, self-perpetuating society of distinguished scholars engaged in scientific and engineering research, dedicated to the furtherance of science and technology and to their use for the general welfare. On the authority of the charter granted to it by the Congress in 1863, the Academy has a mandate that requires it to advise the federal government on scientific and technical matters. Dr. Ralph J. Cicerone is president of the National Academy of Sciences.

The **National Academy of Engineering** was established in 1964, under the charter of the National Academy of Sciences, as a parallel organization of outstanding engineers. It is autonomous in its administration and in the selection of its members, sharing with the National Academy of Sciences the responsibility for advising the federal government. The National Academy of Engineering also sponsors engineering programs aimed at meeting national needs, encourages education and research, and recognizes the superior achievements of engineers. Dr. Charles M. Vest is president of the National Academy of Engineering.

The **Institute of Medicine** was established in 1970 by the National Academy of Sciences to secure the services of eminent members of appropriate professions in the examination of policy matters pertaining to the health of the public. The Institute acts under the responsibility given to the National Academy of Sciences by its congressional charter to be an adviser to the federal government and, on its own initiative, to identify issues of medical care, research, and education. Dr. Harvey V. Fineberg is president of the Institute of Medicine.

The **National Research Council** was organized by the National Academy of Sciences in 1916 to associate the broad community of science and technology with the Academy's purposes of furthering knowledge and advising the federal government. Functioning in accordance with general policies determined by the Academy, the Council has become the principal operating agency of both the National Academy of Sciences and the National Academy of Engineering in providing services to the government, the public, and the scientific and engineering communities. The Council is administered jointly by both the Academies and the Institute of Medicine. Dr. Ralph J. Cicerone and Dr. Charles M. Vest are chair and vice chair, respectively, of the National Research Council.

The **Transportation Research Board** is a division of the National Research Council, which serves the National Academy of Sciences and the National Academy of Engineering. The Board's mission is to promote innovation and progress in transportation through research. In an objective and interdisciplinary setting, the Board facilitates the sharing of information on transportation practice and policy by researchers and practitioners; stimulates research and offers research management services that promote technical excellence; provides expert advice on transportation policy and programs; and disseminates research results broadly and encourages their implementation. The Board's varied activities annually engage more than 5,000 engineers, scientists, and other transportation researchers and practitioners from the public and private sectors and academia, all of whom contribute their expertise in the public interest. The program is supported by state transportation departments, federal agencies including the component administrations of the U.S. Department of Transportation, and other organizations and individuals interested in the development of transportation. **www.TRB.org**

www.national-academies.org

CONTENTS

AUTHOR ACKNOWLEDGMENTS

The research reported herein was performed under NCHRP Project 24–24 by Ocean Engineering Associates, Inc. (OEA) and H.W. Lochner, Inc. (HWL). OEA was the contractor for this study and HWL was a subconsultant.

Dr. Mark Gosselin, P.E., Vice President of OEA, and Dr. D. Max Sheppard, President of OEA, were the co-Project Directors and co-Principal Investigators. The other author and co-Principal Investigator of this report is Mr. Shawn McLemore, P.E., Senior Drainage Engineer with HWL. The work was done under the general supervision of Dr. Gosselin and Mr. McLemore. The authors would also like to acknowledge the work of Mr. Philip Dompe (OEA) and Ms. Jennifer Menendez (HWL) on this project.

ABSTRACT

This report documents and presents the results of a research effort to develop a decision tool for selecting either a one- or two-dimensional hydraulic model when examining flow through bridge crossings. The research began with a literature search and survey of the state of the practice to identify and characterize the site conditions and design requirements that may affect model selection. From this list of factors that influence model selection, a series of “desktop” experiments were constructed that compared one- and two-dimensional model results over a wide range of possible configurations. This research also examined several design criteria to discern their sensitivity to possible inaccuracy in numerical modeling results. From these results, a decision tool in the form of a decision matrix was developed as well as guidelines for its application. This tool provides a formal procedure for selecting the most appropriate model for a particular application incorporating site conditions, design elements, available resources and project constraints.

EXECUTIVE SUMMARY

Engineers responsible for determining hydraulic properties at bridge openings are faced with a myriad of choices regarding how to approach their work. They are faced with a selection not only among different models (e.g., RMA2 vs. FESWMS), but also among fundamentally different *types* of models (e.g., simple analytical solutions vs. one-, two-, or three-dimensional models; finite-element vs. finite-difference models). The engineer faces an even more daunting task: selecting the hydraulic model or method appropriate not only for the design stage, but also appropriate for the site conditions (e.g., embankment skew, multiple openings, etc.). This task is further complicated by the varying availability of data for model setup (e.g., survey data, design flows/stages, etc.). That the engineers applying the models are rarely schooled in the model operation but rather simply its application necessitates the development of guidelines to direct the appropriate model selection.

Current practice emphasizes the use of two-dimensional modeling to examine river systems and bridge crossings to produce more accurate and detailed analyses. Although significant advances in the development of graphical user interfaces have made these models more accessible and easier to apply, these models still require greater amounts of data and generally a greater number of man-hours to setup and apply than do one-dimensional models. Also, little information is available contrasting the relative benefits of one- and two-dimensional models. For the purpose of aiding the hydraulic engineer in model selection, the objective of this research is to develop a decision analysis tool and guidelines for selecting the most appropriate numerical model for analyzing bridge openings in riverine and tidal systems given, as inputs, site conditions and design requirements.

To accomplish this task, this research began with a literature review/survey of the state of the practice to: identify the most commonly employed one- and two-dimensional numerical modeling software for examining hydraulics through bridge openings; identify data sets from actual bridge sites for an example application of the selection tool; and identify and characterize the site conditions and design requirements that may affect model selection. The results of this survey/literature review were then synthesized to form a comprehensive review of the current state of the practice for hydraulic modeling of riverine and tidal bridge crossings, a categorized list of the factors that influence model selection, as well as an overview of the design requirements that influence model selection. This synthesis led to the development of a series of sensitivity tests to evaluate the relative performance of one- and two-dimensional models. These tests covered a wide range of idealized possible site conditions (e.g., converging flow, asymmetric floodplains, etc.). In the experiments, parameters that control the factor in question were meticulously varied to discern the effect of the parameters on the models' relative performance. Additionally, the research evaluated several possible design elements that the engineer may encounter (e.g., determining scour depths, designing rubble riprap protection, etc.) to evaluate the sensitivity of the equations governing the design elements to possible error in the hydraulic parameters (e.g., depth, velocity) determined by the hydraulic model.

Finally, a decision tool was developed from the sensitivity tests and the evaluation of the design elements. The decision tool takes the form of a decision matrix that incorporates all the factors that influence model selection. These include site conditions, design elements, available resources, and project constraints. This report describes this tool as well as presents guidelines for application and an example application.

The utility of the decision tool is that it presents a formal procedure for the selection of the appropriate model to apply rather than rely on an intuitive process. Additionally, it provides the selection procedure in an easy-to-understand and defensible manner for presentation to non-technical laymen or policy makers. With regards to its application, the tool contains enough flexibility to incorporate conditions or constraints not covered in this document. Also, through its application it clearly identifies which feature(s) of the project are most important in the model selection for a specific application.

CHAPTER 1 INTRODUCTION

Hydraulic engineering is an ancient science which dates back to the Egyptians and Babylonians. Until the last few centuries, however, the practice of hydraulic engineering was characterized by the practical and constructional aspects rather than in the understanding of the underlying mechanics. With the development of the foundation of modern mathematics and physics, the 18th, 19th, and early 20th centuries experienced an explosion in the state of the science. Analytical and empirical relationships were developed that described open channel flow, pipe flow, and general fluid motion by the likes of Bernoulli, Chezy, Hagen, Navier, Stokes, Prantl, and others. Unfortunately, developing solutions to hydraulics problems was confined to either simplified/idealized situations or purely empirical relationships.

Enter the digital computer. It is hardly surprising that the development of Computational Fluid Dynamics (CFD) follows hand in hand with the development of the digital computer. Prior to the advent of the computer, few researchers employed numerical methods to solve fluid dynamics problems. Those who did carried out calculations by hand. A single solution often represented an enormous effort and time commitment. Now, these same solutions are obtained in a matter of fractions of seconds.

The foundations for CFD were laid near the beginning of the 20th century by Lewis Fry Richardson. In 1910, he introduced point iterative schemes for numerically solving Laplace's equation and the biharmonic equation. Additionally, he differentiated between problems solved via relaxation schemes and those solved via marching schemes. Several years later in 1928, Courant, Friedrichs, and Lewy addressed the uniqueness and existence of numerical solutions to partial differential equations as well as put forth a stability requirement for the numerical solution of hyperbolic equations. During and immediately following World War II, a significant amount of research was performed in the field of numerical solutions to fluid dynamics problems by researchers such as von Neumann and Richtmyer. Although the primary focus of these researchers was aerodynamics, the contributions that they made to CFD also translate to the solutions of open channel flow problems.

When computers were first employed by hydraulic modelers, their functions mimicked that of powerful calculators. In other words, they simply calculated values from existing, well established formulae for determining flow properties. These applications are termed the first generation of hydraulic modeling (Abbot and Minns, 1998). The second generation of hydraulic models spanned the years from 1960 to 1970. During this time, each model of a particular physical area was constructed individually so that the model applied only to that specific area. Also during this time, the science necessarily migrated away from solutions to empirical formulae to representation of the flow continuum as discrete solutions to continuity equations.

The third generation of hydraulic models began in the 1970s and is still very much with us. This generation is characterized by non-site specific design systems / modeling systems. Whereas the second generation established the scientific paradigm for modeling, the third generation established a new technology paradigm for application of the models. The modeling system provides general tools for examining a wide array of applications

rather than the construction of a single application model. This provides several advantages, amortization of the cost of the technology over numerous applications, iterative fine tuning of the models, and standardization of model output.

The fourth generation of hydraulic modeling was driven by the proliferation of the personal computer in the mid 1980s. The broad access to computing power led to the development of tools (modeling systems) that are employed by engineers who are not necessarily computational hydraulic model developers. This led to the differentiation between tool makers and tool users. Thus, the model system development aimed at creation of tools that appealed to a wider range of end users and that were more application driven. The emphasis in tool development relied more on the control aspects of the code and less on the operational aspects.

Today's modeling systems represent a wide variety of models. Hydraulic engineers are faced with a myriad of choices not only among different models (e.g., RMA2 vs. FESWMS), but also among fundamentally different *types* of models (e.g., simple analytical solutions vs. one-, two-, or three-dimensional models; finite-element vs. finite-difference models). The engineer responsible for analyzing the hydraulics of bridge waterway crossings faces an even more daunting task: selecting the hydraulic model or method appropriate not only for the design stage, but also appropriate for the site conditions (e.g., embankment skew, multiple openings, etc.). This task is further complicated by the varying availability of data for model setup (e.g., survey data, design flows/stages, etc.). That the engineers applying the models are rarely schooled in the model operation but rather simply its application necessitates the development of guidelines to direct the appropriate model selection.

Current practice emphasizes the use of two-dimensional modeling to examine river systems and bridge crossings to produce more accurate and detailed analyses. Although significant advances in the development of graphical user interfaces have made these models more accessible and easier to apply, these models still require greater amounts of data and generally a greater number of man-hours to setup and apply than do one-dimensional models. Also, little information is available contrasting the relative benefits of one- and two-dimensional models. For the purpose of aiding the hydraulic engineer in model selection, the objective of this research is to develop a decision analysis tool and guidelines for selecting the most appropriate numerical model for analyzing bridge openings in riverine and tidal systems given, as inputs, site conditions and design requirements.

RESEARCH TASKS

The work associated with this project comprises two phases. The tasks performed to accomplish the research for Project 24-24 are as follows:

Phase I

The purpose of Phase I of this work was to produce a preliminary decision tool for model selection. This required the following tasks:

1. Conduct a literature review/survey of the state of the practice to
    a. Identify the most commonly employed one- and two-dimensional numerical modeling software for examining hydraulics through bridge openings
    b. Identify data sets from actual bridge sites for an example application of the selection tool
    c. Identify and characterize the site conditions and design requirements that may affect model selection.

2. Synthesize the results of Tasks 1 to form a comprehensive review of the current state of the practice for hydraulic modeling of riverine and tidal bridge crossings, a categorized list of the factors that influence model selection, as well as an overview of the design requirements that influence model selection.

3. Test the sensitivity of several of the more popular models to the factors categorized in Task 2. The sensitivity tests begin by designing "desktop" experiments that meticulously vary parameters that control the factor in question.

4. Prepare a draft decision analysis tool for selecting the most appropriate software to the design requirements and site conditions.

5. Prepare and submit an interim report documenting the results of each task.

Phase II

The purpose of Phase II of the work involved further development of the decision tool. This required the following tasks:

6. Refine the decision tool and provide more descriptive guidelines concerning its application.

7. Perform an example application of the decision tool to a specific case study.

8. Prepare a comprehensive report detailing the entire research effort.

REPORT ORGANIZATION

This report is divided in the following manner: Chapter 2.0 details the survey of the state of the practice. This includes a literature review of numerical modeling applications at bridge sites including comparisons between the two types of models and an email survey of state Departments of Transportation. Chapter 3.0 presents the analysis of the data presented in Chapter 2.0 and the development of a sensitivity testing plan for comparing the numerical models. Chapter 4.0 presents the results of the sensitivity testing including calculated differences. Chapter 5.0 presents sensitivity of design criteria to changes in hydraulic inputs. Chapter 6.0 describes the decision tool including its development and guidelines for its use. Chapter 7.0 presents an example application of the decision tool. This report also contains an appendix which presents the results of the sensitivity study and comparisons between the one- and two-dimensional models.

CHAPTER 2 SURVEY OF THE STATE OF THE PRACTICE

The purpose of a literature review and survey of the state of the practice was multifold. The first objective included identifying the most commonly employed one- and two-dimensional numerical modeling software for examining hydraulics through bridge openings. The second objective includes identifying data sets — which contained measured event flows and stages, survey data, boundary conditions, etc. — from actual bridge sites for the selection tool example application. The final objective includes identifying and characterizing the site conditions and design requirements that may affect model selection.

Given the diverse requirements of this task, the procedure for successful completion had to consist of not only a review of the current literature, but also a survey of the engineers currently performing bridge hydraulic analyses for the state Departments of Transportation and the Federal Highway Administration.

LITERATURE REVIEW

The main objective of the literature review was to compare and contrast the relative benefits/difficulty between the application of one-dimensional and two-dimensional models at bridge crossings under a wide variety of conditions. The literature search revealed that very little literature exists that contrasts these two types of models for such a specific application. As such, the literature review concentrated on three areas: a short description of the commonly applied one- and two-dimensional models, case studies for each of the models, and comparison articles that contrasted one- and two dimensional models for the same site. The models discussed below include the following:

One-dimensional Models

- HEC-2*
- UNET*
- WSPRO*
- HEC-RAS*
- Ad-ICPR
- SWMM
- MIKE11

Two-dimensional Models

- RMA2*
- FESWMS*
- ADCIRC
- MIKE21
- Delft-FLS

* These models were/are free to the public. The remainder are sold privately.

One-dimensional Models

One-dimensional open-channel flow models can simulate steady or unsteady flow in single reaches or complex networks of interconnected channels. The term one-dimensional derives from the model assumptions that the stage, velocity, and discharge vary only in the streamwise direction (USACE, 1993). A one-dimensional model does not explicitly consider transverse effects. Some one-dimensional models attempt to approximate the effects of transverse variation in roughness and velocity through the subdivision of cross sections. Survey of the literature revealed a number of different models for examining flow in open channels and through bridge crossings. This literature

search address only the more commonly available / popular models (i.e., non-proprietary) employed for this specific application (determination of bridge hydraulics). The models addressed herein include: HEC2, UNET, WSPRO, HEC-RAS, Ad-ICPR, SWMM, and MIKE11.

HEC-2

The original computer program HEC-2, Water Surface Profiles, stemmed from a step-backwater program written by Bill S. Eichert in 1964. This early version was developed at the U.S. Army Corps of Engineers, Tulsa District office. In 1966, the Hydrologic Engineering Center (HEC) released the first FORTRAN version of HEC-2 under the name "Backwater Any Cross Section." The Backwater Any Cross Section program possessed the capability of computing water surface profiles in channels with irregularly shaped cross sections. This program represented a significant step in the development of modern computational techniques for hydraulic analysis (USACE, 1990). In 1968, the program was revised and released as HEC-2, Water Surface Profiles. This represented the second in a series of generalized computer programs issued by the HEC. Since the program's first release, addition of new features and improvements have prompted the release of new versions in 1971, 1976 and 1988. In 1984, Alfredo Montalvo adapted HEC-2 to the microcomputer environment. The February 1991 release of HEC-2 (Version 4.6) included the capability to simulate culvert hydraulics using the Federal Highway Administration's (FHWA) culvert procedures. The FHWA procedures were added to HEC-2 by Dodson and Associates of Houston, TX.

The current version of HEC-2 calculates water surface profiles for steady, gradually varied flow in natural or man-made channels. It calculates solutions for both subcritical and supercritical flow profiles. The program can simulate flow around/through various obstructions including bridges, culverts, weirs, and structures in the floodplain. The program's computation scheme involves the solution of the one-dimensional energy equation with energy loss due to friction evaluated with Manning's equation. The computational procedure is known as the standard step method.

The HEC-2 program represented a significant advancement in computational hydraulics. However, the program does contain a number of limitations inherent in one-dimensional, steady-state models:

- Flow is steady;
- Flow is gradually varied;
- Flow is one dimensional (i.e., velocity components in directions other than the model direction are not accounted for); and
- River channels have small slopes, (less than 1:10).

The HEC-2 model assumes steady flow since the time-dependent terms are not included in the energy equation. The flow is assumed to be gradually varied because the energy equation is based on the premise that a hydrostatic pressure distribution exists at each cross section. Flow is assumed to be one-dimensional because the Manning Equation is based on the premise that the total energy head is the same for all points in a cross section.

Engineers have applied the HEC-2 model for a number of different applications, including examination of bridge hydraulics. The code includes provisions for computing energy losses caused by structures (bridges) in two parts. One part consists of the losses that occur in reaches immediately upstream and downstream from the bridge where contraction and expansion of the flow is taking place. The second part consists of losses at the structure itself and is calculated with either the normal bridge method or the special bridge method. The normal bridge method handles a bridge cross section in the same manner as a natural river cross section, except that the area of the bridge below the water surface is subtracted from the total area, and the wetted perimeter is increased where the water is in contact with the bridge structure. The special bridge method computes losses through the structure for low flow, pressure flow, weir flow, or for a combination of these. The profile through the bridge is calculated using hydraulic formulas to determine the change in energy and water surface elevation through the bridge.

Kaatz and James (1997), and Walton and Bradley (1995), and Seckin, et al. (1998) all document HEC-2 applications and/or demonstrate HEC-2 features. Kaatz and James document a comparison of the two bridge routines available in HEC-2 with WSPRO. The study involved comparing predicted backwater during 13 flood events at 9 different bridge sites with measured values. The study found that the HEC-2 normal bridge method produced the most accurate results for the cases examined with an average error of 2%. The study found that the HEC-2 special bridge method computed a backwater that measured an average of 26% less than the measured backwater. Both models accurately represented the water surface elevations associated with the downstream reaches.

UNET

UNET is a one-dimensional, unsteady, open-channel flow model capable of simulating flow in single reaches or complex networks of interconnected channels (USACE, 2001a). The program can model many types of hydraulic controls such as bridges, weirs and culverts. The program can also simulate the exchange of flow over levees with storage areas. Since the model can simulate off-channel storage areas and looped systems, UNET is considered a quasi-two-dimensional model. Dr. Robert L. Barkau performed the primary development of UNET.

In addition to solving the one-dimensional unsteady flow equations in a network system, UNET provides the user with the ability to apply several external and internal boundary conditions, including; flow and stage hydrographs, gated and uncontrolled spillways, bridges, culverts, and levee systems. Cross sectional data are input in a modified HEC-2 forewater format (upstream to downstream). UNET treats bridge crossings in much the same manner as HEC-2 (i.e., via a normal bridge and a special bridge procedure). It includes a normal bridge procedure that calculates bridge backwater by subtracting the area of the embankments and bridge structure from the cross-sectional area and increasing the wetted perimeter by the wetted length of the piers and the bridge superstructure thus decreasing the conveyance. The special bridge procedure models the bridge crossing as an interior boundary condition which substitutes a family of free and submerged rating curves for the unsteady flow equations.

Applications of UNET are far less frequent than those of HEC-2. Teal et al., 1998 applied UNET to examine various flood control alternatives around the city of Slidell, Louisiana. These improvements included altering bridge heights and widths. Chowdhury and Kjelds, 2002 applied UNET to simulate tidal storm surge modeling in a tidal system. The application included examination of bridge hydraulics and wetting and drying of floodplains.

WSPRO

WSPRO computes water-surface profiles for subcritical, critical, or supercritical, one-dimensional, gradually-varied, steady flow. WSPRO's applications include open-channel flow, flow through bridges, flow through culverts, embankment overflow, and multiple-opening stream crossings. WSPRO was primarily developed to provide bridge designers with the capability to analyze alternative bridge openings and/or embankment configurations as well as existing stream crossings. Open-channel computations within WSPRO employ standard step-backwater computational techniques (Shearman, 1990). Computation of single-opening bridge backwater free-surface flows involves an energy-balancing routine, which employs a coefficient of discharge and which estimates an effective flow length. Computation of single-opening bridge backwater pressure flow involves application of orifice-type flow equations as developed by the FHWA. Embankment (road) overflow uses the broad-crested weir equation.

Given its development specifically for analysis of bridge hydraulics, the literature contains numerous examples of WSPRO applications. Mueller, 1993, Kaatz and James, 1997, and Zundel and Jones, 1996 all document WSPRO applications and/or demonstrate WSPRO features. Kaatz and James document a comparison of WSPRO with the two bridge routines available in HEC-2. The study involved comparing predicted backwater during 13 flood events at 9 different bridge sites with measured values. The study found that the WSPRO model generally over predicted the backwater upstream of the bridge. The model performed better at the bridge and downstream of the expansion. Additionally, the study found that for low velocities at the bridge, most of the energy loss occurred as friction loss in the downstream reach; whereas for high velocities, most of the energy loss occurred as expansion loss. The study also showed that energy loss in the upstream reach is a relatively minor component for most of the cases studied.

HEC-RAS

The U.S. Army Corps of Engineers' River Analysis System (HEC-RAS) software allows the user to perform one-dimensional steady and unsteady flow river hydraulics calculations. The HEC-RAS software supersedes the HEC-2 river hydraulics program. It also includes the unsteady flow equation solver developed by Dr. Robert L. Barkau for UNET. The HEC-RAS modeling system is a significant upgrade over both HEC-2 and UNET not only in its improved calculation routines, but more significantly in its graphical user interface (GUI).

The user interacts with HEC-RAS through a GUI. The main focus in the design of the interface was to facilitate software use, while still maintaining a high level of efficiency for the user (USACE, 2001b). The interface provides for the following functions: file

management, data entry and editing, hydraulic analyses, tabulation and graphical displays of input and output data, reporting facilities, and on-line help.

The hydraulic analysis component of the HEC-RAS modeling system comprises two major facets: a steady flow water surface profiles component and an unsteady flow simulation component. The steady flow component calculates water surface profiles for steady gradually varied flow. It can handle a full network of channels, a dendritic system, or a single river reach under subcritical, supercritical, or mixed flow regimes. The basic computational procedure is, unsurprisingly, similar to that described for the HEC-2 software. Similar to HEC-2, HEC-RAS can simulate the effects of various obstructions such as bridges, culverts, weirs, and structures in the flood plain.

The unsteady flow simulation component can simulate one-dimensional unsteady flow through a full network of open channels. The unsteady flow equation solver was adapted from Dr. Robert L. Barkau's UNET model. The unsteady flow component was developed primarily for subcritical flow regime calculations. However, the current version of HEC-RAS can now perform mixed flow regime (subcritical, supercritical, hydraulic jumps, and draw downs) calculations in this component. The hydraulic calculations for cross-sections, bridges, culverts, and other hydraulic structures developed for the steady flow component are incorporated into this component.

Bridge energy losses in HEC-RAS comprise three components. The first component consists of downstream losses associated with an expansion of flow beyond the bridge. The second component involves the losses at the structure itself modeled via several different methods. The third component consists of upstream losses associated with the flow contraction as it approaches the bridge. Contraction and expansion losses between cross sections are determined during the standard step profile calculations.

The HEC-RAS bridge routines allow for bridge analysis via several different methods without changing the bridge geometry. The bridge routines allow for modeling low flow (Classes A, B, and C), low flow and weir flow (with adjustments for submergence), pressure flow (orifice and sluice gate equations), pressure and weir flow, and high flows with the energy equation only. The model also allows for multiple bridge and/or culvert openings at a single location.

HEC-RAS has been applied extensively for examining bridge crossings. Mohammad, et al., 1998 applied HEC-RAS to examine design scour and flows around new piers associated with the retrofit of a bridge in Mendocino County, CA. They also examined the scour and flows associated with cofferdams to be installed during construction of the new piers. This application makes use of the capabilities outlined in Brunner, 1999. Brunner describes the integration of the bridge scour equations, as outlined in HEC-18 (Richardson, et al., 2001), into the HEC-RAS modeling system. The program has the capability of calculating contraction scour, pier scour, and abutment scour at bridge crossings with minimal additional input during model creation.

Ad-ICPR

The Advanced Interconnected Pond Routing (ad-ICPR) model is a one-dimensional, unsteady-state stormwater management model. This model routes runoff hydrographs through complex drainage networks including dendritic, diverging, and looped systems. The primary application of the ad-ICPR model includes the analysis of urban systems. A comprehensive graphical user interface is available for ad-ICPR. The ad-ICPR model can simulate a range of structures (weirs, culverts, gates, etc.). The model also includes provisions for a number of structure rating curves including time-discharge, head-discharge, and stage-discharge without variable tailwater conditions. Bridges can be simulated using the same algorithms as Federal Highway Administration (FHWA) WSPRO.

Ad-ICPR simulates overland flow using runoff hydrographs that can be generated by the Soil Conservation Service (SCS) unit hydrograph method, the Santa Barbara urban hydrograph method, or the kinematic overland flow method. The ad-ICPR model also allows the importing of external hydrograph files generated from other programs.

Few examples of ad-ICPR applications for examining bridge crossings exist in the literature. One such example (Singhofen, 2001) presents the modeling of a complex stormwater drainage system that includes 9 bridges. However, given the models representation of bridges as links between nodes at which water surface elevations are solved, the model is not the ideal choice for detailed examination of bridge hydraulics. Rather, this model may simulate complex systems of open and closed channels and provide boundary conditions for a more explicit solution of the bridge flows via a more detailed model such as HEC-RAS or WSPRO.

SWMM

The U.S. Environmental Protection Agency (EPA) Storm Water Management Model (SWMM) is a tool for simulating urban runoff quantity and quality and flow routing to storm and combined sewers. The model simulates storm events from rainfall and other meteorological inputs and system characteristics to predict water quantity and quality values. The model simulates all aspects of the urban hydrologic and quality cycles including surface and subsurface runoff, transport through the drainage network, and storage and treatment. SWMM also possess the capability of investigating control options with associated cost estimates available for storage and/or treatment. SWMM consists of a number of components, known as “blocks,” which can be linked to run sequentially so that the output of one module provides input to another. The blocks contain the following functions (Camp Dresser & McKee, 2001):

Input Sources - The RUNOFF Block generates surface and subsurface runoff based on arbitrary rainfall and/or snowmelt hyetographs, antecedent conditions, land use, and topography. The TRANSPORT Block provides the option of generating dry-weather flow and infiltration into the sewer system.

Central Cores - The RUNOFF, TRANSPORT, and EXTENDED TRANSPORT (EXTRAN) Blocks route flows and pollutants through the sewer or drainage system.

Correctional Devices - The STORAGE/TREATMENT Block simulates the effects of control devices upon flow and quality. Elementary cost computations are also made.

The EXTRAN Block is a dynamic flow routing model that routes inflow hydrographs through the open channel and/or closed conduit system, computing the time history of flows and heads throughout the system where the assumption of steady flow for computing backwater profiles is violated. EXTRAN represents the drainage system as links and nodes, allowing simulation of parallel or looped pipe networks; weirs, orifices, and pumps; and system surcharges. The program solves the full dynamic equations for gradually varied flow with an explicit forward stepping solution scheme. The RUNOFF Block simulates the runoff rates developed from subareas using a kinematic wave approximation. Hydrologic routing techniques are then used to route the overland flows through a pipe, culvert, channel, and/or lake network.

Similar to the ad-ICPR model, few examples of SWMM applications for examining bridge crossings exist in the literature. Again, since the model represents hydraulic structures as links between nodes at which water surface elevations and flows are solved, the model is not the ideal choice for detailed examination of bridge hydraulics. Rather, this model may simulate complex systems of open and closed channels and provide boundary conditions for a more explicit solution of the bridge flows via a more detailed model such as HEC-RAS or WSPRO.

MIKE11

MIKE11 is a 1-D dynamic flow model for simulating hydrodynamic flows, water quality, and sediment transport in estuaries, rivers, irrigation systems, channels, and other water bodies. Developed in 1979 by the Danish Hydraulic Institute (DHI), MIKE11 applications include detailed design, management, and operation of both simple and complex river and channel systems as well as simulation of stormwater runoff and progressive inundation from river overflows and coastal storm surges.

The MIKE11 modeling system comprises several different hydraulic computational modules. The hydrodynamic (HD) module employs an implicit, finite difference computation scheme for simulating unsteady flows in rivers and estuaries. This allows the model to be applied to branched networks, looped networks, and quasi two-dimensional flow simulations. The methodology assumes a vertically homogeneous flow condition. The model can simulate both subcritical and supercritical flow via a numerical scheme that changes with the local flow conditions. This allows simulation of both steep river flows and tidal estuaries within the same model. The model solves the complete St. Venant non-linear equations of open channel flow between all grid points at specified time steps for the specified boundary conditions. The model also includes the capability of simulating a variety of structures including broad crested weirs, culverts, bridges, and user-defined structures. A number of additional support modules are available for the HD module, including a quasi steady state (HDQSS) module for performing long term simulations, a dam break (DB) module for simulating the failure of one or more dams in a river system, a structure operation (SO) module for simulating operation of control gates and structures, and a flood forecasting (FF) module for performing real-time

automatic updating of flood modeling and correcting for differences in observed and computed hydrographs.

Although few references exist in the literature regarding MIKE 11 applications for examining specifically bridge hydraulic behavior, several examples exist that concern floodway modeling that include bridges in the floodplains. Maunsell McIntyre Pty Ltd., 2001 constructed a MIKE 11 model of Bluewater Creek near Townsville, Australia to perform a flood study and examine risk management options. The model included two major bridges and several culverts. The MIKE 11 model accurately described the flows in the vicinity of the bridges during calibration. Philip Williams & Associates, Ltd., 2002 performed a feasibility study to examine the restoration of marshes in Napa and Solano Counties in California. A component of this study included applying MIKE 11 to describe the flows in the Napa River and Sonoma Creek. Although it did not specifically examine the flows at the bridges over the rivers, the model did include several bridges as part of its schematization. Finally, Juza and Barad, 2000 performed a study of the Cosumnes River in California comparing MIKE 11 with WSPRO and MIKE 21. They found significant local differences between the two one-dimensional models attributed to the difference in solution schemes between the steady state model (WSPRO) and the unsteady, looped model (MIKE 11).

Two-dimensional Models

Two-dimensional models generally refer to the class of two-dimensional, depth-averaged hydrodynamic models that compute water surface elevations and horizontal velocity components for free-surface flows in two dimensional flow fields. In general, these models solve the Reynolds form of the Navier-Stokes equations for turbulent flows via either a finite element or finite difference solution scheme. The finite-difference method represents the water levels at a set of discrete points, for each time step. The typical solution grid is a network of orthogonal straight or curved lines with nodes at the intersections. Currents are normally described at the links between the nodes. The finite-element method divides the solution domain (the water body) into a set of triangular or rectangular elements. The water levels and currents are described as linear or quadratic functions across each finite element. Time is advanced in steps in both solution methods. These models represent an improvement over the one-dimensional models in that the flow direction is not specified a priori (i.e., in the streamwise direction as in the one-dimensional models) but rather solved via the equations of motion. In other word, these models are not hampered by the assumption of lateral homogeneity. Most two-dimensional models operate under the hydrostatic assumption — accelerations in the vertical direction are negligible. Thus the models are two-dimensional in the horizontal plane. Drawbacks of two-dimensional (and three-dimensional) models compared to one-dimensional models include: the models generally do not describe control structures (such as weirs, pumps, and tide gates) as well as one-dimensional models; and, the models may have problems maintaining numerical stability in situations involving rapid wetting and drying cycles. This literature search addresses only the more commonly available / popular models (i.e., non-proprietary) employed for this specific application (determination of bridge hydraulics). The models addressed herein include: RMA2, FESWMS, ADCIRC, MIKE21, and Delft-FLS.

RMA2

RMA2 is a one- and two-dimensional, dynamic, depth-averaged, finite-element, hydrodynamic model. It computes water surface elevations and depth-averaged horizontal velocity for subcritical, free-surface flow in two-dimensional flow fields. Norton, King and Orlob of Water Resources Engineers originally developed RMA2 for the Corps of Engineers' Walla Walla District, in 1973. King and Roig at the University of California, Davis performed further development of the model. King and Norton, of Resource Management Associates (RMA) and the Waterways Experiment Station (WES) Hydraulics Laboratory made subsequent enhancements which produced the current version of the code (Donnell et al., 2001).

The code's governing equations solve conservation of mass and conservation of momentum in the x- and y-directions via one of several available turbulence closure schemes. RMA2 computes a finite element solution of the Reynolds form of the Navier-Stokes equations for turbulent flows. The code treats bottom friction via the Manning's or Chezy equation. Eddy viscosity coefficients define the flow turbulence characteristics. The program contains the capability of solving both steady and unsteady state (dynamic) problems. Model capabilities include: wetting and drying of mesh elements; including Coriolis effects; applying wind stress; simulating five different types of flow control structures; and applying a wide variety of boundary conditions. Model users may specify turbulent exchange coefficients, Manning's n-values, water temperature, or select equations for automatic dynamic assignment of Manning's n-value by depth or Peclet number for automatic dynamic assignment of turbulent exchange coefficients. The equations solved by RMA2 incorporate the hydrostatic assumption. In other words, accelerations in the vertical direction are negligible.

RMA2 is a rigorously tested and well maintained hydrodynamic model with wide applicability. Applications of the model include calculating water levels and flow distribution around islands; flow at bridges having one or more relief openings; in contracting and expanding reaches; into and out of off-channel hydropower plants; at river junctions; and into and out of pumping plant channels; circulation and transport in water bodies with wetlands; and general water levels and flow patterns in rivers; reservoirs; and estuaries.

Several instances of the application of RMA2 exist in the literature. Reed, et al., 1995 and Sheppard and Pritsivelis, 1999 applied RMA2 to examine the effects of varying the shapes of hurricane storm surge hydrographs on currents within the St. Johns River in Jacksonville, Florida and the Indian River Lagoon near Ft. Pierce, Florida. The researchers found that quantities such as rate of rise, rate of fall, and duration of the peak of the offshore storm surge hydrograph had significant effects not only on the water surface elevations, but also the maximum velocities experienced at bridges over estuaries and coastal rivers. They further state that this dependence can translate into an even greater dependence of scour on these parameters. In other studies, Mas et al., 1994 and Miller et al., 1994 applied RMA2 to examine flows in the South Branch of the Potomac River near Petersburg, West Virginia. The researchers simulated flows during several design events to investigate the effects of proposed levees on flows, and the sensitivity of flow patterns on bends, constrictions, and flood induced geomorphic changes at the site.

The studies found that RMA2 predicted significant cross channel variation in water surface elevation and velocity near several river features including bends, levees, and constrictions.

FESWMS

The Federal Highway Administration's Finite Element Surfacewater Modeling System (FESWMS) package comprises two software packages that can model flows in open channels: Flo2DH and Flo1DH. Flo2DH is a two-dimensional finite element surface water computer program for computing flow and water surface elevation behavior in a horizontal plane. Flo1DH is a one-dimensional finite element surface water model for computing unsteady flow and sediment transport in open channels. Flo1DH is currently unavailable to the public according to the FHWA website. Flo2DH simulates water and sediment motion in rivers, estuaries, and coastal regions. Flo2DH solves steady-state and time-dependent two-dimensional depth-averaged surface-water flow and sediment transport equations via the finite element method. As with RMA2, Flo2DH operates under the hydrostatic assumption — vertical velocities and accelerations are negligible. Flo2DH was developed specifically for modeling highway river crossings. As such, it includes many features that other available two-dimensional models do not have, such as pressure flow under bridge decks, flow resistance from bridge piers, local scour at bridge piers, live-bed and clearwater contraction scour at bridges, bridge pier riprap sizing, flow over roadway embankments, flow through culverts, flow through gate structures, and flow through drop-inlet spillways. Additional simulated features of the model (Froehlich, 2002) not necessarily exclusive to FESWMS include: bottom shear stress or bed friction; wind shear stress; Coriolis force; turbulence-induced shear stresses; combined current and wave shear stresses; barometric pressure gradients; tropical cyclone wind fields and barometric pressure fields; coastal storm surge hydrographs; wetting and drying of elements; transport of eight non-cohesive sediment particle size classes; erosion and deposition of transported sediment; armoring of channel beds; wave effects on nearshore sediment transport; supercritical flow and hydraulic jumps; and combined one-dimensional/two-dimensional flow and sediment transport. Notably, recent releases of the hydrodynamic and sediment transport two-dimensional model have featured a new name: FST2DH.

FESWMS is a widely applied and rigorously tested model. In fact, the literature search uncovered more applications of FESWMS to investigate specifically bridge hydraulics than any other model. Examples of these applications include a hydraulic evaluation of the I-65 Bridge at the Alabama River Peninsula (Curry and Pinkston, 1998), a hydraulic analysis of the Baltimore Bridge Street Project (Ports and South, 1995), and examinations of the flows associated with a new bridge over the Ohio River near Owensboro, Kentucky (Ports et al., 1993). In these studies, a specific feature of the waterways prompted the application of FESWMS: flow around a river bend. Each study concluded that the two-dimensional model was successful in describing the flow features (velocity magnitude, depth changes, and angles of attack) associated with this complex flow. Additionally, these models provided an improvement in scour estimation in that the flow angles of attack were solved for rather than inferred.

ADCIRC

ADCIRC (Advanced Circulation Model for Coastal Ocean Hydrodynamics) is a numerical model developed specifically for generating long time periods of hydrodynamic circulation along shelves, coasts, and within estuaries (Luettich and Westerink, 2000). Many researchers contributed to the development of the ADCIRC model including investigators at the University of Notre Dame (J.J. Westerink), the University of North Carolina at Chapel Hill (R.A. Luettich), the University of Texas at Austin (M.F. Wheeler and C. Dawson), the University of Oklahoma (R. Kolar), the State of Texas (Jurji), and the Waterways Experiment Station (N. Scheffner).

ADCIRC solves the equations of motion for a moving fluid on a rotating earth. The equation formulation includes applying the traditional hydrostatic pressure and Boussinesq approximations and discretizing the equations in space via the finite element (FE) method and in time via the finite difference (FD) method (Luettich and Westerink, 2000). The ADCIRC program includes both a two-dimensional depth integrated (2DDI) mode and a three-dimensional (3D) mode. For both, the models solves for elevation via the depth-integrated continuity equation in Generalized Wave-Continuity Equation (GWCE) form. The model solves for velocity via either the 2DDI or 3D momentum equations. These equations retain all the nonlinear terms. ADCIRC includes solution capabilities in either a Cartesian or a spherical coordinate system. The GWCE is solved via either a consistent or a lumped mass matrix and an implicit or explicit time stepping scheme.

Boundary conditions for the model include specified elevation (harmonic tidal constituents or time series); specified normal flow (harmonic tidal constituents or time series); zero normal flow; slip or no slip conditions for velocity; external barrier overflow out of the domain; internal barrier overflow between sections of the domain; surface stress (wind and/or wave radiation stress); atmospheric pressure; or outward radiation of waves (Sommerfield condition). ADCIRC can be forced with: elevation boundary conditions; normal flow boundary conditions; surface stress boundary conditions; tidal potential; or an earth load/self attraction tide.

Both the U.S. Army and Navy have extensively applied ADCIRC for a wide rage of tidal and hurricane storm surge predictions in regions including the western North Atlantic, Gulf of Mexico and Caribbean Sea, the Eastern Pacific Ocean, the North Sea, the Mediterranean Sea, the Persian Gulf, and the South China Sea. The model employs computational models of flow and transport in continental margin waters to predict free surface elevation and currents for a wide range of applications including evaluating coastal inundation, defining navigable depths and currents in near shore regions, to assessing pollutant and/or sediment movement on the continental shelf.

Given its relatively recent public release, relatively few applications of ADCIRC at bridge crossings exist in the literature. Two applications that did surface include Butler and Cialone, 1999 and Edge et al., 1999. Both investigations involve applying ADCIRC as a coastal and ocean model to develop boundary conditions for models that describe flows at the inland bridges. A recent study by Ocean Engineering Associates, 2004 compared the RMA2 and ADCIRC models' capabilities of predicting tidal flows and

hurricane surge flows at inland bridge locations near Lake Worth Inlet, Florida. This study found that ADCIRC performed comparable to RMA2 at predicting both the tides and surge events at two bridges over the Florida Intracoastal Waterway.

MIKE21

Developed at the Danish Hydraulic Institute (DHI), MIKE21 is a software package containing a modeling system for two-dimensional free-surface flows. The hydrodynamic (HD) module of the modeling system simulates the water level variations and flows in response to a variety of forcing functions in lakes, estuaries and coastal areas. It simulates unsteady 2D flows in one layer (vertically homogeneous) fluids. The water levels and flows are resolved on a rectangular finite difference grid covering the area of interest when provided with the bathymetry, bed resistance coefficients, wind field, hydrographic boundary conditions, etc. The module solves the full time-dependent non-linear equations of continuity and conservation of momentum. The solution is obtained using an implicit ADI finite difference scheme of second-order accuracy. Other features simulated by the model include: convective and cross momentum, bottom shear stress, wind shear stress at the surface, barometric pressure gradients, Coriolis forces, momentum dispersion, wave-induced currents, sources and sinks (of mass and momentum), evaporation, wetting and drying, and bridge pier resistance. Hydrographic boundary condition specification includes constant or variable (in time and space) level or flux at each open model boundary, constant or variable sources or sinks anywhere within the model, and initial free surface level map applied over the entire model.

MIKE21 HD applications include a wide range of hydraulic phenomena including tidal hydraulics, wind and wave generated currents, storm surges, flood waves, tidal exchange and currents, secondary circulations, eddies and vortices, harbor seiching, dam breaks, and tidal waves.

Extensive application of MIKE21 occurs primarily outside the United States. However, the model is recently gaining acceptance within the US. Juza and Barad, 2000 and McCowan and Collins, 1999 both examine applications of MIKE21 to investigate floodplain behavior during flood conditions. The DHI website (http://www.dhisoftware.com/mike21c/Description/Examples/Examples_jamuna.htm) does present an example of a MIKE21 application to investigate flows at a bridge crossing. MIKE21 provided the means to determine critical morphological and hydrodynamic conditions during construction of the Jamuna Multipurpose Bridge in Bangladesh. In this application, the hydrodynamic model was run in conjunction with a morphological model to determine changes in the overall characteristics to the braided Jamuna River due to the bridge.

Delft-FLS

The WL | Delft Hydraulics hydrodynamic modeling software package Delft-FLS simulates the dynamic behavior of overland flow over initially dry land, as well as flooding and drying processes on every kind of geometry, including lowlands or mountain areas. Delft-FLS simulates unsteady hydrodynamic flow in two dimensions. It computes flow using the full shallow water equations on a rectilinear, finite difference

grid based on a scheme capable of simulating both subcritical and supercritical flow. Geometrical input data can be specified in a number of ways so that land layout features such as dikes, roads, railroads, waterways, viaducts, culverts, etc., can easily be imported from GIS systems. It simulates the influence of the existing/planned infrastructure on flooding processes. Land use, vegetation characteristics and urban areas are also included. Internal boundary conditions are included to simulate dam break / dike break events. Program features include: flow computation on initially dry land, without using any special drying or wetting procedures; flow computation on very steep slopes, such as dike walls and other man-made structures; flood predictions of dike breaks due to heavy rainfall or other natural hazards; and pre- and post-processing within a GIS environment. Delft-FLS is primarily a flood analysis/planning tool for investigating such flood related events as the time a road is available for evacuation, advance of inundation, water depths (maximal and progression), and flood duration.

As with MIKE21, Delft-FLS is primarily a European model, although the model developers have recently attempted to increase their presence within the US. Very few examples of Delft-FLS applications appear in the literature. One such example, Thomalla, et al., 2002, describes the application of Delft-FLS to examine dynamic storm surge and inundation at two sites along the east coast of England (Kingston-upon-Hull and Canvey Island). The purpose of this study is to characterize the flood vulnerability of the two areas.

Comparisons of One- and Two-dimensional Models

To this point, the literature review has primarily consisted of an overview of the existing one- and two-dimensional models available for examining bridge hydraulics and case studies of the models. The original intent of this literature review was to clearly delineate situations where two-dimensional models were more suitable than one-dimensional models. Unfortunately, one of the lessons learned from this literature review is that researchers and engineers rarely publish findings that state that their approach or methodologies were flawed. Thus, all the case studies found that the applied models accurately represented the flows. Luckily, however, the literature search did unearth a class of articles/studies that provide exactly the type of information originally sought. The one-dimensional versus two-dimensional model comparison articles, though much rarer than the case study class of articles, present the results of applications of both types of models at the same site and contrast the model output.

Walton et al., 1997 describes two such comparisons. The first involves a comparison between RMA2 and HEC-2 at the Sauk River in Washington State where flow in a secondary channel was attacking the left bank upstream of a major highway crossing. After modeling design (100-year) flows in the steady state mode, the researchers concluded that while along-river stages computed via both models generally agreed, the one-dimensional model did not predict either the increased flows or the super-elevation that occurred in the secondary channel. The second comparison involved an application of FESWMS and HEC-RAS at the Tom Music Bridge over Cispus River in Washington. Here, the purpose of the modeling effort was to evaluate hydraulic and scour performance of a replacement bridge. As with the other comparison, the models generally agreed in predicting longitudinal variation of water surface elevations. They departed, however, in

their prediction of the transverse variation. In this instance, significant differences occurred in predictions of current direction and super-elevation at the upstream right bank of the bridge. The bridge's location after a bend in the river contributed to these differences.

Ports et al., 1993 compared WSPRO with FESWMS at a proposed new bridge over the Ohio River near Owensboro, Kentucky. The physical setting of the proposed bridge contains several features that complicate the flow: the proposed bridge crosses the river at approximately halfway through a 90° bend in the river; the crossing lies just upstream from a natural constriction in the channel; and the approach embankment contains five relief bridges all located on the left embankment. The comparison of the models occurred through their predictions of contraction, abutment, and local pier scour computed from the model results. The researchers found little difference at the main bridge for contraction scour, but much larger differences at the relief bridges. At the relief bridges, clear water contraction scour occurs. Thus, the calculations are very sensitive to velocity magnitude. For WSPRO, flows through the bridges are apportioned based on conveyance, whereas in FESWMS they are computed directly. This led to large differences in both flow magnitude and direction at the relief bridge openings. Differences in both abutment scour and local pier scour at the main bridge occurred due to the differences in flow angle of attack. For WSPRO, angle of attack must be assumed based on experience and knowledge of the physical geography. In FESWMS, flow directions are directly computed. Again, large differences resulted which separated scour predictions by as much as 10 ft for some piers.

Thompson, 1989 compared results from HEC-2 and FESWMS at a floodplain encroachment at Les Creek (location not given). The geography of the location consisted of a regular trapezoidal channel bounded by regular overbanks and a broad, asymmetrical (300 ft left, 1050 ft right) floodplain. The encroachment was 300 ft across and located within the right floodplain. The comparison found that the location and magnitude of the maximum backwater differed between the one- and two-dimensional simulations. The FESWMS simulation predicted a greater increase in the water surface due to the encroachment than did the HEC-2 simulation. Although greater, the backwater predicted by FESWMS was more localized. Additionally, the FESWMS simulation predicted transverse variation in the backwater.

Buechter, 2001 compared FESWMS simulation results to those from a one-dimensional model for proposed modifications to William Cannon Drive in Austin, Texas. The modifications included raising the roadway to exceed an intended 25-year flood level; building a new bridge over Onion Creek; constructing a relief opening in the roadway embankment; and building a new bridge over Marble Creek, a tributary of Onion Creek. The one-dimensional model results found no significant upstream impact for the 100-year flood conditions. However, the FESWMS results showed local increases in backwater on the order of 1 ft — a significant violation of the no-rise requirement. Two-dimensional modeling better identified potential impacts associated with the proposed highway reconstruction than did the one-dimensional model.

Juza and Barad, 2000 compared a steady state, one-dimensional model (WSPRO), an unsteady, looped, one-dimensional model (MIKE11) and an unsteady two-dimensional

model (MIKE21) at a reach along the Cosumnes River in California. The researchers found that, in general, WSPRO was not able to describe the interconnections of the main channels, parallel channels, tributaries, and floodplains inherent in the study area. The looped model (MIKE11) performed somewhat better. However, examination of the two-dimensional model results revealed connections and flow pathways not represented in the looped model.

Jia and Alonso, 1994 compared results from HEC-2 and CCHE-2D (a USDA two-dimensional model developed at the University of Mississippi for analysis of river flow, sediment transport and morphological processes) along a 350-m long reach of the Hotophia Creek in Mississippi. The researchers found significant differences around bar encroachments within the reach. Specifically, the results illustrate significant differences in transverse distribution of velocity magnitude between HEC-2 and CCHE-2D near the encroachments. The researchers also found significant differences in water surface elevations near the bars which led to different channel widths.

The comparisons presented above echo several common themes. The one-dimensional and two-dimensional models tend to compare favorably in streamwise quantities, but start to diverge in transverse quantities. This divergence becomes more pronounced the more the assumptions of the one-dimensional model are violated (i.e., flow parallel to the stream centerline). This divergence may have significant impacts in determining floodplain elevations, low member elevations, and vertical extent of channel or abutment protection to name a few. The literature search revealed several features of waterways that cause difficulties for one-dimensional models; namely:

- Complex floodplain geometry;
- Multiple openings;
- Braided or anabranched streams;
- Crossings over/near channel bends; and
- Asymmetric floodplains/encroachments

Waterway features examined by this study should not be limited to only these features, but rather all features that violate the one-dimensional assumptions. These would also include:

- Embankment skew;
- Skewed and/or complex pier configurations;
- Time-dependent flows; and
- Sinuosity (highly meandering vs. straight).

EMAIL SURVEY

The purpose of the email survey was to quickly identify the models employed to examine bridge crossings, discern the problems frequently encountered with model application, and to locate suitable data sets for employing during the verification of the decision tool in a later task. Figure 1 displays the transmitted survey. The survey was sent by e-mail to one or more people in each of the fifty state transportation agencies, Puerto Rico, the

District of Columbia, and to FHWA hydraulics personnel - eighty people in total. Forty-seven people responded to the survey, including at least one person from forty-two of the state highway agencies. Forty-seven out of eighty is a reasonable response rate for this survey. A large percentage of the eighty were one of multiple people at the same agency. The responses indicated that coordination between these people was performed to reduce the response effort. Therefore, the agency response rate is much higher, as indicated by forty-two responses out of fifty from the state highway agencies. The following is a list of the responding states/agencies:

Alaska
Arizona
Arkansas
California
Colorado
Delaware
FHWA – Eastern Lands
FHWA
Georgia
Hawaii
Idaho
Illinois
Indiana
Iowa
Kansas
Louisiana
Maine
Maryland
Michigan
Minnesota
Mississippi
Missouri
Montana
Nevada
New Hampshire
New Mexico
New York
North Carolina
Oklahoma
Ohio
Oregon
Pennsylvania
South Carolina
South Dakota
Tennessee
Texas
Utah
Vermont
Virginia
Wisconsin
Wyoming

We are contacting you as part of the National Cooperative Highway Research Program (NCHRP) Project 24-24, “Criteria for Selecting Numeric Hydraulic Modeling Software”. The objective of this research is to develop a decision analysis tool and guidelines to assist hydraulic engineers in selecting the most appropriate numeric modeling software for analyzing bridge openings in riverine and tidal systems. Your responses will help the research team accomplish this objective.

When you are ready to respond, use your reply option to prepare the return message. Scroll to the questions below and type your responses.

Bridge Hydraulic Modeling Software Survey

1. Please indicate the computer programs used by your agency to model the hydraulics of highway bridges. Place a ‘1’ beside the model most commonly used, a ‘2’ beside the next most commonly used, etc., for both riverine and tidal conditions. Leave a blank beside any models not used.

One dimensional Models		Two Dimensional models	
River	Tidal	River	Tidal
_____ HEC-RAS	_____	_____ FESWMS	_____
_____ WSPRO	_____	_____ RMA2	_____
_____ SWMM	_____	_____ ADCIRC	_____
_____ HEC-2	_____	_____ Mike-21	_____
_____ UNET	_____	_____ Delft-FLS	_____
_____ E-431	_____	_____ POM	_____
_____ Bri-Stars	_____		
_____ HEC-6	_____		
_____ Ad-ICPR	_____		

Others: _____

2. Please describe any problems normally encountered using the models indicated above.

3. Does your agency have guidelines for selecting programs to model the hydraulics of highway bridge crossings?
___ Yes ___ No
If yes, please tell how we may obtain a copy of the guidance.

4. Does your agency prohibit or discourage the use of any programs?
___ Yes ___ No
If yes, which programs? _____
Briefly describe the reason:

5. Do you have any data sets that could be made available to the research team with flows, stages, survey data, and boundary conditions for a:
Riverine highway bridge crossing. ___ Yes ___ No
Tidal highway bridge crossing ___ Yes ___ No

Thank you for taking the time to respond. If you have any suggestions for the research team about possible guidelines for selecting hydraulic models, we would like to hear them. You can include them with your response, or call us at (850) 656-9027.

Figure 1 Email Survey

Table 1 Survey Results — Most Commonly Employed One-dimensional Models

Model	Riverine				Tidal			
	1st	2nd	3rd	4th +	1st	2nd	3rd	4th +
HEC-RAS	36	3			9			
WSPRO	3	13	8		1			
SWMM			1	1	1			
HEC-2		15	6			7		
UNET				1				
E-431				2				
Bri-Stars	1		1	1				
HEC-6			2					

Table 2 Survey Results — Most Commonly Employed Two-dimensional Models

Model	Riverine				Tidal			
	1st	2nd	3rd	4th +	1st	2nd	3rd	4th +
FESWMS	18				6	2		
RMA2		4			2	2		

Table 1 and Table 2 list the results of the first question on the survey which asked for the 1st, then 2nd, etc., most commonly applied numerical models. The results indicated that HEC-RAS is the dominant bridge hydraulics model employed by transportation agencies today. Its predecessor, HEC-2, is also still commonly applied. A reason often cited for its continuing use included the capability of matching existing flood studies. WSPRO is also commonly employed, but application of this model appears to be diminishing similar to HEC-2. The responses indicate that one-dimensional modeling is most common for determining bridge hydraulics. However, from the responses, two-dimensional modeling also appears to provide a feasible alternative in several states. FESWMS is the primary two-dimensional model applied, followed by RMA2. All other models, both one- and two-dimensional, are employed only sporadically. These models included: BrEase (CA), HY8, WSP-2 from Soil Conservation Service, circa 1970's (Ill.), "Hydraulics of Bridge Waterways" (HDS#1) (Iowa), an in-house developed Tiderout program for tidal cases (MD), SWPG (2D) (Nevada), DaveF – 2 Dimensional (NM), TIDEROUT (VA), and WSP water surface profile and scour (WY).

Two primary goals of the survey were to: 1) identify site conditions that influence the choice of particular models, and 2) identify data sets that can be used to verify the selection tool developed in this project.

The survey question that addressed item 1 was broader than our scope; therefore, the responses were wide-ranging. Survey question #2 asked for any problems applying the models. Many of the responses to this question indicated problems with program bugs or other inconveniences, difficulty with finding calibration data, and problems finding experienced engineers to wield the models. The responses also indicated a number of additional site conditions that could influence the model choice:

- Floodplain width
- Degree of contraction
- Combinations of bridge pressure flow and roadway weir flow
- Sites where road parallels the stream and then suddenly crosses it
- Confluences
- Complex sites where flow paths are difficult to visualize

For question #3, 26% of respondents reported having guidelines for selecting programs to model the hydraulics of highway bridge crossings. Most of the agencies with affirmative replies had guidelines posted on the web or available in design documents. For question #4, 47% of respondents reported that their agency prohibits or discourages the use of specific programs. Most respondents replied that they only accepted results from specific models. These most frequently included HEC-RAS, HEC-2, and FESWMS. Interestingly, some states singled out programs that they would not accept including WSPRO and HY-8. Finally, for question #5, 53% of the respondents indicated that they did in fact have data sets available for riverine and/or tidal bridge crossings with the vast majority of those only having data sets for riverine settings. Of those respondents, seven potential sites were identified. These sites included:

- A bridge over Cedar Mills Cr. in Pennsylvania

- Missouri River at Route 54 in Missouri
- Smith Bridge Road over Baker River in New Hampshire
- Ninilichik River on Kenah Peninsula in Alaska
- Cape Fear near Wilmington in North Carolina
- Murphy Creek Bridge in Wyoming
- SC-41 over Black River in South Carolina

After examining the potential sites, it was determined that the best data set available was not identified in the survey, but rather available from the USGS Hydrologic Atlas. Ming et al. (1979) provides maps of a site near Shiloh, Alabama of the Highway 130 Bridge over Buckhorn Creek. The maps provided include measured cross sections of the creek, and measured high watermarks and flow rates of two floods that occurred on March 2-3, 1972 and December 21, 1972. Shown in Figure 2 this meandering creek contains broad floodplains and crosses the bridge at a slight angle. An example of the data available is located in Figure 3.

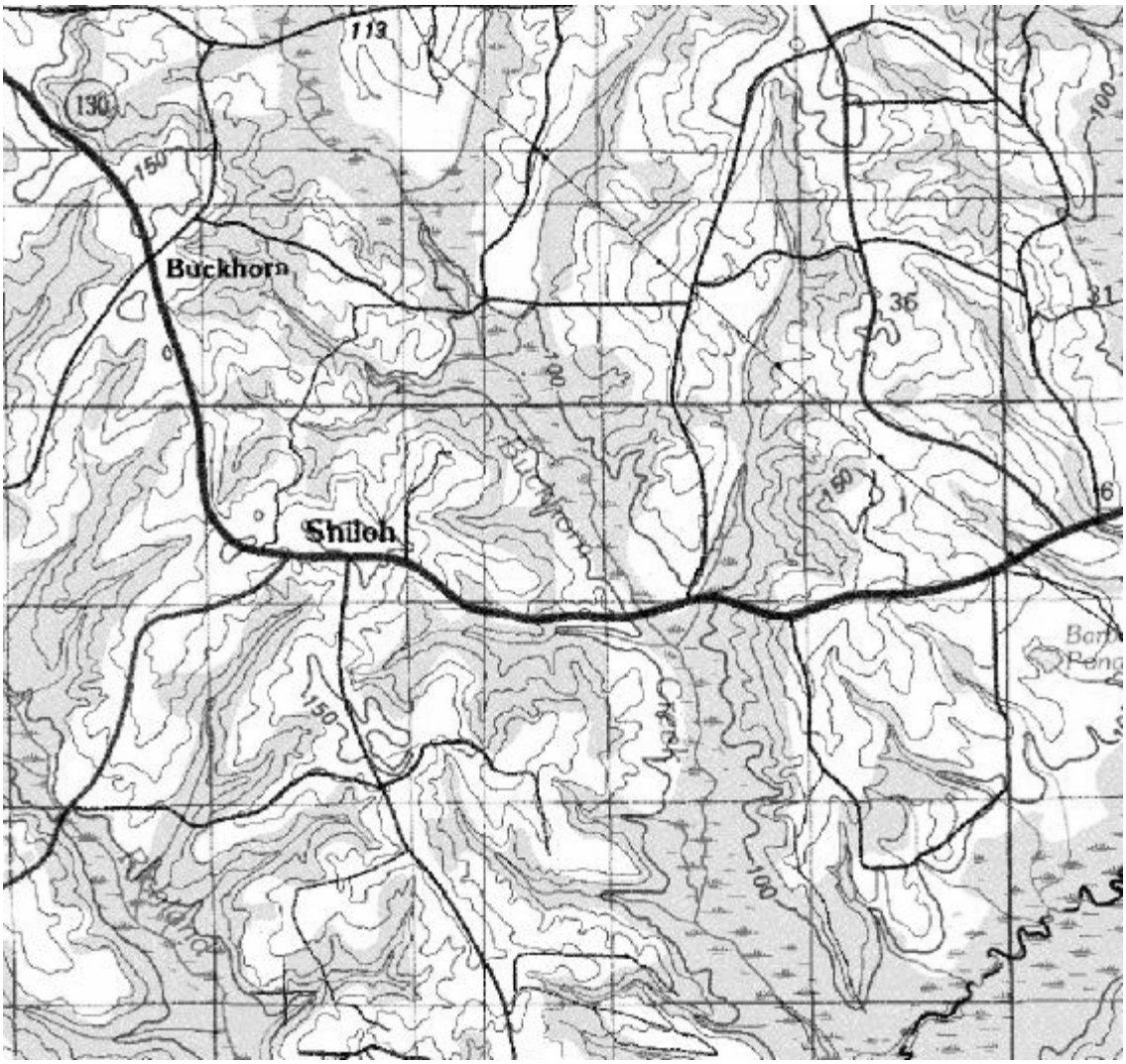

Figure 2 Highway 130 over Buckhorn Creek near Shiloh, AL

Figure 3 Example of Data Available from USGS Hydrologic Atlas

CHAPTER 3 SYNTHESIS OF REVIEW AND DEVELOPMENT OF SENSITIVITY TESTING PLAN

Having identified several of the factors that influence model selection, synthesis of the results of the literature review and survey provides a comprehensive review of the current state of the practice for hydraulic modeling of riverine and tidal bridge crossings, a categorized list of the factors that influence model selection, as well as an overview of the design requirements that influence model selection. The results indicated several general areas of problems encountered when applying hydraulic models at bridge crossings. These areas are summarized below:

Literature Review

- Complex Floodplain Geometry
- Multiple Openings
- Braided or Anabranched Streams
- Crossings over/near Channel Bends
- Asymmetric Floodplains/Encroachments
- Embankment Skew
- Skewed and/or Complex Pier Configurations
- Variable Flow Rates
- Time-Dependant Flows (Riverine Flood Events vs. Hurricane Storm Surges)
- Sinuosity (Highly Meandering Vs. Straight)

Survey

- River Bends
- Confluences
- Wide Floodplain
- Significant Lateral Flow in the Vicinity of the Bridge
- Complex Flow Situations
- Steep Stream Reaches and Mixed Flow Situations
- Distance Inland for Tidal Riverine Sites (for Steady vs. Unsteady Analysis)
- Bays Crossed by Numerous Causeways (for 1-D vs. 2-D)
- Tidal Areas without Well Defined Channels (for 1-D vs. 2-D)
- Complexity of Interconnected Tidal Bodies (for 1-D vs. 2-D)
- Wind
- Multiple Openings
- Overtopping Flow
- Roadway Overtopping with a Perched Bridge
- Combined Pressure and Weir Flow at Bridge
- Severely Contracted Flow (Small Bridge Opening in Very Wide Floodplains)
- Roadway Parallels the Stream then Suddenly Turns and Crosses It
- Determining Drawdown Beneath the Bridge
- Determining Angle of Attack on Piers and Abutments
- Determining FEMA Floodways

Comparison of the lists revealed several common themes. The purpose of this synthesis was to develop a single categorized list of the factors that influence model selection from which to produce a sensitivity testing plan. In developing this list, it is important to be cognizant of the ability to test the factors with the desktop experiments. For example, general comments such as complex floodplain geometry are difficult to quantify and thus would prove highly difficult to include in the sensitivity study. Conversely, factors such as multiple openings and embankment skew are relatively easy to quantify, model, and vary within the sensitivity study. Additionally, one may regard some of the factors as either combinations of more quantifiable factors or a measure of the modeling accuracy. For example, the less precise adjective “complex” may define an instance where several of the factors are present at a bridge crossing. Also, design stage is really a description of the level of acceptable error. Since these types of factors are not assessable within the sensitivity experiments, they were omitted from the list. The list of factors is reduced as follows:

- Multiple Openings
- Bridges Located on River Bends
- Bridges near Confluences
- Bridges with Significant Constrictions
- Overtopping Flow
- Embankment Skew
- Bridges over Meandering Rivers
- Bridges with Asymmetric Floodplains
- Bridges with Large Piers/High Blockage
- Tidal Hydraulics

From this list, it is possible to devise the series of sensitivity experiments from which to draw a comparison of the relative accuracy between the one- and two-dimensional models. The first step in the sensitivity studies was to establish a baseline. The baselines for the sensitivity studies included examination of two idealized channels: a “small” channel and a “large” channel. The channels have trapezoidal geometries in the cross section with gently sloping floodplains (Figure 4). The floodplains end with vertical bluffs at the left and right boundaries. The bridge openings have setbacks from the channel banks and are also trapezoidal in shape (spill-through abutments).

The models include not only the channels at these crossings, but also extend upstream and downstream sufficiently far to satisfy the requirements of the individual sensitivity tests. This distance varies within the sensitivity study to adequately test the factor being examined. The baseline model also included the following boundary conditions: a downstream elevation boundary condition to achieve an approximate depth of 10 ft at the bridge for the small channel and an approximate depth of 15 ft at the bridge for the large channel. The models will also include an upstream flow boundary condition set to 95,000 cfs for the large channel and 5,000 cfs for the small channel. Again, these conditions will vary for some of the factors investigated.

This basic geometry was varied to test each of the factors listed above. Each factor was tested with both the large and small channel under steady-state conditions. The models employed for the sensitivity study included HEC-RAS for the one-dimensional models and FESWMS for the two dimensional models. The tidal hydraulics studies included an application of RMA2 for the two-dimensional model. The series of sensitivity studies are described below.

Multiple Openings

The baseline geometry was altered to include from 1 to 5 openings, alternating the location of the opening from one side to the other.

Bridges Located on River Bends

The baseline geometry was altered to include a bend at the center of the bridge crossing. The crossing remained perpendicular to the channel. The bend varied from 0° (baseline) to 90° in increments of 30°. Additionally, the bend included two radii of curvature: one equal to half the floodplain width and one equal to one quarter of the floodplain width.

Bridges near Confluences

The baseline geometry was altered to include a confluence with a secondary channel. The secondary channel enters the main channel at a 30° and 60° angle. The location of the confluence occurs both immediately upstream and one bridge length upstream. The flow boundary condition on the secondary channel measured 50% and 75% of the main channel.

Bridges with Significant Constrictions

The baseline geometry was altered to include encroachment of the abutments into the channel. The width of the bridge opening (at existing grade) was varied including: baseline, channel banks, 90% of the upstream channel width, and 75% of the upstream channel width.

Overtopping Flow

The baseline geometry remained intact. This study employed flood flow boundary conditions. The downstream boundary conditions vary such that the water surface elevation at the bridge equaled: the low chord elevation, the roadway, and a height equal to the roadway width above the roadway.

Embankment Skew

The baseline geometry was altered to vary the bridge crossing skew to the channel. The skew varies between 15° and 60° in increments of 15°.

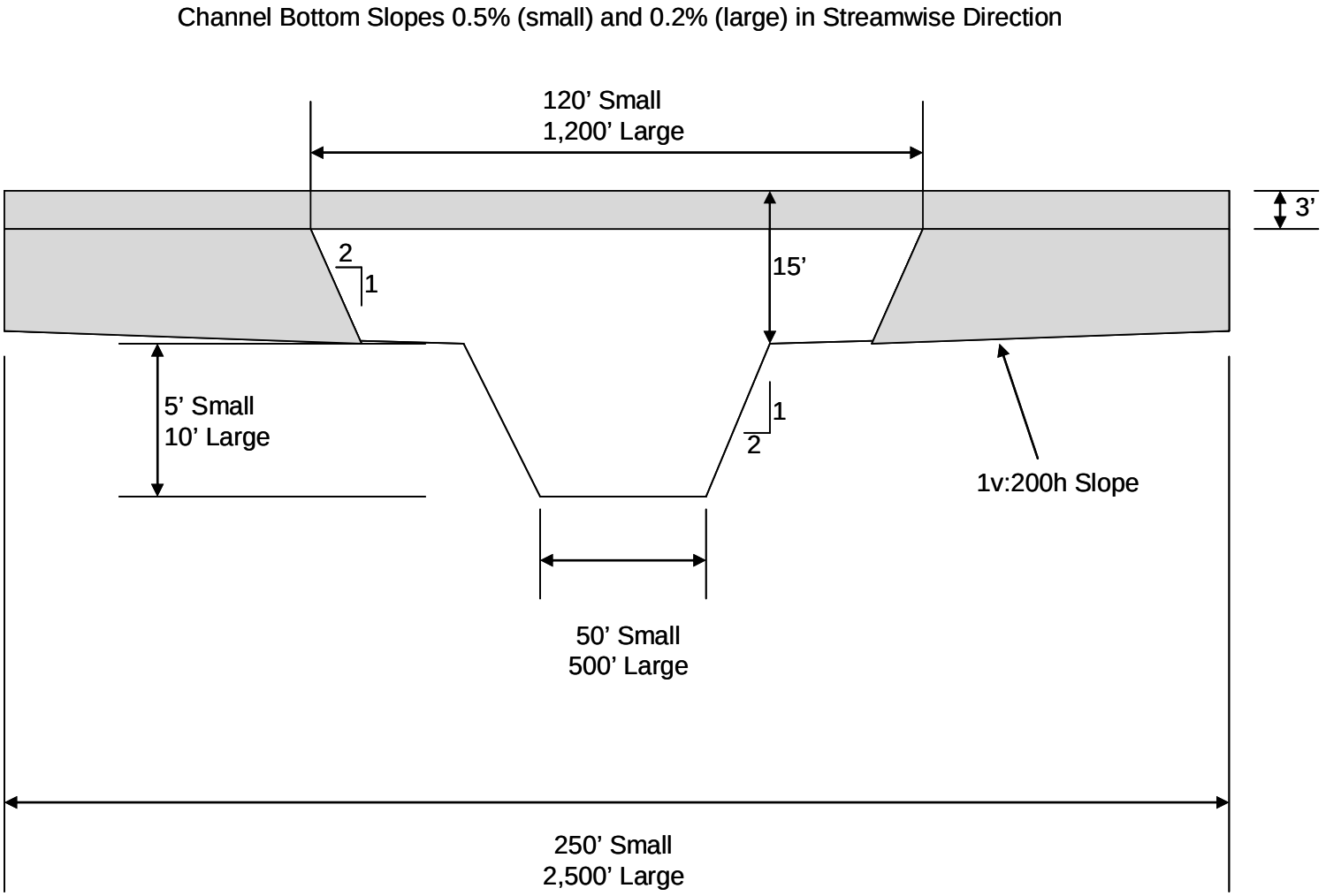

Figure 4 Idealized Channel Dimensions

Bridges over Meandering Rivers

The baseline geometry was altered to vary the sinuosity both upstream and downstream of the bridge crossing. The sinuosity (stream centerline length over length along floodplain) was varied from 1.0 (baseline) to 2.0 in increments of 0.25. The meander was modeled as a sine curve with varying frequency.

Bridges with Asymmetric Floodplains

The baseline geometry was altered to vary the width of the floodplain on one side. The width of the floodplain on one side of the channel was varied from the original width to the channel bank by reducing the width in increments of 25% of the original width.

Bridges with Large Piers/High Blockage

The baseline geometry was altered to include bridge piers. The width of the piers was varied such that the blockage will increase from 5% to 35% of the channel top width (measured bank to bank) in increments of 10%.

Tidal Hydraulics

In addition to the above sensitivity studies, the studies included a series of experiments to compare one- and two-dimensional models in tidal environments. Given the large number of responses that made reference to these types of problems, tidal situations require some treatment within this project. Unfortunately, given the wide variety of possible geometries associated with coastal areas, creating one, or even several, idealized case(s) for sensitivity testing proved to be a formidable task. In an attempt to simplify this problem, this test is designed to test the appropriateness of the models for application in these instances. A simple and complex (in the judgment of the researchers) tidal situation was designed and tested during normal tidal and hurricane storm surge (design) conditions.

As described, the sensitivity study involved 88 individual conditions (including both medium and large channels) for a total of 176 individual simulations (including both one- and two-dimensional models). These studies are the subject of the ensuing chapter. Contour plots of the results from the experiments were generated and included in the Appendix. These contour plots were compared via difference contours and percentage difference plots. Additionally, the time spent during the setup and execution of the models was recorded in order to evaluate ease of application of the two models.

In addition to the sensitivity tests, the review identified several design considerations to be examined for their sensitivity to hydraulic inputs. These include the following:

- Riprap Sizing for Scour, Abutment, or Slope Protection
- Armor Units for Scour, Abutment, or Slope Protection
- Concrete Block for Scour, Abutment, or Slope Protection
- Abutment Scour Calculation

- Pier Scour Calculation
- FEMA “No-Rise” Studies
- Bendway Weirs

Chapter 5.0 describes the sensitivity of these issues to hydraulic inputs.

CHAPTER 4 SENSITIVITY TESTING AND MODEL COMPARISON

The sensitivity tests involved application of HEC-RAS for the one-dimensional modeling and FESWMS for the two-dimensional modeling. The lone exception to this involved the tidal hydraulics sensitivity tests. These tests involved the application of RMA2 for the two-dimensional modeling. The sensitivity tests involved the development of the one- and two-dimensional models independent of each other. In other words, no attempt was made to "calibrate" the HEC-RAS models to the FESWMS models or vice versa. Upon completion of the simulations, the model results were compared to each other. These comparisons included development of contour plots of velocity magnitude and water surface elevation as well as difference contours and percentage change contours between the modeling efforts. Additionally, the time spent applying each of the models for each simulation was recorded. This record is perhaps the best indicator of the ease of applicability/effort/cost associated with each models' application. This chapter provides a description of each of the sensitivity tests, the results of the simulations, and a discussion of the results.

MODELING PHILOSOPHY

The most efficient approach to model development involved performing the two-dimensional modeling for each simulation first. Upon completion of an individual study, only the model mesh was then provided to the engineer performing the one-dimensional modeling. The one-dimensional model was then constructed by pulling cross sections from the two-dimensional model mesh. This ensured that the two models employed the same elevation data as inputs. Essentially the two-dimensional model provided the digital terrain map for the one-dimensional model.

Development of the two-dimensional models first involved creation of the model geometry in AutoCAD. AutoCAD not only provided a means to quickly modify geometries for each of the individual model meshes, but also contains the mathematical tools to create some of the complex geometries associated with some of the models (e.g., sinusoidally meandering rivers). Elevation data was generated via an Excel spreadsheet. Again, this program contains the mathematical tools necessary for the more complex geometries. The AutoCAD drawings were then exported to dxf files and imported into the FESWMS interface SMS (Surfacewater Modeling System). The dxf provided the basis to create the model meshes. Mesh creation involved locating nodes along the top and bottom of the channel banks. Additionally, attempts were made to include several nodes across the bottom of the channel as well as between the top of the channel bank and the beginning of the bridge abutment. The meshes included increased resolution along the bridge abutments. Mesh resolution decreased with increasing distance from the bridge. Node location along the roadway embankments was determined through trial and error. Each simulation was run initially to determine the water surface elevation at the bridge. Then nodes were moved to locations just below these elevations along the embankments. This reduced the error associated with wetting/drying of elements by properly accounting for the wetted cross section at the bridge. Additional modeling parameters associated with the two-dimensional simulations included the following:

- Average water density equaled 1.937 slugs/ft^3;

- Unit flow convergence equaled 0.01 to 0.001 (in general);
- Unit water depth convergence equaled 0.01 to 0.001 (in general);
- Depth tolerance for drying equaled 0.25 to 0.5 ft;
- Manning's n equaled 0.025 for the channel, 0.045 for the roadway embankments, and 0.75 for the overbank areas;
- Manning's n did not vary with depth; and
- Constant eddy viscosities of 5 to 10 ft^2/sec in the channel and 10 to 50 ft^2/sec on the embankments.

Also, in general, the simulations involved employing a small relaxation factor and a high number of iterations to ensure convergence.

Development of the one-dimensional models involved employing the Energy (Standard Step) Bridge Method within HEC-RAS. In general, the required cross sections near the bridge were located as defined within the HEC-RAS User's Manual. Cross Sections 1 and 4 were located using equations found in the HEC-RAS Applications Guide. The expansion and contraction coefficients were set to the standard values of 0.1 and 0.3. The geometry and roughness values equaled those in the two-dimensional model with the exception of the higher roughness value associated with the abutments. Additional cross sections were included up- and downstream of the bridge cross sections to model the same reach length as the two-dimensional model. Interpolated cross sections were inserted as needed to fill in between the reach boundaries and the bridge. Boundary conditions of flow and starting water surface elevation matched those employed in the two-dimensional model.

MODEL SETUP

The first step in the sensitivity studies was to establish a baseline. The sensitivity studies began with two idealized channels: a "small" channel and a "large" channel. The channels have trapezoidal geometries in the cross section with gently sloping floodplains. The floodplains end with vertical bluffs at the left and right boundaries. The bridge openings have setbacks from the channel banks and are trapezoidal in shape (spill through abutments). Figure 4 illustrates both the large and small idealized channels.

The models included not only the channels at these crossings, but also extend upstream and downstream sufficiently far to satisfy the requirements of the individual sensitivity tests. This distance varied within the sensitivity study to adequately test the factor being examined. The baseline model also includes the following boundary conditions: a downstream elevation boundary condition to achieve an approximate depth of 10 ft at the bridge for the small channel and an approximate depth of 15 ft at the bridge for the large channel. The models also include an upstream flow boundary condition set to 95,000 cfs for the large channel and 5,000 cfs for the small channel. Again, these conditions vary for some of the factors investigated.

Upon completion of the baseline testing, this basic geometry was varied to test each of the factors listed above. Each factor was tested with both the large and small channel under steady-state conditions with the exception of the tidal hydraulics sensitivity tests.

The series of sensitivity studies are described below. Notably, each section described below presents example results from both the one- and two-dimensional models. The appendix contains contours of velocity magnitude and water surface elevation from both model results for every simulation. In order to display the HEC-RAS output on contours, points along the cross sections were output and plotted in SMS. The appendix also contains comparison plots. For these plots, the FESWMS output was interpolated onto the HEC-RAS cross sections to provide an accurate comparison. It should be noted that one of the advantages of the two-dimensional models is the more resolved spatial coverage throughout the domain. However, in the interest of examining only locations resolved in both models, the plots only show contours from points in both domains.

Baseline Models

Two baseline models were constructed according to the geometry presented in Figure 4. Figure 5 presents the large channel one-dimensional model and Figure 6 presents the water surface elevation solution along the channel centerline. Figure 7 presents the small channel two-dimensional model mesh and Figure 8 presents the solution via contours of velocity magnitude overlaid with velocity vectors indicating flow direction. Figure 9 presents a comparison of the difference in velocity magnitude for the large channel baseline model (FESWMS results minus HEC-RAS results). In the figure, contours of positive values indicate areas where the two-dimensional model predict higher velocities than the one-dimensional model and contours of negative values indicate areas where the two-dimensional model predicts lower velocities. Notably, the models tend to agree along the channel centerline. Large percentage differences do occur near the embankments where the flow becomes more two-dimensional. The one-dimensional model approaches this geometry assuming flow is perpendicular to the specified cross sections. Additionally, near the bridge, specification of ineffective areas serves to create areas of storage with zero flow along the floodplains upstream and downstream of the embankments. As such, the model will not resolve the local acceleration of the flow parallel to the embankment that occurs as the flow is forced through the bridge opening. Since the two-dimensional model does resolve this behavior. Thus, it will predict higher velocity magnitudes along the embankments.

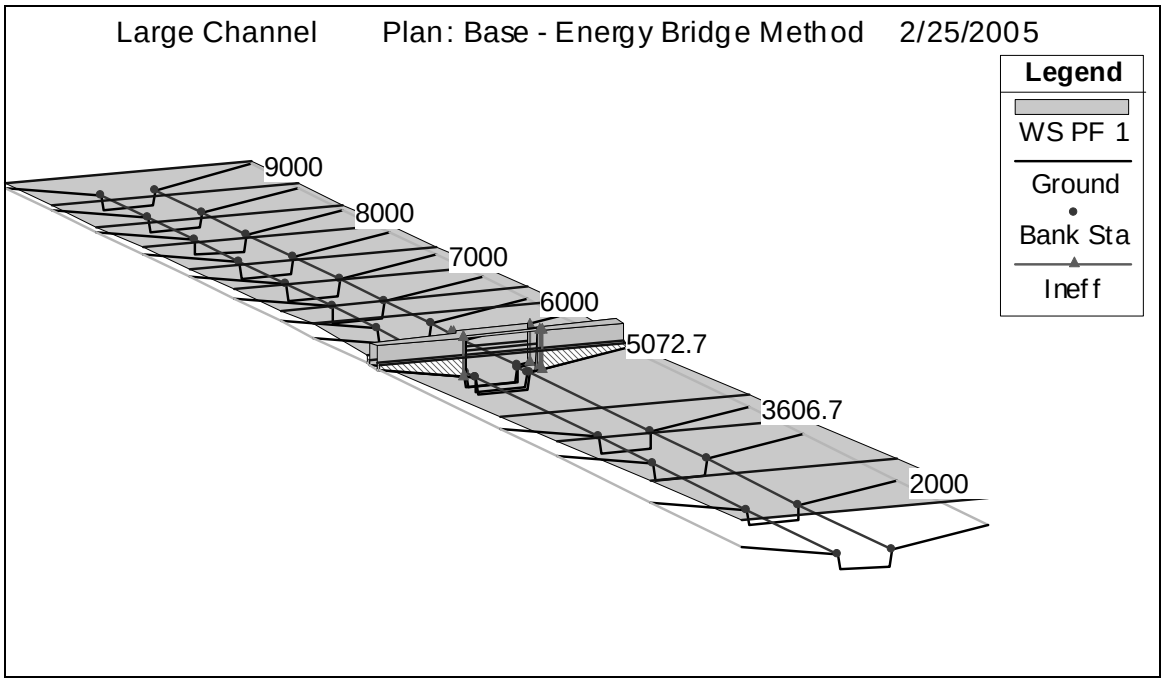

Figure 5 Large Channel Baseline One-dimensional Model Setup

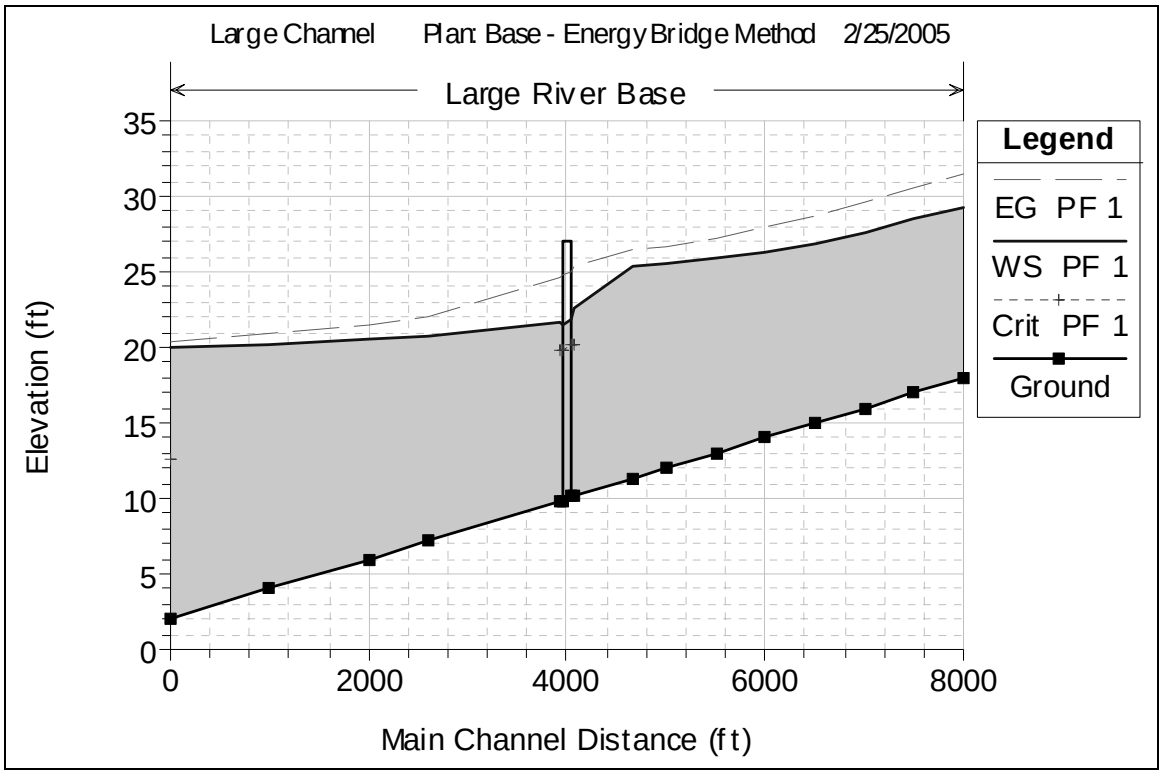

Figure 6 Large Channel Baseline One-dimensional Model Results

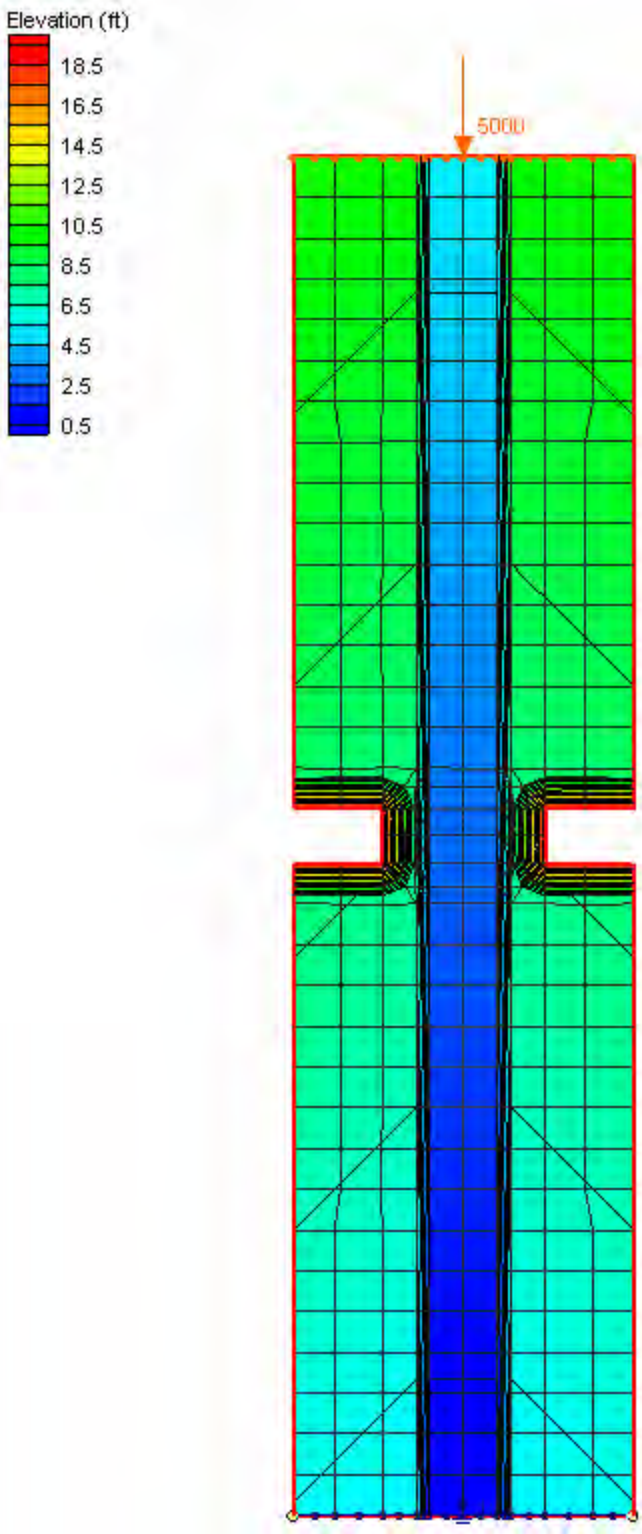

Figure 7 Small Channel Baseline Two-dimensional Model Mesh

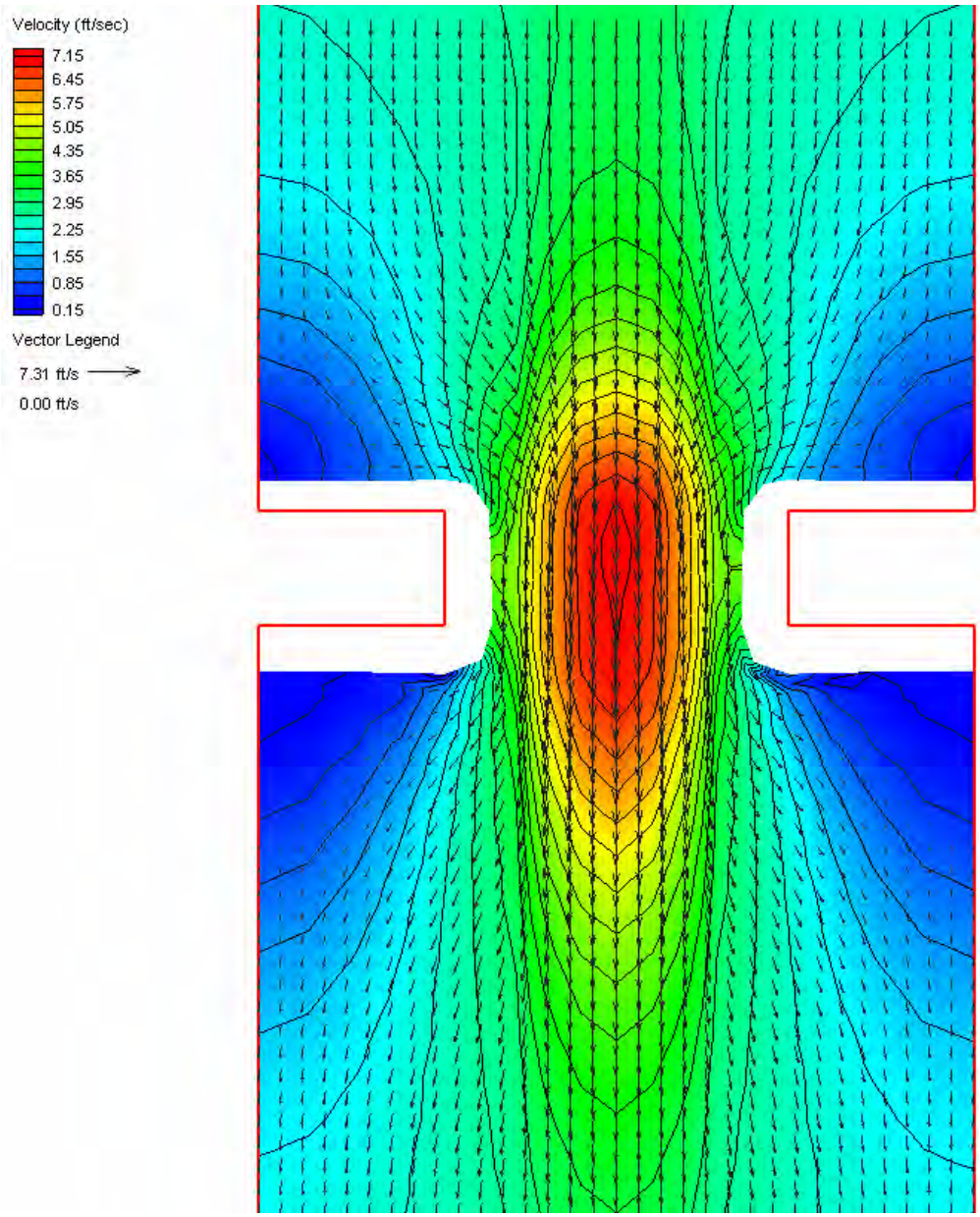

Figure 8 Small Channel Baseline Two-dimensional Model Results

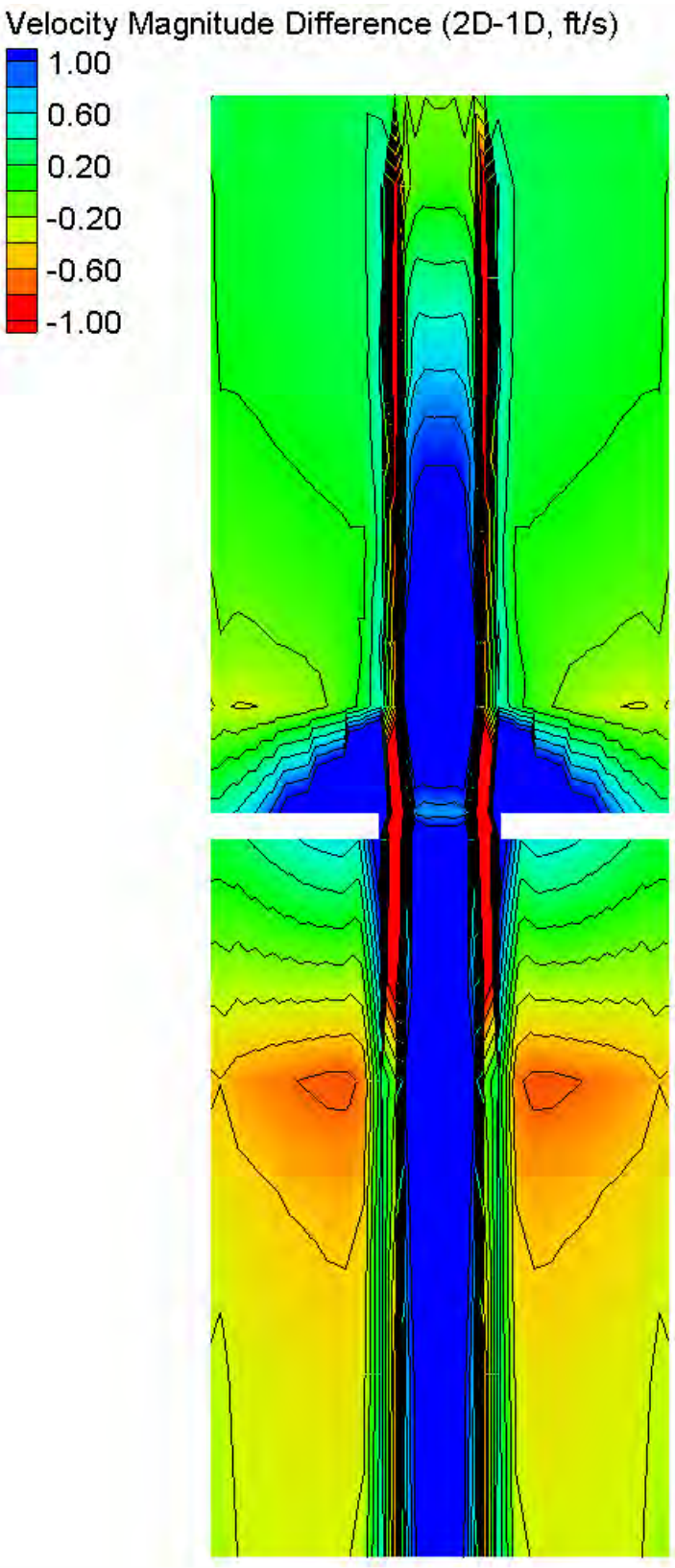

Figure 9 Velocity Magnitude Difference for Large Channel Baseline Models

Multiple Openings

The multiple opening experiments call for 1 to 5 openings in the elevated roadway (*causeways)* alternating the location of the opening from one side of the main opening to the other. In both the large and small channel models, the geometric parameters from the Baseline (Figures 4 and 6) are employed with some exceptions. For the two-dimensional models, the floodplain was expanded to provide the required space for the alternating openings. Additionally, the roadway was included in the model mesh. By including the roadway in the mesh, each alternative employs the same mesh with only minor modifications to the elevations and material properties when each opening is added. The one-dimensional models also required minor modification from the baseline models. These included the widening of the flood plain and the modifications to the bridge and the ineffective areas. Twenty models were generated for this experiment: ten for the large channel and ten for the small channel. Figure 10 through Figure 13 present examples of the model geometries and simulation results. Figure 14 presents the differences in velocity magnitude results at the bridge for the large channel multiple openings (four) models as percentage difference [100%*(2-D – 1-D)/2-D]. Notably, the models exhibit good agreement at the main channel and reasonable agreement at the side openings. As with the baseline tests, the models do not compare well in the areas along the upstream and downstream faces of the embankments.

Two methods are available in HEC-RAS to model multiple openings. The first is the program's multiple opening capability and the second is the program's divided flow capability. The multiple opening capability was used for all cases. The multiple opening capability within HEC-RAS evaluates each opening as a separate entity. The flow is divided between the openings and the computed upstream energies for each opening are compared. If the upstream energy grade lines are not within an allowed tolerance, the flow is redistributed in an iterative process until the energies are within the allowed tolerance. The two-dimensional model approach to this geometry differs. As flow approaches the openings, stagnation points that form along the embankment skew the flow upstream toward the different openings. The modeled flow through each opening results from the solution of the two-dimensional conservation of momentum equations which will locally balance the approach flow distribution and the local frictional losses.

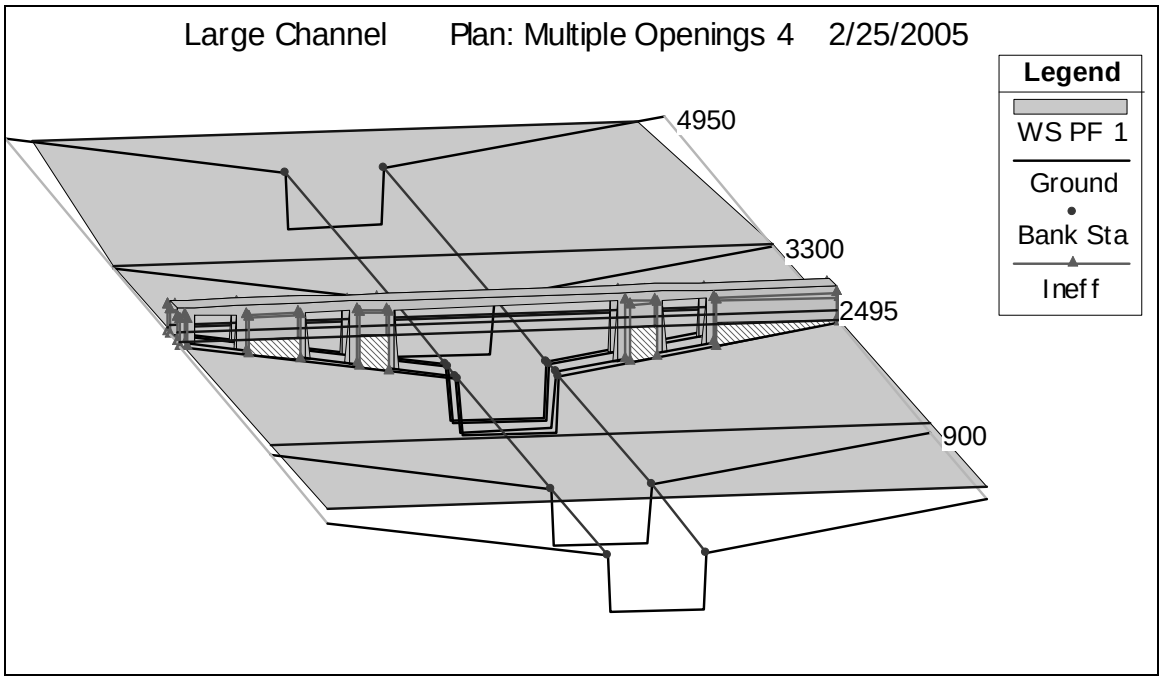

Figure 10 Large Channel Multiple Openings (Four) One-dimensional Model Setup

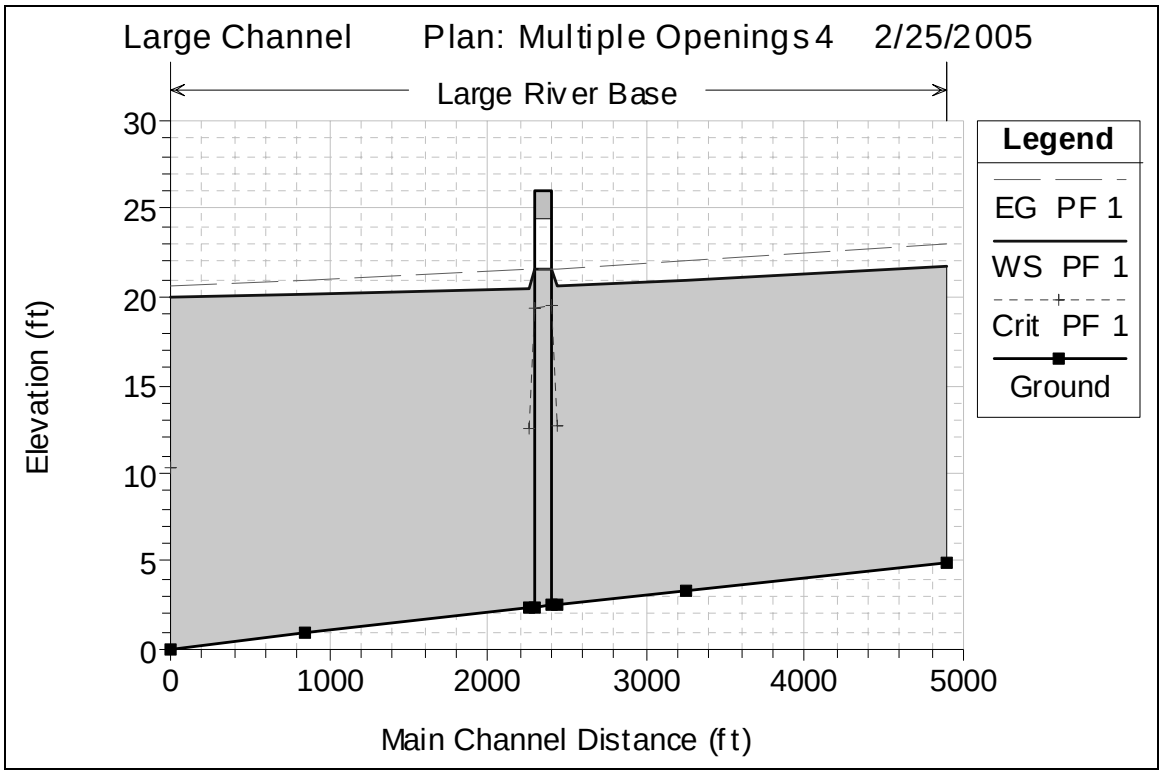

Figure 11 Large Channel Multiple Openings (Four) One-dimensional Model Results

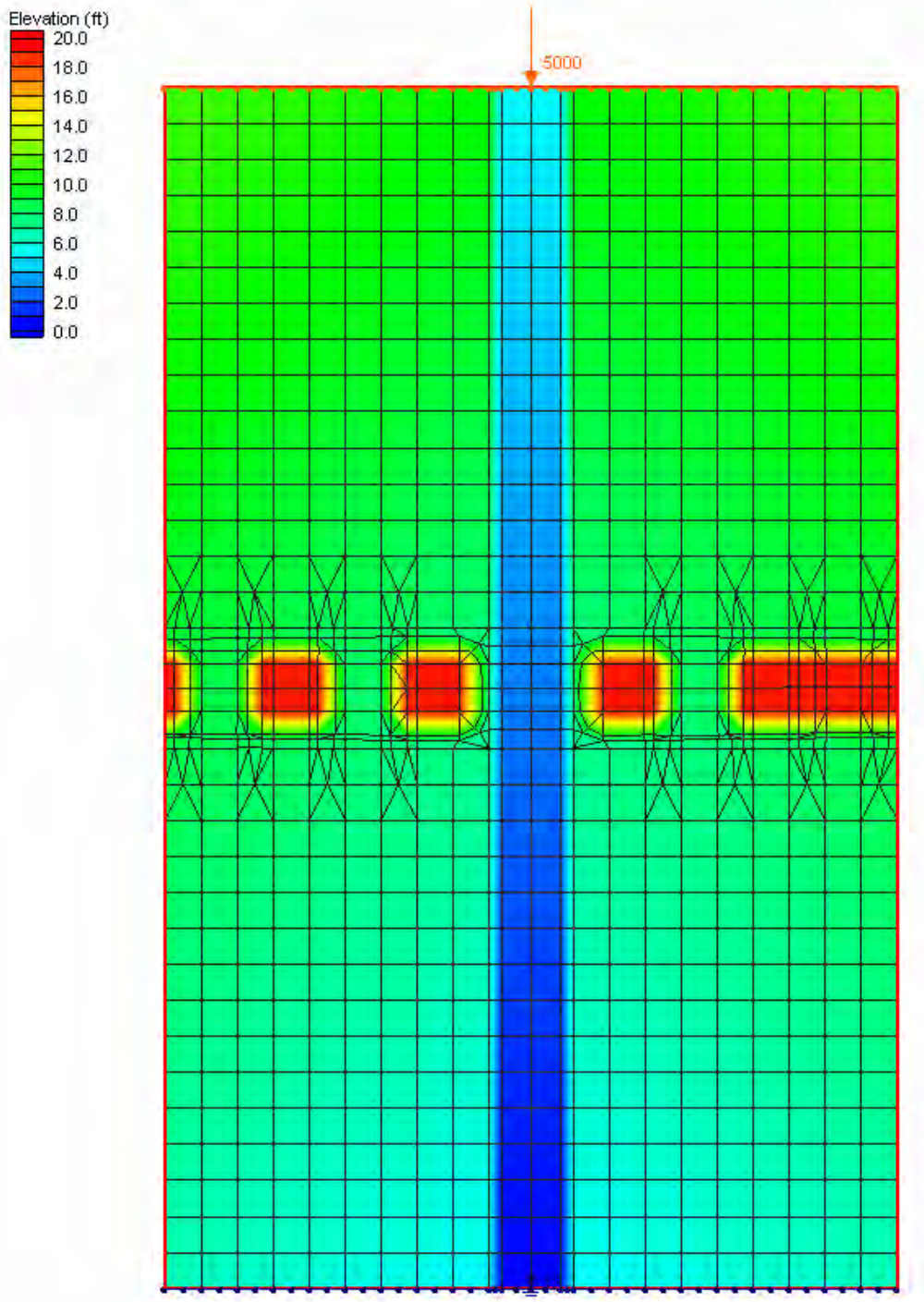

Figure 12 Small Channel Multiple Openings (Four) Two-dimensional Model Mesh

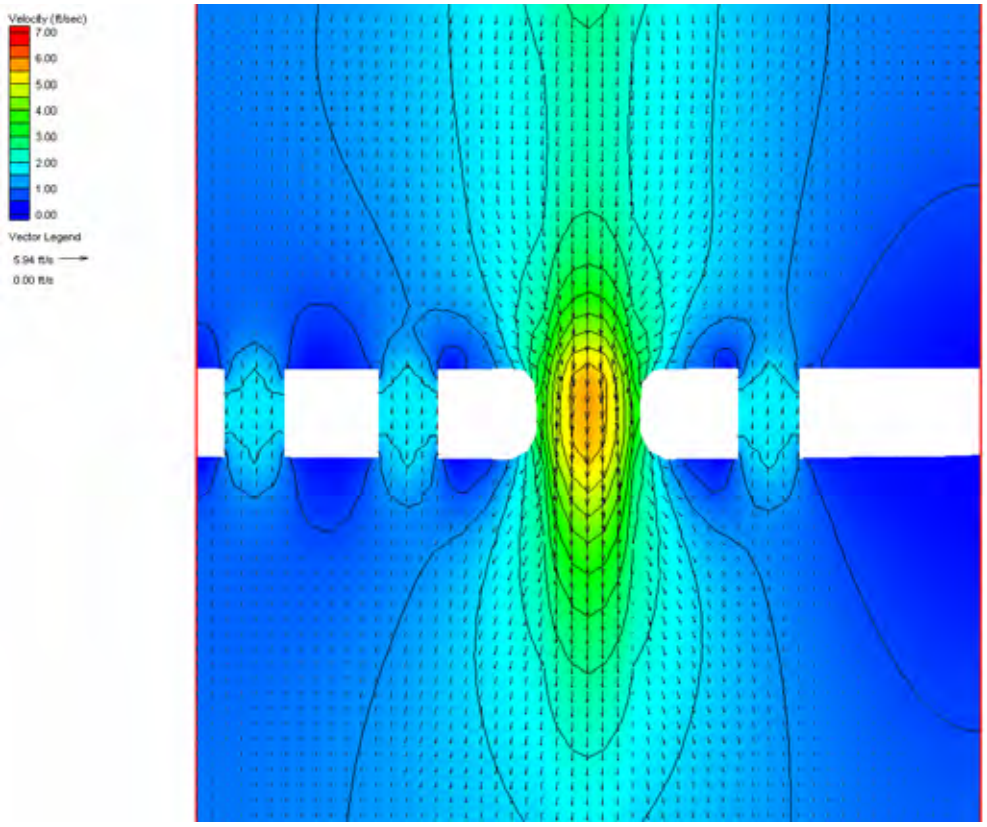

Figure 13 Small Channel Multiple Openings (Four) Two-dimensional Model Results

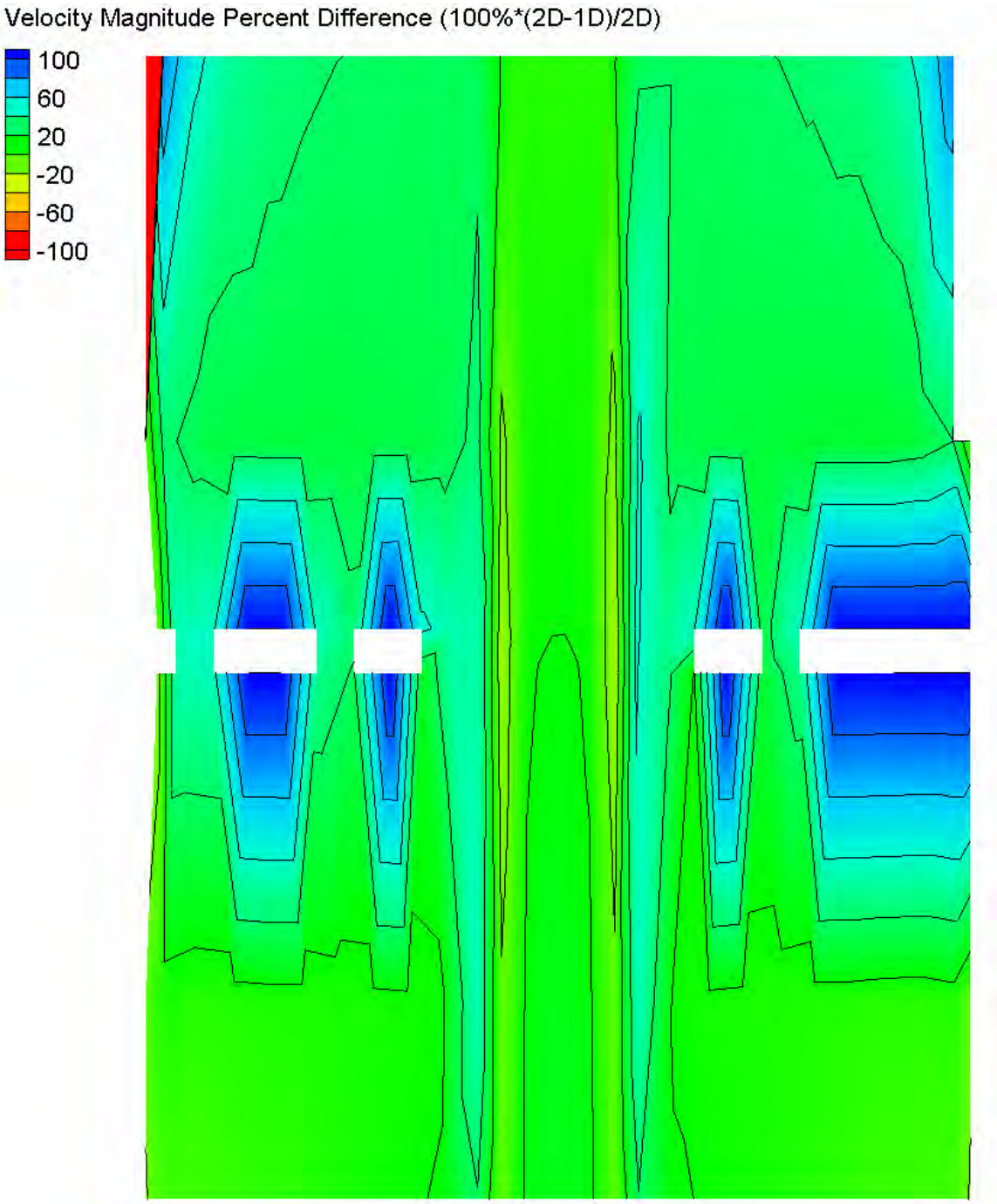

Figure 14 *Velocity Magnitude Percentage Change Comparison for Large Channel Multiple Openings (Four) Models*

Bridges Located on River Bends

These experiments investigate a bend at the center of the bridge crossing. The bend varies from 0° to 90° in 30° increments, with two radii of curvature: one equal to half the floodplain width and one equal to one quarter of the flood plain width. Twenty-four models were generated for this experiment, 12 for the large channel and 12 for the small channel. Figure 15 through Figure 18 illustrate examples of the two-dimensional model meshes and simulation results — velocity vectors overlaid on velocity magnitude contours. One-dimensional model development involved altering the locations of the upstream and downstream cross sections so as to not intersect the roadway embankments. Figure 19 illustrates a comparison of the water surface elevation solutions from the one- and two-dimensional models. The contours illustrate the results from the two-dimensional model minus the one-dimensional model results. From the figure, the one dimensional model is not accurately predicting the super elevation that can occur along the outside of the bend. Here, the one-dimensional solution is limited by the assumption of uniform water surface elevation across a cross section. Unlike the two-dimensional model, it will not accurately predict the secondary flows that result from the change in direction of the flow.

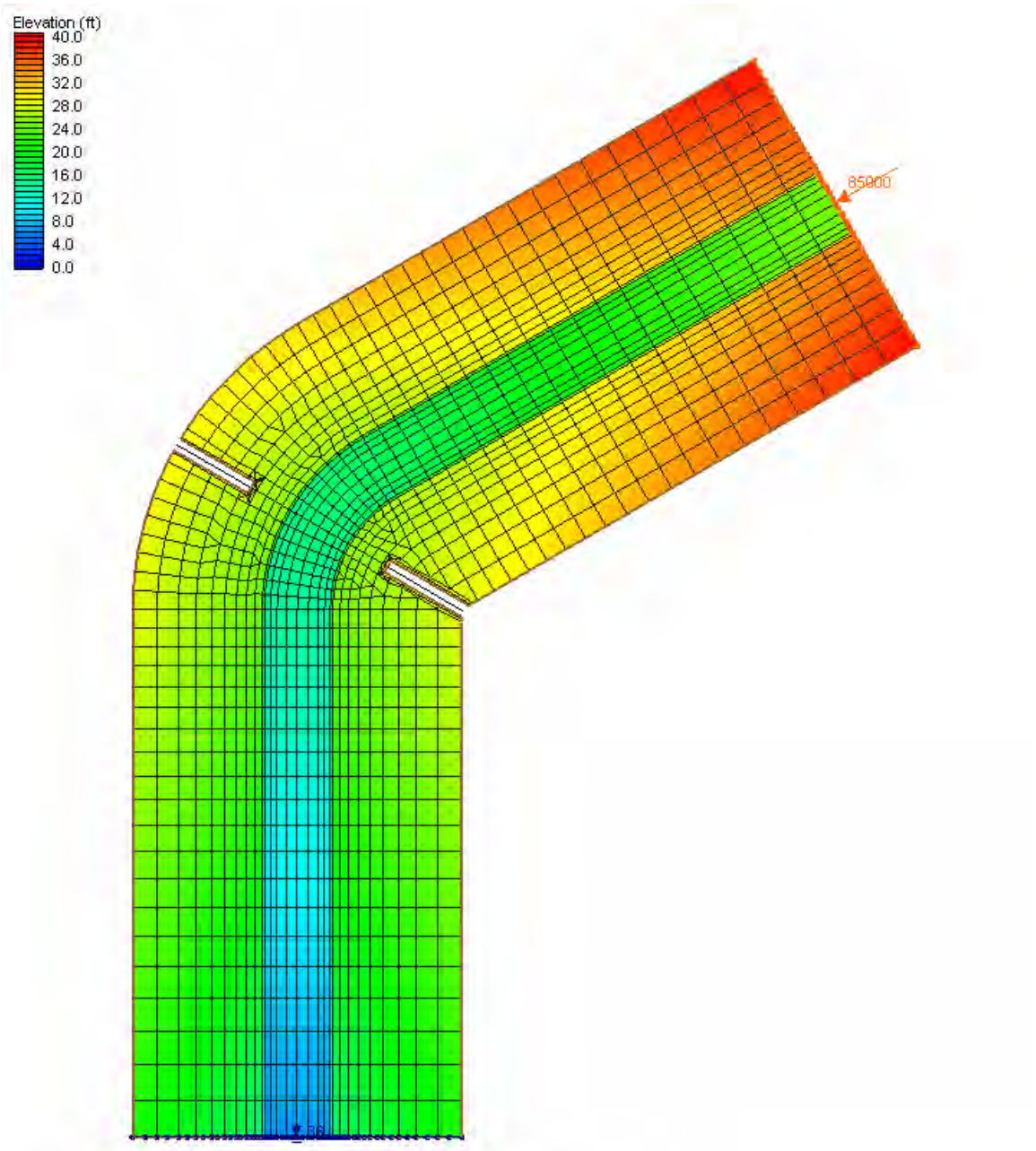

Figure 15 *Large Channel 60° River Bend Half Floodplain Radius Two-dimensional Model Mesh*

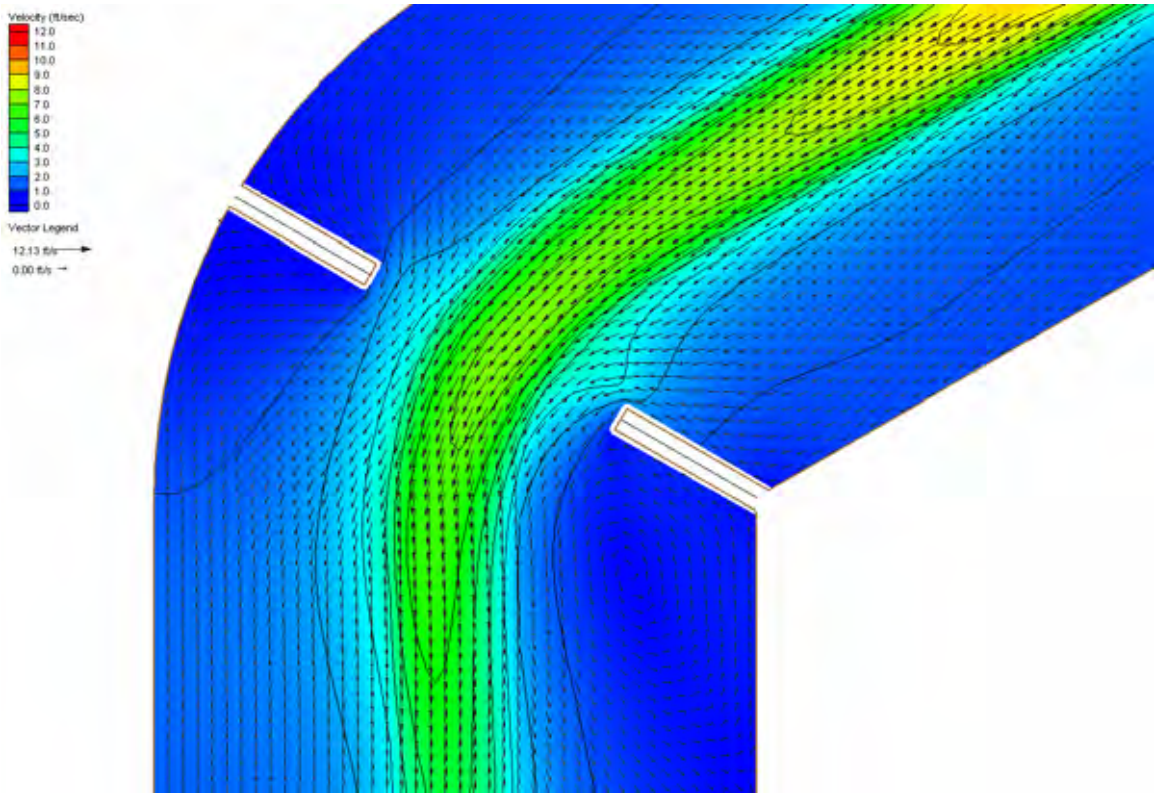

Figure 16 Large Channel 60° River Bend Half Floodplain Radius Two-dimensional Model Results

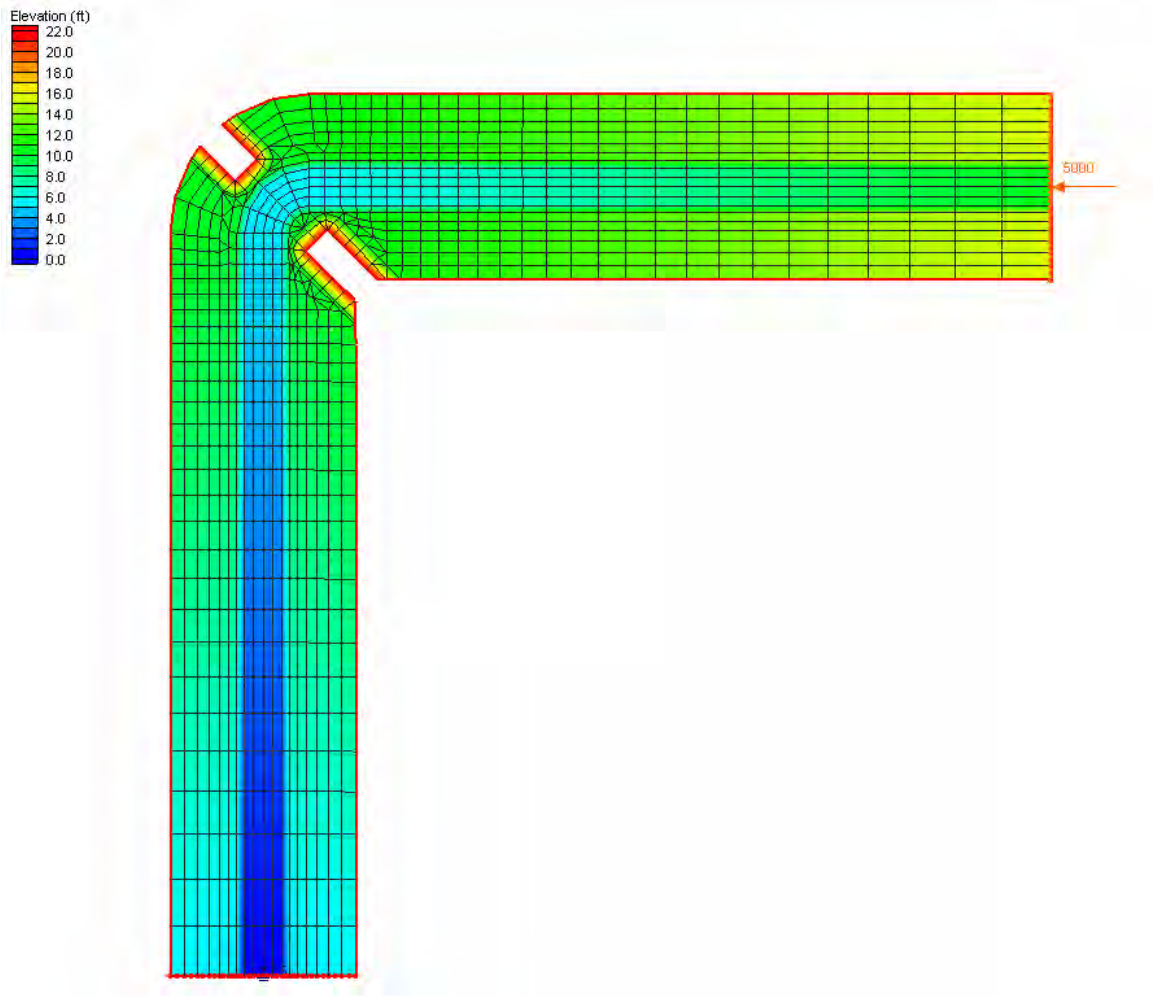

Figure 17 *Small Channel 90° River Bend Quarter Floodplain Radius Two-dimensional Model Mesh*

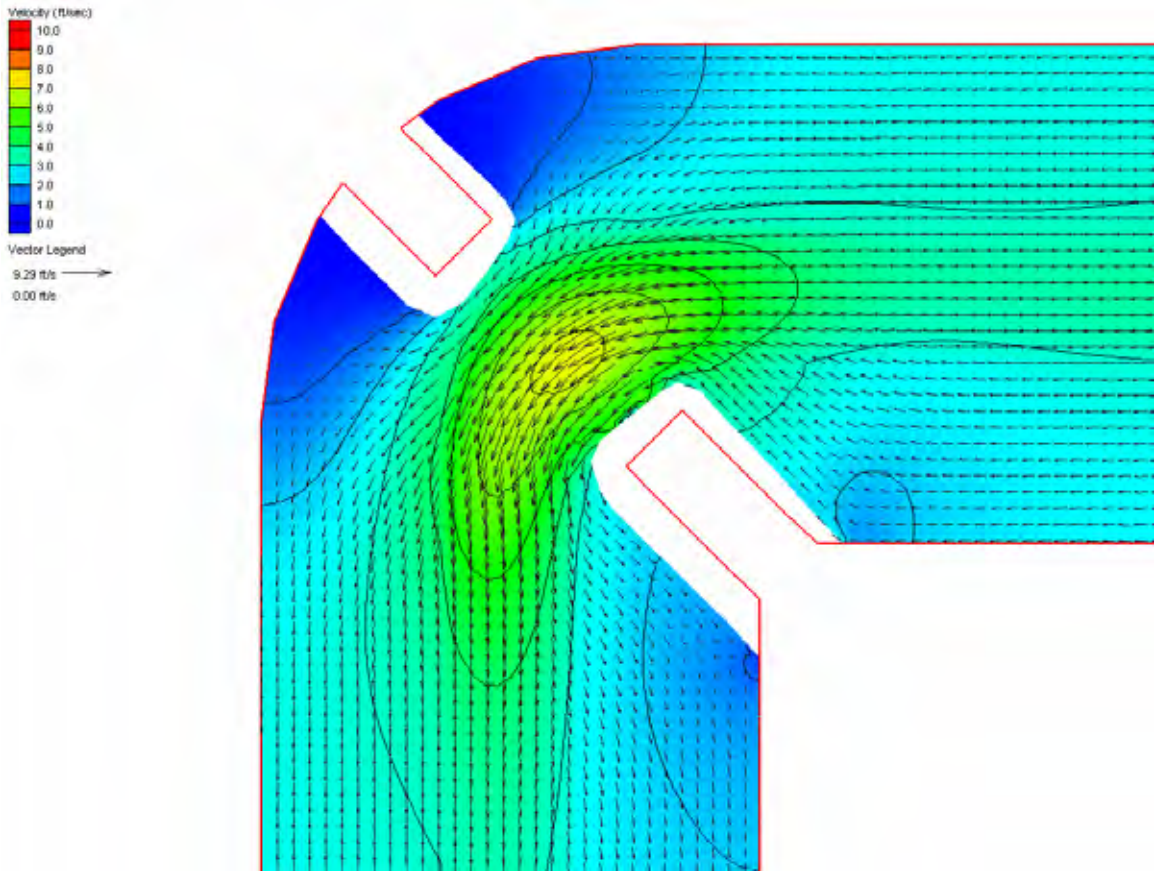

Figure 18 *Small Channel 90° River Bend Quarter Floodplain Radius Two-dimensional Model Results*

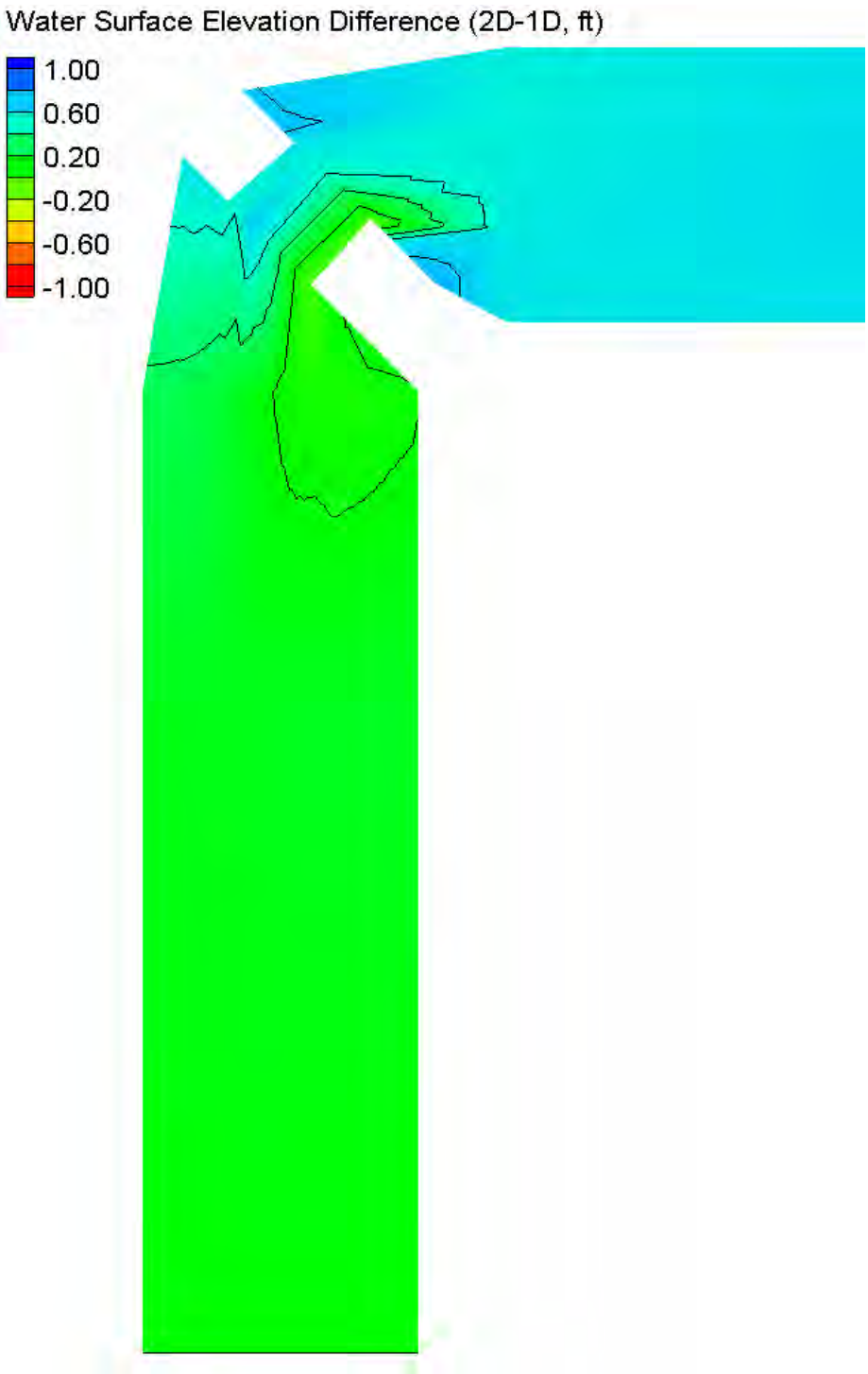

Figure 19 *Water Surface Elevation Comparison for Small Channel 90° River Bend Quarter Floodplain Radius Models*

Bridges near Confluences

These experiments involved evaluating confluences entering the main channel at two different locations, two angles, and two flows. Thirty-two models were generated for this experiment. In the models, the secondary channel enters the main channel at a 30° and 60° angle. The location of the confluence occurs immediately upstream and one bridge length upstream. The flow boundary condition on the secondary channel measured 50% and 75% of the main channel. Figure 20 through Figure 24 present examples of the model setups/meshes and simulation results for this sensitivity test. Figure 25 illustrates a comparison via the velocity magnitude percentage difference for the large channel 60° confluence at the bridge with 75% flow boundary condition models. The contours illustrate the difference between the two-dimensional and one-dimensional velocity magnitudes normalized by the two-dimensional velocity magnitude, or functionally as [100%*(2-D – 1-D)/2-D]. The figure shows a significant difference in the overall flow field both near the confluence and the bridge where the flow is highly two-dimensional. This results from that HEC-RAS outputs velocity based on flow perpendicular to the cross section while FESWMS provides the magnitude regardless of direction. This indicates that in this case there is significant flow parallel to the bridge face. This results in significant disagreement in outputted velocity magnitude.

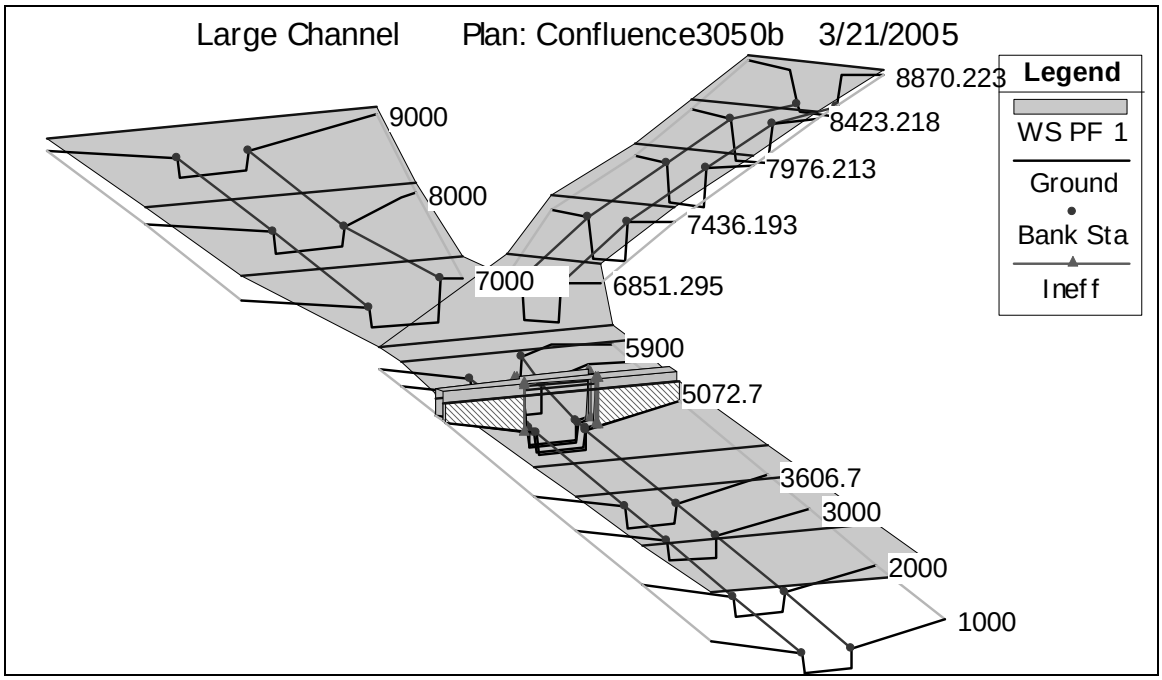

Figure 20 Large Channel 30° Confluence at Bridge with 50% Flow Boundary Condition One-dimensional Model Setup

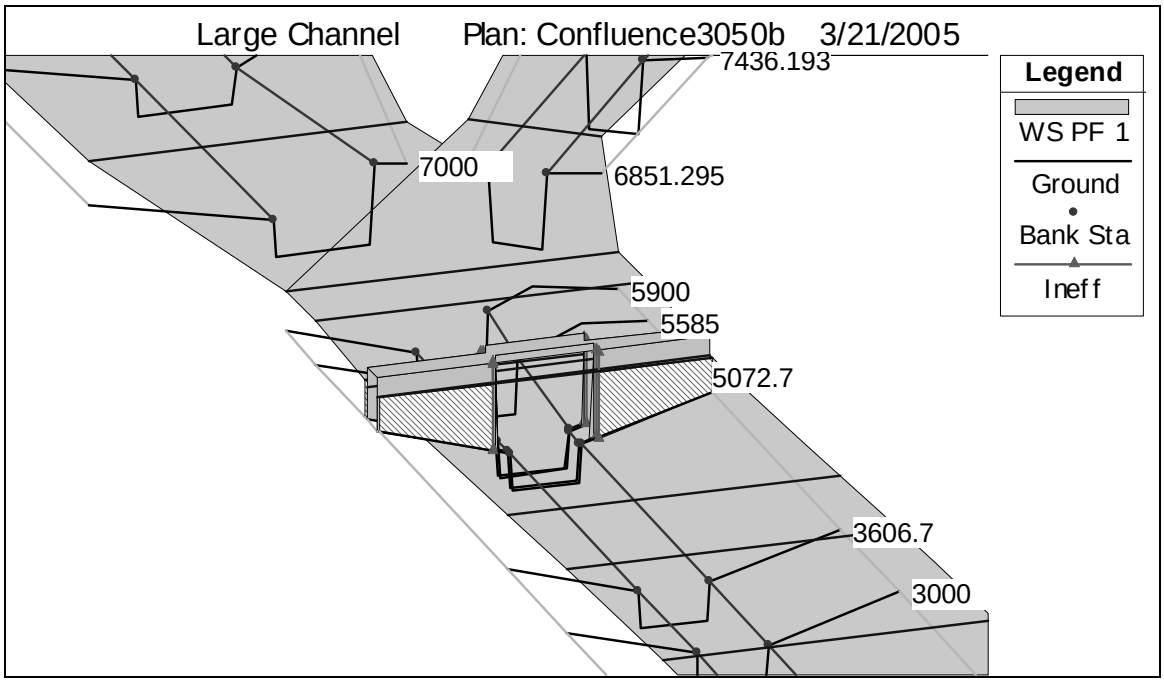

Figure 21 Enlargement of Large Channel 30° Confluence at Bridge with 50% Flow Boundary Condition One-dimensional Model Setup

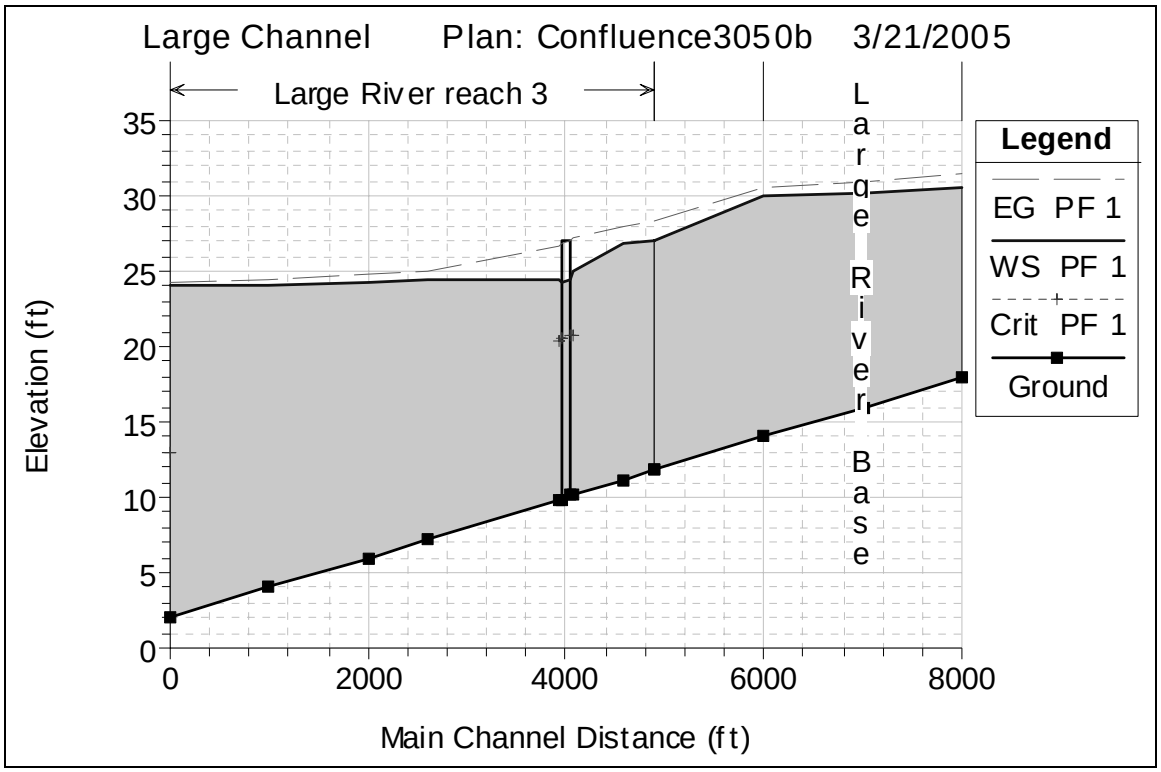

Figure 22 *Large Channel 30° Confluence at Bridge with 50% Flow Boundary Condition One-dimensional Model Results*

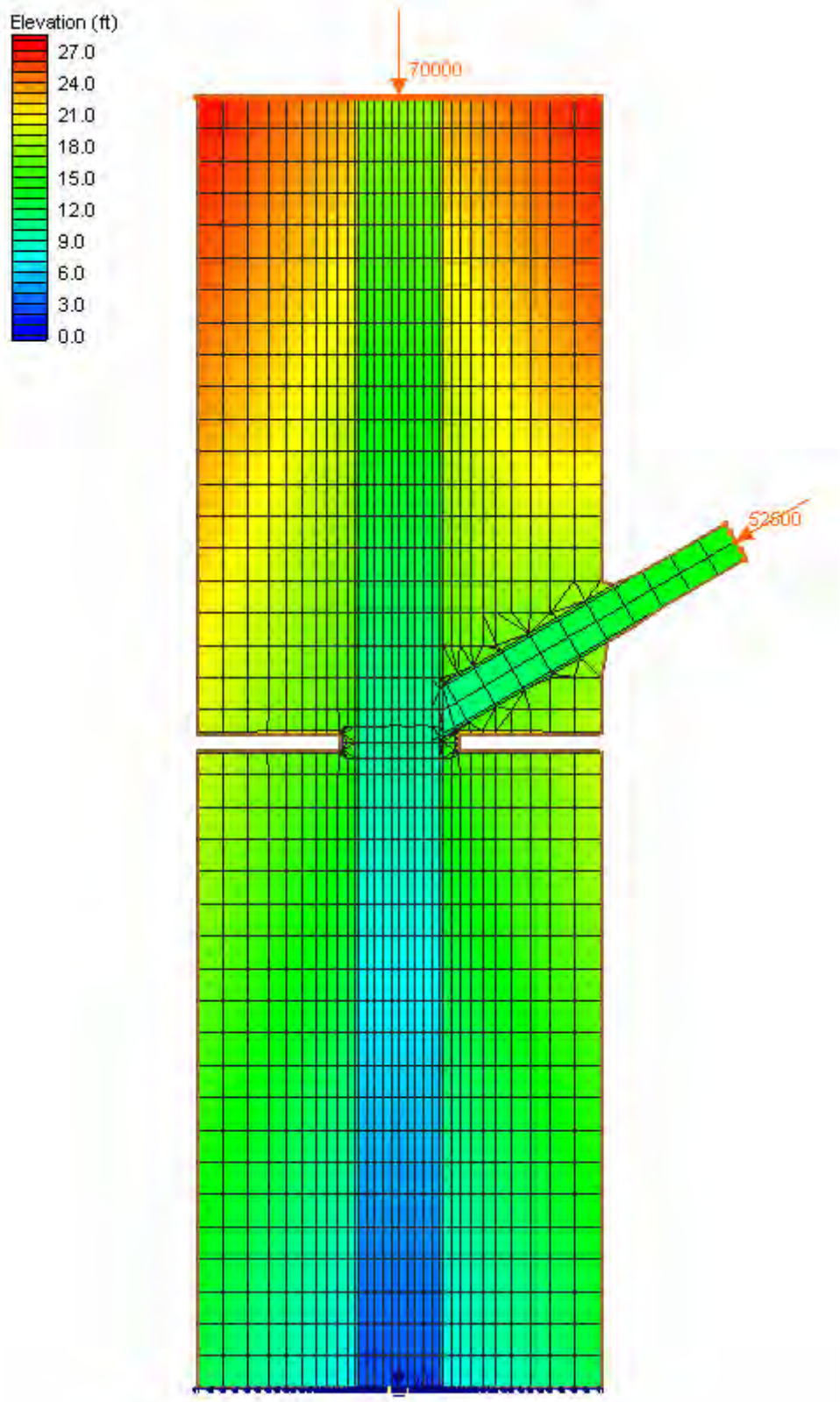

Figure 23 *Large Channel 60° Confluence at Bridge with 75% Flow Boundary Condition Two-dimensional Model Mesh*

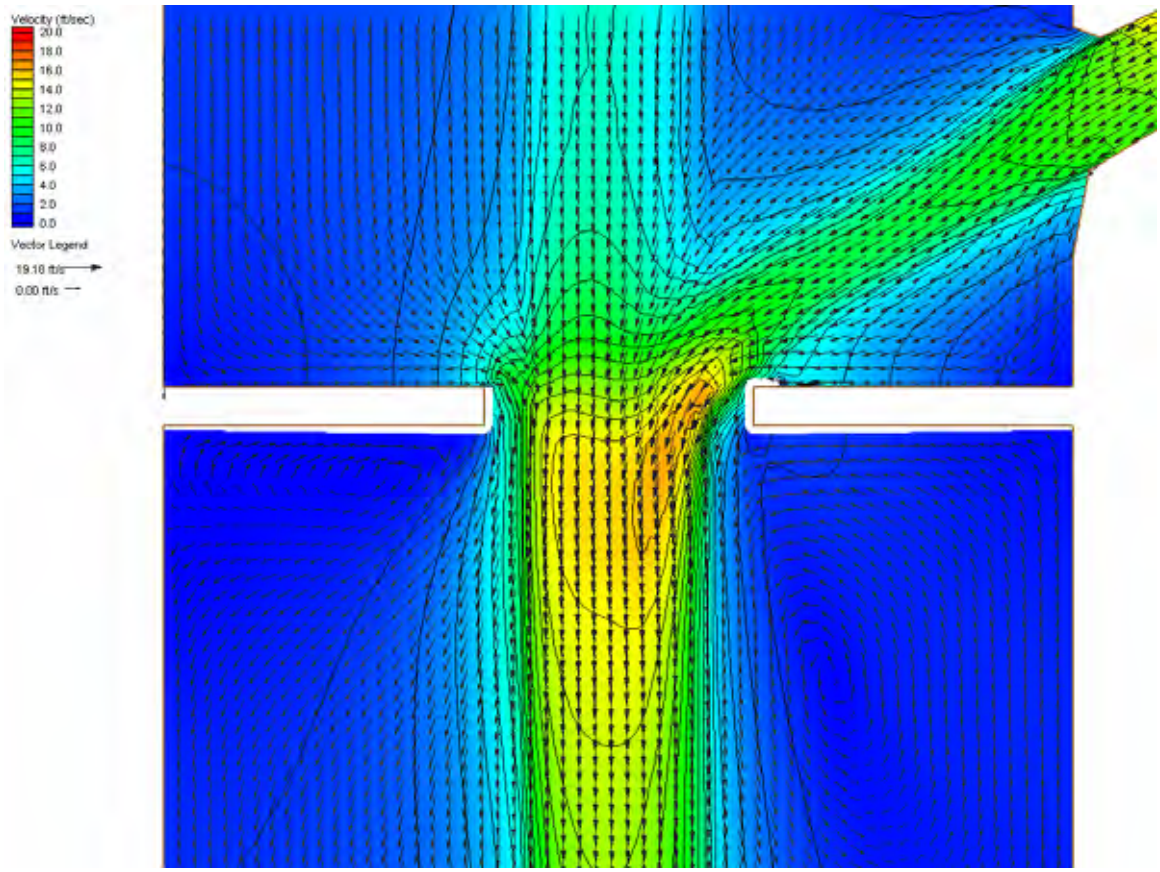

Figure 24 *Large Channel 60° Confluence at Bridge with 75% Flow Boundary Condition Two-dimensional Model Results*

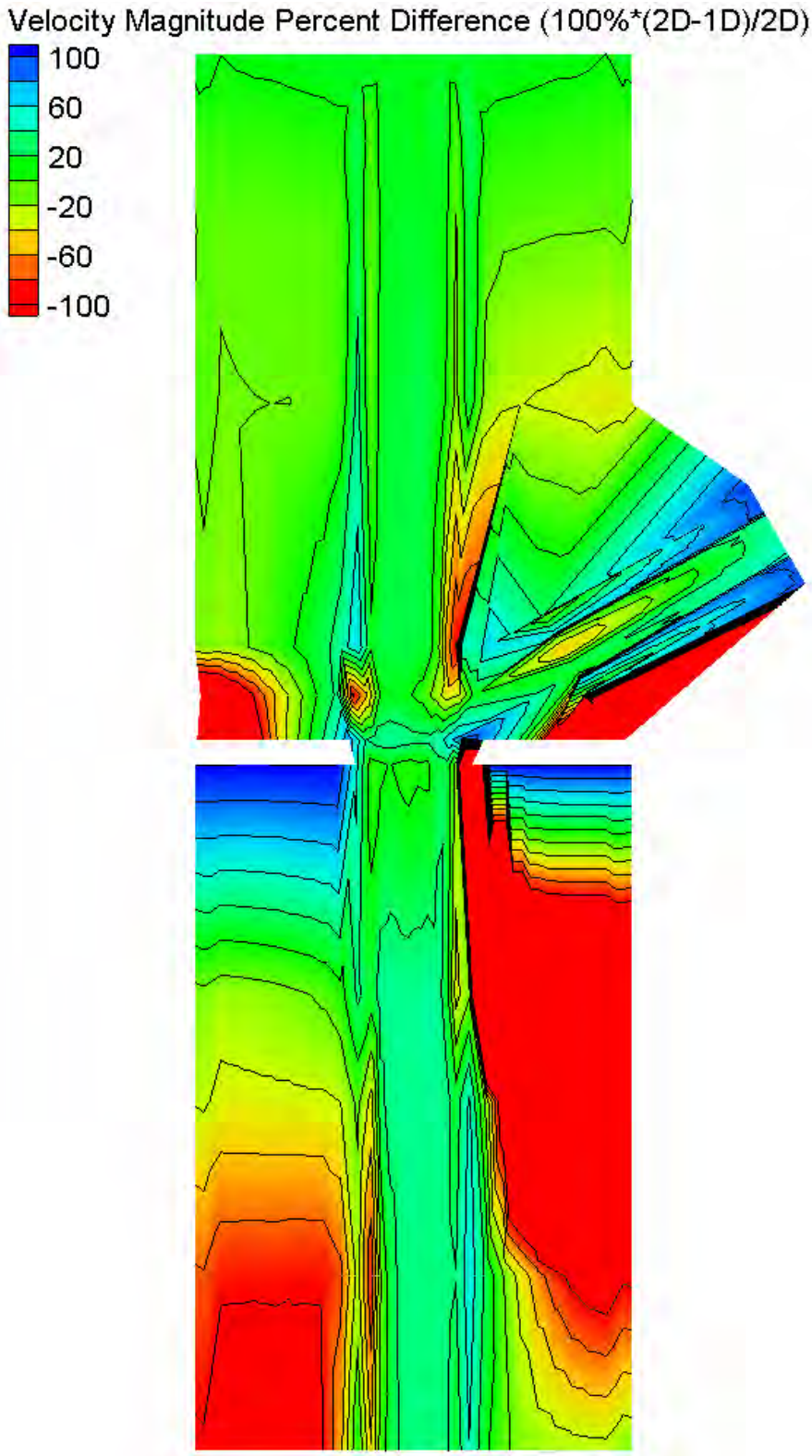

Figure 25 *Velocity Magnitude Percentage Difference Comparison at Upstream Bridge Face for Large Channel 60° Confluence at Bridge with 75% Flow Boundary Condition Models*

Bridges with Significant Constrictions

The experiments for the bridges creating significant constrictions evaluate the effect of variations in the width of the bridge opening. These included examining a reduction of the baseline bridge opening (at existing grade) to the channel banks, 90% of the upstream channel width, and 75% of the upstream channel width. Twelve models were generated for this experiment. Figure 26 through Figure 29 depict examples of the model meshes and simulation results for this sensitivity study. Figure 30 displays a comparison of the velocity magnitude percentage difference (calculated as described in previous sections) for the large channel with constriction (opening equals 75% of upstream channel width) models. The figure shows the one-dimensional model predicting significantly lower velocities at the bridge opening. The effects of a constriction at a bridge can be included in a one-dimensional via the expansion and contraction losses between cross sections. The expansion and contraction coefficients are multiplied by the difference between the velocity head at each cross section. A more significant constriction will cause a larger difference between the velocity heads of the bridge section and the up and downstream cross sections, which will cause a greater expansion and contraction loss. Increasing the expansion and contraction coefficients can further increase the magnitude of the expansion and contraction losses.

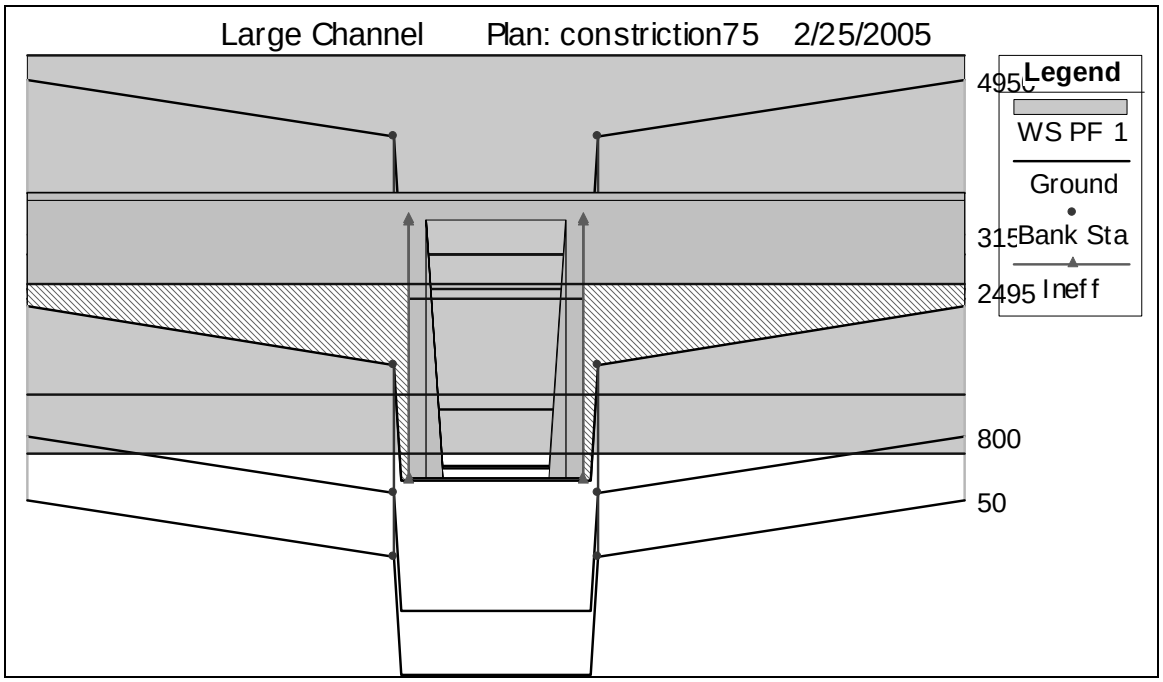

Figure 26 Large Channel with Constriction (Opening Equals 75% of Upstream Channel Width) One-dimensional Model Setup

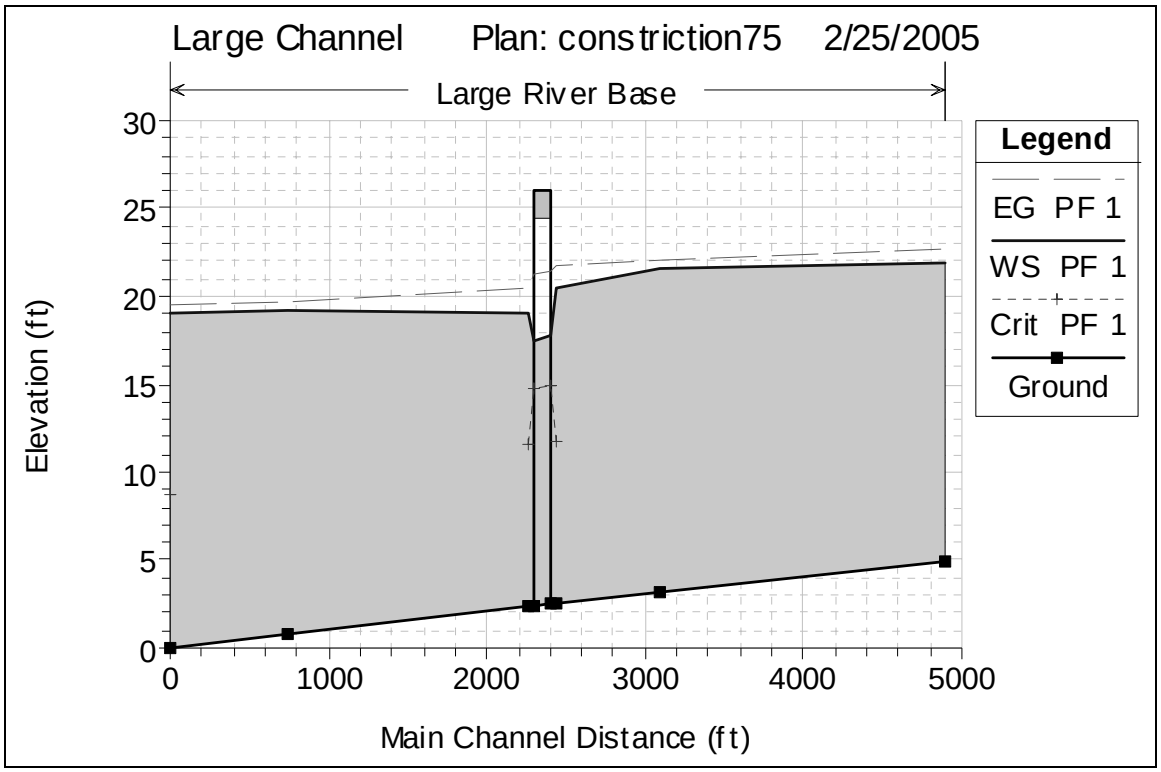

Figure 27 Large Channel with Constriction (Opening Equals 75% of Upstream Channel Width) One-dimensional Model Results

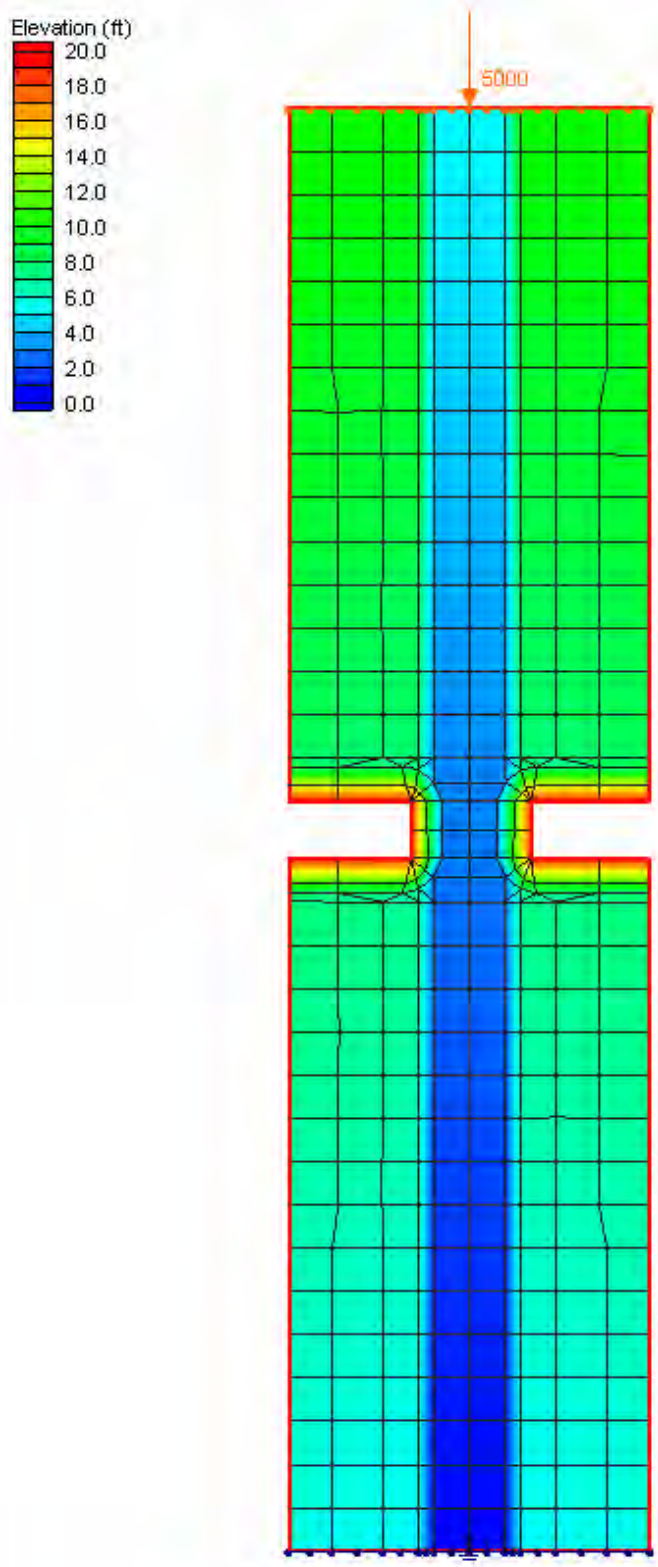

Figure 28 Small Channel with Constriction (Opening Equals 75% of Upstream Channel Width) Two-dimensional Model Mesh

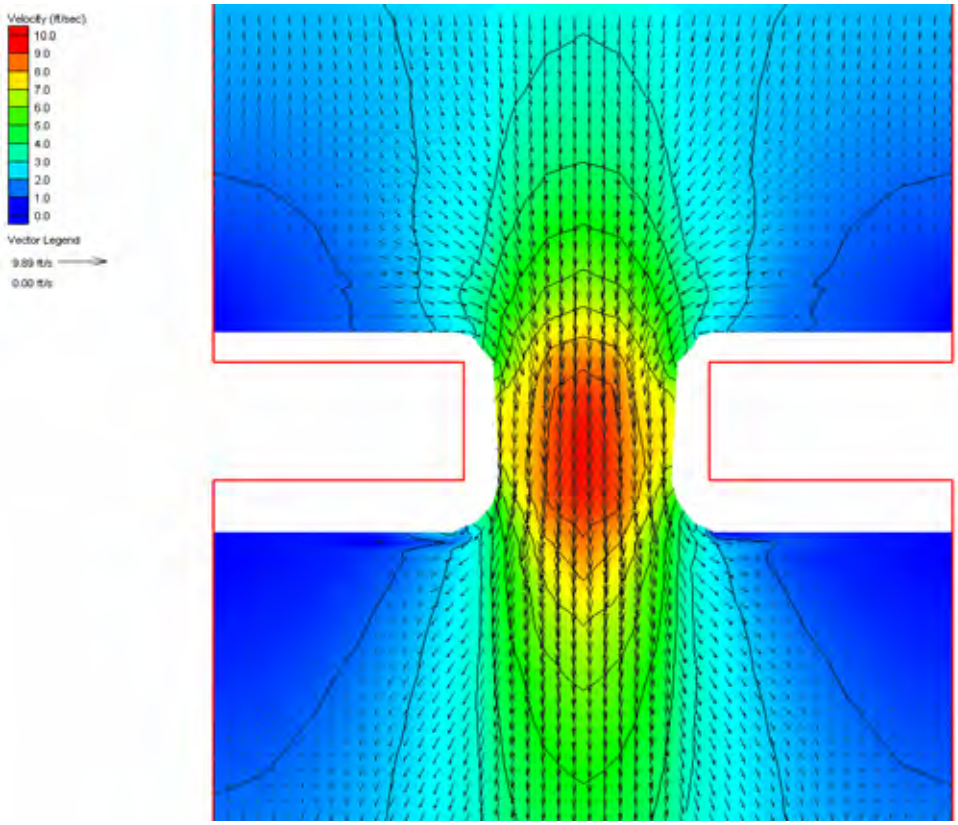

Figure 29 *Small Channel with Constriction (Opening Equals 75% of Upstream Channel Width) Two-dimensional Model Results*

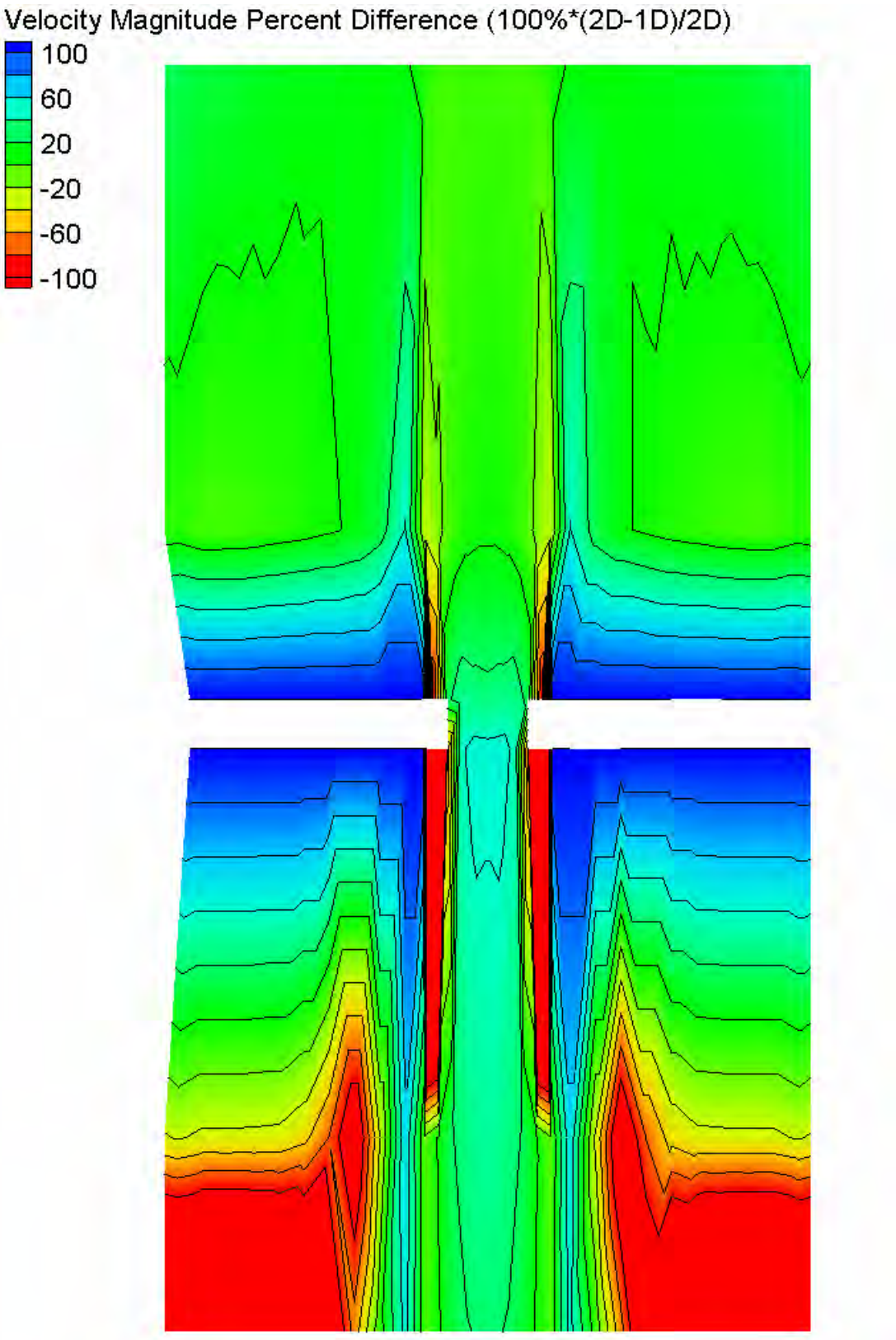

Figure 30 *Velocity Magnitude Percentage Difference for Large Channel with Constriction (Opening Equals 75% of Upstream Channel Width) Models*

Overtopping Flows

For the overtopping experiments, the baseline geometry remained intact. The downstream boundary condition was varied such that the water surface elevation at the bridge equaled the roadway and a distance equal to 10% of the roadway width above the roadway (10 ft and 7 ft). Unfortunately, evaluation of the low chord (pressure flow) conditions proved unsuccessful due to instabilities with the ceiling function in FESWMS. Representatives from BOSS International (a former vendor of SMS which provides support for the models employed in SMS) indicated that although the ceiling function works, significant instabilities still exist when employing this function. Help was also sought from Dr. Larry Arneson of the FHWA Western Resource Center (a member of the review panel for this project). He provided several techniques to attempt, but none proved successful. Given this obviously unacceptable result, this experiment was excluded from the two dimensional modeling sensitivity tests. As such, it is recommended that for pressure flow situations, for stability reasons alone, the one-dimensional model is preferable. For the one-dimensional models, the pressure/weir method was used for high flow. When the flow gets too high, the program switches back to the energy method. A total of eight models were created for this experiment. Figure 31 and Figure 32 present examples of the simulation results for this sensitivity test. Figure 33 presents a comparison of the velocity magnitude as a percentage difference for the large channel overtopping (10 ft above roadway) models. The contours were developed by dividing the difference in velocity magnitudes (2-D minus 1-D) and normalizing by the two-dimensional results. The models exhibit reasonable agreement both within the channel and along the overbanks. In the FESWMS model, since it was not possible to include the bridge deck in the calculations, the simulations should exhibit slightly larger velocities within the channel at the bridge. This is due to the lower losses via this flow path given the relatively larger area as compared with the HEC-RAS model. This was in fact the case. Also, the velocity vectors associated with this simulation indicate that the flow was decidedly one-dimensional in nature. As such, good agreement between the models was both expected and proved.

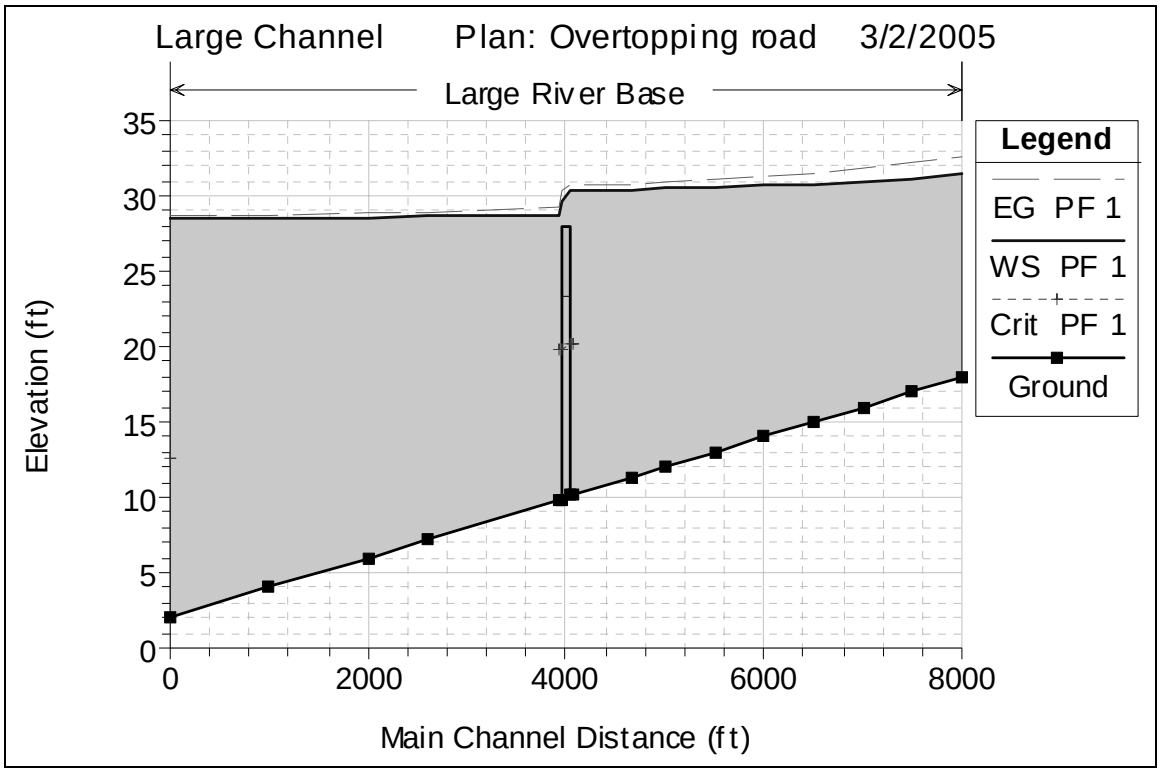

Figure 31 Large Channel Overtopping (10 ft above Roadway) One-dimensional Model Results

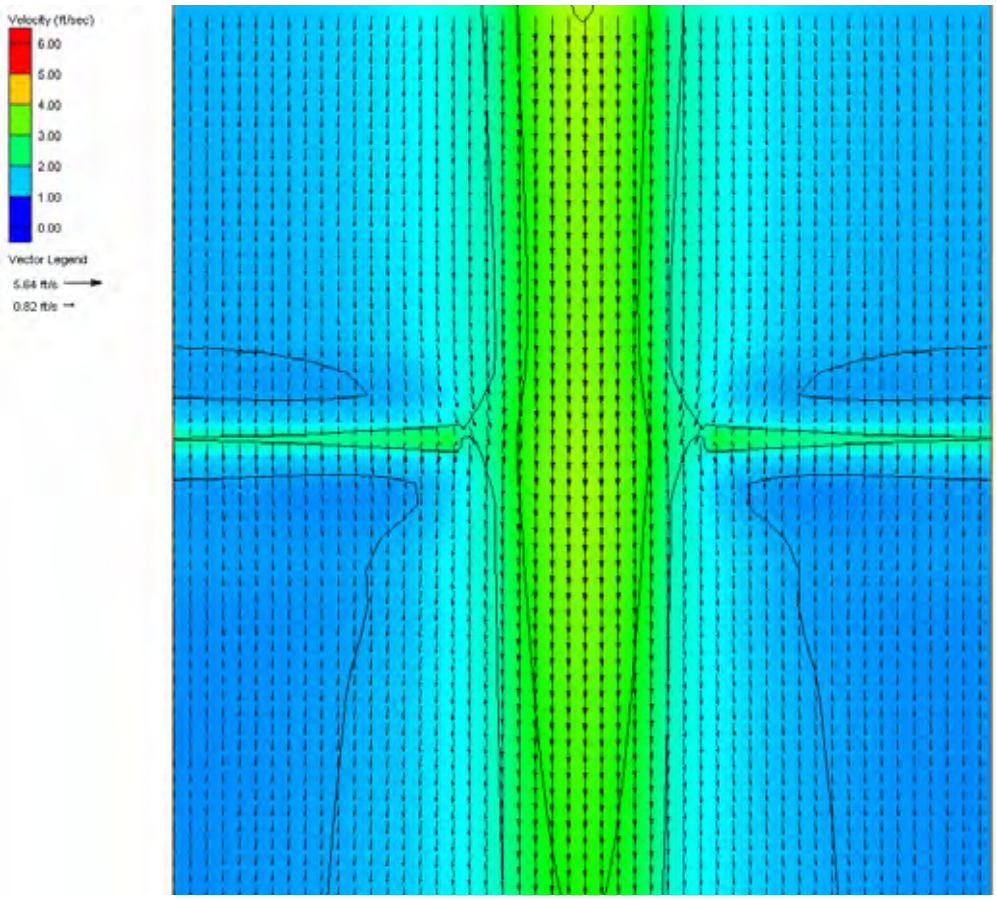

Figure 32 Large Channel Overtopping (10 ft above Roadway) Two-dimensional Model Results

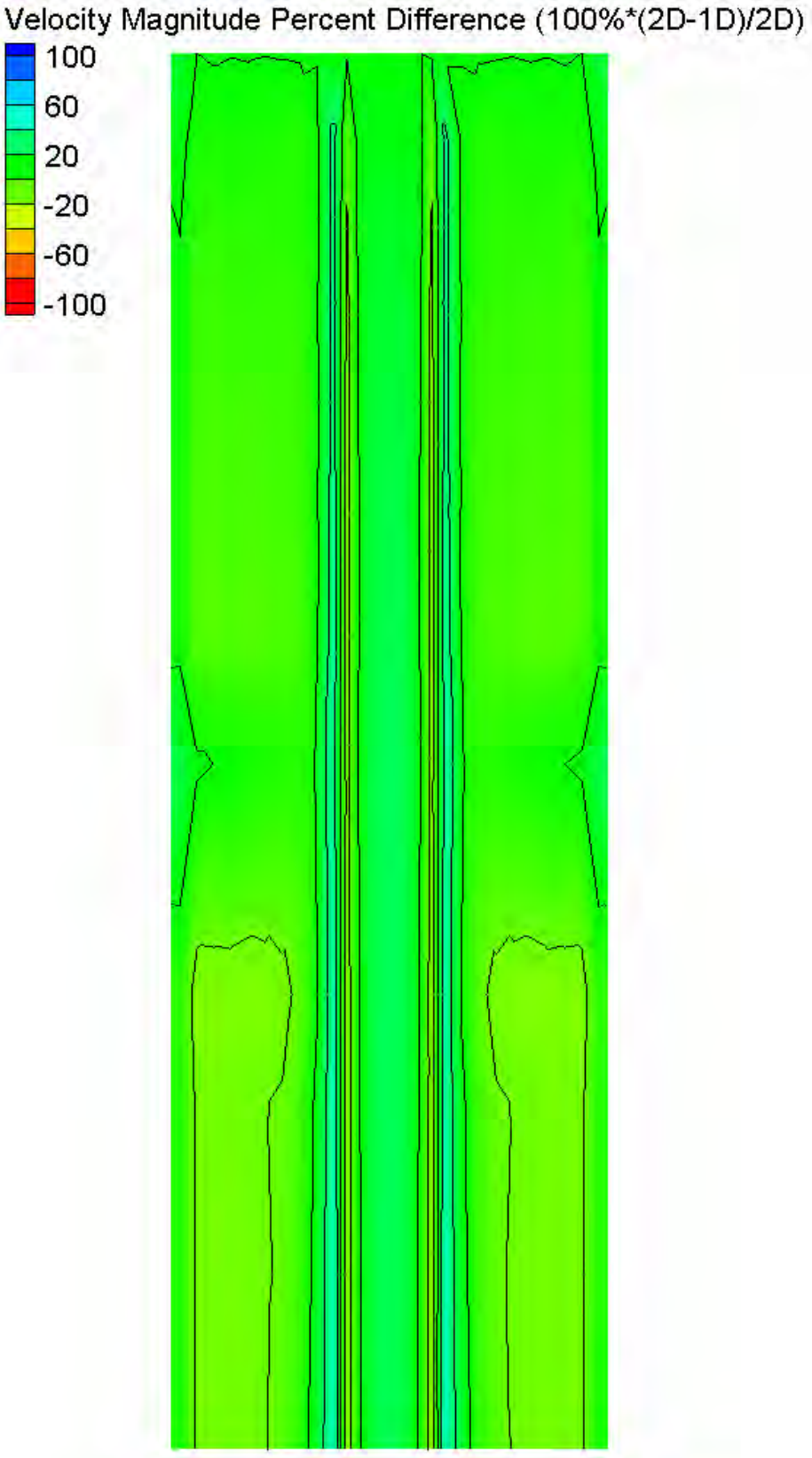

Figure 33 *Velocity Magnitude Percentage Difference for Large Channel Overtopping (10 ft above Roadway) Models*

Embankment Skew

This experiment involved altering the baseline geometry to vary the bridge crossing skew to the channel. The skew varied between 15° and 60° in increments of 15°. For the one-dimensional models, the skew cases required two different modeling approaches. The 15° and 30° cases were modeled by selecting the four cross sections parallel to the bridge and then applying the skew feature within HEC-RAS on all four cross sections and the bridge. The cases with bridges skewed greater than 30° were modeled without incorporating a bridge into the model. Cross sections were defined at various points in the vertical range of the bridge to model its geometry. Several of these cross sections were "dog-legged" such that they lay perpendicular to the flow (see Figure 34). Manning's n values were varied horizontally to incorporate the abutments. Sixteen models were produced for this experiment. Figure 35 and Figure 36 illustrate an example of a two-dimensional model mesh and simulation results — velocity vectors overlaid on velocity magnitude contours — for one of the sensitivity tests. Figure 37 presents a comparison of the velocity magnitude results in percentage difference for the large channel with 45° skewed bridge crossing simulations. From the figure, this one-dimensional modeling technique performed surprisingly well within the channel when compared to the two-dimensional modeling results. Not surprisingly, the model did not perform well in the areas along the embankments where the flow is more two-dimensional in structure.

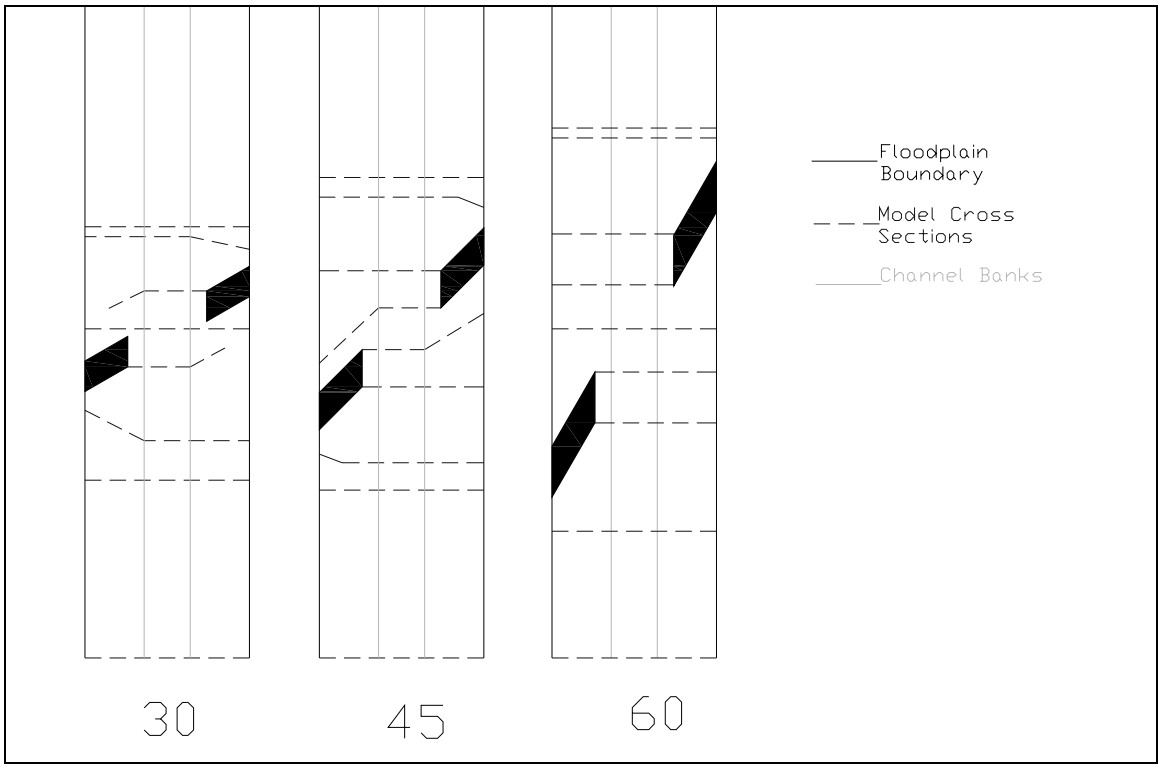

Figure 34 Cross Section Locations for the Small Channel Embankment Skew (30°, 45°, and 60°) One-dimensional Model Setups

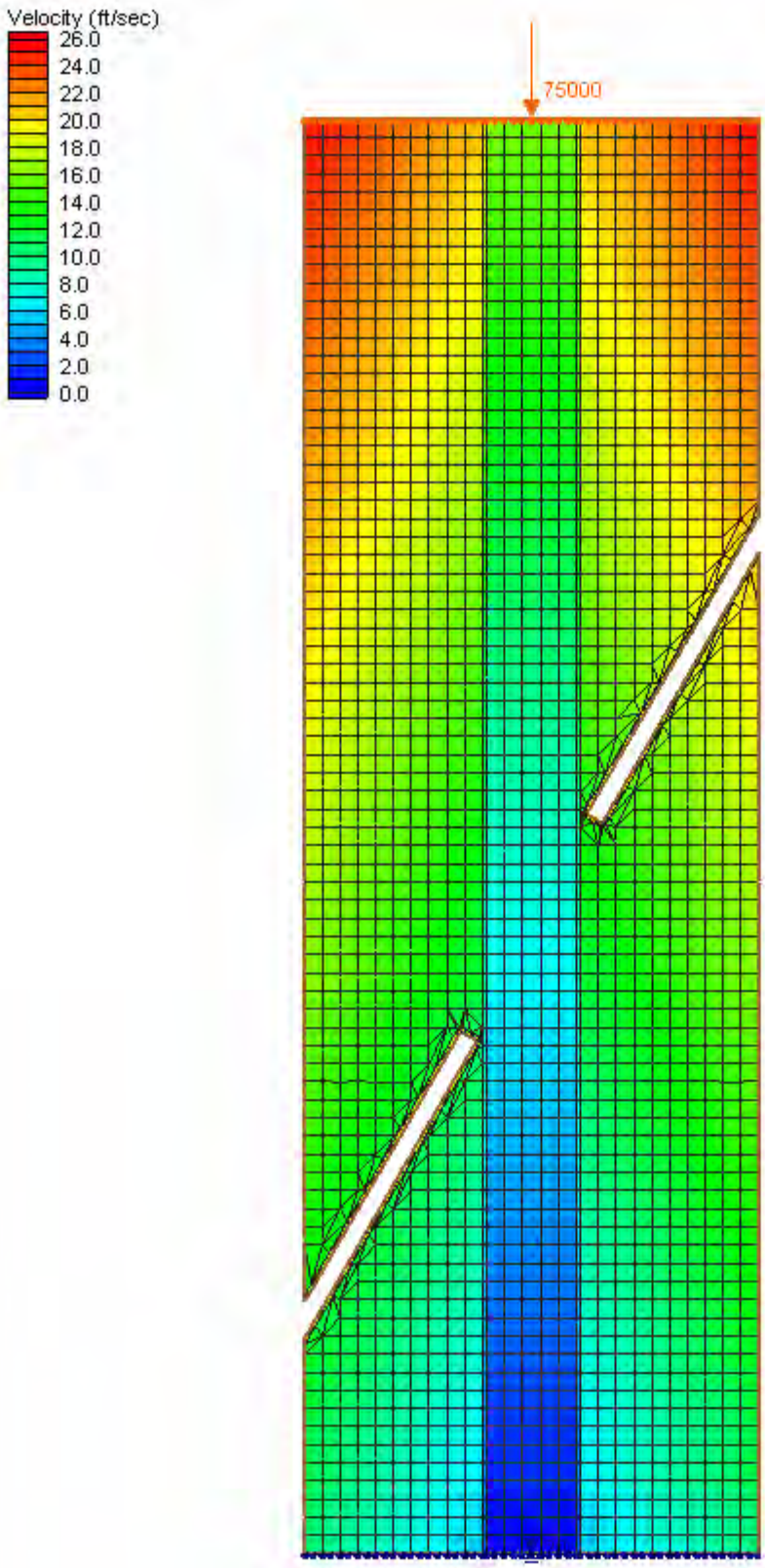

Figure 35 *Large Channel with 60° Skewed Bridge Crossing Two-dimensional Model Mesh*

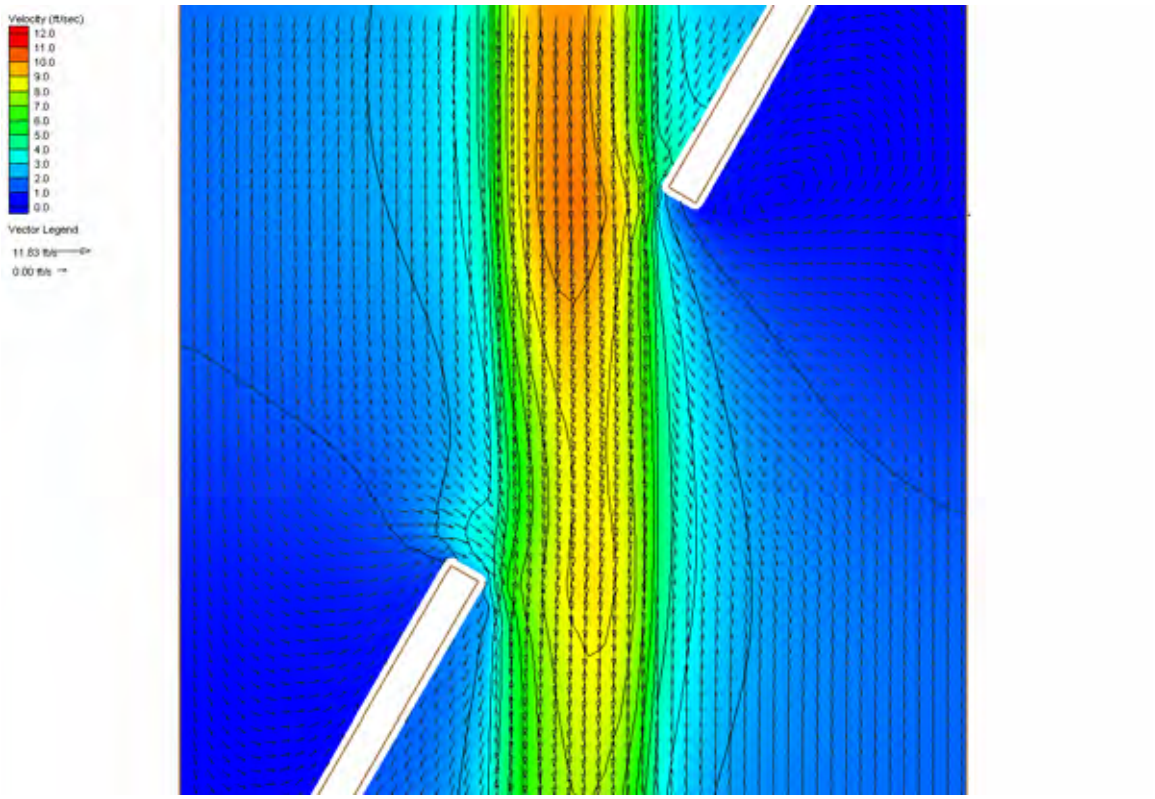

Figure 36 *Large Channel with 60° Skewed Bridge Crossing Two-dimensional Model Results*

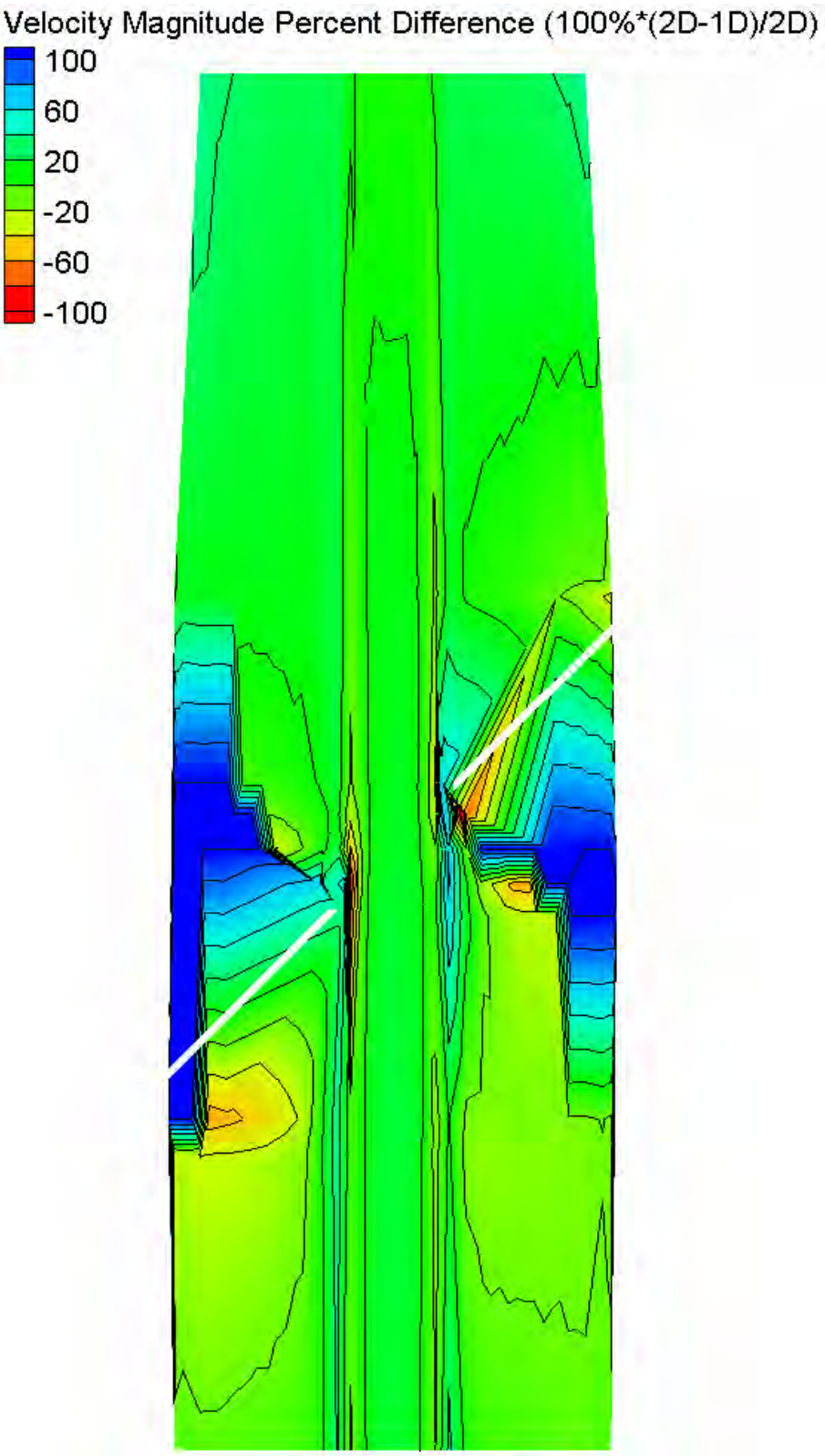

Figure 37 *Velocity Magnitude Percentage Difference Comparison for Large Channel with 45° Skewed Bridge Crossing Models*

Bridges over Meandering Rivers

This experiment involved altering the baseline geometry to vary the sinuosity both upstream and downstream of the bridge crossing. The channel banks were modeled as a sine curve with varying frequency. The sinuosity (stream centerline length over length along floodplain) was varied from 1.0 (baseline) to 2.0 in increments of 0.25. For the one-dimensional models, a cross section was located at each bend in the river. If cross sections fell between two bends, they were mathematically skewed in HEC-RAS such that they lay perpendicular to the (assumed) flow direction. The bridge was also skewed if it fell between two bends. Sixteen models were generated for this experiment. Figure 35 and Figure 36 illustrate an example of a two-dimensional model mesh and simulation results — velocity vectors overlaid on velocity magnitude contours — for one of the sensitivity tests. Figure 37 presents a comparison of the velocity magnitude percentage difference for the large channel meandering (S=1.25) simulations. The saw tooth pattern exhibited in the figure results from the FESWMS results interpolated onto the HEC-RAS cross sections. From the figure, the one-dimensional model tended to over estimate the velocities on the outside bends in the meanders. This is attributed to the fact that the one-dimensional model forces the flow to follow the channel centerline thus keeping the flow within the channels. In contrast, with the two-dimensional models, the flow travels over the banks in a more uniform direction (as compared with the one-dimensional model). Thus, when the flows encounter the channel after having traveled over the floodplain, the expansion in depth leads to a lower velocity.

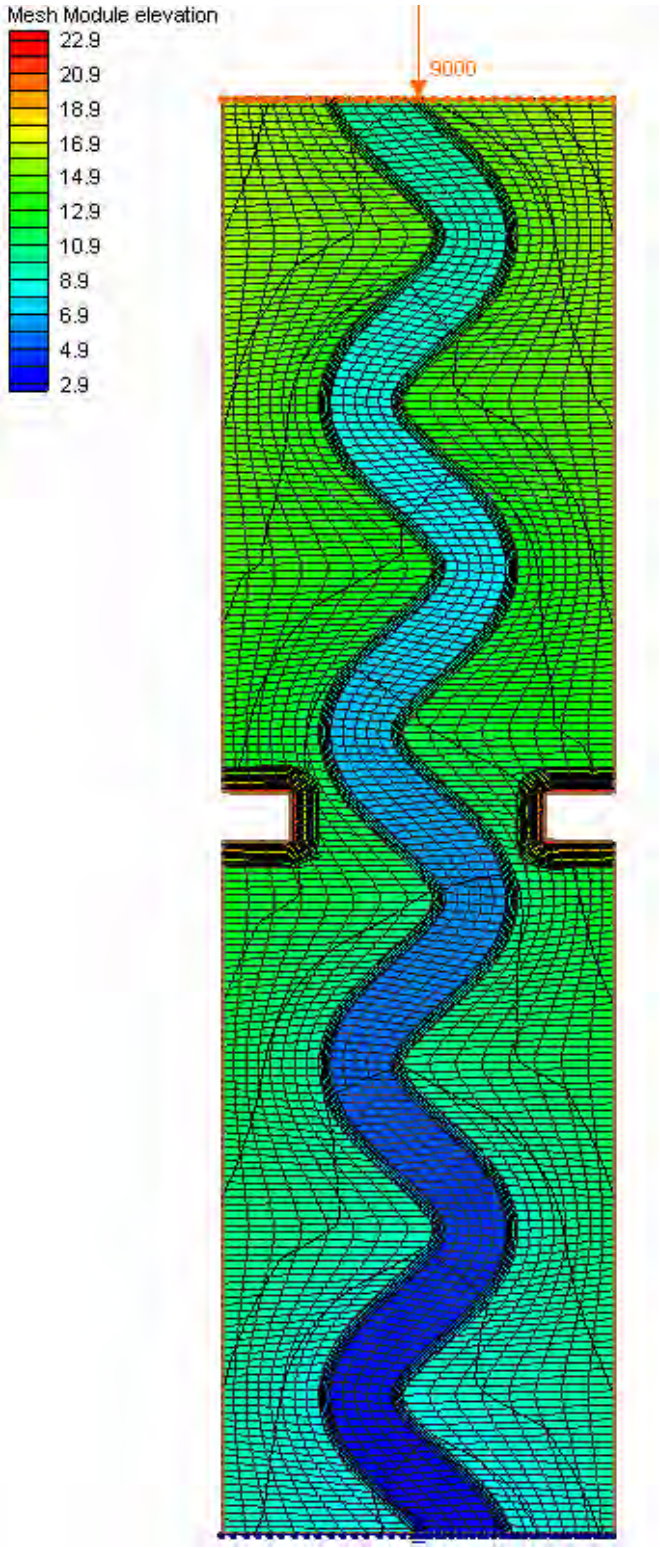

Figure 38 Small Channel with 1.25 Sinuosity Two-dimensional Model Mesh

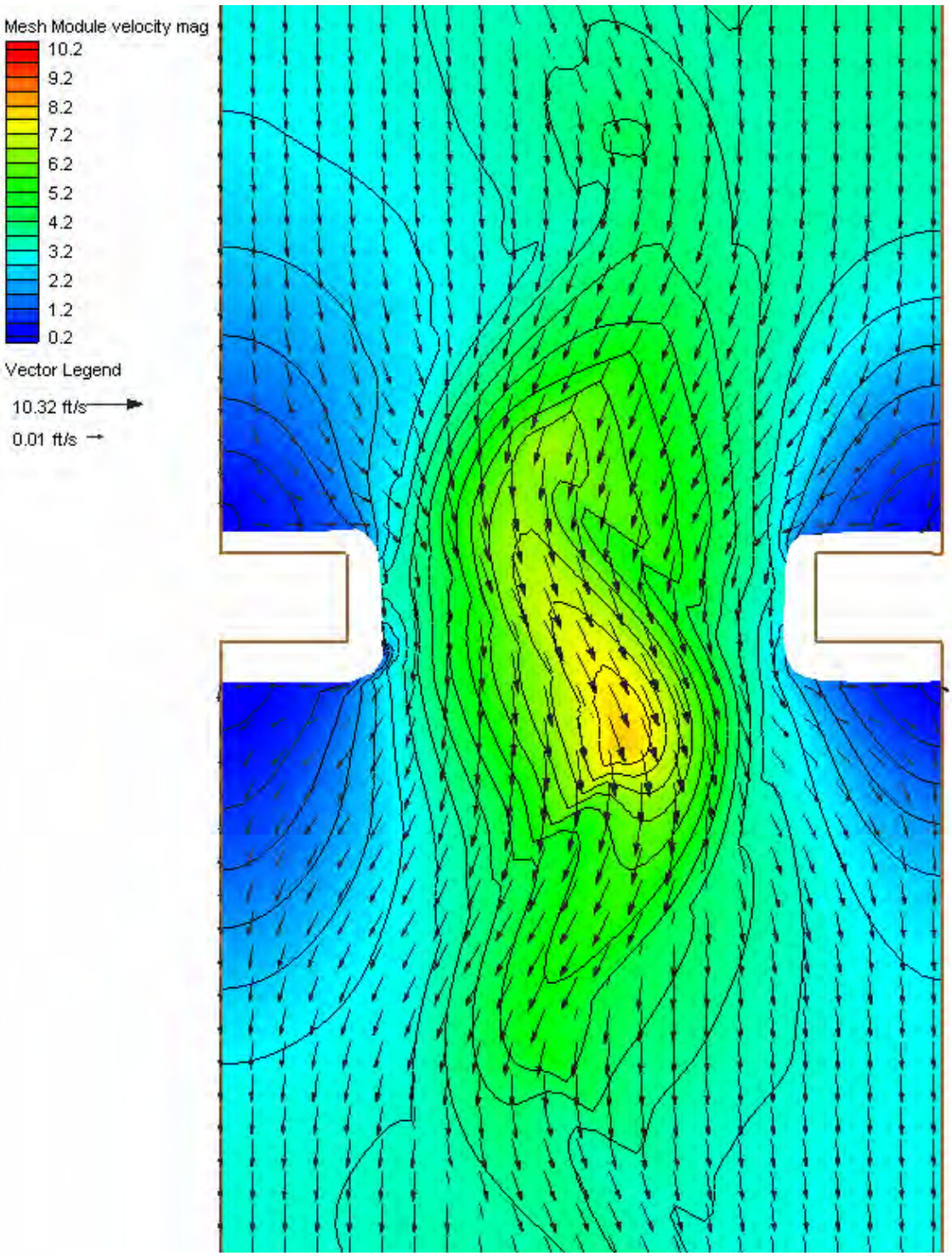

Figure 39 Small Channel with 1.25 Sinuosity Two-dimensional Model Results

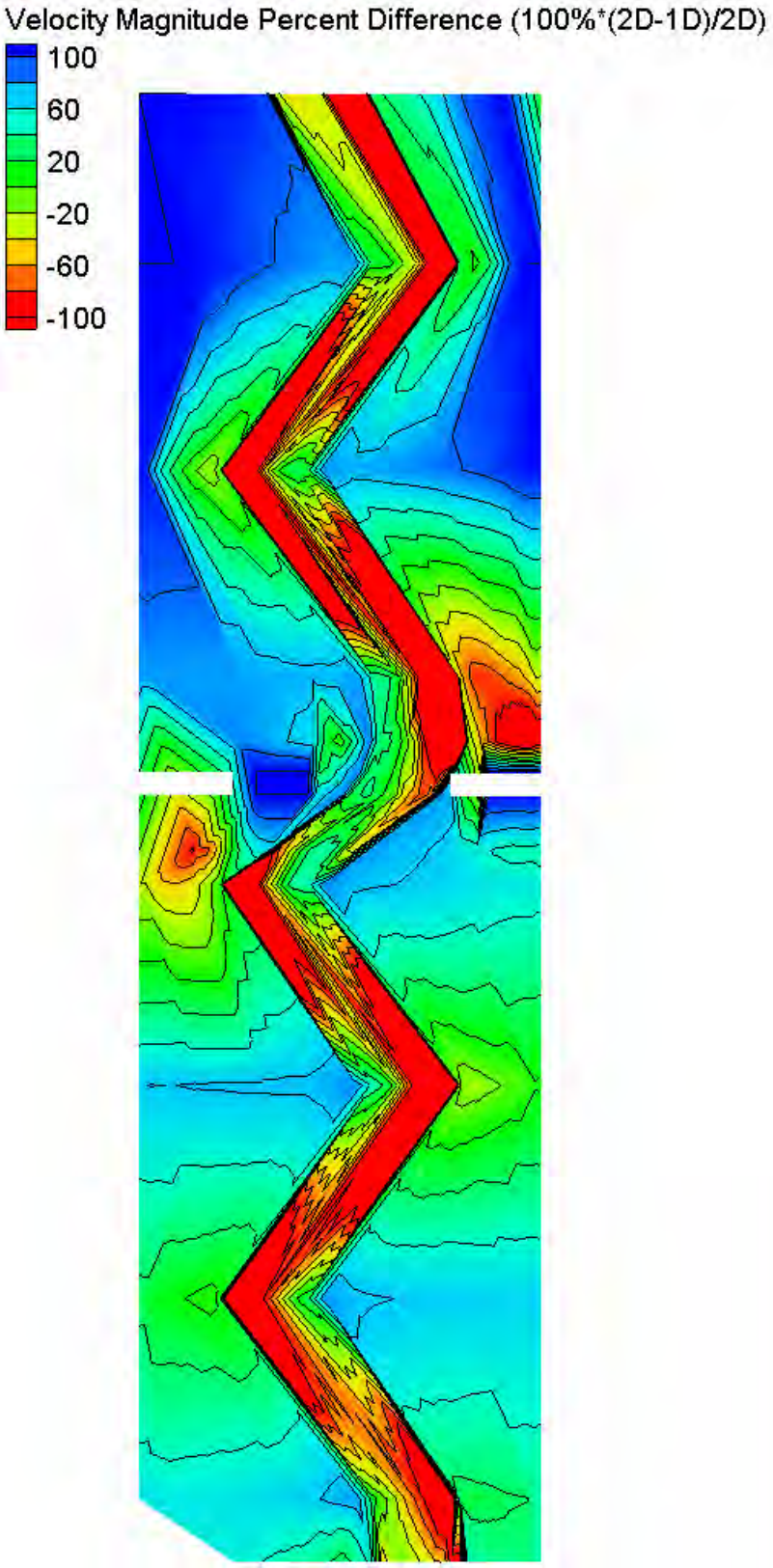

Figure 40 *Water Surface Elevation Comparison along Channel Centerline for Large Channel Meandering (S=1.25) Models*

Asymmetric Floodplains

This experiment involved altering the baseline geometry to vary the width of the floodplain on one side. The width of the floodplain on one side of the channel was varied from the original width to the channel bank by reducing the width in increments of 25% of the original width. Sixteen models were developed for this experiment. Figure 41 and Figure 42 present an example of a model mesh and simulation results — velocity vectors overlaid on velocity magnitude contours — for the large channel with 50% floodplain reduction two-dimensional model simulation. Figure 43 presents a comparison of the velocity magnitude solutions for the large channel with 25% reduction asymmetric floodplain simulations. As with the baseline models, the one-dimensional model does not exhibit good agreement in the areas along the abutments where the flow structure is more two-dimensional.

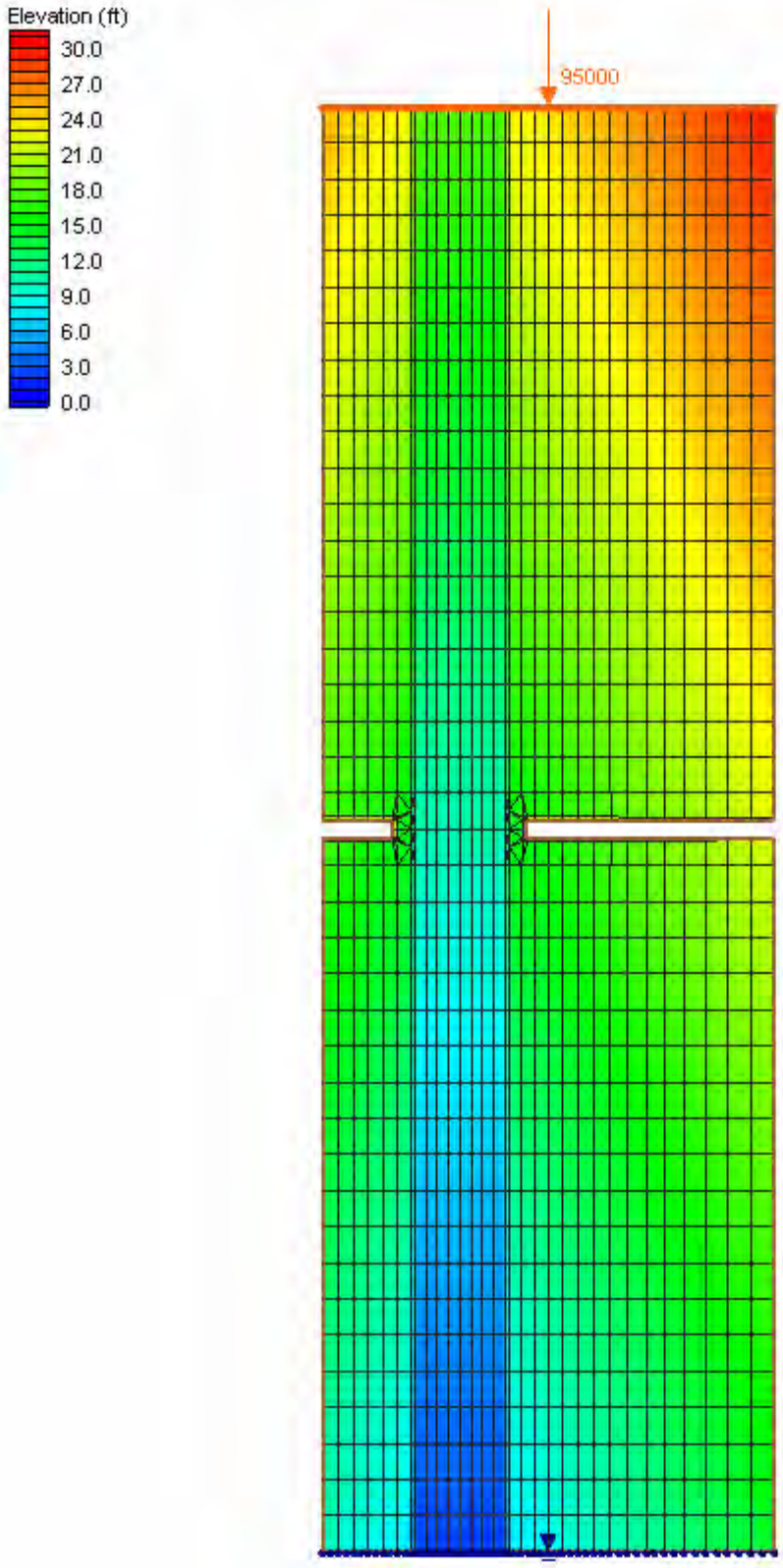

Figure 41 *Large Channel with 50% Reduction Asymmetric Floodplain Two-dimensional Model Mesh*

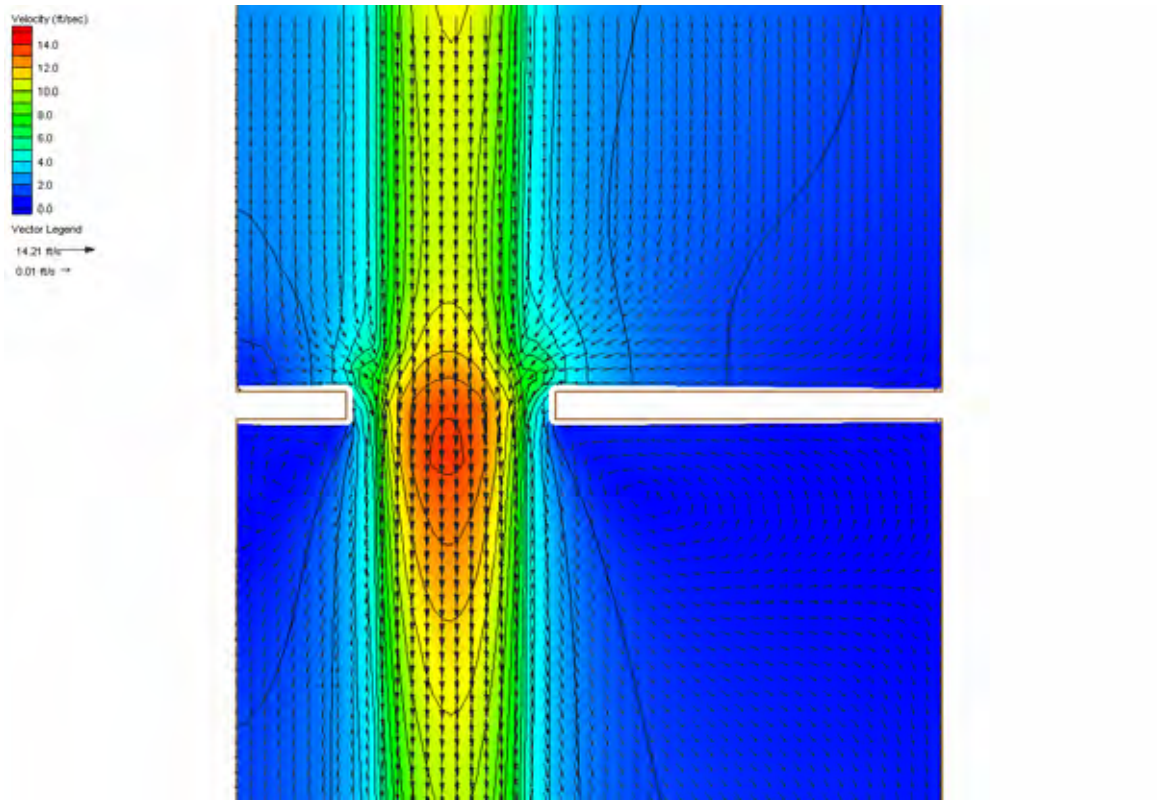

Figure 42 *Large Channel with 50% Reduction Asymmetric Floodplain Two-dimensional Model Results*

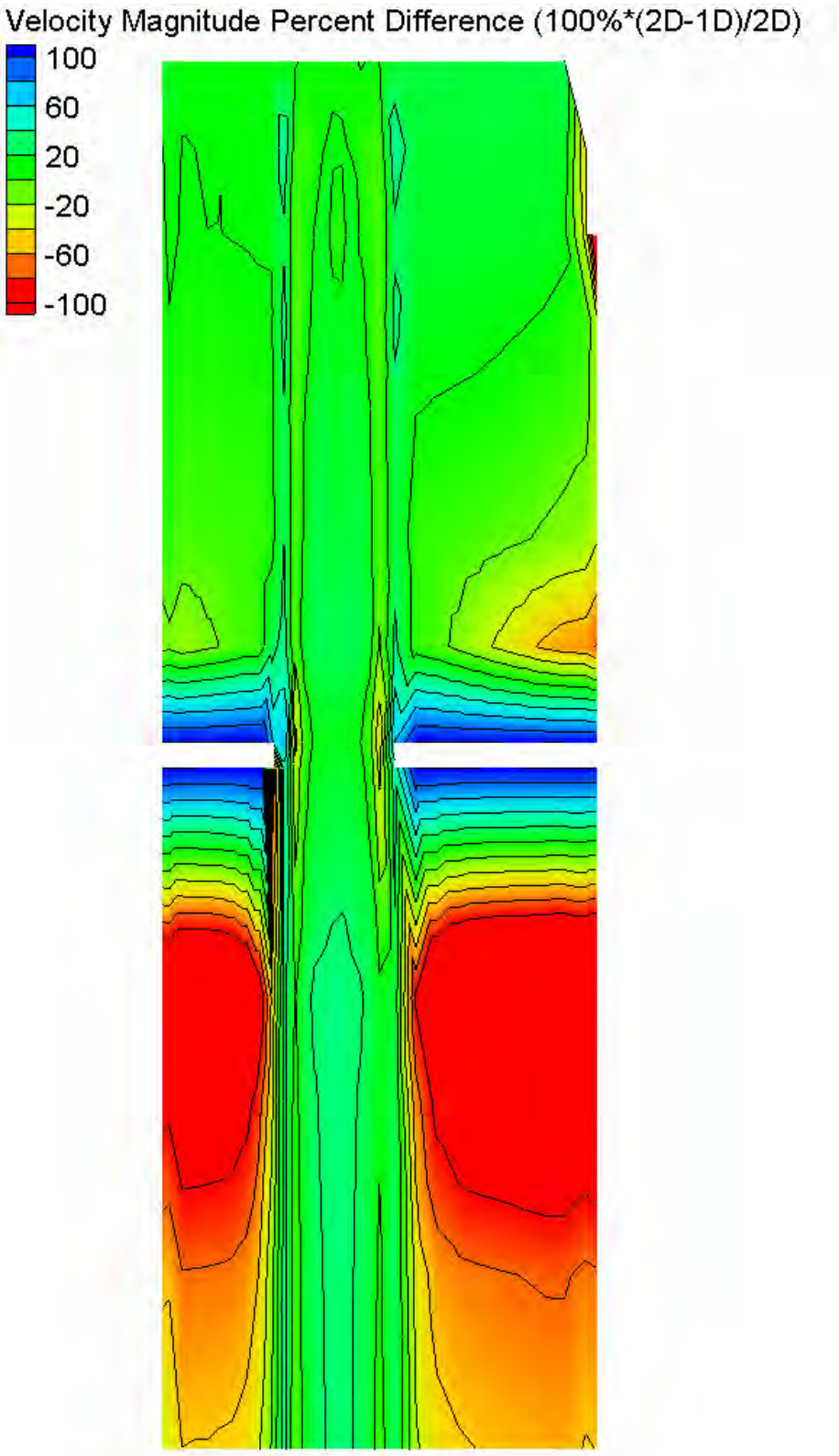

Figure 43 *Velocity Magnitude Percentage Difference Comparison for Large Channel with 25% Reduction Asymmetric Floodplain Models*

Bridges with Large Piers/High Blockage

For these sets of sensitivity tests, the intention was to examine the effects of high blockage at the bridge associated with large piers. The baseline geometry was altered to include these bridge piers. The width of the piers was varied such that the blockage increased from 5% to 35% of the channel top width in increments of 10%. For the two-dimensional model, the piers were incorporated by deleting elements within the mesh occupied by the piers. This set of tests involved performing 16 simulations. Figure 44 and Figure 45 present an example of the model setups for the large channel with large bridge piers (35% reduction in bridge opening top width) one- and two-dimensional simulation. Figure 46 displays a comparison of the large channel with large bridge piers (35% reduction in bridge opening top width) one-dimensional model results with the two dimensional large channel baseline simulation. From the comparison, the models compare well at the bridge cross section, but poorly downstream of the piers. In this case, the one-dimensional model incorporates the frictional losses from the piers through an increase in the wetted perimeter. By modeling the piers through element deletion, the two-dimensional model does not account for frictional losses if a slip boundary condition along the model edges is employed. Rather, losses from the piers are attributed to the momentum losses associated with the creation of the secondary flows around the piers and in the wake region.

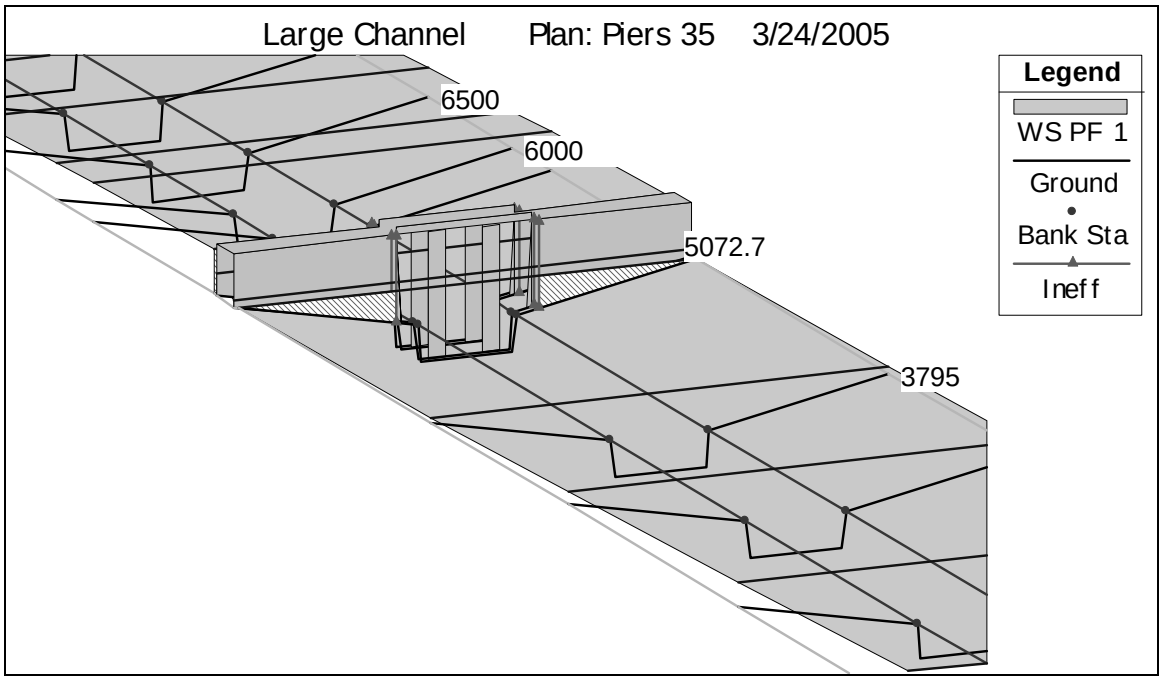

Figure 44 Large Channel with Large Bridge Piers (35% Reduction in Bridge Opening Top Width) One-dimensional Model Setup

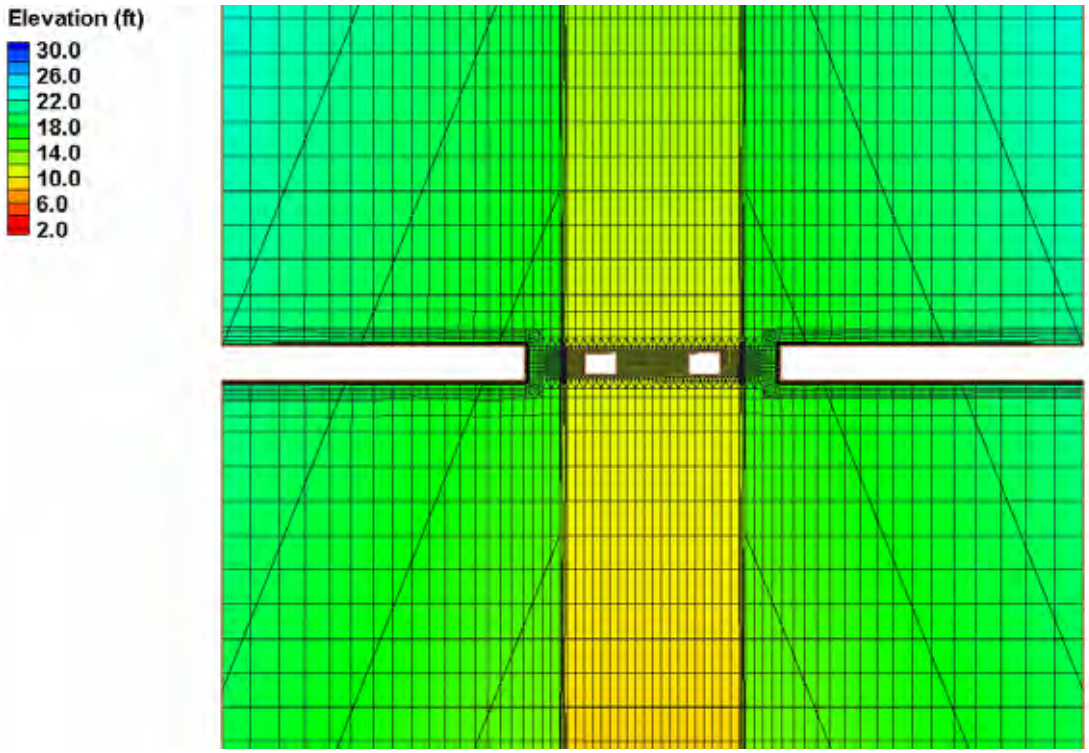

Figure 45 *Large Channel with Large Bridge Piers (35% Reduction in Bridge Opening Top Width) Two-dimensional Model Setup*

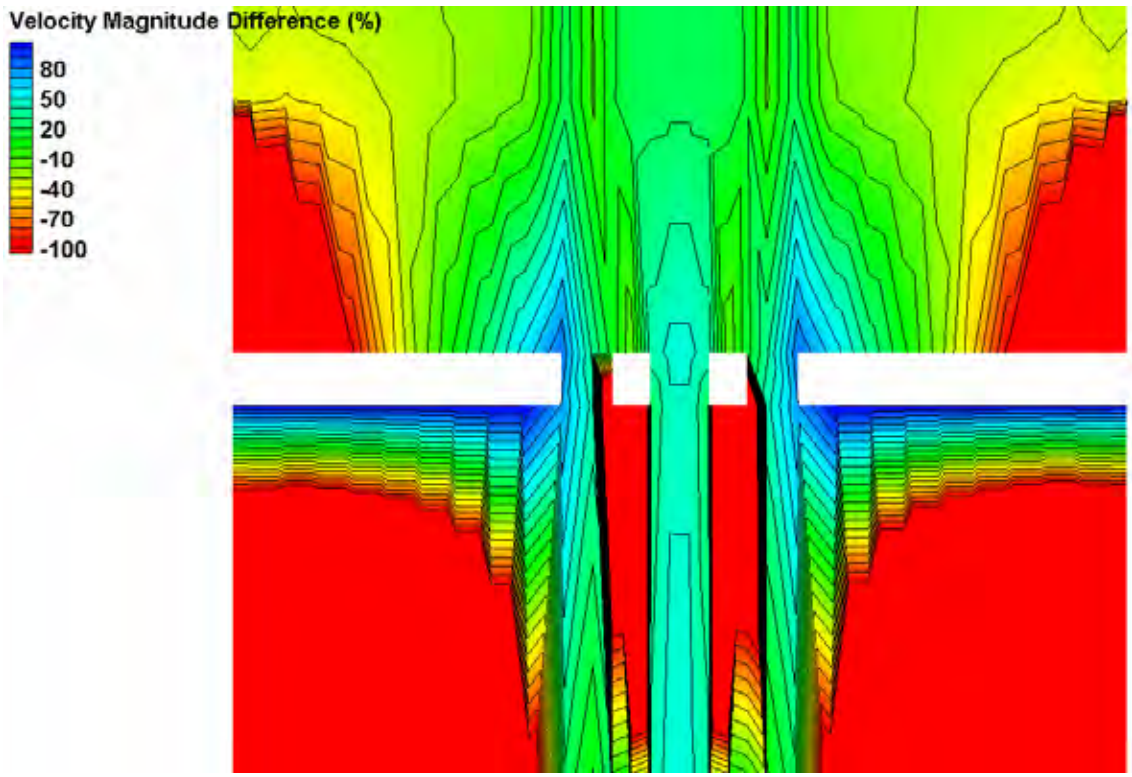

Figure 46 *Velocity Magnitude Percentage Difference Comparison at the Upstream Bridge Face with Large Bridge Piers (35% Reduction in Bridge Opening Top Width)*

Tidal Hydraulics

This series of experiments compared one- and two-dimensional models in tidal environments. They included simple and complex (in the judgment of the researchers) tidal geometries during normal tidal and hurricane storm surge conditions. The model boundary conditions included only one time series that contained both the surge and the tide. Figure 47 and Figure 48 illustrate the simple and complex tidal waterway two-dimensional meshes. The locations of the bridges are indicated in yellow. These were the locations at which the one- and two-dimensional models were compared. Figure 49 presents the two-dimensional simulation output far the complex tidal waterway test during the time of maximum velocity at the southern inlet. Figure 50 presents a comparison of the water surface elevation simulation results at the southern inlet for the complex tidal waterway test. Not surprisingly, since the location of the elevation boundary condition resides not far from the inlets, the two models compare favorably throughout the simulation.

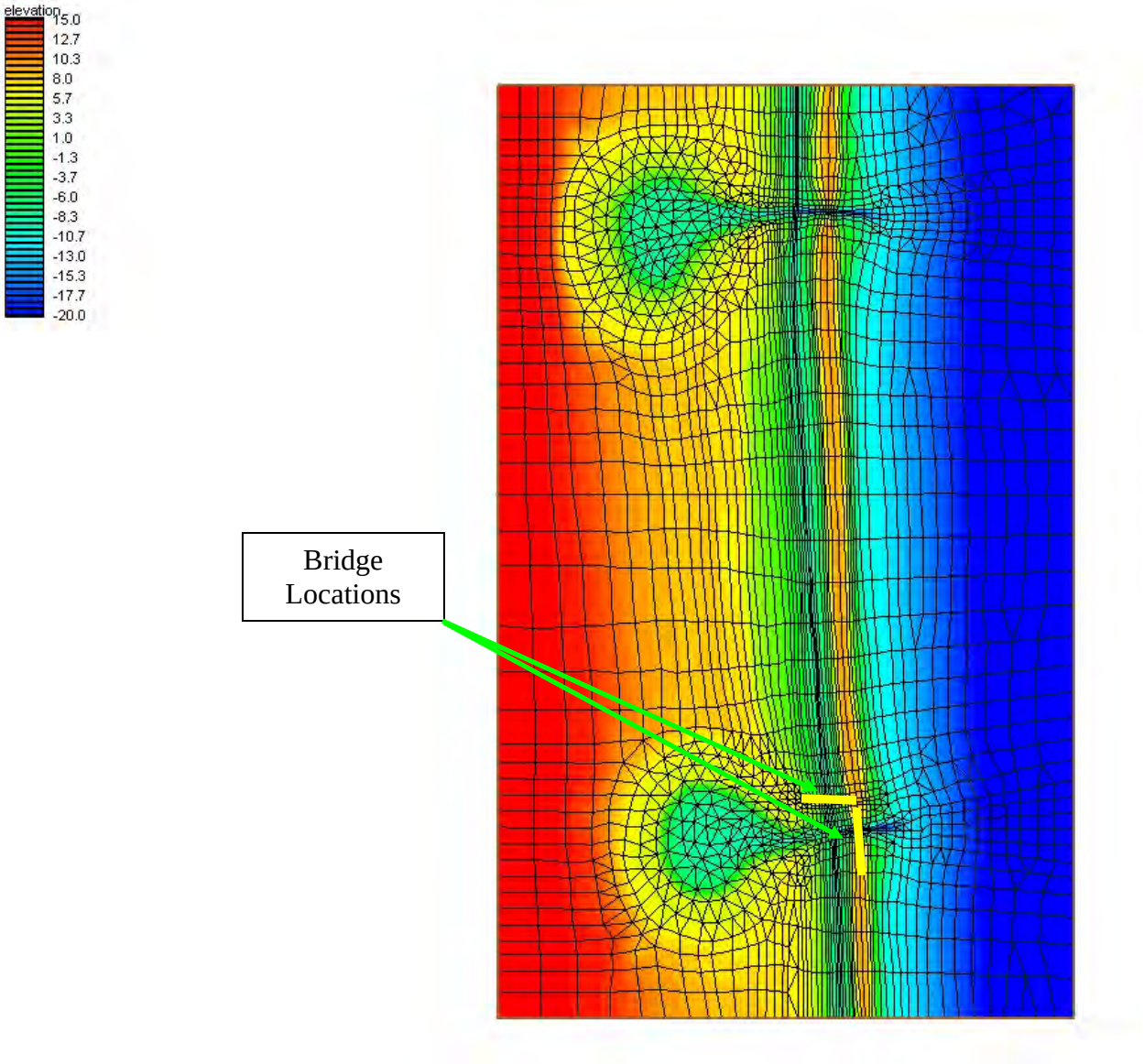

Figure 47 Simple Tidal Waterway Two-dimensional Model Mesh

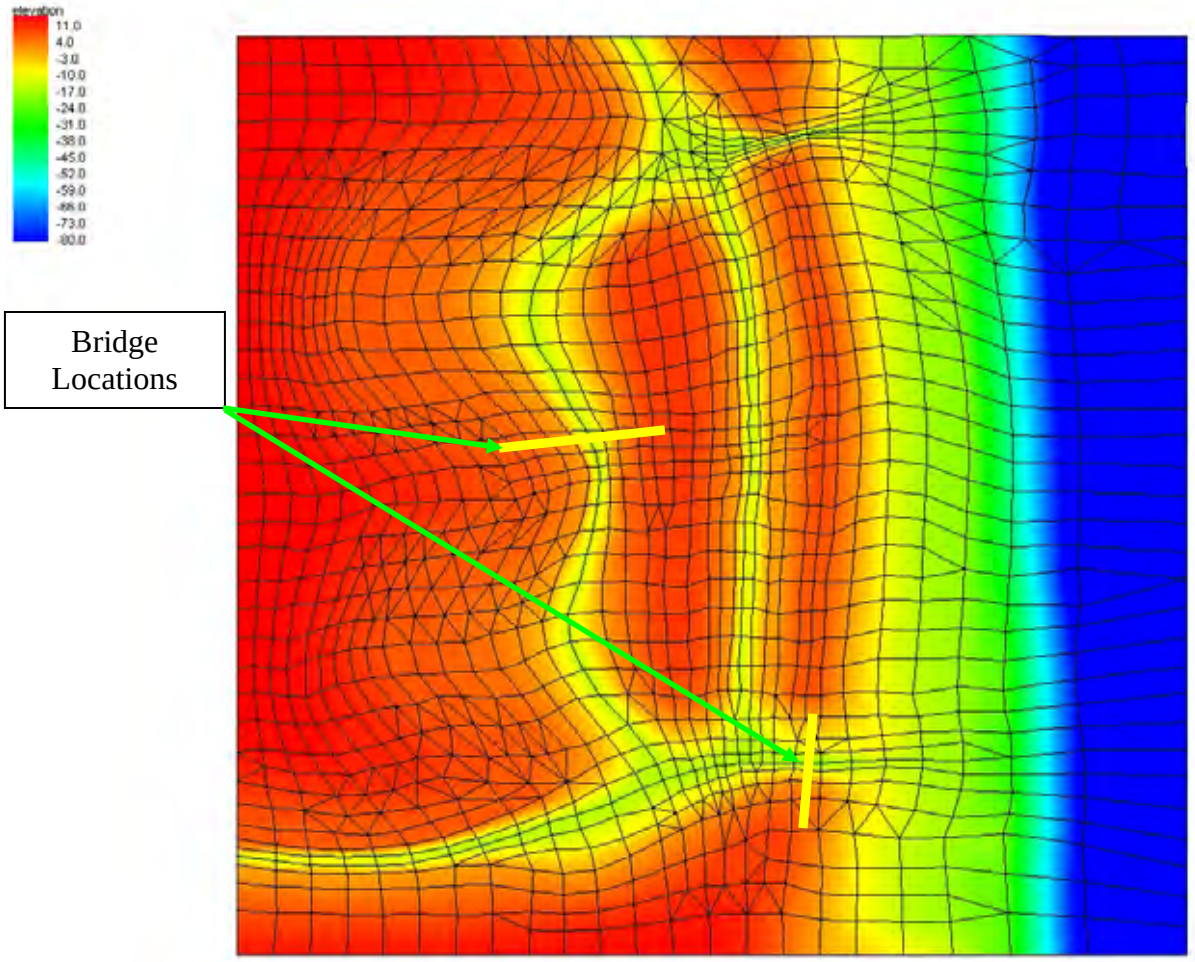

Figure 48 Complex Tidal Waterway Model Mesh

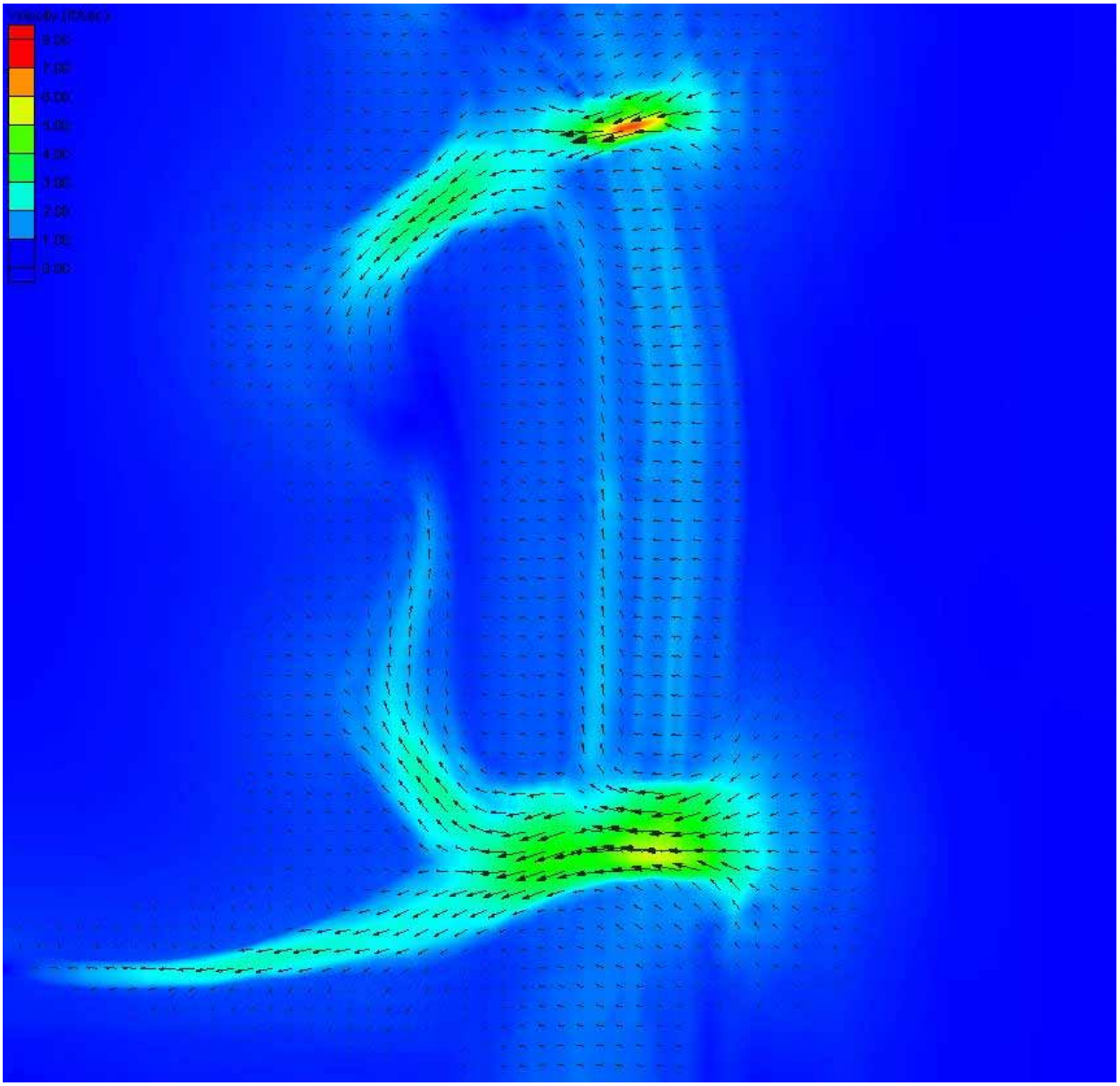

Figure 49 Complex Tidal Waterway Two-dimensional Model Results at Time of Maximum Velocity at Southern Inlet (Time=54 hrs)

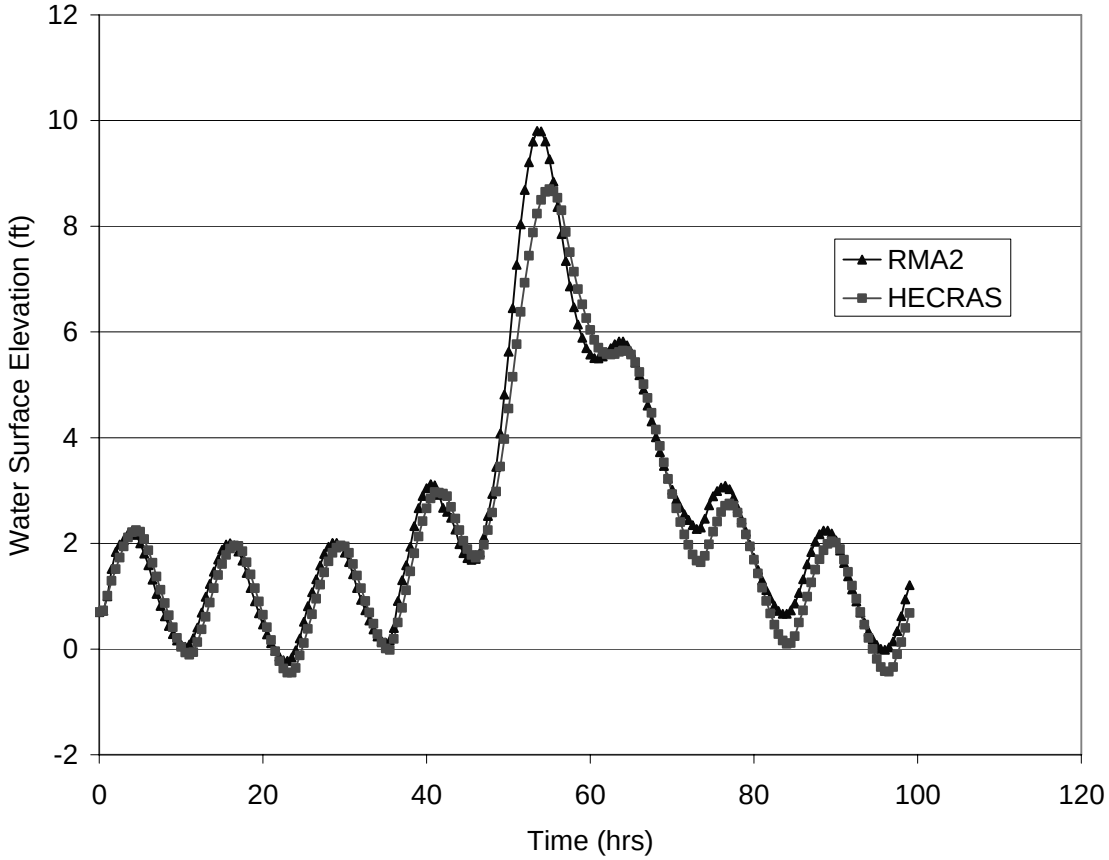

Figure 50 *Water Surface Elevation Comparison at Southern Inlet for Complex Tidal Waterway Models*

SENSITIVITY TEST RESULTS

Testing the sensitivity of the varied parameters required comparison of the output from both the one- and two-dimensional models on several levels. The appendix contains contours of velocity magnitude and water surface elevation from both model results for every simulation. In order to display the HEC-RAS output on contours, points along the cross sections were output and plotted in SMS. The appendix also contains comparison plots. For these plots, the FESWMS output was interpolated onto the HEC-RAS cross sections to provide an accurate comparison. It should be noted that one of the advantages of the two-dimensional models is the more resolved spatial coverage throughout the domain. However, in the interest of examining only locations resolved in both models, the plots only show contours from points in both domains. An additional factor examined in the sensitivity testing was the time spent during the setup and execution of the models in order to evaluate ease of application of the two models.

The model results reflect several general trends when compared. First, the one-dimensional models did not perform well in any of the cases in predicting the velocity direction at the bridge cross section. This, of course, is based on the assumption that the directions associated with the two-dimensional model are more accurate than those assumed with the one-dimensional model. This poor performance is not surprising given that the assumed angle of attack was perpendicular to the bridge centerline. As such, except for at the very center of the crossing, flow entering the opening from the floodplains will inevitably skew from this assumed direction.

In general, the model comparisons reveal that the more one-dimensional the flow becomes, the closer the prediction between the two models. Again, this result is not surprising. However, it does lead to some non-intuitive results. For example, in the multiple opening tests, the more openings added at the bridge crossings, the differences in the model become smaller. This results from the fact that more flow along the floodplains is allowed to flow parallel to the channel centerline rather than turn into the channel at the crossing. As such, the flow becomes more one-dimensional in a global sense, and hence the better the agreement. Below is a discussion of each of the model results.

Multiple Openings

Qualitatively, the multiple openings simulations compared favorably (i.e., relatively the same) between the one- and two-dimensional modeling results. The velocity magnitudes, water surface elevations, and angles of attack all fell within acceptable levels for the large channel simulations with only slightly poorer performance for the small channel simulations. As mentioned previously, comparisons of the models improved in all categories as more openings were added. This is attributed to the tendency of the flow around the bridge to act more “one-dimensional” in the floodplains as less of the flow was blocked.

Bridges Located on River Bends

In general, the large channel simulations compared better than the small channel simulations. This may be attributed to the larger radius of curvature associated with the wider floodplains on the large channel model. Also, the greater the bend, the poorer the agreement between the models became.

Bridges near Confluences

The simulations involving confluences exhibited poor agreement for all cases for both the large and small channel simulations. In general, the greater the flow and the greater the angle, the poorer the agreement between the models became. In some cases, there were significant deviations in both velocity magnitude and water surface elevation near the bridge.

Bridges with Significant Constrictions

In these tests, the simulations involving locating the abutments at the banks provided acceptable agreement. However, once the embankments encroached on the channel, significant divergence in the results occurred. In general, the large channel simulations agreed better than the small channel simulations, especially in the comparison of velocity magnitude at the contraction distance upstream of the bridge and in the velocity direction at the bridge.

Overtopping Flow

Since efforts with the ceiling function in FESWMS proved fruitless, the bridge decks were not included in the model. From the results, the major overtopping simulations agreed slightly better than the minor overtopping simulations. Also, the small channel simulations agreed slightly better than the large channel simulations. As with the multiple opening cases, the more overtopping that occurs, the more “one-dimensional” the flow becomes, especially in the floodplains. This bears out in the results as the major overtopping results agreed better than the minor overtopping results.

Embankment Skew

These sets of tests provided some challenges for the one-dimensional model setup. For embankment skews greater than 30°, standard practice recommends against employing standard bridge routine methods to determine the bridge hydraulics. For the one-dimensional simulations of skews greater than 30°, the HEC-RAS models were set up by running cross sections perpendicular to the channel centerline rather than parallel to the bridge face at the crossing. The cross sections would then stop once they reached the roadway. Interestingly, this technique actually improved the agreement between the one- and two-dimensional models. From the model results, the large channel simulations agreed better than the small channel simulations. Also, although the velocity magnitude agreement improved with the change in modeling technique, the agreement in angle of attack worsened.

Bridges over Meandering Rivers

There were significant differences in the results between the one- and two-dimensional model simulations for the meandering cases. The results exhibited very poor agreement in all categories for all modeled sinuosities. These tests exhibited the largest differences in velocity magnitude, water surface elevation, and velocity direction of all the tests conducted. Upon further consideration, the setup for this test may have placed unrealistic constraints on the modeled geometry. In an attempt to maintain similar floodplain widths across all tests, the floodplain width constriction set an upper bound on the amplitude of the sine wave. As such, with a given sinuosity, the wavelength was bounded as well. This caused rapid fluctuation in direction over a very short distance, which did not allow the flow enough time/distance to align with the channel. In reality, sinuous channels are usually located along much wider floodplains (as compared with the amplitudes of the fluctuations in direction).

Bridges with Asymmetric Floodplains

For these sets of tests, the one-dimensional models tended to replicate the velocities at the bridge crossing as compared with the two-dimensional models, but not along the embankments. Interestingly, the models exhibited reasonable agreement in water surface elevation.

Bridges with Large Piers/High Blockage

From the contours in the Appendix, the large pier simulations performed similar to the constriction tests. The greater the constriction, the less favorable the comparison became. By comparison, the one-dimensional model under predicts the acceleration of the flow both along the embankment and through the cross section.

Tidal Hydraulics

The results from the tidal model simulations were compared in several ways. First, velocity profiles at the bridge cross sections were compared at the time of maximum velocity. Next, the time series of velocity magnitude and water surface elevation at each bridge location were divided into two components (a tide and a surge) and compared over the entire record. Finally, the differences in the peak values over the entire time series were calculated. From the results, the agreement between two models was better than expected. The two agreed surprisingly well in terms of water surface elevation. Velocity magnitude and velocity direction, however, exhibited some significant differences, especially at the inlets in the model. Not surprisingly, the tide portion of the simulation exhibited less difference in the results than did the surge portion of the simulation on average. Results from these simulations may be misleading. Whereas this comparison performed well, in situations where multiple flow paths can influence a bridge site during extreme storm surge events, the results may be quite different. This is especially true in areas with low wide floodplains, marshy areas, and areas near low barrier islands.

Expended Time Comparison

One of the surprising results of this study is the comparison of the time spent to setup and run the models.

Table 3 below breaks down the hour spent by sensitivity test. Before performing a one to one comparison of the results, one should be aware of several caveats. First, no hours were recorded for trying to debug simulations that were not ultimately employed in the sensitivity testing. For example, although considerable time was spent attempting to get the deck ceiling option to work, the table below does not reflect this time since the pressure flow simulation was omitted from the tests. Also, there is a significant difference between the experience levels of the employees performing the modeling. The two-dimensional modeler has more than a decade of experience with these types of models, holds a masters degree, and is a registered Professional Engineer, whereas the one-dimensional modeler is a recent graduate, holds a bachelor's degree, and is an E.I. As such, there is a significant salary difference between the two employees. In a general sense, it is highly likely that two-dimensional modelers will have more experience, and hence larger salaries, industry-wide. This must be kept in mind when examining the results.

The surprising aspect of the results is that the two-dimensional modeling took less time to perform than did the one-dimensional modeling (208 hours as compared with 285 hours not including the large pier blockage simulations). This is a reflection both on the experience of the modeler as well as the tools available for constructing and running two-dimensional models. The results also show that a significant amount of time spent by the one-dimensional modeler was on the tidal hydraulics cases. The complexity of these types of models and the unfamiliarity of most one-dimensional modelers with these environments can lead to significant investments of time in these types of simulations. Excluding these simulations from the comparisons leads to totals of 232.5 hours for the one-dimensional modeling and 175 hours for the two-dimensional modeling. These translate to an average hours spent per model of 3.1 and 2.4. Therefore, on average, the one-dimensional models took 32% longer to complete. Granted, the results will vary depending on the experience of the modeler performing the work. However, it is startling that the hours are comparable. This certainly refutes the long-held belief that two-dimensional modeling consumes more resources than does one-dimensional modeling. It should be noted, however, that the meshes for these idealized tests are, in general, much easier to construct than a "real world" situation.

Table 3 Expended Time Comparison for Sensitivity Tests

Sensitivity Test	One-dimensional		Two-dimensional	
	Hours Expended	**Hours/Model**	**Hours Expended**	**Hours/Model**
Baseline	12.5	6.3	8.0	4.0
Multiple Openings	14.0	1.4	16.0	1.6
Bridges Located on River Bends	42.0	3.5	32.0	2.7
Bridges near Confluences	75.0	4.7	36.0	2.3
Bridges with Significant Constrictions	3.0	0.5	16.0	2.7
Overtopping Flow	8.0	2.0	4.0	1.0
Embankment Skew	25.0	3.1	24.0	3.0
Bridges over Meandering Rivers	42.0	5.3	28.0	3.5
Bridges with Asymmetric Floodplains	11.0	1.4	12.0	1.5
Bridges with Large Piers/High Blockage	5.0	0.6	NA	NA
Tidal Hydraulics	52.5	26.3	32.0	16.0
Total	290.0		208.0	

CHAPTER 5 DESIGN CRITERIA AND OTHER PROJECT CONSIDERATIONS

Other factors which enter into the decision process of an engineer when selecting a numerical model include potential design applications that the engineer may examine in conjunction with the hydraulic modeling, as well as resource related and other considerations. Design considerations may include a type of study (e.g., a FEMA "no-rise" study, a FHWA scour evaluation, etc.) or the construction of a specific structure (e.g., bendway weirs, bank slope protection, etc.). Resource considerations may include schedule constraints, modeler experience, or data availability. This chapter addresses the important parameters associated with the different types of studies/structures. Additionally, it contains an examination of the design equations for different types of possible construction and how uncertainty with the predicted hydraulic parameters may affect the overall design. This discussion is intended to educate the engineer as to risks associated with uncertainties in prediction of bridge hydraulic parameters. Finally, it addresses critical evaluation of resources available to the engineer performing the work as well as other considerations to factor into the decision process.

DESIGN CRITERIA CONSIDERATIONS

The synthesis of the literature review/survey identified the following design issues associated with bridge hydraulic modeling:

- Riprap Sizing for Scour, Abutment, or Slope Protection
- Armor Units for Scour, Abutment, or Slope Protection
- Concrete Block for Scour, Abutment, or Slope Protection
- Abutment Scour Calculation
- Pier Scour Calculation
- FEMA "No-Rise" Studies
- Bendway Weirs/Stone Spurs

Each of these issues is discussed below. To employ the information contained in this section, the engineer should examine the figures contained in the Appendix to determine relative performance of the modeling approaches in the locations specific to their application. Armed with this information, the engineer can then consult this section to determine whether the relative difference in the estimation of the hydraulic parameters produces acceptable differences (in the form of percentage error) in the design equations.

Riprap

Riprap experiences widespread use for abutment protection, bank slope protection, and local pier scour protection at or near bridge sites. Sizing riprap involves specifying design flow at the placement site. This is usually done through numerical modeling. As such, errors in estimation of the input parameters can influence the riprap specifications.

For example, HEC-23 (Lagasse et al., 2001) contains the standard for design of rock riprap at abutments. Sizing the stone (for Froude Numbers less than 0.8) is accomplished through application of the Ishbash Equation:

$$\frac{D_{50}}{y} = \frac{K}{(S_s - 1)}\left[\frac{V^2}{gy}\right]$$

where D_{50} is the median stone diameter, V is the characteristic average velocity in the contracted section, S_s is the specific gravity of the rock riprap, g is gravity, y is the depth of flow in the contracted bridge opening, and K is a constant specific to the type of opening (spill-through vs. vertical wall abutments). Rearranging this equation yields the following:

$$D_{50} = CV^2;\ \text{where}\ C = \frac{K}{g(S_s - 1)}$$

Notably, this equation is independent of depth. Performing an error analysis on this equation yields the following:

$$E_{D50} = (1 + E_v)^2 + 1$$

where E_V is the percentage change in velocity and E_{D50} is the percentage change in median stone diameter. Graphing this equation produces the relationship depicted in Figure 51. The figure illustrates that small changes in predicted velocity may result in large changes in predicted median stone size. Extending this analysis to weight of the stone, which varies with the cube of diameter, illustrates even more sensitivity to velocity. For example, an engineer performs hydraulic modeling to develop a stone size for a spill-through abutment. The engineer's model predicted a velocity of 11.0 ft/s, however, for the engineers specific application, the model tends to over estimate velocity by as much as 20-30%. If one assumes a specific gravity of 2.65 for the riprap, an 11.0 ft/s flow results in a median stone diameter of 2.0 ft and a median weight of 1,377 lbs (based on a cube for the sake of argument). However, if the engineer has over estimated the velocity by 22%, a 9.0 ft/s flow would result in a median stone diameter of 1.4 ft and a median weight of 413 lbs. Therefore, a 22% over estimation of velocity resulted in a 49% over estimation of diameter and a 233% over estimation of median weight. This can have significant impacts to the overall cost of a project. This example illustrates that for this application, the engineer would have been better served to select a model that more accurately predicts velocity even if it means sacrificing accuracy in predicting water surface elevation.

The equation for sizing riprap at piers for local pier scour protection is similar in form to the Ishbash equation. It only differs by a constant. As such, it will exhibit the same error behavior as that for sizing riprap at abutments.

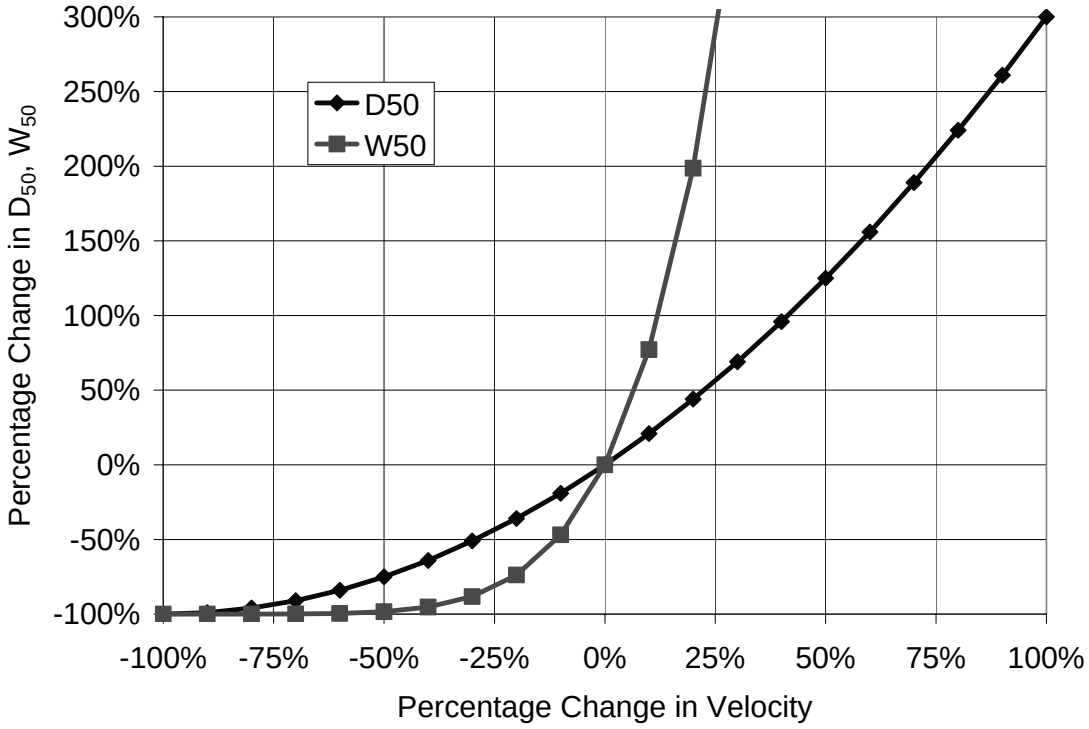

Figure 51 Ishbash Equation Sensitivity to Velocity

Armor Units

HEC-23 (Lagasse et al., 2001) provides design guidelines for protection comprised of armor units. According to the document, "Concrete armor units are man-made 3-dimensional shapes fabricated for soil stabilization and erosion control. These structures have been used in environments where riprap availability is limited or where large rock sizes are required to resist extreme hydraulic forces. They have been used as revetments on shorelines, channels, streambanks and for scour protection at bridges. Some examples of armor units include Toskanes, A-Jacks®, tetrapods, tetrahedrons, dolos and Core-loc™."

As an example of the influence of hydraulic parameters on the design of armor units, the design guidelines for the Toskane armor units for pier scour protection are examined. According to HEC-23 (Lagasse et al., 2001), the equivalent spherical diameter, Du, of a Toskane unit is directly proportional to the velocity. Determining the number of units per unit area is inversely proportional to Du^2. Given this dependence, Figure 52 presents the errors in equivalent diameter and number of units per area as a function of estimated velocity. From the figure, small changes in velocity can significantly affect the number of units required for a project.

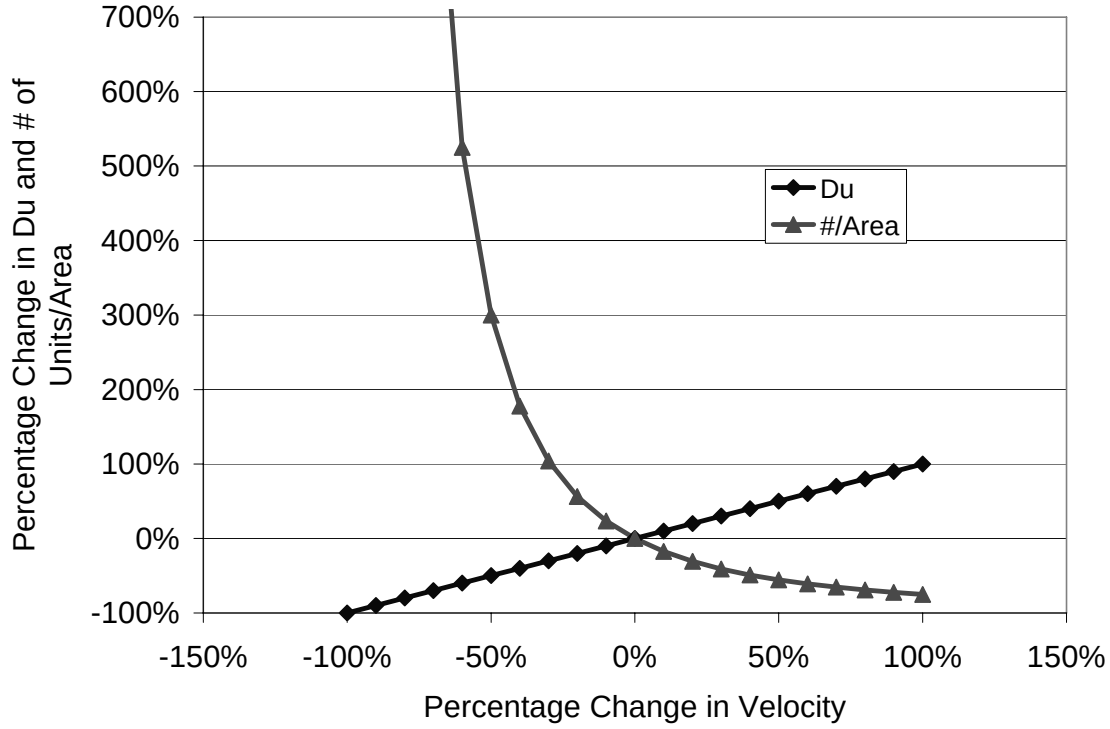

Figure 52 Toskane Design Dependence on Velocity

Concrete Blocks

Articulating concrete block (ACB) provides an alternative to traditional riprap in many protection applications. There are several manufacturers of ACB and each provides their own design guidelines. Common to most guidelines are the determination of shear stress, lift forces, and drag forces for the sizing and selection of the appropriate block system. By combining Manning's equation and the conservation of momentum equation, it can be shown that shear stress is proportional to velocity squared and inversely proportional to depth to the 1/3. Figure 53 displays the sensitivity to shear stress to hydraulic inputs. Similarly, lift and drag forces are usually calculated as a function of velocity squared. Figure 54 displays this dependence as a function of velocity.

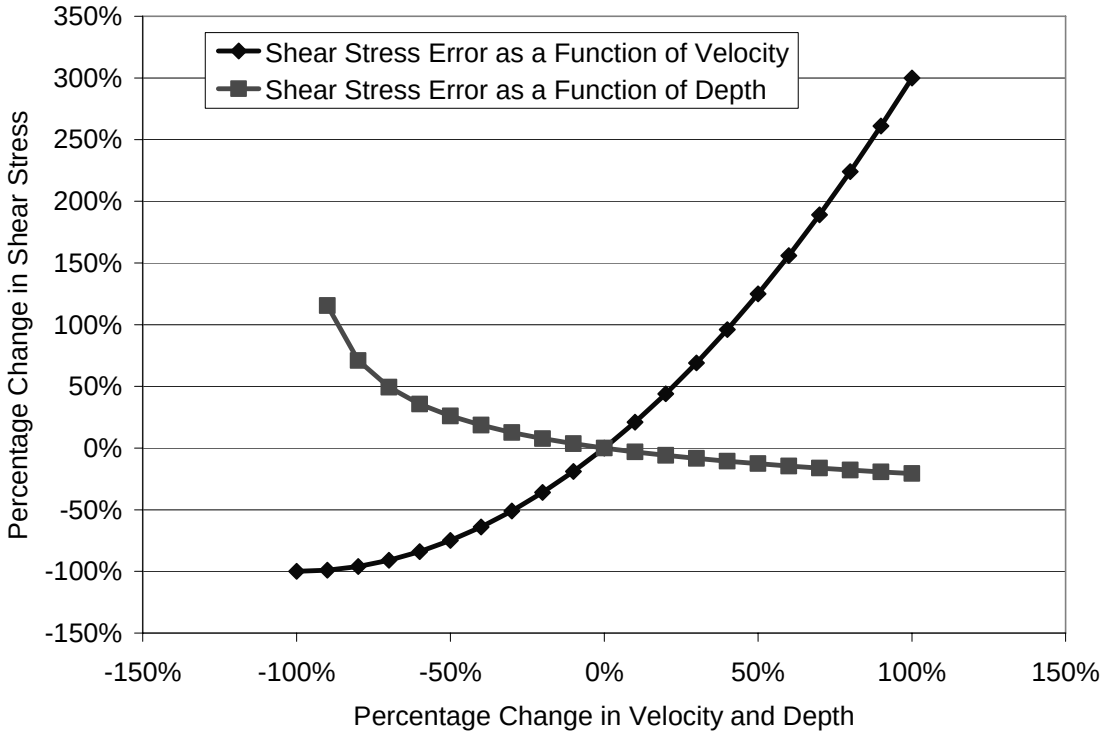

Figure 53 Shear Stress Sensitivity to Hydraulic Inputs

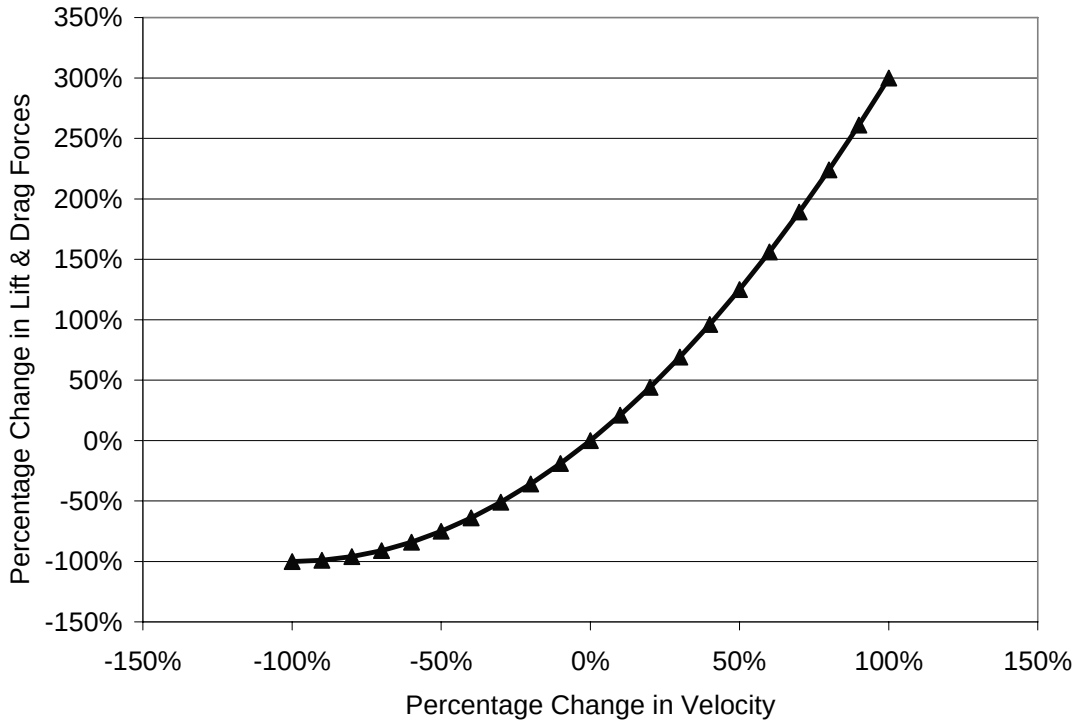

Figure 54 Lift and Drag Force Sensitivity to Velocity

Abutment Scour Calculation

According to the FHWA, calculation of abutment scour at a bridge site follows either the Froehlich equation or the HIRE equation. To demonstrate the sensitivity of these calculations to hydraulic inputs, the HIRE equation is examined. The HIRE equation lists as follows:

$$\frac{y_s}{y_1} = 4Fr_1^{0.33}\frac{K_1}{0.55}K_2$$

and y_s is the scour depth, K_1 is the abutment shape coefficient, K_2 is the coefficient for skew angle of abutment to flow, y_1 is the depth of flow at the abutment on the overbank, and Fr_1 is the Froude Number based on the velocity and depth adjacent to and upstream of the abutment. From the equation, scour depth is a proportional to velocity to the 0.33 and proportional to depth to the 0.835. Figure 55 displays this dependence. Here, the figure shows the relative insensitivity of abutment scour to velocity. A 100% change in velocity would only produce a 26% change in scour depth.

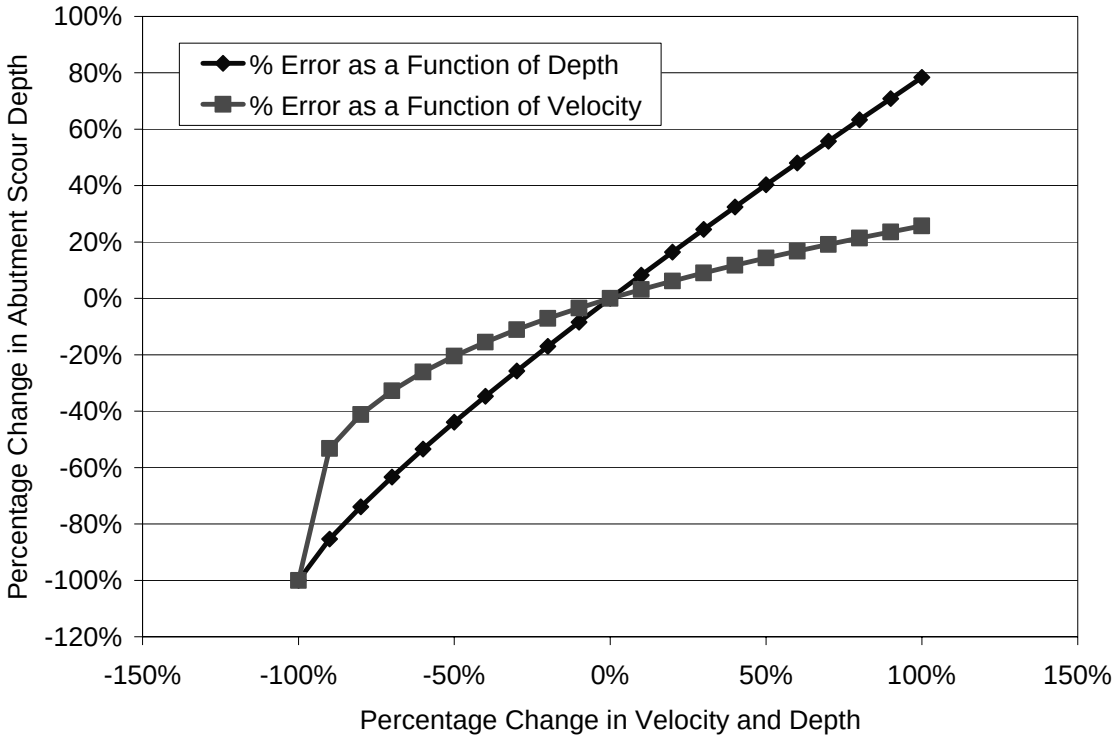

Figure 55 Abutment Scour Equations Sensitivity to Hydraulic Inputs

From the above figure, it is important to note that equations that employ both depth and velocity present a unique problem in error analysis. In general, if the depth is over estimated, the velocity is under estimated. These two would counter balance and tend to reduce the overall error. However, since the sensitivity to depth in the above equation is greater than the sensitivity to velocity, accurate prediction of depth is the more desirable factor in a model for this equation.

Pier Scour Calculation

Scour calculation at piers typically follows the HEC-18 methodology. This equation is a function of approach flow depth, approach flow velocity, and angle of attack. The CSU equation for scour around a single pile takes the following form:

$$\frac{y_s}{y_1} = 2.0 K_1 K_2 K_3 K_4 \left(\frac{a}{y_1}\right)^{0.65} Fr_1^{0.43}$$

where y_s is the local pier scour, y_1 is the approach flow depth, K_1 is the correction factor for pier nose shape, K_2 is the correction factor for angle of attack of flow, K_3 is the correction factor for bed condition, K_4 is the correction factor for armoring by bed material size, a is the pier width and Fr_1 is the Froude number of the approach flow. From the equation, the scour depth is a function of velocity to the 0.43 and depth to the 0.135. Figure 56 shows this dependence. Interestingly, the pier scour is relatively insensitive to both velocity and depth. A 100% change in velocity produces only a 35% change in scour depth and a 100% change in depth produces only a 10% change in scour depth.

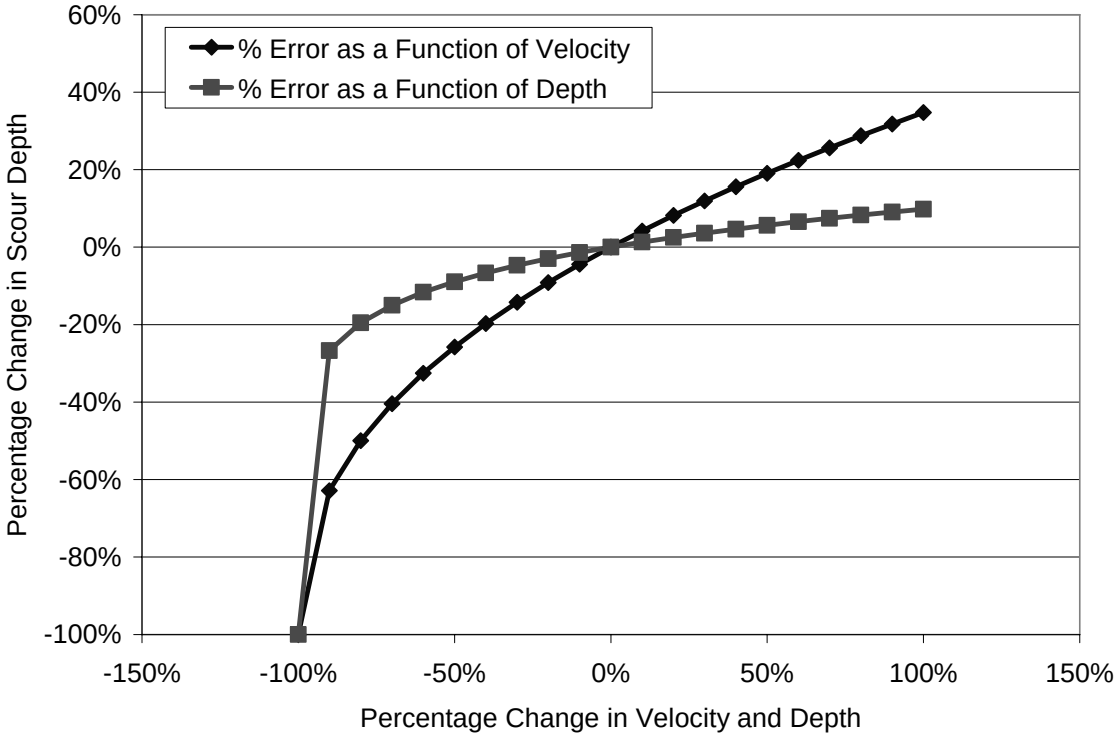

Figure 56 Pier Scour Sensitivity to Changes in Approach Flow Velocity and Depth

One of the correction factors, K_2, addresses angle of attack. This factor is a function of angle of attack via the following equation:

$$K_2 = \left(\cos\theta + \frac{L}{a} \sin\theta \right)^{0.65}$$

where θ is the angle of attack and L is the length of the pier in the streamwise direction. Given the non-linearity associated with the dependence on angle of attack, percentage changes in scour depth are dependent on the initial estimate. Figure 57 displays a sensitivity curve for a pier with a length to width ratio of eight for several initial estimates of angle of attack.

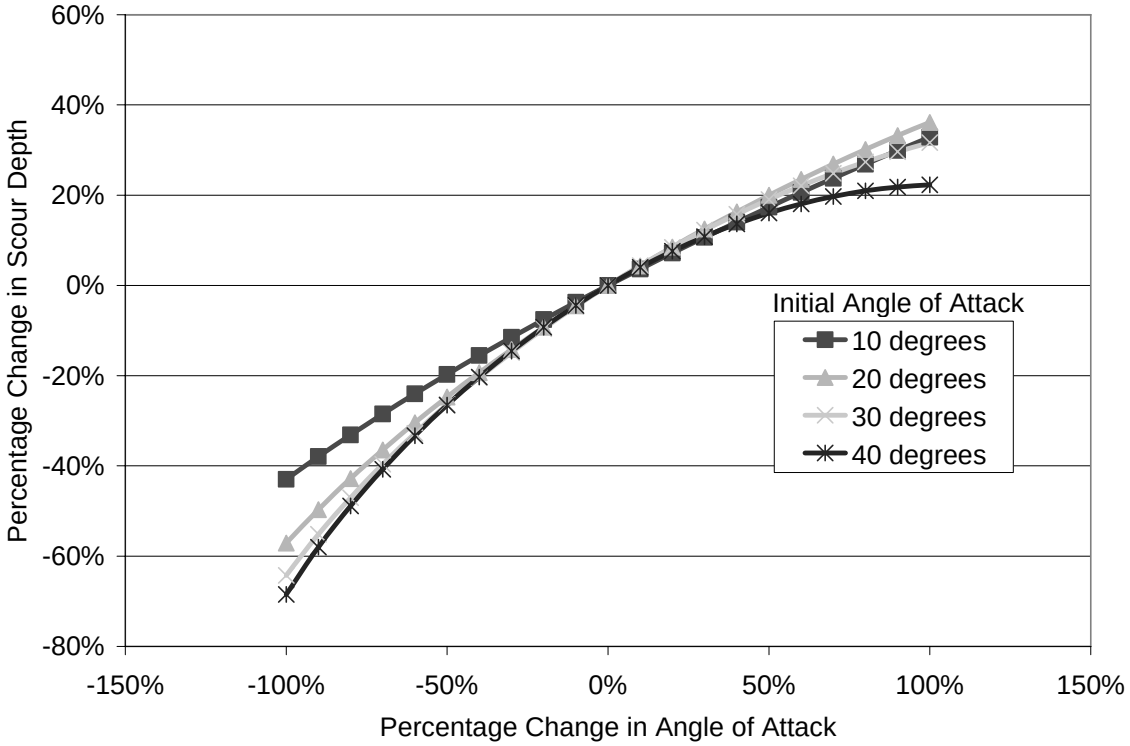

Figure 57 Pier Scour Sensitivity to Angle of Attack for L/a = 8

FEMA "No-Rise" Studies

Prior to construction of bridges near or over regulatory floodways, a hydraulic engineer is often asked to perform hydraulic modeling to ensure that the new construction will not impact pre-project base flood elevations. Based on this requirement accurate determination of water surface elevations in and around the bridge is paramount. In situations such as these, the engineer is advised to select the model that provides the most accurate backwater determination given the different project features described in the previous chapter. The engineer is also advised to consult the Appendix to determine how these different elements affect the solution of water surface elevation in and around the bridge.

Bendway Weirs/Stone Spurs

Bendway weirs and stone spurs are structures that are installed somewhat perpendicular to the shoreline along the outside bend in a river to protect from bank erosion. According to HEC-23 (Lagasse et al., 2001), "spurs are typically visible above the flow line and are designed so that flow is either diverted around the structure, or flow along the bank line is reduced as it passes through the structure. Bendway weirs are normally not visible, especially at stages above low water, and are intended to redirect flow by utilizing weir hydraulics over the structure. Flow passing over the bendway weir is redirected such that it flows perpendicular to the axis of the weir and is directed towards the channel centerline."

Given the inherent two-dimensional nature of flow around spurs and bendway weirs, application of a two-dimensional model is the best tool for examining flow structure, optimizing placement, and sizing stone. The hydraulic engineer is advised not to employ a one-dimensional model for these applications.

OTHER PROJECT CONSIDERATIONS

In deciding upon what model to select, the responsible engineer must make a critical evaluation of their available resources for successfully completing the project as well as outside constraints such as project schedule and data availability. The resources include the software available to the engineer performing the work and more importantly the experience of the engineers employing the software. Since this project does not distinguish between different available software packages, this report will not address this topic. However, the responsible engineer is advised that certain critical features of a specific project can dominate the selection process via which software package contains that particular feature. An example of this may be capability of HEC-RAS to predict supercritical flow when selecting between HEC-RAS and RMA2.

The resource that is most germane to this discussion is that of modeler experience. If the modeler is the one making the selection, that engineer is certainly aware of their comfort level regarding the two different approaches. If a project manager is making the decision and has more than one engineer with varying levels of experience available, assessing capabilities is less straight forward. There are a number of indicators as to a modeler's ability to successfully complete a project. Foremost is the number of years experience

with the model. Also relevant is the engineer's demonstrated performance with the model as rated by past project performance as well as internal and external QA/QC reviews. The project manager deciding on the appropriate approach should weigh each of these in their assessment of their staff's experience with both types of models.

Other considerations that factor into the decision making process are data availability and schedule constraints. One common critique of two-dimensional modeling, is that it requires too much additional data to perform. This is a common misconception. A two-dimensional model can be constructed from exactly the same data as can a one-dimensional model. The model will simply require the same assumption as does the one-dimensional model: i.e., prismatic changes between subsequent cross sections. That said, when there is little resolution of bathymetry and topography that can influence flow, there may be no distinct advantage to applying a two-dimensional model. In other words, in a general sense, increases in availability of data increases the advantage of employing a two-dimensional model. This is a distinctly different concept than the widely held belief that the requirements of a two-dimensional model limits its use. To judge the data availability constraints of a project, the engineer must therefore critically evaluate whether the available data: 1) meets the requirements of the models and 2) provides any differentiation between the two model applications. Additionally, several data sources and techniques exist for augmenting two-dimensional data sets beyond acquired survey data. Several governmental agencies (e.g., NGDS, NOAA, USGS) provide coarse resolution data online that can provide descriptions of floodplains or larger waterbodies. Also, the engineer can digitize geo-referenced bathymetric/topographic maps or navigation charts to extend data sets. Although tools for accomplishing this have become increasingly easy to apply, this still involves a time commitment that must be factored into model setup.

A final consideration that should be factored in is schedule. The engineer/project manager must be familiar enough with their abilities and staff's abilities to evaluate the time requirements associated with the modeling effort. For example, tracking the time spent on the sensitivity study indicated that the more experienced modeler was able to complete the two-dimensional modeling in approximately the same amount of time that it took the less experienced modeler to complete the one-dimensional modeling. Additionally, the two-dimensional modeler finished the tidal simulations in significantly less time. From this example, if one employed these two modelers and were presented with a riverine project, there may be little difference in which model to select based on time constraints alone. However, if the project called for tidal flows, the two-dimensional modeler has exhibited a distinct difference. As the example illustrates, the best indicator for evaluating the relative performance regarding scheduling constraints between the two model approaches is the modeler's performance on projects of similar types.

CHAPTER 6 DECISION TOOL

Selection of the appropriate type of numerical model to apply to specific site conditions, design applications, data availability, and modeler's experience is a complex process that is not easily condensed to a simple procedure. Rather, the modeler must sift through several decision factors and weigh the relative importance of each. The most appropriate tool for accomplishing this job is a decision matrix. A decision matrix is a chart that allows one to systematically identify, analyze, and rate the strength of relationships between sets of information. The matrix is especially useful for analyzing large numbers of decision factors and assessing each factor's relative importance.

CONCEPTUAL STRUCTURE

Designing a decision matrix involves the application of four steps. Step one involves identifying alternatives. In this case, the alternatives are employing either a one-dimensional or two dimensional model. Step two involves the identification of decision/selection criteria. The previous chapters have discussed several of the criteria relevant to this decision. They can be reduced to three types: criteria involving the site conditions, criteria involving design considerations, and criteria involving other project related considerations. Concerning the site conditions, the criteria include those features examined in the sensitivity study presented earlier. These include multiple openings, river bends, asymmetric floodplains, etc. The criteria involving design considerations include the purpose of the model application. Examples of these purposes include: design of abutment protection, calculation of scour depths, evaluation of FEMA "no-rise" requirements, etc. The final category relates to all other criteria associated with the project. These may include time constraints, data availability, and modeler experiences with each of the numerical model types.

The next step (Step three) in the development of the tool involves the assignment of weights to each of the decision criteria. This step requires the engineer to critically evaluate the application and rate the relative importance of each of the decision factors. This decision tool will provide guidance to the engineer regarding how to assess this importance. Step four of the decision matrix design involves development of a scoring system by which the engineer can rate the performance of each of the models relative to each of the decision criteria. The scoring will involve assigning numerical values from, for example, 1 (low applicability or performance) to 5 (high applicability or performance). Developing the score will involve assimilating the information presented in the previous chapters regarding the sensitivity testing as well as the sensitivity of the different design equations to the model results. For example, if the engineer is designing riprap bank protection on the outside of a river bend upstream of or at the bridge, the scoring for the one-dimensional model for the decision criteria of "Riprap Bank Protection" would be relatively low whereas the scoring for the two dimensional model would be relatively high. However, if the protection were located well downstream of the bridge and the bend, the scoring for the two models might be relatively even.

Table 4 presents an example decision matrix. For this matrix, the user is deciding between two alternatives based on three decision criteria. In the development of the tool, the user has assigned weights of 5, 4, and 1 to the criteria. The user then rated the performance/applicability of each of the alternatives relative to each of the criteria. In the application of this tool, the weights are multiplied by the score and then totaled for each alternative. The alternative with the higher total is the recommended alternative. In this example, each alternative received the same scores in that each received a 1, 3, and 5 in one of the criteria. However, since Alternative B received a higher score in what was deemed the more important criteria (Decision Criteria 1), it is the recommended alternative.

Table 4 Example Decision Matrix

		Score	
Criteria	Weighting Factor	Alternative A	Alternative B
Decision Criteria 1	5	3 (X5) = 15	5 (X5) = 25
Decision Criteria 2	4	5 (X4) = 20	3 (X4) = 12
Decision Criteria 3	1	1 (X1) = 1	1 (X1) = 1
Totals		**15 + 20 + 1 = 36**	**25 + 12 + 1 = 38**

Scoring: 1 = low
3 = medium
5 = high

TOOL APPLICATION/DEVELOPMENT

Each application of the decision tool should involve the development of the decision matrix. This document provides the framework from which to develop the decision matrix.

Step 1: Identification of Alternatives

Given the stated purpose of this study, the alternatives include: 1) Employing a one-dimensional model; and 2) Employing a two-dimensional model. The discussion presented in previous chapters has limited itself to general one- versus two-dimensional model applications. The engineer may wish to customize the alternatives by evaluating specific individual models. However, the engineer performing this evaluation must be familiar enough with the relative performance of the models with respect to the decision criteria. The discussion presented herein will concern only one- and two-dimensional models in general.

Step 2: Identification of Decision Criteria

The purpose of the preceding chapters was to present sufficient discussion of the various factors that lead to model selection. These, in essence, are the decision criteria. As stated previously, the decision criteria fall into one of three categories: 1) criteria related to site conditions, 2) criteria related to design considerations, and 3) criteria related to other project considerations. Before selecting decision criteria, the engineer should assemble all available information concerning the project site and the design requirements. From this information the engineer can evaluate which criteria are relevant to the subject project. This document provides criteria that were introduced in the previous chapters. The engineer can add additional criteria, but only if the engineer is sufficiently familiar with the relative performance/applicability of the models that he/she is choosing between.

Decision criteria related to site conditions include those conditions evaluated during the sensitivity tests. The engineer developing the decision matrix should evaluate the site conditions and select which of the following criteria apply:

- Multiple Openings
- Bridges Located on River Bends
- Bridges near Confluences
- Bridges with Significant Constrictions
- Overtopping Flow
- Embankment Skew
- Bridges over Meandering Rivers
- Bridges with Asymmetric Floodplains
- Bridges with Large Piers/High Blockage
- Tidal Hydraulics

Decision criteria related to design requirements include those introduced during the evaluation of the design equations. The engineer developing the decision matrix should include all design elements associated with the project from the list below:

- Riprap
- Armor Units
- Concrete Block
- Abutment Scour Calculation
- Pier Scour Calculation
- FEMA “No-Rise”
- Bendway Weirs

Decision criteria related to other project considerations include those factors not specifically related to the site or design (technical) elements. Rather they include elements related to project management or personnel. The engineer constructing the decision matrix should include all the following criteria:

- Modeler Experience
- Scheduling
- Data Availability

Step 3: Weighting the Criteria

Once the appropriate criteria are selected, the engineer proceeds to assigning weighting factors to each of the criteria. The engineer needs to critically evaluate the project within the context of each of the decision criteria. The purpose of the evaluation is to determine the relative importance of each with respect to the other criteria within the same category. Weights are assigned relative to what is deemed the more important or governing criteria of the subject project. For example, take the situation where a new bridge is constructed over a waterway. The state of the site location requires that the engineer calculate abutment scour. However, the plan for the bridge also requires rubble riprap abutment protection. As such, the accuracy of the abutment scour calculation is less important than accurately sizing the rubble riprap for the protection. Therefore, the weighting value of the riprap criteria will be higher than that associated with the abutment scour calculation. Another example of relative importance is found when examining the SC-41 Bridge over the Black River (Figure 3). From the figure, when selecting decision criteria, the engineer should include: (1) multiple openings, (2) bridges located on river bends, (3) embankment skew, and (4) bridges with asymmetric floodplains since all of these features are present. However, since the relief bridge is quite small and located far from the main opening, and since the bridge is located upstream of the bend rather than on it, the engineer should weight criteria (1) and (2) lower than criteria (3) and (4). As developed, recommended values for weights should range from 1 to 10. These values should provide ample range to differentiate between the importance of the individual criteria within each category and with respect to the other categories.

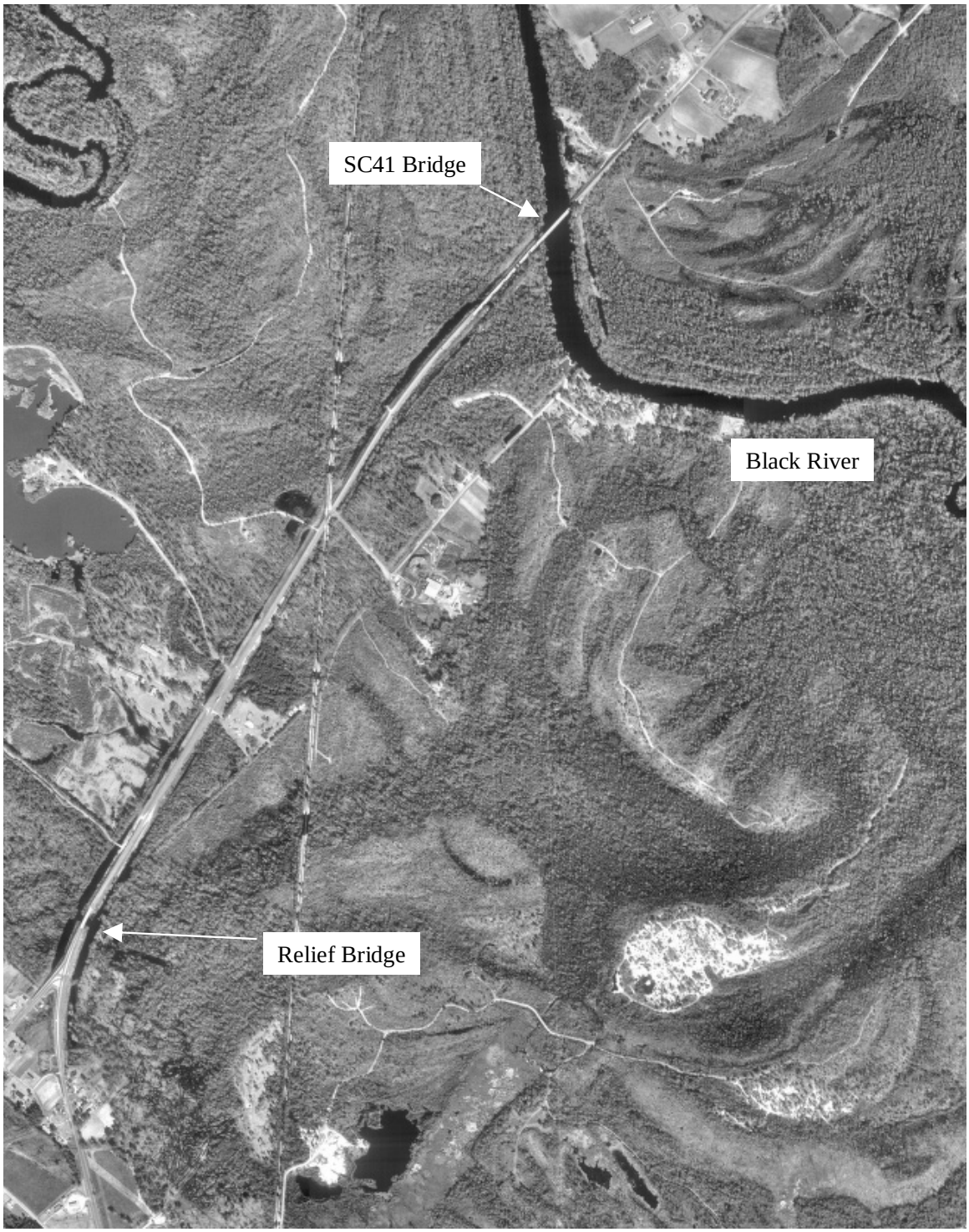

Figure 58 S.C.-41 Bridge over the Black River, South Carolina

Step 4: Scoring System/Tool Application

As constructed, scoring the decision criteria involves assigning numerical values equal to 1 (low performance/applicability), 3 (medium performance/applicability), or 5 (high performance/applicability). This system is deemed simple enough for the engineer to apply based on the information provided in this document yet still provide enough differentiation to identify the proper model to apply. For each criterion, the engineer should reference the appropriate section in this document and become familiar with each model's performance relative to the criteria. Given the categorization of the criteria, the first category (Site Conditions) should be judged on each models' relative performance over the entire model domain. The next group of criteria (Design Requirements) refers to the models' performance at specific locations. Given a specific design element, the engineer should examine the performance of the model at the planned location as well as examine the sensitivity of the design equation to model results. The final group is dependent upon the engineer's (or engineering team's) qualifications as well as the project specifics. The engineer must make a judgment based on his/her past experience with projects of this type relative to the requirements of the subject project.

Table 5 presents the developed decision tool. To apply this tool, the engineer first selects which criteria (rows) are applicable. Notably, the table includes blank rows under each category if the engineer wishes to evaluate other criteria not included in this document. Next, the engineer assigns weights from 1 to 10 in column 2 for each selected criteria. The engineer then assigns scores to both types of models in columns 3 and 5. The engineer then fills in columns 4 and 6 with the multiples of the scores times the weights. These multiples are added up for each model and the sum is entered in the final row. The model with the highest score is the recommended model for the project. Notably, if the scores are very close (within a few points), the engineer may wish to either reevaluate the criteria or add additional criteria to provide more differentiation.

Notably, this research project is based on the assumption that, in general, the two-dimensional models produce more accurate and useful results if for no other reason but that they are not limited by an assumption of unidirectional flow and provide more complete spatial coverage. As such, one would expect that the two-dimensional model would score equal to or higher than the one-dimensional model for all criteria in the first two categories. Viewed in this light, the decision tool becomes a way to evaluate whether the technical aspects of a project outweigh time, data availability, and experience short comings to justify applying a two-dimensional model over a one-dimensional model.

Table 5 Decision Tool

Design Criteria	Weight	One Dimensional Model		Two Dimensional Model	
		Score 1=low 3=medium 5=high	Weight x Score	**Score** 1=low 3=medium 5=high	Weight x Score
Site Conditions	**(1-10)**				
Multiple Openings					
Bridges Located on River Bends					
Bridges near Confluences					
Bridges with Significant Constrictions					
Overtopping Flow					
Embankment Skew					
Bridges over Meandering Rivers					
Bridges with Asymmetric Floodplains					
Bridges with Large Piers/High Blockage					
Tidal Hydraulics					
Design Requirements	**(1-10)**				
Riprap					
Armor Units					
Concrete Block					
Abutment Scour Calculation					
Pier Scour Calculation					
FEMA “No-Rise”					
Bendway Weirs					
Other Considerations	**(1-10)**				
Modeler Experience					
Scheduling					
Data Availability					
Totals (Sum of Weight x Score)					

GUIDELINES FOR TOOL APPLICATION

Application of the decision tool begins with an examination of the decision criteria. To begin, the engineer should collect data regarding the project location that provides information on the channel and floodplain features as well as the existing or proposed bridge. This will include aerial photographs, topographic maps, bridge plans, conceptual bridge designs, etc. From this information, the engineers should list the site condition features relevant to this application. Notably, the engineer may wish to add site condition features not included in the above list if they are deemed applicable. Next, the engineer should list the design requirements associated with the subject project. Again, there may be requirements not included in the tool's list that the engineer may wish to add. The final criteria group under the heading "Other Considerations" should be included with all tool applications. Additionally, the engineer may add additional criteria under this heading that are not considered in this report.

After identifying the relevant criteria to the subject project, the engineer should progress to weighting the criteria on a scale from 1 to 10. Weighting should involve first examining each criteria in terms of importance to the other identified criteria within each of the three groups. Then, the weighting must be judged between the groups. Consider the following example. A project involves determining the design hydraulic conditions at an existing tidal bridge for a scour evaluation. The channel is relatively straight and the abutments are located on high bluffs outside the floodplain. The engineer performing the work has considerable experience with both one- and two-dimensional models. Additionally, the engineer has considerable topographic and bathymetric data available and ample time available. Under this scenario, pier scour calculation and tidal hydraulics should be weighted high (9-10) whereas modeler experience, data availability, and schedule should receive low rankings (1-3). With an increasing number of identified criteria, the engineer can incorporate more differentiation between the criteria. The engineer should also examine the sensitivity study tests to aid in assigning weights. For example, an embankment skew of 45° should receive a higher weighting than a skew of only 10°.

Once the weights of the criteria have been assigned, the next step in tool application involves scoring the criteria. As constructed, the tool involves assigning a score of 1, 3, or 5 which corresponds to a low, medium, or high performance of the model. For the site conditions criteria, the engineer should consult both the description of the sensitivity test results listed in Chapter 4.0 as well as the figures contained in the appendix. When examining the figures, the engineer should examine the test results in the areas most relevant to the project. For example, if the engineer is calculating pier scour, the most relevant area is the bridge opening. If the engineer is designing abutment protection, the most relevant areas are near the abutments. The engineer should examine each of the area relevant to the design and judge the performance of the model relative to the individual criteria as a whole. For example, in the case of a significant embankment skew, the one-dimensional model performs well at the center of the bridge, but poorly near the roadway embankments. If the project involves both local pier scour and abutment scour protection design, the overall performance of the one-dimensional model may be judged as medium (=3). As another example, an engineer is examining a pressure flow scour situation at a bridge. In this case, the instabilities inherent in the ceiling function in FESWMS may lower the two-dimensional model's ranking for overtopping flows to a 1.

Following examination of the site conditions, the next step involves examination of the design criteria. Here, the engineer should consult the sensitivity analysis located in Chapter 5.0. This analysis provides information regarding how sensitive the design equations are to changes in hydraulic inputs. If the equations are relatively insensitive, then the rankings for the two models should be equal. However, if there is significant sensitivity, the engineer should again consult the appendices to examine the relative performance of the two models in the relevant area and judge the model accordingly. Notably, in the site conditions group of criteria, the model's performance is judged in general over the entire domain of interest. In the design requirements group, the models are judged relative to both the set of design requirements at specific locations and the performance at that location. This allows the engineer to incorporate further differentiation at specific locations within the project domain.

For the scoring of the remaining criteria associated with the project, the engineer should critically evaluate the schedule, data availability, modeler experience available to them. Chapter 5.0 also contains a discussion regarding evaluation of these factors.

After scoring the criteria for both models, total scores are developed by multiplying the weights by the scores and finding the sum for each model. The total with the greater score is the recommended model for the application. The difference between the two scores can reveal much about the differentiation between the two models for a particular application. For example, a difference of more than 40 points for an application that only identified five decision criteria provides a strong indicator for one model over another. However, a difference of less than 5 points for an application that involved ten decision criteria indicates that either model may be adequate. In this case, the engineer is advised to either reexamine the criteria weighting to provide more differentiation between the two models or to add additional criteria.

CHAPTER 7 EXAMPLE APPLICATION

The following example illustrates an application of the decision tool. The site of the application was identified from both the literature review and the distributed survey. The location is the Highway 130 Bridge over Buckhorn Creek near Shiloh, Alabama. The site is described in the USGS Hydrologic Atlas by Ming et al. (1979). This reference provides maps of a site and includes measured cross sections of the creek, and measured high watermarks and flow rates of two floods that occurred on March 2-3, 1972 and December 21, 1972. As shown in Figure 59 and Figure 60, the area is characterized by wide floodplains with an asymmetry. The creek itself meanders in its approach to and downstream of the crossing, but remains relatively straight through the bridge. The creek crosses beneath the bridge near the west abutment.

For this example, the project considered is a bridge replacement project along the same alignment that will include design of rubble riprap abutment protection and calculation of local pier scour. There will be no change in the location of the abutments or bridge opening. As such, it is assumed that calculation of change in backwater is not an issue. The piers considered for the project are in-line pile bents comprised of 6 24-inch (0.61 m) square concrete piles spaced 8.0 ft (2.44 m) apart centerline to centerline. The replacement bridge length will be 75 m and will include 9 piers spaced 7.5 m apart.

Before applying the tool, a critical review of the project location, project elements, and available resources/other considerations is required. From the aerials and topographic maps, the channel exhibits some asymmetry in the floodplains with the channel traveling along the west side of the floodplain. The floodplain width on the west side (103 m) measures only 60% of the floodplain on the east side (170 m). The channel does exhibit some meandering both upstream and downstream of the site. The sinuosity of the channel is measured at 1.18.

As mentioned previously, the project requirements entail riprap abutment scour protection and calculation of local pier scour. The available data include surveyed cross sections at the bridge and upstream and downstream of the site as well as any data available from on-line sources. Unfortunately, only a coarse resolution DTM of the site was available from the USGS. Detailed resolution of the area would involve digitizing contours from the USGS topographic map and merging this data with the surveyed cross sections.

The project manager applying the tool has two engineers available for performing the modeling. The one-dimensional modeler has over twenty years of modeling experience in a variety of situations. The two-dimensional modeler has approximately eight years experience with the two-dimensional model. The project manager considers both sufficiently experienced in applying their respective models in situations of this type. However, the project manager recognizes that in order to take advantage of the increased resolution of the overall flow field, an application of the two-dimensional model will involve digitizing the USGS maps. Unfortunately, the project manager has recently been assigned a new drafting technician that is fresh out of school who does not have demonstrable experience with this type of work. Additionally, with the deadlines associated with this project and the prior commitments of the two modelers, the project manager recognizes that the one-dimensional modeler should have plenty of time to complete the project, but the two-dimensional modeler may be pressed for time.

Figure 59 Aerial Photograph of Highway 130 Bridge over Buckhorn Creek

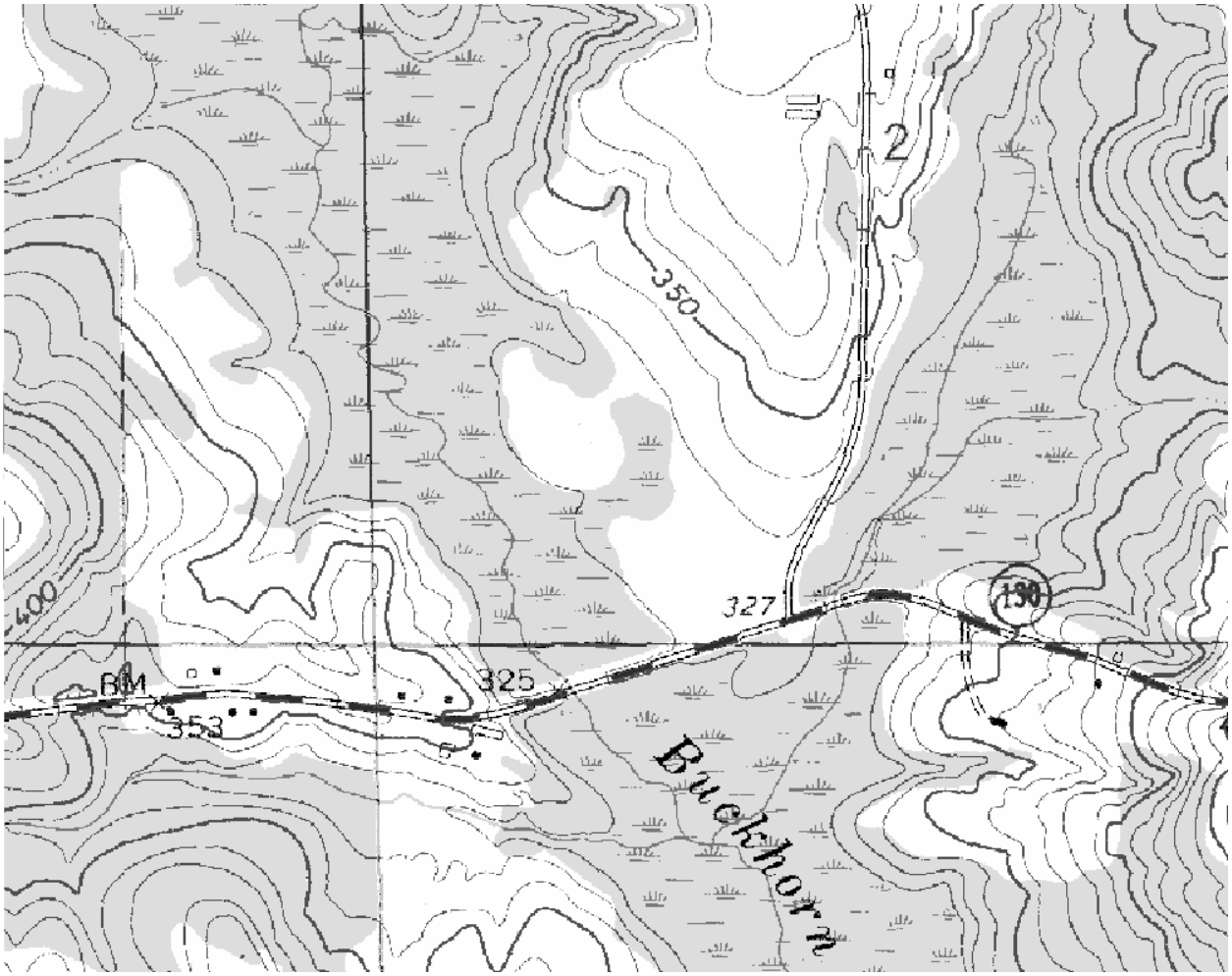

Figure 60 USGS Quadrangle Map of Highway 130 Bridge over Buckhorn Creek

STEP 1: IDENTIFICATION OF ALTERNATIVES

After having examined all the relevant features of the project, the project manager next turns to step one of tool application: identification of alternatives. In this example, the manager is choosing between an application of FESWMS and HEC-RAS.

STEP 2: IDENTIFICATION OF DECISION CRITERIA

Step two of the application involves identification of the decision criteria. From the critical review, the manager has identified the following criteria:

- Asymmetric Floodplains
- Bridges over Meandering Rivers
- Riprap
- Pier Scour Calculation
- Modeler Experience
- Scheduling
- Data Availability

STEP 3: WEIGHTING THE CRITERIA

The next step in tool application involves weighting the criteria. Two site conditions criteria were identified: Asymmetric Floodplains and Bridges over Meandering Rivers. The manager recognizes that although there is evidence of meandering upstream and downstream of the bridge, the creek is relatively straight at the bridge cross section. Additionally, the upstream and downstream meandering is not significant. The manager also recognizes that there is moderate to high asymmetry to the floodplain. As such, the weighting of the meandering criteria should be relatively low (assigned a value of 2) while the asymmetry weight should be moderate to high (assigned a value of 7).

The design criteria identified include use of riprap and calculation of pier scour. For this job, the initial designs called for significant amounts of riprap along both the abutments and embankments upstream and downstream of the bridge. Regarding the pier scour calculations, the initial geotechnical characterization has indicated that there are no issues associated with increasing pile tip elevations. As such increases in scour estimates would only influence the bridge design in regards to the increased length of the piles. Given the relatively simple geometry of the substructure, this additional length does not significantly affect design. With this in mind, the manager assigns a low weight to the pier scour calculation criteria (a value of 3) and a high weight to the riprap criteria (a value of 9).

In assigning weights to the other considerations criteria, the project manager decides that schedule is extremely important to the overall success to the project. In fact, there may be severe financial impacts if the project is delivered late. The modeling itself is relatively straight forward and should not require a particularly high level of expertise. Concerning data availability, ample data exists to perform both one- and two-dimensional modeling. Given this situation, modeler

experience and data availability are assigned low weights (values of 3) and schedule is assigned a high weight (a value of 10). Table 6 illustrates the results of the weight assignments.

STEP 4: SCORING SYSTEM

The next step in the tool application involves scoring the different models for each of the criteria. For the site conditions criteria, the manager references the different cases in the Appendix to judge the performance of the model for the overall domain. For the meandering criteria, the manager checks the small channel meandering case for a sinuosity of 1.25. The manager notes that the one-dimensional model performed poorly when compared with the two-dimensional model when comparing velocity magnitude. However, given that the channel is relatively straight through the bridge, the manager also checks the small baseline model. The manager notes that for the baseline comparison the models compare well. Given this, the manager assigns a score of 3 (medium) for the one-dimensional model and 5 (high) for the two-dimensional model.

For the asymmetry criteria, the manager checks the small channel asymmetry case of 50% reduction. From the comparison, the manager notes that the one-dimensional model performed relatively well within the channel but not as well in the floodplains. As such, the manager assigns a score of 3 (medium) to the one-dimensional model, and 5 (high) to the two-dimensional model.

For the design requirements criteria, the manager begins by checking the sensitivity of the design equations to the hydraulic model inputs located in Chapter 5.0. Then, the manager again checks the figures in the appendix. This time, the manager looks specifically at the hydraulic input solutions in the areas where the design elements are located. For the riprap criteria, the manager notes that the design equations are very sensitive to velocity magnitude. The manager then examines the velocity magnitude comparisons for the cases identified in the site conditions: small channel meandering (sinuosity = 1.25), baseline, and asymmetric floodplains (50% reduction). The manager notes that the one-dimensional model performed poorly predicting the velocity magnitude along the upstream and downstream face of the abutments for all cases. However, the manager also recognizes that the design velocity magnitude for the riprap will occur at the bridge opening constriction where the velocities are the highest. At this location, the models compare relatively well. Based on this information, the manager decides to assign scores of 3 to both the one- and two-dimensional model. This decision is based on the fact that both models predicted similar velocity magnitudes in the overbanks through the bridge cross section.

Table 6 Example Decision Tool after Weight Assignment

Design Criteria	Weight	One Dimensional Model		Two Dimensional Model	
		Score 1=low 3=medium 5=high	Weight x Score	**Score** 1=low 3=medium 5=high	Weight x Score
Site Conditions	**(1-10)**				
Bridges over Meandering Rivers	***2***				
Bridges with Asymmetric Floodplains	***7***				
Design Requirements	**(1-10)**				
Riprap	***9***				
Pier Scour Calculation	***3***				
Other Considerations	**(1-10)**				
Modeler Experience	***3***				
Scheduling	***10***				
Data Availability	***3***				
Totals (Sum of Weight x Score)					

For the pier scour calculation criteria, the manager consults the design equation section and notes that the HEC-18 equations are only mildly sensitive to velocity magnitude. When examining the angle of attack sensitivity, the manager notes that for an expected angle of attack of 10° or less, the K_2 coefficient is not particularly sensitive. Doubling the angle of attack would only result in a 40% change. The manager then consults the Appendix for the identified cases. From the figures, the manager notes that for the majority of the piers, the angle of attack predicted by the two-dimensional model for the flow at the bridge compares well with the assumed (parallel to the channel centerline) angle of attack for the one-dimensional model. Additionally, the velocity magnitudes for the majority of the piers also compare well. Given this information, the manager assigns scores of 3 (medium) to both models.

The final category involves the manager's assessment of the resources available and the project constraints. The manager has confidence that both modelers can adequately model the subject project. As such, the manager assigns scores of 5 to both modelers. Concerning schedules, the manager is concerned that the two-dimensional modeler may be constrained for time. Additionally, the manager is concerned that the relative inexperience of the new drafting technician who would be involved in generating additional data for the two-dimensional modeling effort may affect project schedule. Despite this, the manager believes that the two-dimensional modeling can meet the schedule, just that there is no room for error. The manager has no such reservations concerning a one-dimensional modeling effort. Therefore, the manager assigns scores of 5 (high) to the one-dimensional model and 3 (medium) to the two-dimensional model. Finally, all data necessary for performing the modeling is available for either effort. As such, the manager assigns scores of 5 (high) to both models. Table 7 presents the tool after the scores have been assigned.

At this point, the manager can identify which model is appropriate for this project by multiplying the scores by the weights and summing this product for each model. Table 8 displays the results and identification of the appropriate model. From the table, the tool identified the one-dimensional model as appropriate for this project. Given the small difference in the score, however, either modeling effort should suffice. Notably, from the table, the better performance of the two-dimensional model was overshadowed by concerns about the scheduling. If these concerns did not exist, the tool would have identified the two-dimensional model as the appropriate model.

Table 7 Example Decision Tool after Scoring

Design Criteria	Weight	One Dimensional Model		Two Dimensional Model	
		Score 1=low 3=medium 5=high	Weight x Score	**Score** 1=low 3=medium 5=high	Weight x Score
Site Conditions	**(1-10)**				
Bridges over Meandering Rivers	2	***3***		***5***	
Bridges with Asymmetric Floodplains	7	***3***		***5***	
Design Requirements	**(1-10)**				
Riprap	9	***3***		***3***	
Pier Scour Calculation	3	***3***		***3***	
Other Considerations	**(1-10)**				
Modeler Experience	3	***5***		***5***	
Scheduling	10	***5***		***3***	
Data Availability	3	***5***		***5***	
Totals (Sum of Weight x Score)					

Table 8 Example Decision Tool after Model Selection

Design Criteria	Weight	One Dimensional Model		Two Dimensional Model	
		Score 1=low 3=medium 5=high	Weight x Score	**Score** 1=low 3=medium 5=high	Weight x Score
Site Conditions	**(1-10)**				
Bridges over Meandering Rivers	2	3	***6***	5	***10***
Bridges with Asymmetric Floodplains	7	3	***21***	5	***35***
Design Requirements	**(1-10)**				
Riprap	9	3	***27***	3	***27***
Pier Scour Calculation	3	3	***9***	3	***9***
Other Considerations	**(1-10)**				
Modeler Experience	3	5	***15***	5	***15***
Scheduling	10	5	***50***	3	***30***
Data Availability	3	5	***15***	5	***15***
Totals (Sum of Weight x Score)			***143***		***141***

VALIDATION OF SELECTED MODEL

To test whether the decision tool identified the correct model, both models were applied to this site. Models were calibrated to the data contained in the Hydrologic Atlas for the March 2-3, 1972 event. The design conditions for the site were assumed to match the conditions for the December 21, 1972 flood event. Table 9 displays the boundary conditions for both the calibration simulation and the design conditions simulation. Both modeling approaches made assumptions regarding model setup and calibration that are consistent in the manner with which they would be approached for an actual design project. Additionally, the Hydrologic Atlas provided estimates of Manning's n as a function of depth for this location. The estimates were based on modeling performed by Schneider et al (1976) for these flood events. The reference recommends a Manning's n that varies from 0.15 if the depth is less than 0.6 m to 0.1 if the depth is greater than 1.0 m. The value varies linearly for depths between 0.6 and 1.0 m. Figure 61 and Figure 62 display the model setups for both the HEC-RAS and FESWMS simulations. The Hydrologic Atlas provided cross sections at nine locations that spanned upstream and downstream of the bridge. This data provided the basis for the one-dimensional model setup. Construction of the two-dimensional model involved digitizing a USGS topographic map and merging this data with the surveyed cross sections. This process did indeed take longer than originally anticipated given the manual work required to merge the sets in a logical manner.

For the design simulations, the hydraulic parameters that are most important to the design requirements are both angle of attack and velocity magnitude for the pier scour calculations and velocity magnitude near the abutments for the riprap. Figure 63 and Figure 64 display the design simulation output results. From the figures, the HEC-RAS modeling predicted a maximum velocity magnitude of 1.3 m/s as compared with the FESWMS prediction of 1.4 m/s (only a 7 % difference). Both of these compare well with the maximum measurement of 1.43 m/s (at the 0.2 water depth) along the west side of the opening. Additionally, the FESWMS model predicts a maximum angle of attack of 6° as compared with the assumed 0° angle of attack with the HEC-RAS model. Given these results for this situation, the tool correctly predicted that there is little difference in the simulation results given the constraints. However, it should be noted that the one-dimensional model did not perform well throughout the model. In fact, it over estimated the backwater by more than 0.5 m near the upstream boundary condition whereas the two-dimensional model matched the measured values. In comparing the velocities upstream and downstream of the bridge, the velocity compared relatively well downstream of the bridge, however, there was divergence in the predictions upstream of the bridge. This is not surprising given the one-dimensional model's over estimation in backwater. Although the difference in backwater is concerning, this difference does not affect this example since the purpose was to examine conditions at the bridge. The example is built on the assumption that the opening associated with the bridge replacement remains the same and thus does not examine changes in backwater. Additional resources could have been spent to address this difference (e.g., by changing ineffective area or tuning the roughness), however, it would not have enhanced the example application.

Table 9 Boundary Condition for Validation Modeling

Boundary Condition	Calibration	Design
	March 2-3, 1972	December 21, 1972
Flow Rate (m^3/s)	63.7	118
Downstream Elevation (m)	95.9	96.7

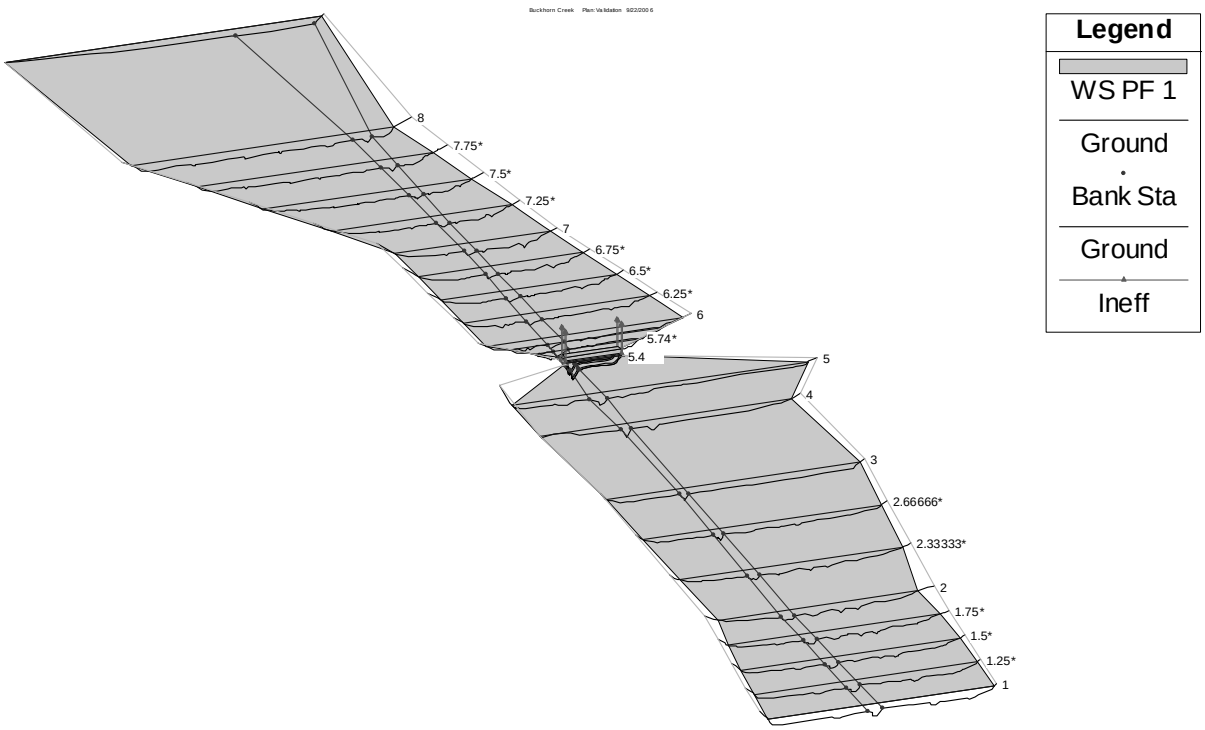

Figure 61 HEC-RAS Model Setup

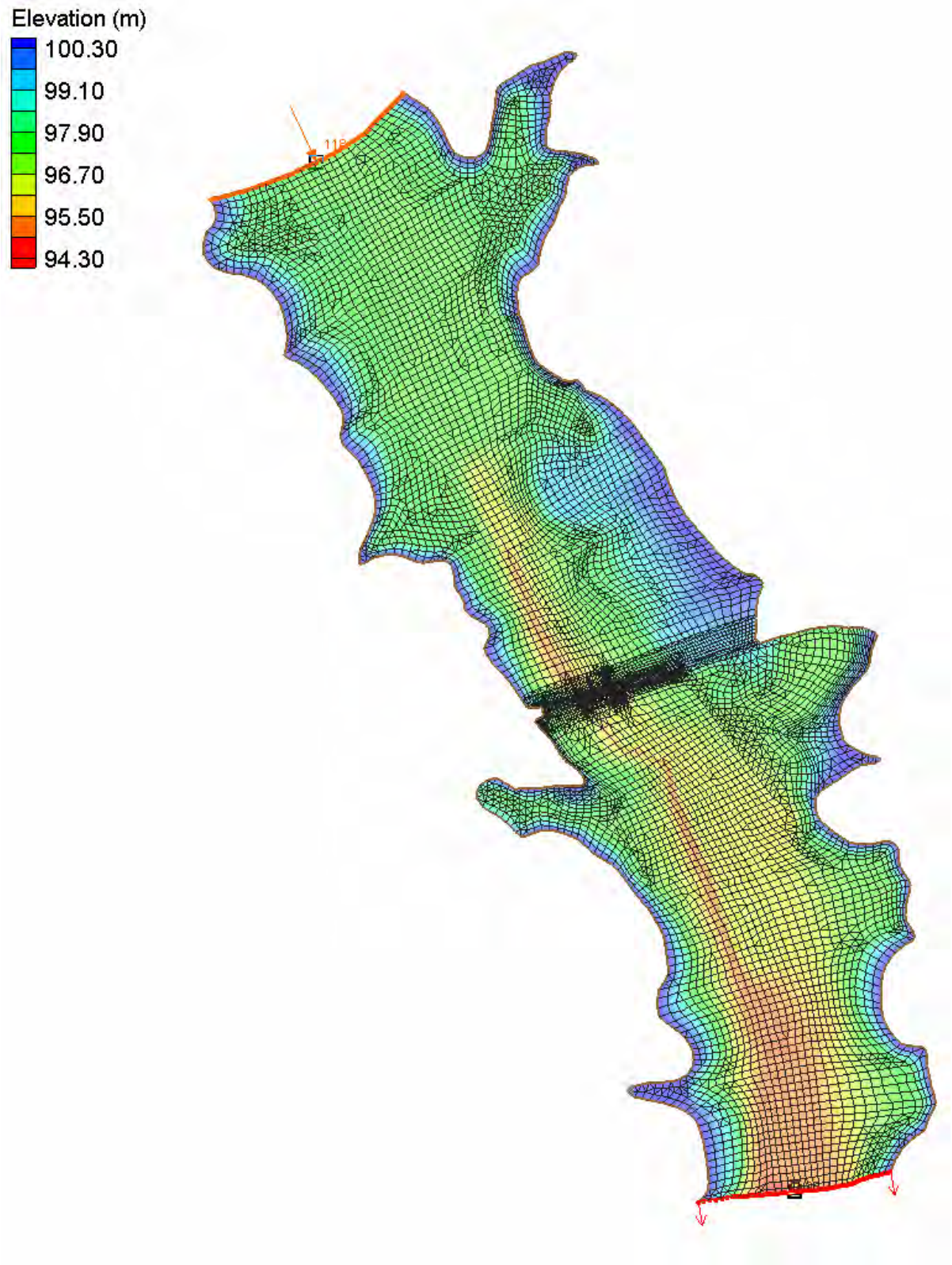

Figure 62 FESWMS Model Mesh

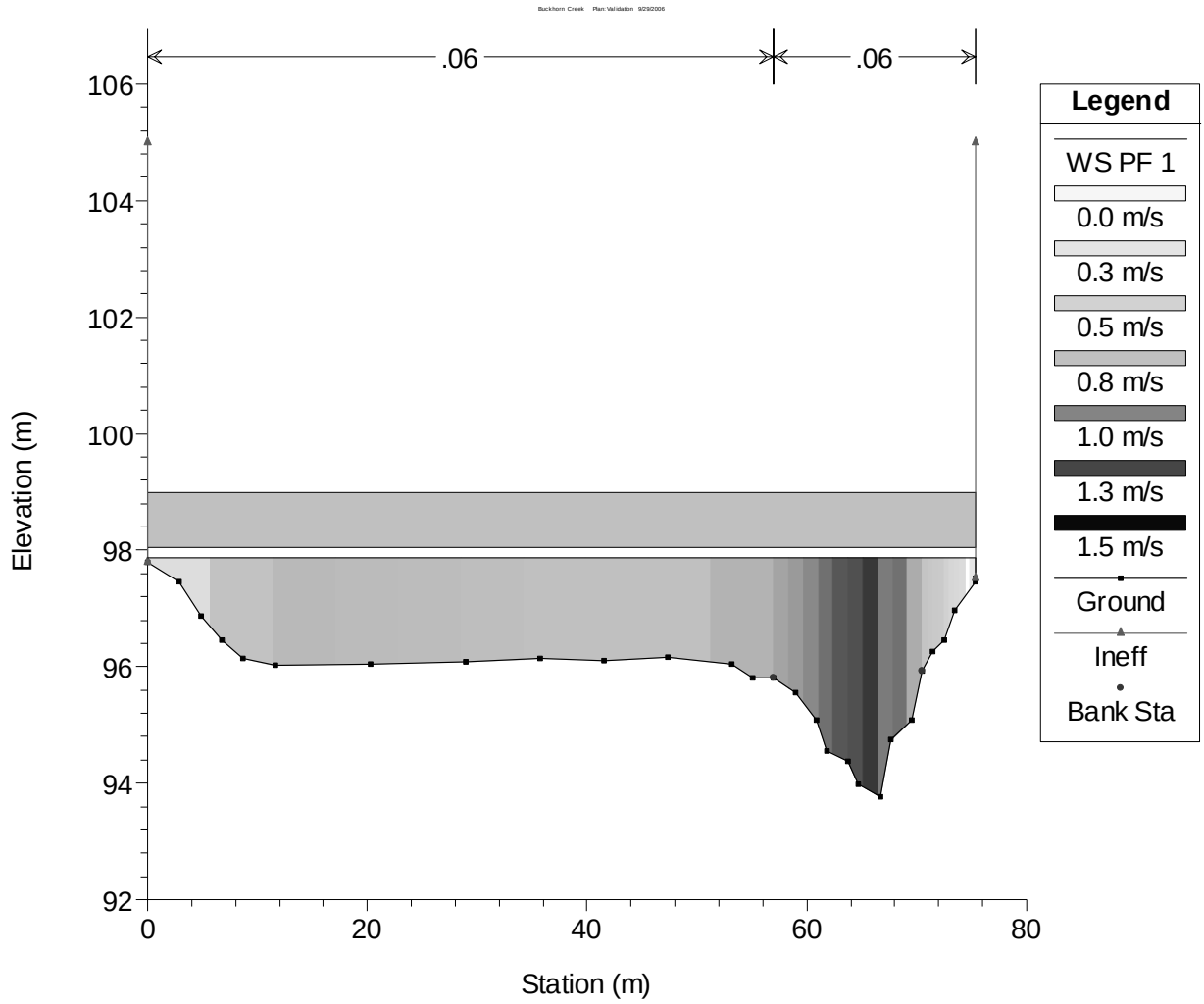

Figure 63 Design Simulation HEC-RAS Velocity Magnitude at Bridge

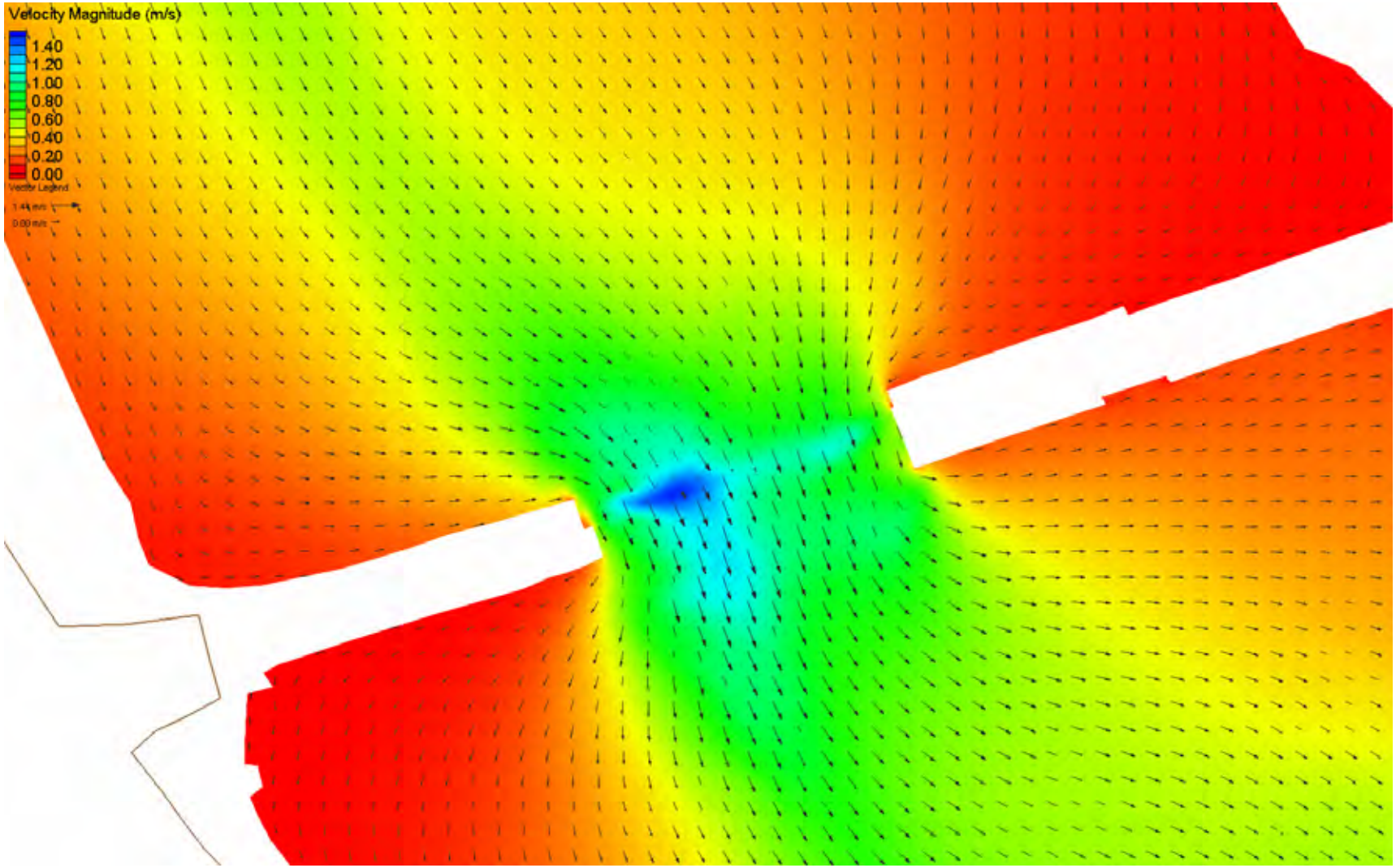

Figure 64 Design Simulation FESWMS Velocity Magnitude at Bridge

CHAPTER 8 CONCLUSIONS AND RECOMMENDATIONS

This report has documented the development of a decision tool to identify the most appropriate modeling approach (one-dimensional or two-dimensional) to apply to a specific application regarding determining the hydraulics associated with a bridge crossing. It incorporates the given site conditions as well as specific design elements associated with the project, available resources, and project constraints. Development of the tool began with a literature review/survey of the state of the practice to: identify the most commonly employed one- and two-dimensional numerical modeling software for examining hydraulics through bridge openings; identify data sets from actual bridge sites for an example application of the selection tool; and identify and characterize the site conditions and design requirements that may affect model selection. The results of this survey/literature review were then synthesized to form a comprehensive review of the current state of the practice for hydraulic modeling of riverine and tidal bridge crossings, a categorized list of the factors that influence model selection, as well as an overview of the design requirements that influence model selection. This synthesis led to the development of a series of sensitivity tests to evaluate the relative performance of one- and two-dimensional models. These tests covered a wide range of idealized possible site conditions (e.g., converging flow, asymmetric floodplains, etc.). In the experiments, parameters that control the factor in question were meticulously varied to discern the effect of the parameters on the models' relative performance. Additionally, the research evaluated several possible design elements that the engineer may encounter (e.g., determining scour depths, designing rubble riprap protection, etc.) to evaluate the sensitivity of the equations governing the design elements to possible error in the hydraulic parameters (e.g., depth, velocity) determined by the hydraulic model. Finally, a decision tool was developed from the sensitivity tests and the evaluation of the design elements. The decision tool takes the form of a decision matrix that incorporates all the factors that influence model selection. These include site conditions, design elements, available resources, and project constraints.

In addition to the decision tool, this document also contains a significant amount of information regarding the relative performance between one- and two-dimensional models over a wide range of varying site conditions. Additionally, this report provides information regarding the sensitivity of design equations to hydraulic parameters. As such, this document can aid the hydraulic engineer in their understanding of the consequences of model selection even if the tool is not directly applied.

The utility of the decision tool is that it presents a formal procedure for the selection of the appropriate model to apply rather than rely on an intuitive process. Additionally, it provides the selection procedure in an easy-to-understand and defensible manner for presentation to the non-technical or to policy makers. With regards to its application, the tool contains enough flexibility to incorporate conditions or constraints not covered in this document. Also, through its application it clearly identifies which feature(s) of the project are most important in the model selection for a specific application.

REFERENCES

1. Abbot, M. B. and Minns, A. W., *Computational Hydraulics, 2nd Edition*. Ashgate Publishing Co., Burlington, VT (1998) 557 pp.
2. US Army Corps of Engineers, *River Hydraulics*, Engineer Manual 1110-2-1416, Waterways Experimental Station, Hydraulics Laboratory, Vicksburg, MS (1993).
3. U.S. Army Corps of Engineers, *HEC-2 Water Surface Profiles, User's Manual*, Hydrologic Engineering Center, Davis, CA, CPD-2A, (1990, Revised 1991).
4. Kaatz, K.J. and James, W.P., "Analysis of Alternatives for Computing Backwater at Bridges." In *Journal of Hydraulic Engineering*, Vol. 123, No. 9. ASCE, (1997) pp. 784-792.
5. Walton, R. and Bradley, J.B., "HEC-2 Modifications for Bridge Scour Analyses." In *Water Resources Engineering (Proceedings of the First International Conference held in San Antonio, TX, August 14-18, 1995)* William H. Espey, Jr. and Phil G. Combs (editors). ASCE, New York, (1995).
6. Seckin, G., Yurtal, R., and Haktanir, T., "Contraction and Expansion Losses Through Bridge Constrictions." *Journal of Hydraulic Engineering*, Vol. 124, No. 5, (May 1998) ASCE, pp. 546-549.
7. US Army Corps of Engineers, *UNET, One-Dimensional Unsteady Flow Through a Full Network of Open Channels, User's Manual*. Hydrologic Engineering Center, Davis, California. CPD-66, Version 4.0, (2001a).
8. Teal, M.J., Powell, N., Gomez, E. and Williams, D.T., "A Conceptual Flood Control Plan for a Complex Channel System Using UNET," In *Water Resources Engineering '98* (Proceedings of the International Water Resources Engineering Conference held in Memphis, Tennessee, August 3-7, 1998.) Steven R. Abt, Jayne Young-Pezeshk, and Chester C. Watson (editors). ASCE, Reston, VA (1998).
9. Chowdhury, S. and Kjelds, J.T., "Simulation of Coastal Flooding and Levee Failure with MIKE 11" In *Solutions to Coastal Disasters '02* (Conference proceedings of Solutions to Coastal Disasters Conference 2002, held in San Diego, California, February 24-27, 2002) Lesley Ewing and Louise Wallendorf, (editors). ASCE, Reston, VA, (2002).
10. Shearman, J.O. (1990) *User's Manual for WSPRO--A Computer Model for Water Surface Profile Computations*, FHWA-IP-89-027.
11. Mueller, D.S., "Bridge-Scour Analysis Using the Water-Surface Profile (WSPRO) Model". In *Hydraulic Engineering '93* (Proceedings of the 1993 Conference held in San Francisco, California, July 25-30, 1993) by Hsieh Wen Shen, S. T. Su, and Feng Wen, (editors), ASCE, New York (1993).
12. Zundel, A.K. and Jones, N.L. "A Graphical Environment for Multi-Dimensional Surface Water Modeling." In *North American Water and Environment Congress & Destructive Water*, Chenchayya Bathala, (editor), ASCE, New York (1996).
13. US Army Corps of Engineers, *HEC-RAS, River Analysis System, User's Manual, Version 3.1.* Hydrologic Engineering Center, Davis, CA, (2001b).

14. Mohammad, E., Williams, D.T., Crossett-Avila, C., and McBride, D., "HEC-RAS Hydraulic and Scour Analysis of Ten Mile River Bridge Under the Caltrans Seismic Retrofit Program." In *Water Resources Engineering '98* (Proceedings of the International Water Resources Engineering Conference held in Memphis, Tennessee, August 3-7, 1998.) Steven R. Abt, Jayne Young-Pezeshk, and Chester C. Watson (editors), ASCE, Reston, VA, (1998).

15. Brunner, G.W., "Using HEC-RAS to Compute Scour at Bridges." In *Stream Stability and Scour at Highway Bridges* (Compendium of papers presented at conferences sponsored by the Water Resources Engineering (Hydraulics) Divsion of ASCE) E.V. Richardson and P.F. Lagasse (editors), ASCE, Reston, VA, (1999).

16. Richardson, E. F., Harrison, L. J., and Davis, S. R., *Evaluating Scour at Bridges Fourth Edition.* FHWA NHI 01-001, HEC-18, Springfield, VA, (2001), pp. 378.

17. Singhofen, P.J. "Calibration and Verification of Stormwater Models." Presented at the Florida Association of Stormwater Utilities 2001 Annual Conference, (June 20-22, 2001).

18. Camp Dresser & McKee, *Evaluation of Integrated Surface Water and Groundwater Modeling Tools.* Camp Dresser & McKee Inc., Water Resources, Research & Development Program Report, (2001).

19. Maunsell McIntyre Pty Ltd. *Bluewater Creek Flood Study*. Thuringowa City Council Report. Thuringowa, Australia, (2001).

20. Philip Williams & Associates, Ltd. *Napa-Sonoma Marsh Restoration Feasibility Study, Napa and Solano Counties, California, Hydrodynamic Modeling Analyses of Existing Conditions – Phase 1.* PWA Technical Report, PWA Ref. # 1174 – 8, (2002).

21. Juza, B., and Barad, M.F. "Dynamic and Steady State Modeling Approaches to Riverine Hydraulic Studies Using 1-D, Looped 1-D, and 2-Dimensional Topological Discretizations." In Proceedings of Hydroinformatics 2000, Iowa City, Iowa (2000).

22. Donnell, Barbara P., Letter, Joseph V., and McAnally, W. H., *User's Guide for RMA2 Version 4.5*. US Army, Engineer Research and Development Center, Waterways Experiment Station, Coastal and Hydraulics Laboratory, Vicksburg, MS, (2001).

23. Reed, C.W., Harr, S. and Sheppard, D.M., "Sensitivity of Bridge Scour Producing Currents to Storm Surge Parameters." In *Water Resources Engineering (Proceedings of the First International Conference held in San Antonio, TX, August 14-18, 1995)* William H. Espey, Jr. and Phil G. Combs (editors), ASCE, New York, (1995).

24. Sheppard, D.M. and Pritsivelis, A., "Sensitivity of Currents and Water Evaluations in Tidal Waters to Storm Surge Parameters." In *Stream Stability and Scour at Highway Bridges.* Everett V. Richardson and Peter F. Lagasse (editors), ASCE, Reston, VA, (1999).

25. Mas, D.M.L., Miller, A.J., Smith, J.A. and Chung, W., "Analysis of Levee Design in a Mountain River Using Two-Dimensional Flow Modeling." In *Hydraulic Engineering '94* (Proceedings of the 1994 Conference held in Buffalo, New York, August 1-5, 1994), George V. Cotroneo and Ralph R. Rumer, (editors), ASCE, New York, (1994).

26. Miller, A.J., Mas, D.M.L., Smith, J.A. and Chung, W. "Boundary Conditions and Flow Patterns in a Mountain River." In *Hydraulic Engineering '94* (Proceedings of the 1994 Conference held in Buffalo, New York, August 1-5, 1994), George V. Cotroneo and Ralph R. Rumer, (editors), ASCE, New York, (1994).

27. Froehlich, D.C. (2002) *User's Manual for FESWMS Flo2DH, Two-dimensional Depth-averaged Flow and Sediment Transport Model, Release 3*. Publication No. FHWA-RD-03-053. FHWA, McLean, VA, (2002), pp. 203.

28. Curry, J. and Pinkston, L., "Hydraulic Evaluation of I-65 at the Alabama River Peninsula." In *Water Resources Engineering '98* (Proceedings of the International Water Resources Engineering Conference held in Memphis, Tennessee, August 3-7, 1998.) Steven R. Abt, Jayne Young-Pezeshk, and Chester C. Watson (editors), ASCE, Reston, VA, (1998).

29. Ports, M.A. and South, N.R., "A Practical Application of Two-Dimensional Hydraulic Analysis for the Baltimore Street Bridge Rehabilitation Project." In Water Resources Engineering (Proceedings of the First International Conference held in San Antonio, TX, August 14-18, 1995) William H. Espey, Jr. and Phil G. Combs (editors), ASCE, New York, (1995).

30. Ports, M.A., Turner, T.G., and Froehlich, D.C., "Practical Comparison of One-Dimensional and Two-Dimensional Hydraulic Analyses for Bridge Scour." In *Hydraulic Engineering '93* (Proceedings of the 1993 Conference held in San Francisco, California, July 25-30, 1993) by Hsieh Wen Shen, S. T. Su, and Feng Wen, (editors), ASCE, New York, (1993).

31. Luettich, R.A. and Westerink, J.J., *ADCIRC, A (Parallel) ADvanced CIRCulation Model for Oceanic, Coastal and Estuarine Waters.* http://www.marine.unc.edu/C_CATS/adcirc/document/users_manual_pdf_version/ADCIRC_manual.pdf, (2000).

32. Butler, H.L. and Cialone, M.A., "Technology Advancements for Estimating Storm-Induced Currents." In *Stream Stability and Scour at Highway Bridges* (Compendium of papers presented at conferences sponsored by the Water Resources Engineering (Hydraulics) Divsion of ASCE) E.V. Richardson and P.F. Lagasse (editors), ASCE, Reston, VA, (1999).

33. Edge, B.L., Vignet, S.N., and Fisher, J.S., "Determination of Bridge Scour Velocity in an Estuary." In *Stream Stability and Scour at Highway Bridges* (Compendium of papers presented at conferences sponsored by the Water Resources Engineering (Hydraulics) Divsion of ASCE) E.V. Richardson and P.F. Lagasse (editors), ASCE, Reston, VA, (1999).

34. Ocean Engineering Associates, "Hydrodynamic Model Comparison, ADCIRC vs. RMA2, FDOT Hurricane Storm Surge Modeling." Florida Department of Transportation Research Report, Tallahassee, FL, (2004).

35. McCowan, A.D. and Collins, N., "The use of Mike 21 for full two-dimensional flood impact assessment." Users Conference DHI, Horsholm, (1999).

36. Thomalla, F., Brown, J., Kelman, I., Möller, I., Spence, R., and Spencer, T., "Towards an integrated approach for coastal flood impact assessment." In *Solutions to Coastal Disasters '02* (Conference proceedings of Solutions to Coastal Disasters Conference 2002, held in San Diego, California, February 24-27, 2002). Lesley Ewing and Louise Wallendorf (editors). ASCE, Reston, VA, (2002).

37. Walton, R., Bradley, J.B. and Grindeland, T.R., "1-D or 2-D Models for River Hydraulic Studies?" In *Managing Water: Coping with Scarcity and Abundance* (Proceedings of Theme A: Water for a Changing Global Community; The 27th Congress of the International Association for Hydraulic Research, San Francisco, CA, Aug. 10-15, 1997) Marshall English and Andras Szollosi-Nagy (editors), ASCE, New York, (1997).

38. Thompson, J.C., "1-D and 2-D Analysis of Flood Plain Encroachment." In *Hydraulic Engineering*, Michael Ports (editor), ASCE (1989), pp. 911-916.

39. Buechter, M.T., "Something Here Doesn't Smell Right: Two-Dimensional Floodplain Study of Onion Creek." In *Bridging the Gap: Meeting the World's Water and Environmental Resources Challenges* (State of the Practice—Proceedings of the World Water and Environmental Resources Congress, May 20-24, 2001, Orlando, Florida) Don Phelps and Gerald Shelke (editors), ASCE, Reston, VA, (2001).

40. Jia, Y. and Alonso, C.V., "One- and Two-Dimensional Analysis of Flow in Hotophia Creek, MS." In *Hydraulic Engineering '94.* (Proceedings of the 1994 Conference held in Buffalo, New York, August 1-5, 1994) George V. Cotroneo and Ralph R. Rumer (editors), ASCE, New York, (1994).

41. Ming, C. O., Colson, B. E., and Arcement, George J. (1979) *Hydrologic Atlas, Backwater at bridges and densely wooded flood plains, Buckhorn Creek near Shiloh, Alabama*. USGS Report #607, M(200) Hy no.607.

42. Lagasse, P.F., Zevenbergen, L.W., Schall, J.D., and Clopper, P.E., *Bridge Scour and Stream Instability Countermeasures, Experience, Selection and Design Guidance, Second Edition*. FHWA NHI 01-003, HEC-23. Springfield, VA, (2001), pp. 398.

43. Schneider, V. R., Board, J. W., Colson, B. E., Lee, F. N., and Druffel, L., *Computation of Backwater and Discharge at Width Constrictions of Heavily Vegetated Flood Plains.* U.S. Geological Survey Water Resources Inv. 76-129, Springfield, Virginia, (1976).

APPENDIX A

SENSITIVITY TEST MODEL RESULTS AND COMPARISONS

This Appendix contains the results from the sensitivity tests for the one- and two-dimensional models. The results are presented organized by sensitivity test and then by large channel and small channel results. The contour plots of the one-dimensional models were generated by creating scatter sets of the HEC-RAS solution files and importing them into SMS (Surfacewater Modeling System). The comparison plots contained herein were generated by interpolating the FESWMS model results onto the HEC-RAS scatter set points and then performing the differencing. Obviously, the FESWMS models contain more resolution of the flow field. However, the difference and percentage difference contours illustrate only the differences between the models at locations resolved by both models.

Each section in this appendix contains all simulations associated with a particular sensitivity study. The plots in each section illustrate the following:

- Water surface elevation solution for the HEC-RAS model
- Velocity magnitude for the HEC-RAS model
- Water surface elevation for the FESWMS model
- Velocity magnitude and velocity vectors for the FESWMS model
- Water surface elevation difference between the two models (FESWMS – HEC-RAS)
- Velocity magnitude difference between the two models (FESWMS – HEC-RAS)
- Velocity magnitude percentage change between the two models (100%*(FESWMS – HEC-RAS)/FESWMS)

Notably, the velocity vectors are not displayed for the HEC-RAS model. Velocity directions for these models are assumed perpendicular to the HEC-RAS cross sections.

The sensitivity test results are listed in this appendix in the following order:

Baseline Models

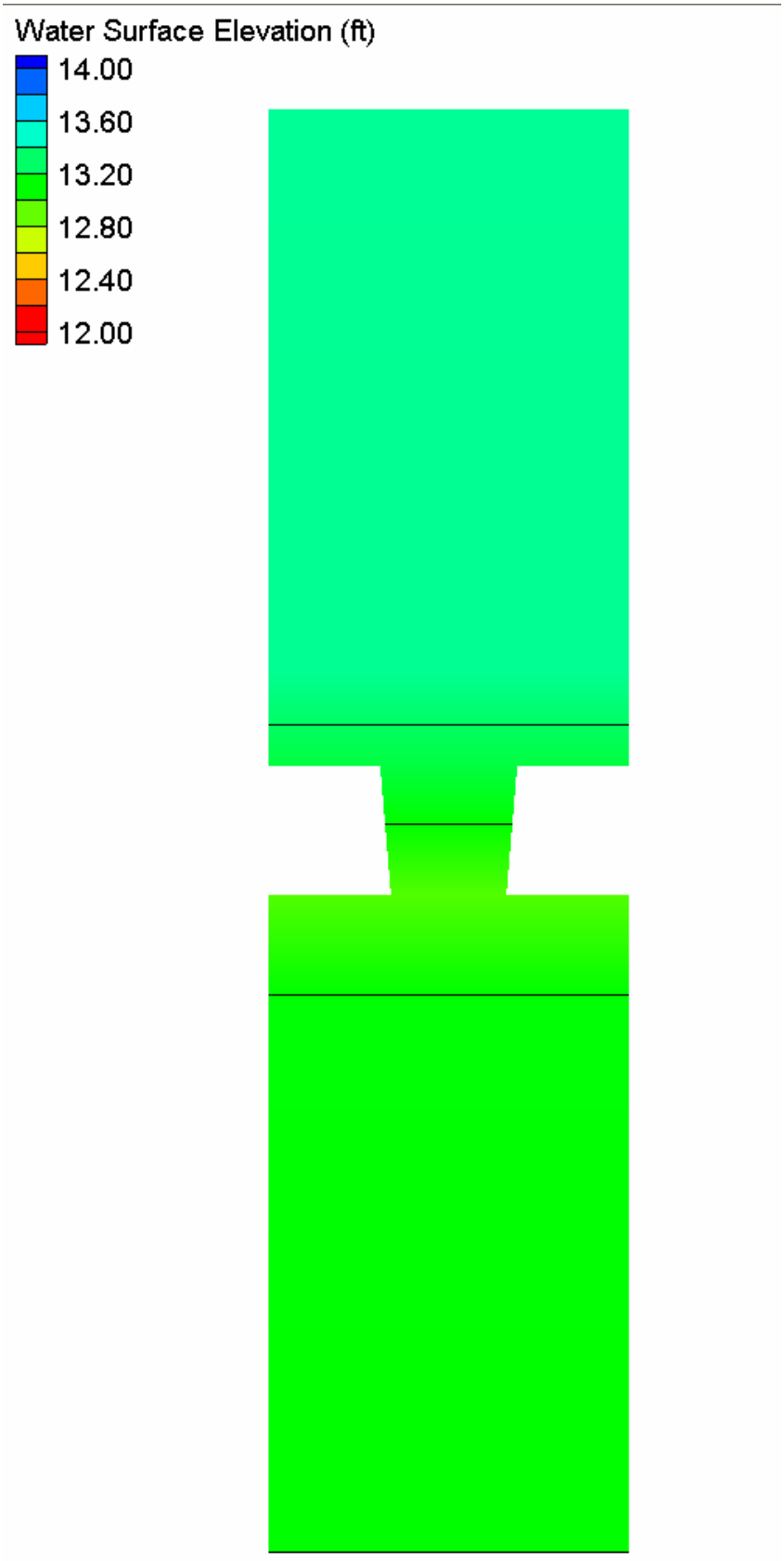

HEC-RAS Water Surface Elevation Contours – Small Channel – Baseline

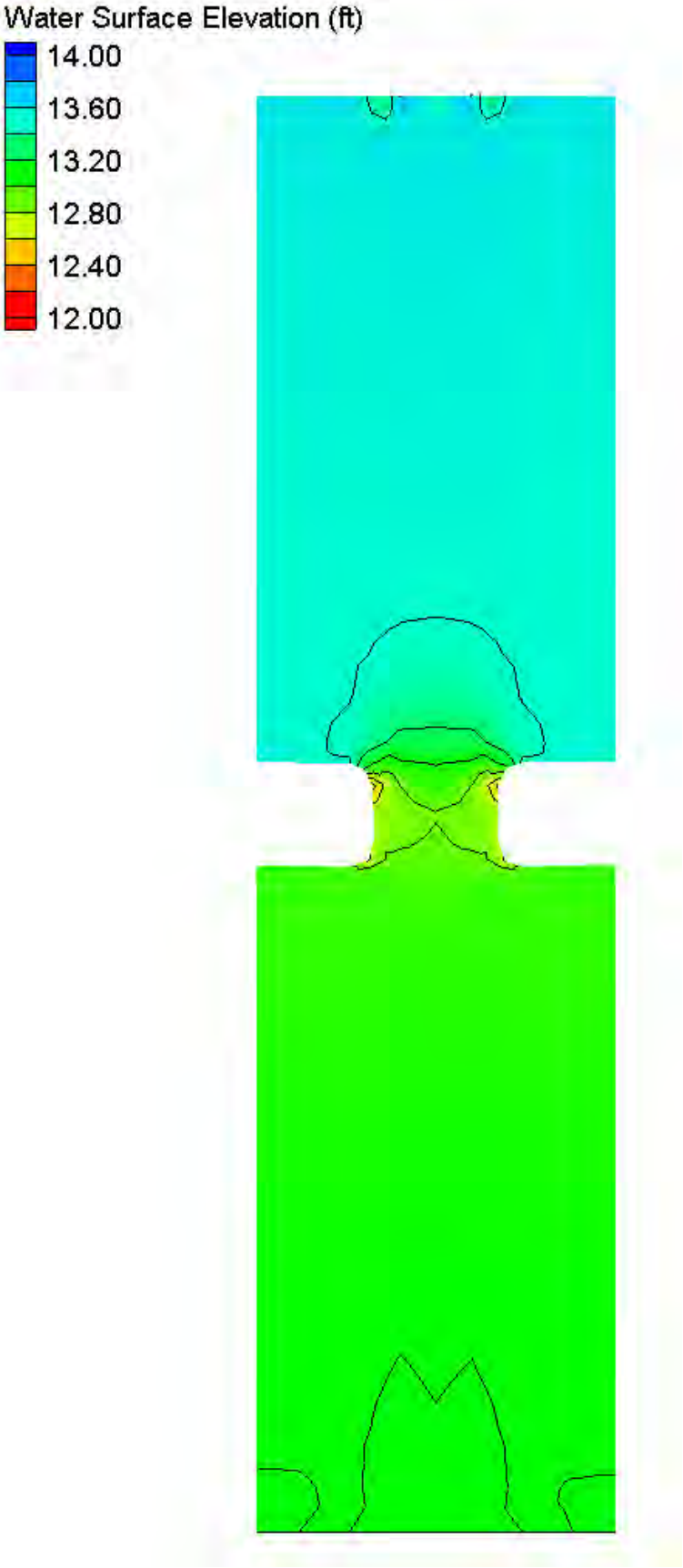

FESWMS Water Surface Elevation Contours – Small Channel – Baseline

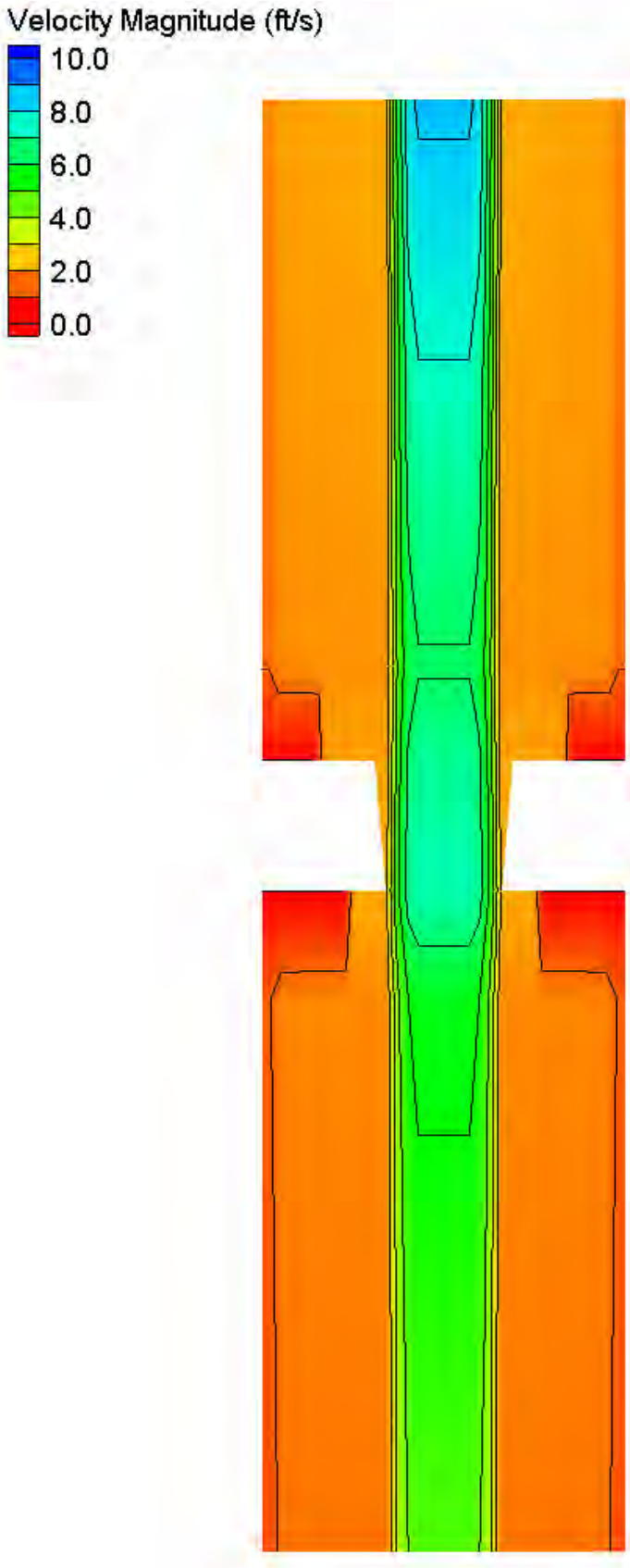

HEC-RAS Velocity Magnitude Contours – Small Channel – Baseline

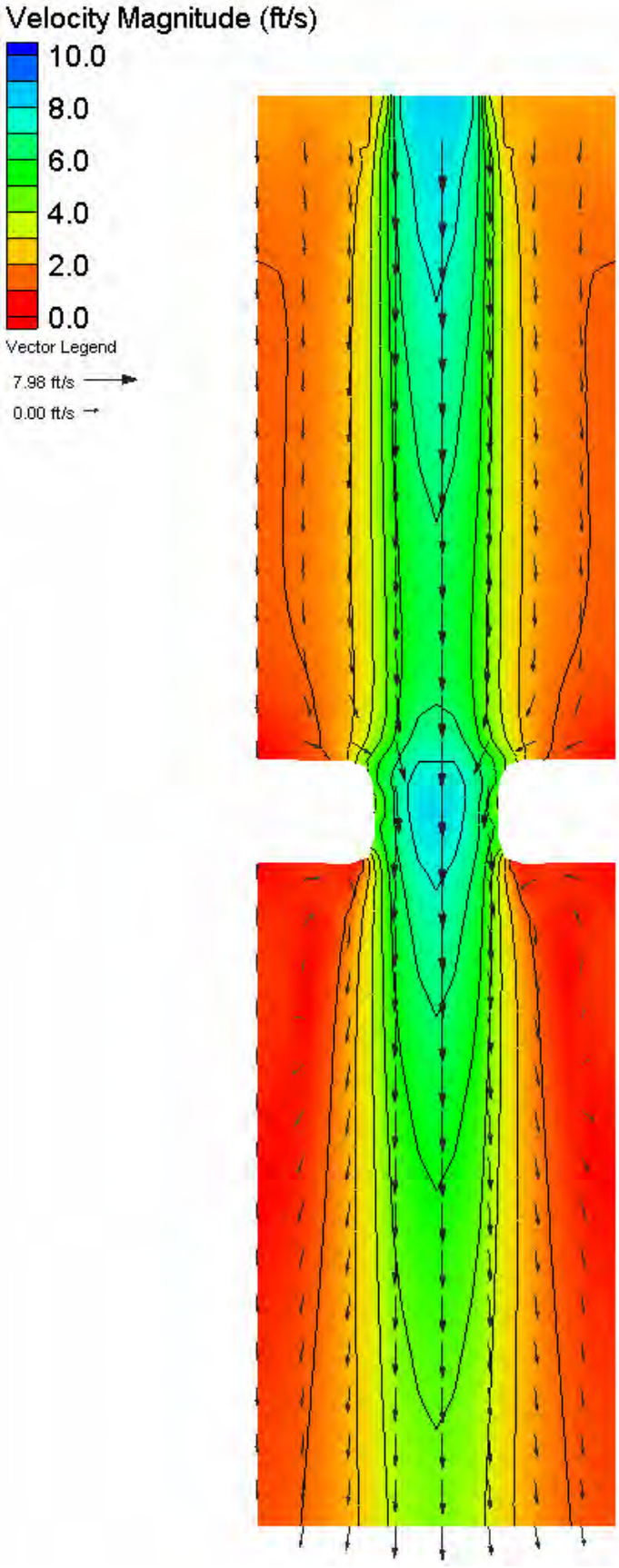

FESWMS Velocity Magnitude Contours – Small Channel – Baseline

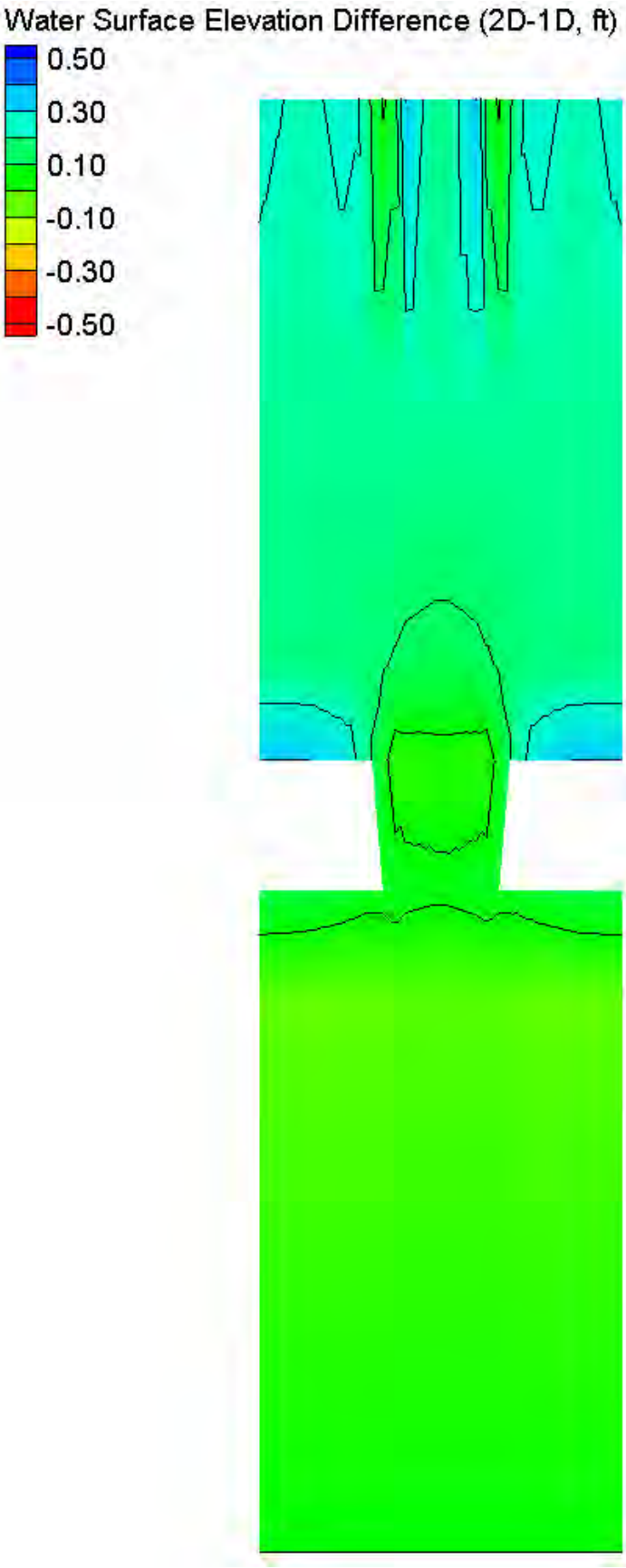

Water Surface Elevation Difference Contours – Small Channel – Baseline

Velocity Magnitude Difference Contours – Small Channel – Baseline

Velocity Magnitude Percent Difference Contours – Small Channel – Baseline

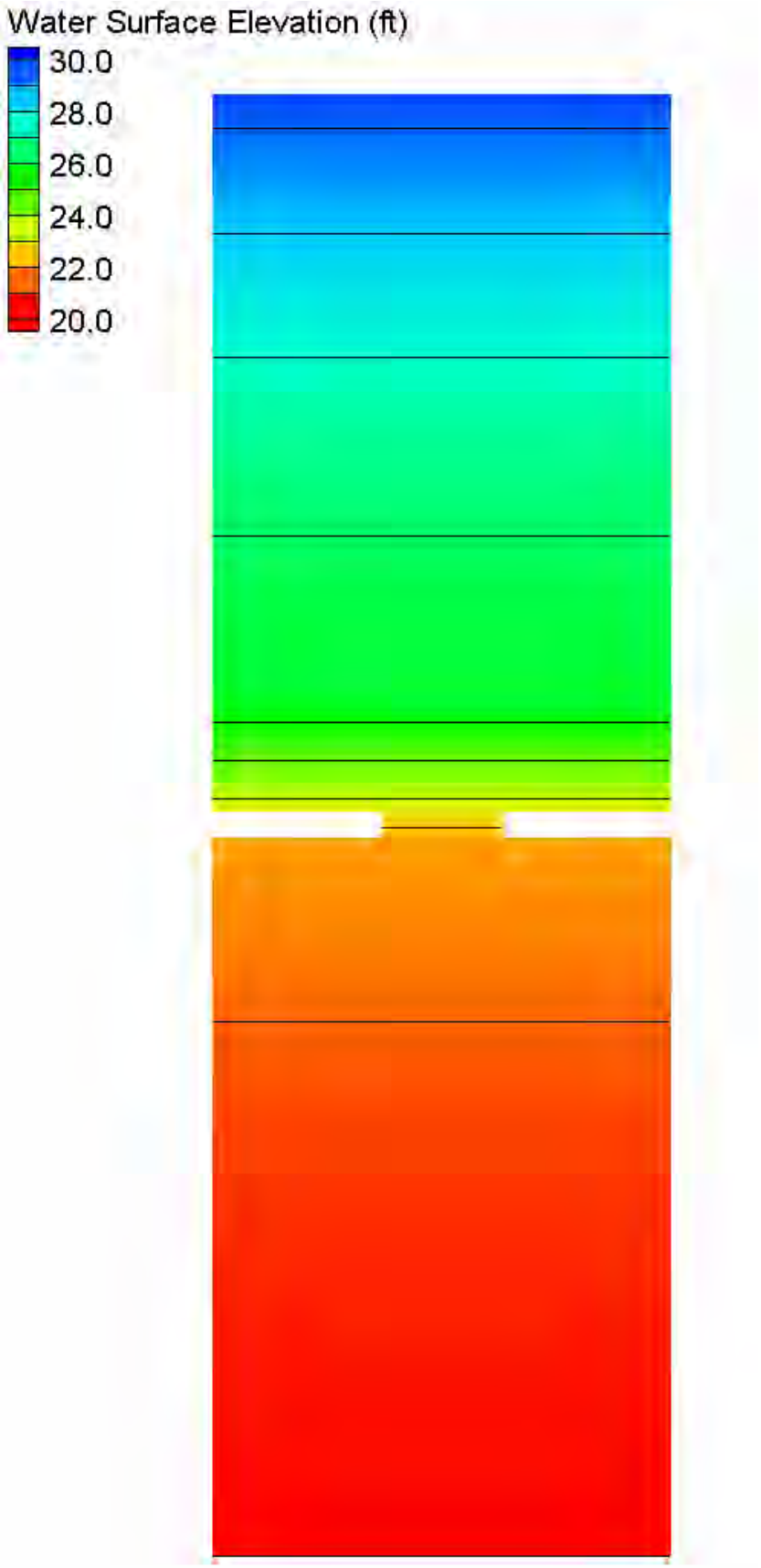

HEC-RAS Water Surface Elevation Contours – Large Channel – Baseline

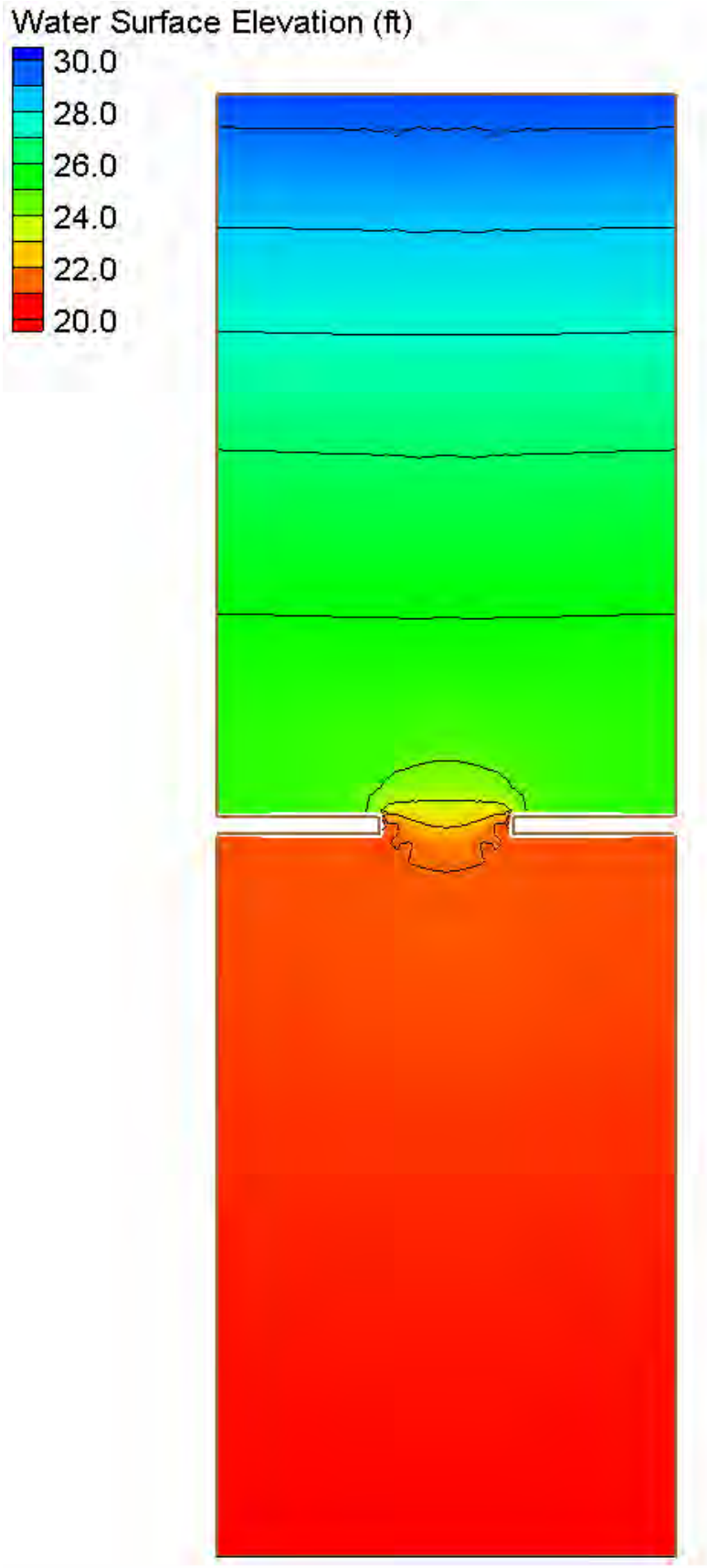

FESWMS Water Surface Elevation Contours – Large Channel – Baseline

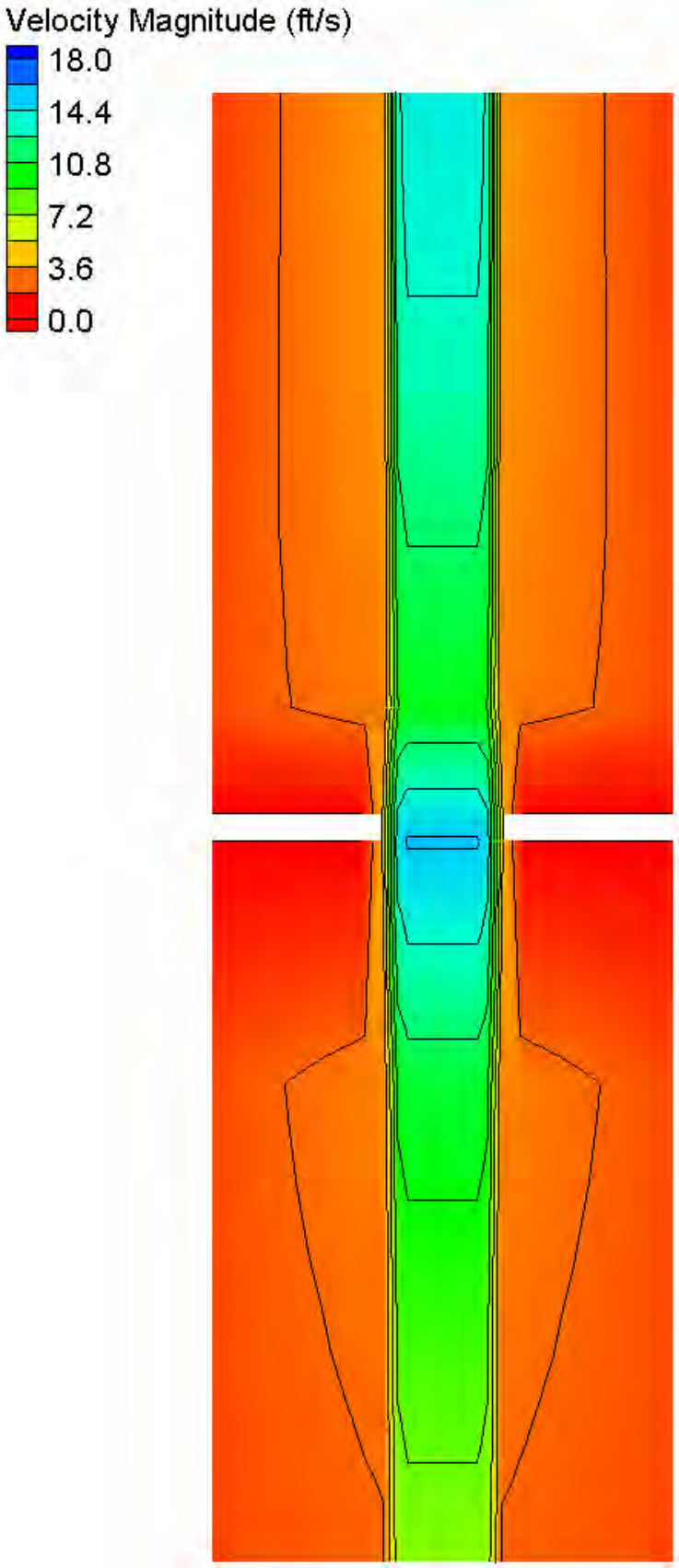

HEC-RAS Velocity Magnitude Contours – Large Channel – Baseline

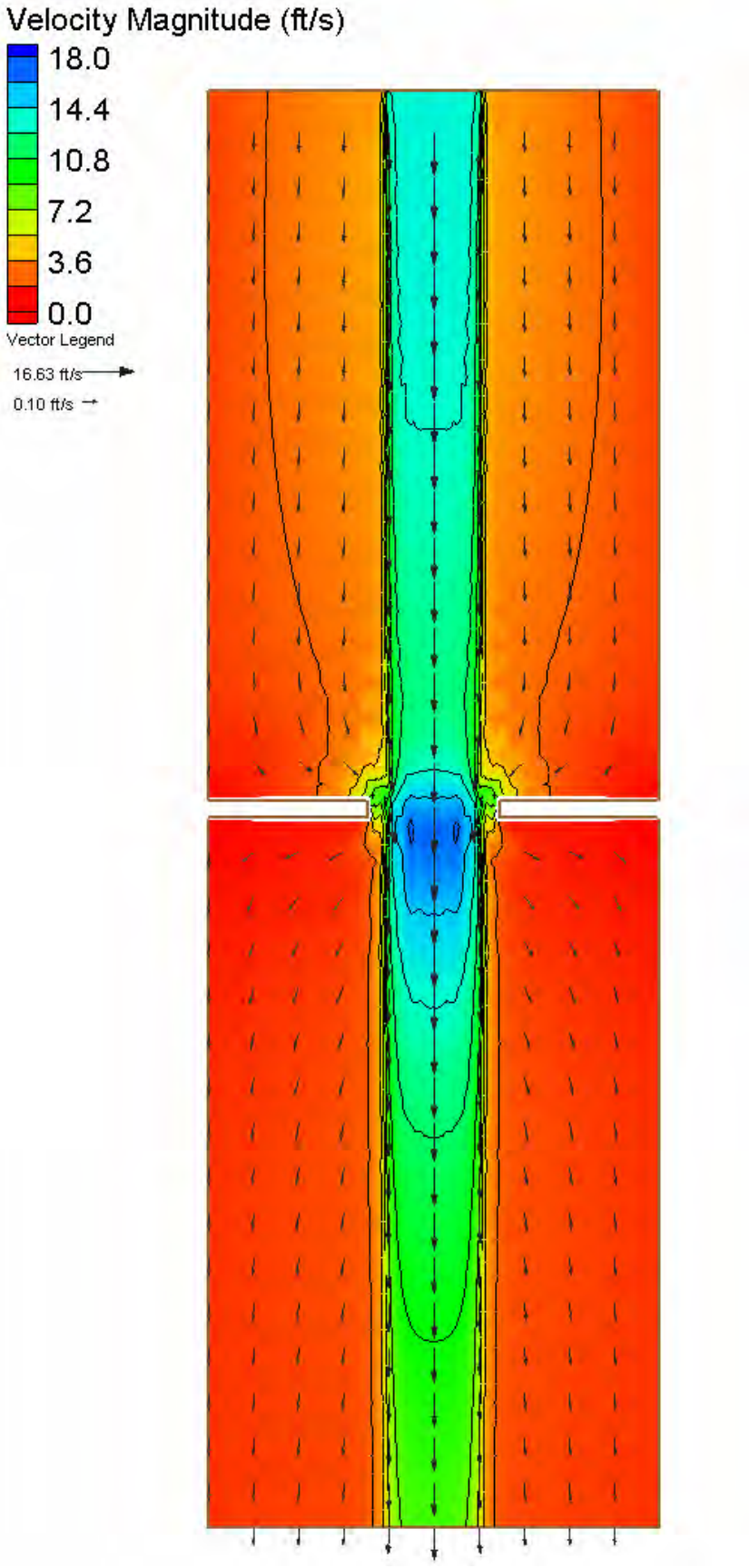

FESWMS Velocity Magnitude Contours – Large Channel – Baseline

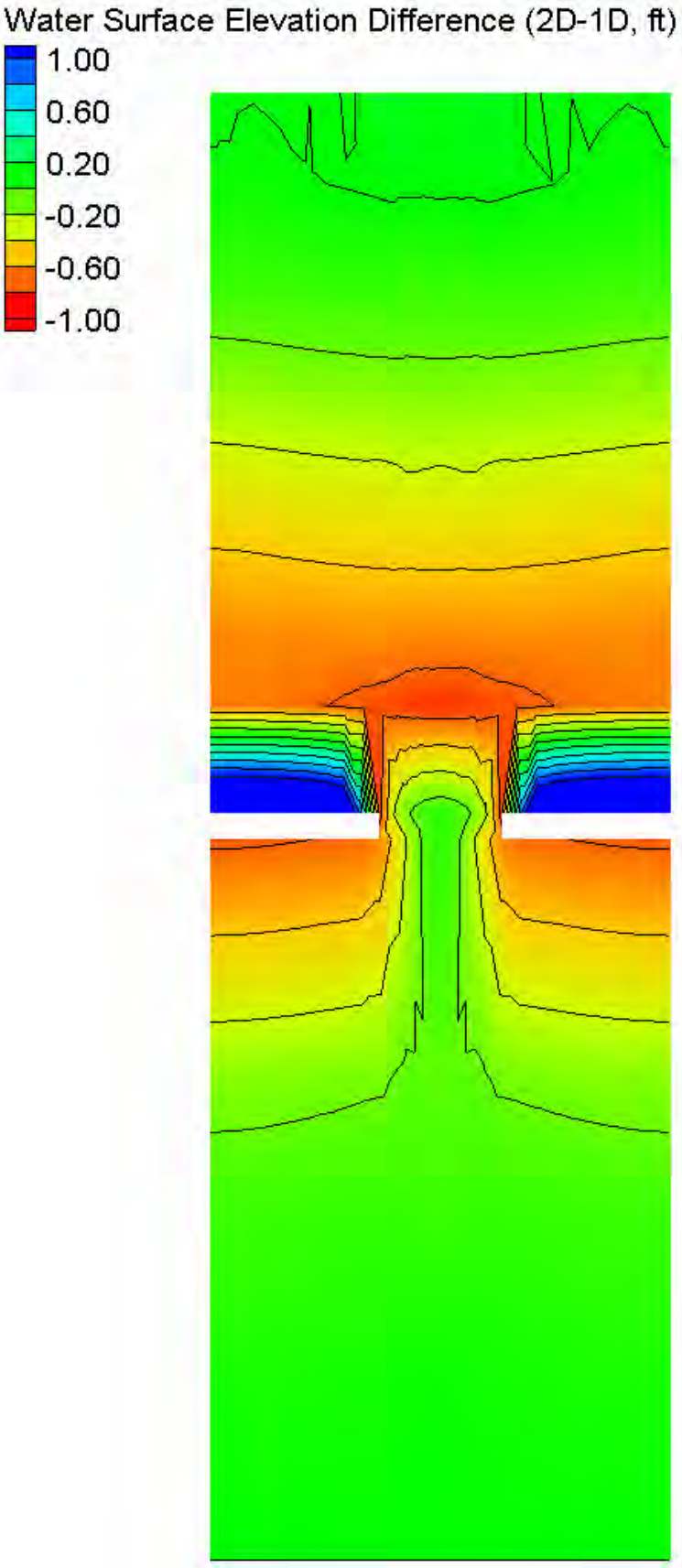

Water Surface Elevation Difference Contours – Large Channel – Baseline

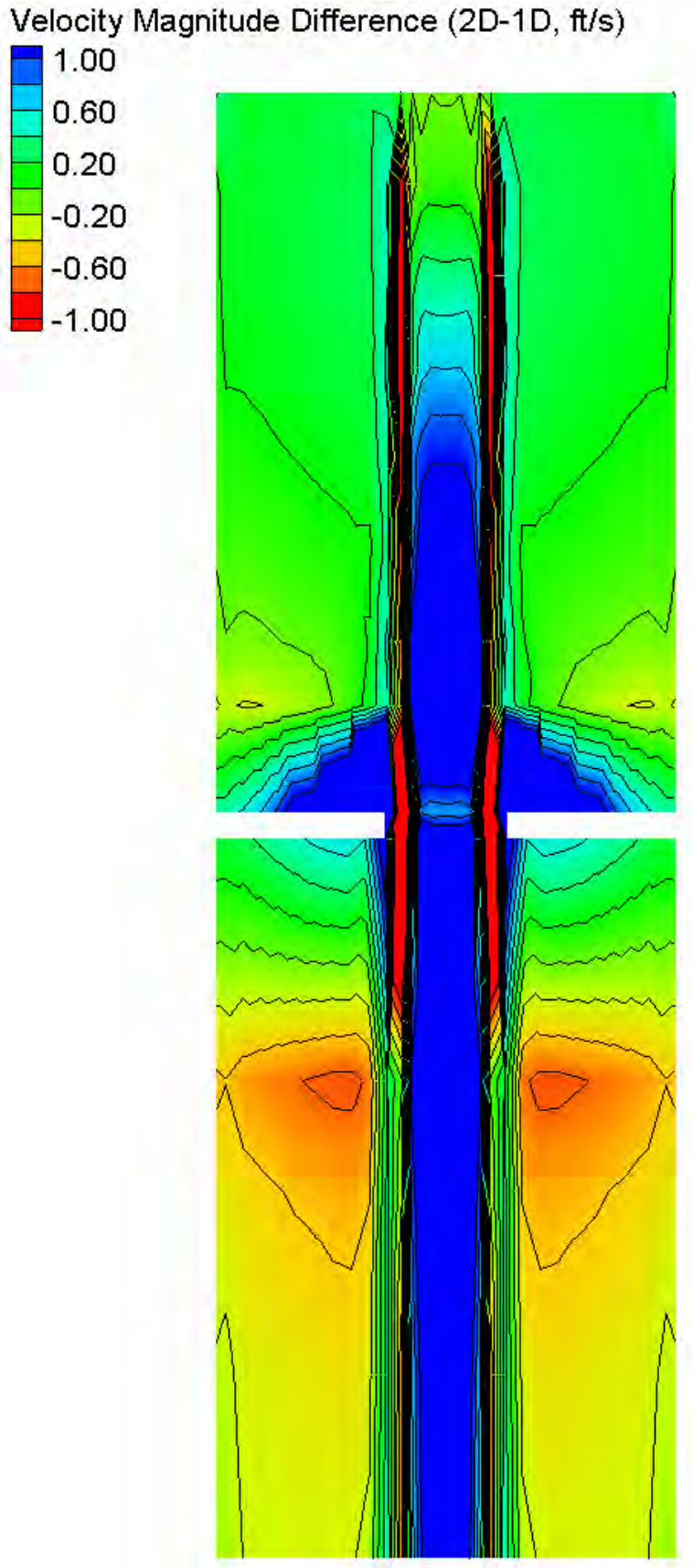

Velocity Magnitude Difference Contours – Large Channel – Baseline

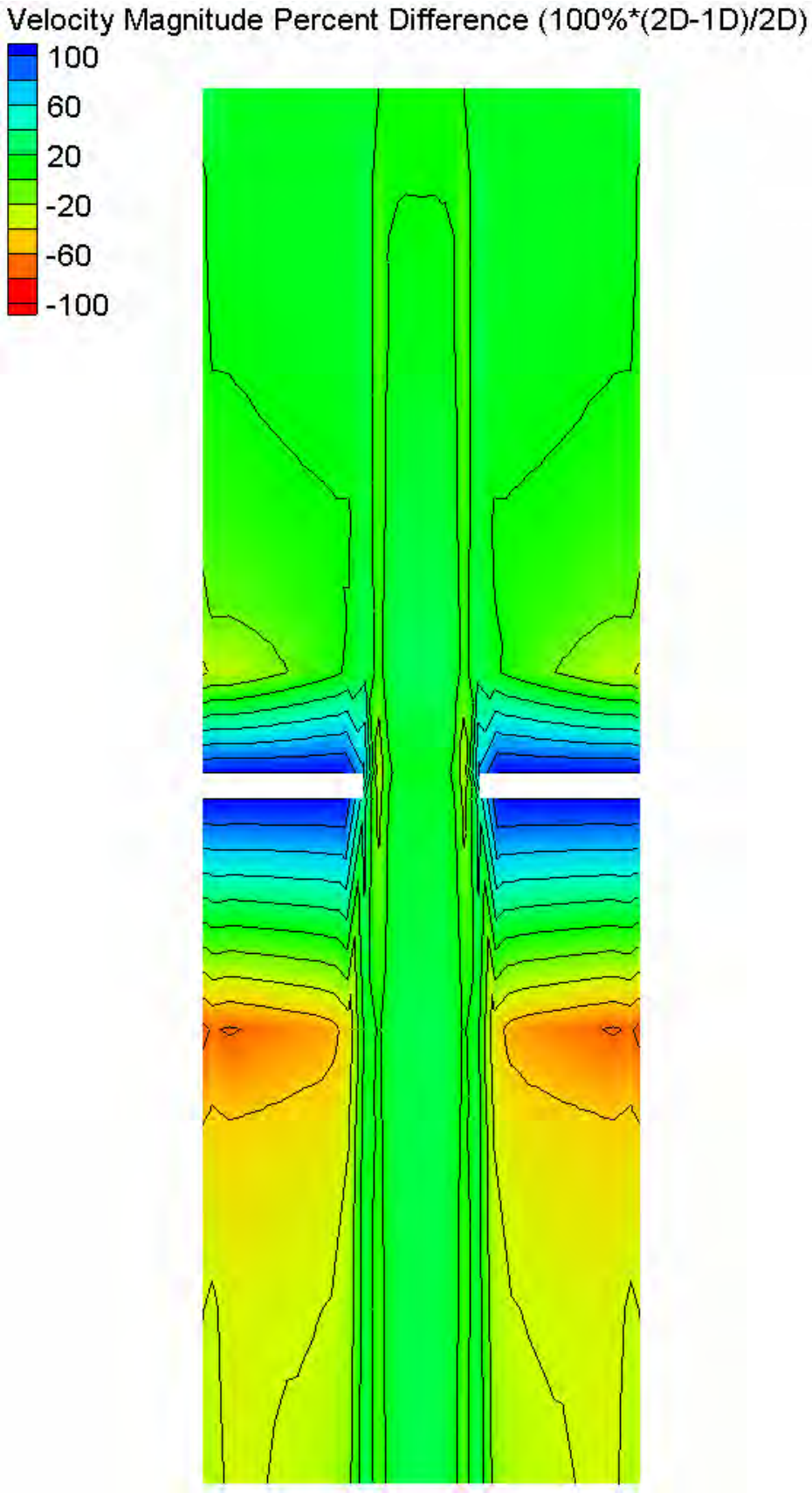

Velocity Magnitude Percent Difference Contours – Large Channel – Baseline

Multiple Openings

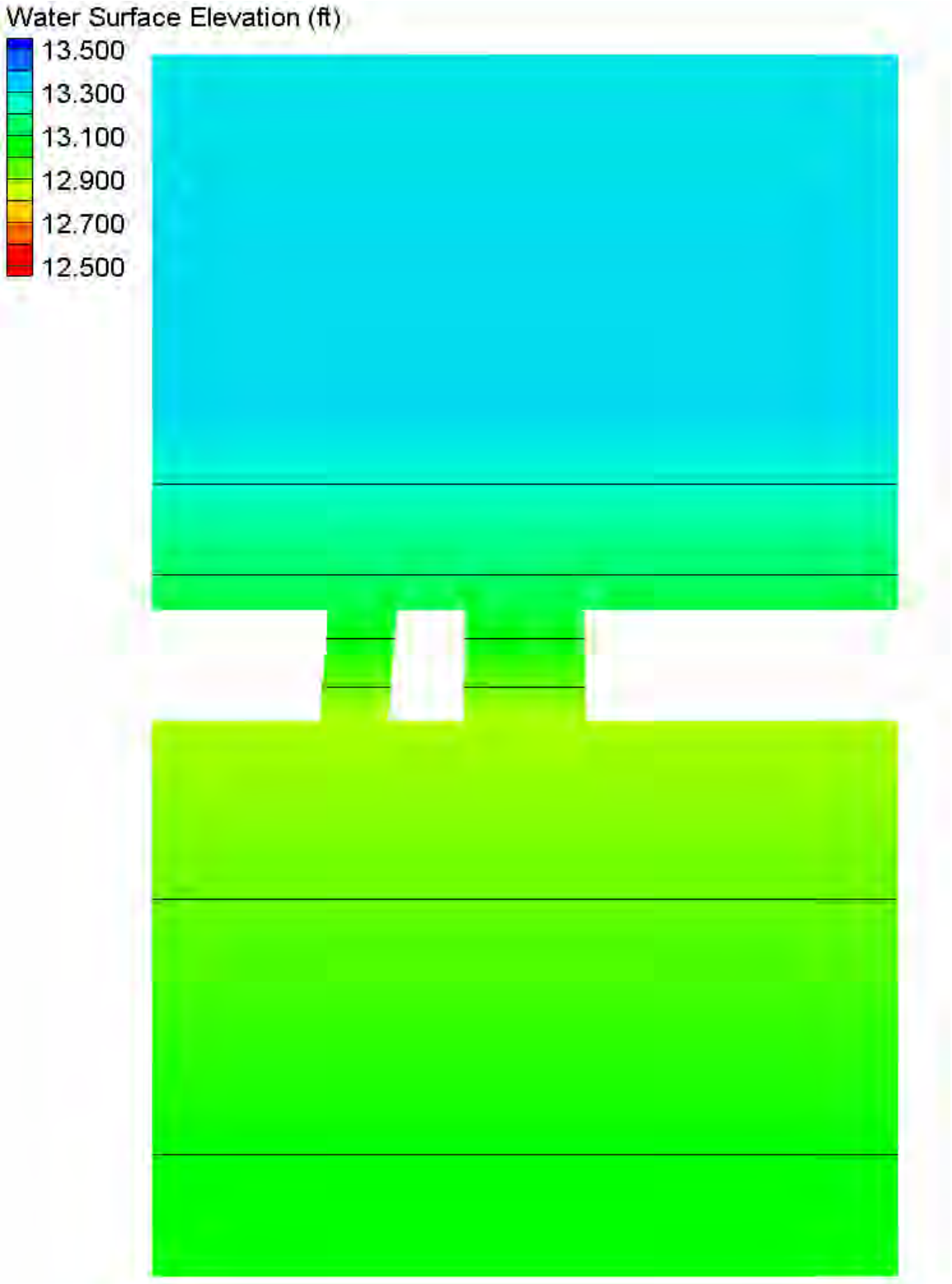

HECRAS Water Surface Elevation Contours – Small Channel – Multiple Openings (2)

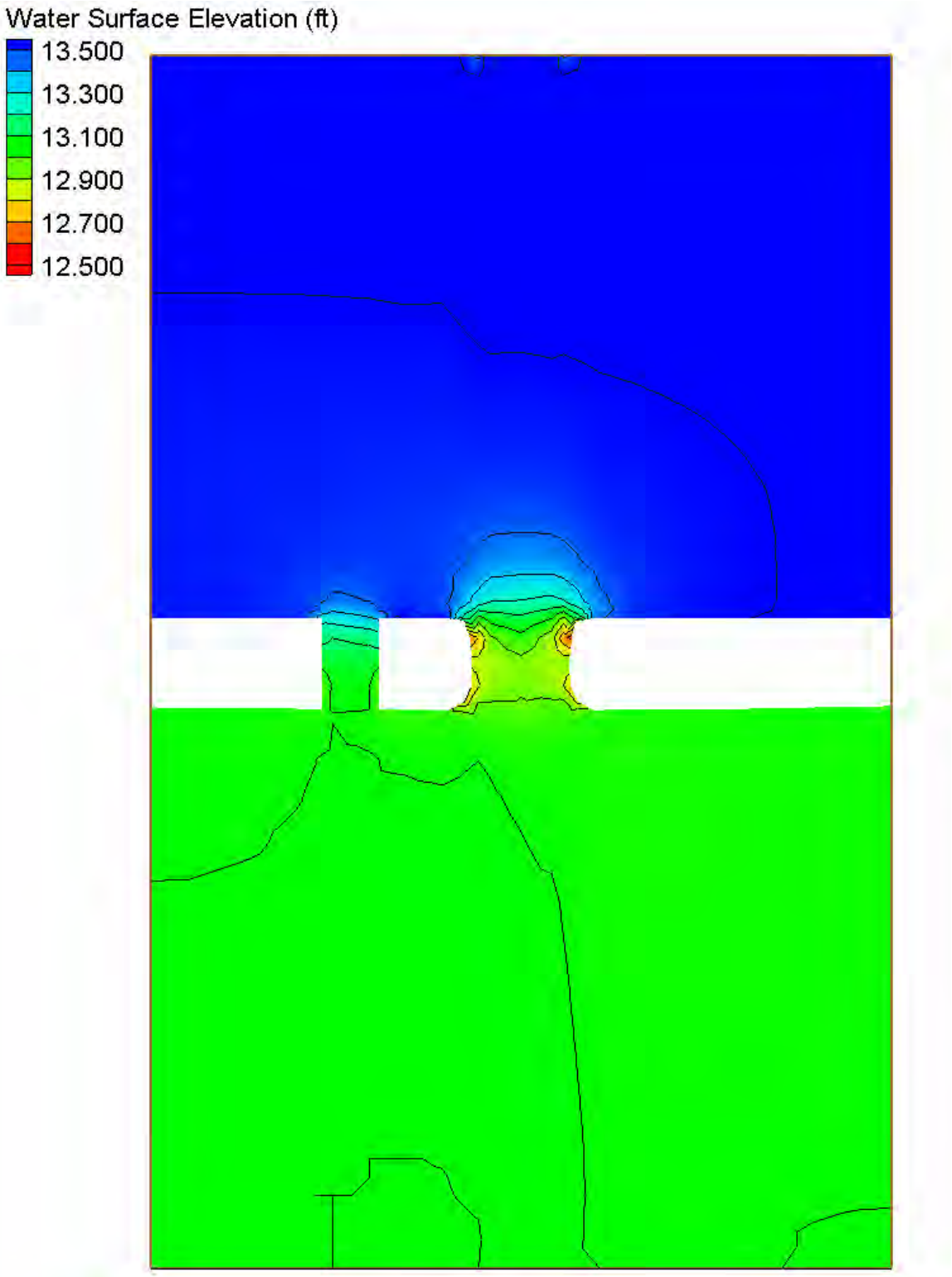

FESWMS Water Surface Elevation Contours – Small Channel – Multiple Openings (2)

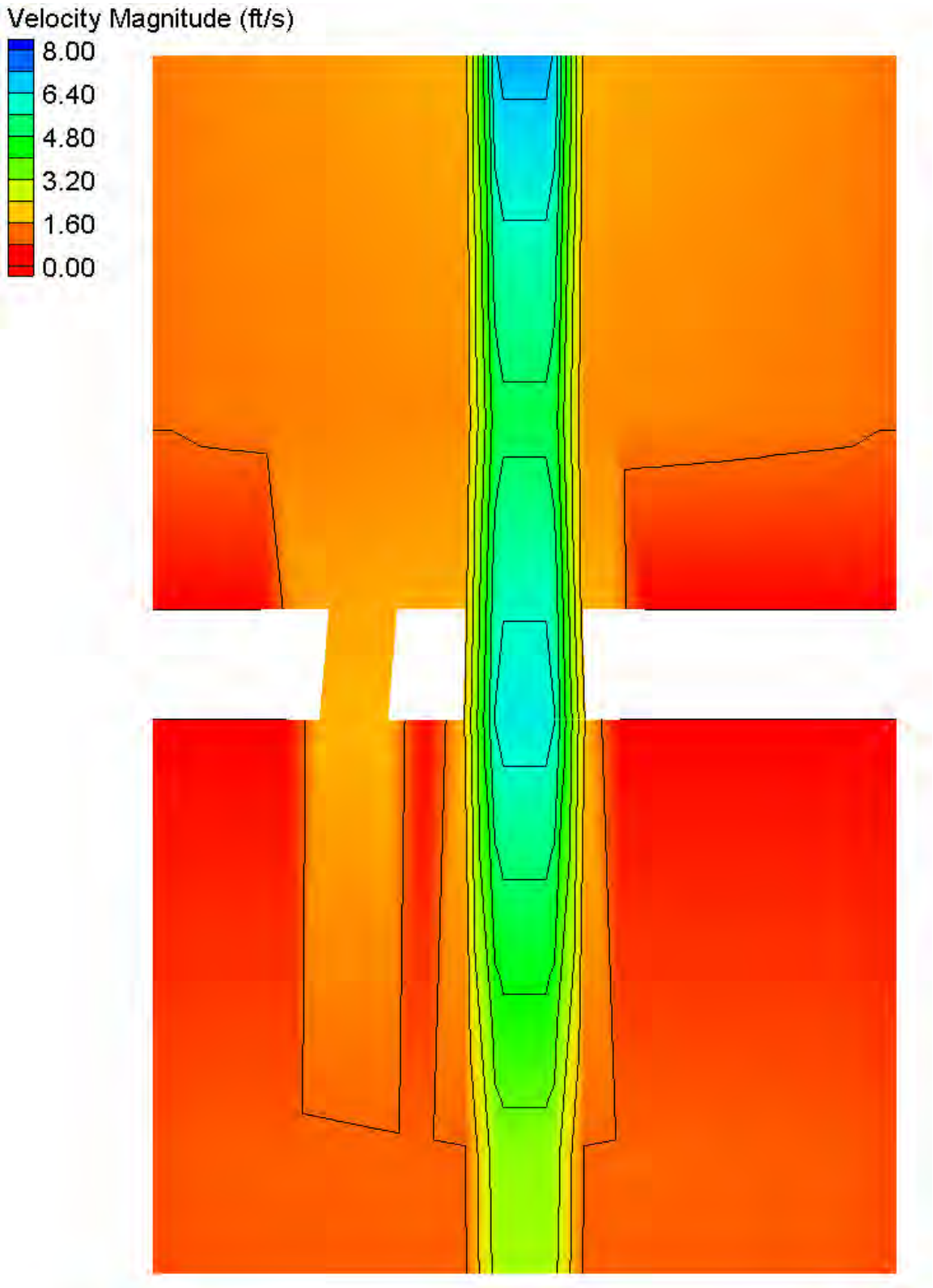

HEC-RAS Velocity Magnitude Contours – Small Channel – Multiple Openings (2)

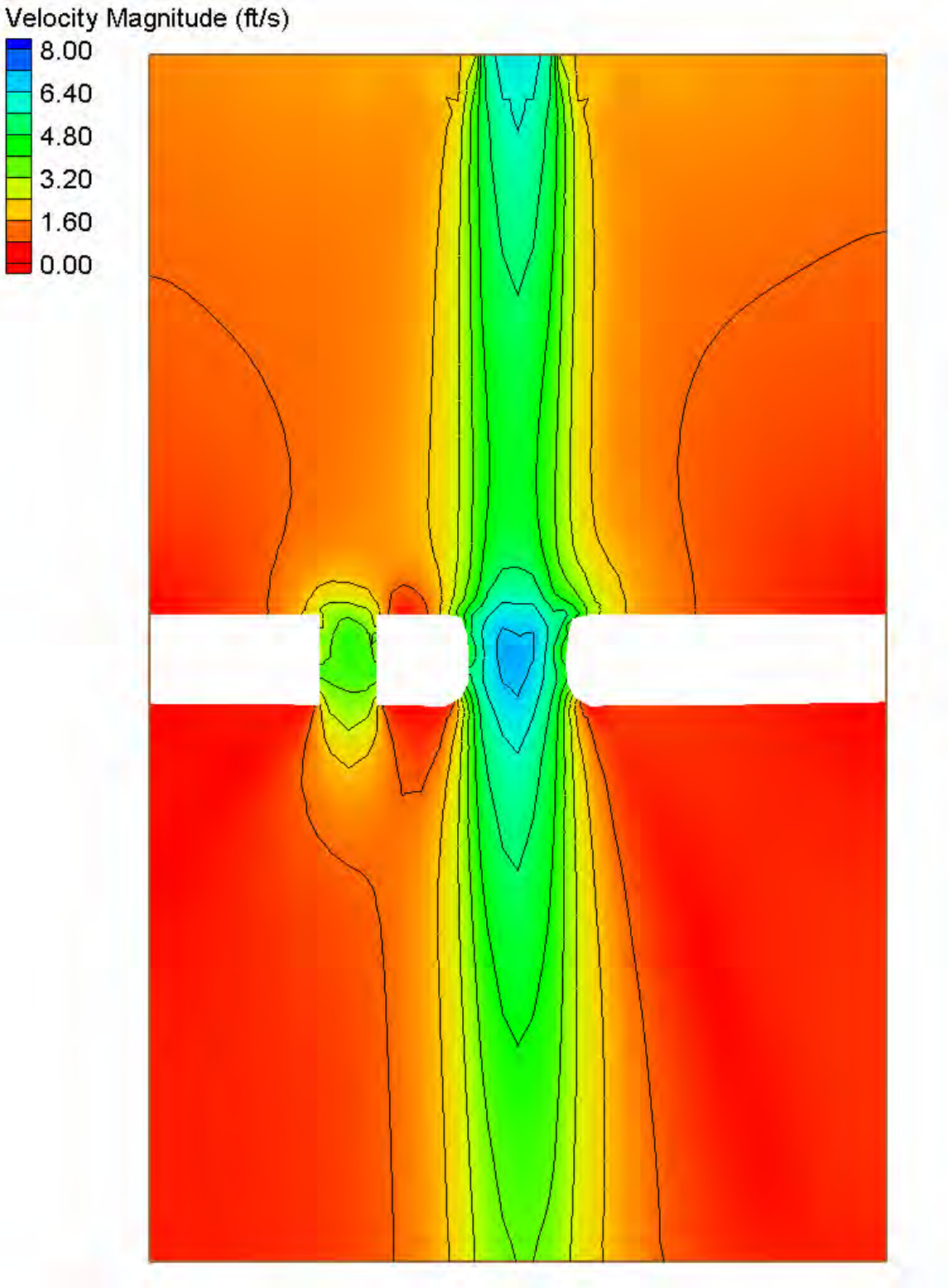

FESWMS Velocity Magnitude Contours – Small Channel – Multiple Openings (2)

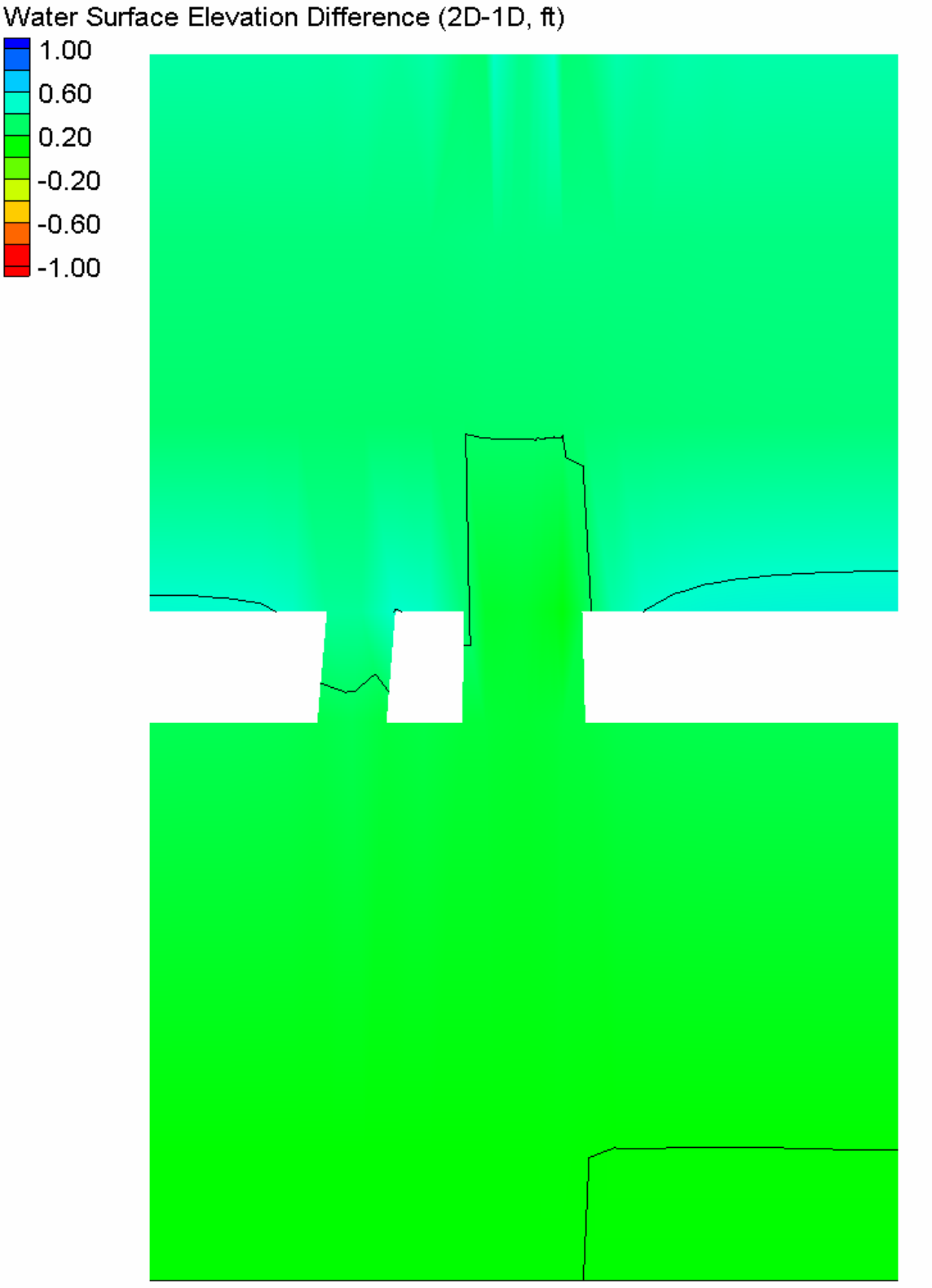

Water Surface Elevation Difference Contours – Small Channel – Multiple Openings (2)

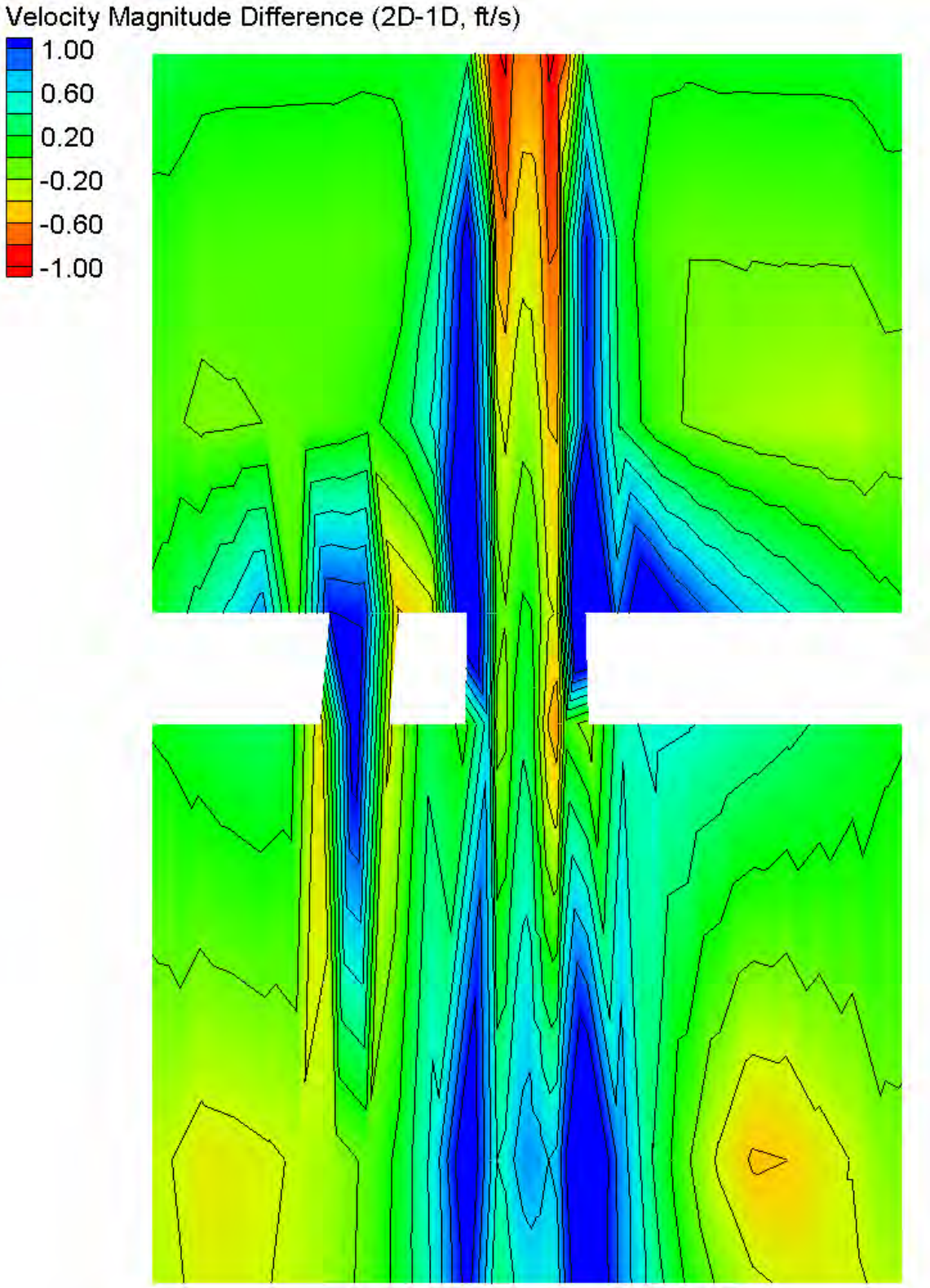

Velocity Magnitude Difference Contours – Small Channel – Multiple Openings (2)

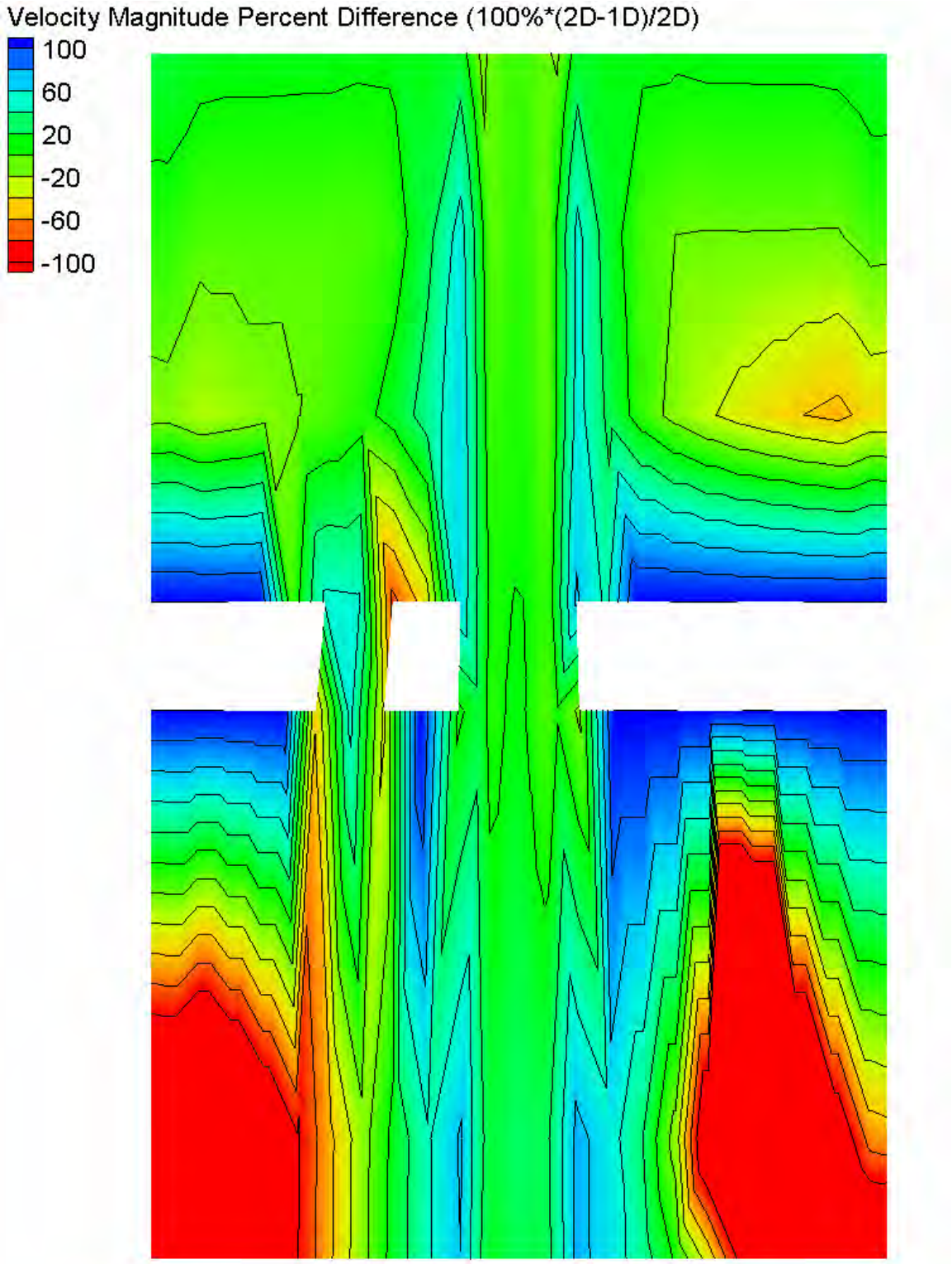

Velocity Magnitude Percent Difference Contours – Small Channel – Multiple Openings (2)

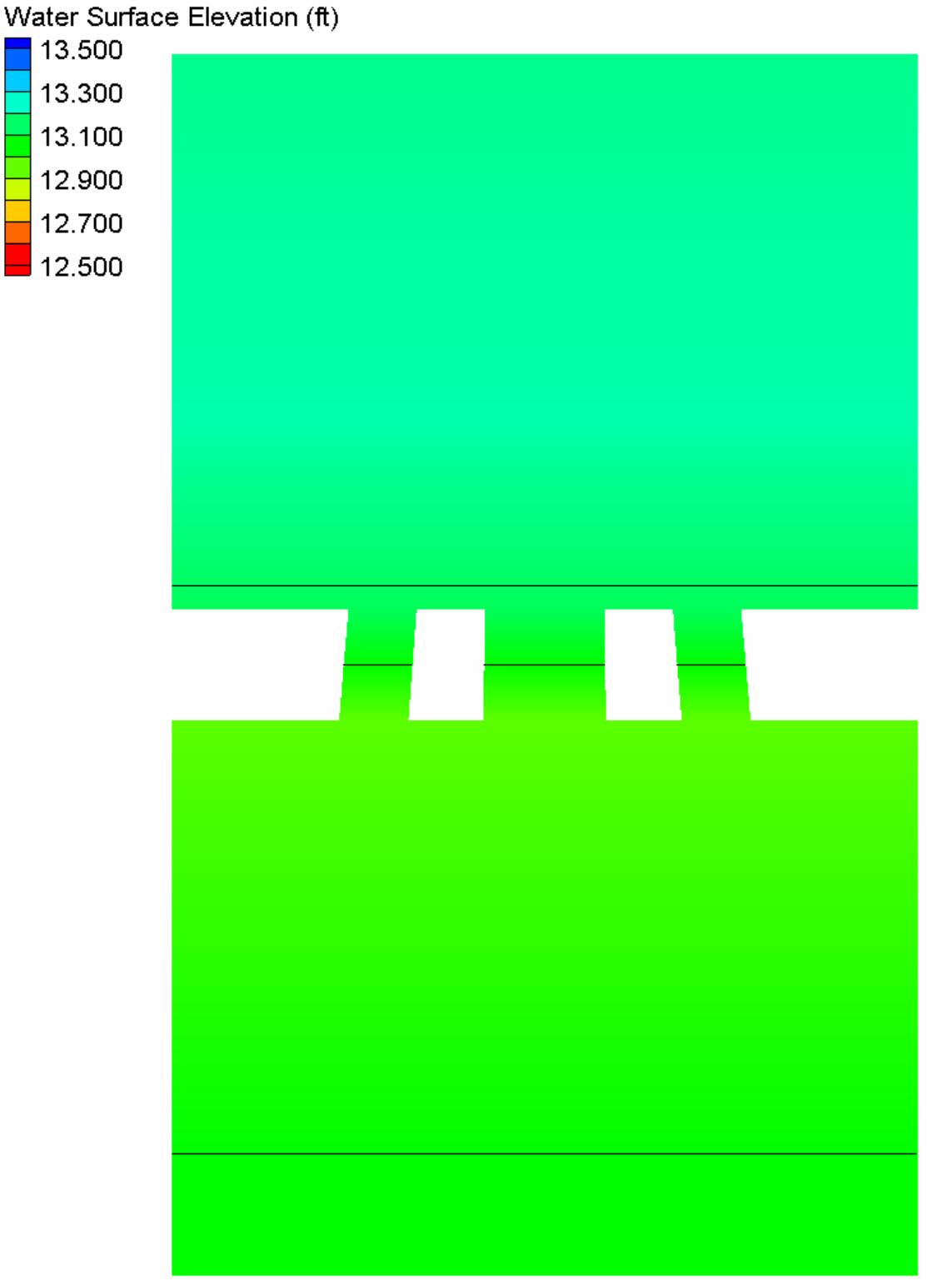

HEC-RAS Water Surface Elevation Contours – Small Channel – Multiple Openings (3)

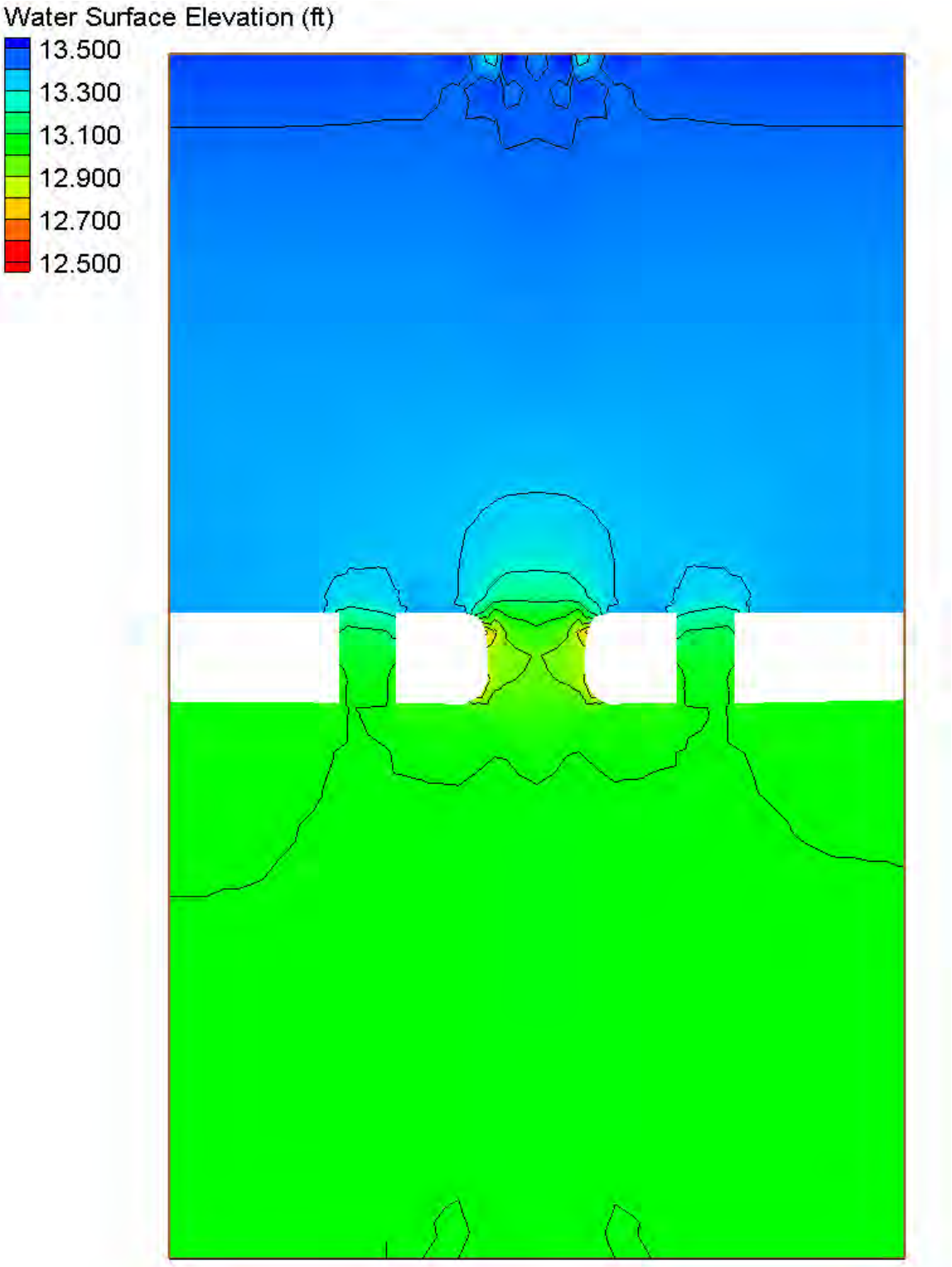

FESWMS Water Surface Elevation Contours – Small Channel – Multiple Openings (3)

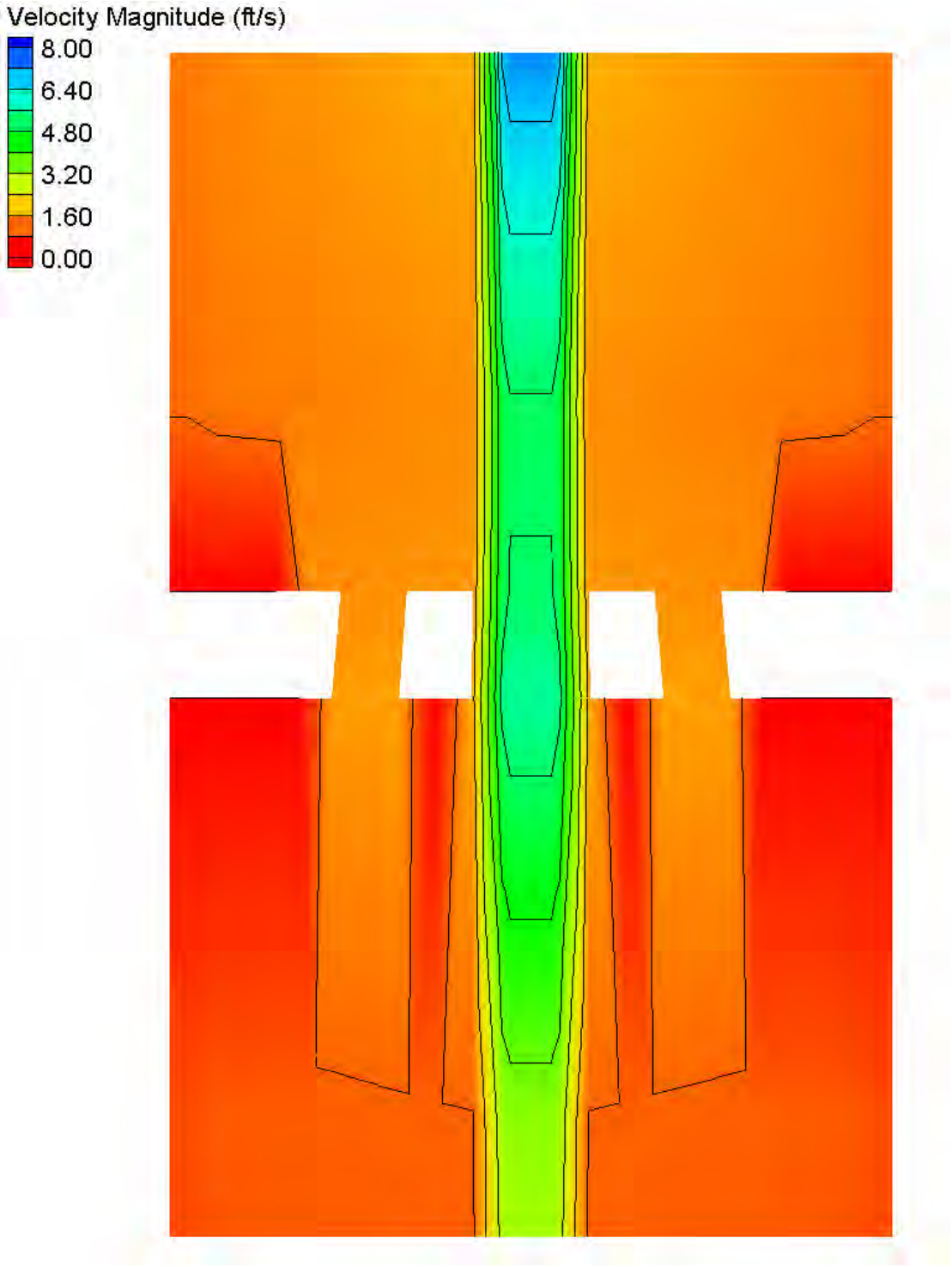

HEC-RAS Velocity Magnitude Contours – Small Channel – Multiple Openings (3)

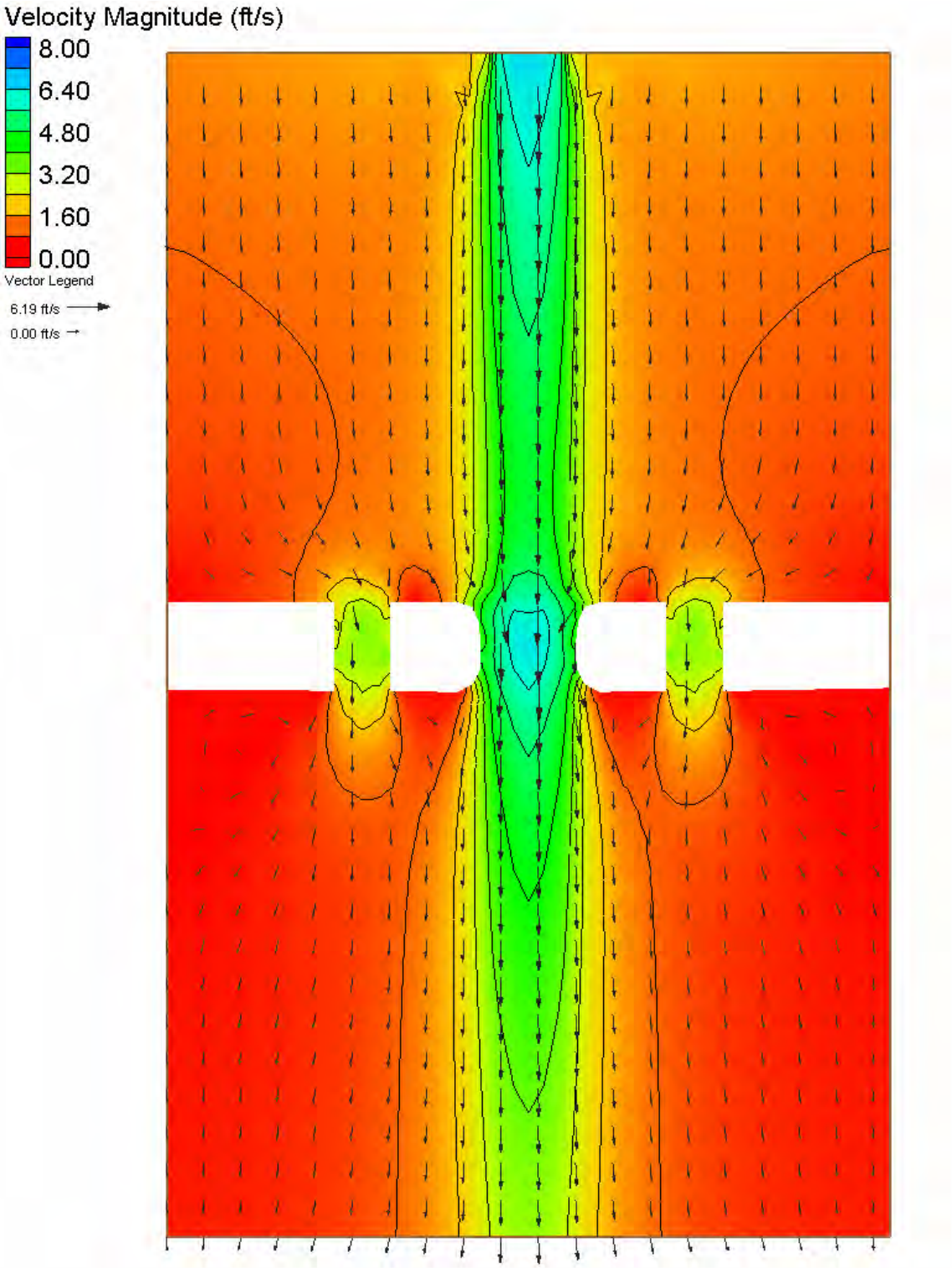

FESWMS Velocity Magnitude Contours – Small Channel – Multiple Openings (3)

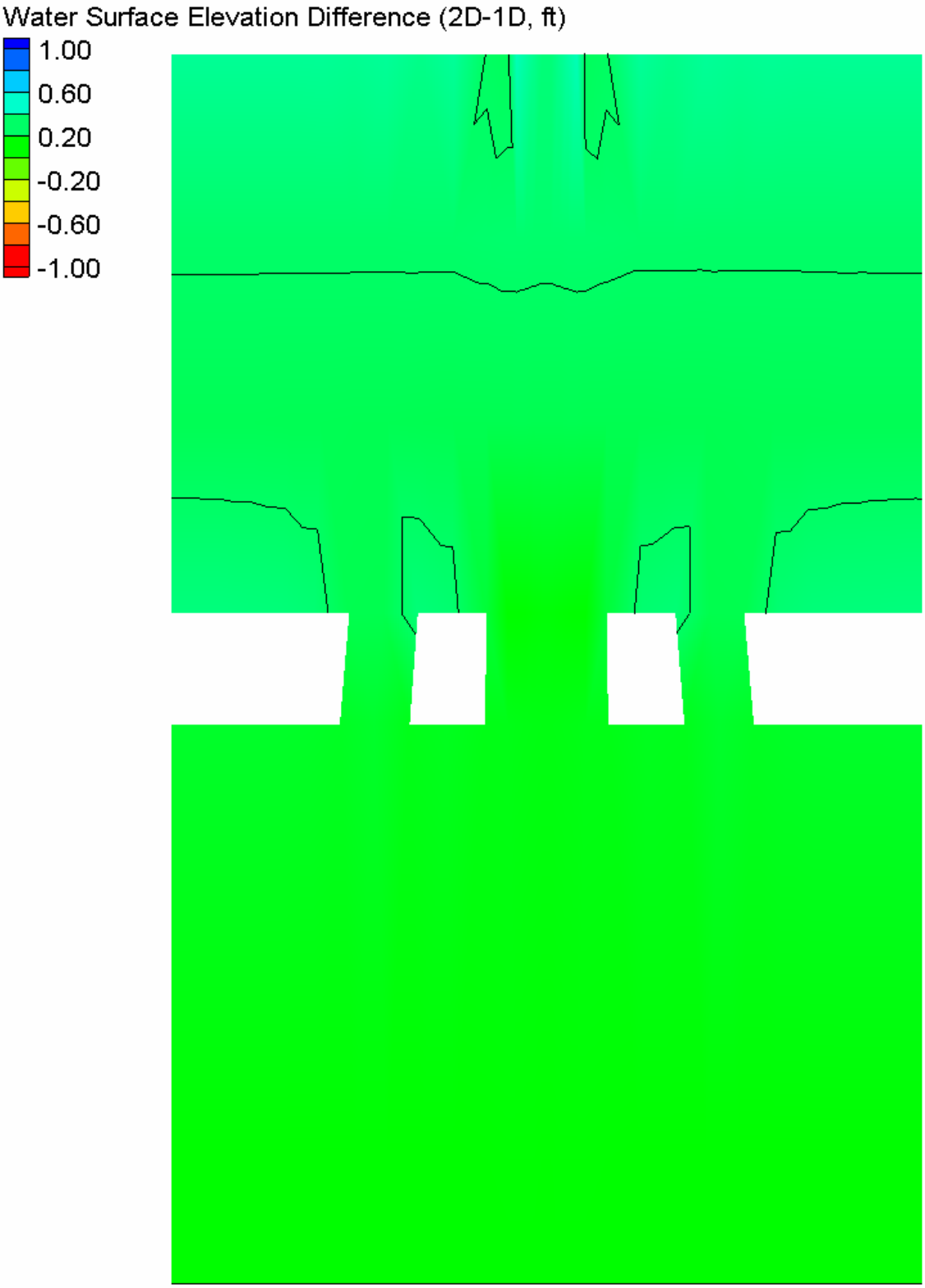

Water Surface Elevation Difference Contours – Small Channel – Multiple Openings (3)

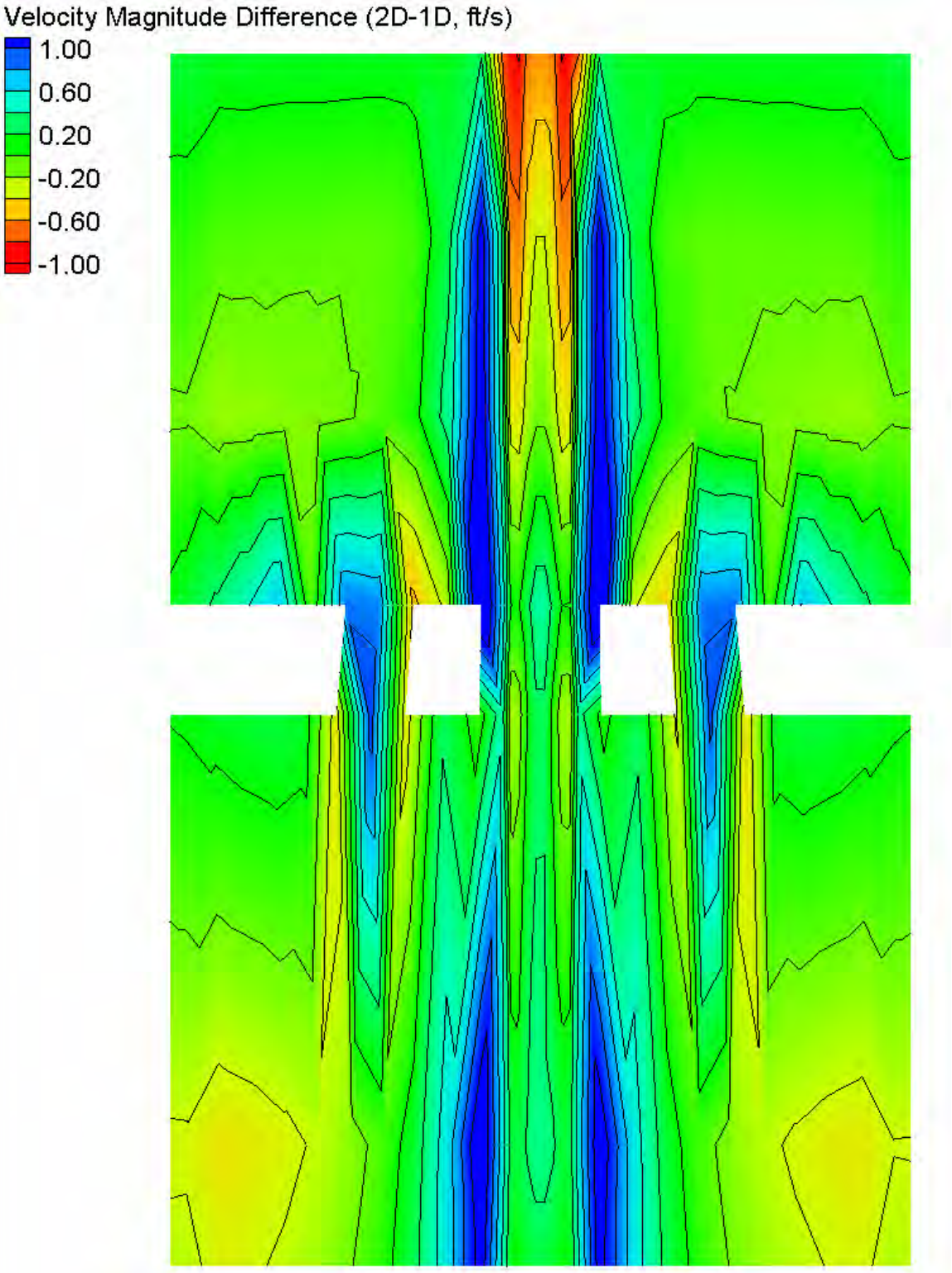

Velocity Magnitude Difference Contours – Small Channel – Multiple Openings (3)

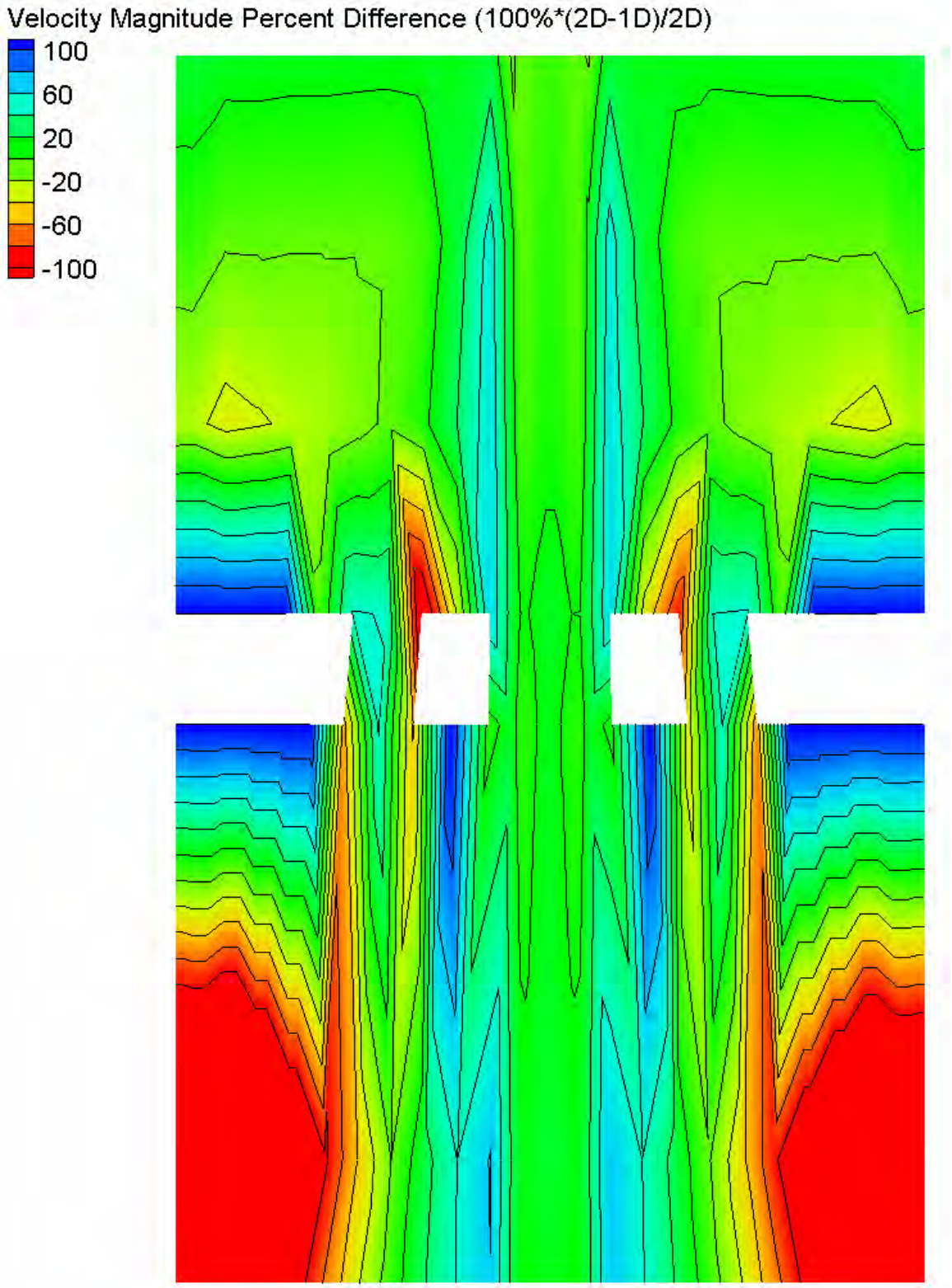

Velocity Magnitude Percent Difference Contours – Small Channel – Multiple Openings (3)

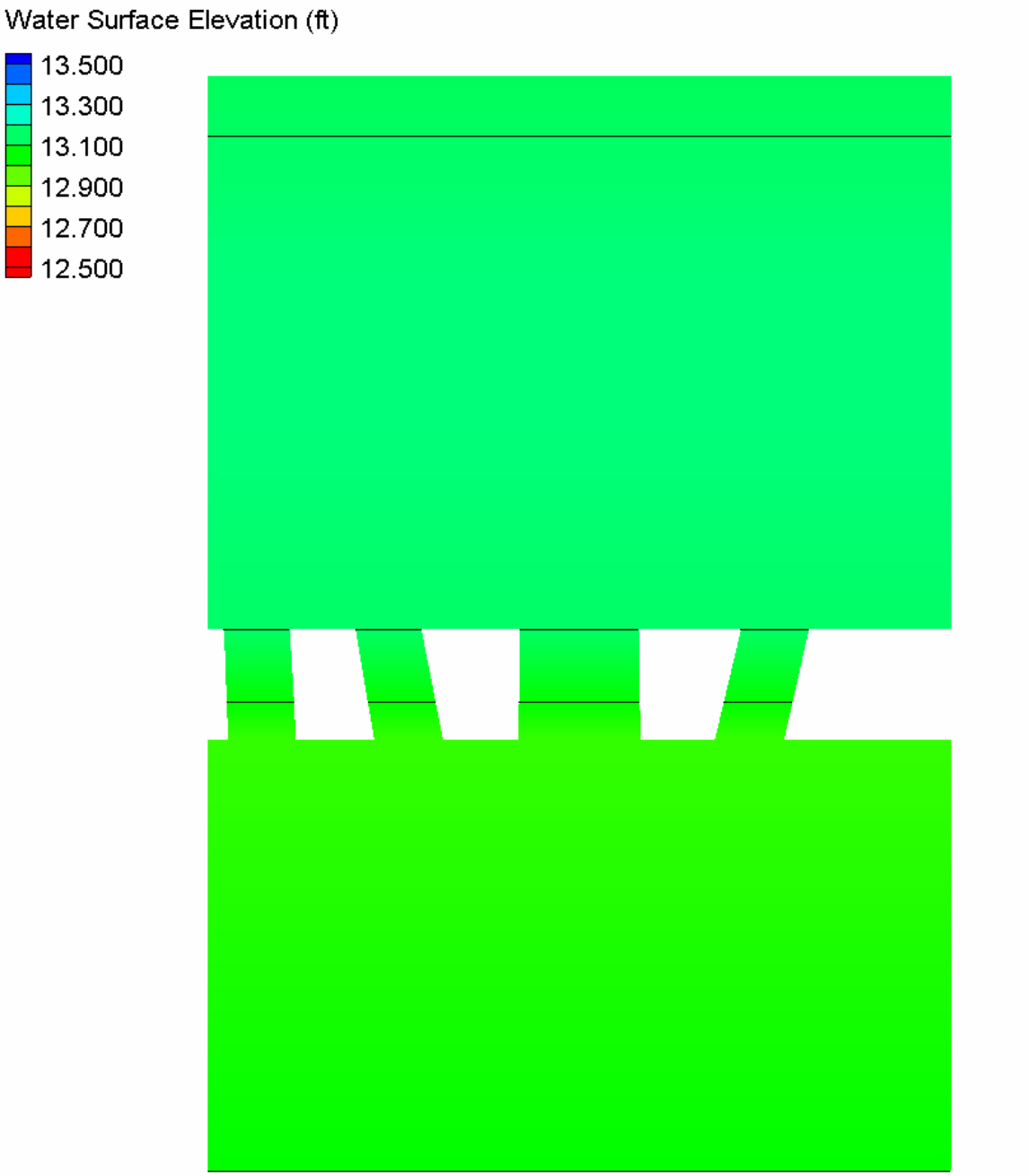

HEC-RAS Water Surface Elevation Contours – Small Channel – Multiple Openings (4)

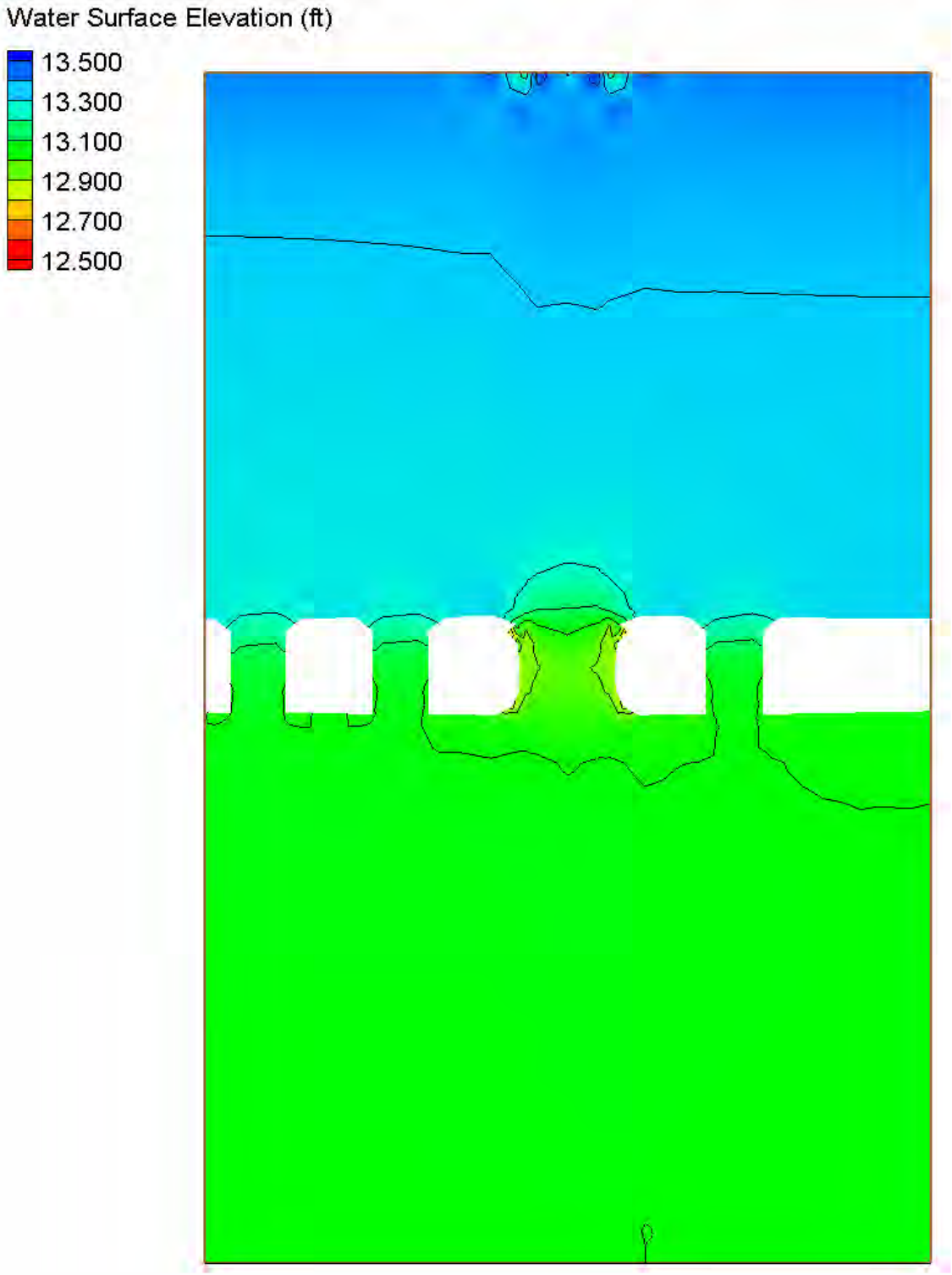

FESWMS Water Surface Elevation Contours – Small Channel – Multiple Openings (4)

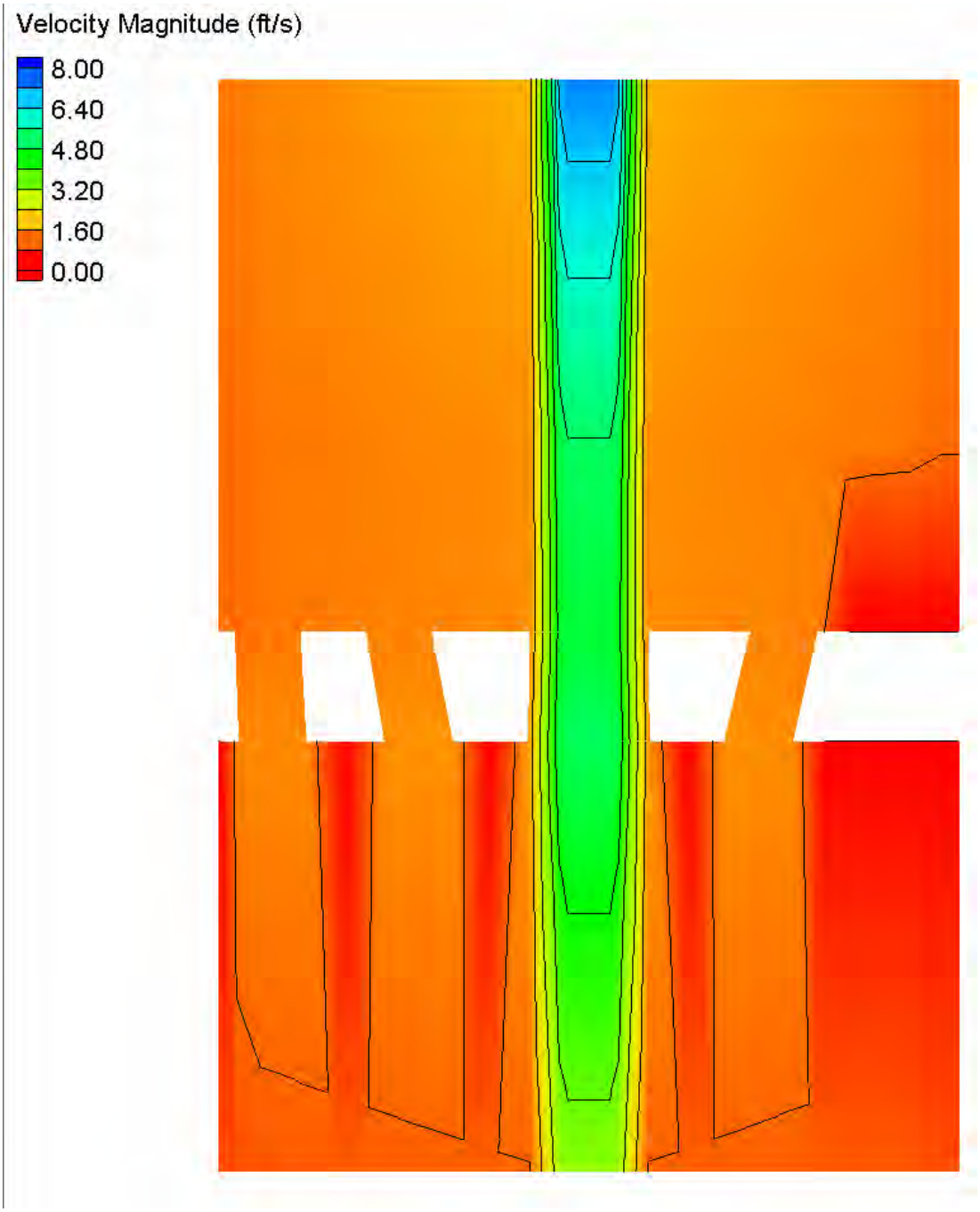

HEC-RAS Velocity Magnitude Contours – Small Channel – Multiple Openings (4)

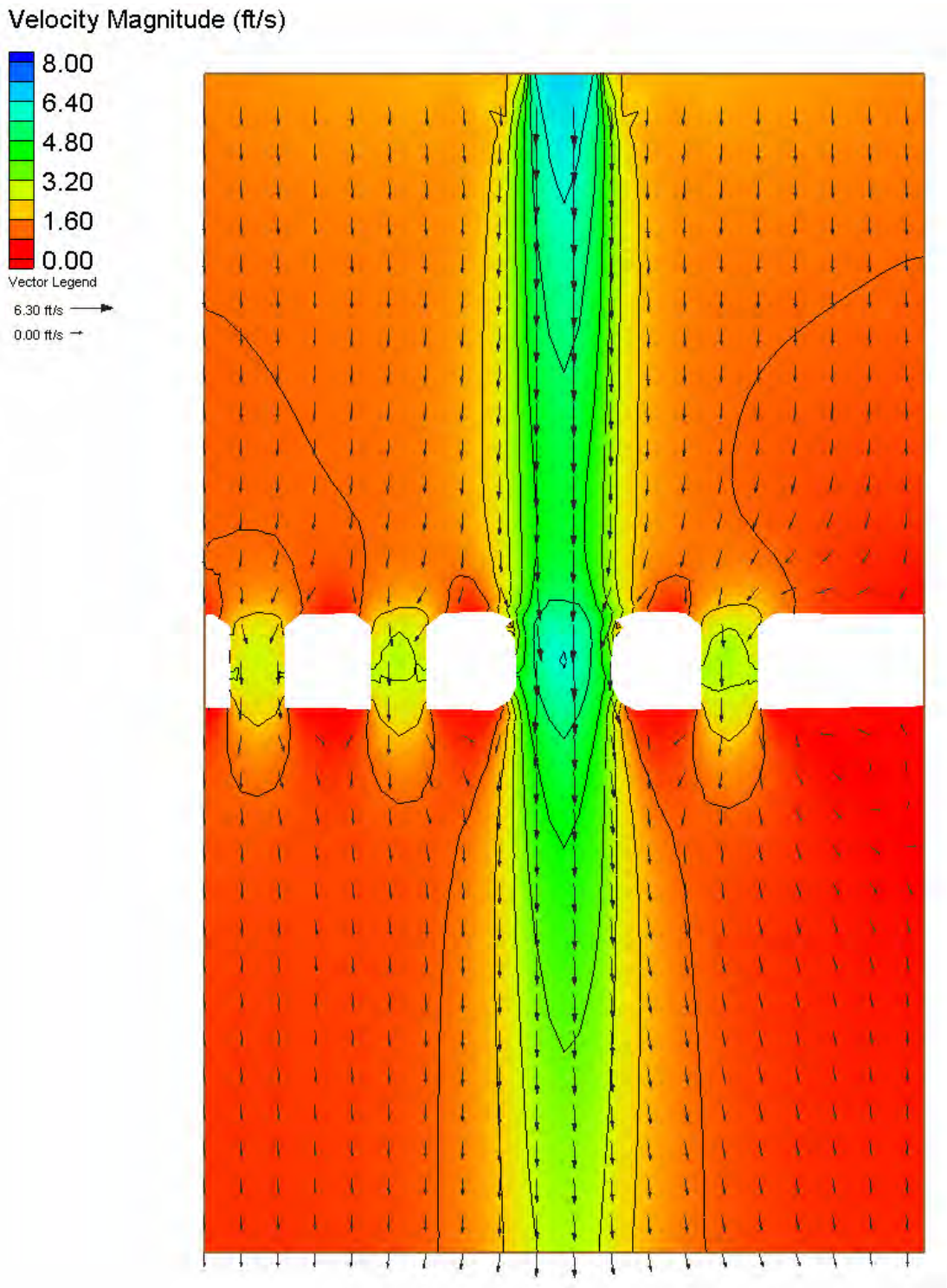

FESWMS Velocity Magnitude Contours – Small Channel – Multiple Openings (4)

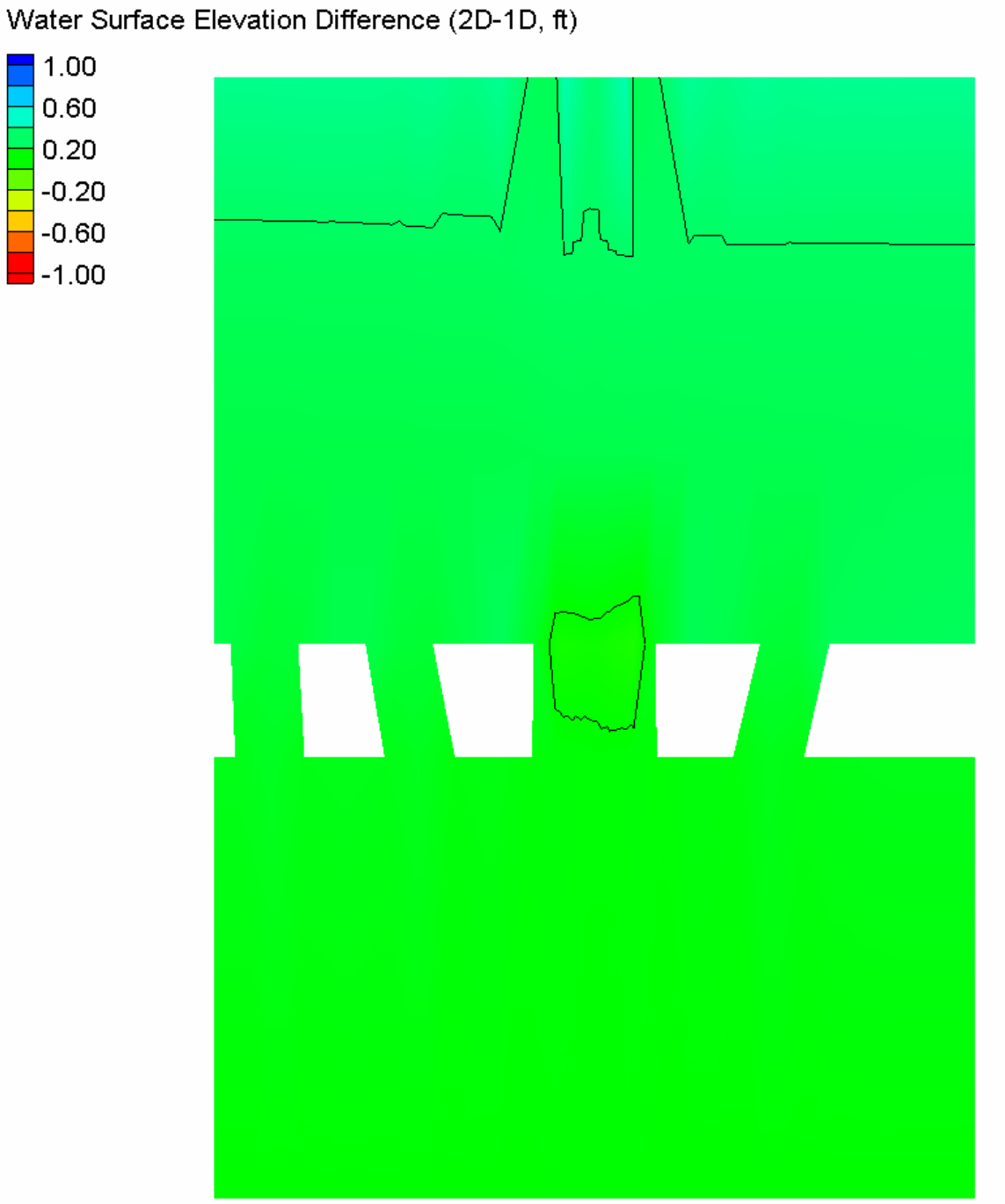

Water Surface Elevation Difference Contours – Small Channel – Multiple Openings (4)

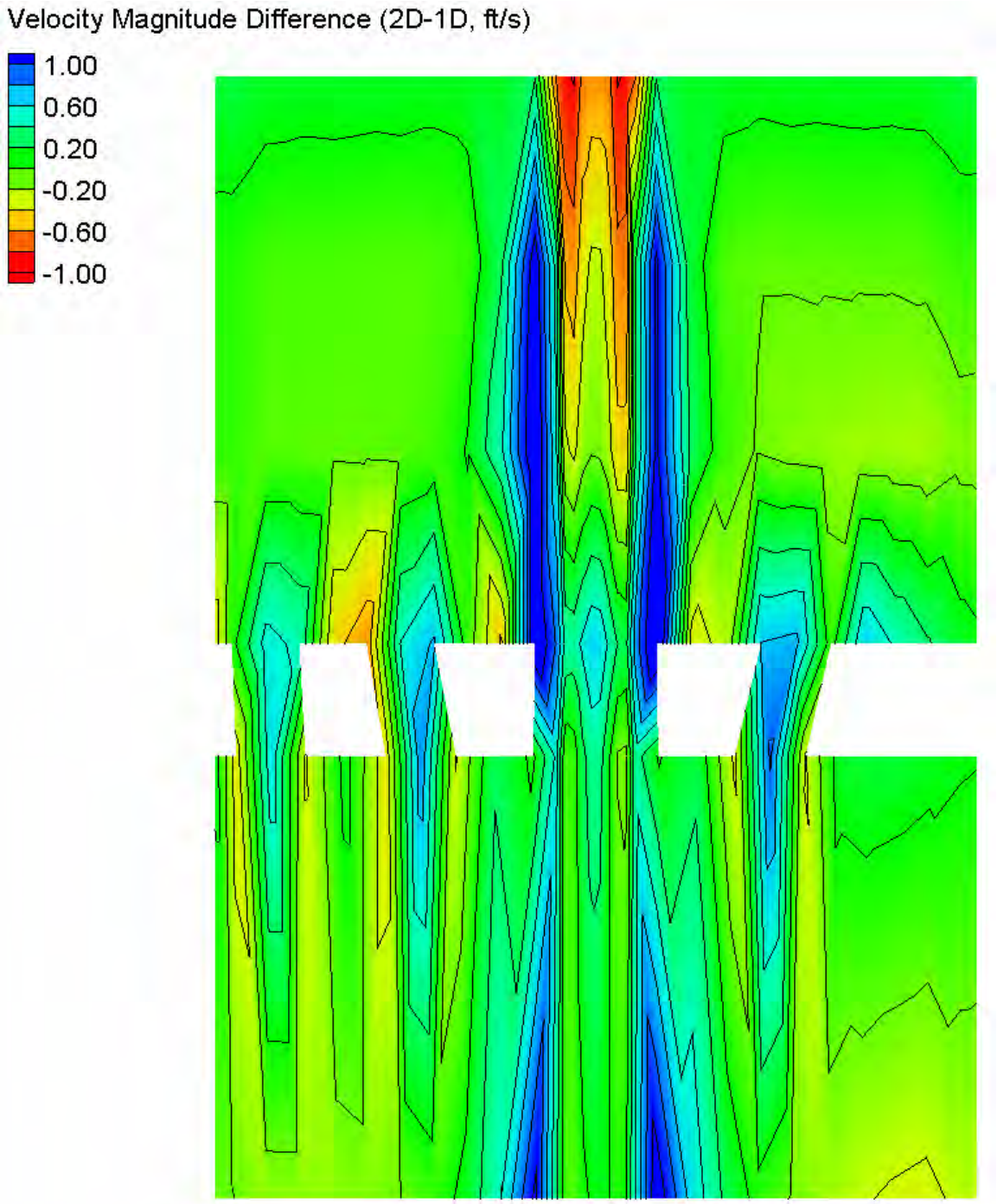

Velocity Magnitude Difference Contours – Small Channel – Multiple Openings (4)

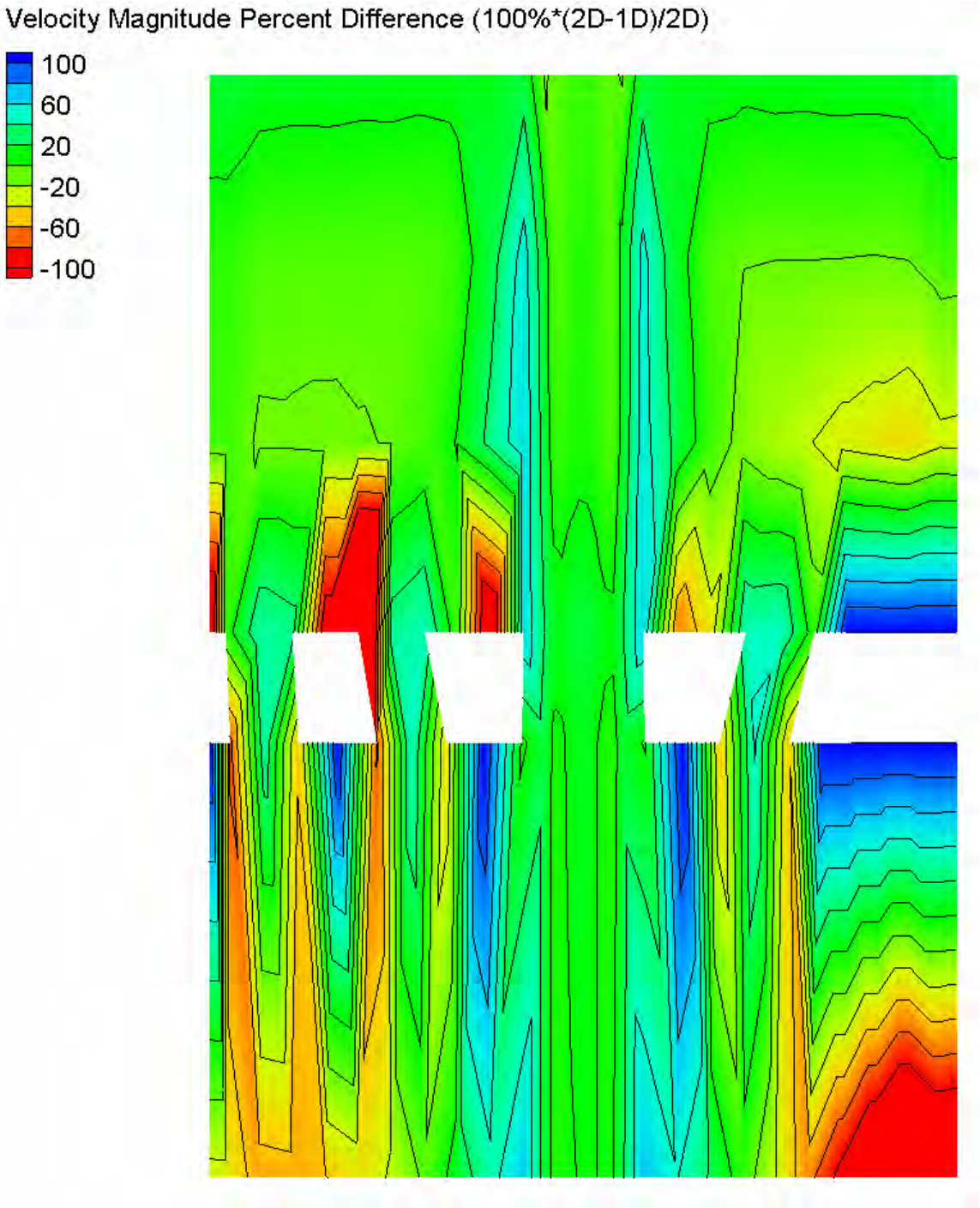

Velocity Magnitude Percent Difference Contours – Small Channel – Multiple Openings (4)

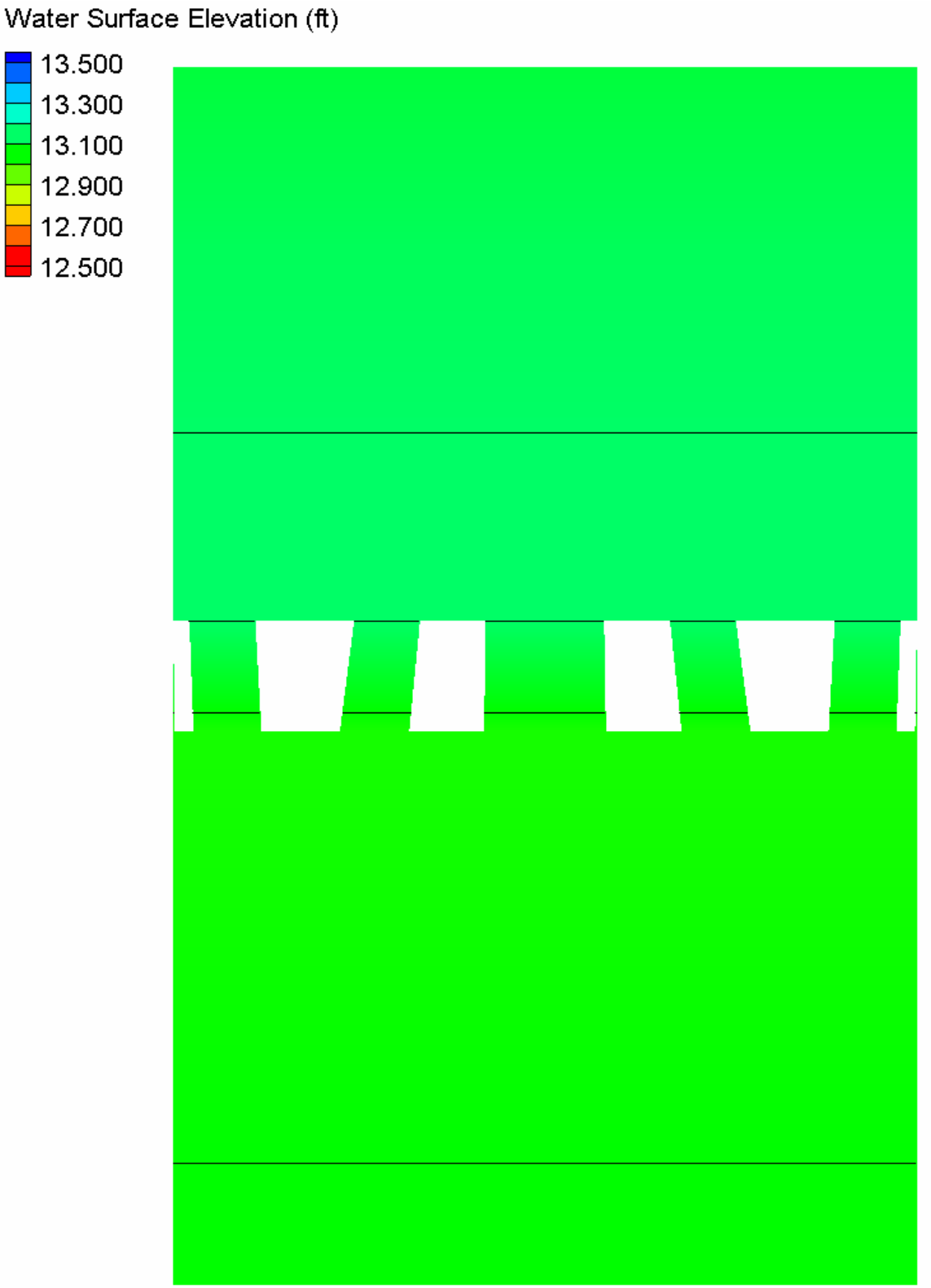

HEC-RAS Water Surface Elevation Contours – Small Channel – Multiple Openings (5)

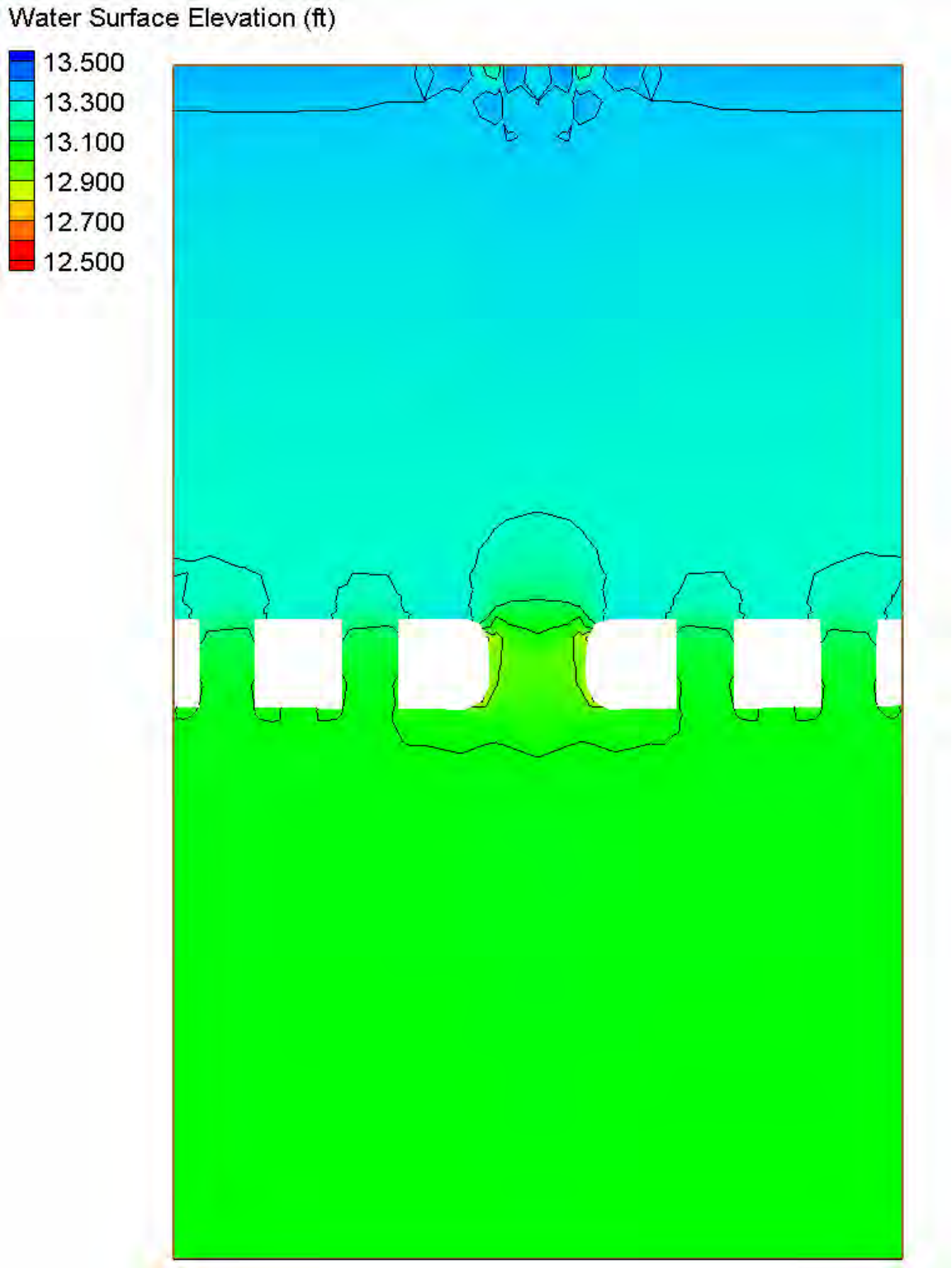

FESWMS Water Surface Elevation Contours – Small Channel – Multiple Openings (5)

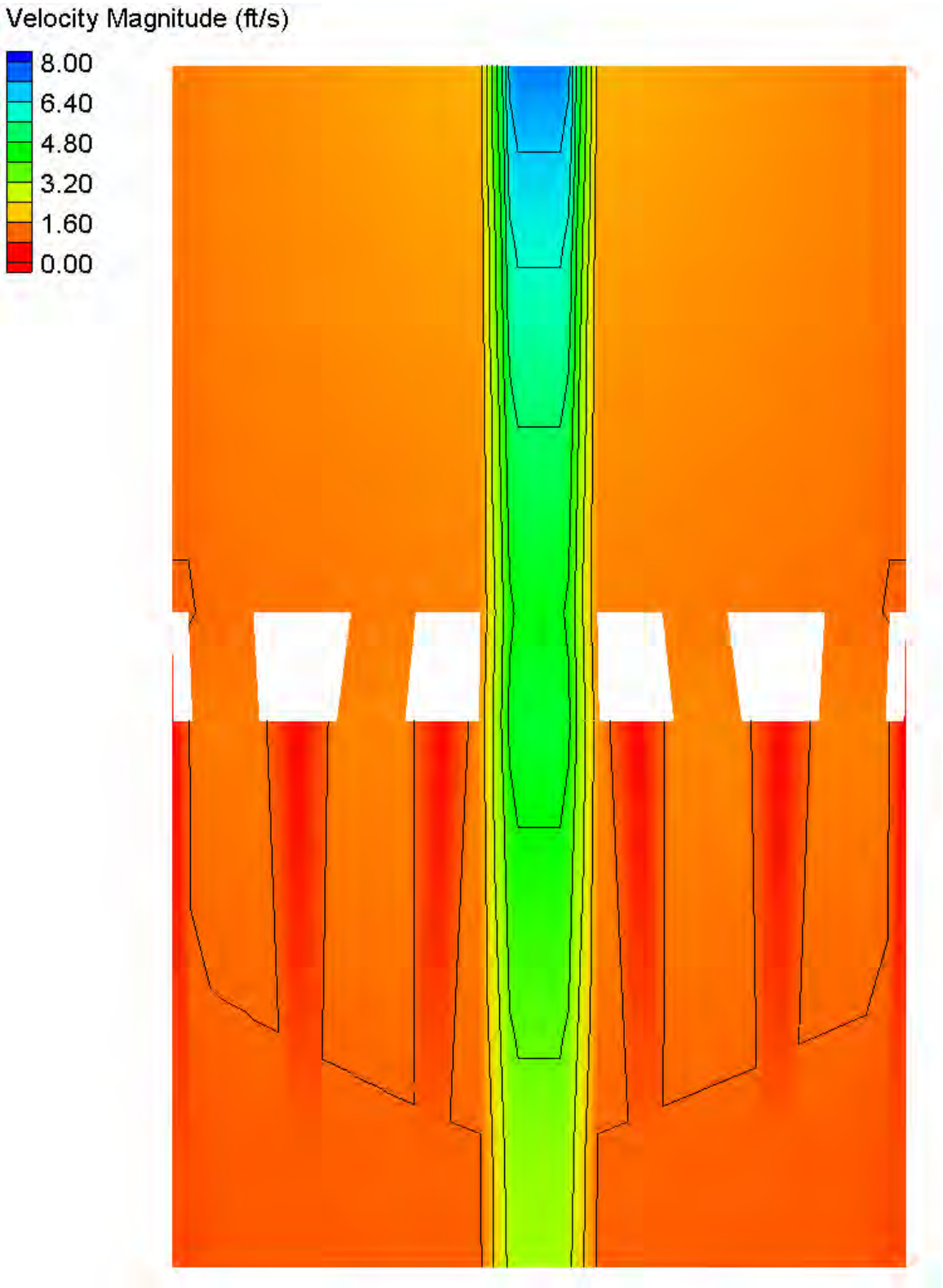

HEC-RAS Velocity Magnitude Contours – Small Channel – Multiple Openings (5)

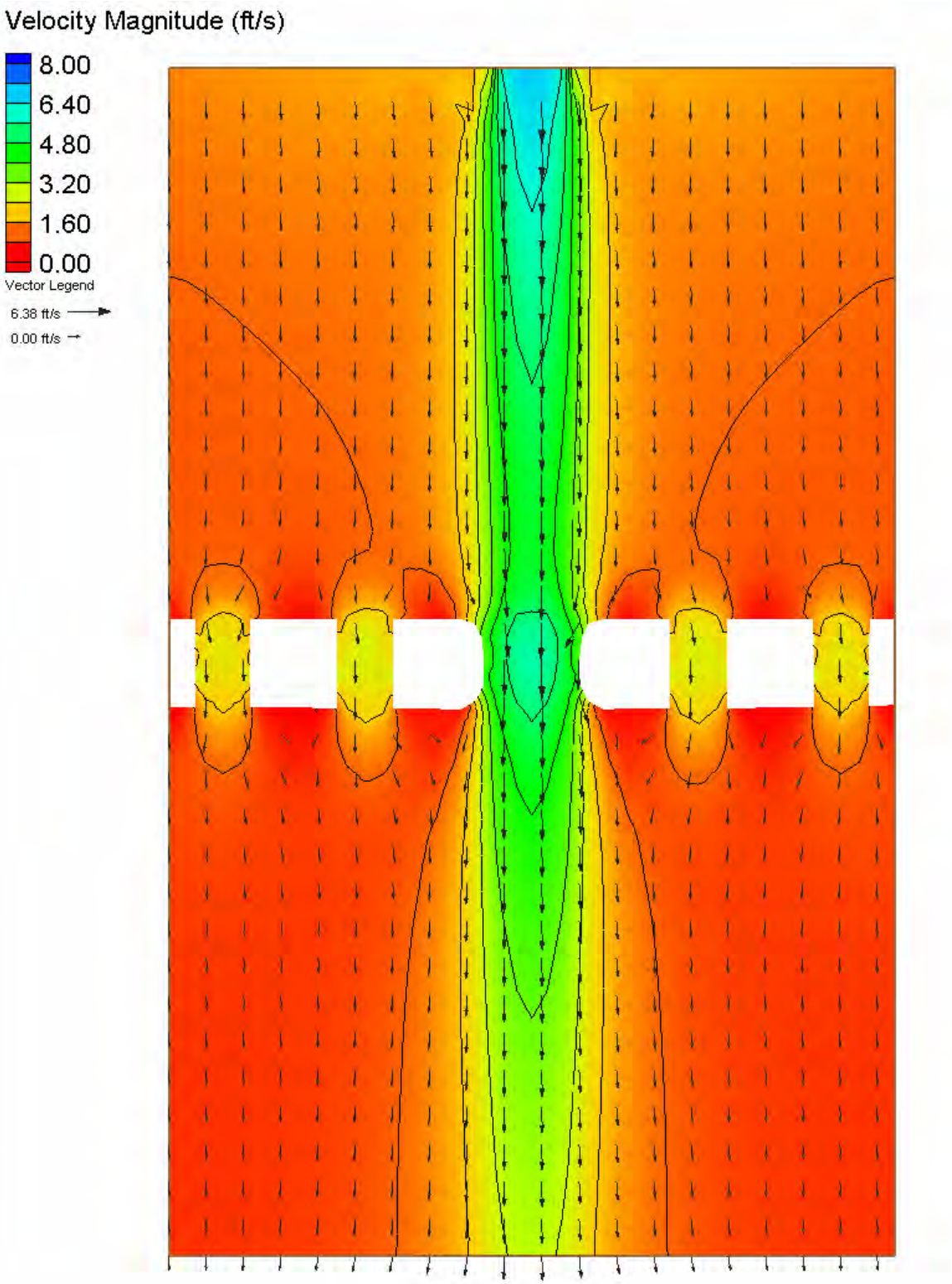

FESWMS Velocity Magnitude Contours – Small Channel – Multiple Openings (5)

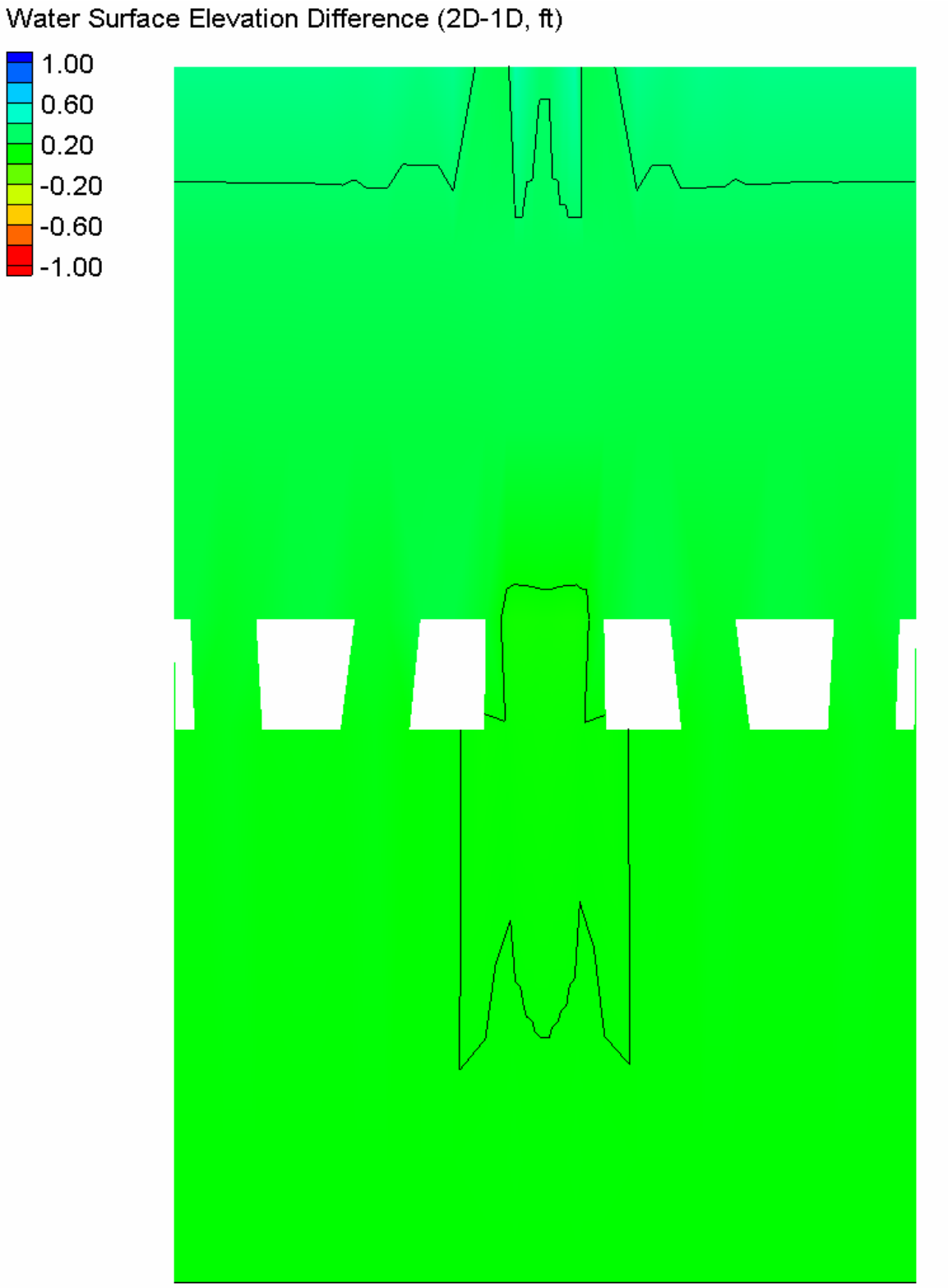

Water Surface Elevation Difference Contours – Small Channel – Multiple Openings (5)

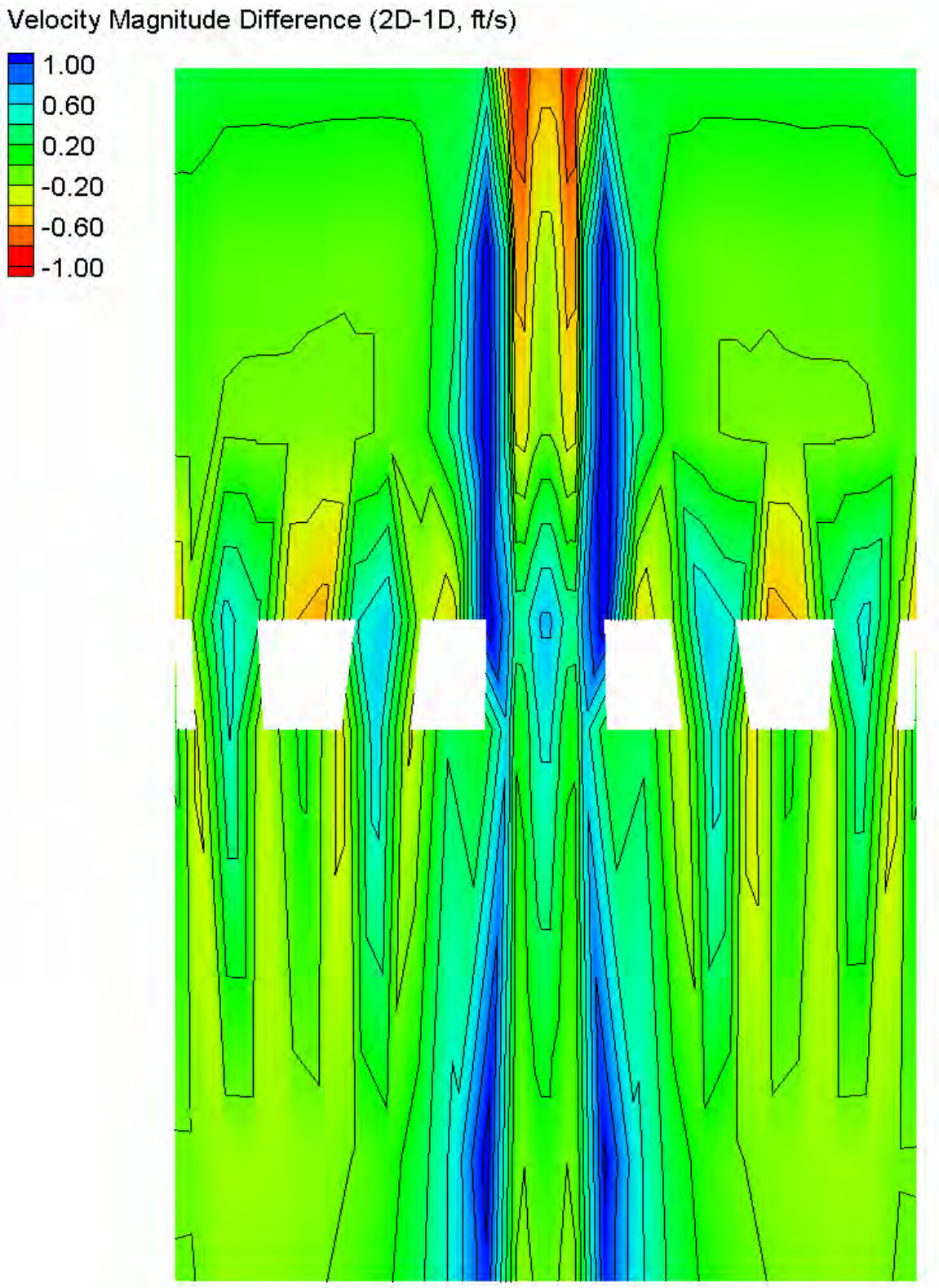

Velocity Magnitude Difference Contours – Small Channel – Multiple Openings (5)

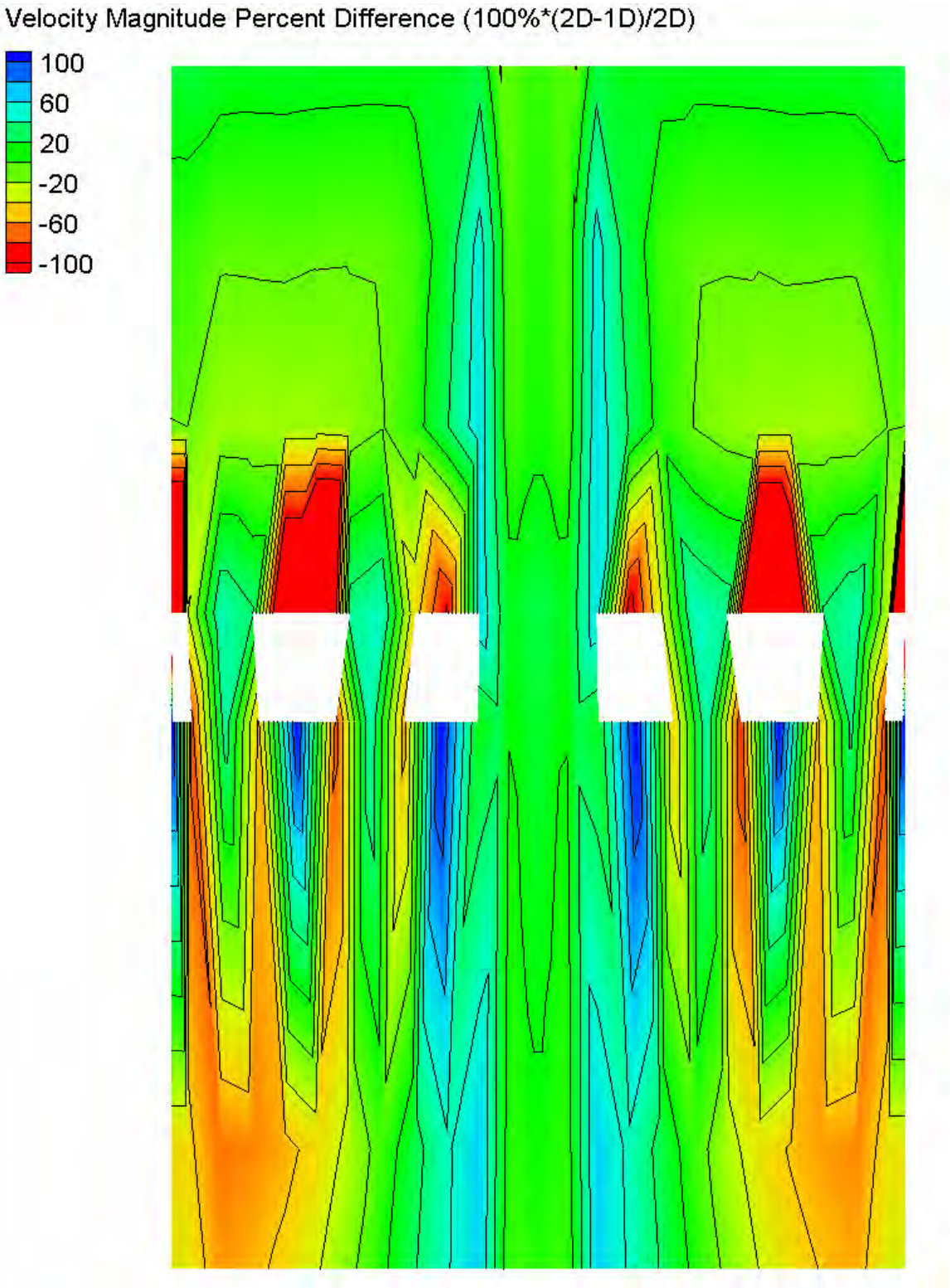

Velocity Magnitude Percent Difference Contours – Small Channel – Multiple Openings (5)

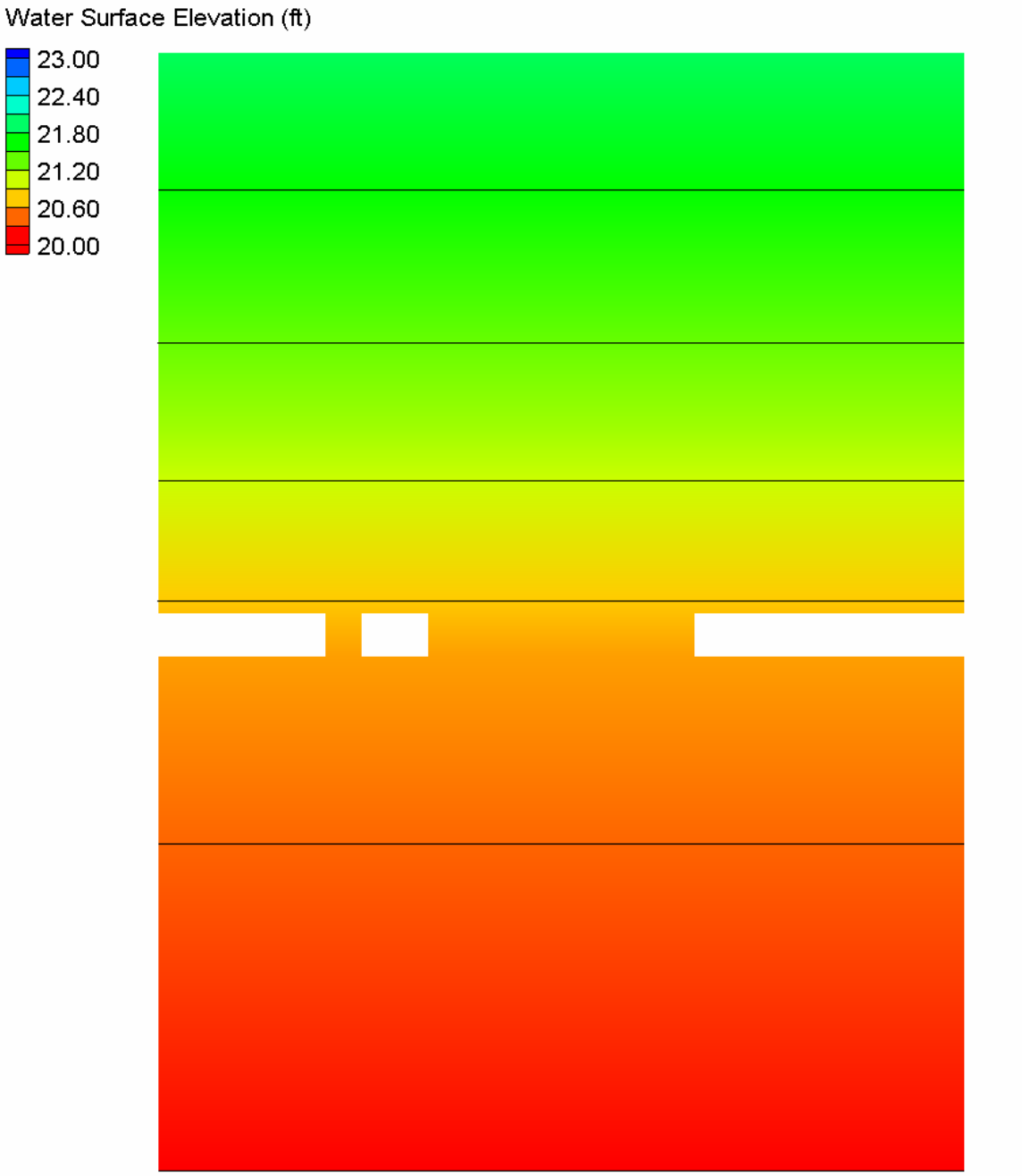

HEC-RAS Water Surface Elevation Contours – Large Channel – Multiple Openings (2)

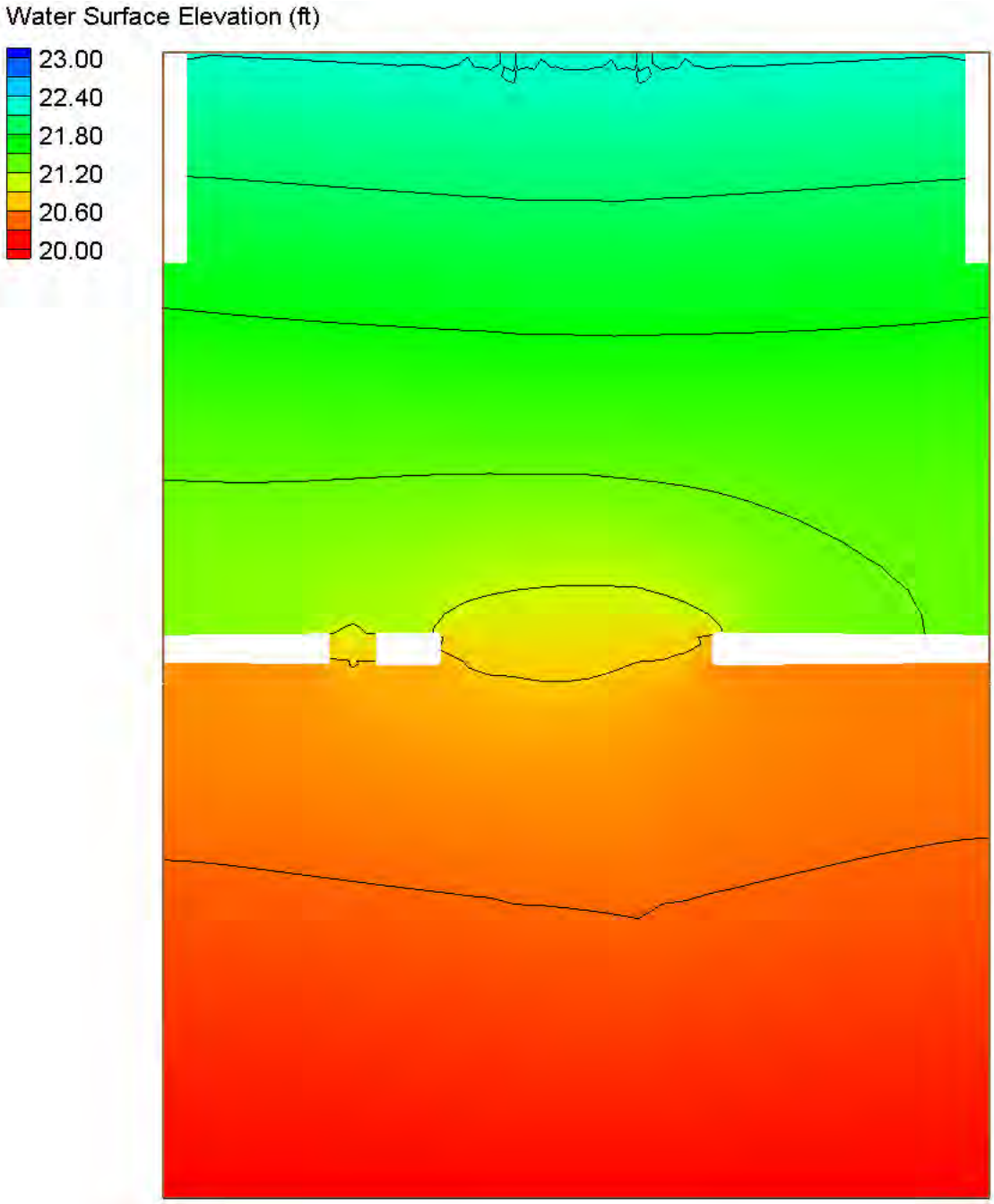

FESWMS Water Surface Elevation Contours – Large Channel – Multiple Openings (2)

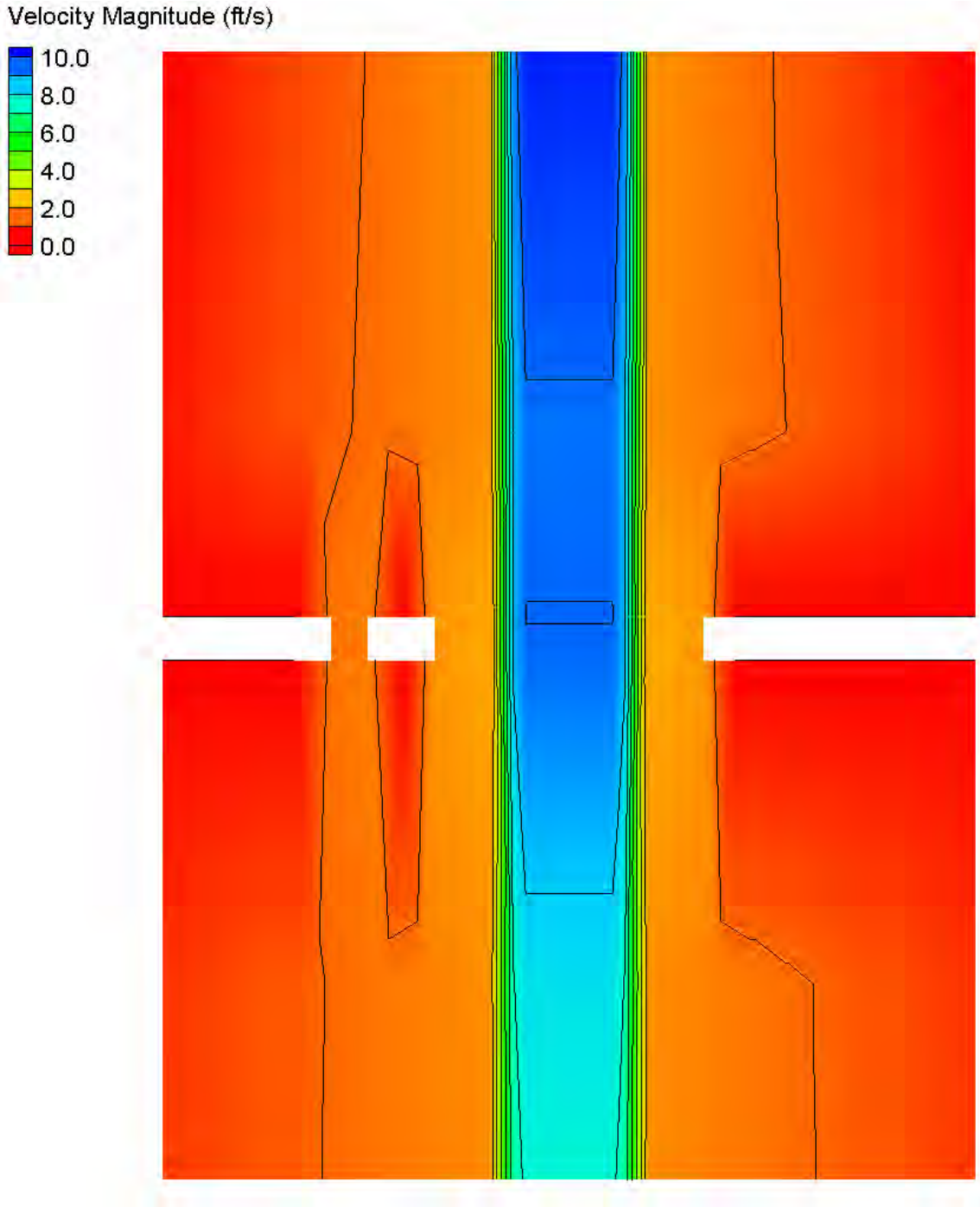

HEC-RAS Velocity Magnitude Contours – Large Channel – Multiple Openings (2)

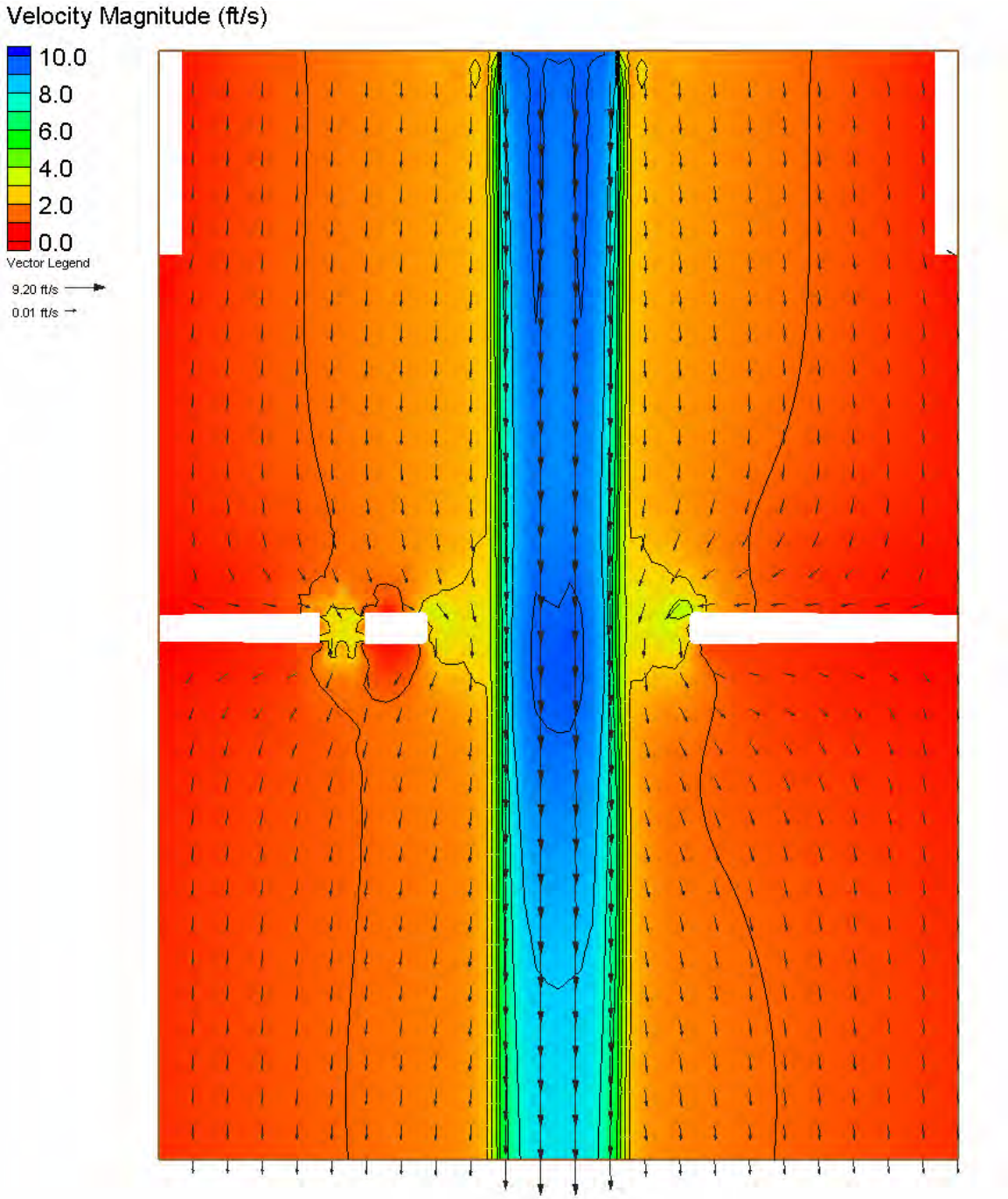

FESWMS Velocity Magnitude Contours – Large Channel – Multiple Openings (2)

Water Surface Elevation Difference Contours – Large Channel – Multiple Openings (2)

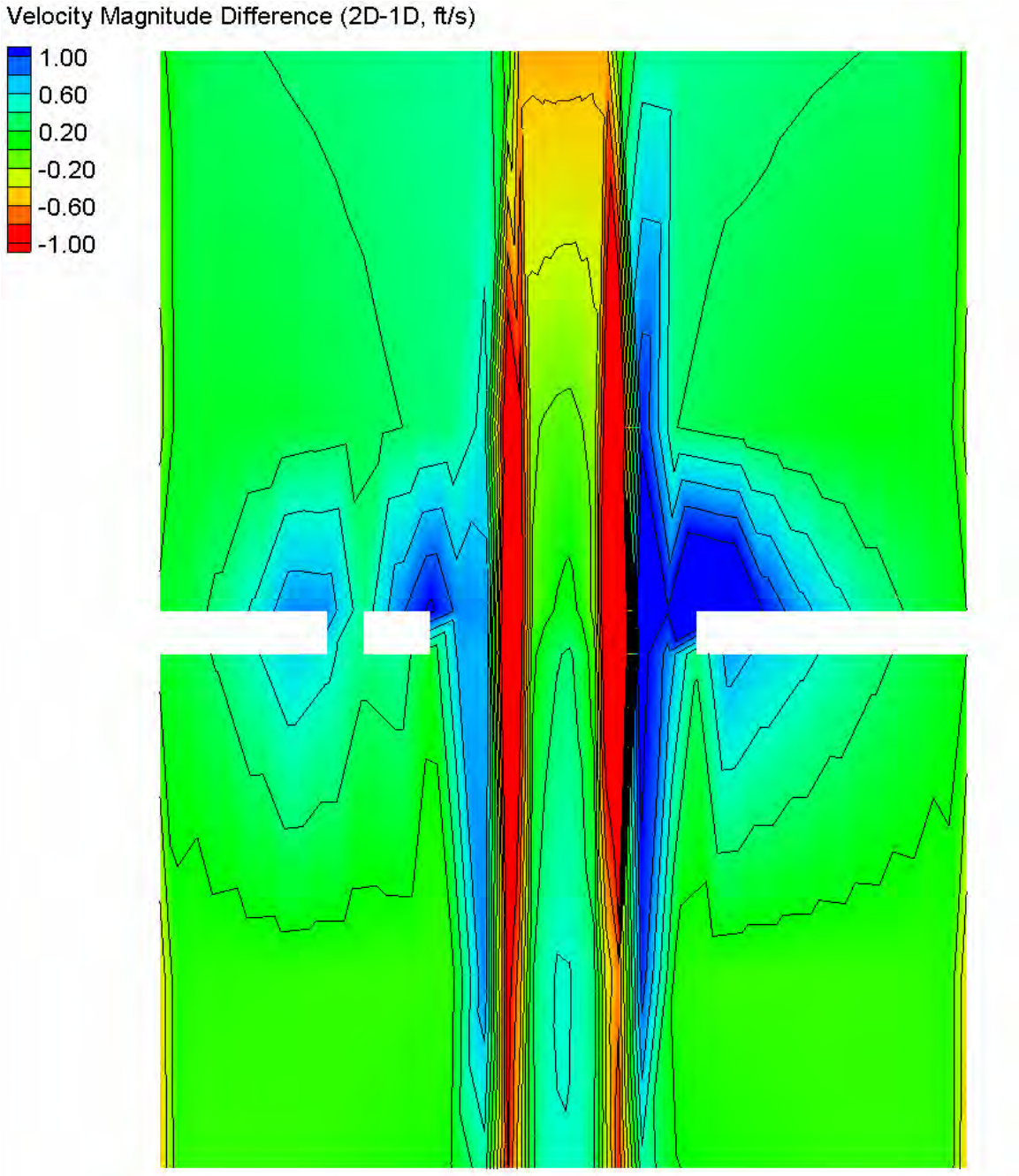

Velocity Magnitude Difference Contours – Large Channel – Multiple Openings (2)

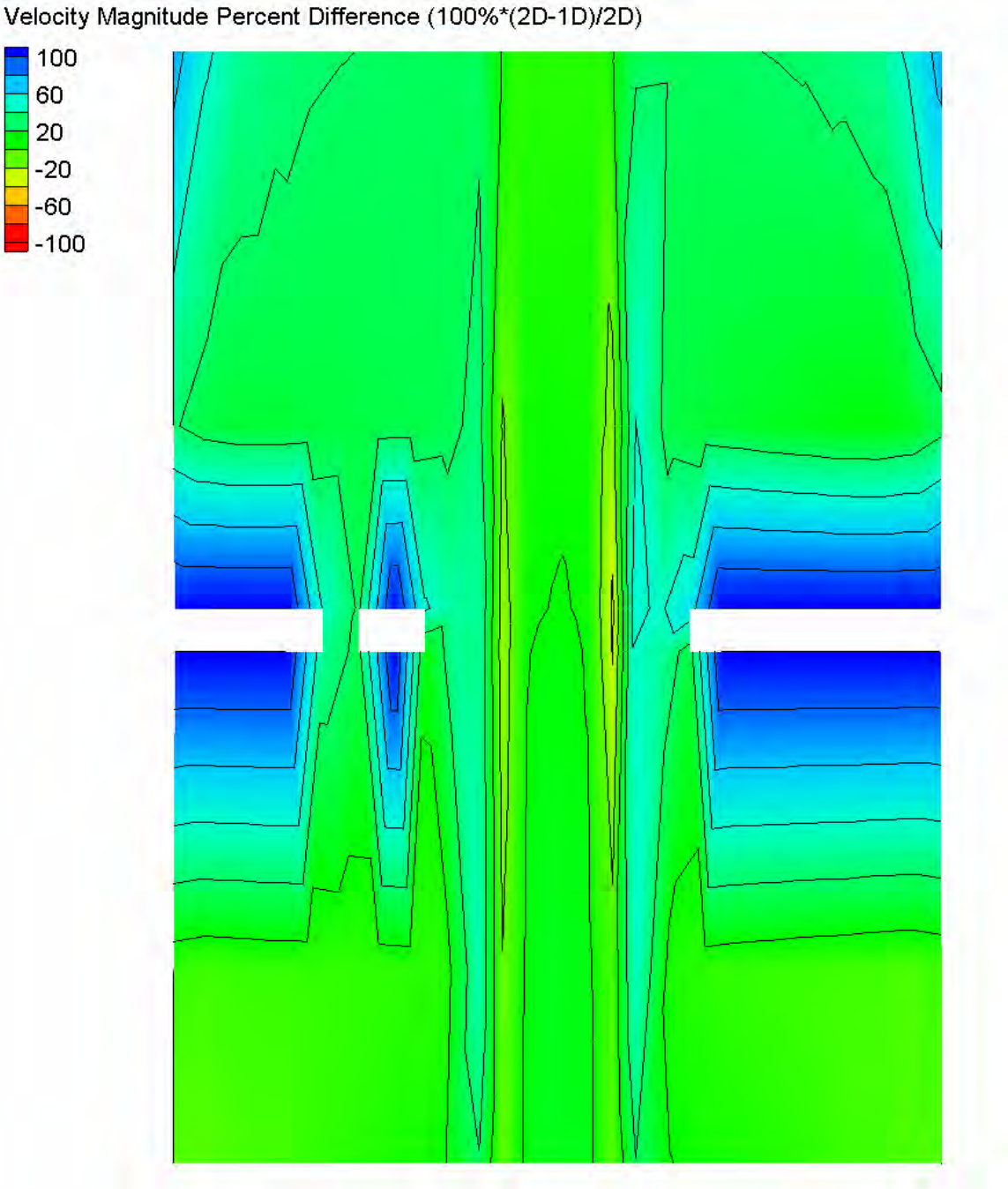

Velocity Magnitude Percent Difference Contours – Large Channel – Multiple Openings (2)

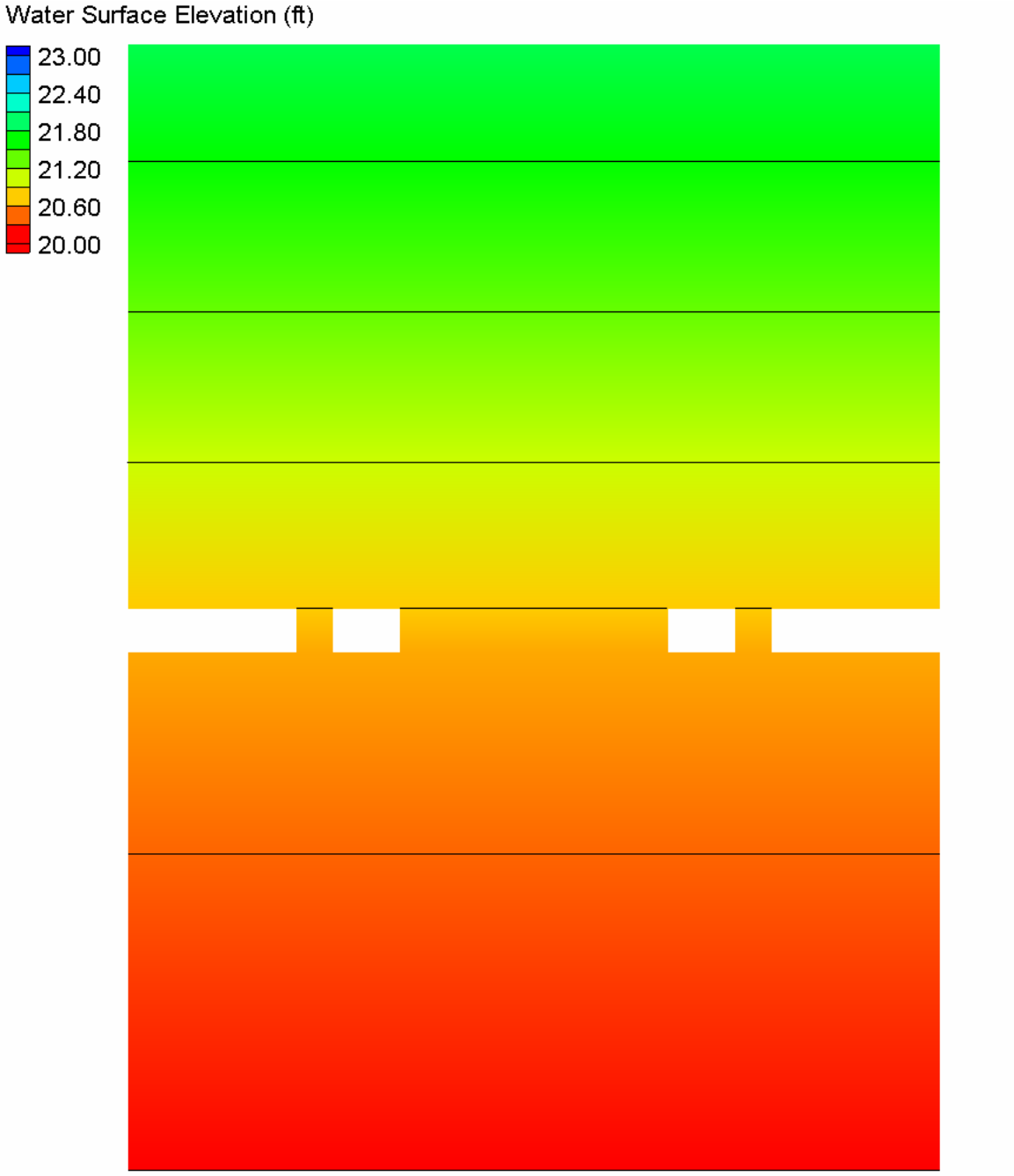

HEC-RAS Water Surface Elevation Contours – Large Channel – Multiple Openings (3)

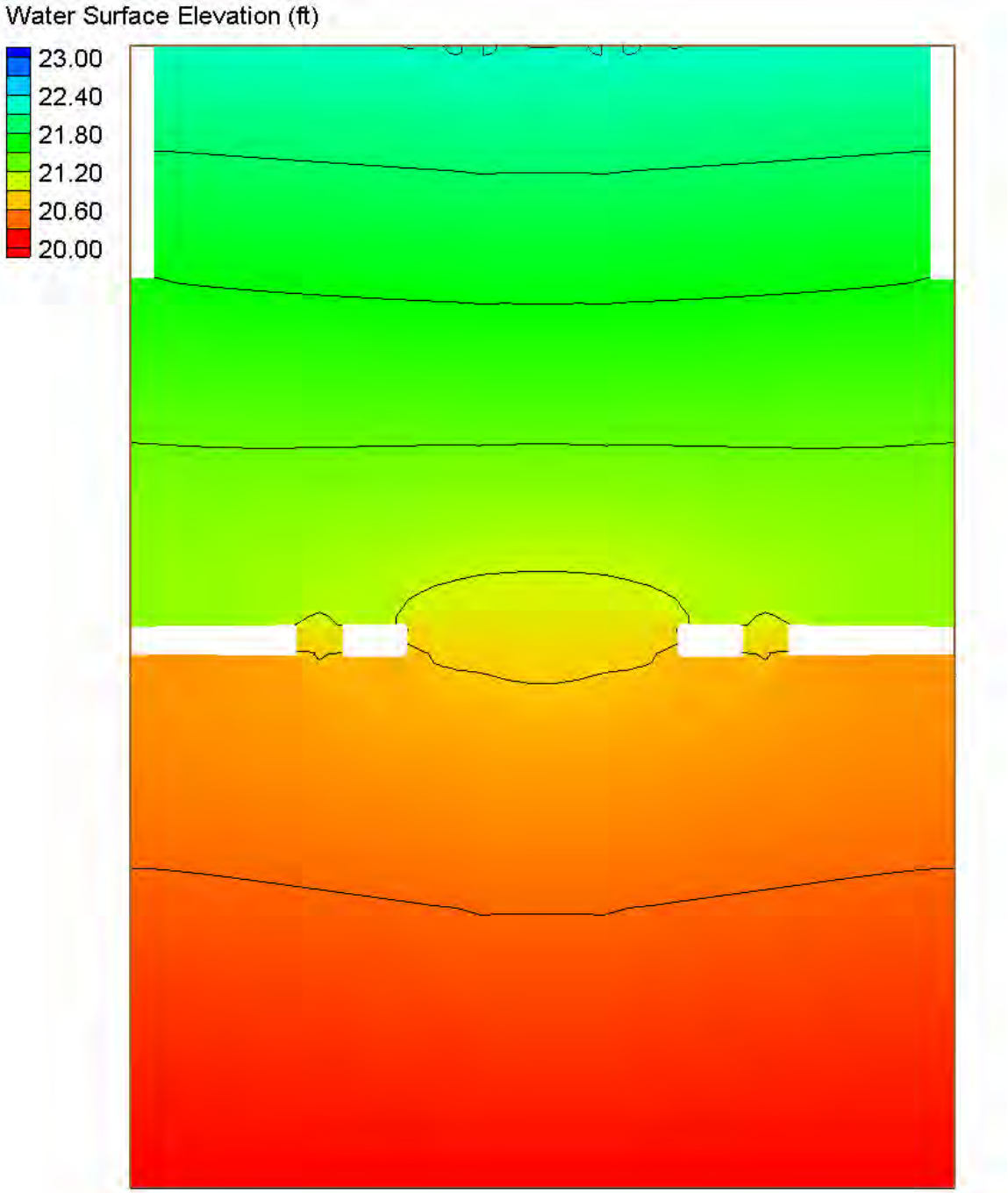

FESWMS Water Surface Elevation Contours – Large Channel – Multiple Openings (3)

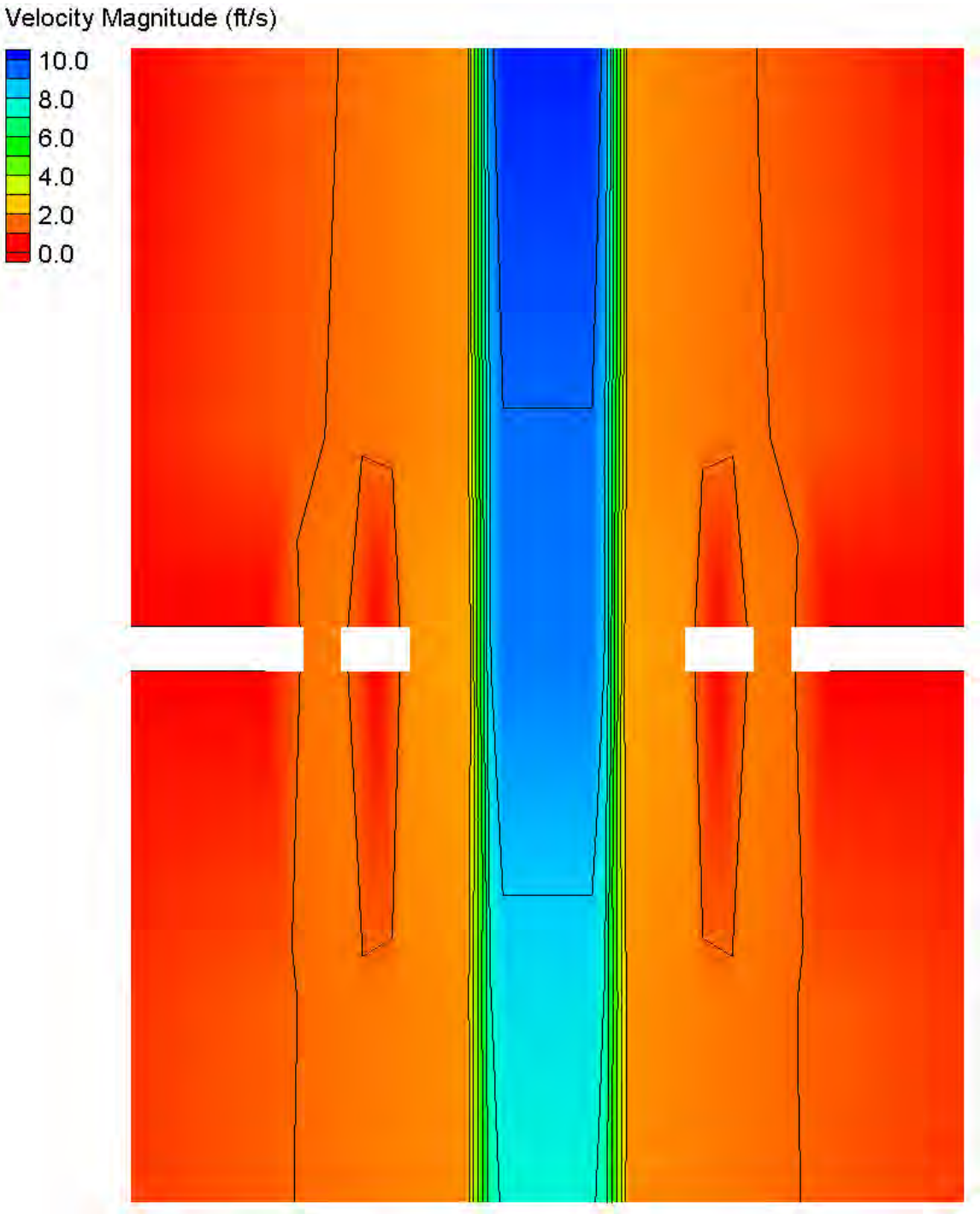

HEC-RAS Velocity Magnitude Contours – Large Channel – Multiple Openings (3)

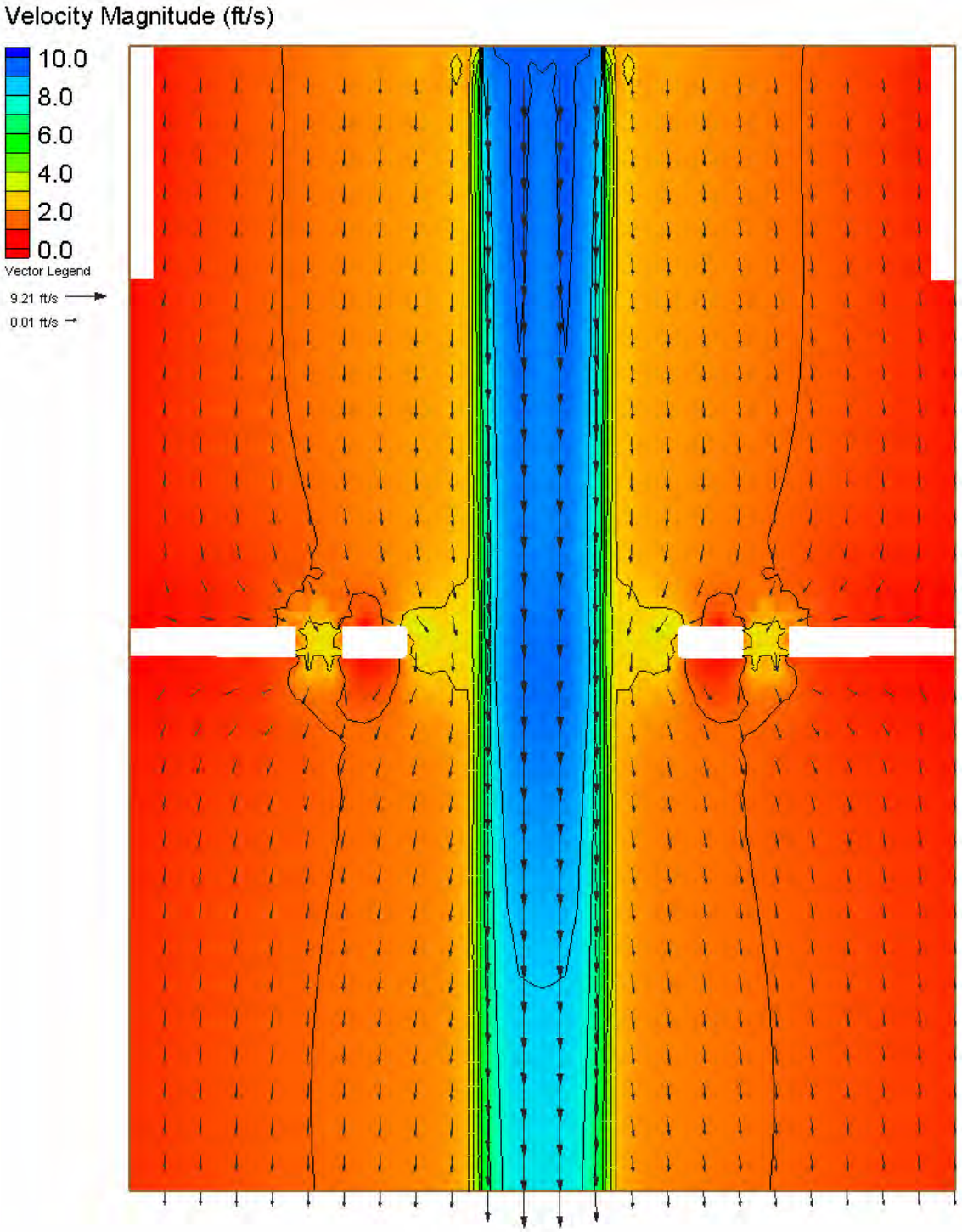

FESWMS Velocity Magnitude Contours – Large Channel – Multiple Openings (3)

Water Surface Elevation Difference Contours – Large Channel – Multiple Openings (3)

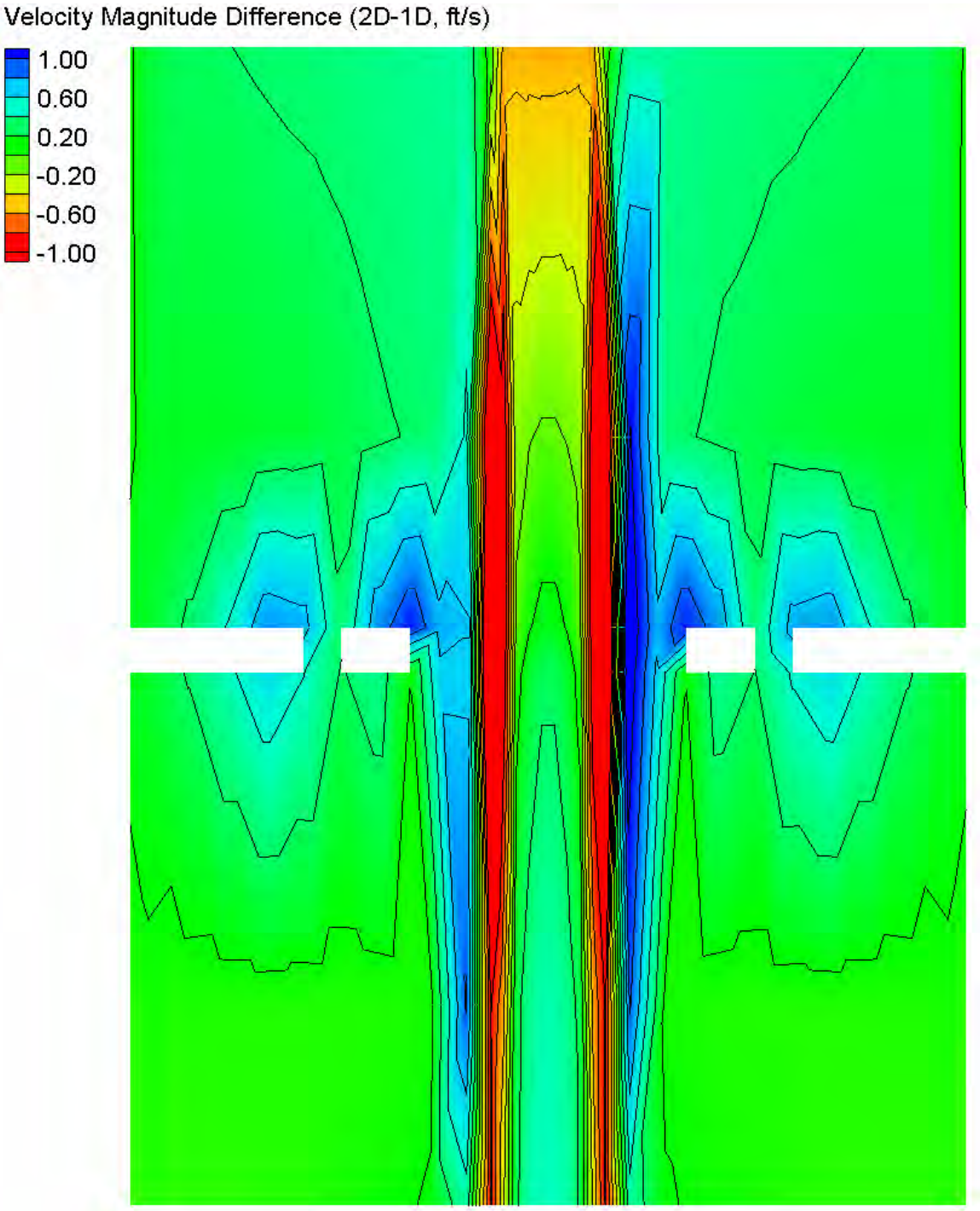

Velocity Magnitude Difference Contours – Large Channel – Multiple Openings (3)

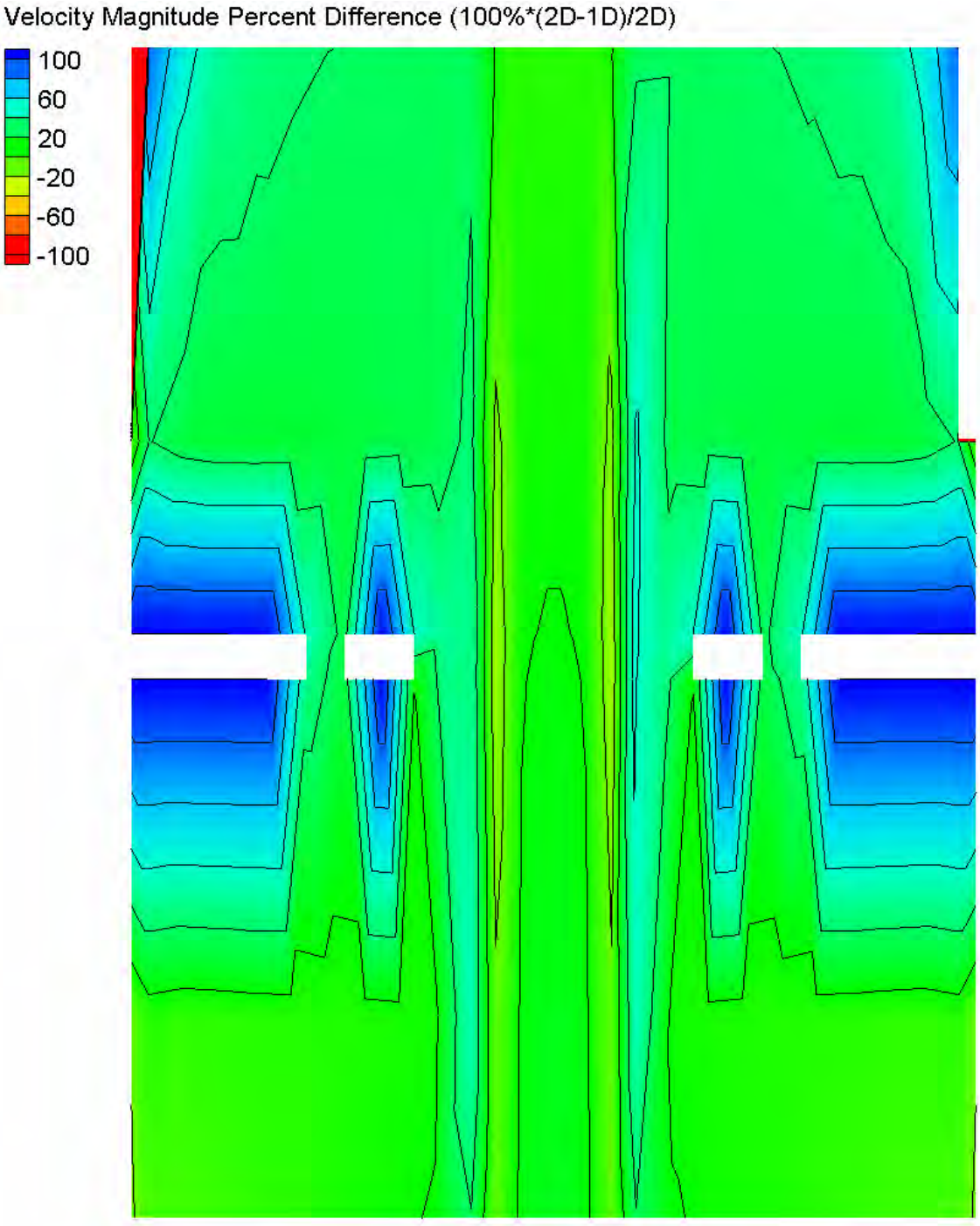

Velocity Magnitude Percent Difference Contours – Large Channel – Multiple Openings (3)

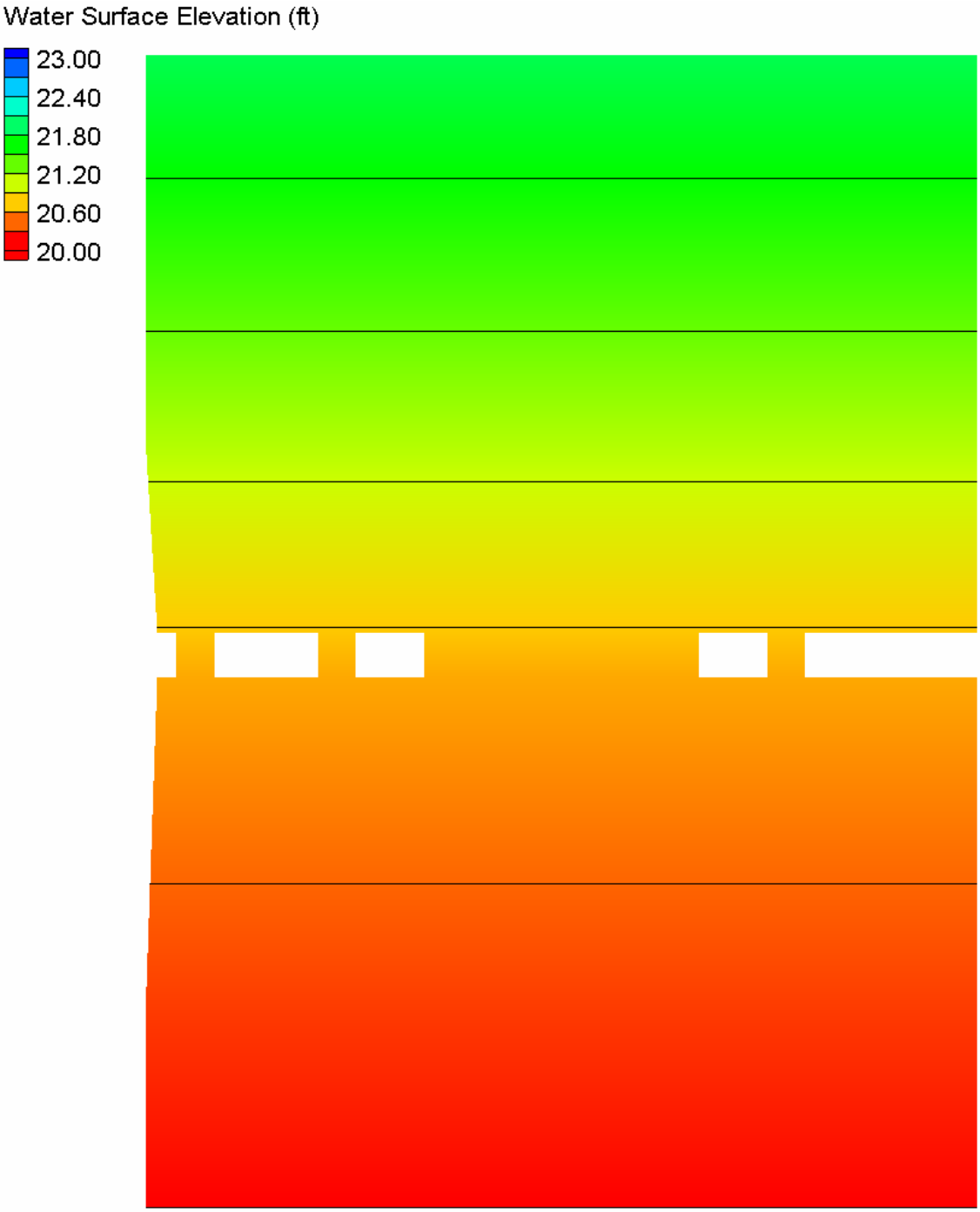

HEC-RAS Water Surface Elevation Contours – Large Channel – Multiple Openings (4)

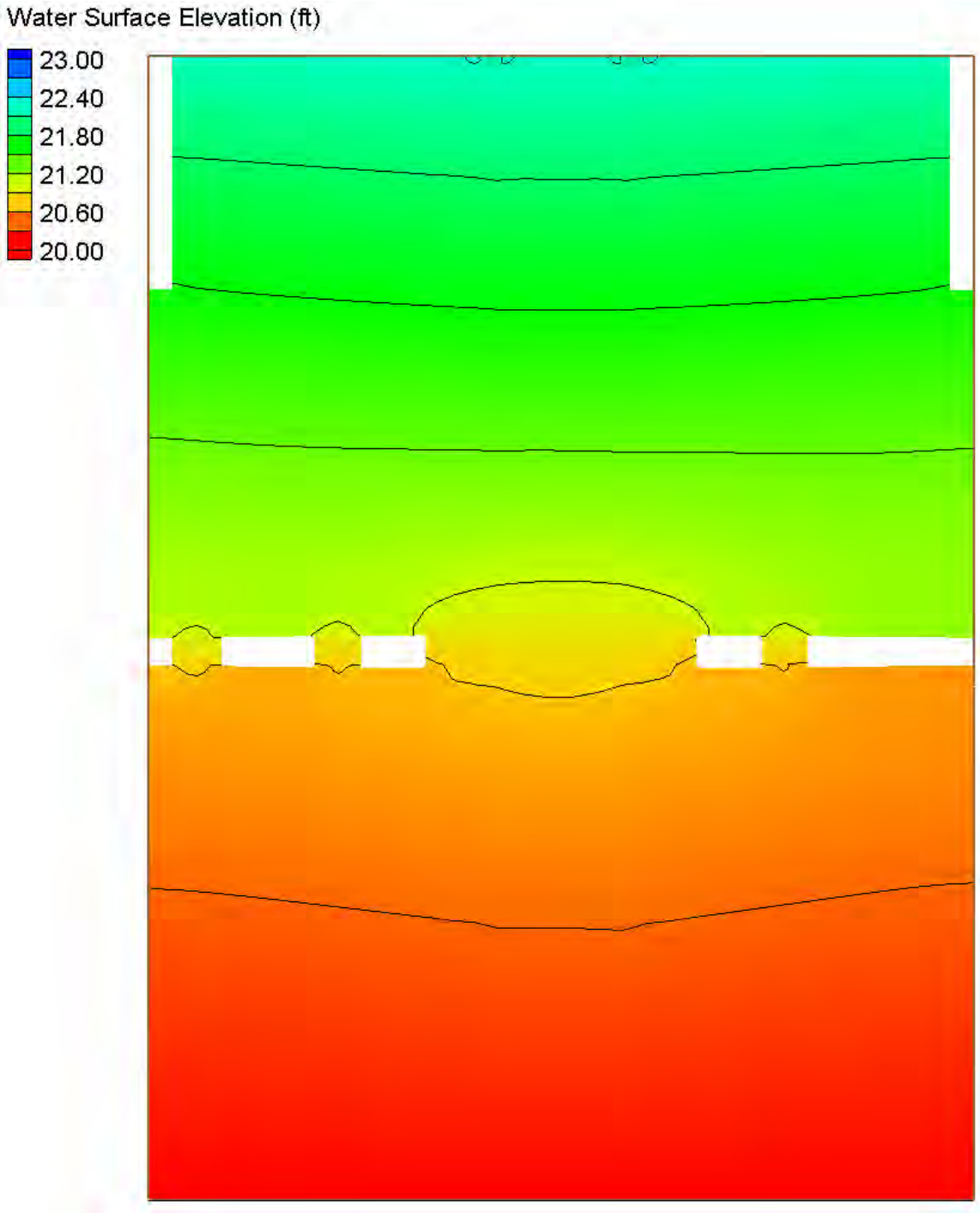

FESWMS Water Surface Elevation Contours – Large Channel – Multiple Openings (4)

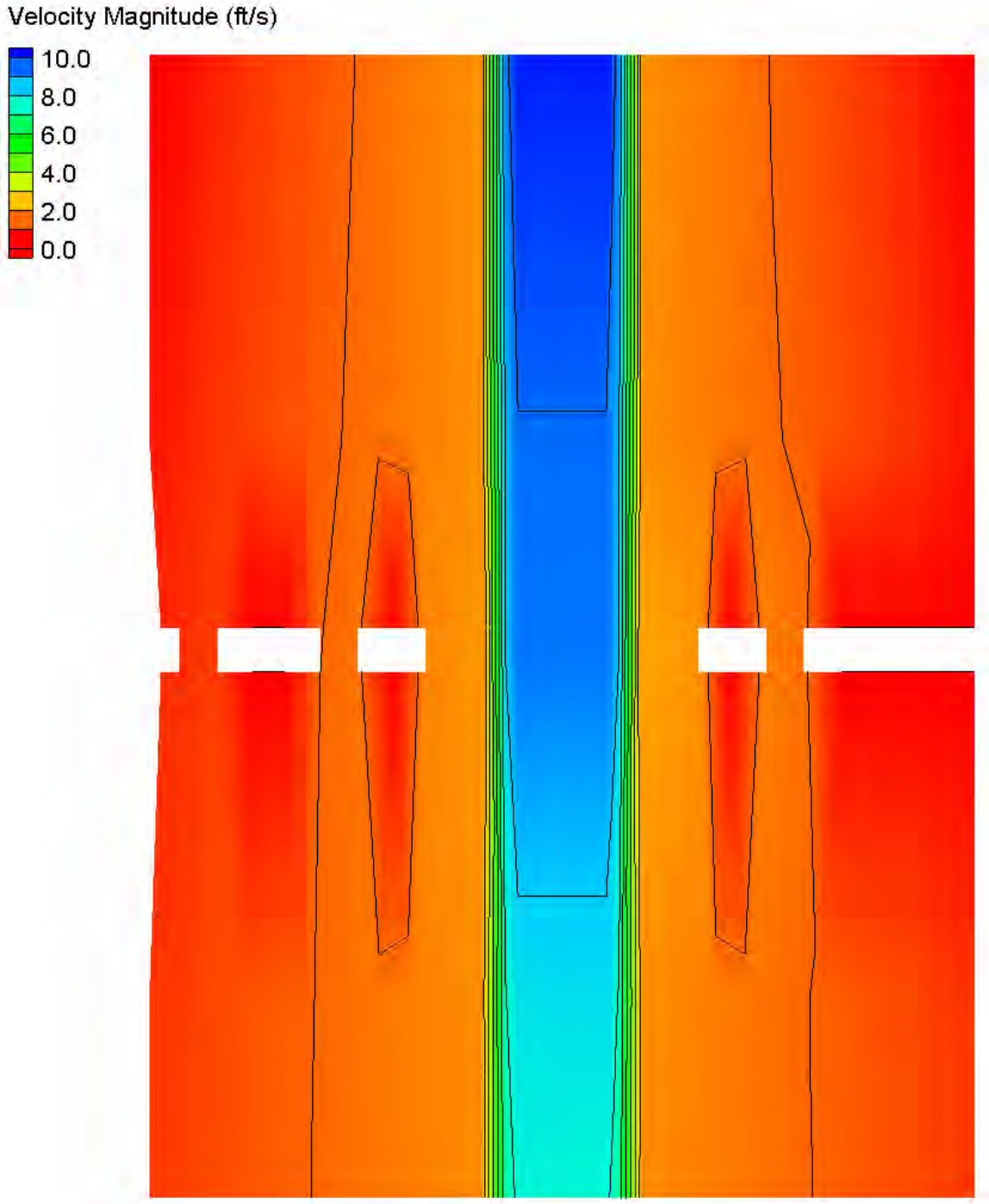

HEC-RAS Velocity Magnitude Contours – Large Channel – Multiple Openings (4)

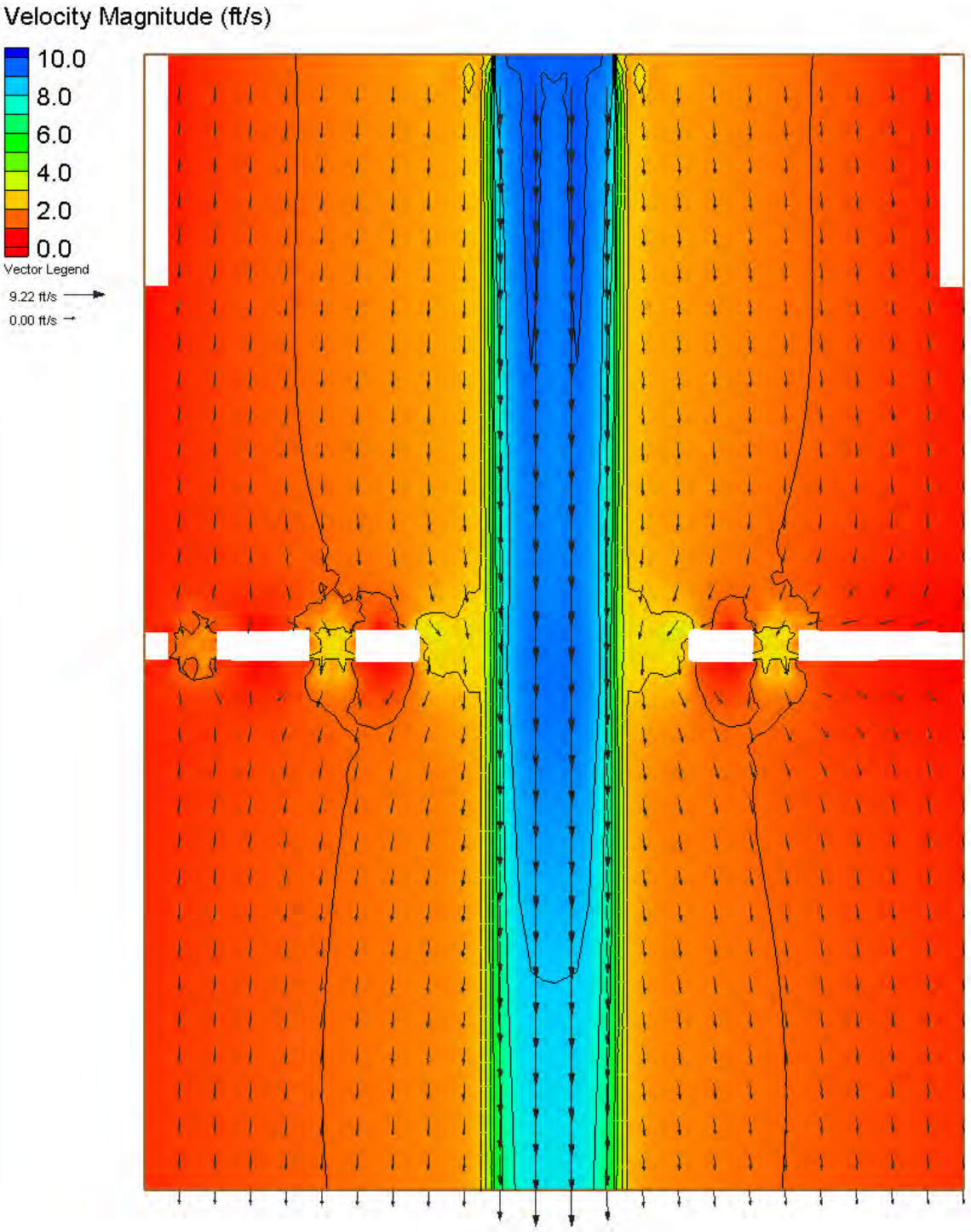

FESWMS Velocity Magnitude Contours – Large Channel – Multiple Openings (4)

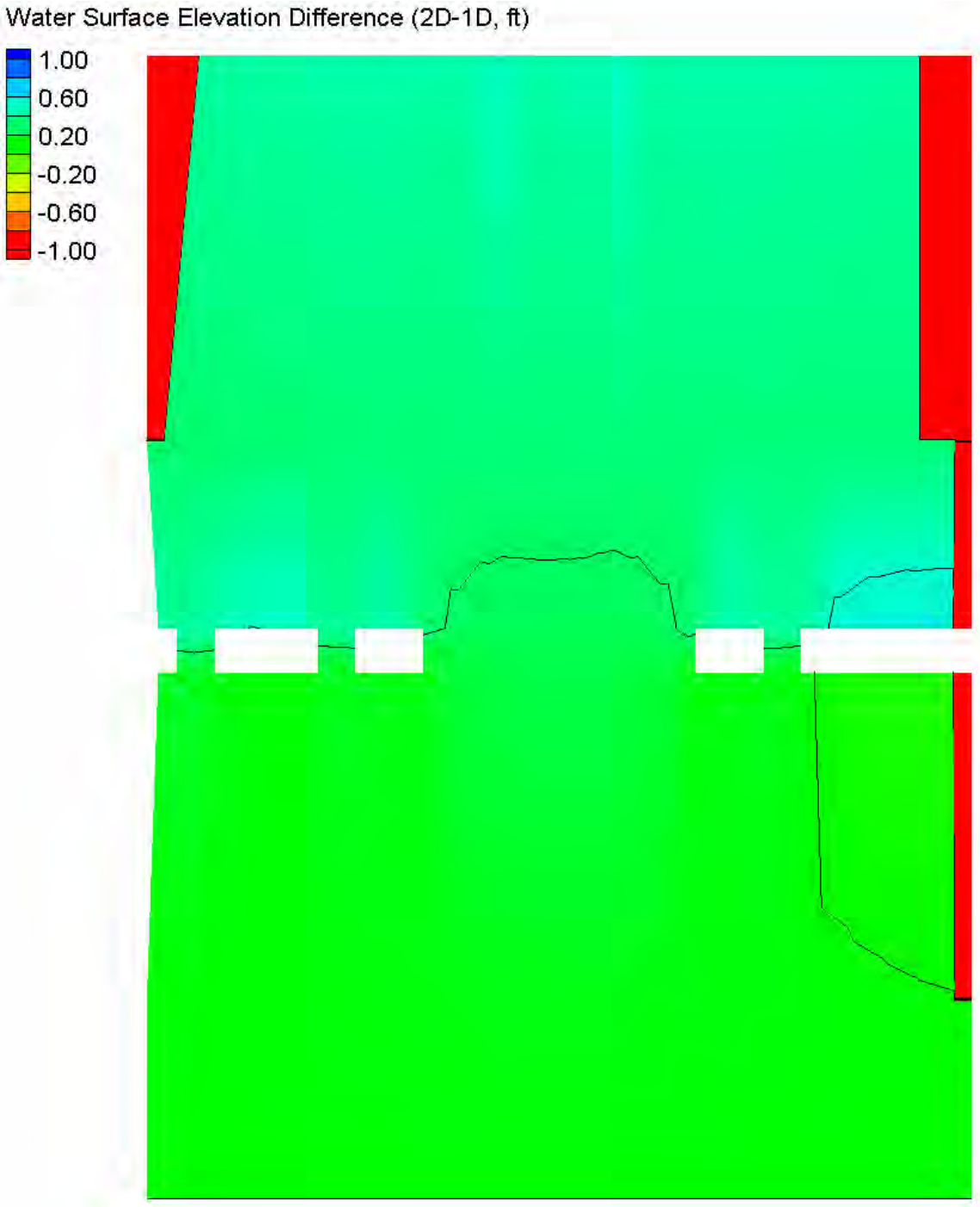

Water Surface Elevation Difference Contours – Large Channel – Multiple Openings (4)

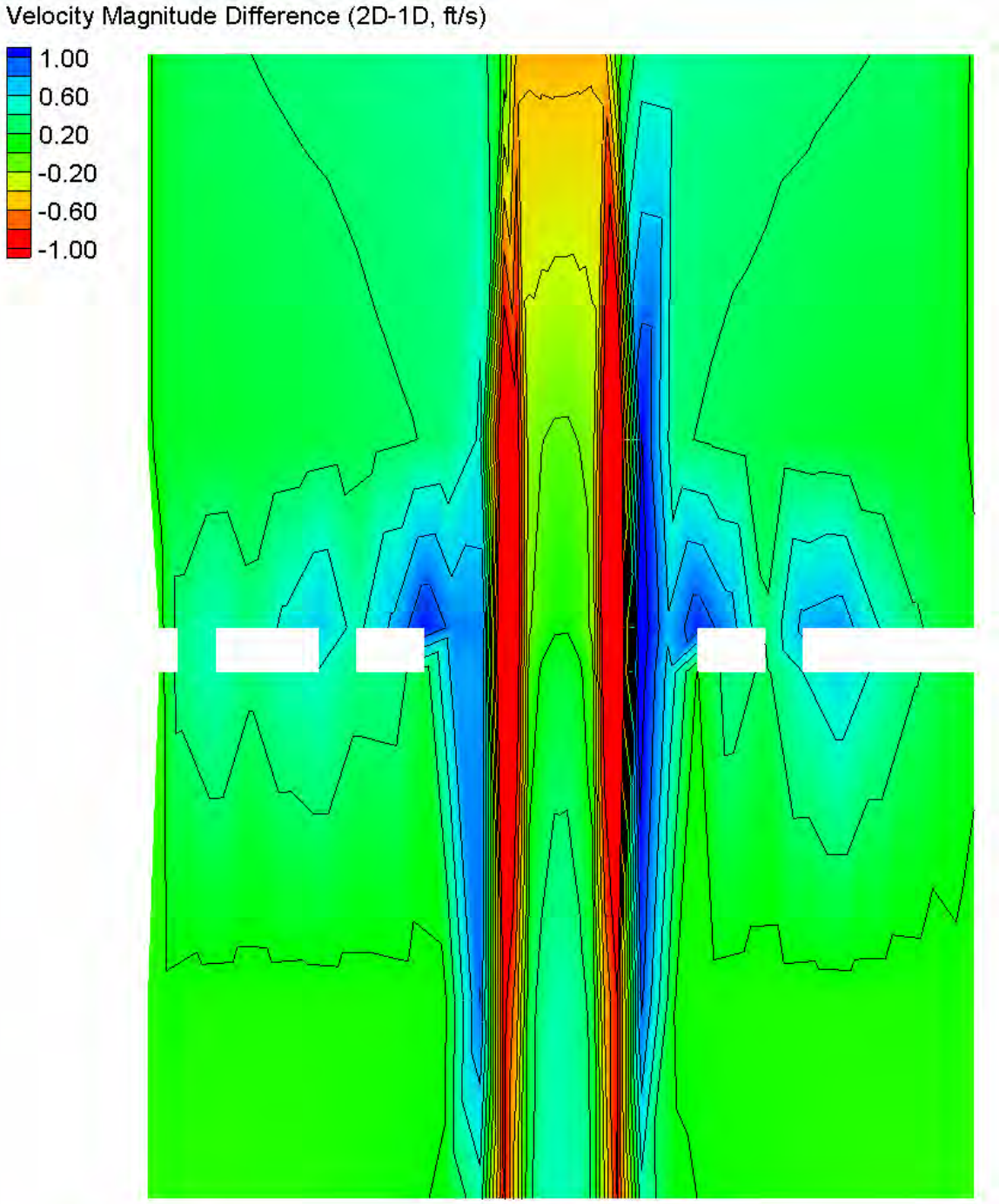

Velocity Magnitude Difference Contours – Large Channel – Multiple Openings (4)

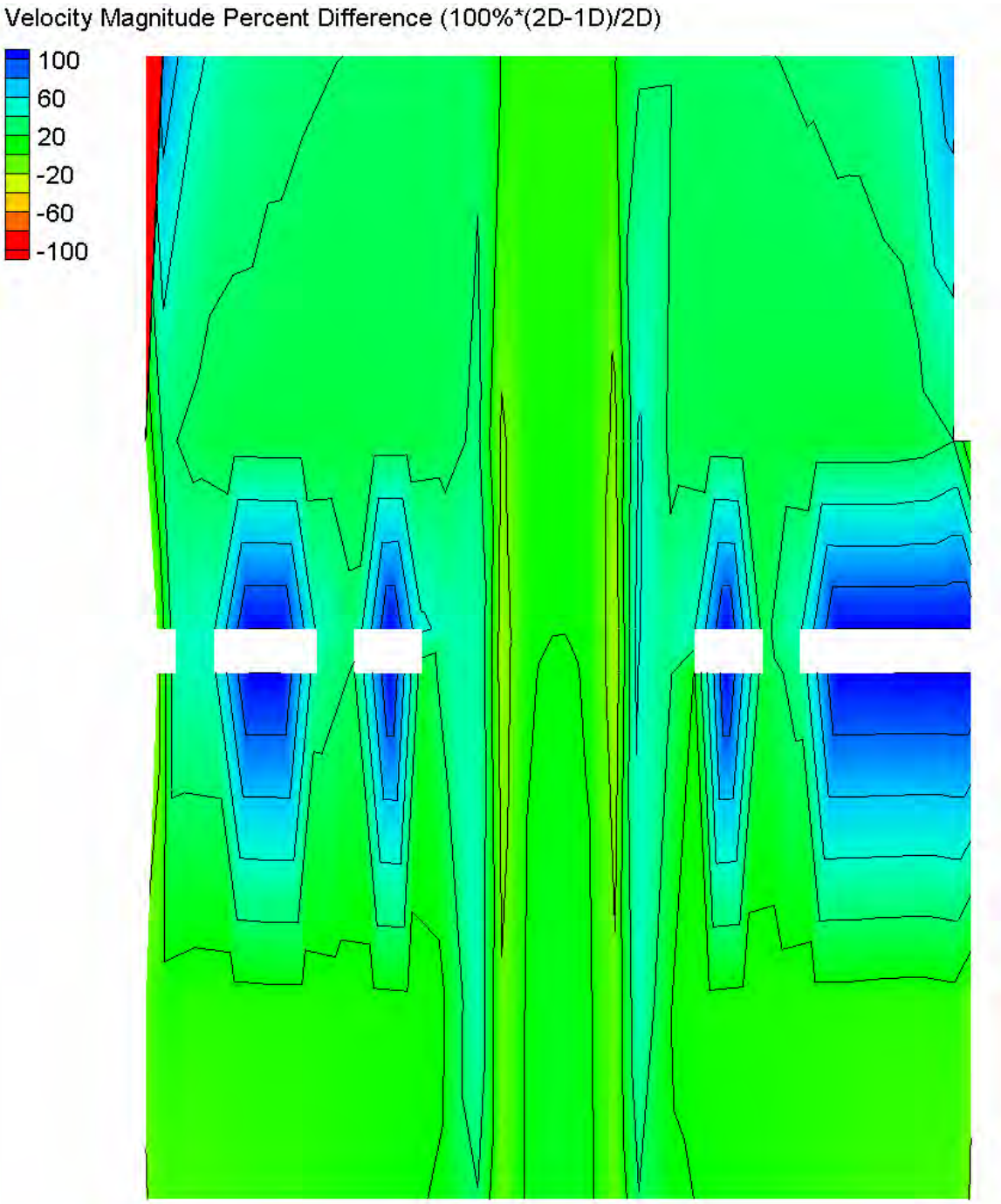

Velocity Magnitude Percent Difference Contours – Large Channel – Multiple Openings (4)

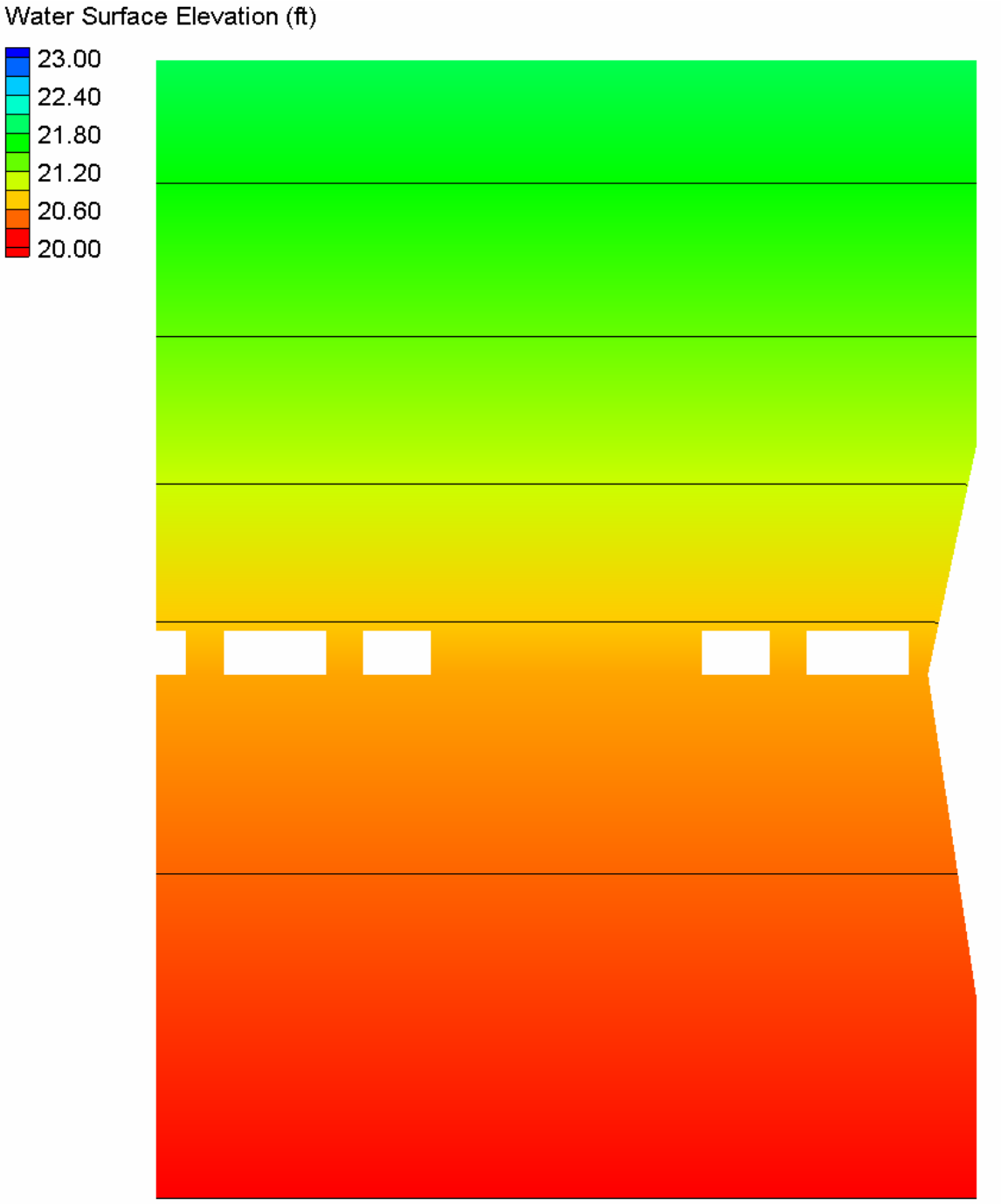

HEC-RAS Water Surface Elevation Contours – Large Channel – Multiple Openings (5)

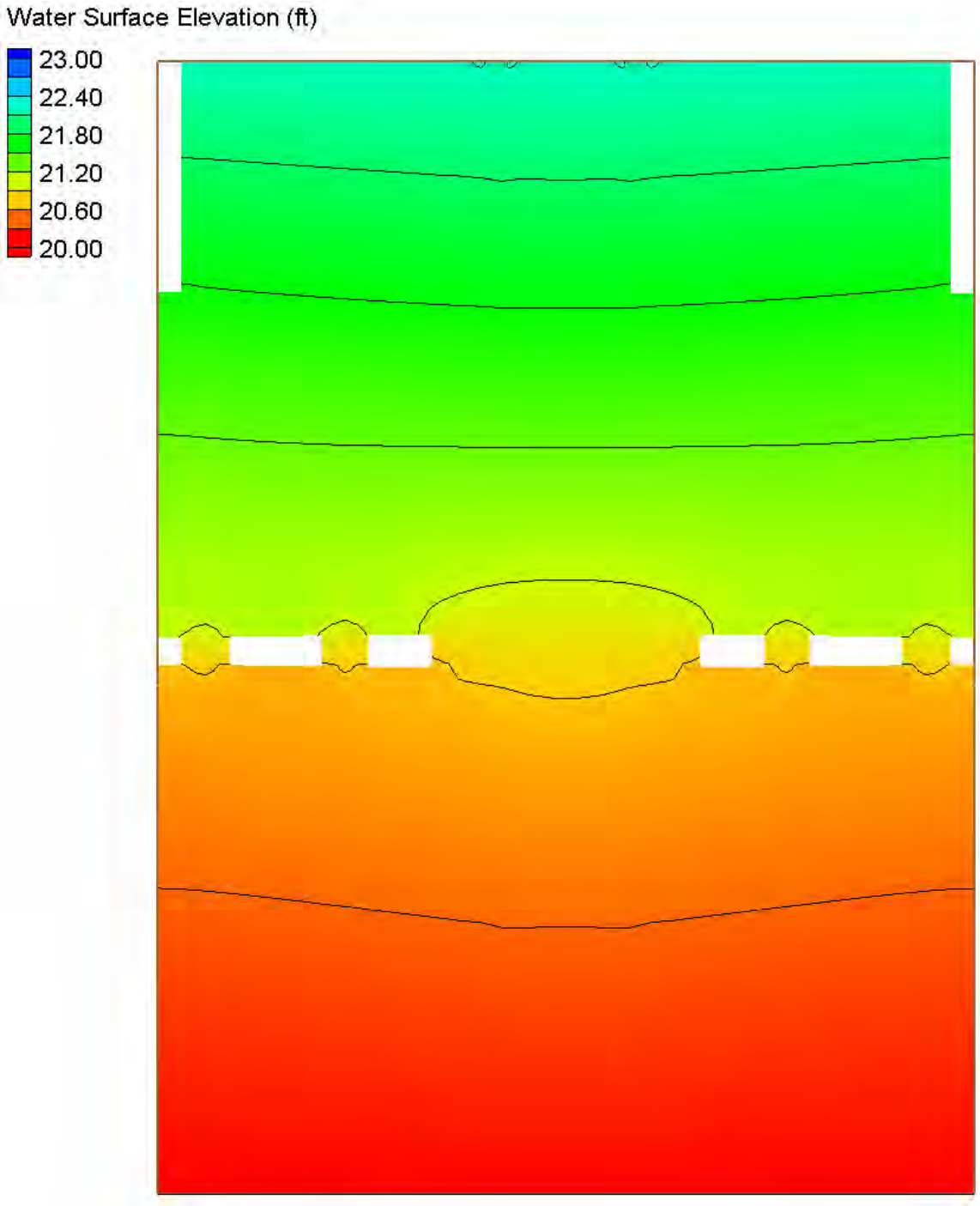

FESWMS Water Surface Elevation Contours – Large Channel – Multiple Openings (5)

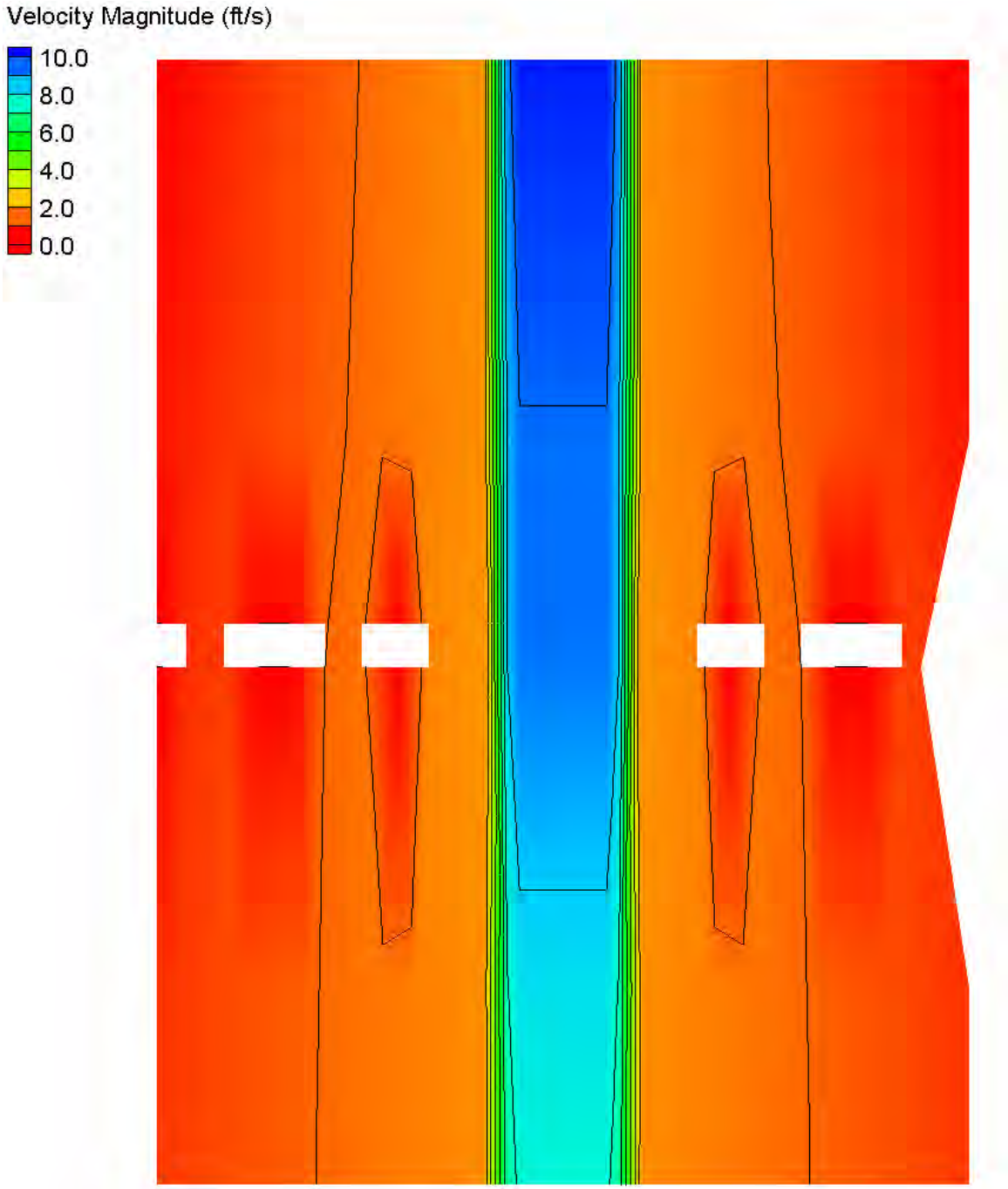

HEC-RAS Velocity Magnitude Contours – Large Channel – Multiple Openings (5)

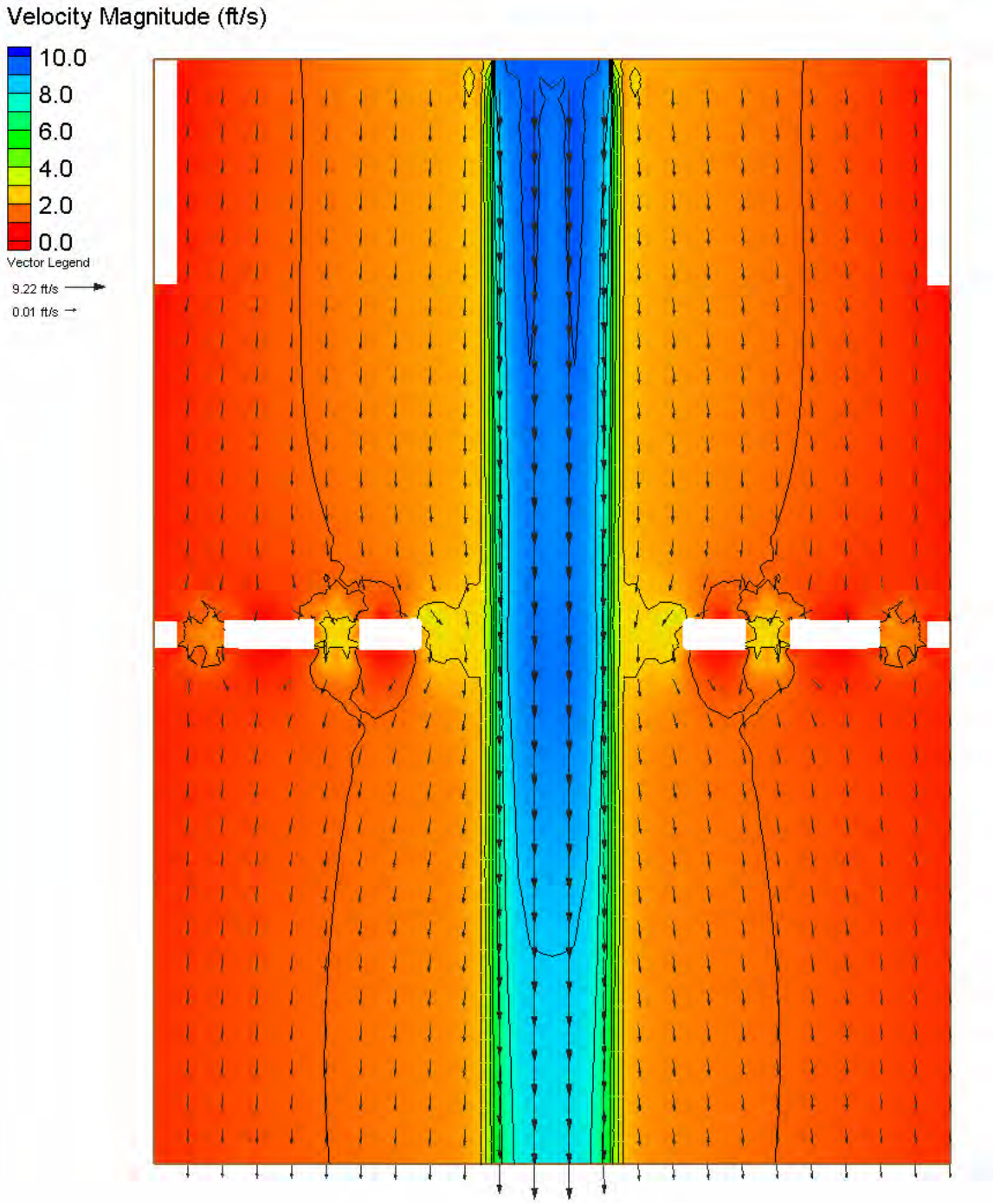

FESWMS Velocity Magnitude Contours – Large Channel – Multiple Openings (5)

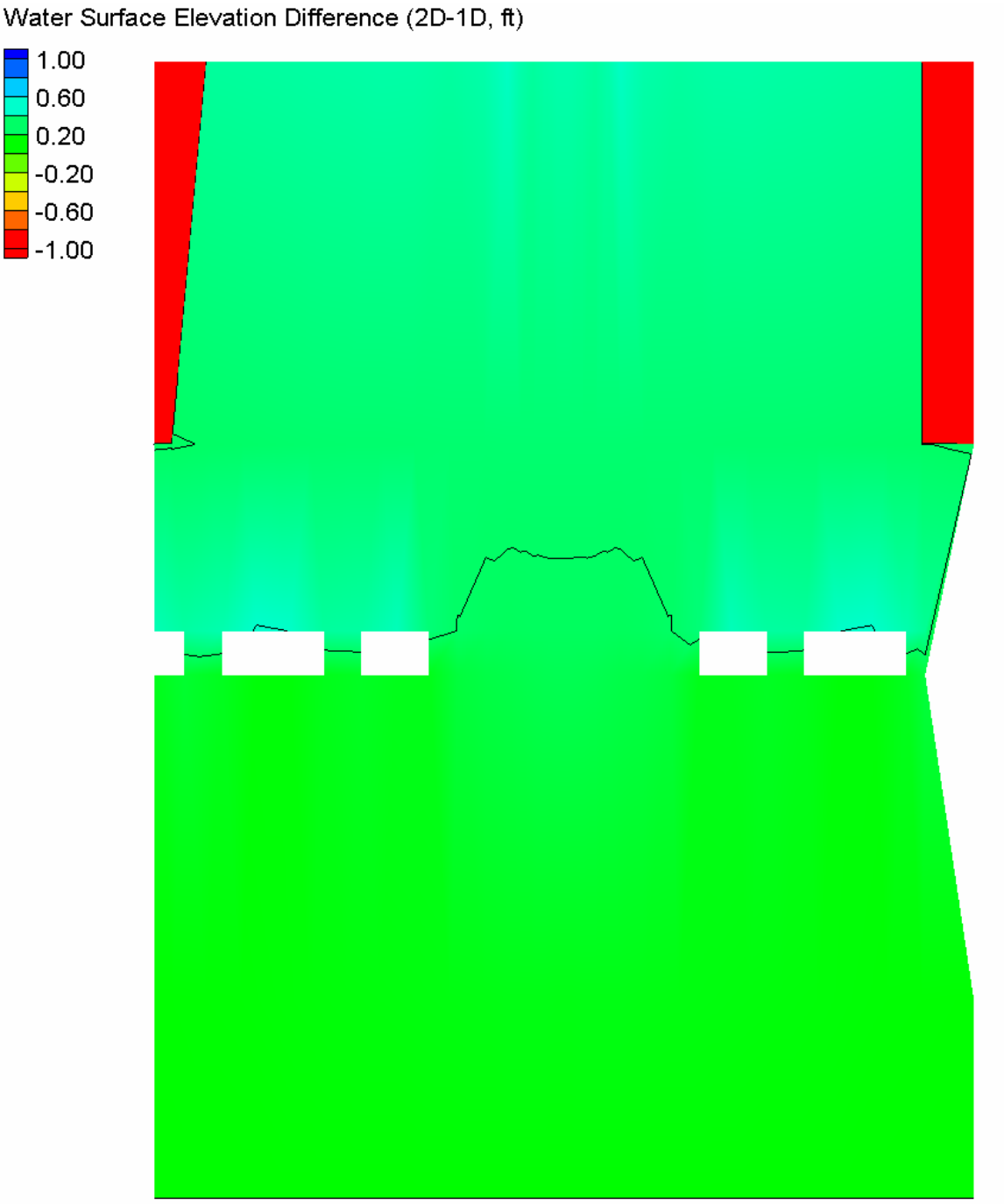

Water Surface Elevation Difference Contours – Large Channel – Multiple Openings (5)

Velocity Magnitude Difference Contours – Large Channel – Multiple Openings (5)

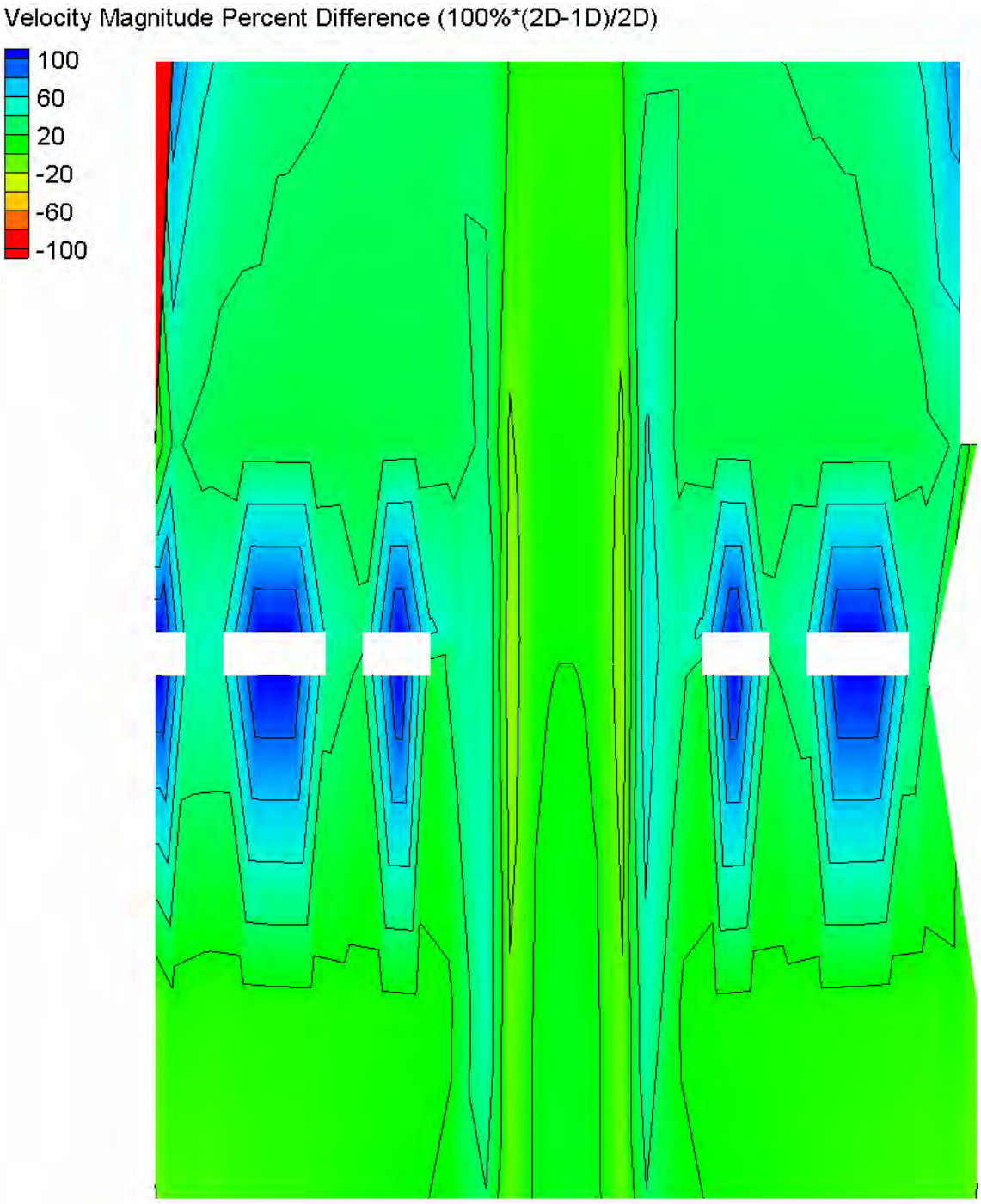

Velocity Magnitude Percent Difference Contours – Large Channel – Multiple Openings (5)

Bridges Located on River Bends

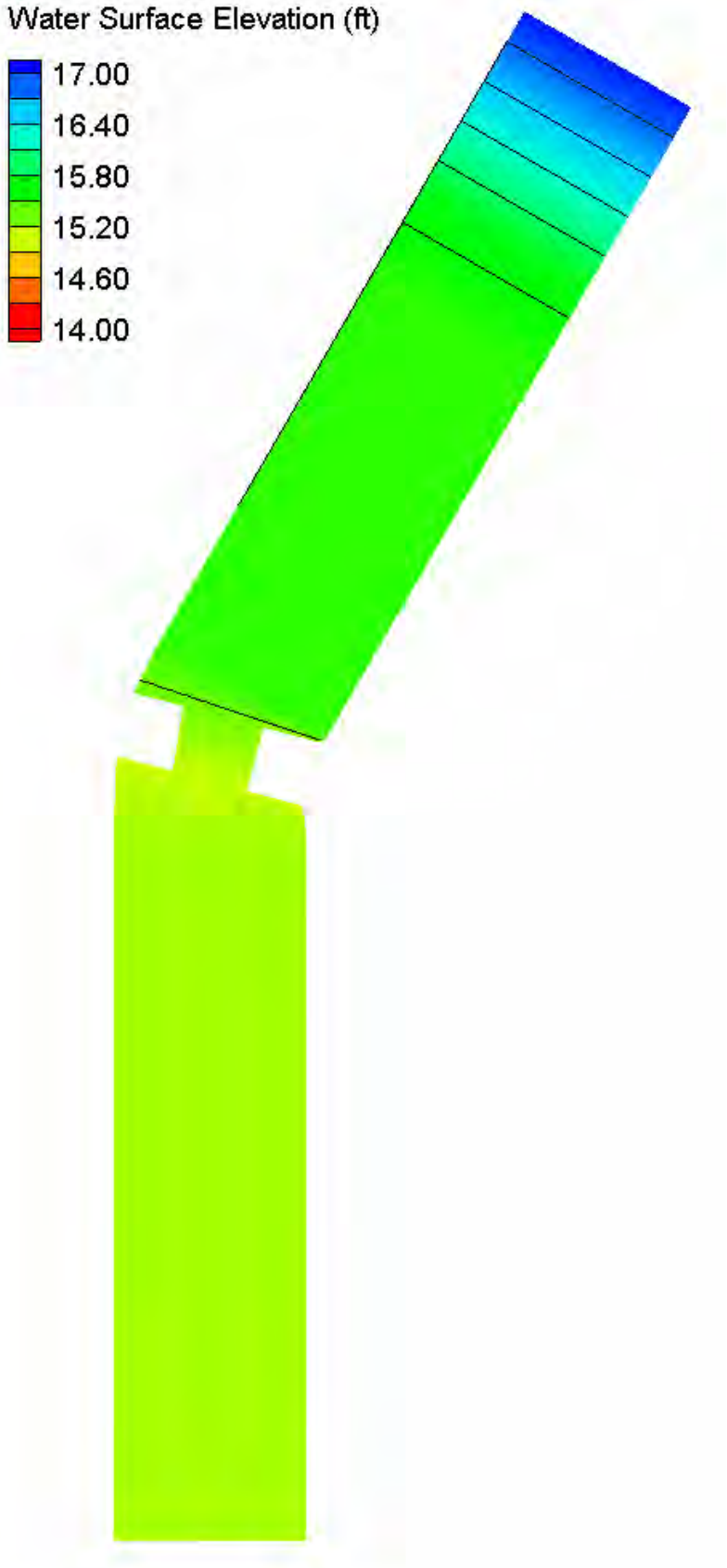

HEC-RAS Water Surface Elevation Contours – Small Channel – River Bends (30°, ½ radius)

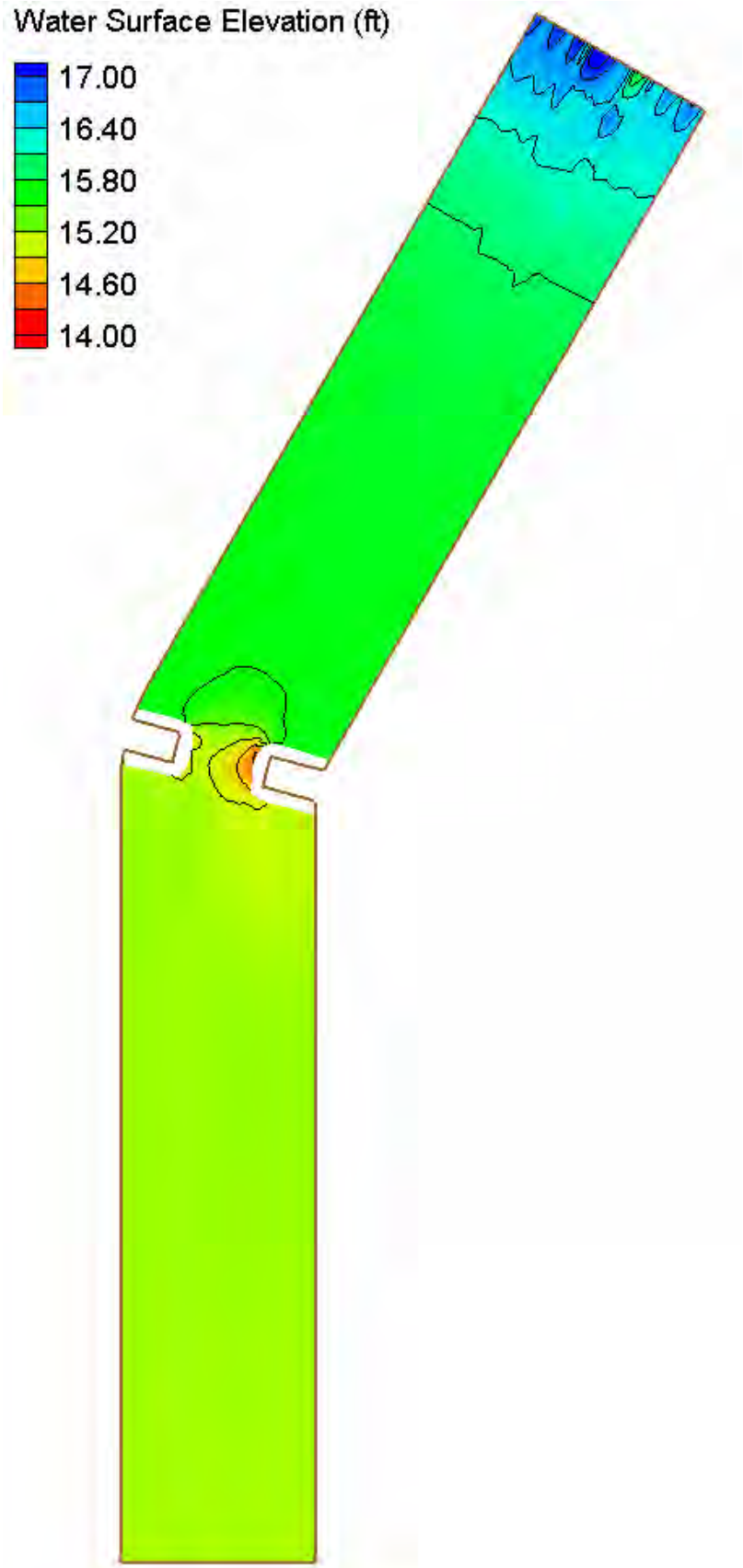

FESWMS Water Surface Elevation Contours – Small Channel – River Bends (30°, ½ radius)

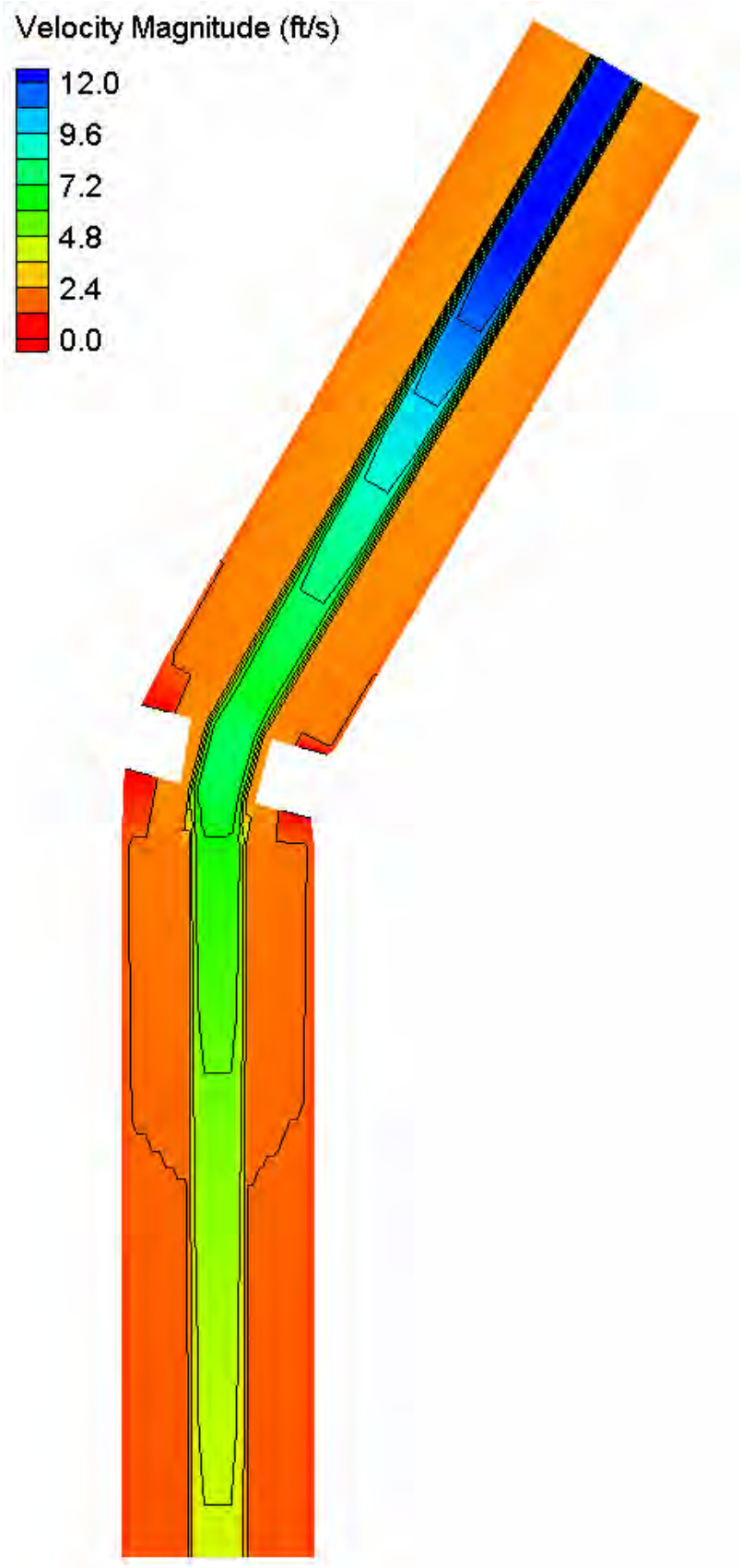

HEC-RAS Velocity Magnitude Contours – Small Channel – River Bends (30°, ½ radius)

FESWMS Velocity Magnitude Contours – Small Channel – River Bends (30°, ½ radius)

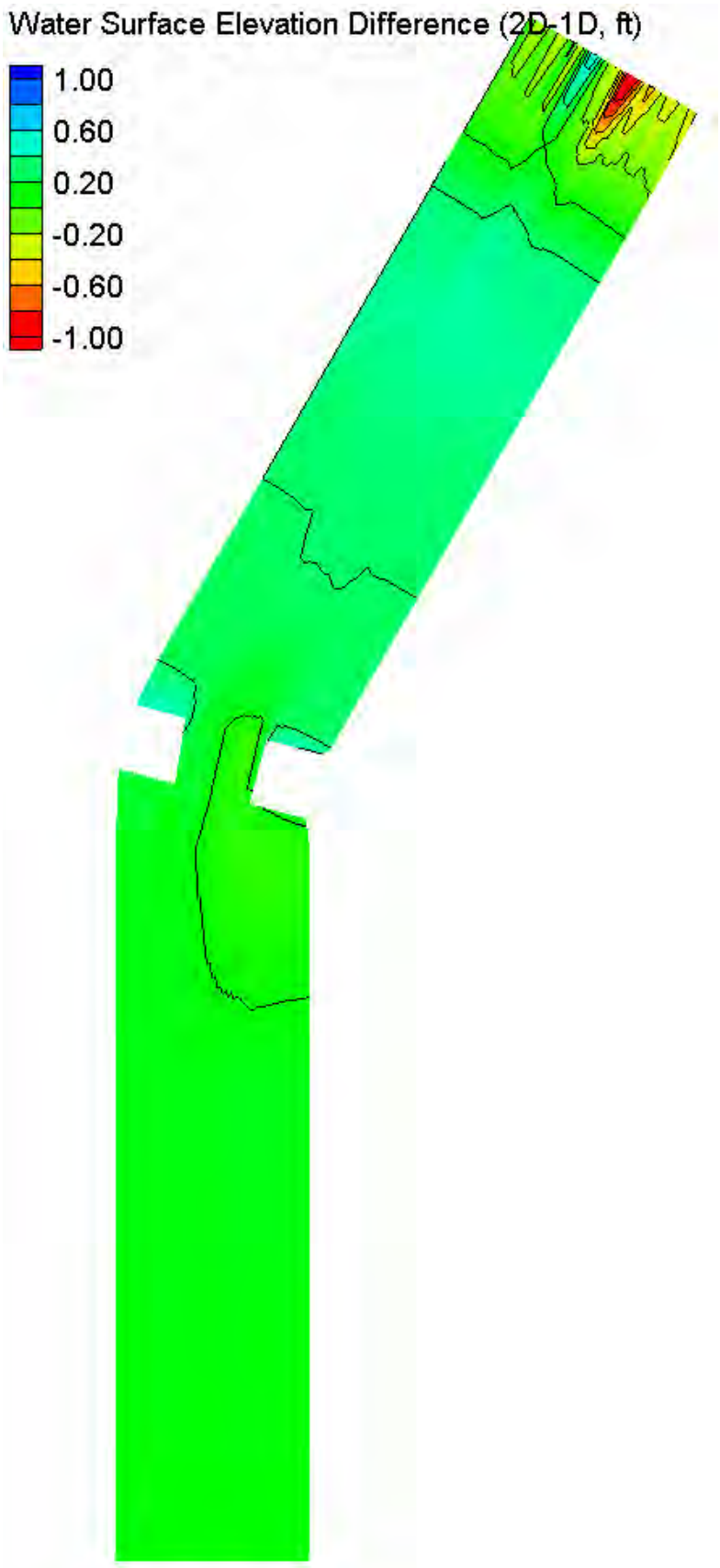

Water Surface Elevation Difference Contours – Small Channel – River Bends (30°, ½ radius)

Velocity Magnitude Difference Contours – Small Channel – River Bends (30°, ½ radius)

Velocity Magnitude Percent Difference Contours – Small Channel – River Bends (30°, ½ radius)

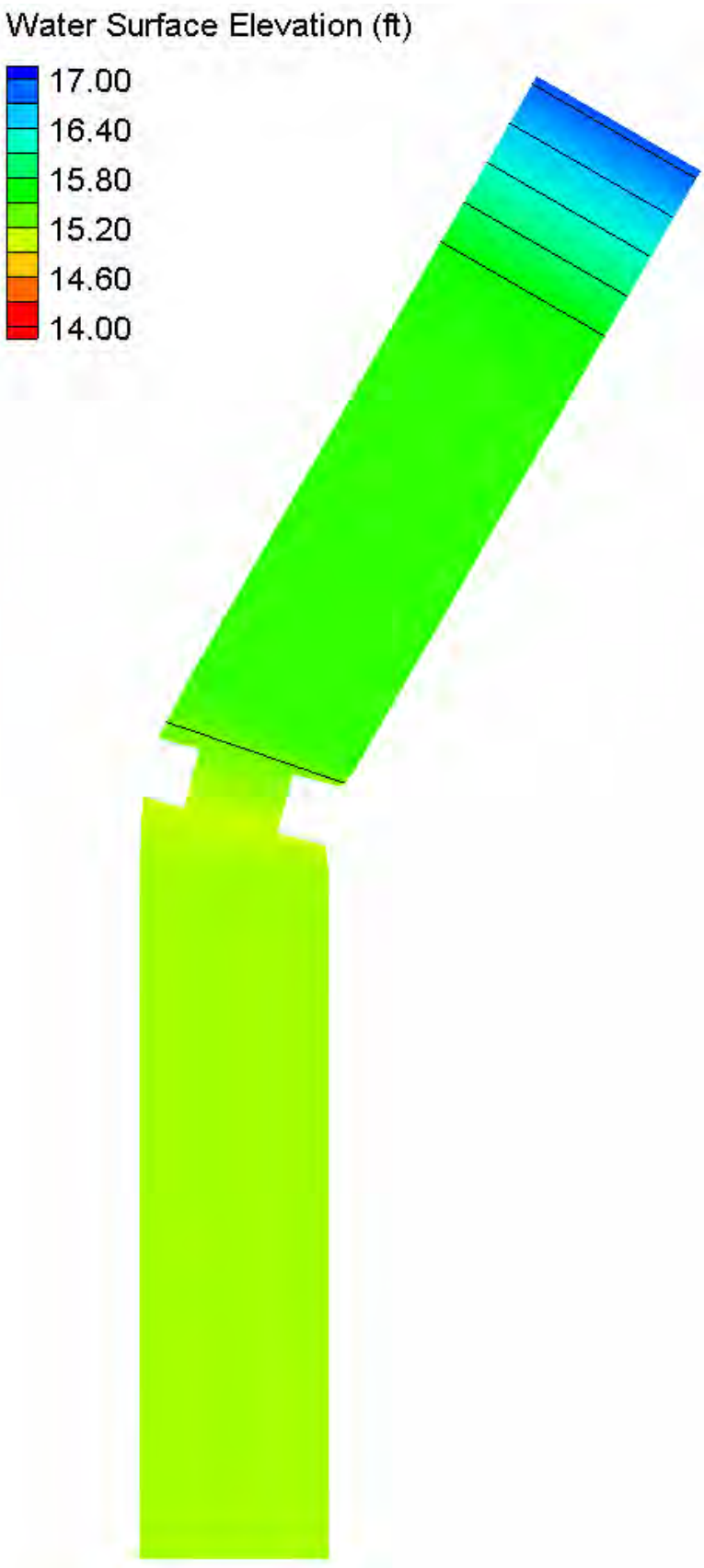

HEC-RAS Water Surface Elevation Contours – Small Channel – River Bends (30°, ¼ radius)

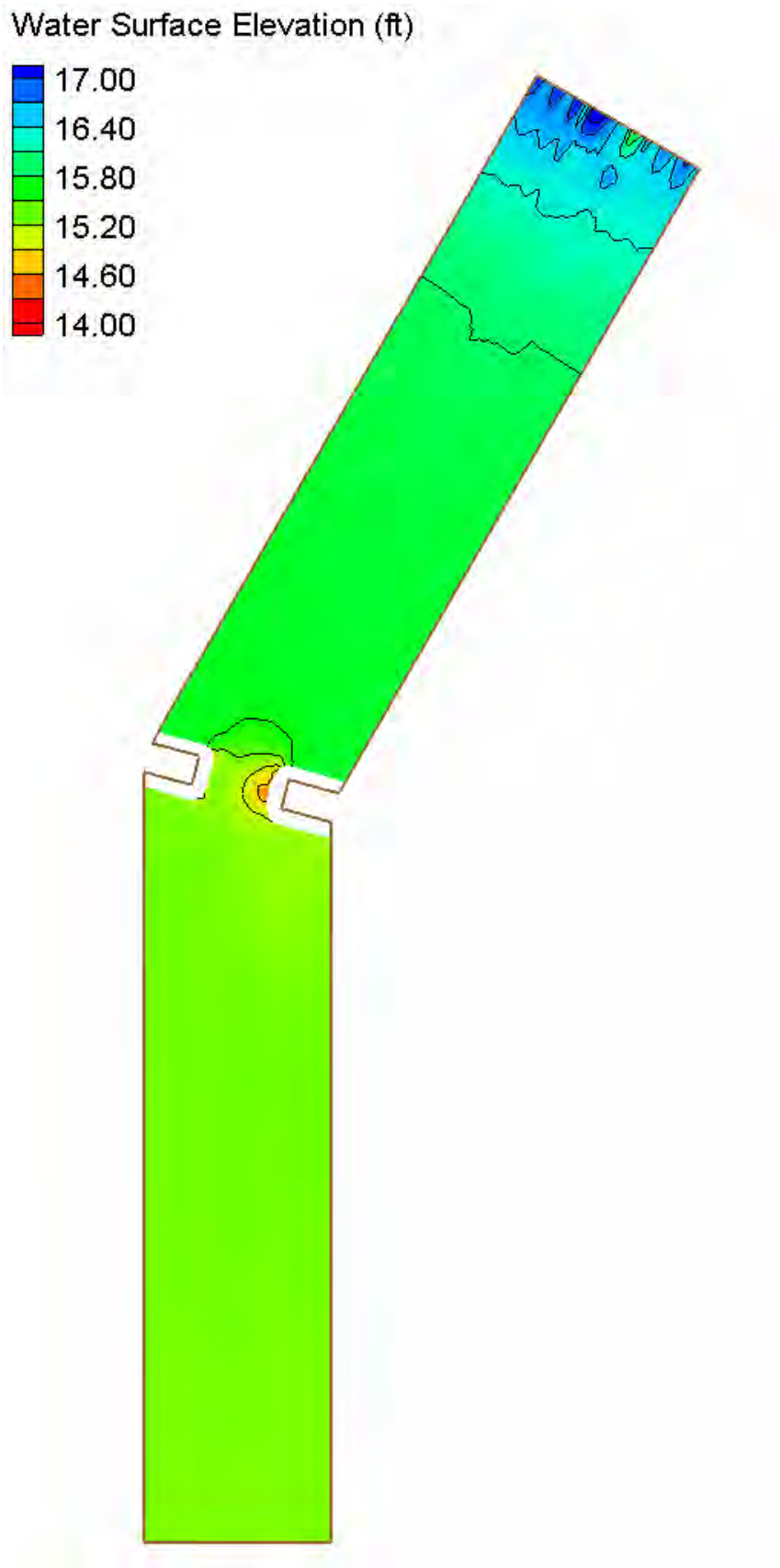

FESWMS Water Surface Elevation Contours – Small Channel – River Bends (30°, ¼ radius)

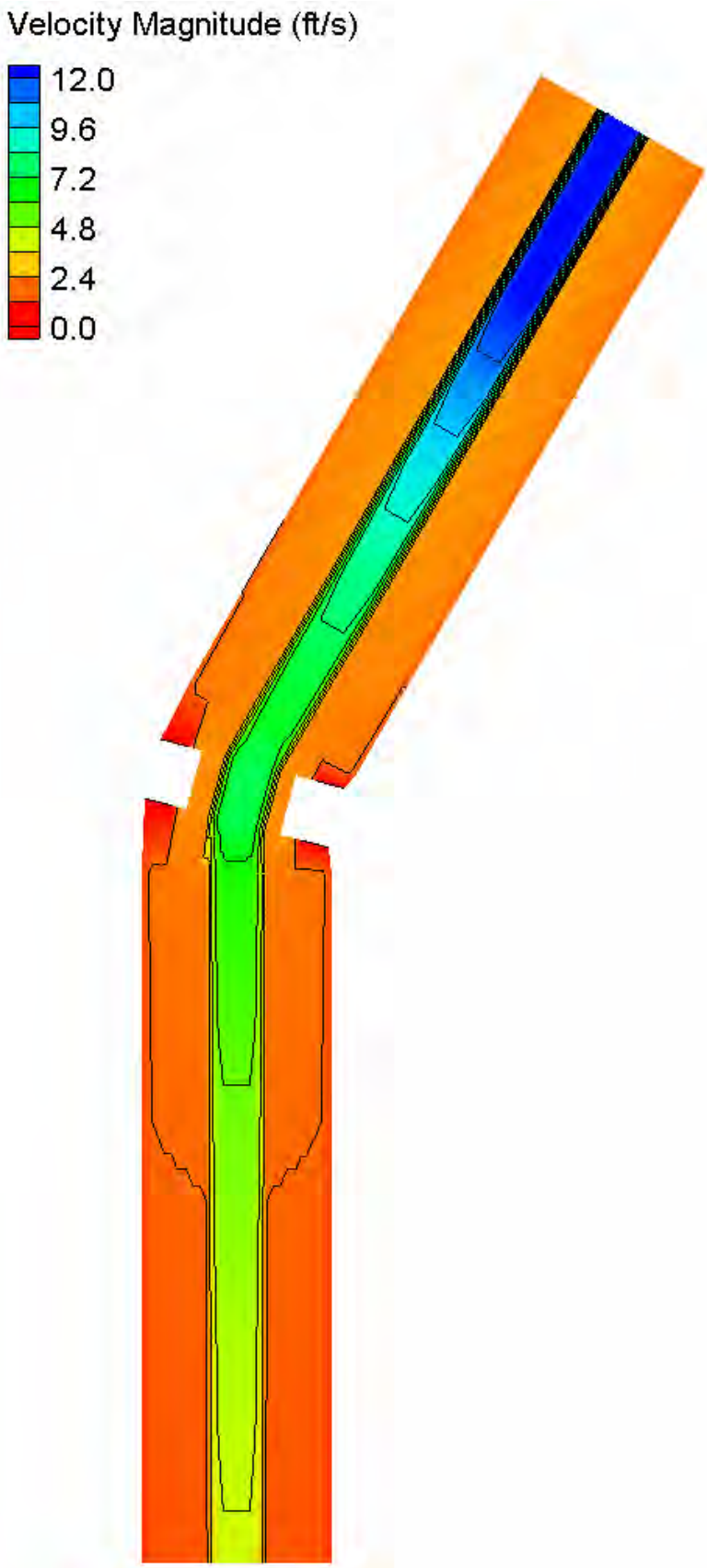

HEC-RAS Velocity Magnitude Contours – Small Channel – River Bends (30°, ¼ radius)

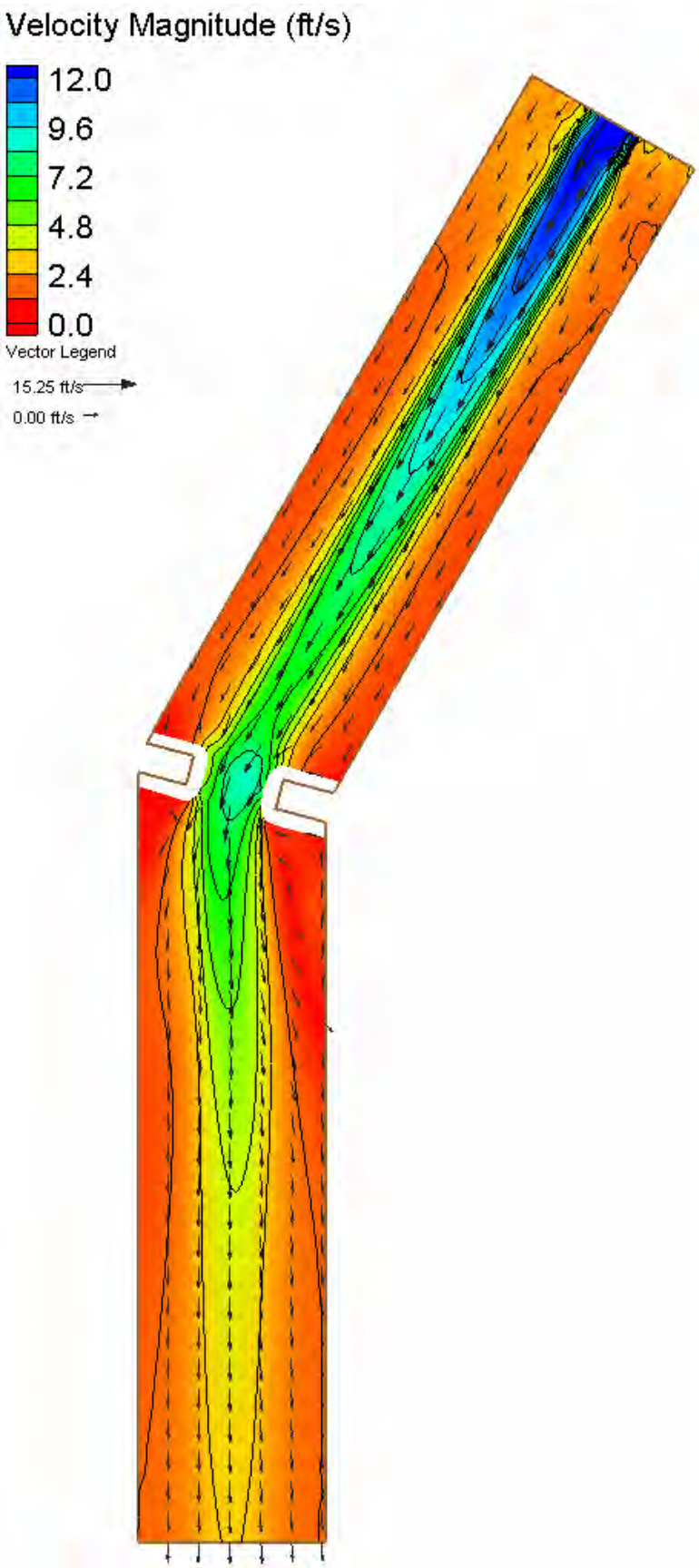

FESWMS Velocity Magnitude Contours – Small Channel – River Bends (30°, ¼ radius)

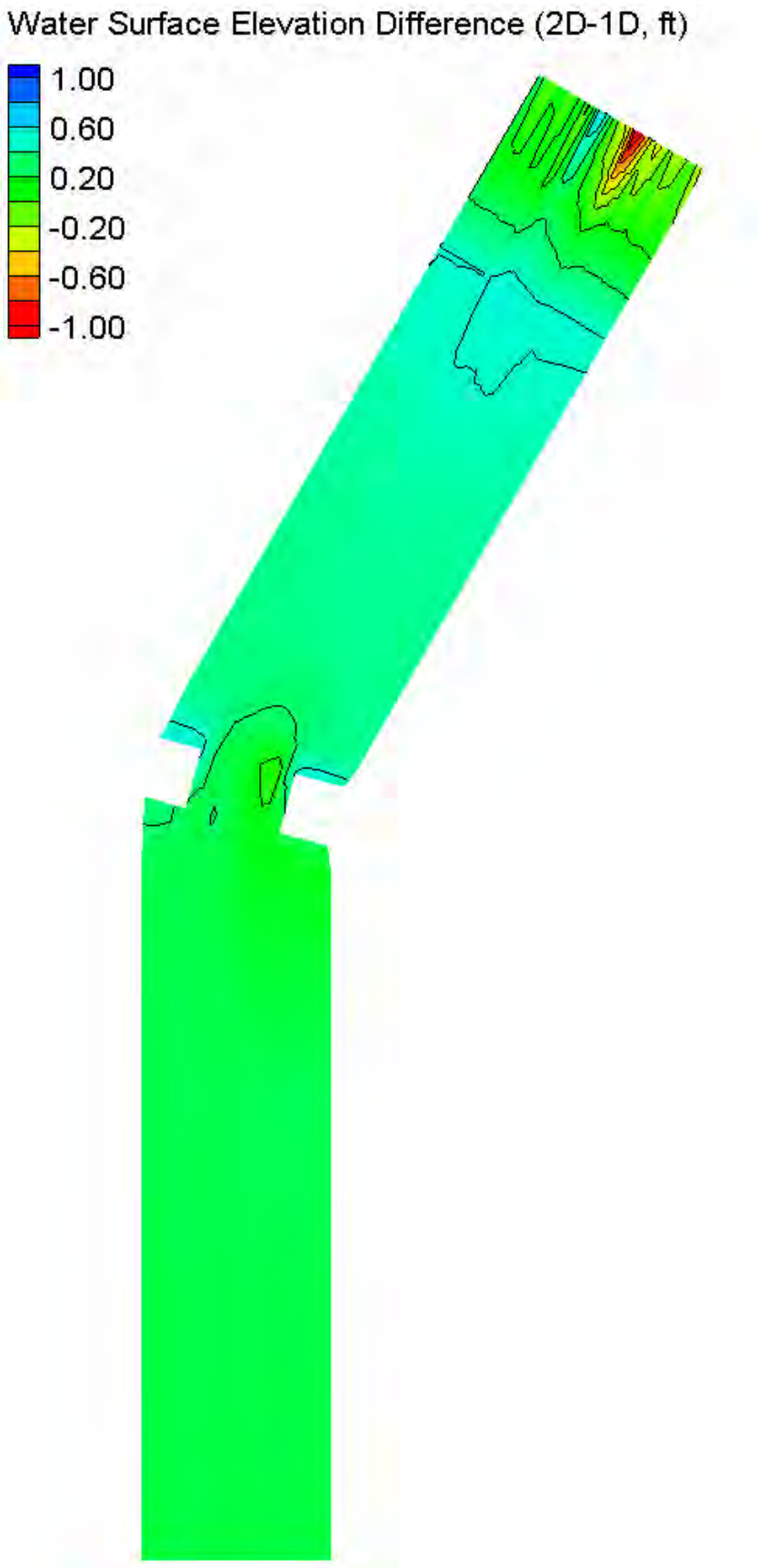

Water Surface Elevation Difference Contours – Small Channel – River Bends (30°, ¼ radius)

Velocity Magnitude Difference Contours – Small Channel – River Bends (30°, ¼ radius)

Velocity Magnitude Percent Difference Contours – Small Channel – River Bends (30°, ¼ radius)

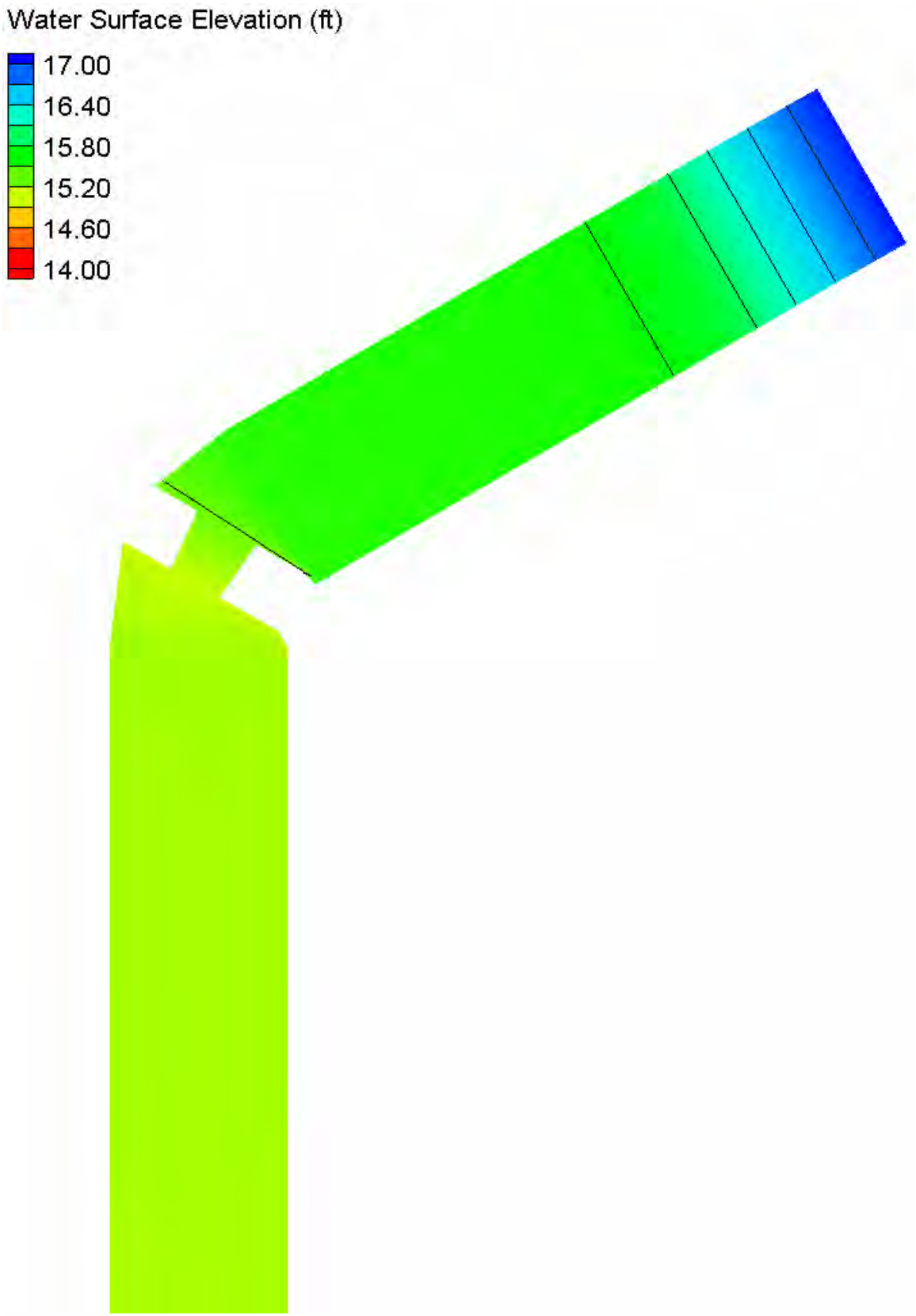

HEC-RAS Water Surface Elevation Contours – Small Channel – River Bends (60°, ½ radius)

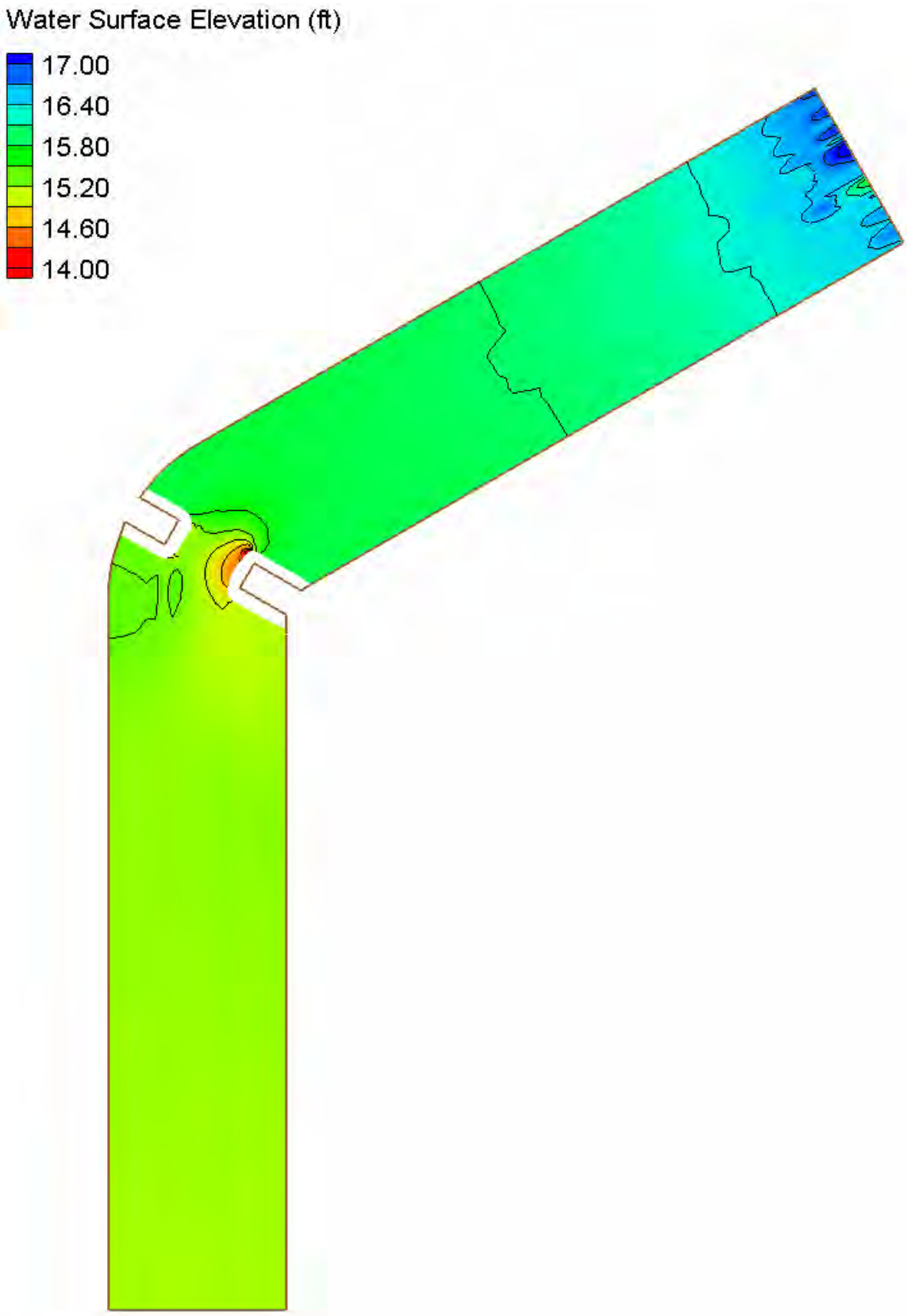

FESWMS Water Surface Elevation Contours – Small Channel – River Bends (60°, ½ radius)

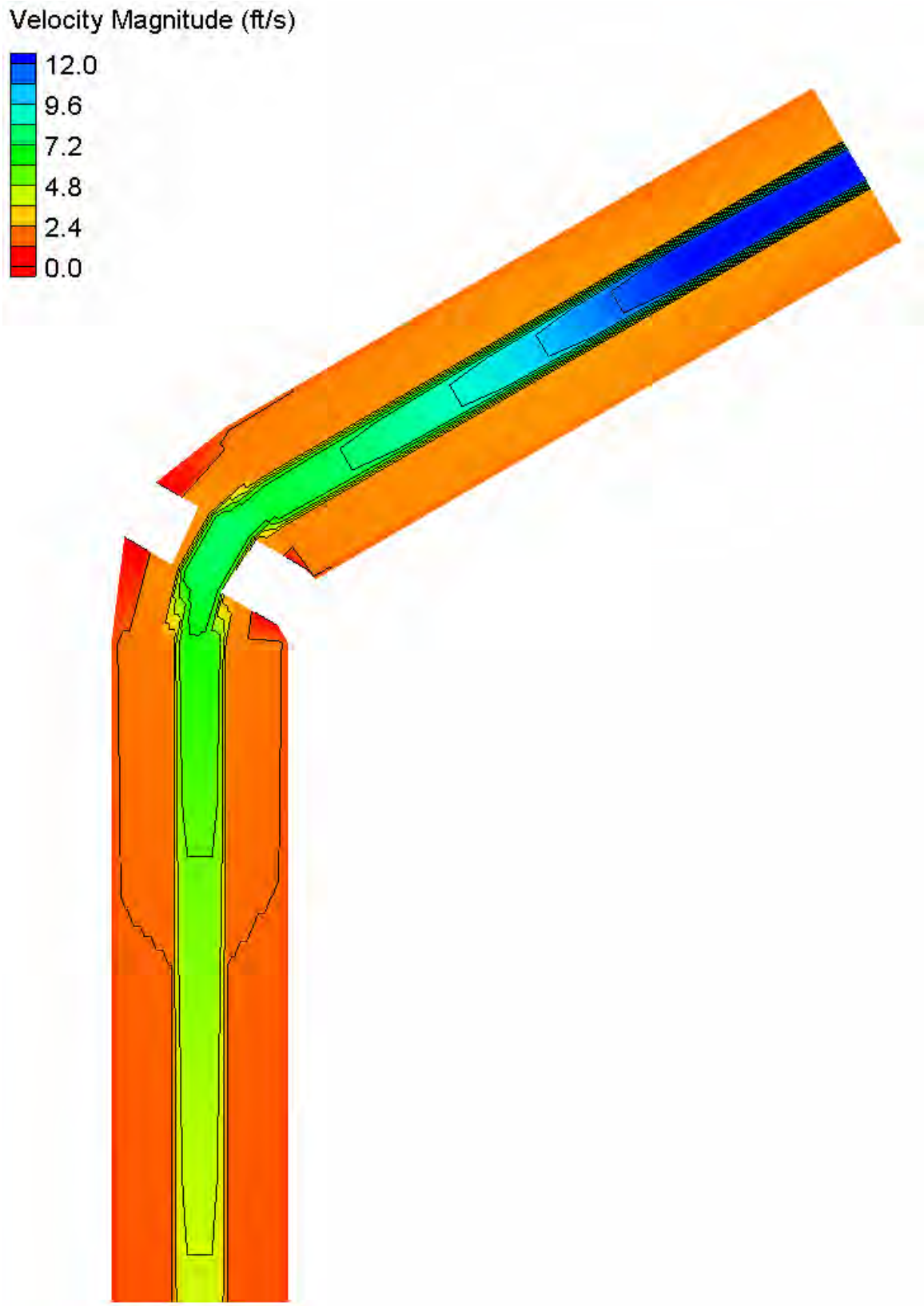

HEC-RAS Velocity Magnitude Contours – Small Channel – River Bends (60°, ½ radius)

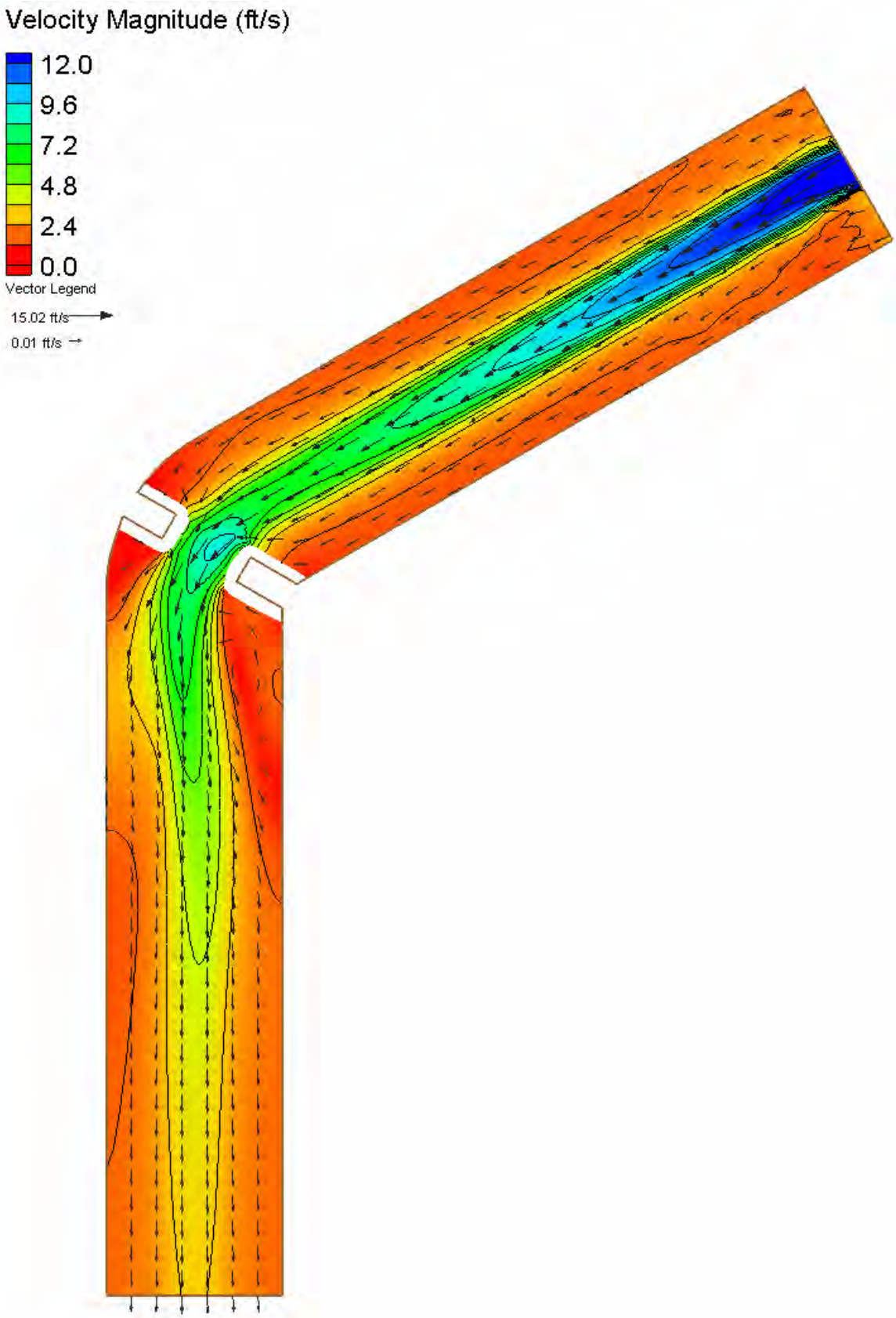

FESWMS Velocity Magnitude Contours – Small Channel – River Bends (60°, ½ radius)

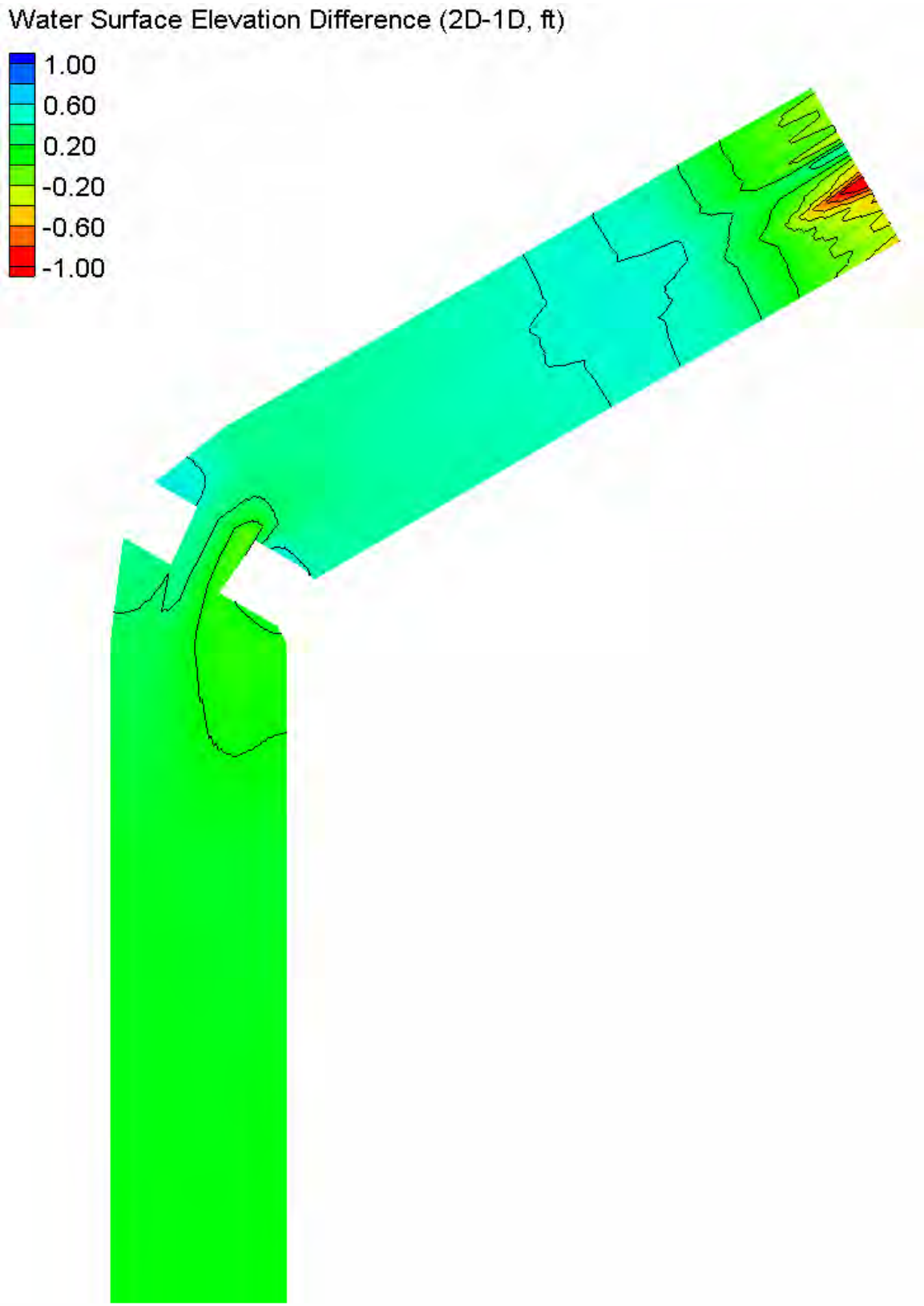

Water Surface Elevation Difference Contours – Small Channel – River Bends (60°, ½ radius)

Velocity Magnitude Difference Contours – Small Channel – River Bends (60°, ½ radius)

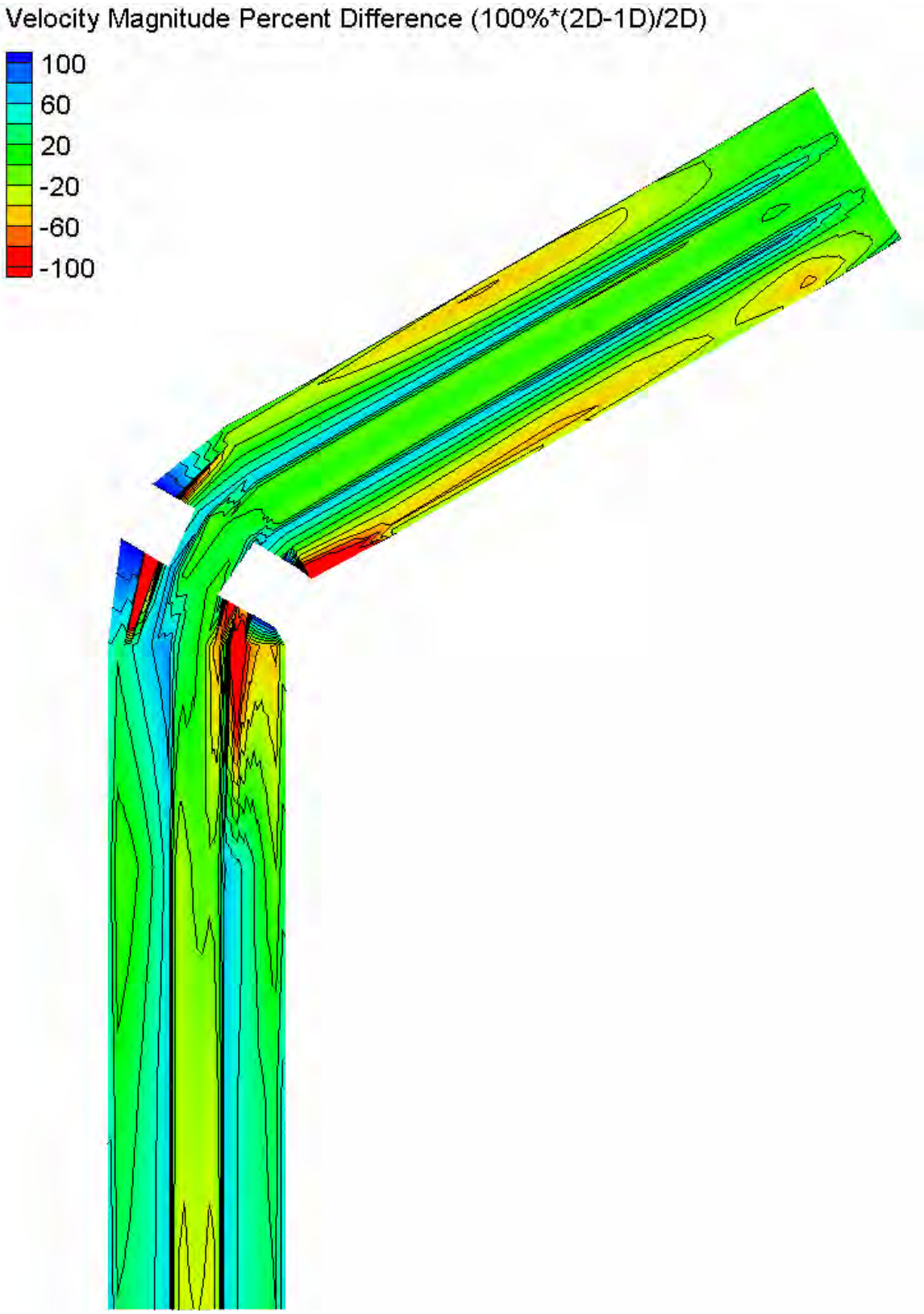

Velocity Magnitude Percent Difference Contours – Small Channel – River Bends (60°, ½ radius)

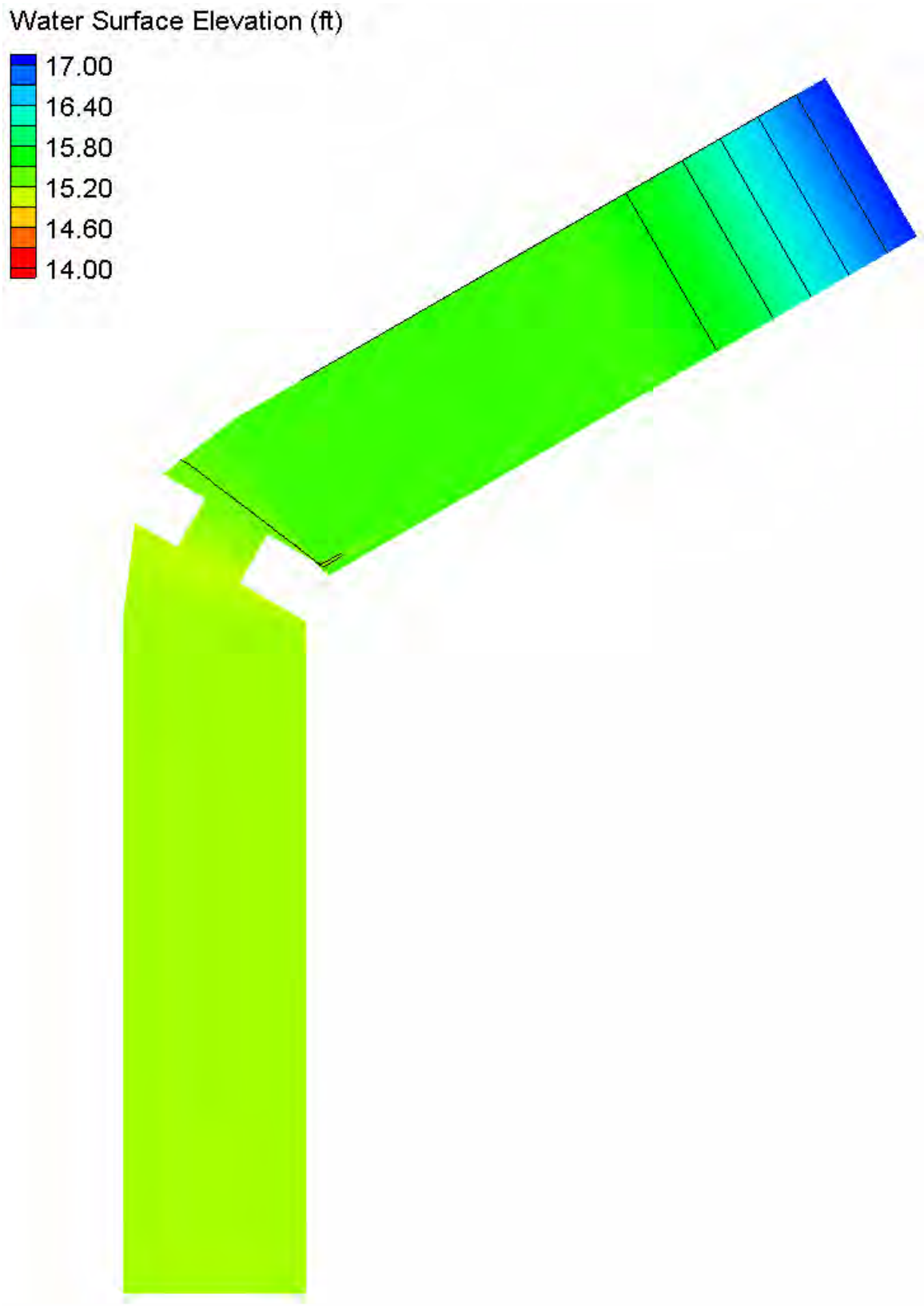

HEC-RAS Water Surface Elevation Contours – Small Channel – River Bends (60°, ¼ radius)

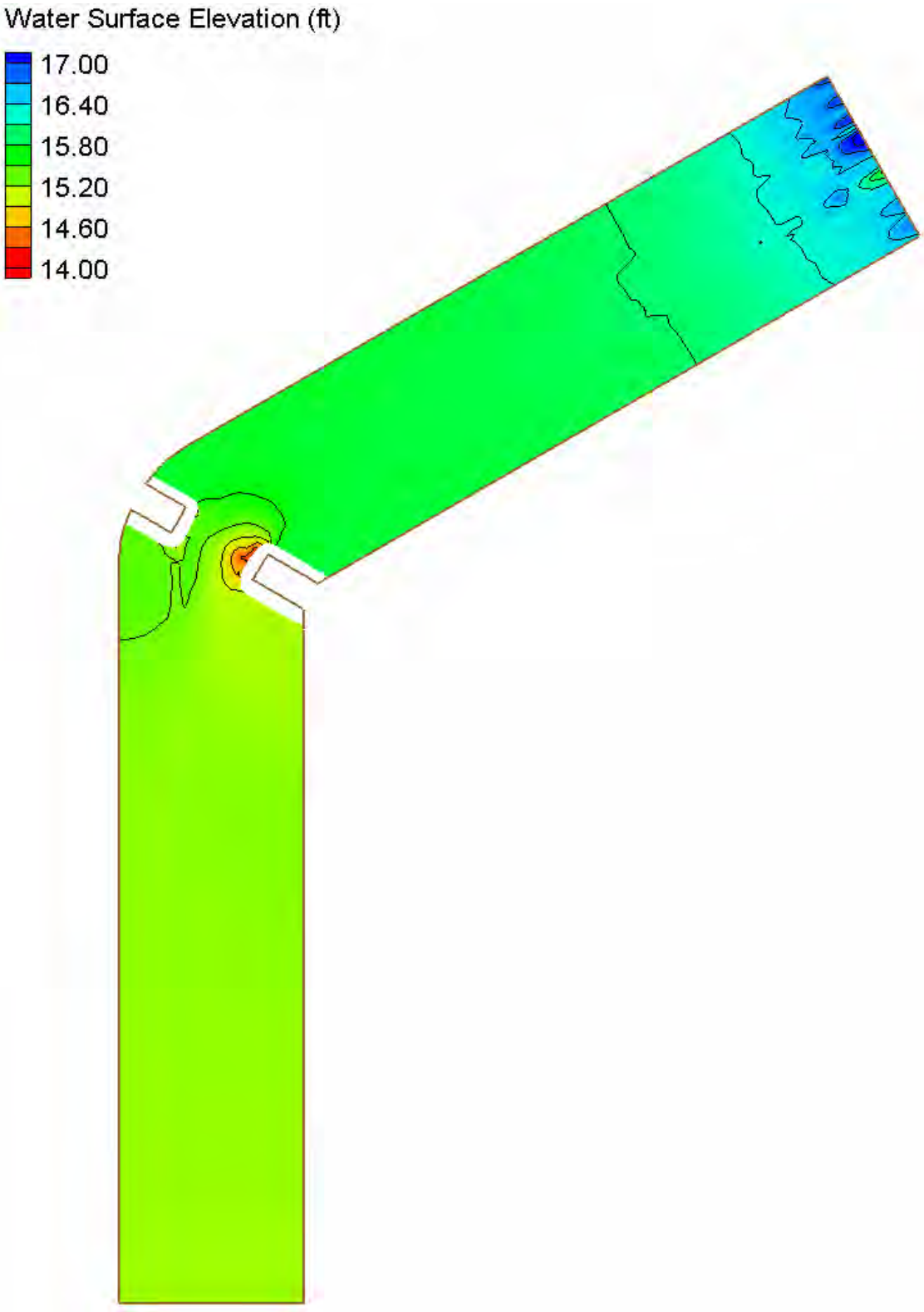

FESWMS Water Surface Elevation Contours – Small Channel – River Bends (60°, ¼ radius)

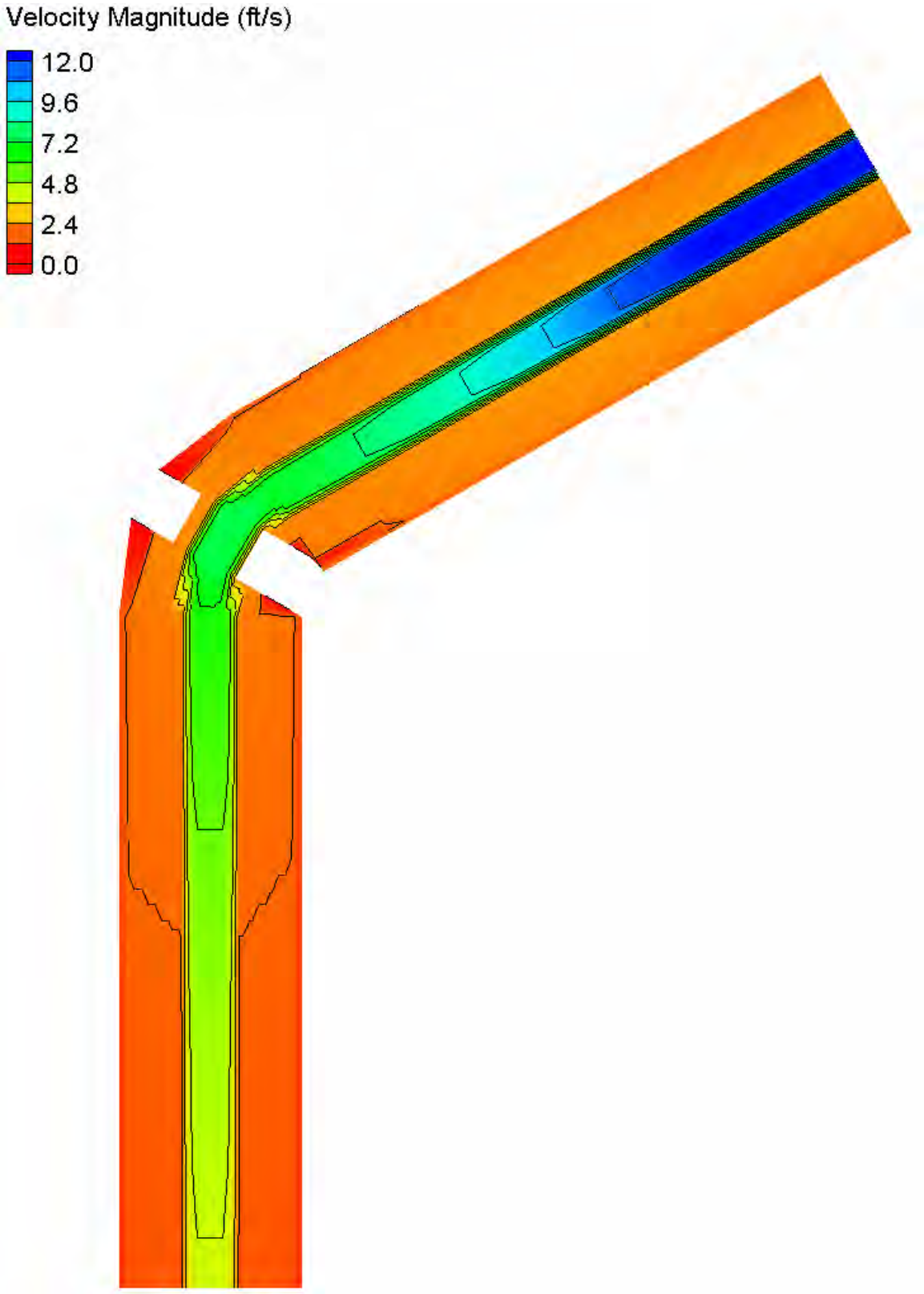

HEC-RAS Velocity Magnitude Contours – Small Channel – River Bends (60°, ¼ radius)

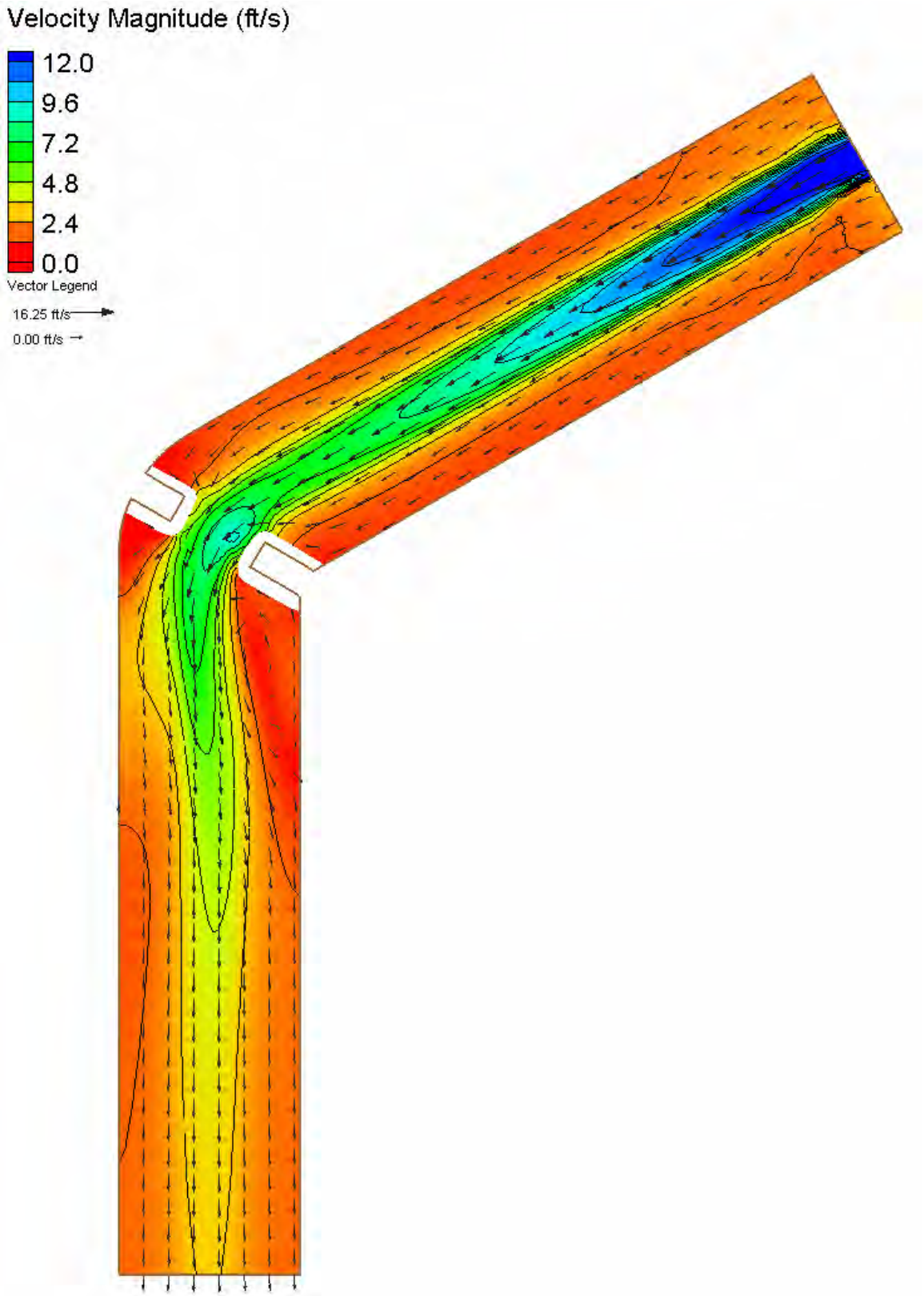

FESWMS Velocity Magnitude Contours – Small Channel – River Bends (60°, ¼ radius)

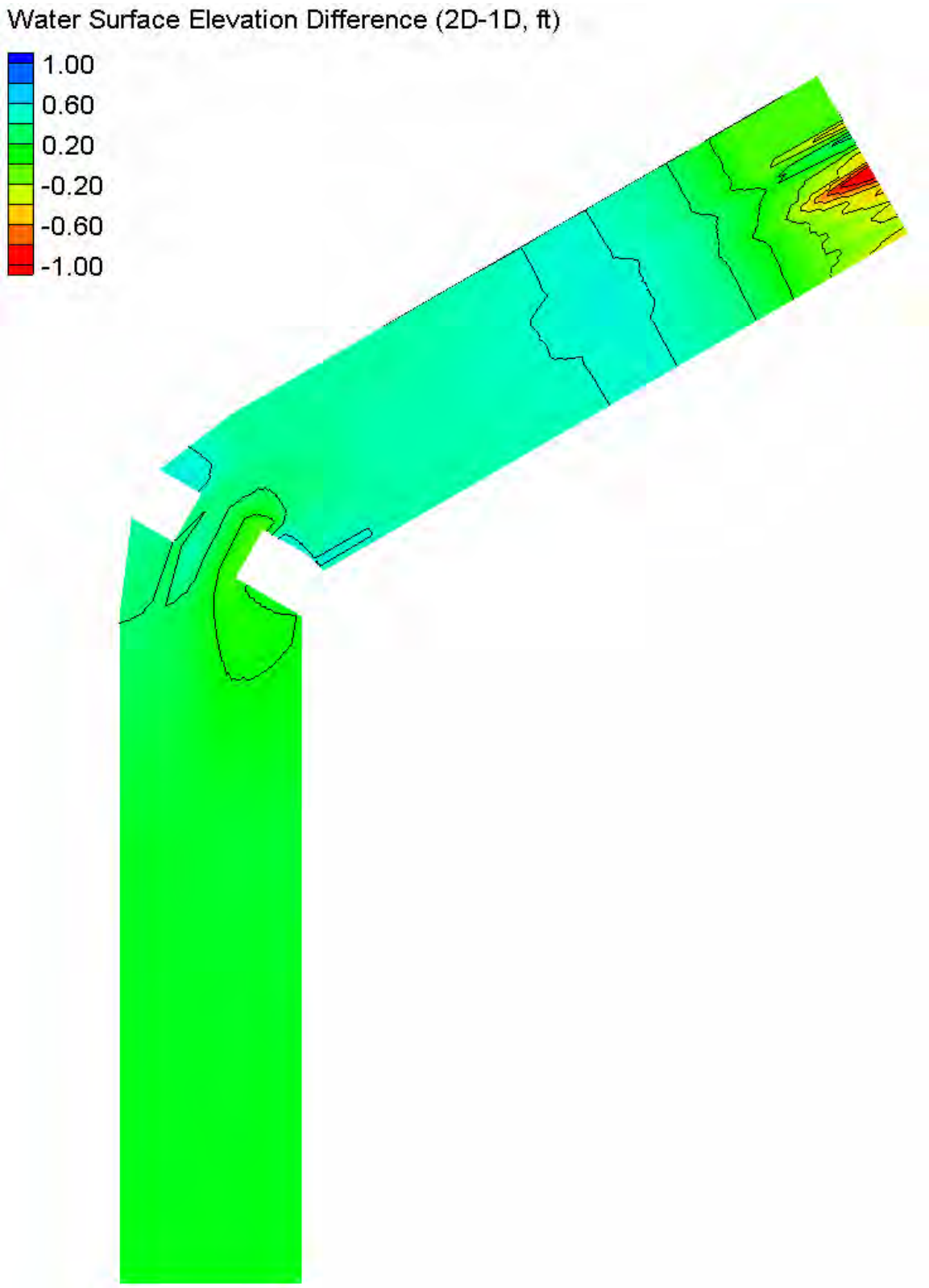

Water Surface Elevation Difference Contours – Small Channel – River Bends (60°, ¼ radius)

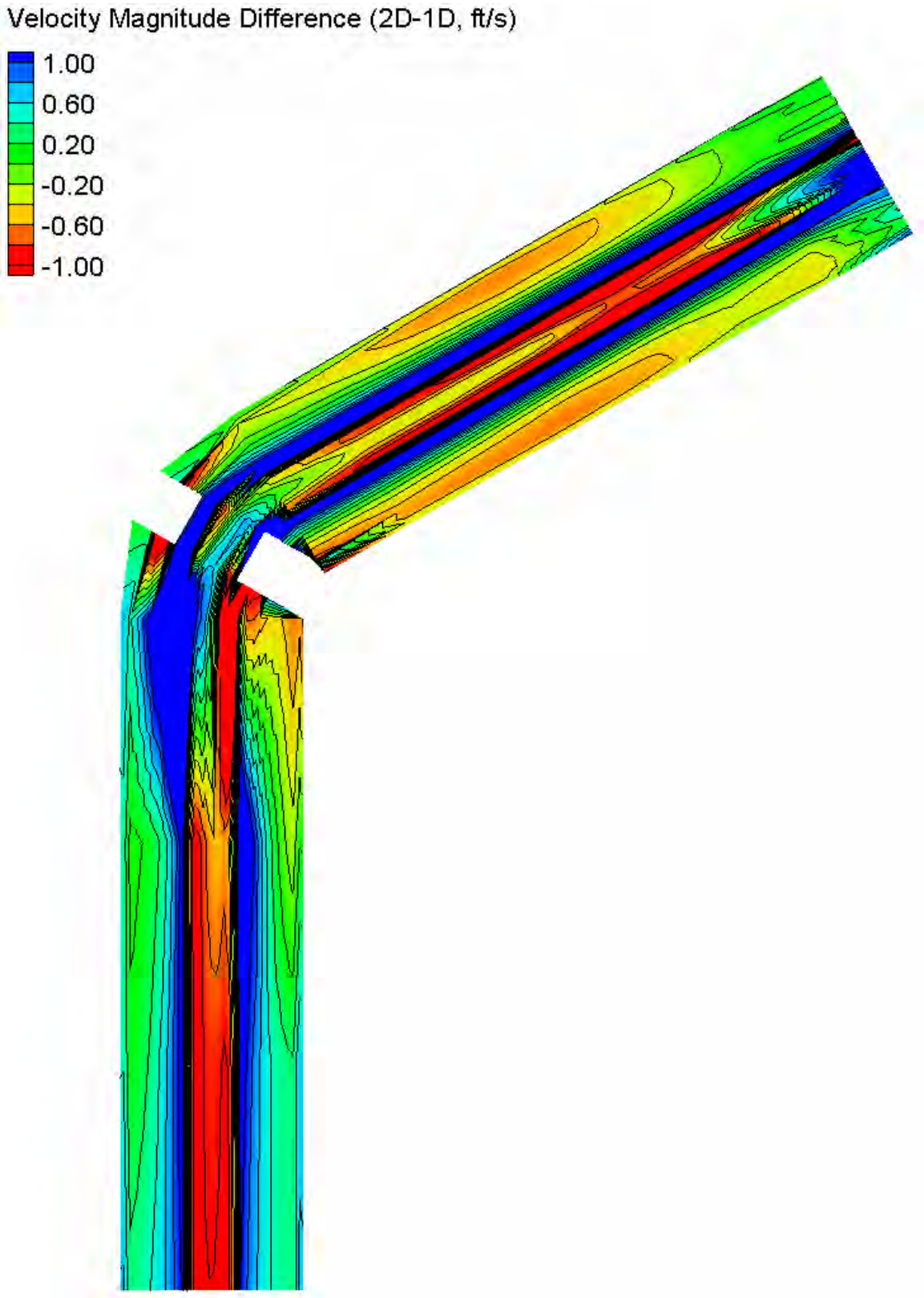

Velocity Magnitude Difference Contours – Small Channel – River Bends (60°, ¼ radius)

Velocity Magnitude Percent Difference Contours – Small Channel – River Bends (60°, ¼ radius)

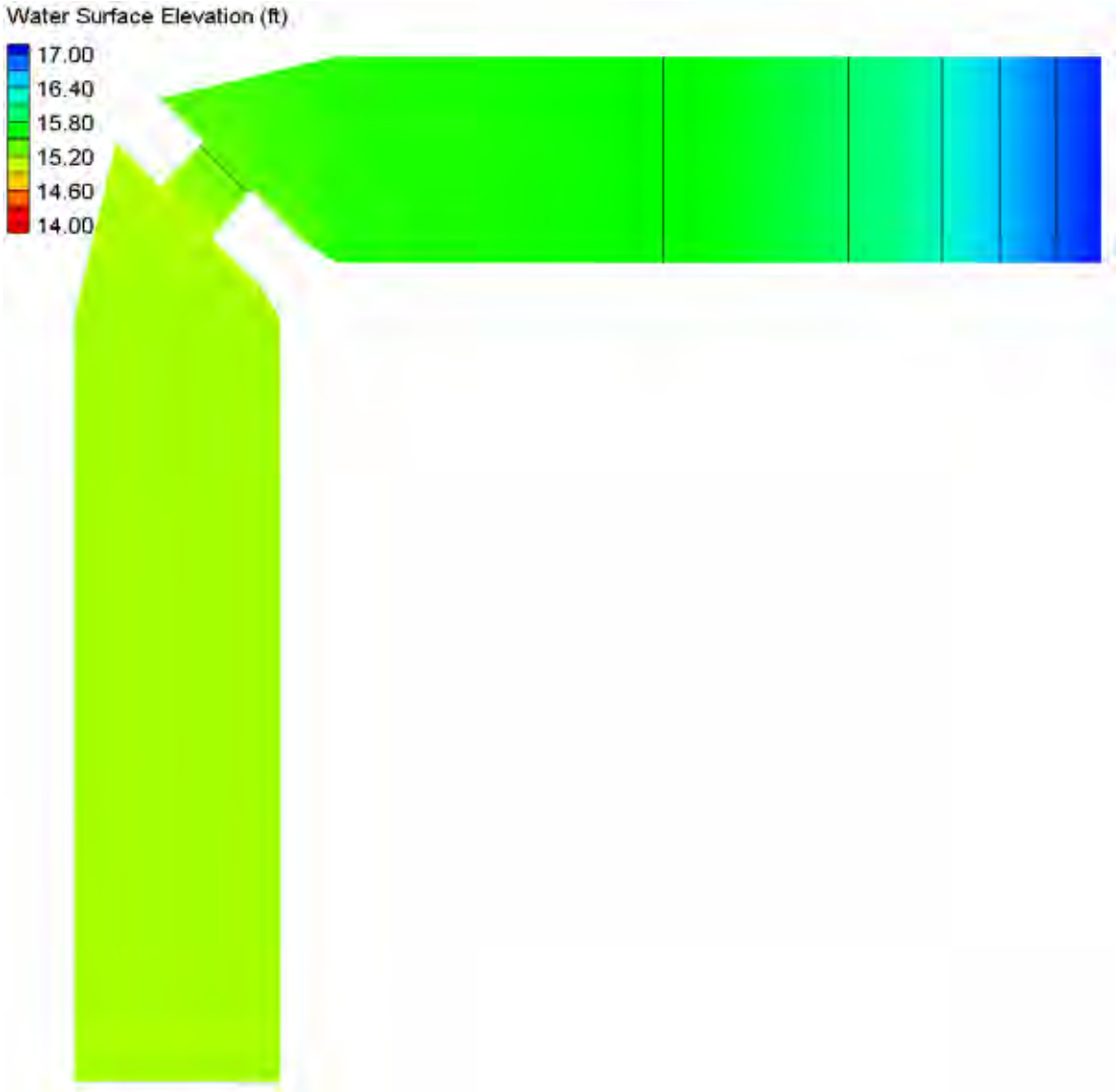

HEC-RAS Water Surface Elevation Contours – Small Channel – River Bends (90°, ½ radius)

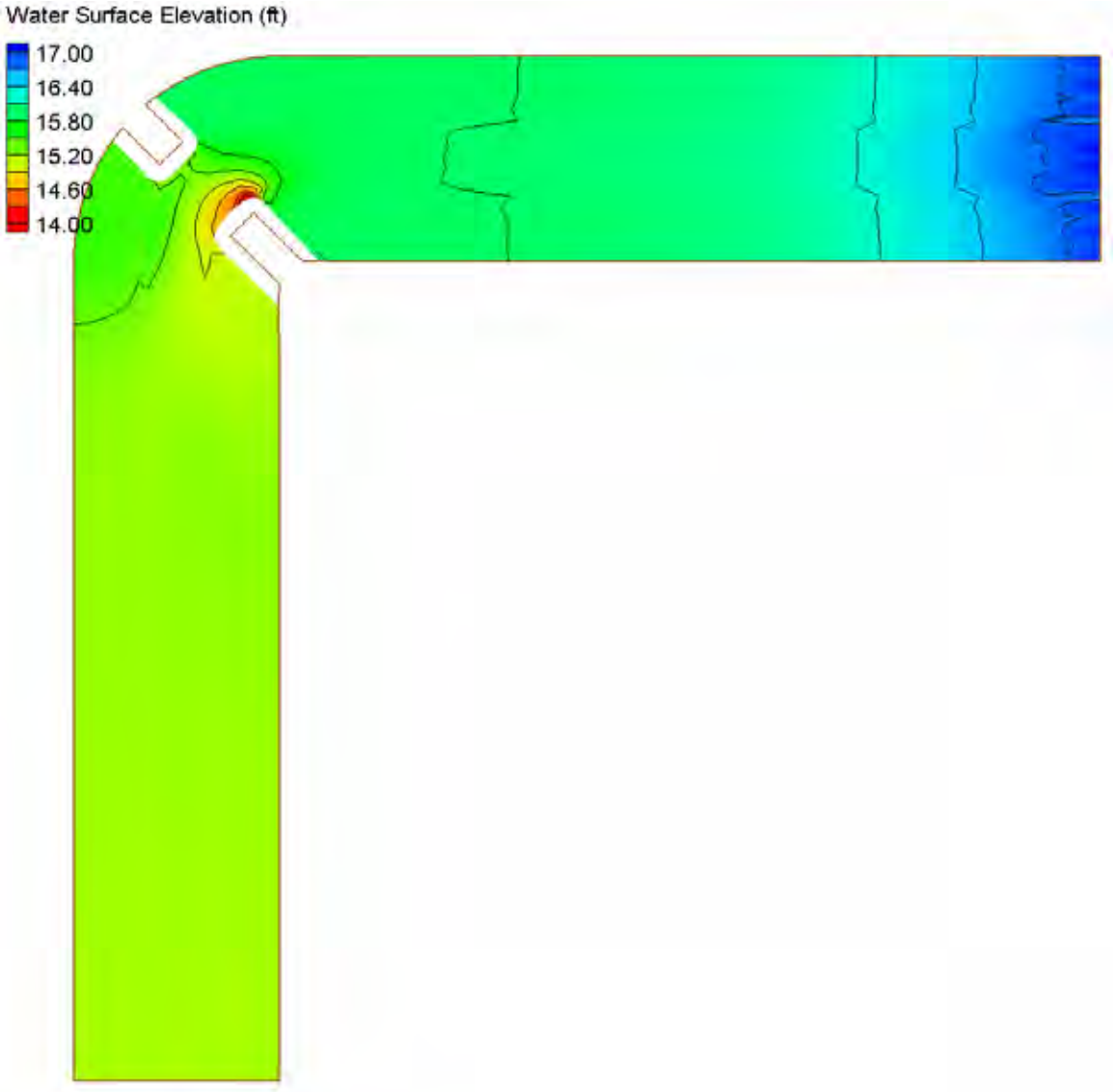

FESWMS Water Surface Elevation Contours – Small Channel – River Bends (90°, ½ radius)

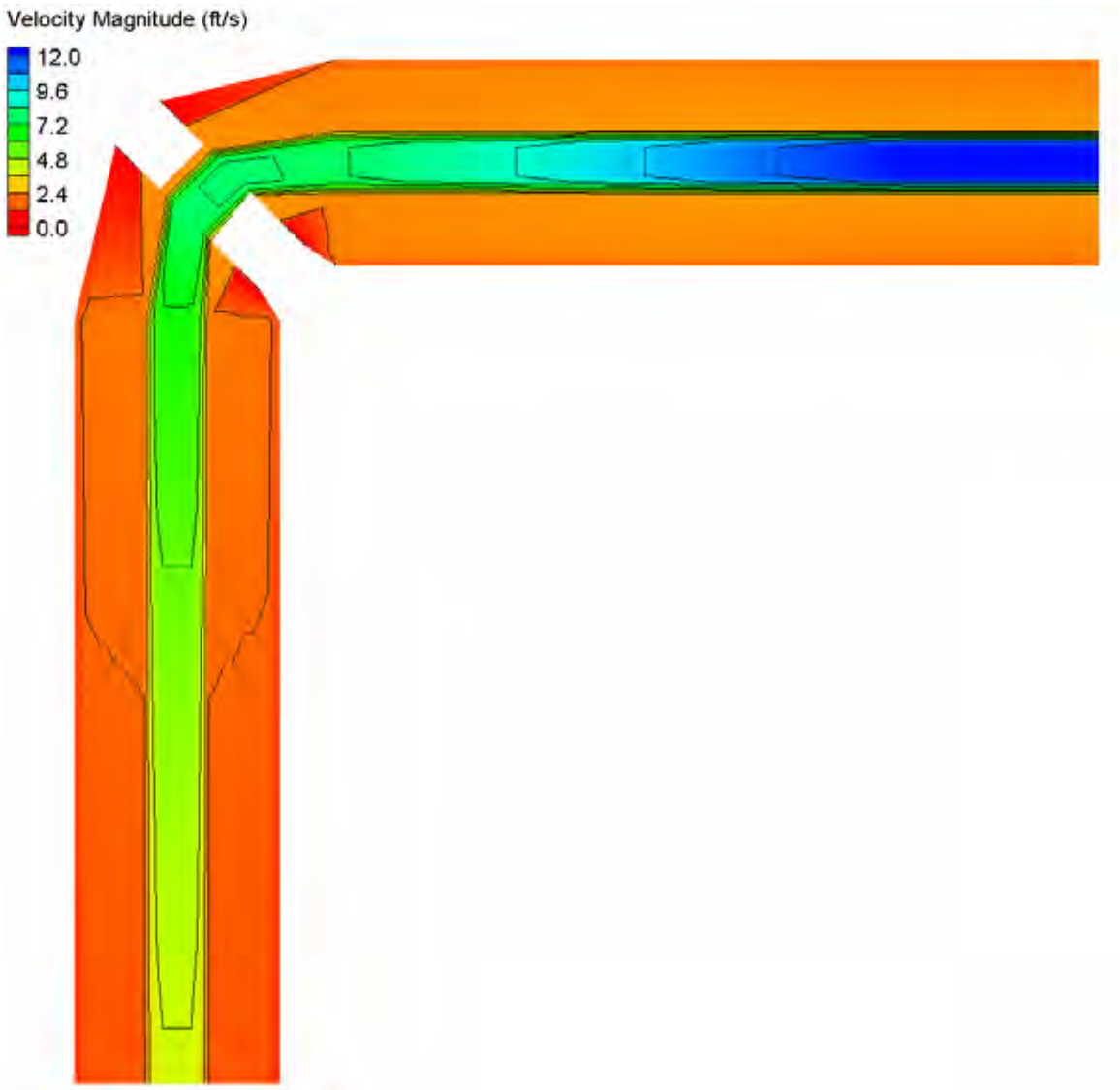

HEC-RAS Velocity Magnitude Contours – Small Channel – River Bends (90°, ½ radius)

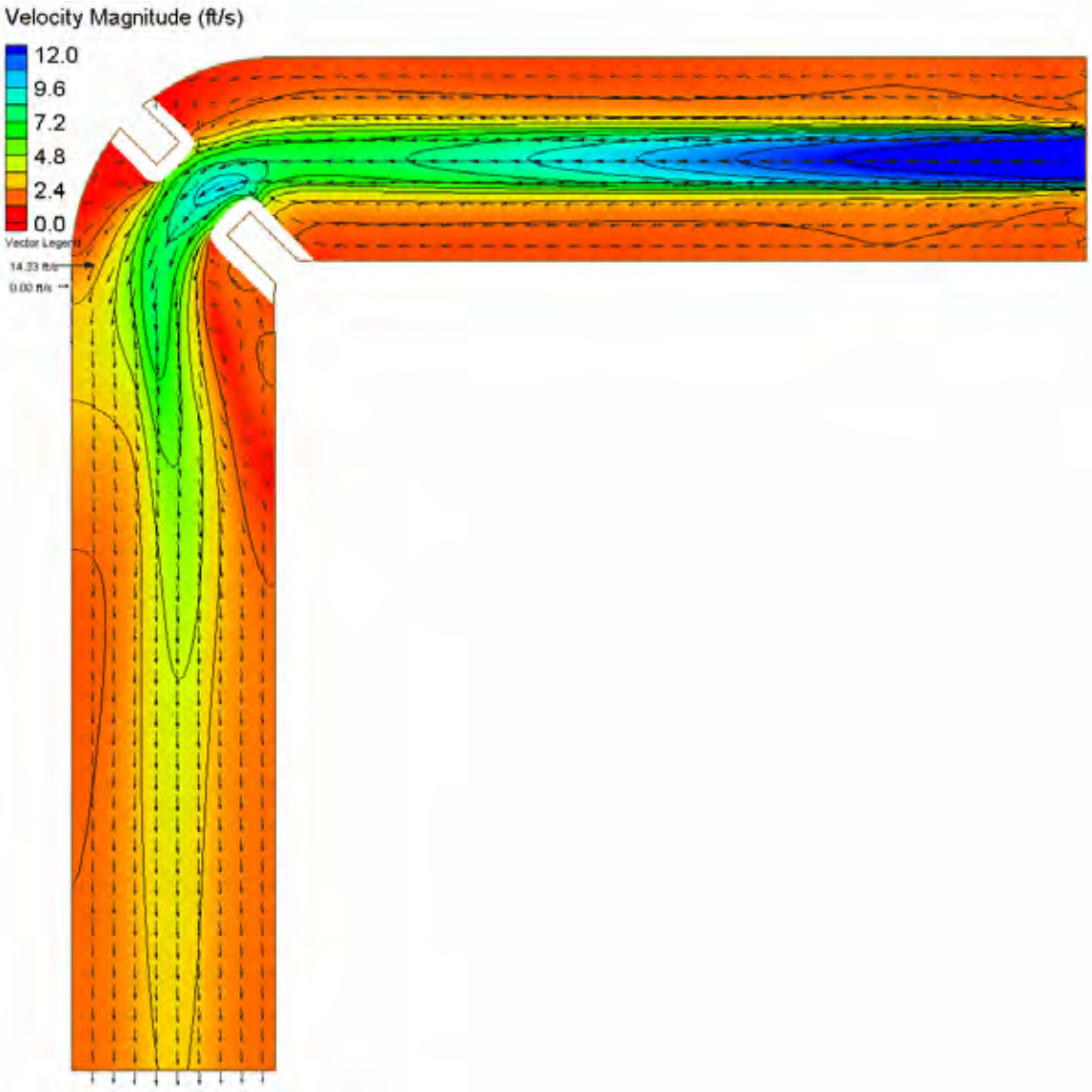

FESWMS Velocity Magnitude Contours – Small Channel – River Bends (90°, ½ radius)

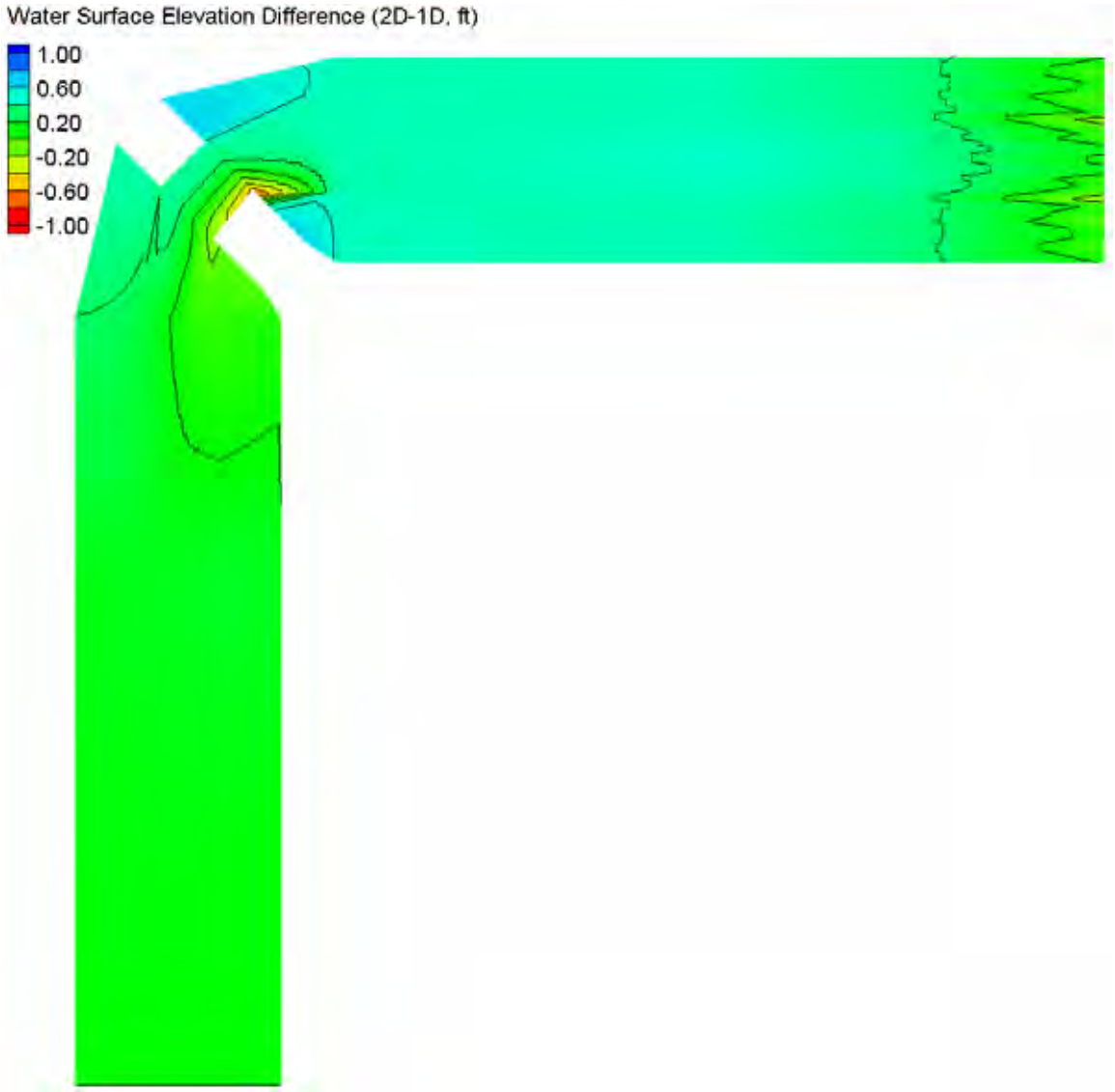

Water Surface Elevation Difference Contours – Small Channel – River Bends (90°, ½ radius)

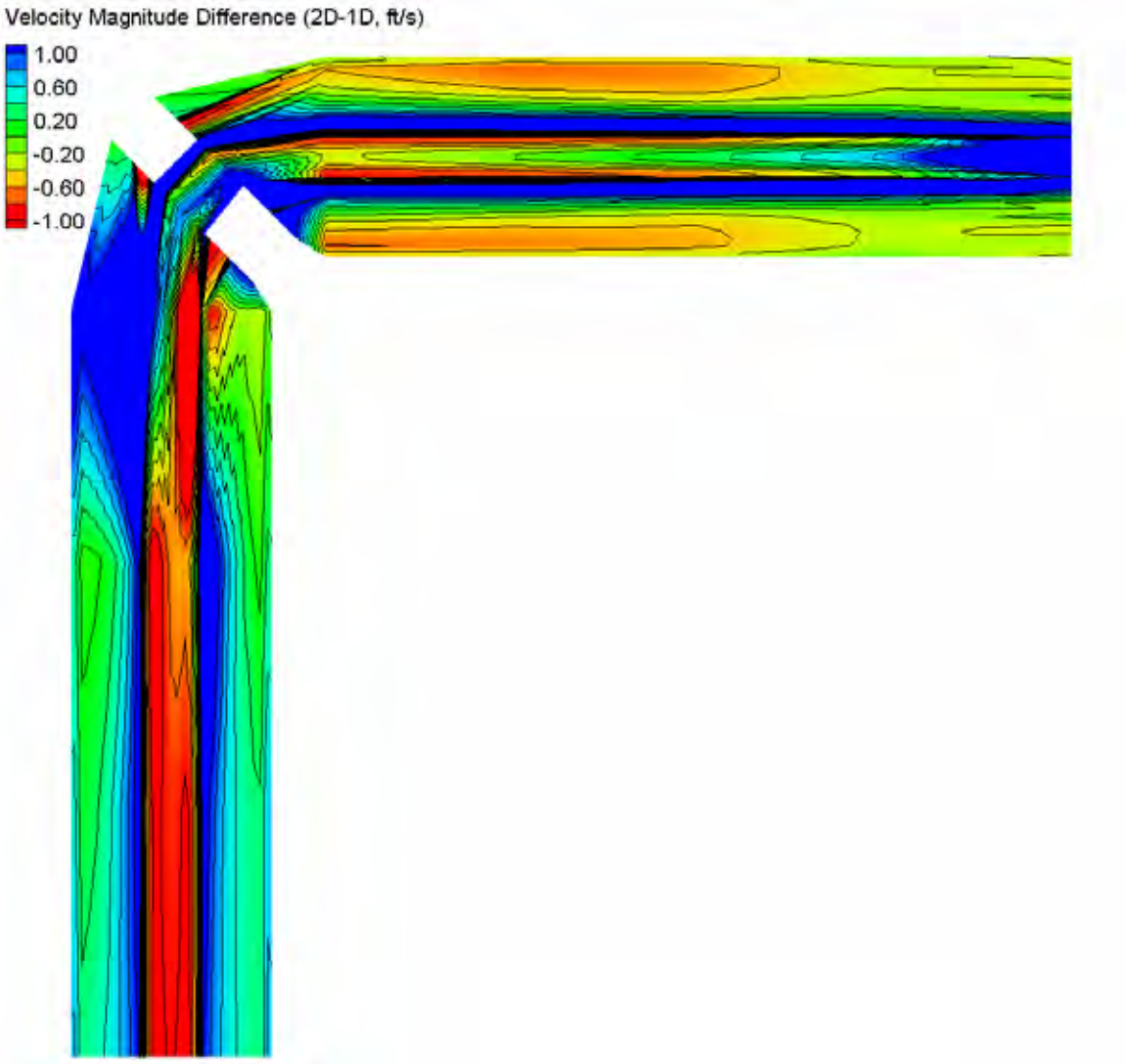

Velocity Magnitude Difference Contours – Small Channel – River Bends (90°, ½ radius)

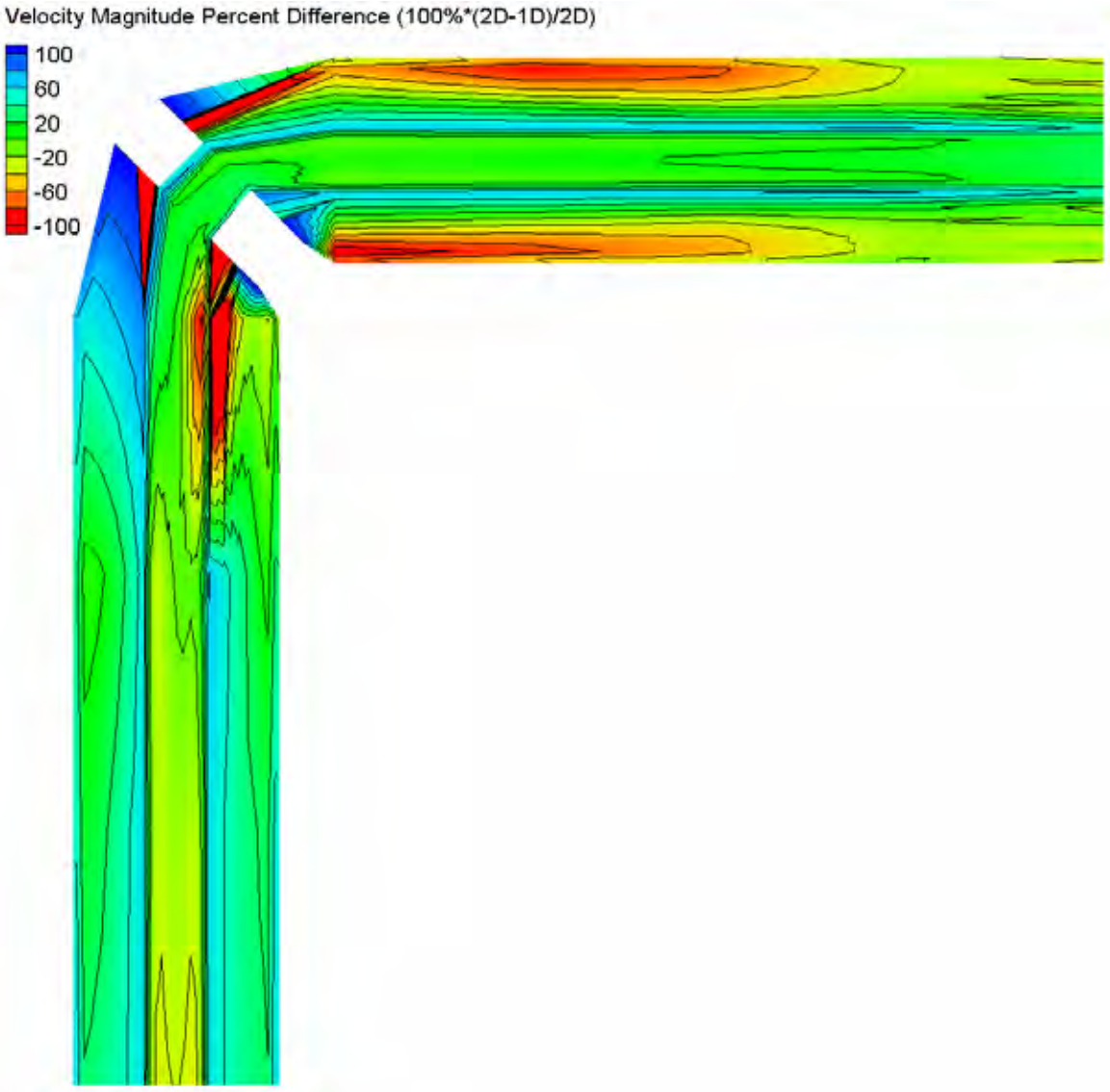

Velocity Magnitude Percent Difference Contours – Small Channel – River Bends (90°, ½ radius)

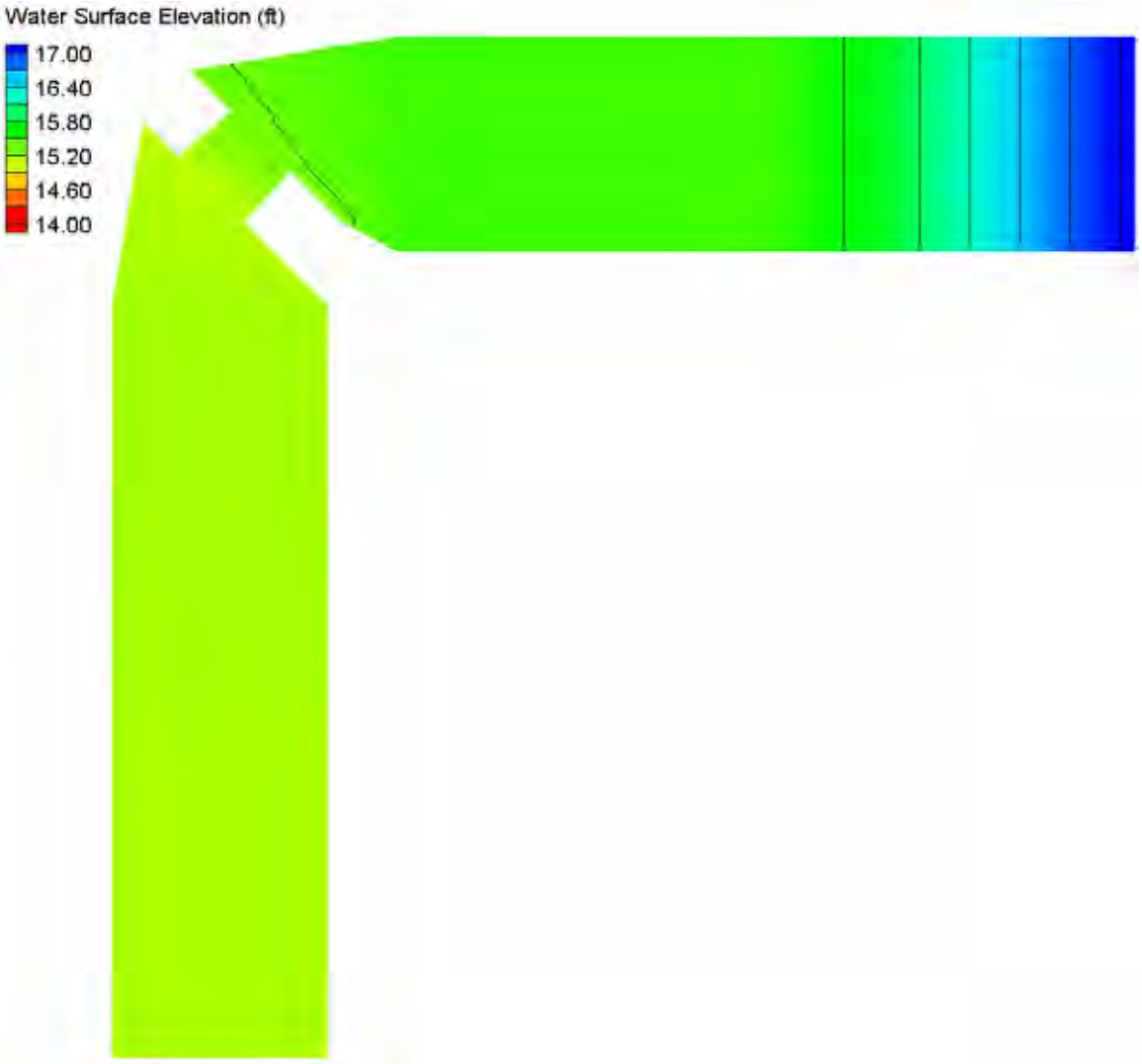

HEC-RAS Water Surface Elevation Contours – Small Channel – River Bends (90°, ¼ radius)

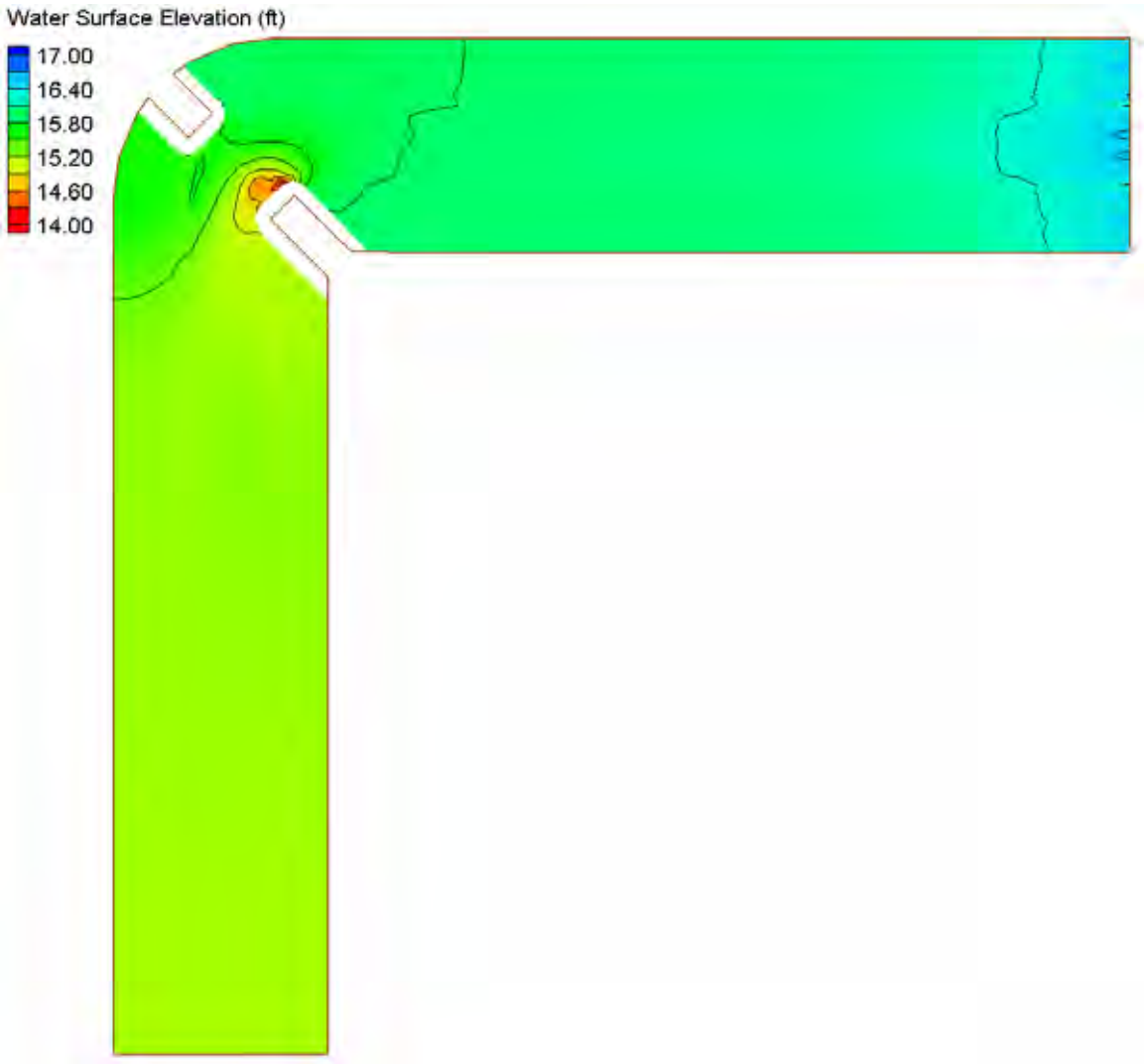

FESWMS Water Surface Elevation Contours – Small Channel – River Bends (90°, ¼ radius)

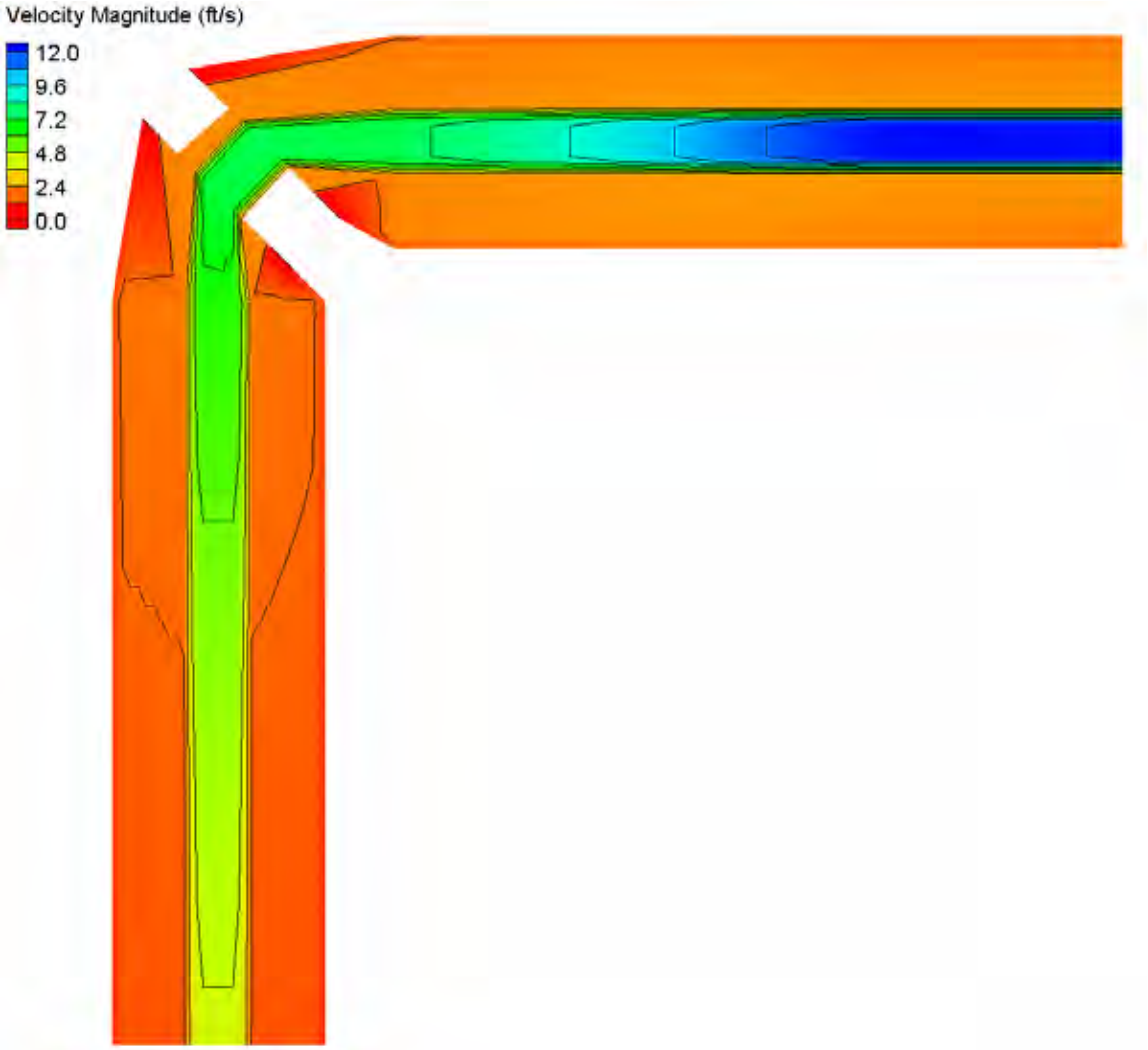

HEC-RAS Velocity Magnitude Contours – Small Channel – River Bends (90°, ¼ radius)

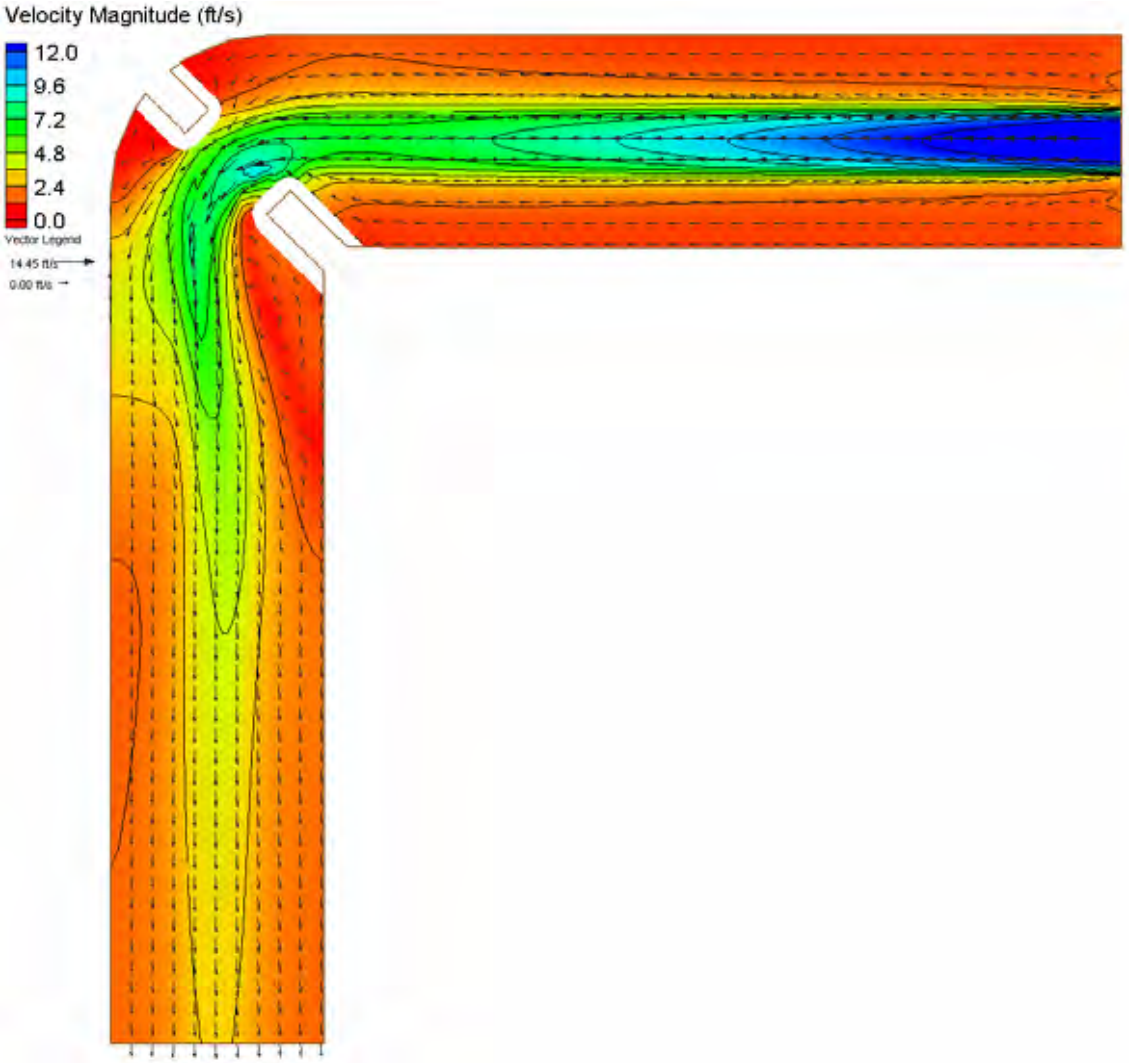

FESWMS Velocity Magnitude Contours – Small Channel – River Bends (90°, ¼ radius)

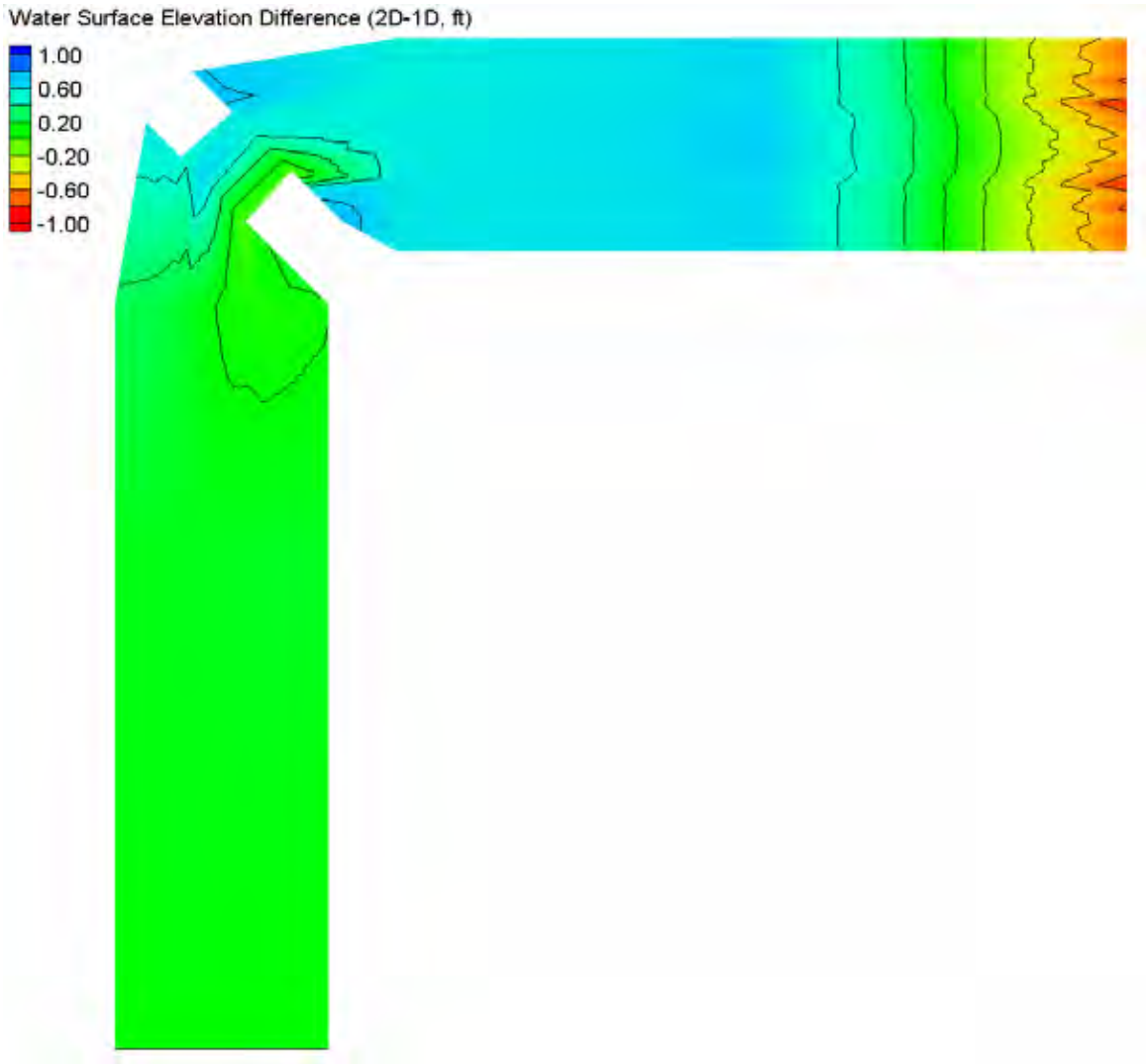

Water Surface Elevation Difference Contours – Small Channel – River Bends (90°, ¼ radius)

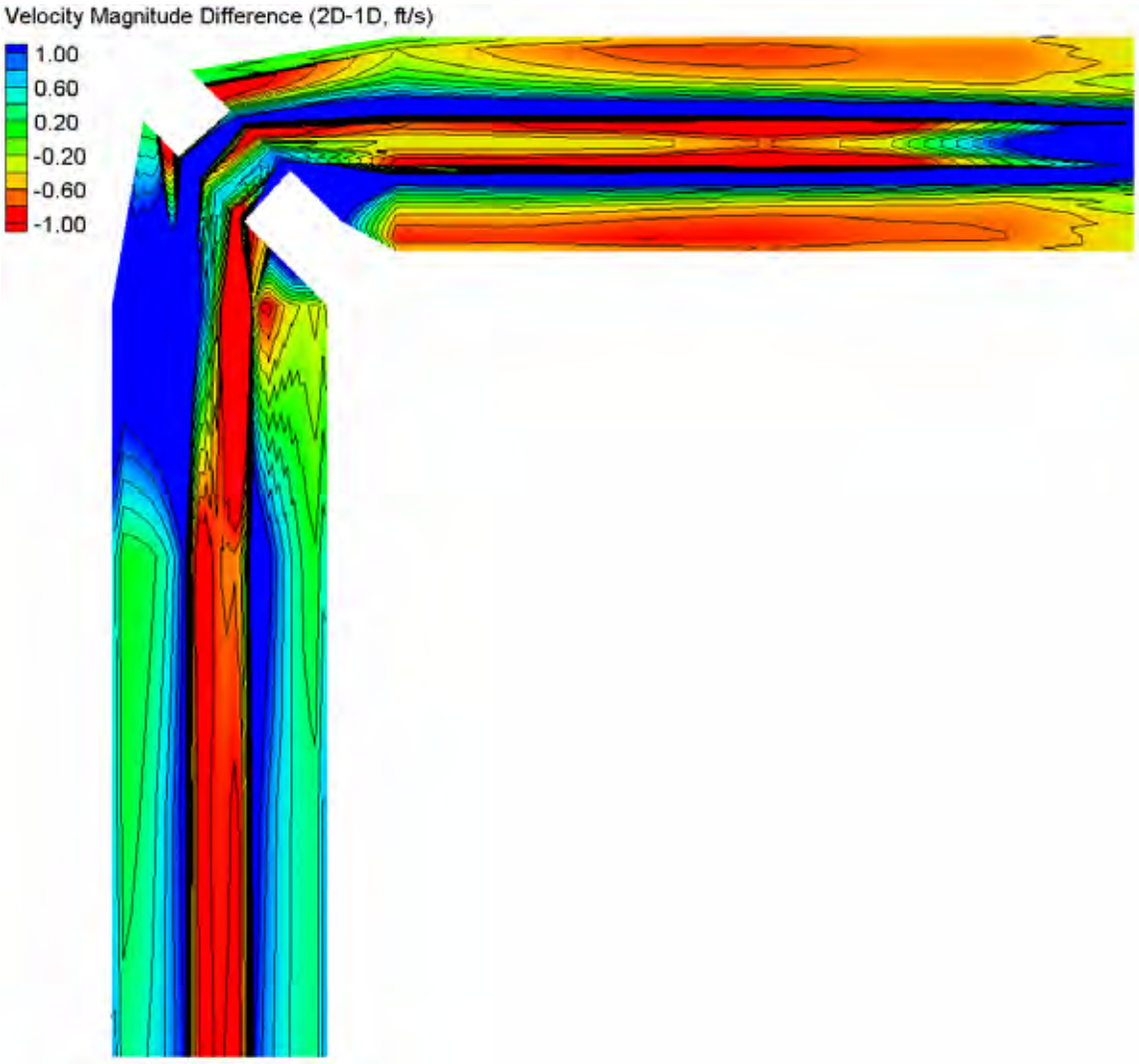

Velocity Magnitude Difference Contours – Small Channel – River Bends (90°, ¼ radius)

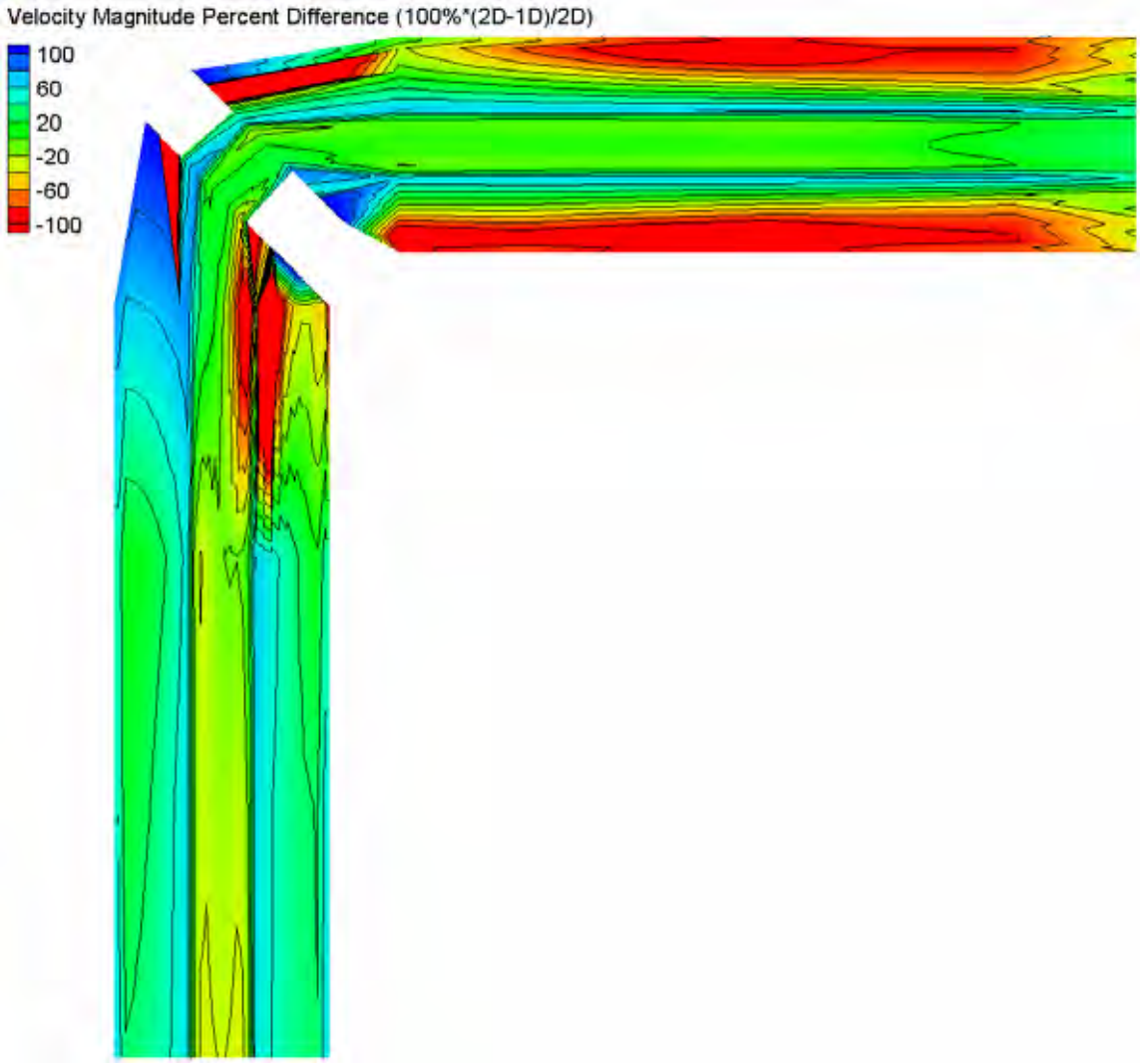

Velocity Magnitude Percent Difference Contours – Small Channel – River Bends (90°, ¼ radius)

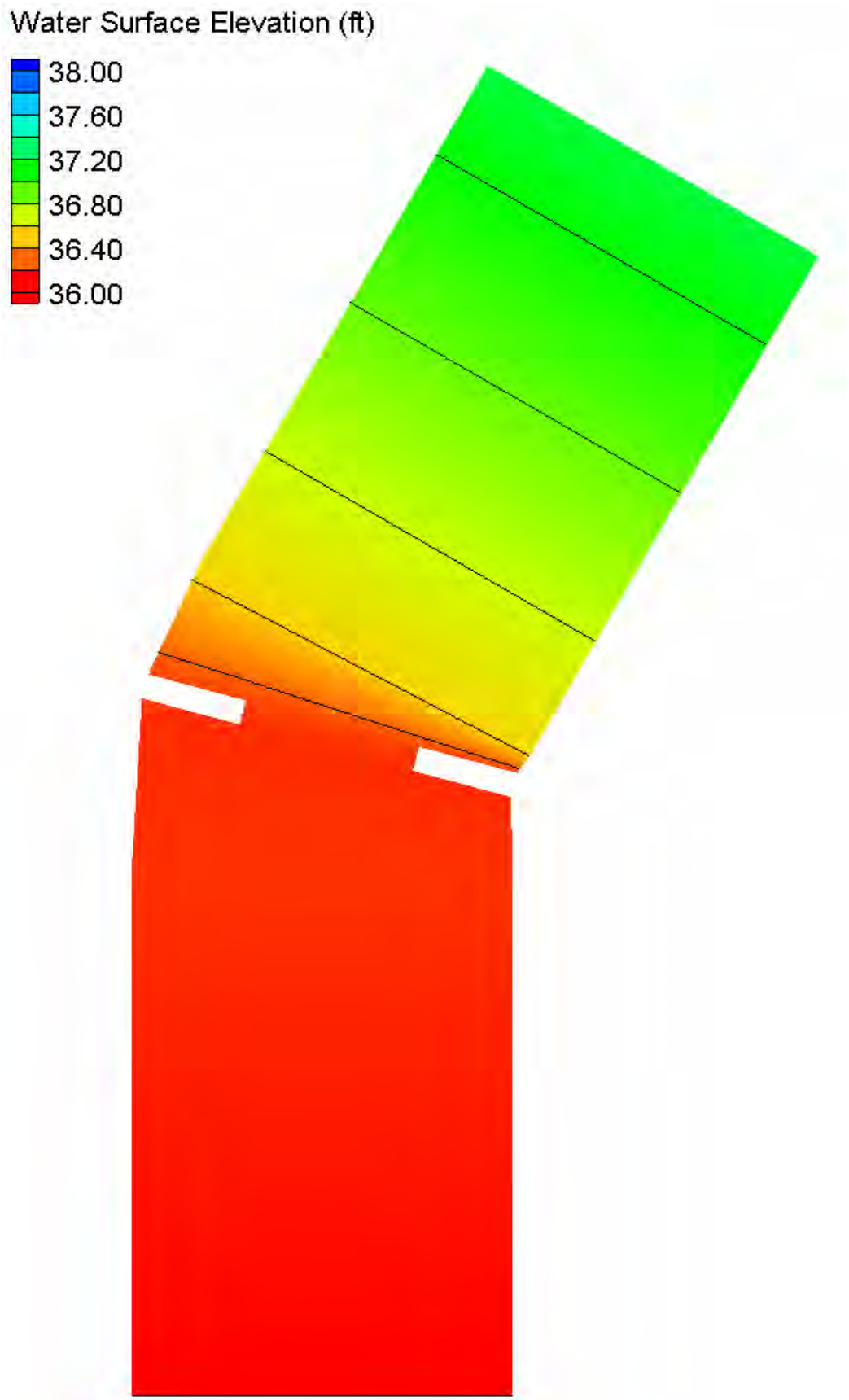

HEC-RAS Water Surface Elevation Contours – Large Channel – River Bends (30°, ½ radius)

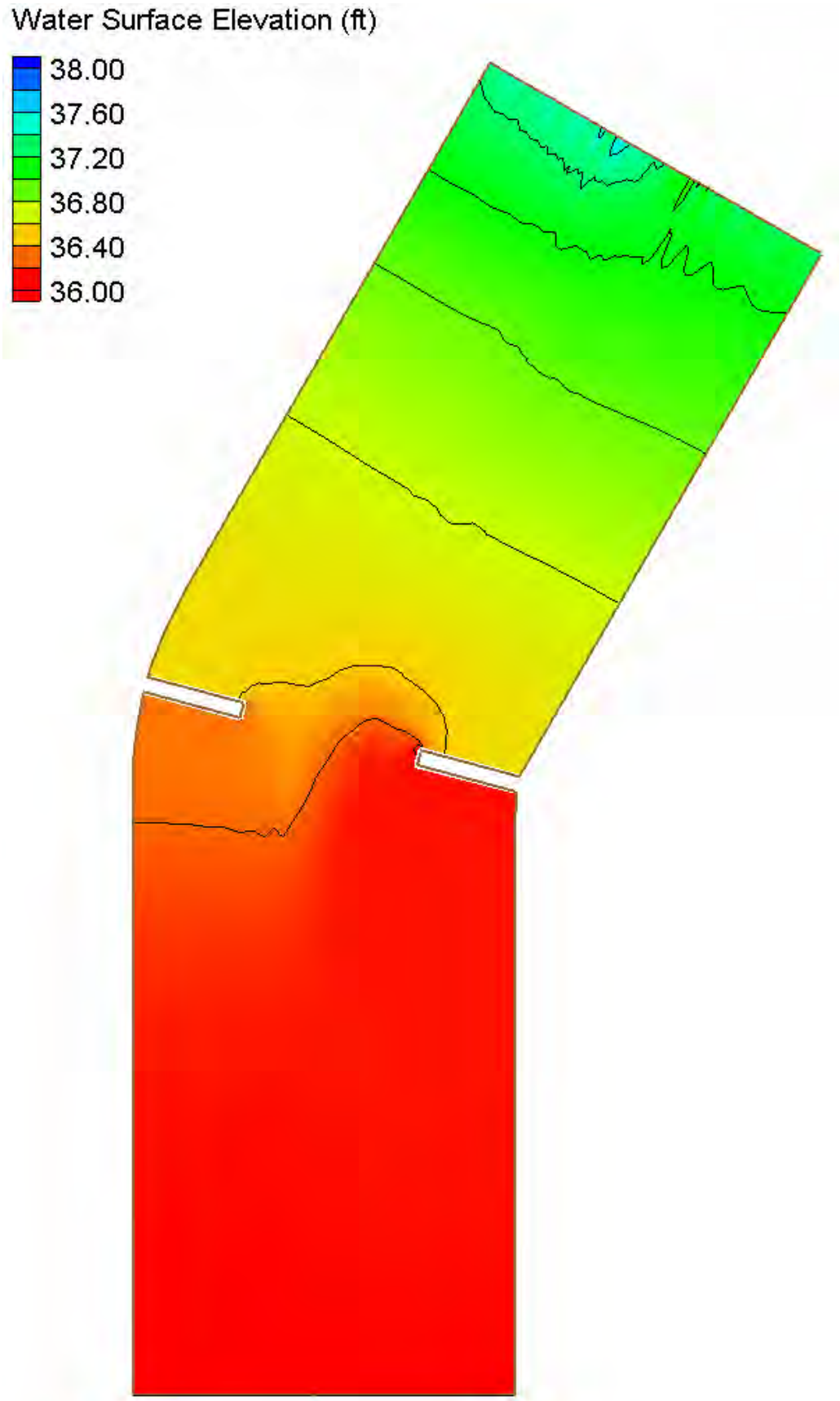

FESWMS Water Surface Elevation Contours – Large Channel – River Bends (30°, ½ radius)

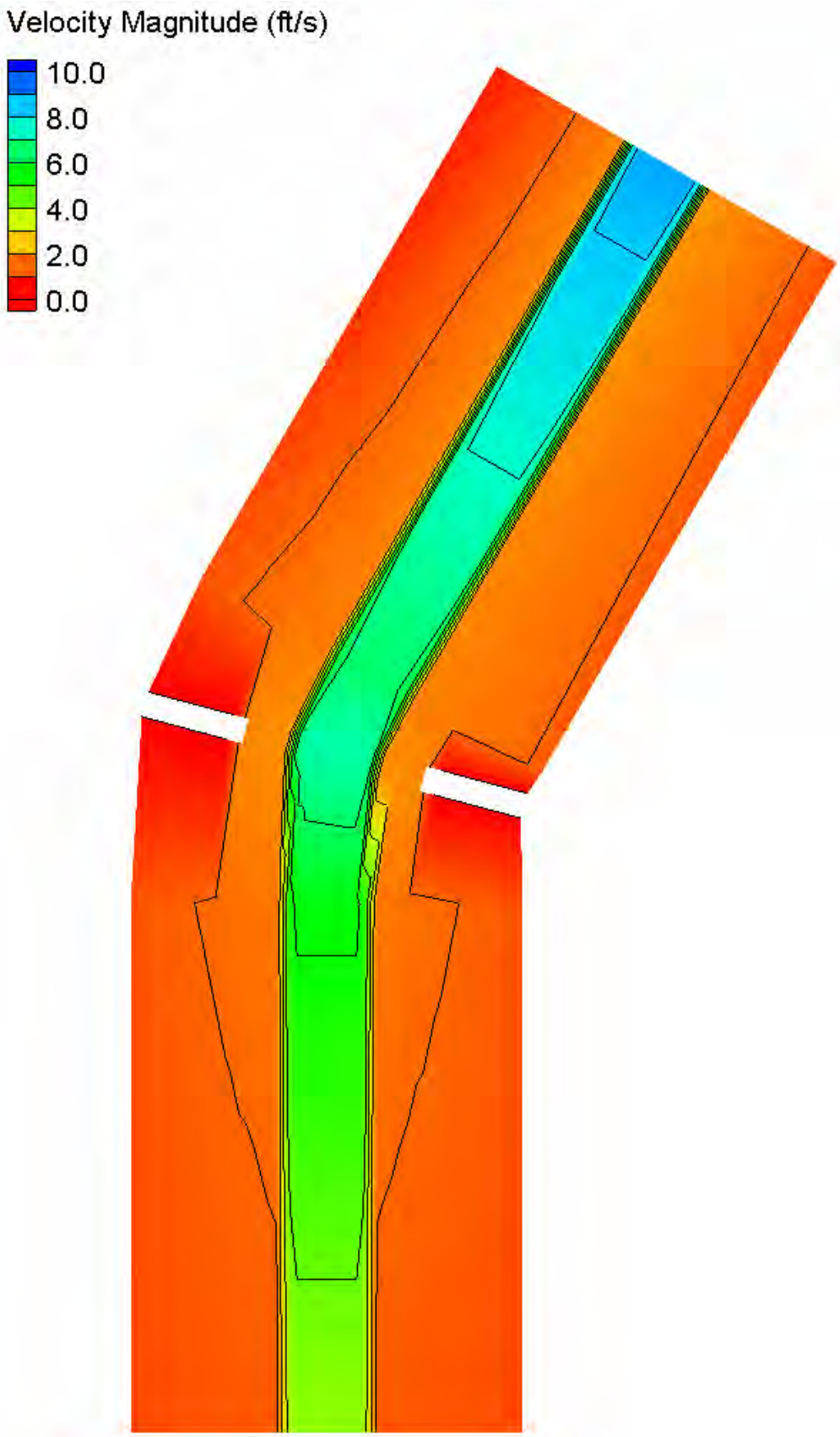

HEC-RAS Velocity Magnitude Contours – Large Channel – River Bends (30°, ½ radius)

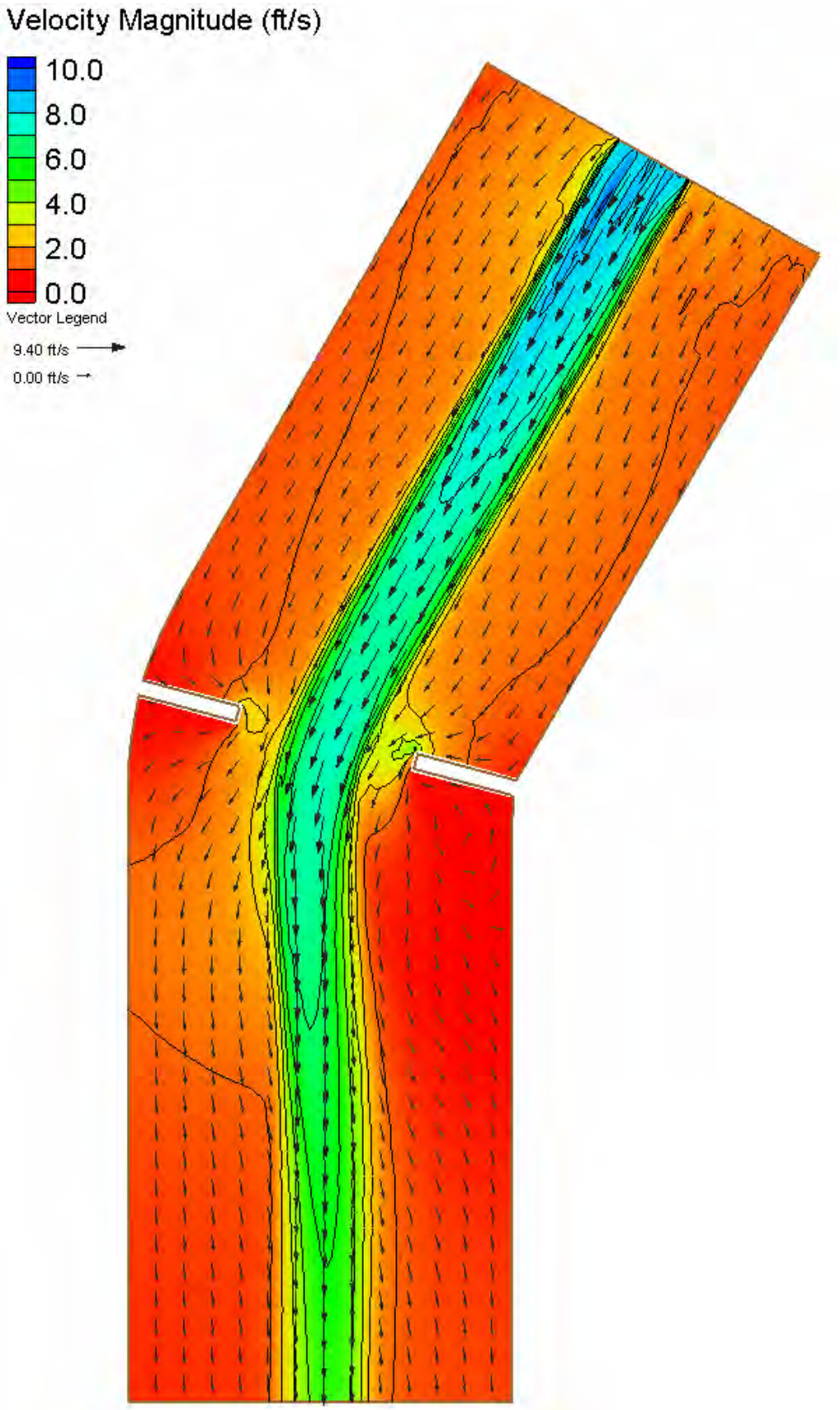

FESWMS Velocity Magnitude Contours – Large Channel – River Bends (30°, ½ radius)

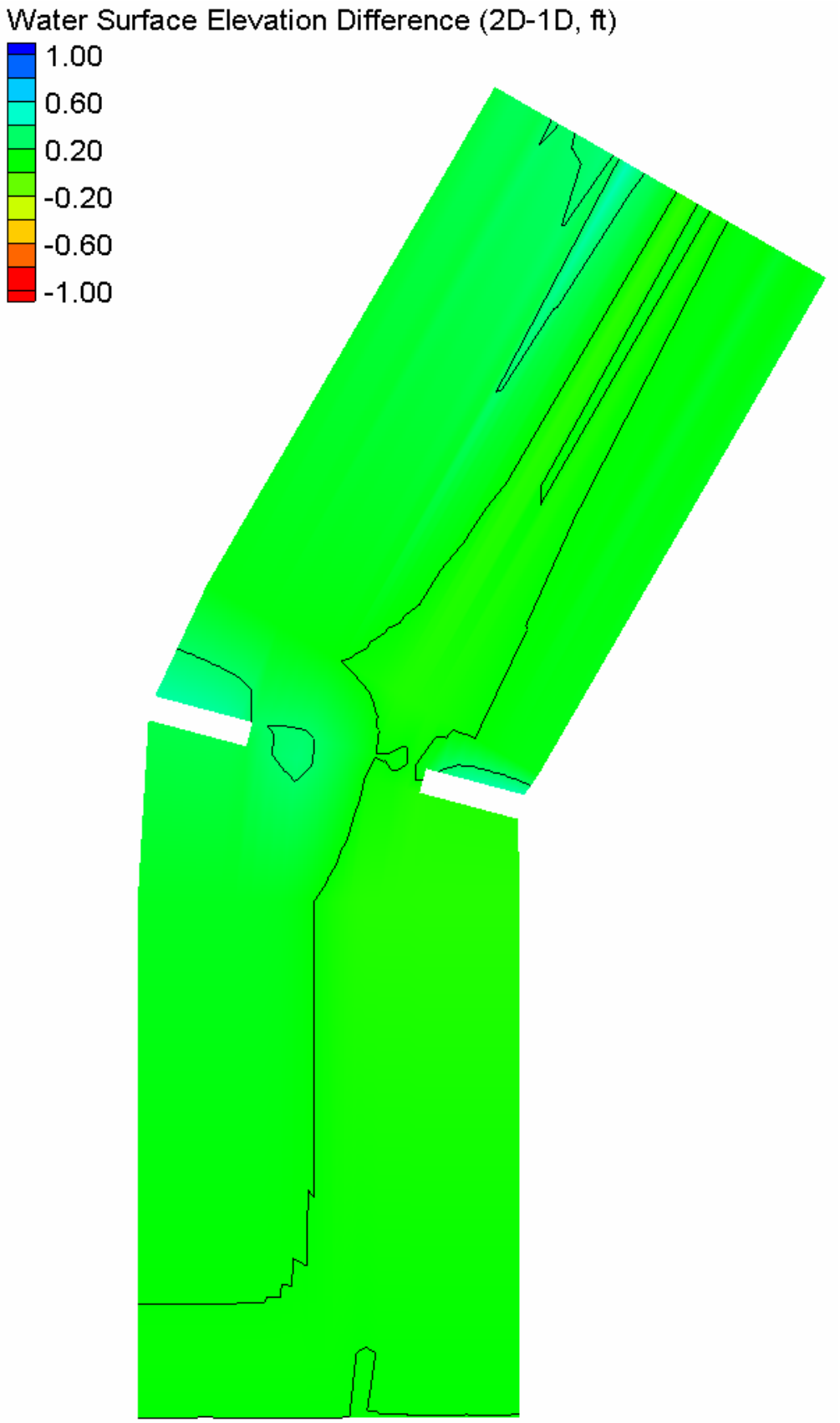

Water Surface Elevation Difference Contours – Large Channel – River Bends (30°, ½ radius)

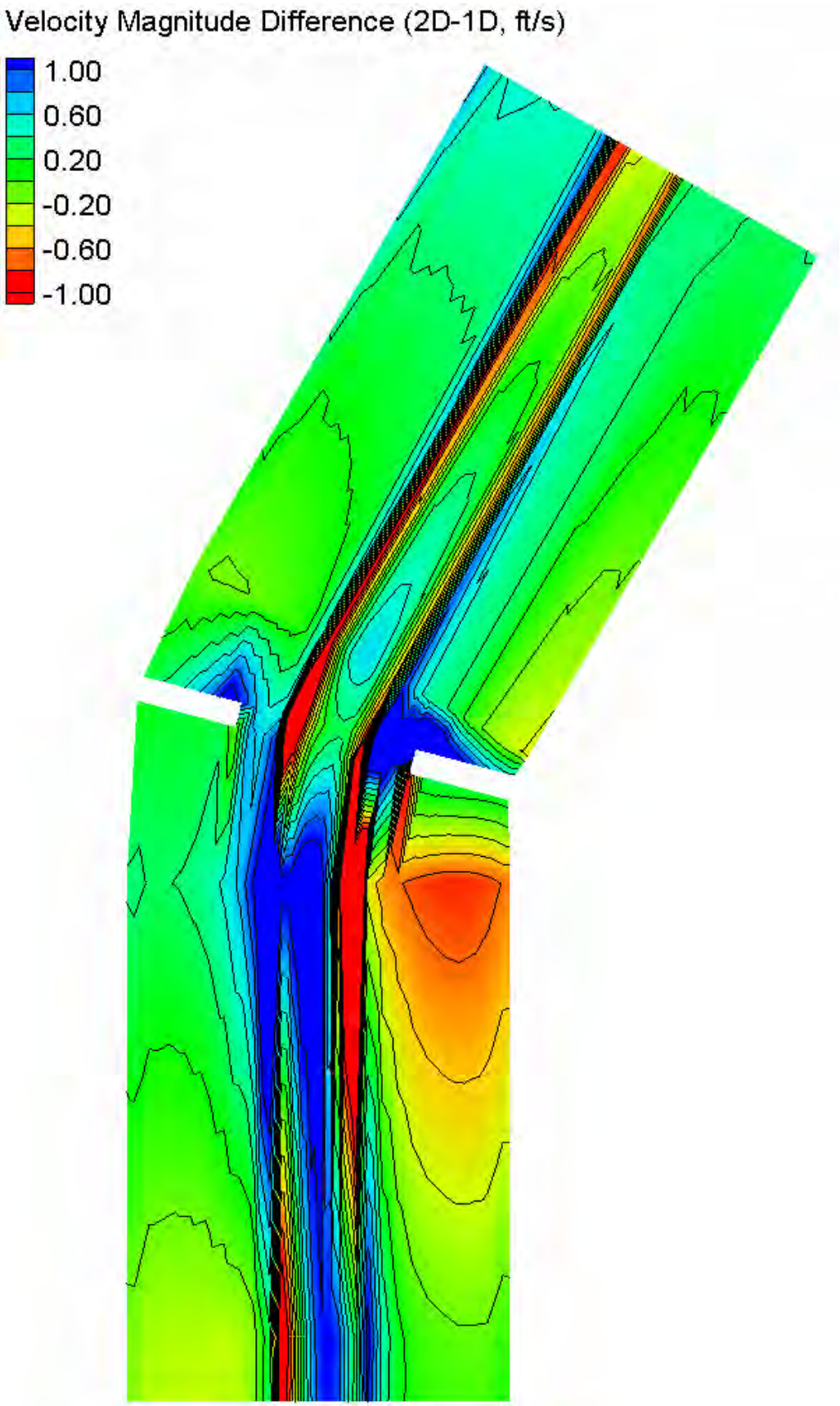

Velocity Magnitude Difference Contours – Large Channel – River Bends (30°, ½ radius)

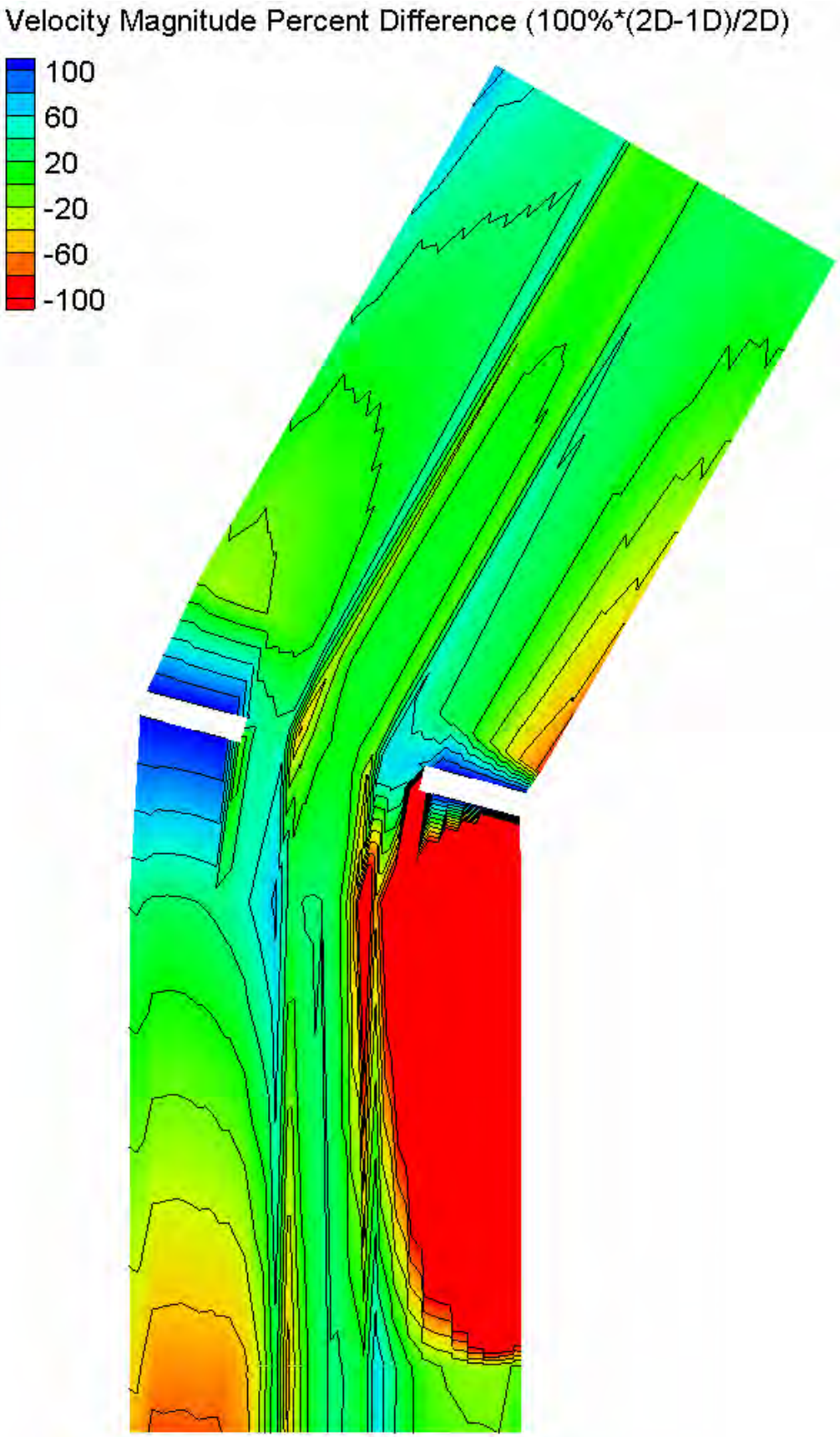

Velocity Magnitude Percent Difference Contours – Large Channel – River Bends (30°, ½ radius)

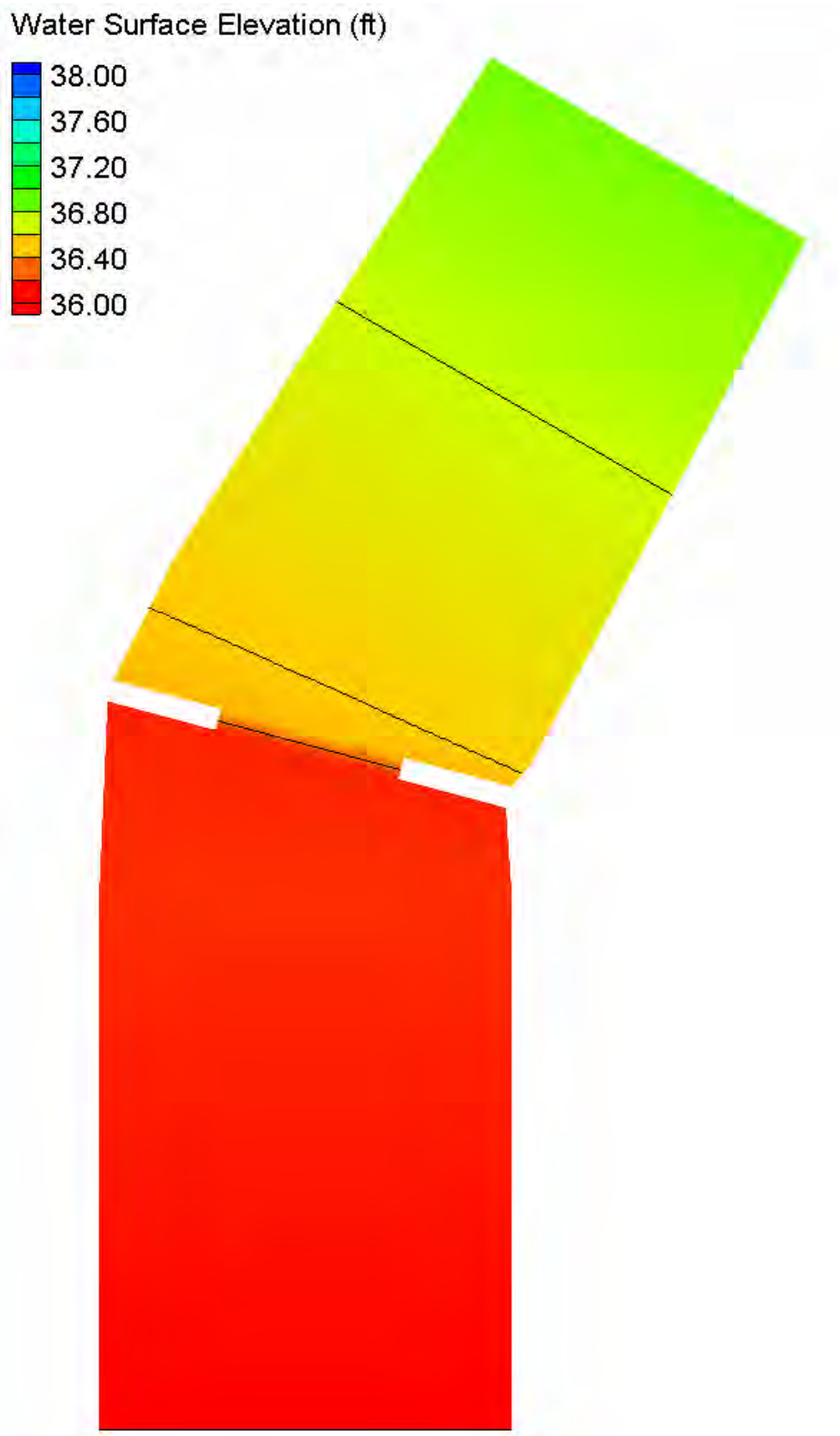

HEC-RAS Water Surface Elevation Contours – Large Channel – River Bends (30°, ¼ radius)

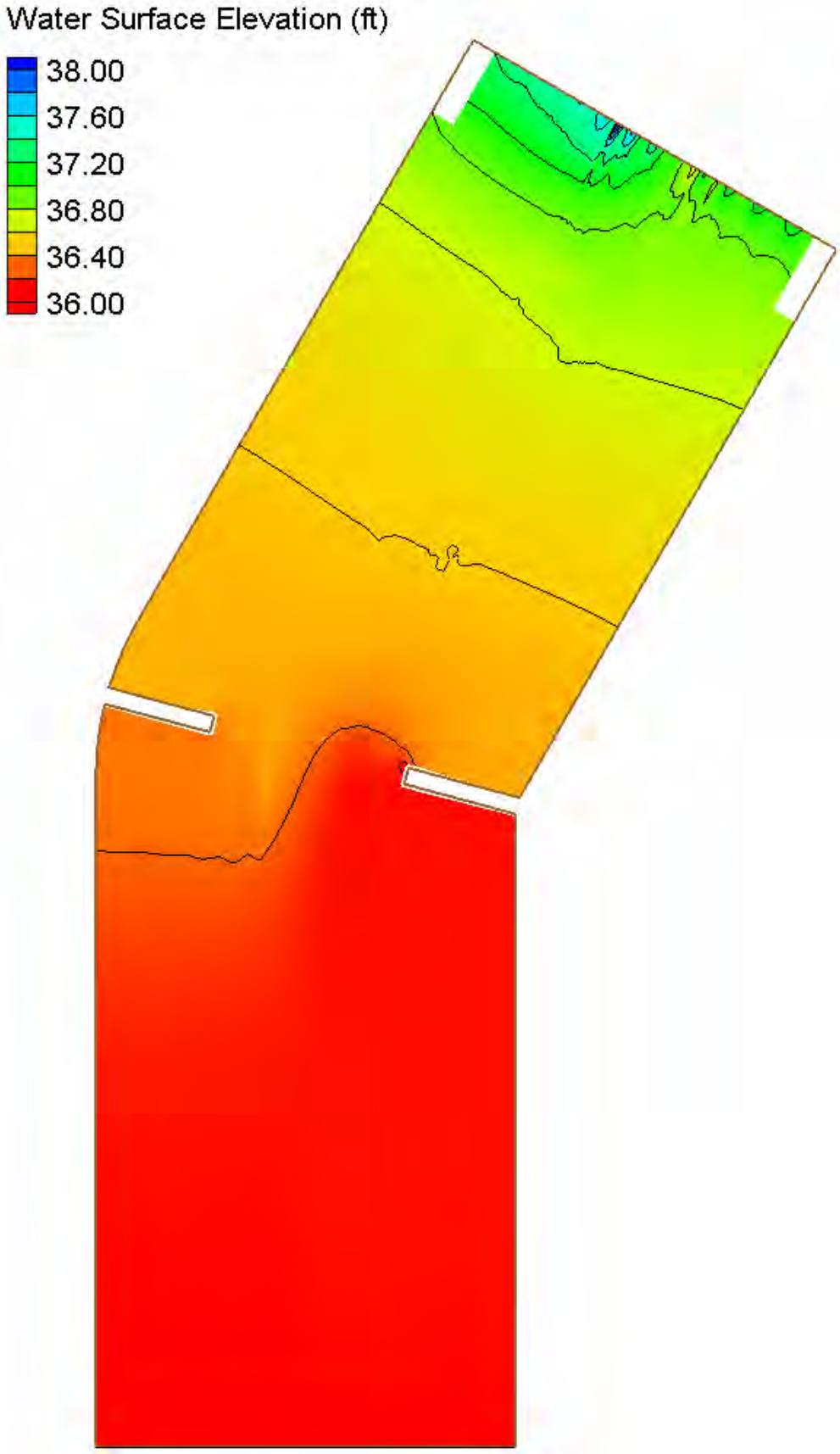

FESWMS Water Surface Elevation Contours – Large Channel – River Bends (30°, ¼ radius)

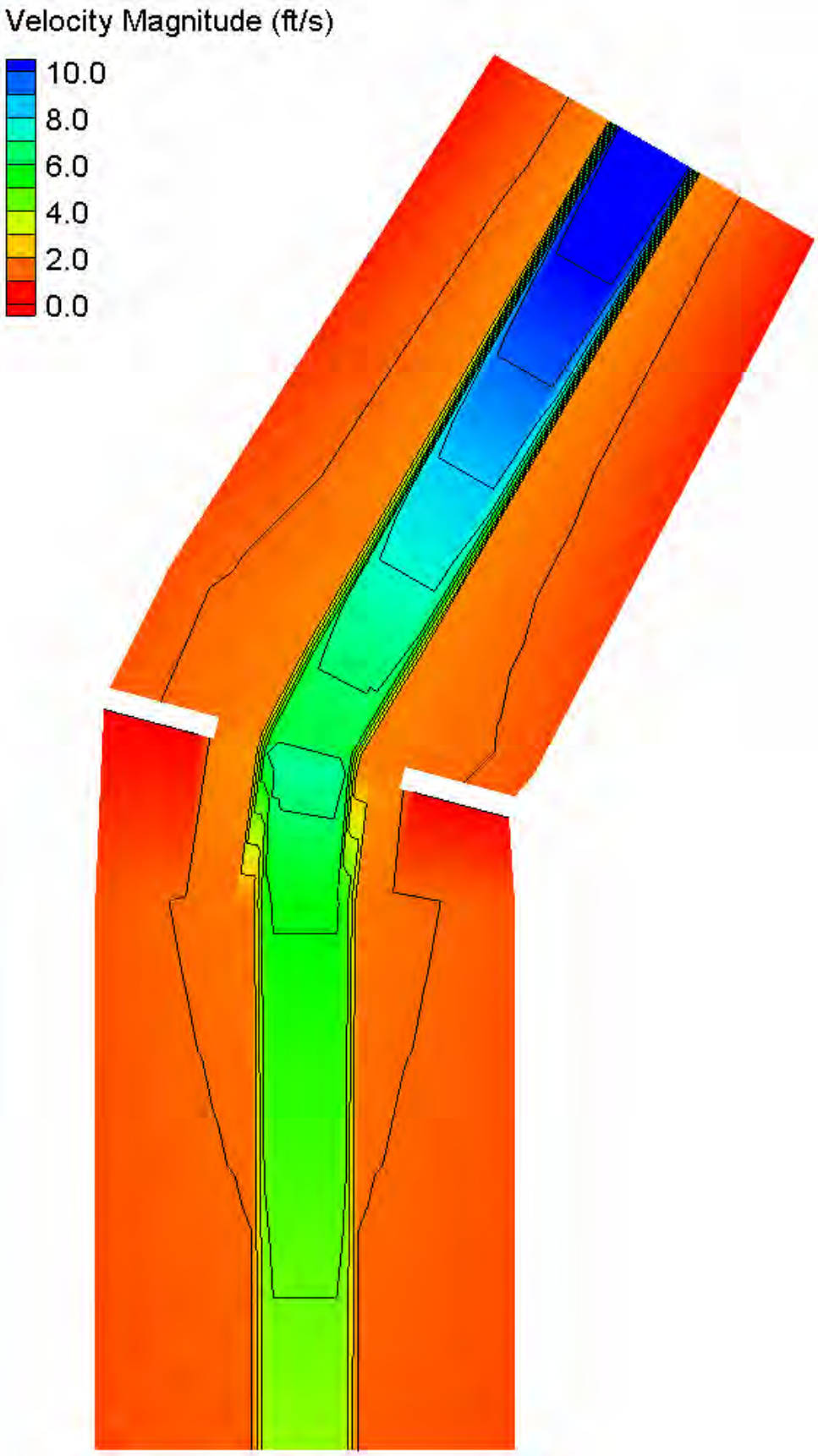

HEC-RAS Velocity Magnitude Contours – Large Channel – River Bends (30°, ¼ radius)

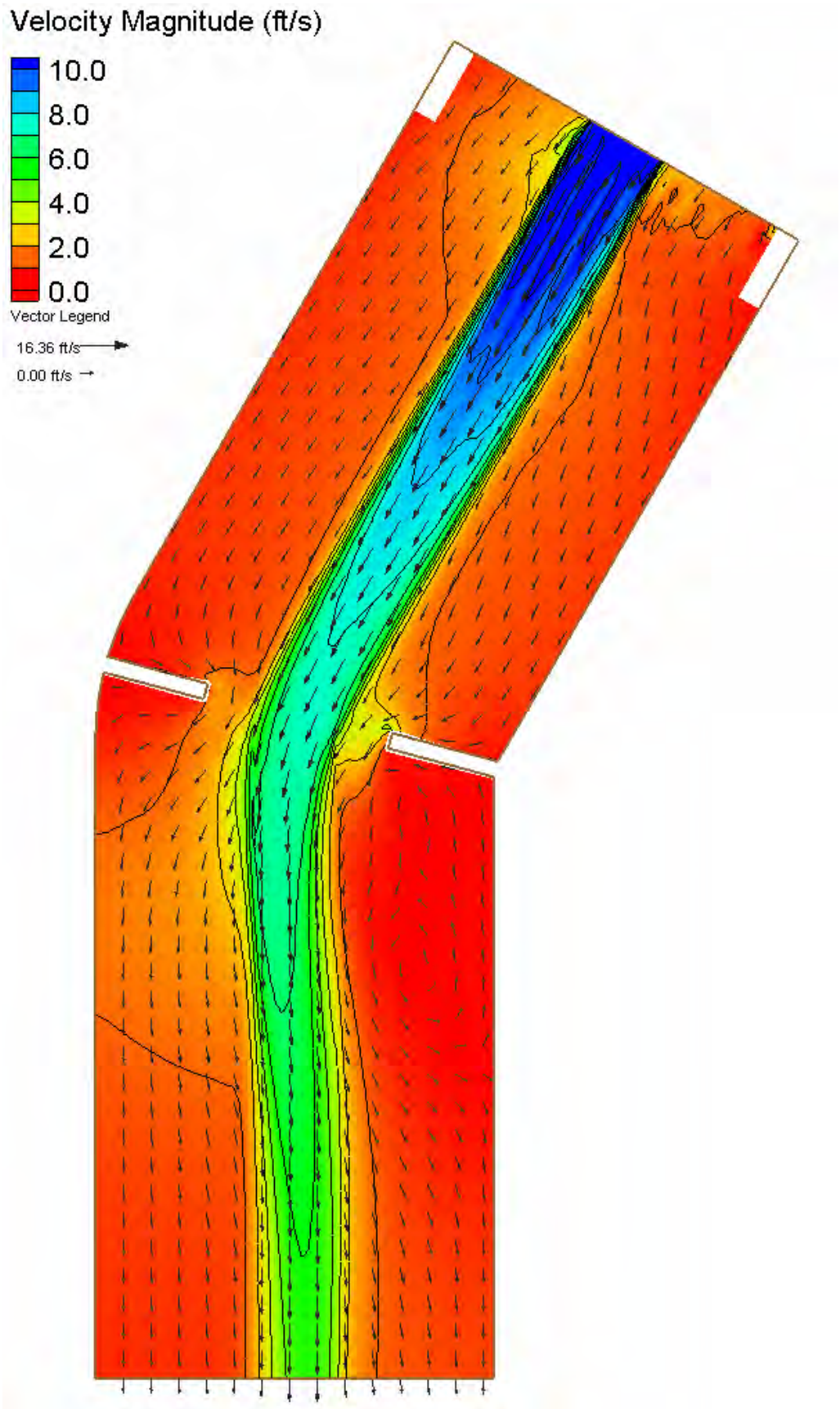

FESWMS Velocity Magnitude Contours – Large Channel – River Bends (30°, ¼ radius)

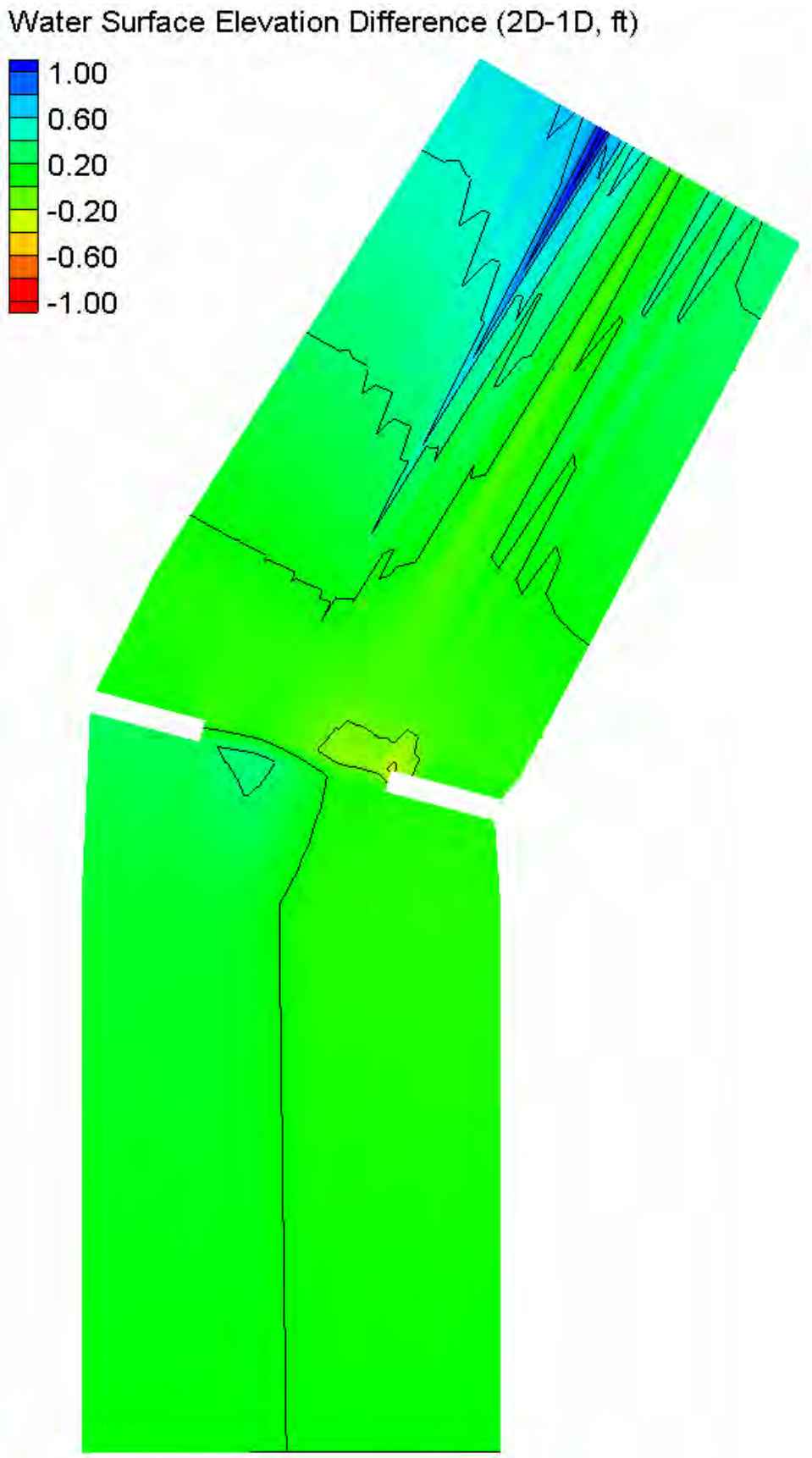

Water Surface Elevation Difference Contours – Large Channel – River Bends (30°, ¼ radius)

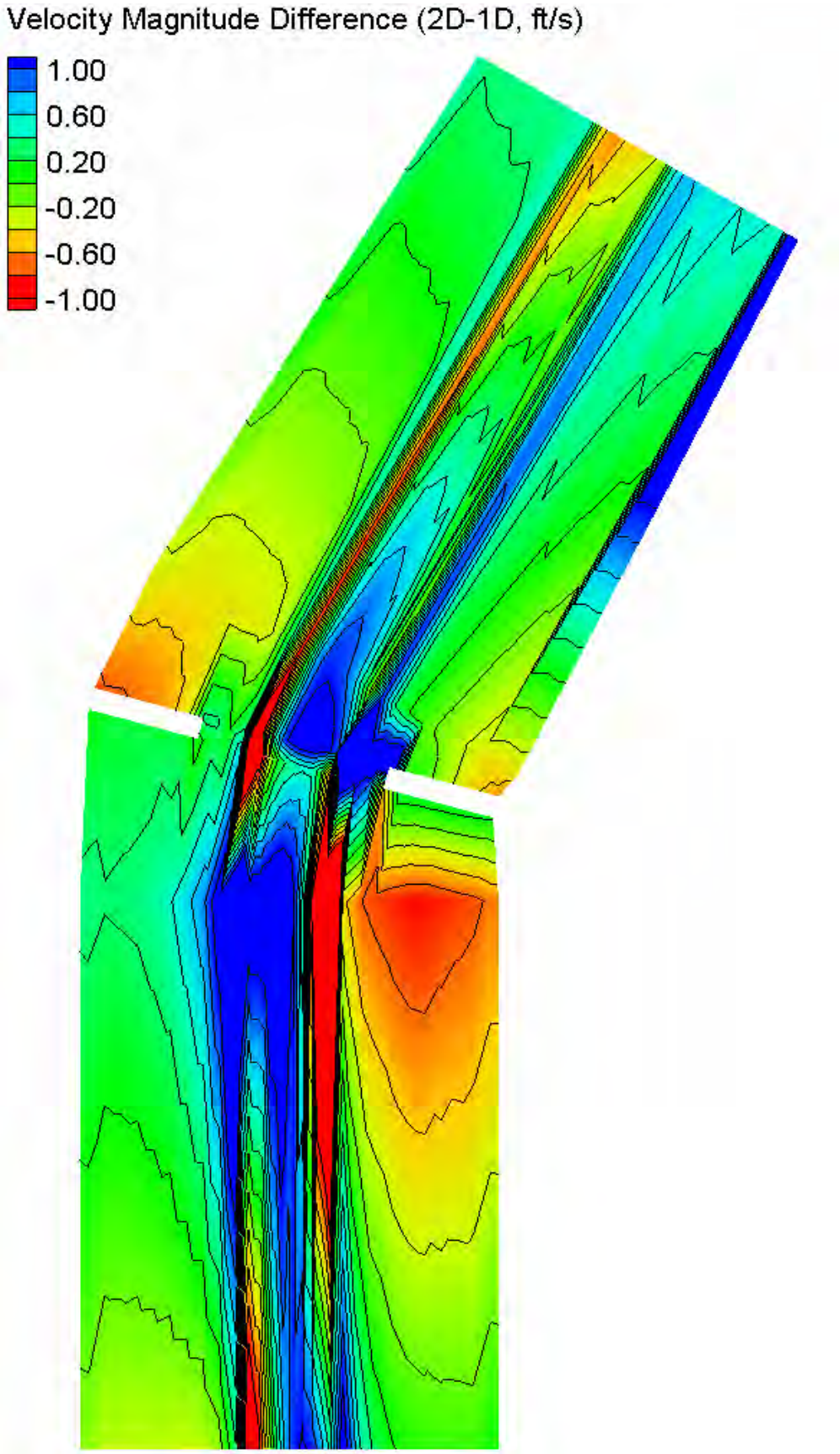

Velocity Magnitude Difference Contours – Large Channel – River Bends (30°, ¼ radius)

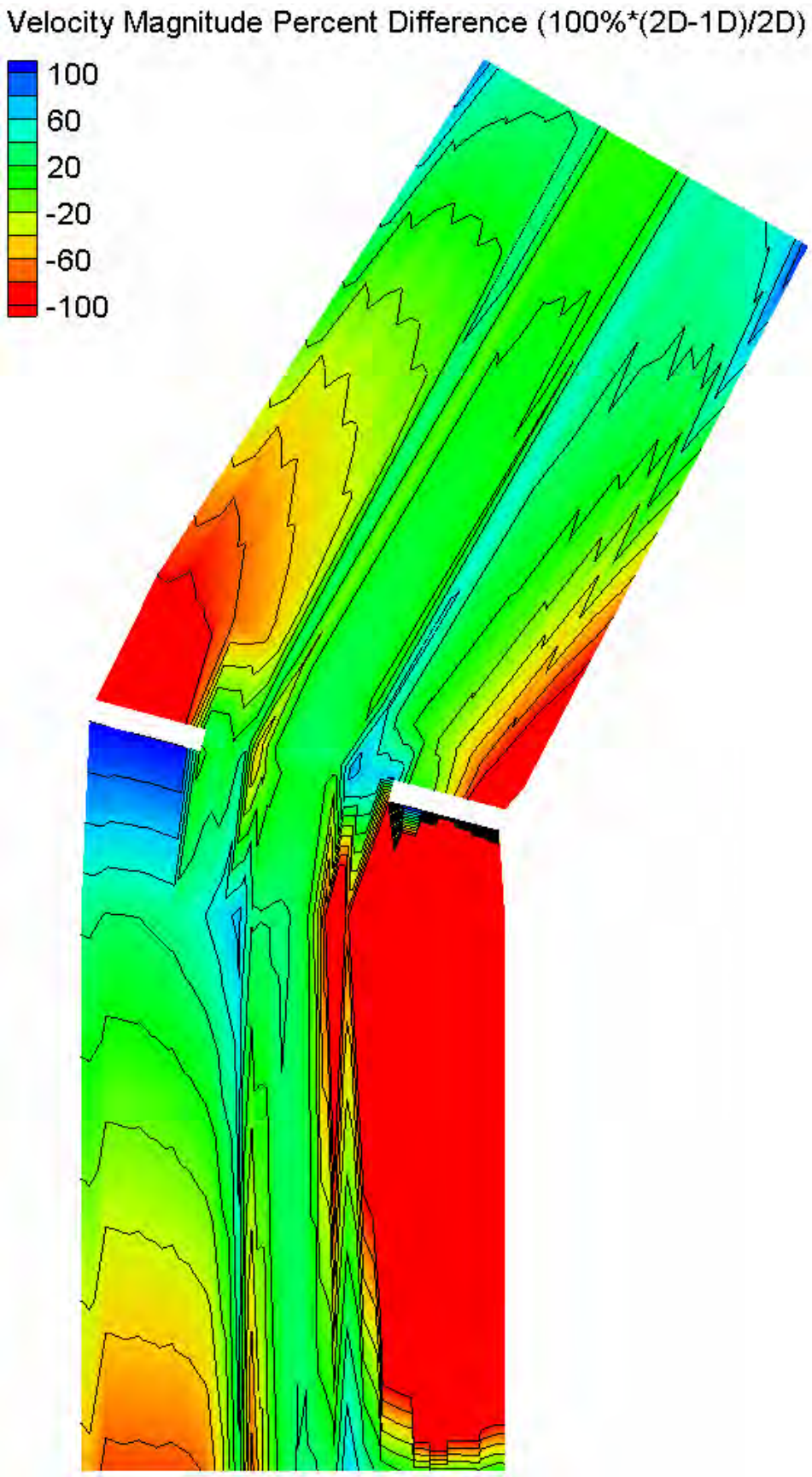

Velocity Magnitude Percent Difference Contours – Large Channel – River Bends (30°, ¼ radius)

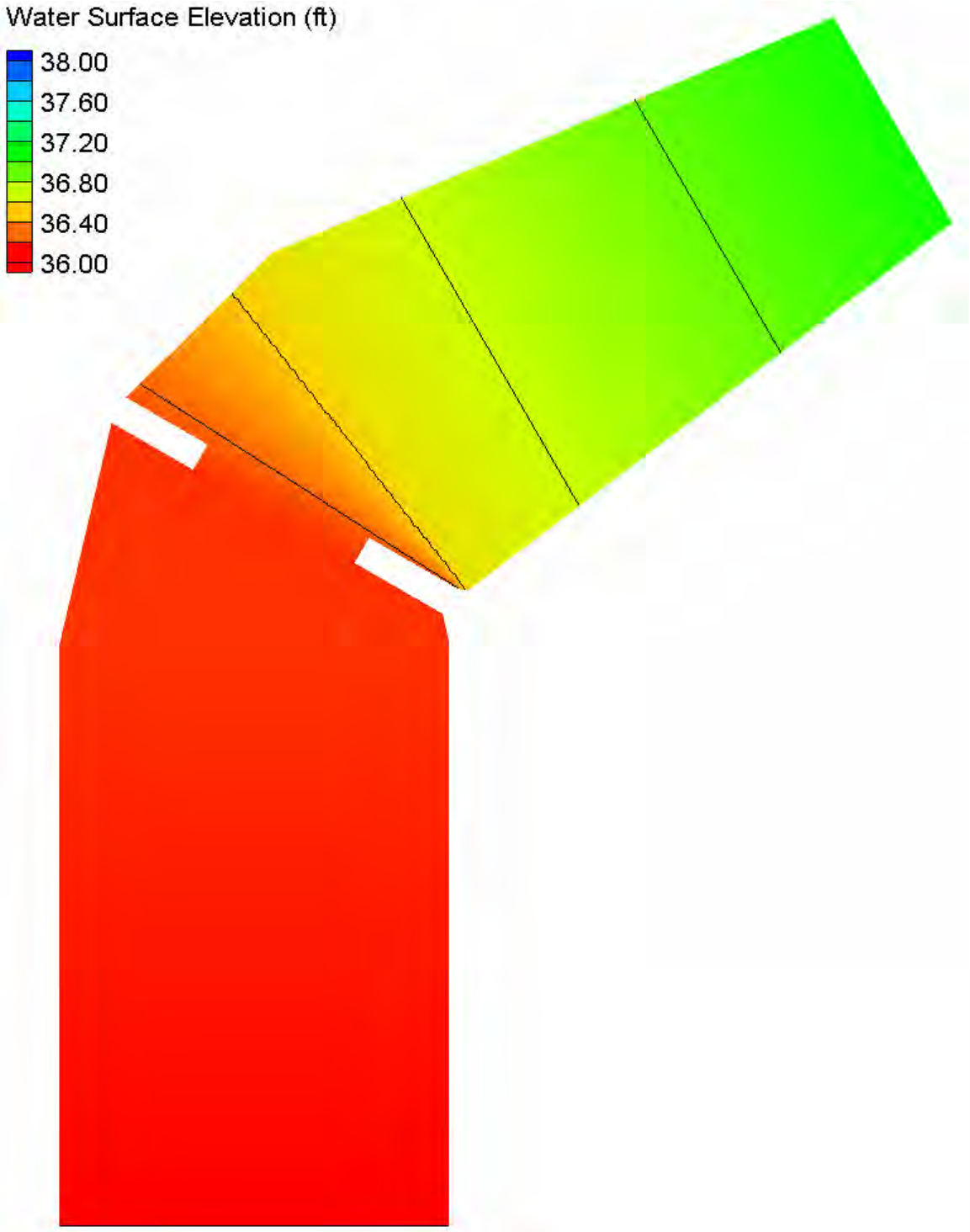

HEC-RAS Water Surface Elevation Contours – Large Channel – River Bends (60°, ½ radius)

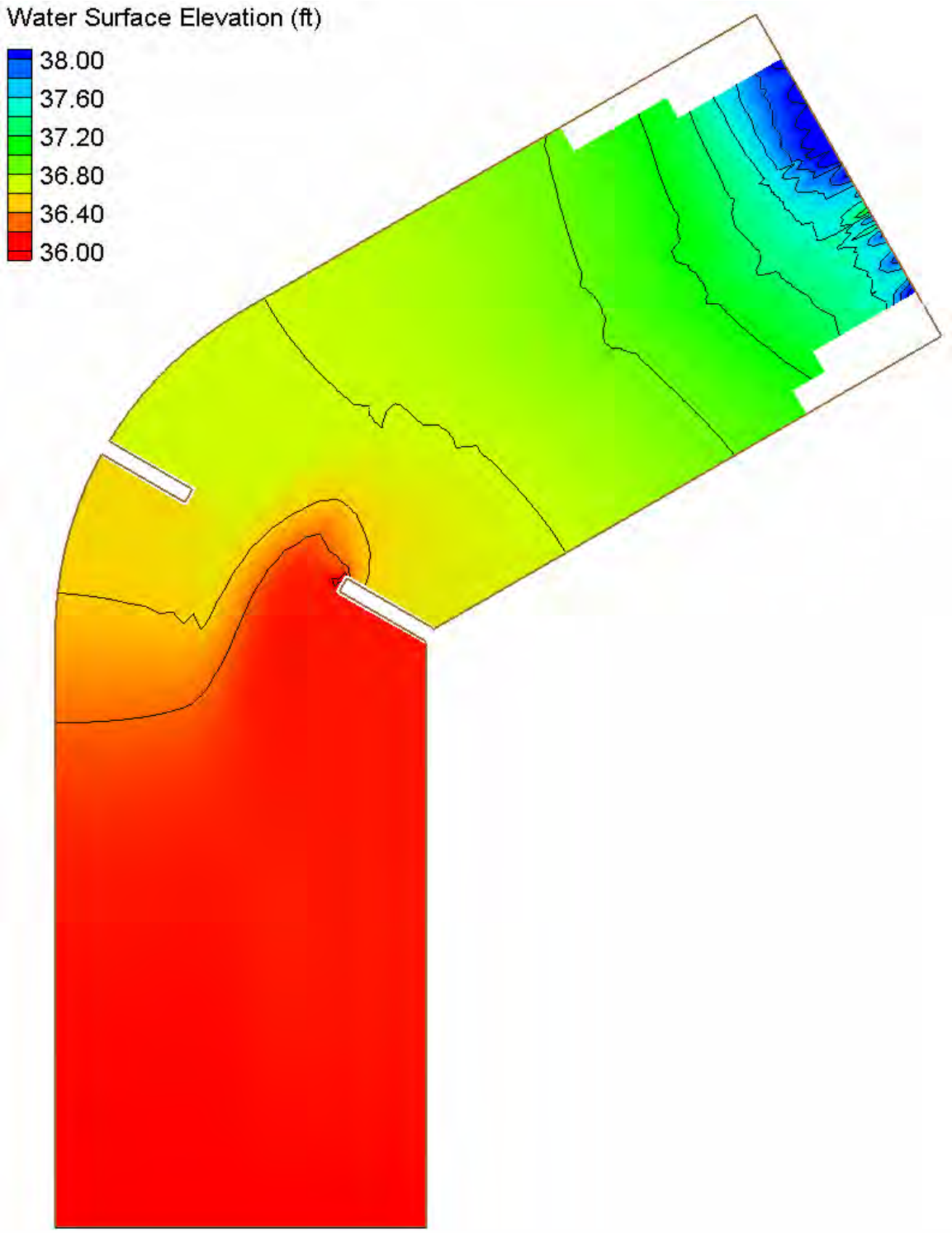

FESWMS Water Surface Elevation Contours – Large Channel – River Bends (60°, ½ radius)

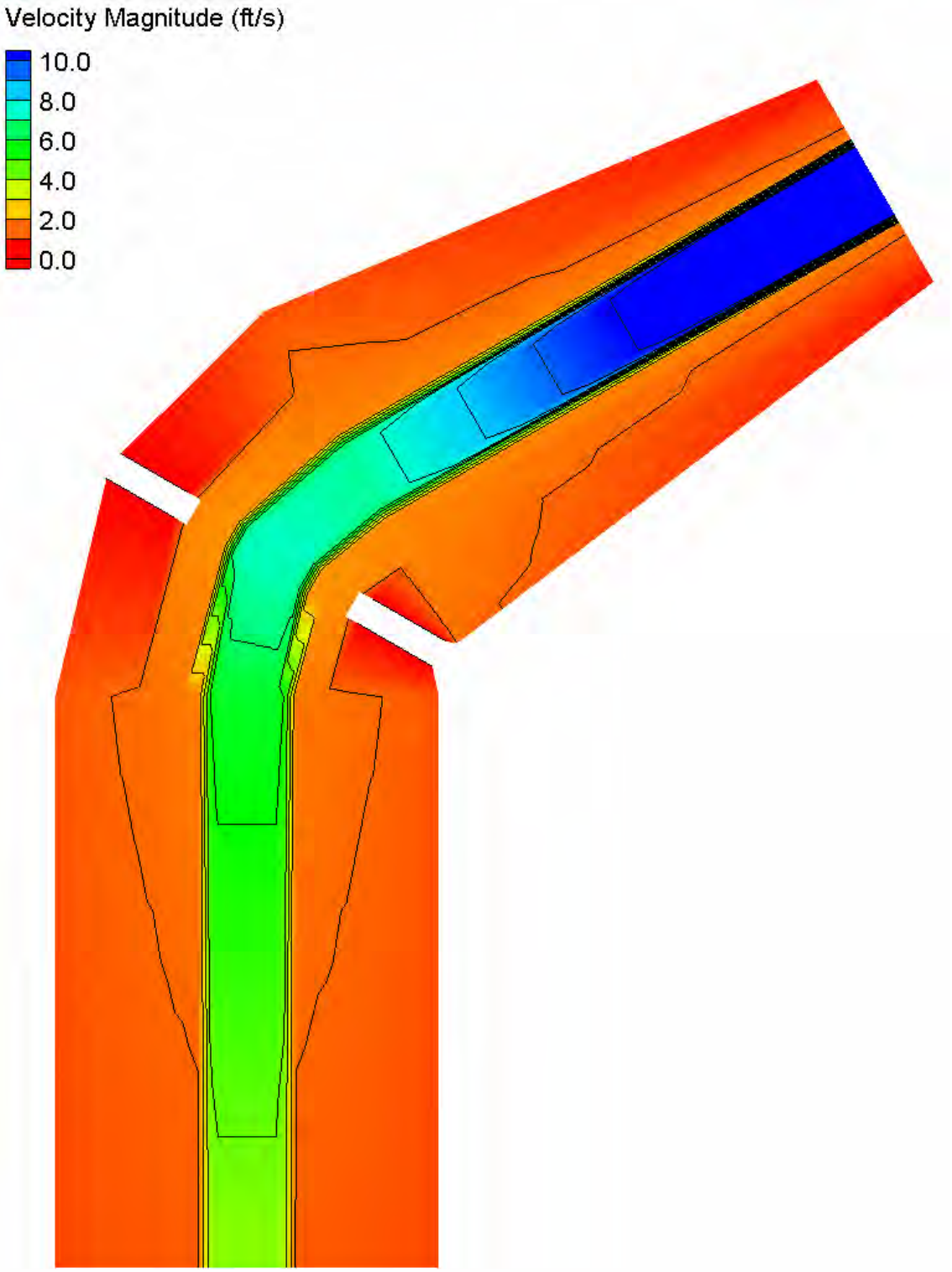

HEC-RAS Velocity Magnitude Contours – Large Channel – River Bends (60°, ½ radius)

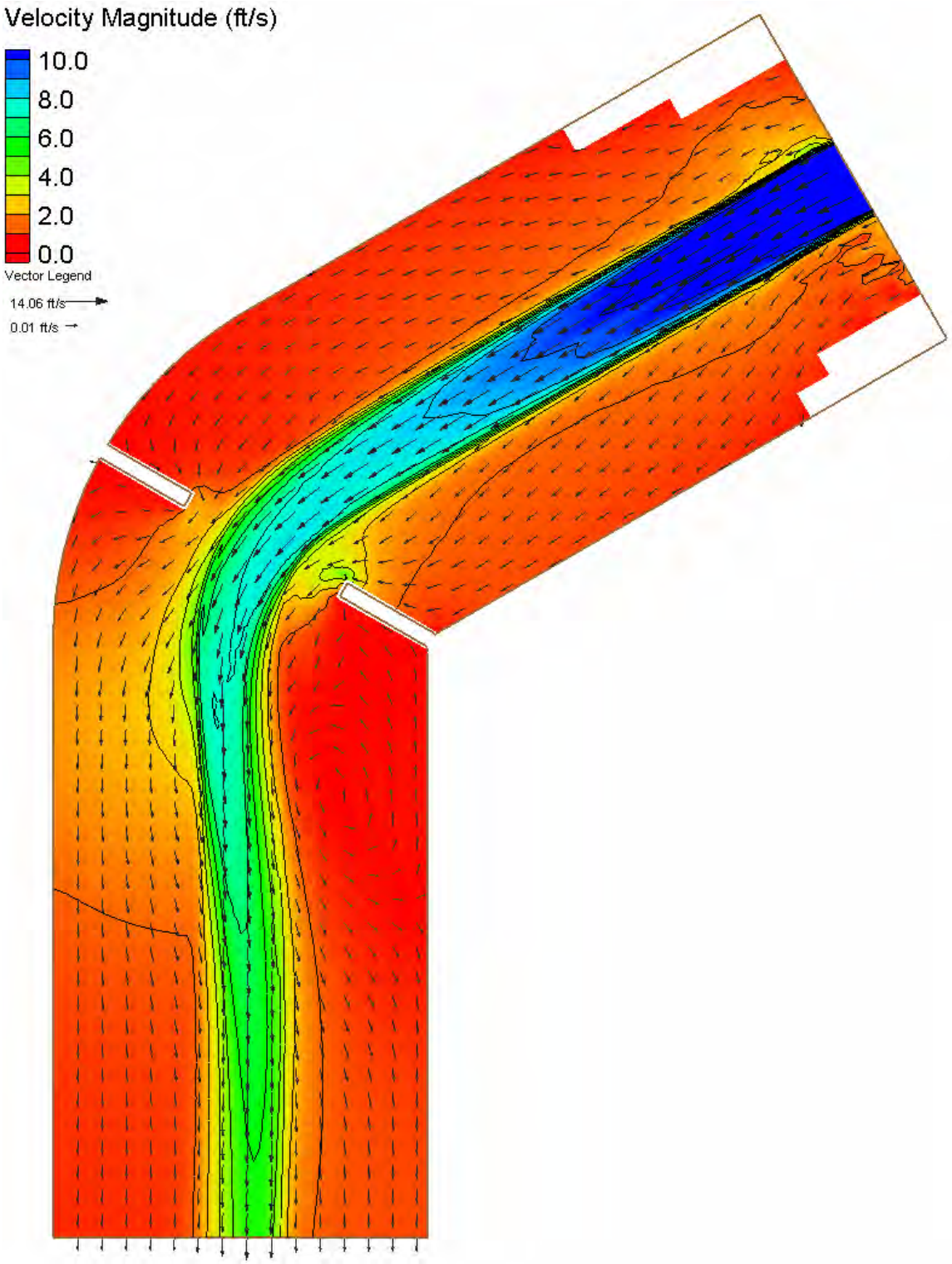

FESWMS Velocity Magnitude Contours – Large Channel – River Bends (60°, ½ radius)

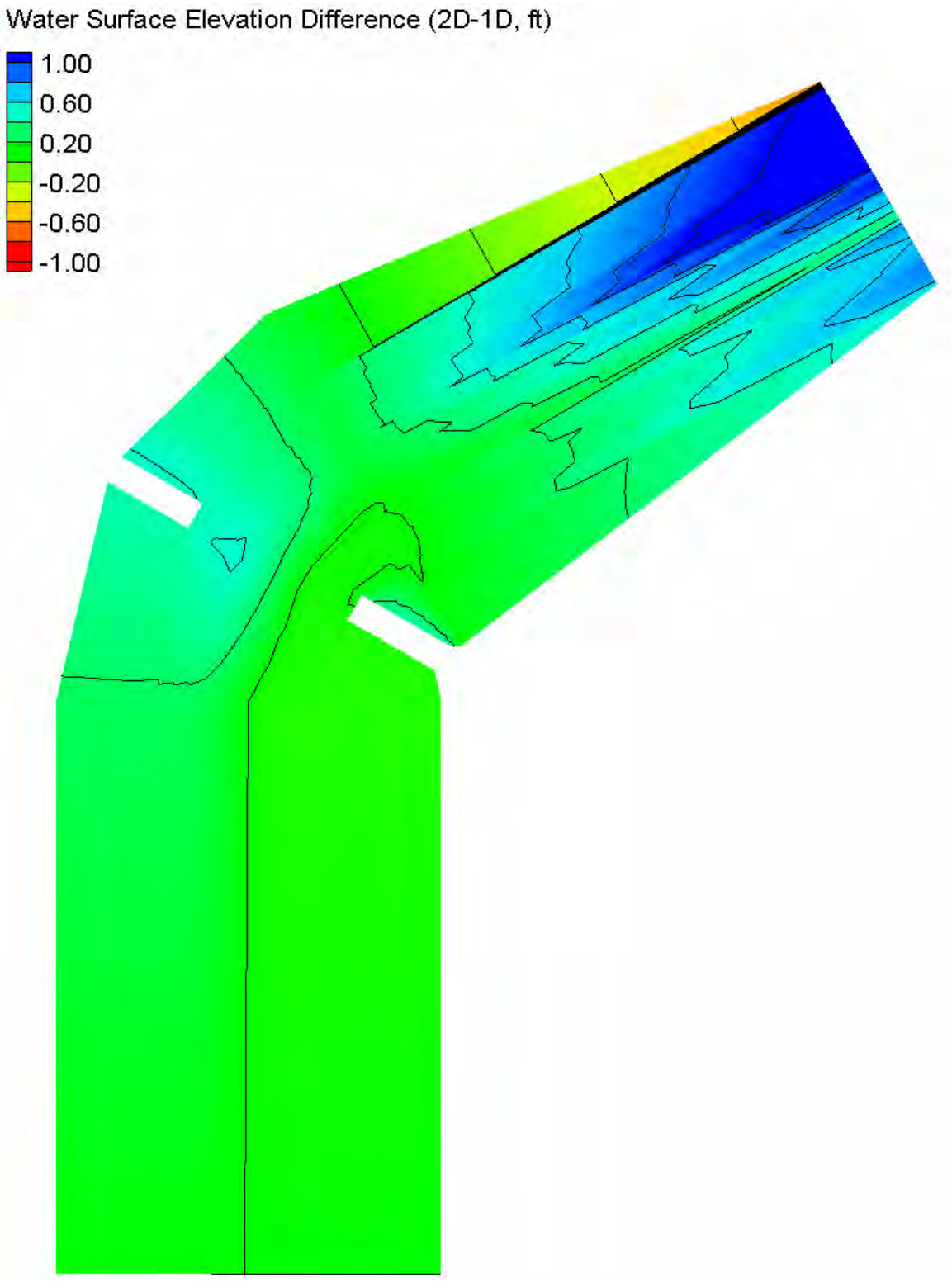

Water Surface Elevation Difference Contours – Large Channel – River Bends (60°, ½ radius)

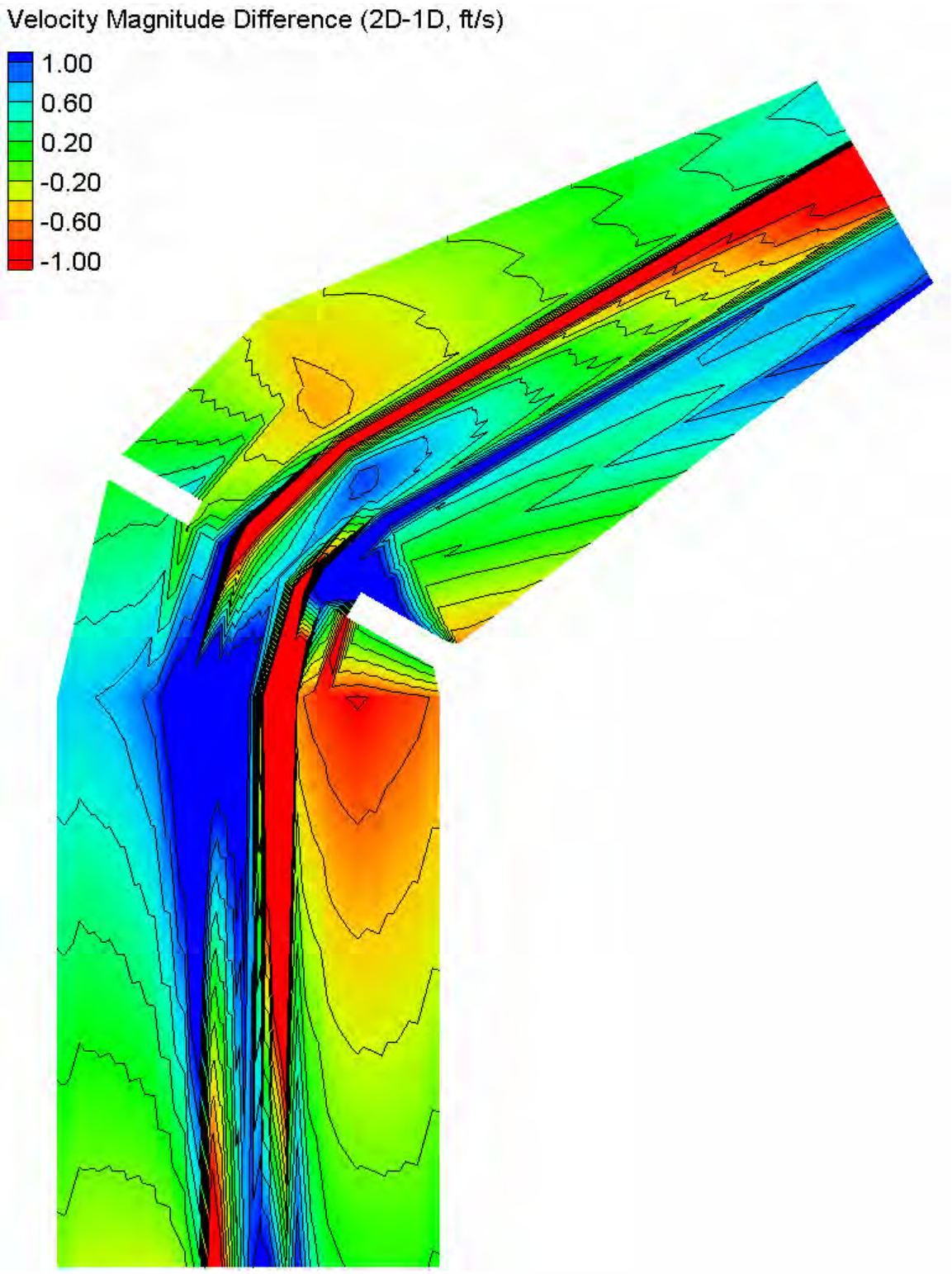

Velocity Magnitude Difference Contours – Large Channel – River Bends (60°, ½ radius)

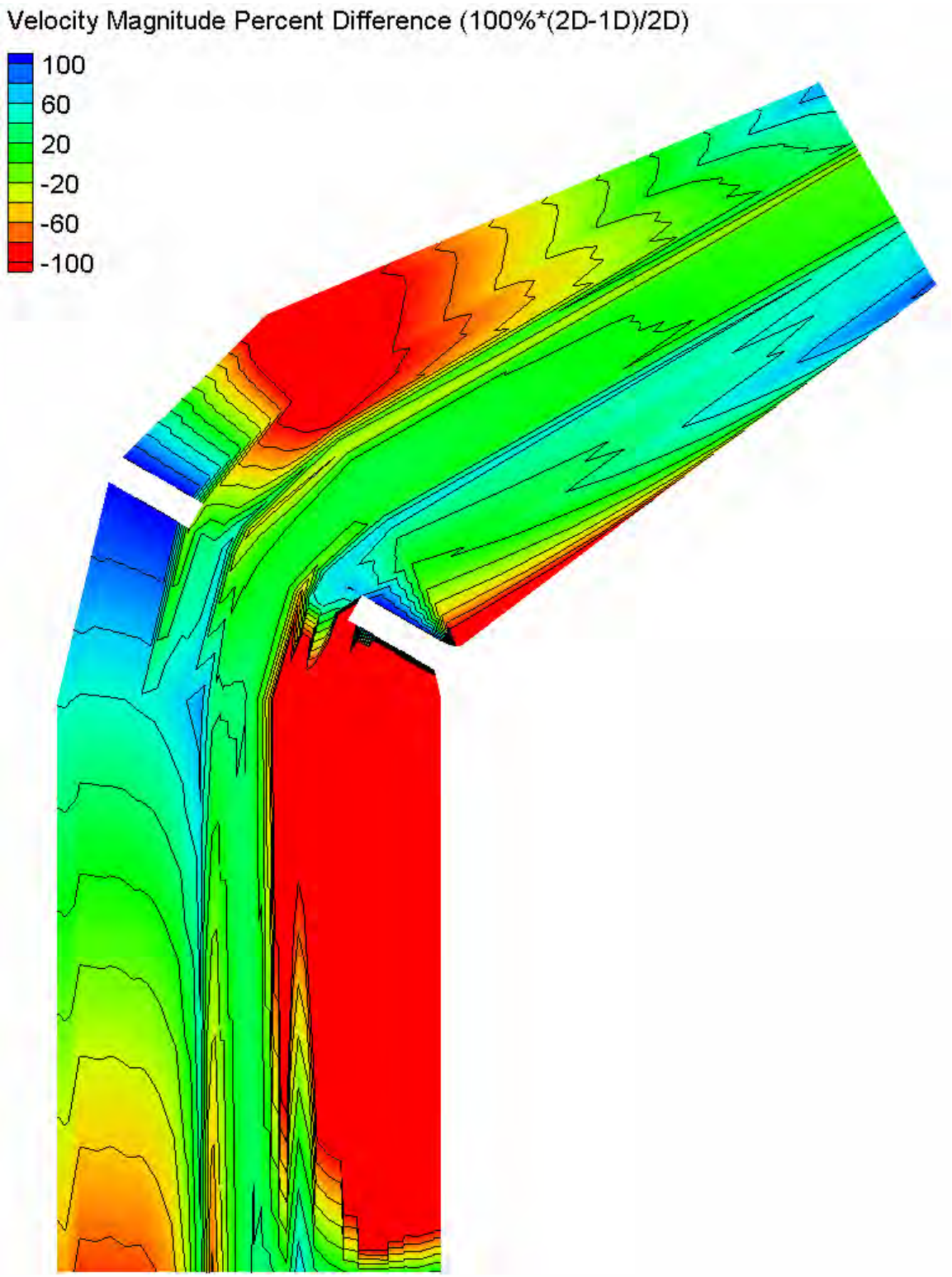

Velocity Magnitude Percent Difference Contours – Large Channel – River Bends (60°, ½ radius)

HEC-RAS Water Surface Elevation Contours – Large Channel – River Bends (60°, ¼ radius)

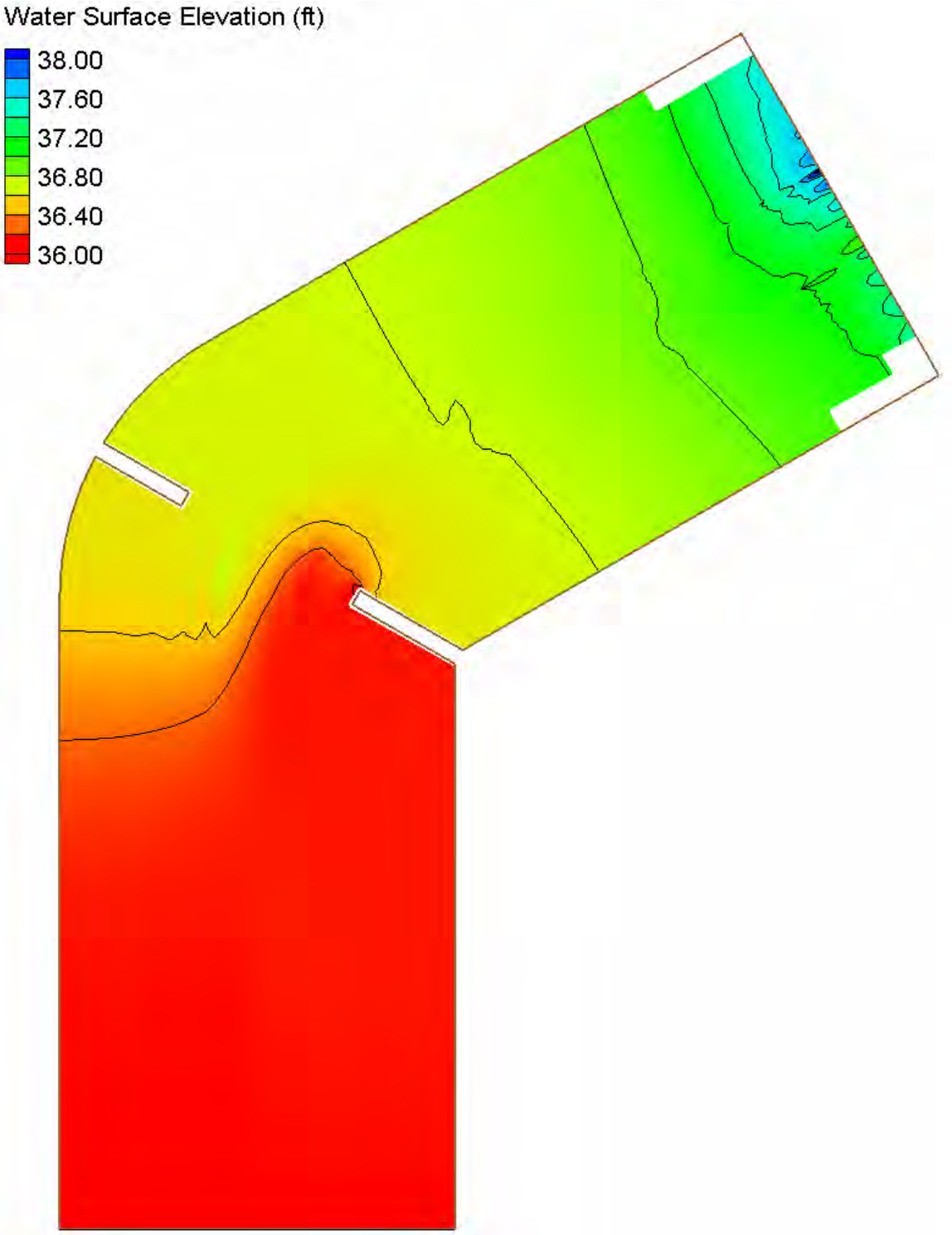

FESWMS Water Surface Elevation Contours – Large Channel – River Bends (60°, ¼ radius)

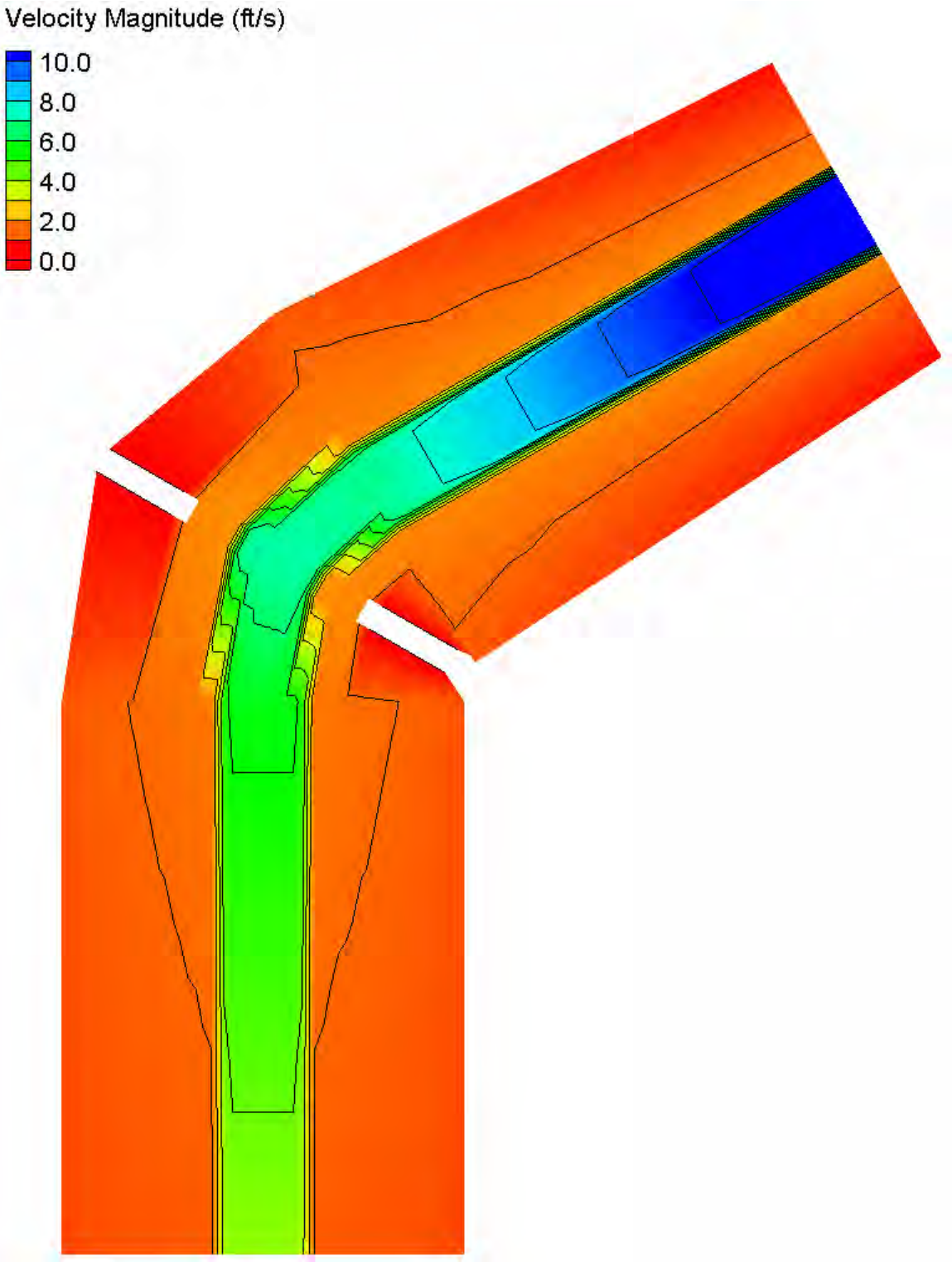

HEC-RAS Velocity Magnitude Contours – Large Channel – River Bends (60°, ¼ radius)

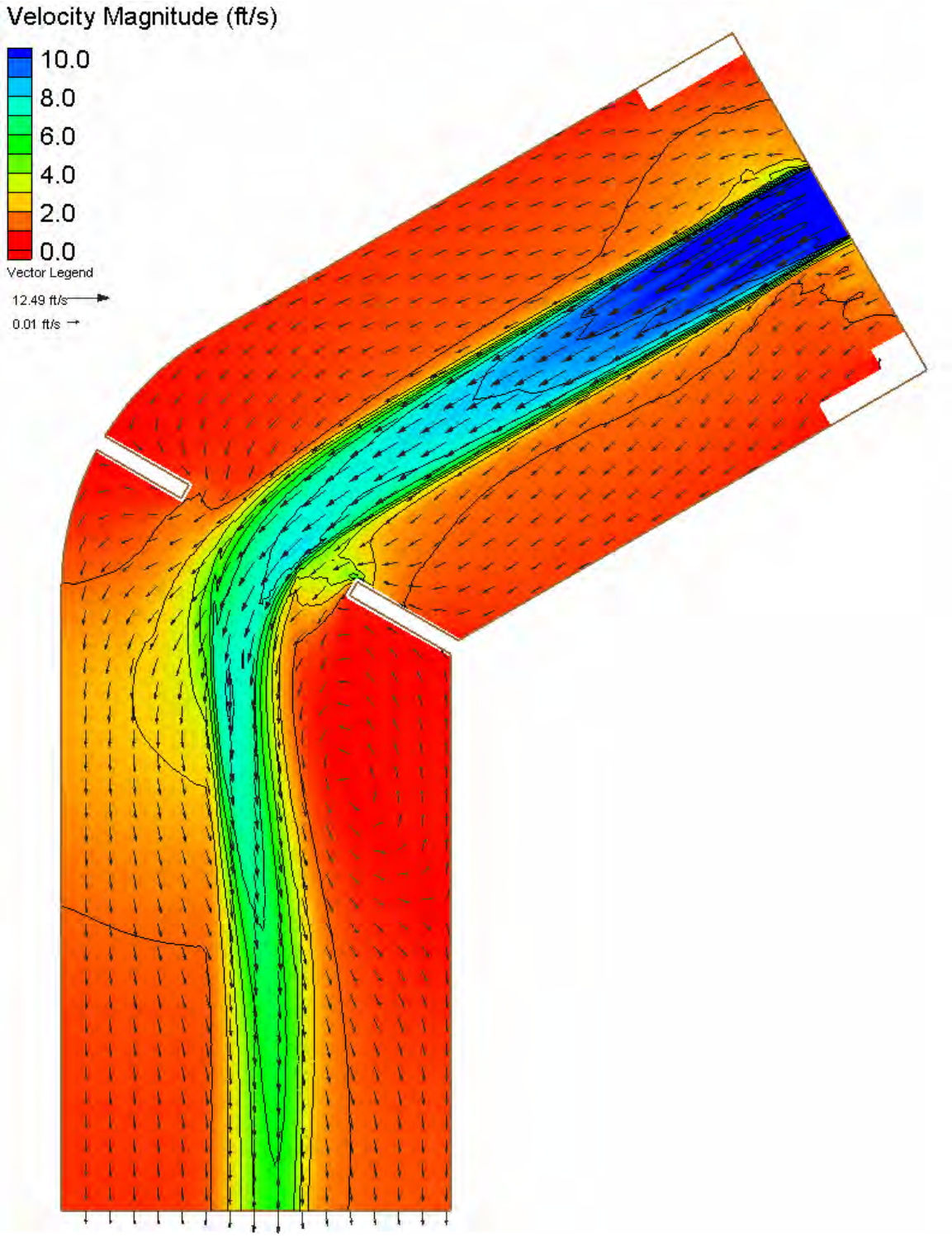

FESWMS Velocity Magnitude Contours – Large Channel – River Bends (60°, ¼ radius)

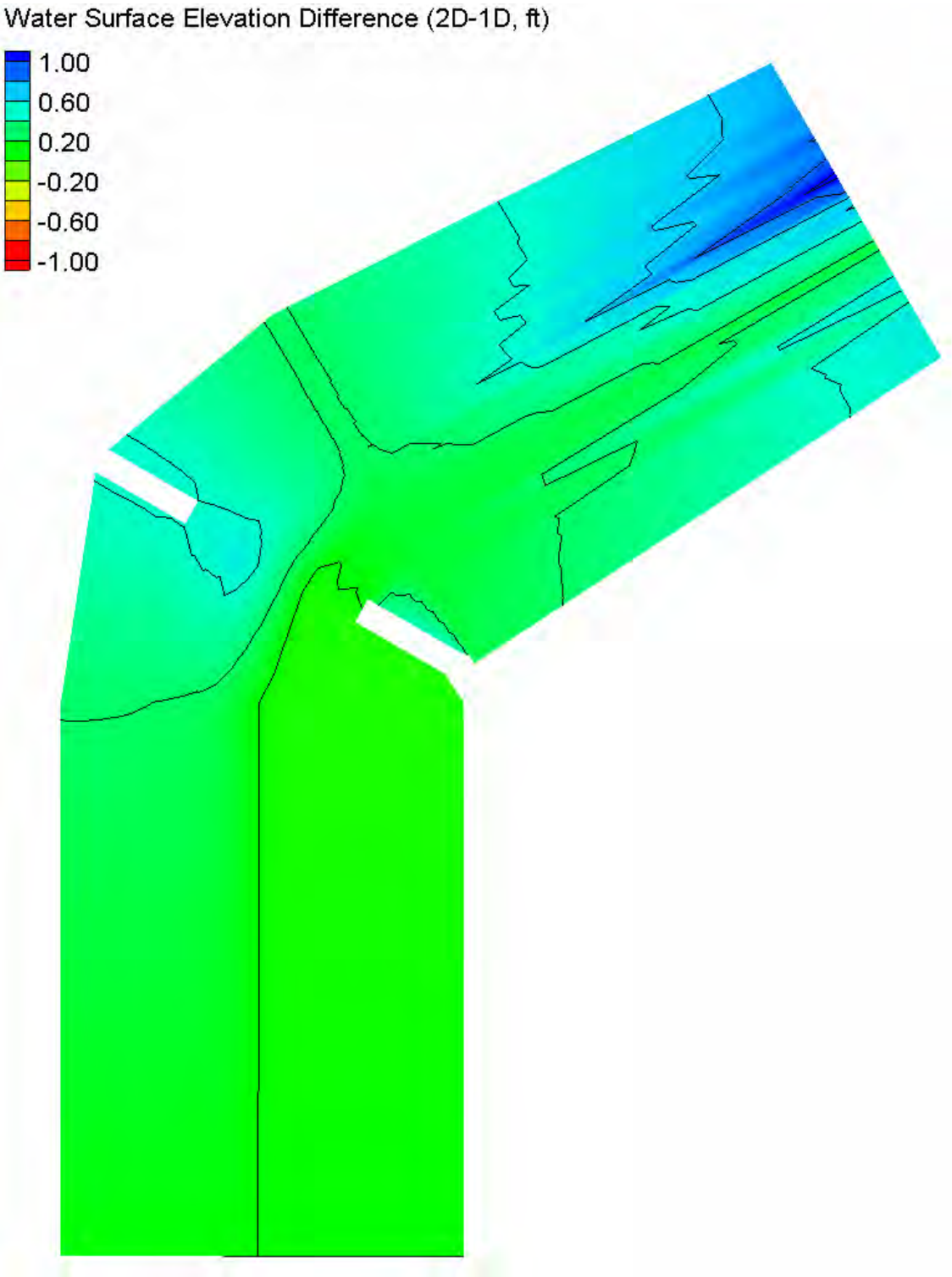

Water Surface Elevation Difference Contours – Large Channel – River Bends (60°, ¼ radius)

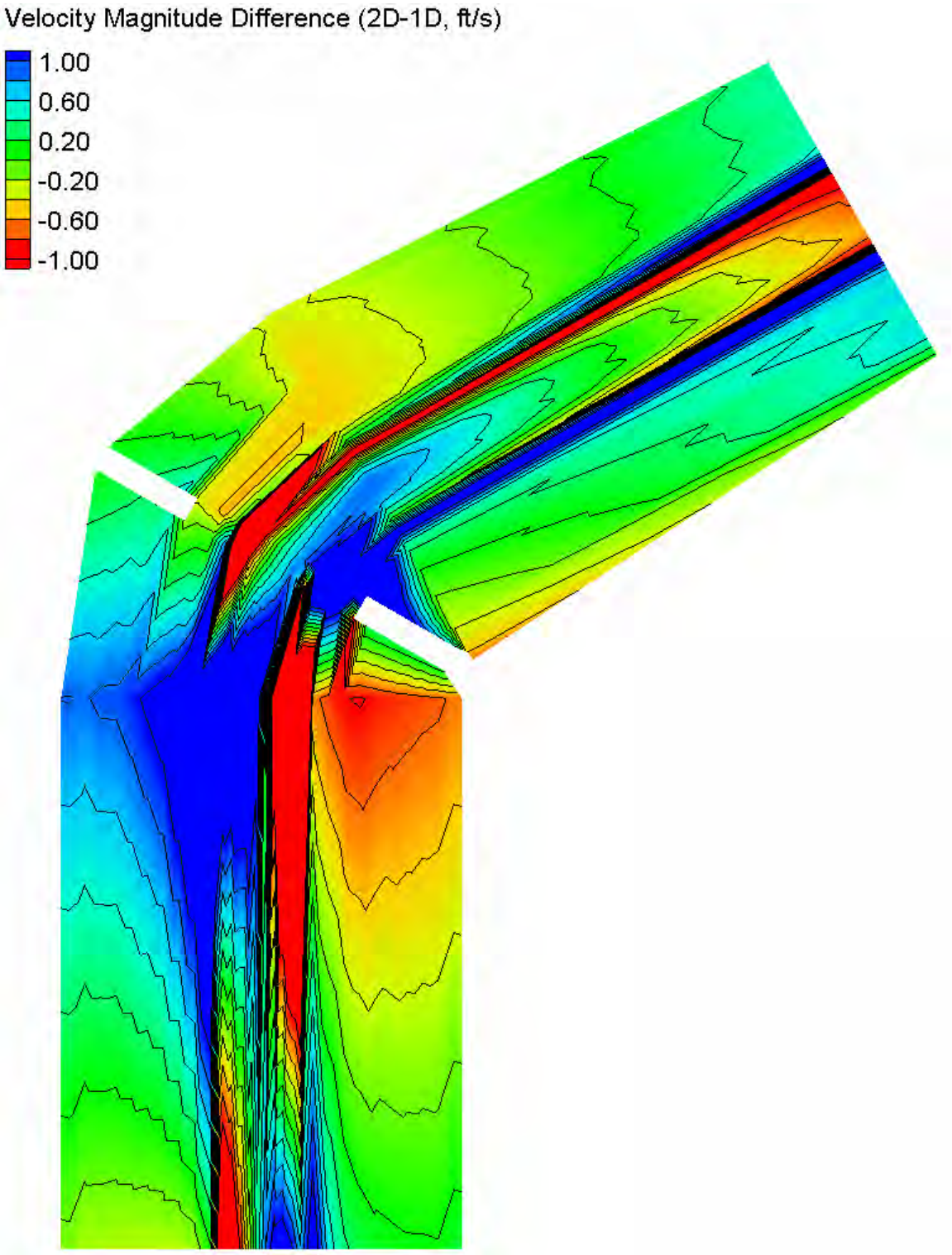

Velocity Magnitude Difference Contours – Large Channel – River Bends (60°, ¼ radius)

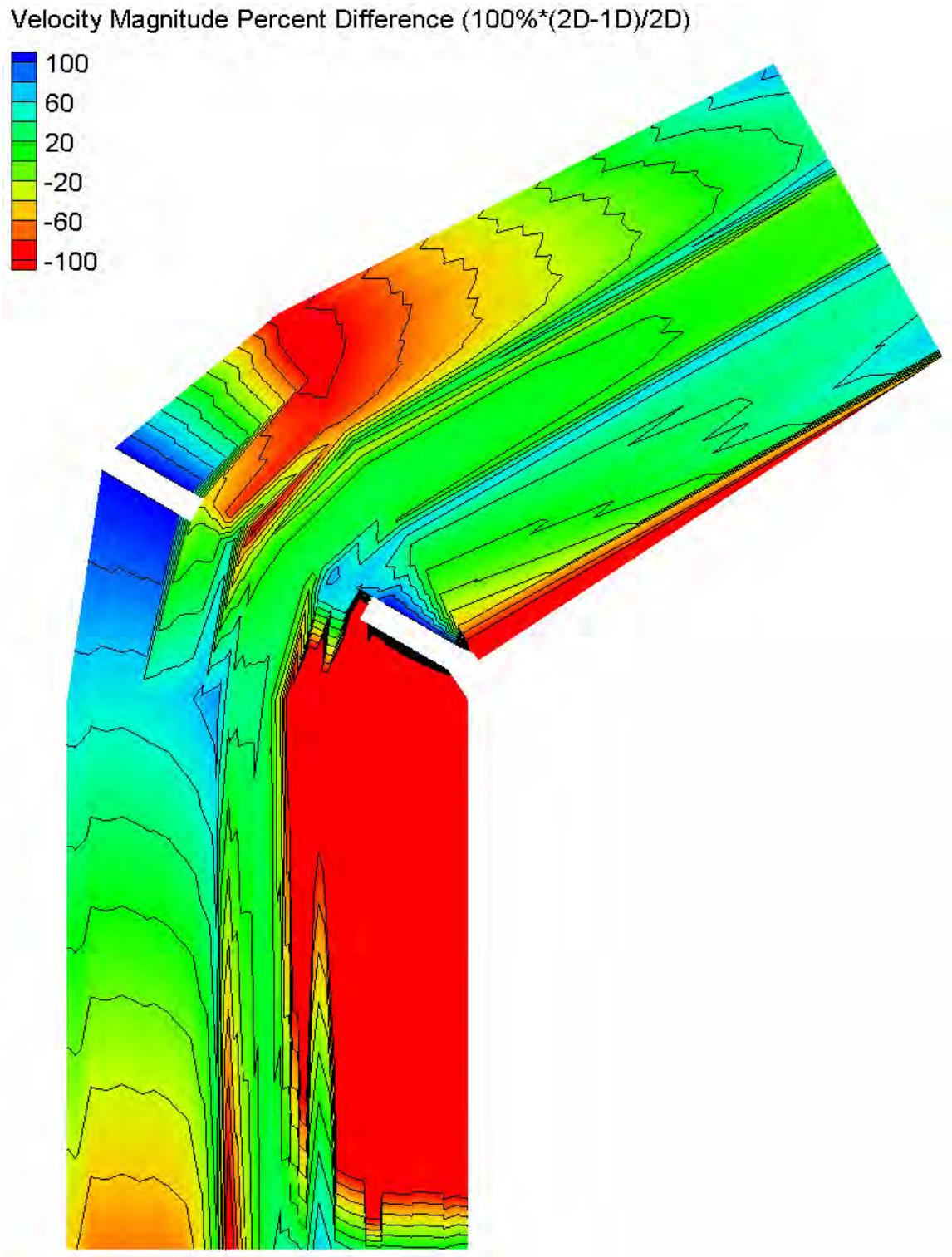

Velocity Magnitude Percent Difference Contours – Large Channel – River Bends (60°, ¼ radius)

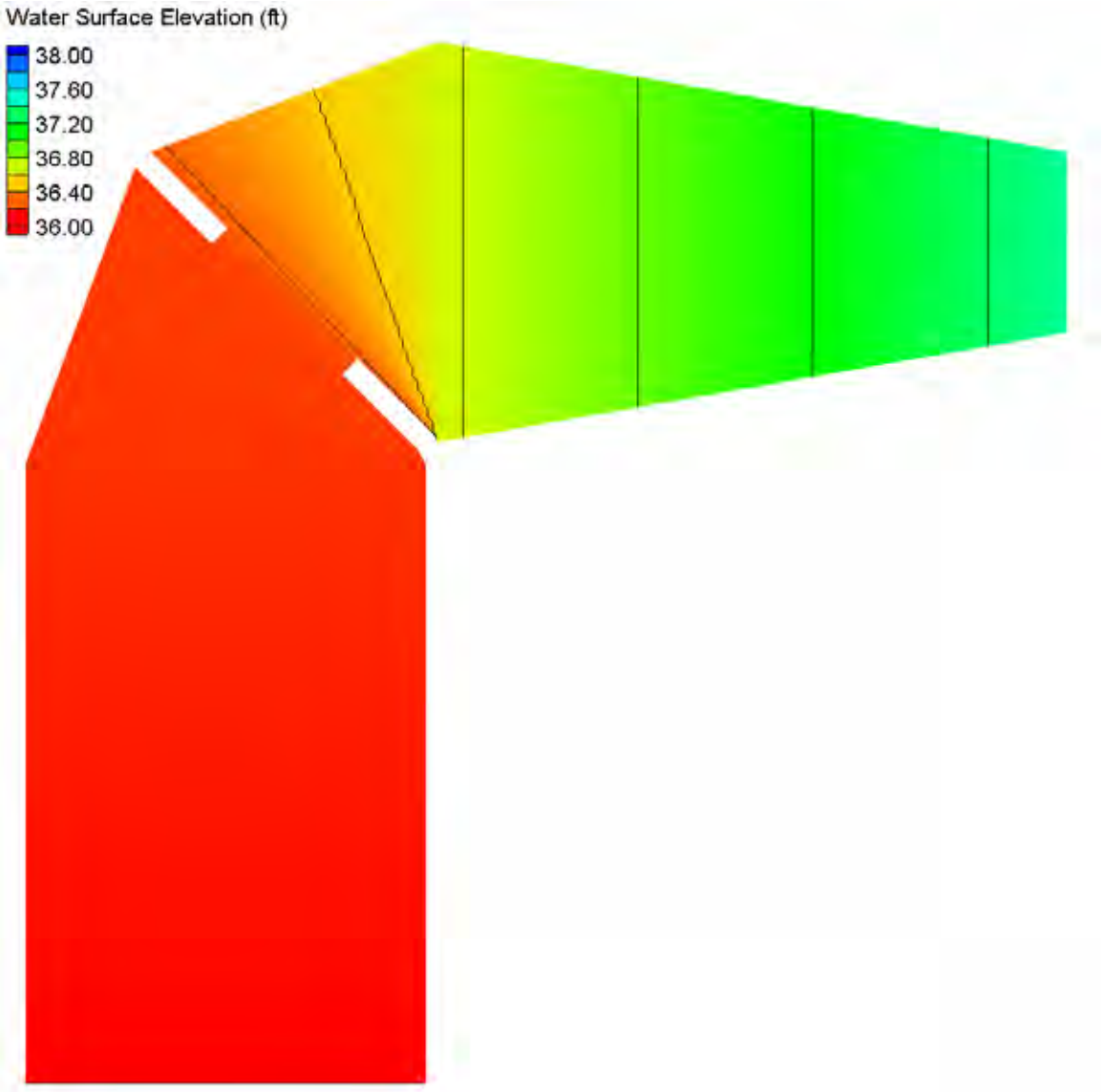

HEC-RAS Water Surface Elevation Contours – Large Channel – River Bends (90°, ½ radius)

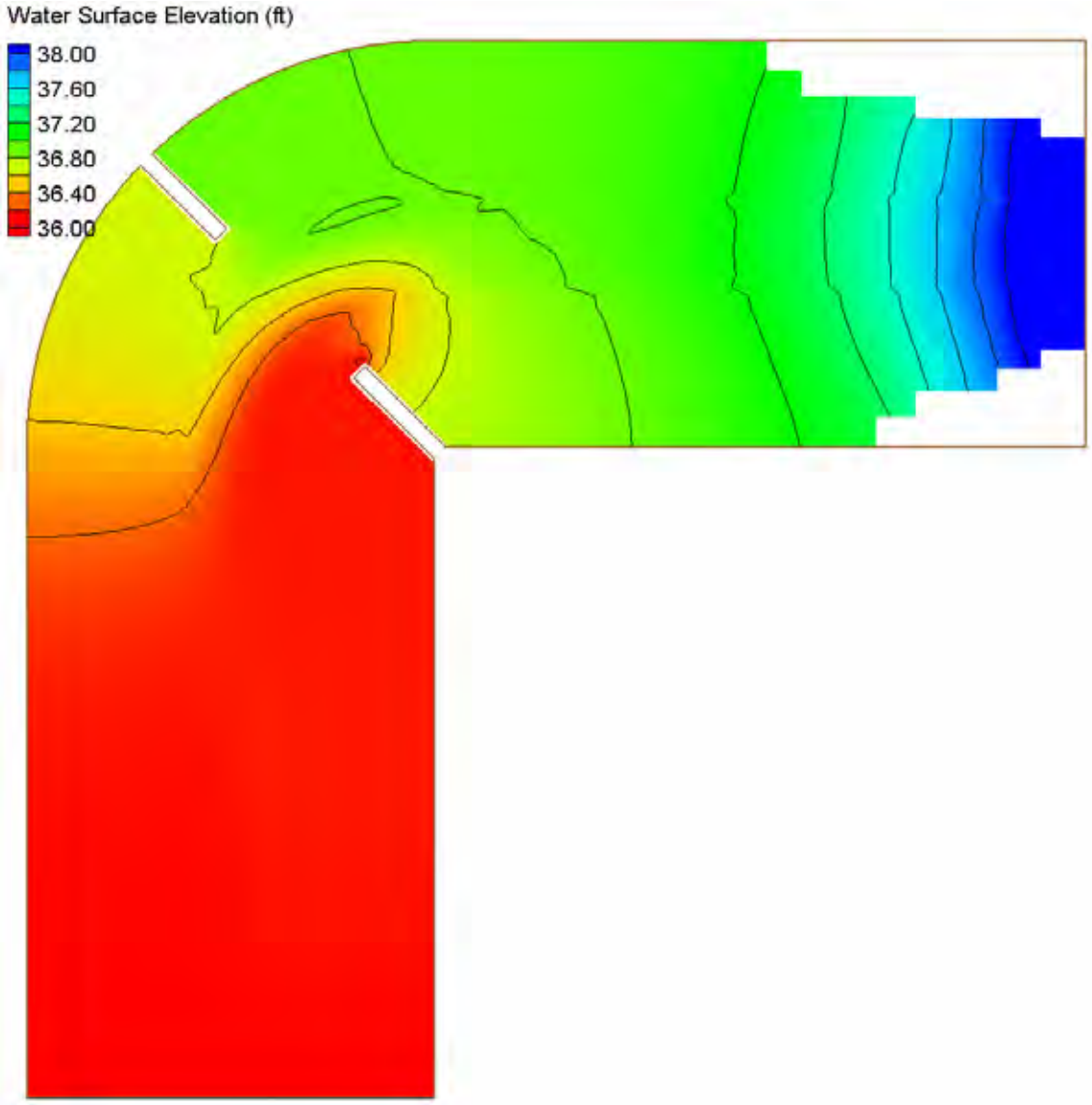

FESWMS Water Surface Elevation Contours – Large Channel – River Bends (90°, ½ radius)

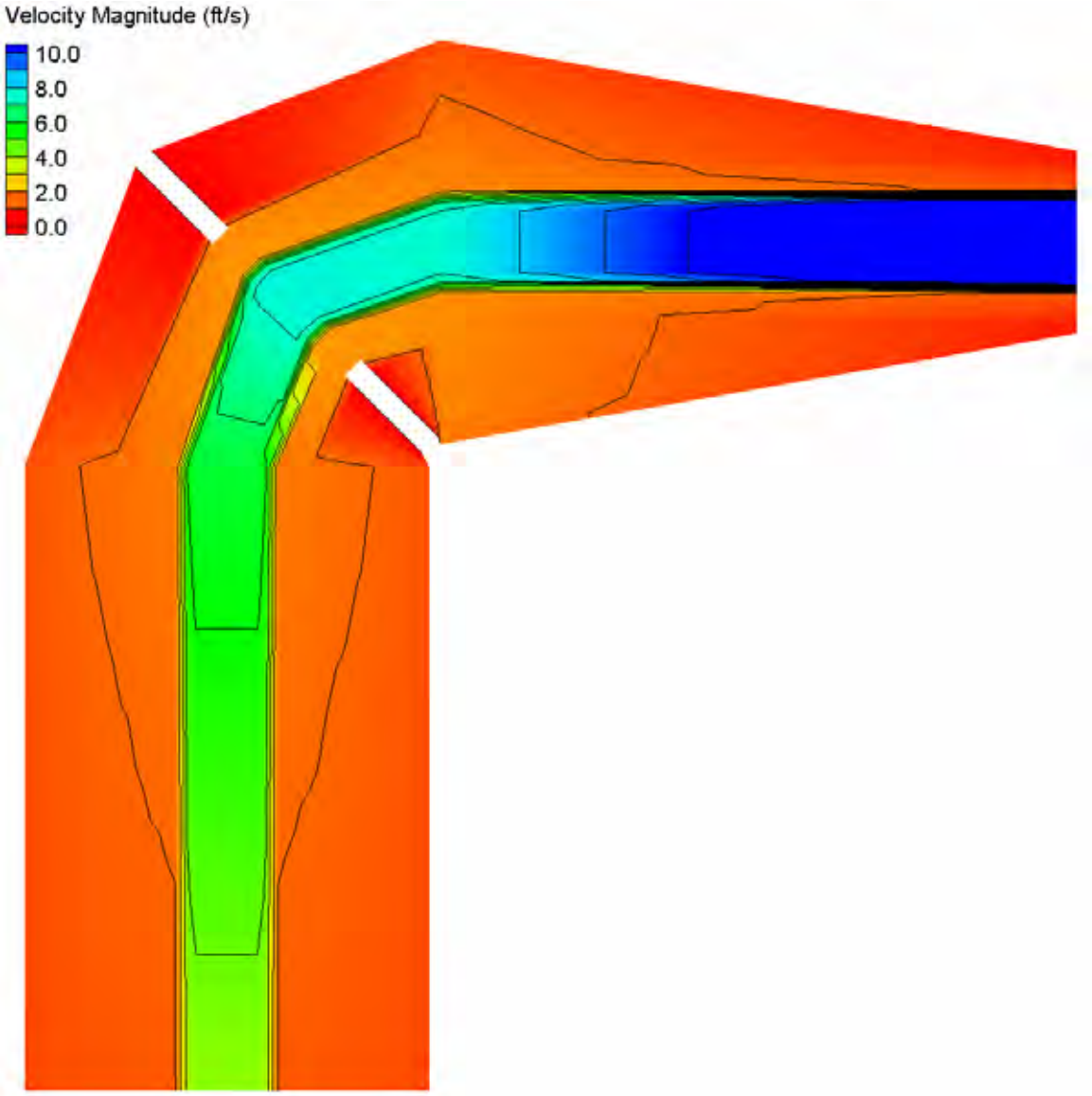

HEC-RAS Velocity Magnitude Contours – Large Channel – River Bends (90°, ½ radius)

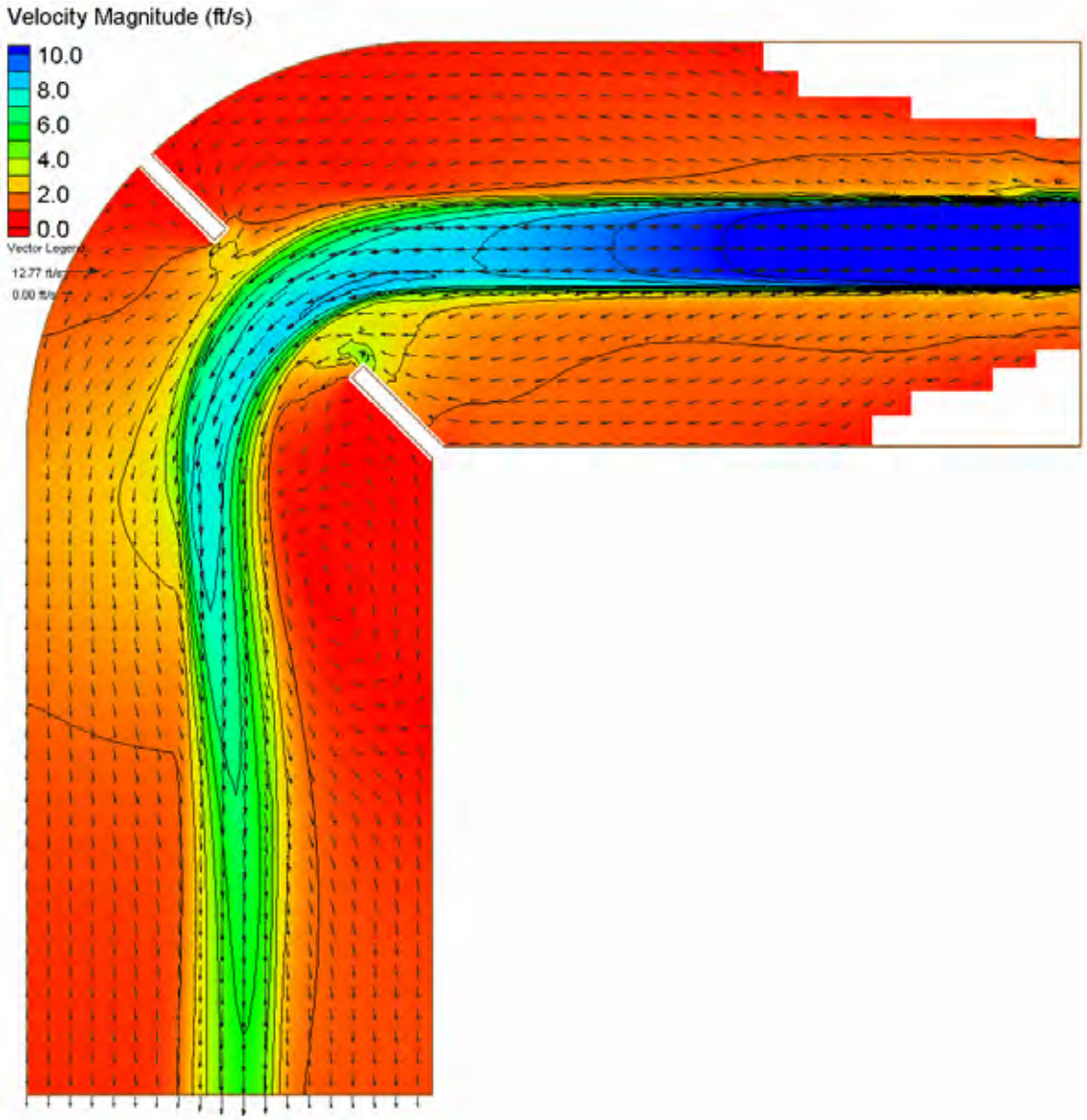

FESWMS Velocity Magnitude Contours – Large Channel – River Bends (90°, ½ radius)

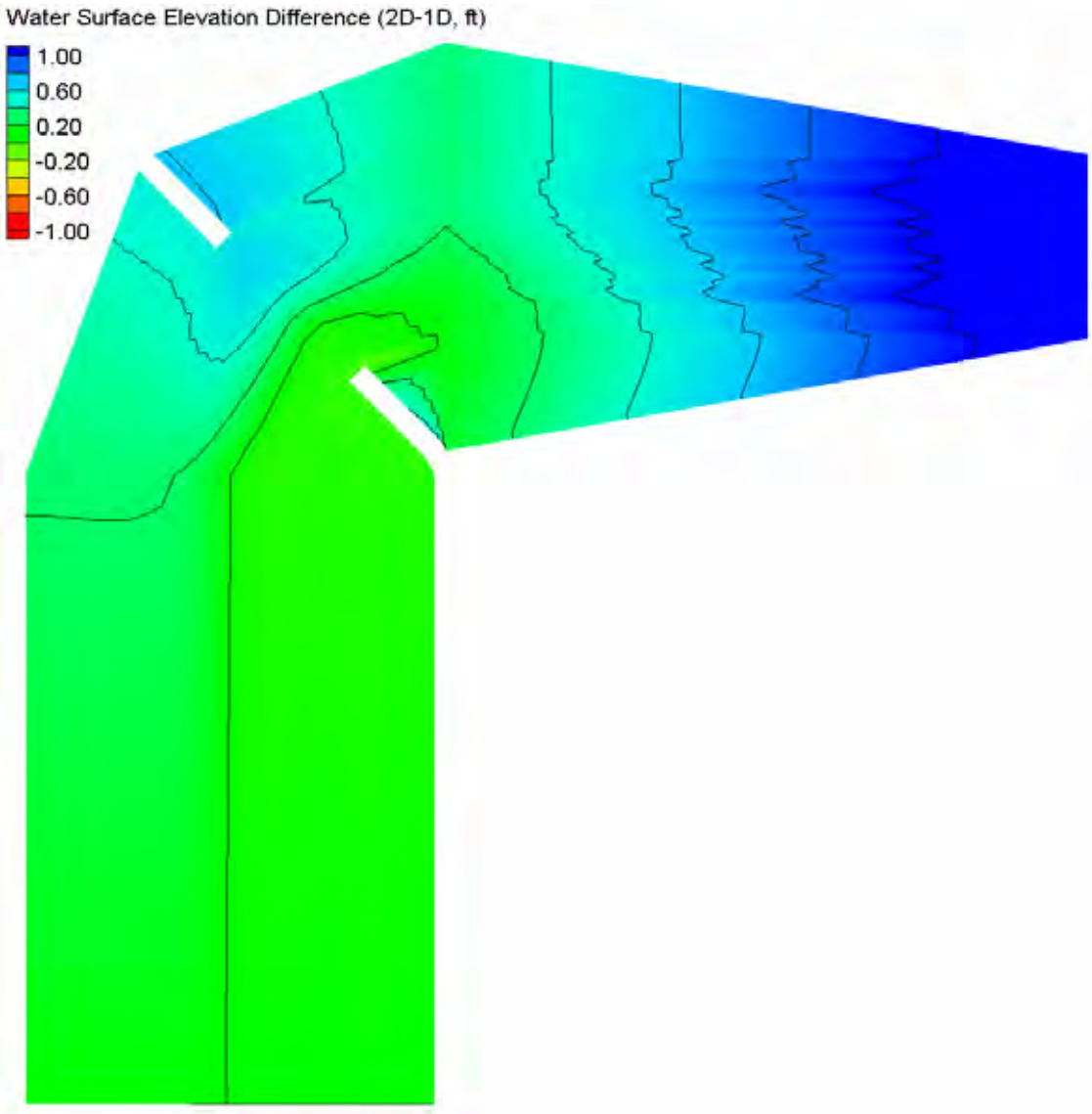

Water Surface Elevation Difference Contours – Large Channel – River Bends (90°, ½ radius)

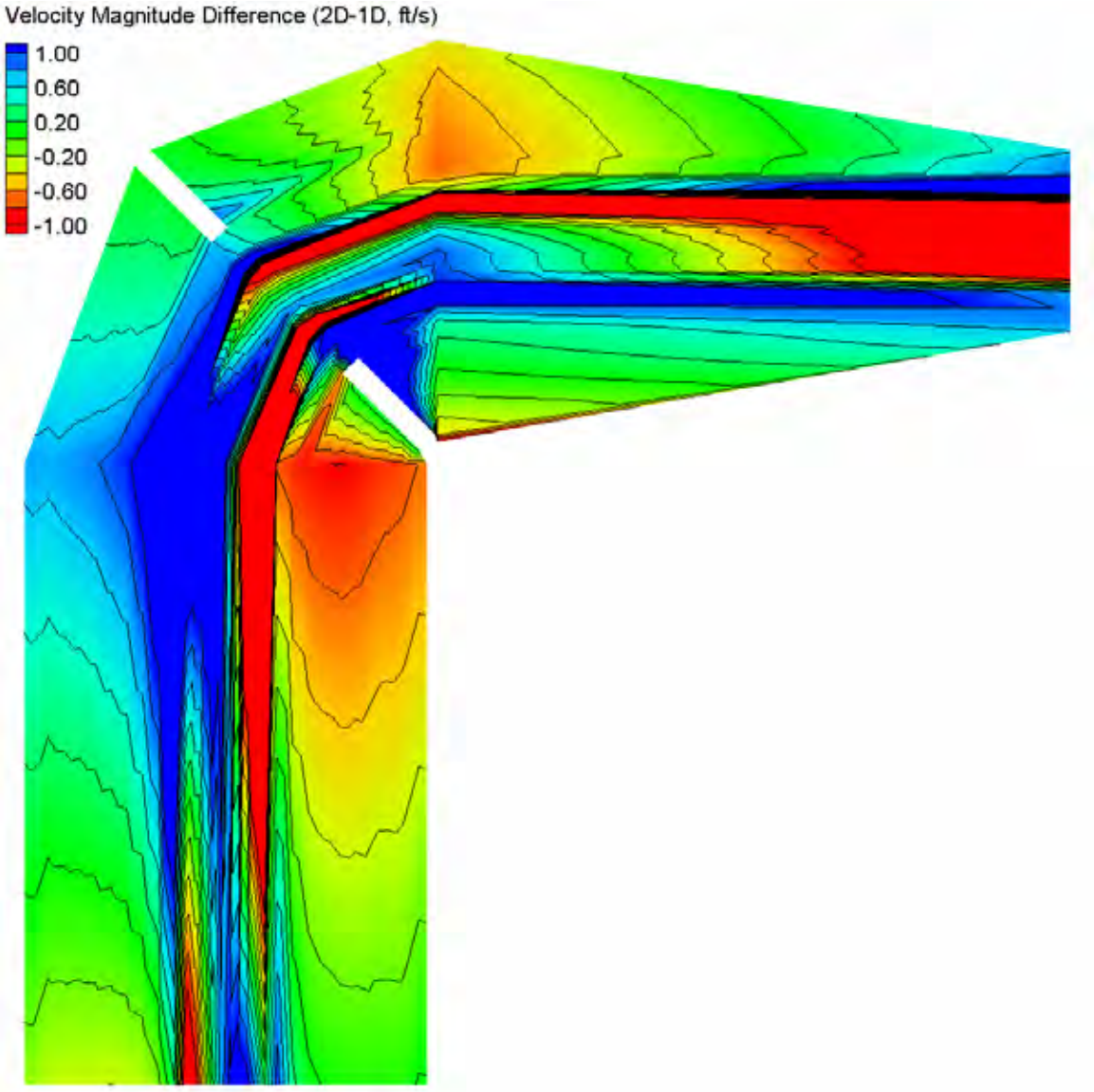

Velocity Magnitude Difference Contours – Large Channel – River Bends (90°, ½ radius)

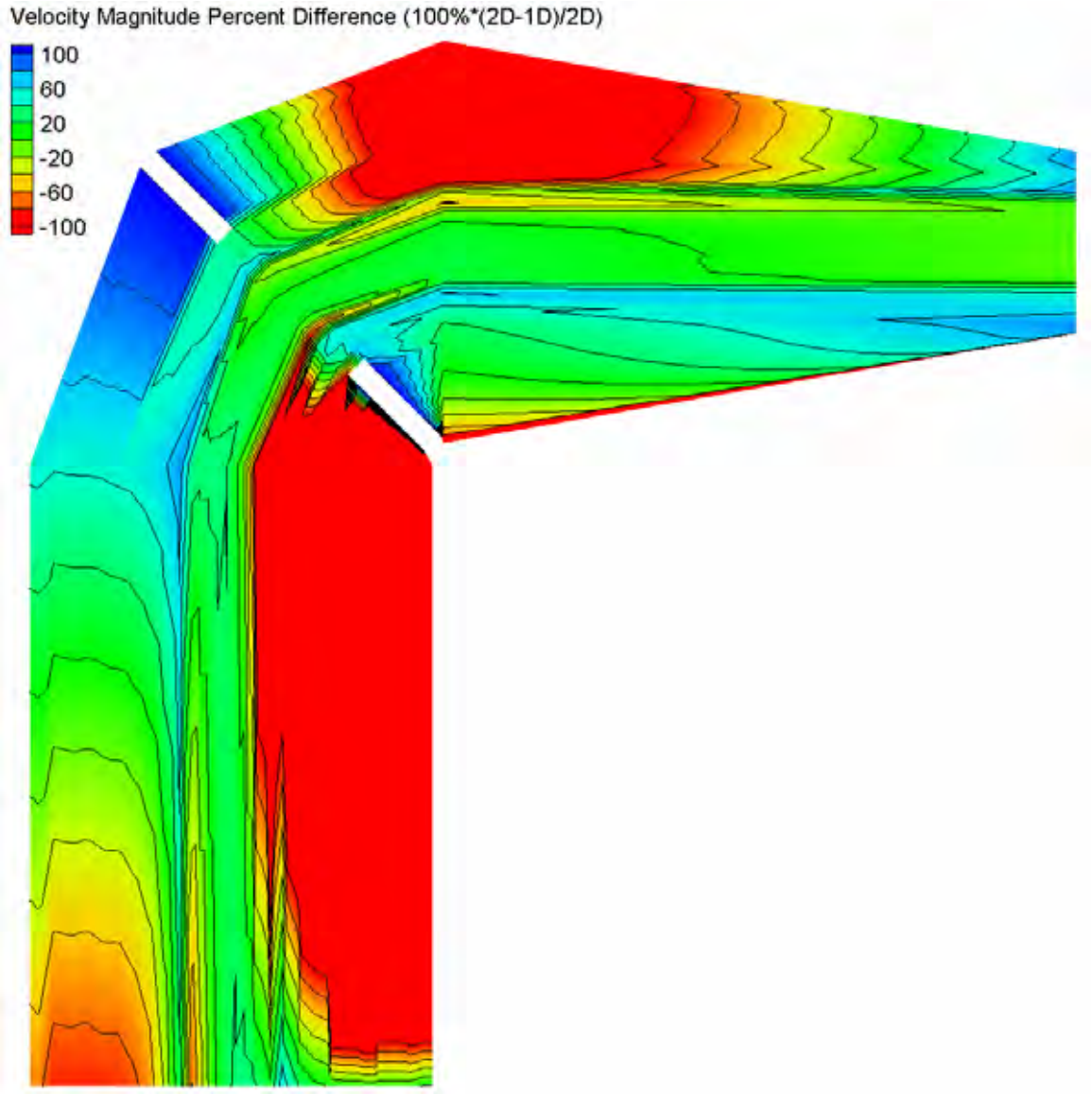

Velocity Magnitude Percent Difference Contours – Large Channel – River Bends (90°, ½ radius)

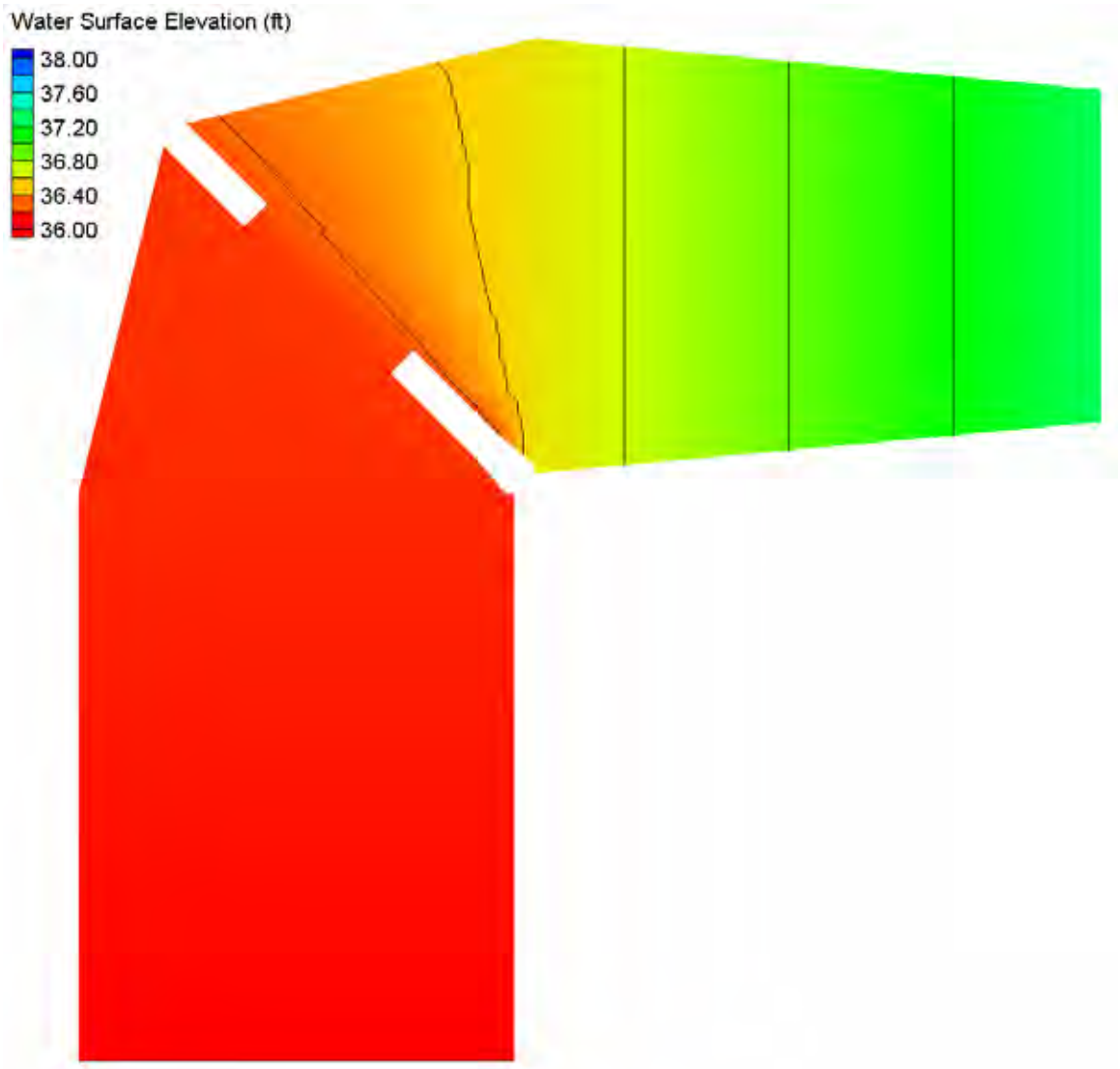

HEC-RAS Water Surface Elevation Contours – Large Channel – River Bends (90°, ¼ radius)

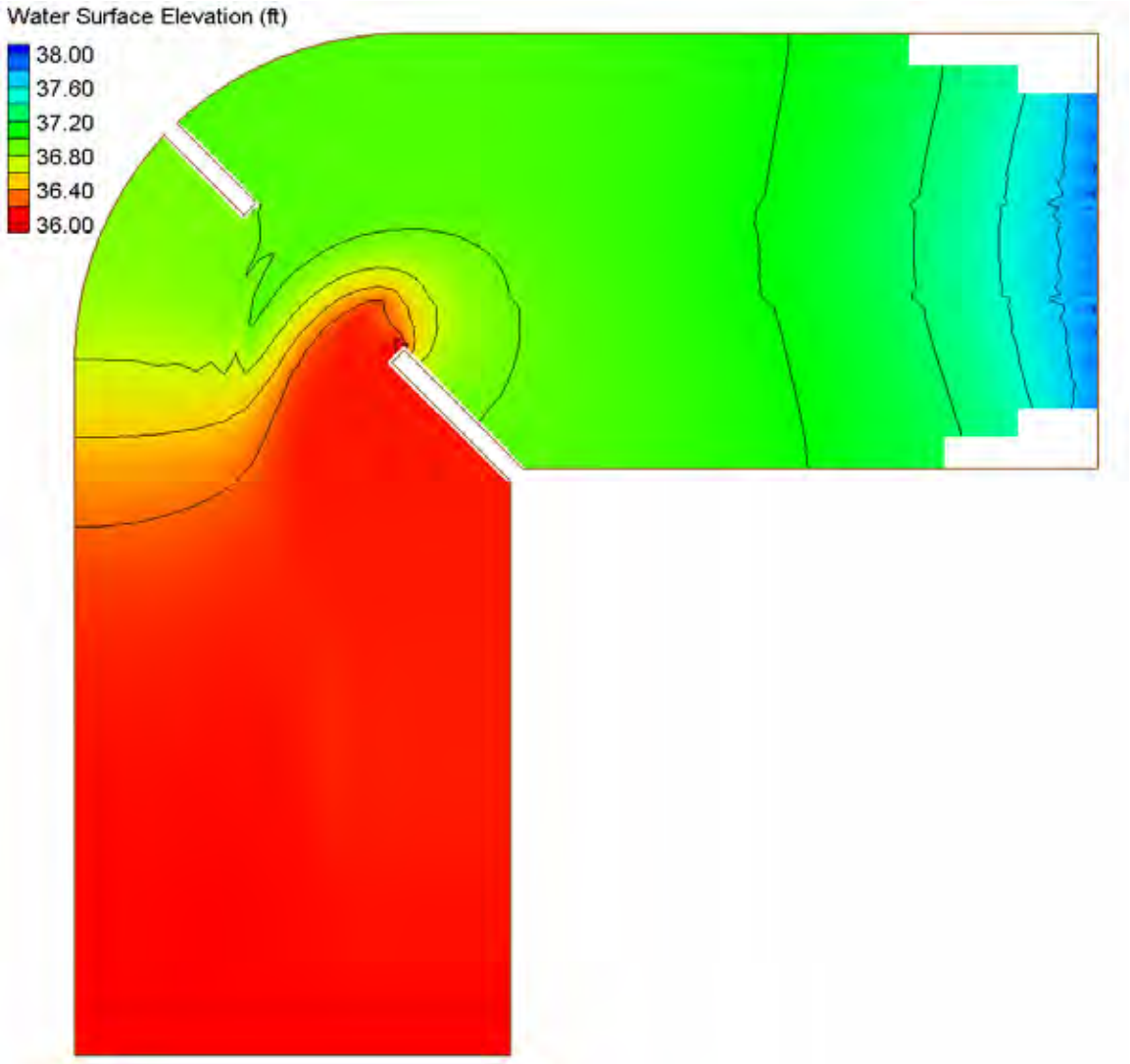

FESWMS Water Surface Elevation Contours – Large Channel – River Bends (90°, ¼ radius)

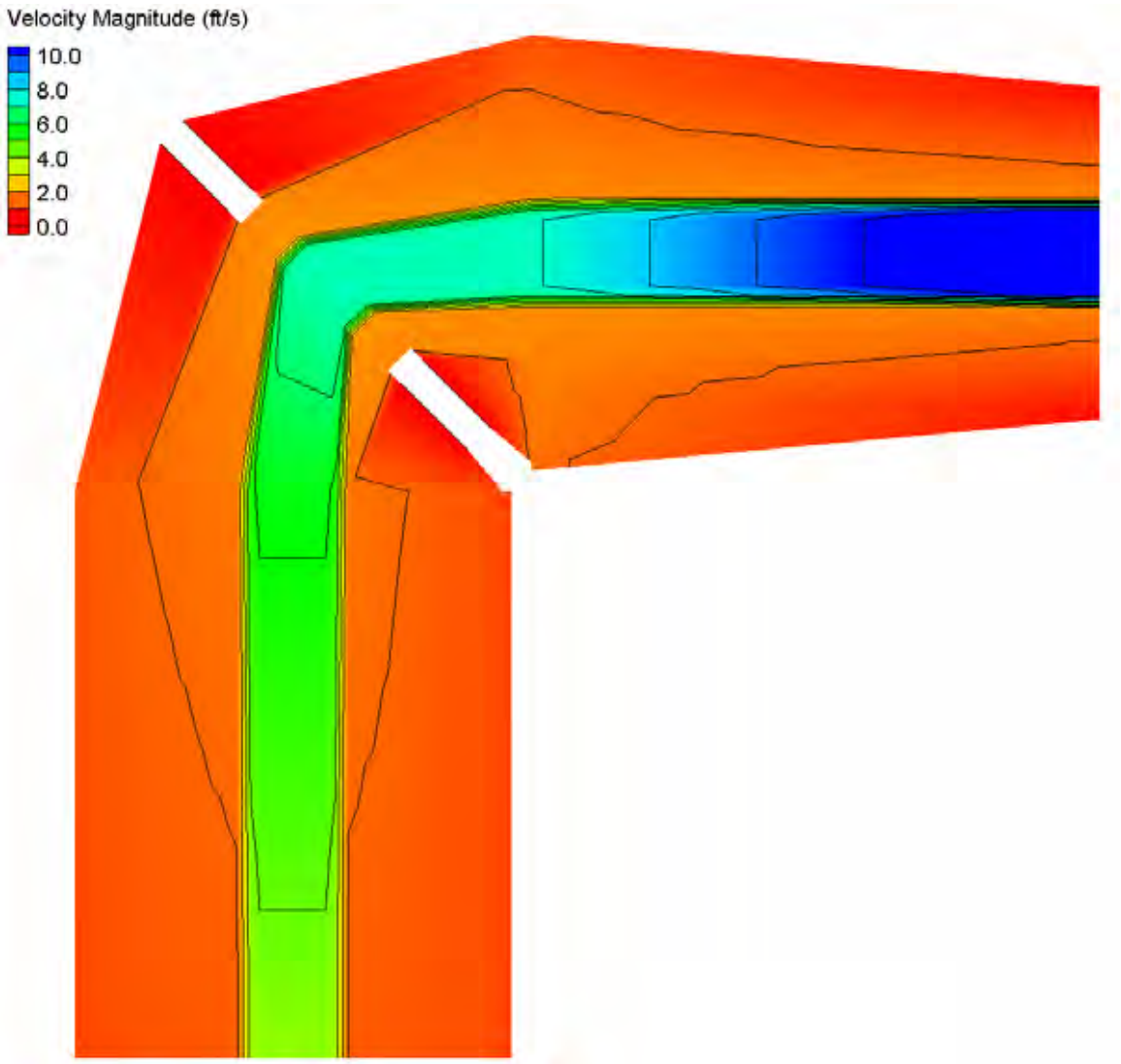

HEC-RAS Velocity Magnitude Contours – Large Channel – River Bends (90°, ¼ radius)

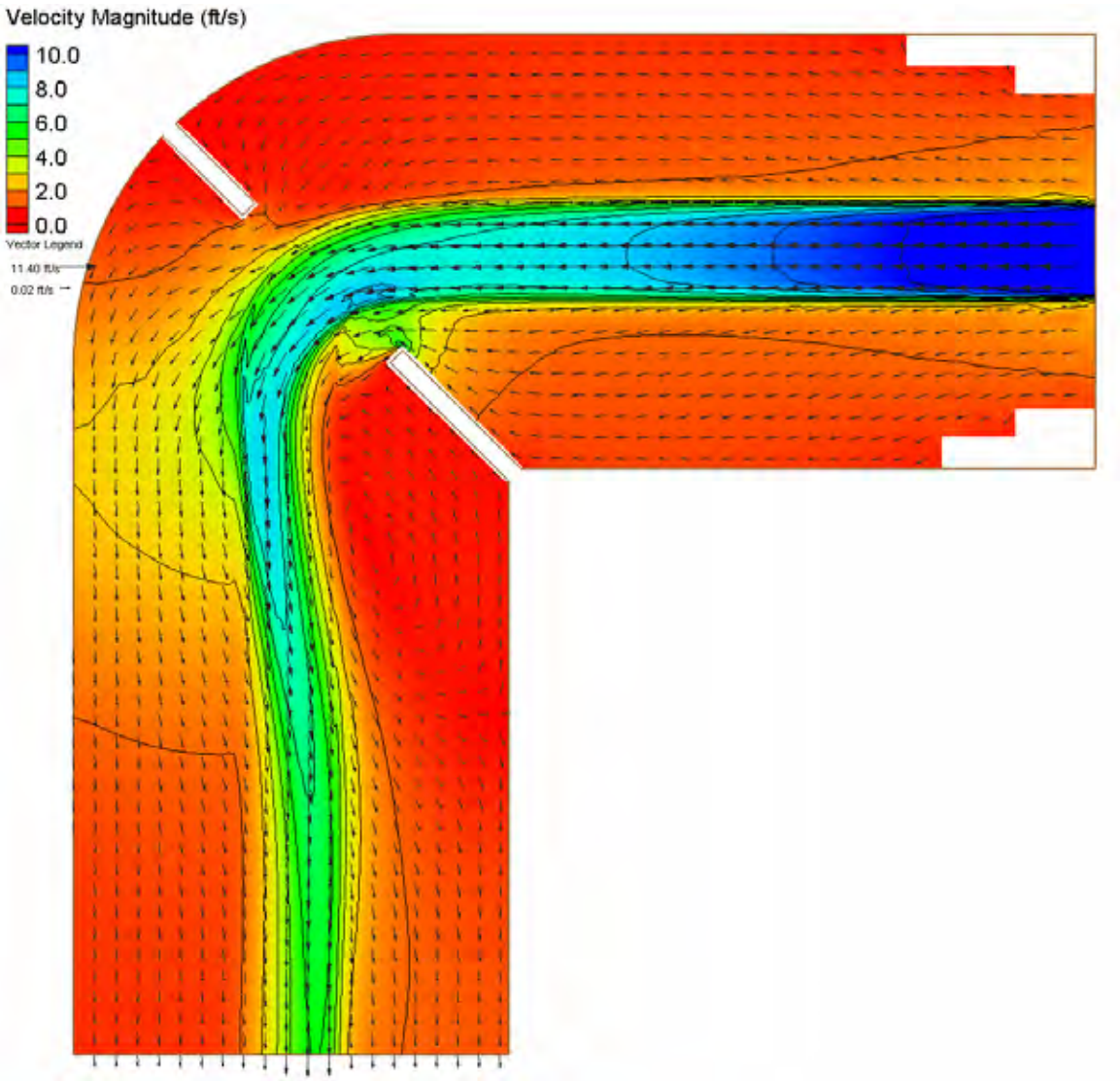

FESWMS Velocity Magnitude Contours – Large Channel – River Bends (90°, ¼ radius)

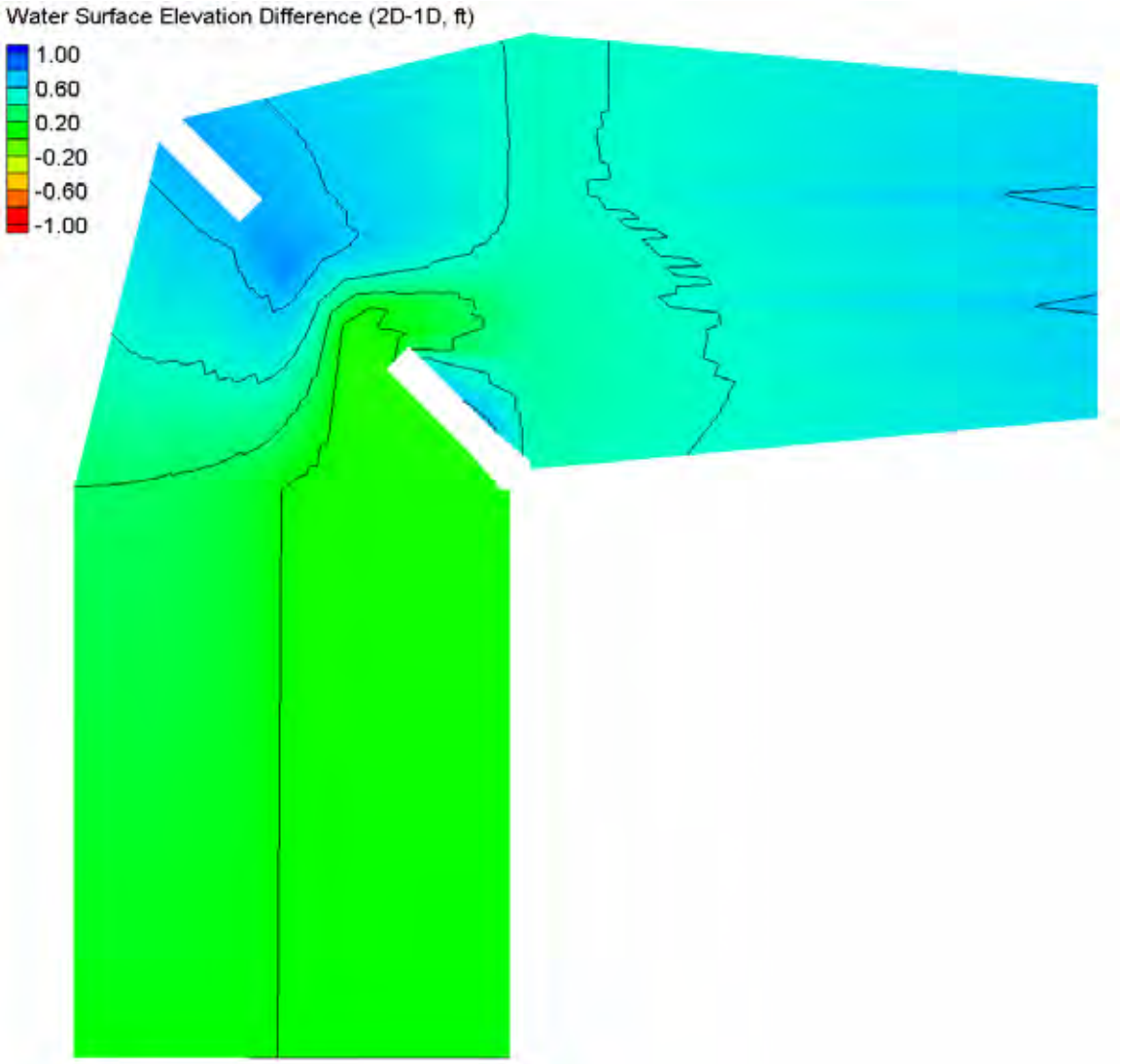

Water Surface Elevation Difference Contours – Large Channel – River Bends (90°, ¼ radius)

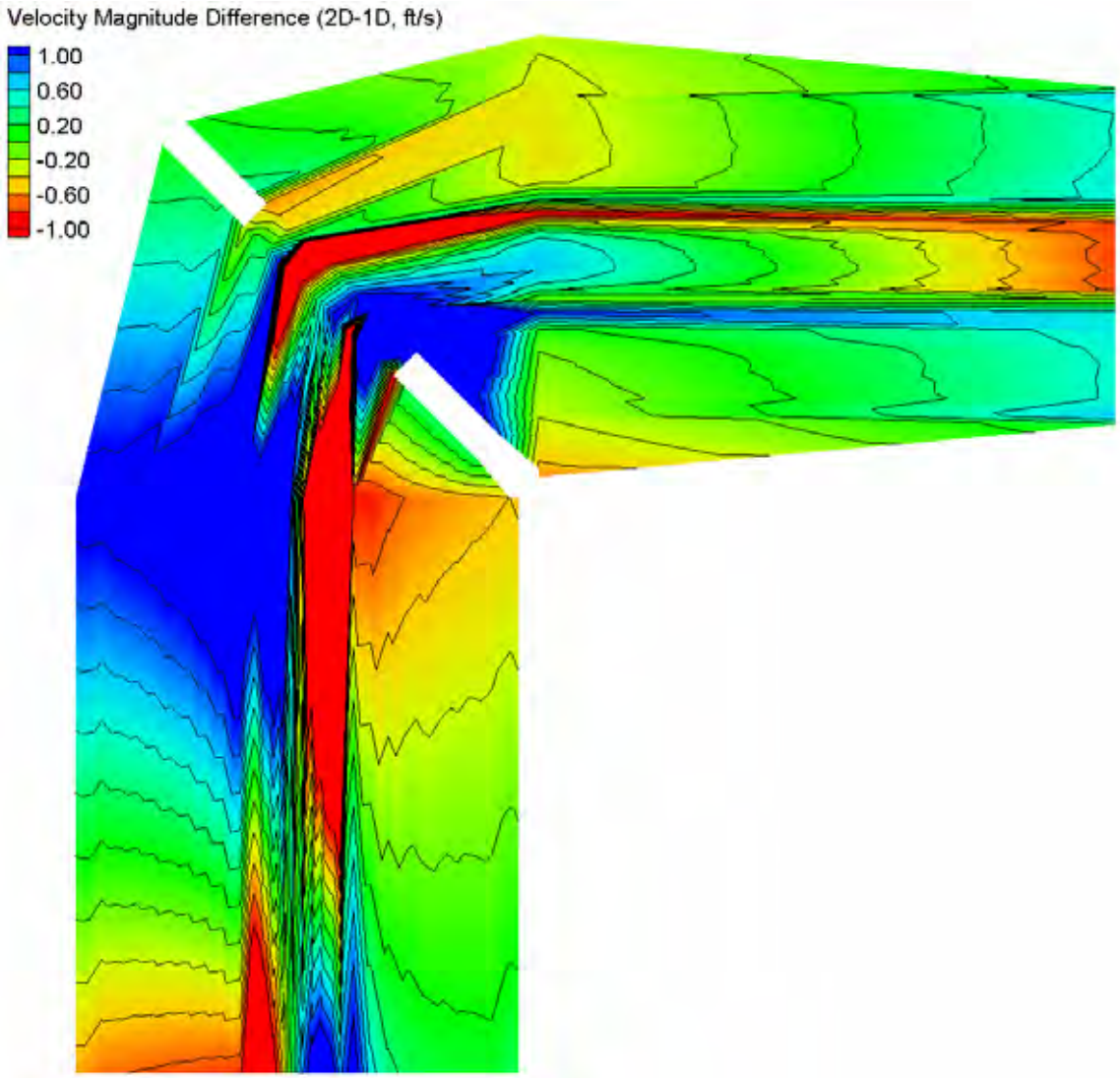

Velocity Magnitude Difference Contours – Large Channel – River Bends (90°, ¼ radius)

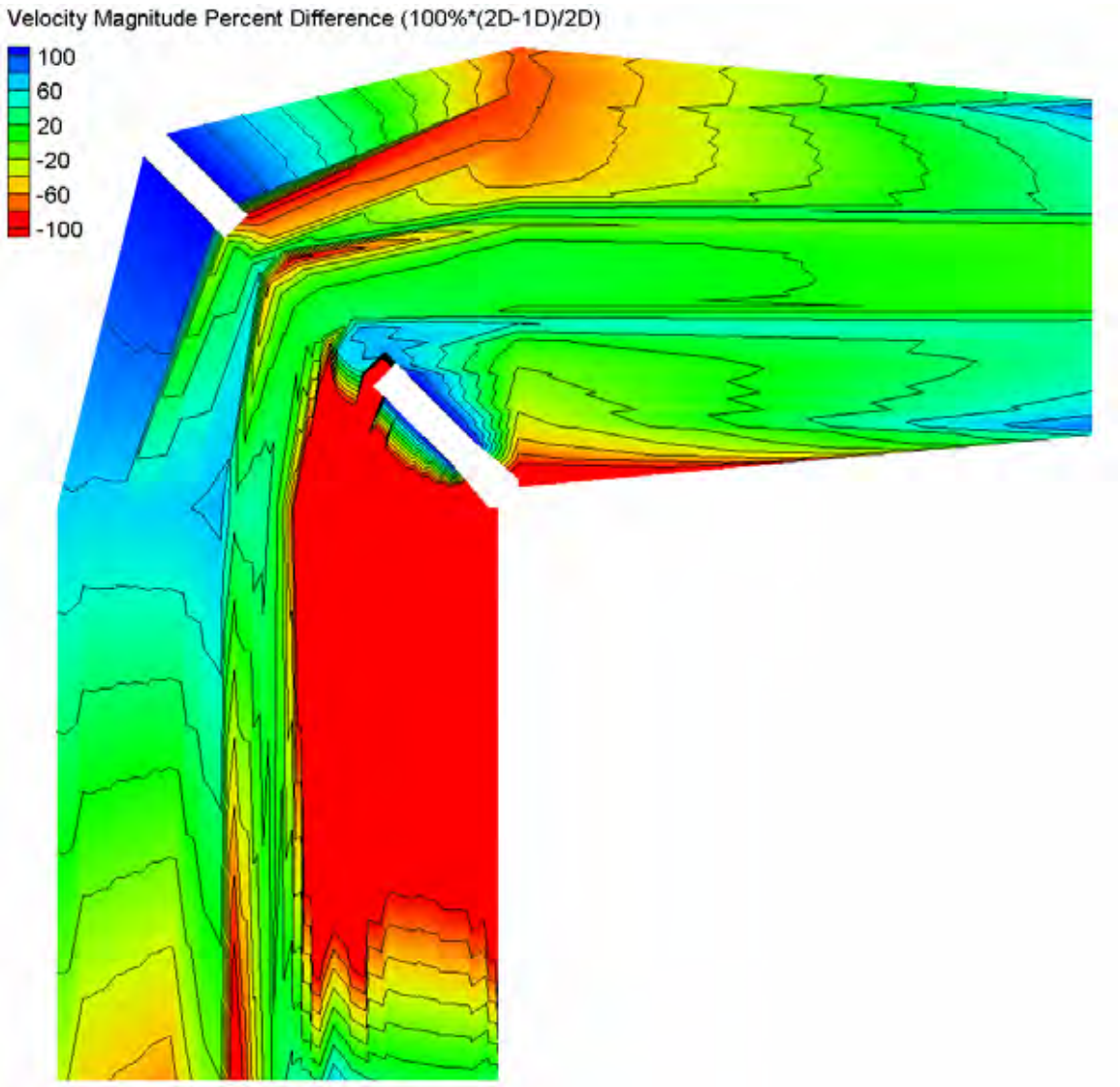

Velocity Magnitude Percent Difference Contours – Large Channel – River Bends (90°, ¼ radius)

Bridges Near Confluences

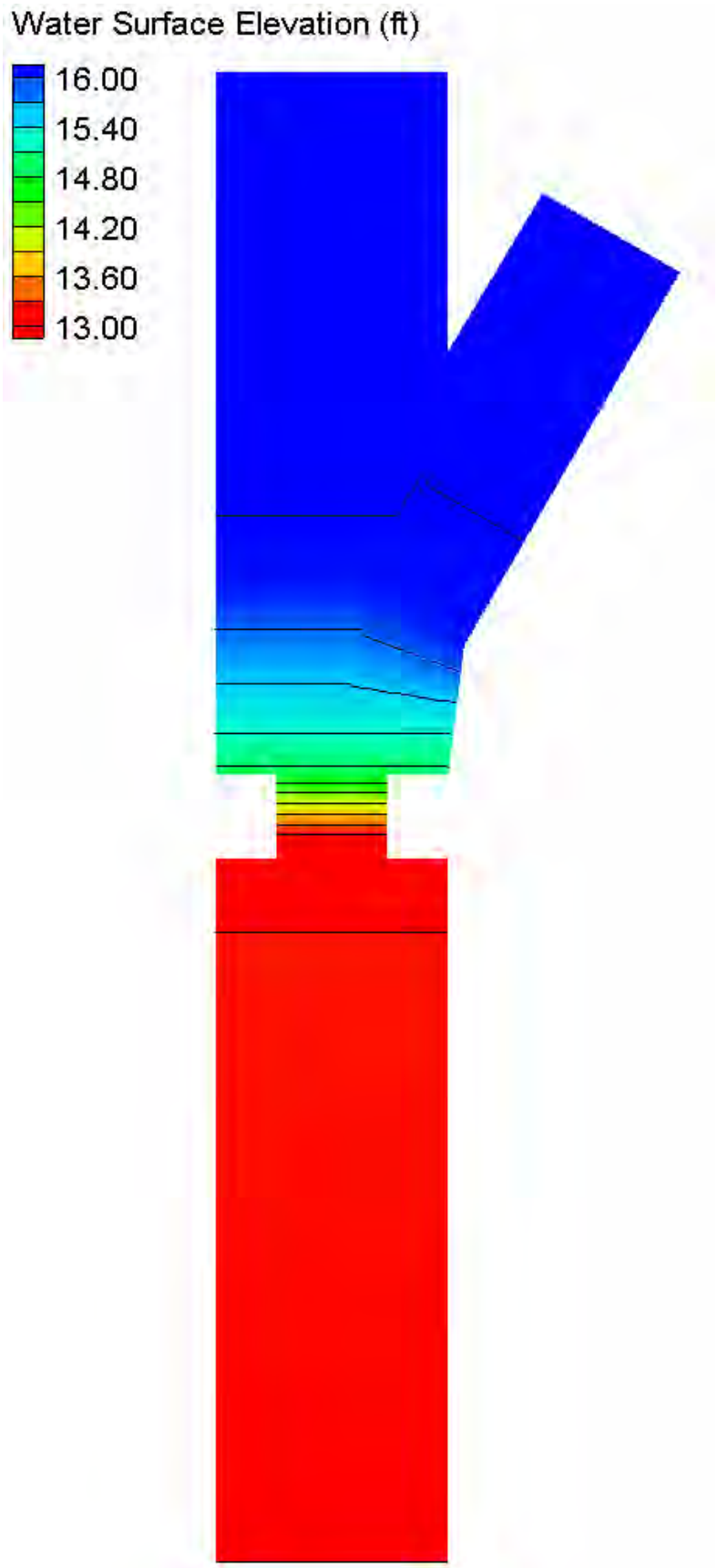

HEC-RAS Water Surface Elevation Contours – Small Channel – Confluences (30°, 50% flow, one bridge length upstream)

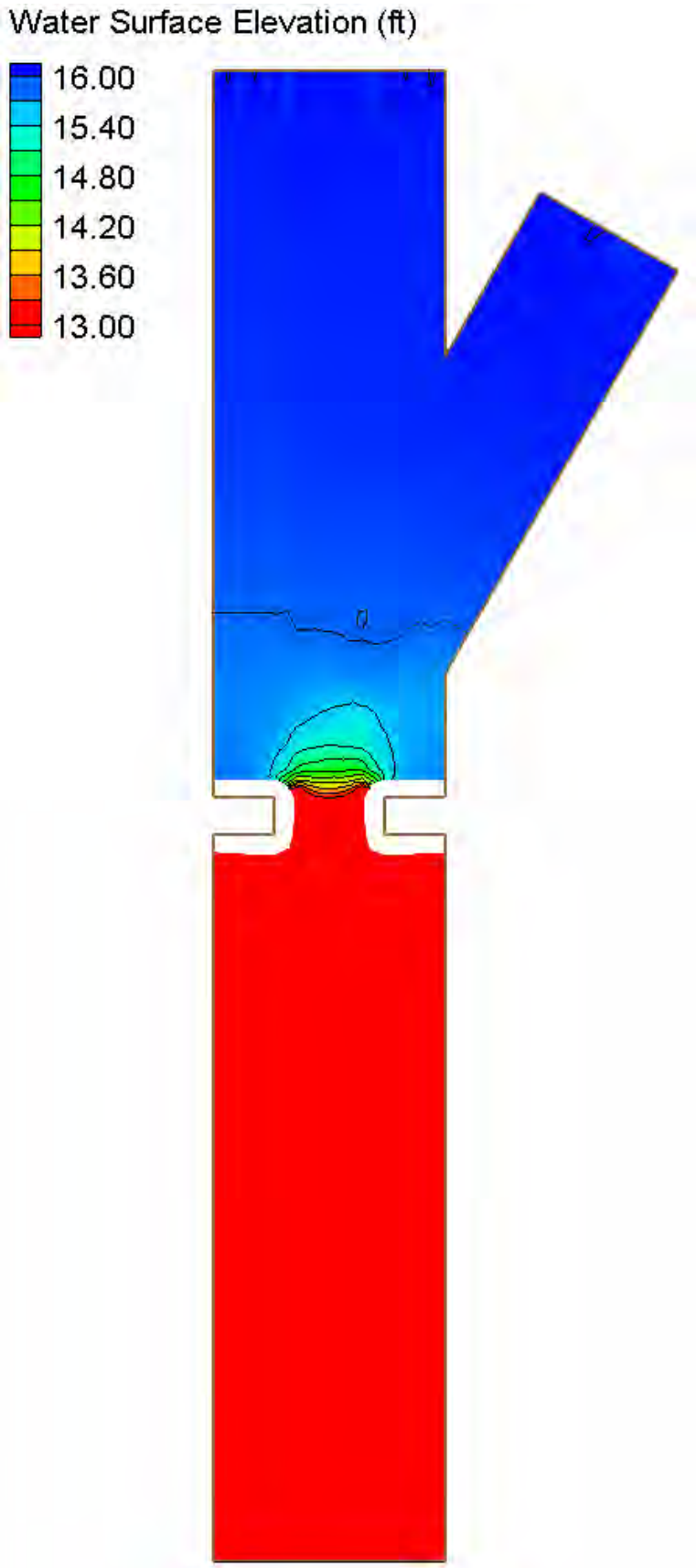

FESWMS Water Surface Elevation Contours – Small Channel – Confluences (30°, 50% flow, one bridge length upstream)

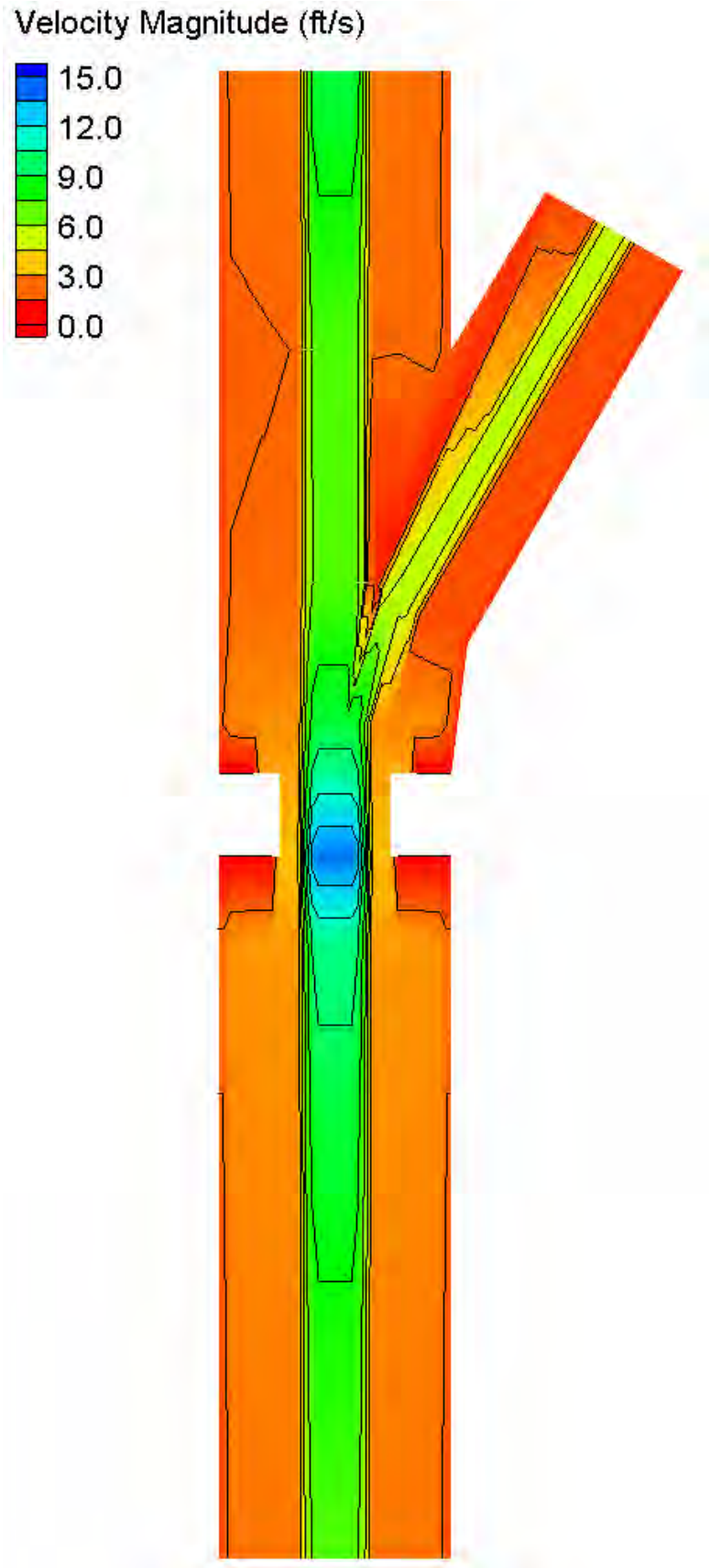

HEC-RAS Velocity Magnitude Contours – Small Channel – Confluences (30°, 50% flow, one bridge length upstream)

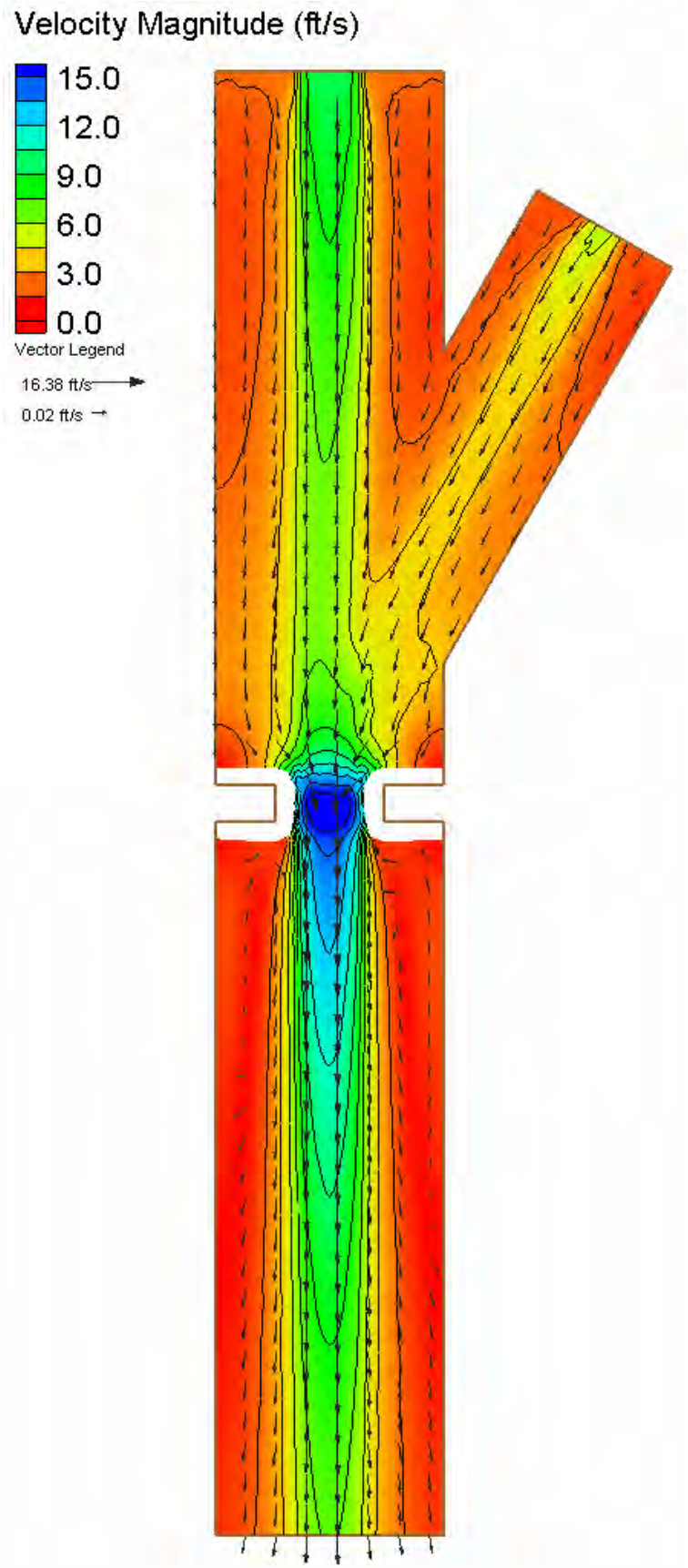

FESWMS Velocity Magnitude Contours – Small Channel – Confluences (30°, 50% flow, one bridge length upstream)

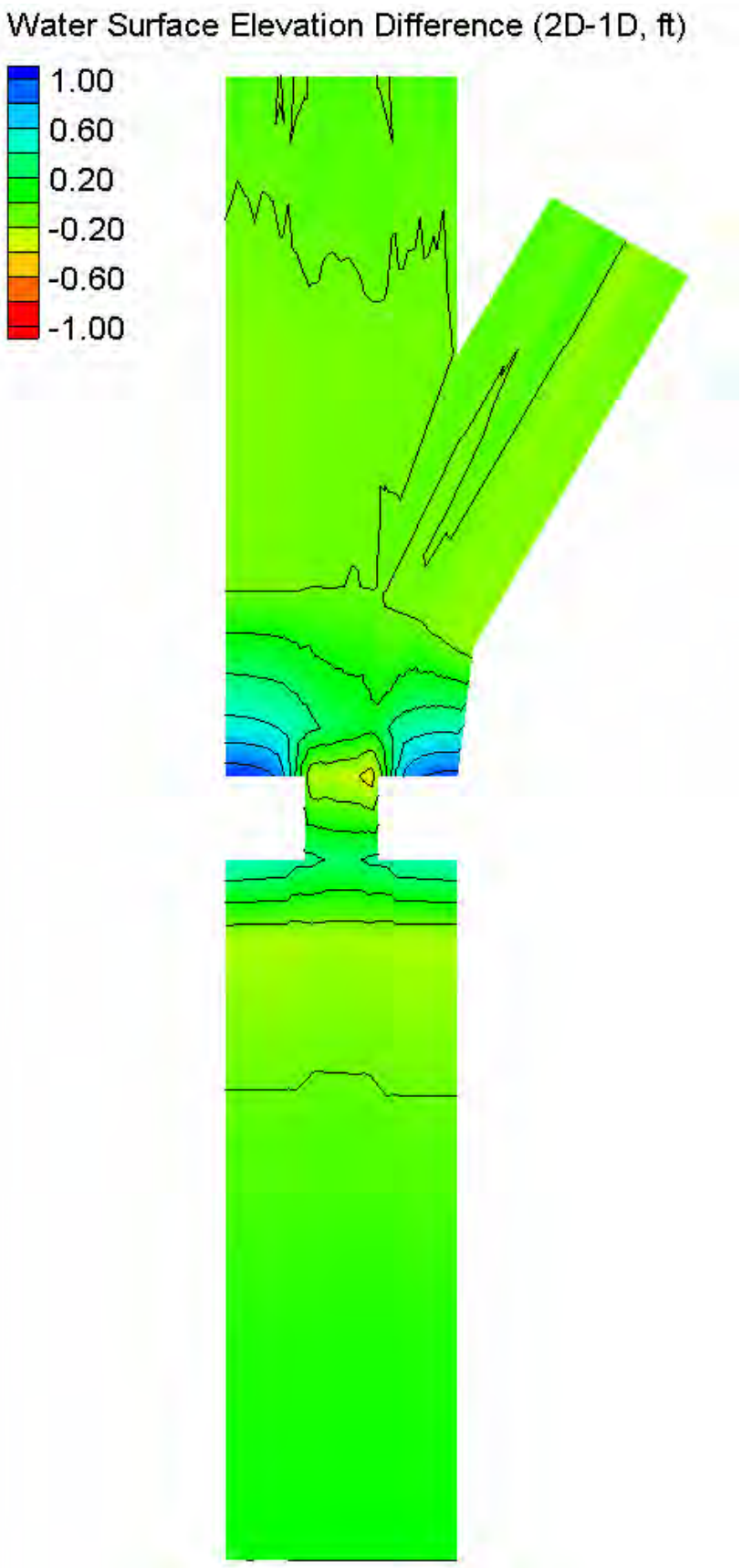

Water Surface Elevation Difference Contours – Small Channel – Confluences (30°, 50% flow, one bridge length upstream)

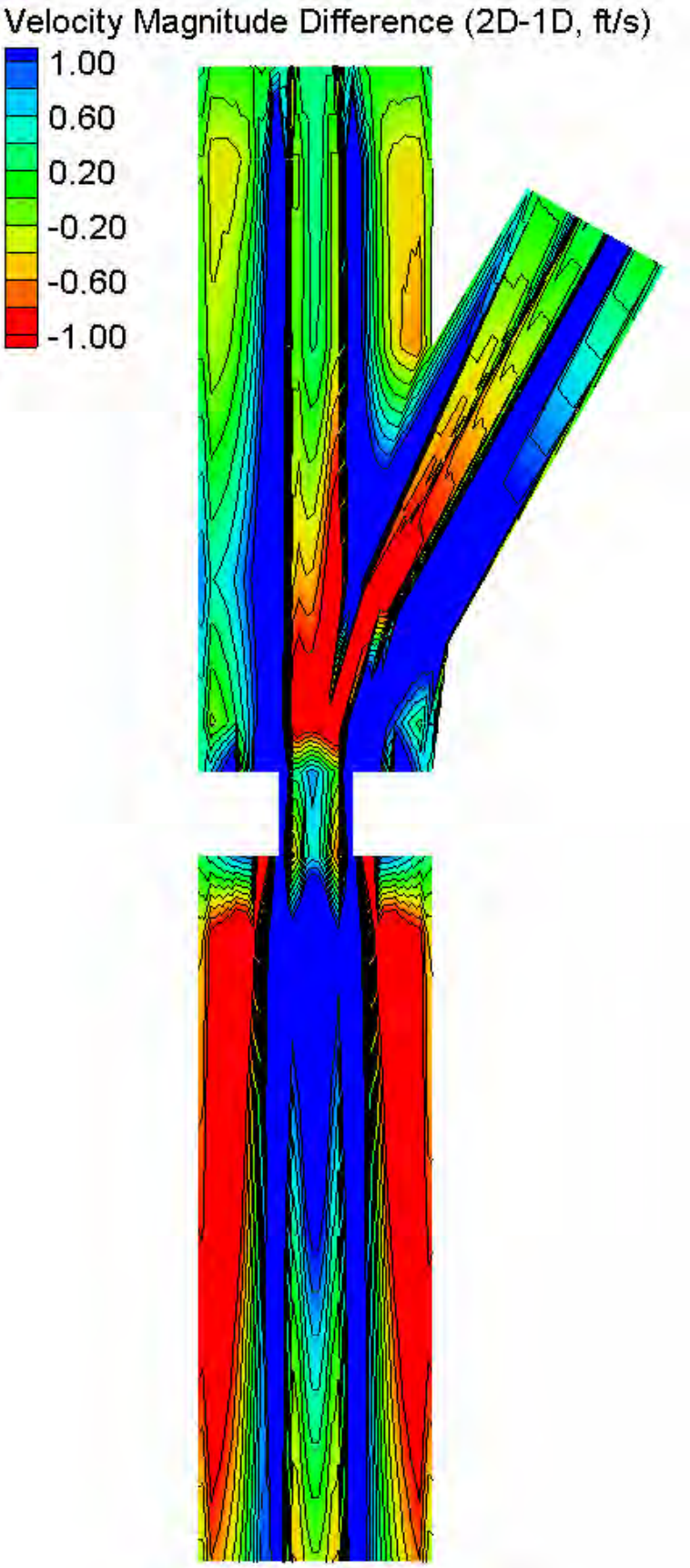

Velocity Magnitude Difference Contours – Small Channel – Confluences (30°, 50% flow, one bridge length upstream)

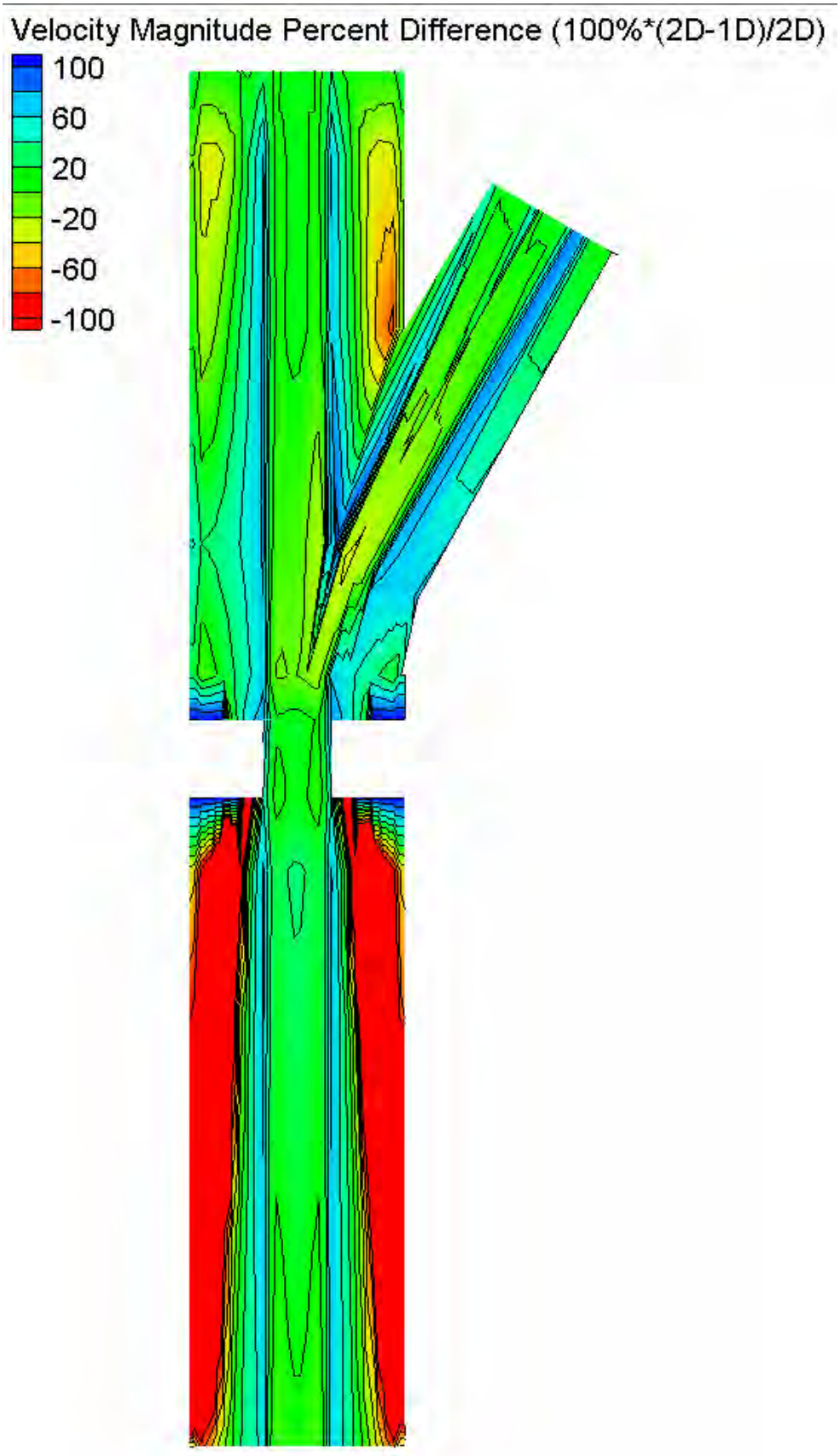

Velocity Magnitude Percent Difference Contours – Small Channel – Confluences (30°, 50% flow, one bridge length upstream)

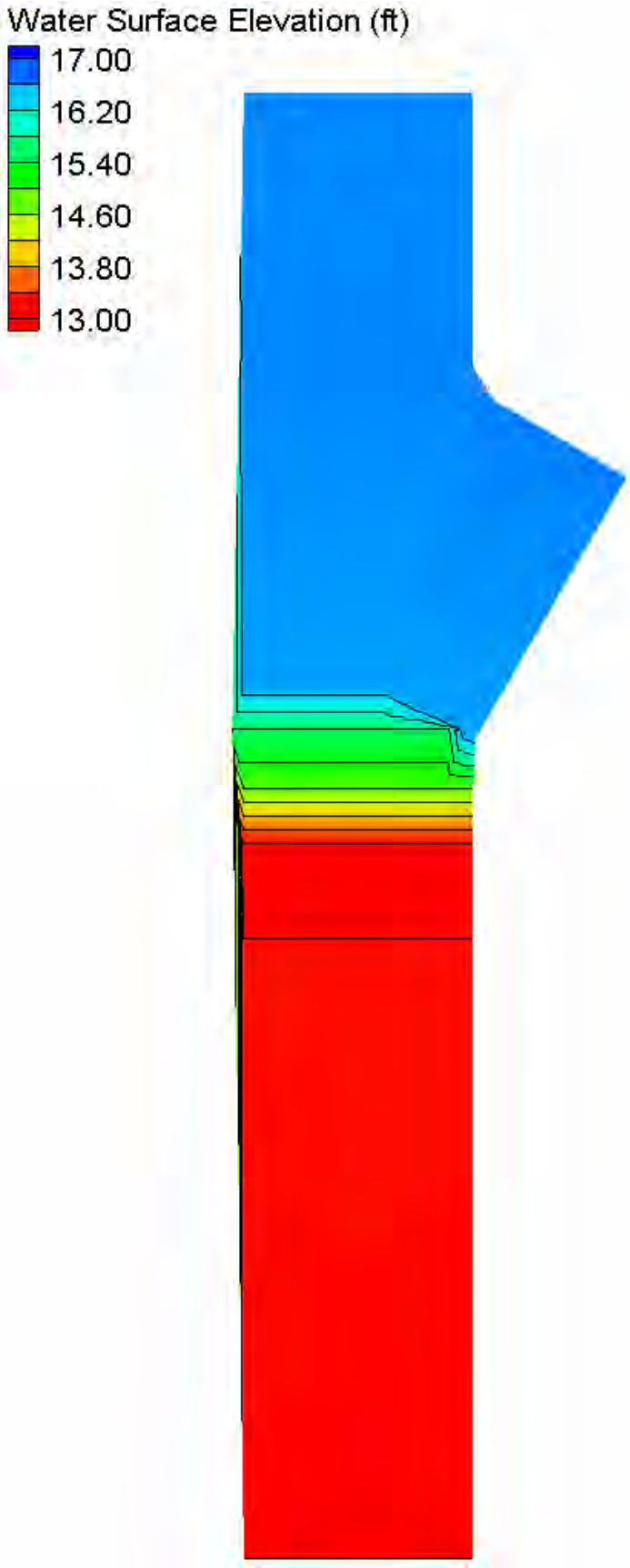

HEC-RAS Water Surface Elevation Contours – Small Channel – Confluences (30°, 50% flow, immediately upstream)

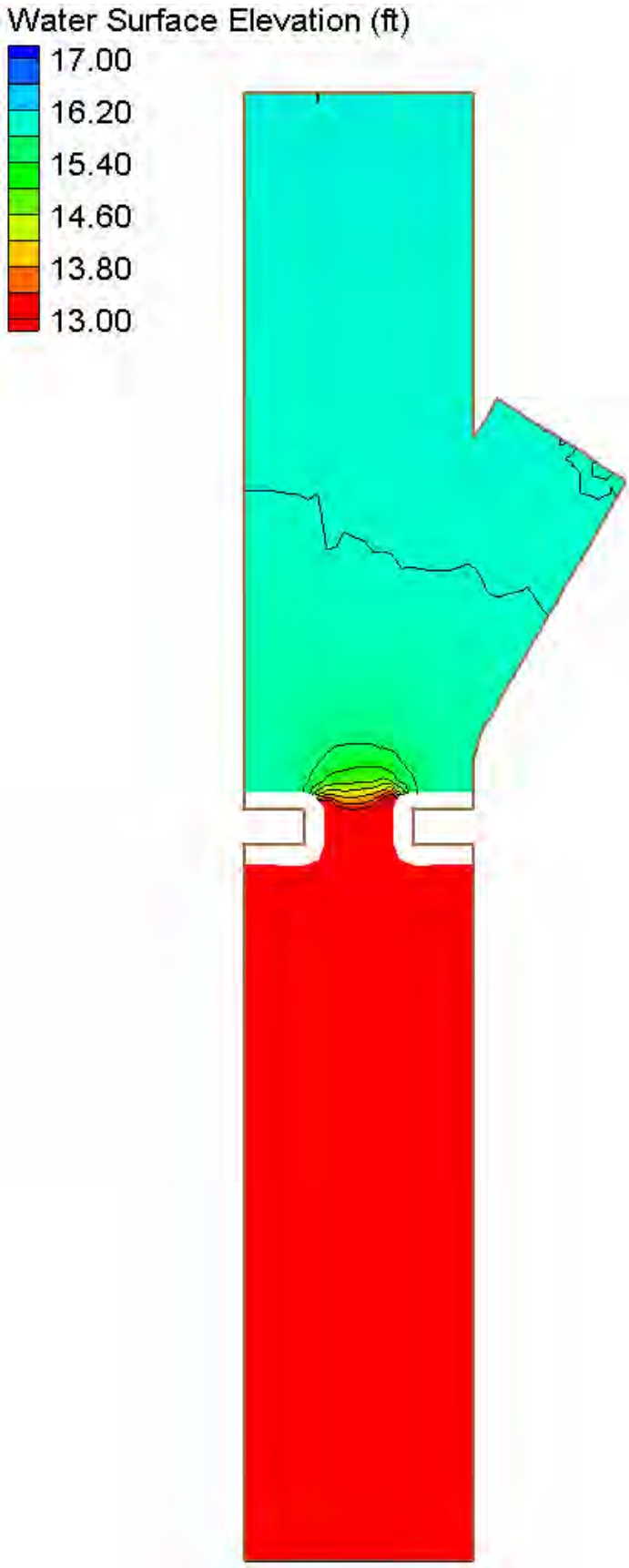

FESWMS Water Surface Elevation Contours – Small Channel – Confluences (30°, 50% flow, immediately upstream)

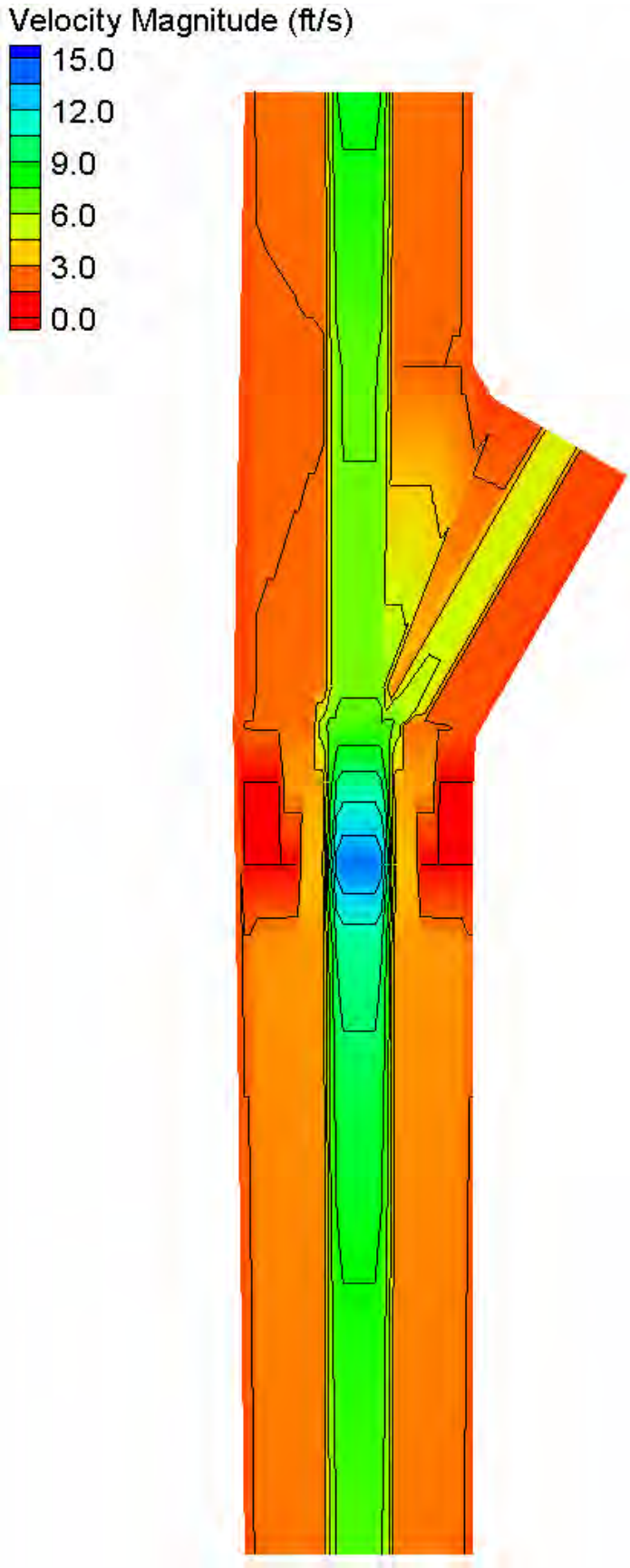

HEC-RAS Velocity Magnitude Contours – Small Channel – Confluences (30°, 50% flow, immediately upstream)

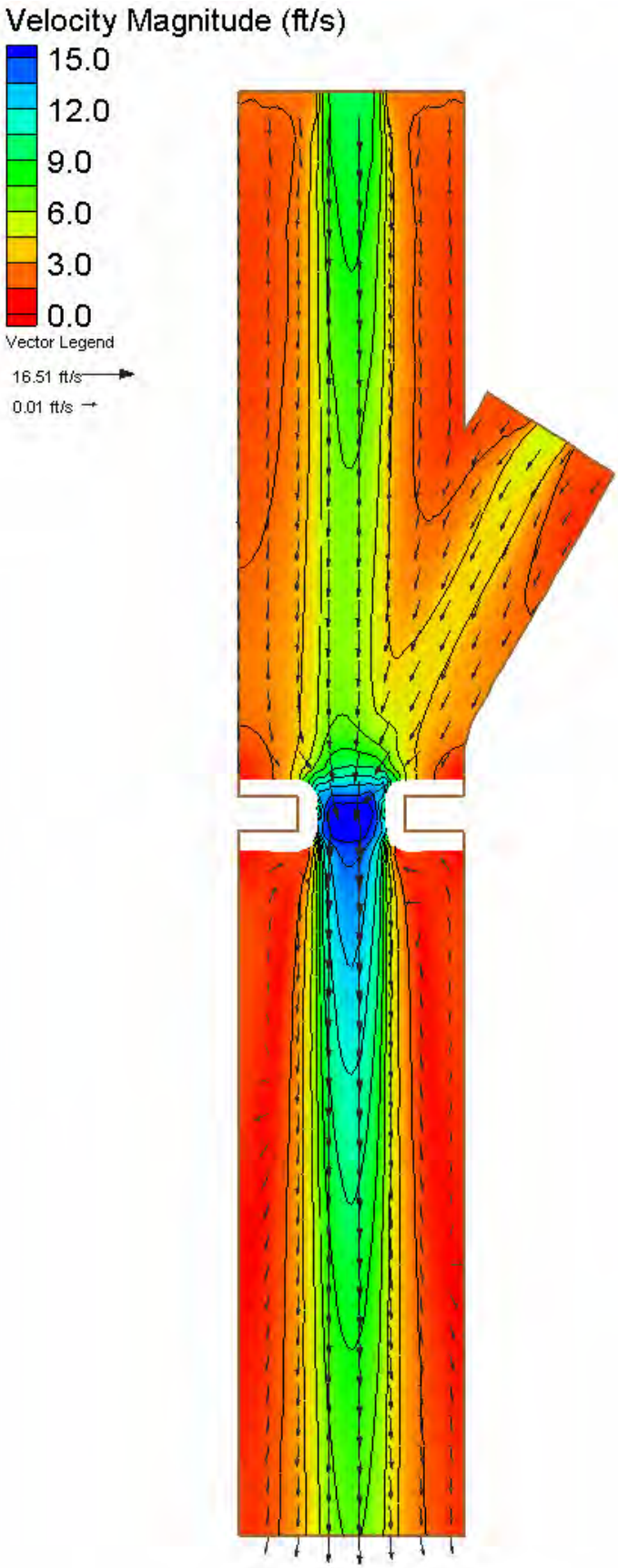

FESWMS Velocity Magnitude Contours – Small Channel – Confluences (30°, 50% flow, immediately upstream)

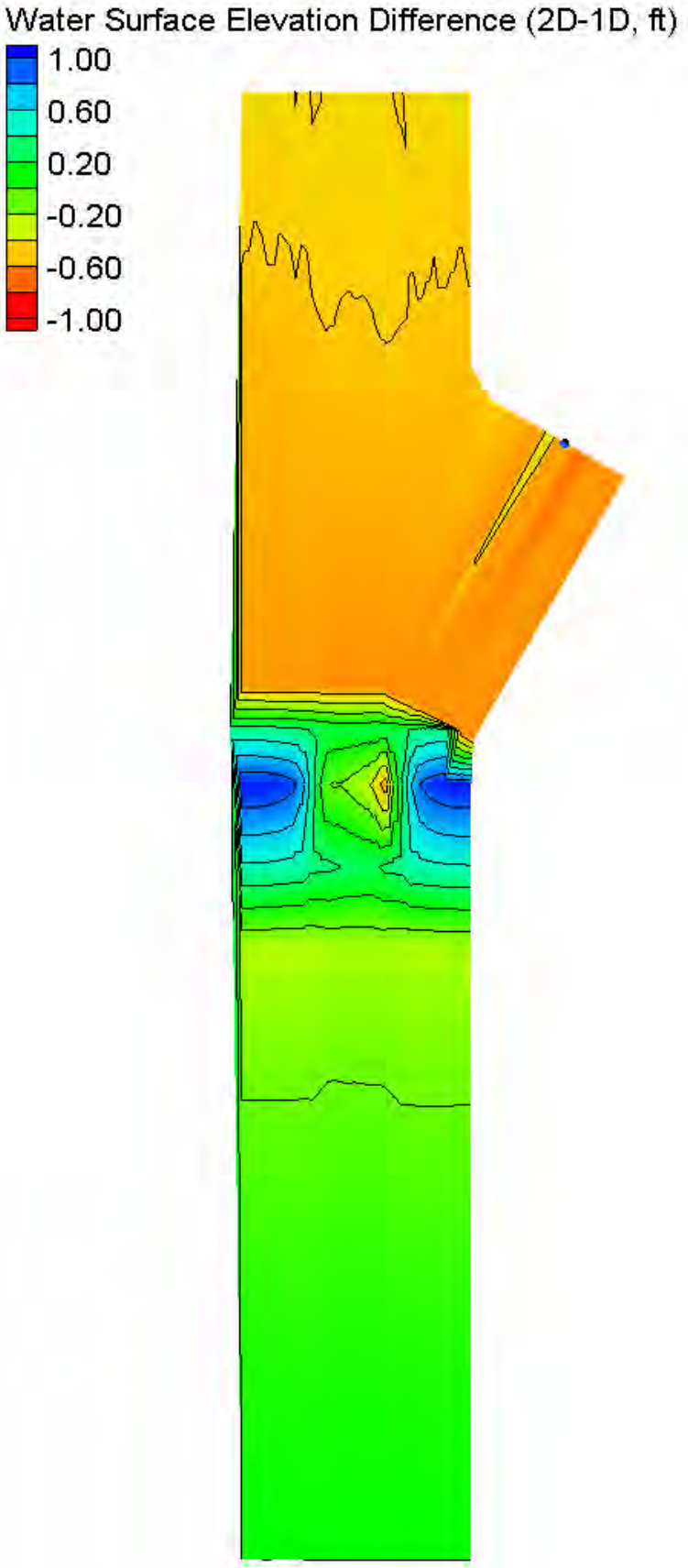

Water Surface Elevation Difference Contours – Small Channel – Confluences (30°, 50% flow, immediately upstream)

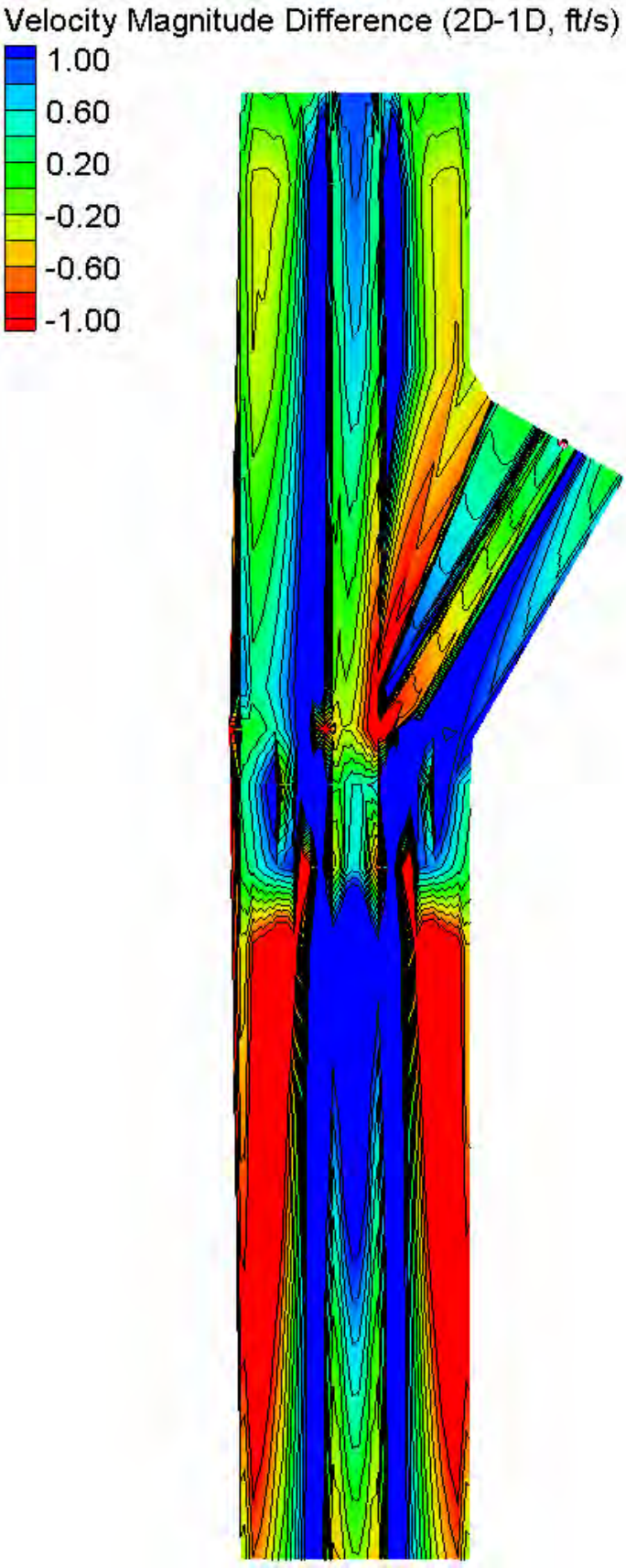

Velocity Magnitude Difference Contours – Small Channel – Confluences (30°, 50% flow, immediately upstream)

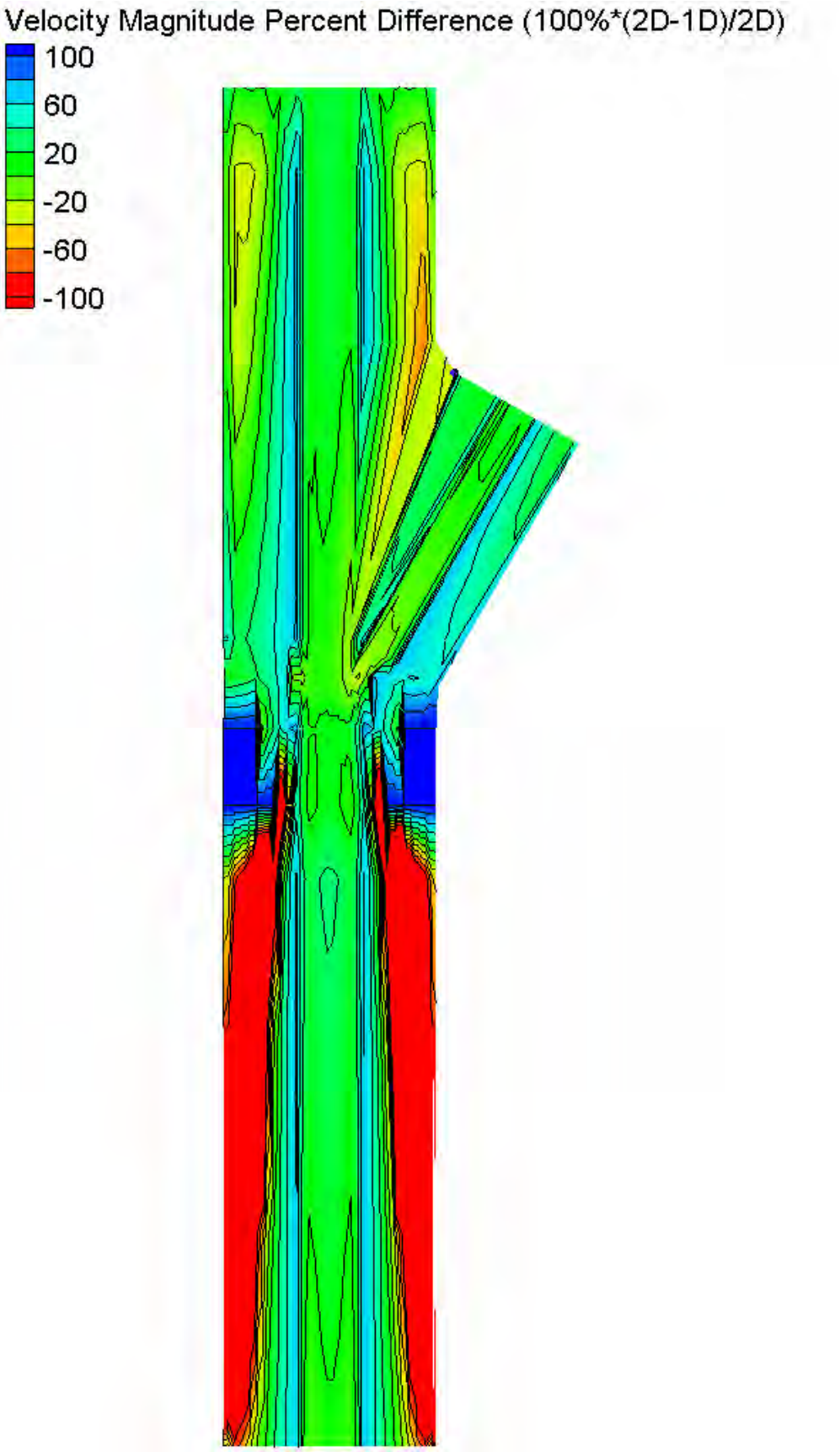

Velocity Magnitude Percent Difference Contours – Small Channel – Confluences (30°, 50% flow, immediately upstream)

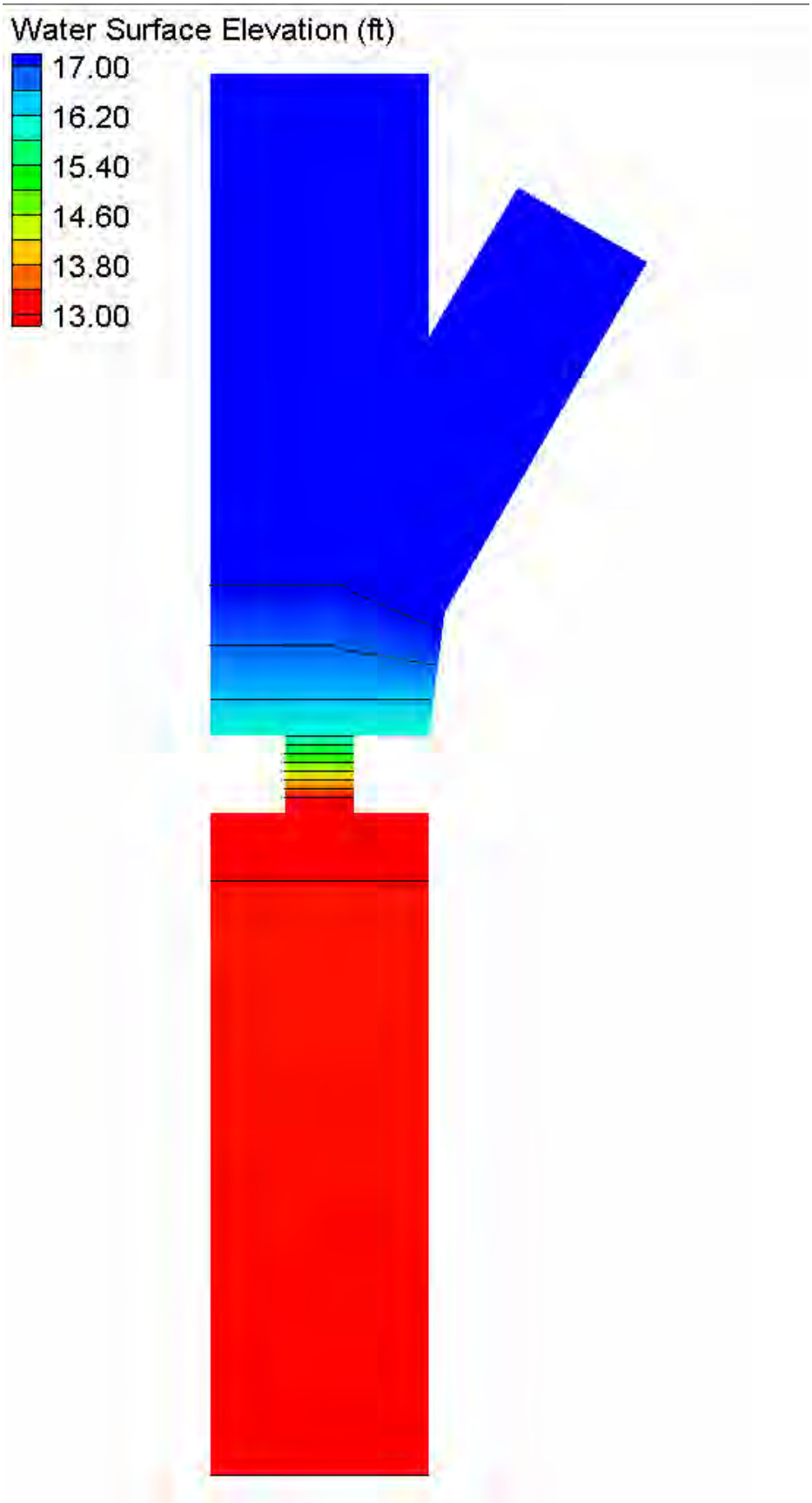

HEC-RAS Water Surface Elevation Contours – Small Channel – Confluences (30°, 75% flow, one bridge length upstream)

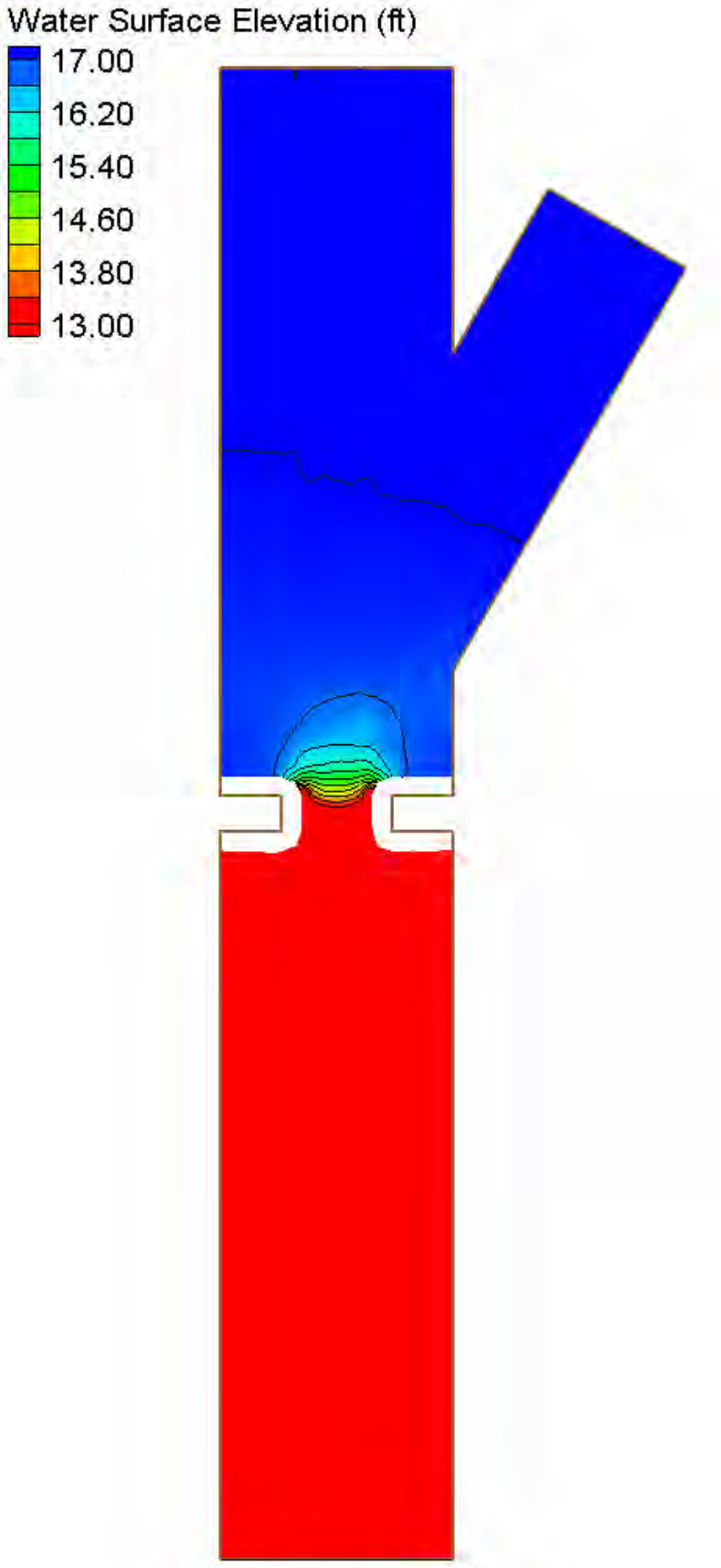

FESWMS Water Surface Elevation Contours – Small Channel – Confluences (30°, 75% flow, one bridge length upstream)

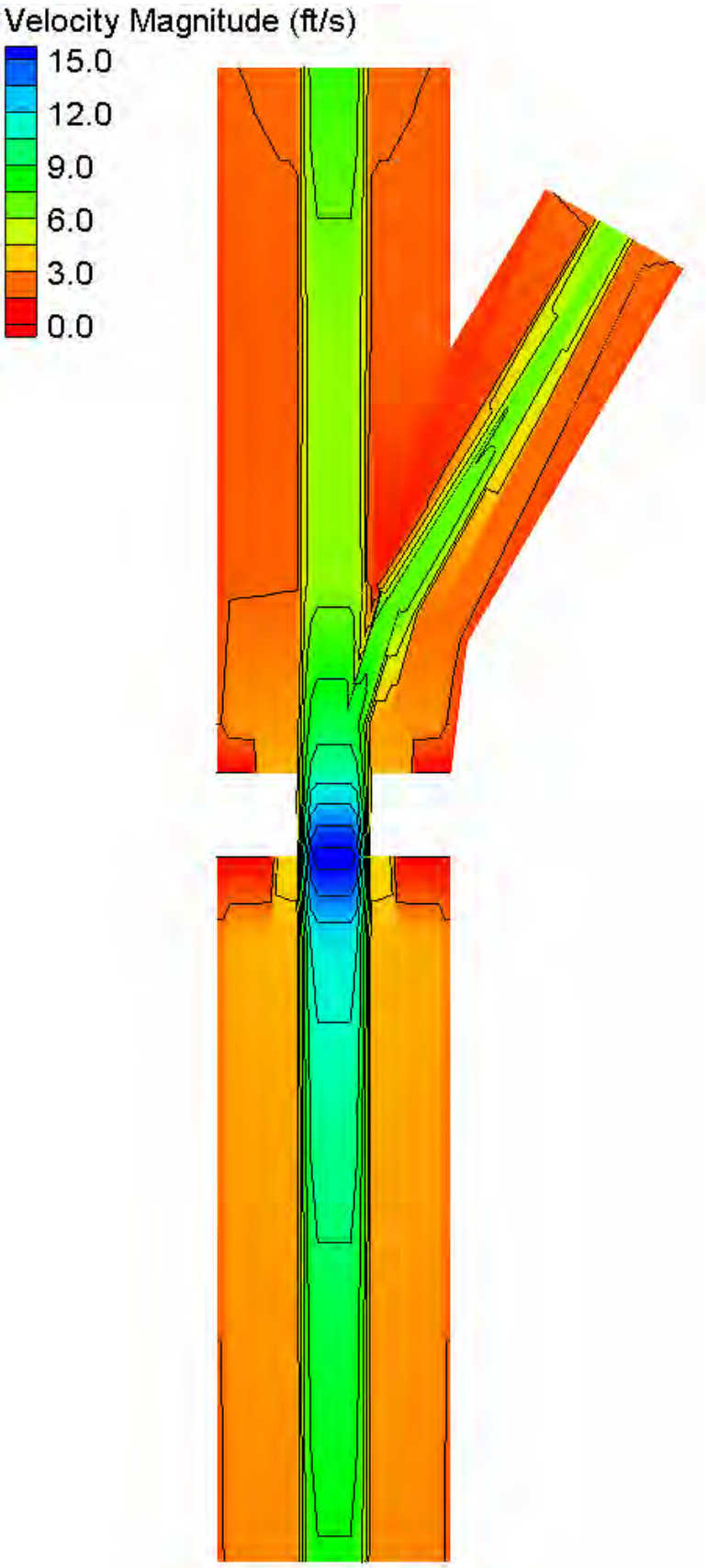

HEC-RAS Velocity Magnitude Contours – Small Channel – Confluences (30°, 75% flow, one bridge length upstream)

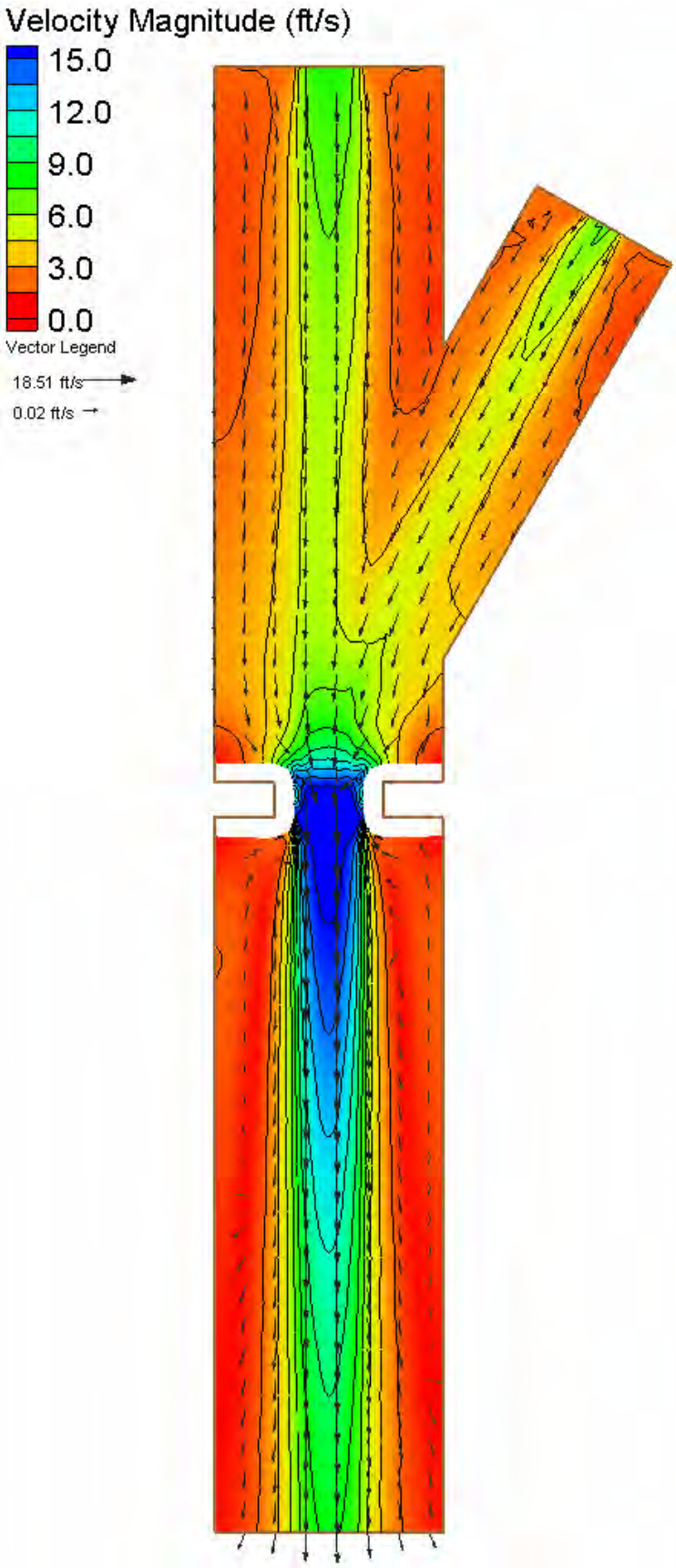

FESWMS Velocity Magnitude Contours – Small Channel – Confluences (30°, 75% flow, one bridge length upstream)

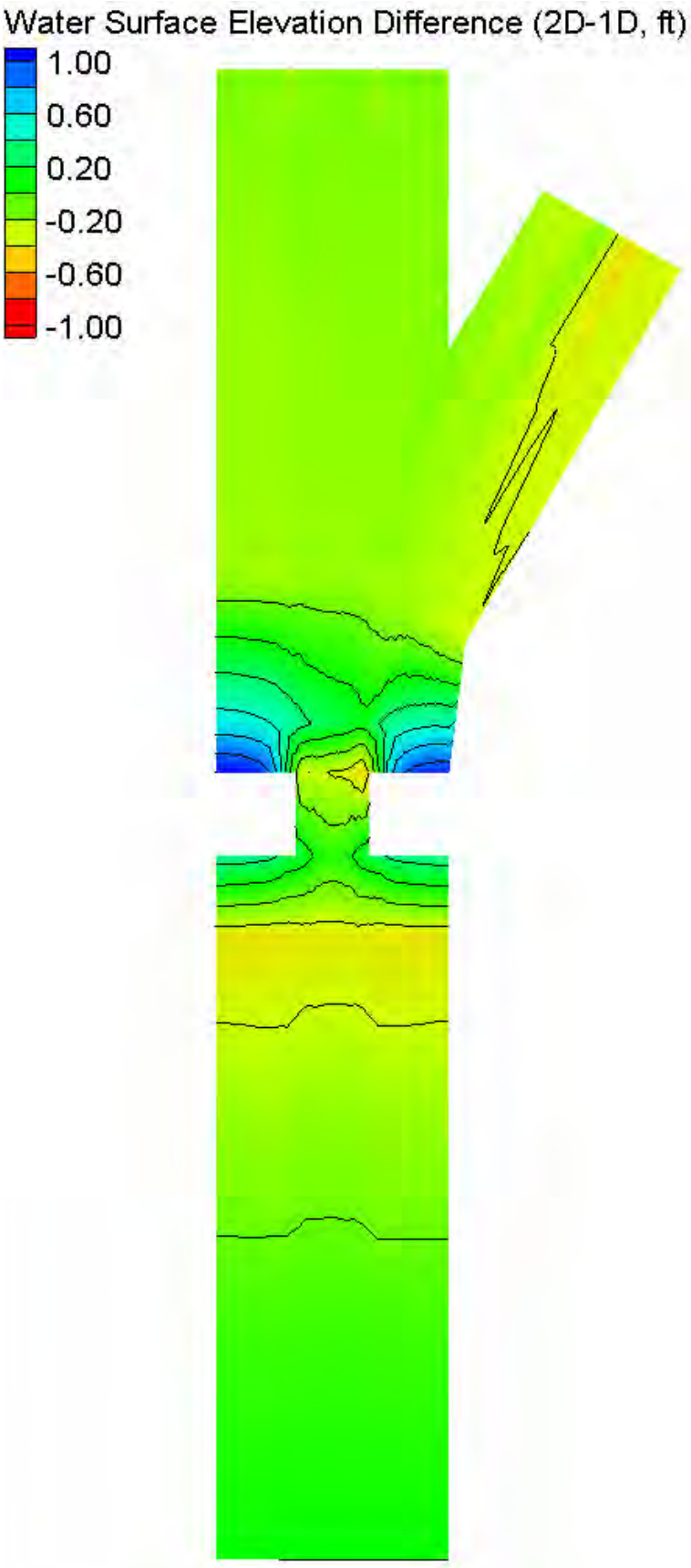

Water Surface Elevation Difference Contours – Small Channel – Confluences (30°, 75% flow, one bridge length upstream)

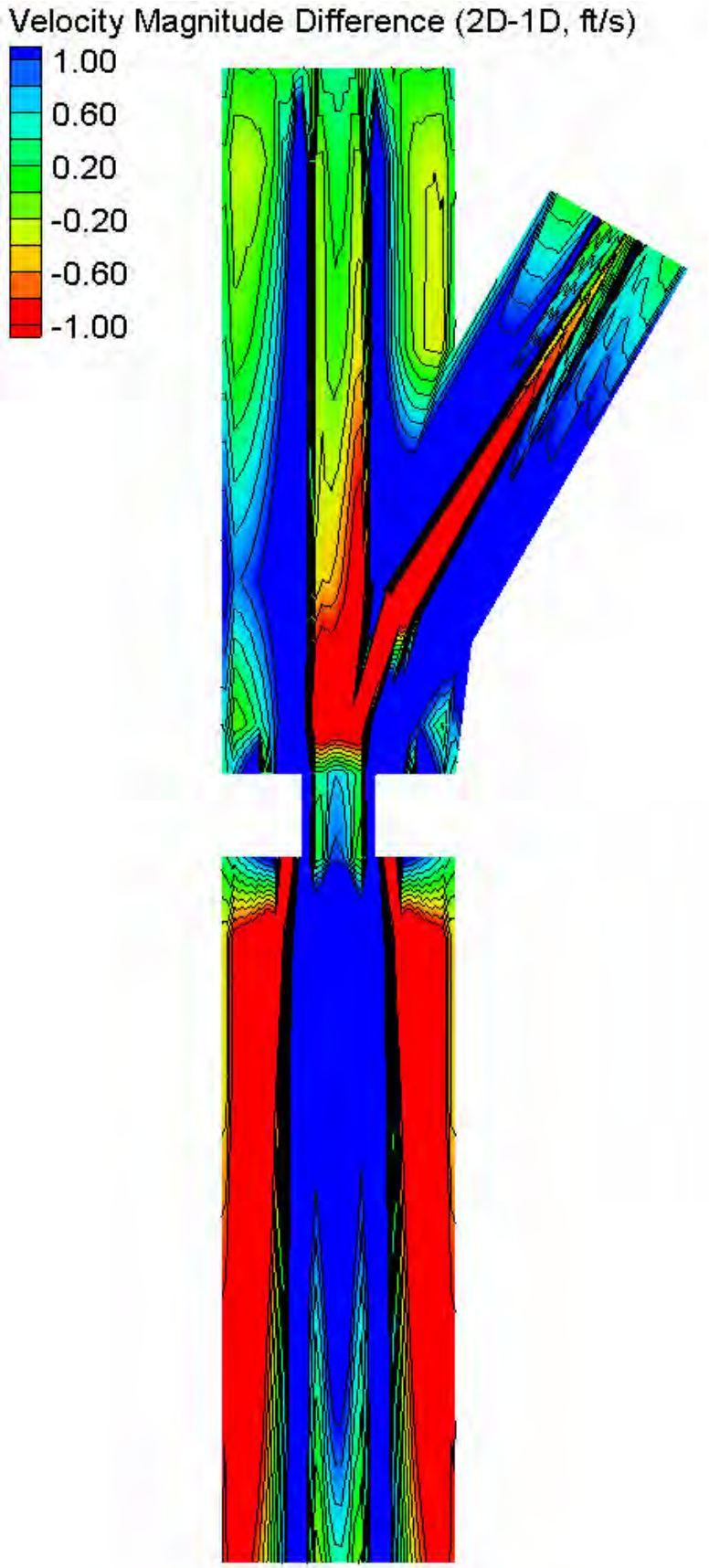

Velocity Magnitude Difference Contours – Small Channel – Confluences (30°, 75% flow, one bridge length upstream)

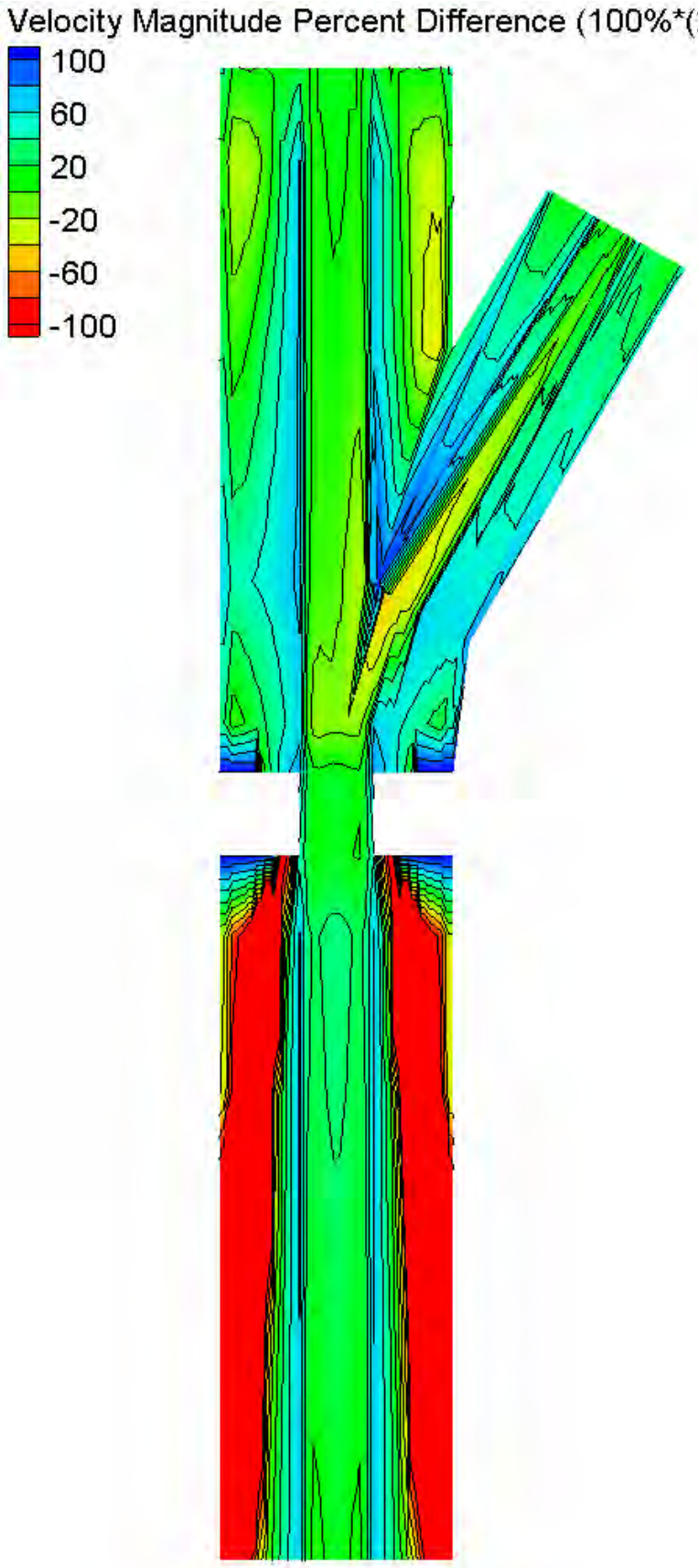

Velocity Magnitude Percent Difference Contours – Small Channel – Confluences (30°, 75% flow, one bridge length upstream)

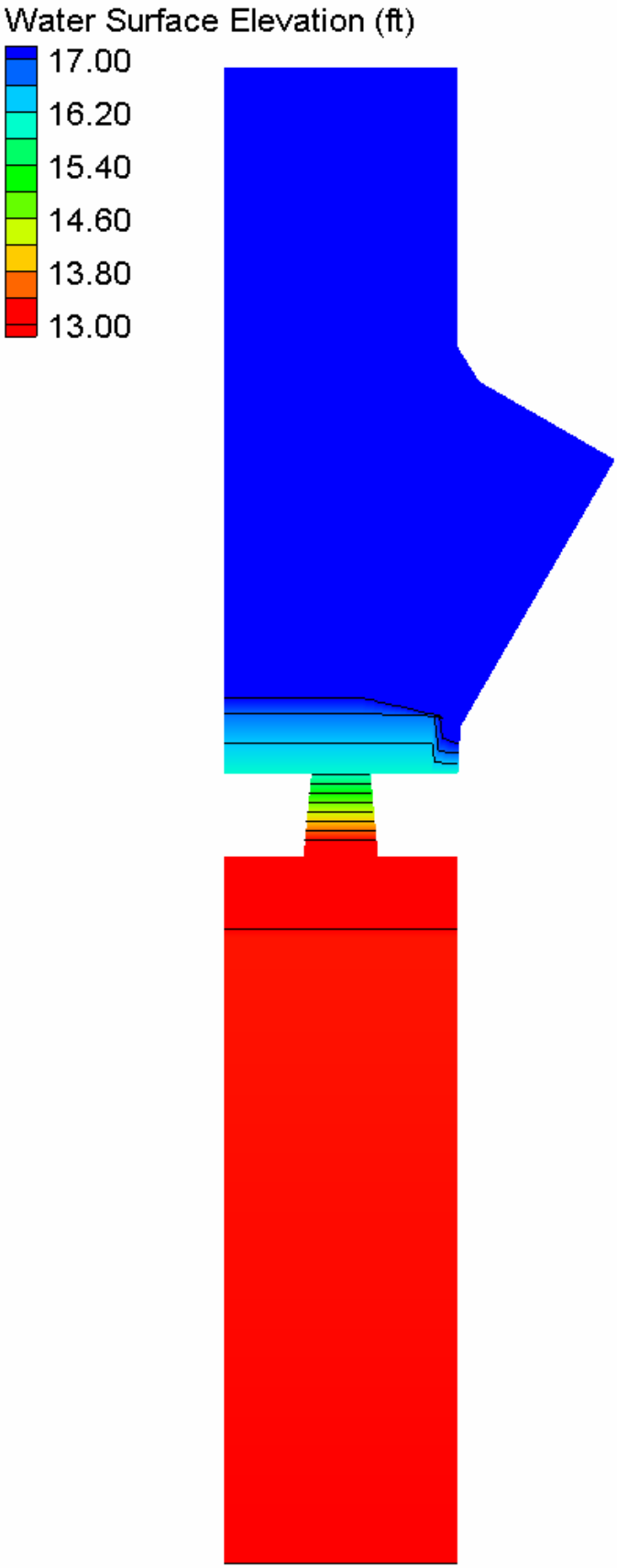

HEC-RAS Water Surface Elevation Contours – Small Channel – Confluences (30°, 75% flow, immediately upstream)

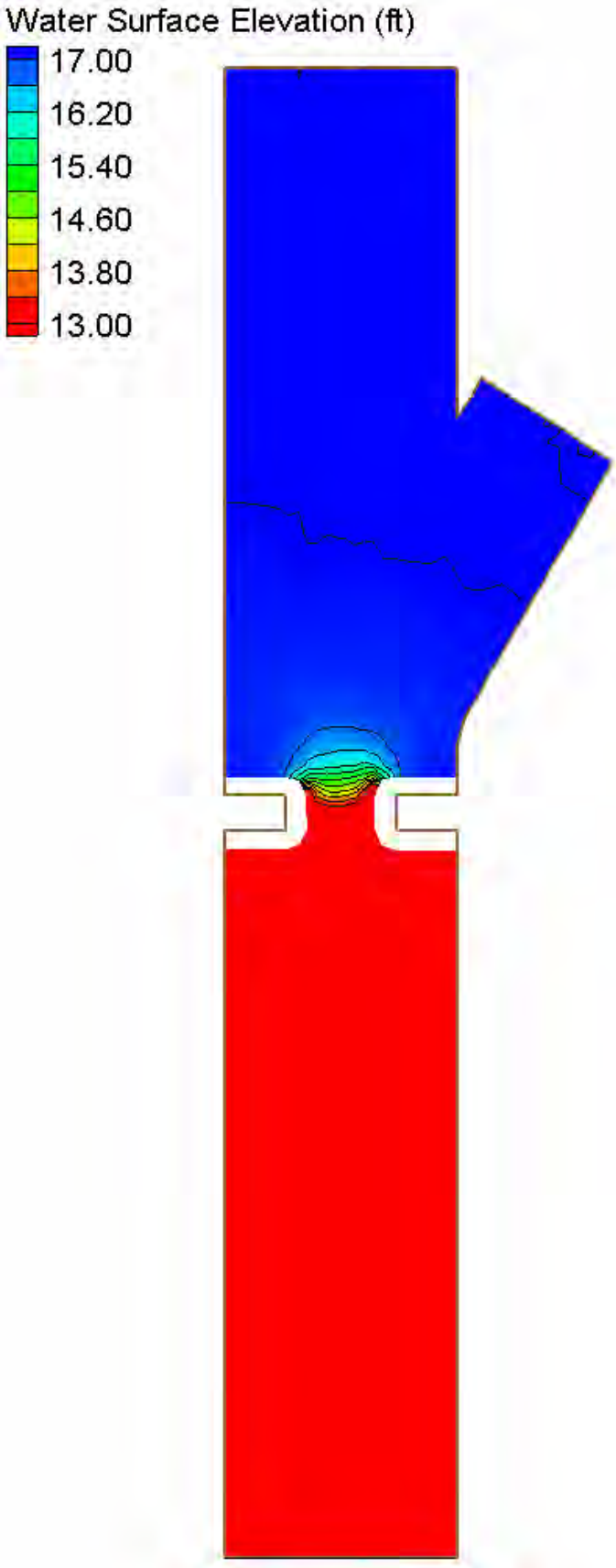

FESWMS Water Surface Elevation Contours – Small Channel – Confluences (30°, 75% flow, immediately upstream)

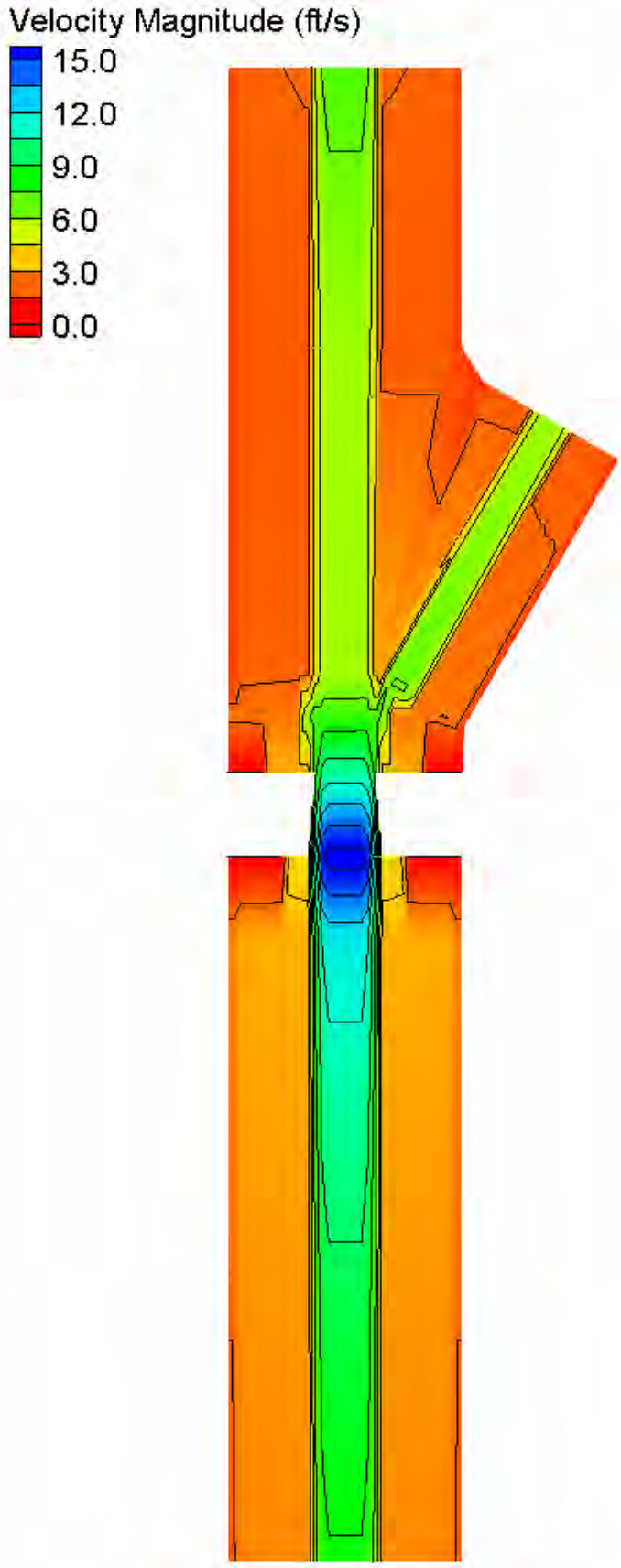

HEC-RAS Velocity Magnitude Contours – Small Channel – Confluences (30°, 75% flow, immediately upstream)

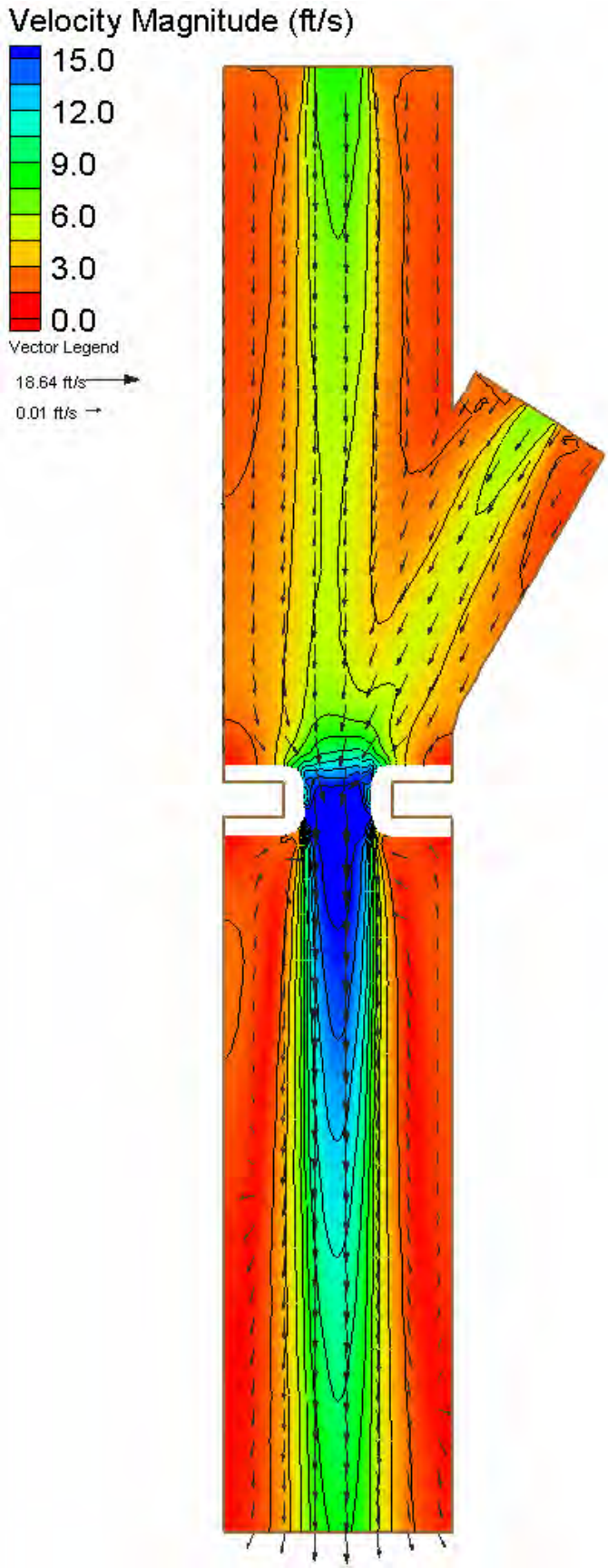

FESWMS Velocity Magnitude Contours – Small Channel – Confluences (30°, 75% flow, immediately upstream)

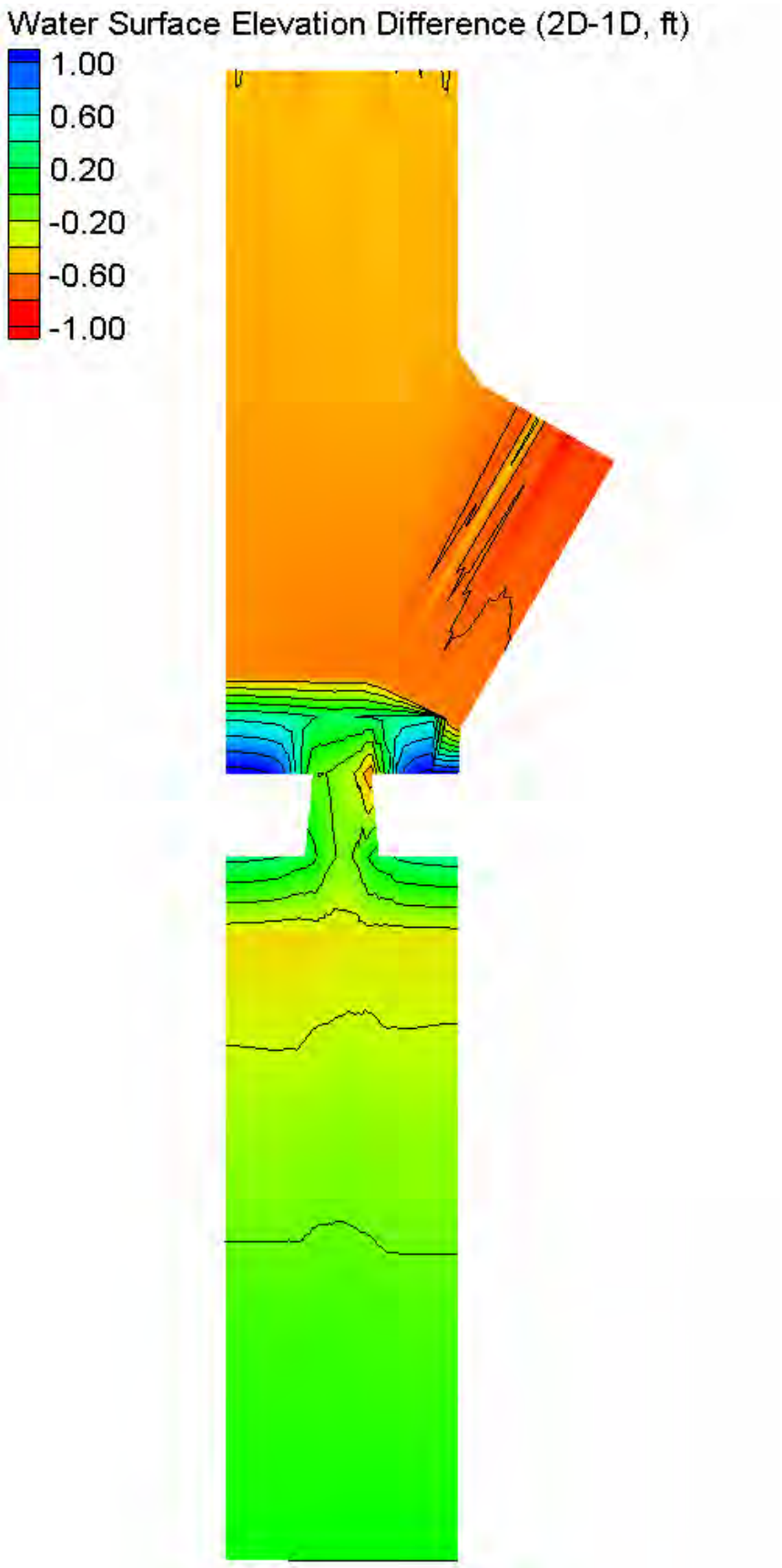

Water Surface Elevation Difference Contours – Small Channel – Confluences (30°, 75% flow, immediately upstream)

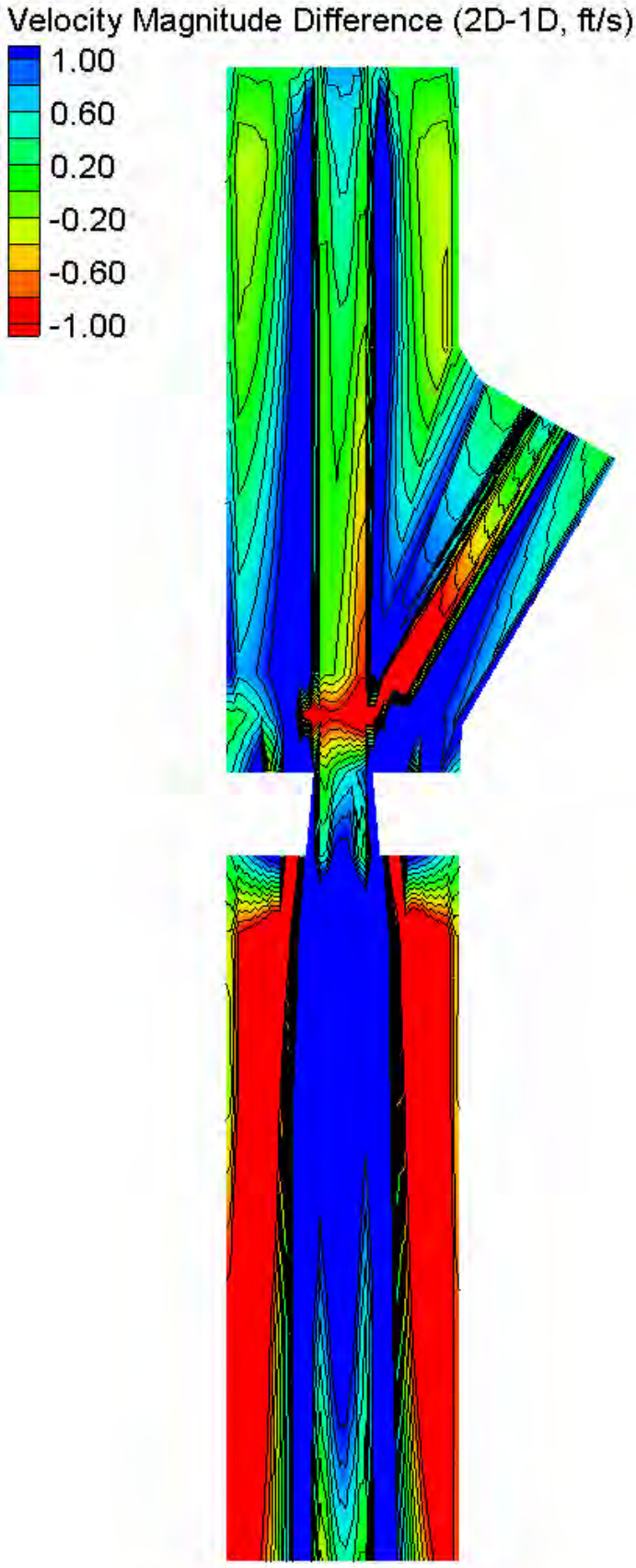

Velocity Magnitude Difference Contours – Small Channel – Confluences (30°, 75% flow, immediately upstream)

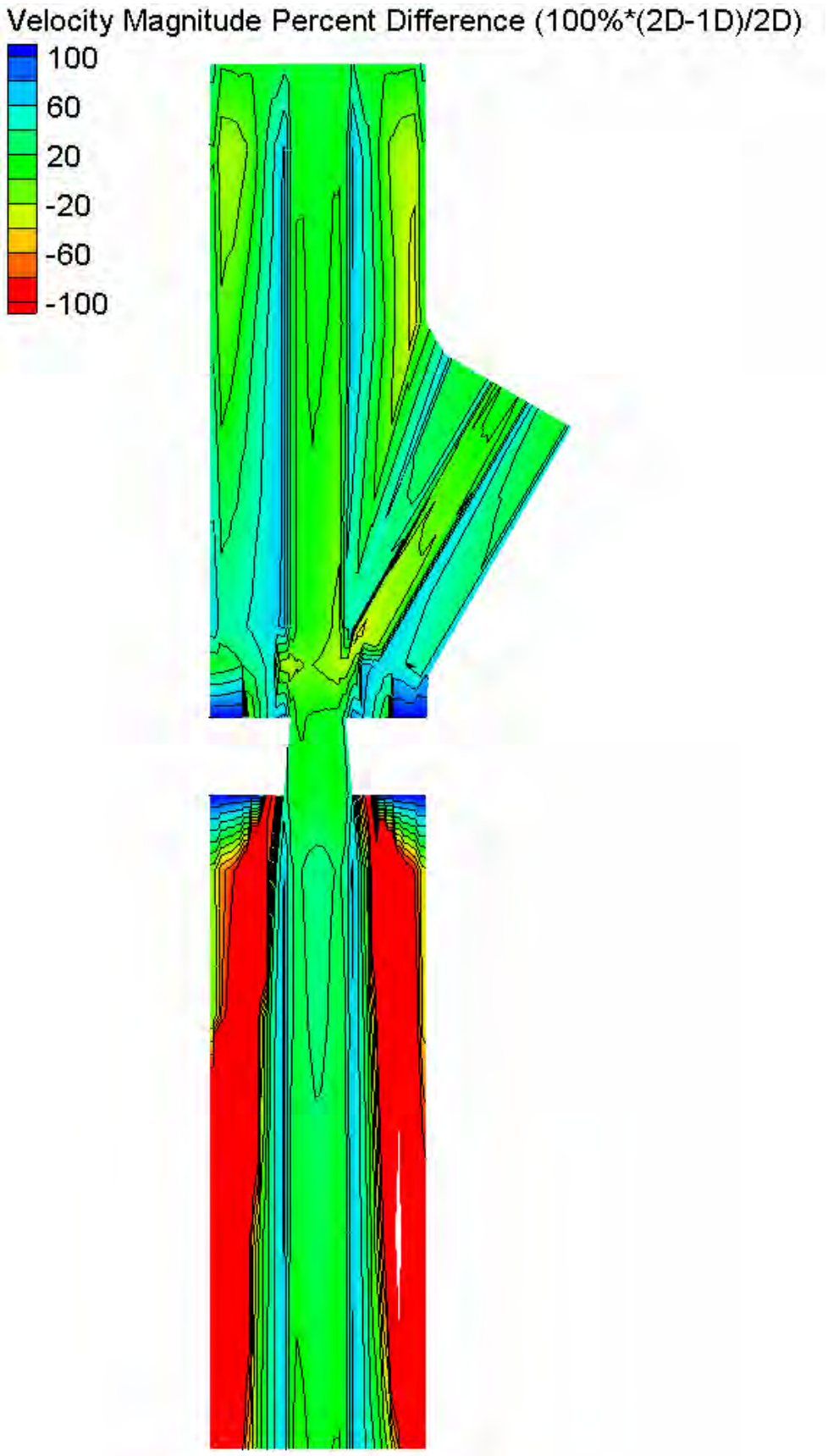

Velocity Magnitude Percent Difference Contours – Small Channel – Confluences (30°, 75% flow, immediately upstream)

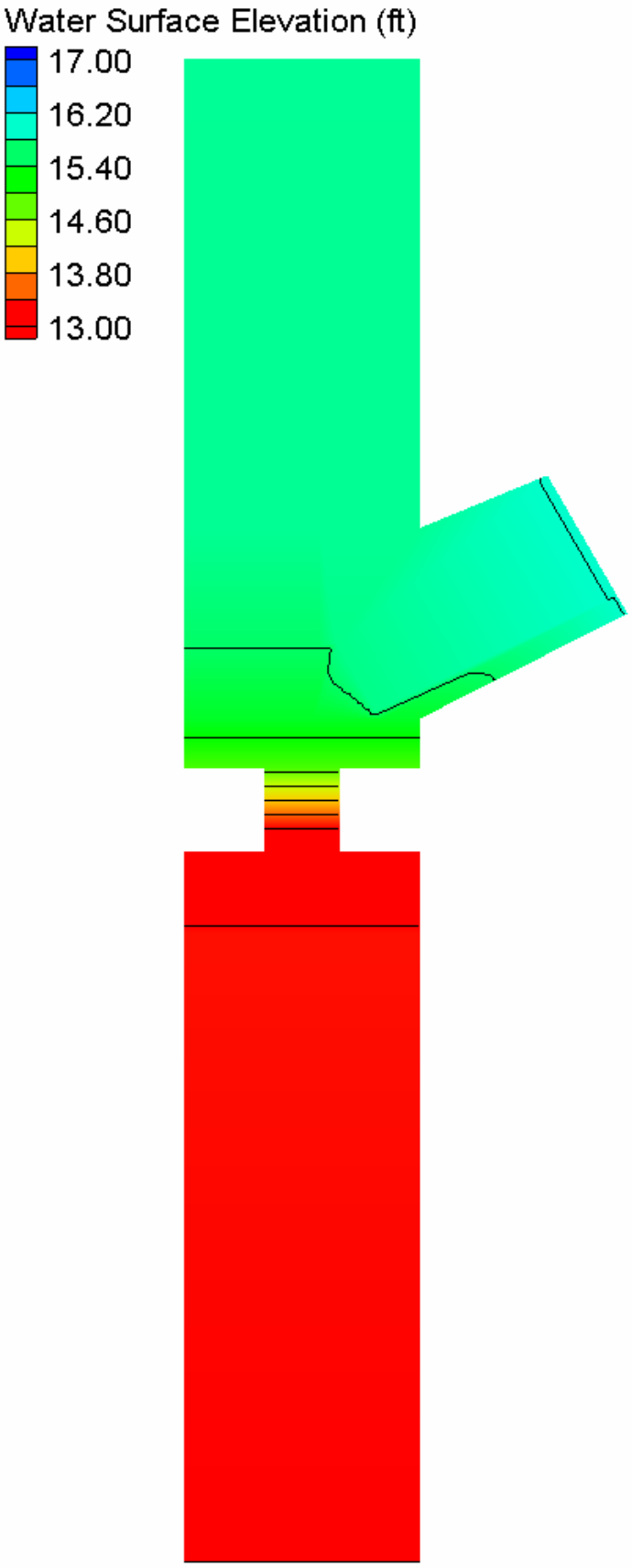

HEC-RAS Water Surface Elevation Contours – Small Channel – Confluences (60°, 50% flow, one bridge length upstream)

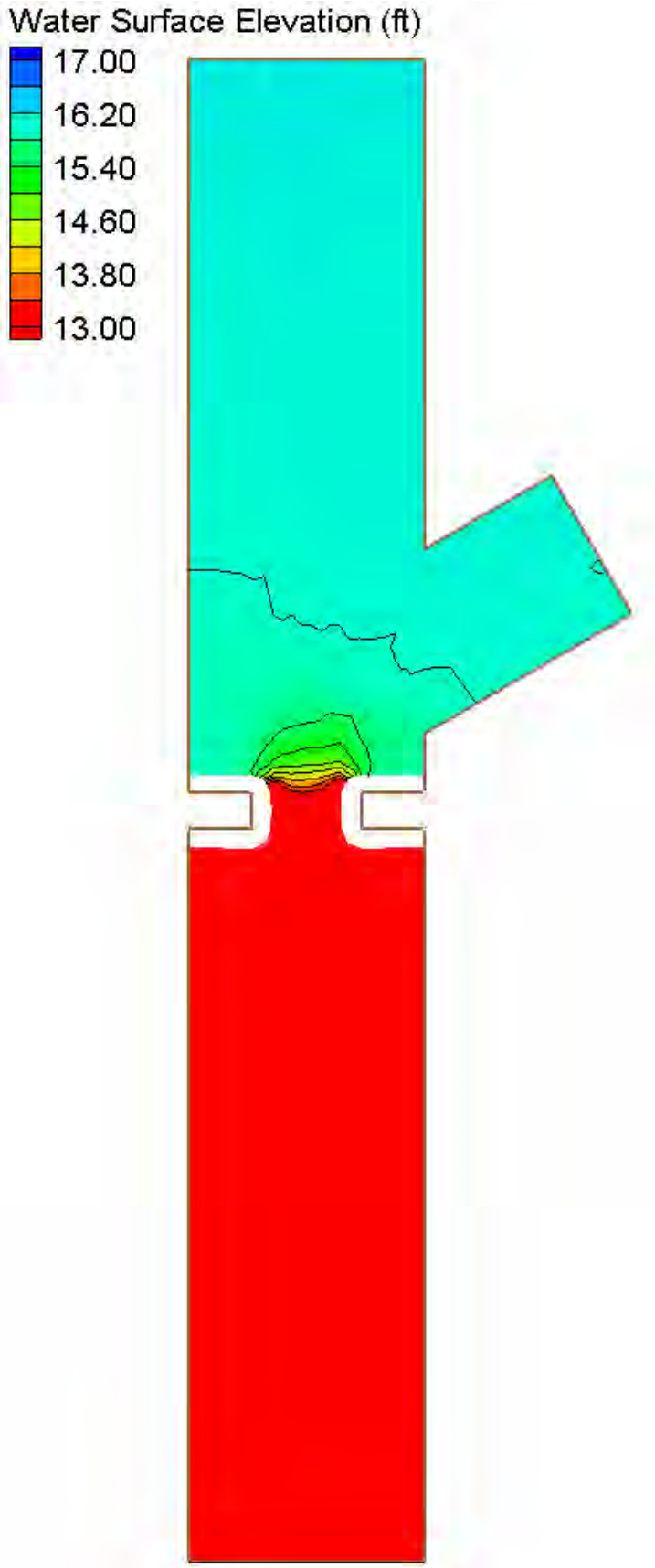

FESWMS Water Surface Elevation Contours – Small Channel – Confluences (60°, 50% flow, one bridge length upstream)

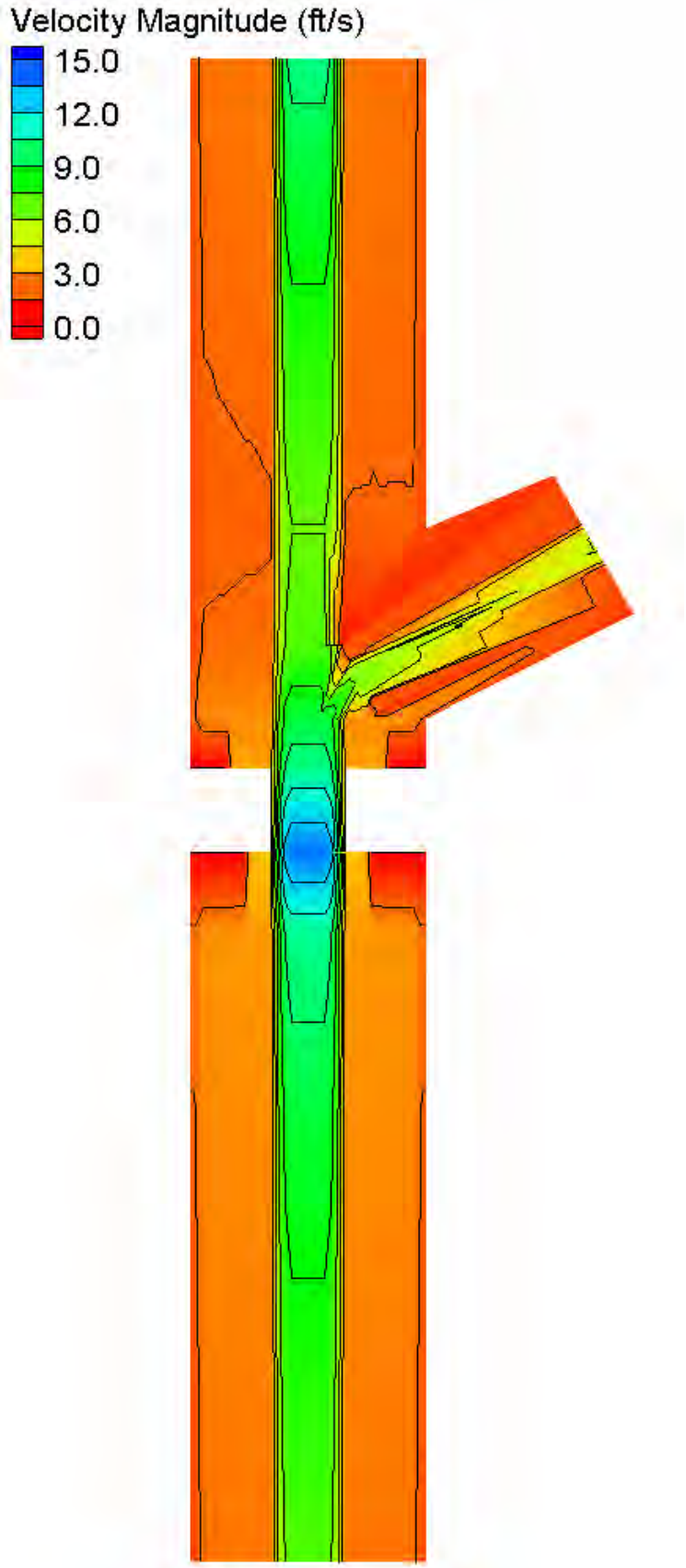

HEC-RAS Velocity Magnitude Contours – Small Channel – Confluences (60°, 50% flow, one bridge length upstream)

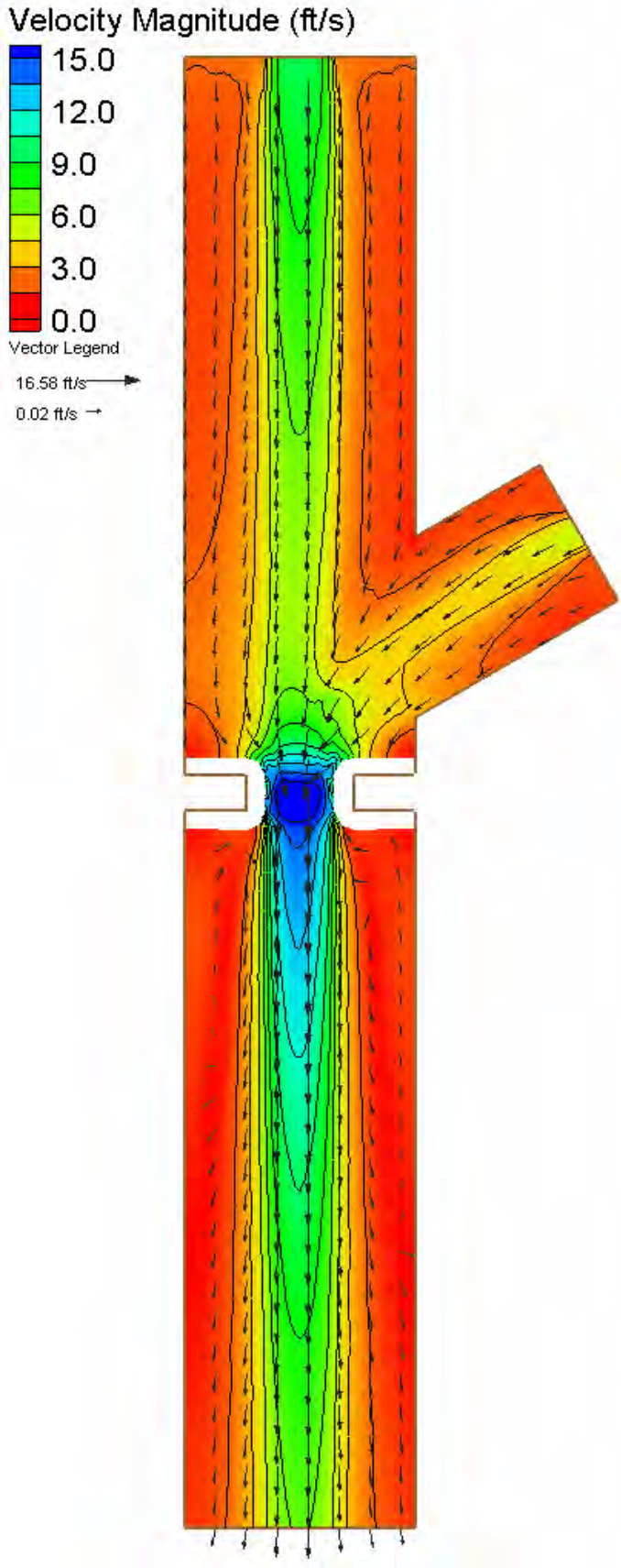

FESWMS Velocity Magnitude Contours – Small Channel – Confluences (60°, 50% flow, one bridge length upstream)

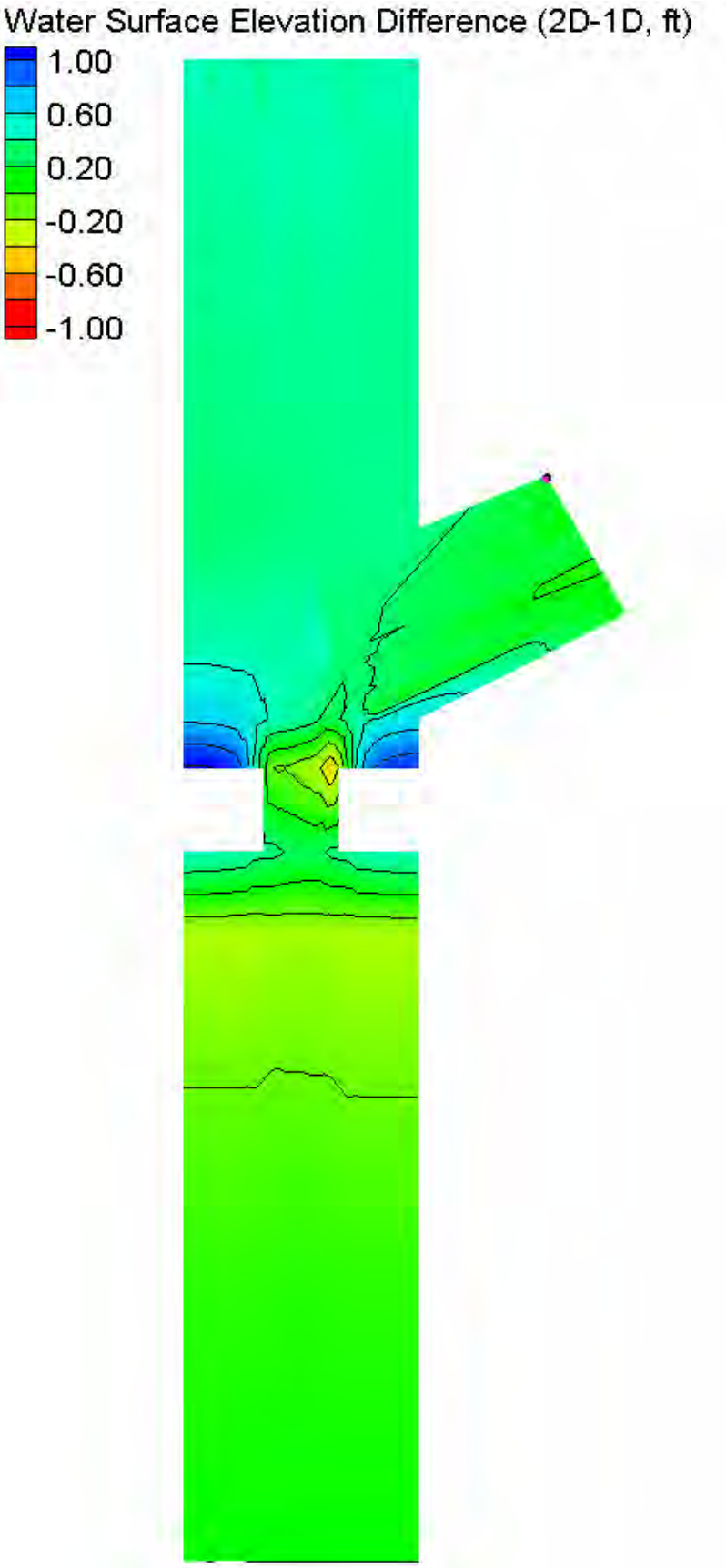

Water Surface Elevation Difference Contours – Small Channel – Confluences (60°, 50% flow, one bridge length upstream)

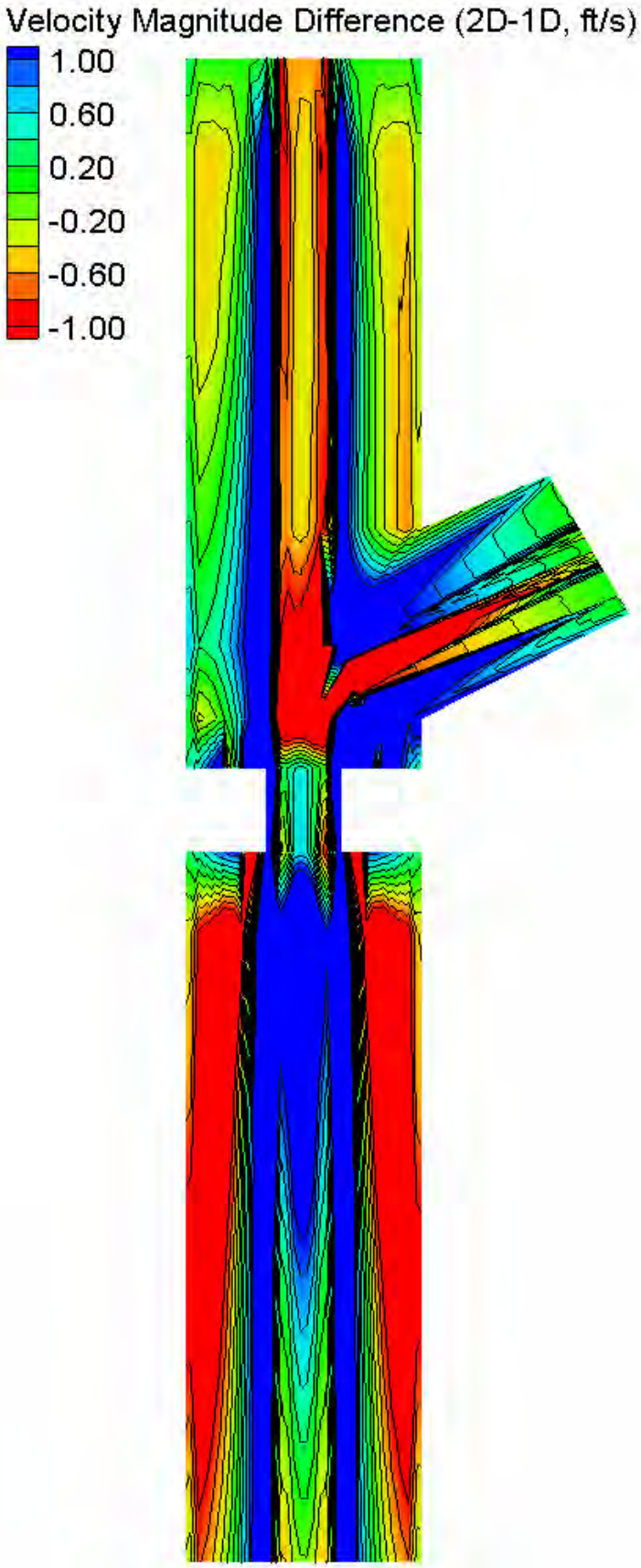

Velocity Magnitude Difference Contours – Small Channel – Confluences (60°, 50% flow, one bridge length upstream)

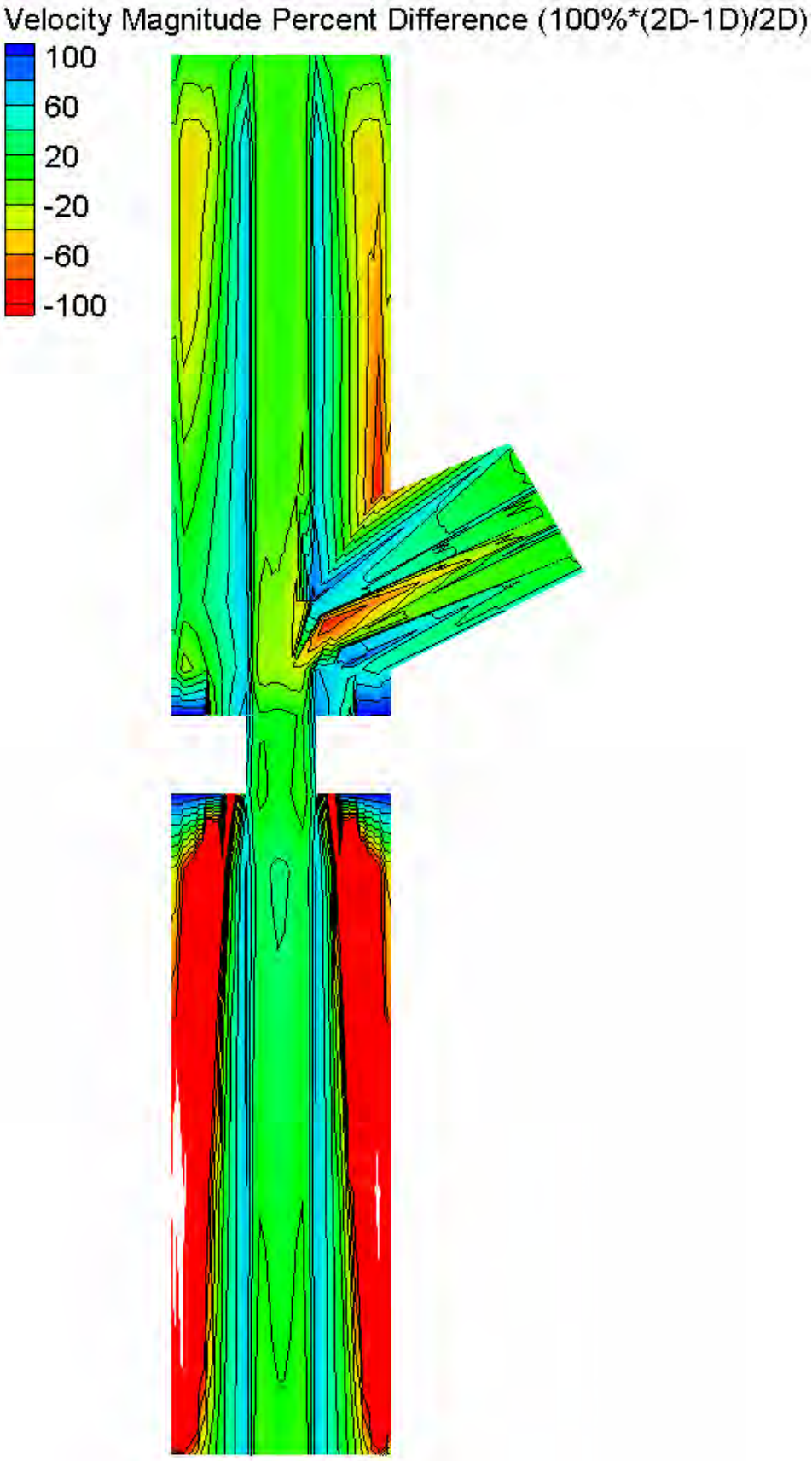

Velocity Magnitude Percent Difference Contours – Small Channel – Confluences (60°, 50% flow, one bridge length upstream)

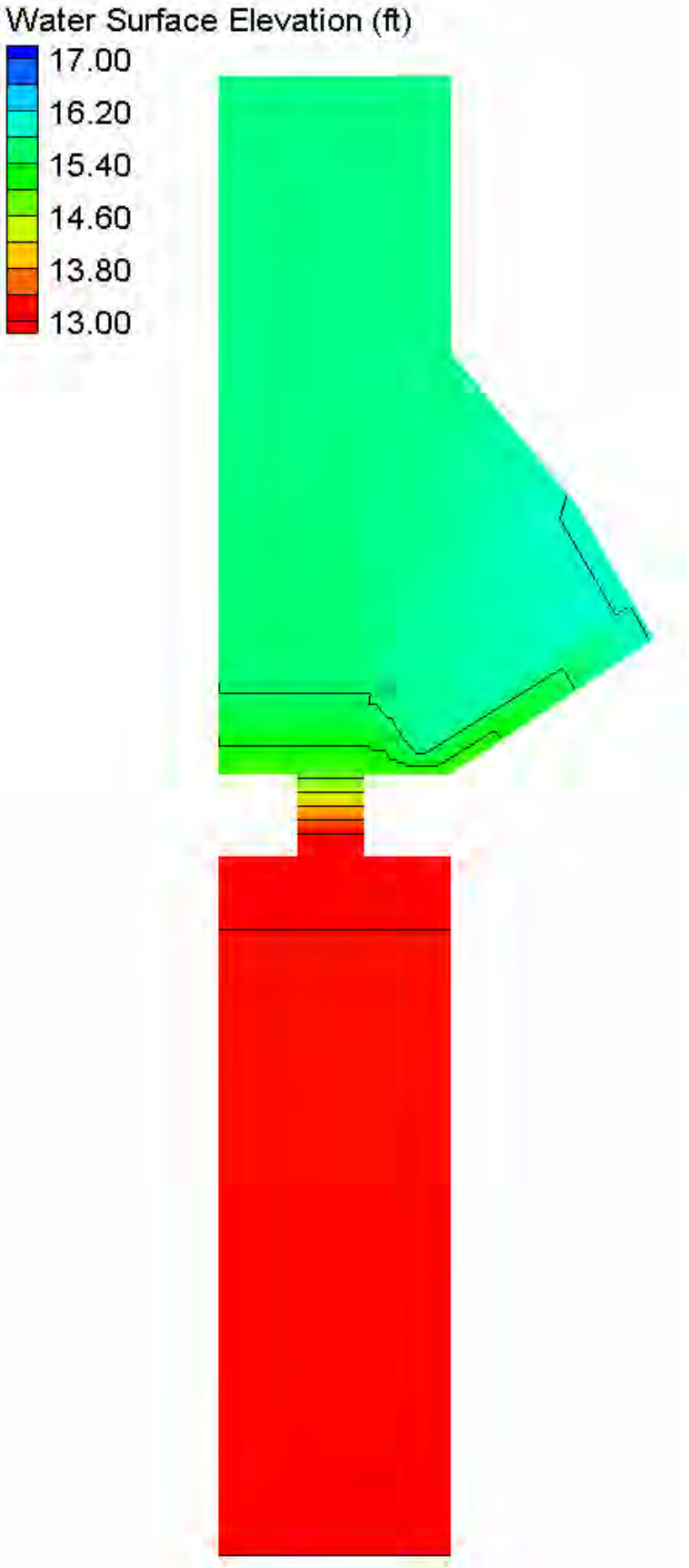

HEC-RAS Water Surface Elevation Contours – Small Channel – Confluences (60°, 50% flow, immediately upstream)

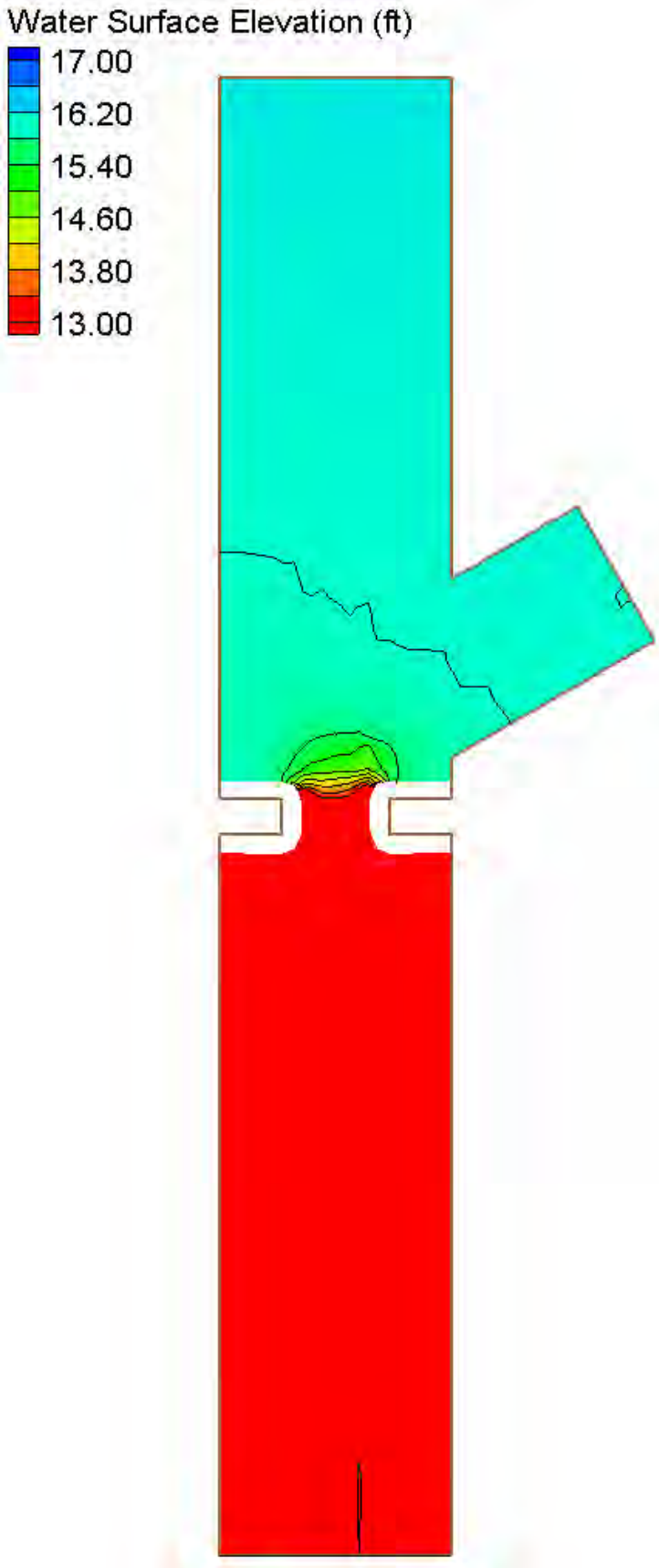

FESWMS Water Surface Elevation Contours – Small Channel – Confluences (60°, 50% flow, immediately upstream)

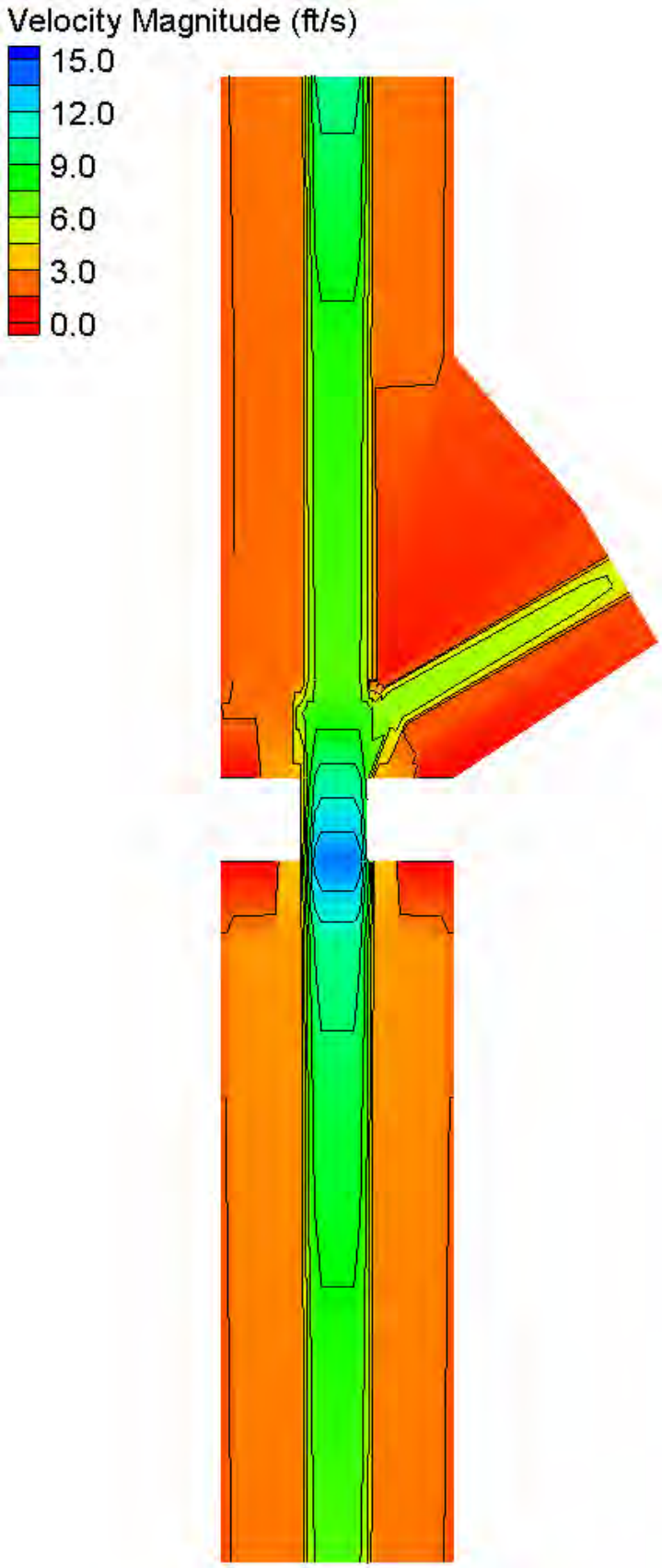

HEC-RAS Velocity Magnitude Contours – Small Channel – Confluences (60°, 50% flow, immediately upstream)

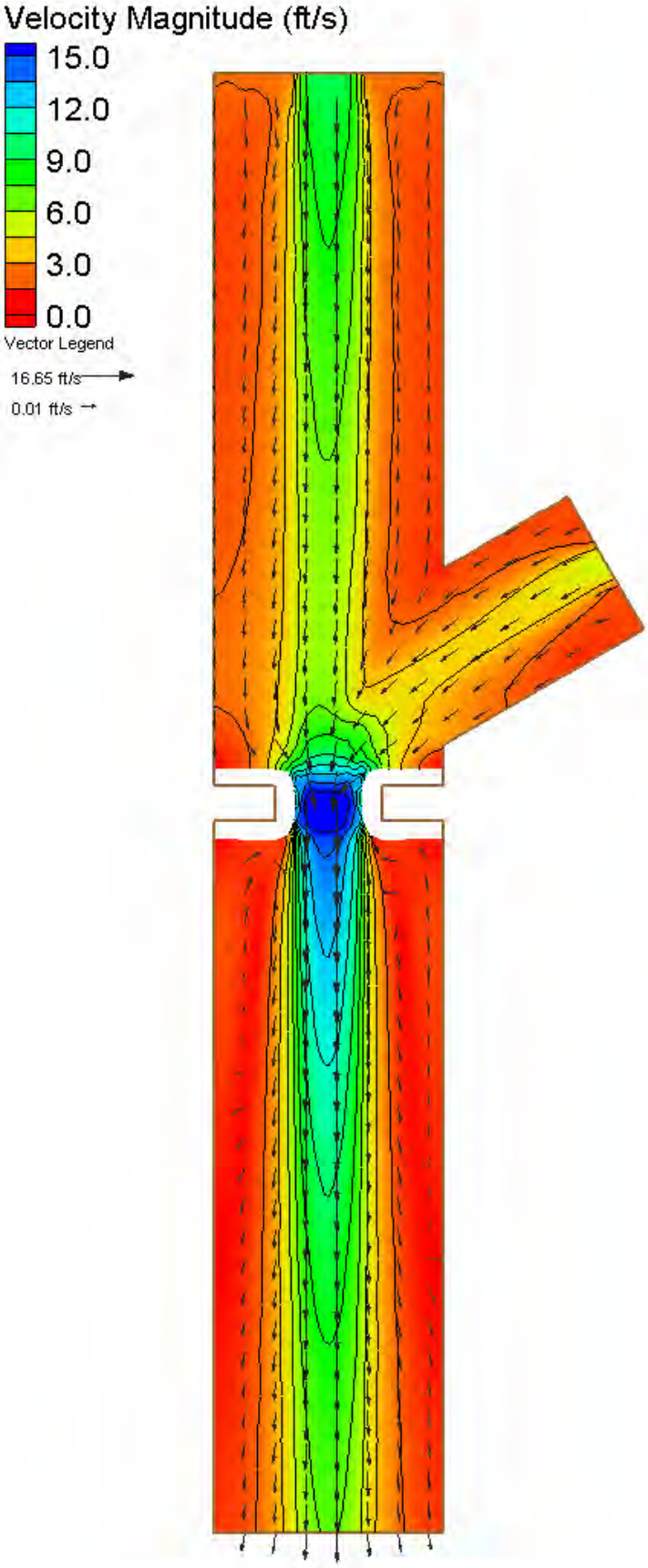

FESWMS Velocity Magnitude Contours – Small Channel – Confluences (60°, 50% flow, immediately upstream)

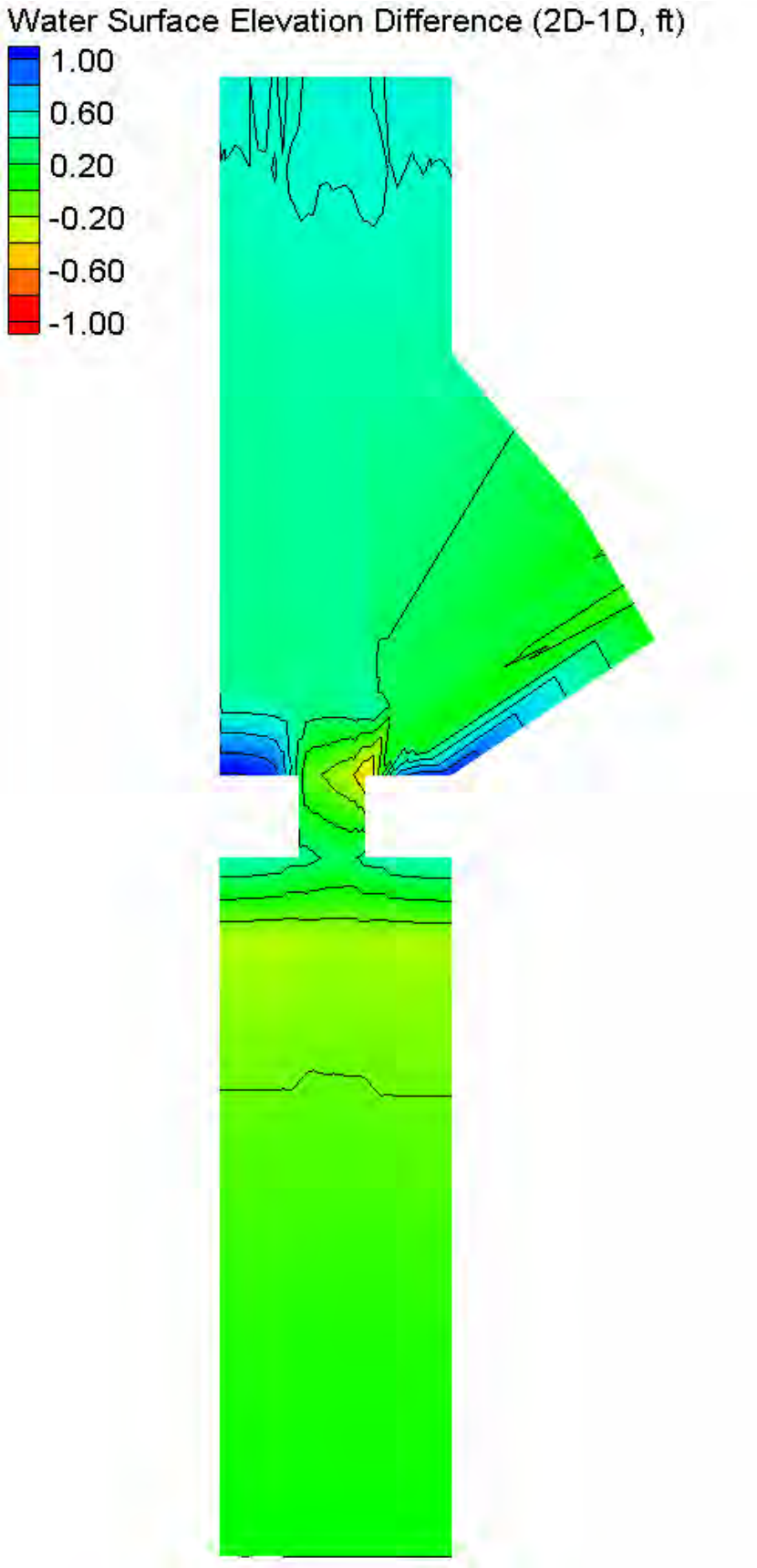

Water Surface Elevation Difference Contours – Small Channel – Confluences (60°, 50% flow, immediately upstream)

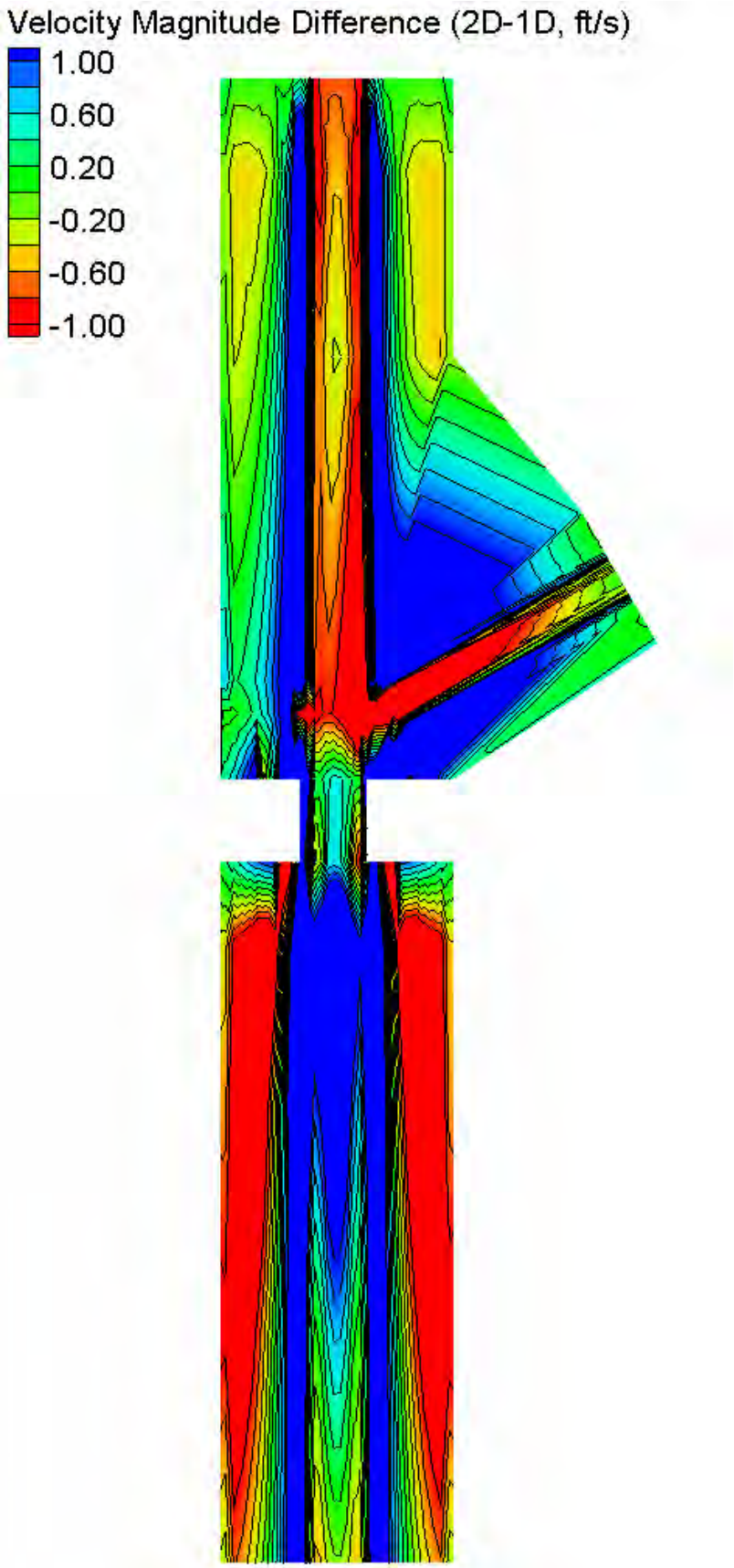

Velocity Magnitude Difference Contours – Small Channel – Confluences (60°, 50% flow, immediately upstream)

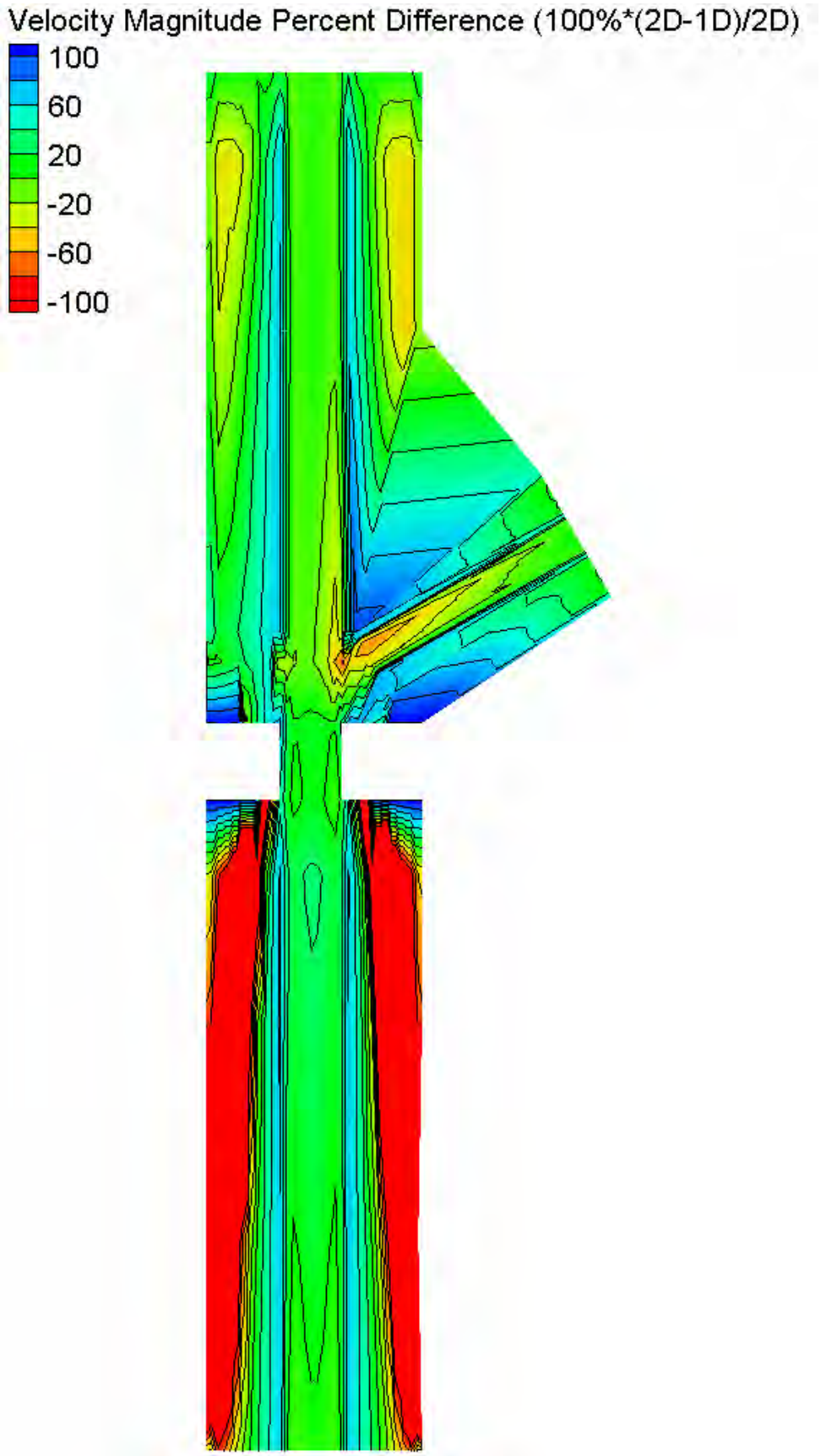

Velocity Magnitude Percent Difference Contours – Small Channel – Confluences (60°, 50% flow, immediately upstream)

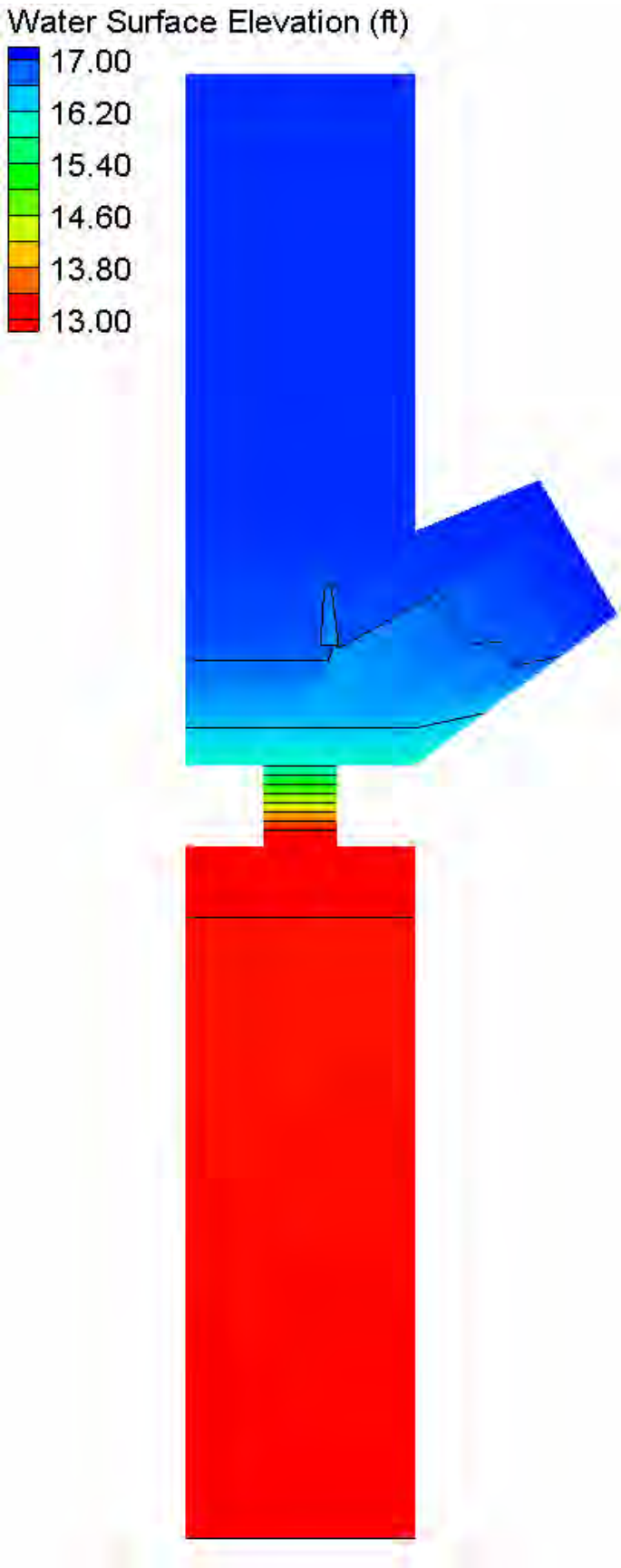

HEC-RAS Water Surface Elevation Contours – Small Channel – Confluences (60°, 75% flow, one bridge length upstream)

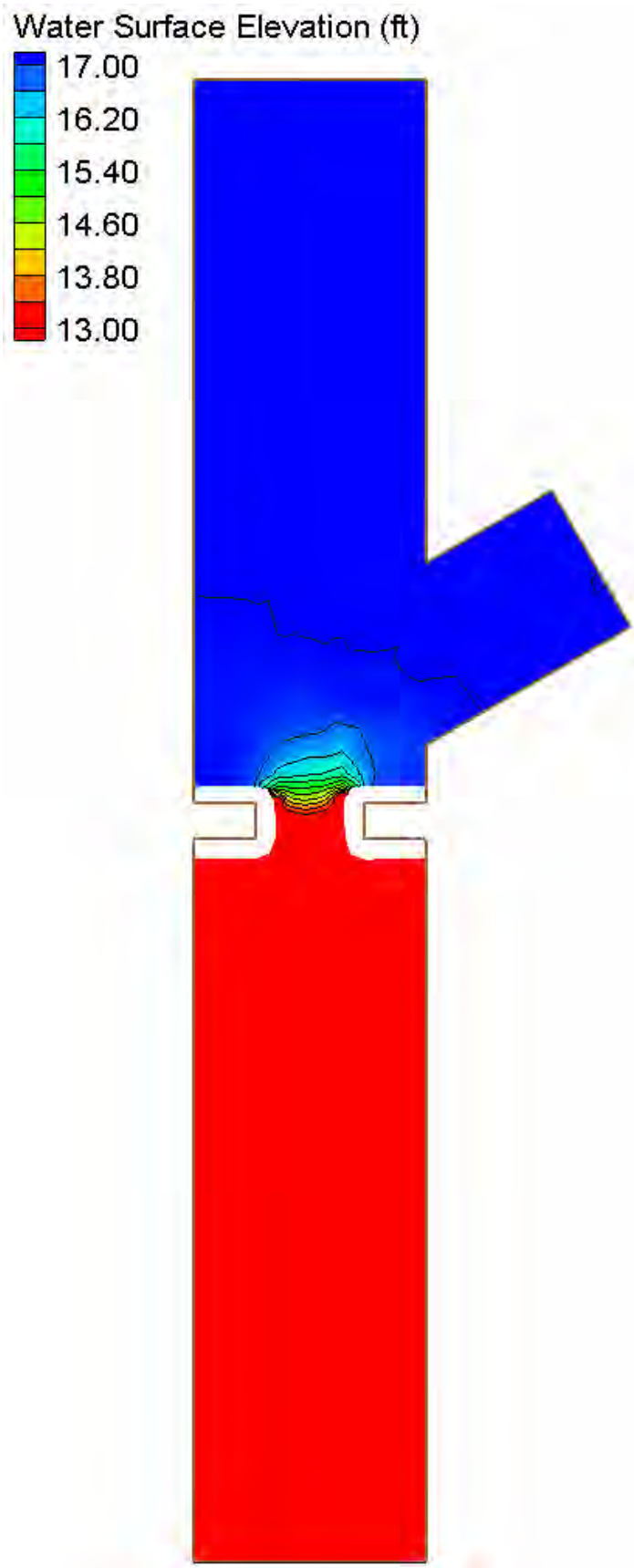

FESWMS Water Surface Elevation Contours – Small Channel – Confluences (60°, 75% flow, one bridge length upstream)

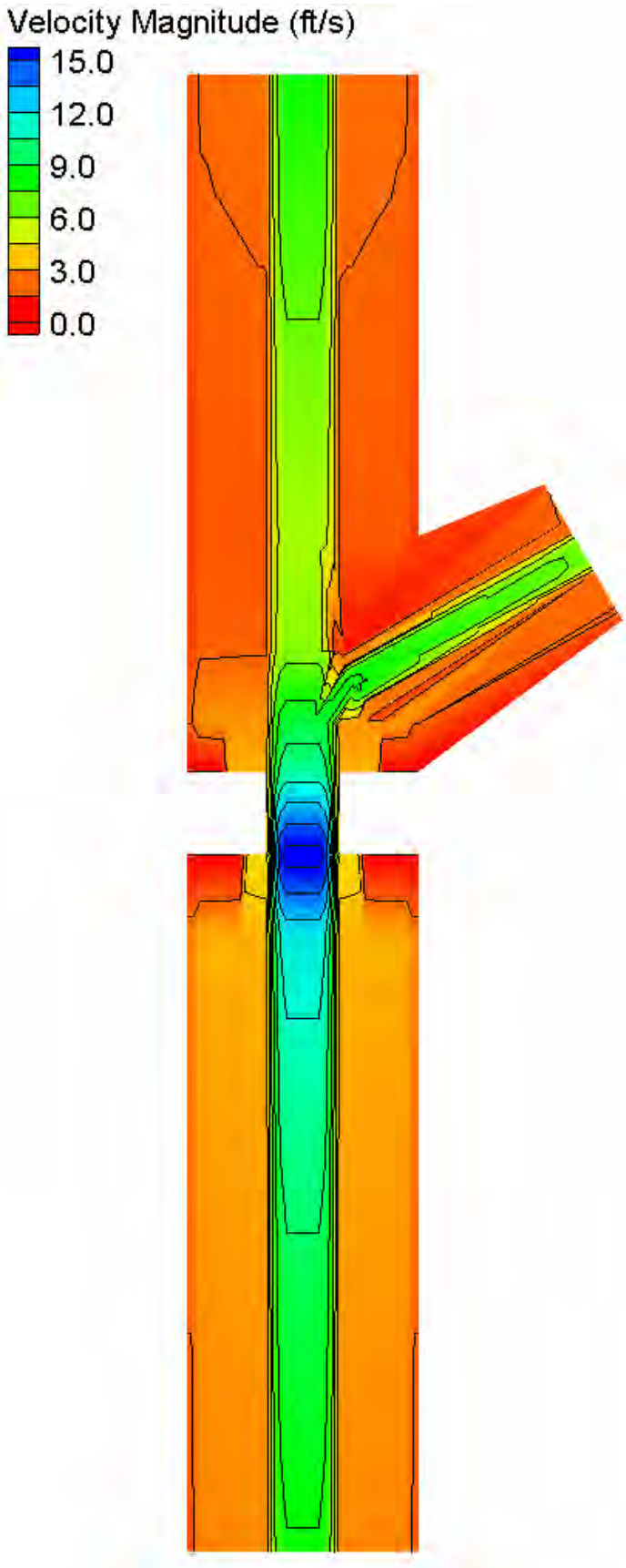

HEC-RAS Velocity Magnitude Contours – Small Channel – Confluences (60°, 75% flow, one bridge length upstream)

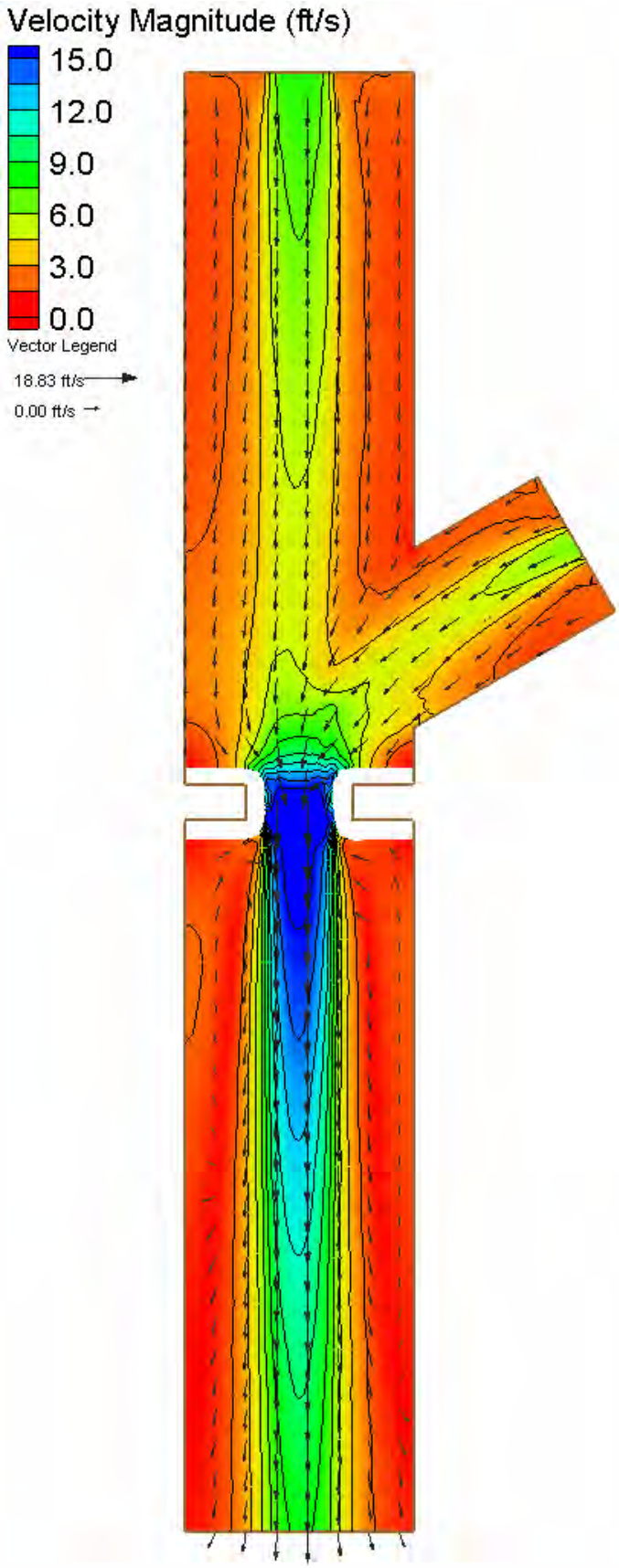

FESWMS Velocity Magnitude Contours – Small Channel – Confluences (60°, 75% flow, one bridge length upstream)

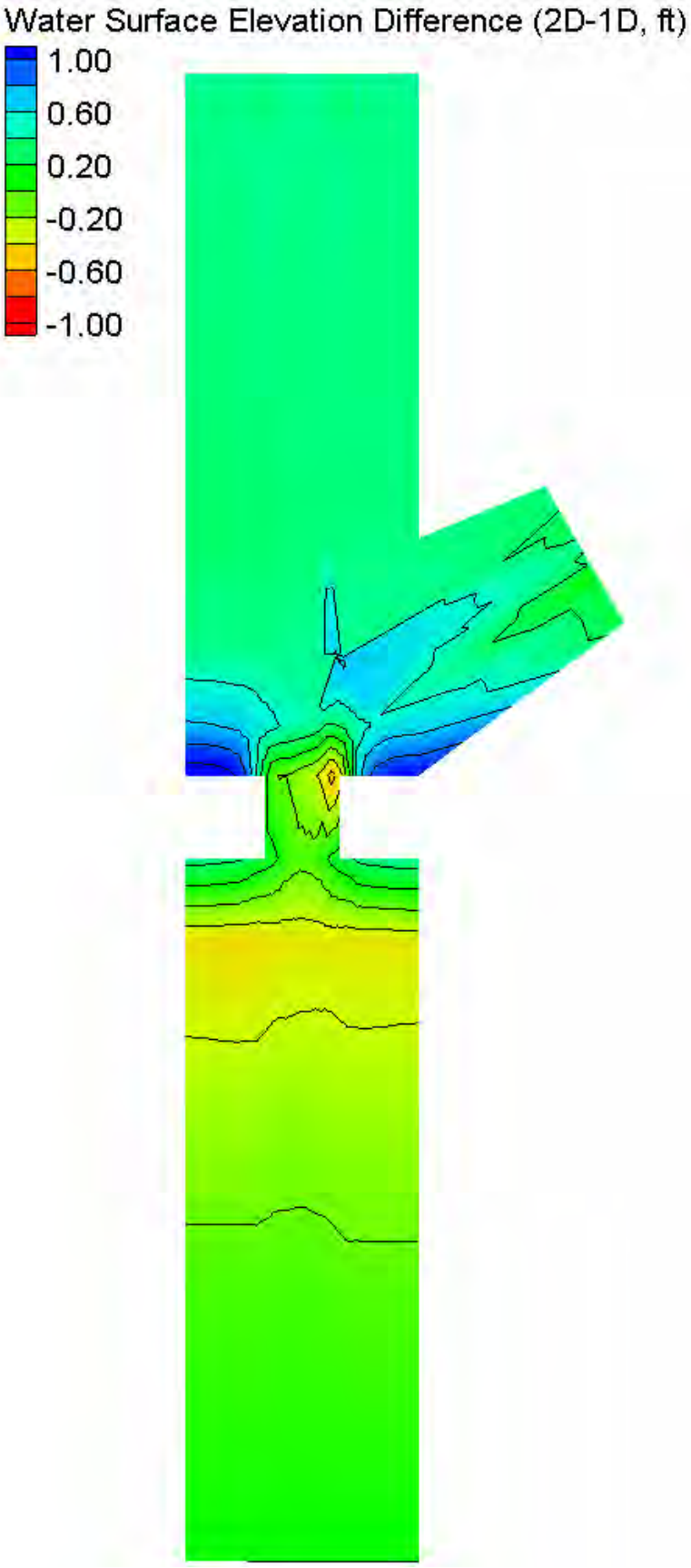

Water Surface Elevation Difference Contours – Small Channel – Confluences (60°, 75% flow, one bridge length upstream)

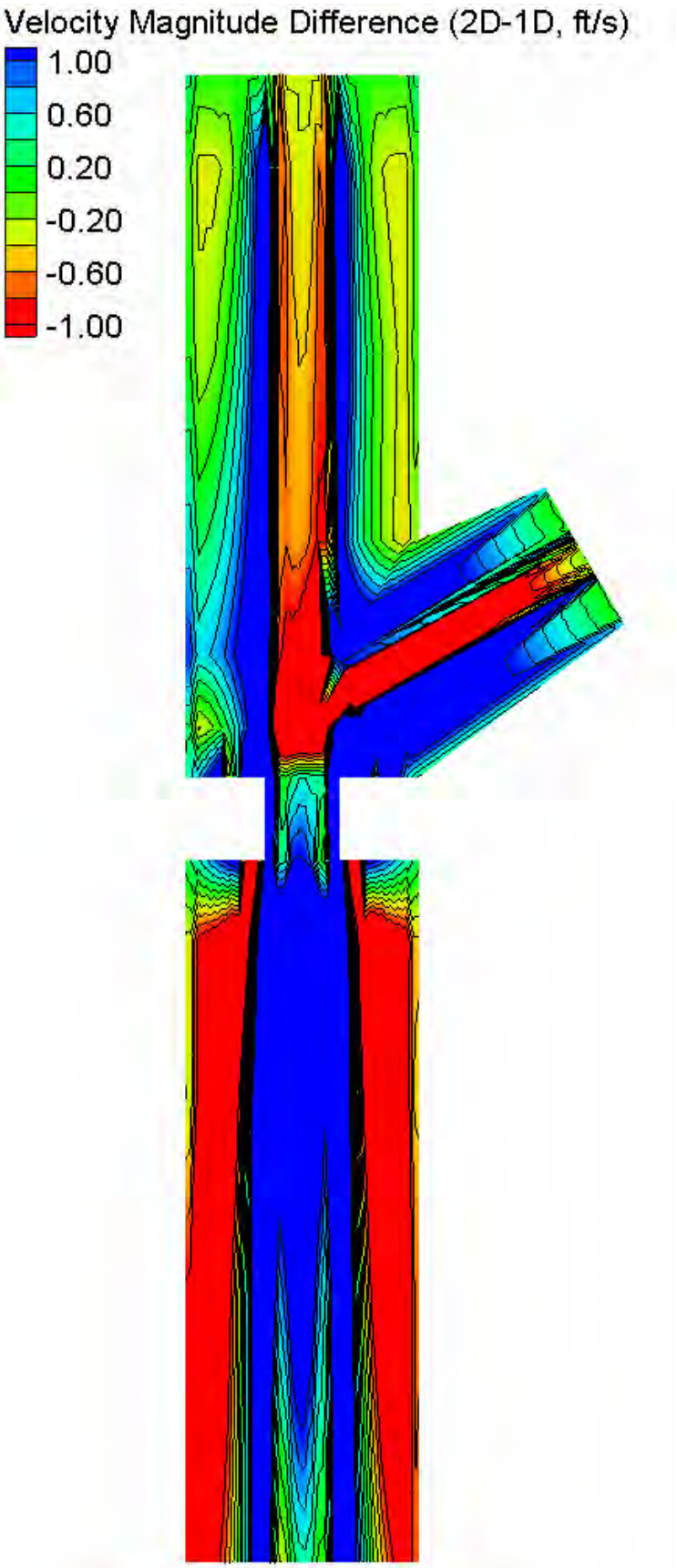

Velocity Magnitude Difference Contours – Small Channel – Confluences (60°, 75% flow, one bridge length upstream)

Velocity Magnitude Percent Difference Contours – Small Channel – Confluences (60°, 75% flow, one bridge length upstream)

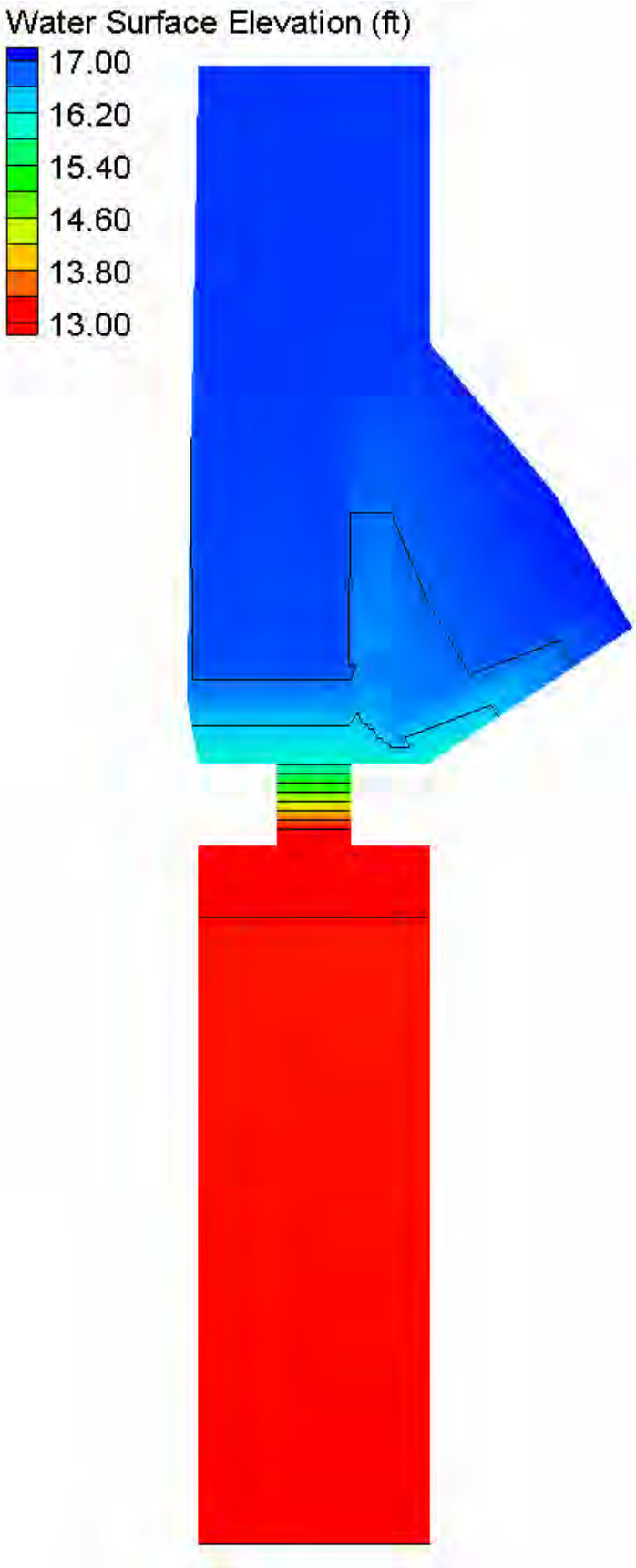

HEC-RAS Water Surface Elevation Contours – Small Channel – Confluences (60°, 75% flow, immediately upstream)

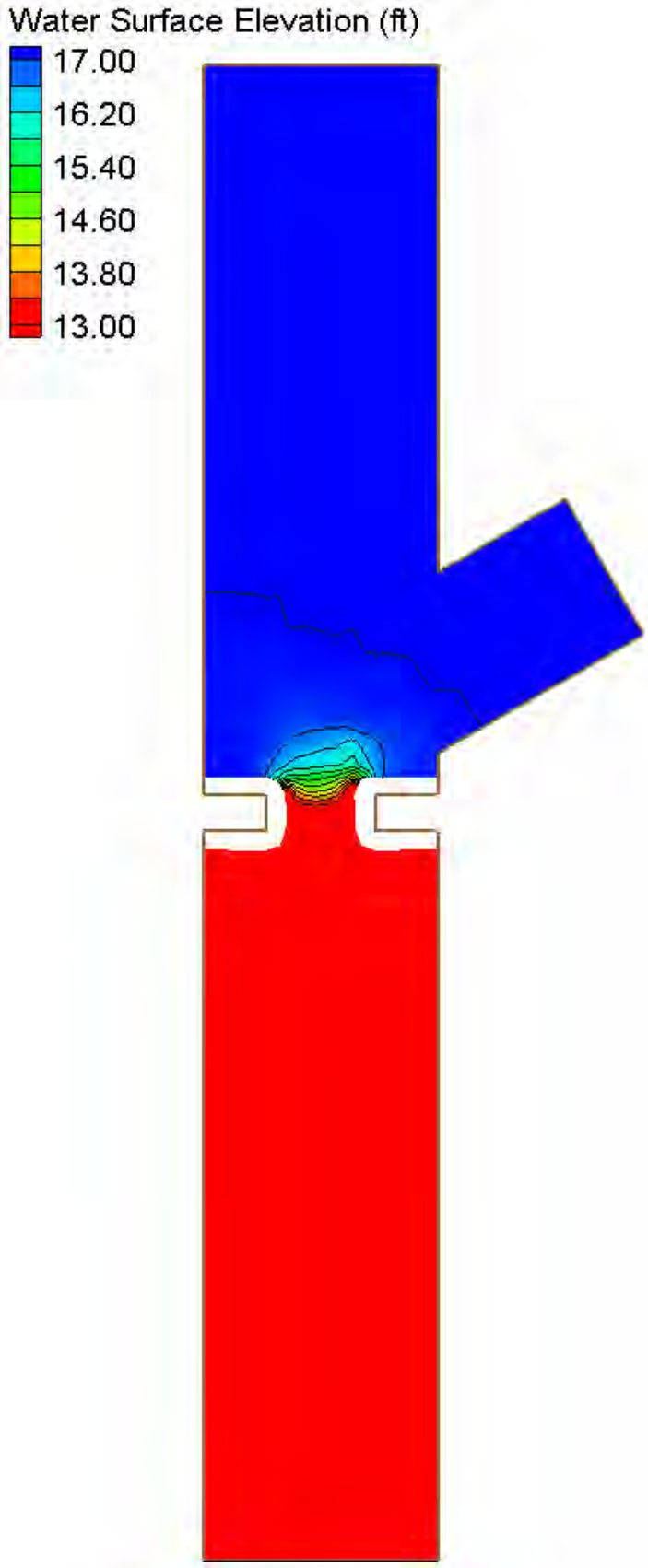

FESWMS Water Surface Elevation Contours – Small Channel – Confluences (60°, 75% flow, immediately upstream)

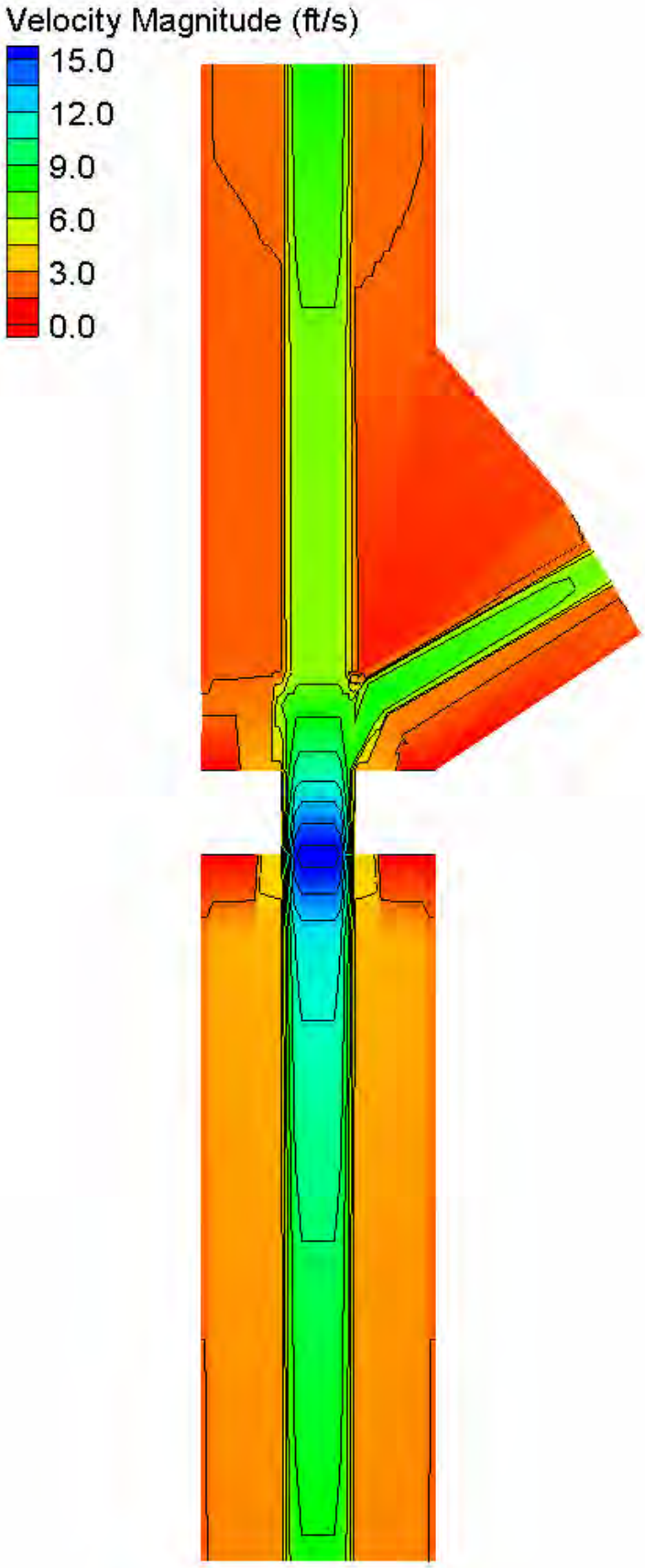

HEC-RAS Velocity Magnitude Contours – Small Channel – Confluences (60°, 75% flow, immediately upstream)

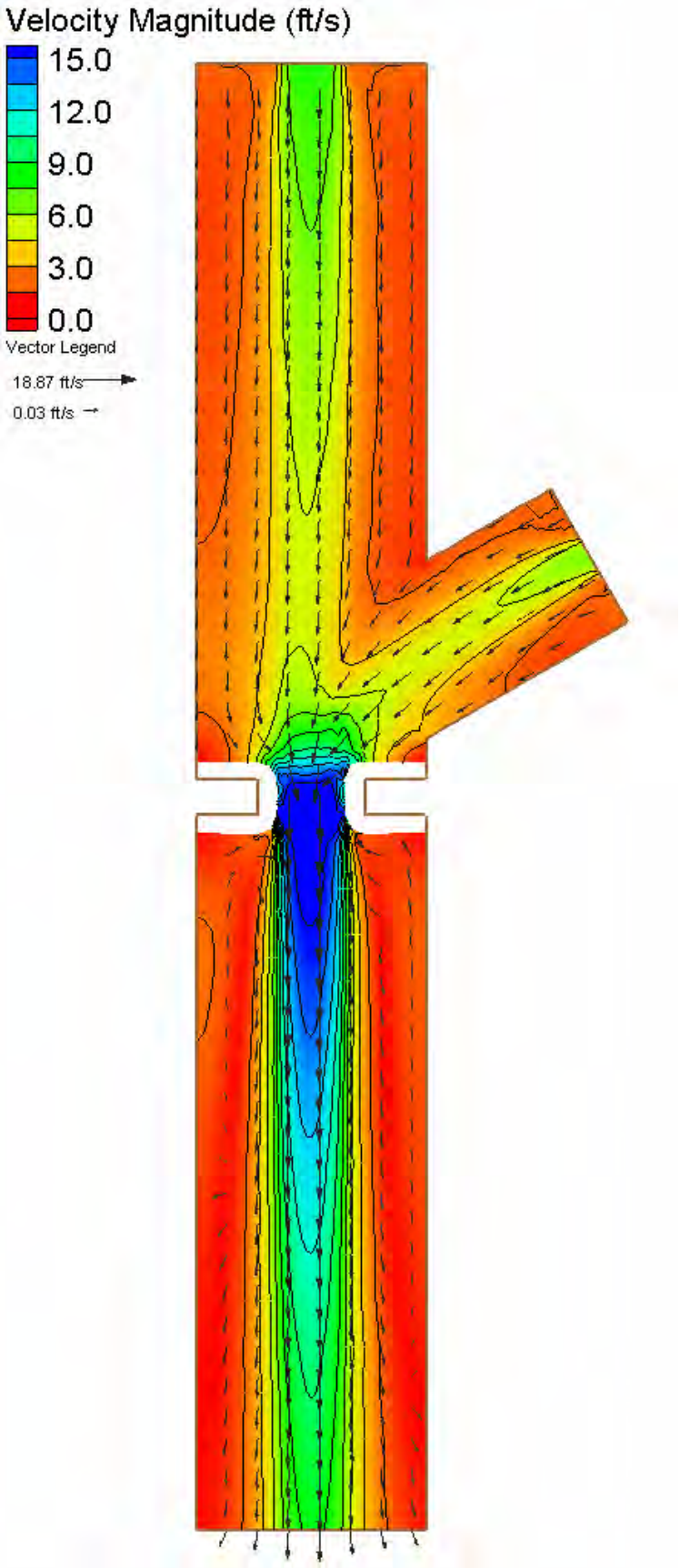

FESWMS Velocity Magnitude Contours – Small Channel – Confluences (60°, 75% flow, immediately upstream)

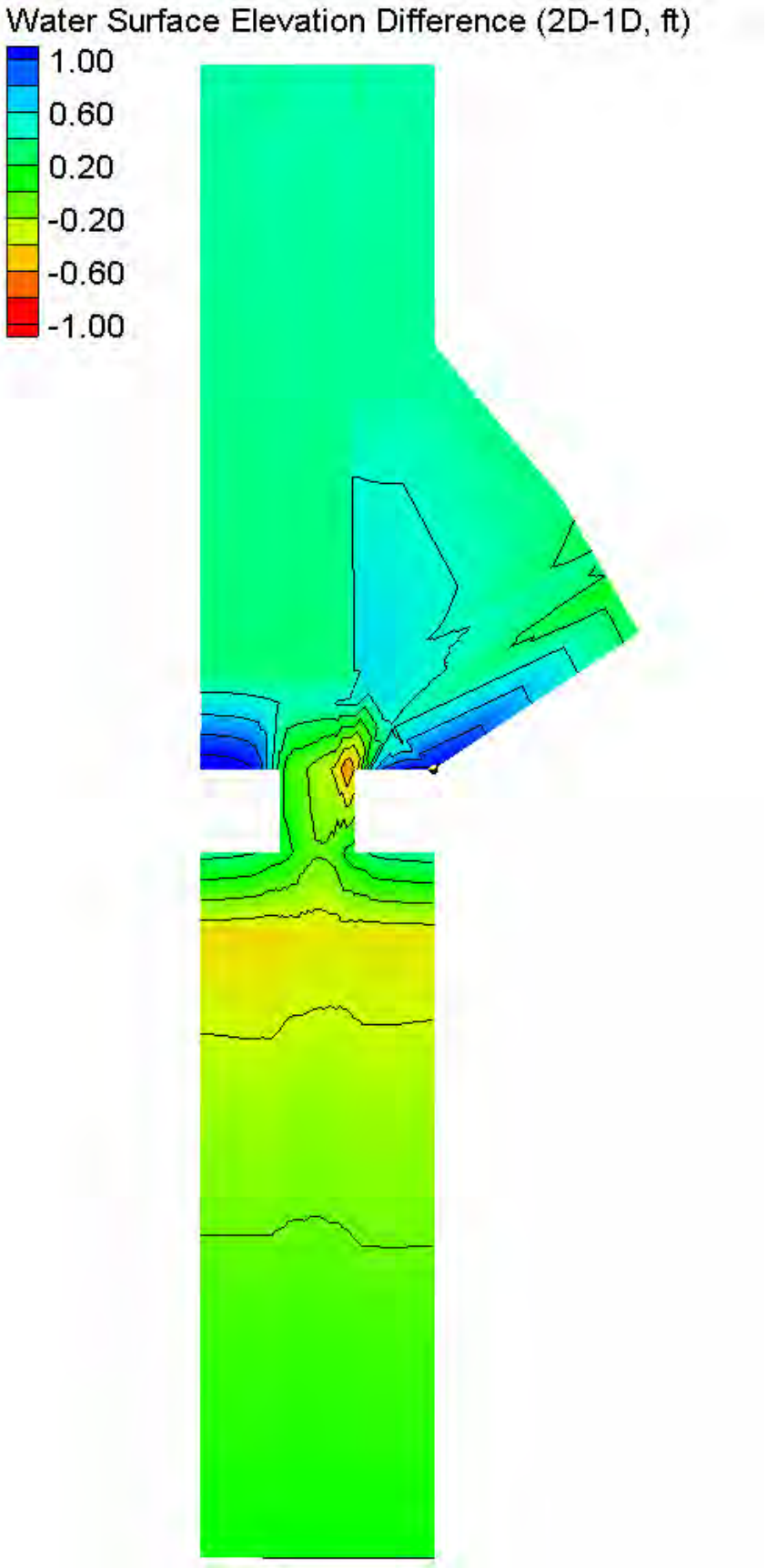

Water Surface Elevation Difference Contours – Small Channel – Confluences (60°, 75% flow, immediately upstream)

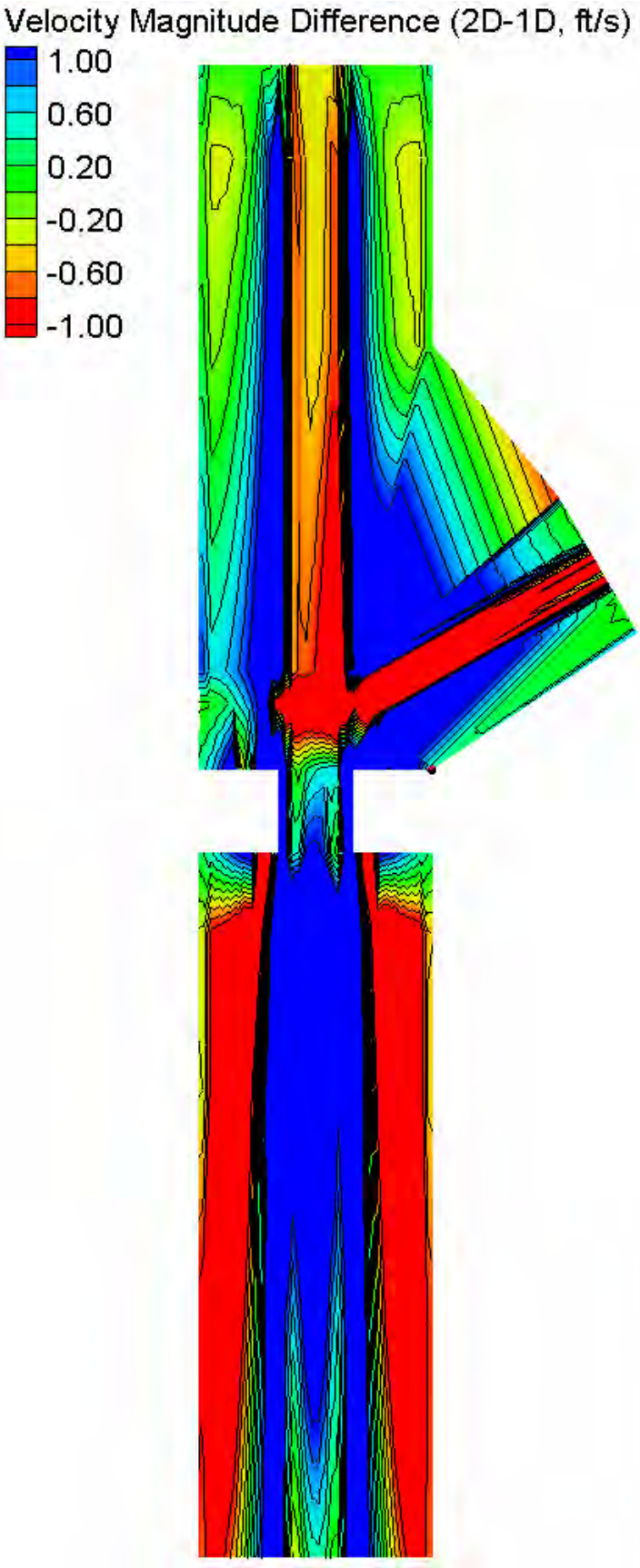

Velocity Magnitude Difference Contours – Small Channel – Confluences (60°, 75% flow, immediately upstream)

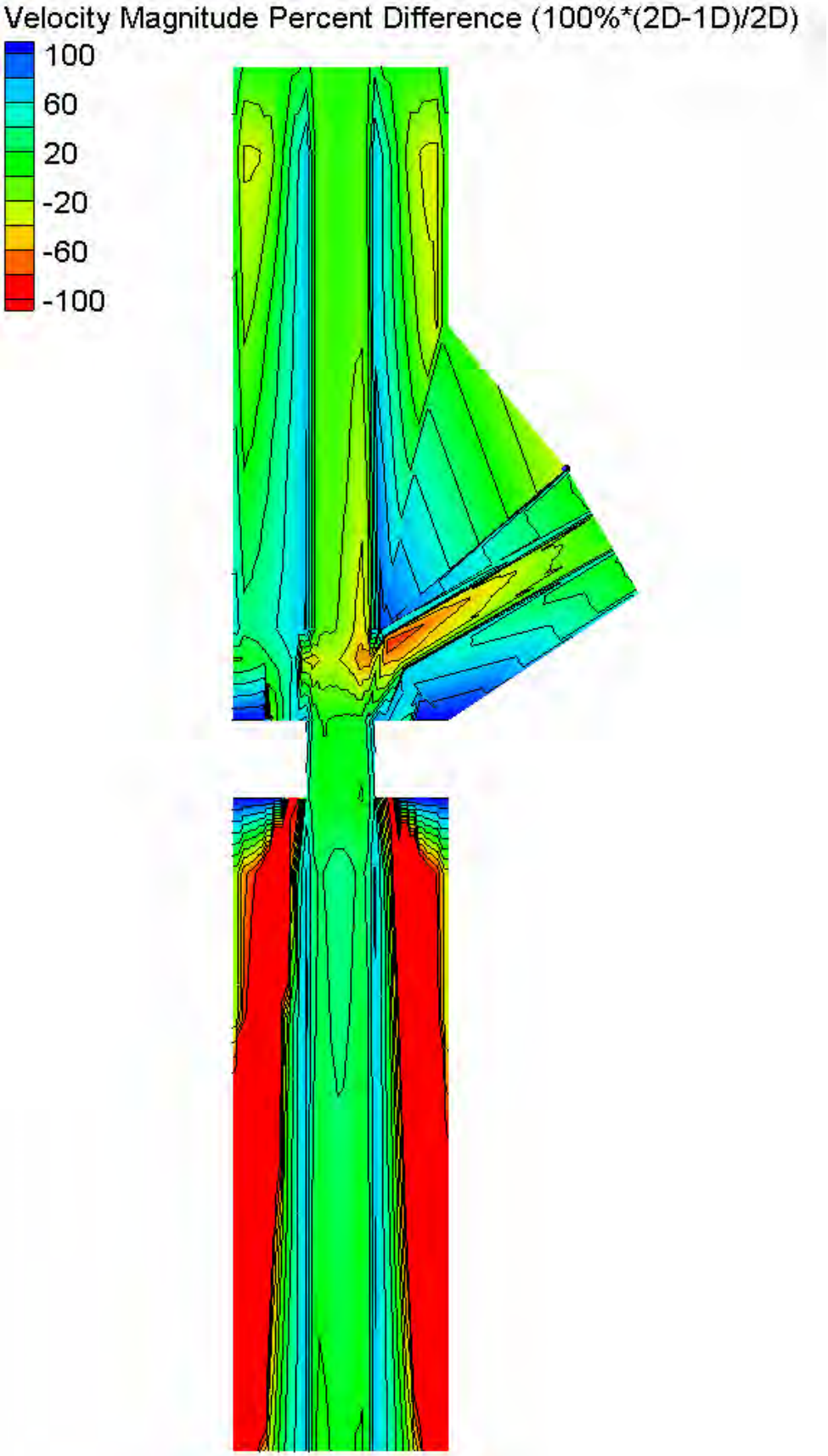

Velocity Magnitude Percent Difference Contours – Small Channel – Confluences (60°, 75% flow, immediately upstream)

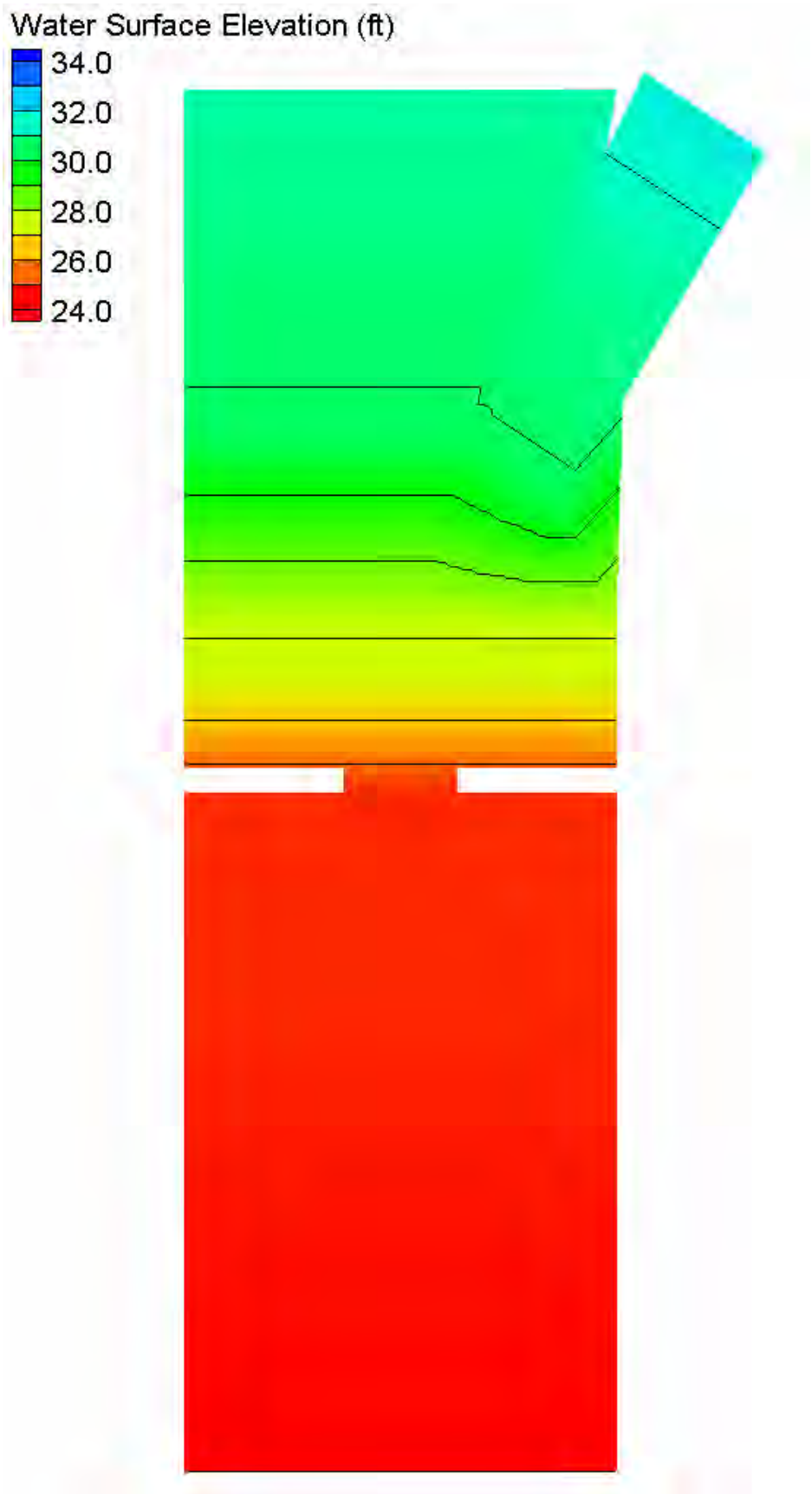

HEC-RAS Water Surface Elevation Contours – Large Channel – Confluences (30°, 50% flow, one bridge length upstream)

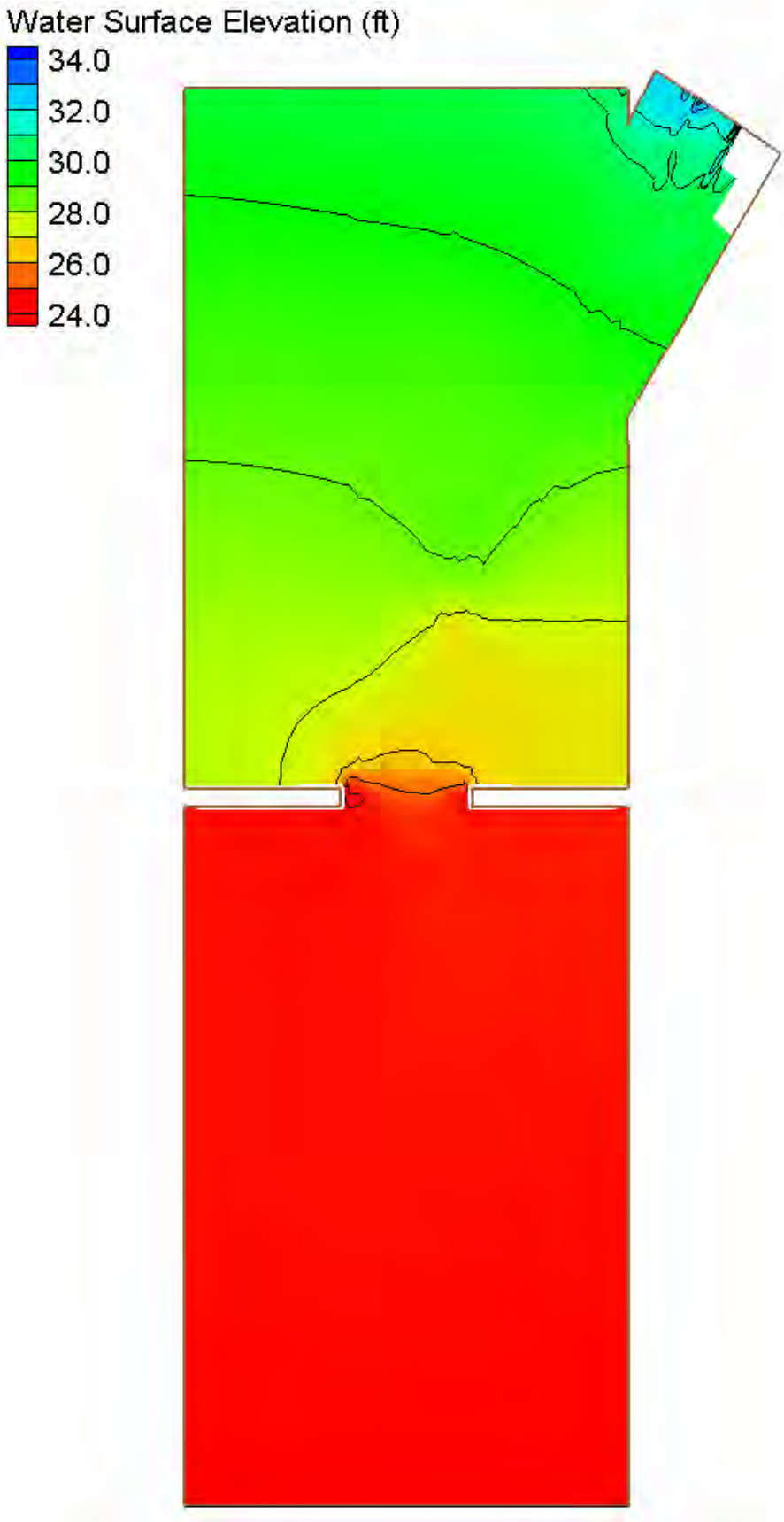

FESWMS Water Surface Elevation Contours – Large Channel – Confluences (30°, 50% flow, one bridge length upstream)

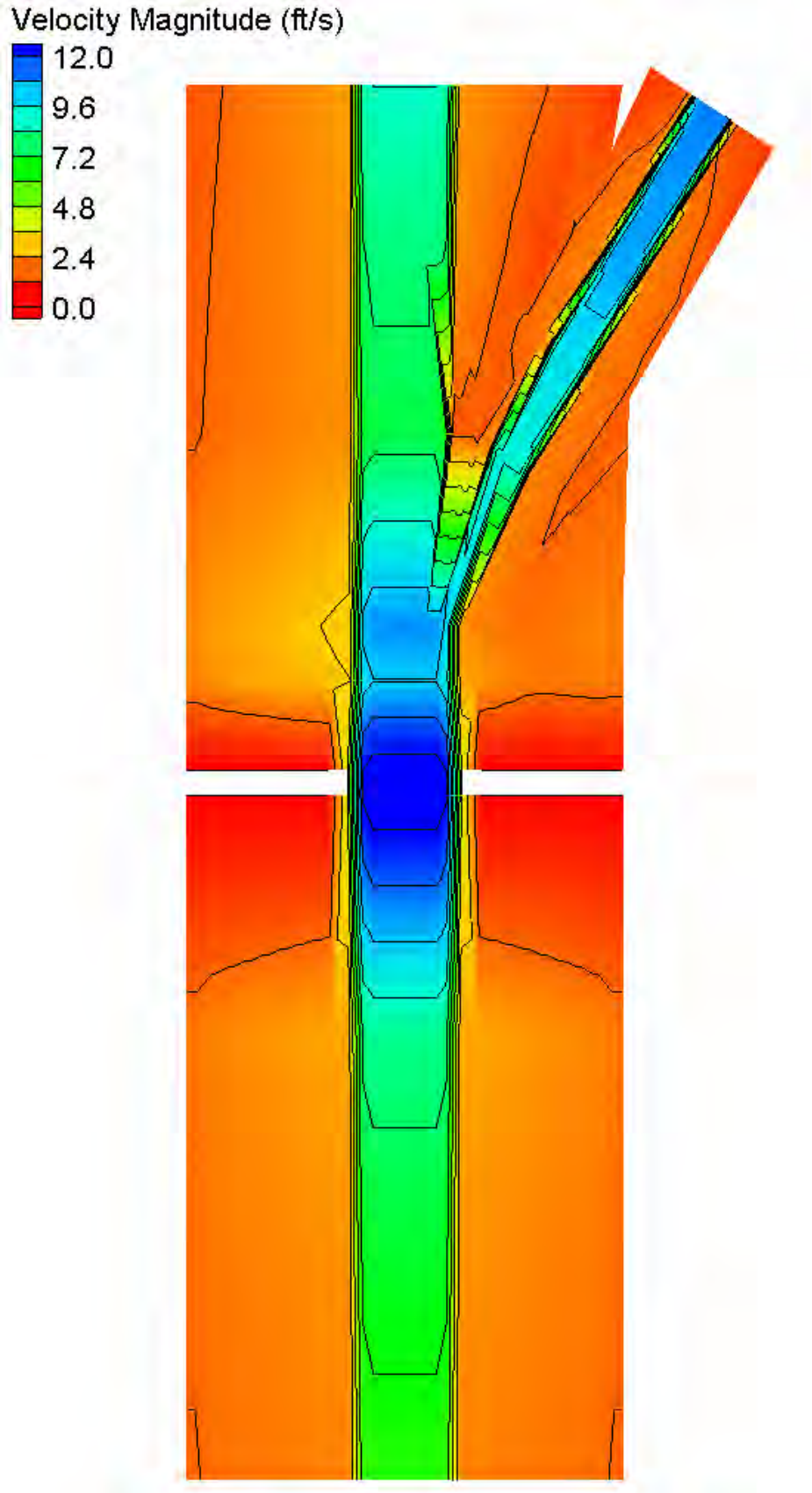

HEC-RAS Velocity Magnitude Contours – Large Channel – Confluences (30°, 50% flow, one bridge length upstream)

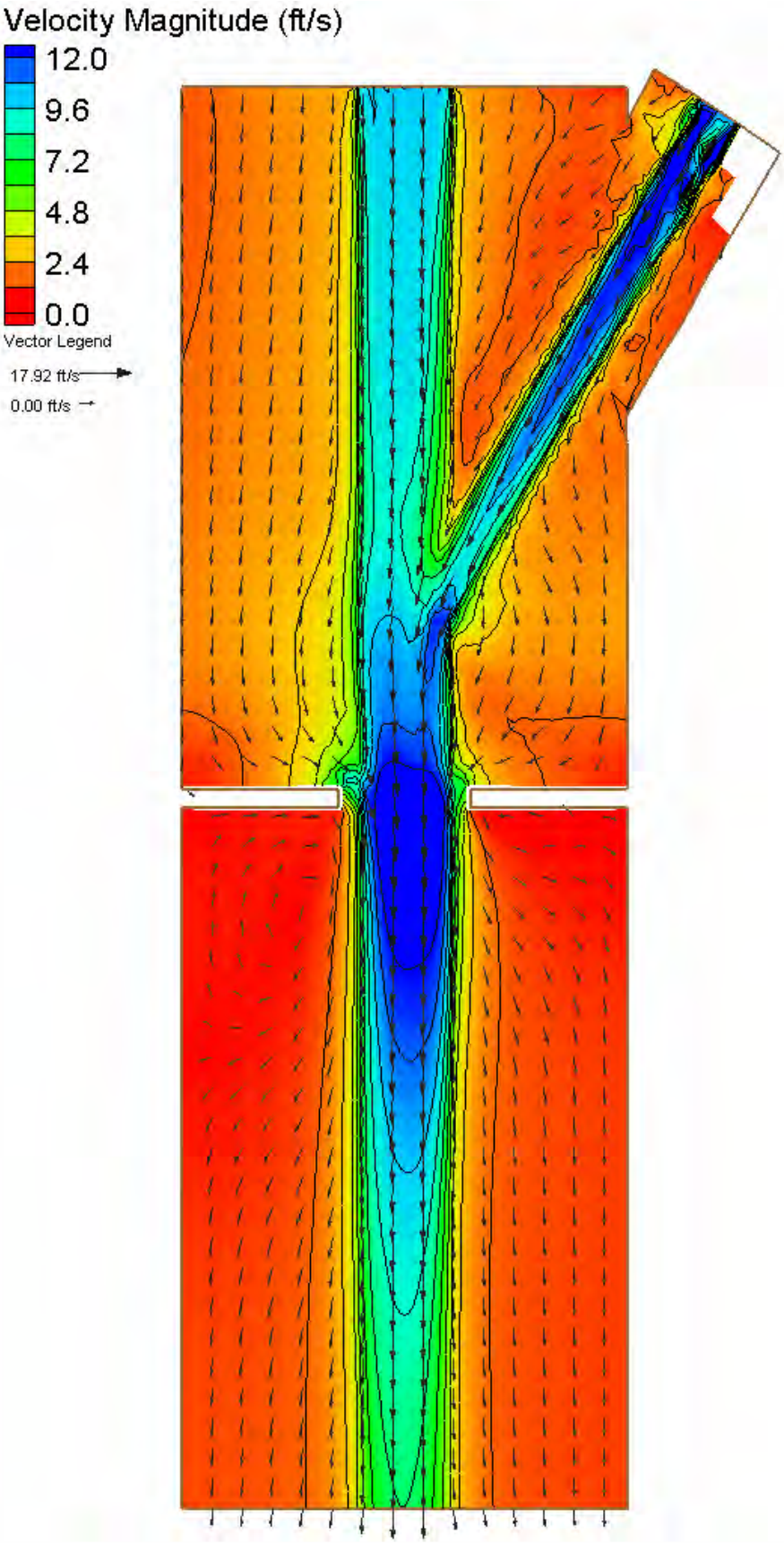

FESWMS Velocity Magnitude Contours – Large Channel – Confluences (30°, 50% flow, one bridge length upstream)

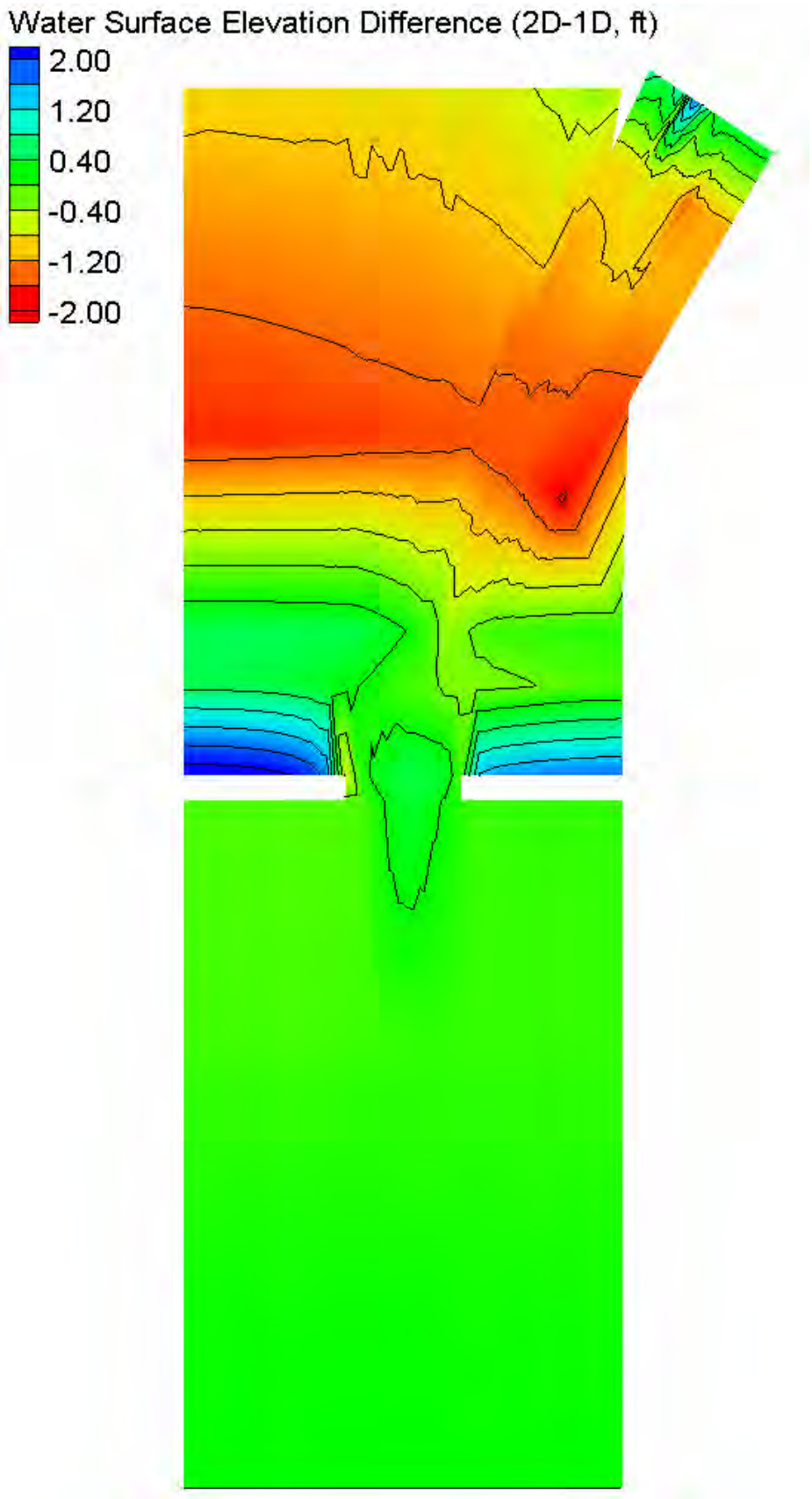

Water Surface Elevation Difference Contours – Large Channel – Confluences (30°, 50% flow, one bridge length upstream)

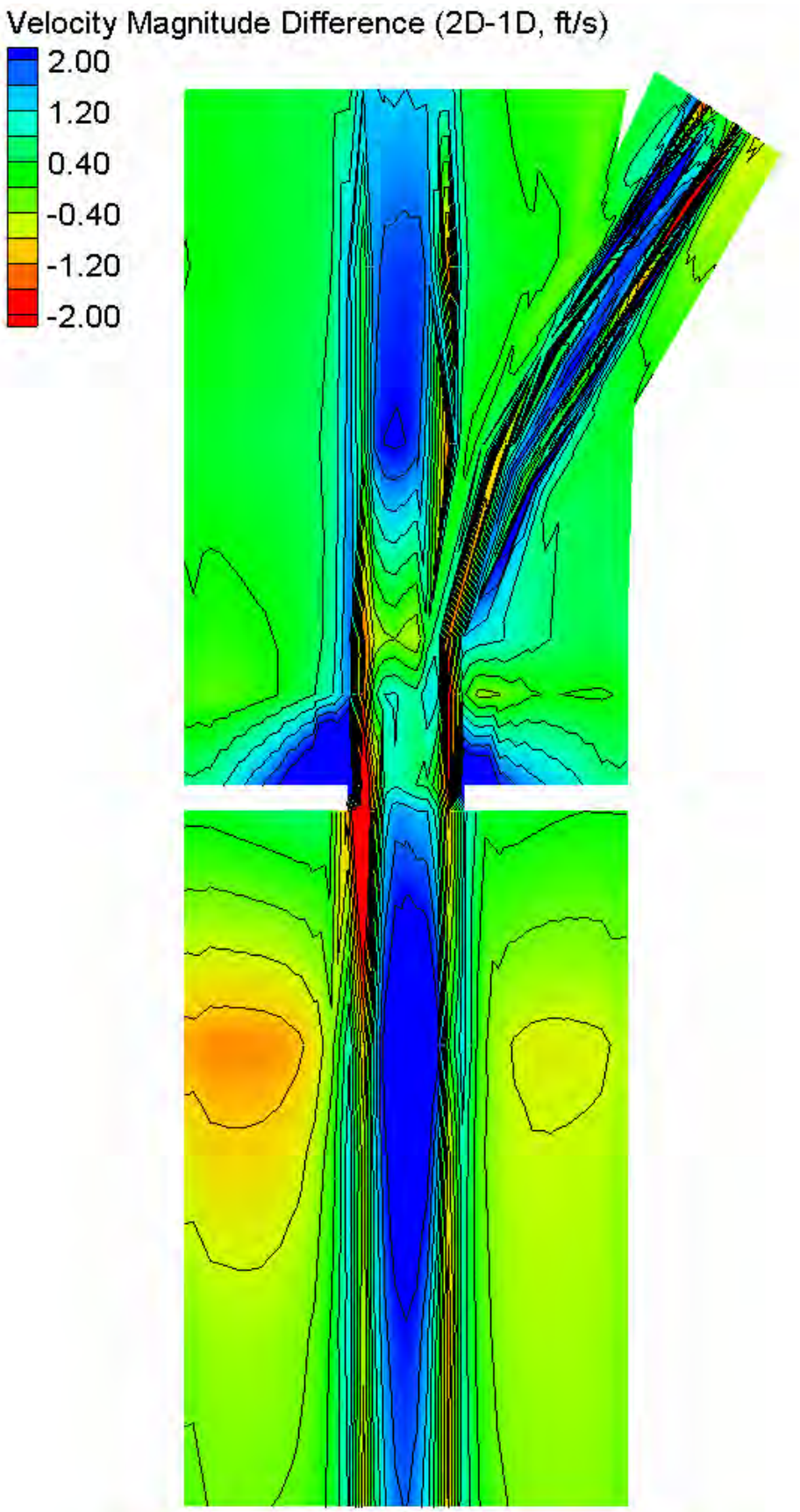

Velocity Magnitude Difference Contours – Large Channel – Confluences (30°, 50% flow, one bridge length upstream)

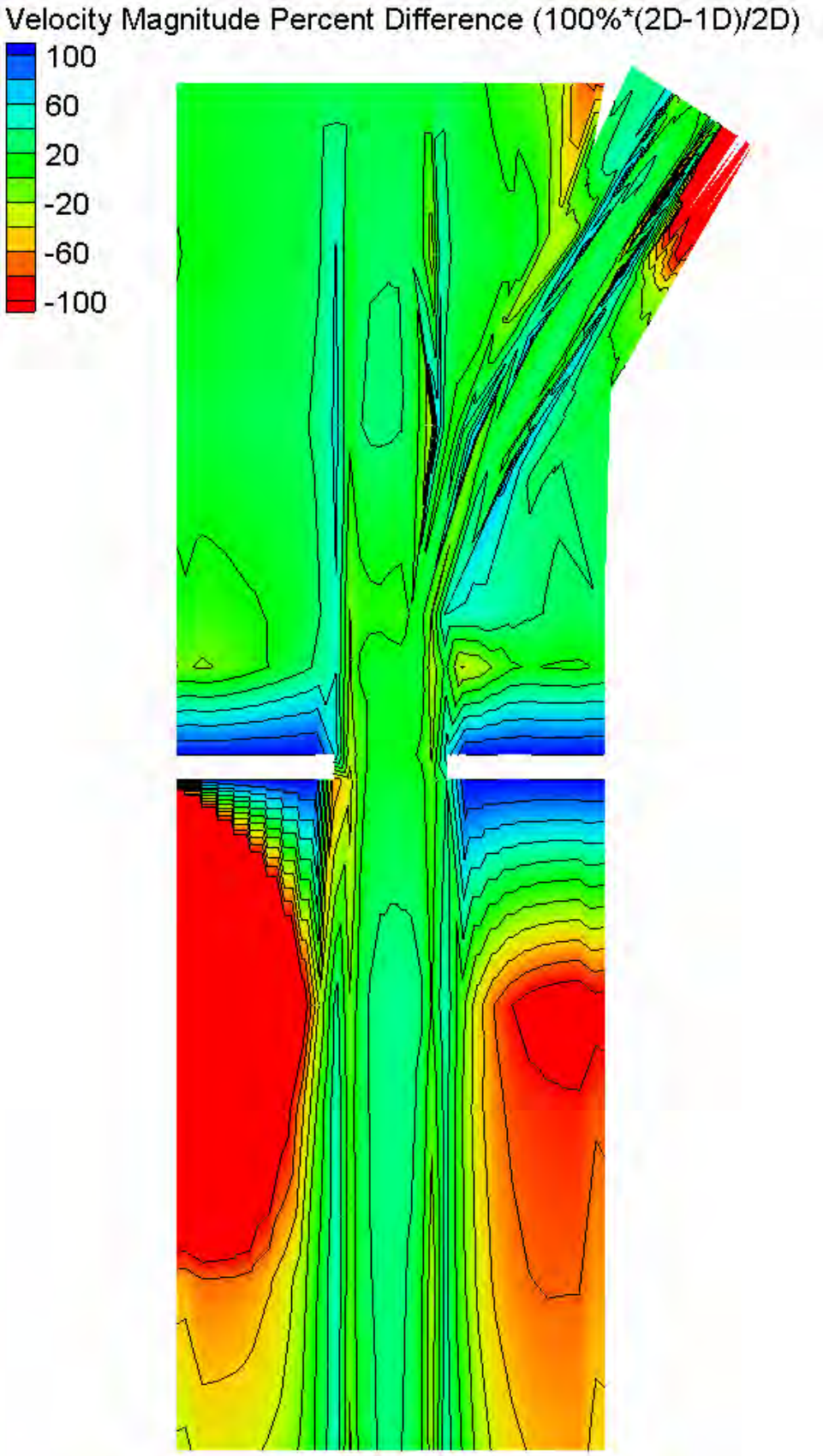

Velocity Magnitude Percent Difference Contours – Large Channel – Confluences (30°, 50% flow, one bridge length upstream)

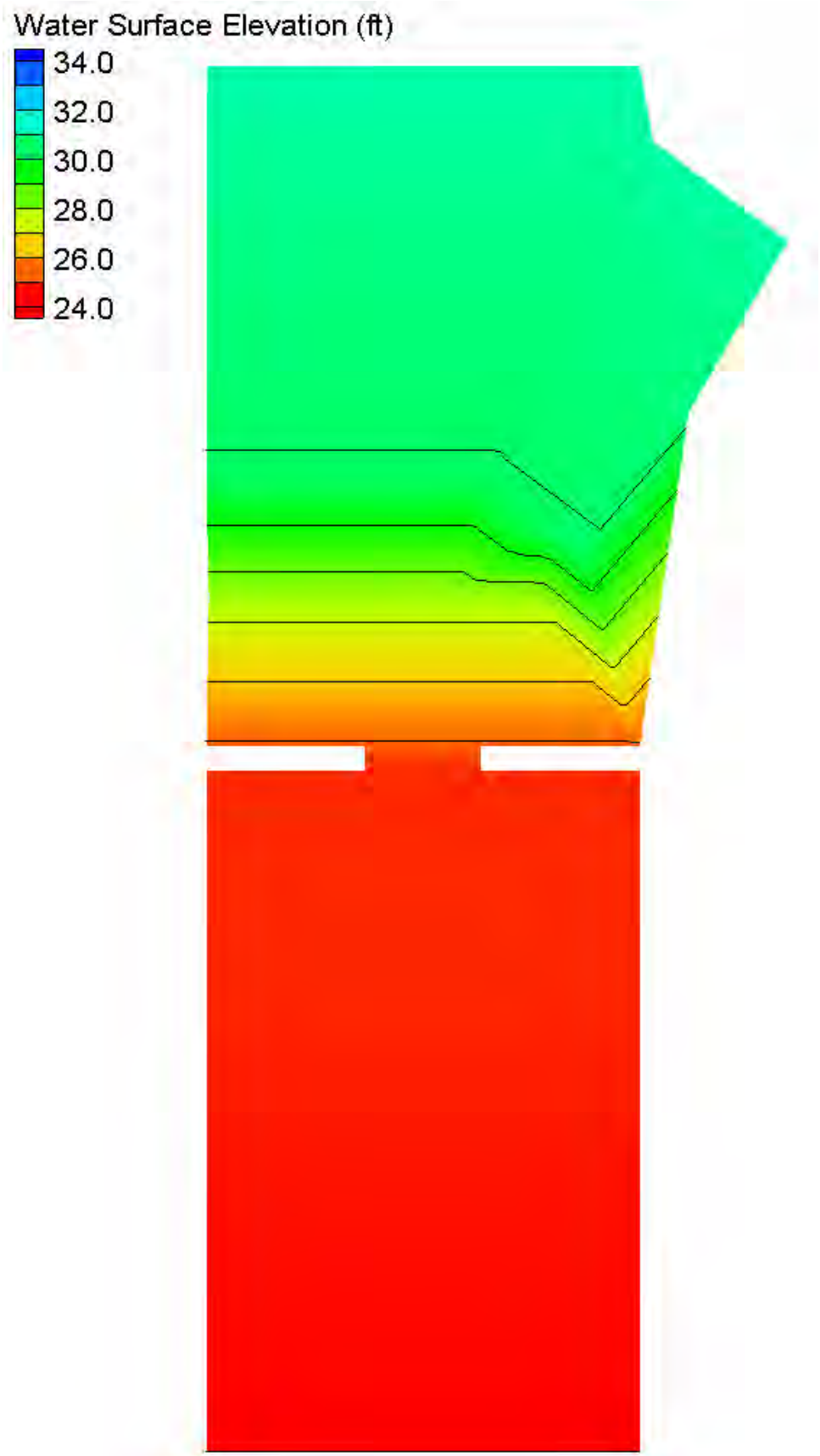

HEC-RAS Water Surface Elevation Contours – Large Channel – Confluences (30°, 50% flow, immediately upstream)

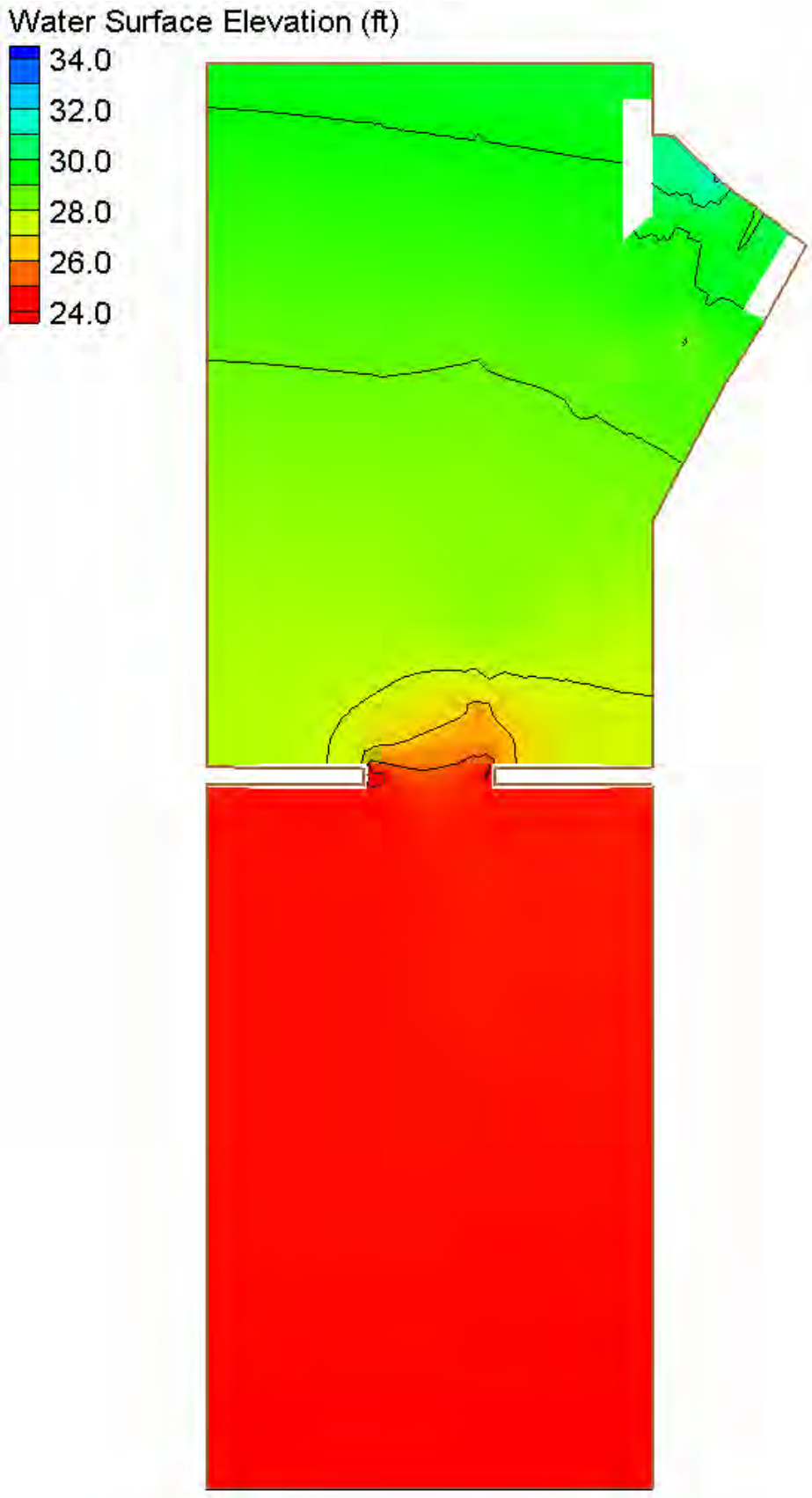

FESWMS Water Surface Elevation Contours – Large Channel – Confluences (30°, 50% flow, immediately upstream)

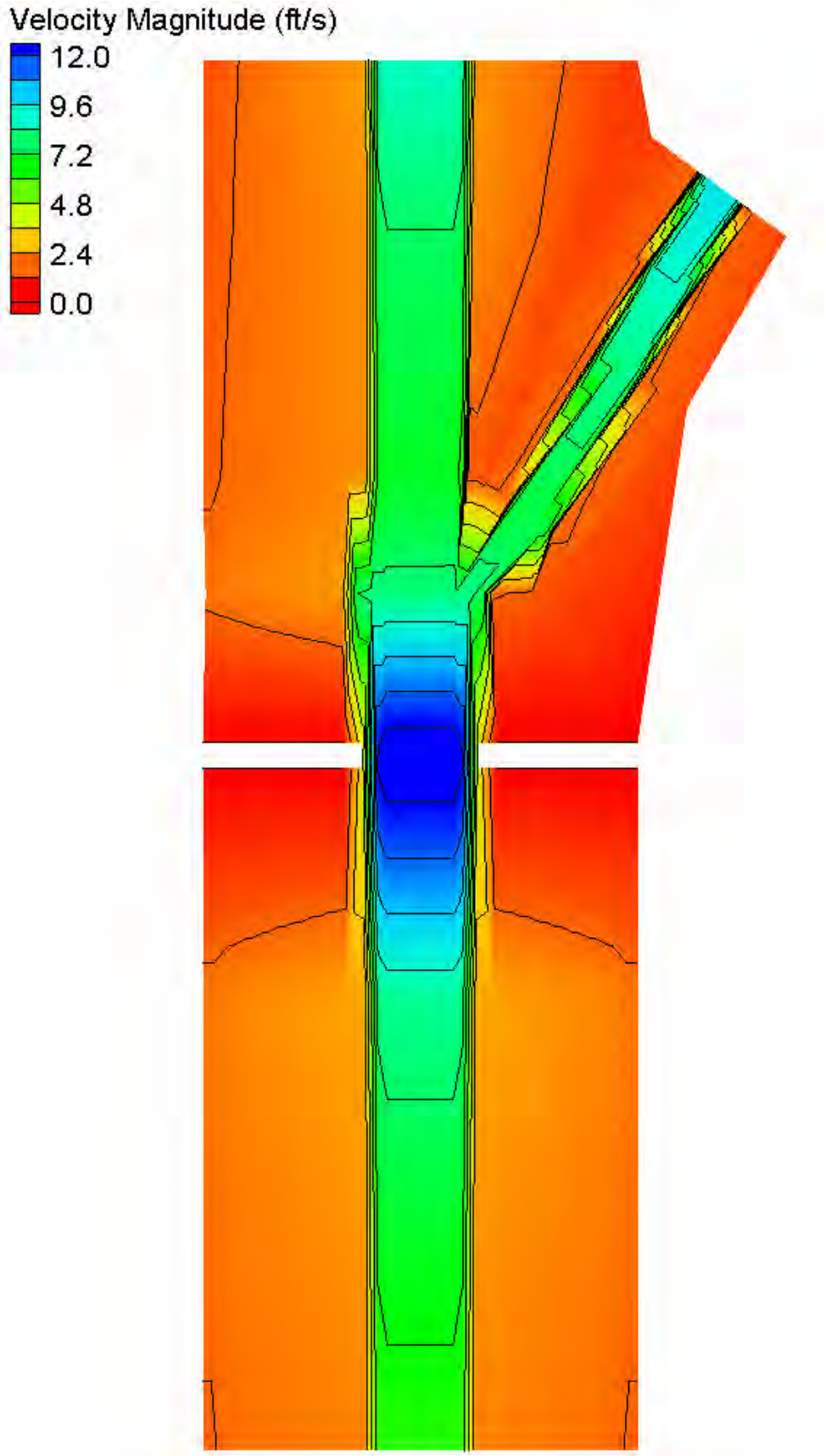

HEC-RAS Velocity Magnitude Contours – Large Channel – Confluences (30°, 50% flow, immediately upstream)

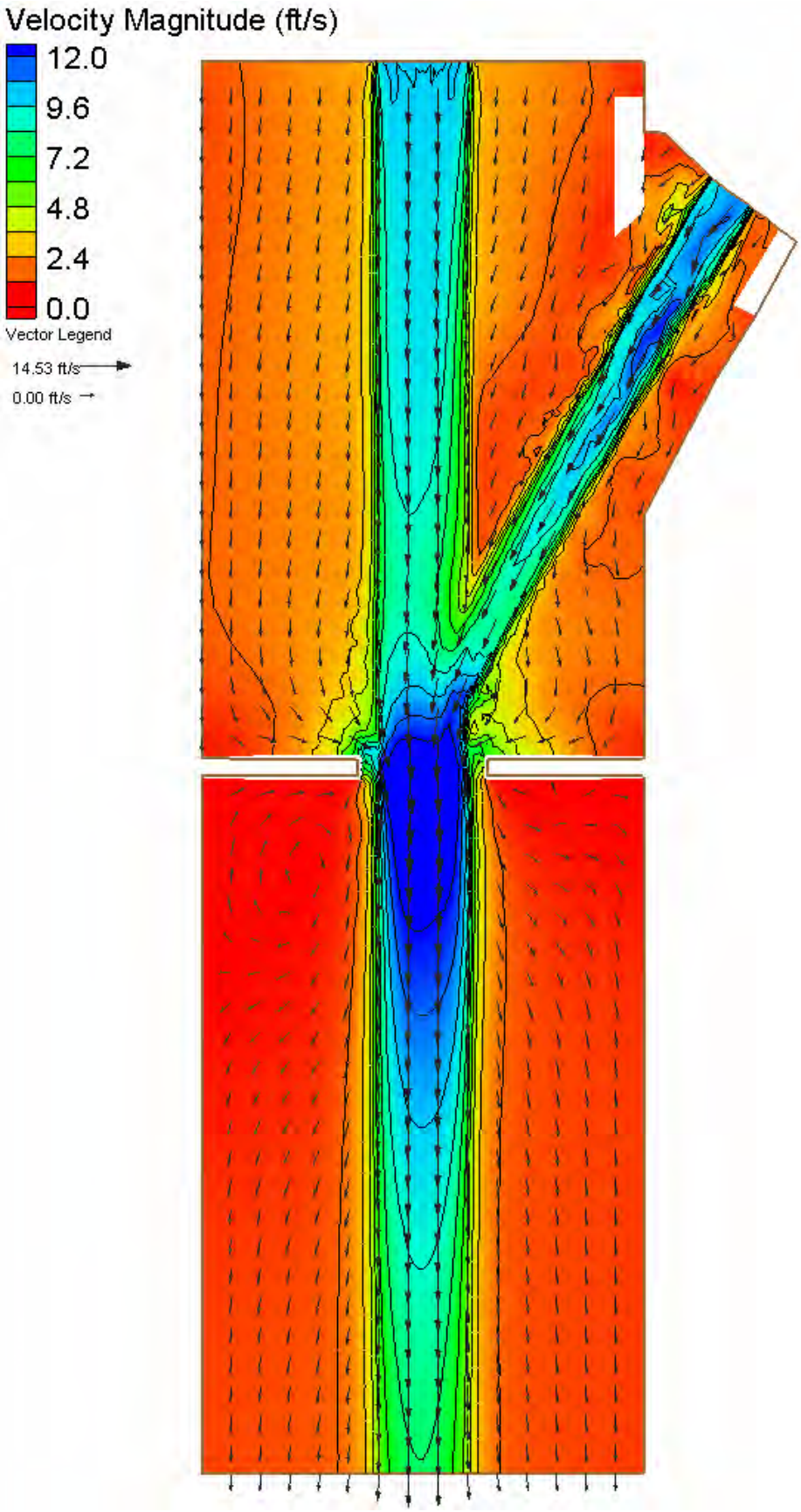

FESWMS Velocity Magnitude Contours – Large Channel – Confluences (30°, 50% flow, immediately upstream)

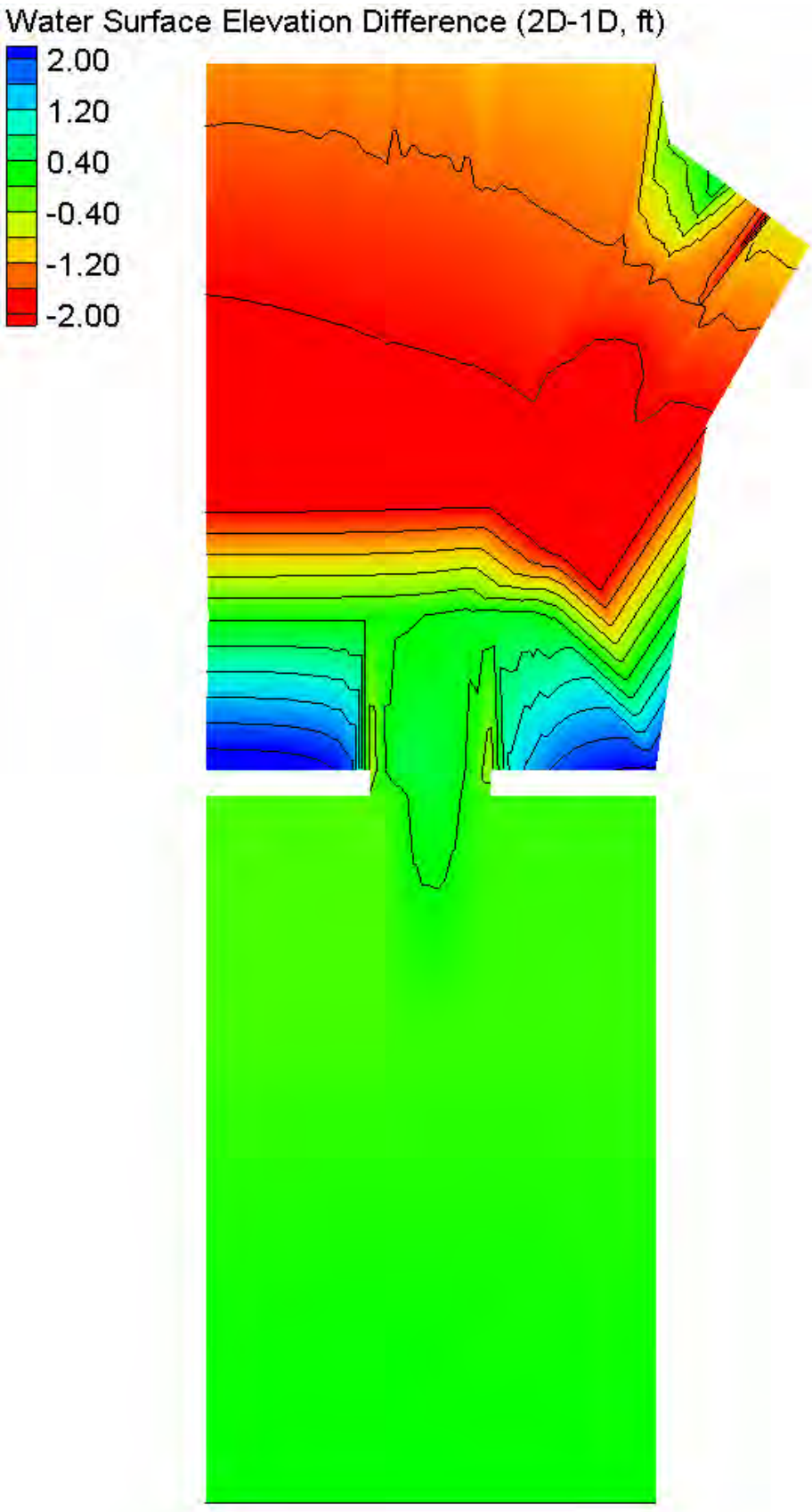

Water Surface Elevation Difference Contours – Large Channel – Confluences (30°, 50% flow, immediately upstream)

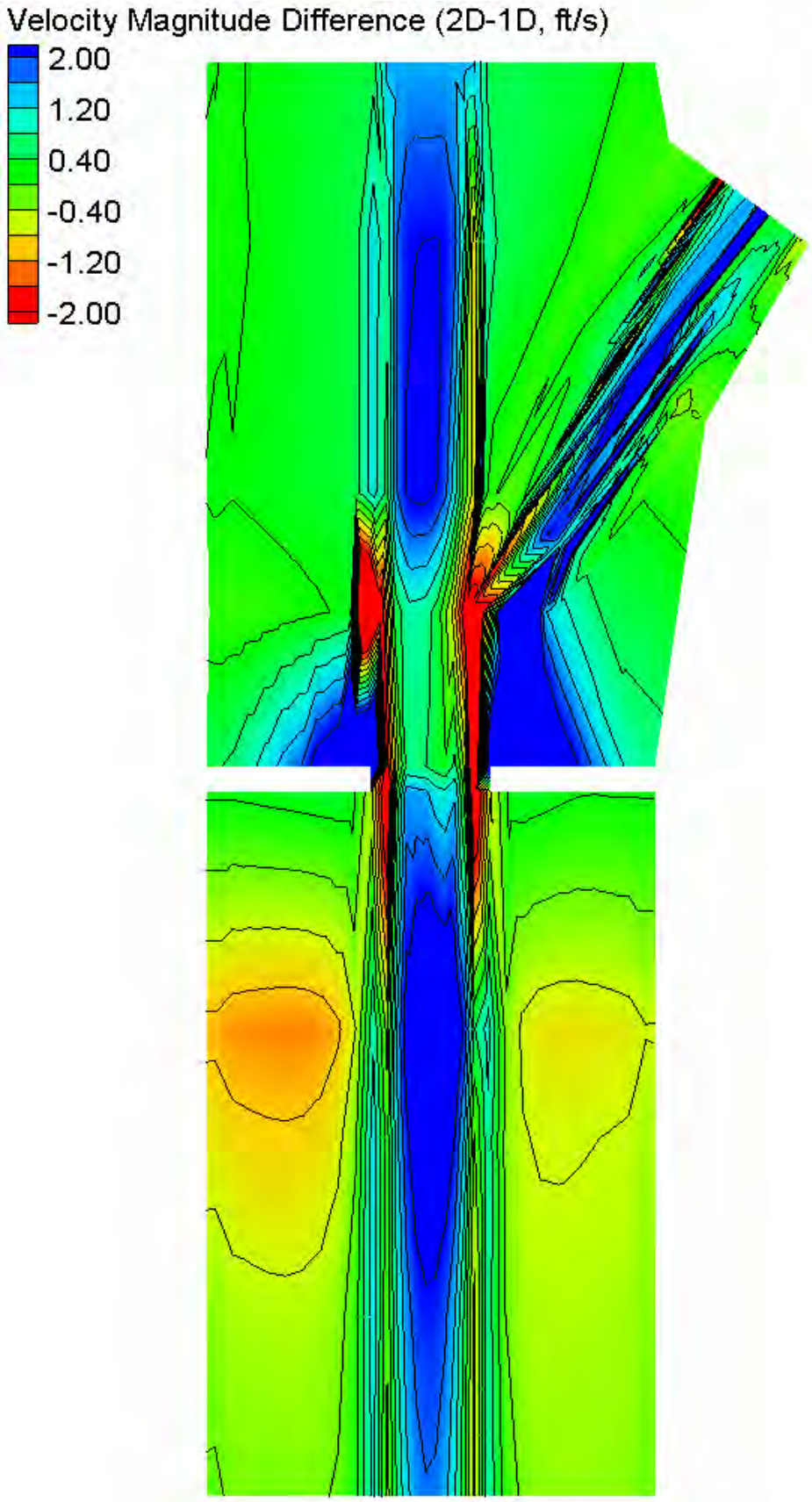

Velocity Magnitude Difference Contours – Large Channel – Confluences (30°, 50% flow, immediately upstream)

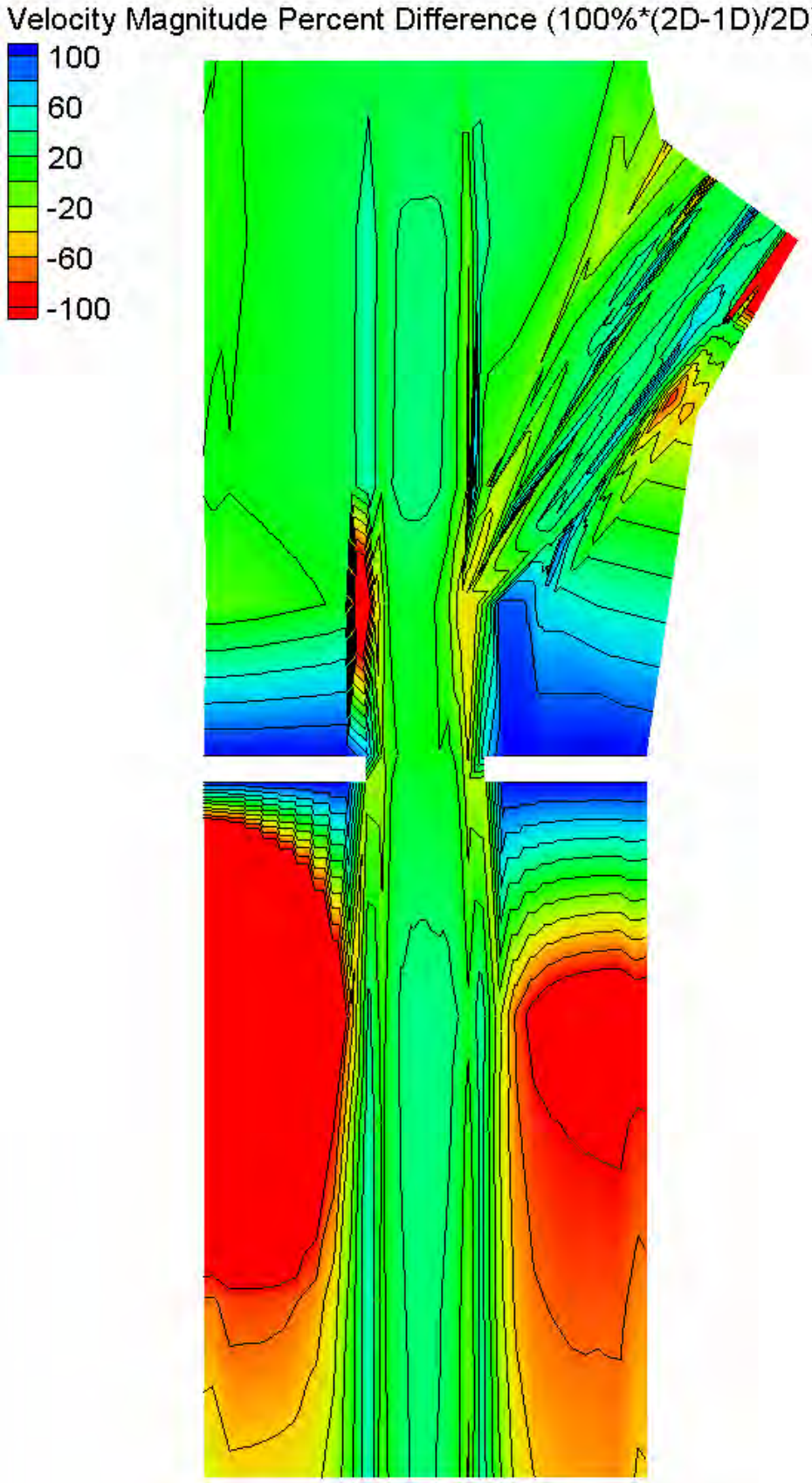

Velocity Magnitude Percent Difference Contours – Large Channel – Confluences (30°, 50% flow, immediately upstream)

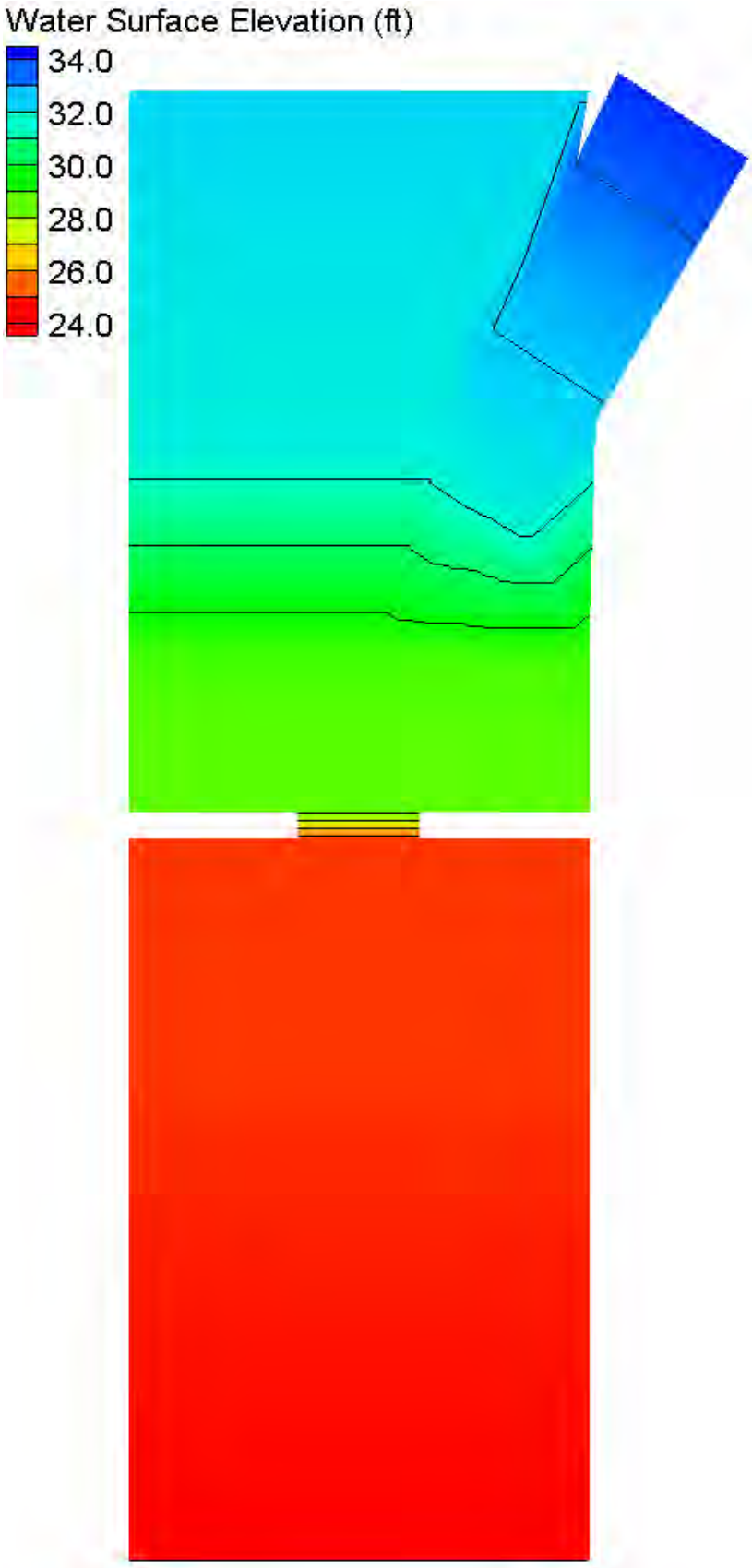

HEC-RAS Water Surface Elevation Contours – Large Channel – Confluences (30°, 75% flow, one bridge length upstream)

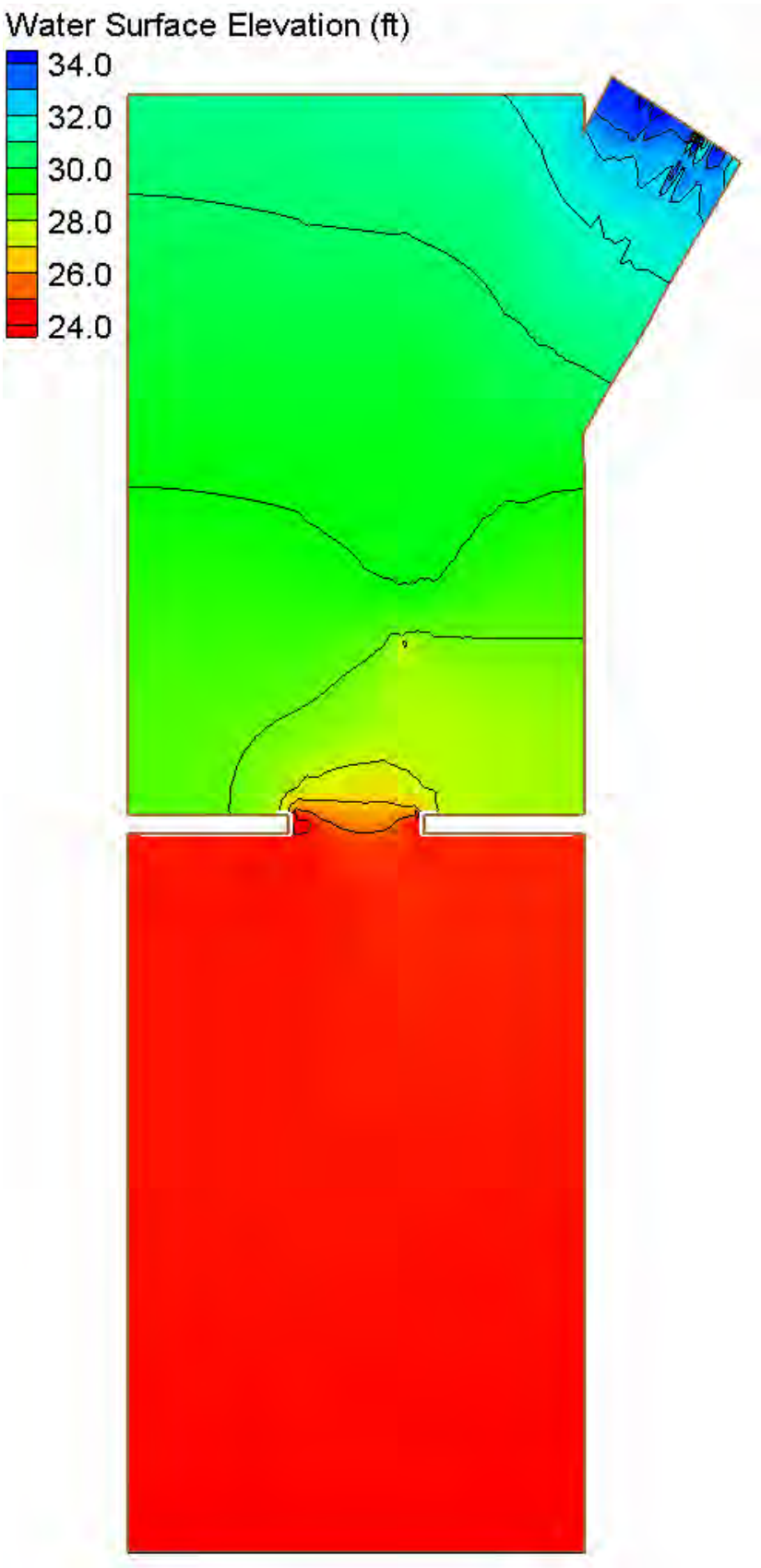

FESWMS Water Surface Elevation Contours – Large Channel – Confluences (30°, 75% flow, one bridge length upstream)

HEC-RAS Velocity Magnitude Contours – Large Channel – Confluences (30°, 75% flow, one bridge length upstream)

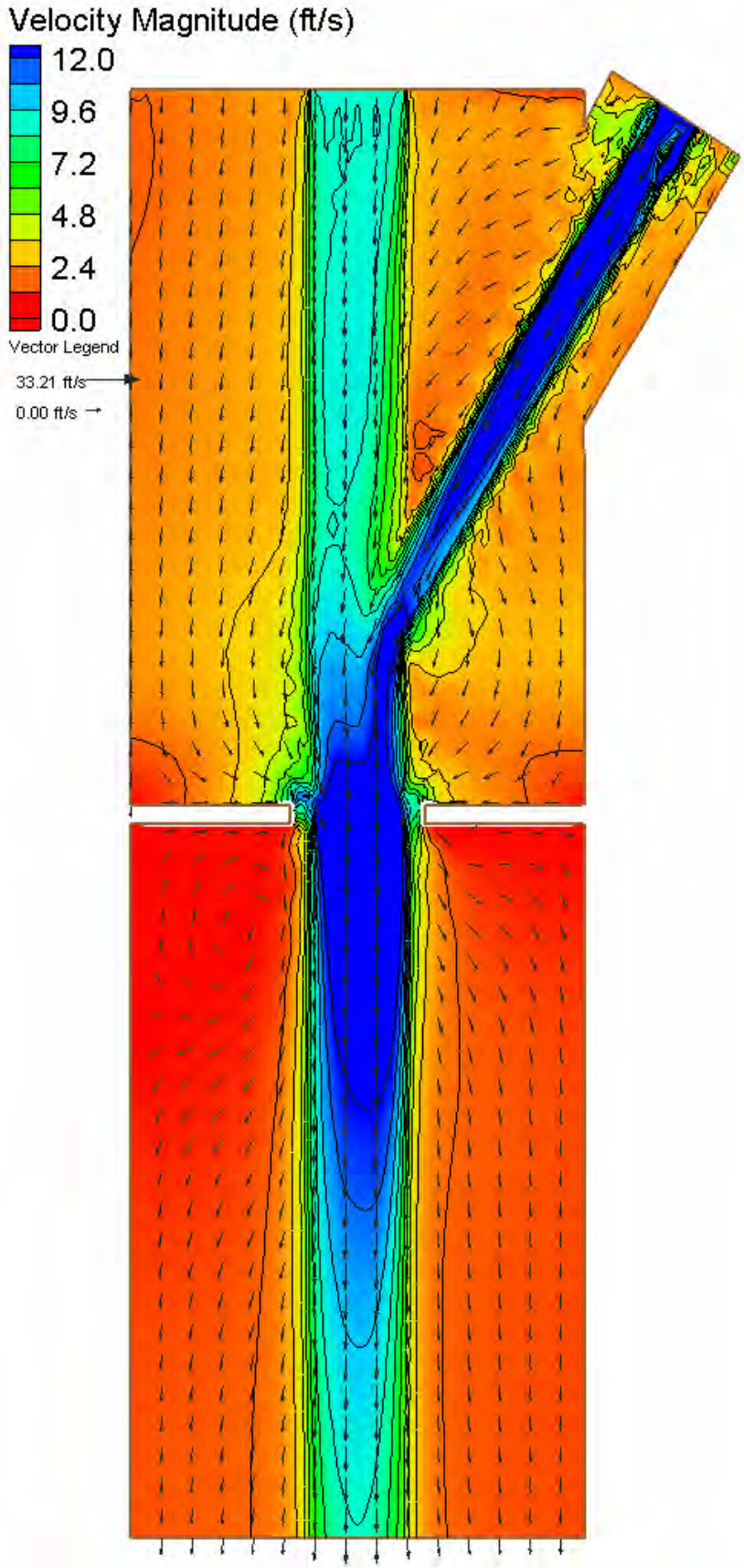

FESWMS Velocity Magnitude Contours – Large Channel – Confluences (30°, 75% flow, one bridge length upstream)

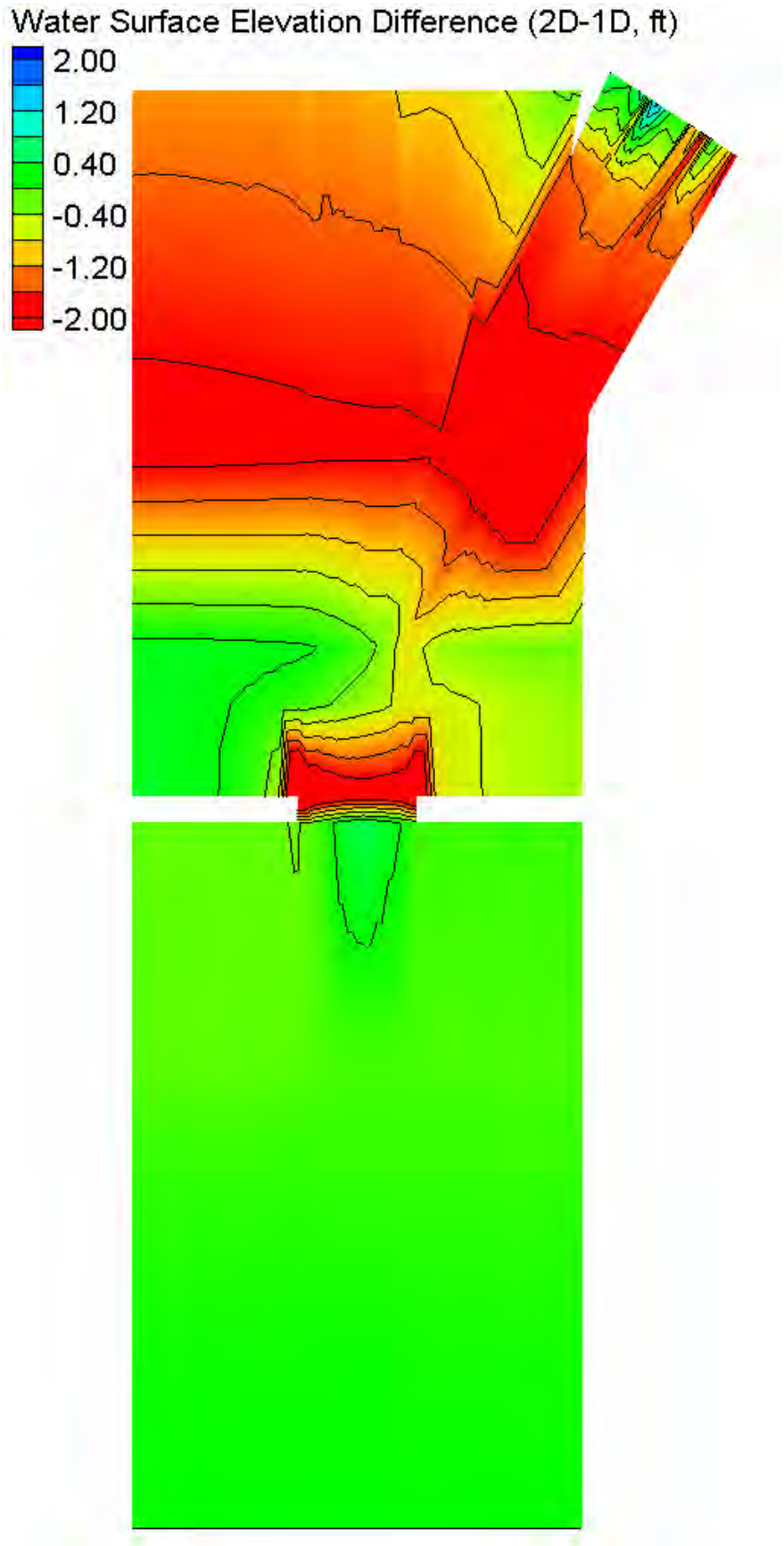

Water Surface Elevation Difference Contours – Large Channel – Confluences (30°, 75% flow, one bridge length upstream)

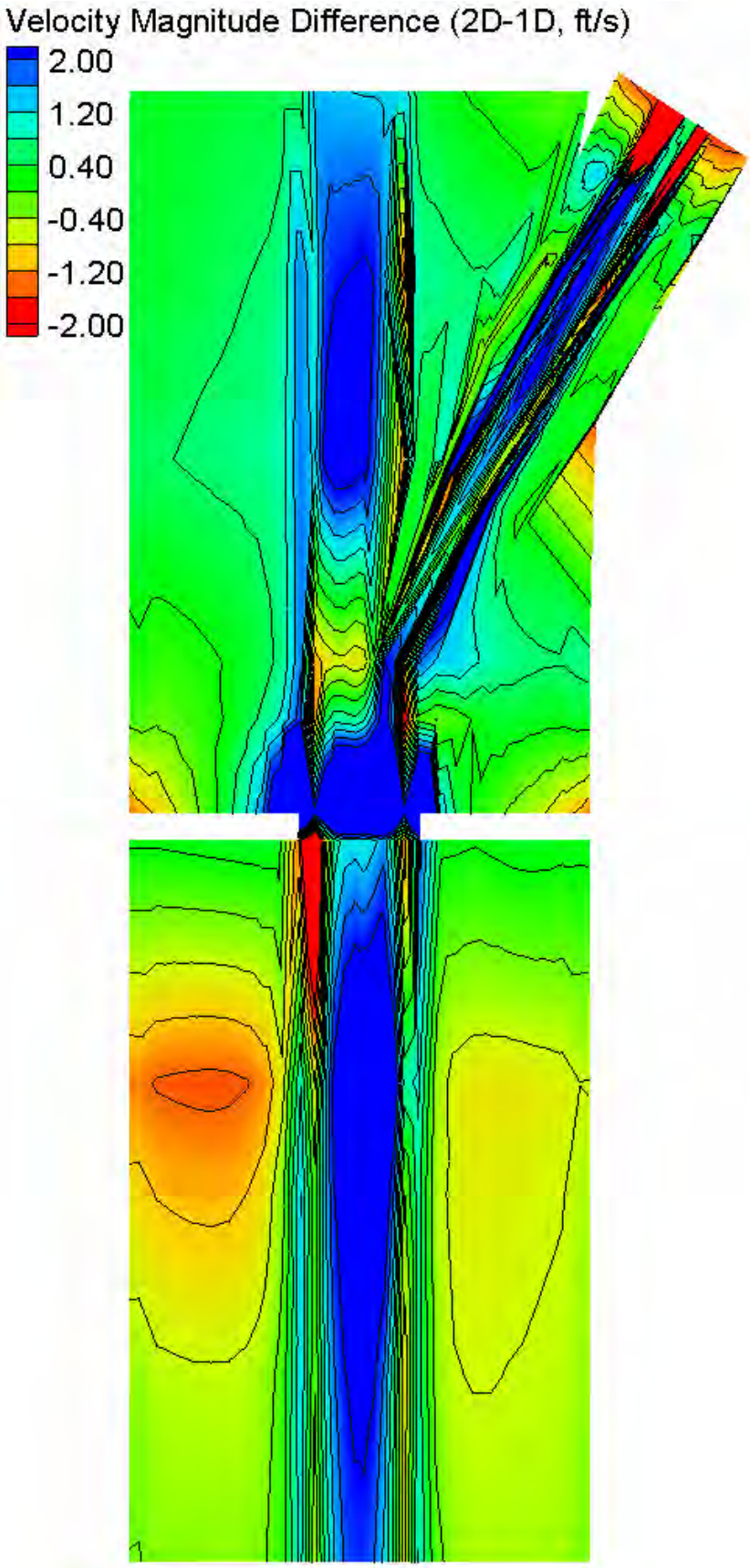

Velocity Magnitude Difference Contours – Large Channel – Confluences (30°, 75% flow, one bridge length upstream)

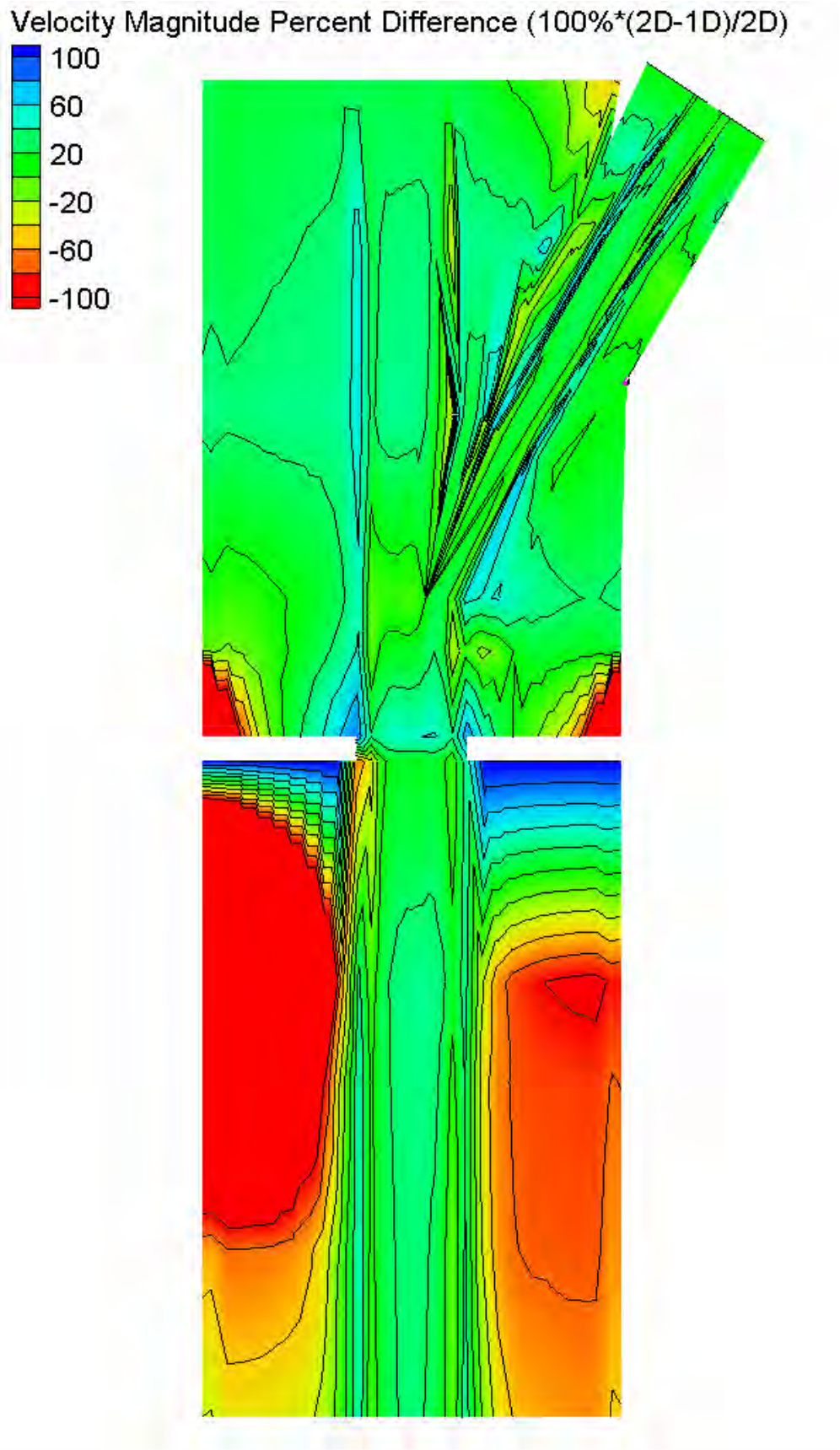

Velocity Magnitude Percent Difference Contours – Large Channel – Confluences (30°, 75% flow, one bridge length upstream)

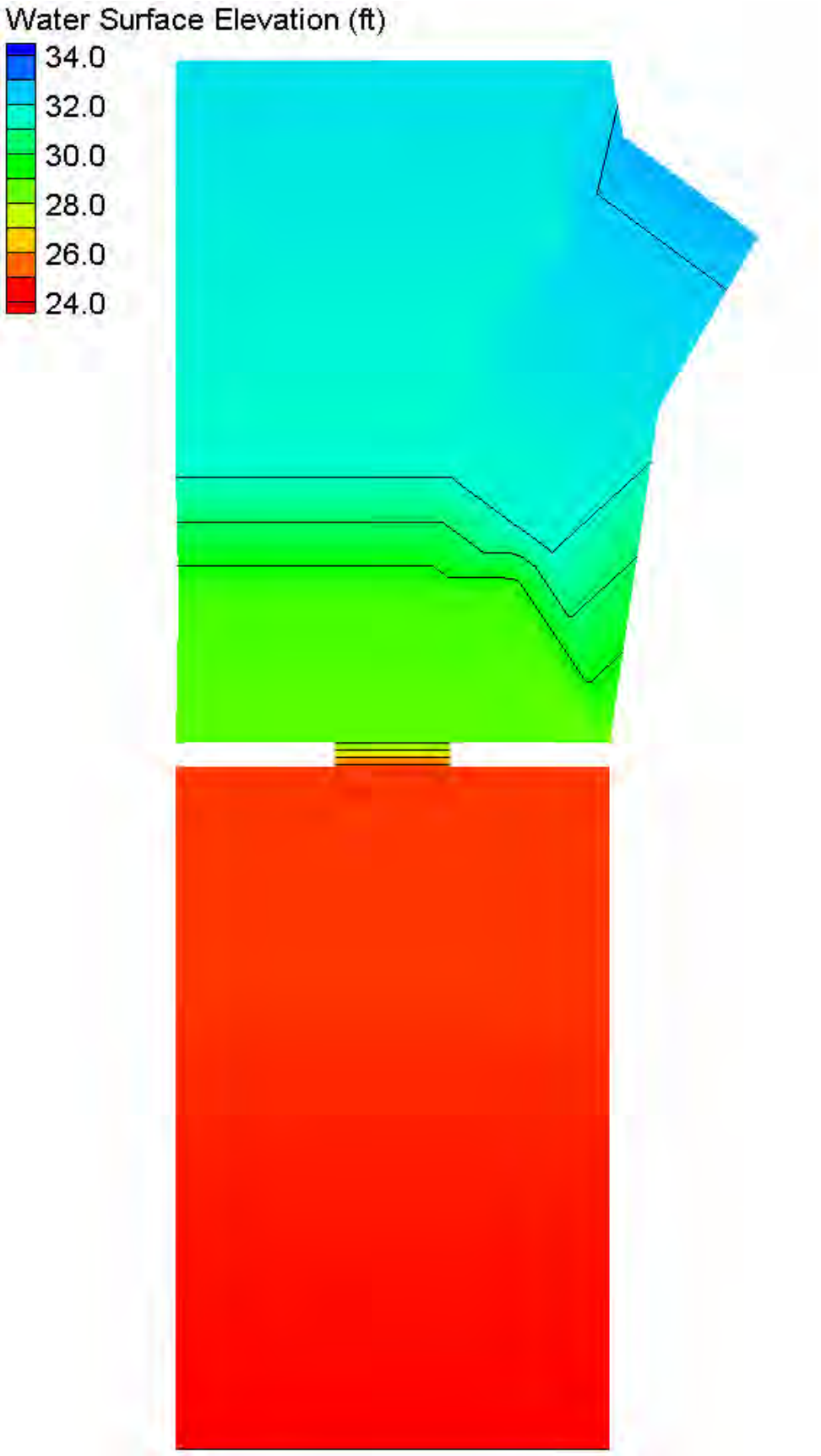

HEC-RAS Water Surface Elevation Contours – Large Channel – Confluences (30°, 75% flow, immediately upstream)

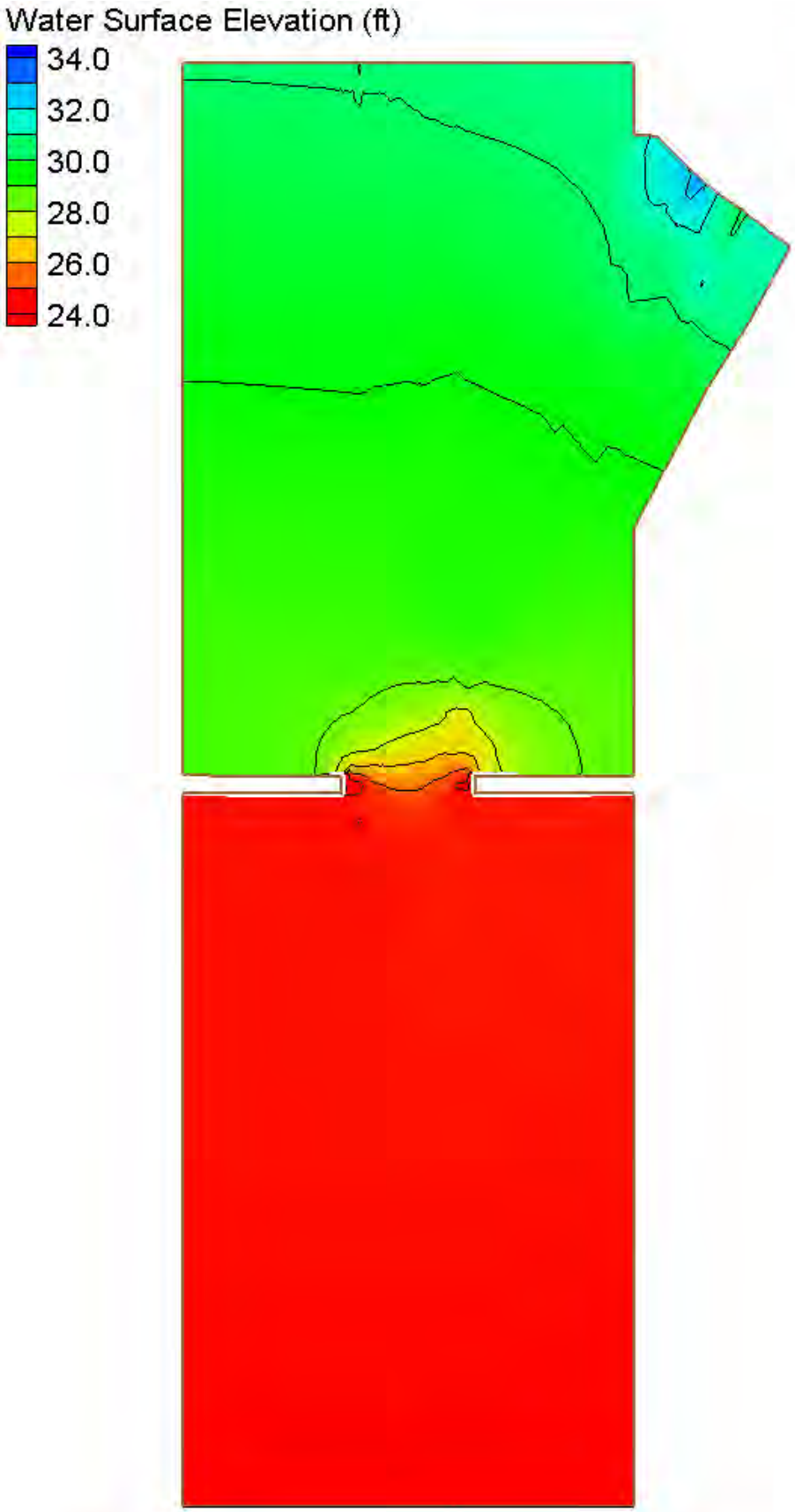

FESWMS Water Surface Elevation Contours – Large Channel – Confluences (30°, 75% flow, immediately upstream)

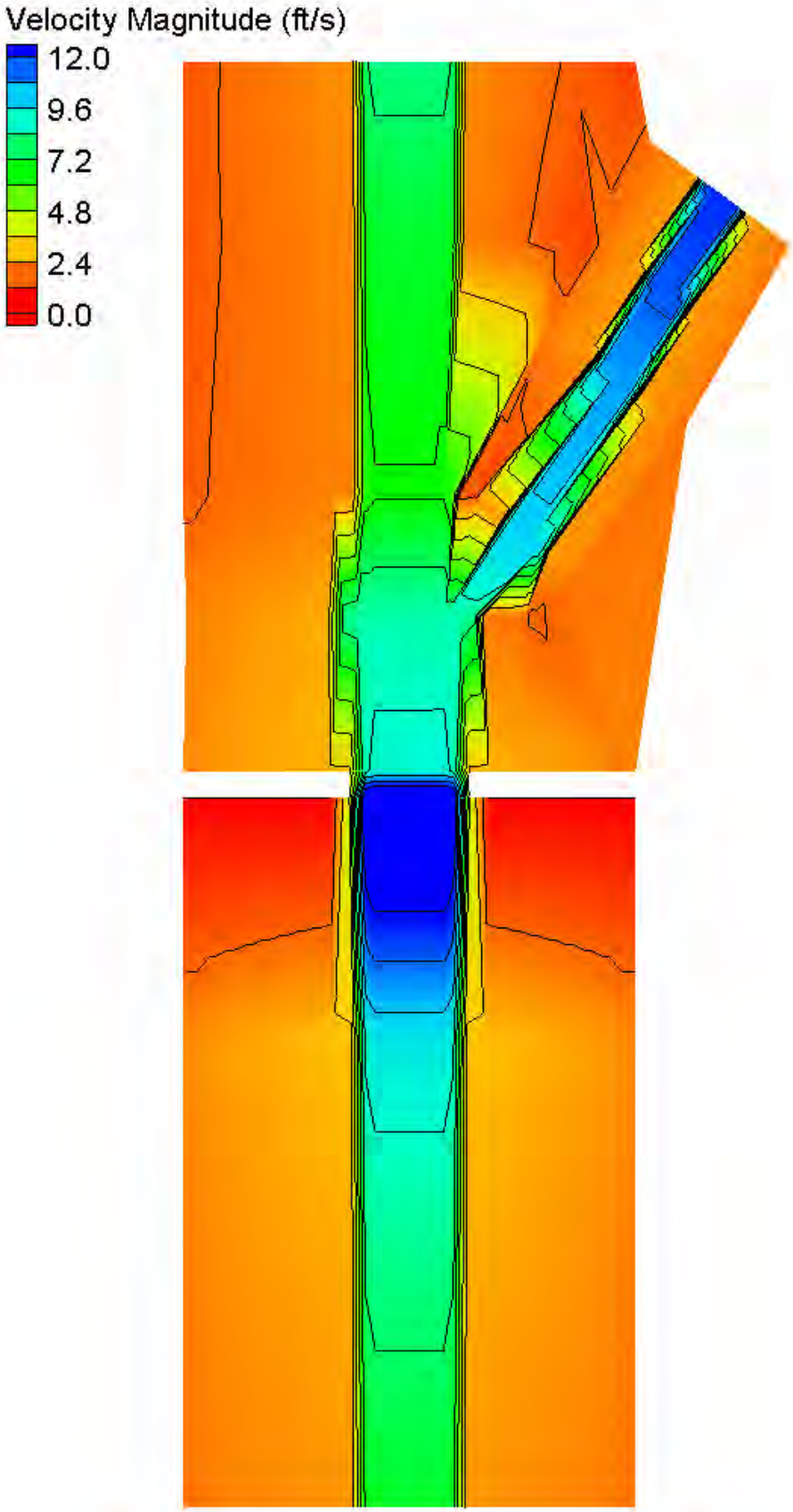

HEC-RAS Velocity Magnitude Contours – Large Channel – Confluences (30°, 75% flow, immediately upstream)

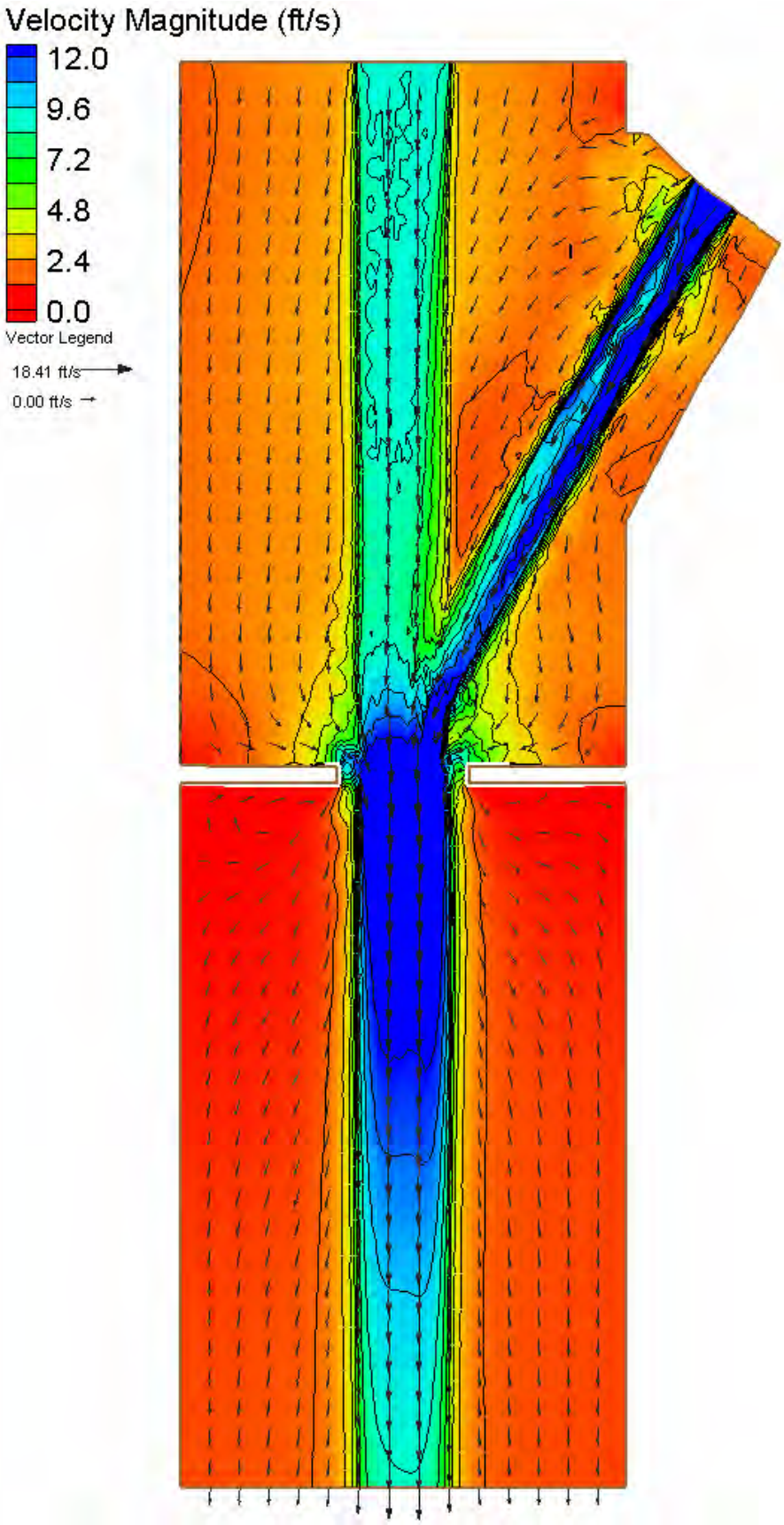

FESWMS Velocity Magnitude Contours – Large Channel – Confluences (30°, 75% flow, immediately upstream)

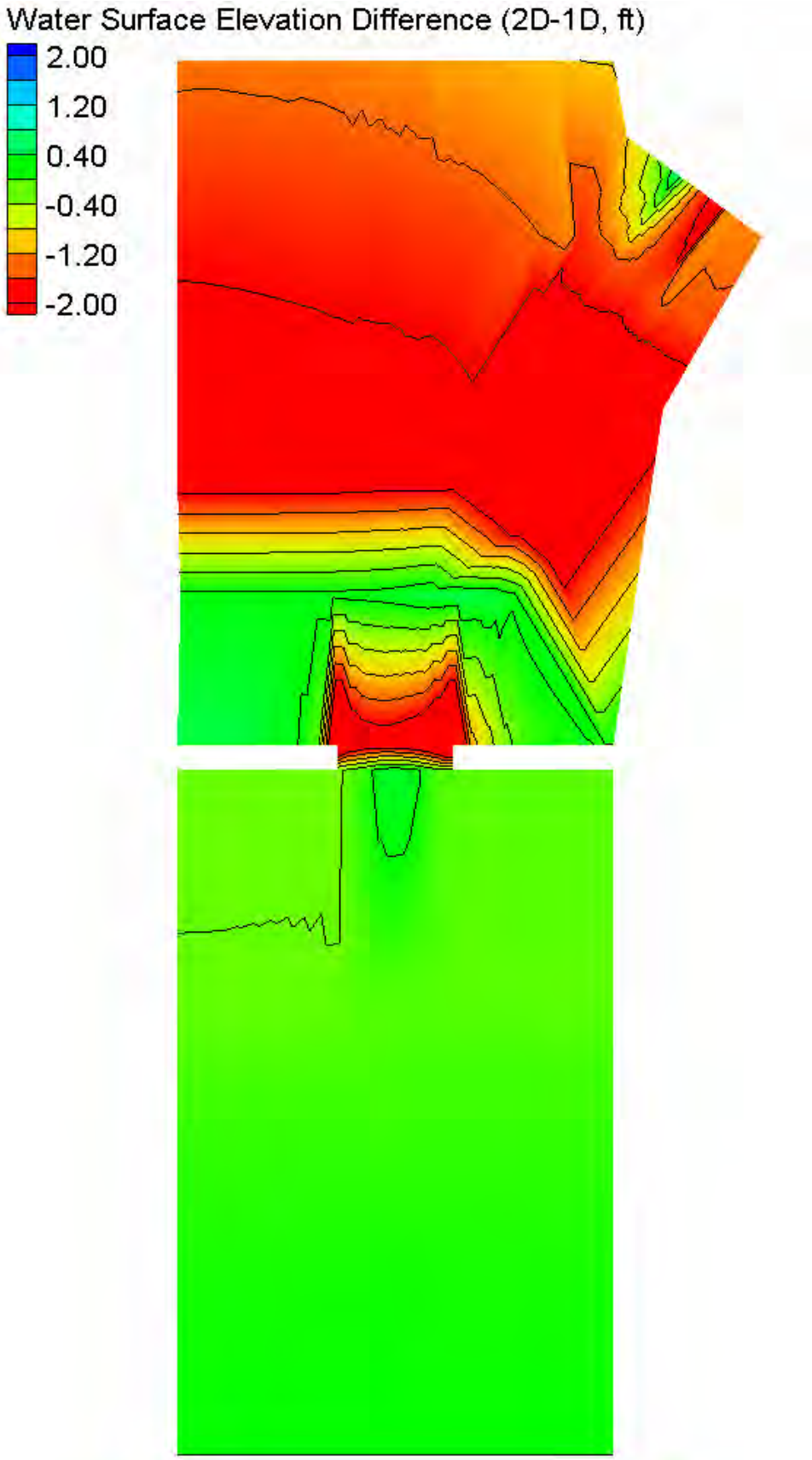

Water Surface Elevation Difference Contours – Large Channel – Confluences (30°, 75% flow, immediately upstream)

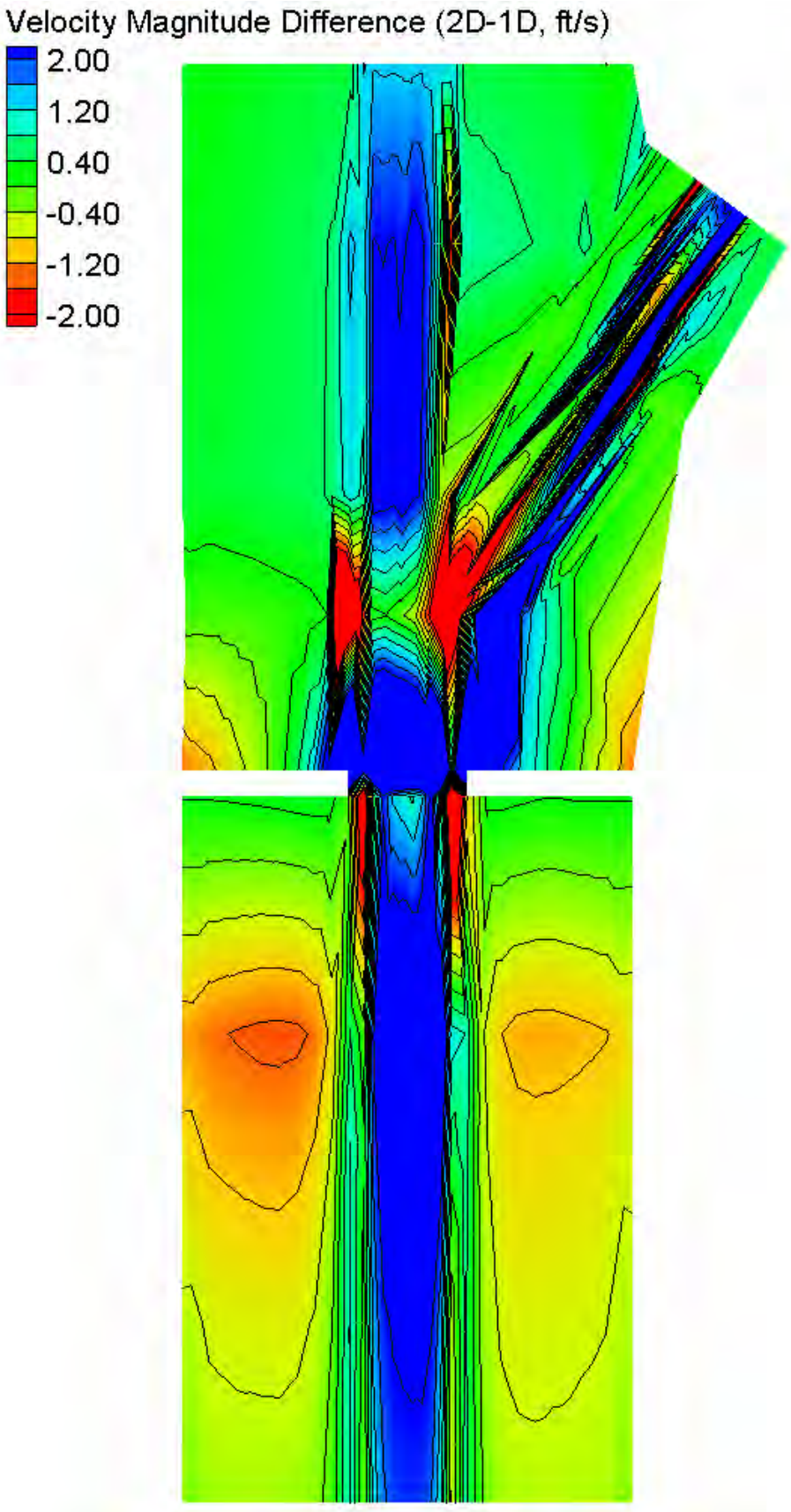

Velocity Magnitude Difference Contours – Large Channel – Confluences (30°, 75% flow, immediately upstream)

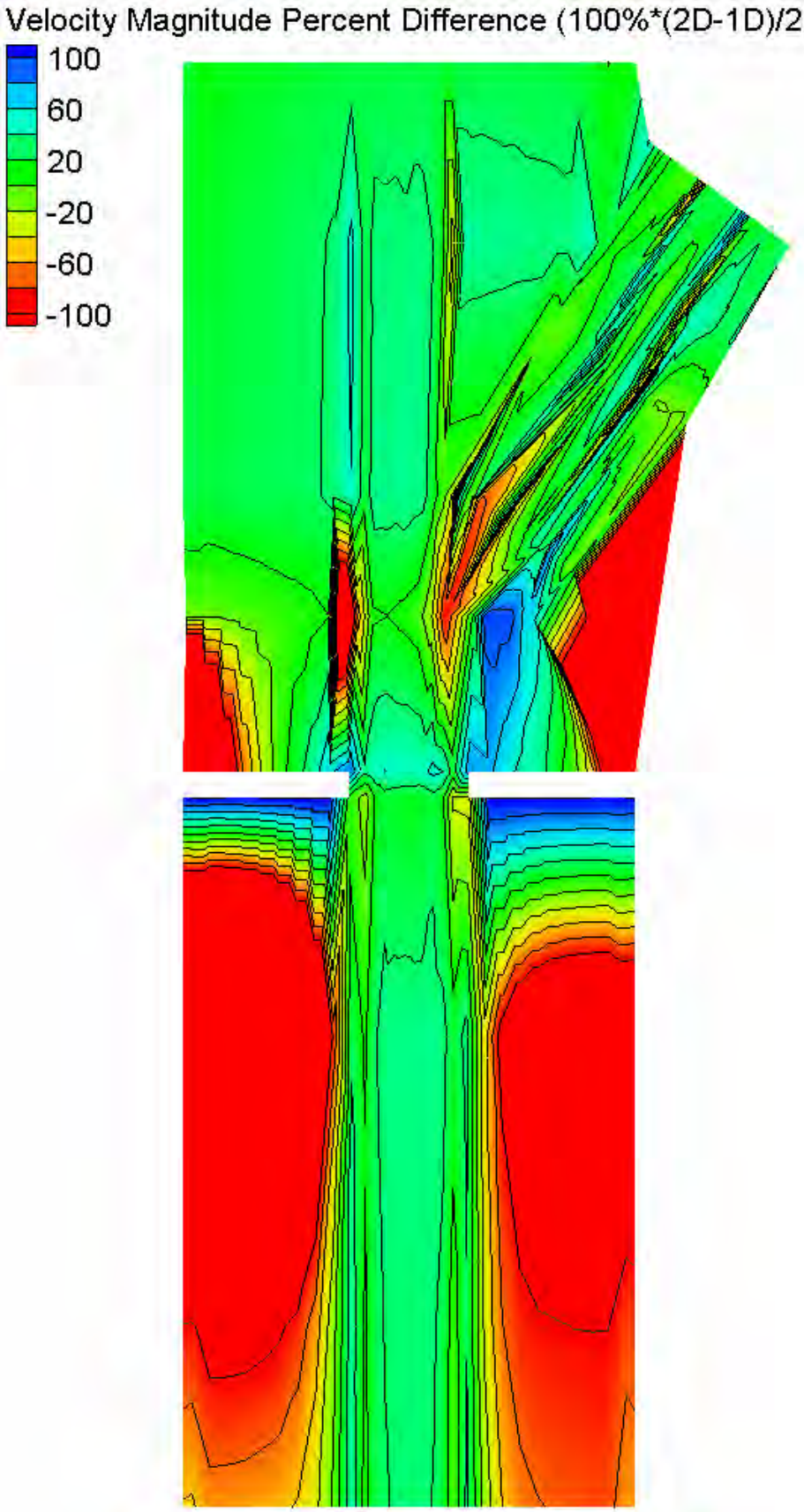

Velocity Magnitude Percent Difference Contours – Large Channel – Confluences (30°, 75% flow, immediately upstream)

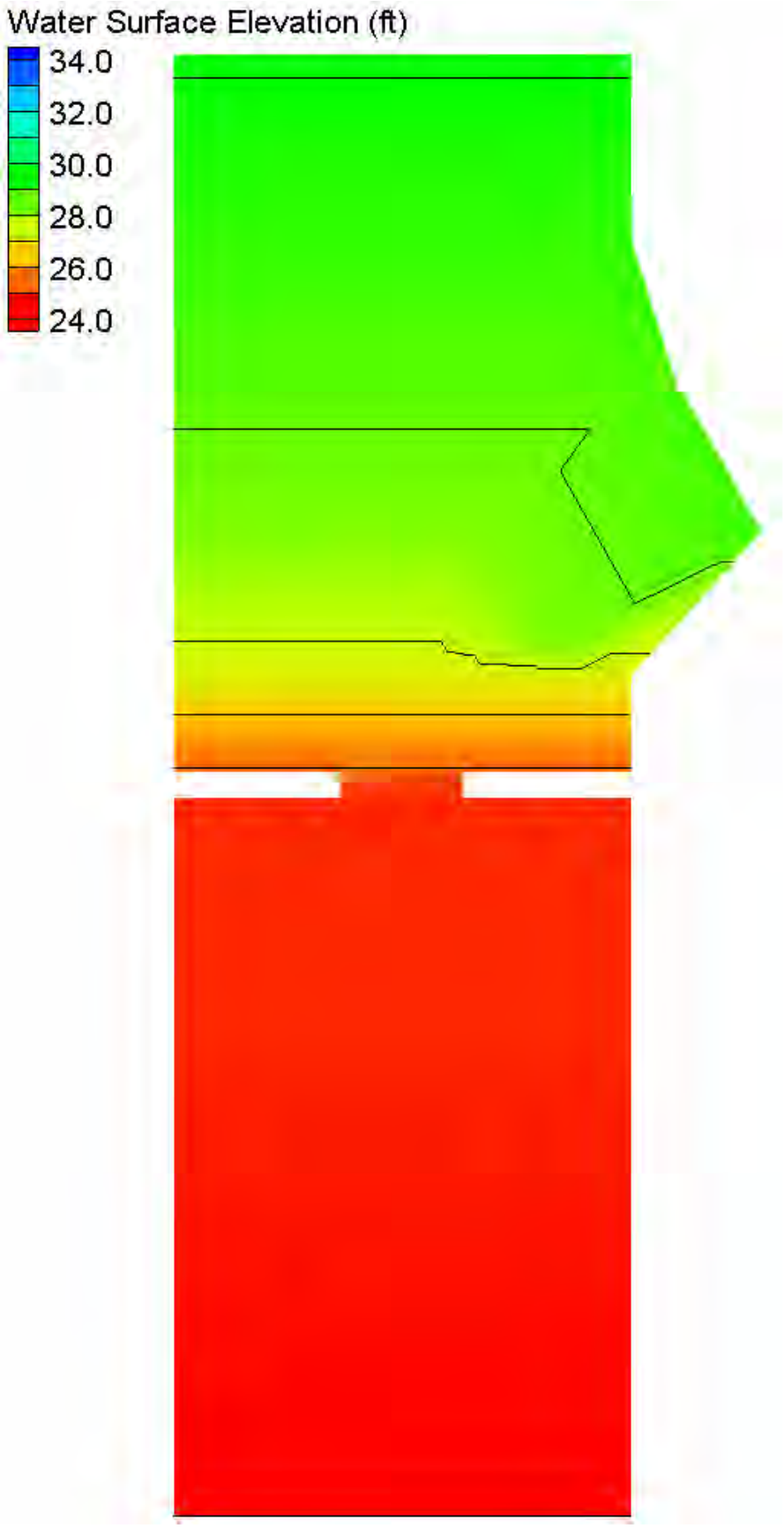

HEC-RAS Water Surface Elevation Contours – Large Channel – Confluences (60°, 50% flow, one bridge length upstream)

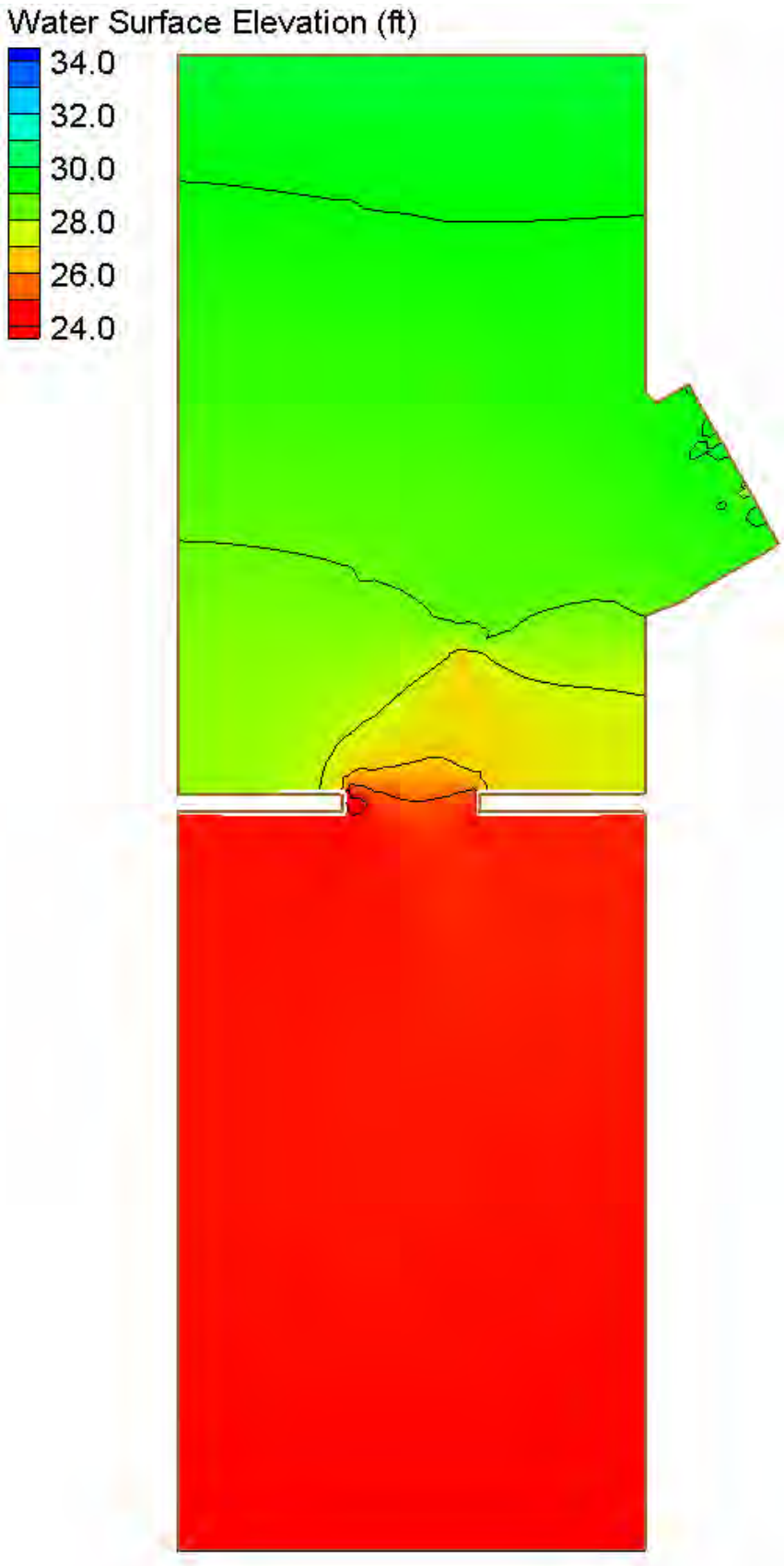

FESWMS Water Surface Elevation Contours – Large Channel – Confluences (60°, 50% flow, one bridge length upstream)

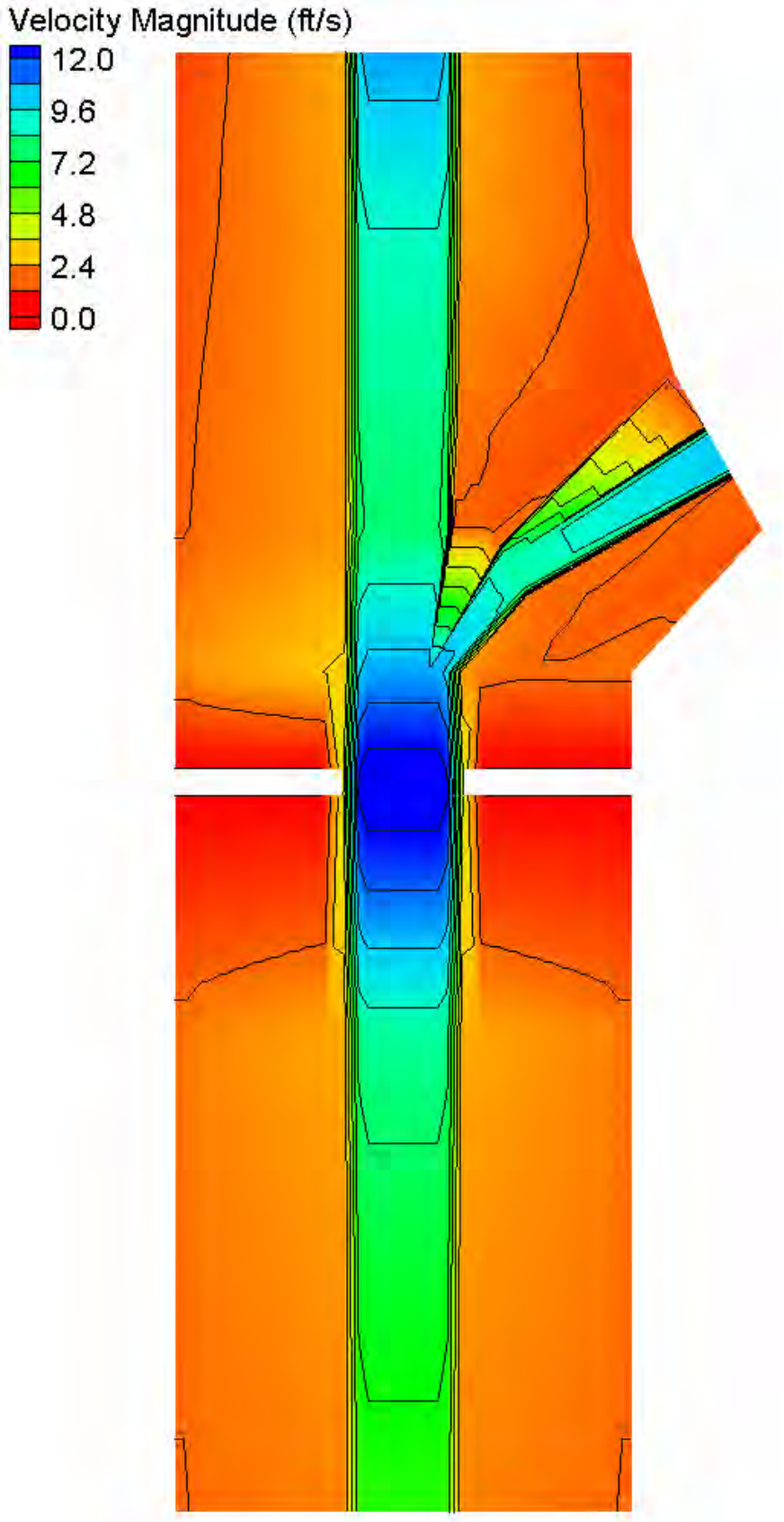

HEC-RAS Velocity Magnitude Contours – Large Channel – Confluences (60°, 50% flow, one bridge length upstream)

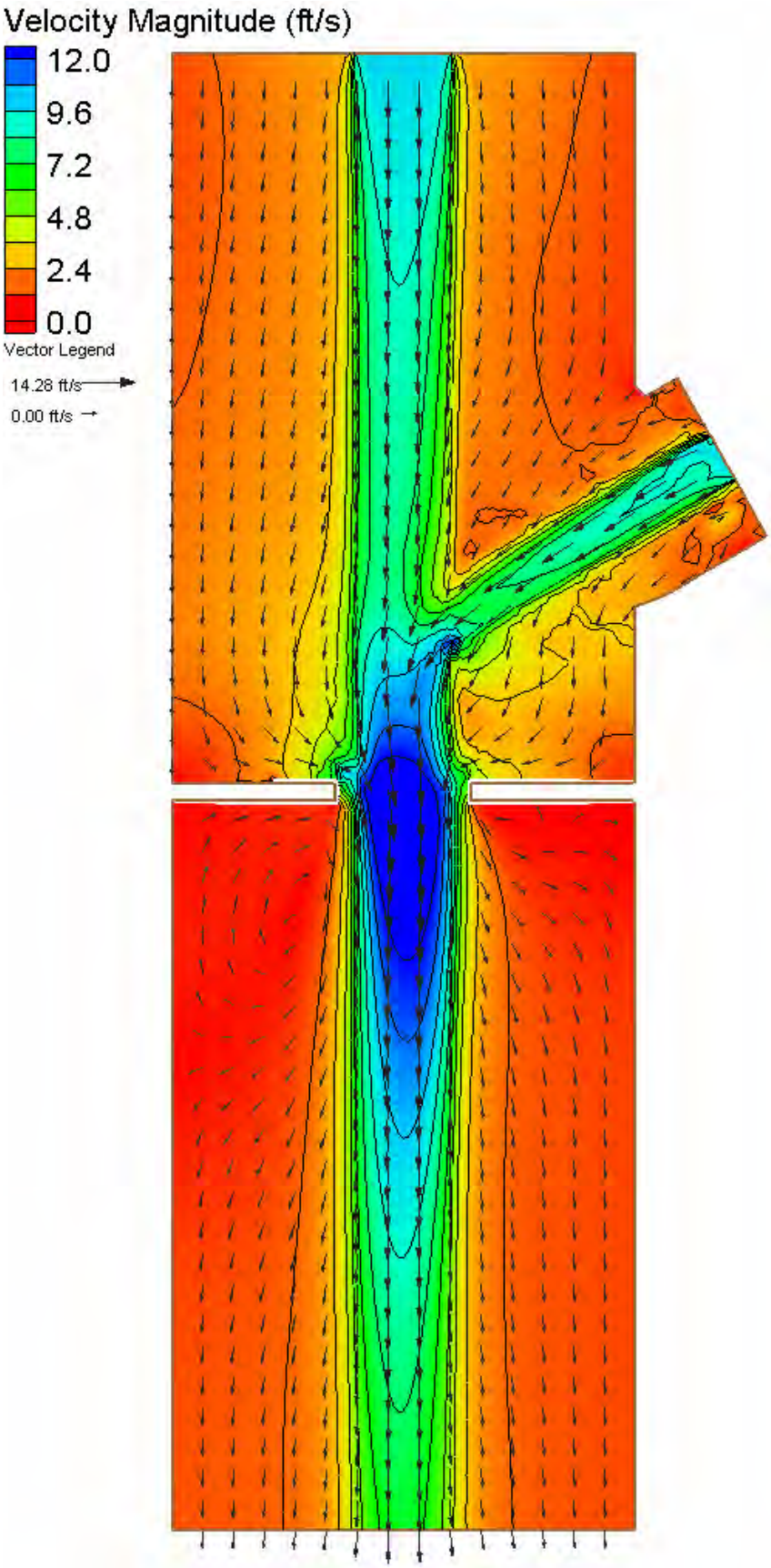

FESWMS Velocity Magnitude Contours – Large Channel – Confluences (60°, 50% flow, one bridge length upstream)

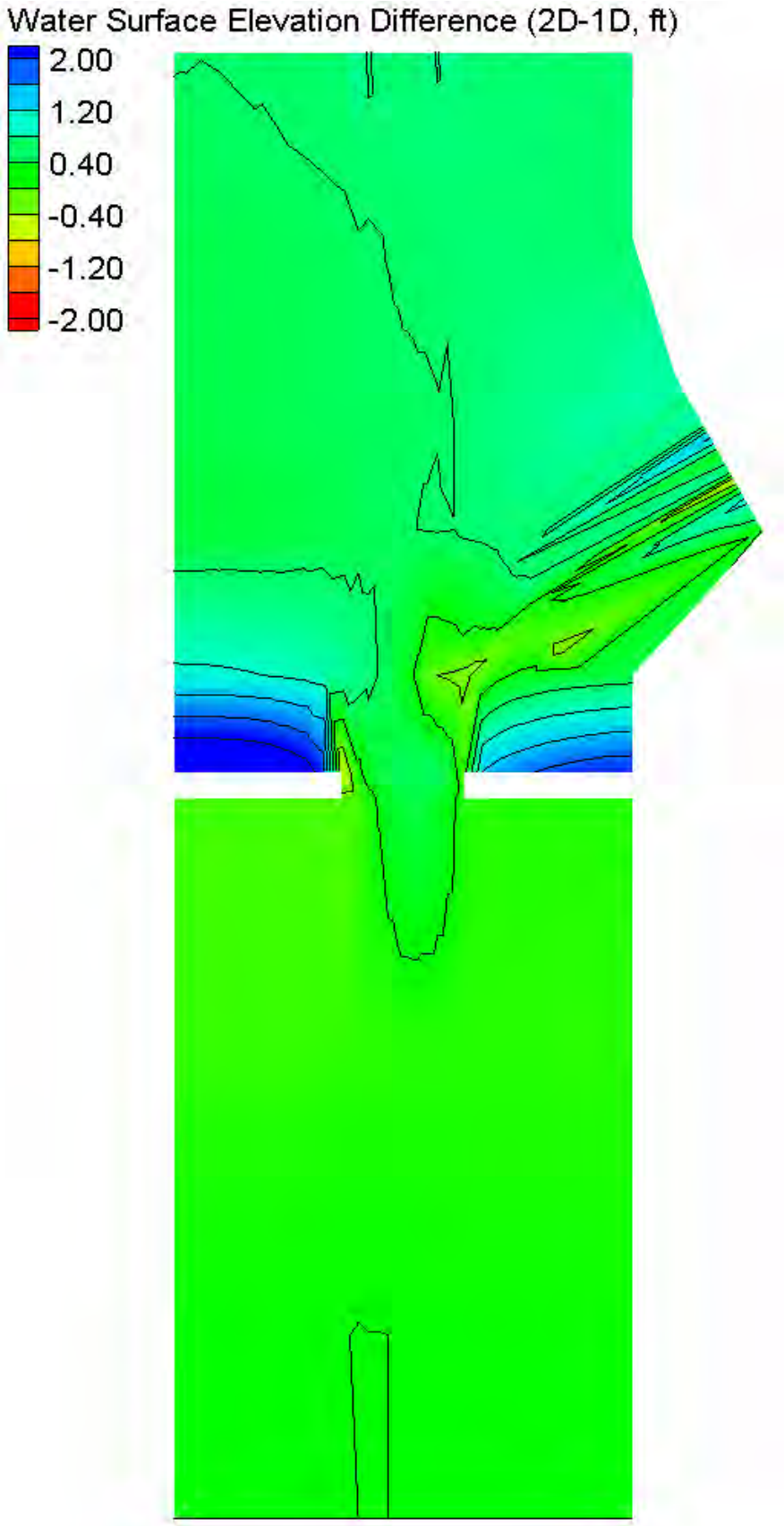

Water Surface Elevation Difference Contours – Large Channel – Confluences (60°, 50% flow, one bridge length upstream)

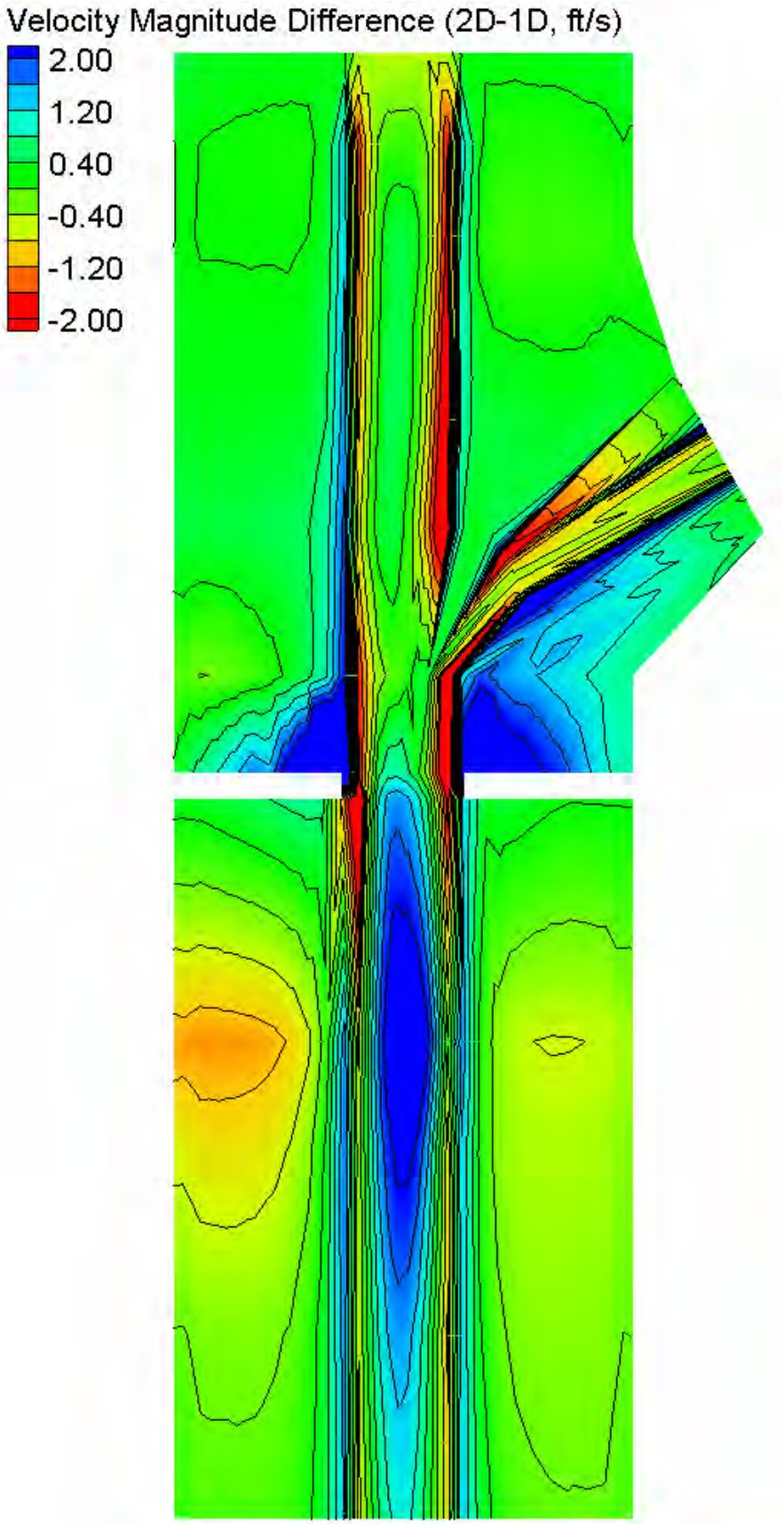

Velocity Magnitude Difference Contours – Large Channel – Confluences (60°, 50% flow, one bridge length upstream)

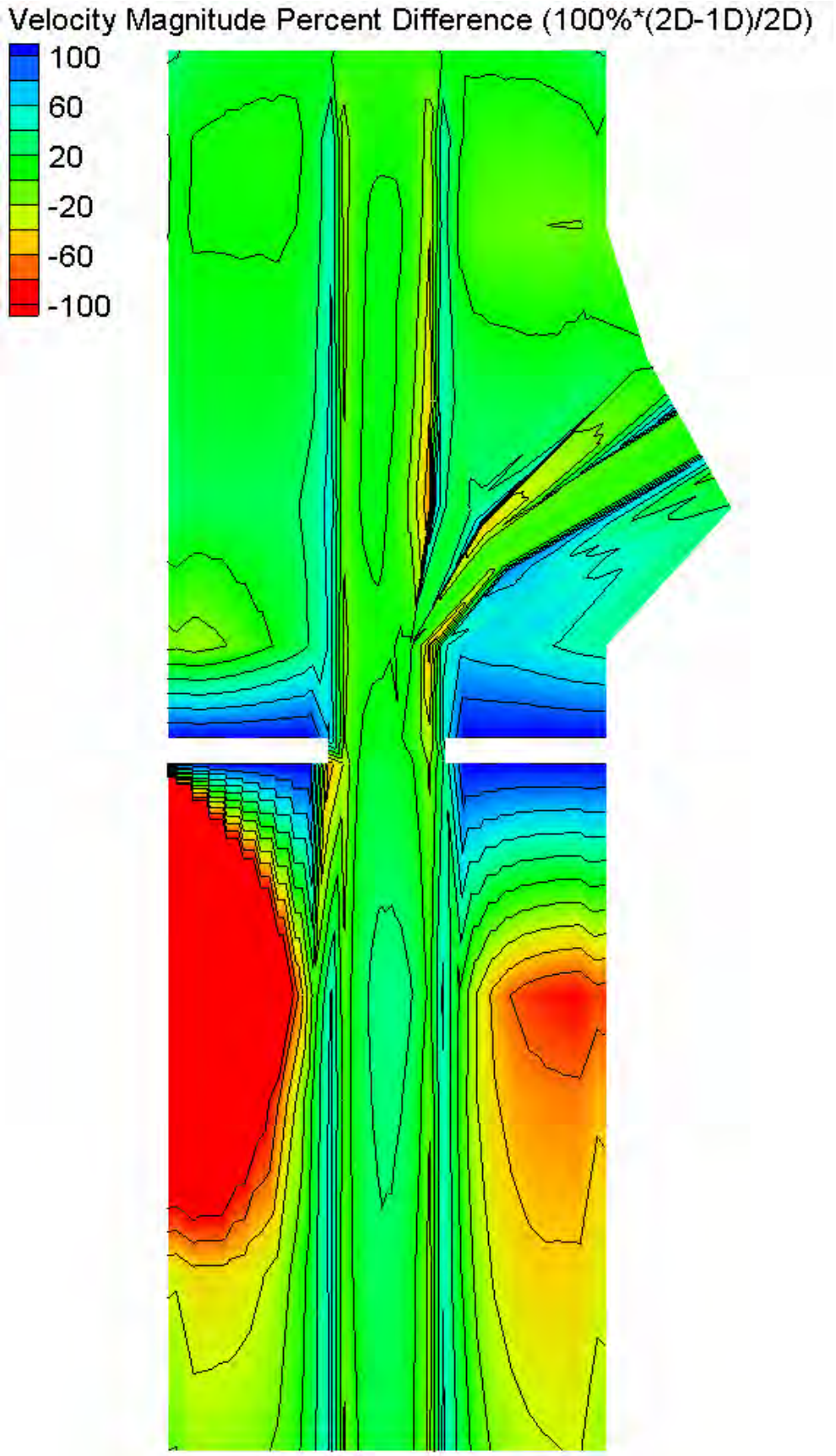

Velocity Magnitude Percent Difference Contours – Large Channel – Confluences (60°, 50% flow, one bridge length upstream)

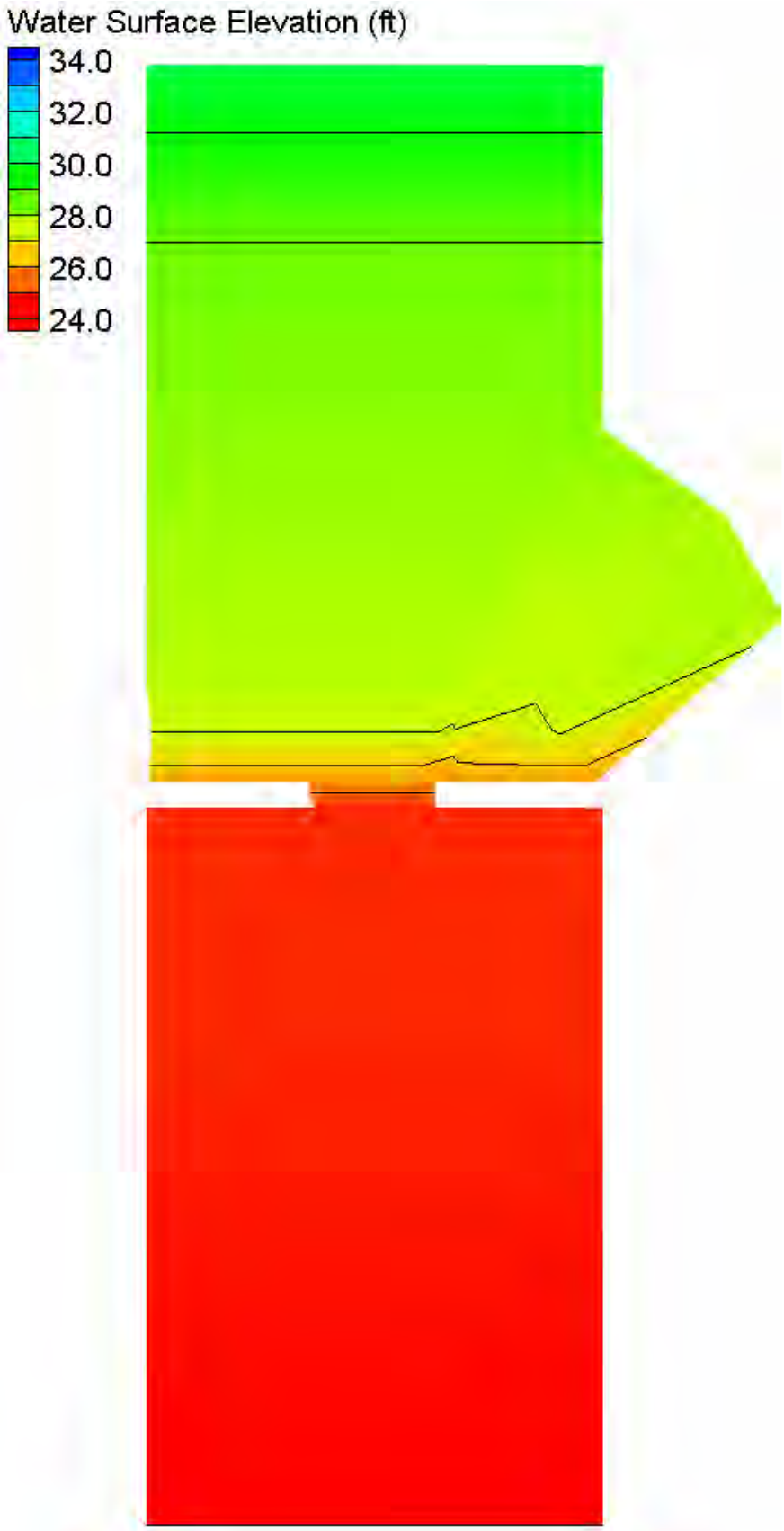

HEC-RAS Water Surface Elevation Contours – Large Channel – Confluences (60°, 50% flow, immediately upstream)

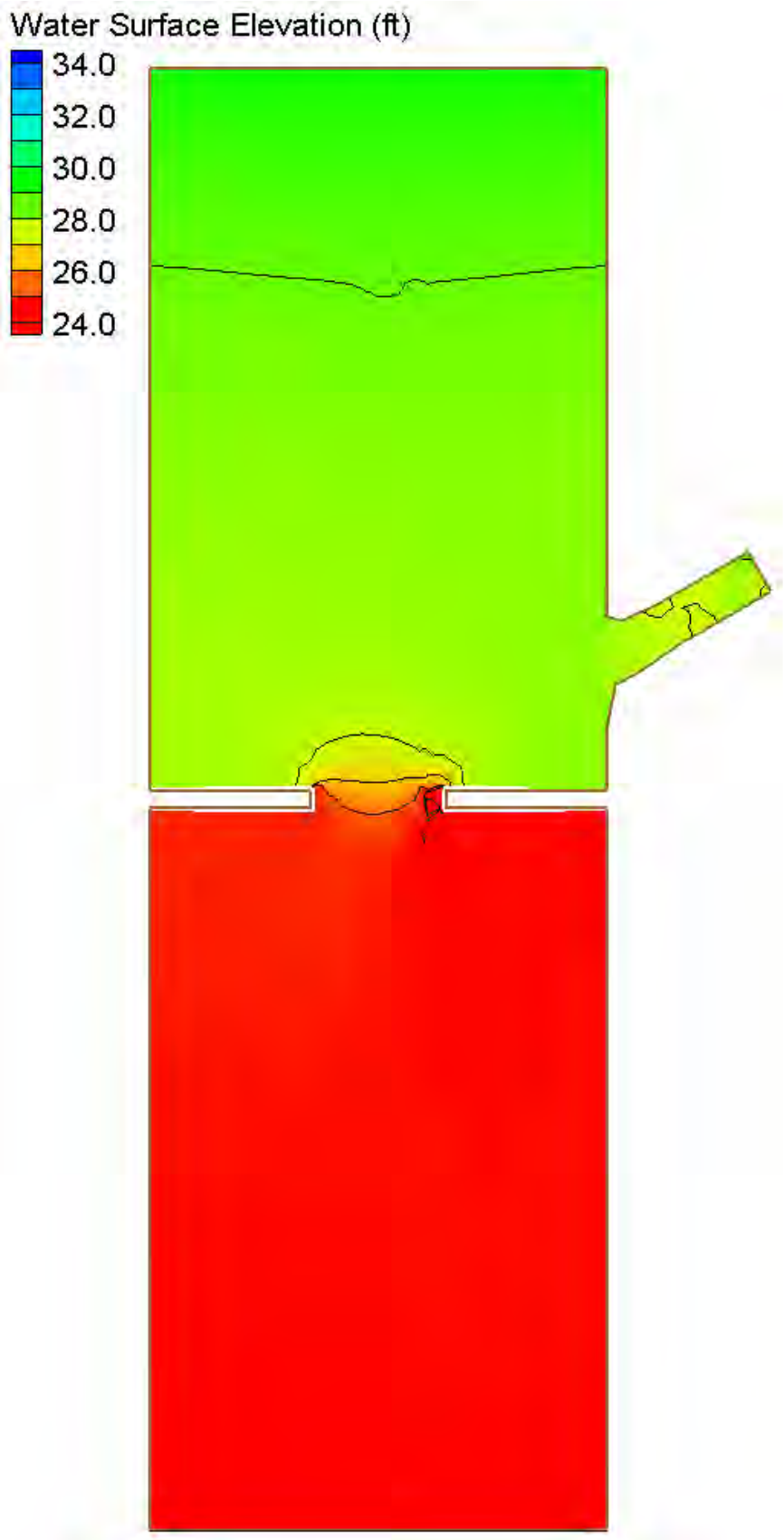

FESWMS Water Surface Elevation Contours – Large Channel – Confluences (60°, 50% flow, immediately upstream)

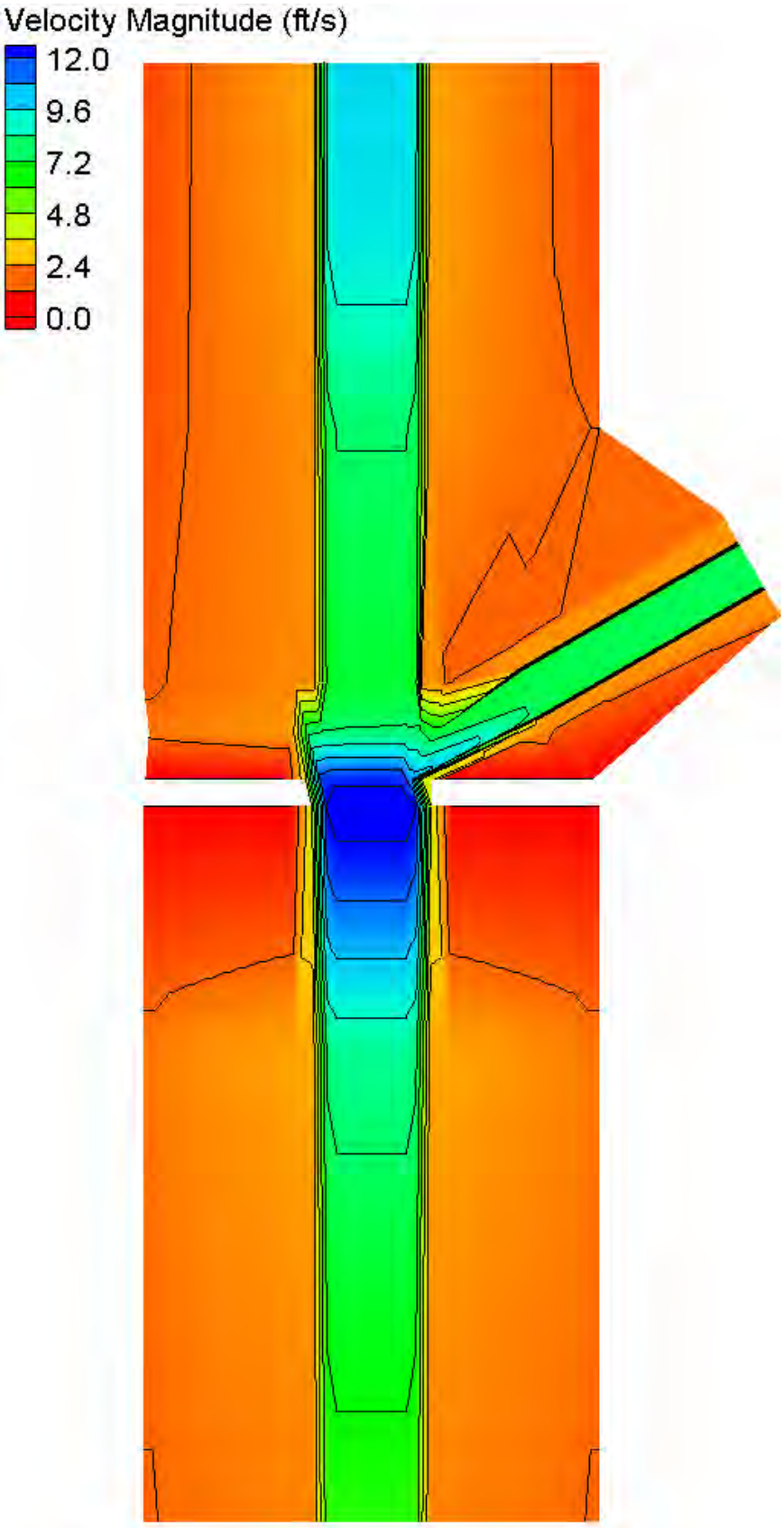

HEC-RAS Velocity Magnitude Contours – Large Channel – Confluences (60°, 50% flow, immediately upstream)

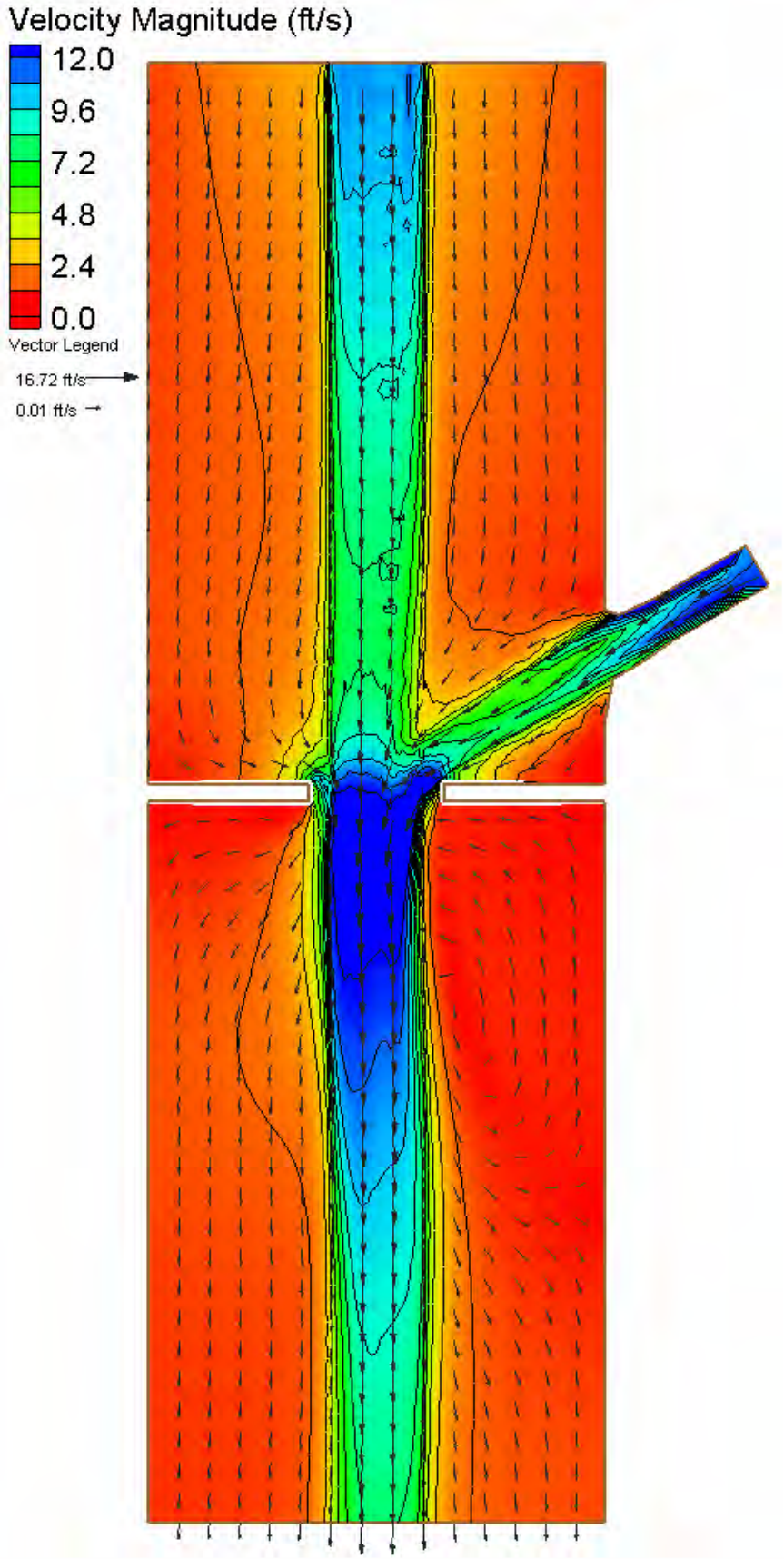

FESWMS Velocity Magnitude Contours – Large Channel – Confluences (60°, 50% flow, immediately upstream)

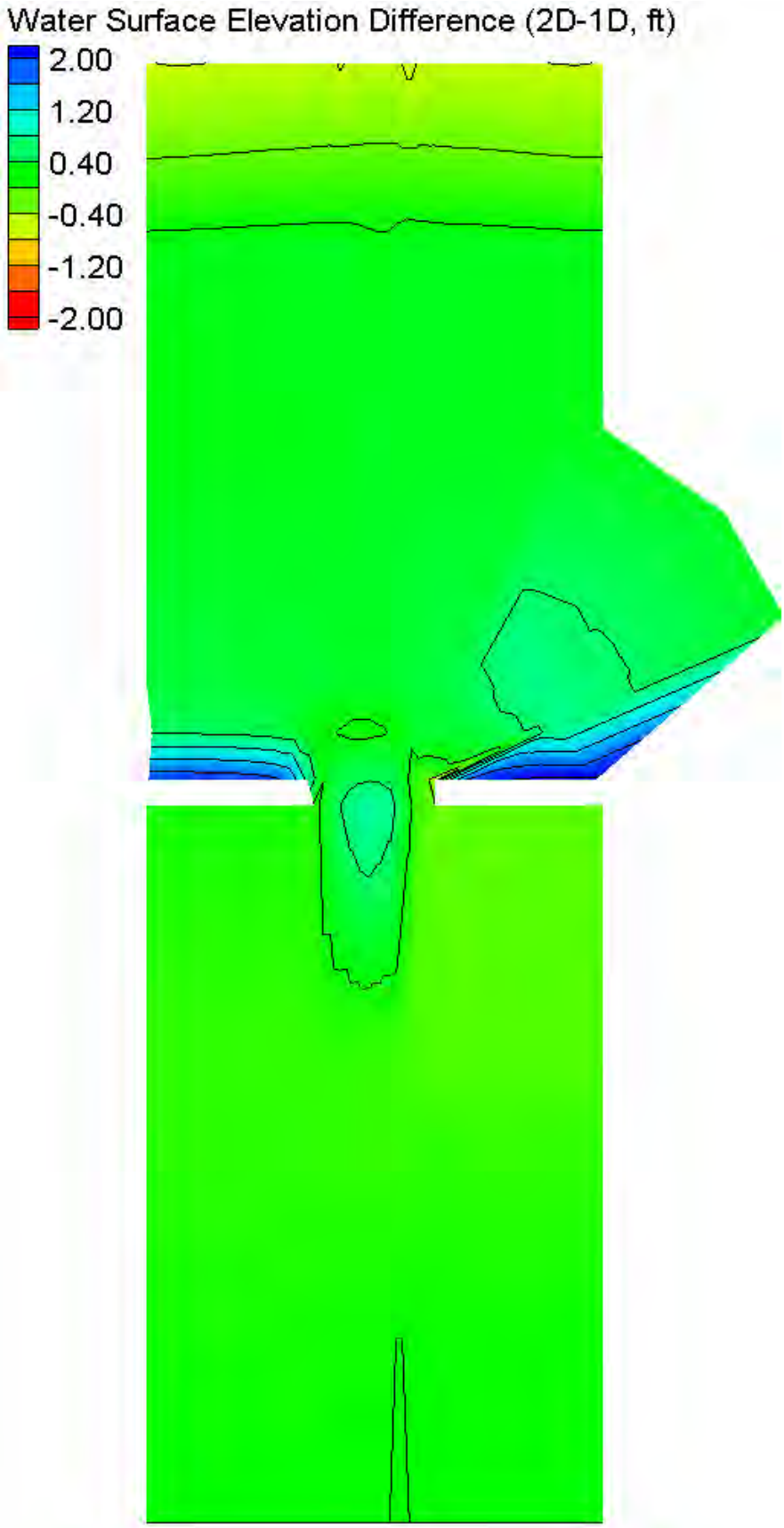

Water Surface Elevation Difference Contours – Large Channel – Confluences (60°, 50% flow, immediately upstream)

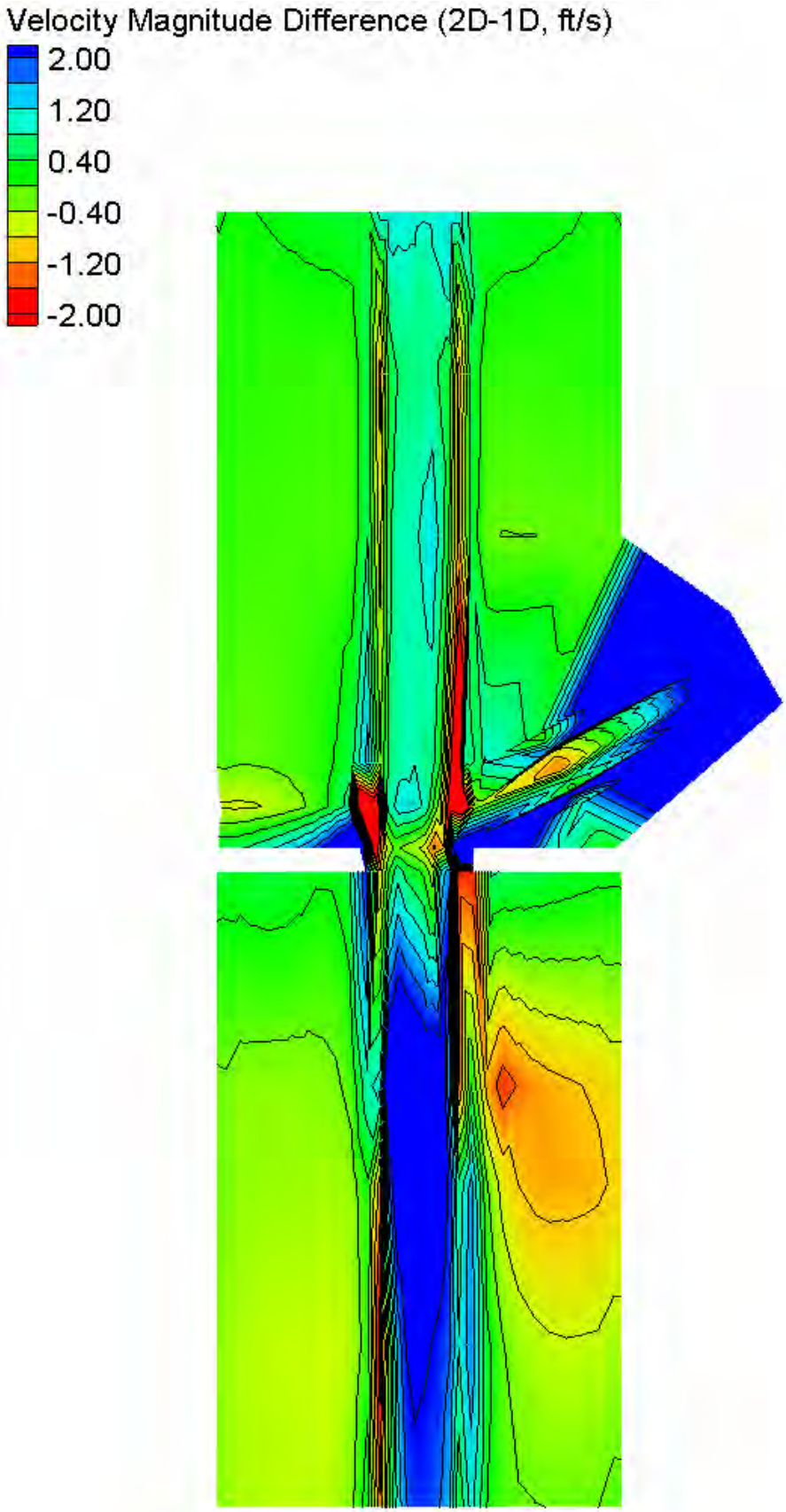

Velocity Magnitude Difference Contours – Large Channel – Confluences (60°, 50% flow, immediately upstream)

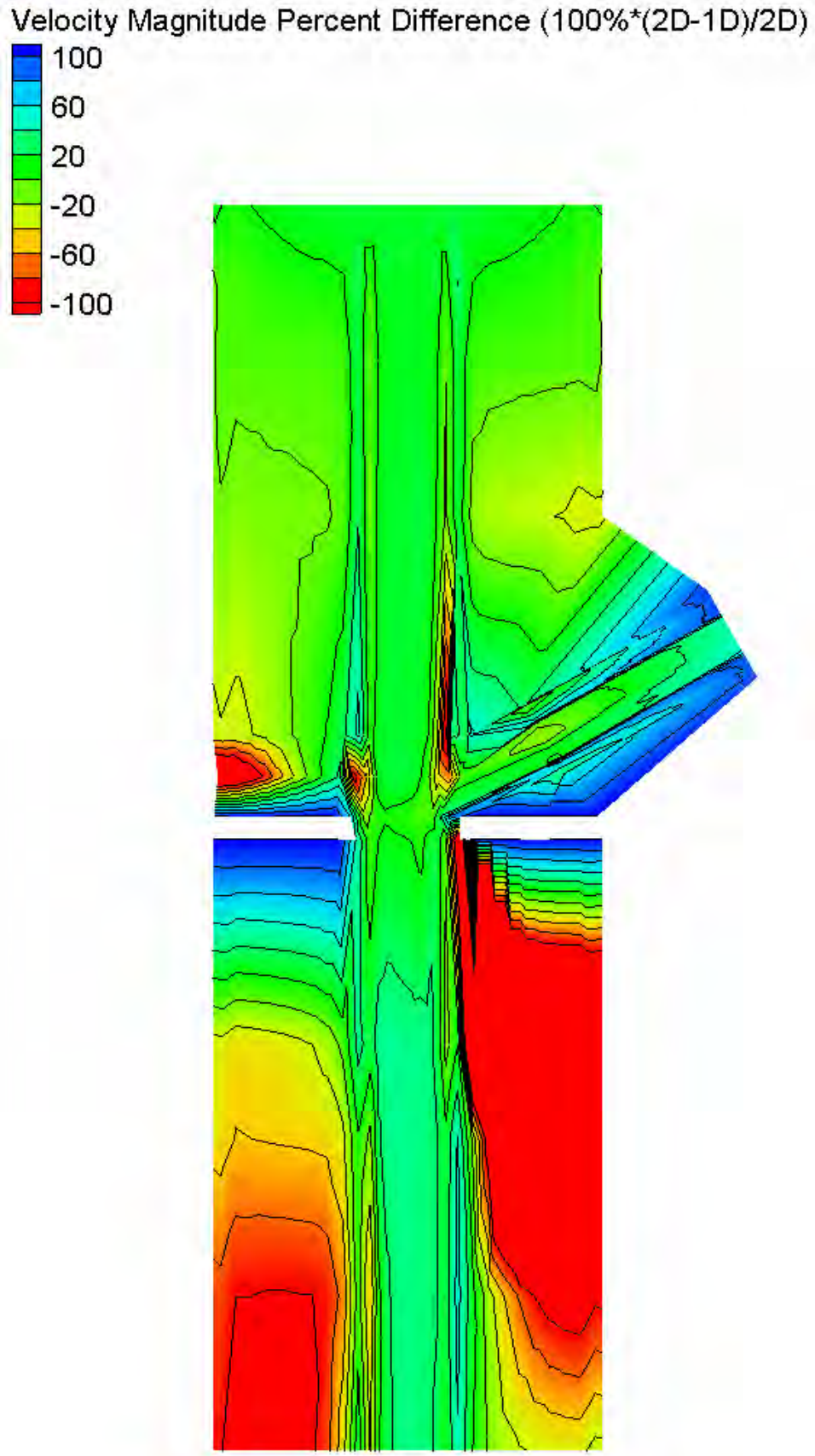

Velocity Magnitude Percent Difference Contours – Large Channel – Confluences (60°, 50% flow, immediately upstream)

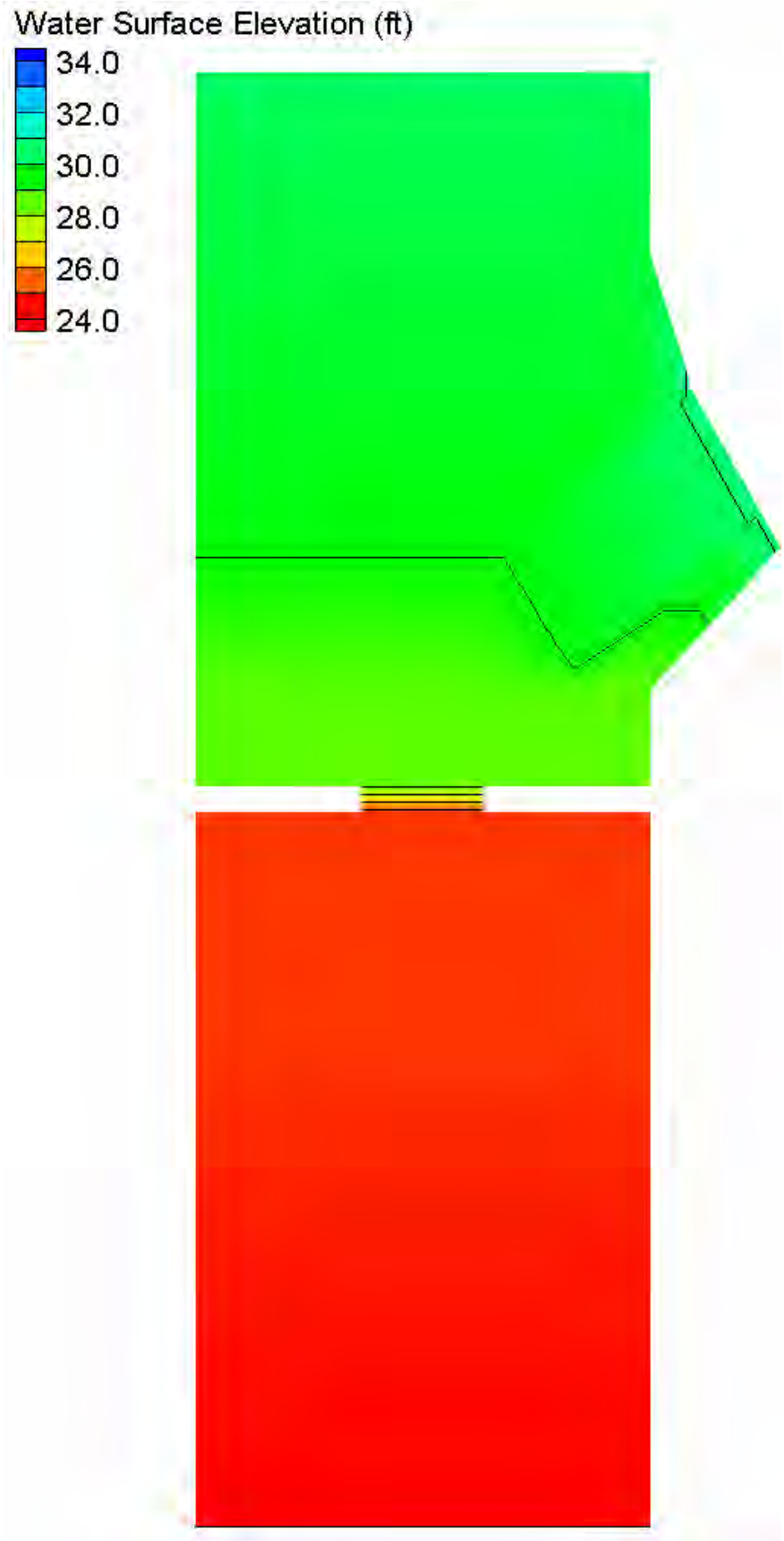

HEC-RAS Water Surface Elevation Contours – Large Channel – Confluences (60°, 75% flow, one bridge length upstream)

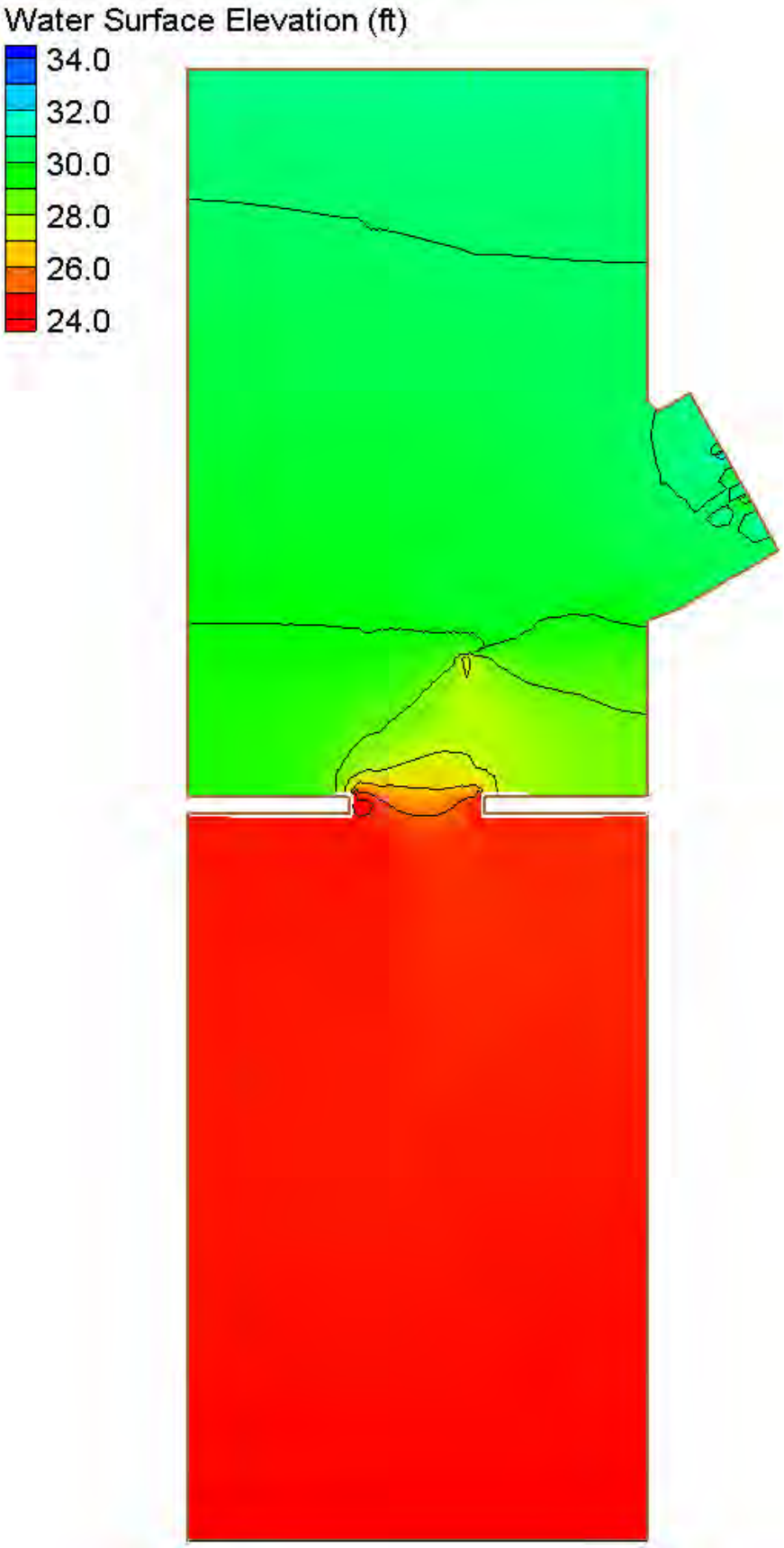

FESWMS Water Surface Elevation Contours – Large Channel – Confluences (60°, 75% flow, one bridge length upstream)

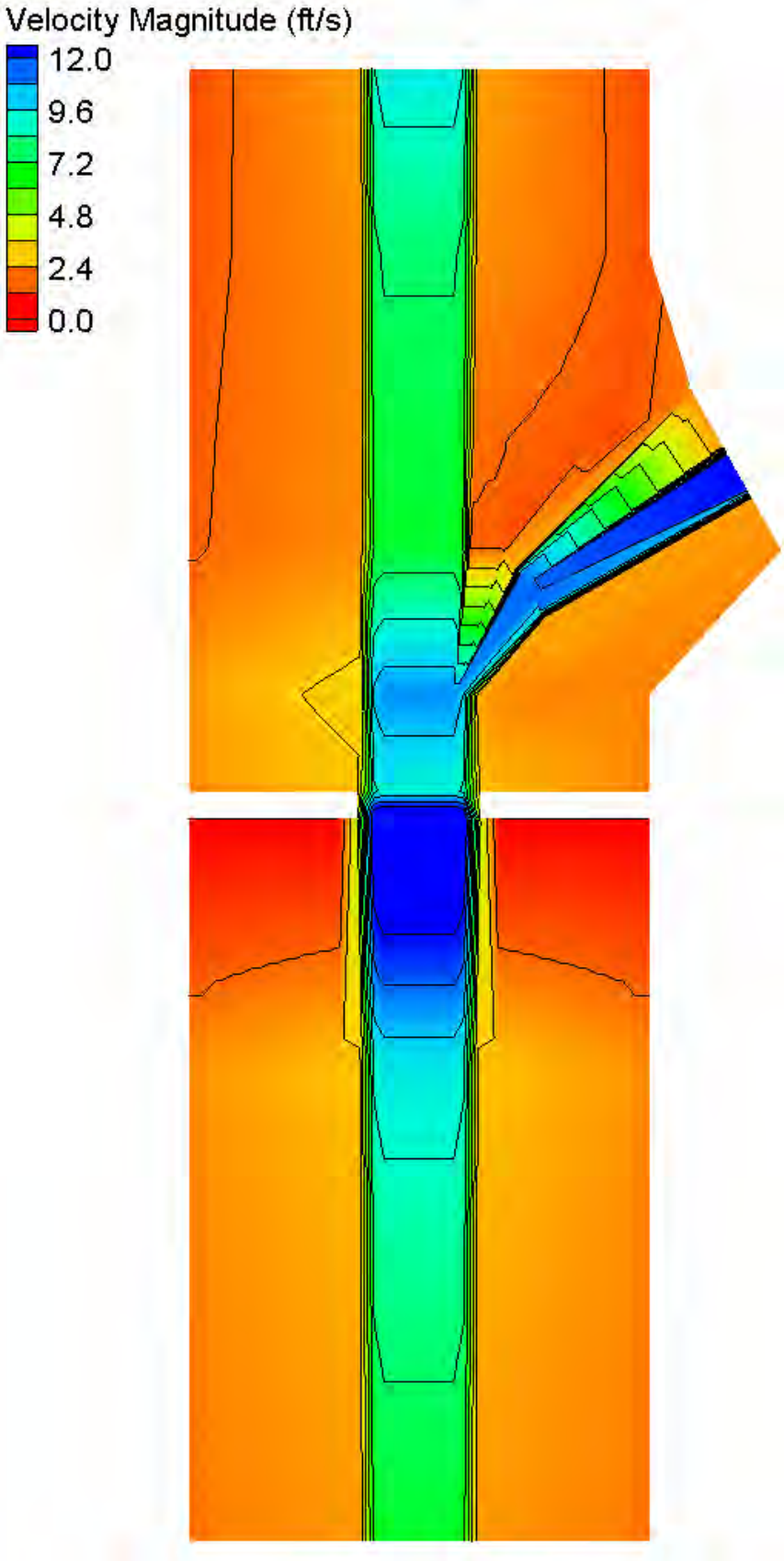

HEC-RAS Velocity Magnitude Contours – Large Channel – Confluences (60°, 75% flow, one bridge length upstream)

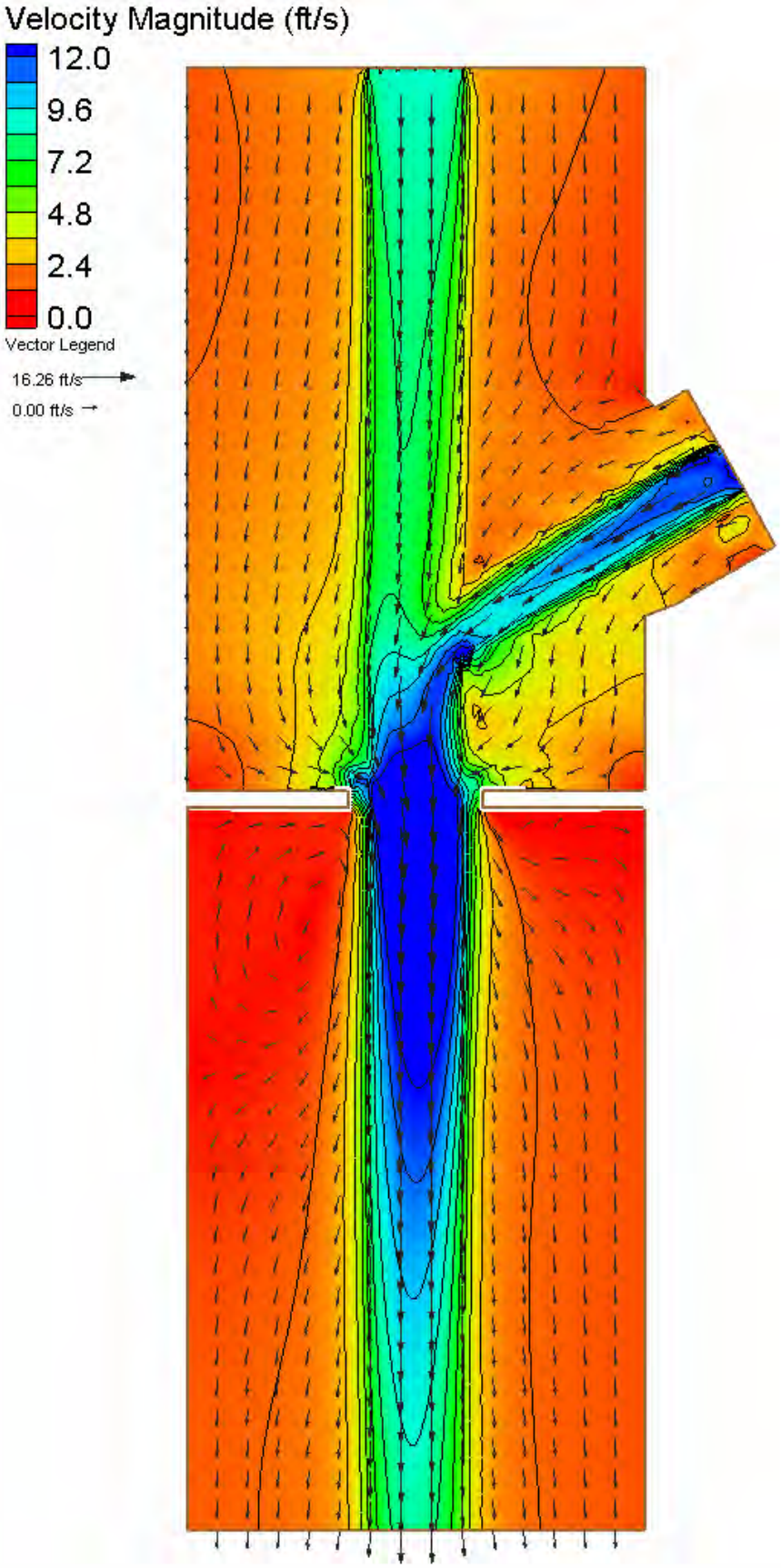

FESWMS Velocity Magnitude Contours – Large Channel – Confluences (60°, 75% flow, one bridge length upstream)

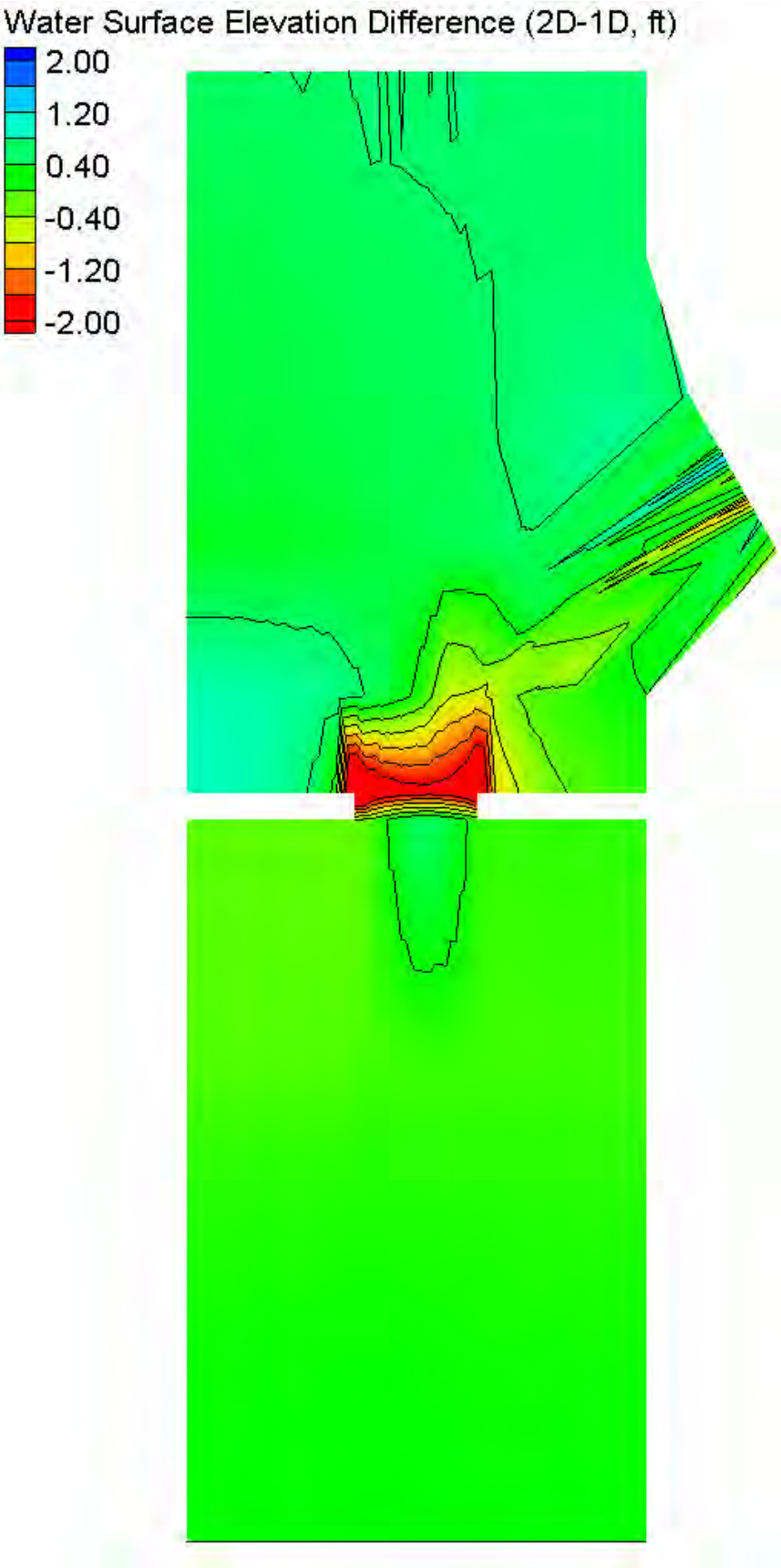

Water Surface Elevation Difference Contours – Large Channel – Confluences (60°, 75% flow, one bridge length upstream)

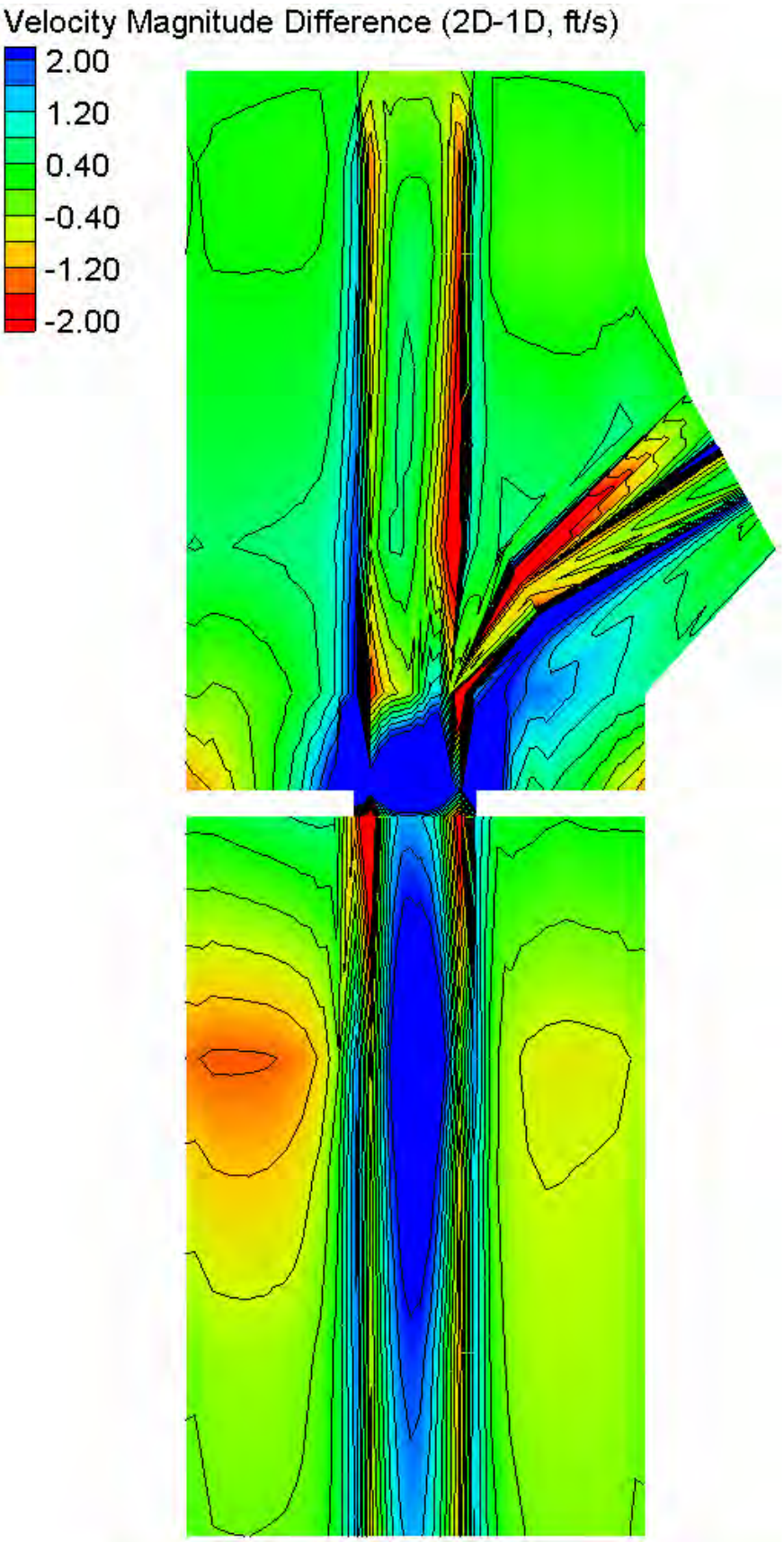

Velocity Magnitude Difference Contours – Large Channel – Confluences (60°, 75% flow, one bridge length upstream)

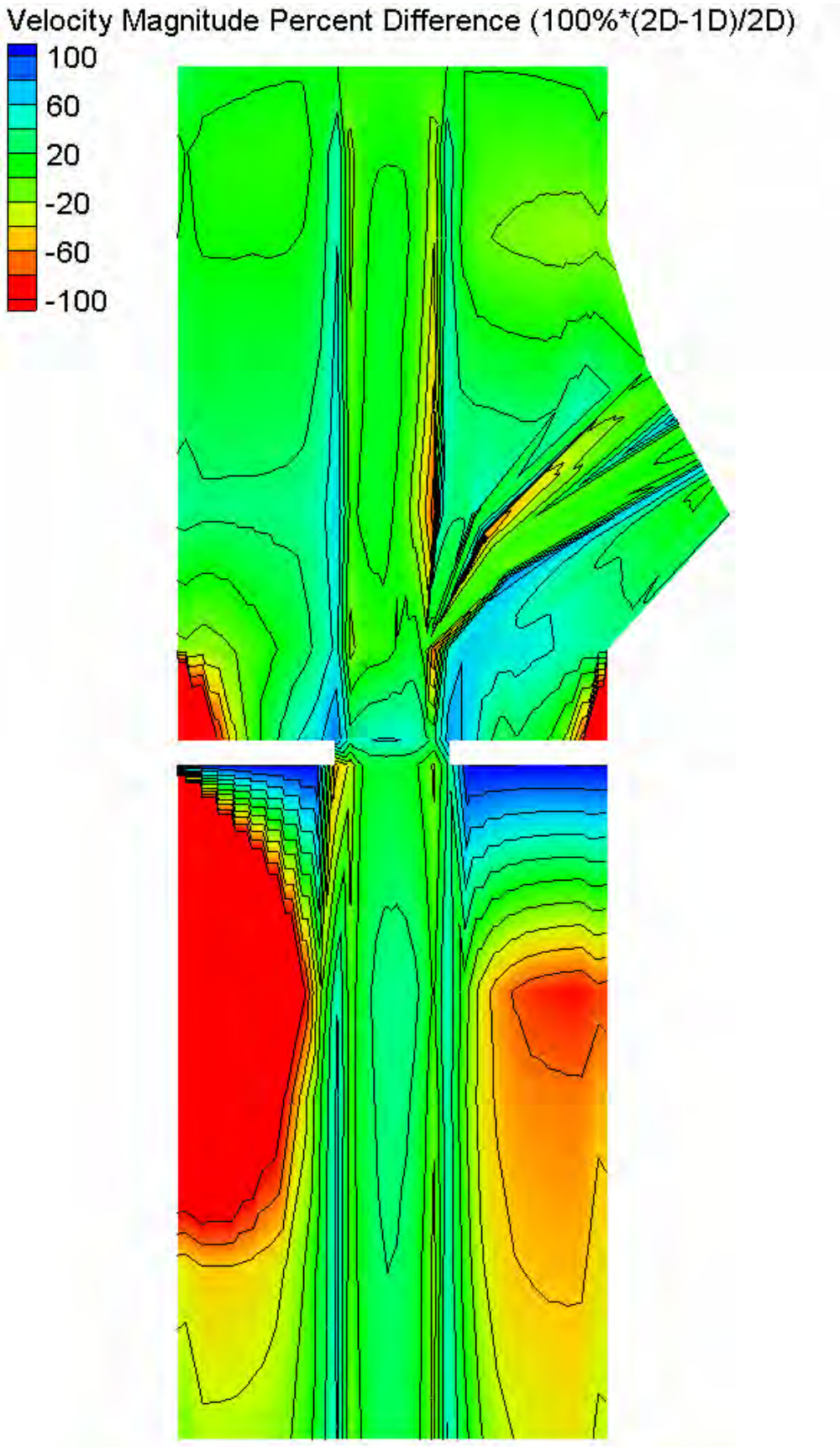

Velocity Magnitude Percent Difference Contours – Large Channel – Confluences (60°, 75% flow, one bridge length upstream)

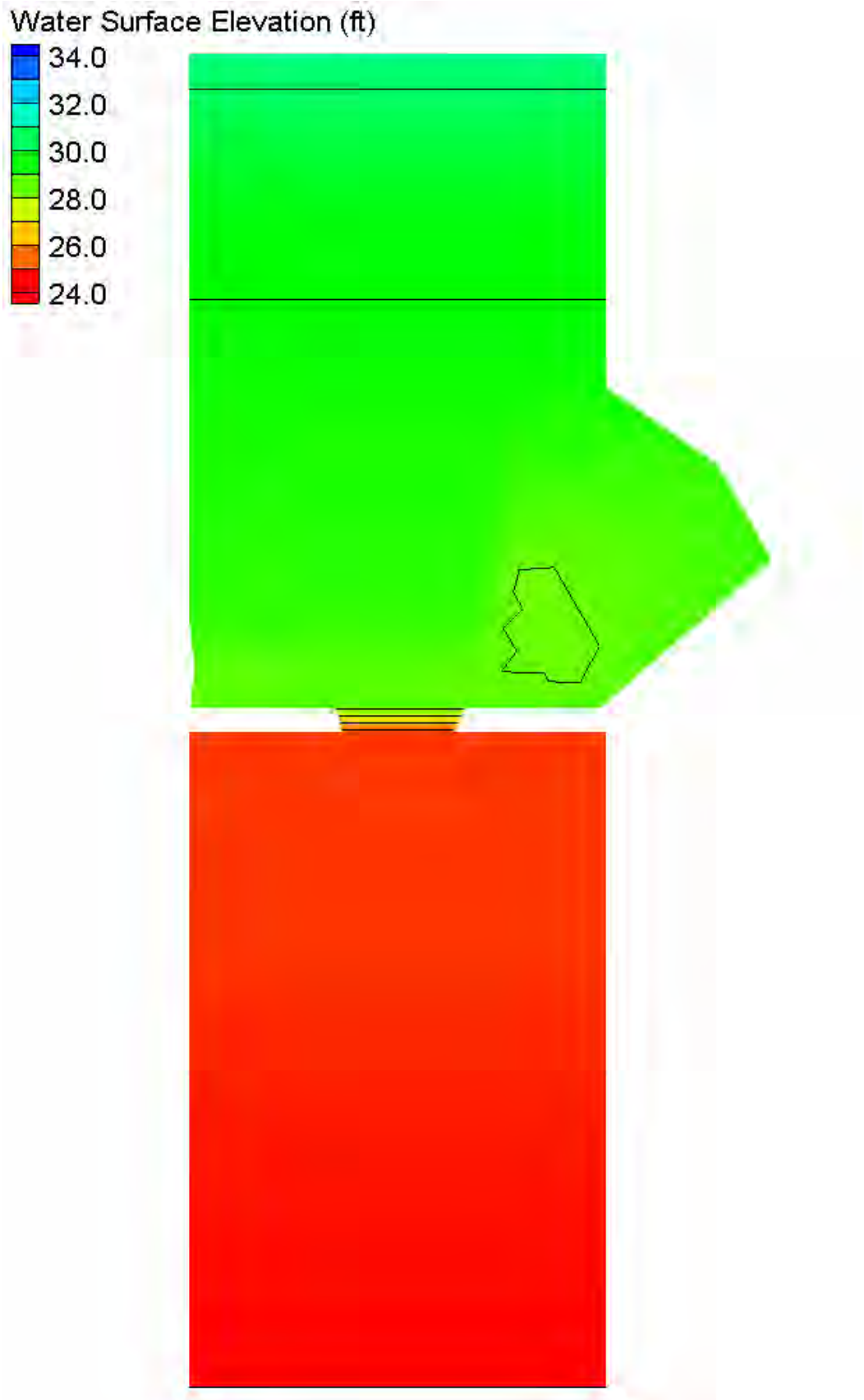

HEC-RAS Water Surface Elevation Contours – Large Channel – Confluences (60°, 75% flow, immediately upstream)

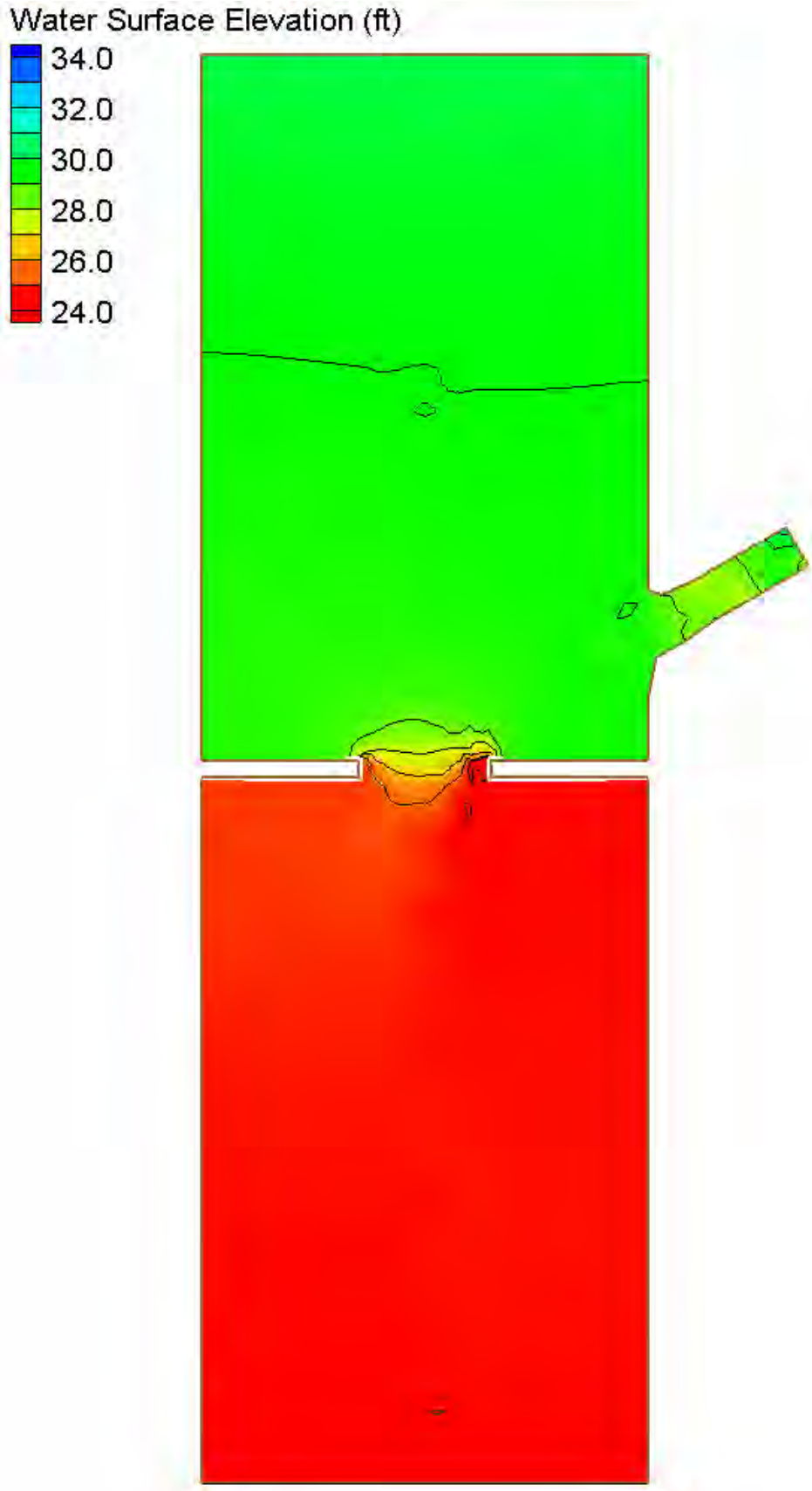

FESWMS Water Surface Elevation Contours – Large Channel – Confluences (60°, 75% flow, immediately upstream)

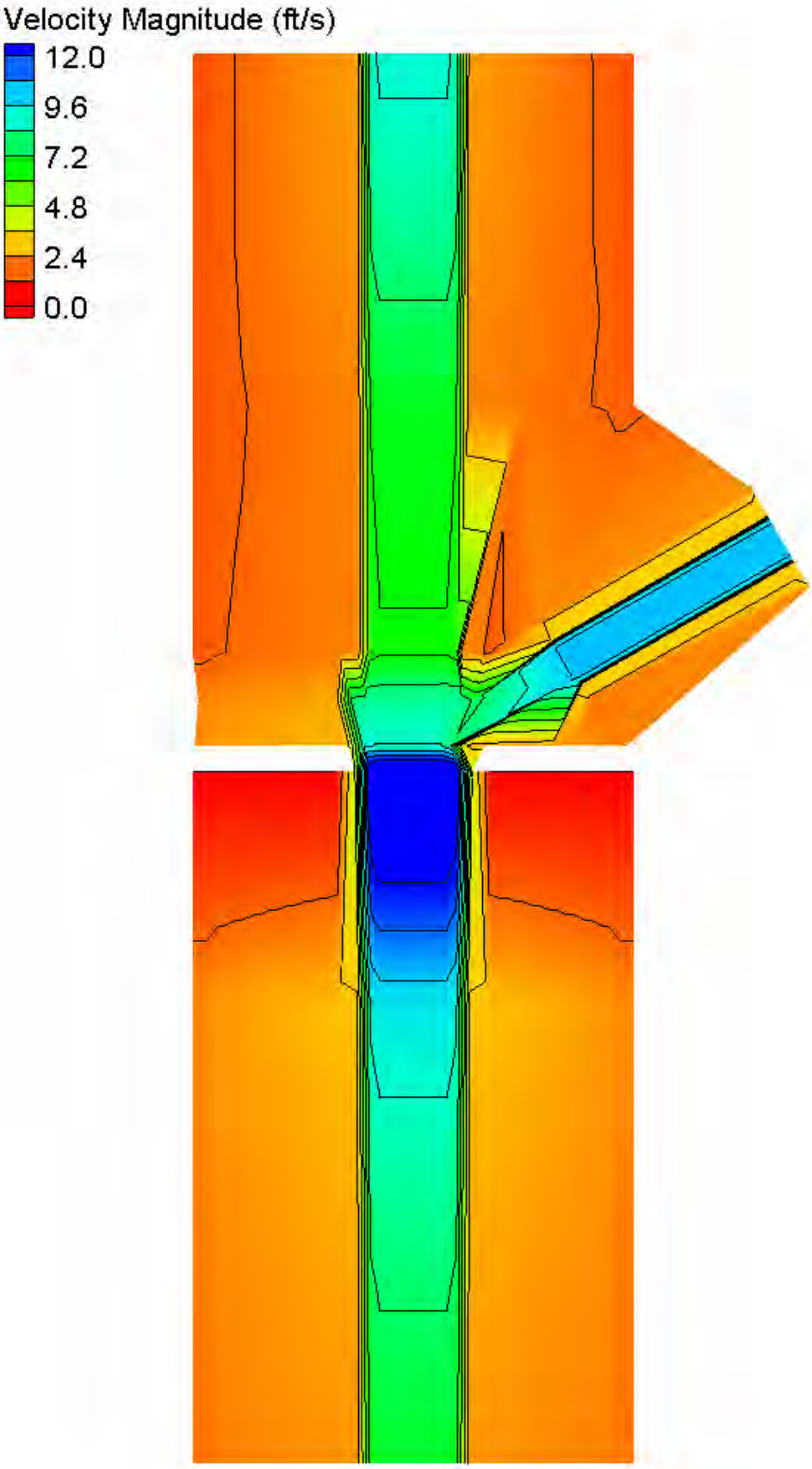

HEC-RAS Velocity Magnitude Contours – Large Channel – Confluences (60°, 75% flow, immediately upstream)

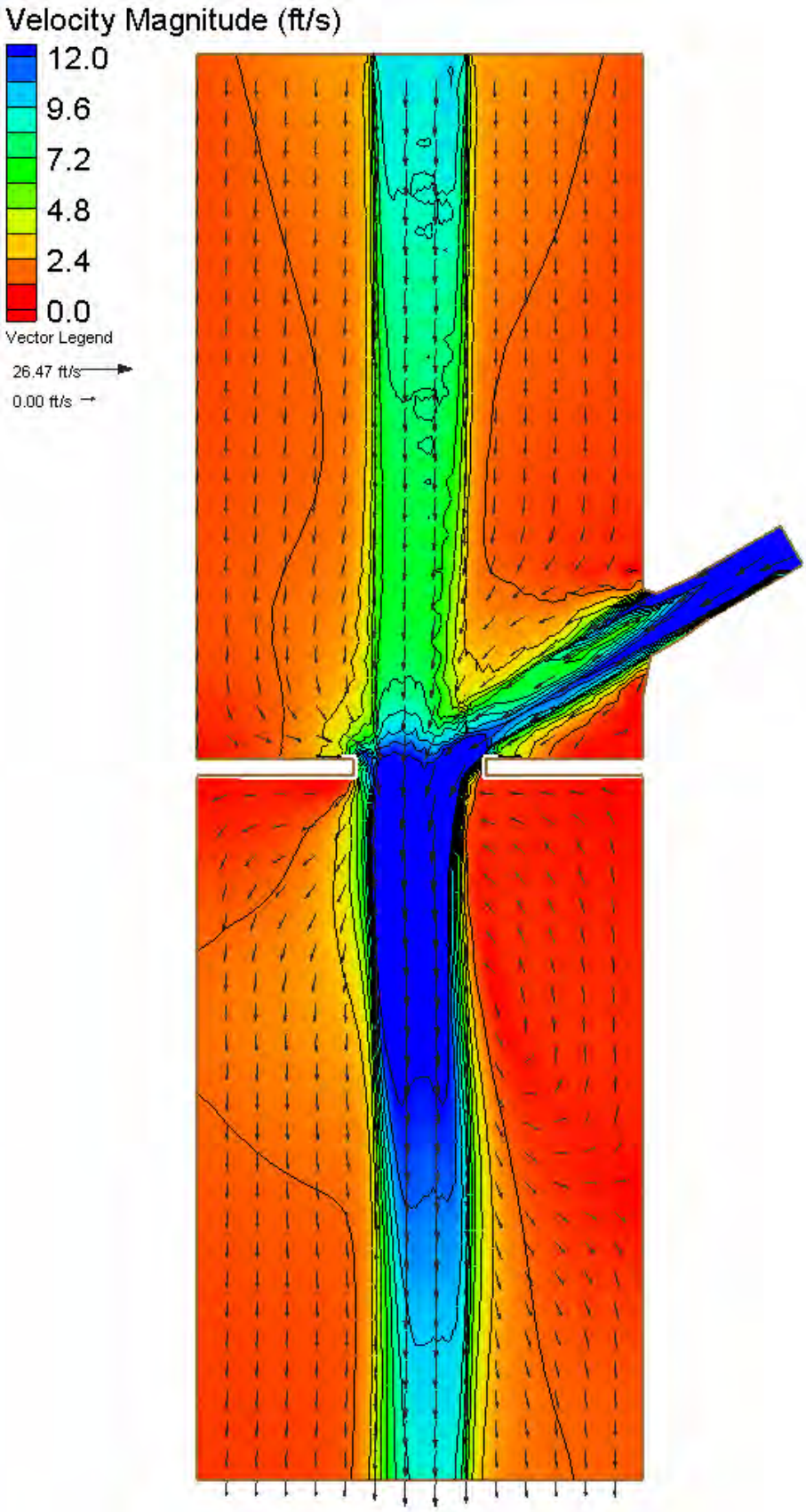

FESWMS Velocity Magnitude Contours – Large Channel – Confluences (60°, 75% flow, immediately upstream)

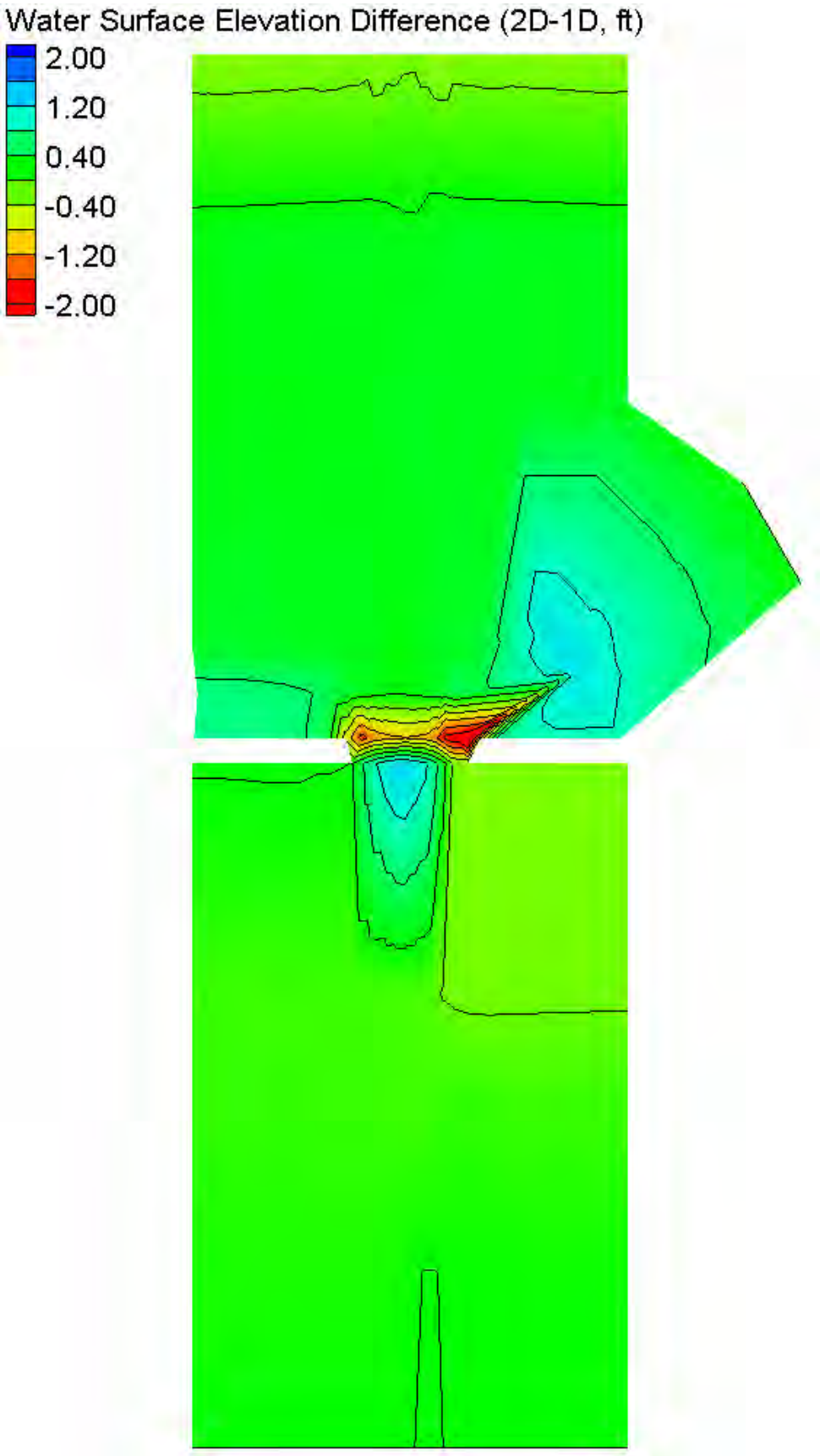

Water Surface Elevation Difference Contours – Large Channel – Confluences (60°, 75% flow, immediately upstream)

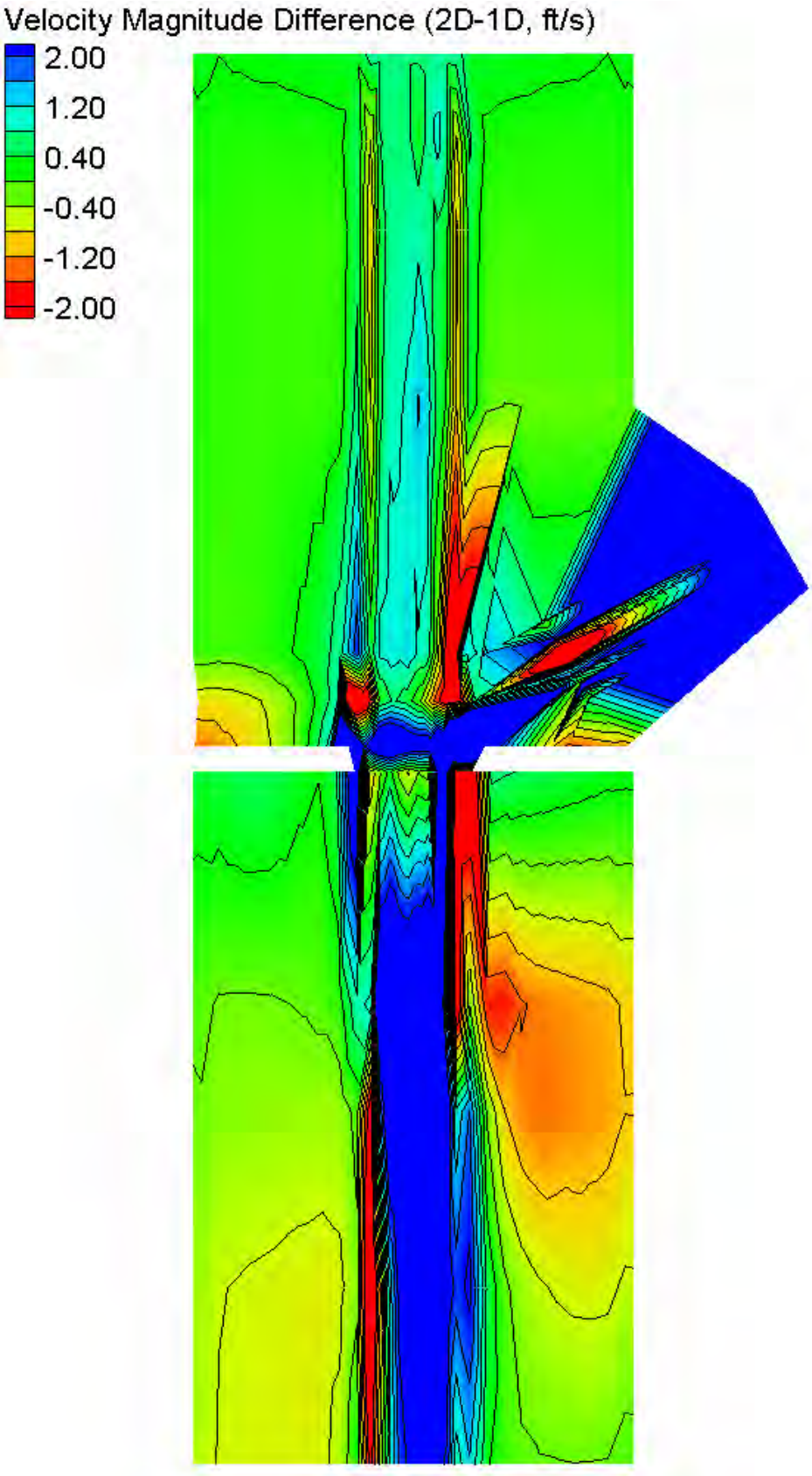

Velocity Magnitude Difference Contours – Large Channel – Confluences (60°, 75% flow, immediately upstream)

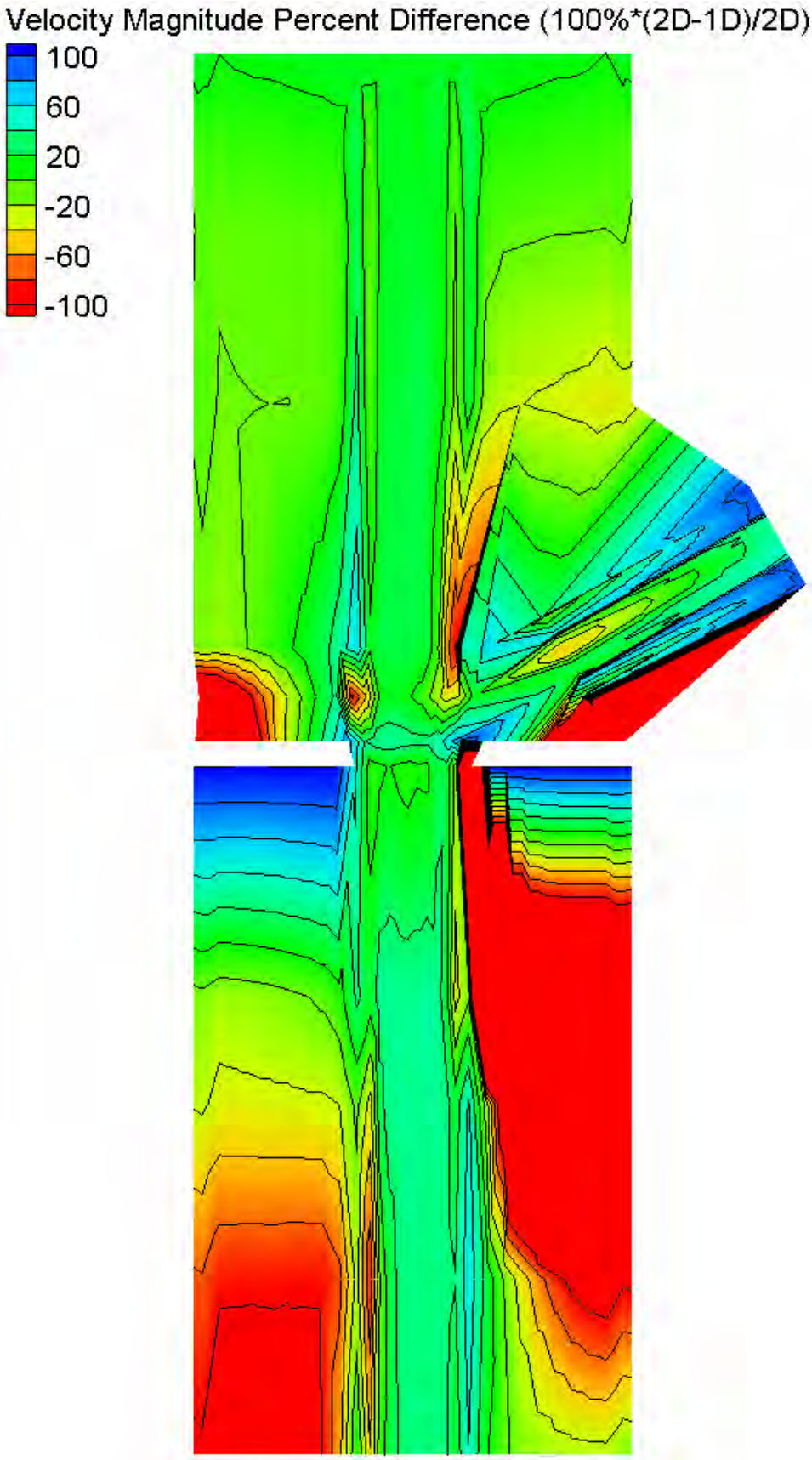

Velocity Magnitude Percent Difference Contours – Large Channel – Confluences (60°, 75% flow, immediately upstream)

Bridges with Significant Constrictions

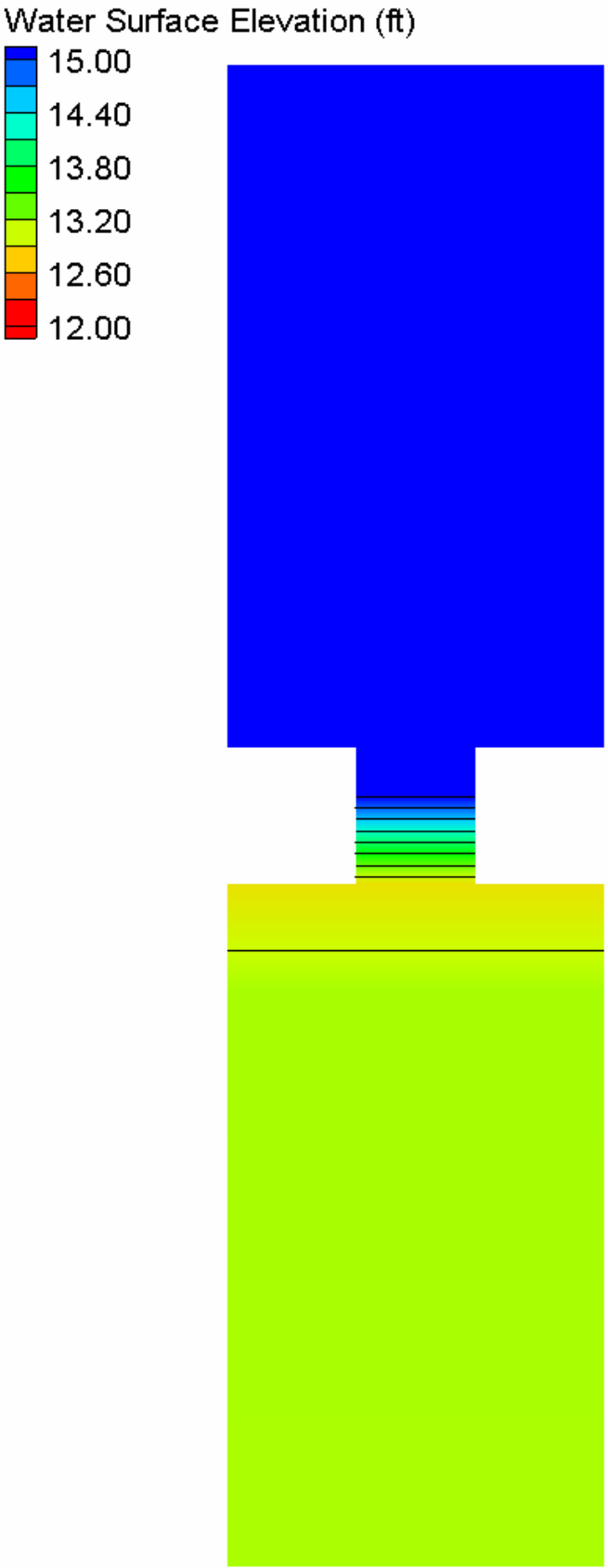

HEC-RAS Water Surface Elevation Contours – Small Channel – Constrictions (75%)

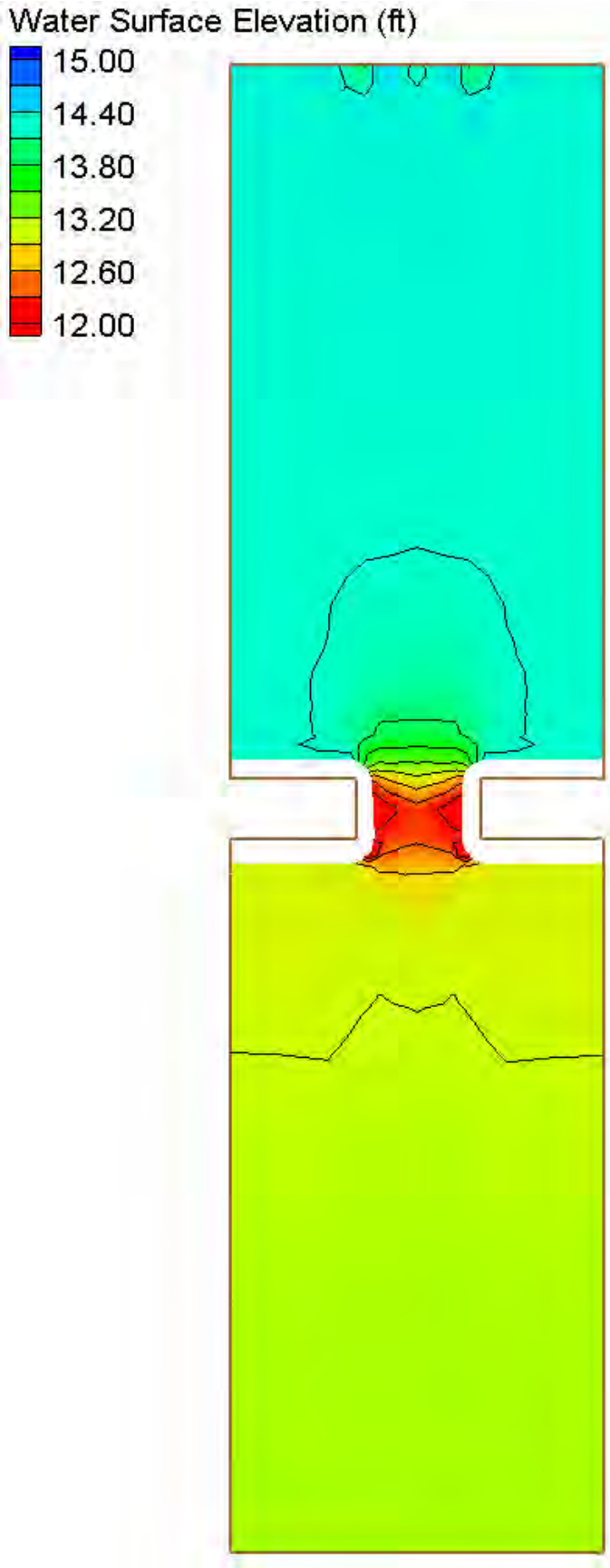

FESWMS Water Surface Elevation Contours – Small Channel – Constrictions (75%)

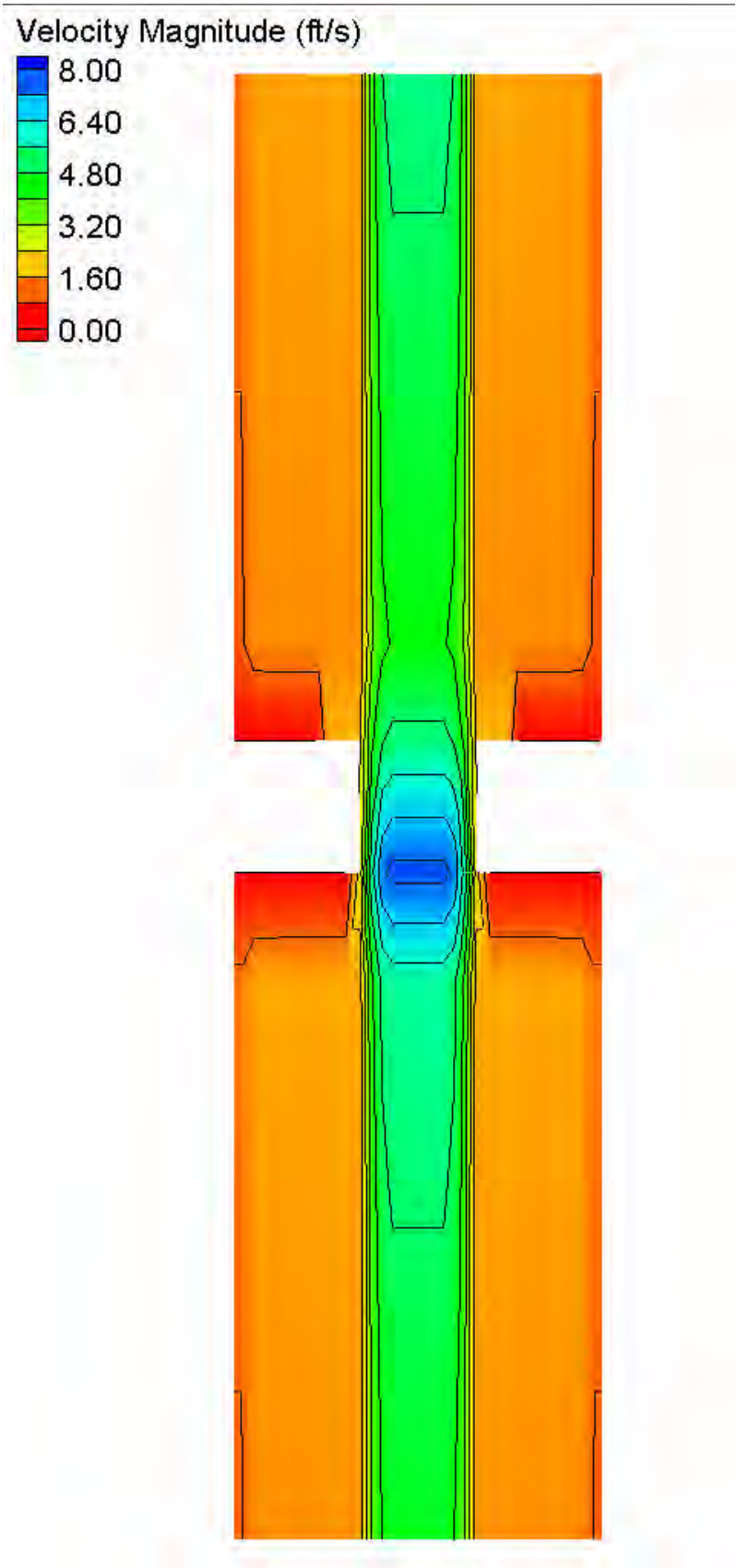

HEC-RAS Velocity Magnitude Contours – Small Channel – Constrictions (75%)

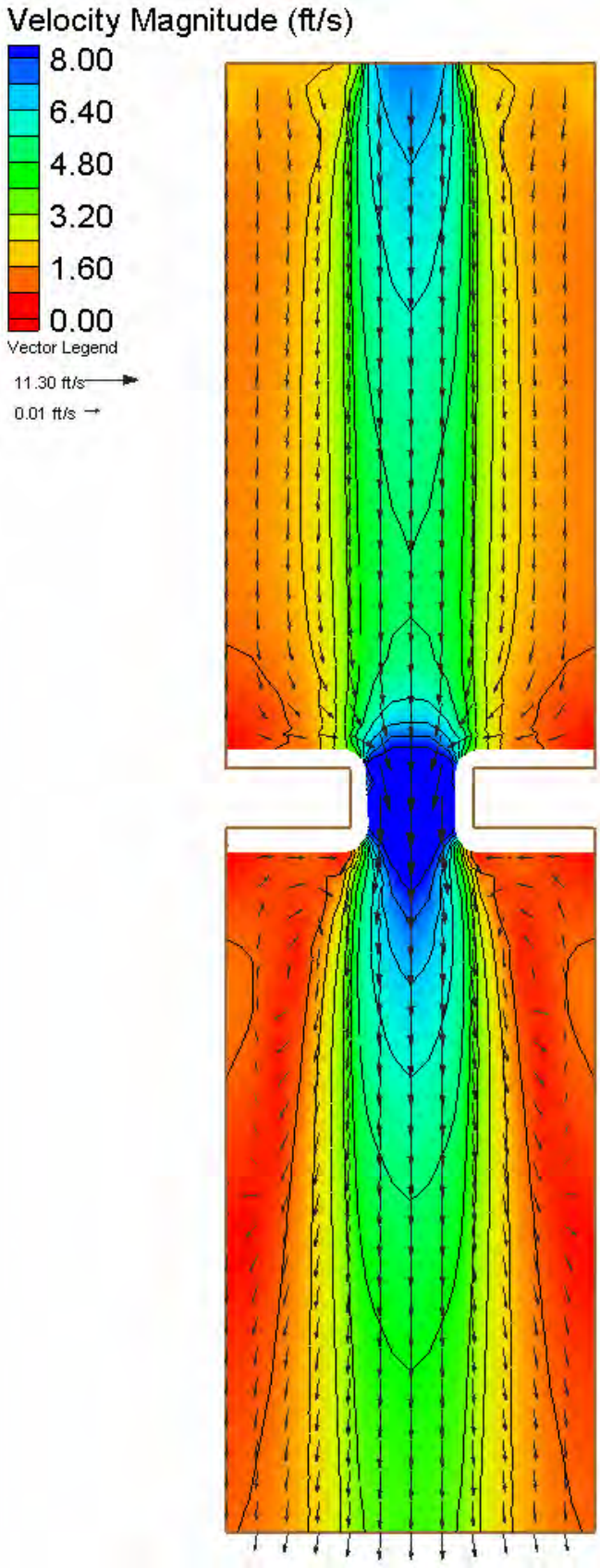

FESWMS Velocity Magnitude Contours – Small Channel – Constrictions (75%)

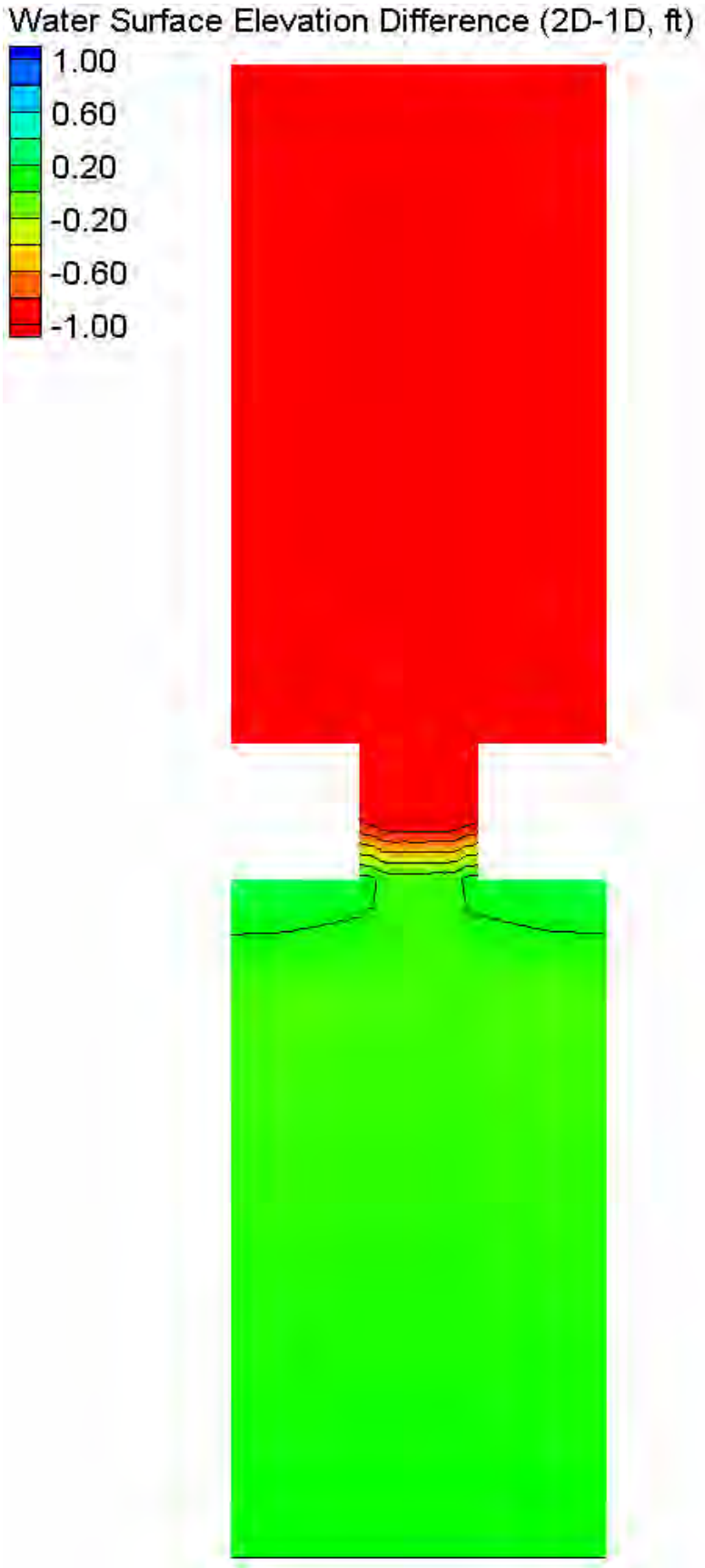

Water Surface Elevation Difference Contours – Small Channel – Constrictions (75%)

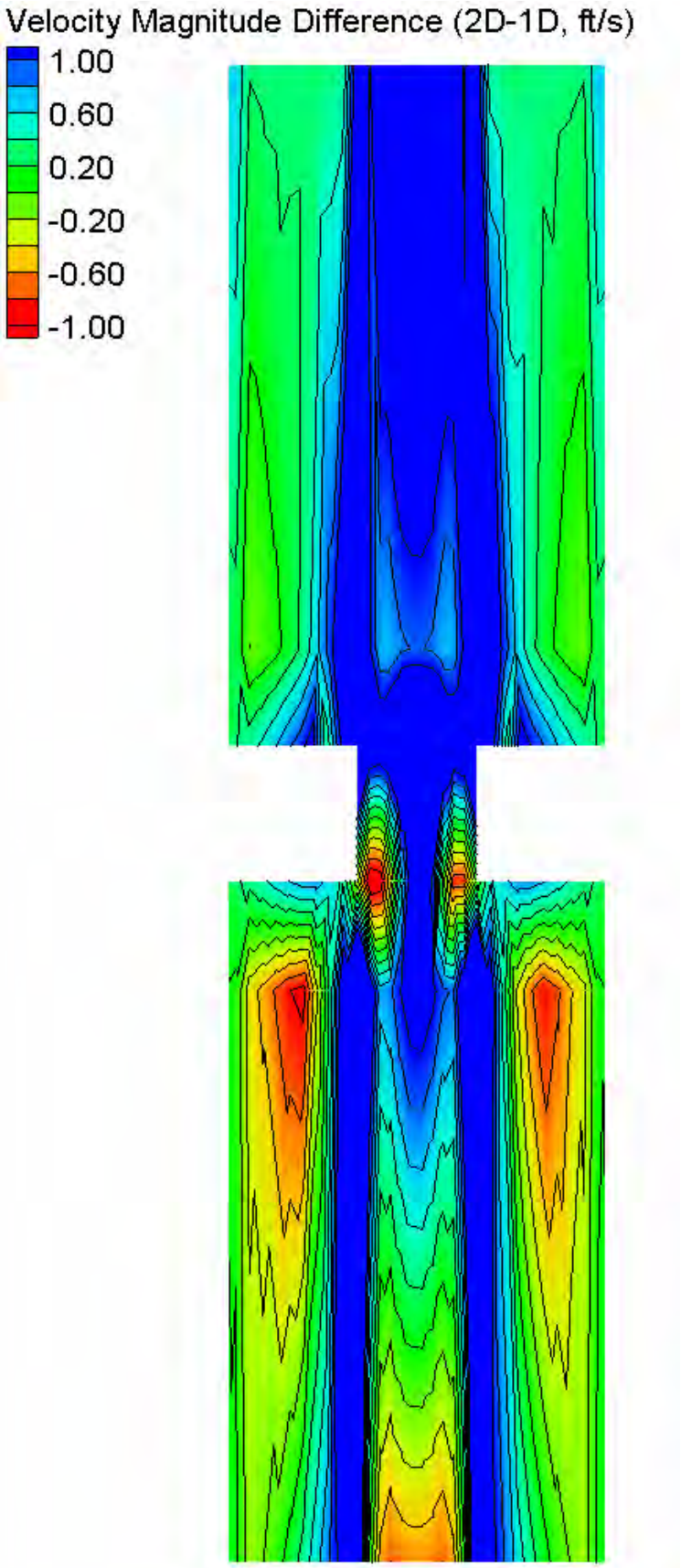

Velocity Magnitude Difference Contours – Small Channel – Constrictions (75%)

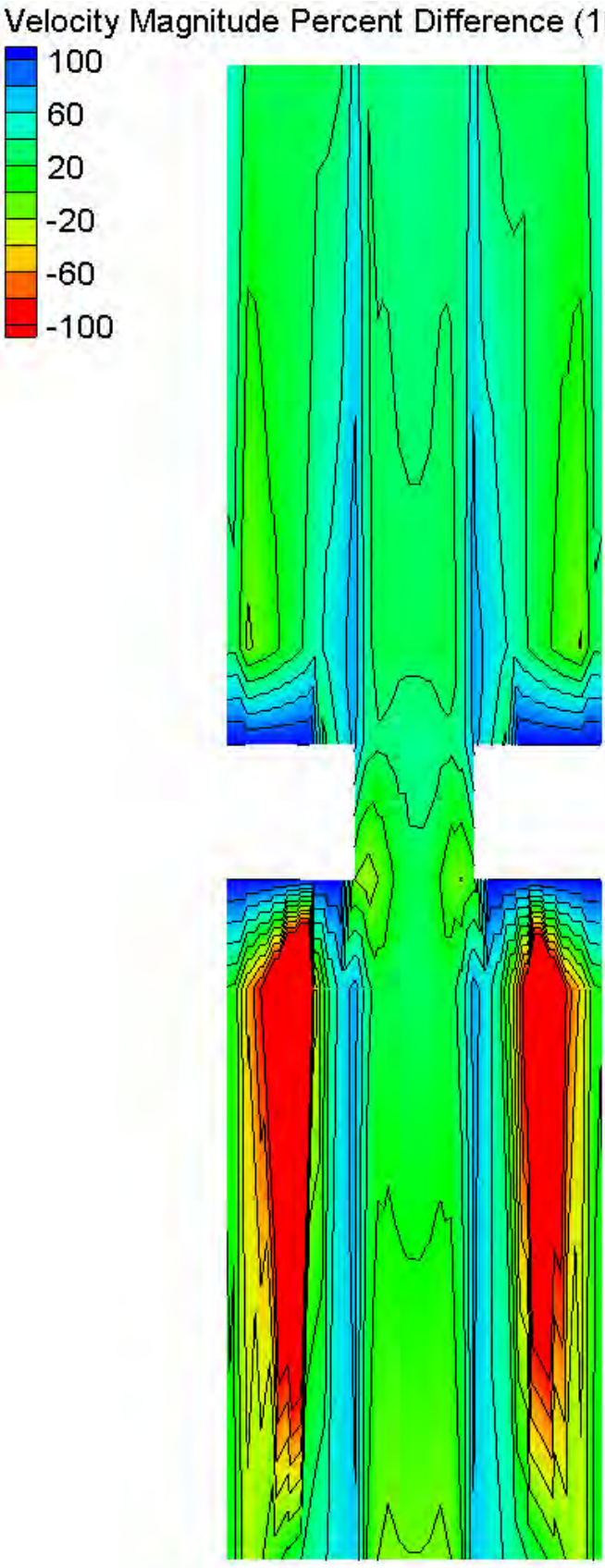

Velocity Magnitude Percent Difference Contours – Small Channel – Constrictions (75%)

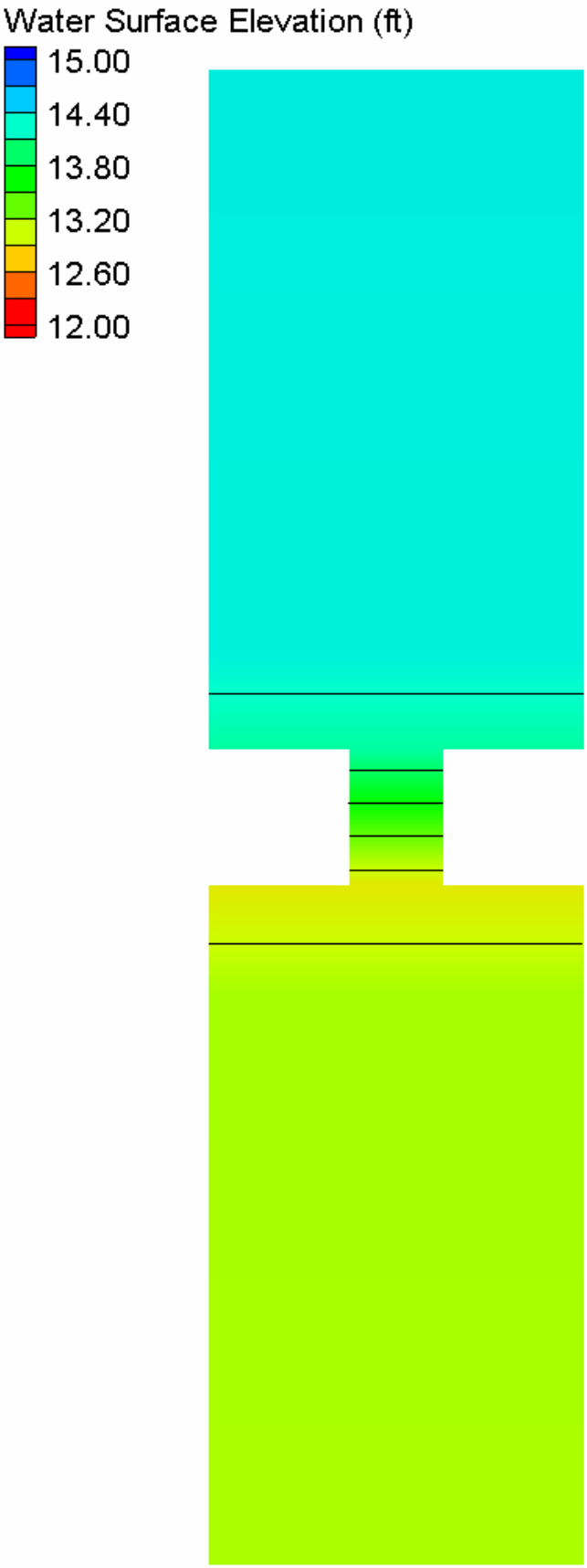

HEC-RAS Water Surface Elevation Contours – Small Channel – Constrictions (90%)

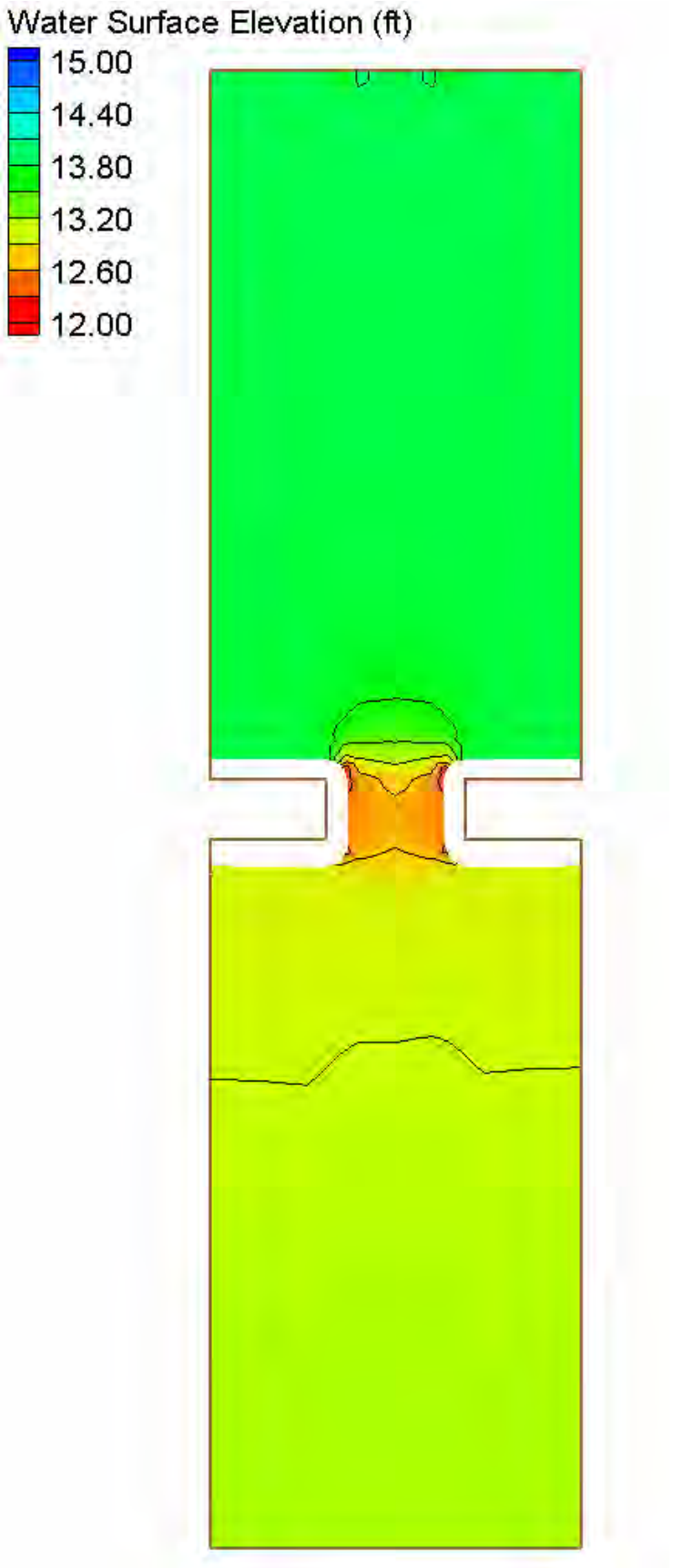

FESWMS Water Surface Elevation Contours – Small Channel – Constrictions (90%)

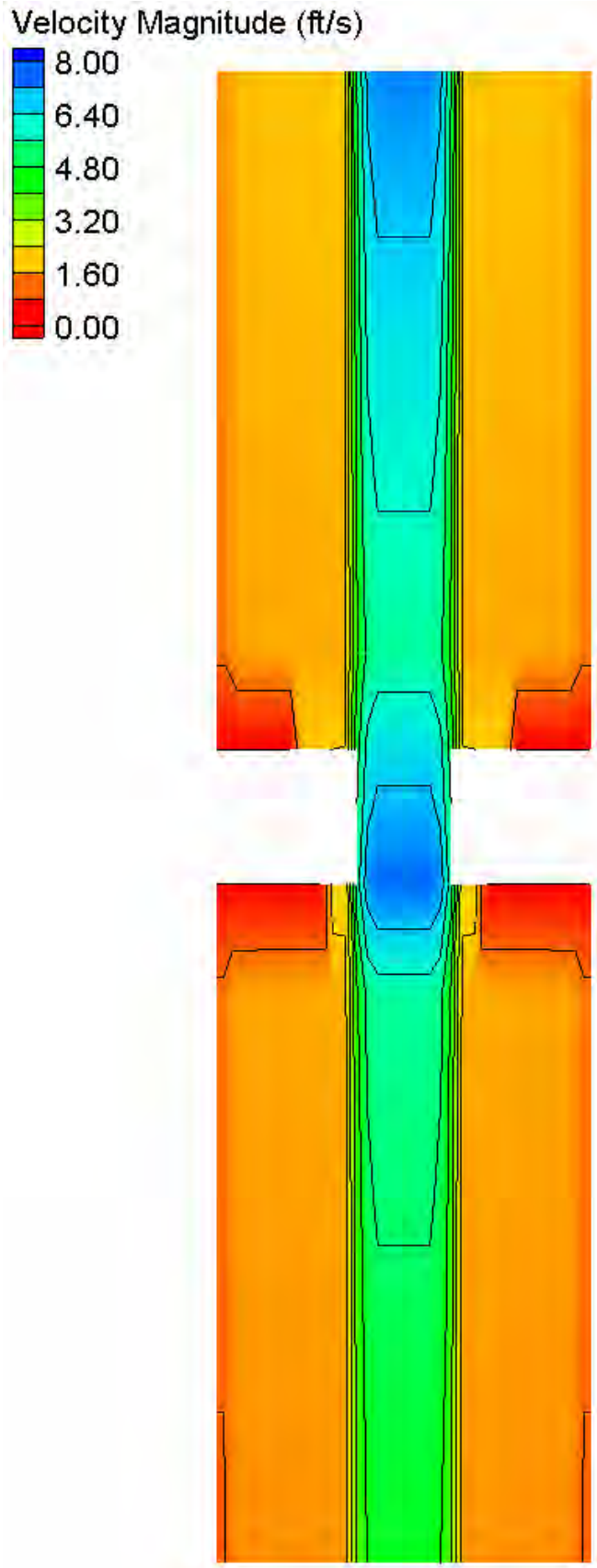

HEC-RAS Velocity Magnitude Contours – Small Channel – Constrictions (90%)

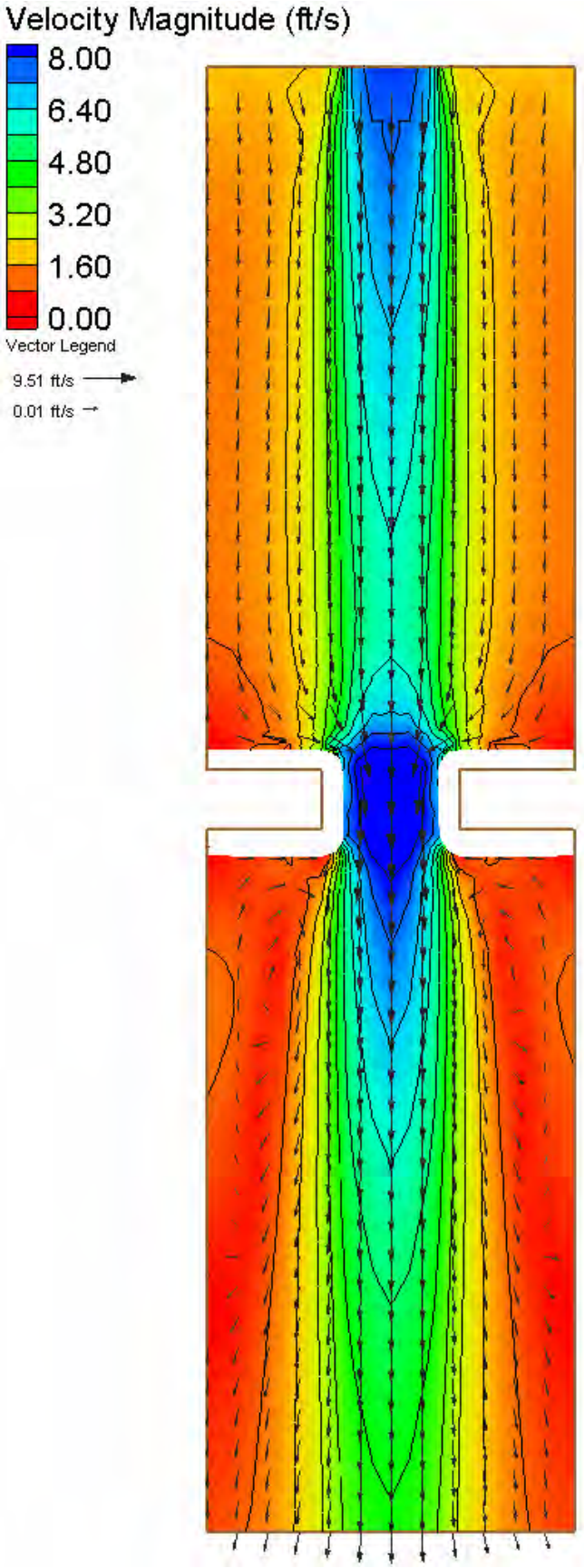

FESWMS Velocity Magnitude Contours – Small Channel – Constrictions (90%)

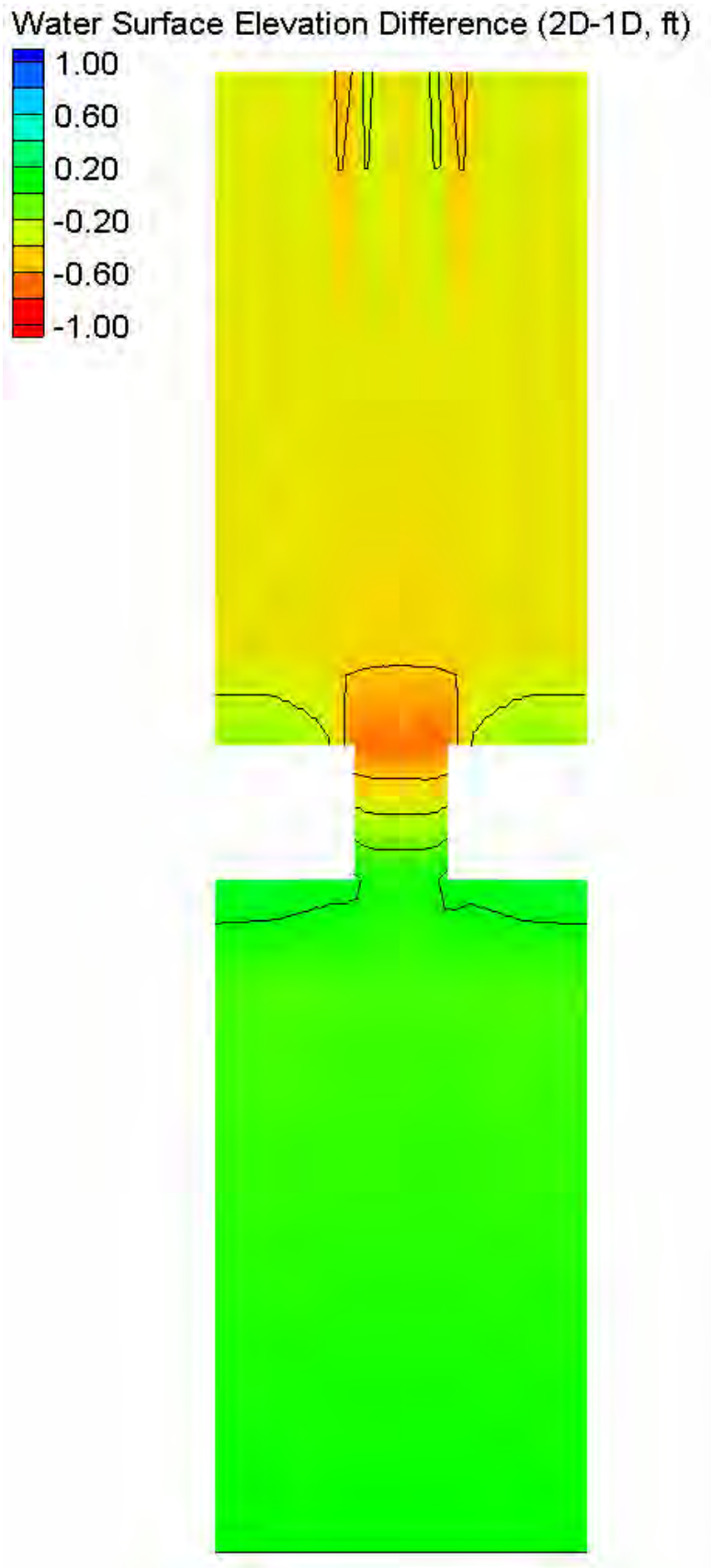

Water Surface Elevation Difference Contours – Small Channel – Constrictions (90%)

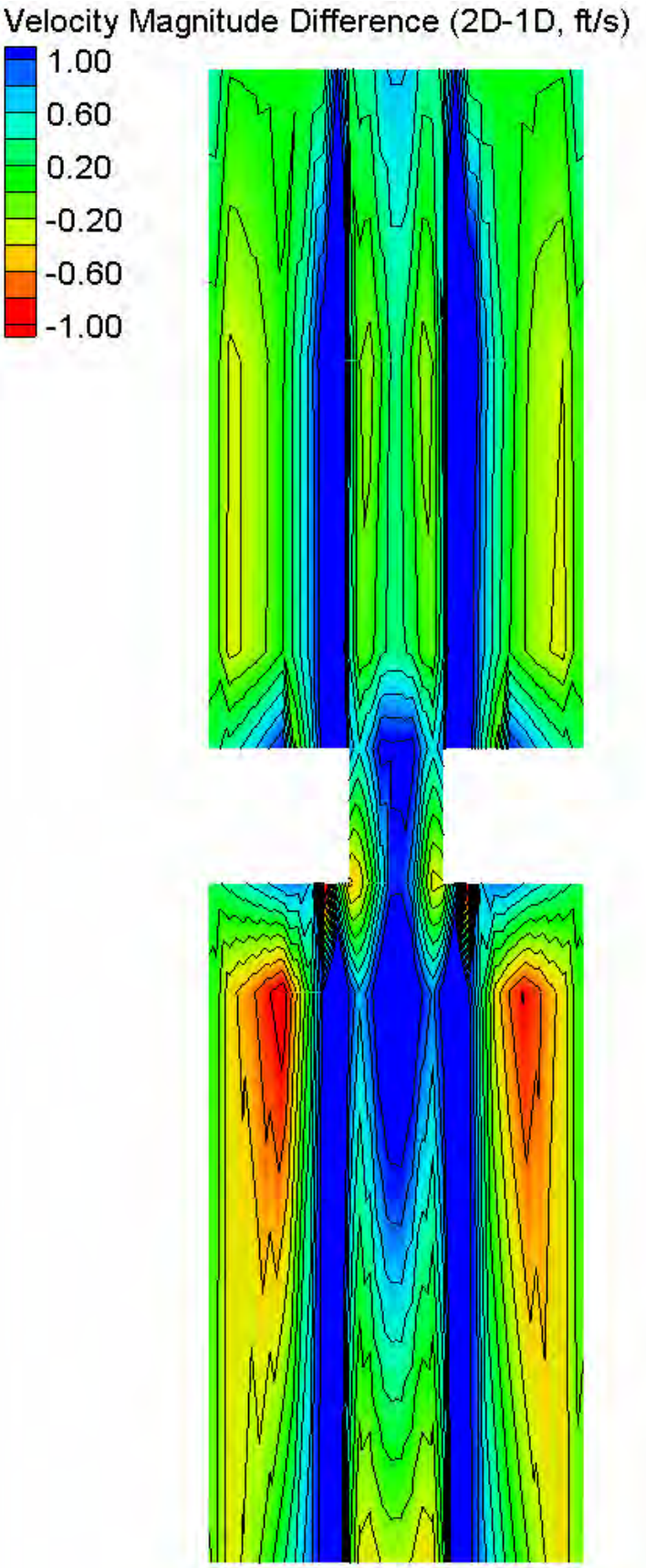

Velocity Magnitude Difference Contours – Small Channel – Constrictions (90%)

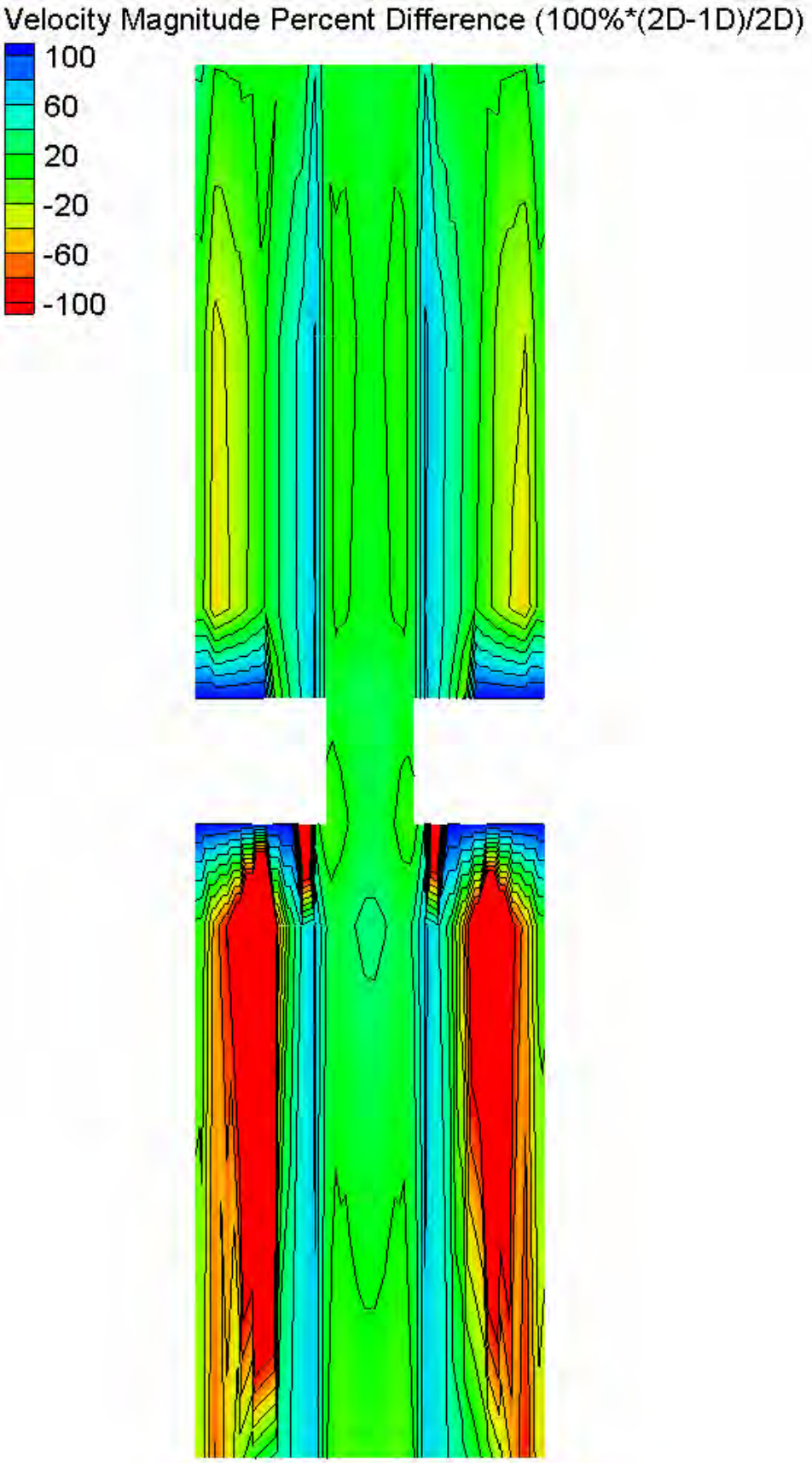

Velocity Magnitude Percent Difference Contours – Small Channel – Constrictions (90%)

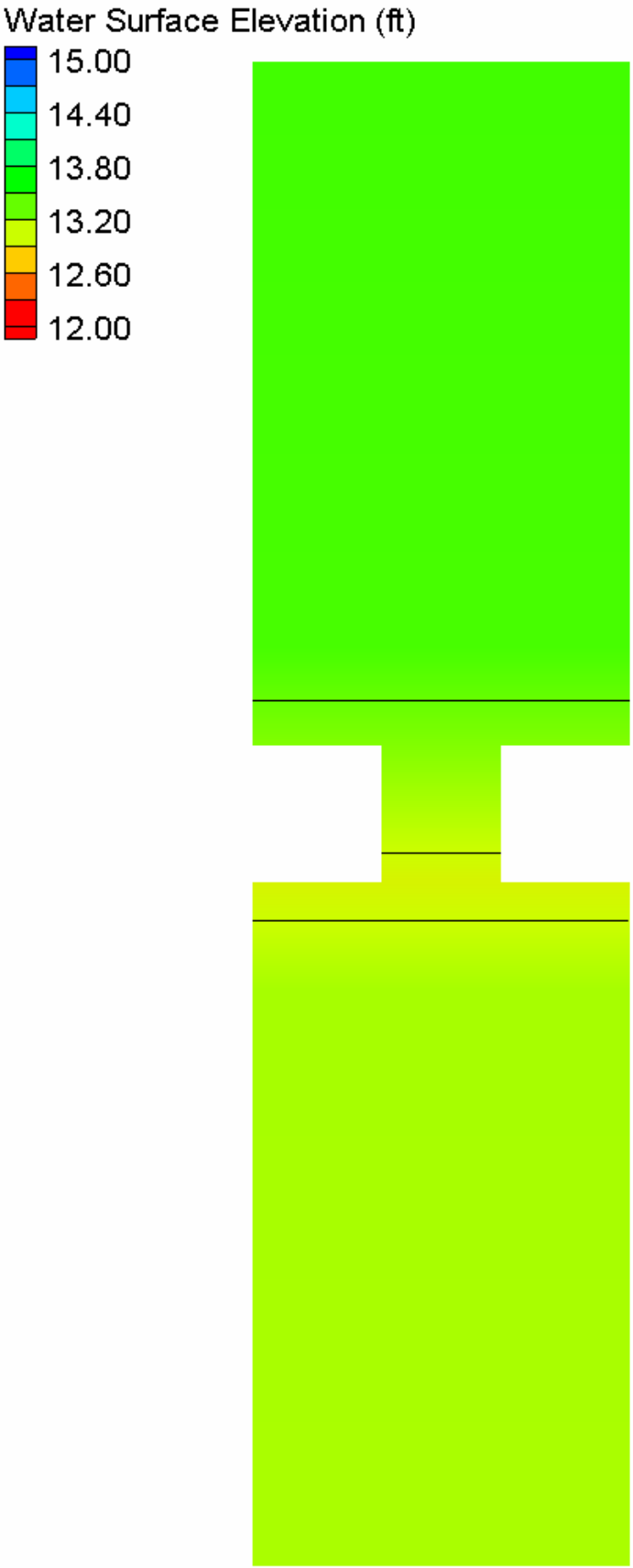

HEC-RAS Water Surface Elevation Contours – Small Channel – Constrictions (at banks)

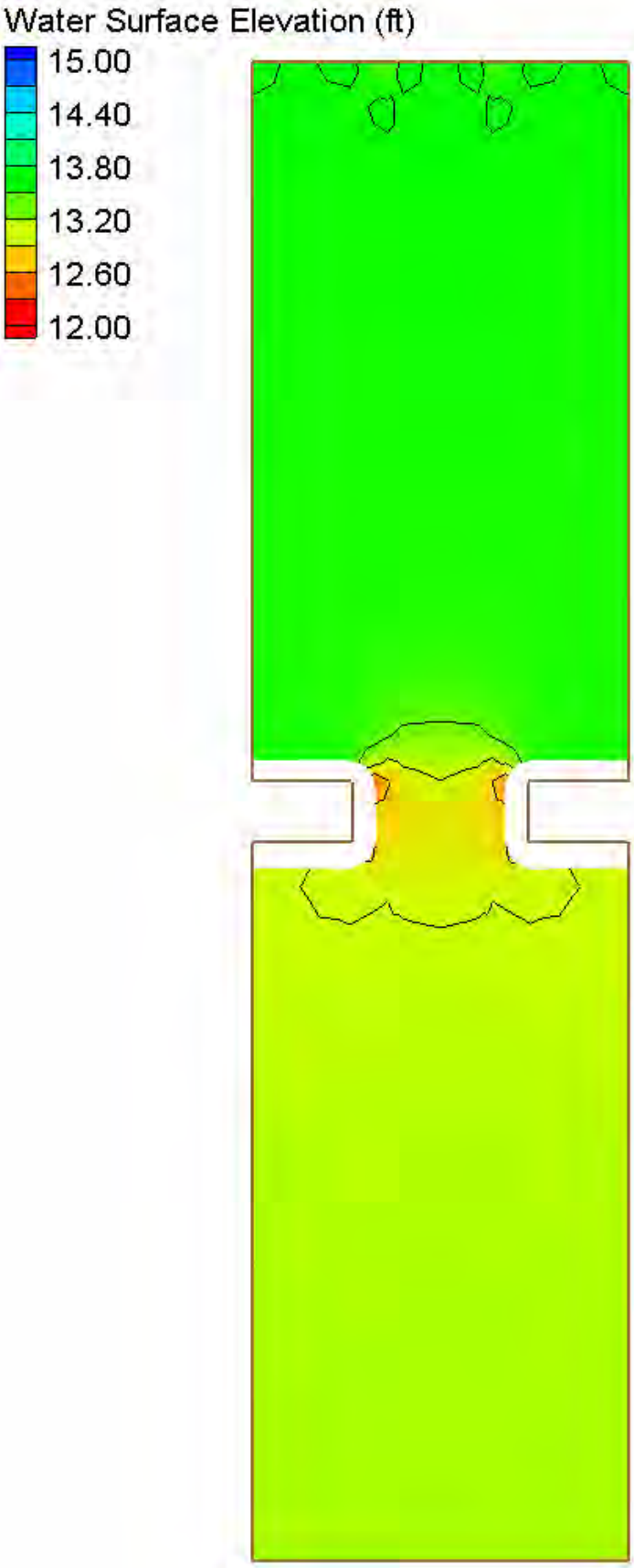

FESWMS Water Surface Elevation Contours – Small Channel – Constrictions (at banks)

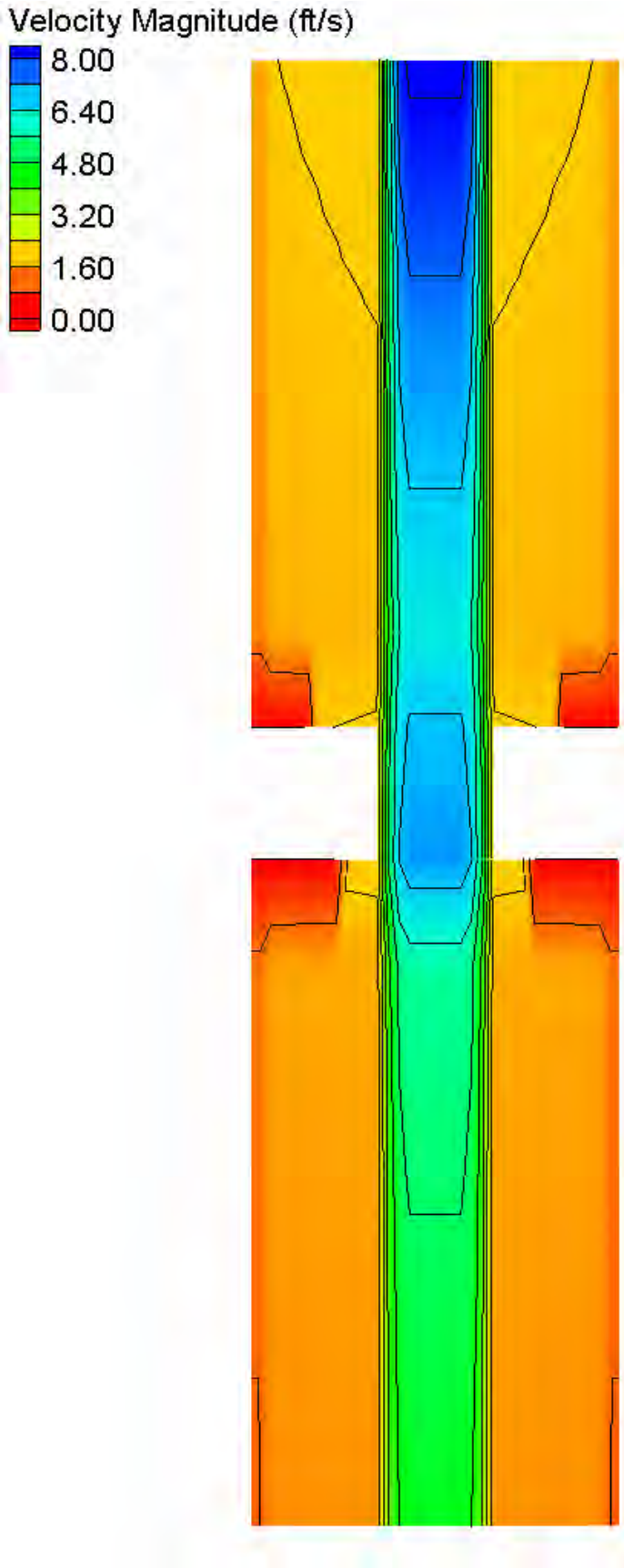

HEC-RAS Velocity Magnitude Contours – Small Channel – Constrictions (at banks)

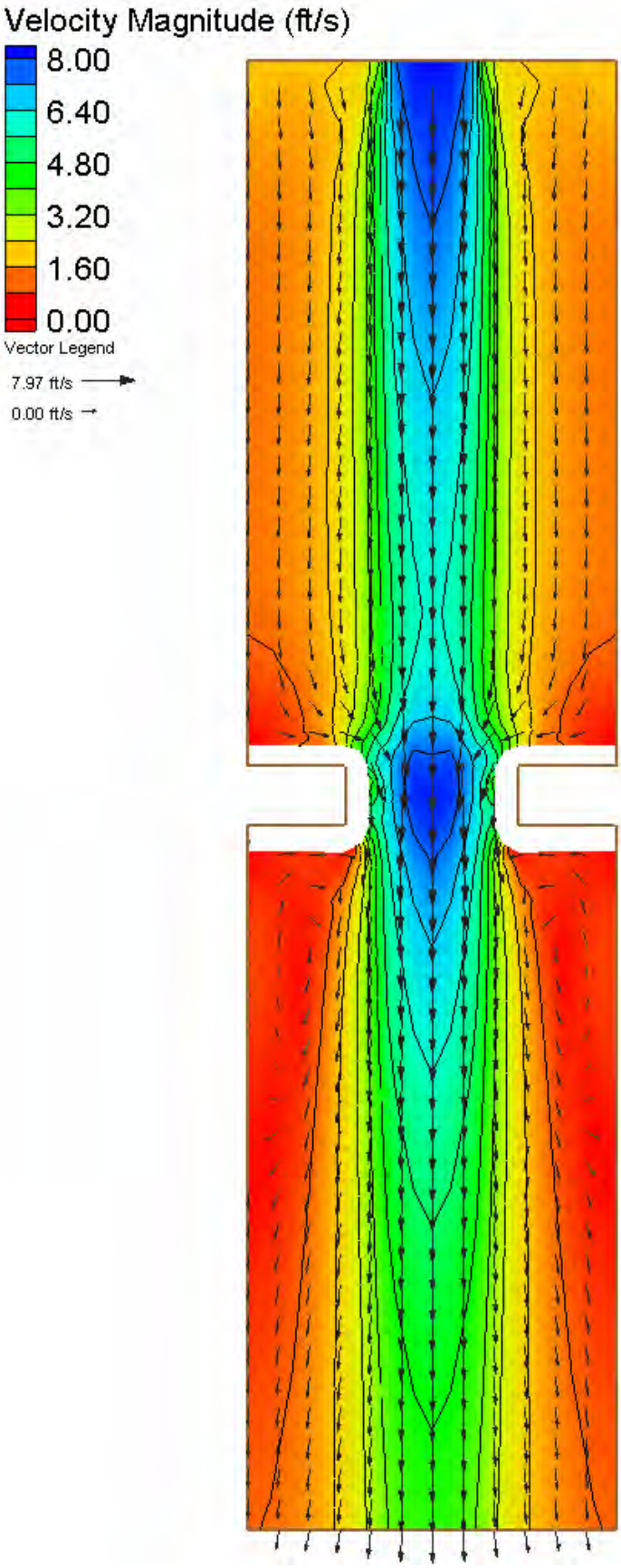

FESWMS Velocity Magnitude Contours – Small Channel – Constrictions (at banks)

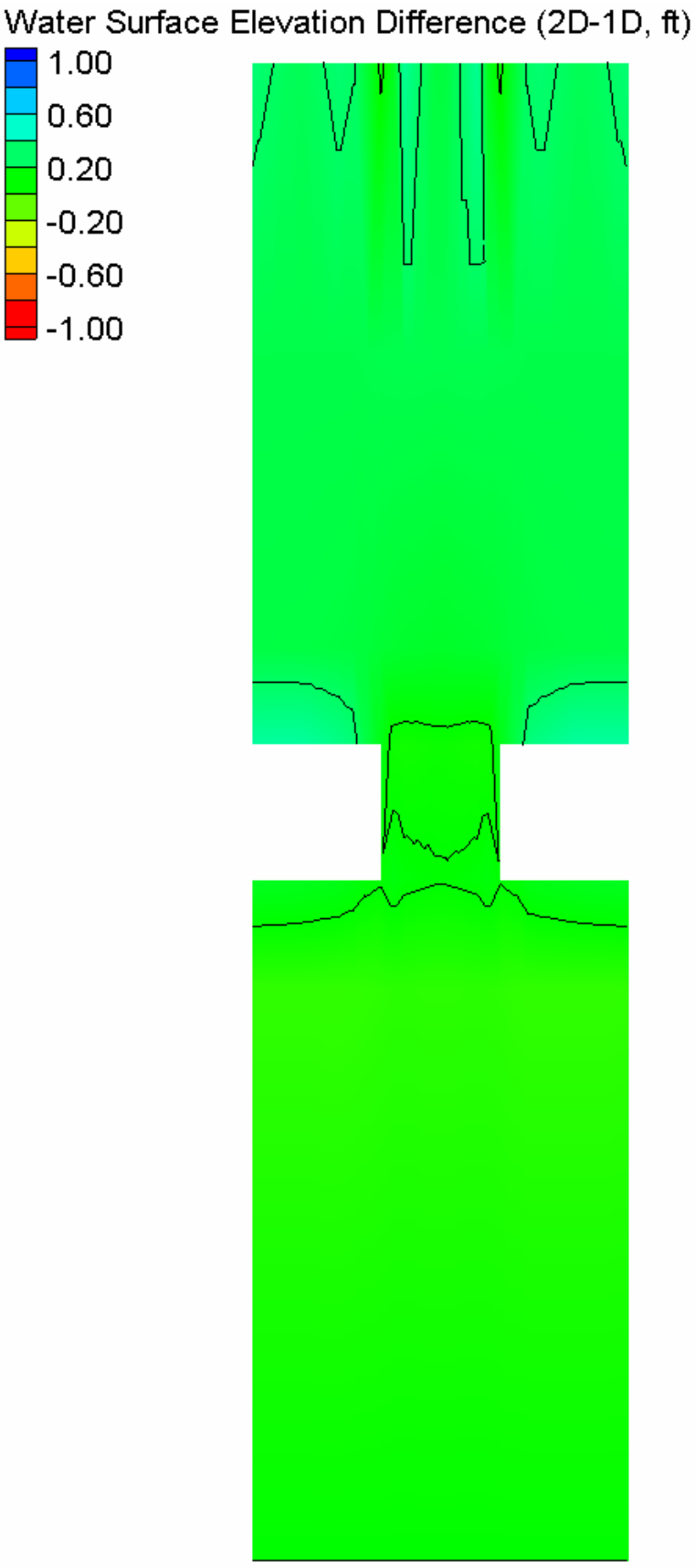

Water Surface Elevation Difference Contours – Small Channel – Constrictions (at banks)

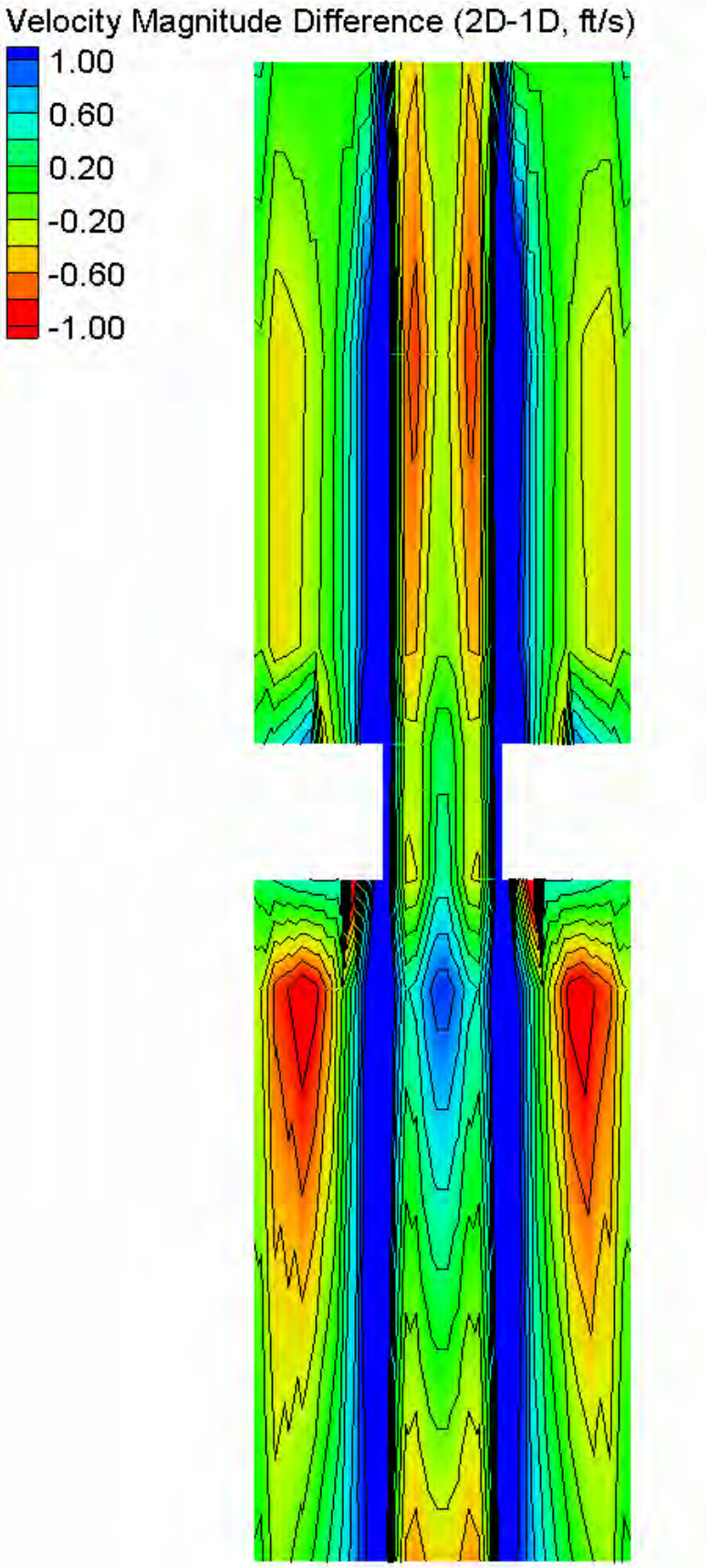

Velocity Magnitude Difference Contours – Small Channel – Constrictions (at banks)

Velocity Magnitude Percent Difference Contours – Small Channel – Constrictions (at banks)

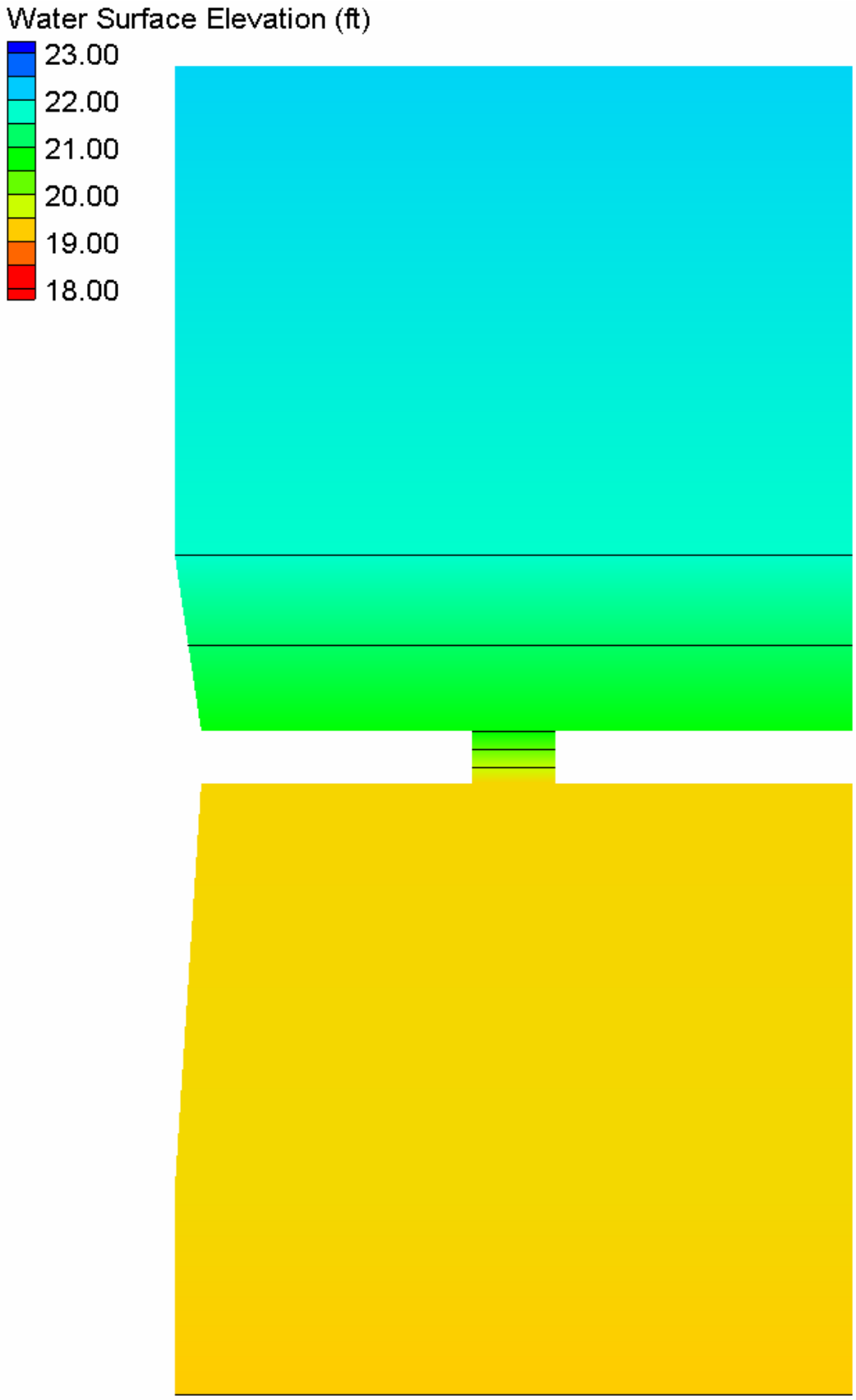

HEC-RAS Water Surface Elevation Contours – Large Channel – Constrictions (75%)

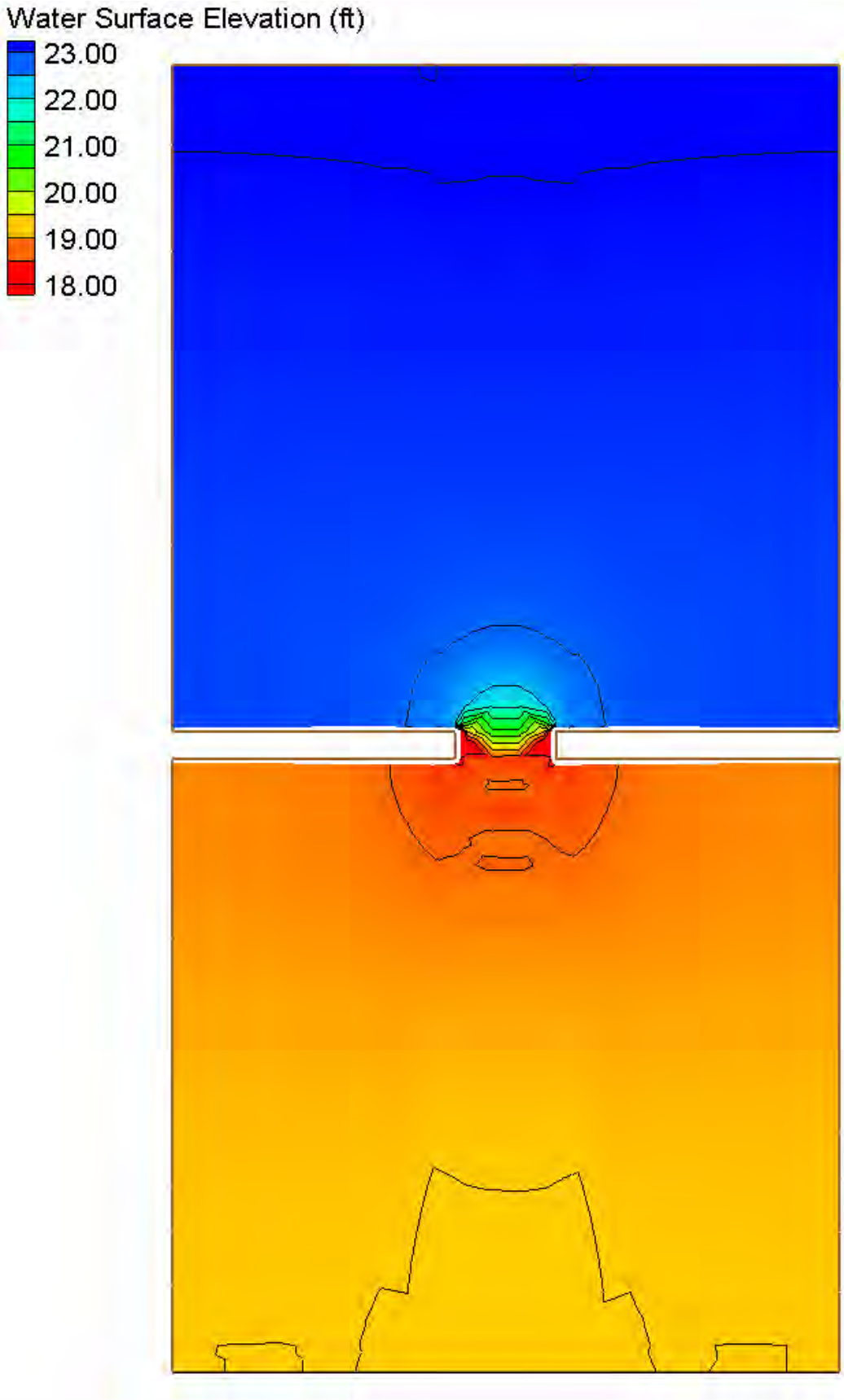

FESWMS Water Surface Elevation Contours – Large Channel – Constrictions (75%)

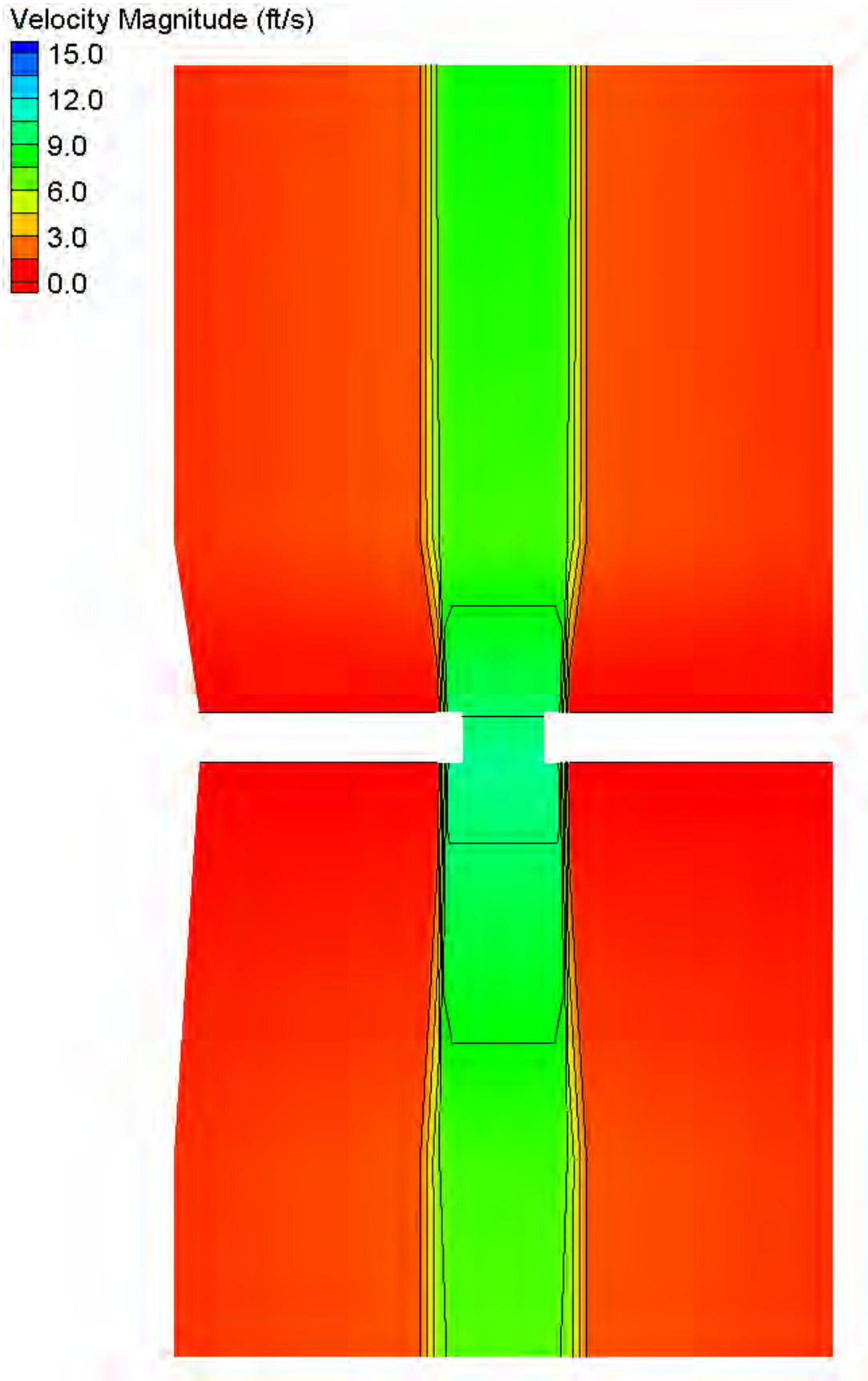

HEC-RAS Velocity Magnitude Contours – Large Channel – Constrictions (75%)

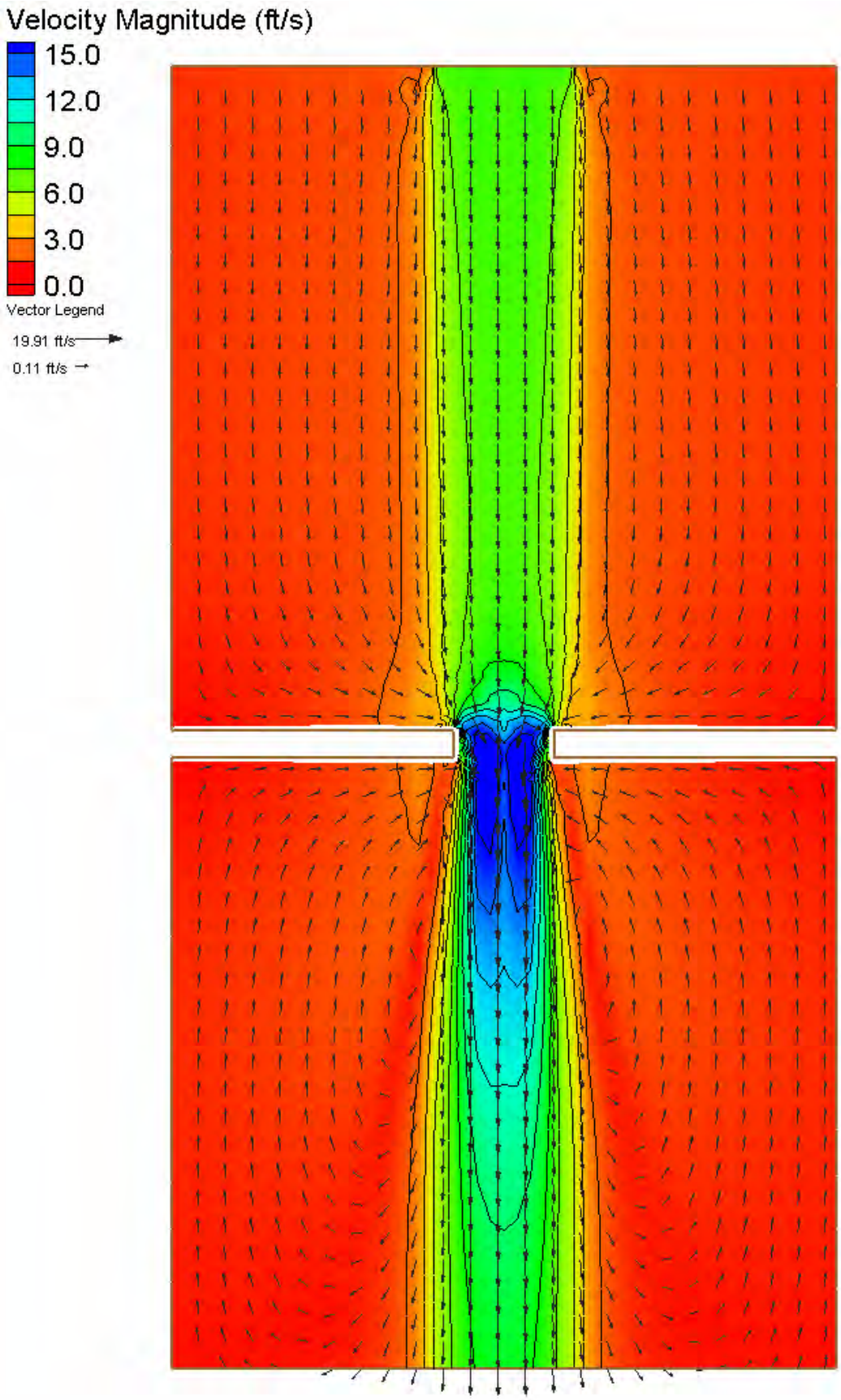

FESWMS Velocity Magnitude Contours – Large Channel – Constrictions (75%)

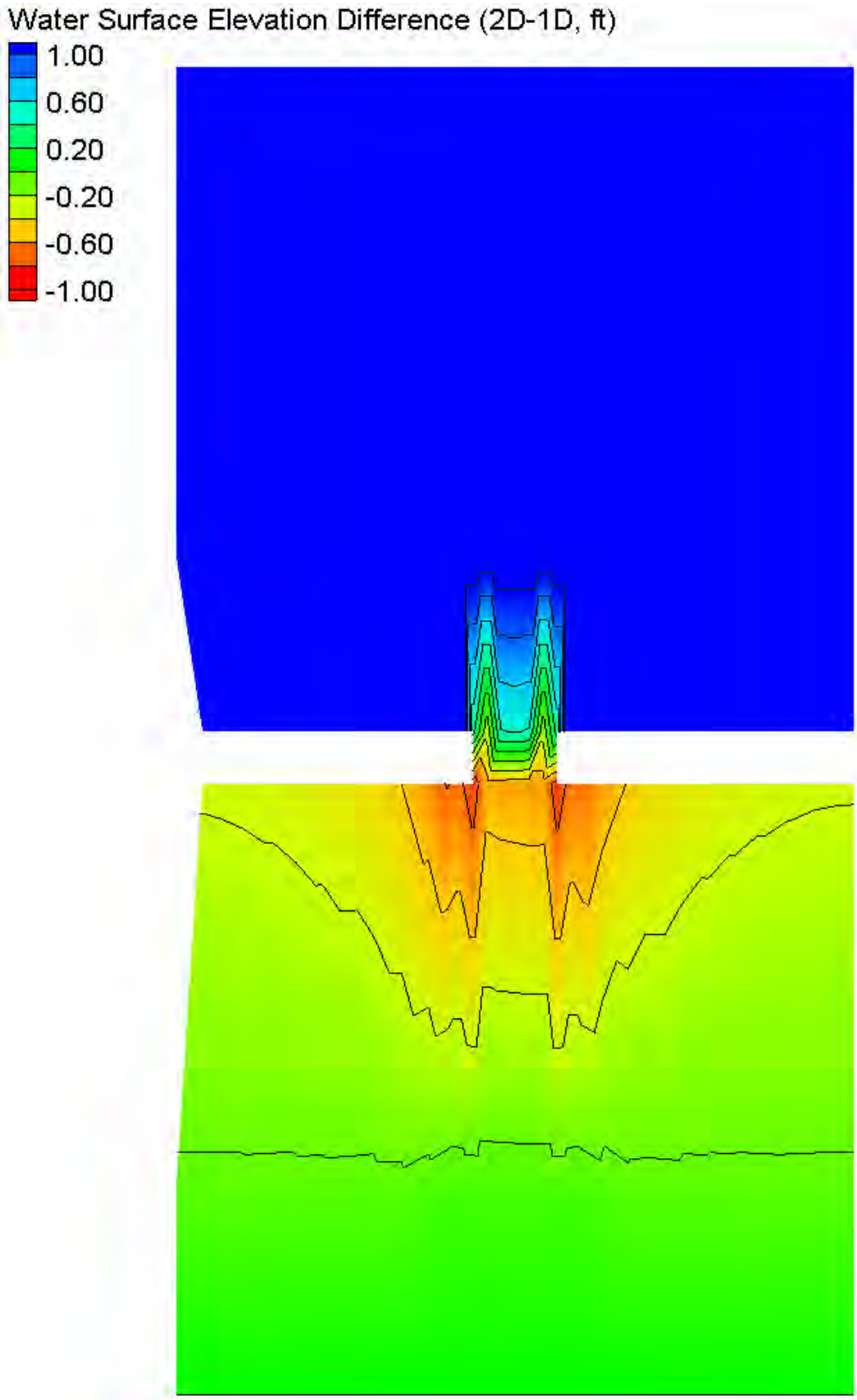

Water Surface Elevation Difference Contours – Large Channel – Constrictions (75%)

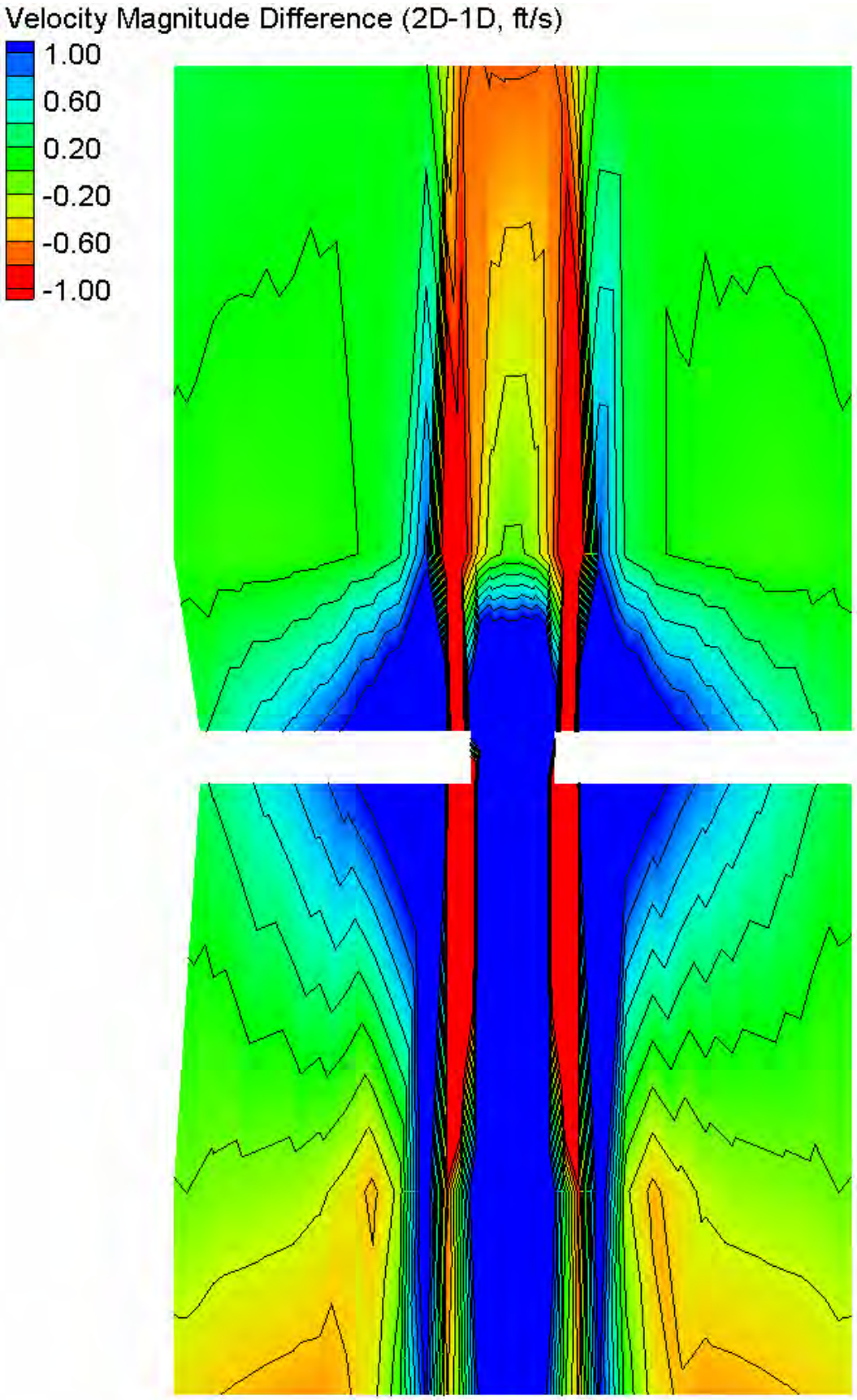

Velocity Magnitude Difference Contours – Large Channel – Constrictions (75%)

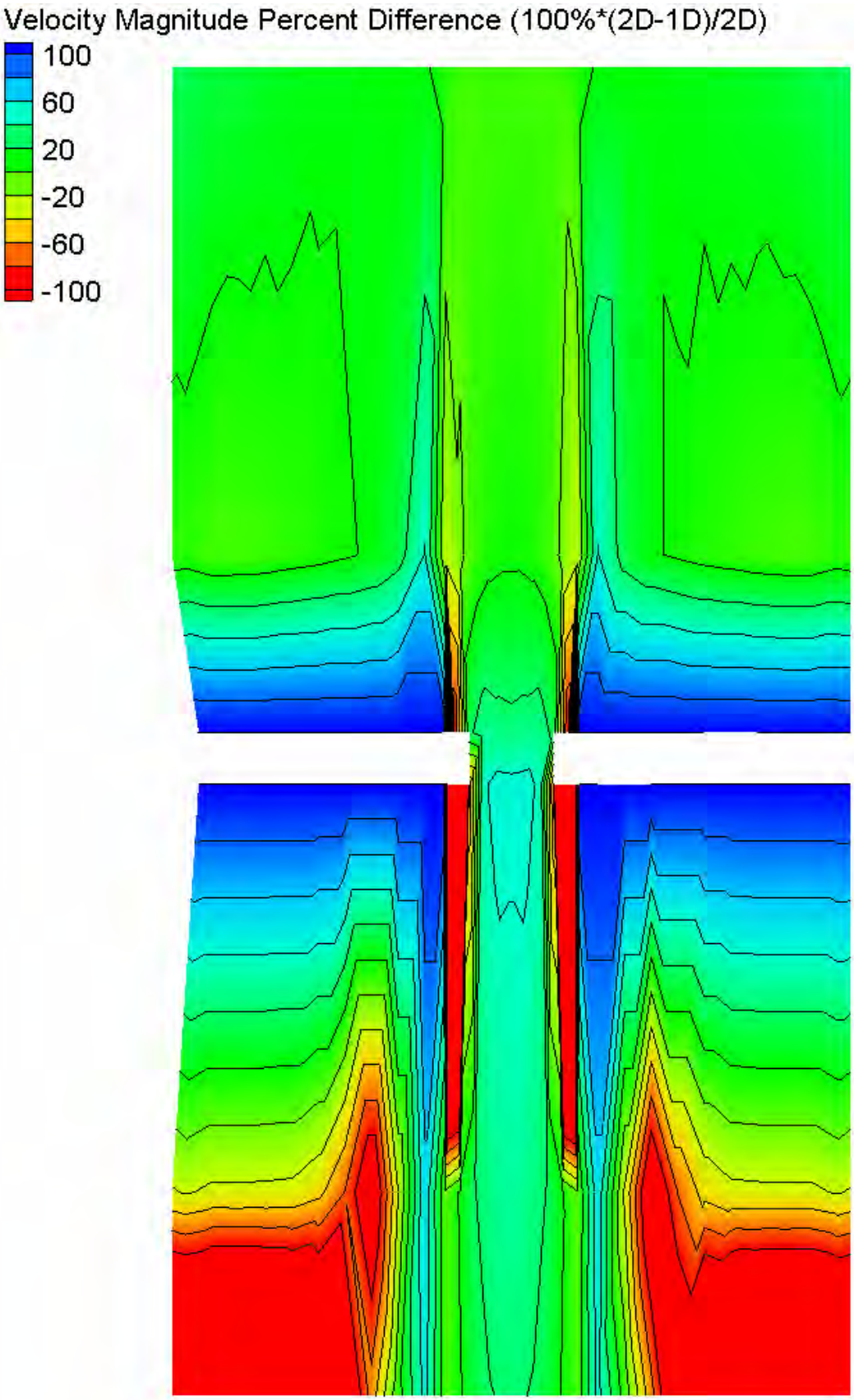

Velocity Magnitude Percent Difference Contours – Large Channel – Constrictions (75%)

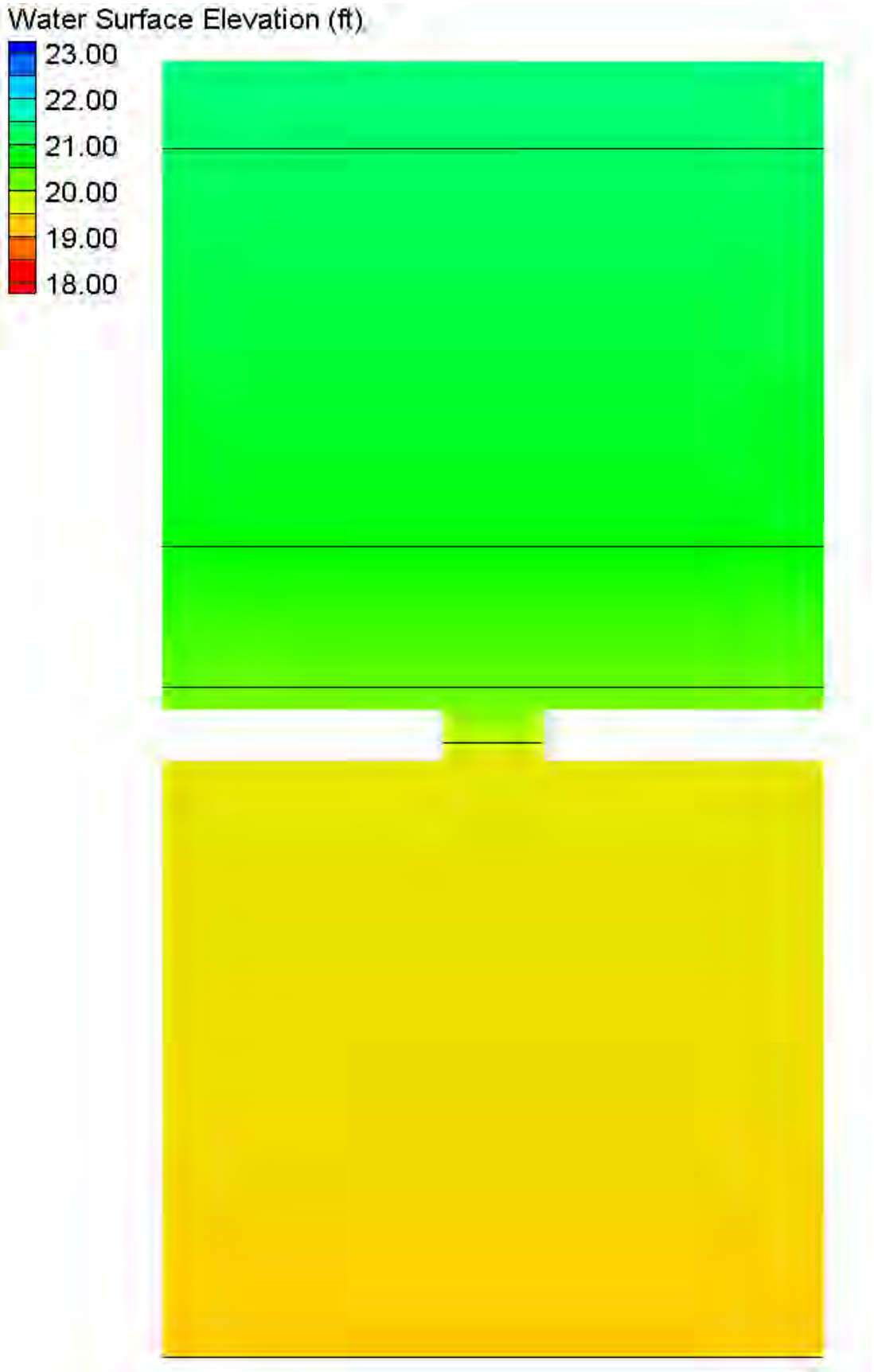

HEC-RAS Water Surface Elevation Contours – Large Channel – Constrictions (90%)

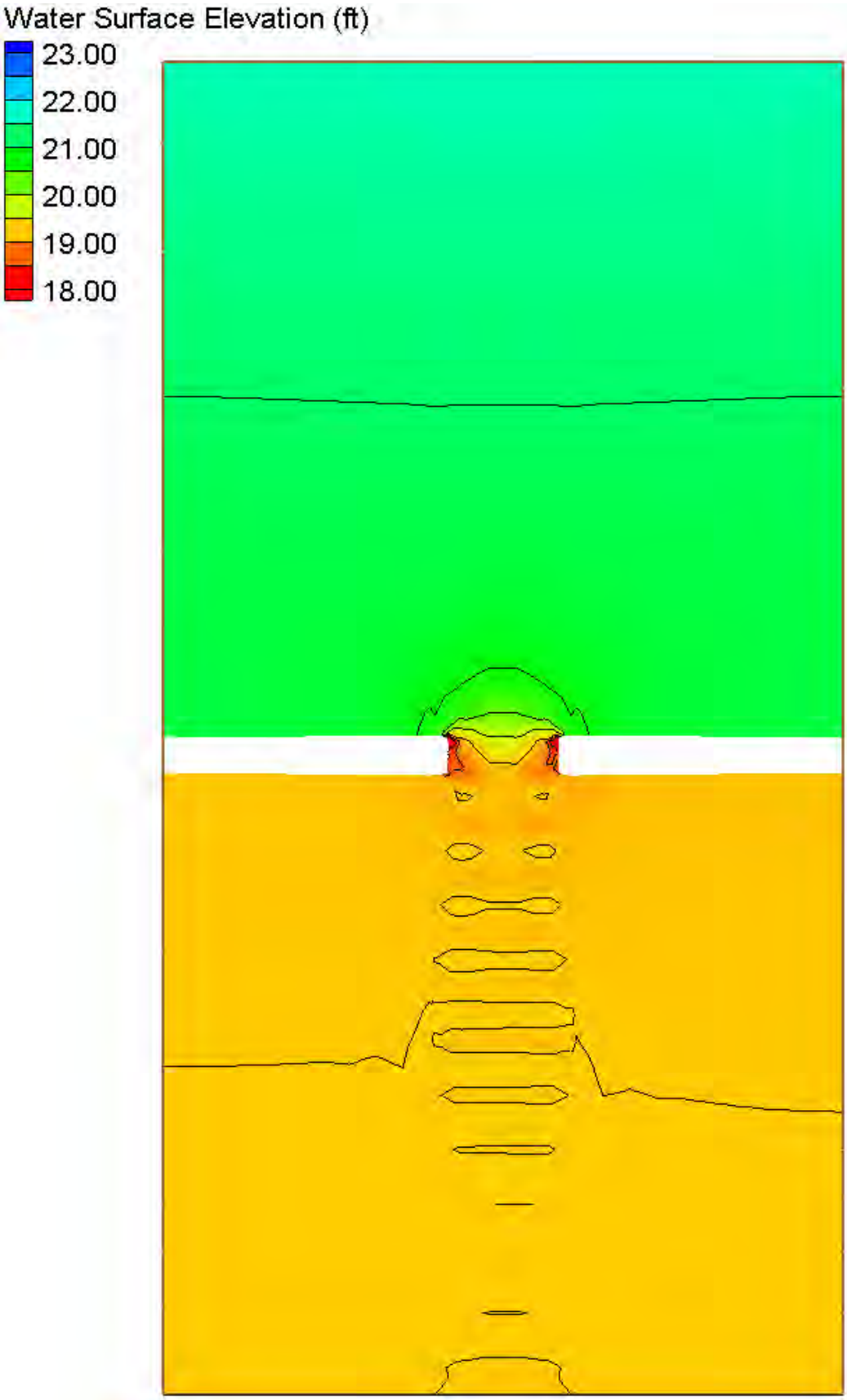

FESWMS Water Surface Elevation Contours – Large Channel – Constrictions (90%)

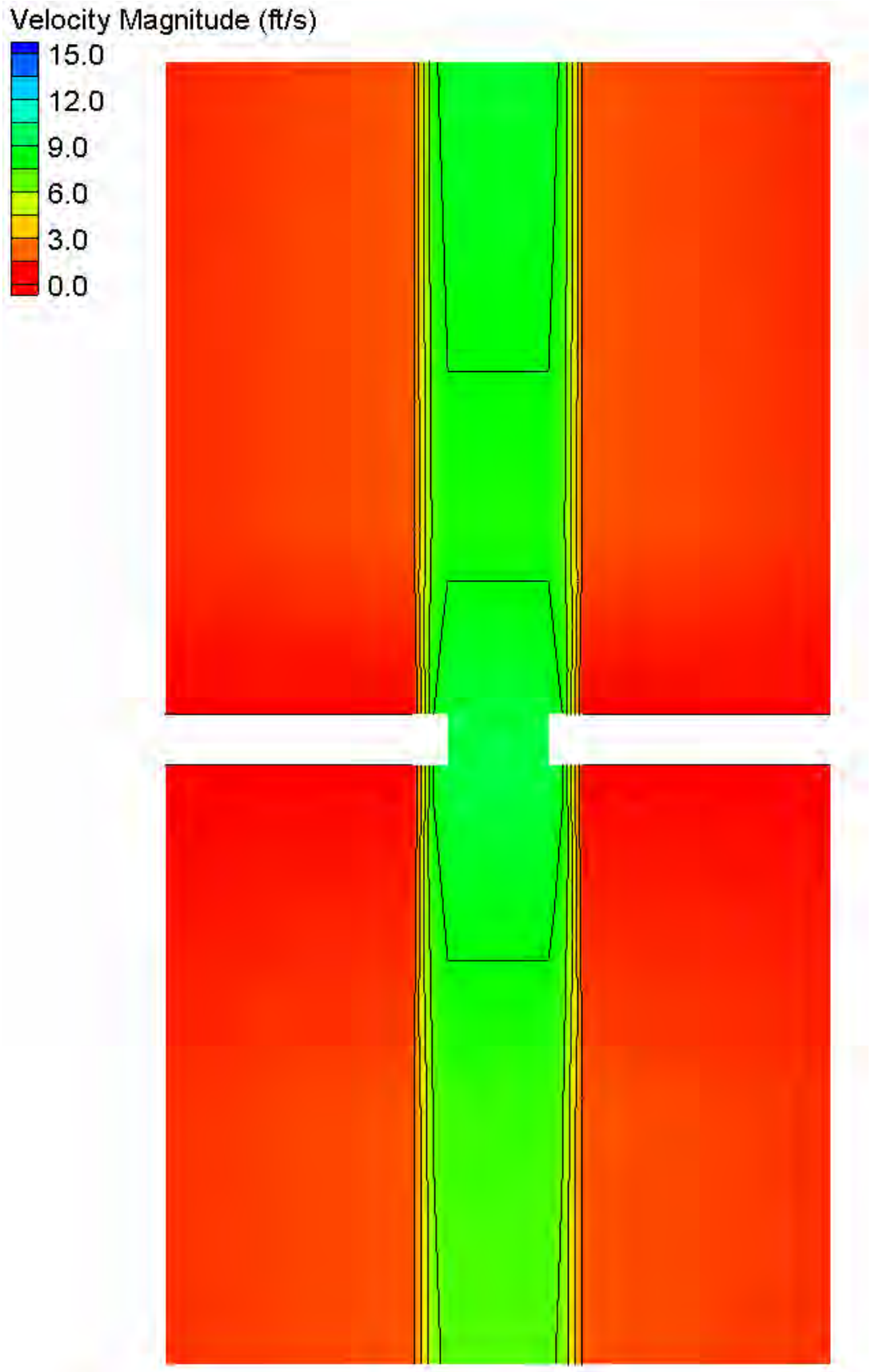

HEC-RAS Velocity Magnitude Contours – Large Channel – Constrictions (90%)

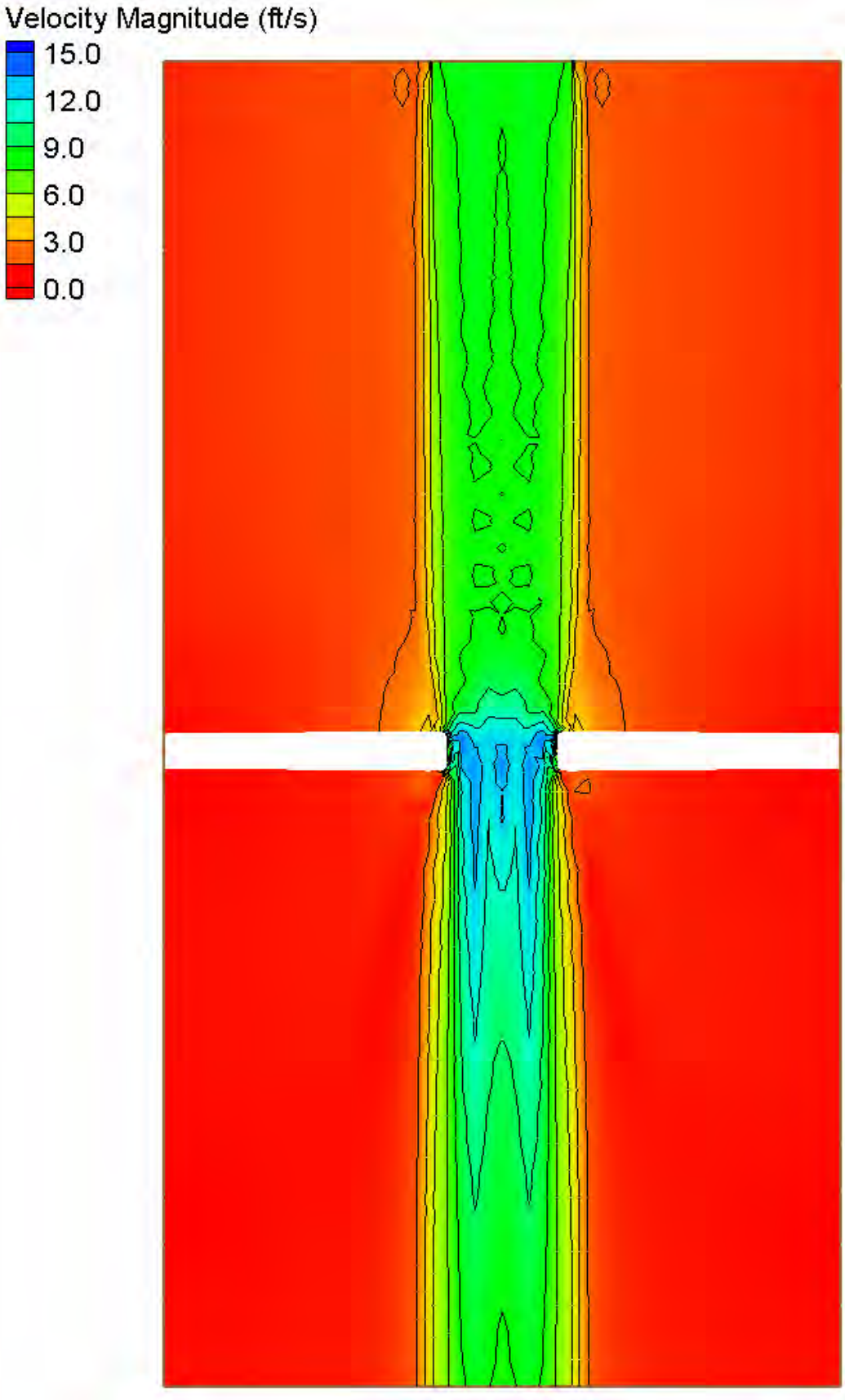

FESWMS Velocity Magnitude Contours – Large Channel – Constrictions (90%)

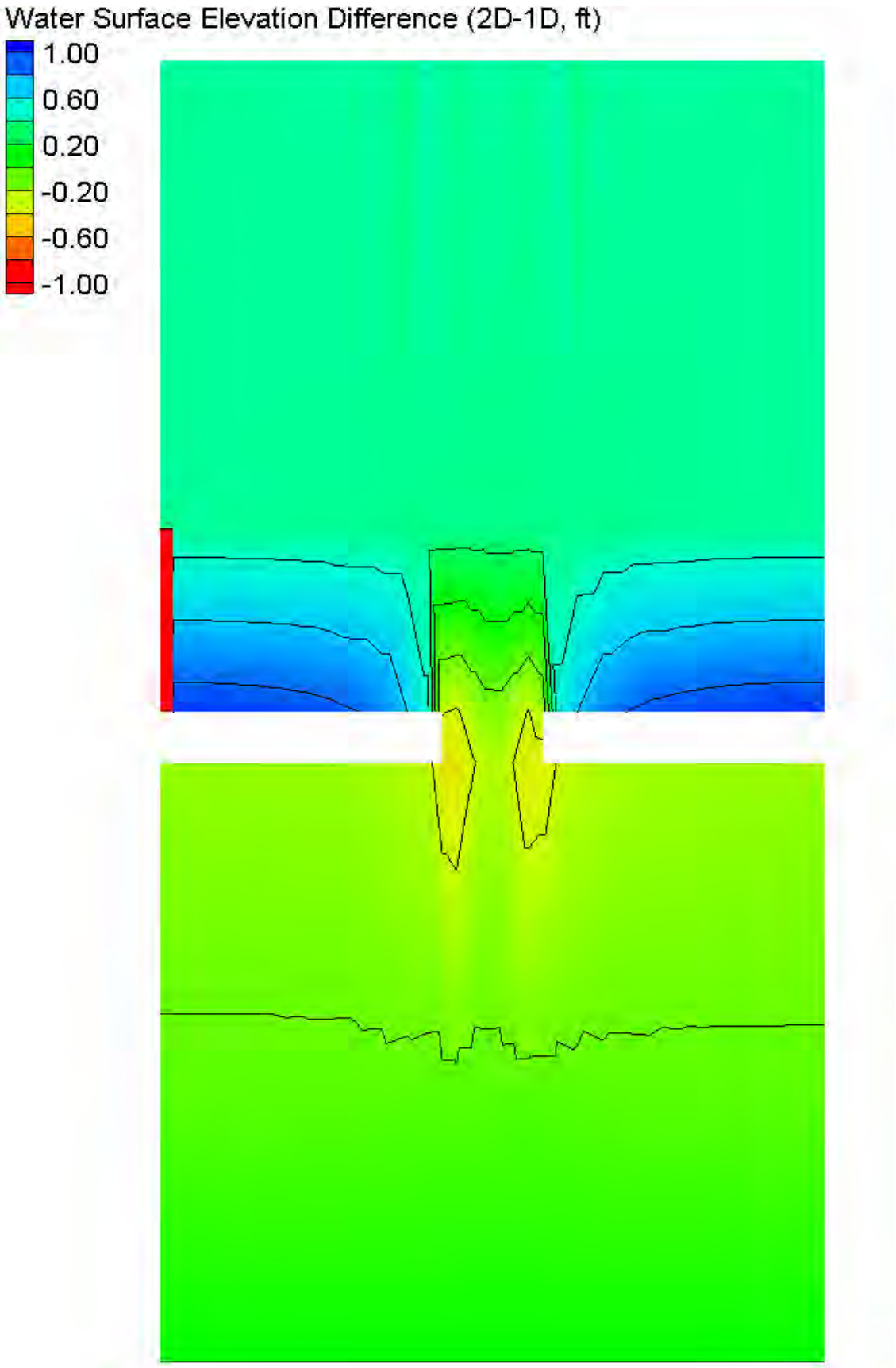

Water Surface Elevation Difference Contours – Large Channel – Constrictions (90%)

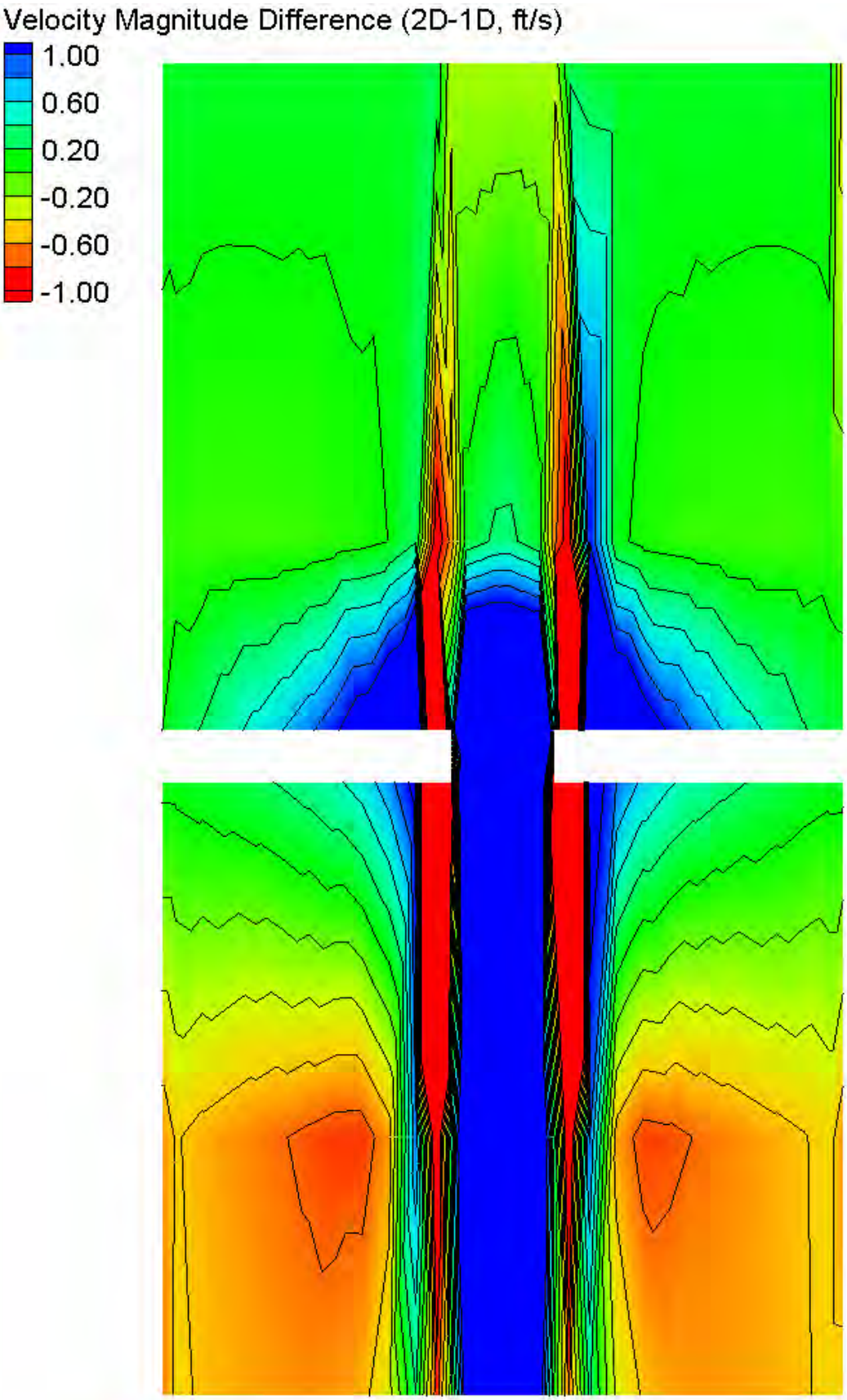

Velocity Magnitude Difference Contours – Large Channel – Constrictions (90%)

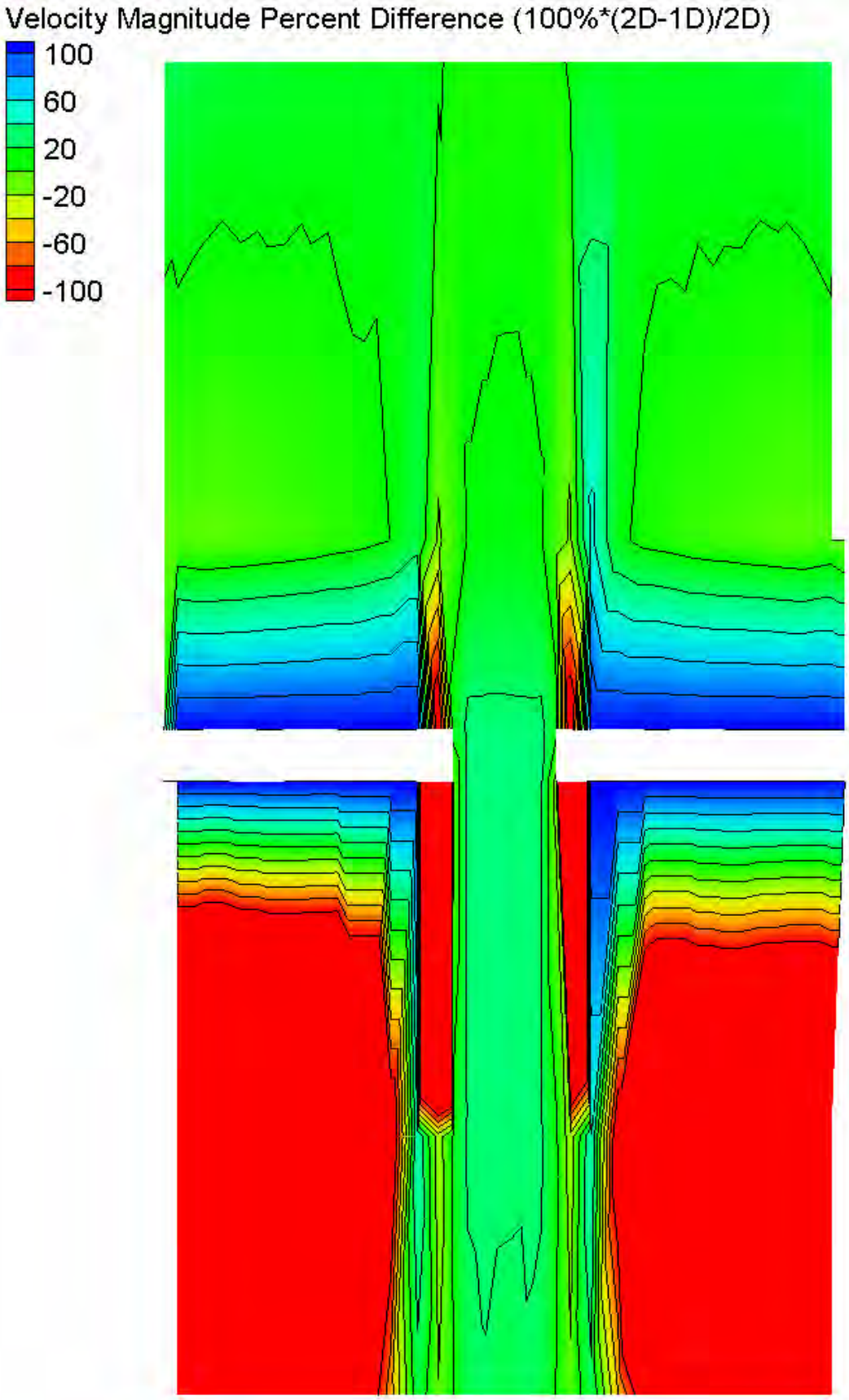

Velocity Magnitude Percent Difference Contours – Large Channel – Constrictions (90%)

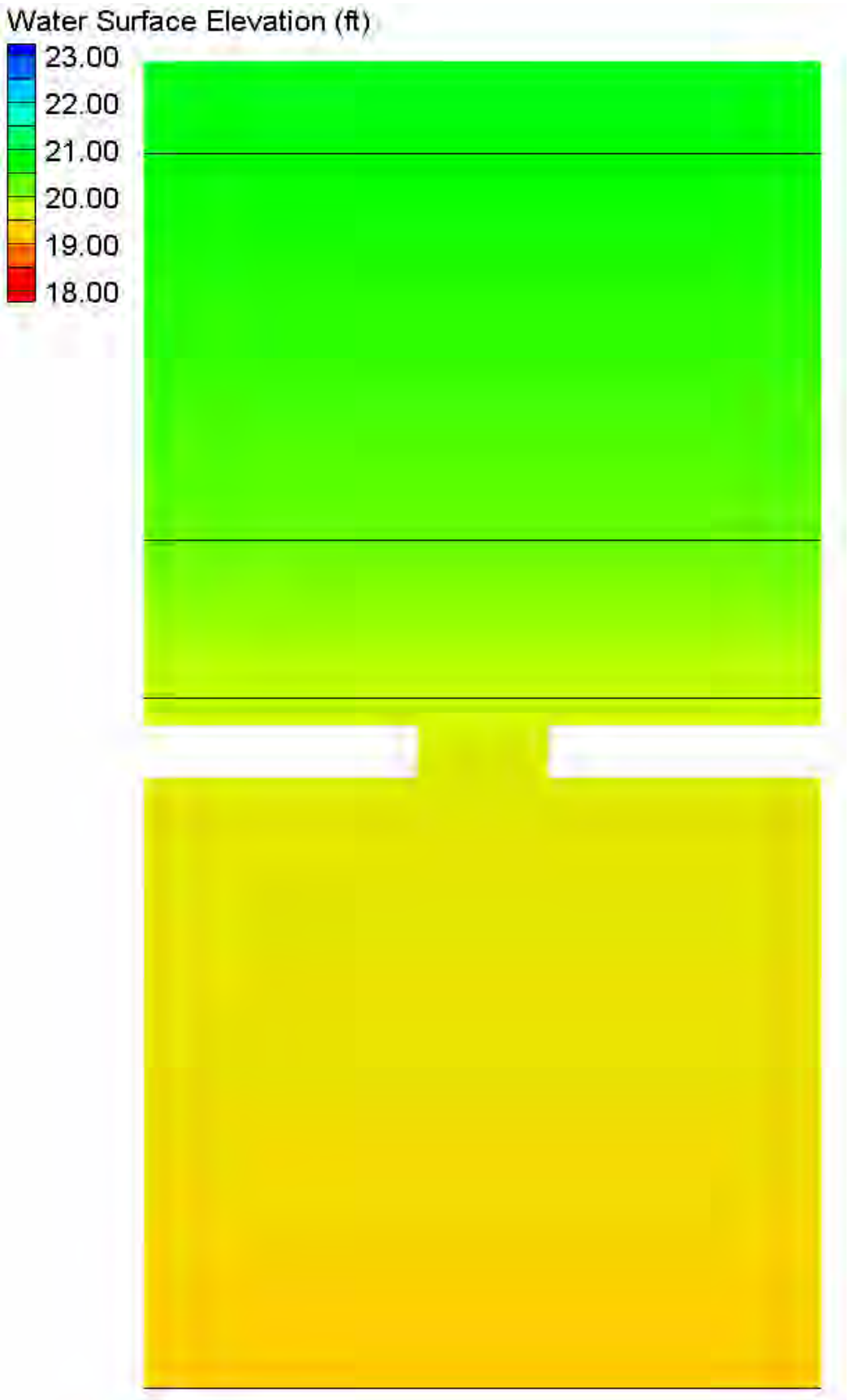

HEC-RAS Water Surface Elevation Contours – Large Channel – Constrictions (at banks)

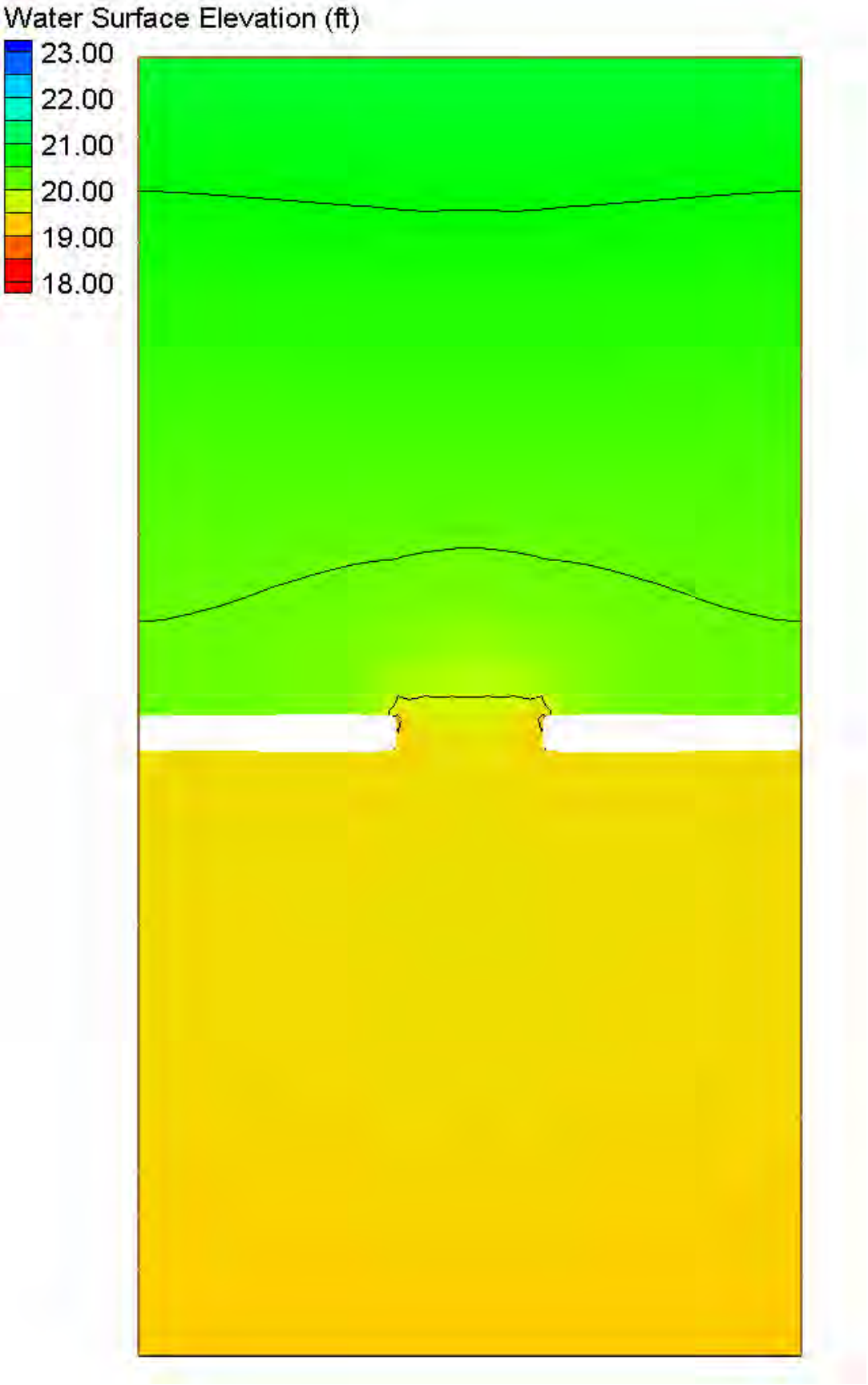

FESWMS Water Surface Elevation Contours – Large Channel – Constrictions (at banks)

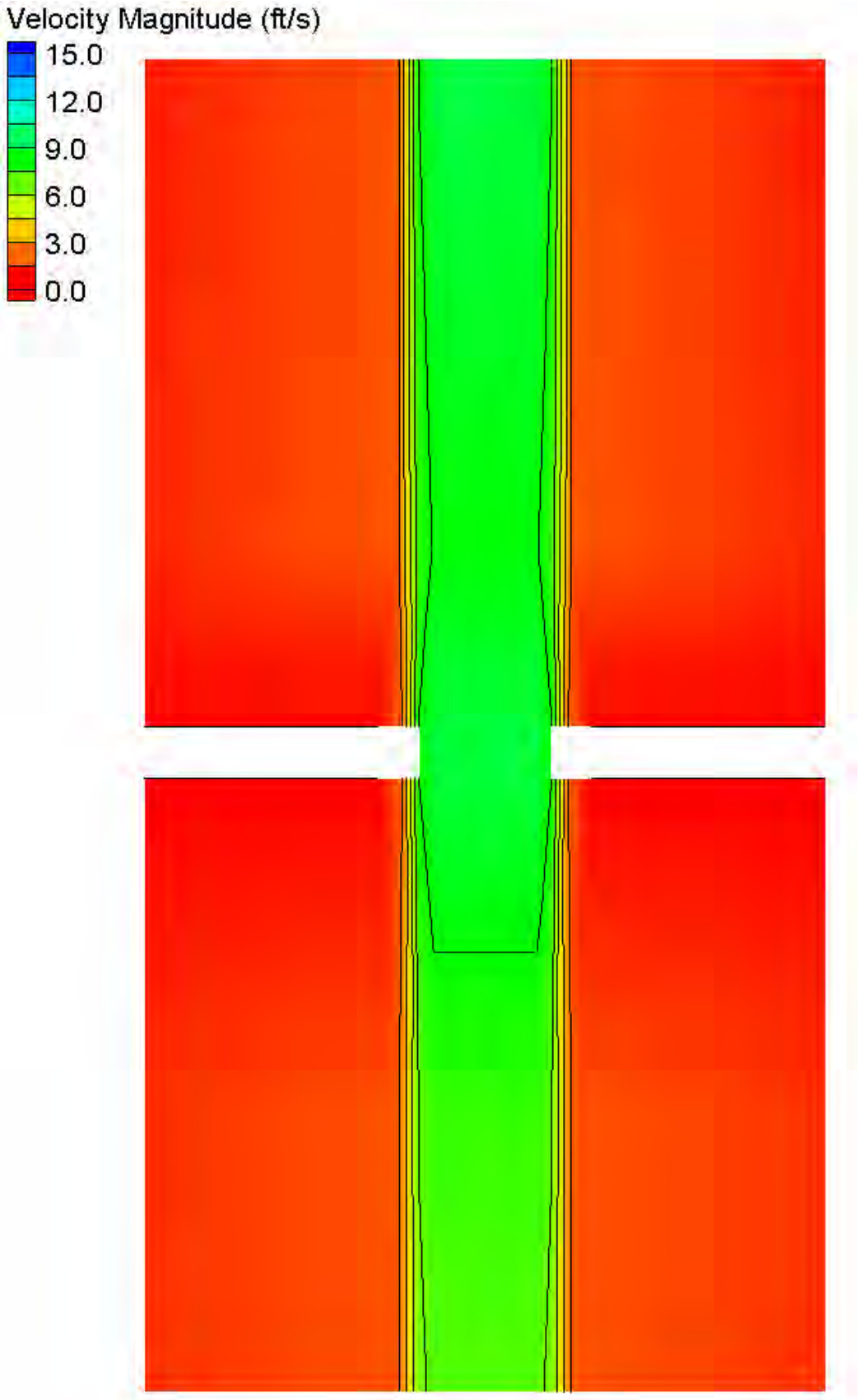

HEC-RAS Velocity Magnitude Contours – Large Channel – Constrictions (at banks)

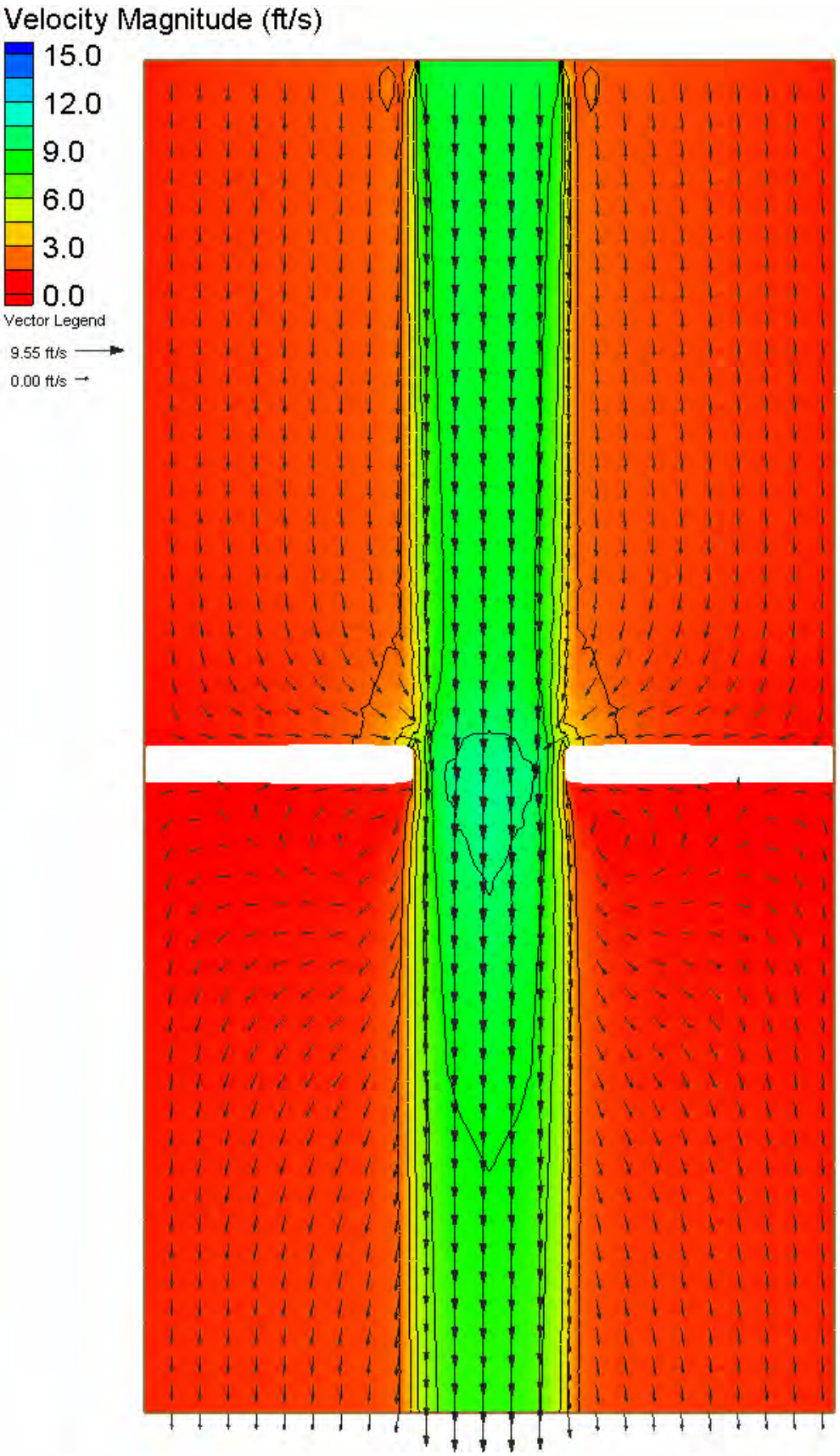

FESWMS Velocity Magnitude Contours – Large Channel – Constrictions (at banks)

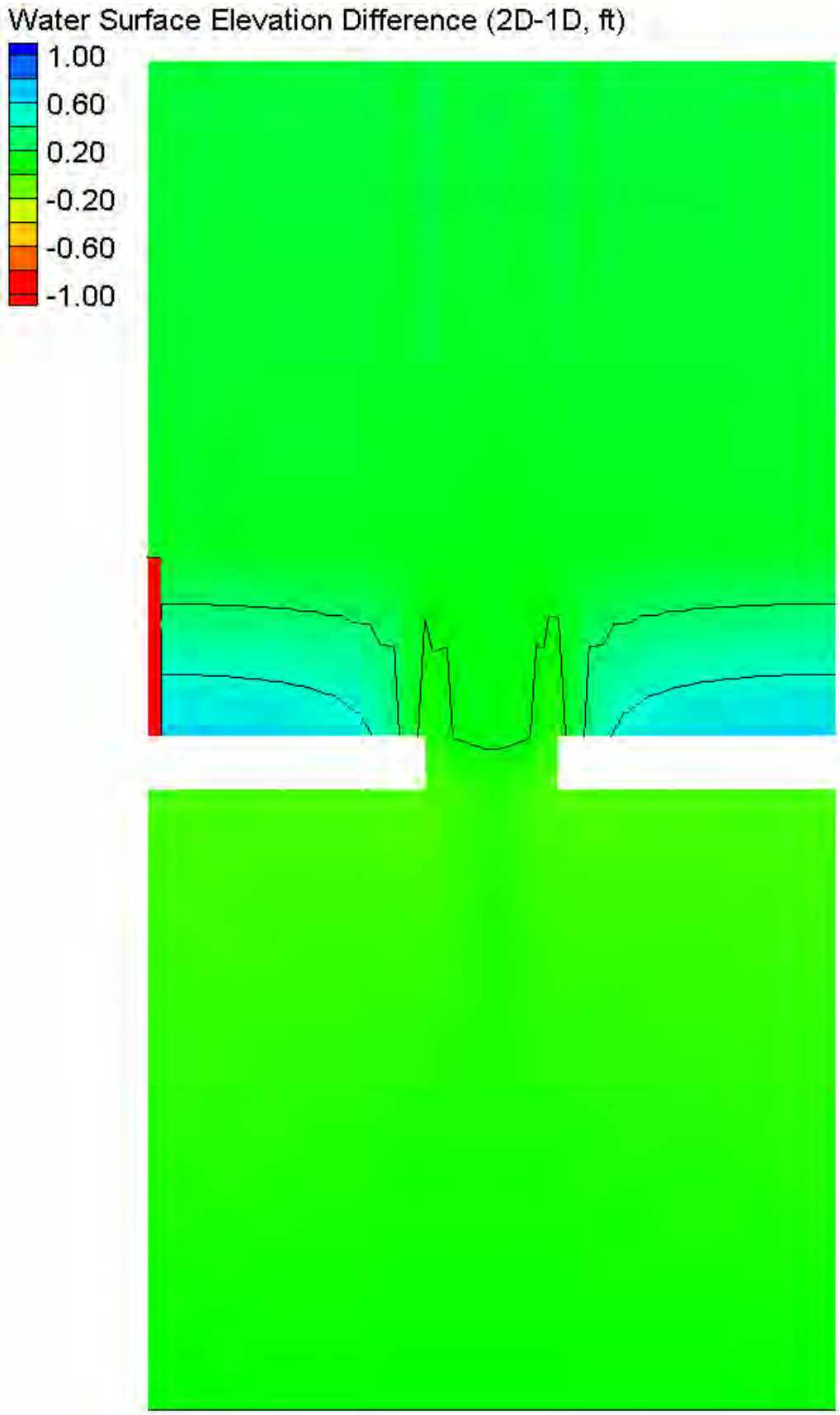

Water Surface Elevation Difference Contours – Large Channel – Constrictions (at banks)

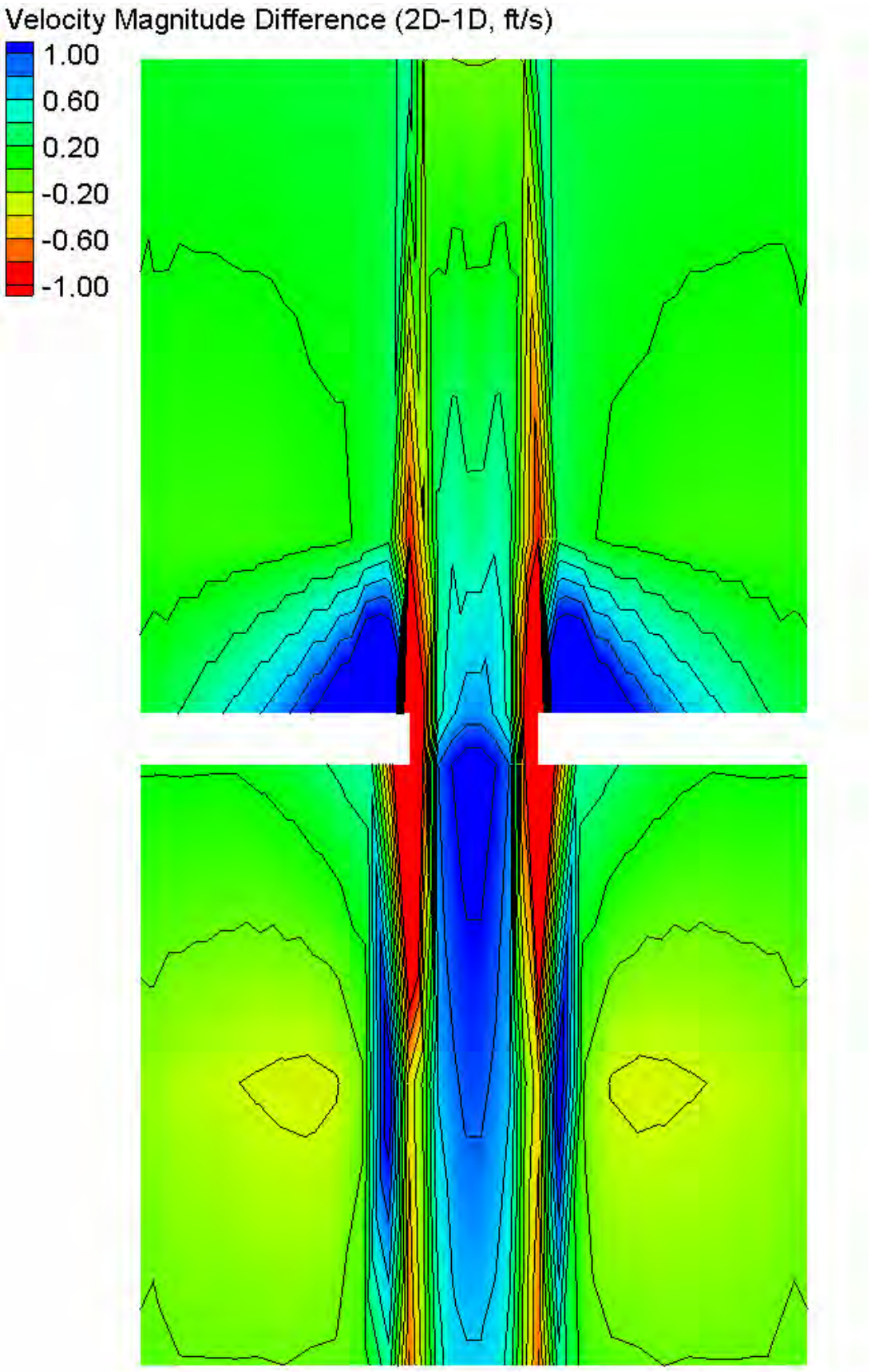

Velocity Magnitude Difference Contours – Large Channel – Constrictions (at banks)

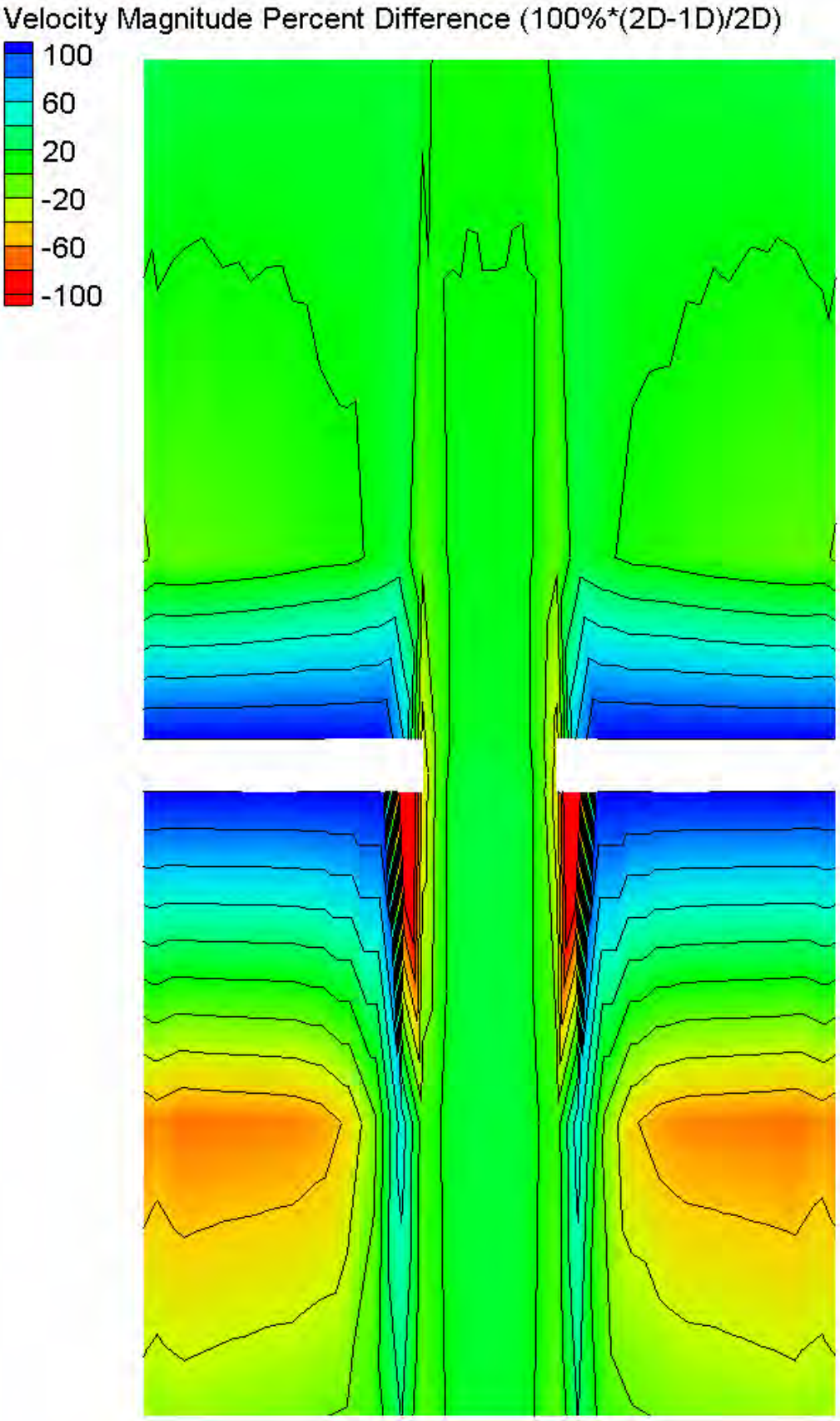

Velocity Magnitude Percent Difference Contours – Large Channel – Constrictions (at banks)

Overtopping Flows

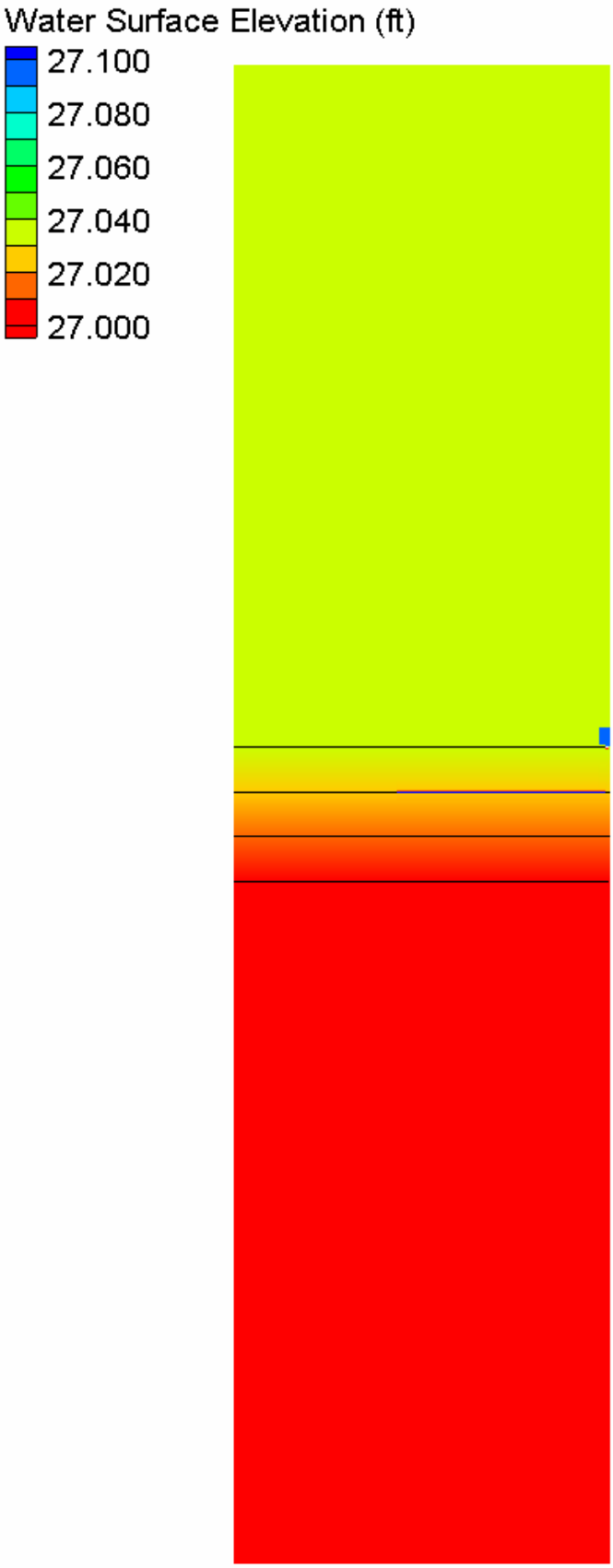

HEC-RAS Water Surface Elevation Contours – Small Channel – Overtopping (+10 ft)

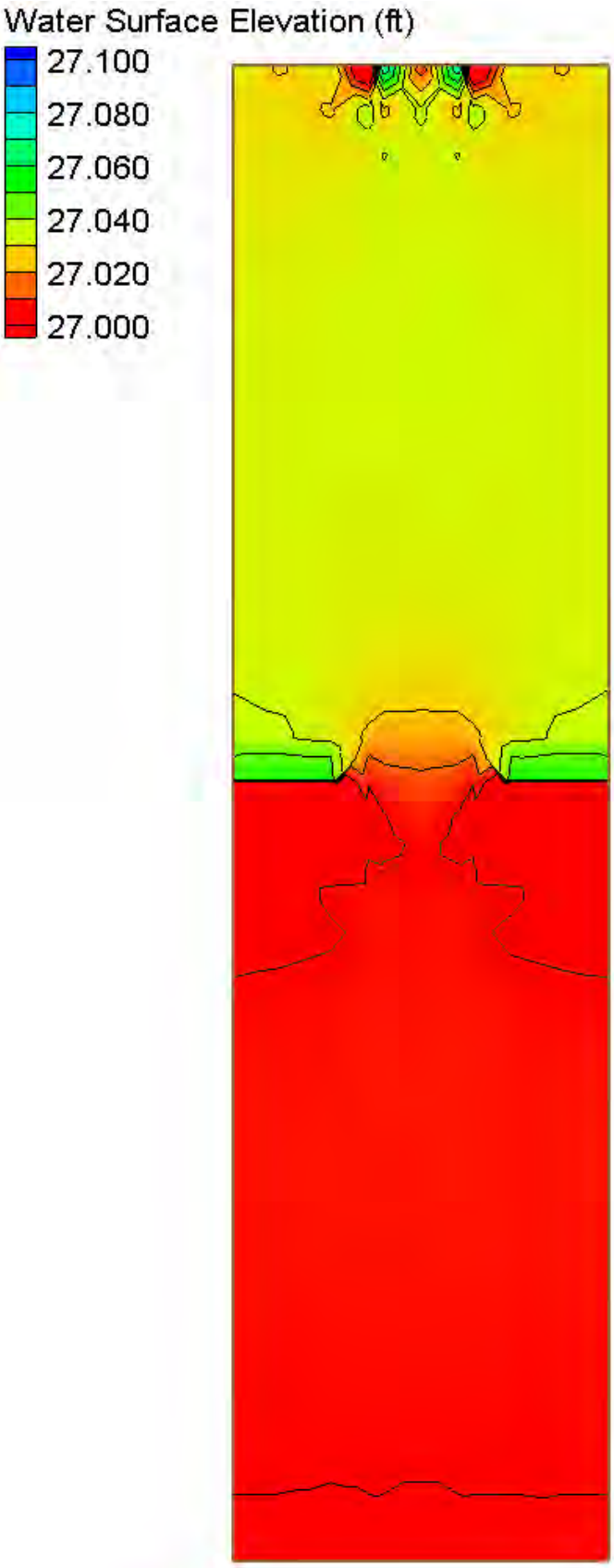

FESWMS Water Surface Elevation Contours – Small Channel – Overtopping (+10 ft)

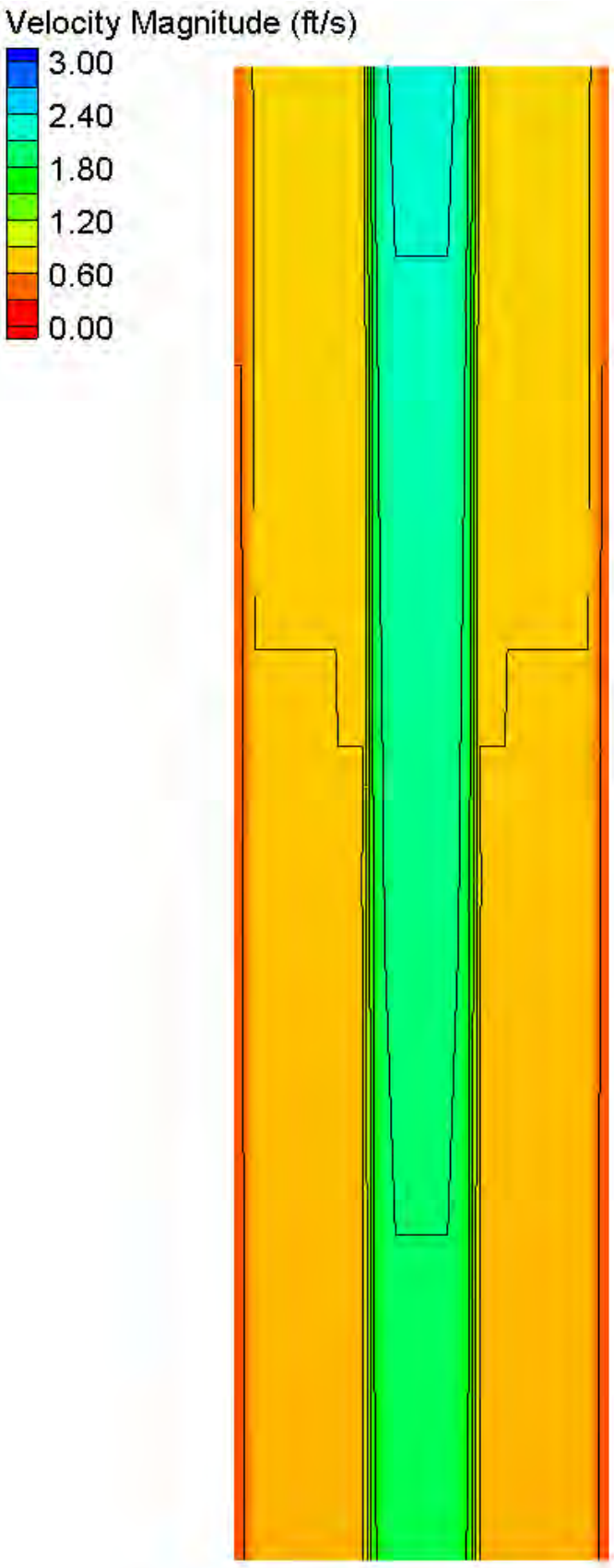

HEC-RAS Velocity Magnitude Contours – Small Channel – Overtopping (+10 ft)

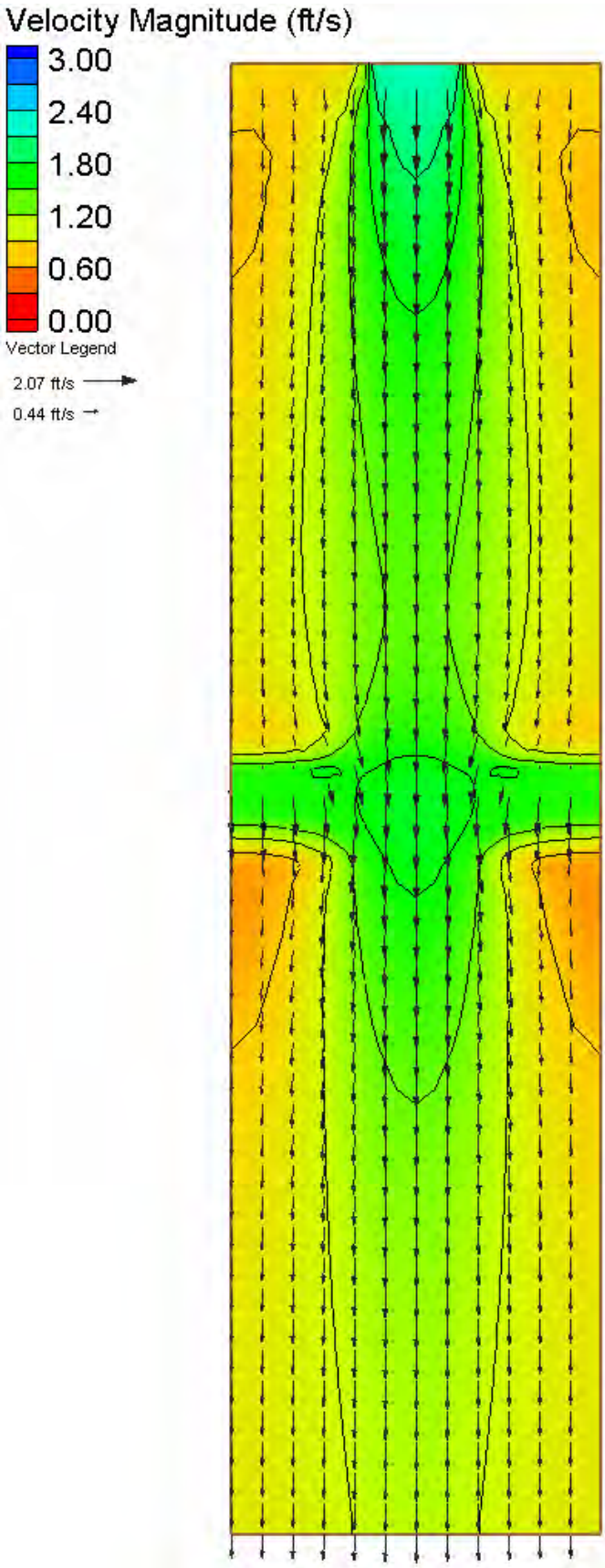

FESWMS Velocity Magnitude Contours – Small Channel – Overtopping (+10 ft)

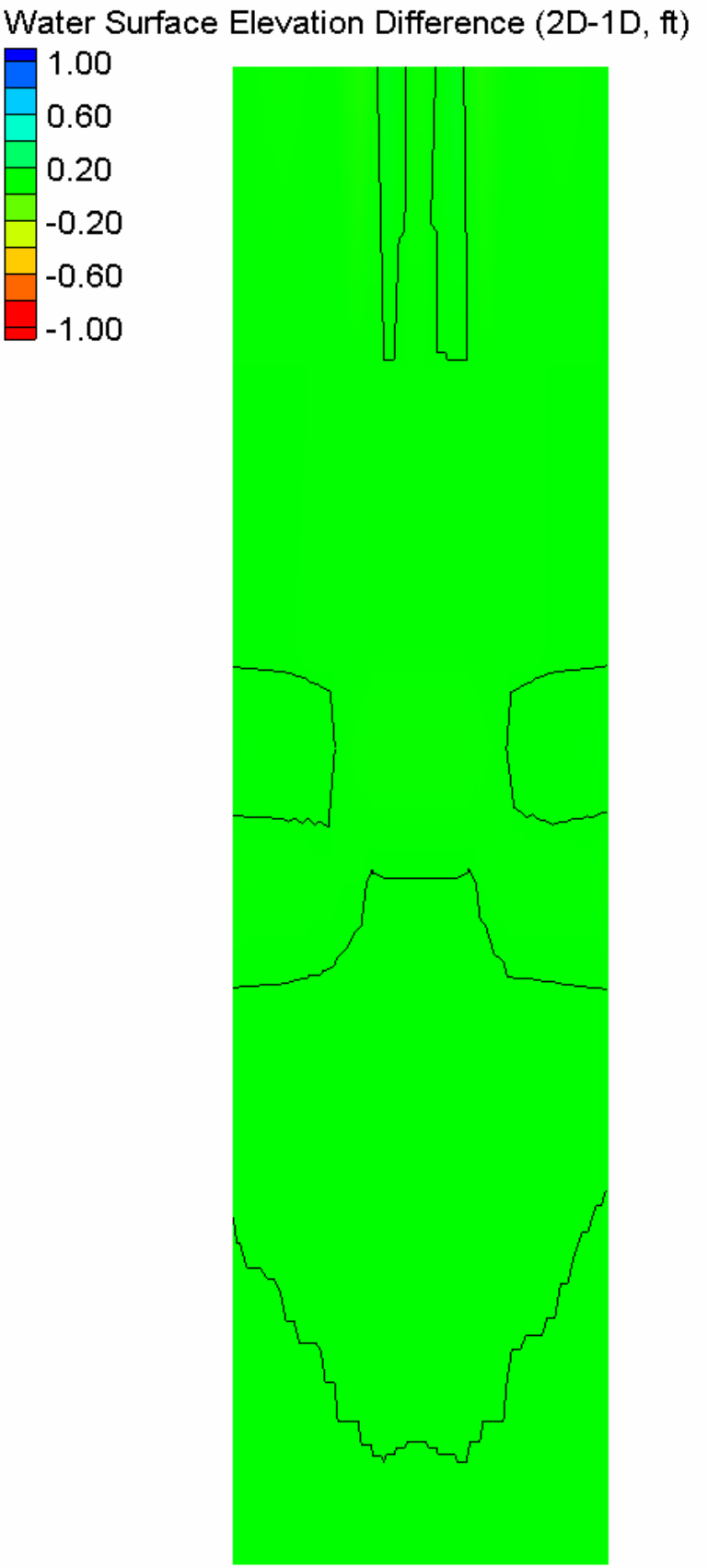

Water Surface Elevation Difference Contours – Small Channel – Overtopping (+10 ft)

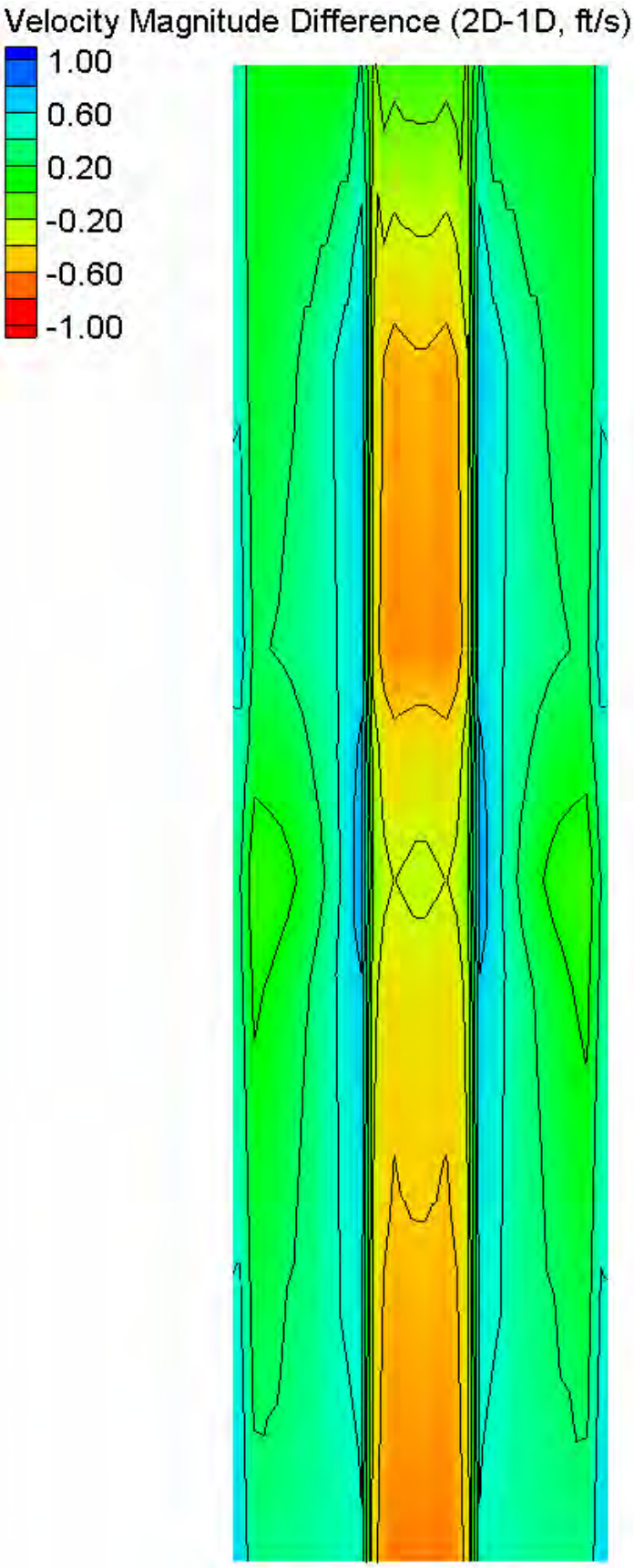

Velocity Magnitude Difference Contours – Small Channel – Overtopping (+10 ft)

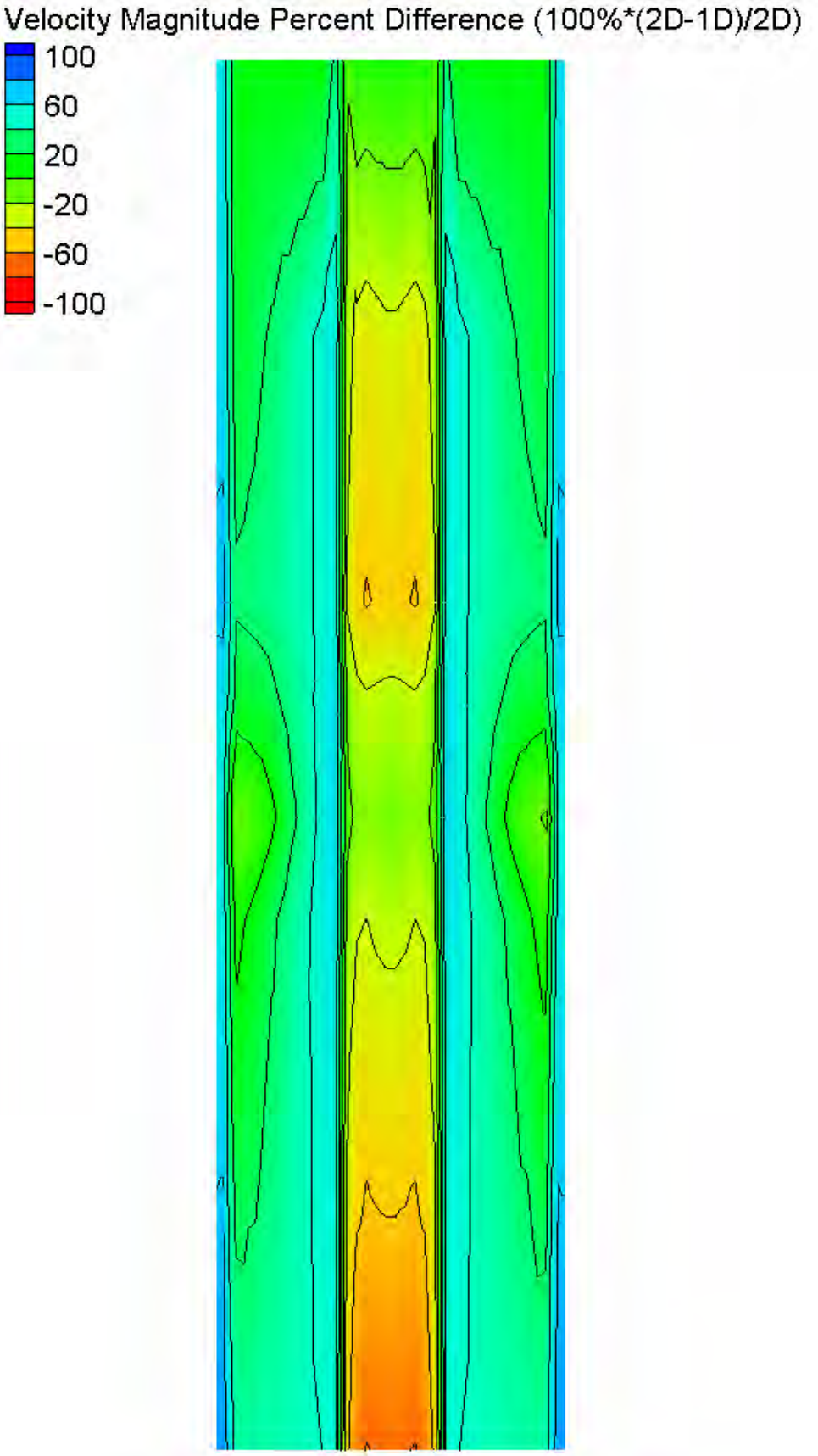

Velocity Magnitude Percent Difference Contours – Small Channel – Overtopping (+10 ft)

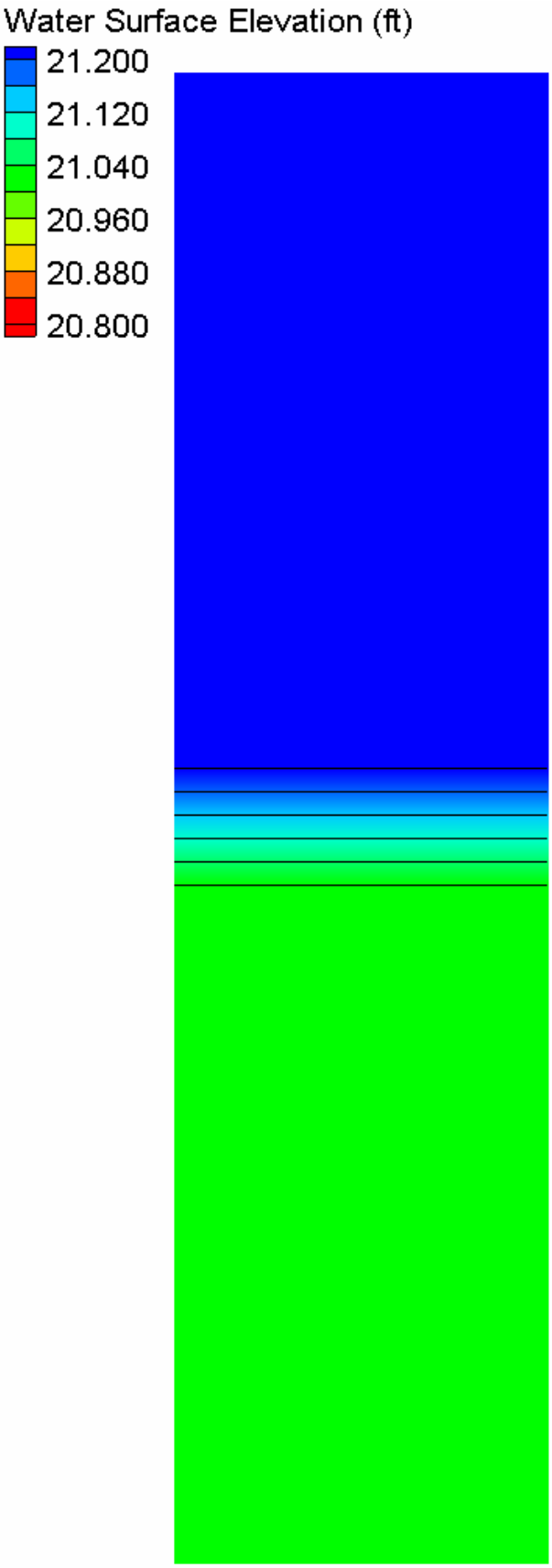

HEC-RAS Water Surface Elevation Contours – Small Channel – Overtopping (low chord)

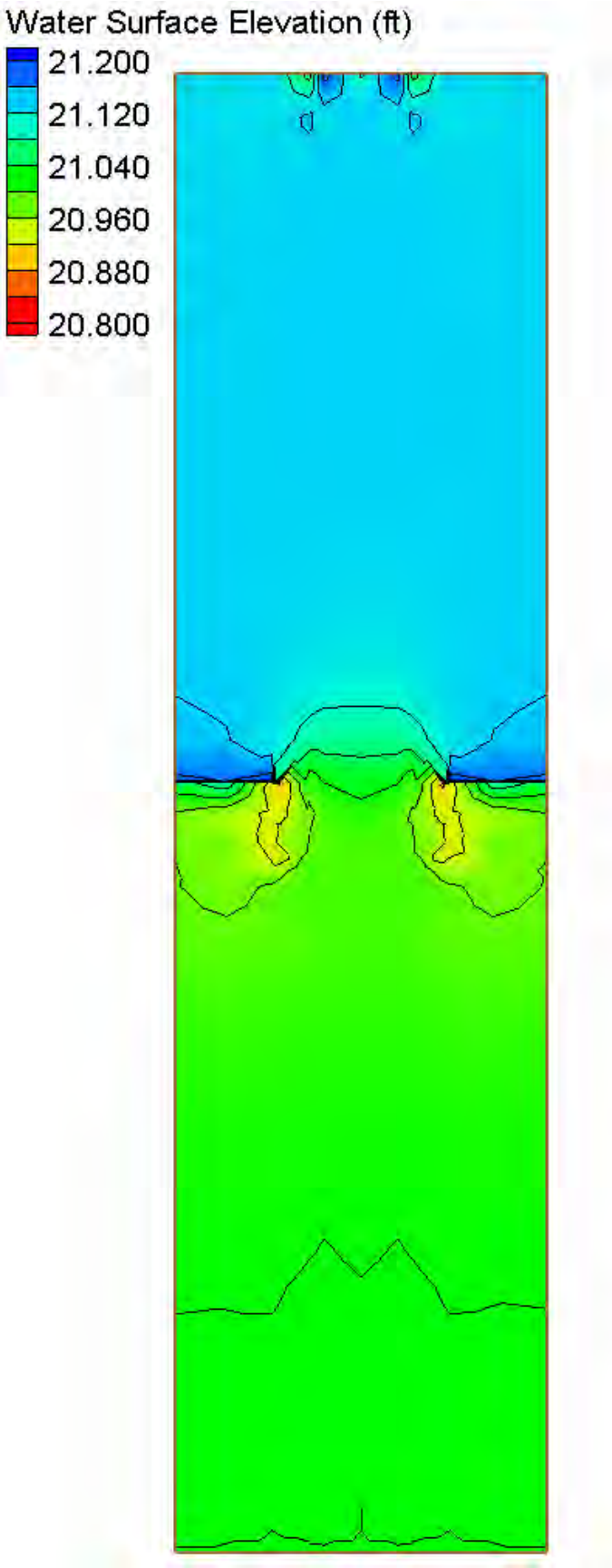

FESWMS Water Surface Elevation Contours – Small Channel – Overtopping (low chord)

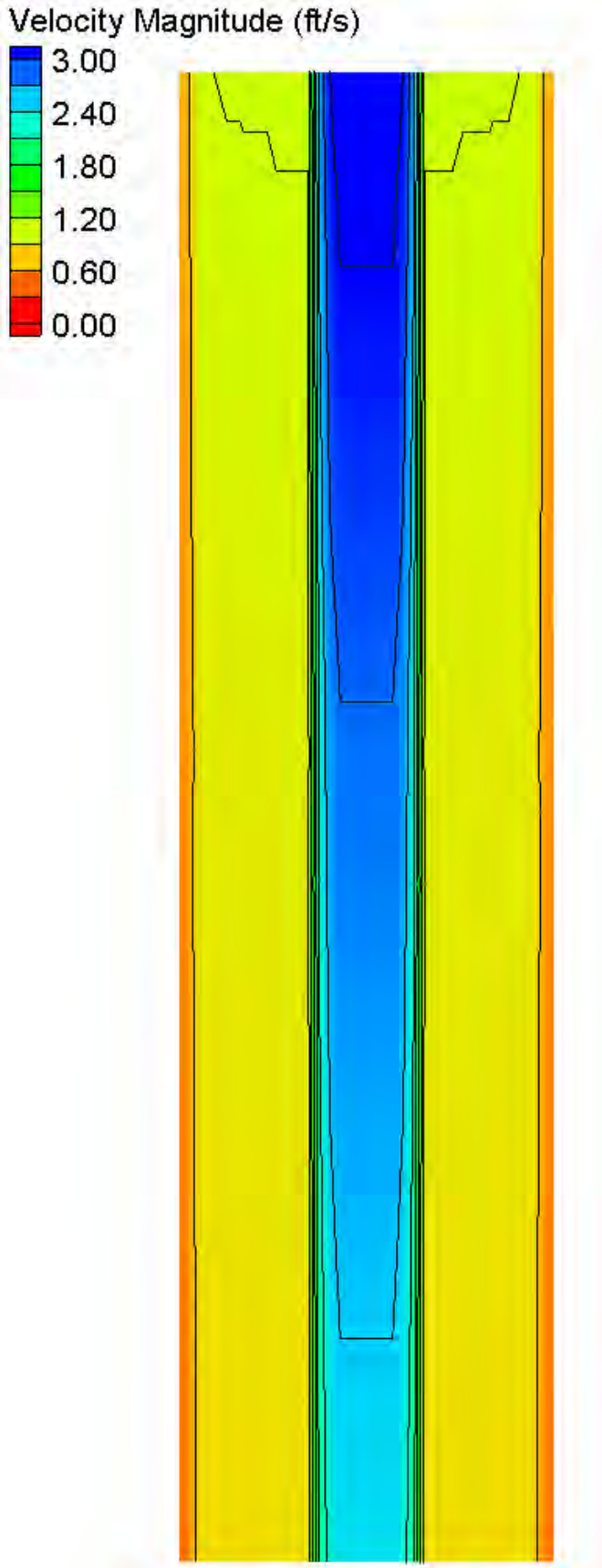

HEC-RAS Velocity Magnitude Contours – Small Channel – Overtopping (low chord)

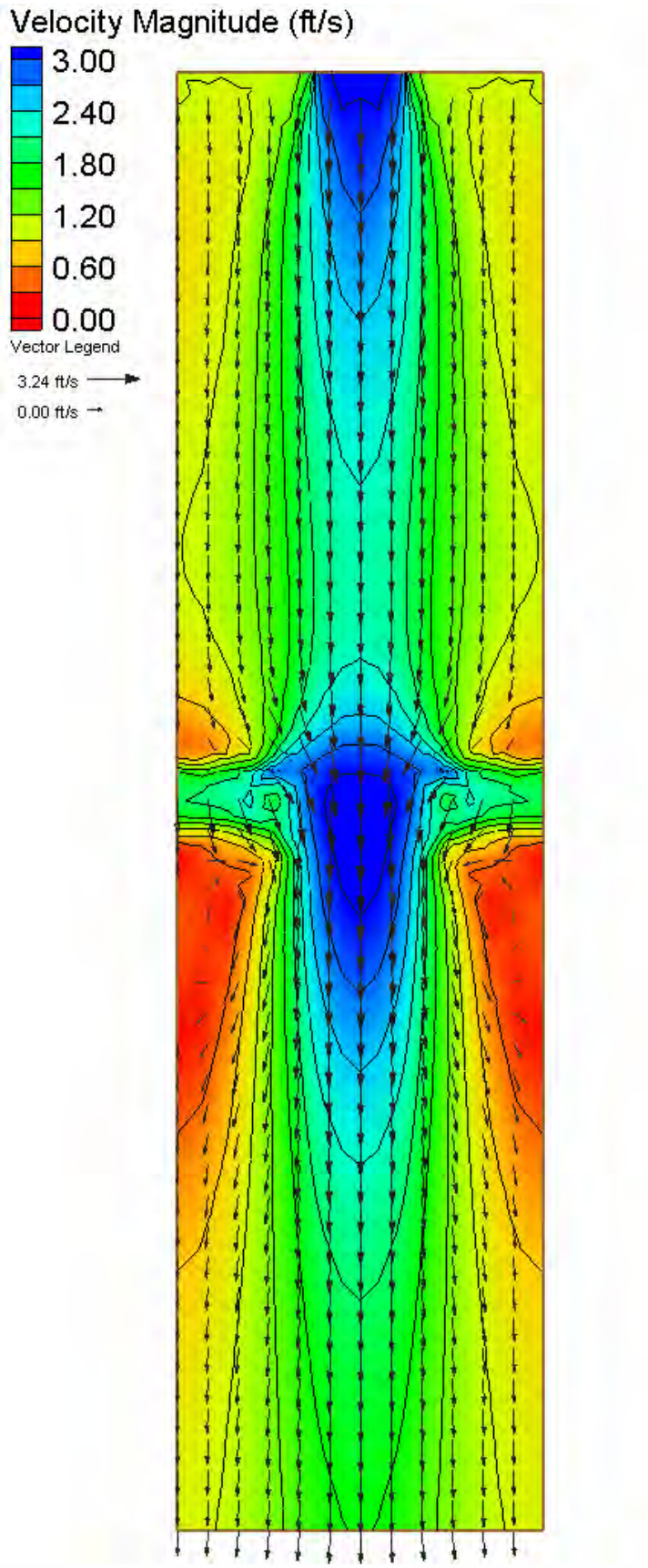

FESWMS Velocity Magnitude Contours – Small Channel – Overtopping (low chord)

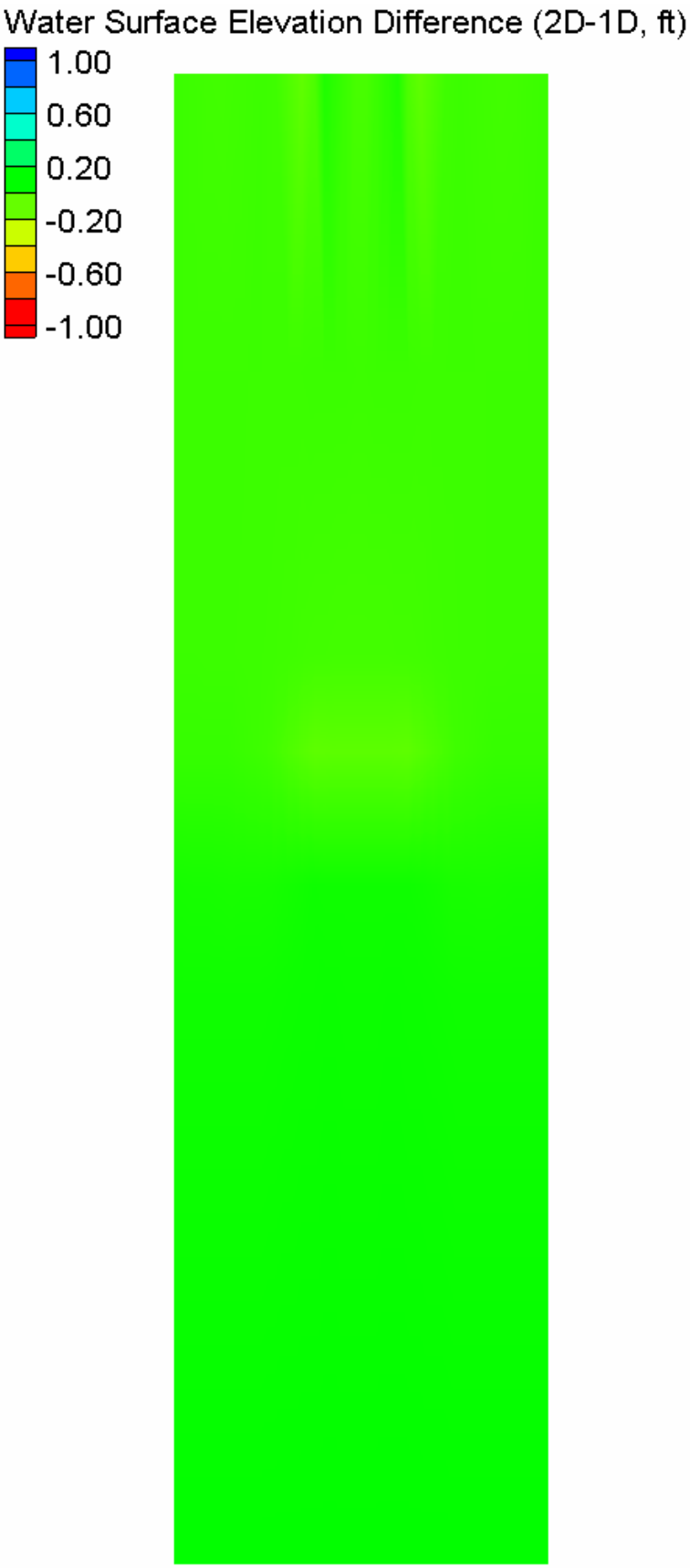

Water Surface Elevation Difference Contours – Small Channel – Overtopping (low chord)

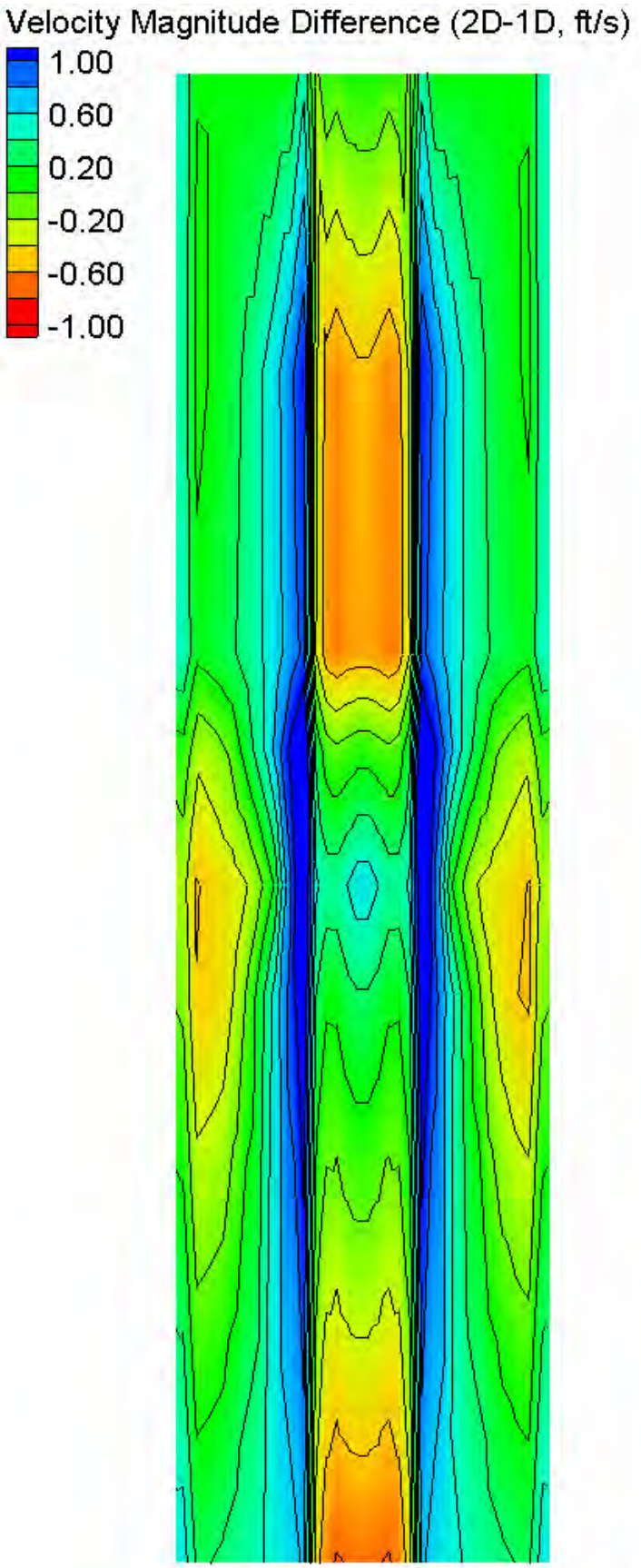

Velocity Magnitude Difference Contours – Small Channel – Overtopping (low chord)

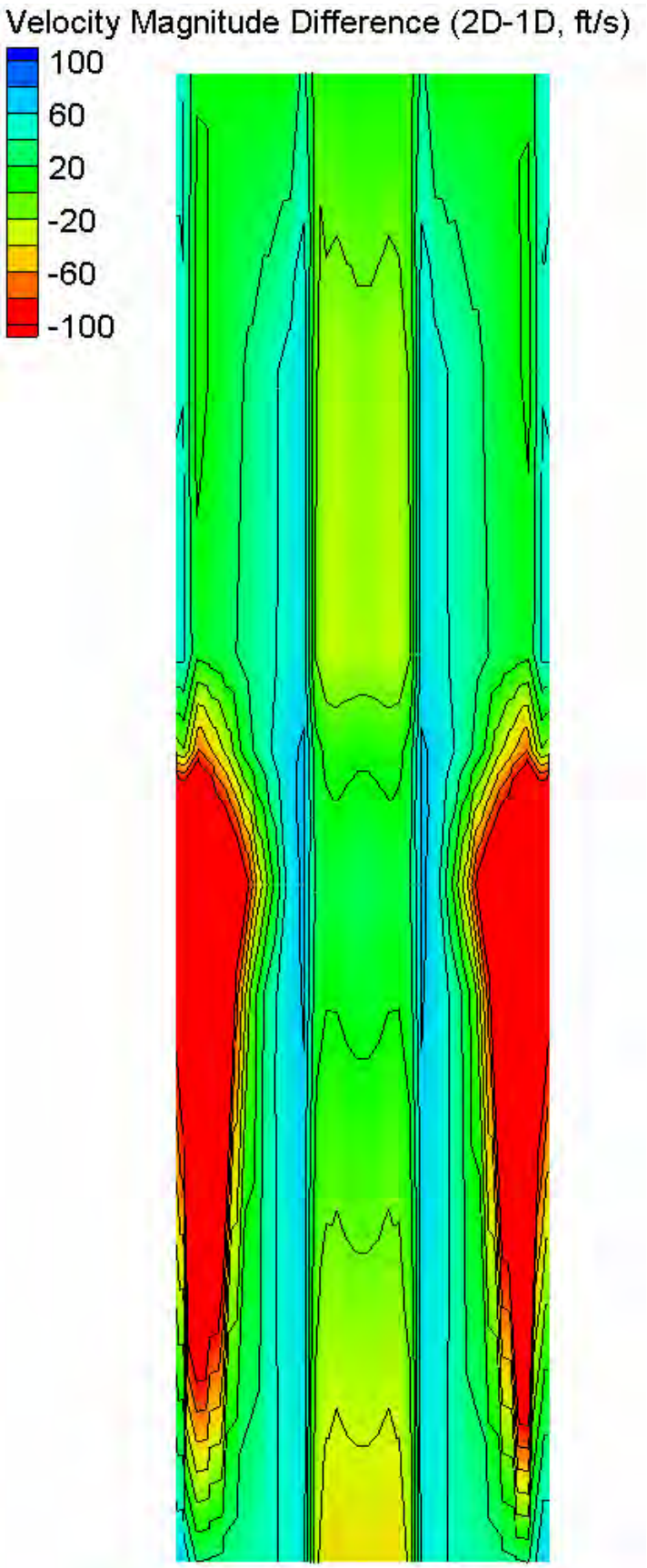

Velocity Magnitude Percent Difference Contours – Small Channel – Overtopping (low chord)

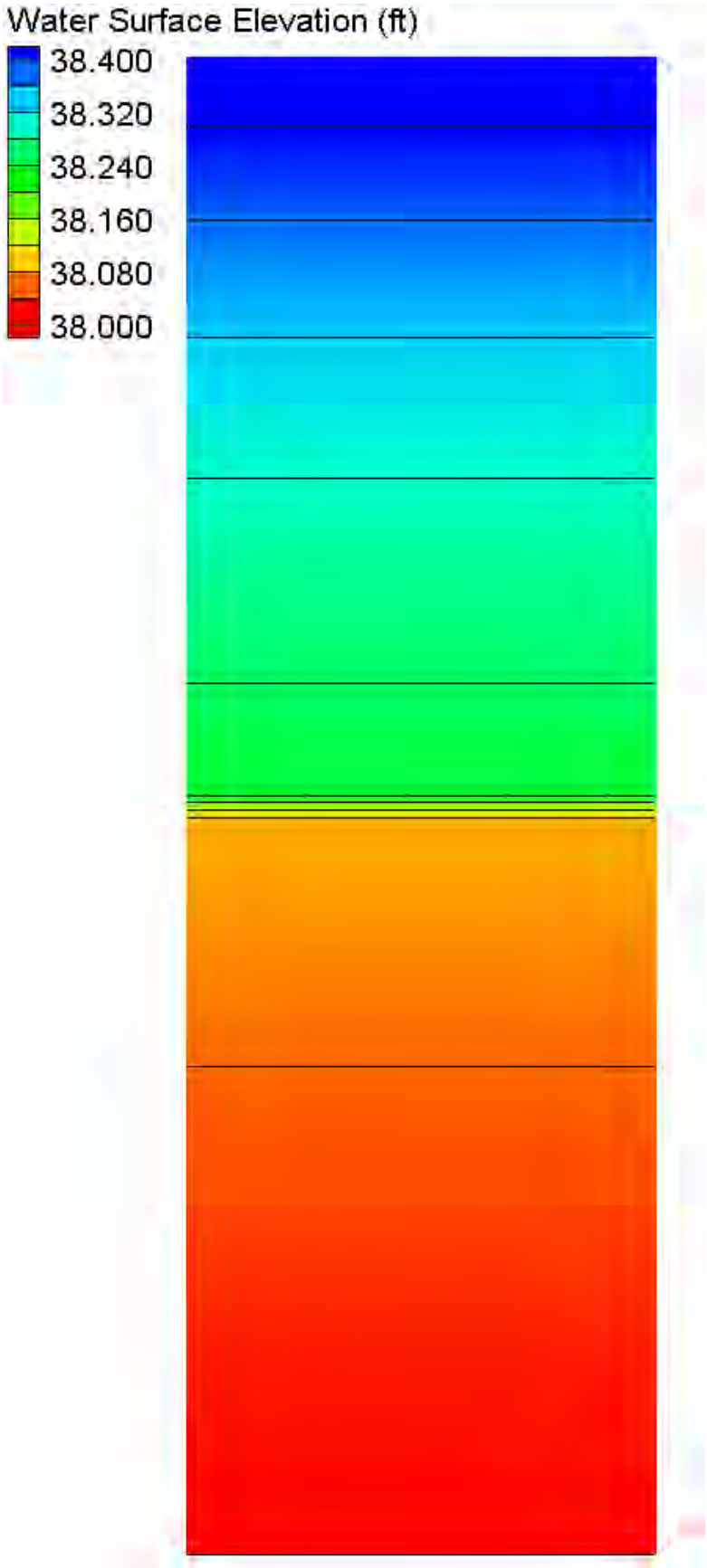

HEC-RAS Water Surface Elevation Contours – Large Channel – Overtopping (+10 ft)

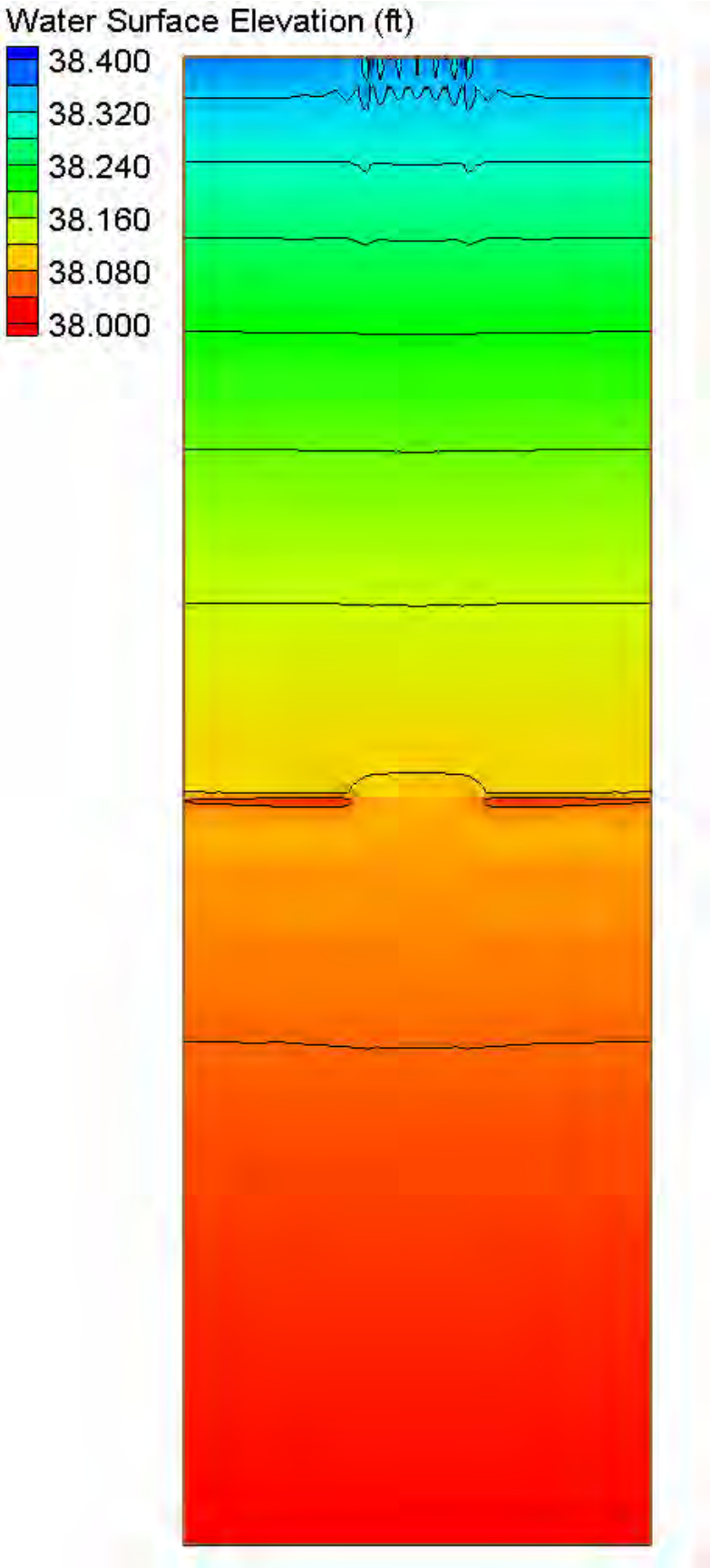

FESWMS Water Surface Elevation Contours – Large Channel – Overtopping (+10 ft)

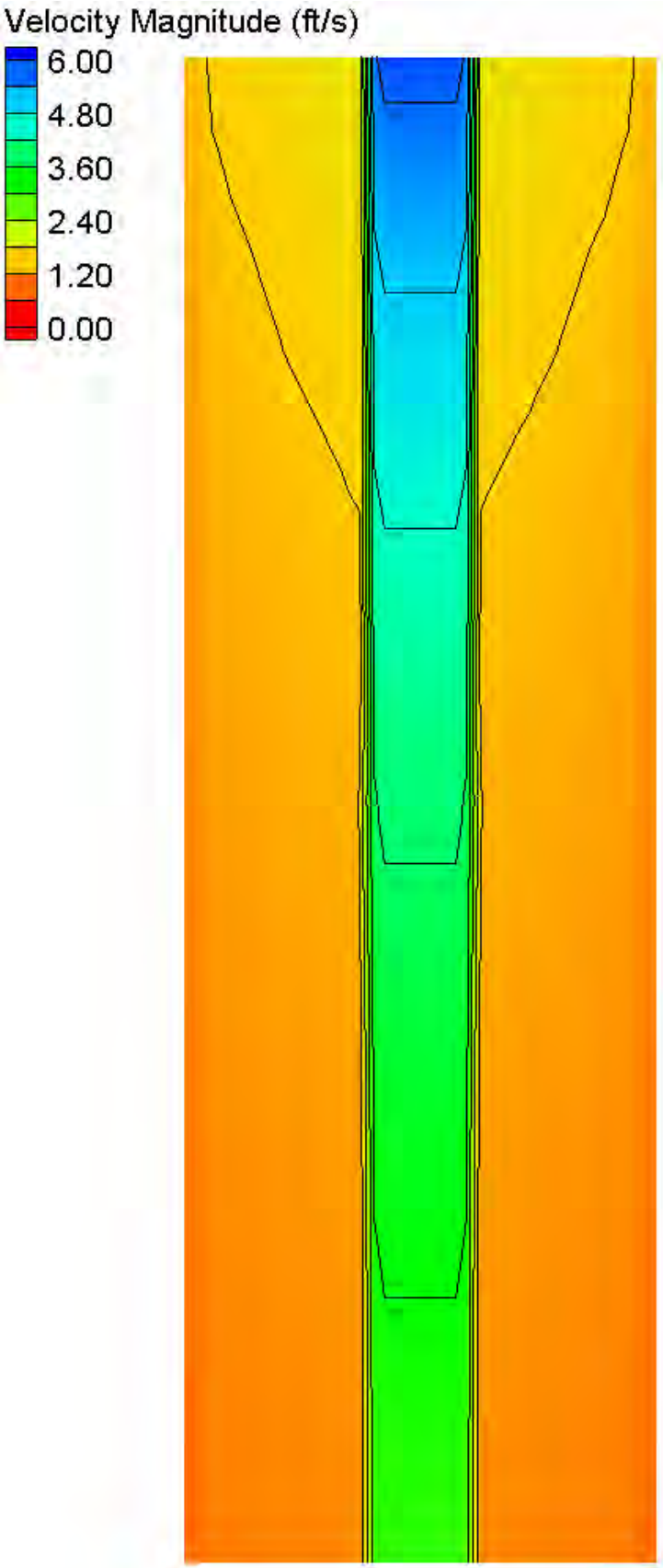

HEC-RAS Velocity Magnitude Contours – Large Channel – Overtopping (+10 ft)

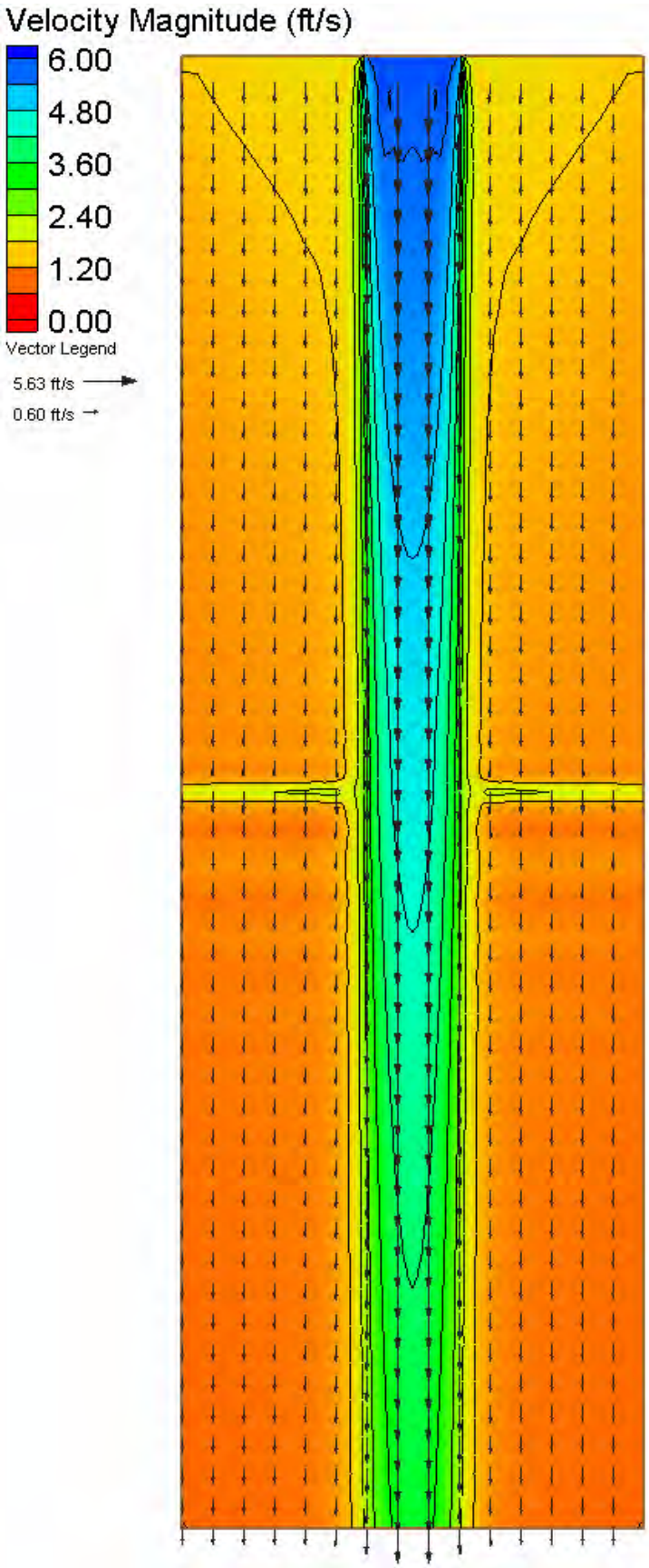

FESWMS Velocity Magnitude Contours – Large Channel – Overtopping (+10 ft)

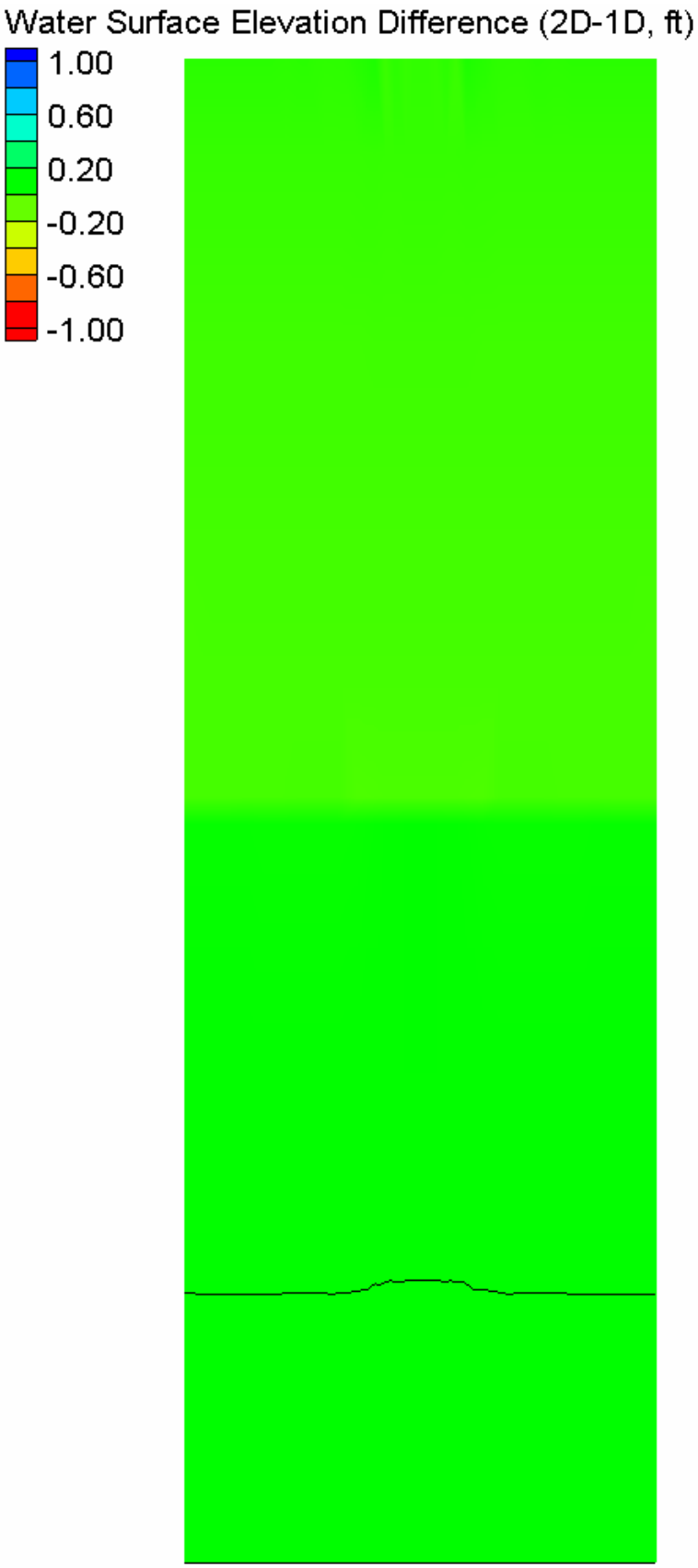

Water Surface Elevation Difference Contours – Large Channel – Overtopping (+10 ft)

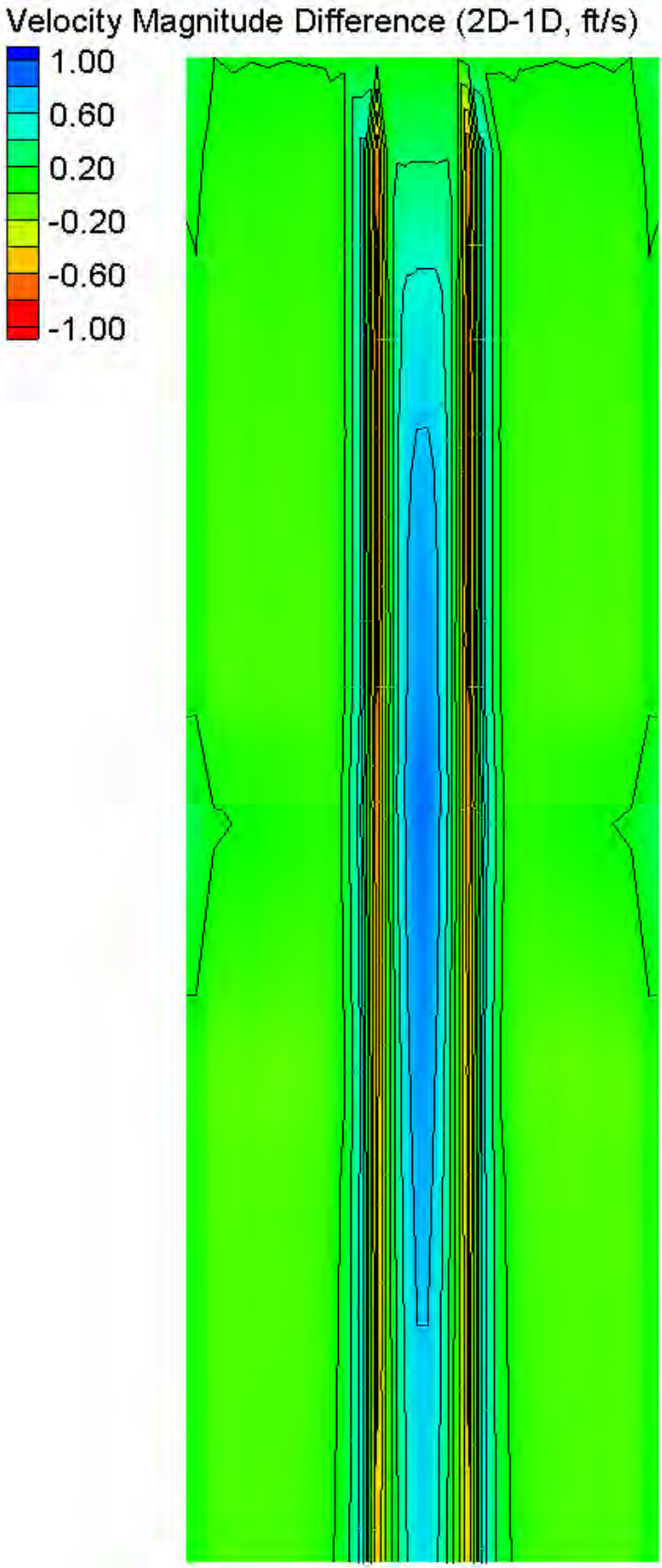

Velocity Magnitude Difference Contours – Large Channel – Overtopping (+10 ft)

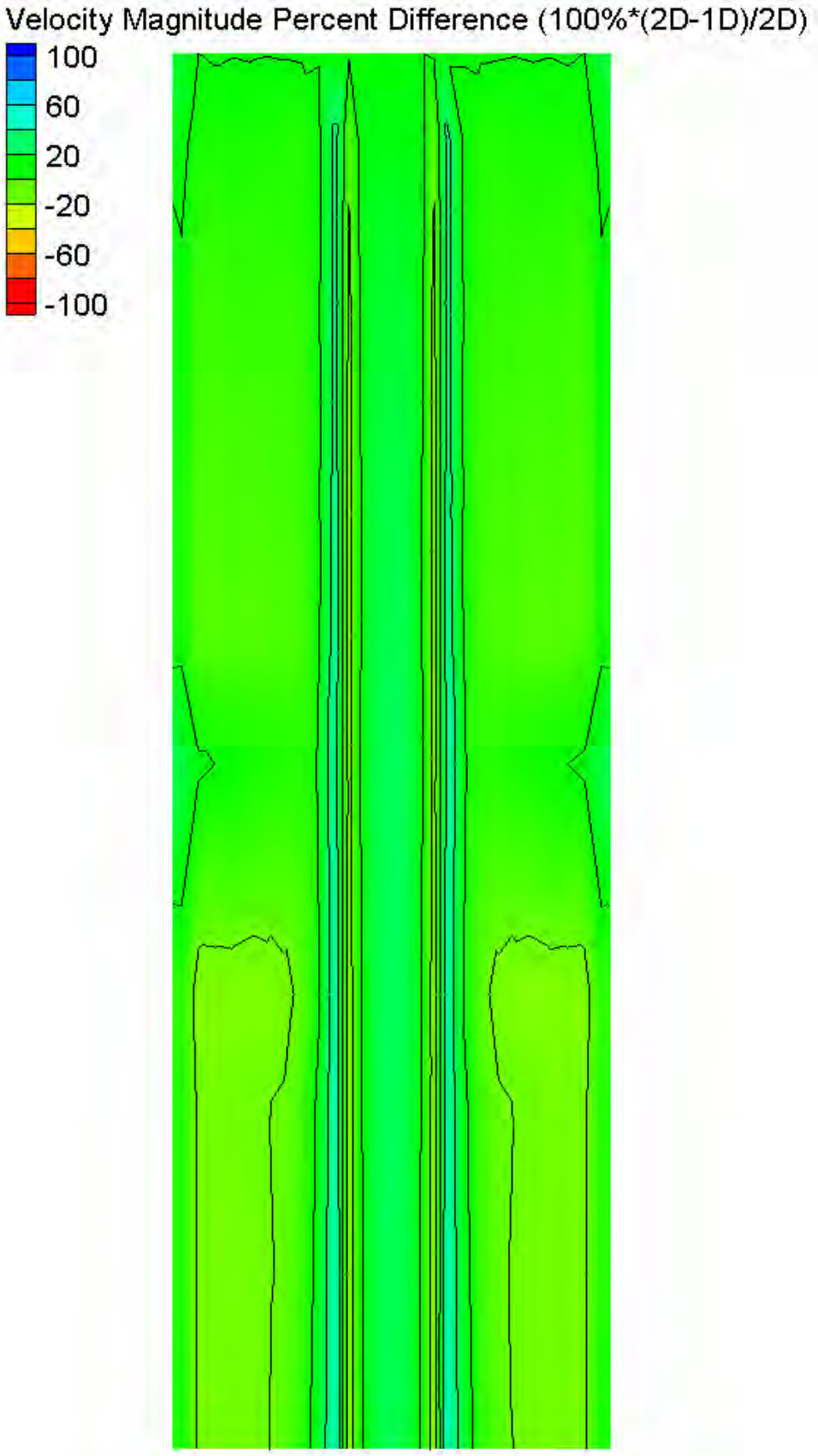

Velocity Magnitude Percent Difference Contours – Large Channel – Overtopping (+10 ft)

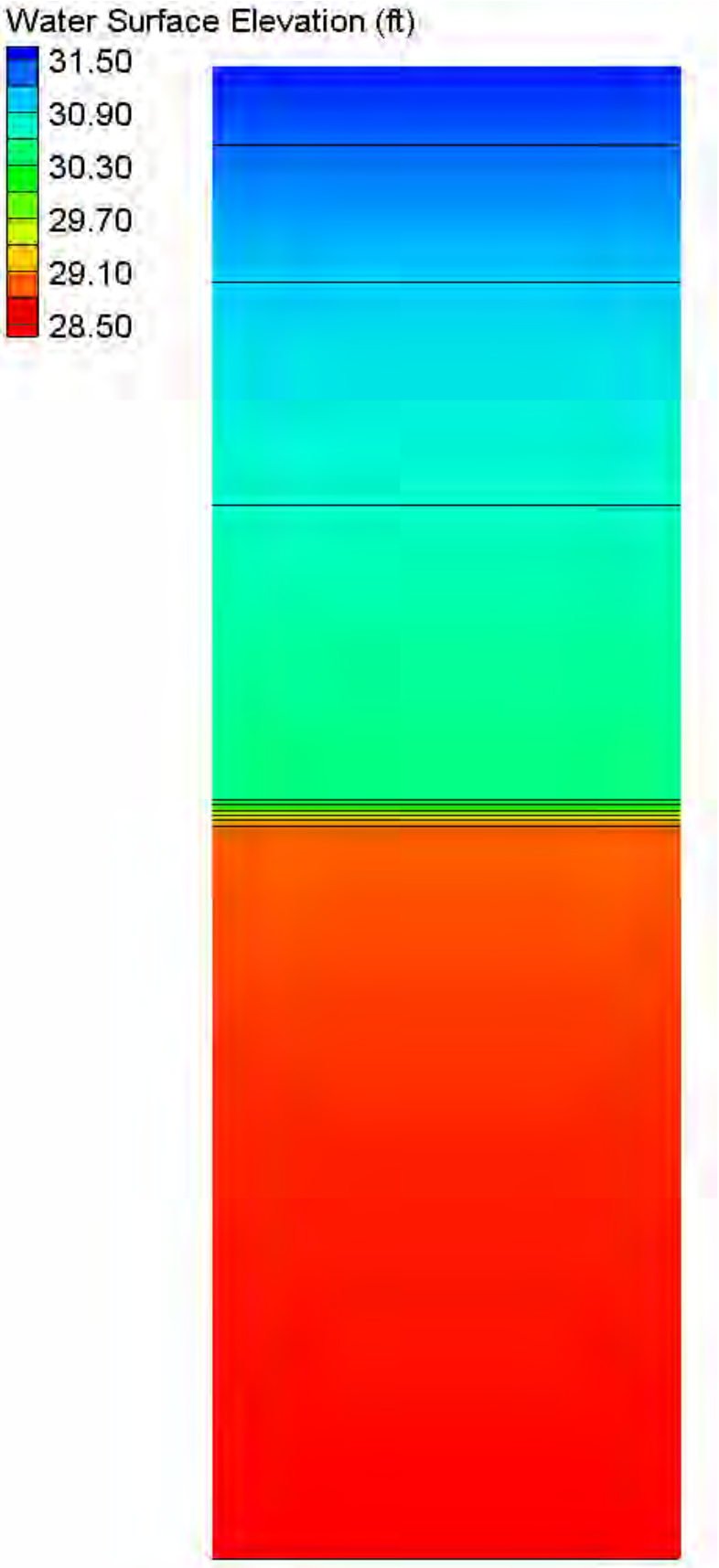

HEC-RAS Water Surface Elevation Contours – Large Channel – Overtopping (low chord)

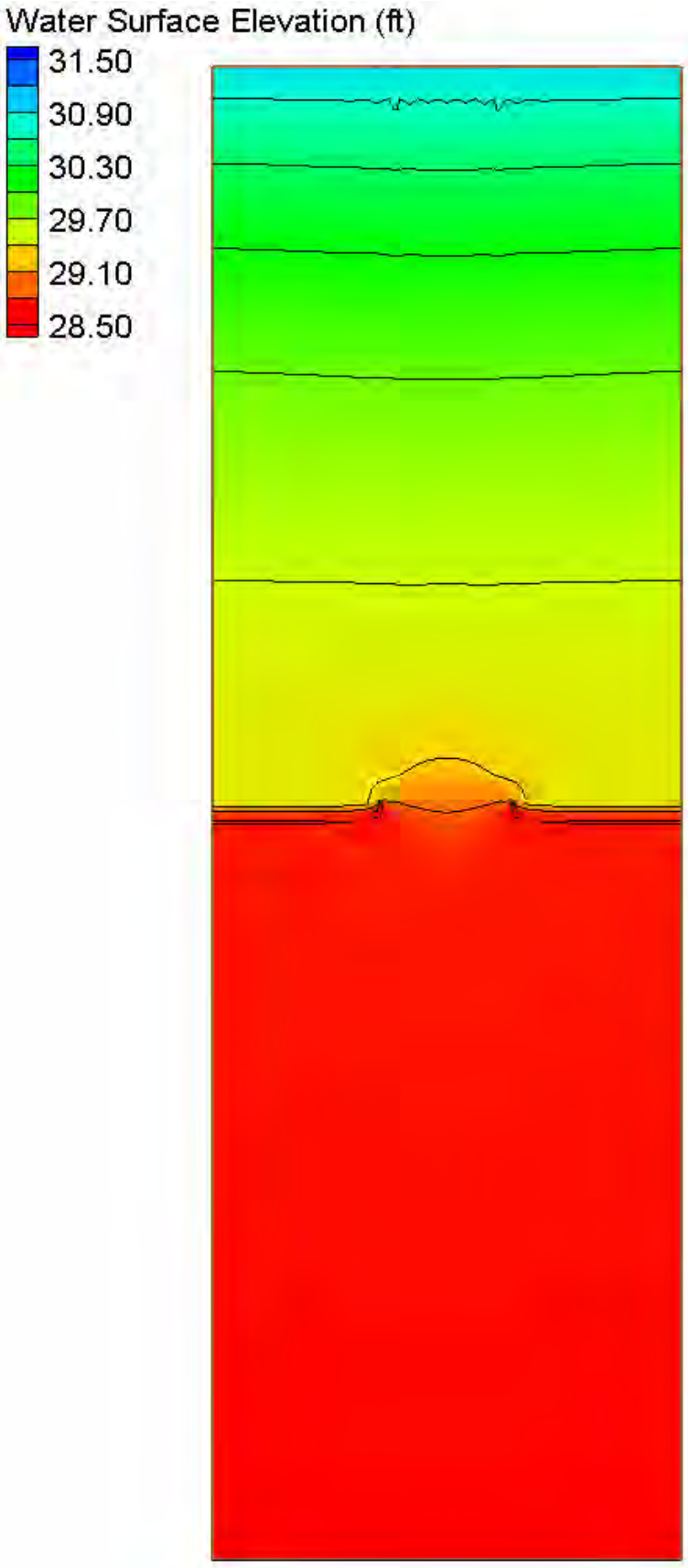

FESWMS Water Surface Elevation Contours – Large Channel – Overtopping (low chord)

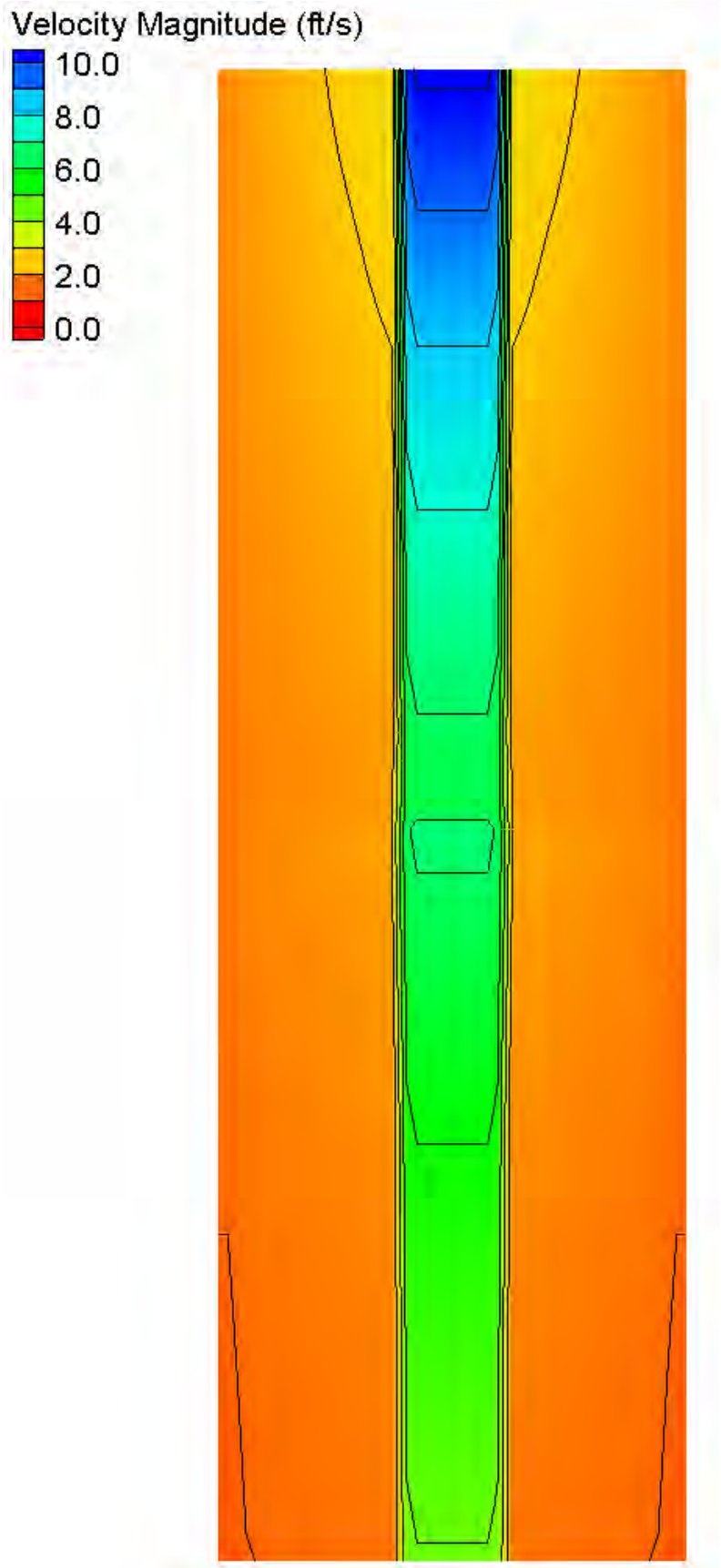

HEC-RAS Velocity Magnitude Contours – Large Channel – Overtopping (low chord)

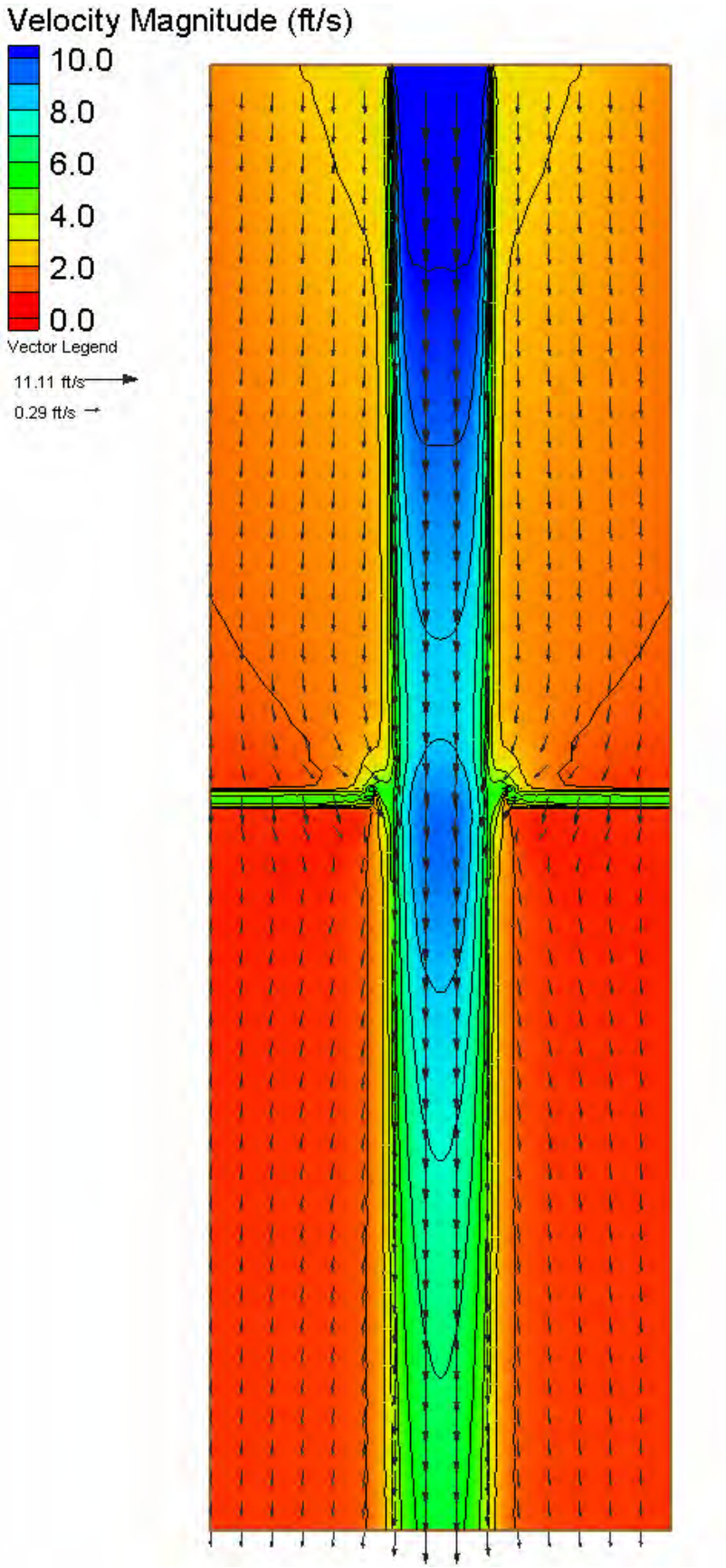

FESWMS Velocity Magnitude Contours – Large Channel – Overtopping (low chord)

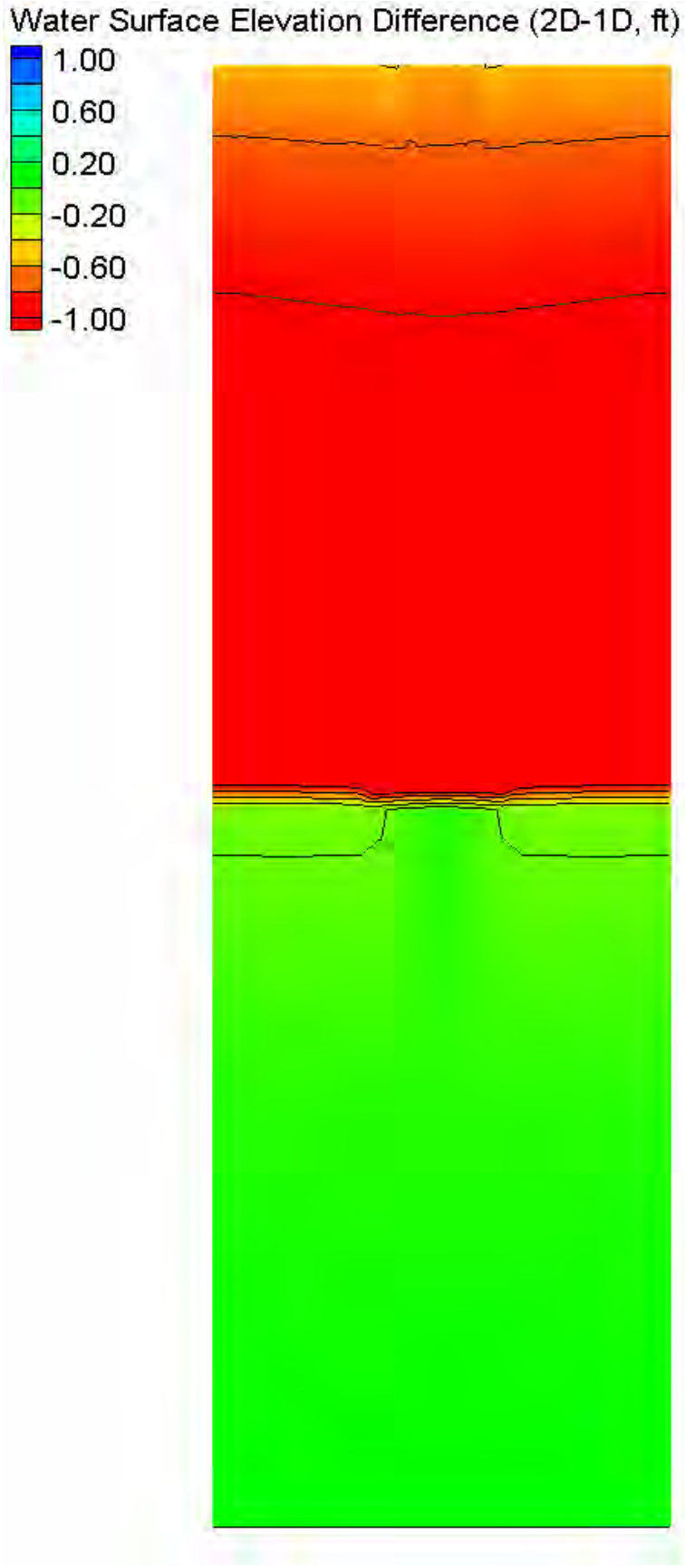

Water Surface Elevation Difference Contours – Large Channel – Overtopping (low chord)

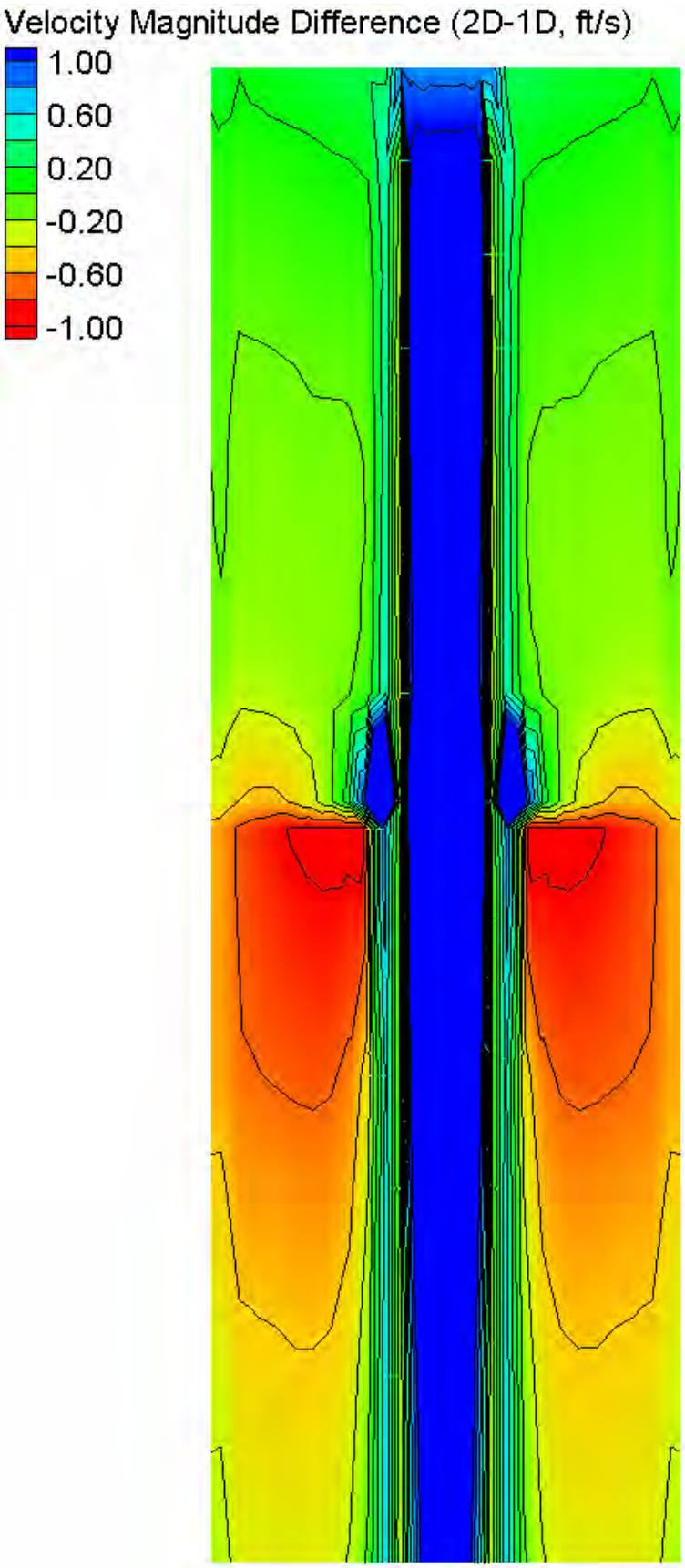

Velocity Magnitude Difference Contours – Large Channel – Overtopping (low chord)

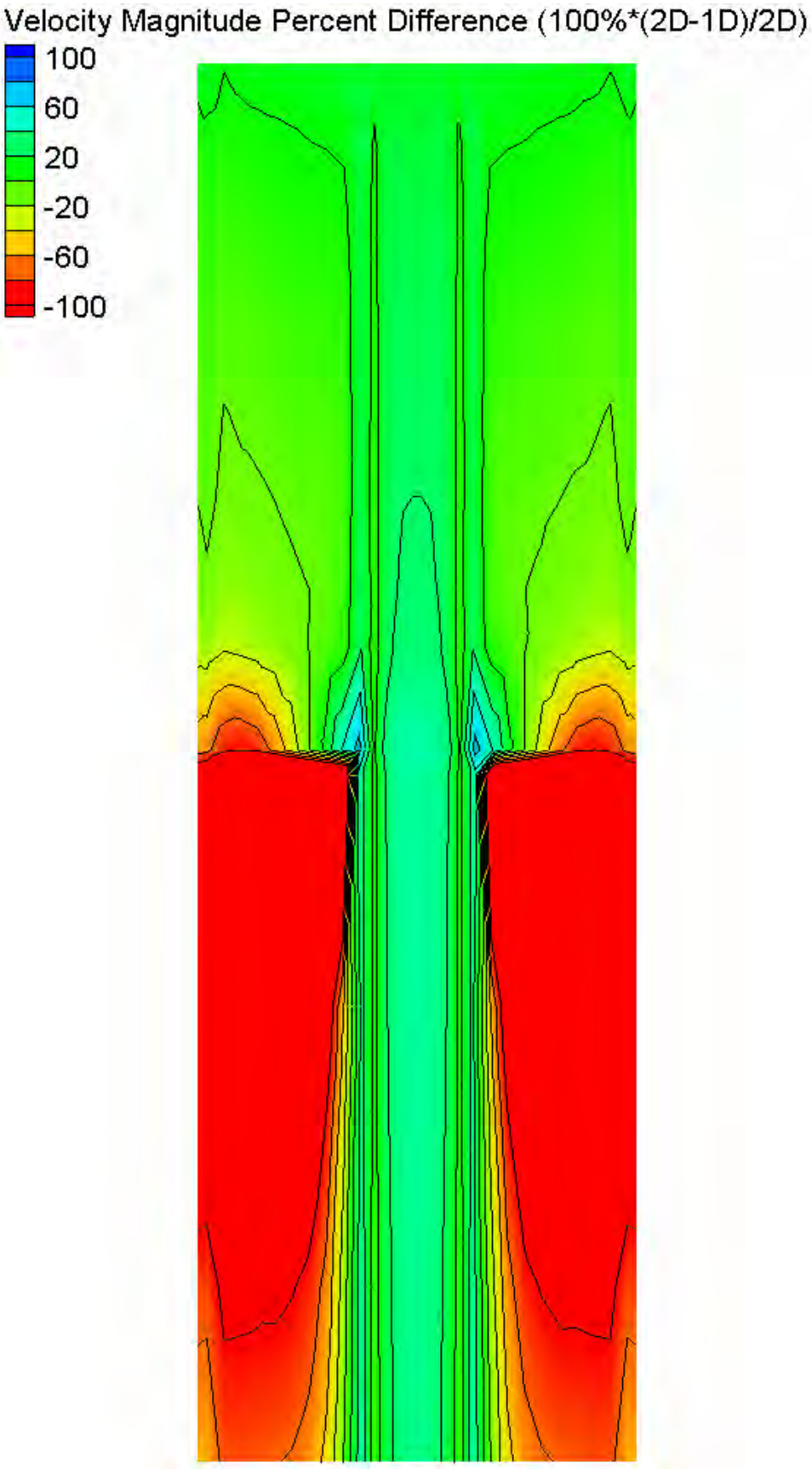

Velocity Magnitude Percent Difference Contours – Large Channel – Overtopping (low chord)

Embankment Skew

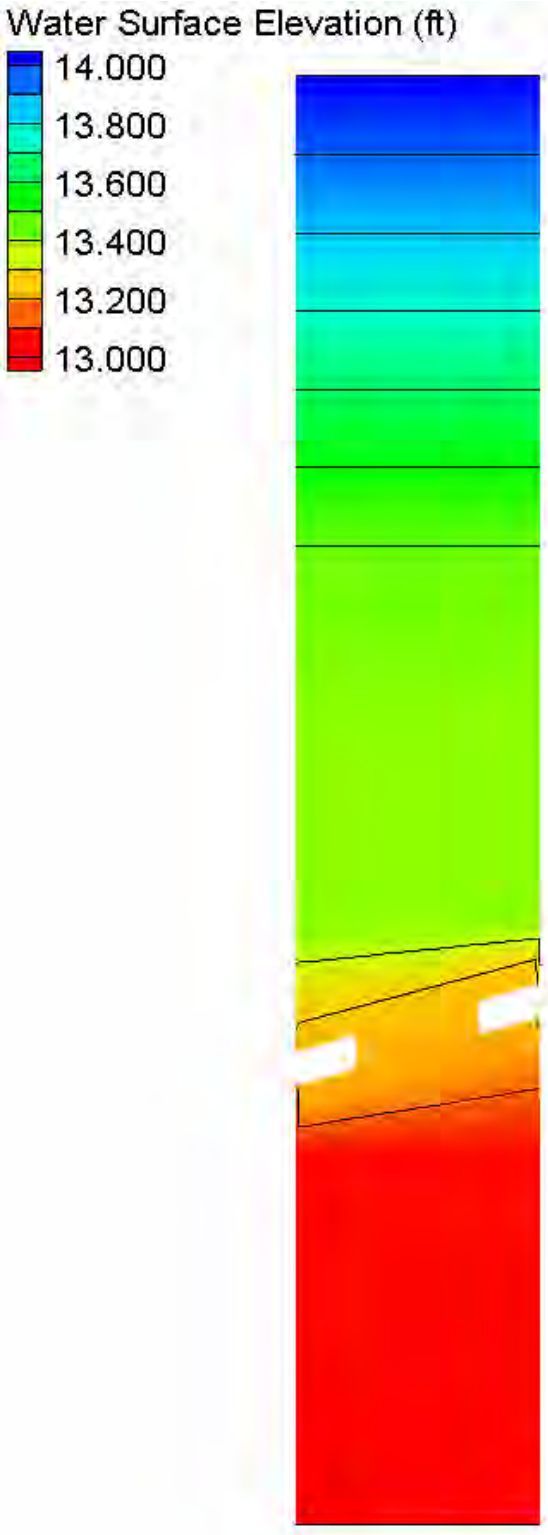

HEC-RAS Water Surface Elevation Contours – Small Channel – Embankment Skew (15°)

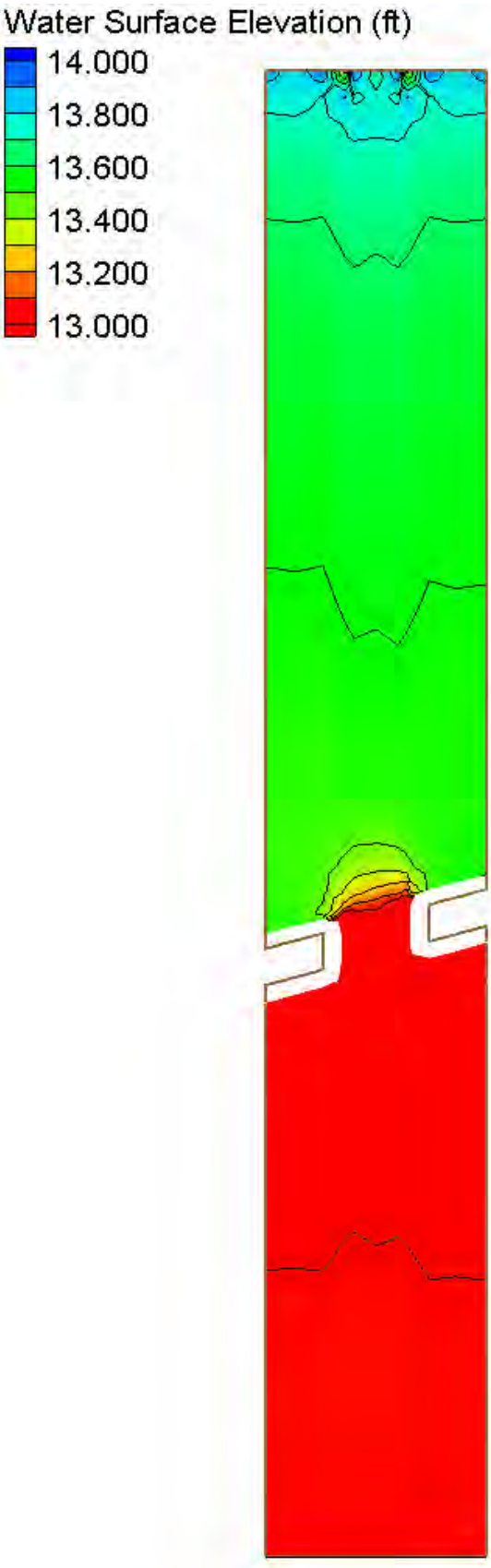

FESWMS Water Surface Elevation Contours – Small Channel – Embankment Skew (15°)

HEC-RAS Velocity Magnitude Contours – Small Channel – Embankment Skew (15°)

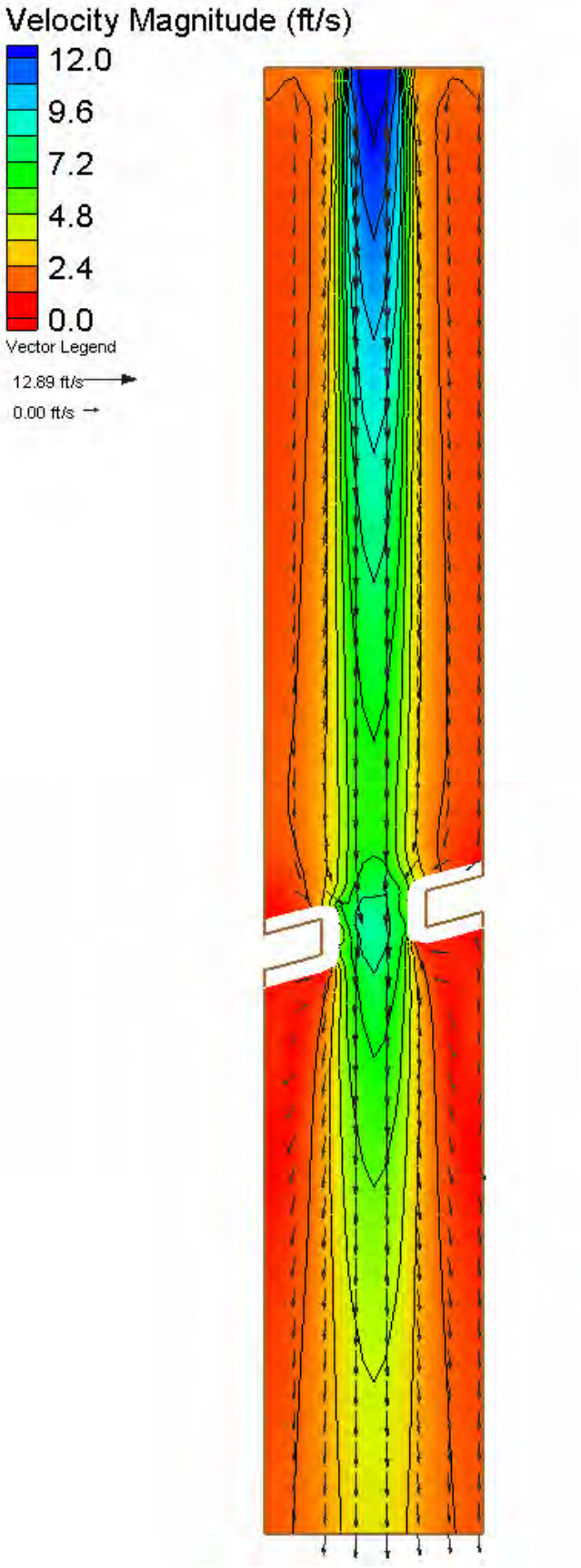

FESWMS Velocity Magnitude Contours – Small Channel – Embankment Skew (15°)

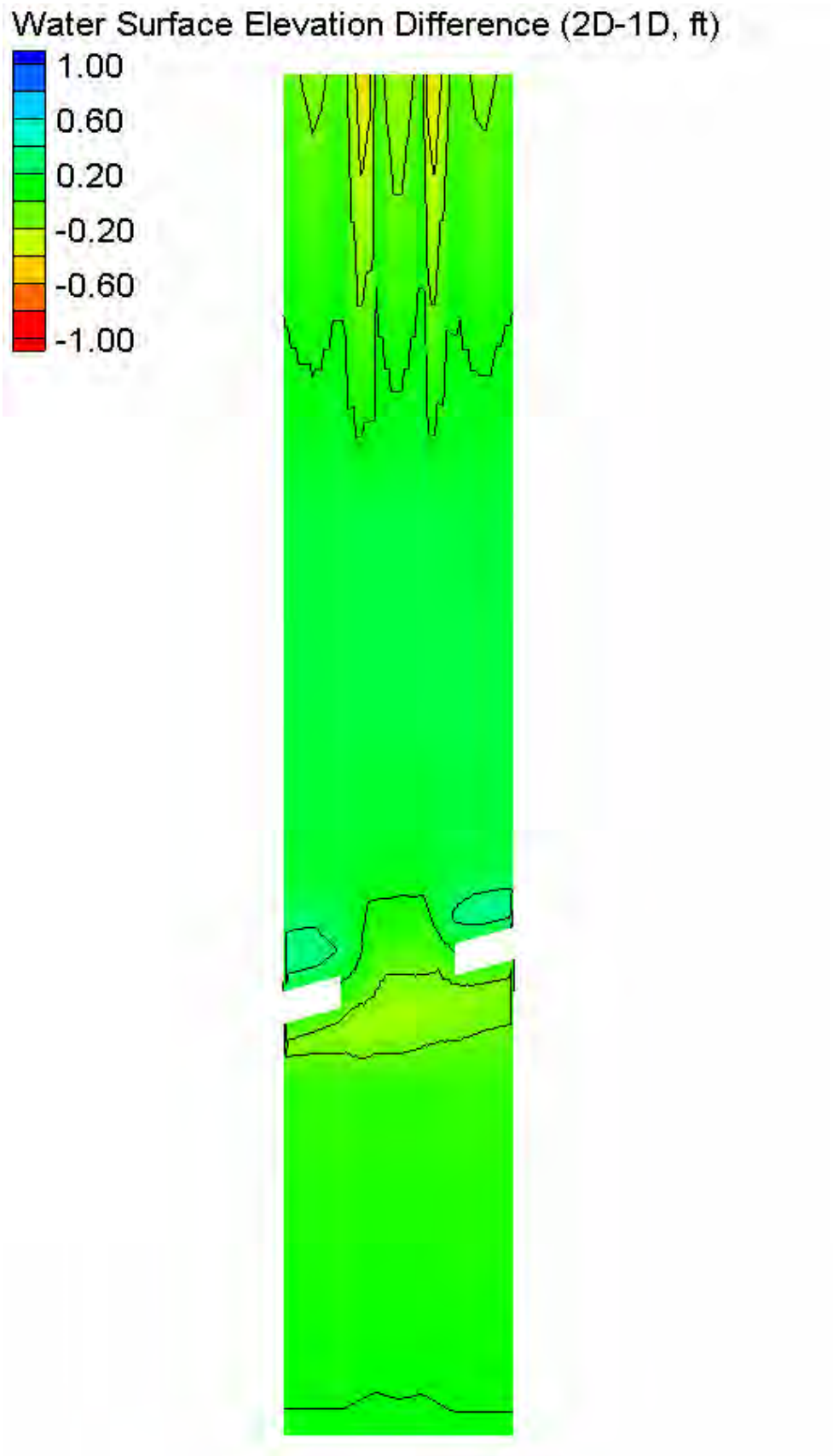

Water Surface Elevation Difference Contours – Small Channel – Embankment Skew (15°)

Velocity Magnitude Difference Contours – Small Channel – Embankment Skew (15°)

Velocity Magnitude Percent Difference Contours – Small Channel – Embankment Skew (15°)

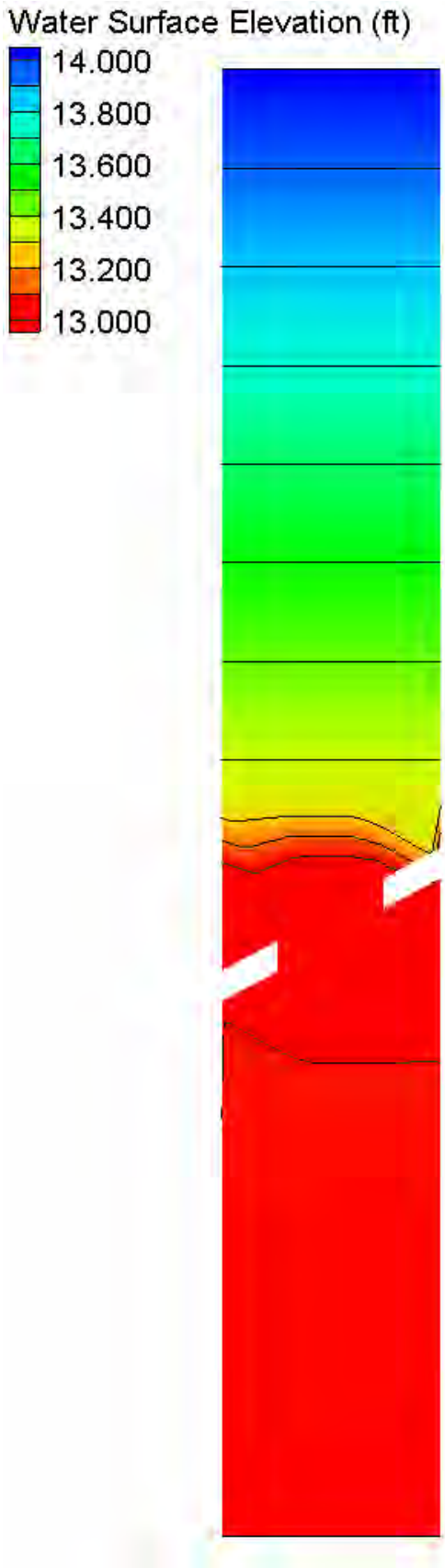

HEC-RAS Water Surface Elevation Contours – Small Channel – Embankment Skew (30°)

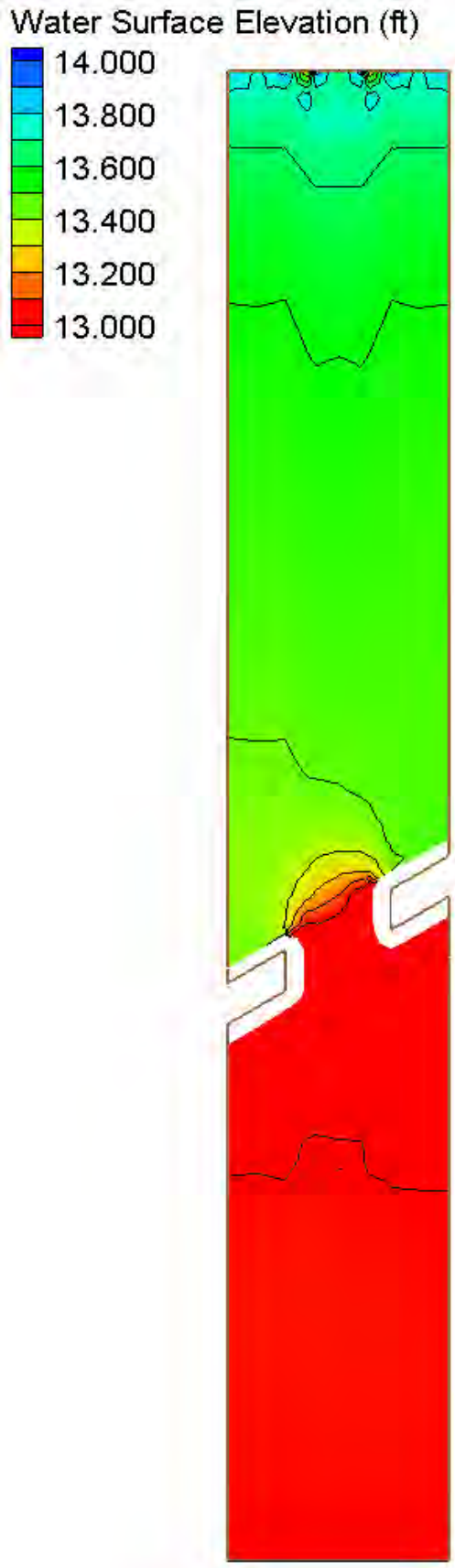

FESWMS Water Surface Elevation Contours – Small Channel – Embankment Skew (30°)

HEC-RAS Velocity Magnitude Contours – Small Channel – Embankment Skew (30°)

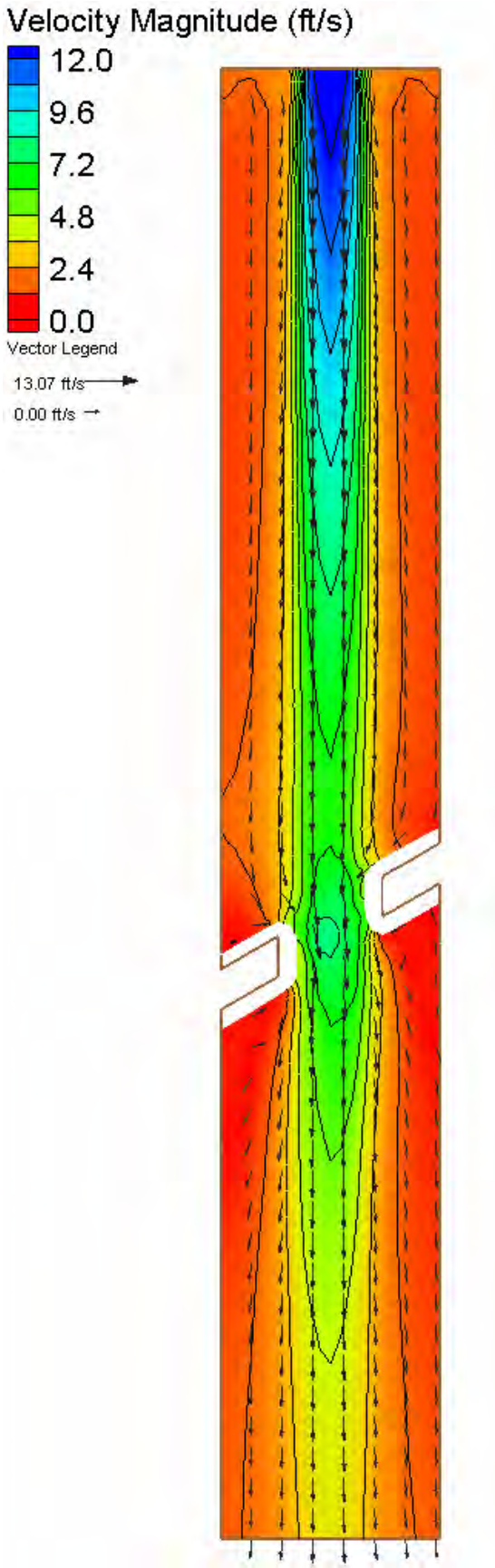

FESWMS Velocity Magnitude Contours – Small Channel – Embankment Skew (30°)

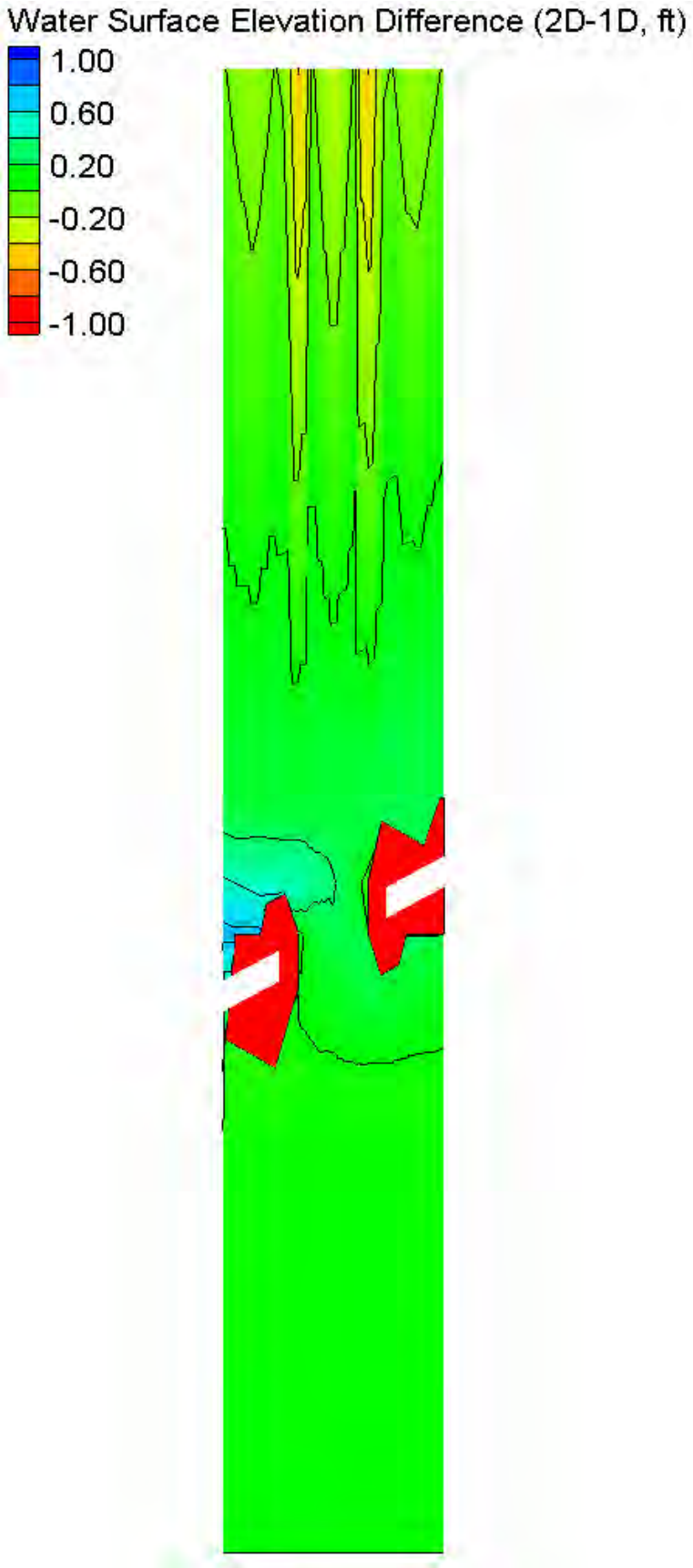

Water Surface Elevation Difference Contours – Small Channel – Embankment Skew (30°)

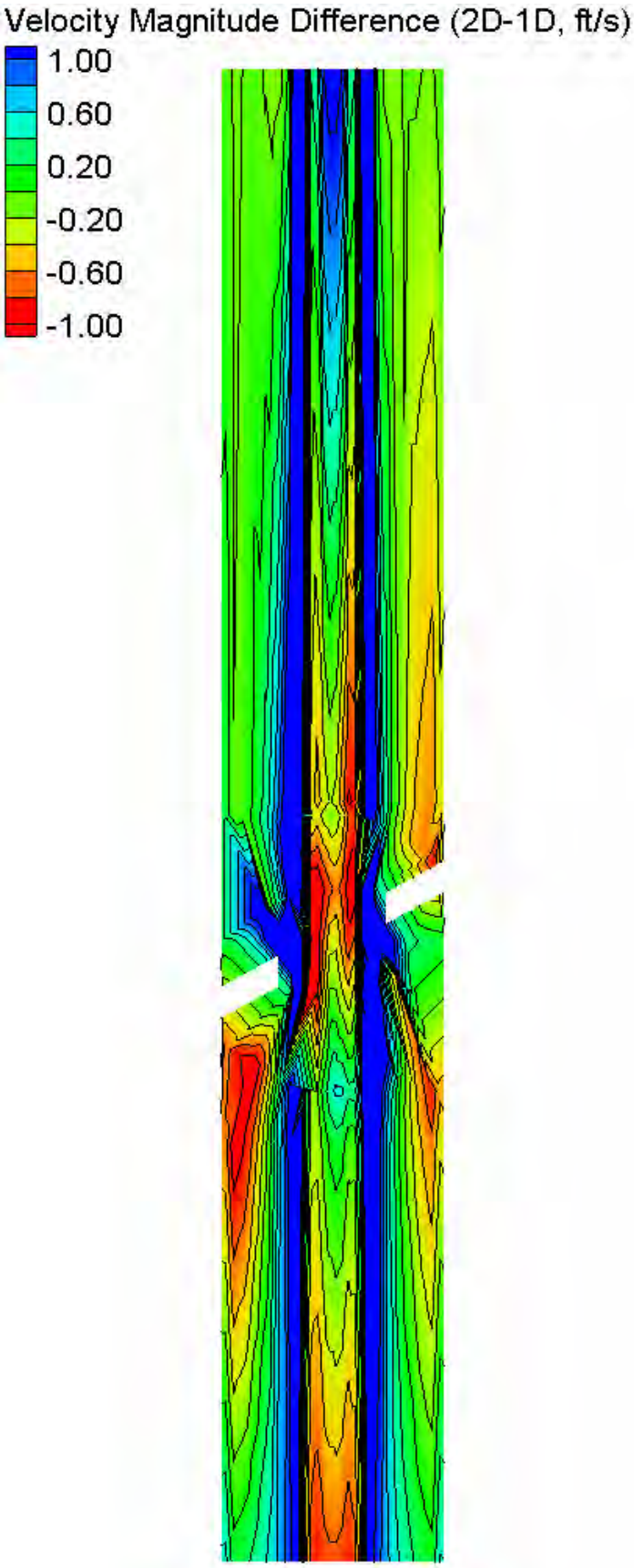

Velocity Magnitude Difference Contours – Small Channel – Embankment Skew (30°)

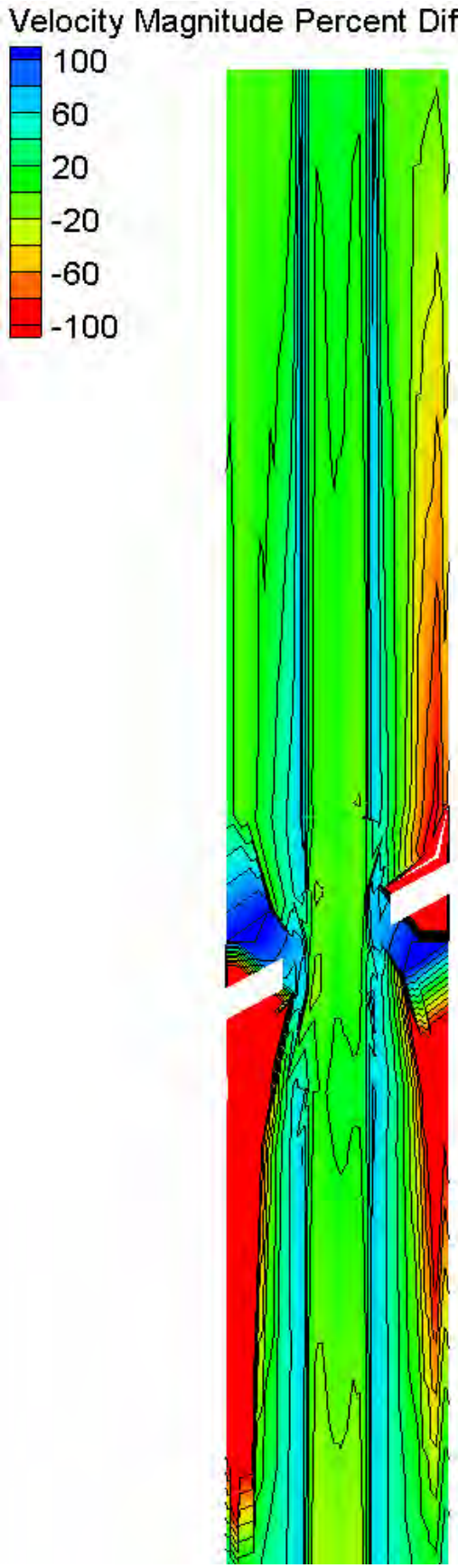

Velocity Magnitude Percent Difference Contours – Small Channel – Embankment Skew (30°)

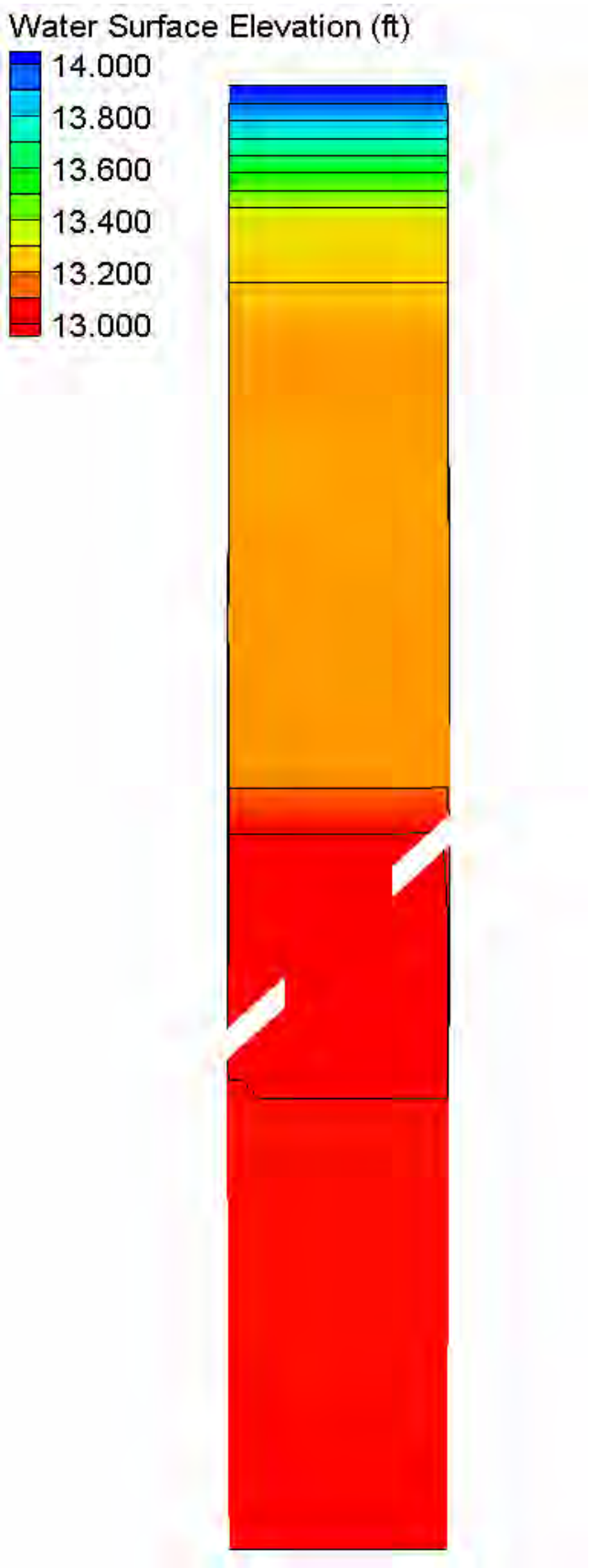

HEC-RAS Water Surface Elevation Contours – Small Channel – Embankment Skew (45°)

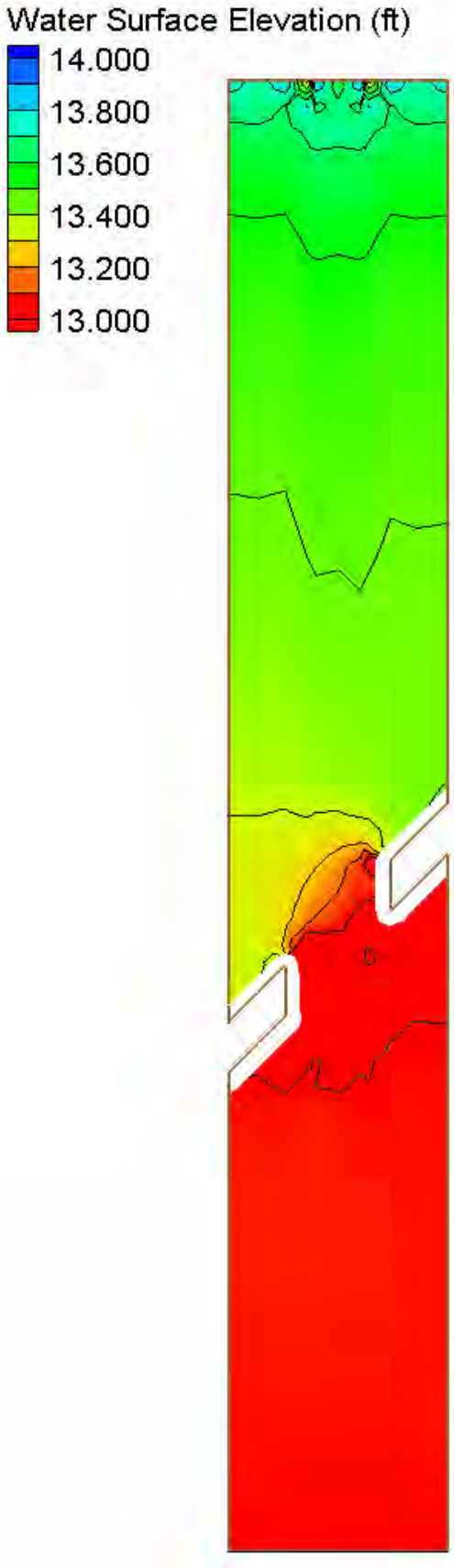

FESWMS Water Surface Elevation Contours – Small Channel – Embankment Skew (45°)

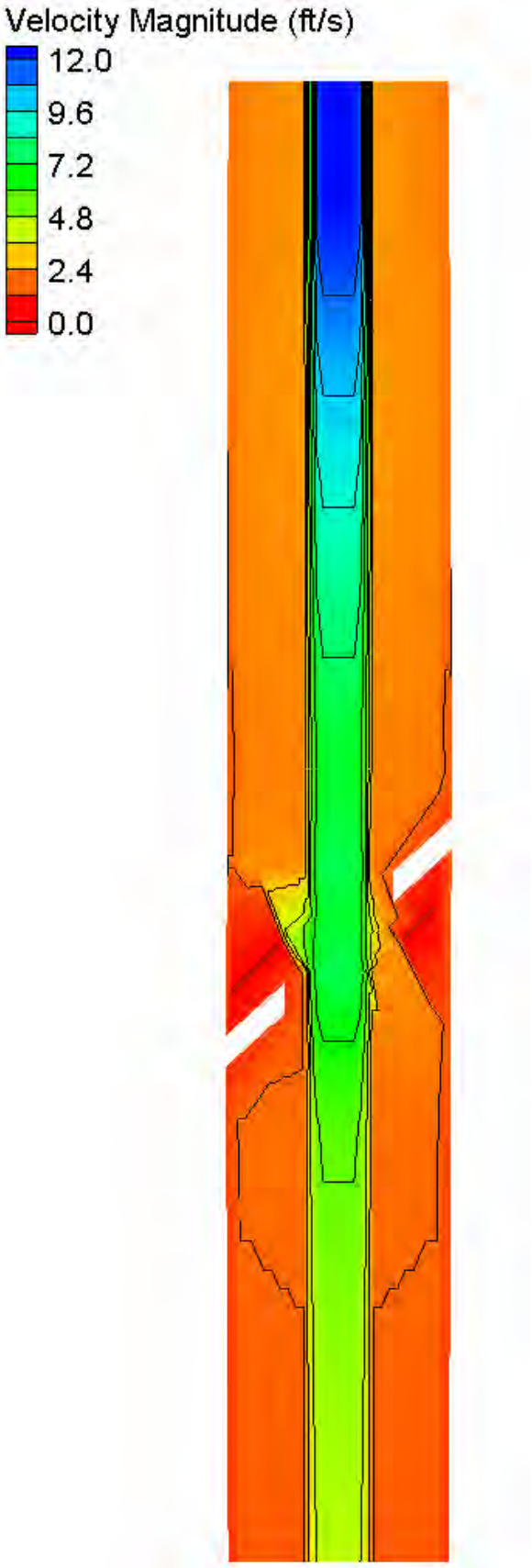

HEC-RAS Velocity Magnitude Contours – Small Channel – Embankment Skew (45°)

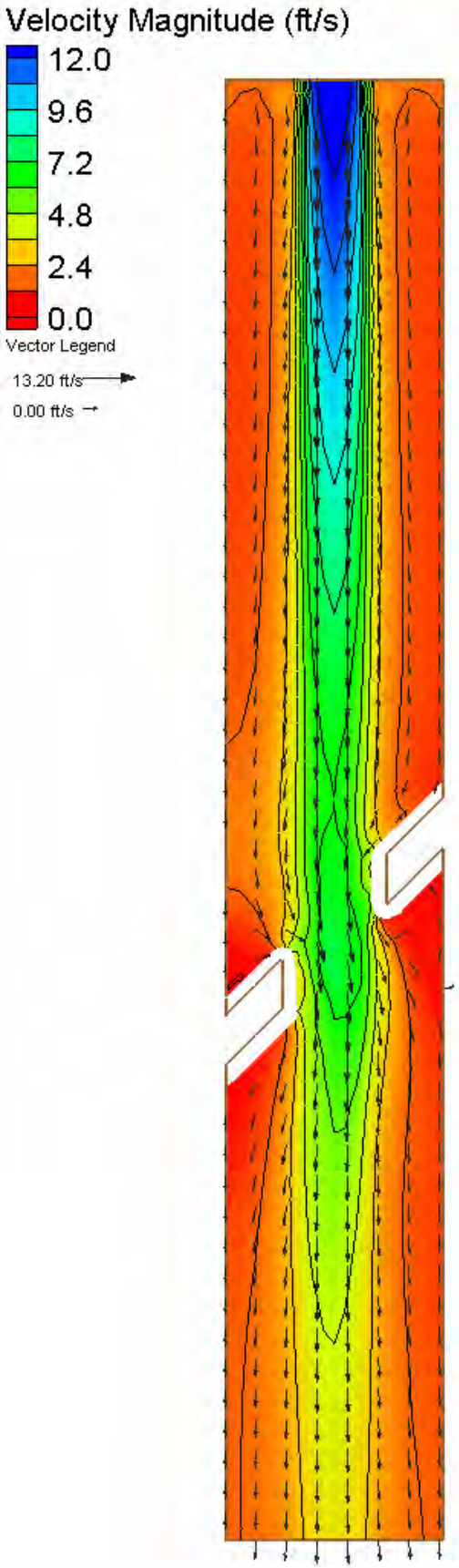

FESWMS Velocity Magnitude Contours – Small Channel – Embankment Skew (45°)

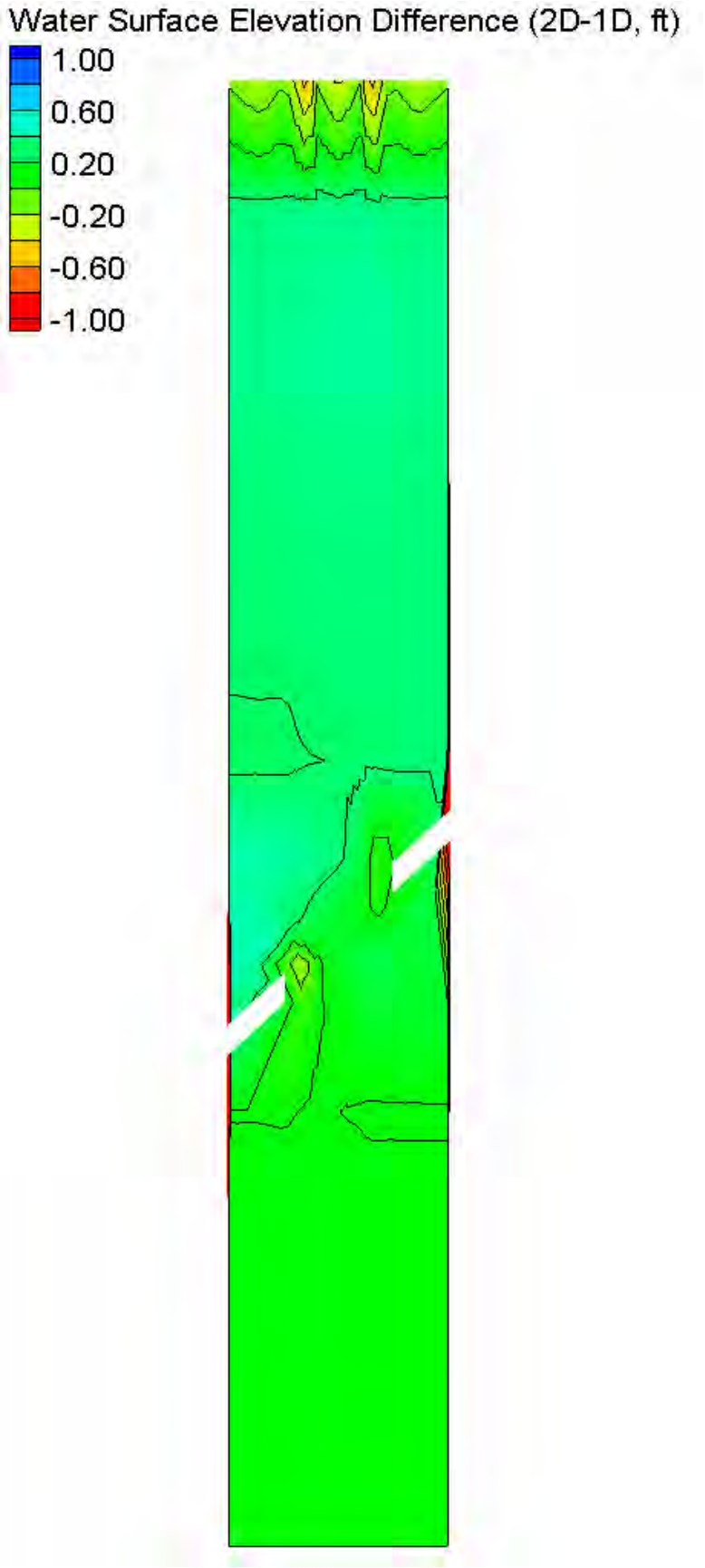

Water Surface Elevation Difference Contours – Small Channel – Embankment Skew (45°)

Velocity Magnitude Difference Contours – Small Channel – Embankment Skew (45°)

Velocity Magnitude Percent Difference Contours – Small Channel – Embankment Skew (45°)

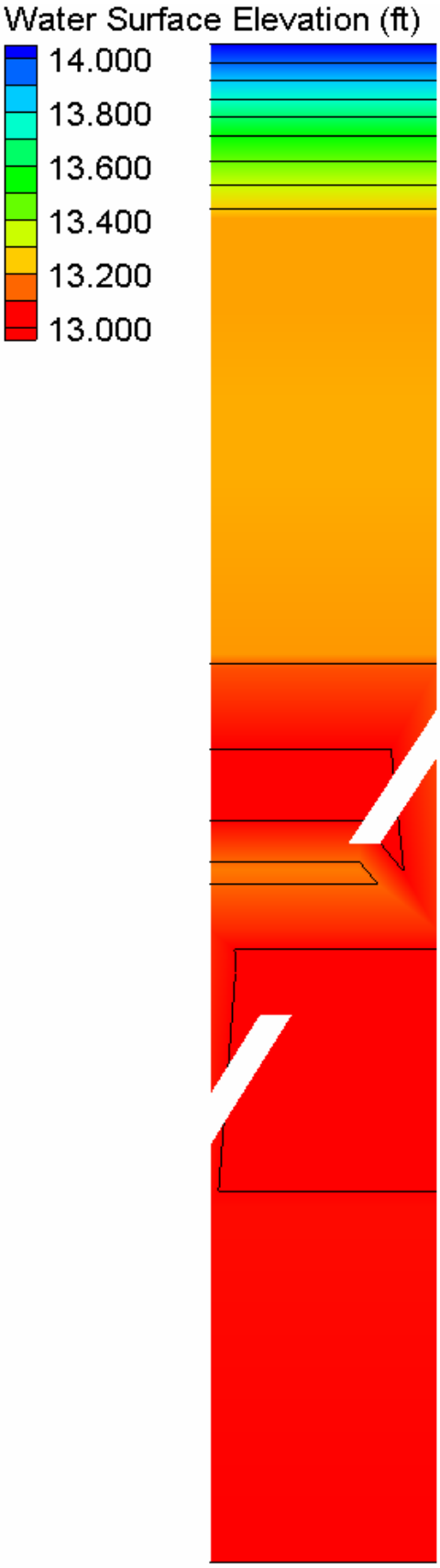

HEC-RAS Water Surface Elevation Contours – Small Channel – Embankment Skew (60°)

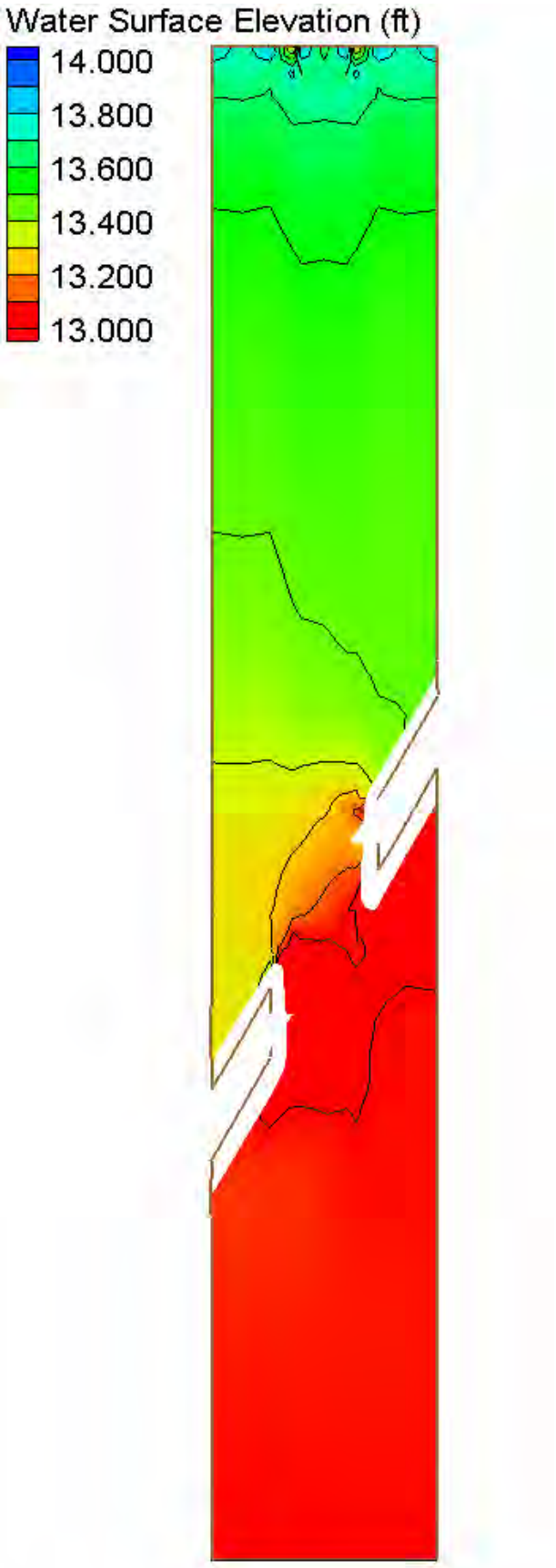

FESWMS Water Surface Elevation Contours – Small Channel – Embankment Skew (60°)

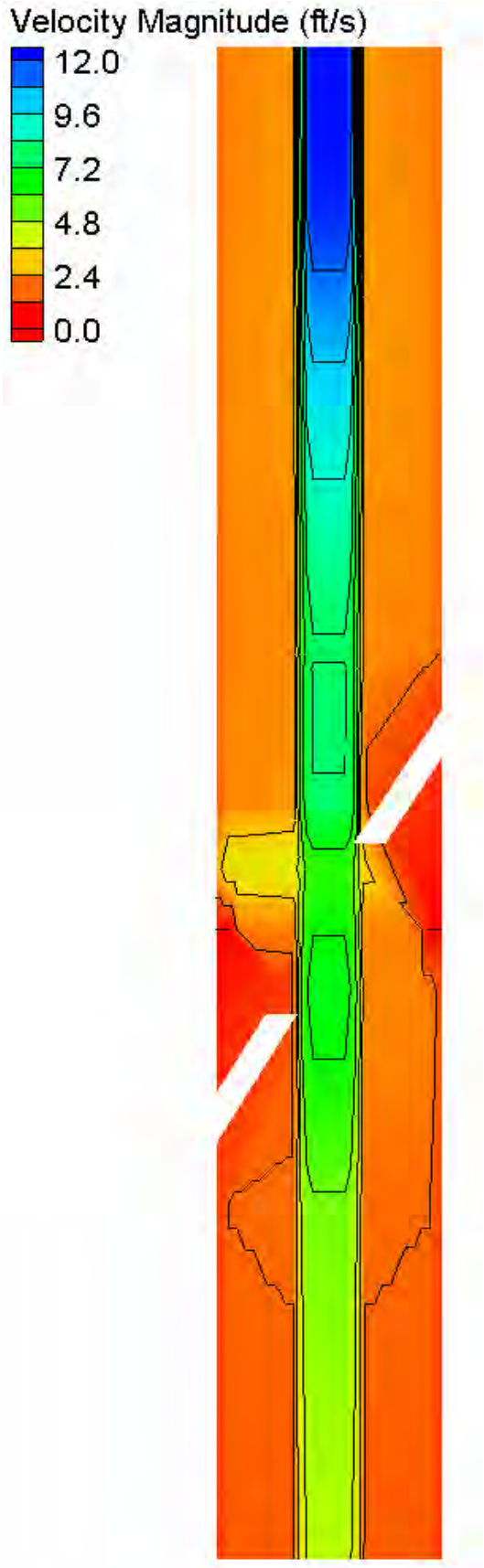

HEC-RAS Velocity Magnitude Contours – Small Channel – Embankment Skew (60°)

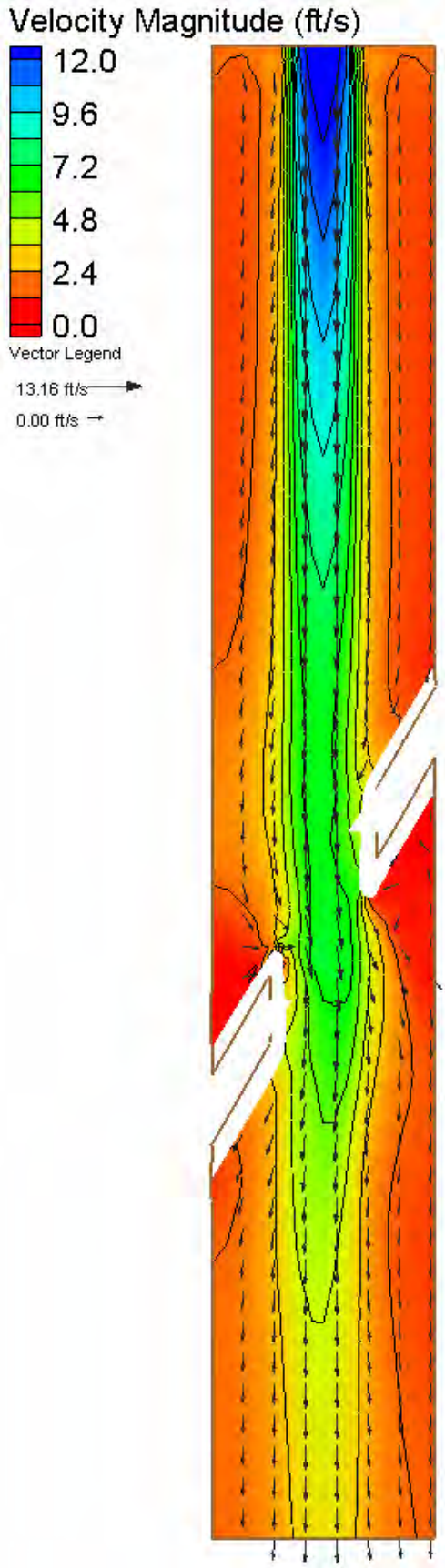

FESWMS Velocity Magnitude Contours – Small Channel – Embankment Skew (60°)

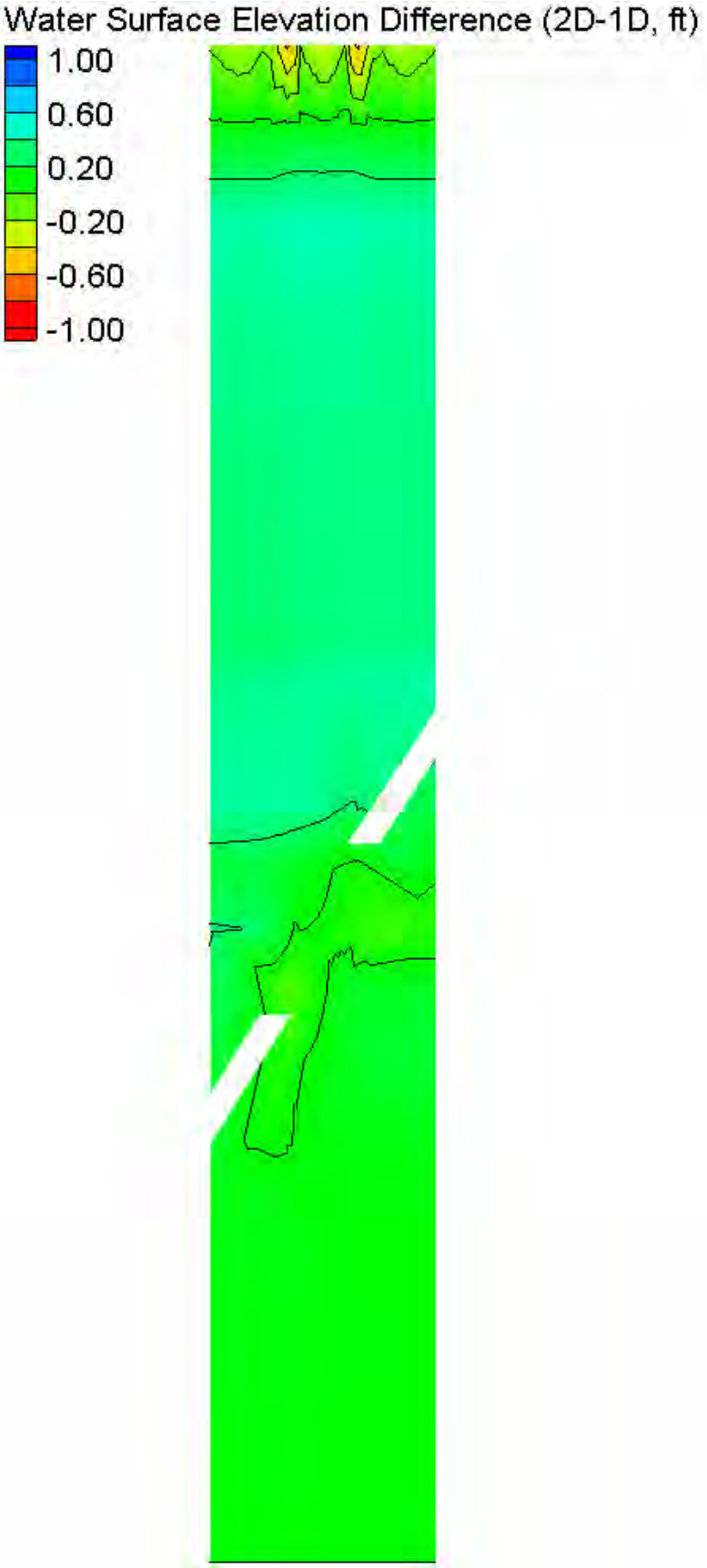

Water Surface Elevation Difference Contours – Small Channel – Embankment Skew (60°)

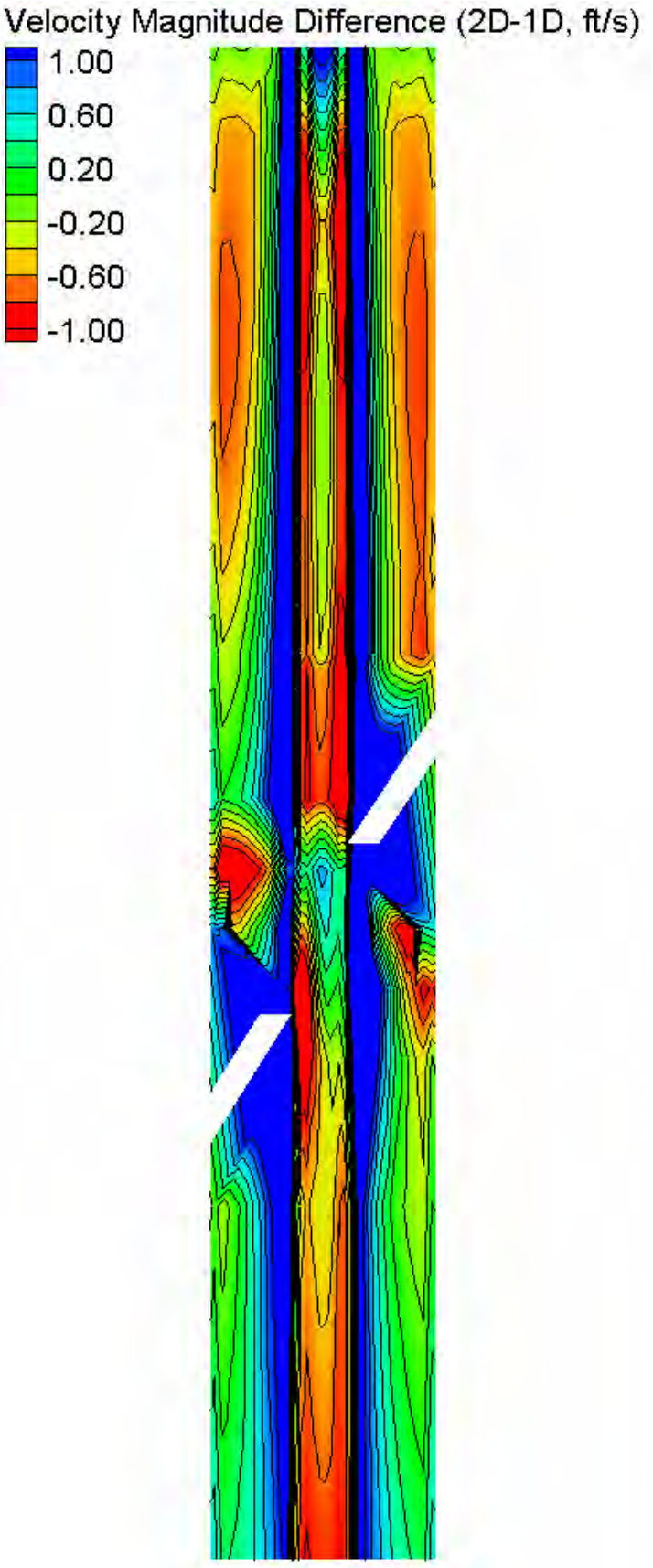

Velocity Magnitude Difference Contours – Small Channel – Embankment Skew (60°)

Velocity Magnitude Percent Difference Contours – Small Channel – Embankment Skew (60°)

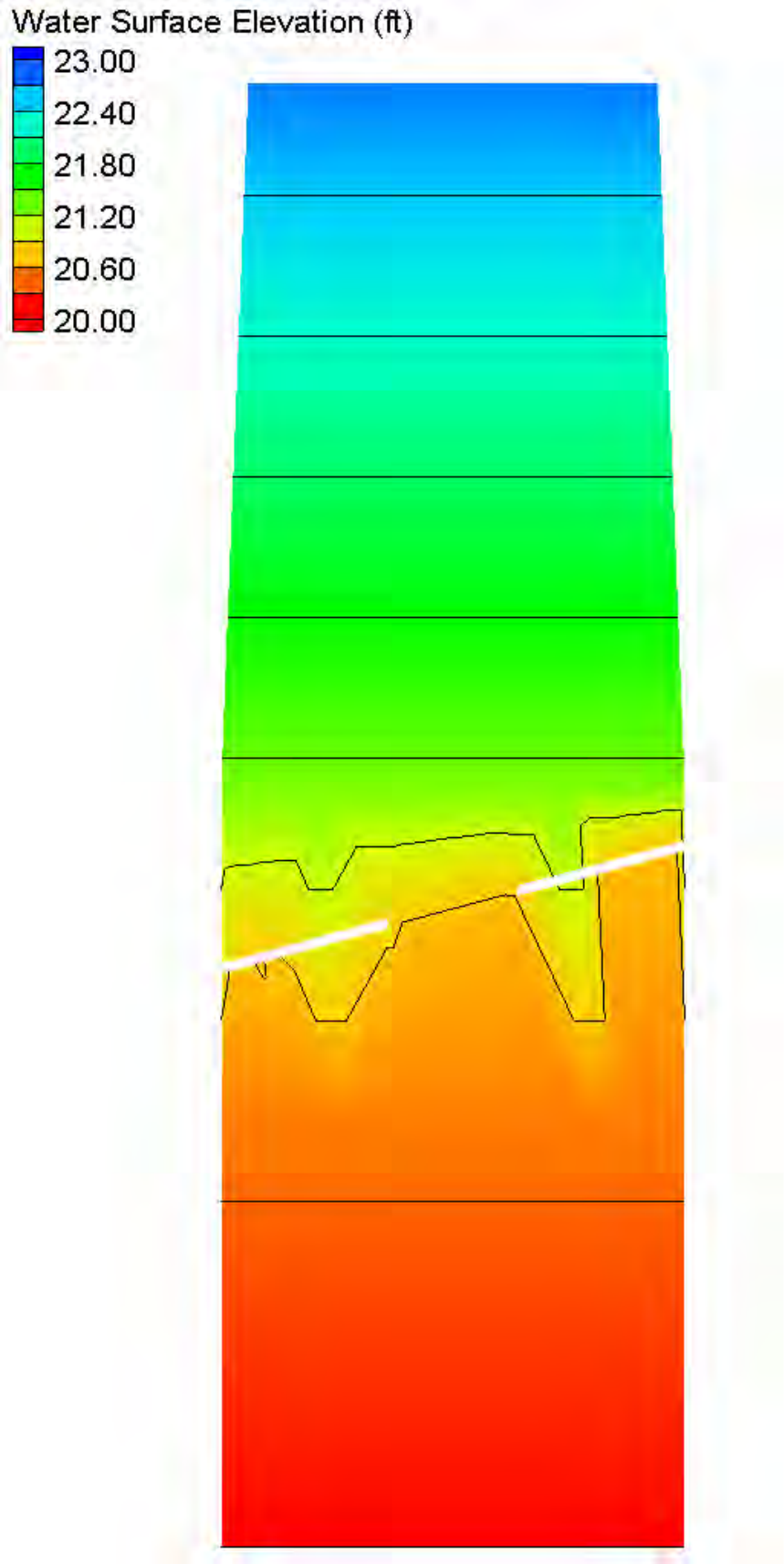

HEC-RAS Water Surface Elevation Contours – Large Channel – Embankment Skew (15°)

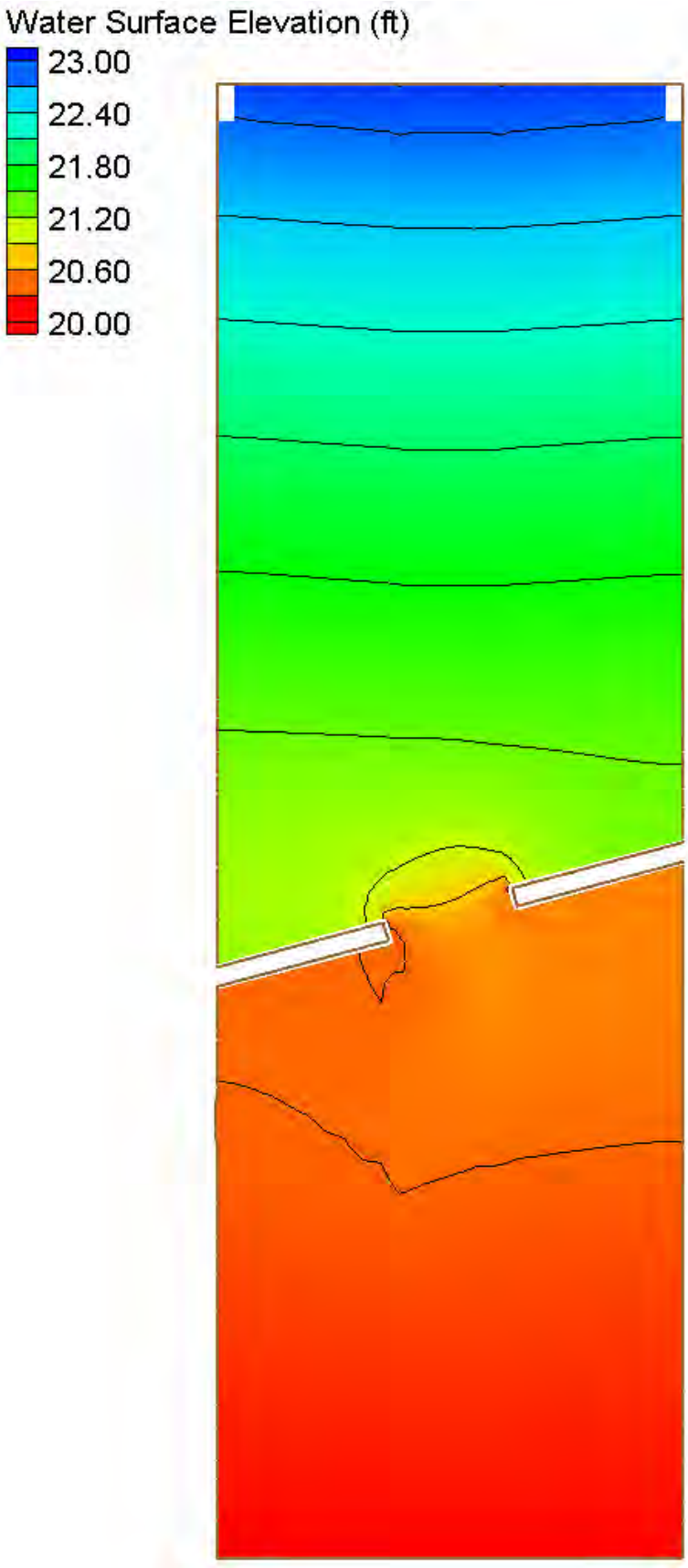

FESWMS Water Surface Elevation Contours – Large Channel – Embankment Skew (15°)

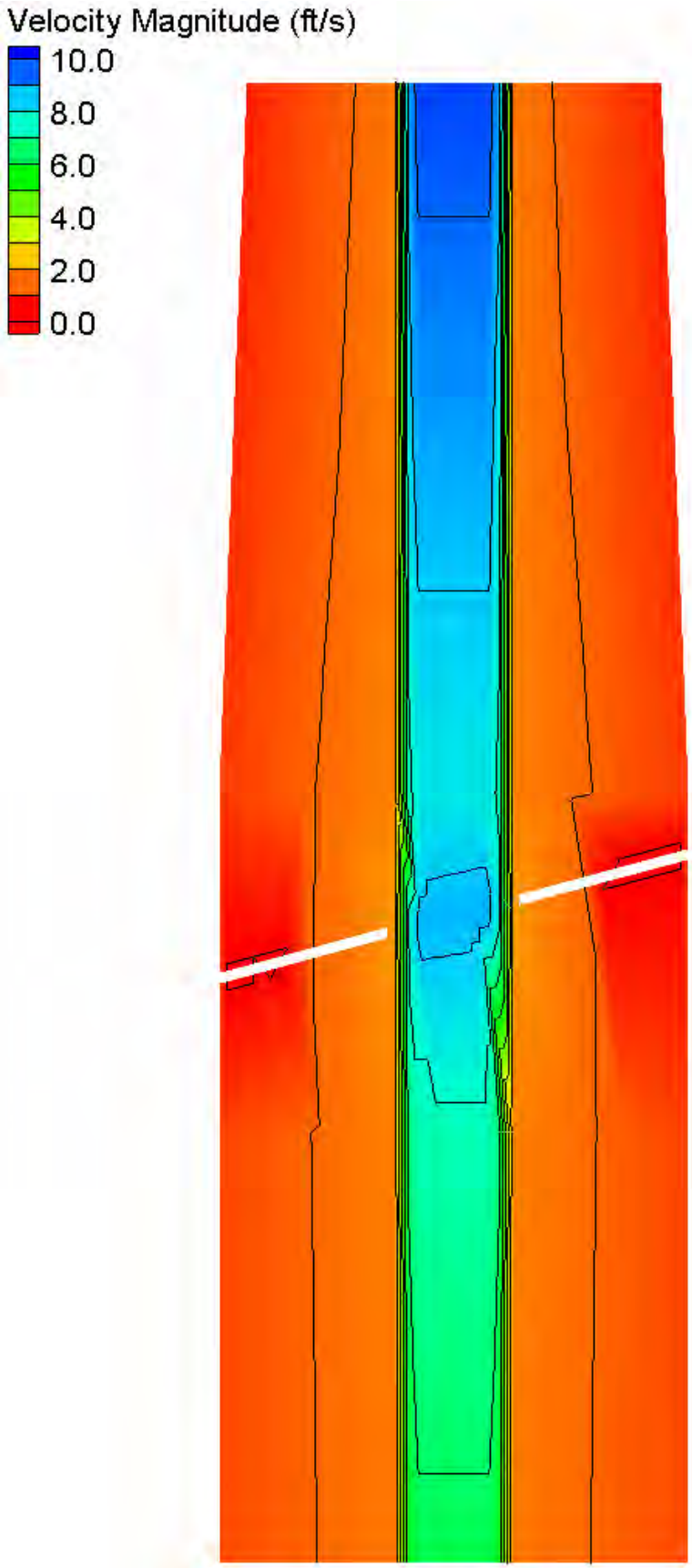

HEC-RAS Velocity Magnitude Contours – Large Channel – Embankment Skew (15°)

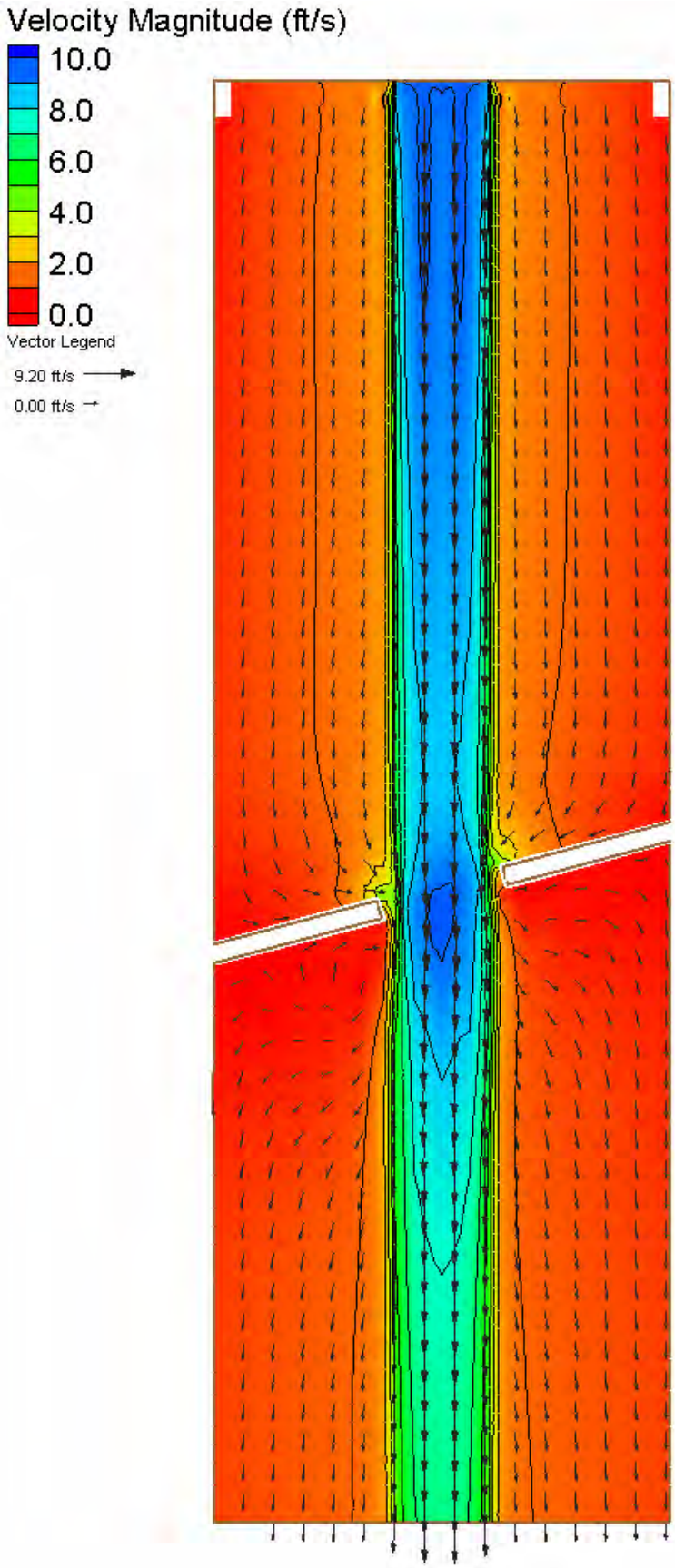

FESWMS Velocity Magnitude Contours – Large Channel – Embankment Skew (15°)

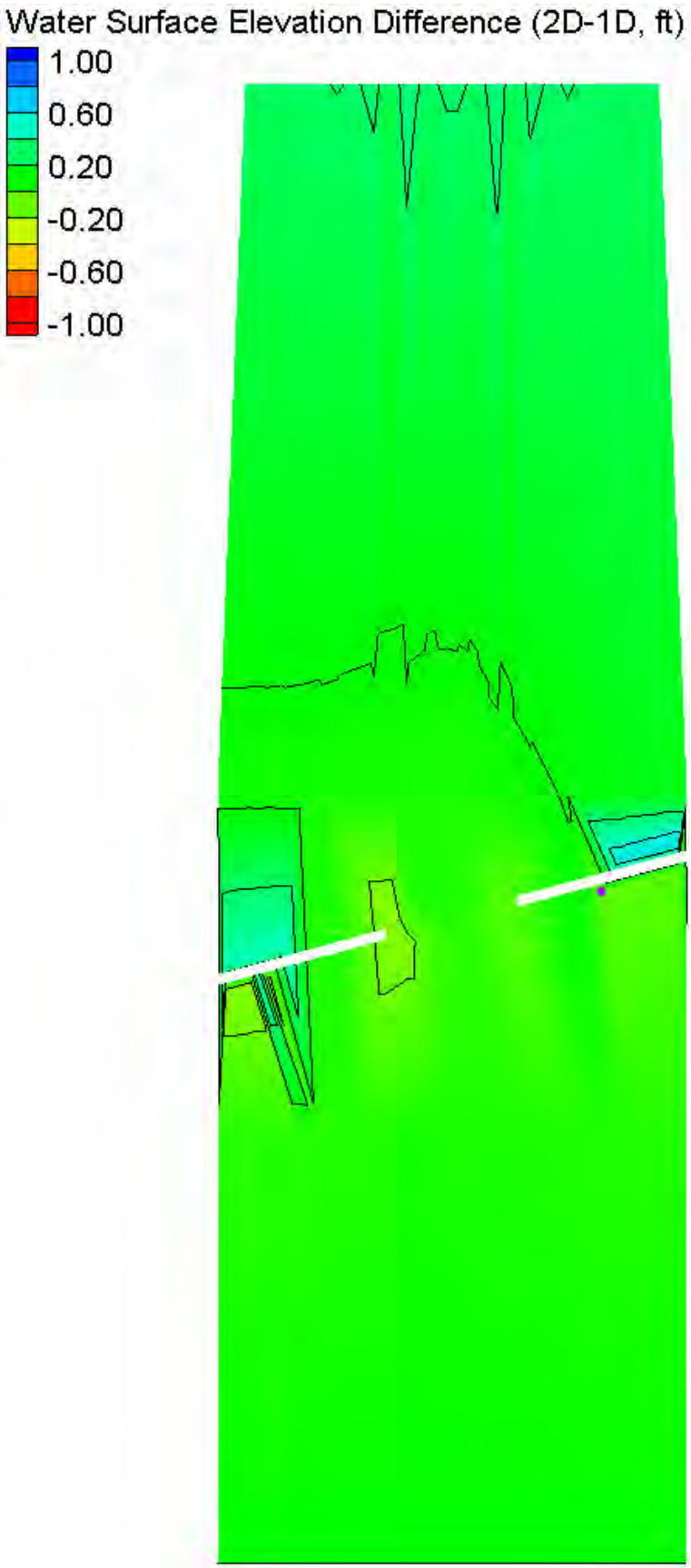

Water Surface Elevation Difference Contours – Large Channel – Embankment Skew (15°)

Velocity Magnitude Difference Contours – Large Channel – Embankment Skew (15°)

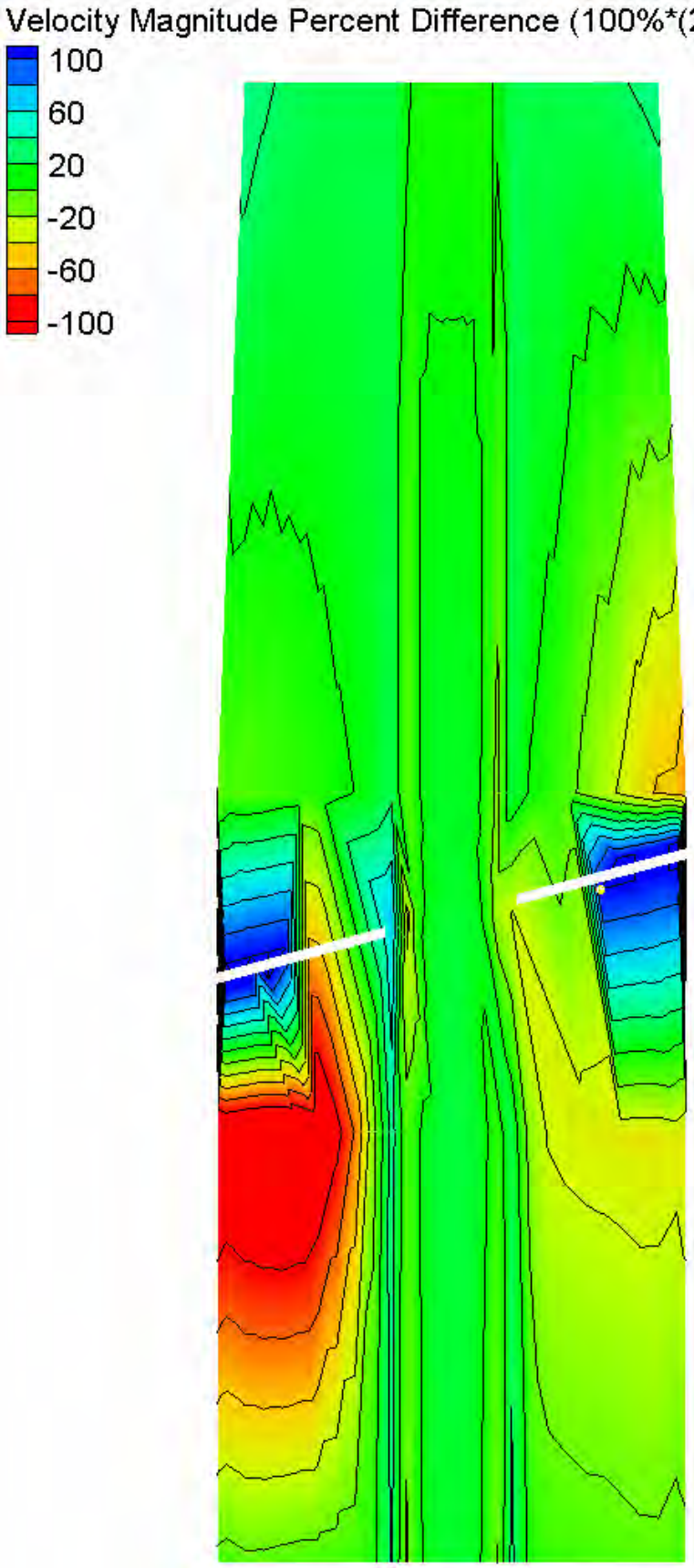

Velocity Magnitude Percent Difference Contours – Large Channel – Embankment Skew (15°)

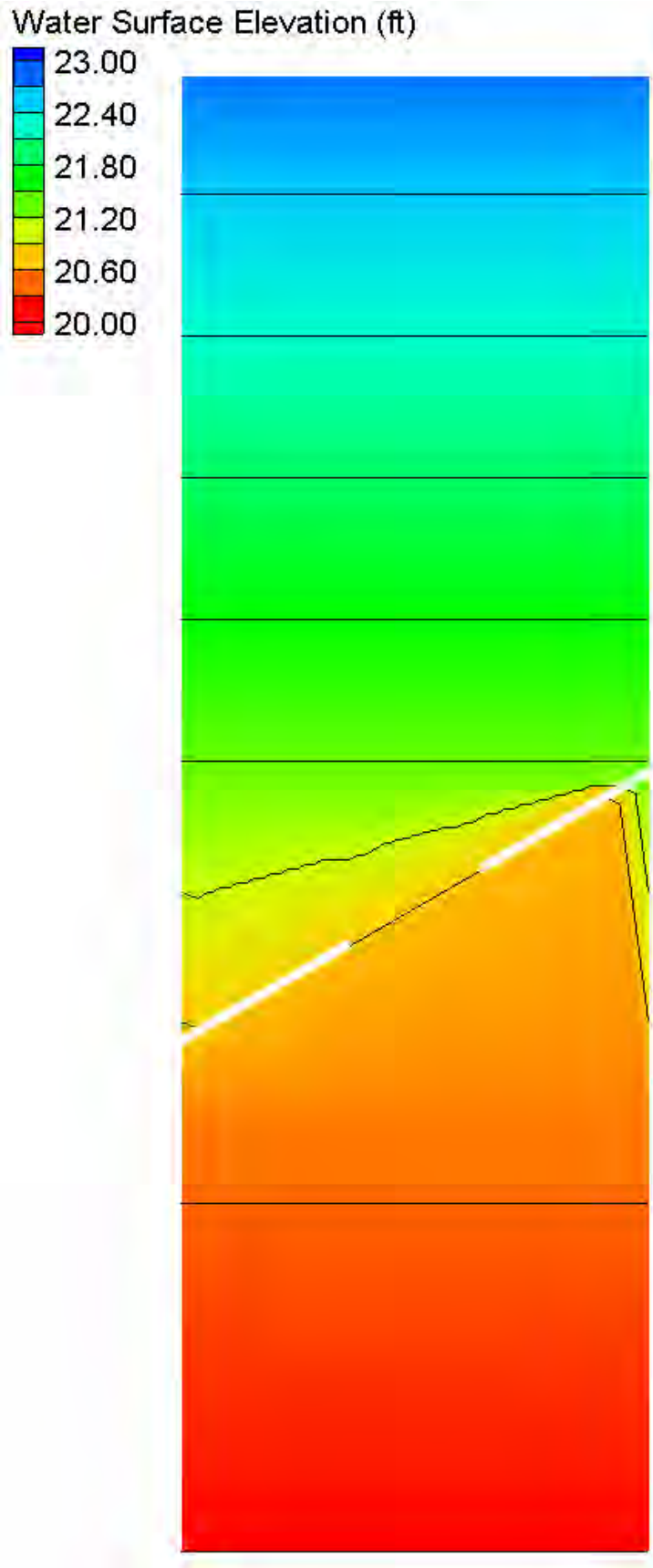

HEC-RAS Water Surface Elevation Contours – Large Channel – Embankment Skew (30°)

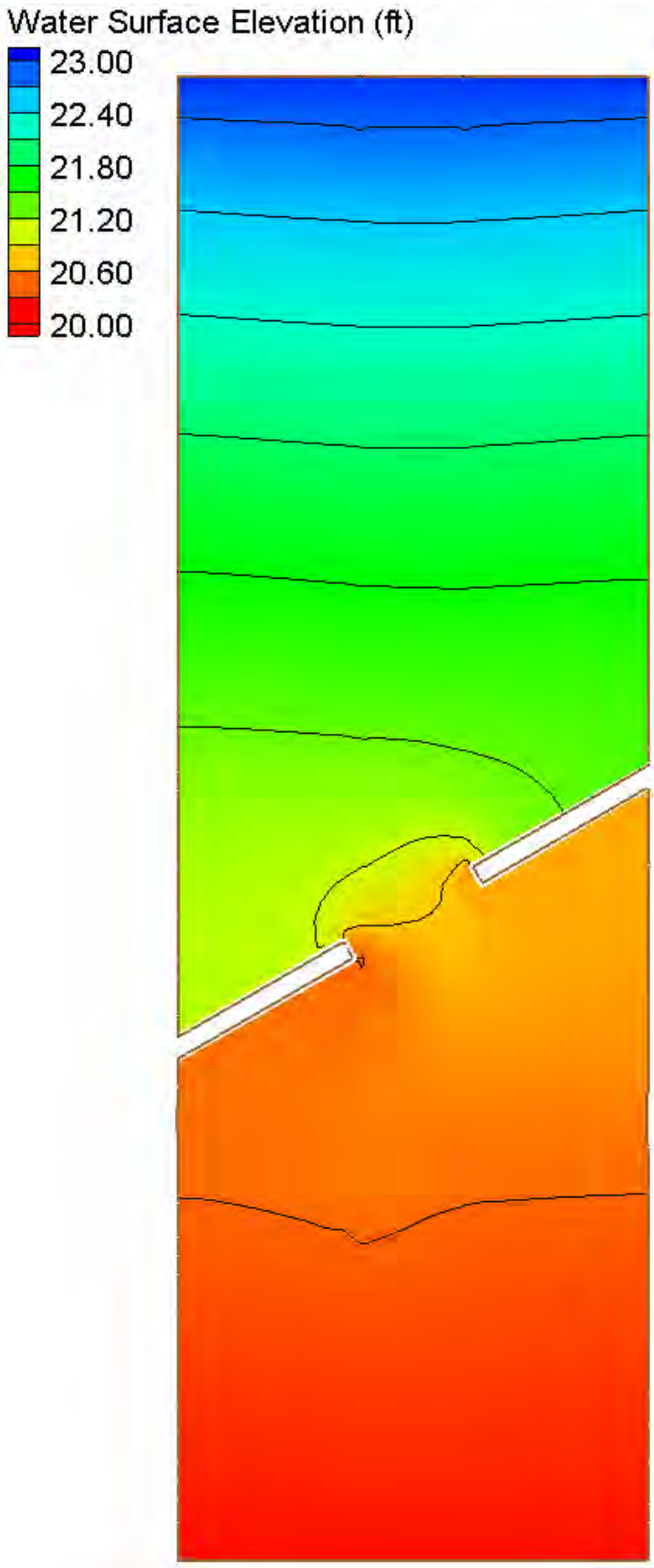

FESWMS Water Surface Elevation Contours – Large Channel – Embankment Skew (30°)

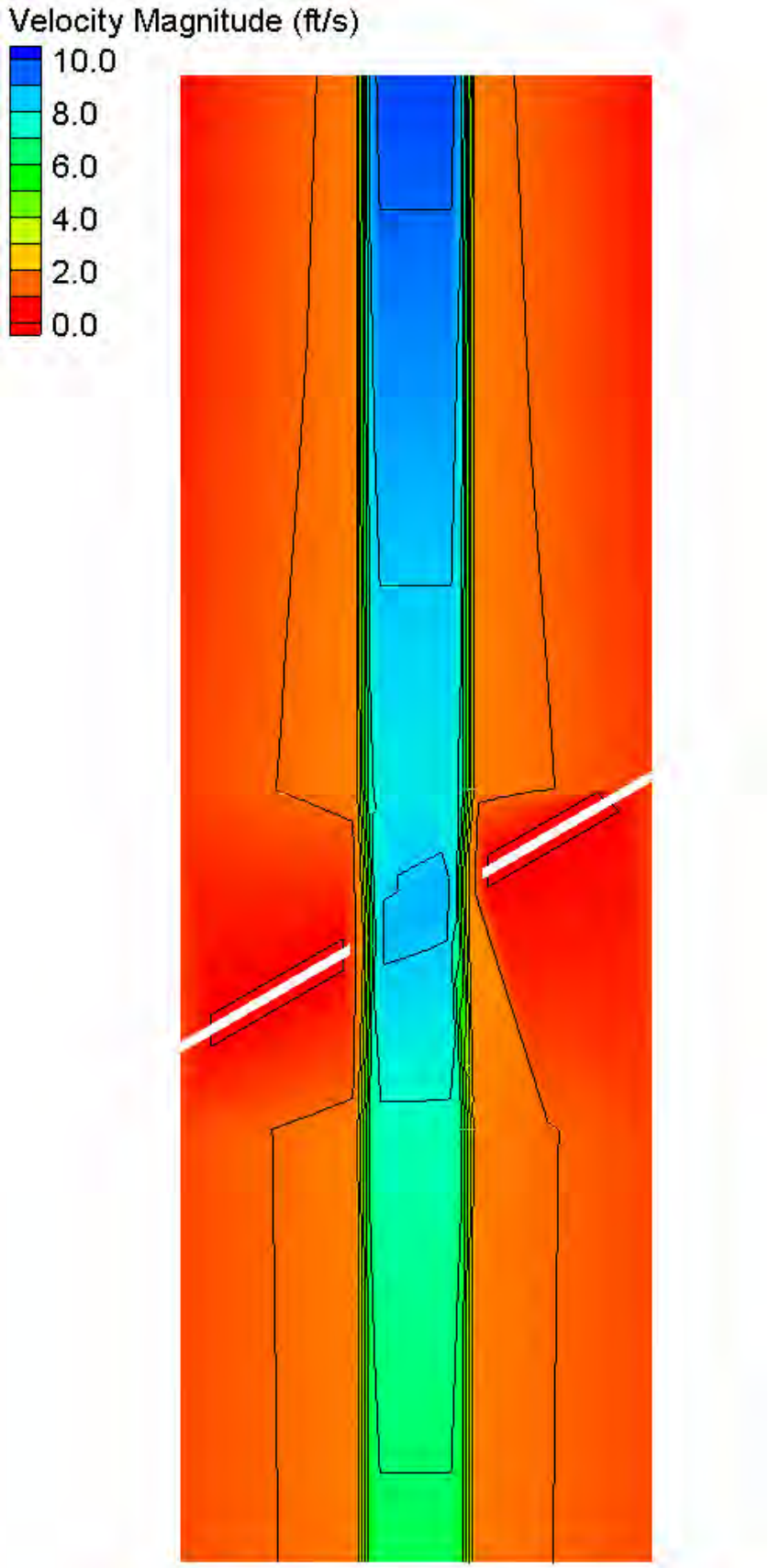

HEC-RAS Velocity Magnitude Contours – Large Channel – Embankment Skew (30°)

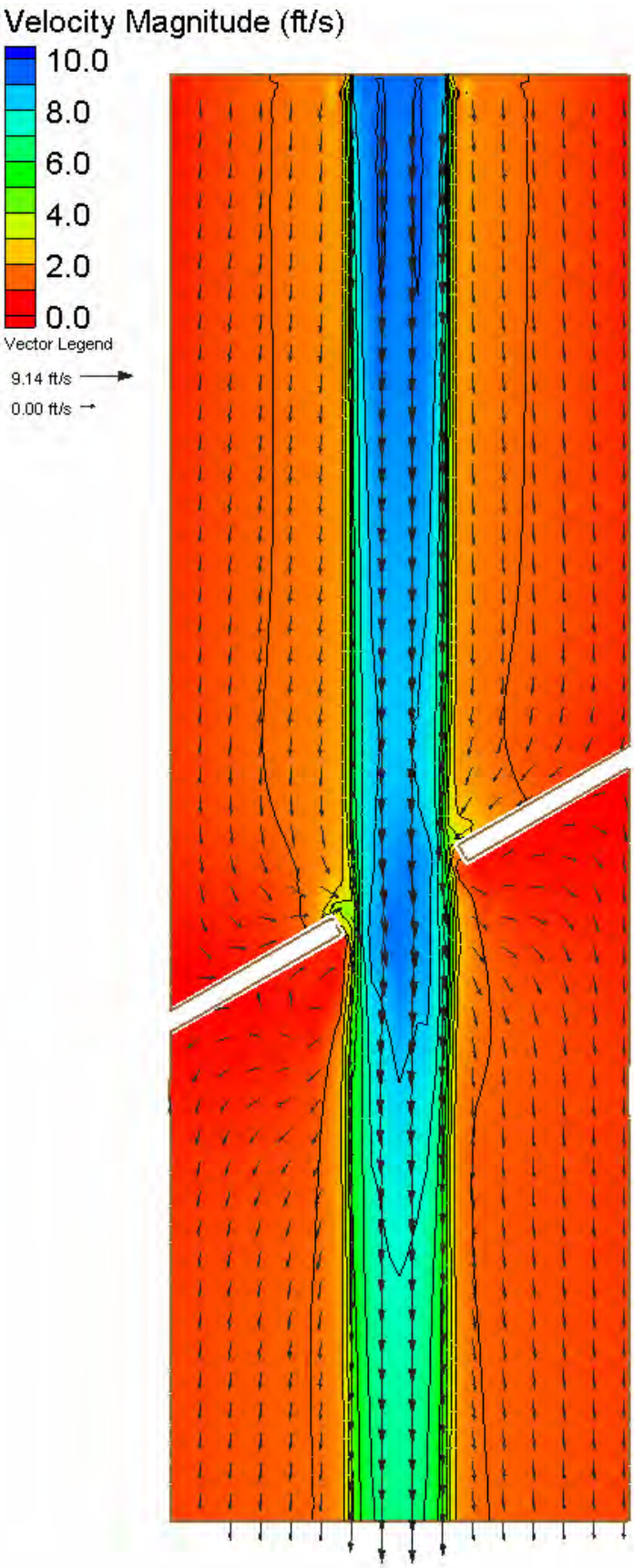

FESWMS Velocity Magnitude Contours – Large Channel – Embankment Skew (30°)

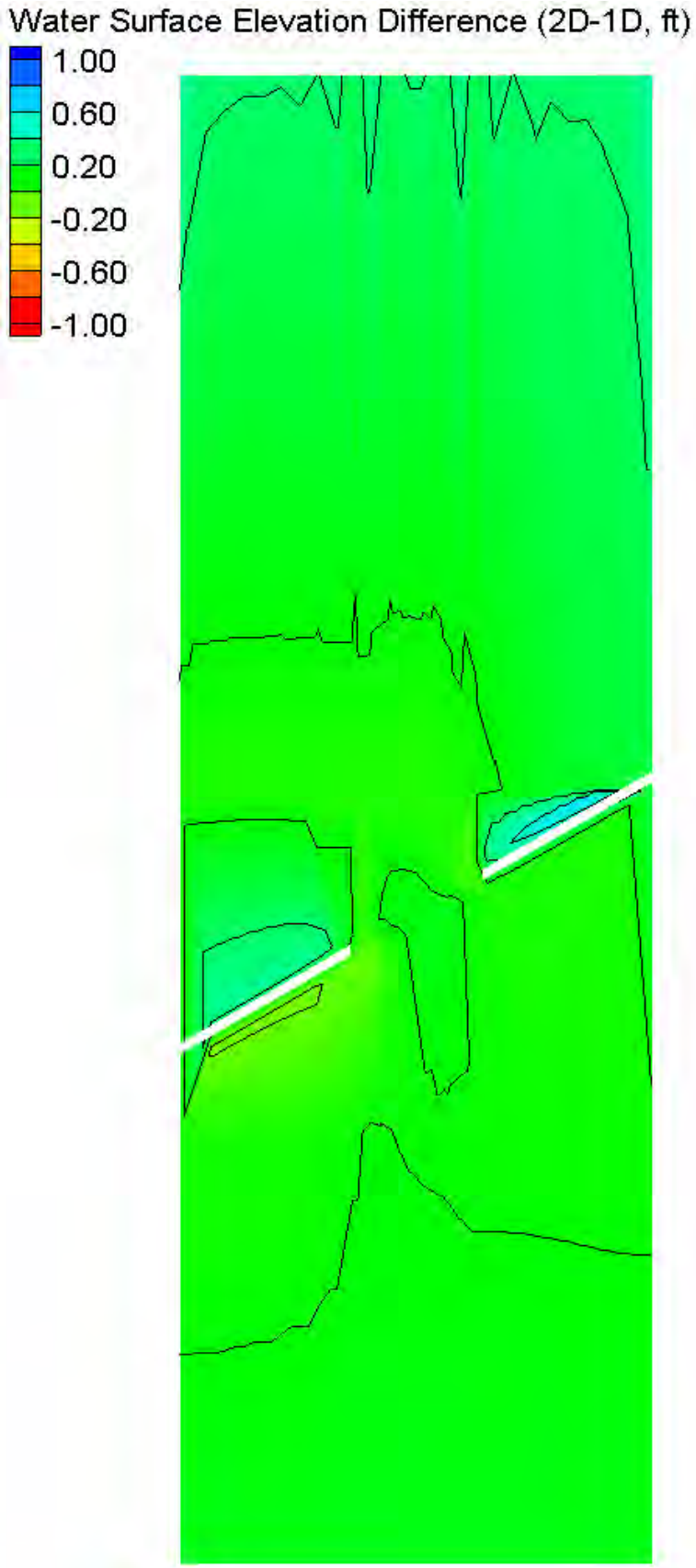

Water Surface Elevation Difference Contours – Large Channel – Embankment Skew (30°)

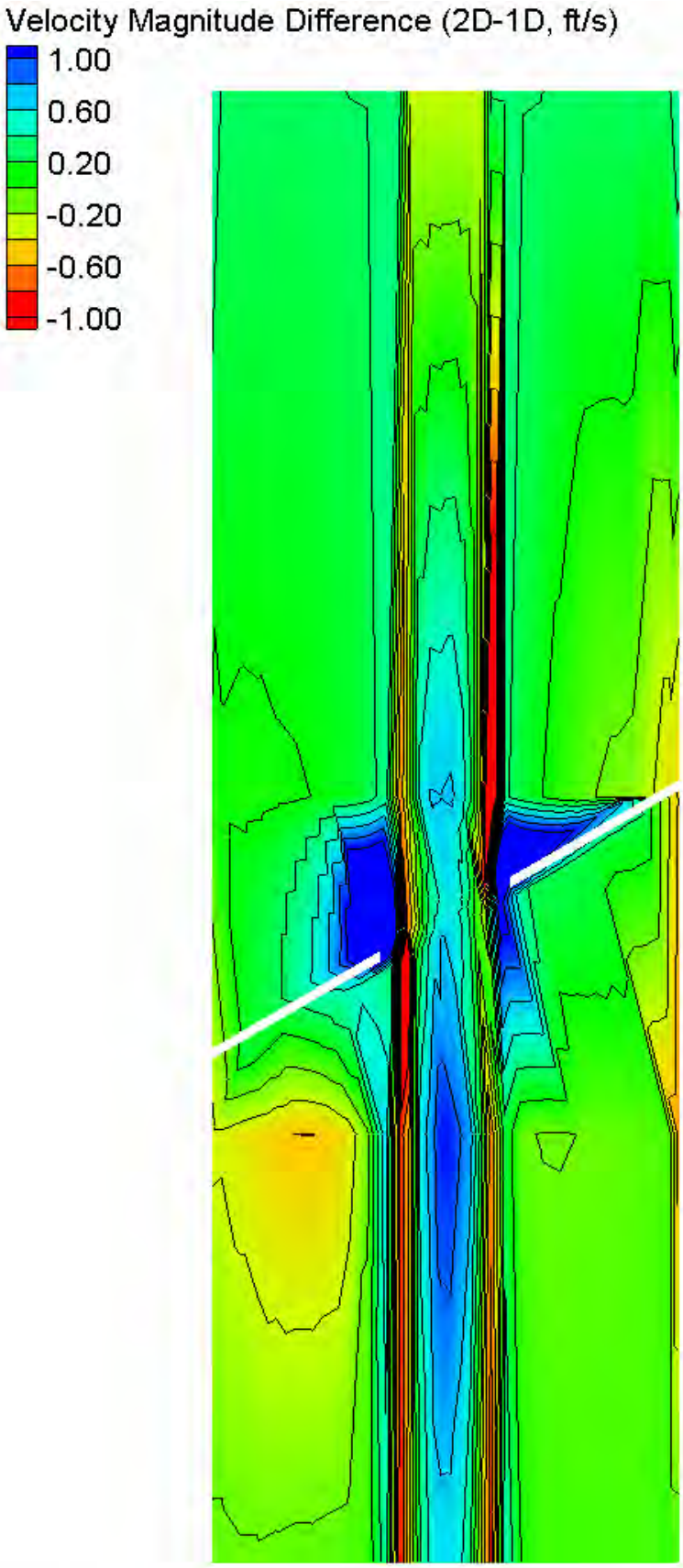

Velocity Magnitude Difference Contours – Large Channel – Embankment Skew (30°)

Velocity Magnitude Percent Difference Contours – Large Channel – Embankment Skew (30°)

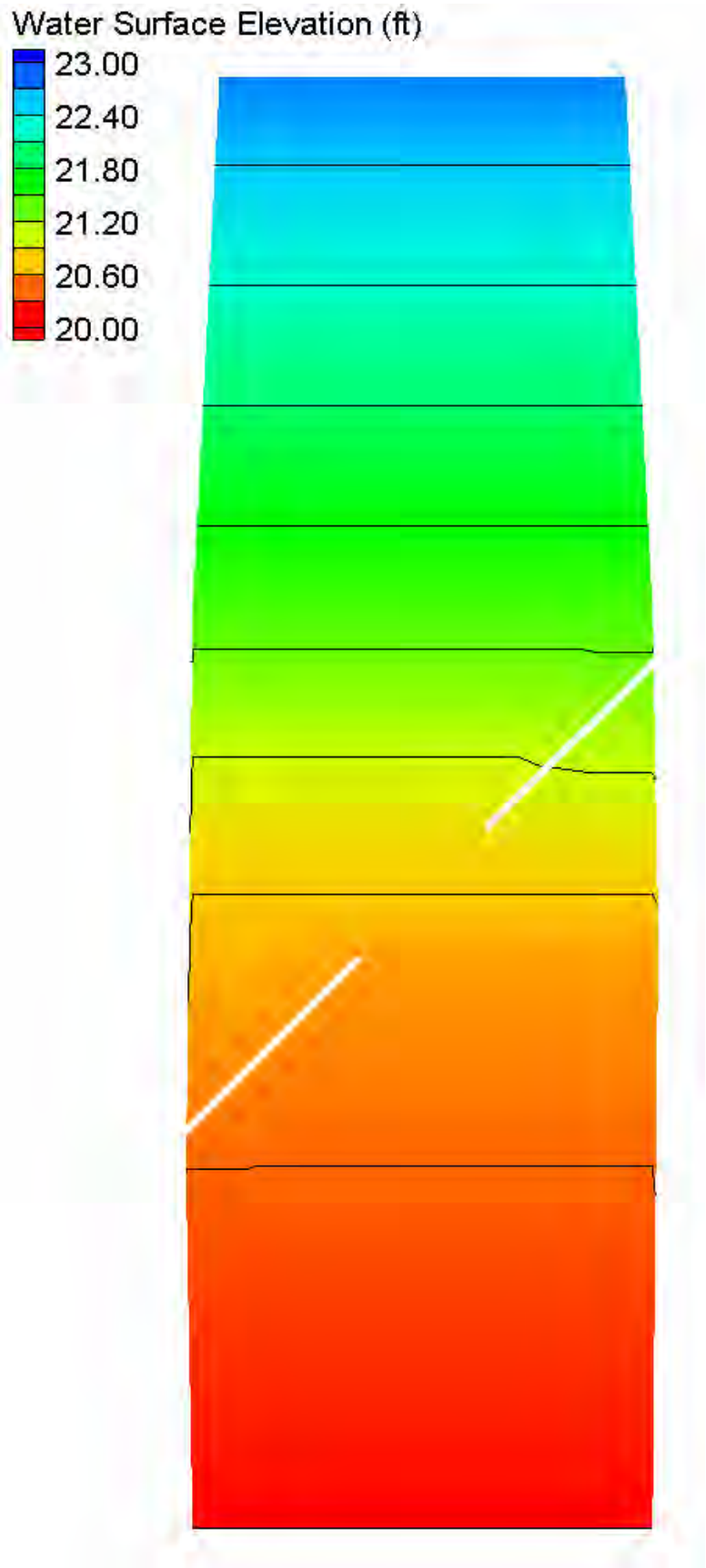

HEC-RAS Water Surface Elevation Contours – Large Channel – Embankment Skew (45°)

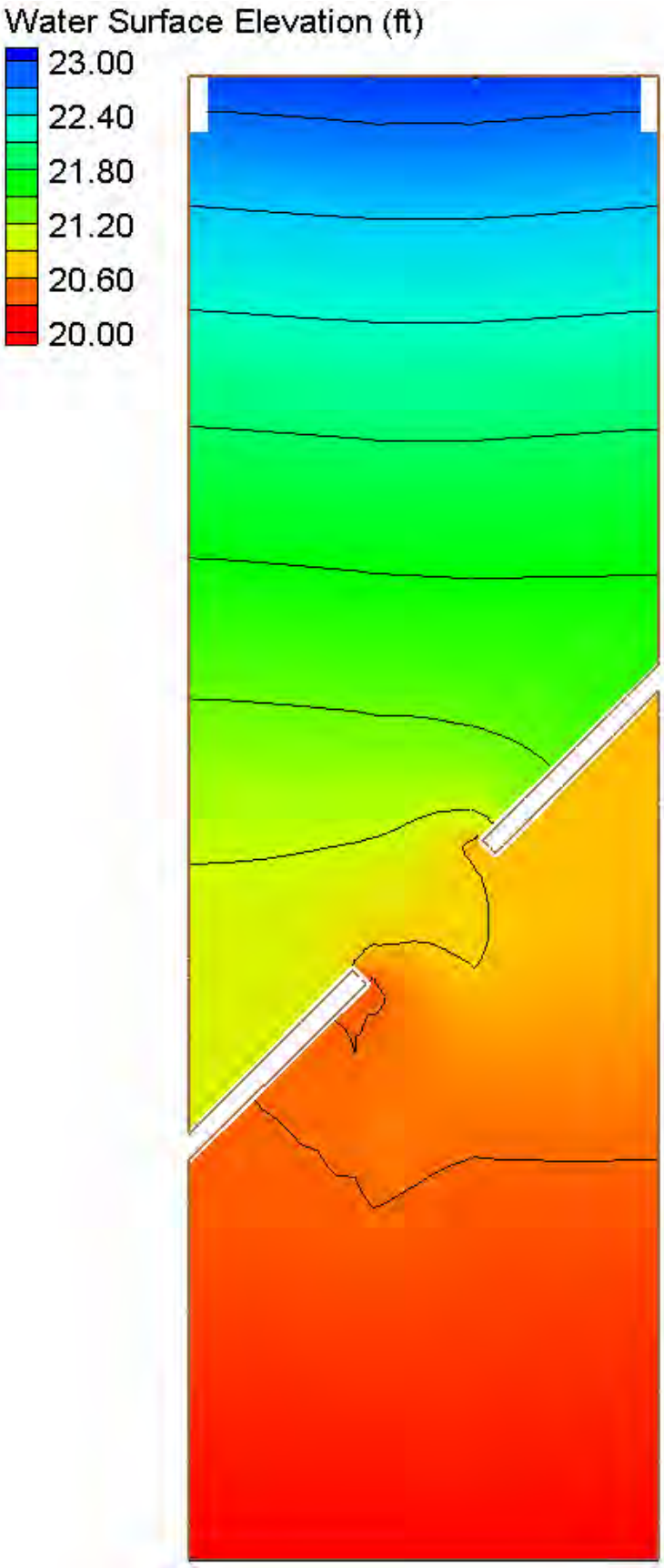

FESWMS Water Surface Elevation Contours – Large Channel – Embankment Skew (45°)

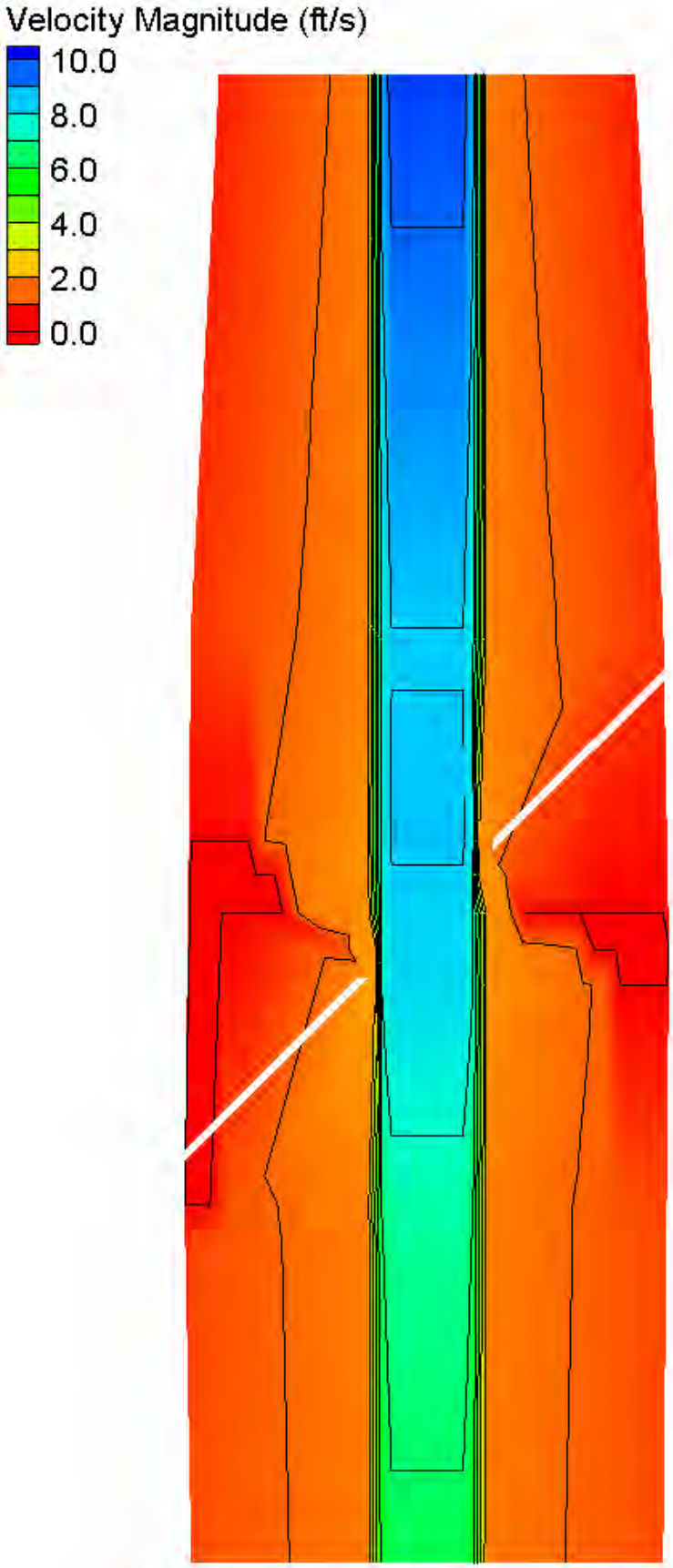

HEC-RAS Velocity Magnitude Contours – Large Channel – Embankment Skew (45°)

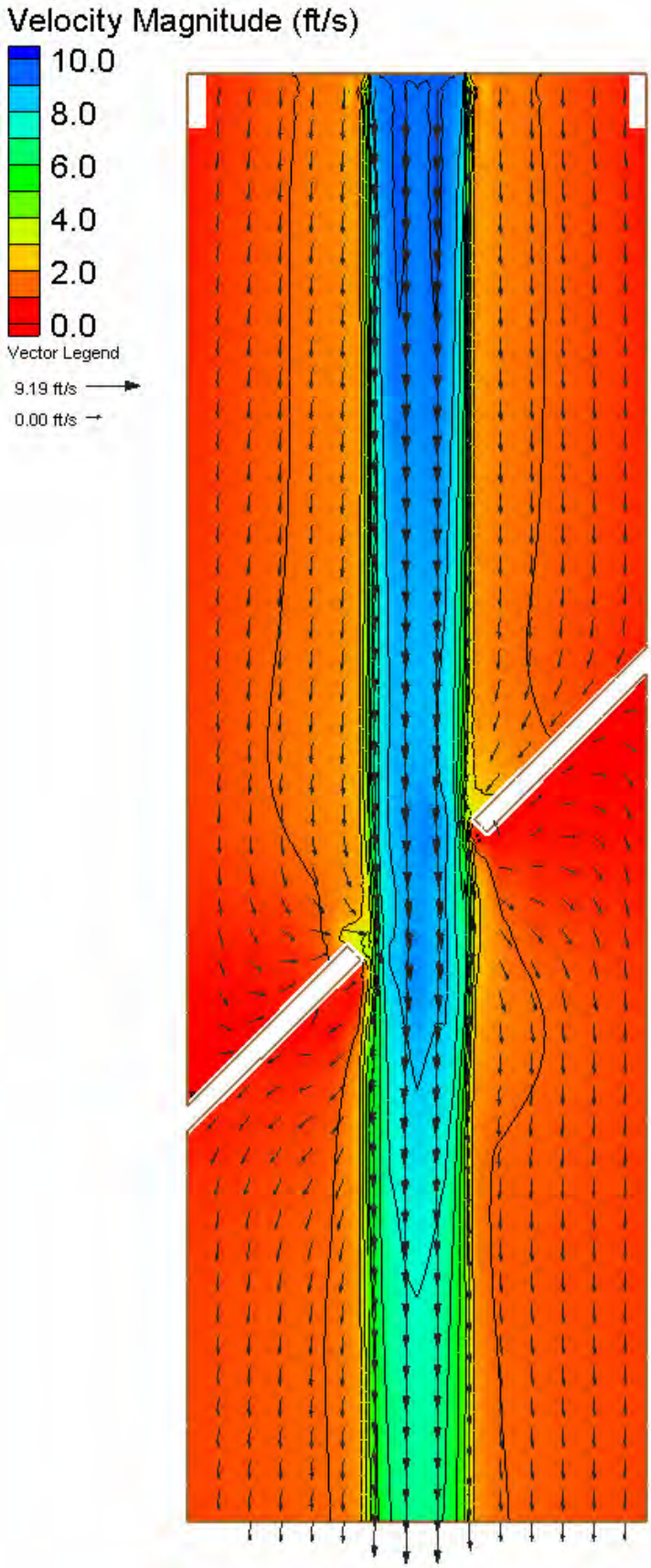

FESWMS Velocity Magnitude Contours – Large Channel – Embankment Skew (45°)

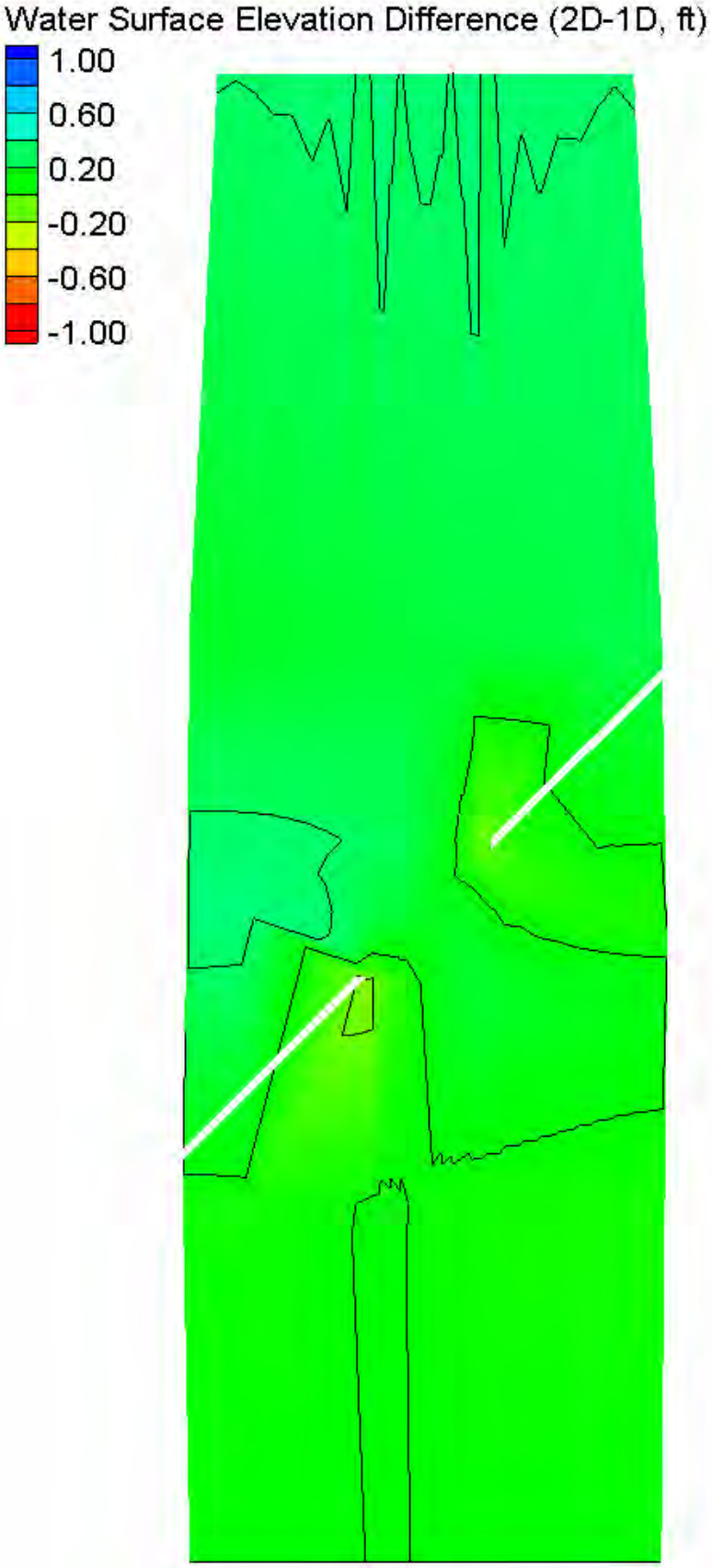

Water Surface Elevation Difference Contours – Large Channel – Embankment Skew (45°)

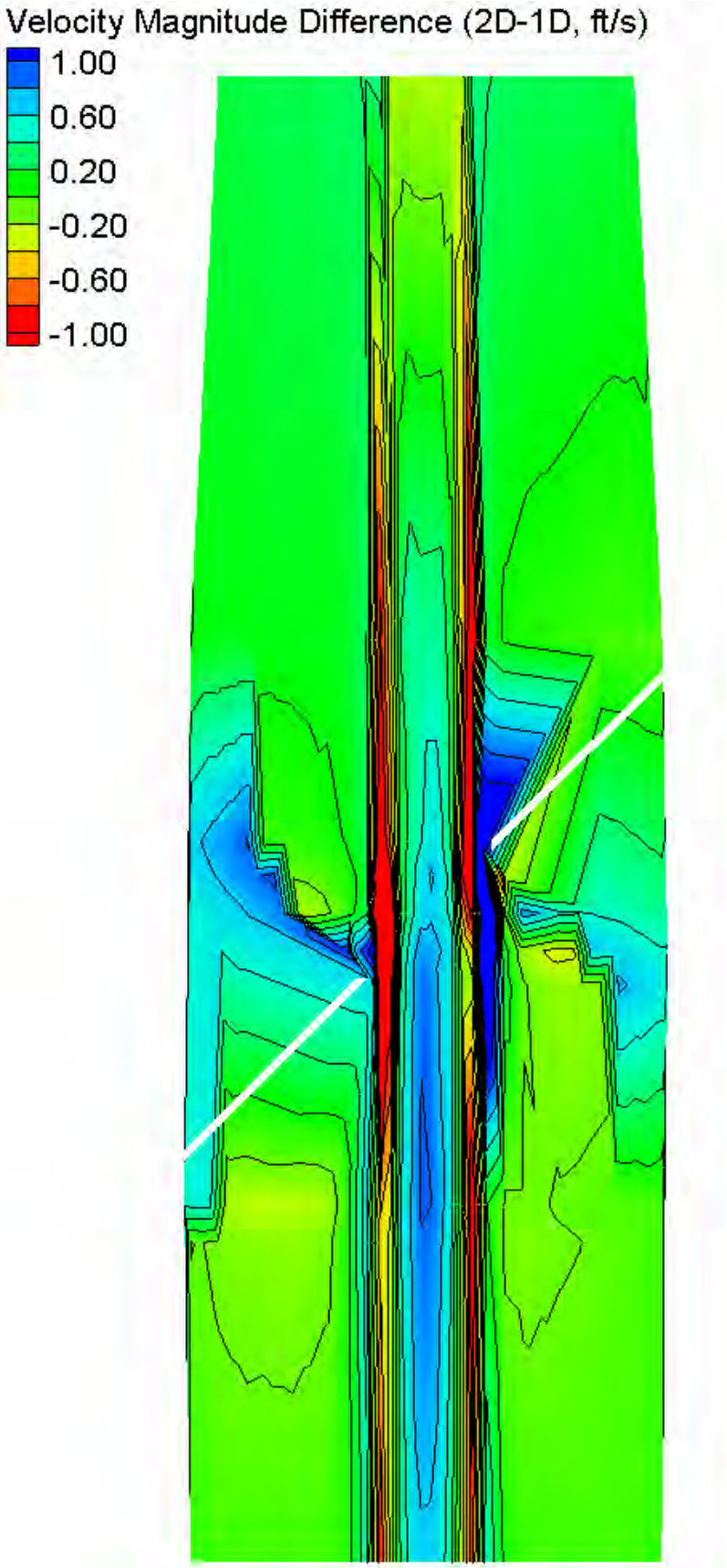

Velocity Magnitude Difference Contours – Large Channel – Embankment Skew (45°)

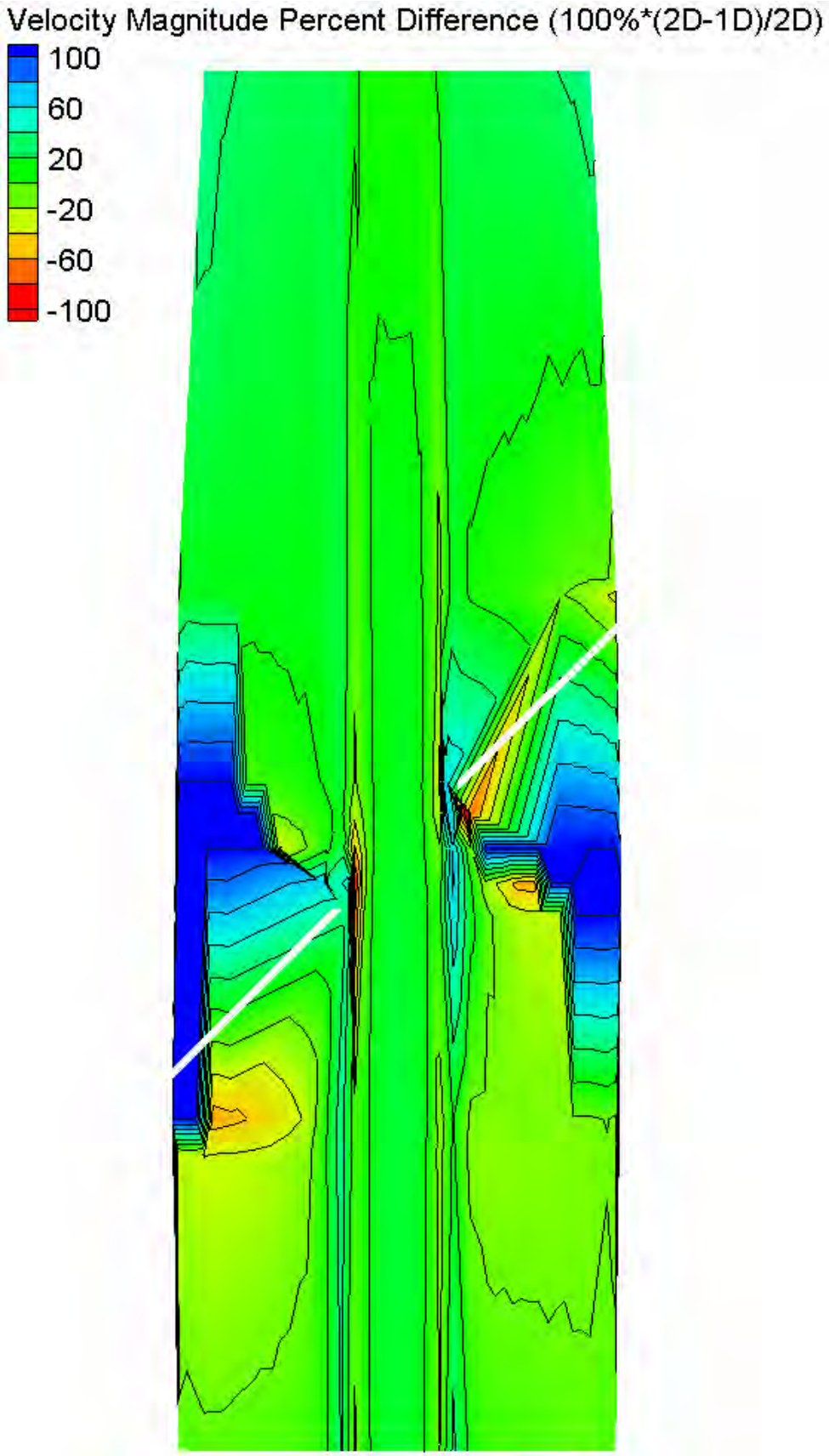

Velocity Magnitude Percent Difference Contours – Large Channel – Embankment Skew (45°)

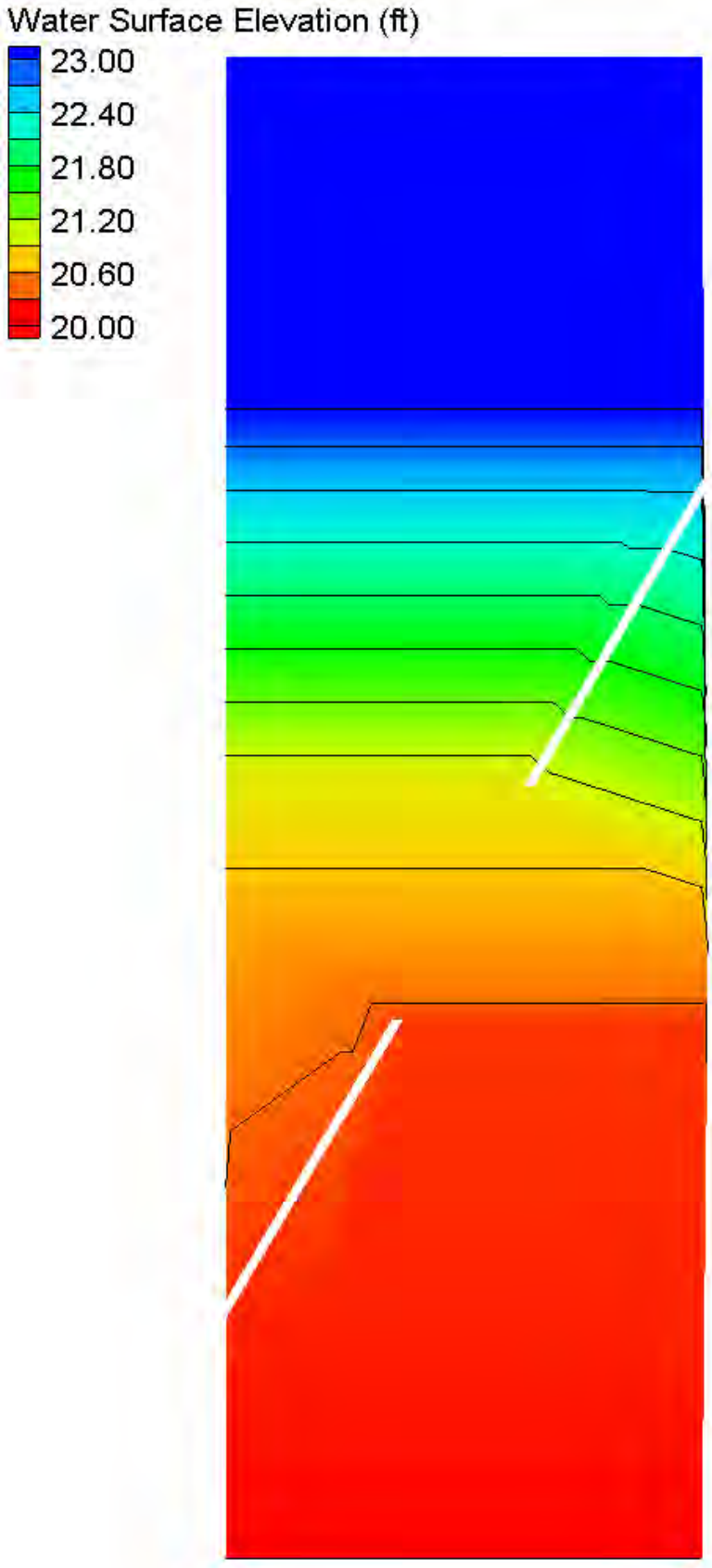

HEC-RAS Water Surface Elevation Contours – Large Channel – Embankment Skew (60°)

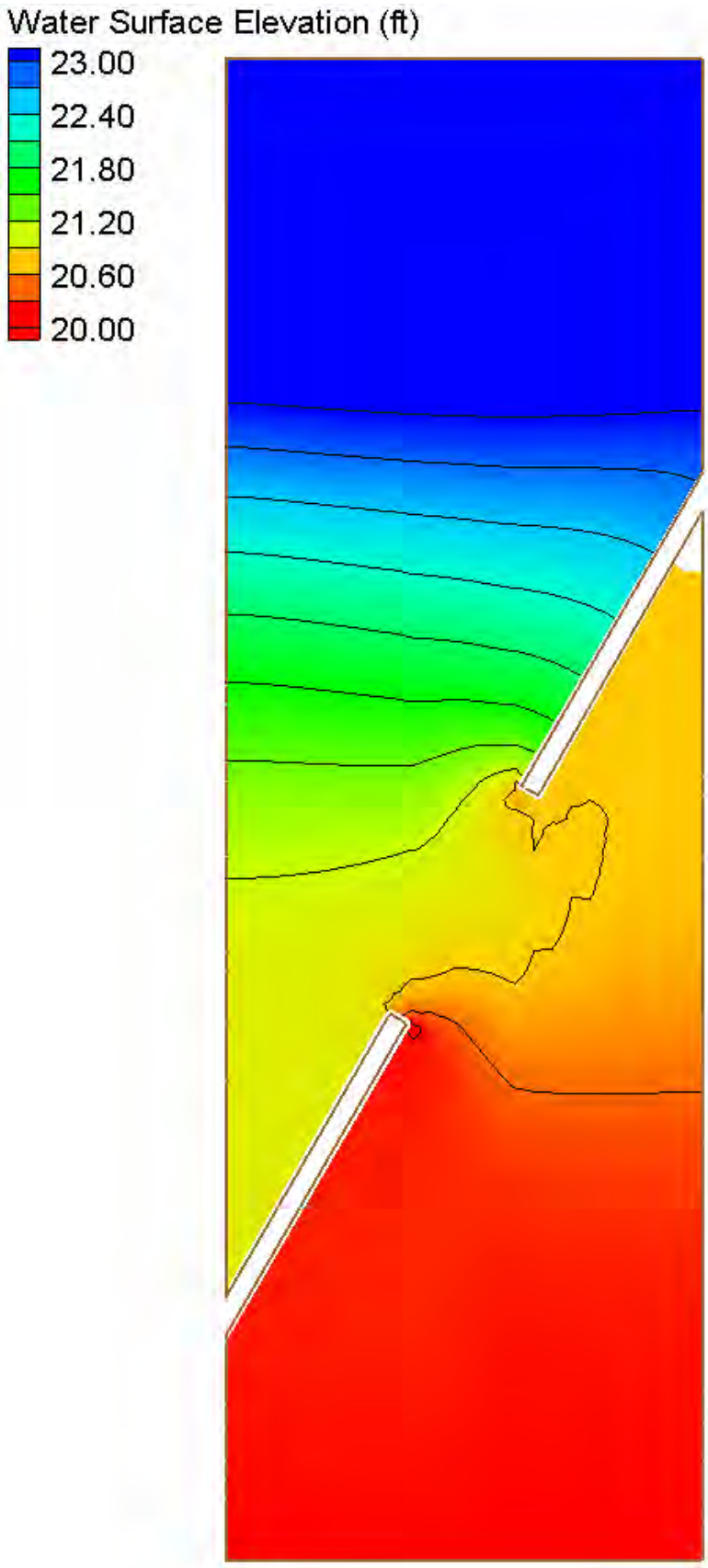

FESWMS Water Surface Elevation Contours – Large Channel – Embankment Skew (60°)

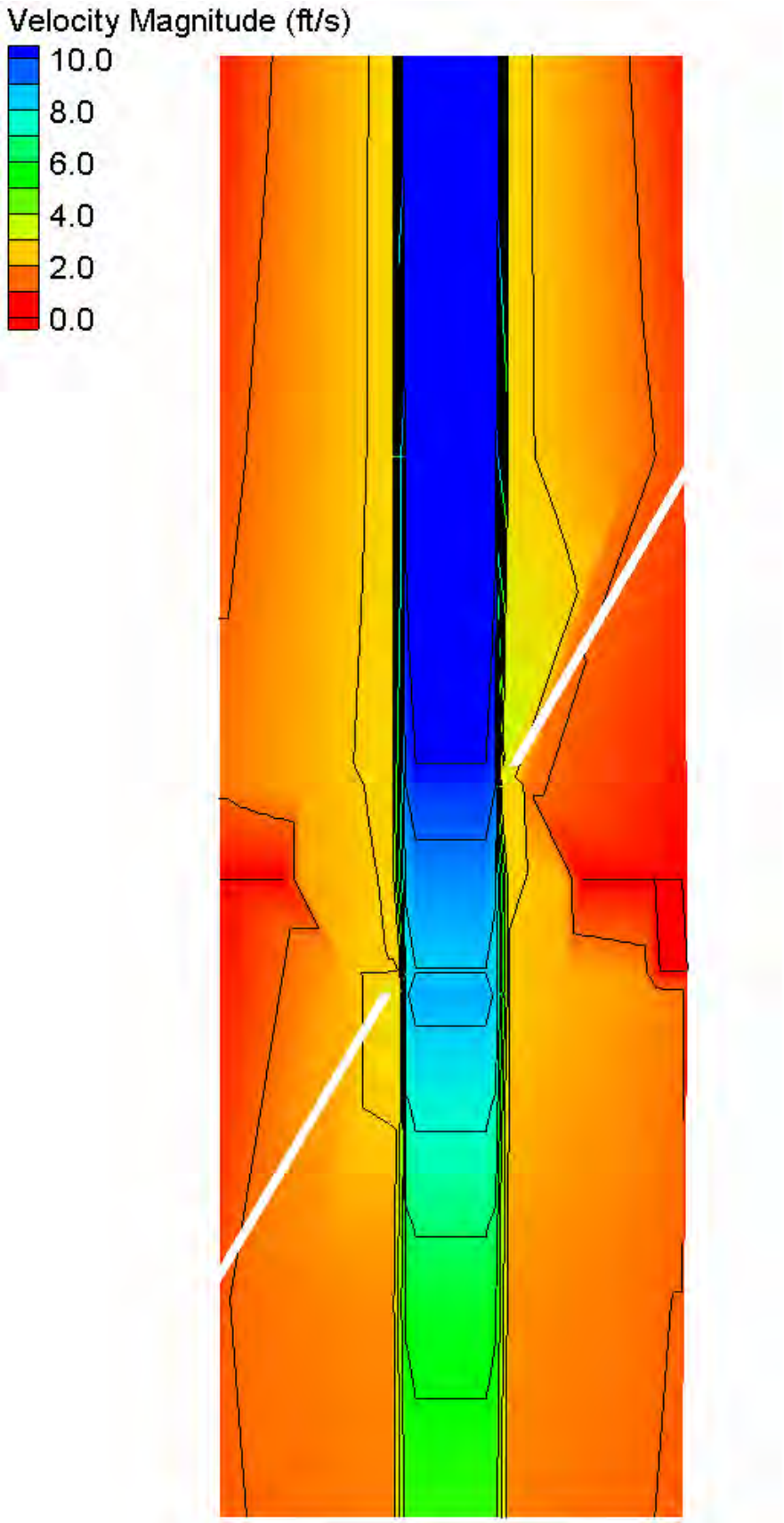

HEC-RAS Velocity Magnitude Contours – Large Channel – Embankment Skew (60°)

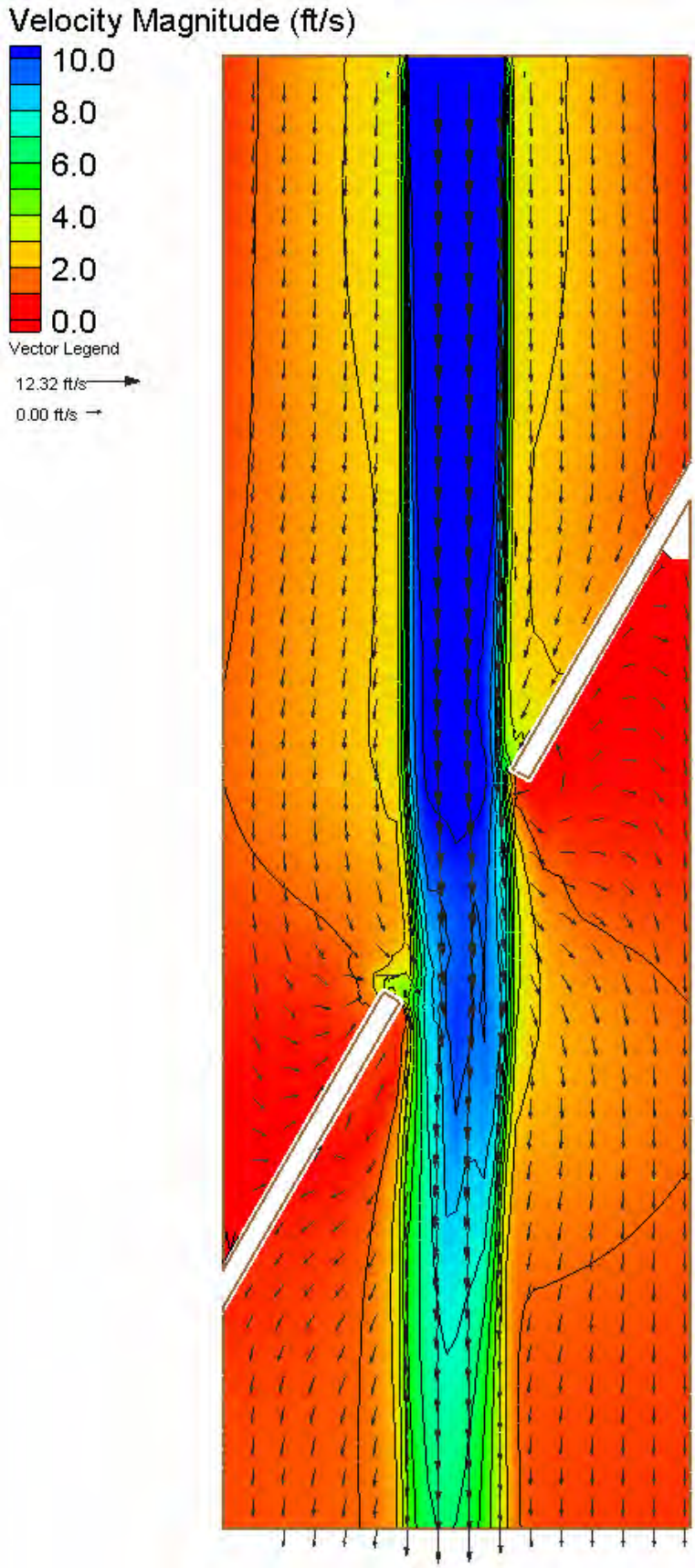

FESWMS Velocity Magnitude Contours – Large Channel – Embankment Skew (60°)

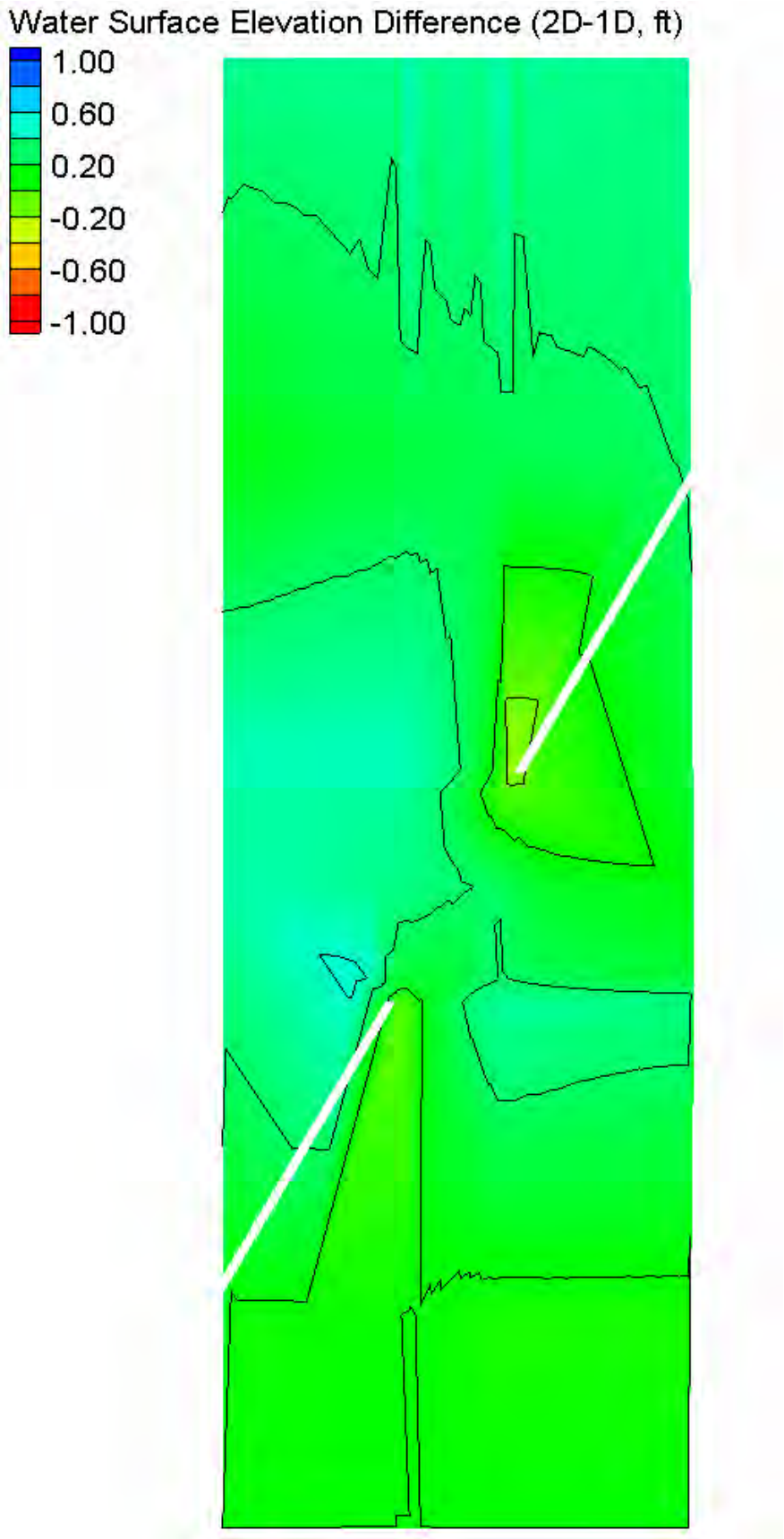

Water Surface Elevation Difference Contours – Large Channel – Embankment Skew (60°)

Velocity Magnitude Difference Contours – Large Channel – Embankment Skew (60°)

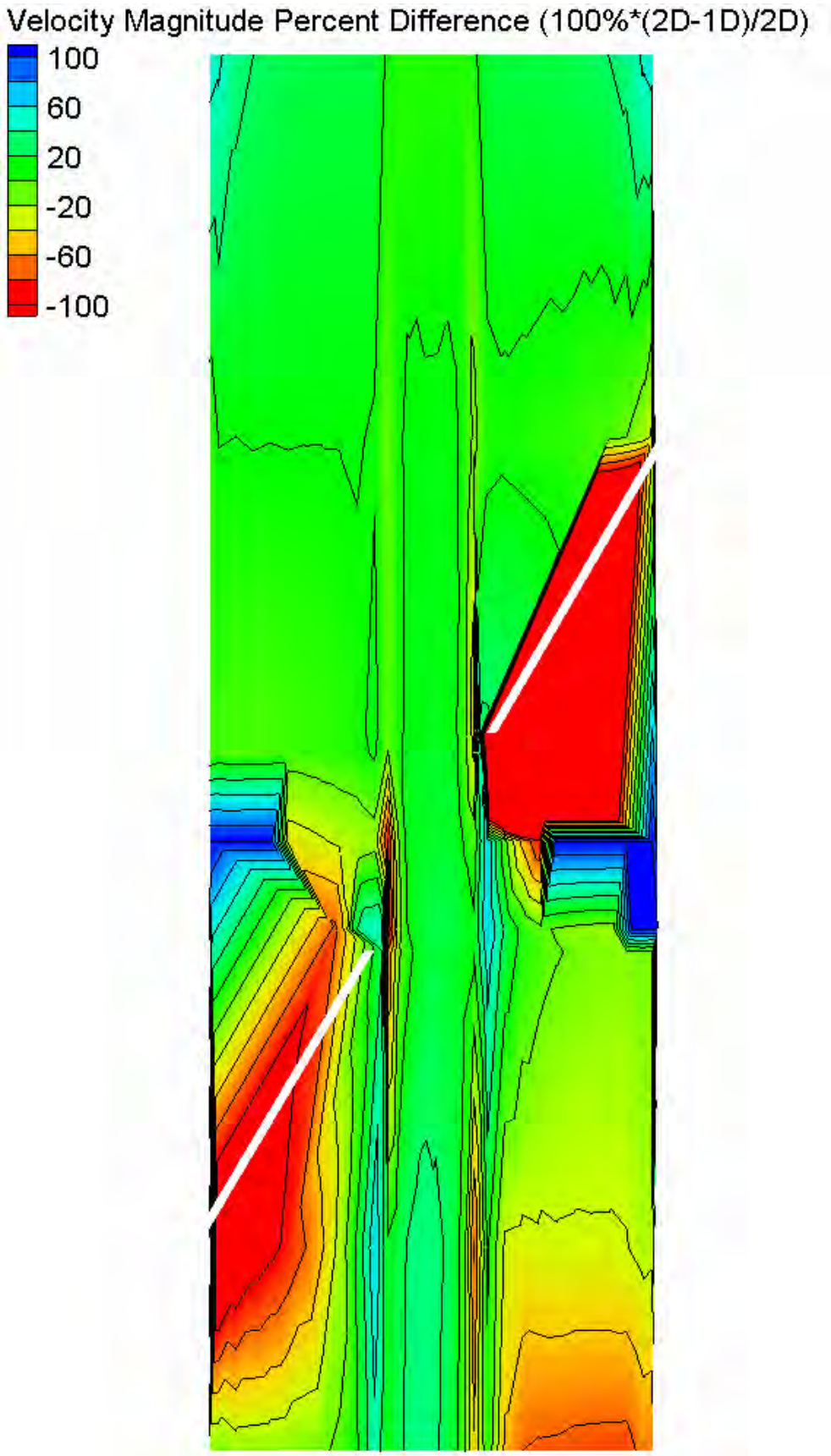

Velocity Magnitude Percent Difference Contours – Large Channel – Embankment Skew (60°)

Bridges over Meandering Rivers

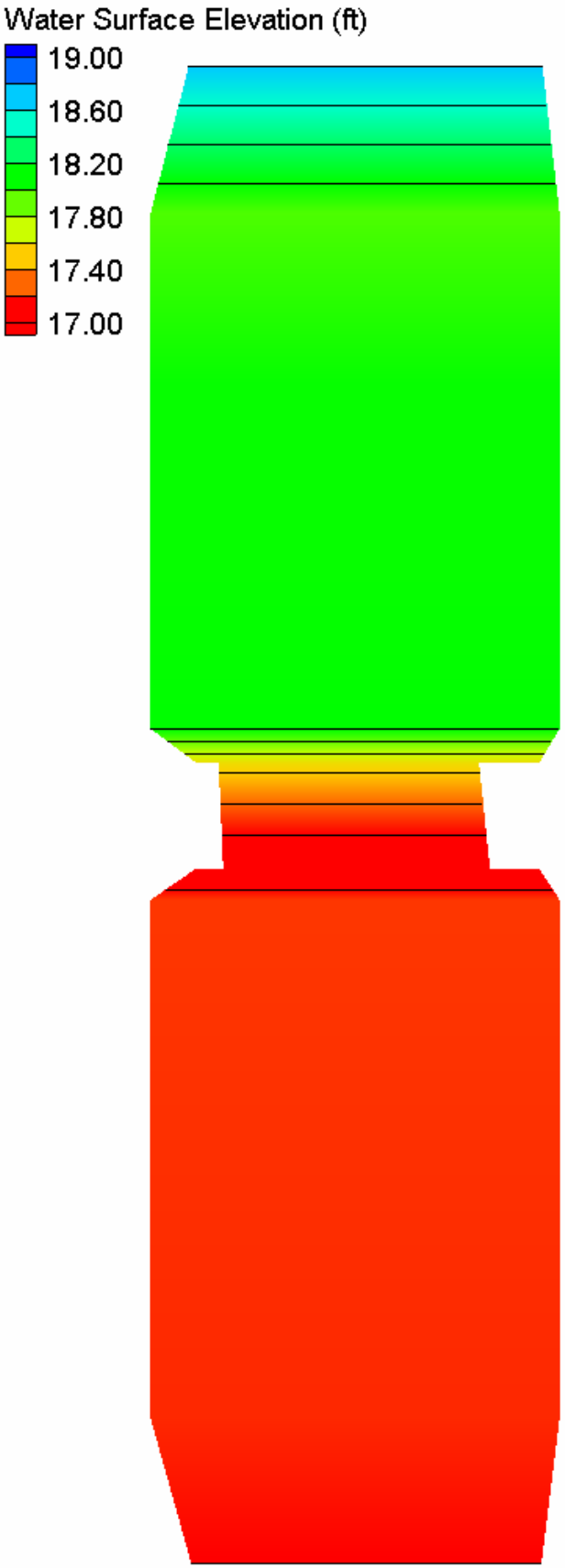

HEC-RAS Water Surface Elevation Contours – Small Channel – Meandering (1.25 sinuosity)

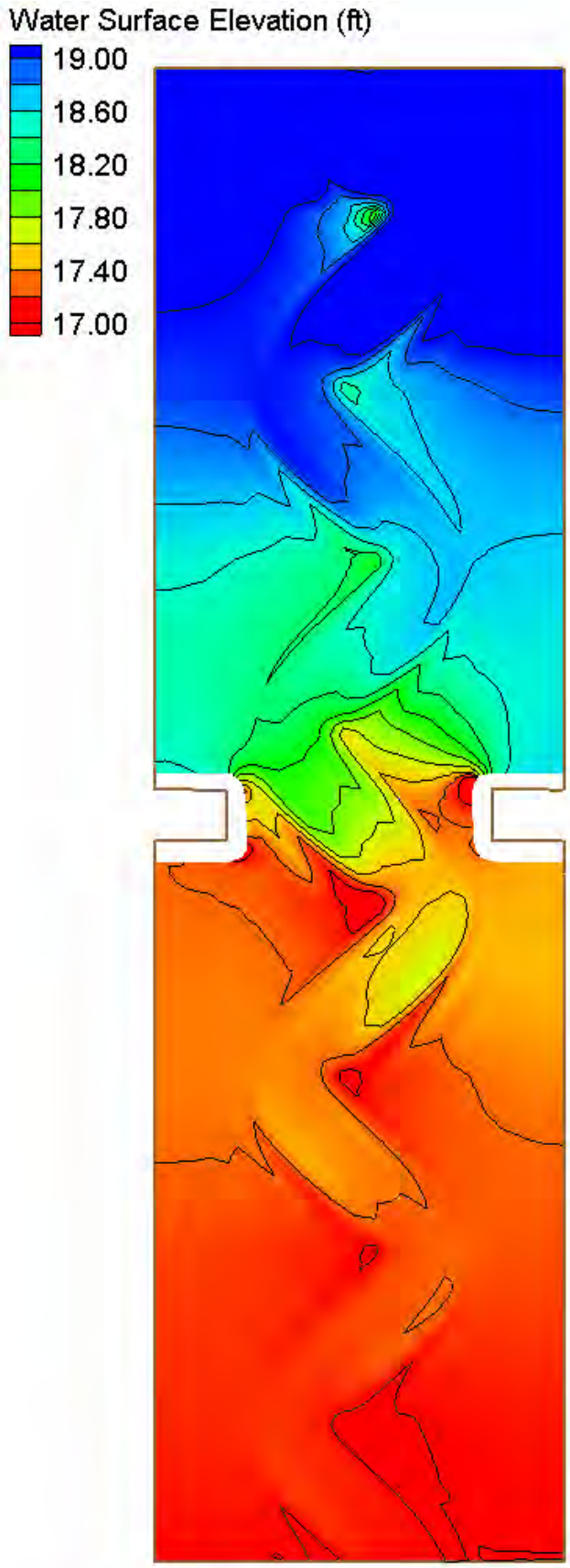

FESWMS Water Surface Elevation Contours – Small Channel – Meandering (1.25 sinuosity)

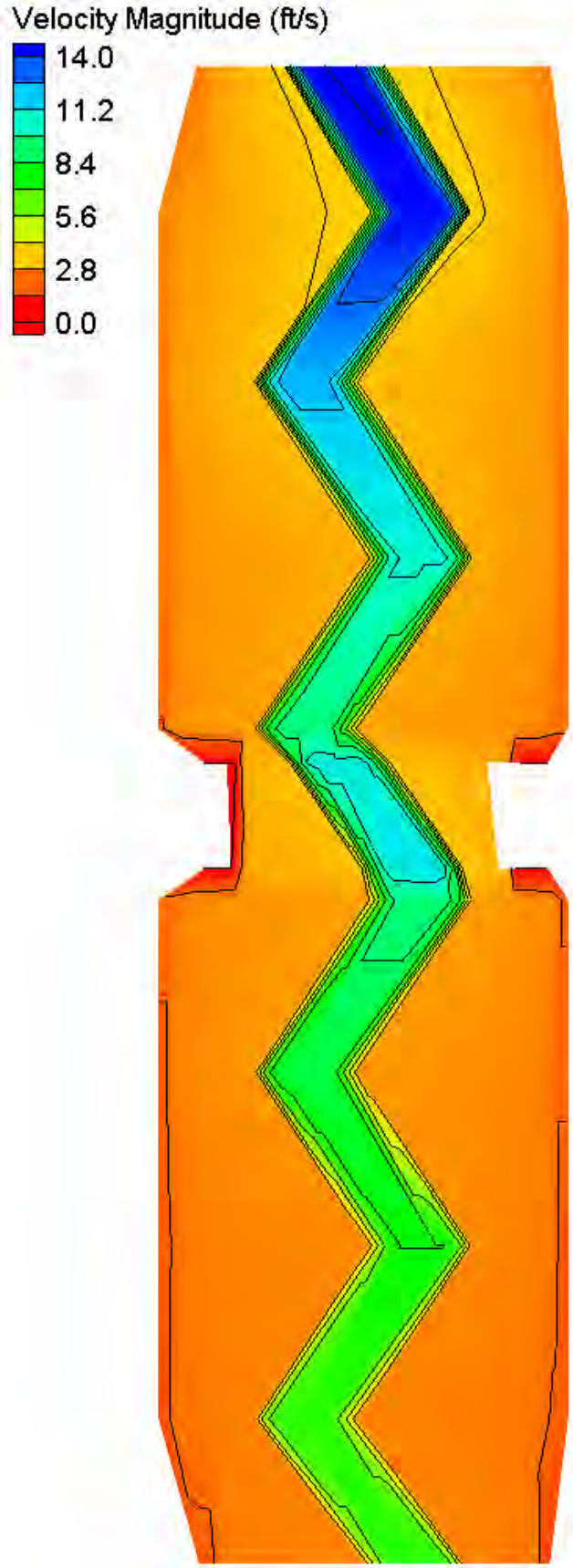

HEC-RAS Velocity Magnitude Contours – Small Channel – Meandering (1.25 sinuosity)

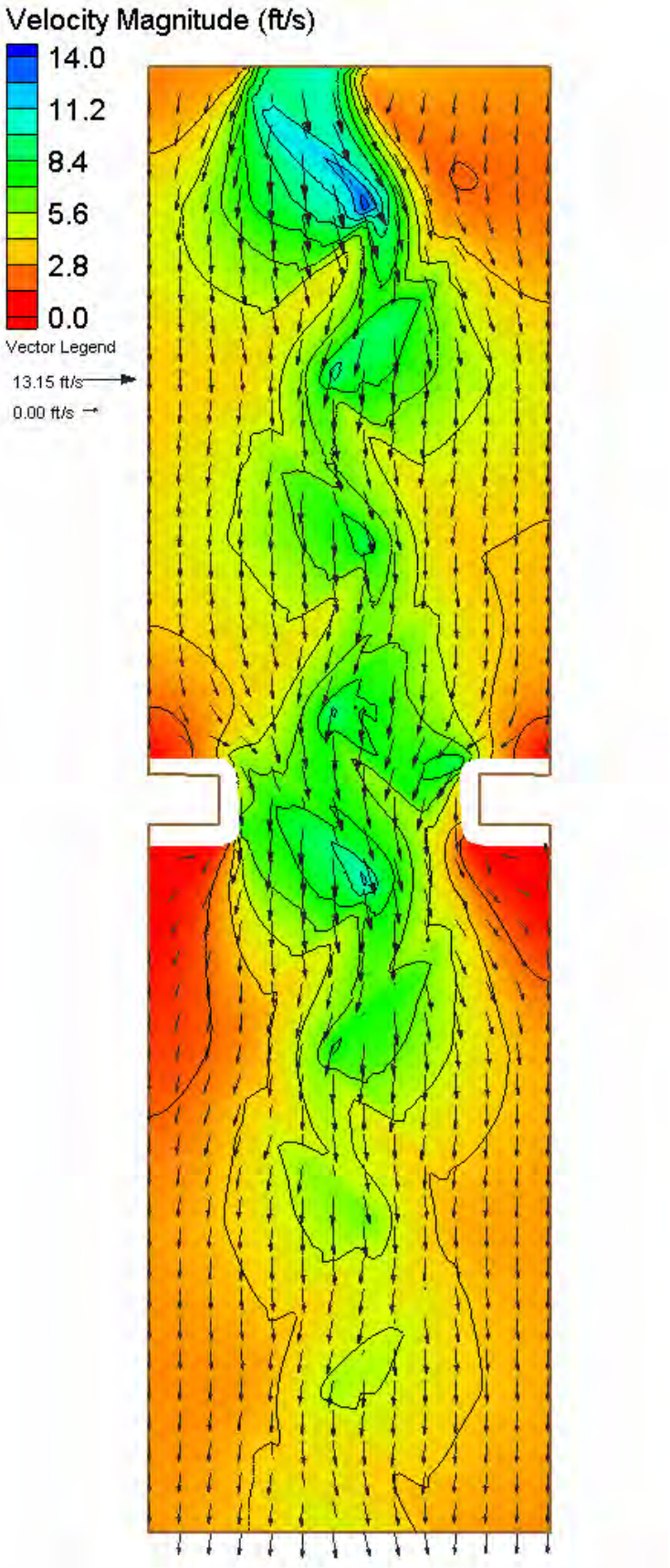

FESWMS Velocity Magnitude Contours – Small Channel – Meandering (1.25 sinuosity)

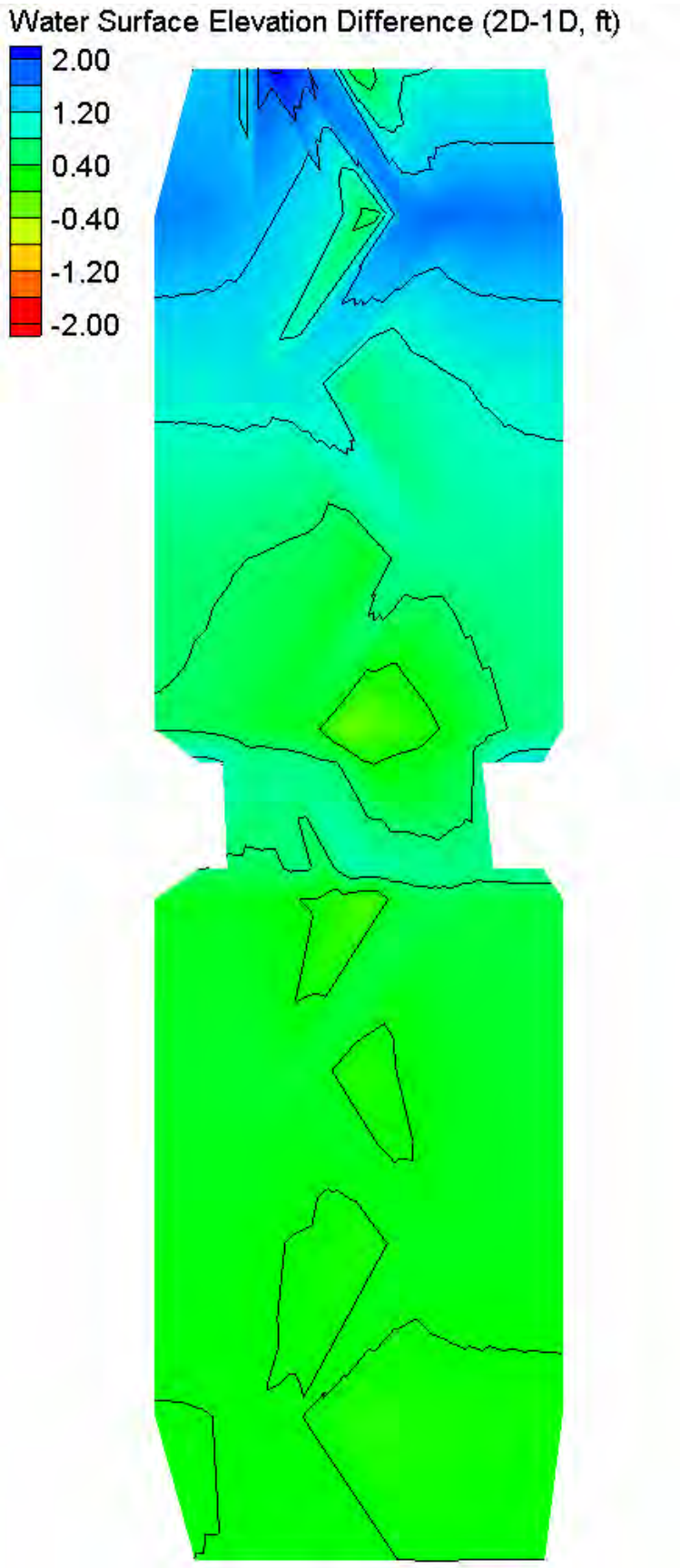

Water Surface Elevation Difference Contours – Small Channel – Meandering (1.25 sinuosity)

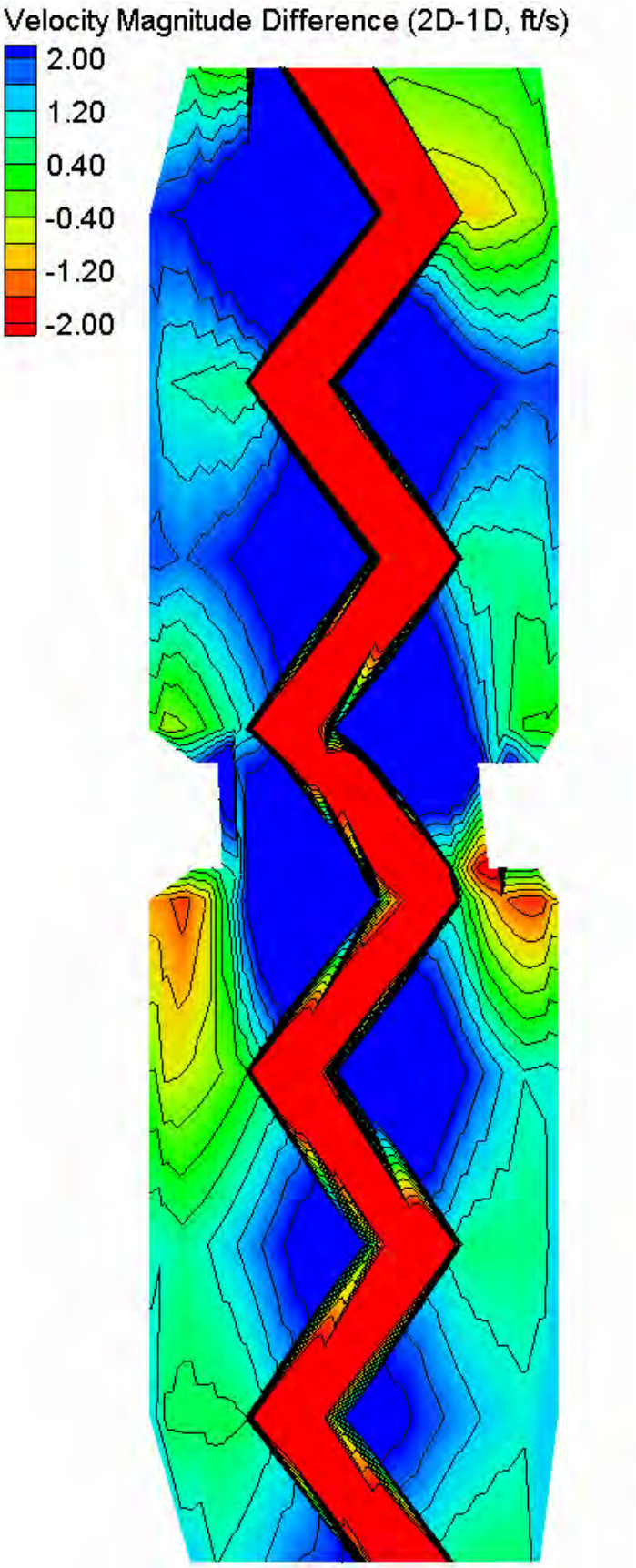

Velocity Magnitude Difference Contours – Small Channel – Meandering (1.25 sinuosity)

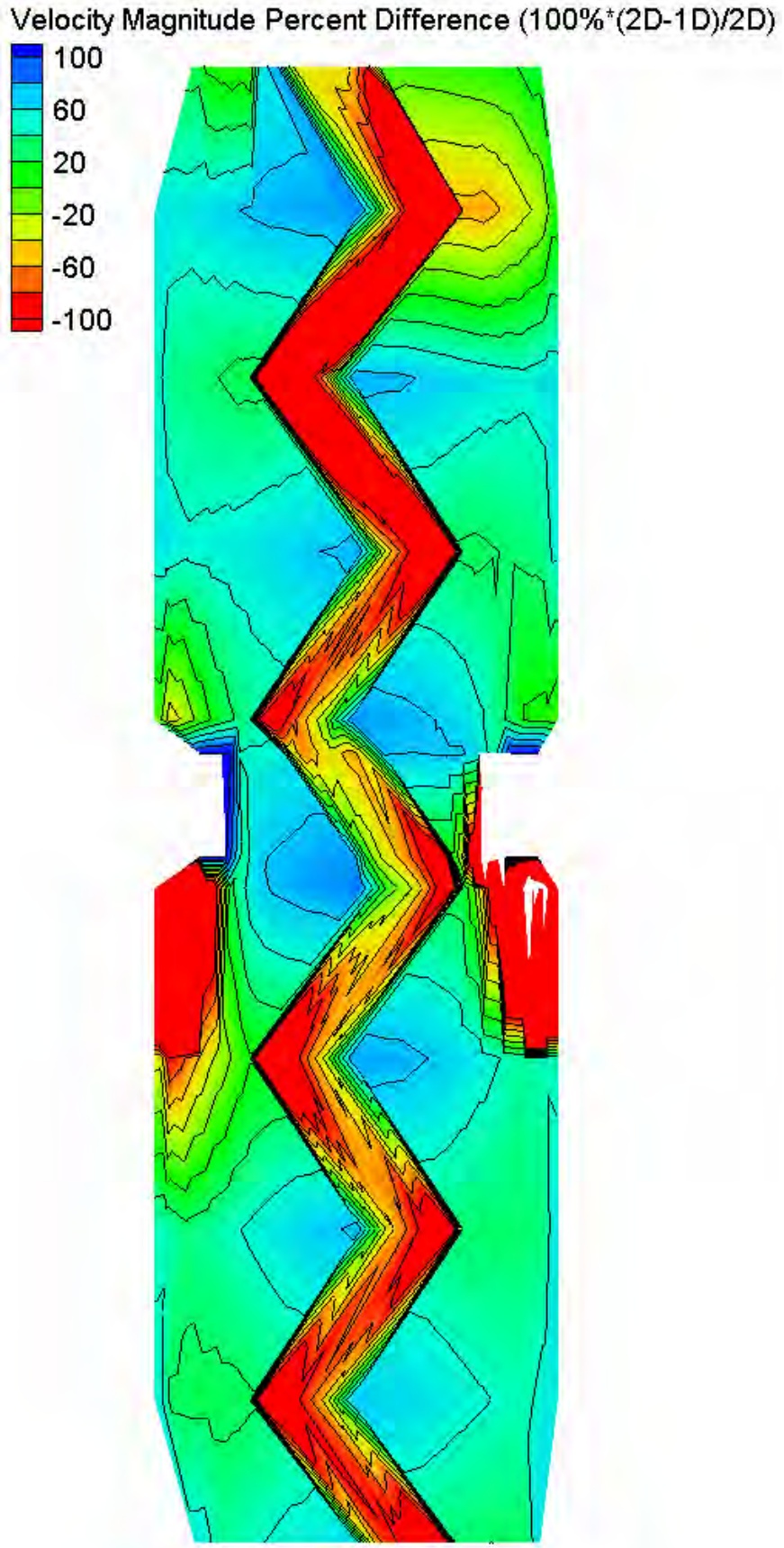

Velocity Magnitude Percent Difference Contours – Small Channel – Meandering (1.25 sinuosity)

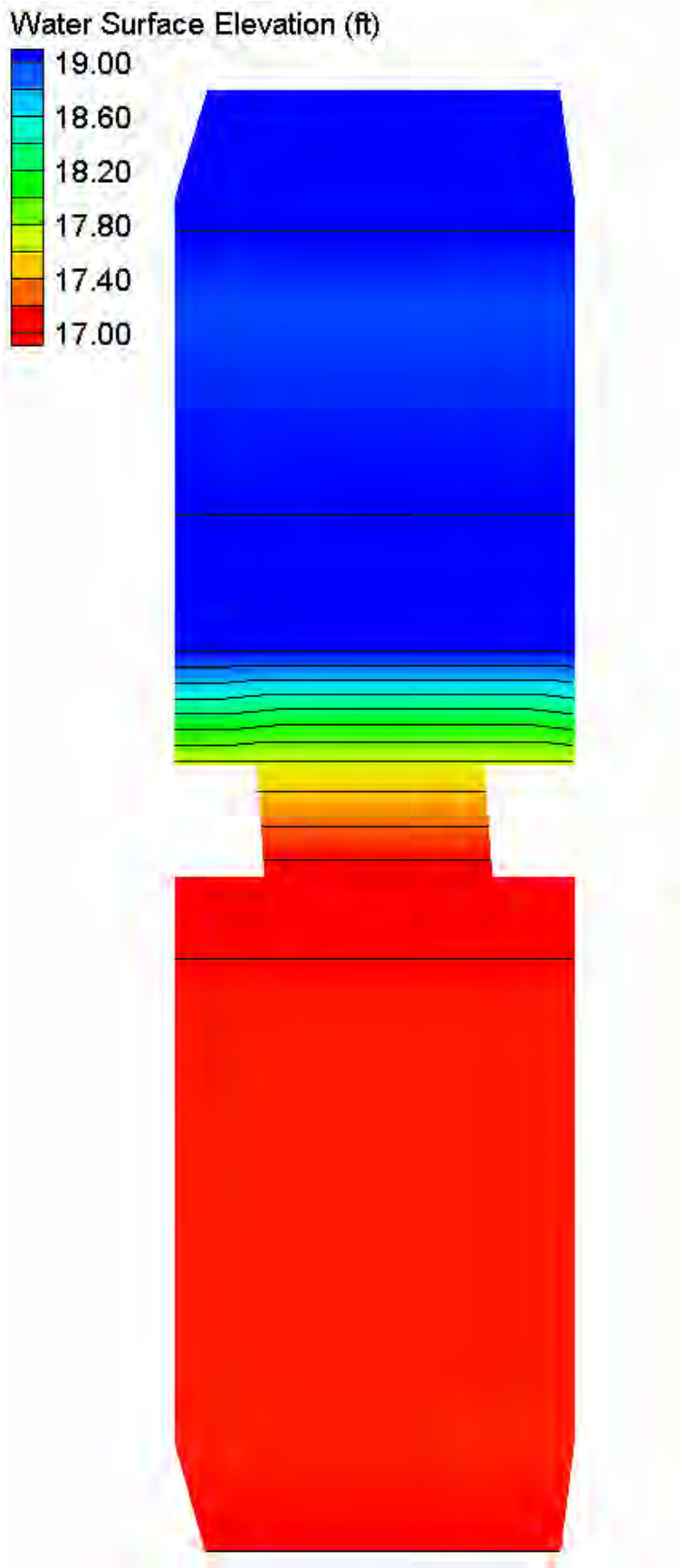

HEC-RAS Water Surface Elevation Contours – Small Channel – Meandering (1.5 sinuosity)

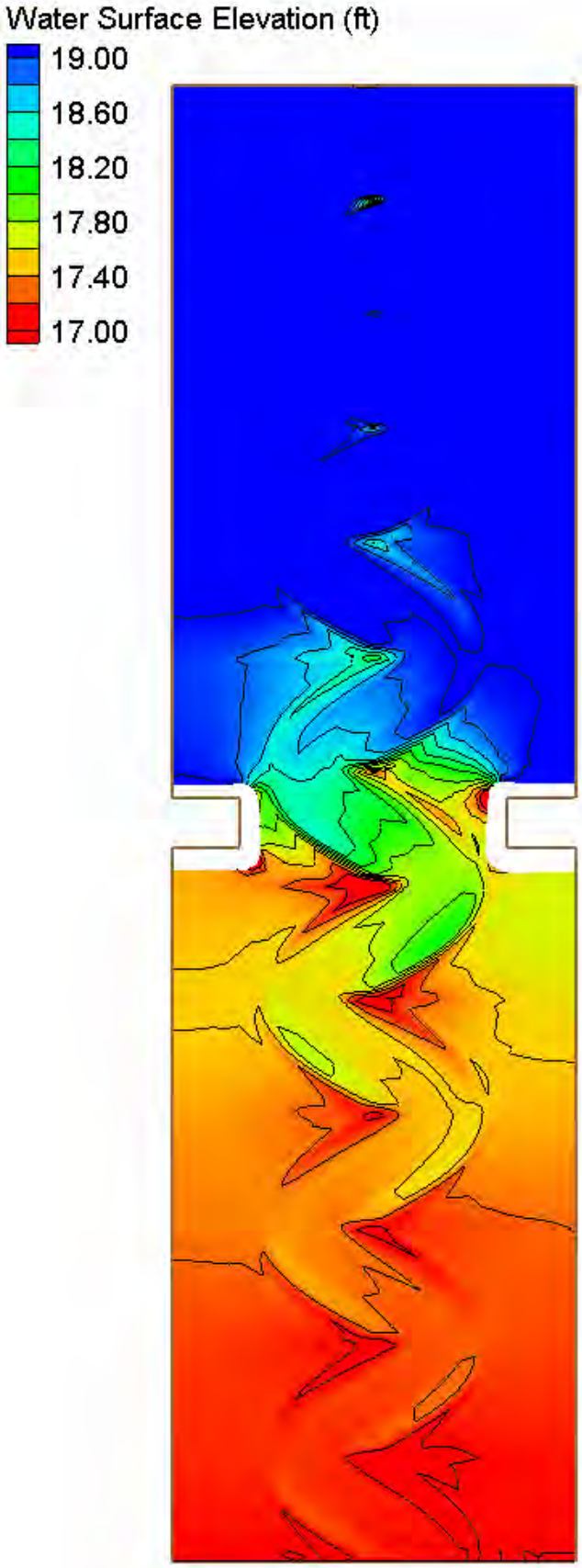

FESWMS Water Surface Elevation Contours – Small Channel – Meandering (1.5 sinuosity)

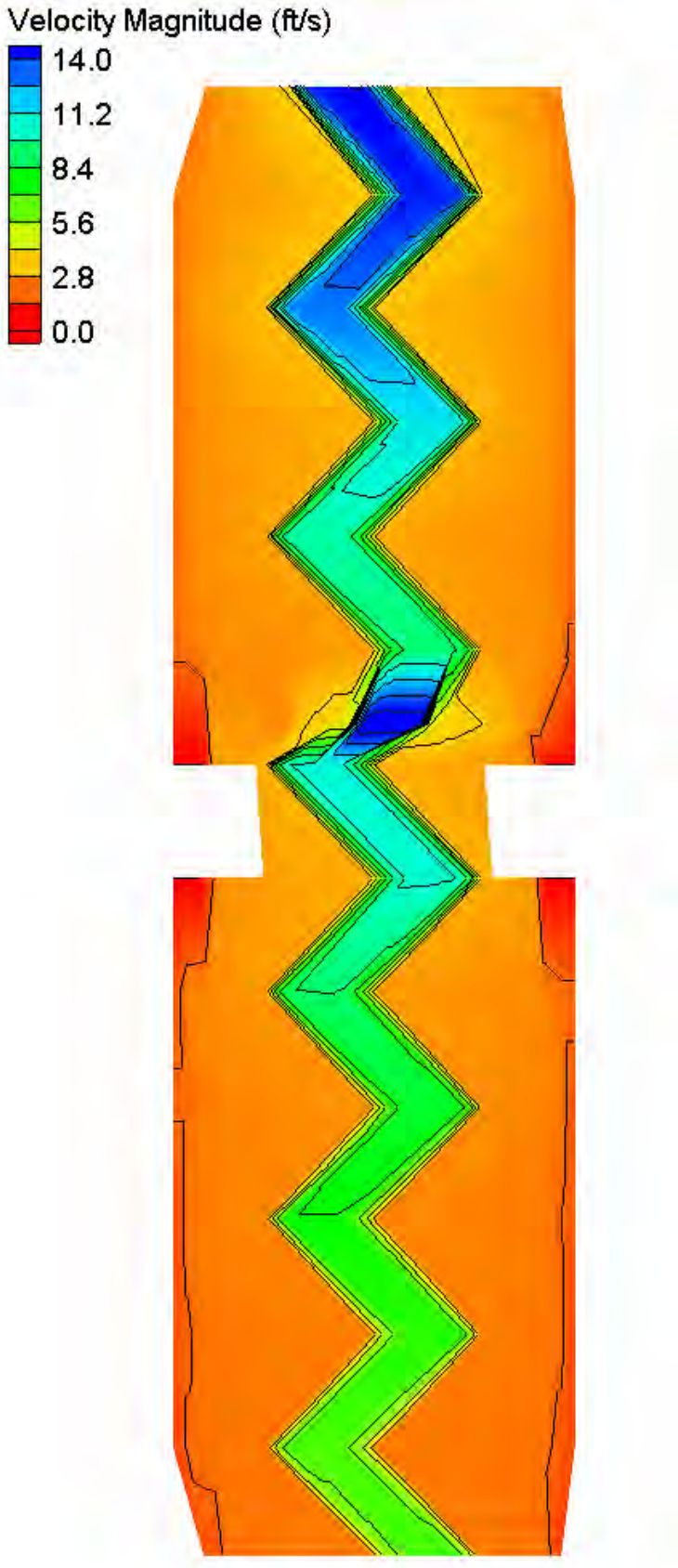

HEC-RAS Velocity Magnitude Contours – Small Channel – Meandering (1.5 sinuosity)

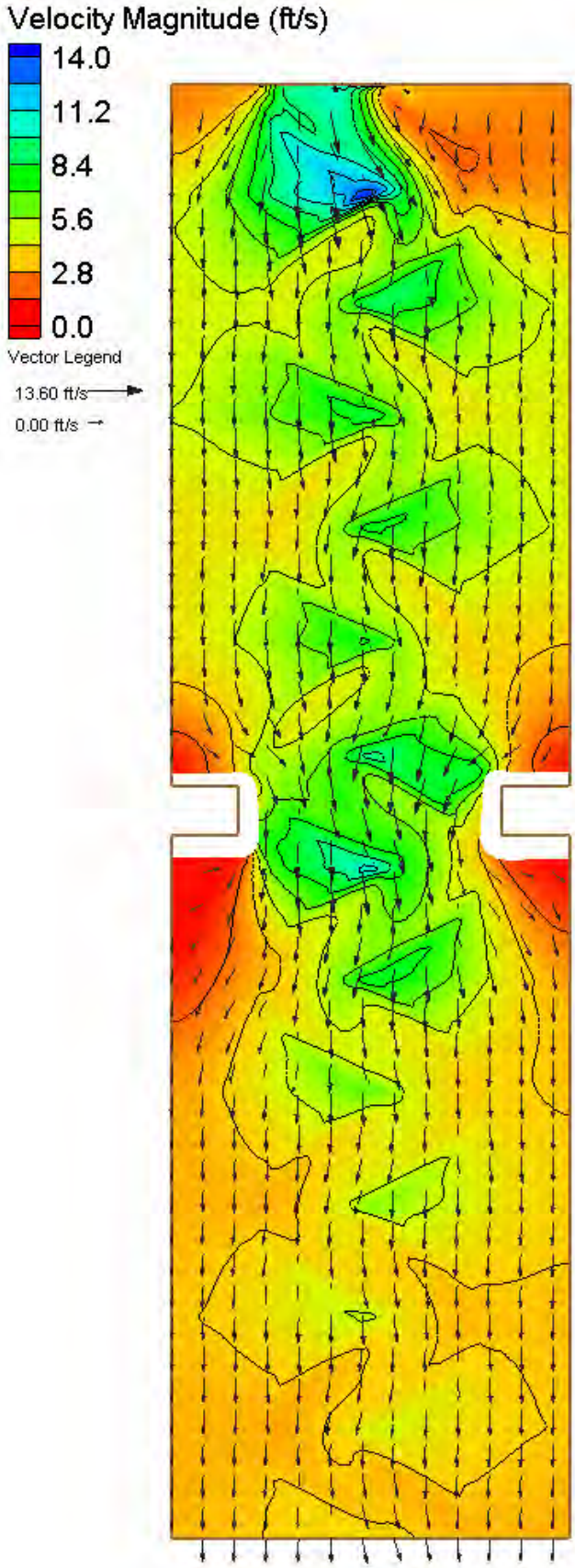

FESWMS Velocity Magnitude Contours – Small Channel – Meandering (1.5 sinuosity)

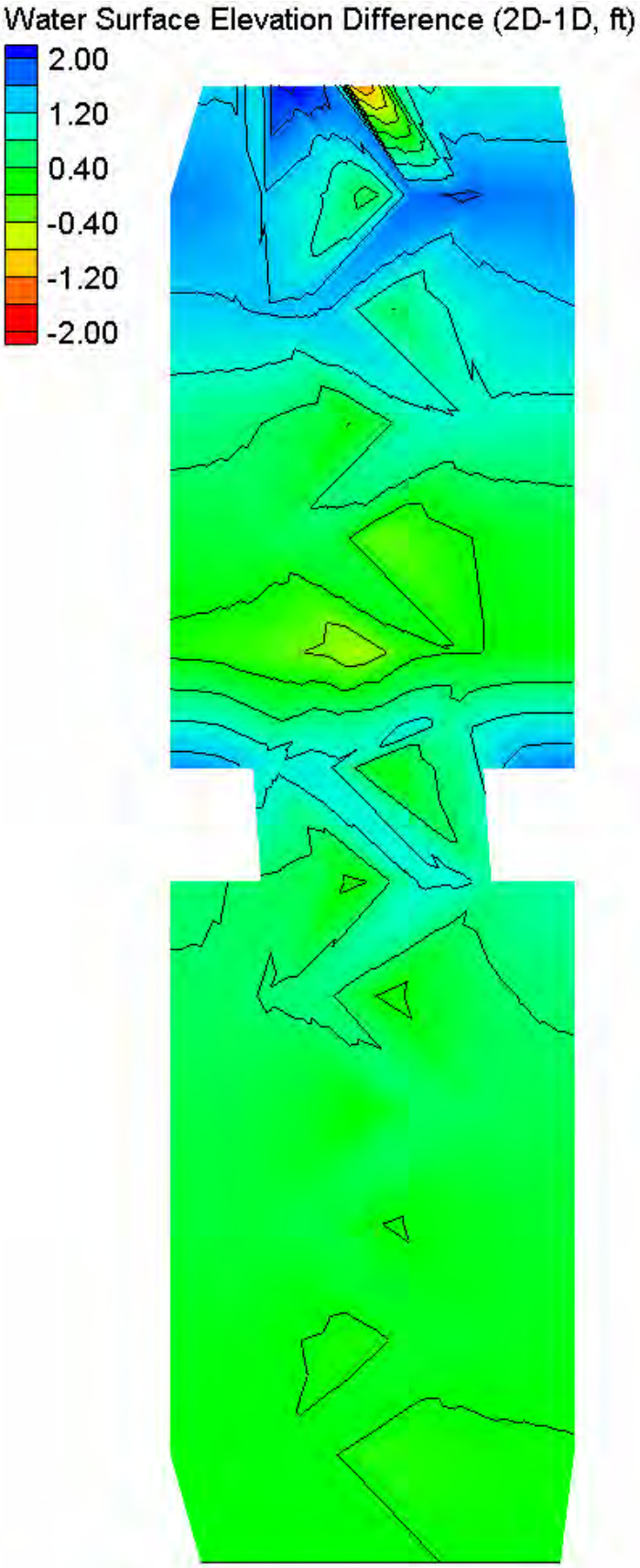

Water Surface Elevation Difference Contours – Small Channel – Meandering (1.5 sinuosity)

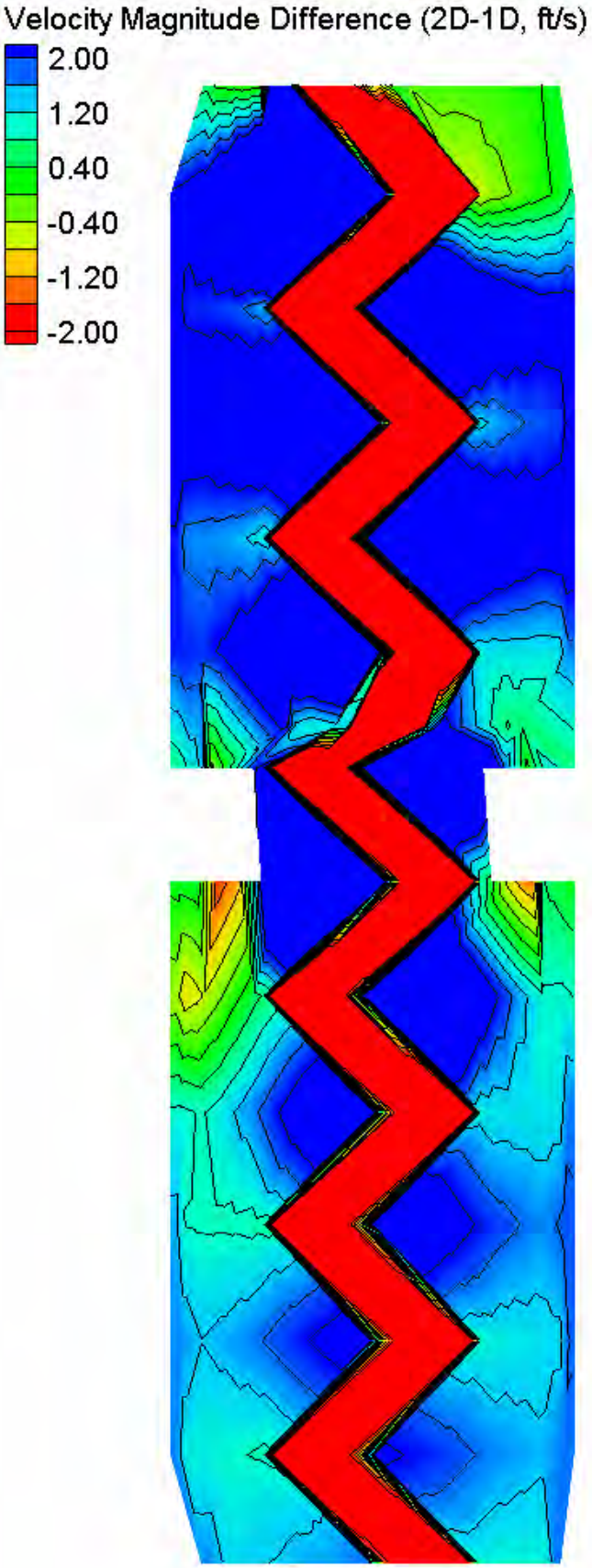

Velocity Magnitude Difference Contours – Small Channel – Meandering (1.5 sinuosity)

Velocity Magnitude Percent Difference Contours – Small Channel – Meandering (1.5 sinuosity)

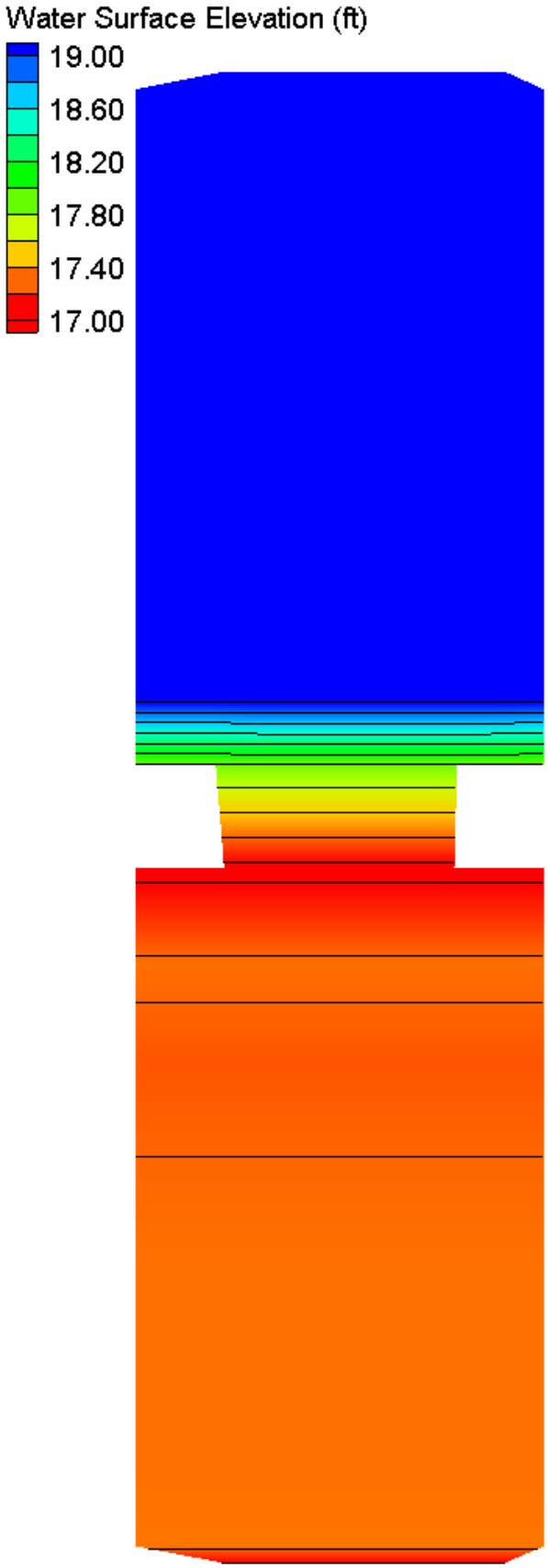

HEC-RAS Water Surface Elevation Contours – Small Channel – Meandering (1.75 sinuosity)

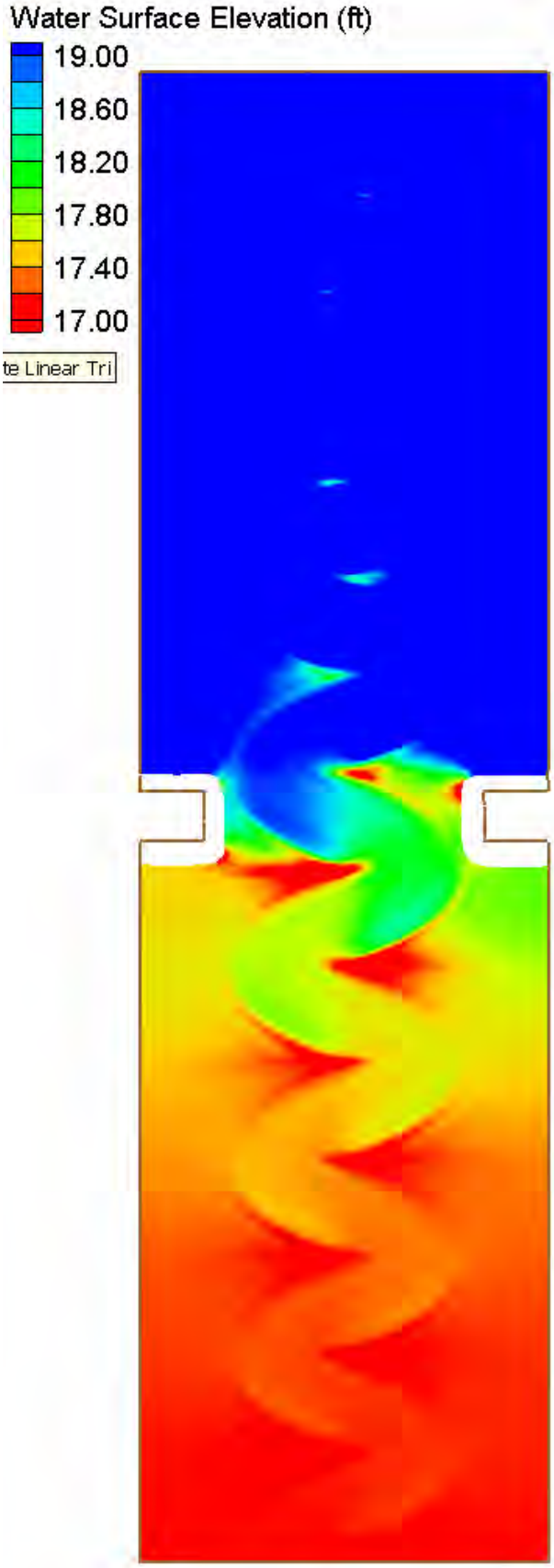

FESWMS Water Surface Elevation Contours – Small Channel – Meandering (1.75 sinuosity)

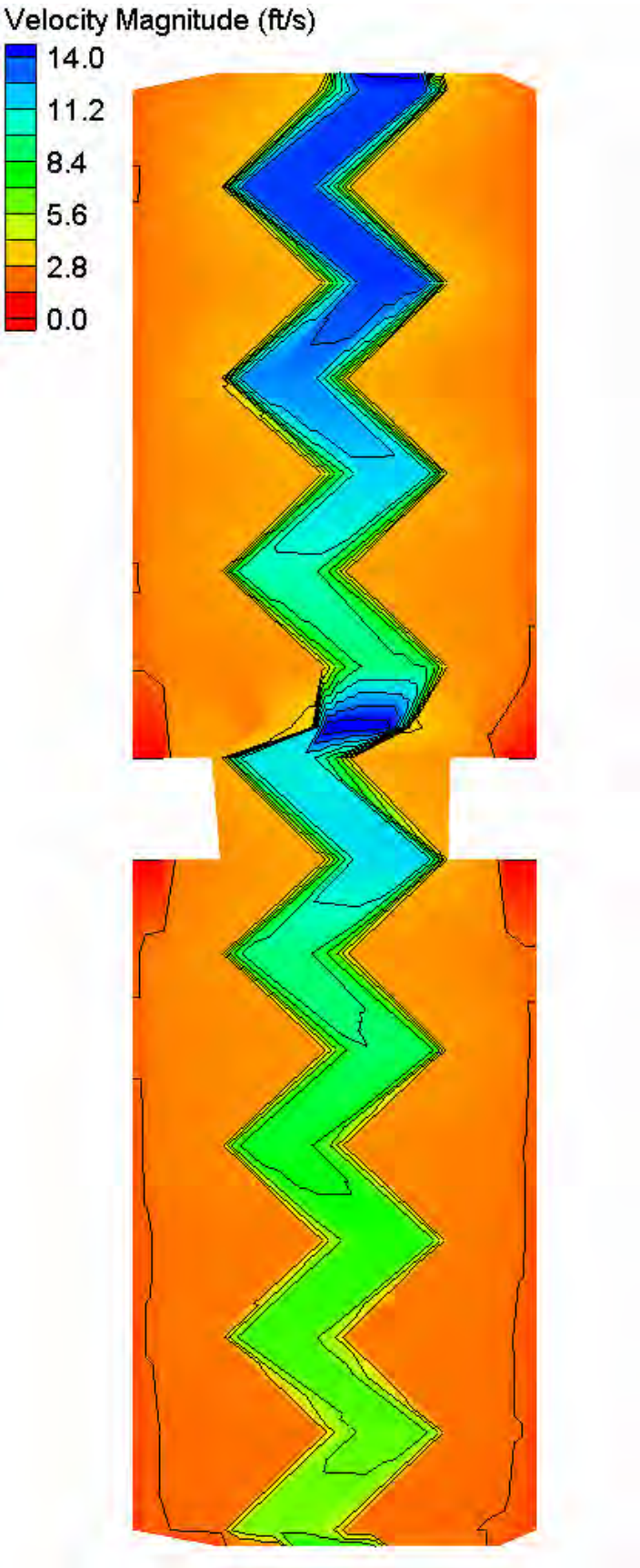

HEC-RAS Velocity Magnitude Contours – Small Channel – Meandering (1.75 sinuosity)

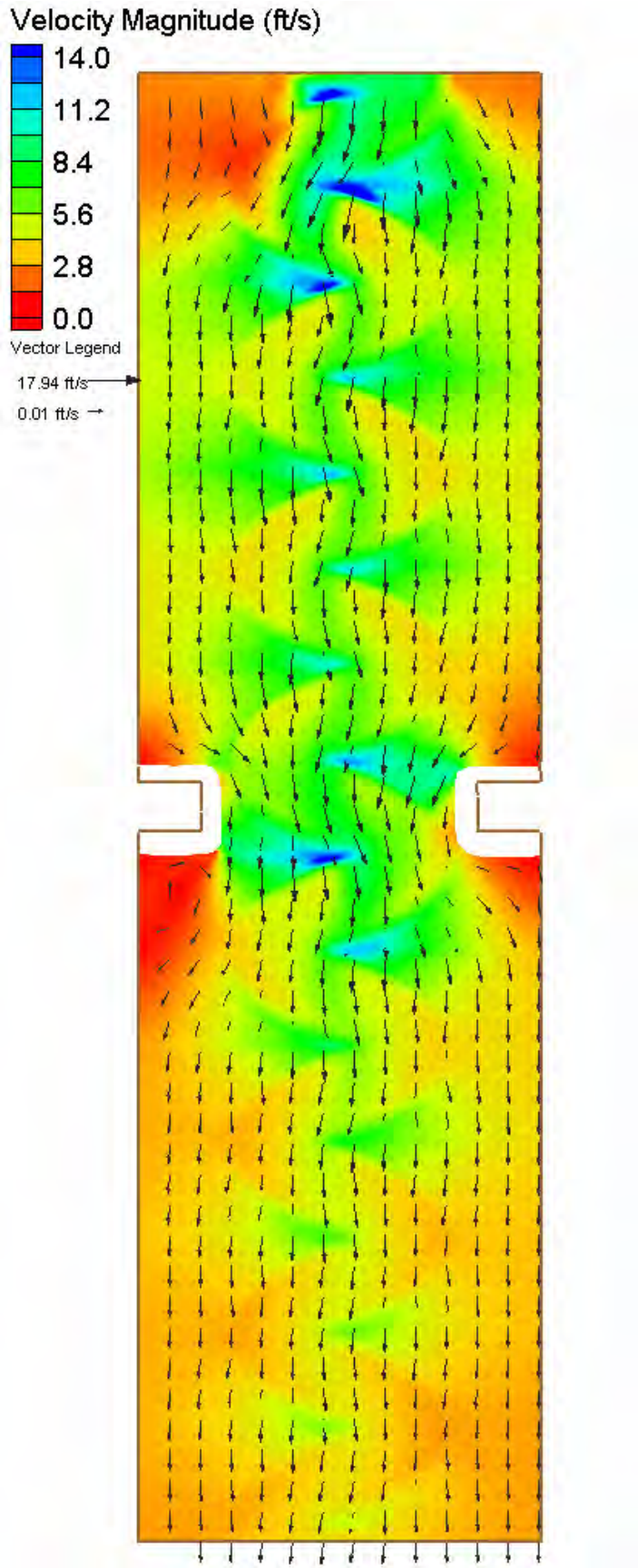

FESWMS Velocity Magnitude Contours – Small Channel – Meandering (1.75 sinuosity)

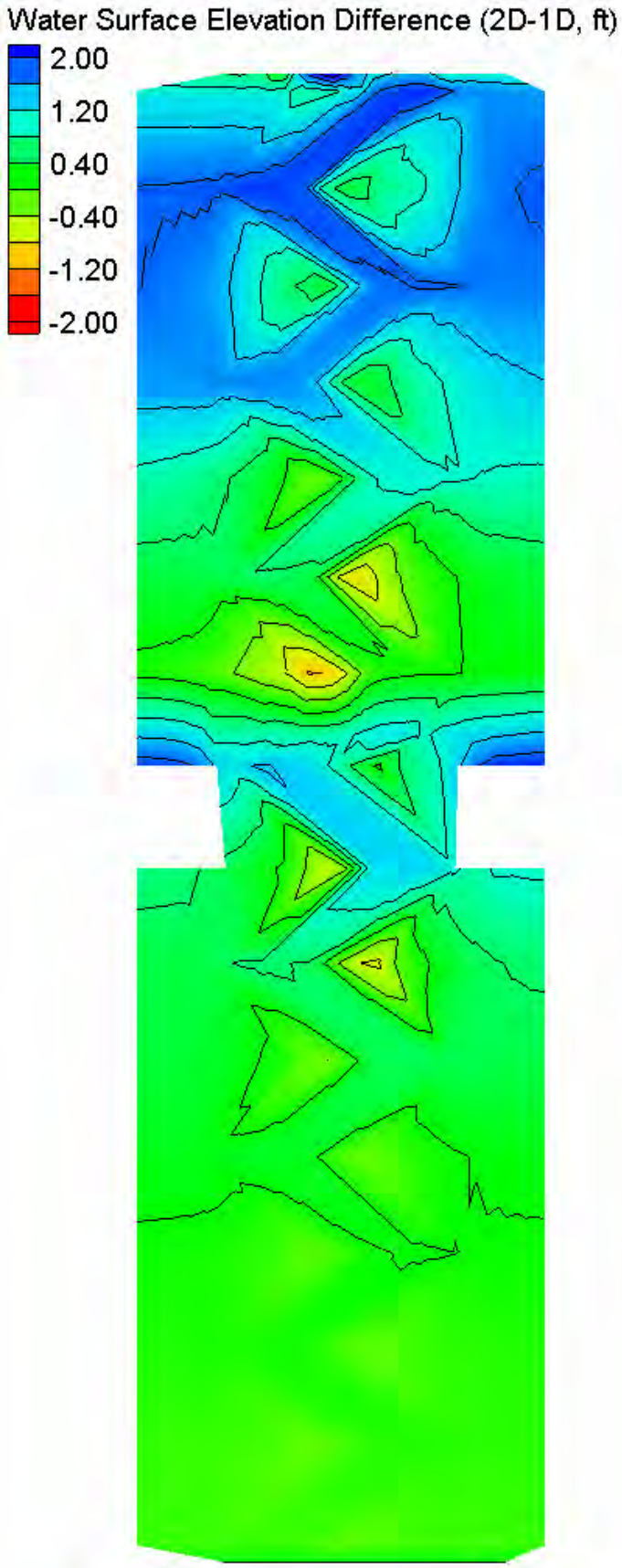

Water Surface Elevation Difference Contours – Small Channel – Meandering (1.75 sinuosity)

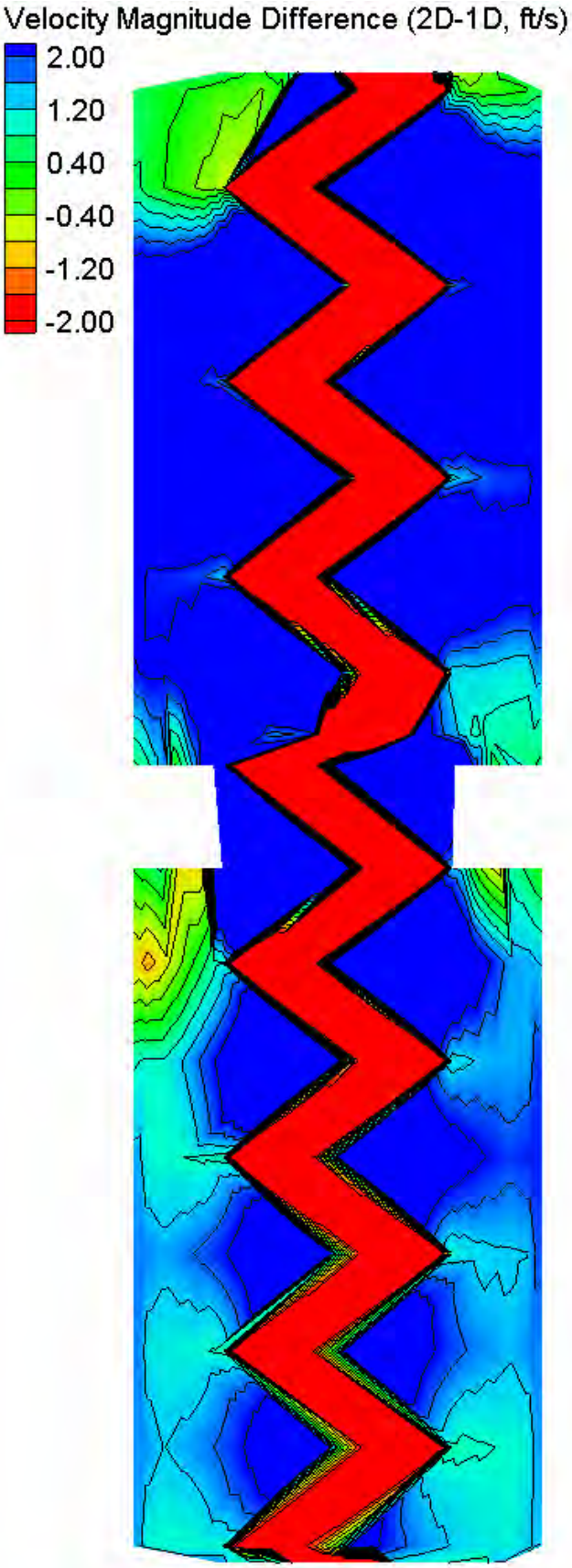

Velocity Magnitude Difference Contours – Small Channel – Meandering (1.75 sinuosity)

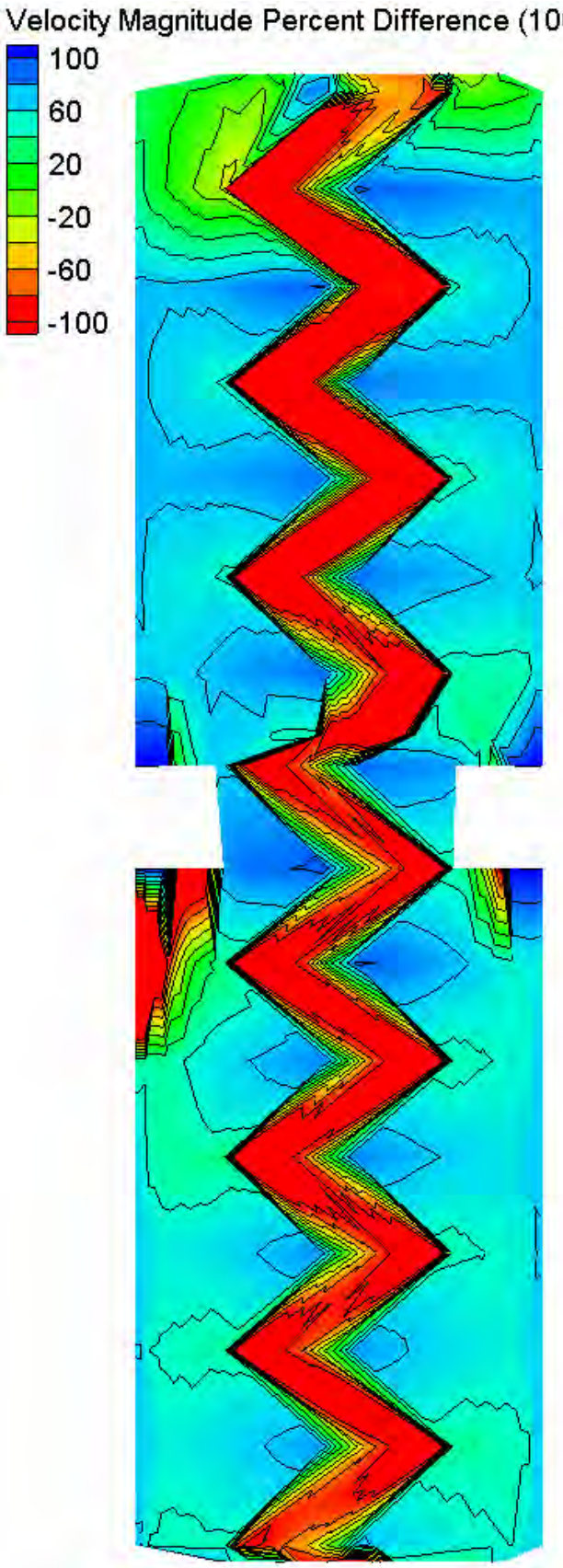

Velocity Magnitude Percent Difference Contours – Small Channel – Meandering (1.75 sinuosity)

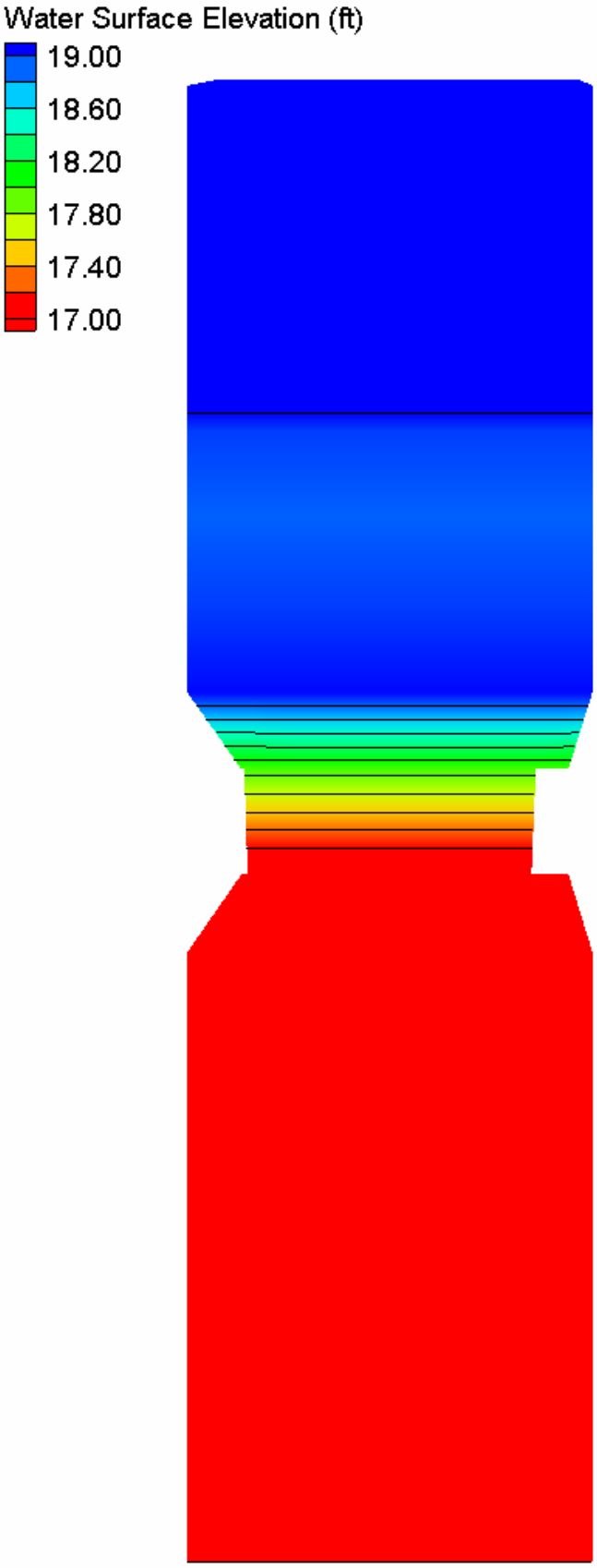

HEC-RAS Water Surface Elevation Contours – Small Channel – Meandering (2.0 sinuosity)

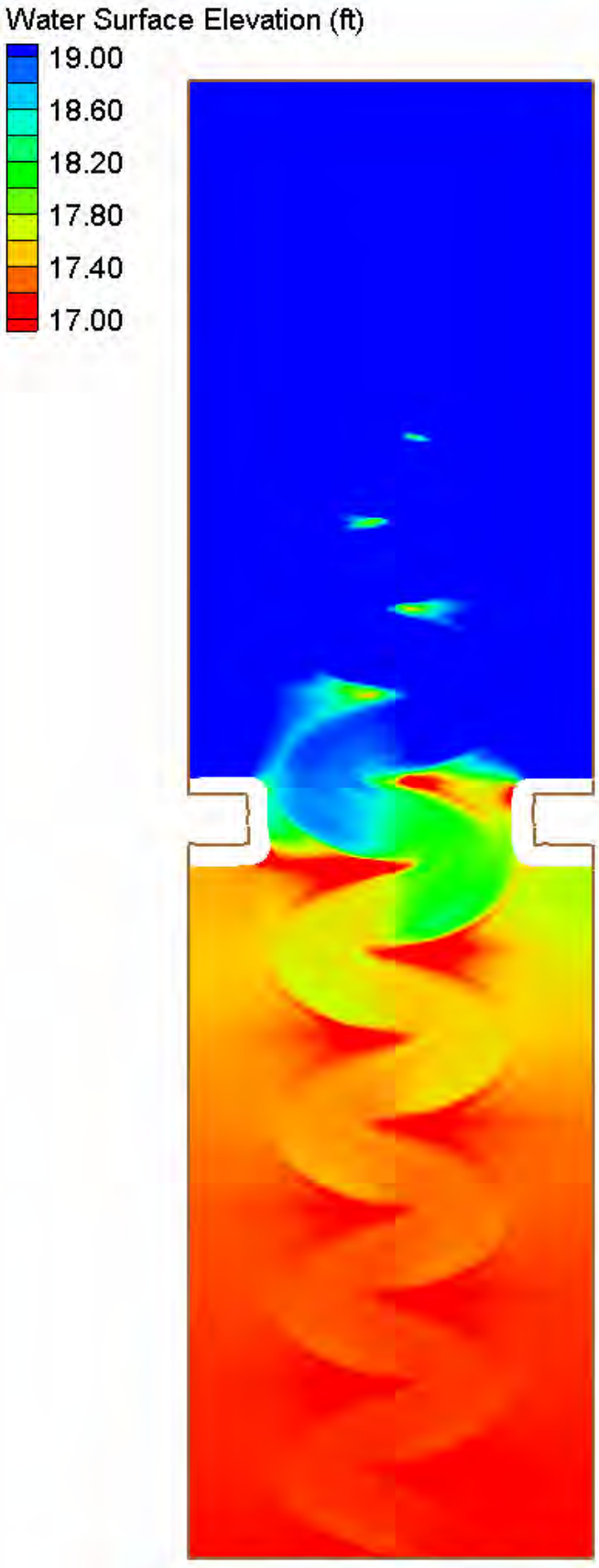

FESWMS Water Surface Elevation Contours – Small Channel – Meandering (2.0 sinuosity)

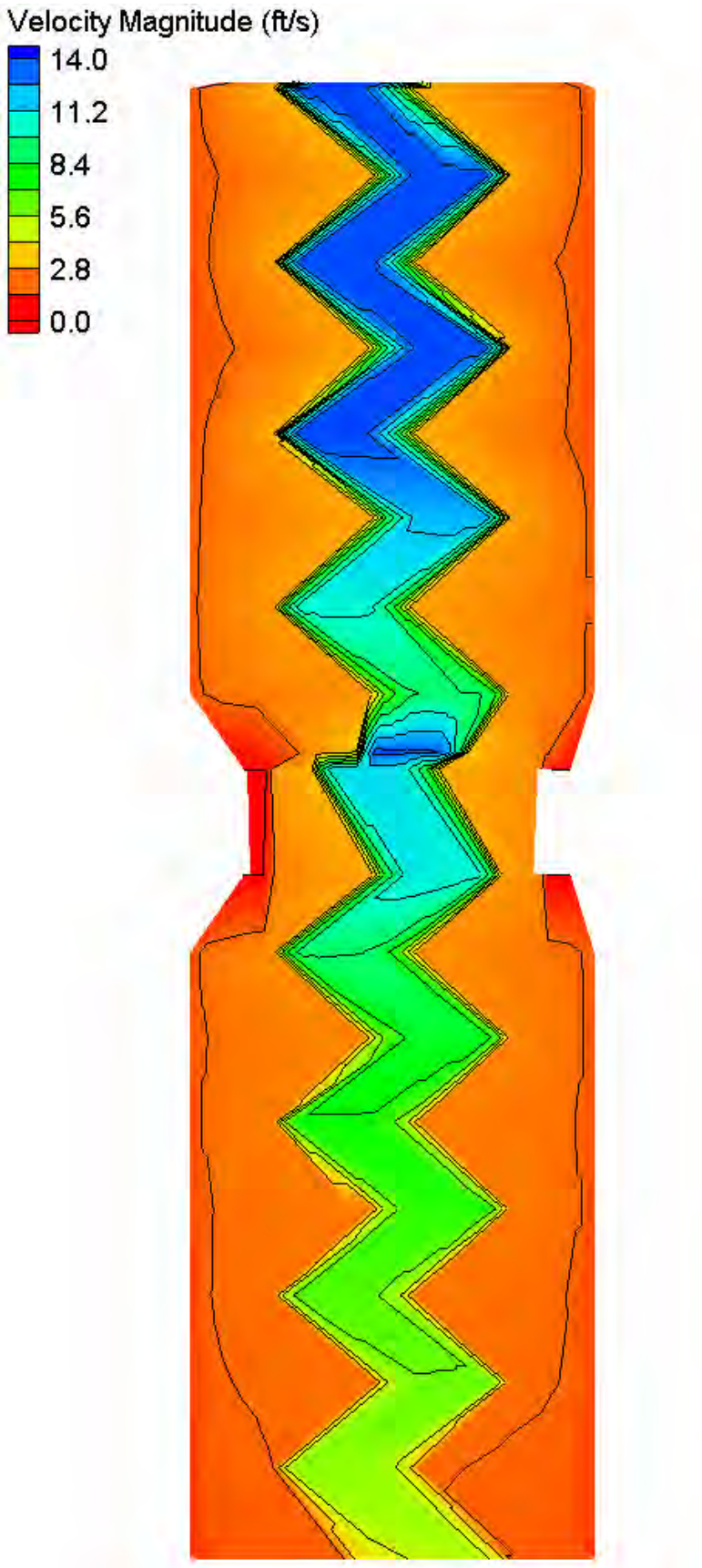

HEC-RAS Velocity Magnitude Contours – Small Channel – Meandering (2.0 sinuosity)

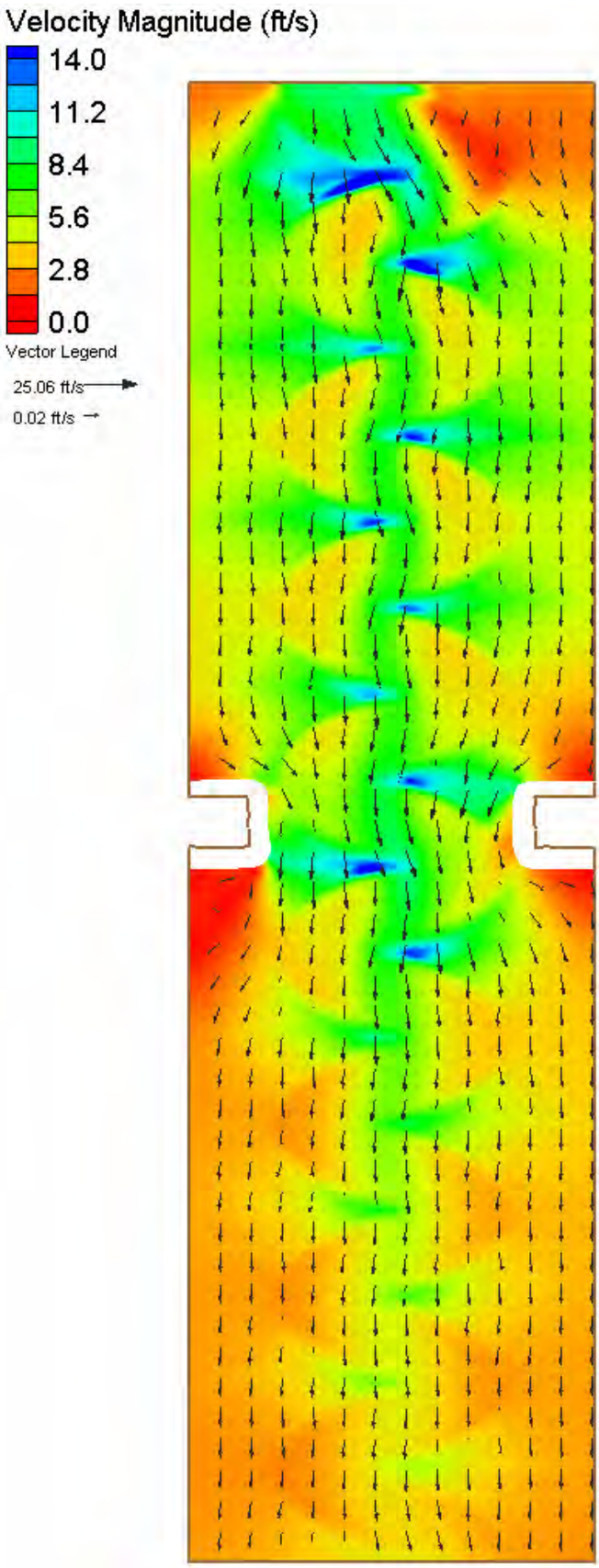

FESWMS Velocity Magnitude Contours – Small Channel – Meandering (2.0 sinuosity)

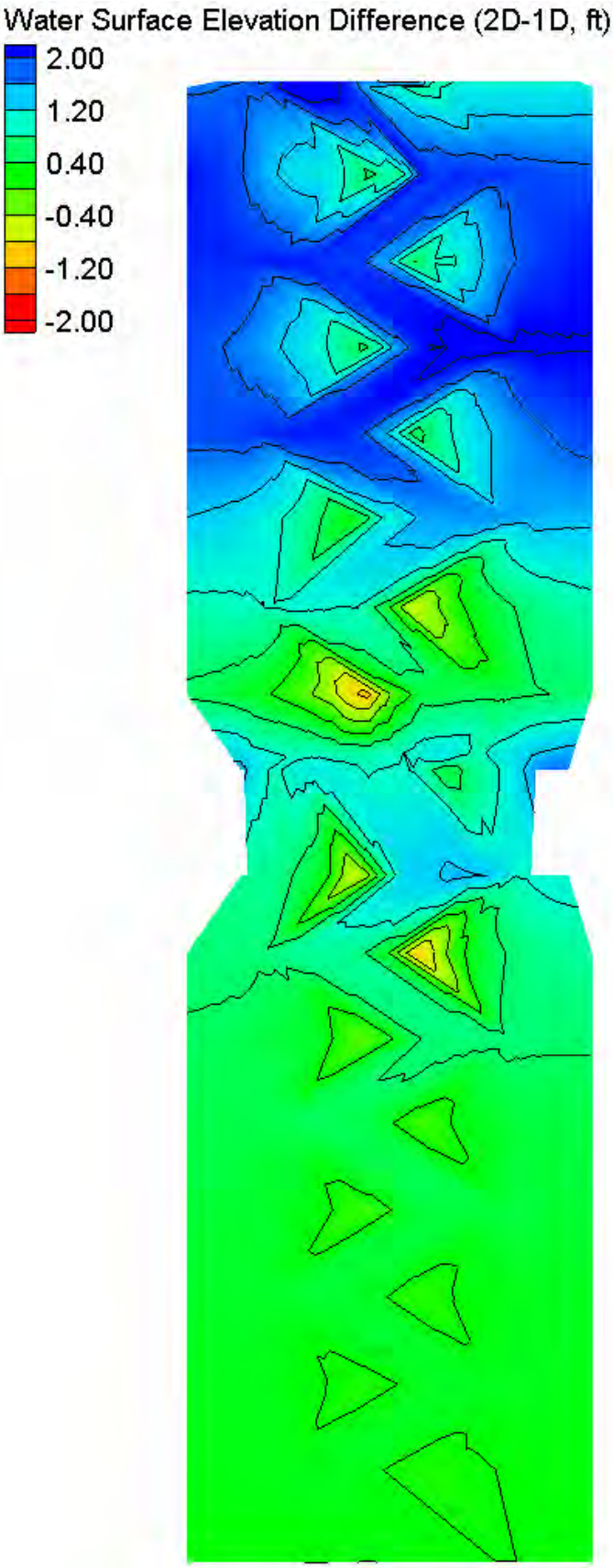

Water Surface Elevation Difference Contours – Small Channel – Meandering (2.0 sinuosity)

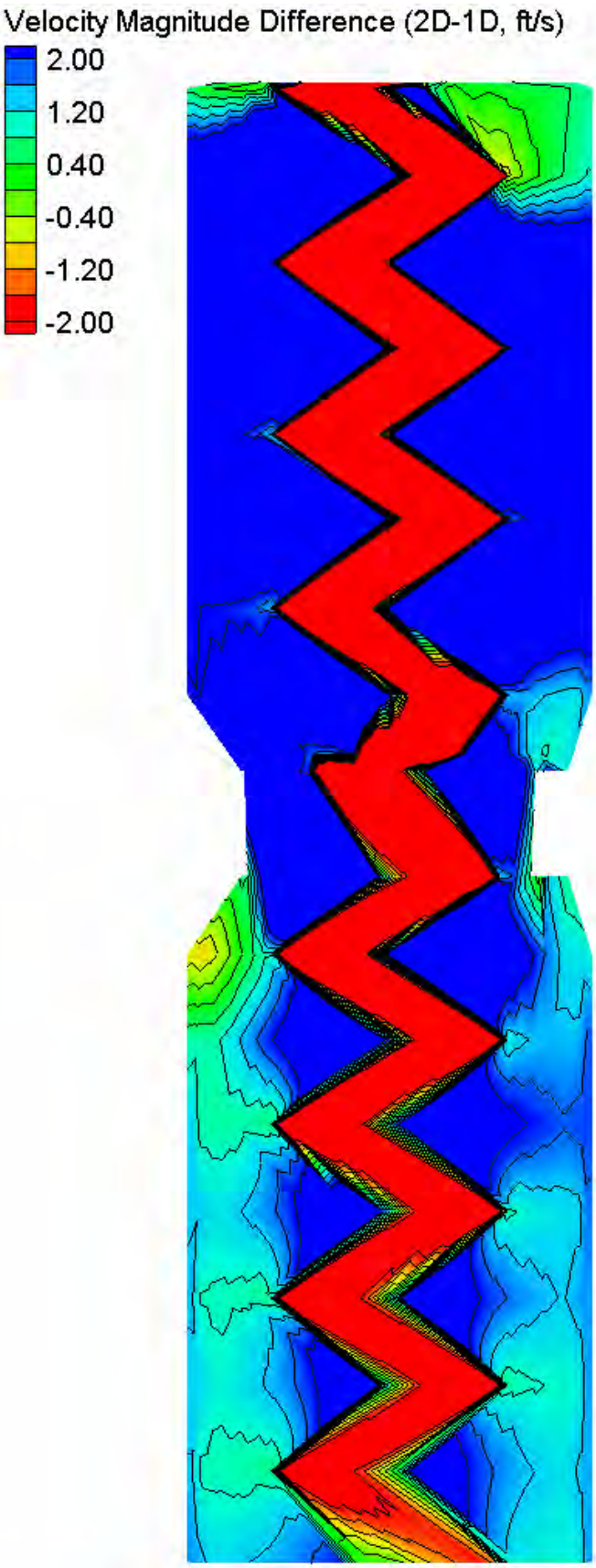

Velocity Magnitude Difference Contours – Small Channel – Meandering (2.0 sinuosity)

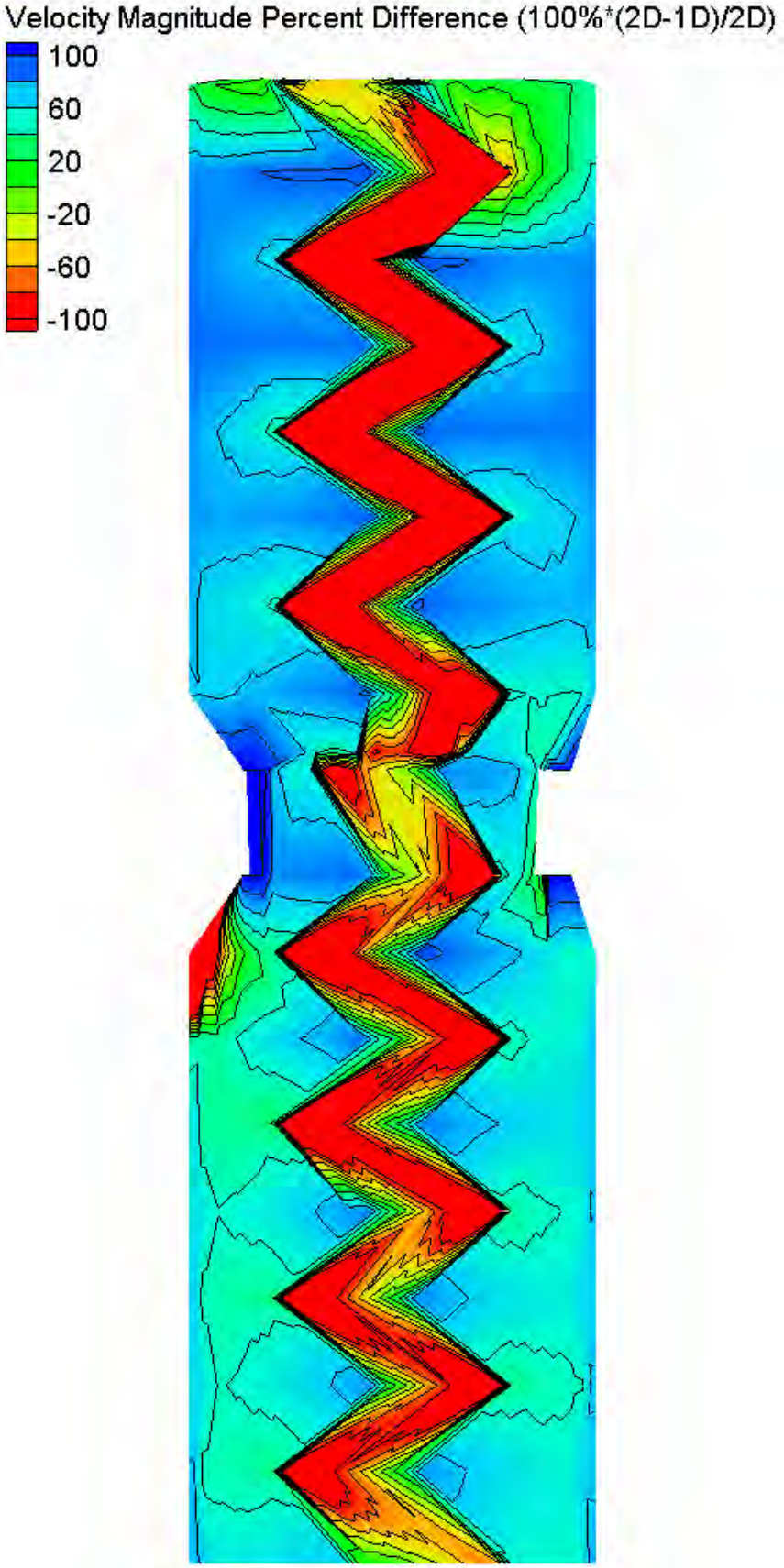

Velocity Magnitude Percent Difference Contours – Small Channel – Meandering (2.0 sinuosity)

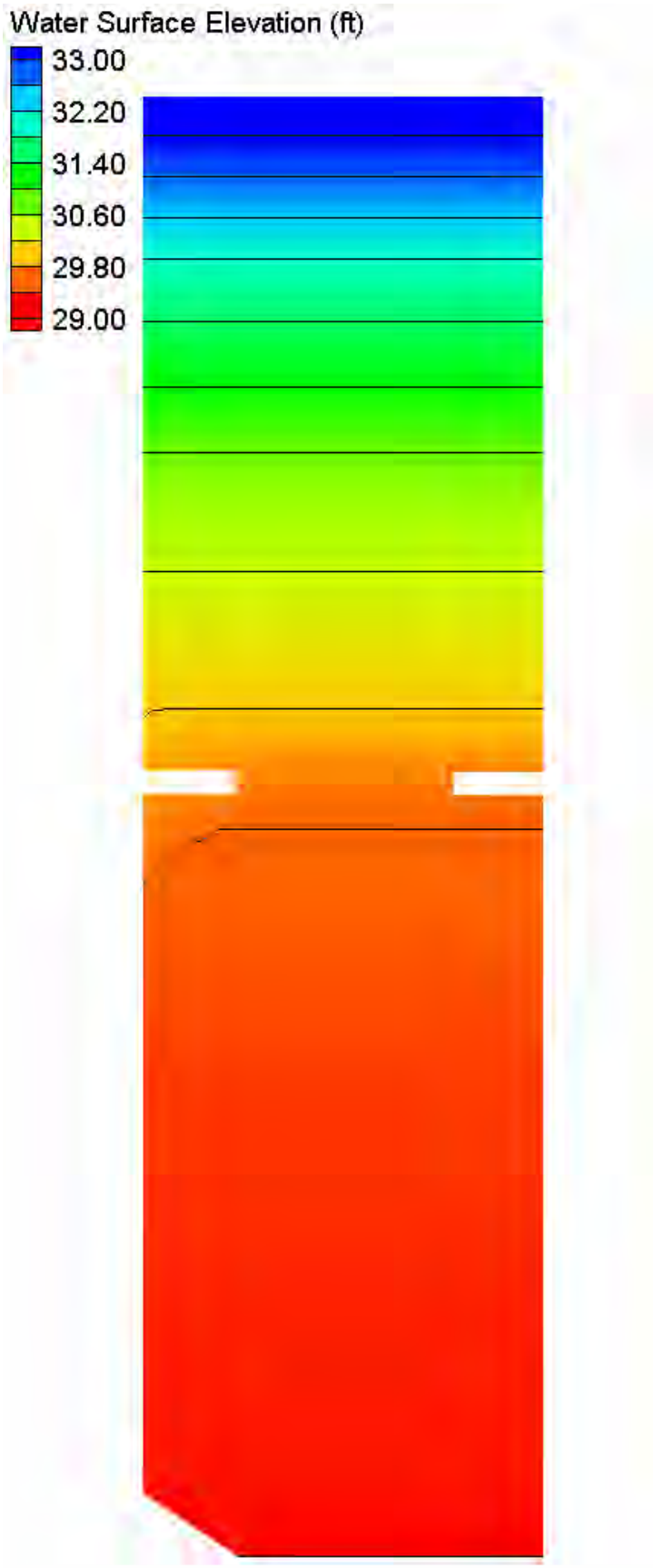

HEC-RAS Water Surface Elevation Contours – Large Channel – Meandering (1.25 sinuosity)

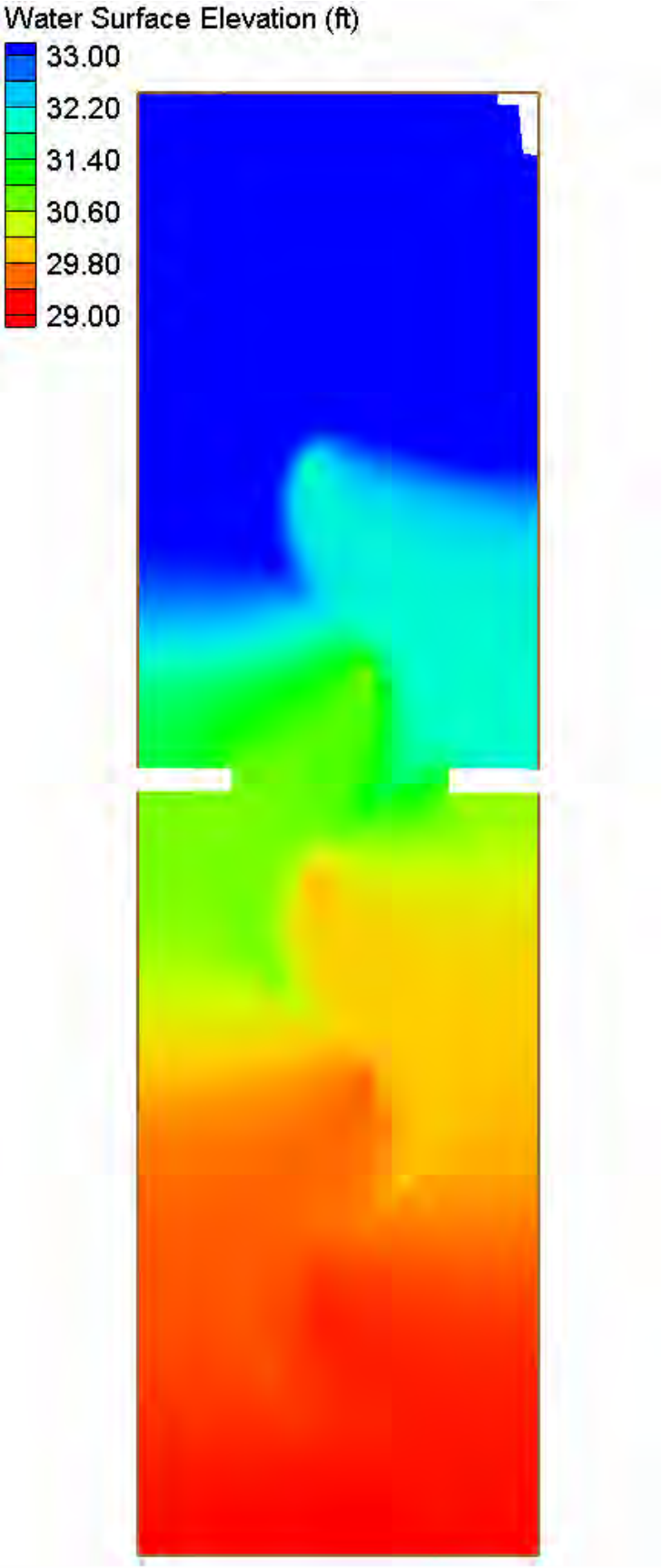

FESWMS Water Surface Elevation Contours – Large Channel – Meandering (1.25 sinuosity)

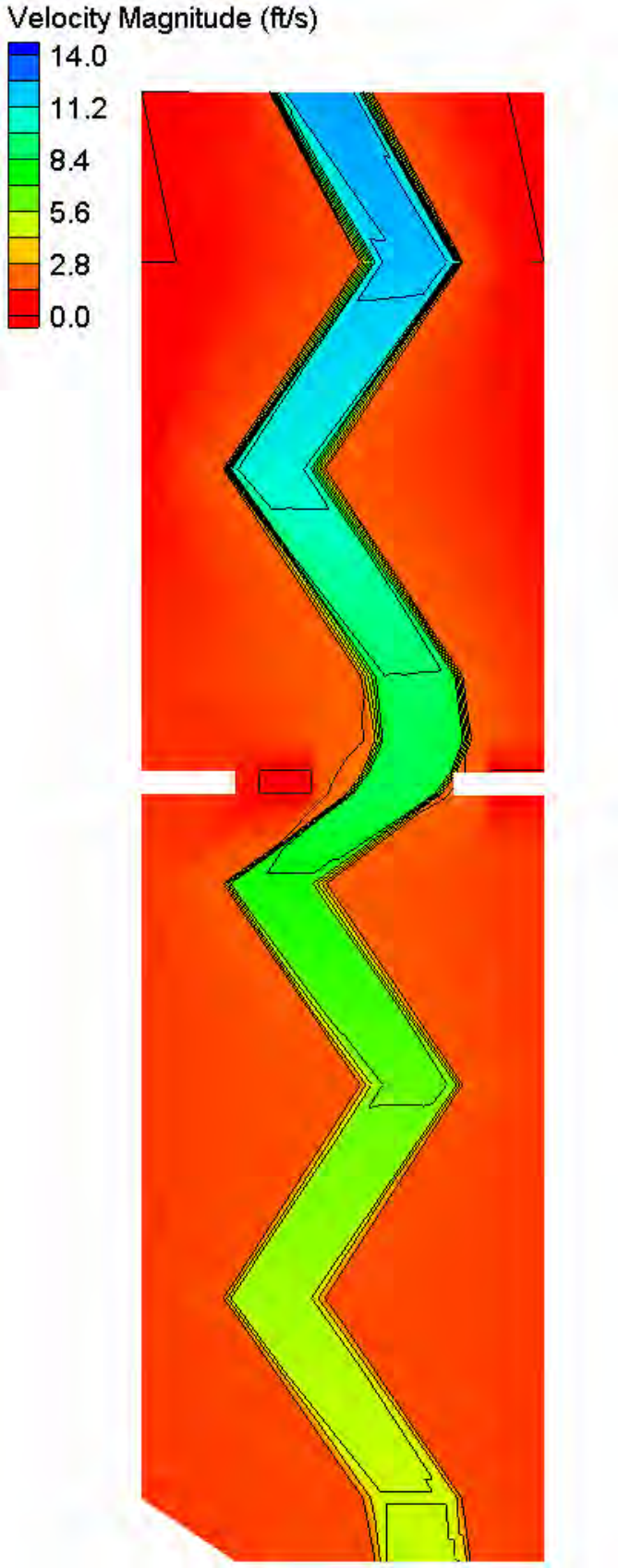

HEC-RAS Velocity Magnitude Contours – Large Channel – Meandering (1.25 sinuosity)

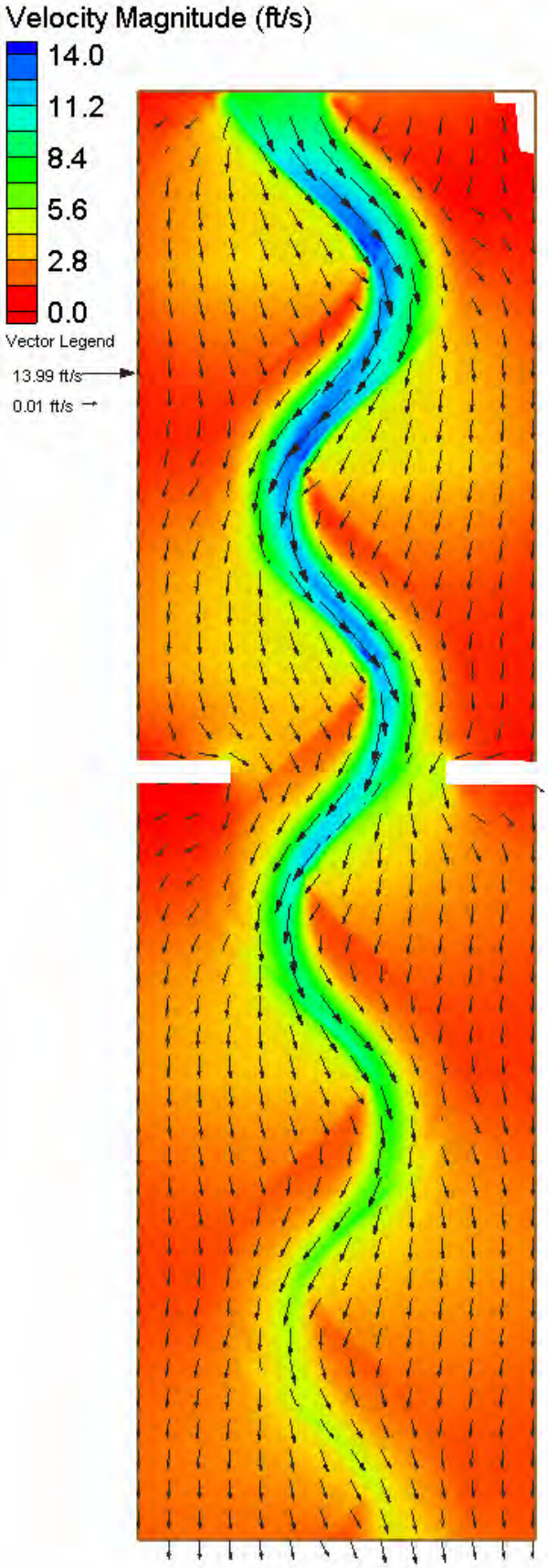

FESWMS Velocity Magnitude Contours – Large Channel – Meandering (1.25 sinuosity)

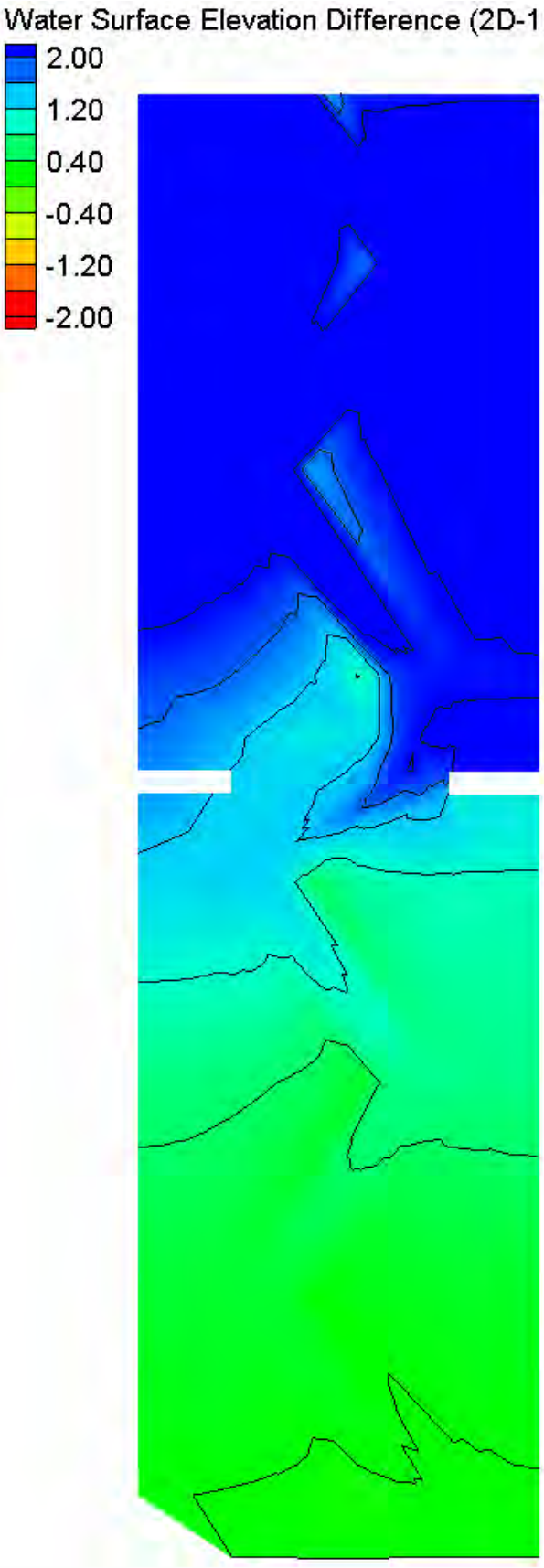

Water Surface Elevation Difference Contours – Large Channel – Meandering (1.25 sinuosity)

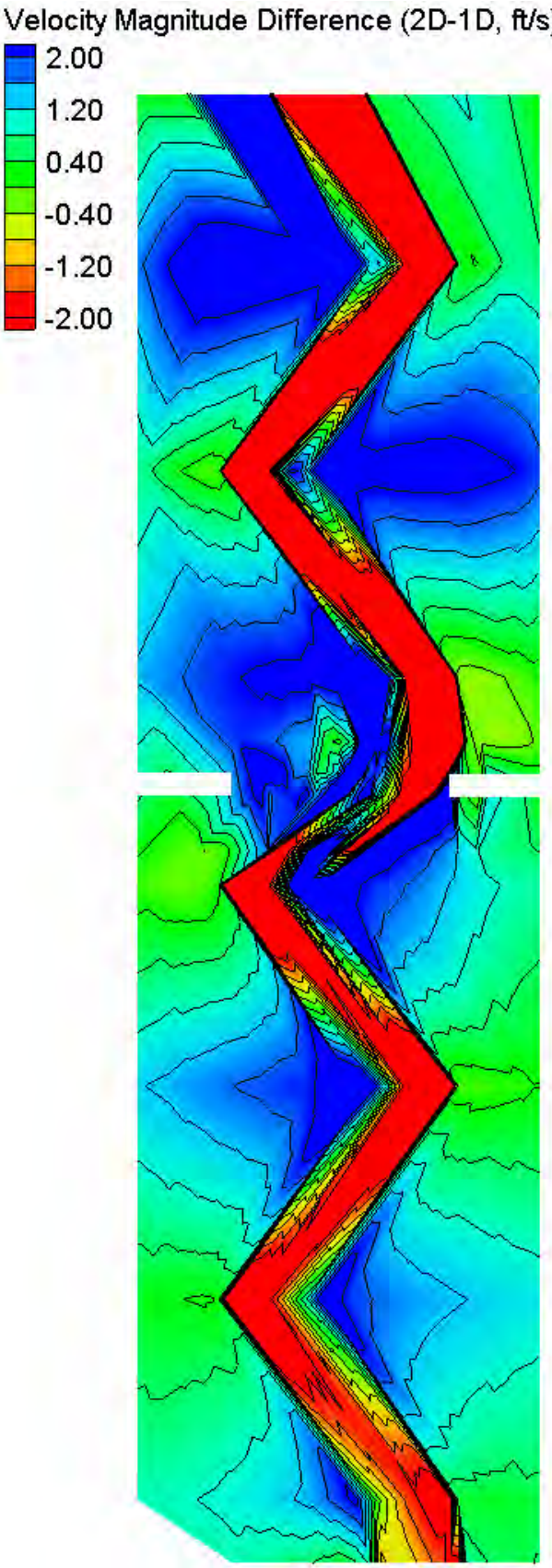

Velocity Magnitude Difference Contours – Large Channel – Meandering (1.25 sinuosity)

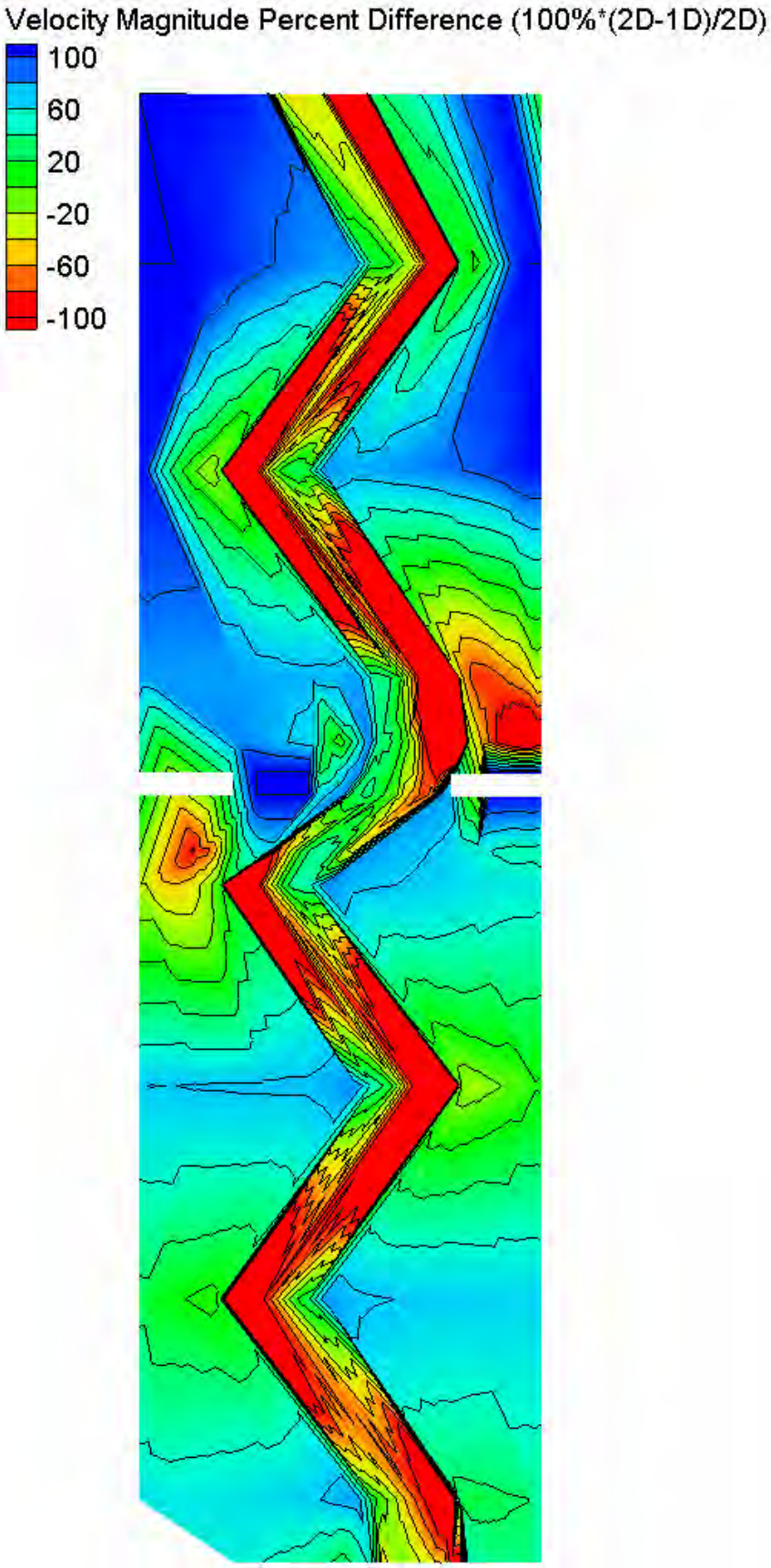

Velocity Magnitude Percent Difference Contours – Large Channel – Meandering (1.25 sinuosity)

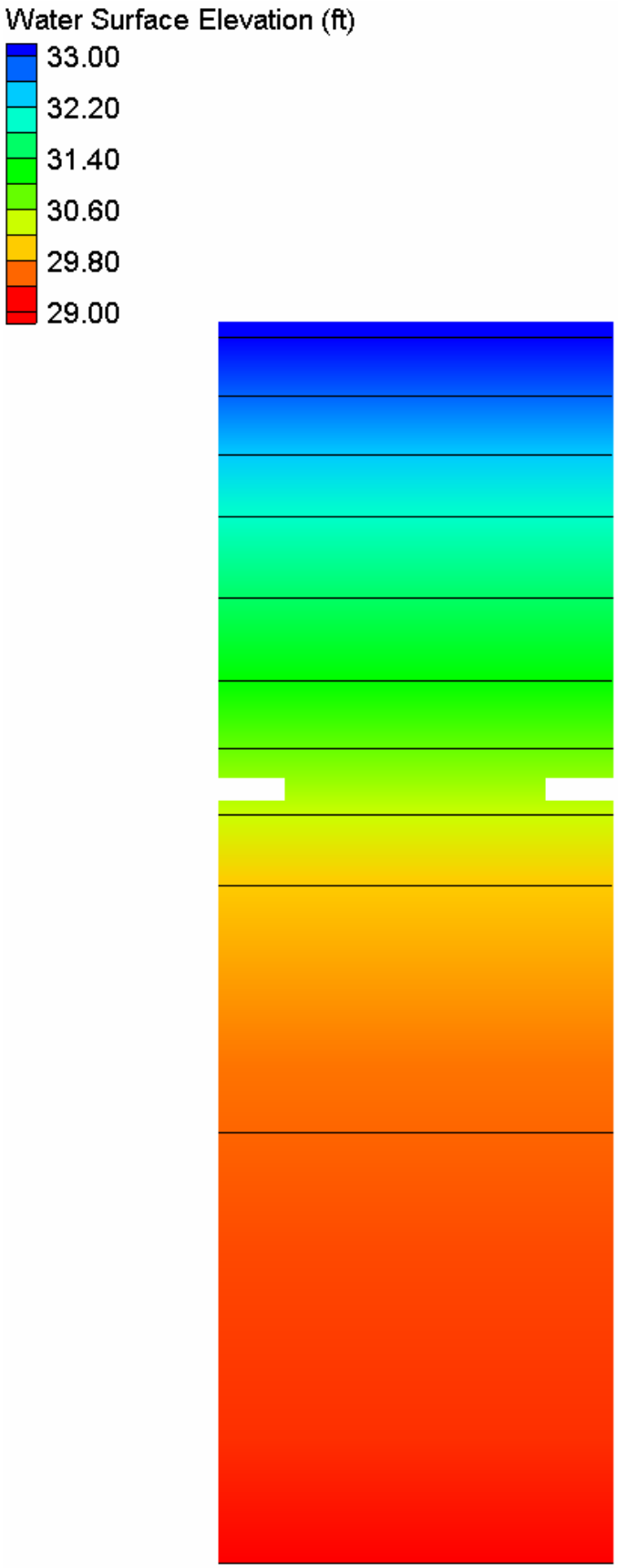

HEC-RAS Water Surface Elevation Contours – Large Channel – Meandering (1.5 sinuosity)

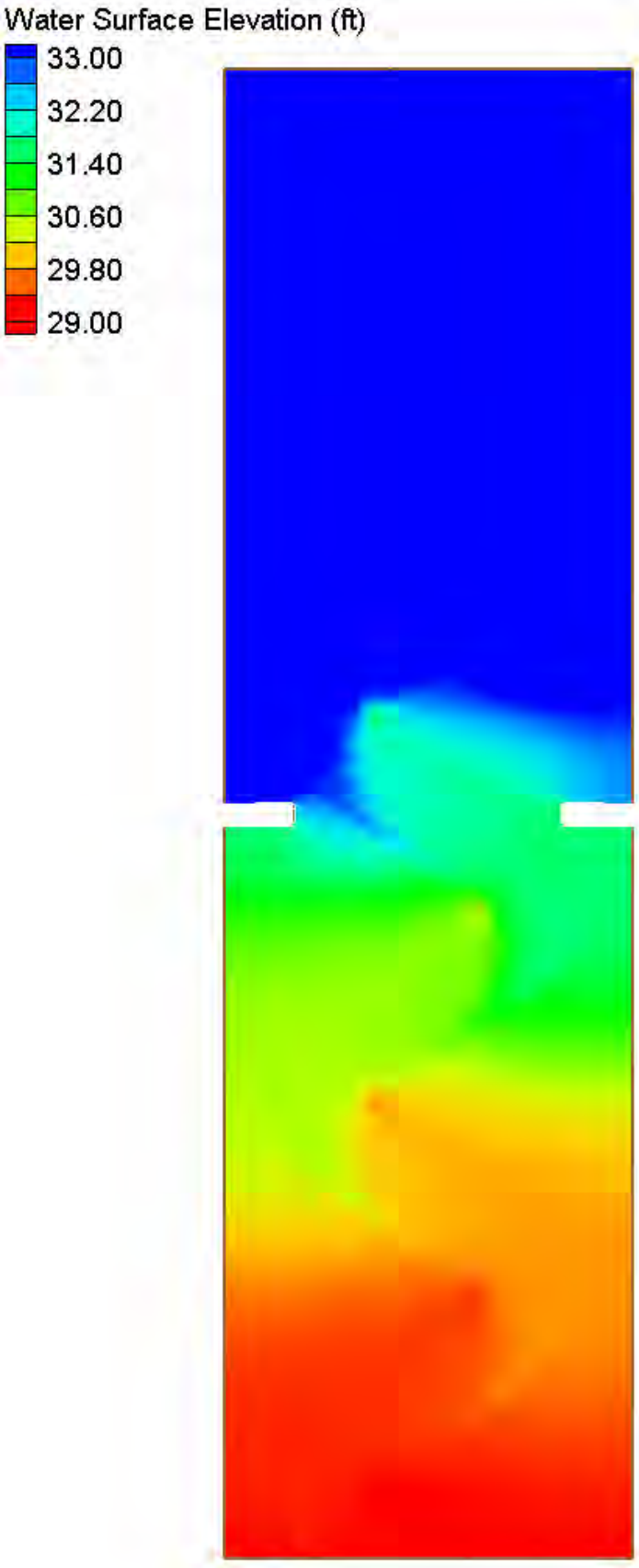

FESWMS Water Surface Elevation Contours – Large Channel – Meandering (1.5 sinuosity)

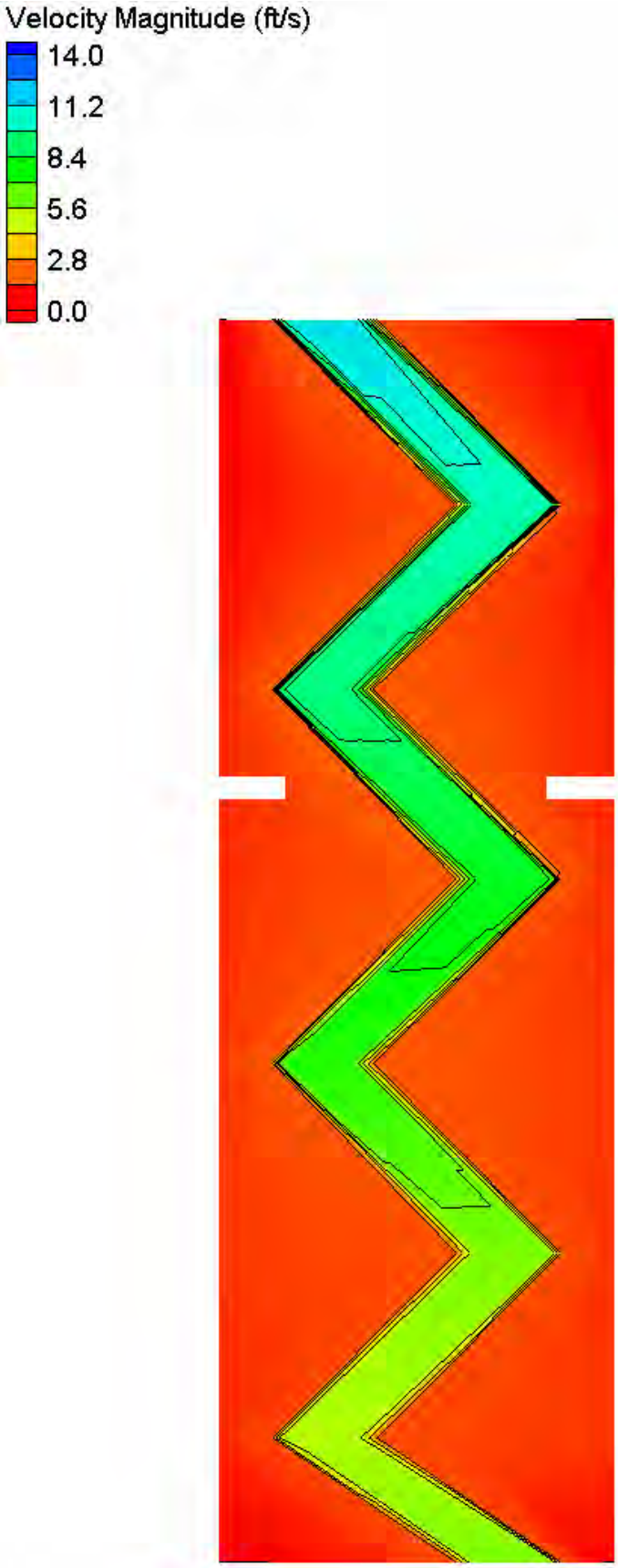

HEC-RAS Velocity Magnitude Contours – Large Channel – Meandering (1.5 sinuosity)

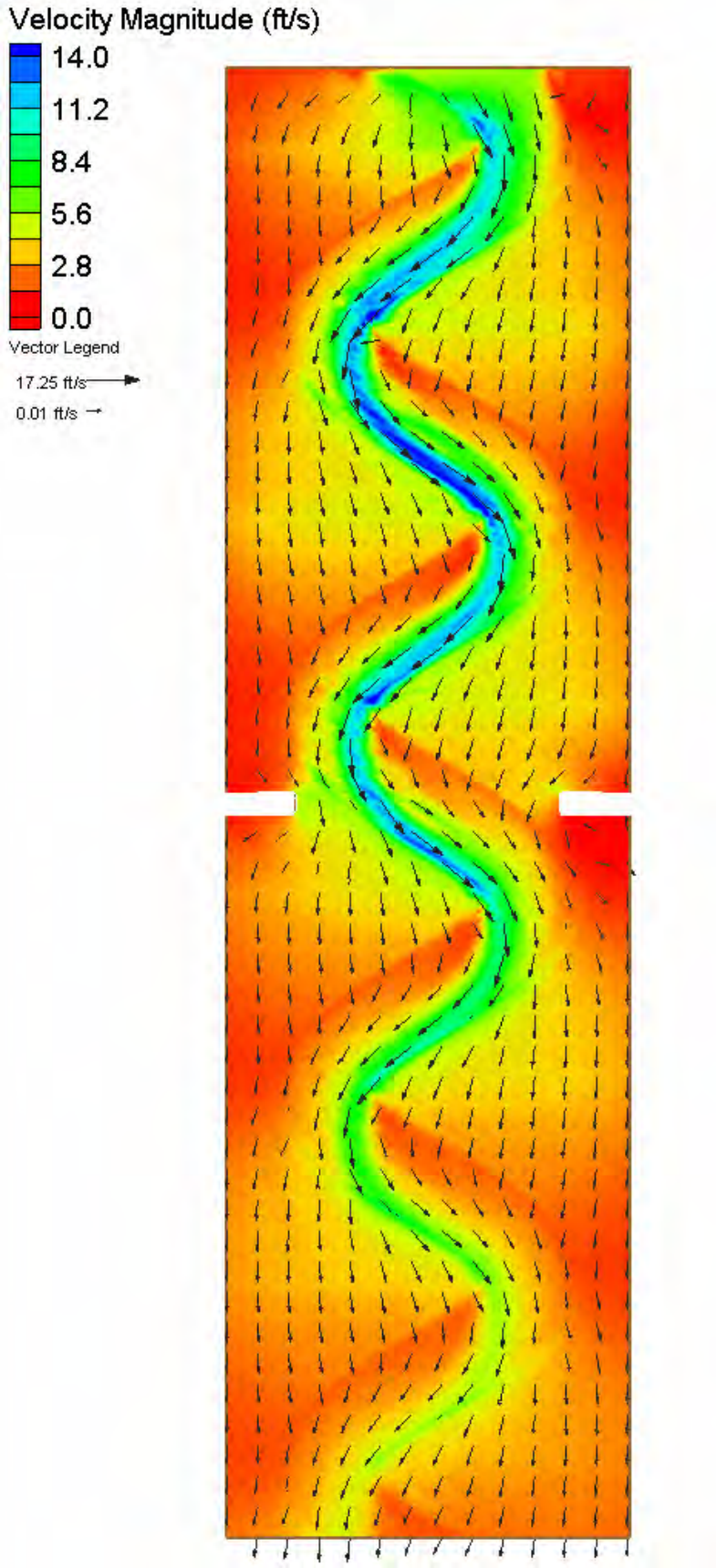

FESWMS Velocity Magnitude Contours – Large Channel – Meandering (1.5 sinuosity)

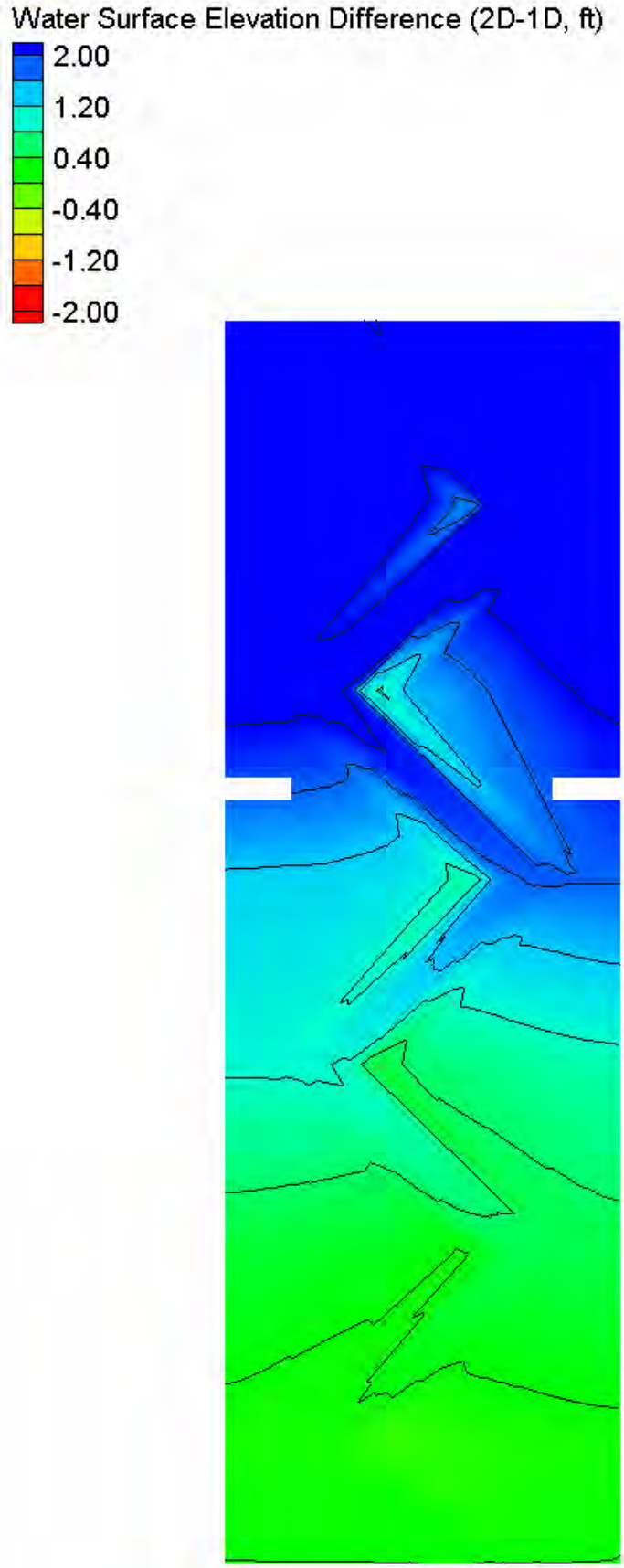

Water Surface Elevation Difference Contours – Large Channel – Meandering (1.5 sinuosity)

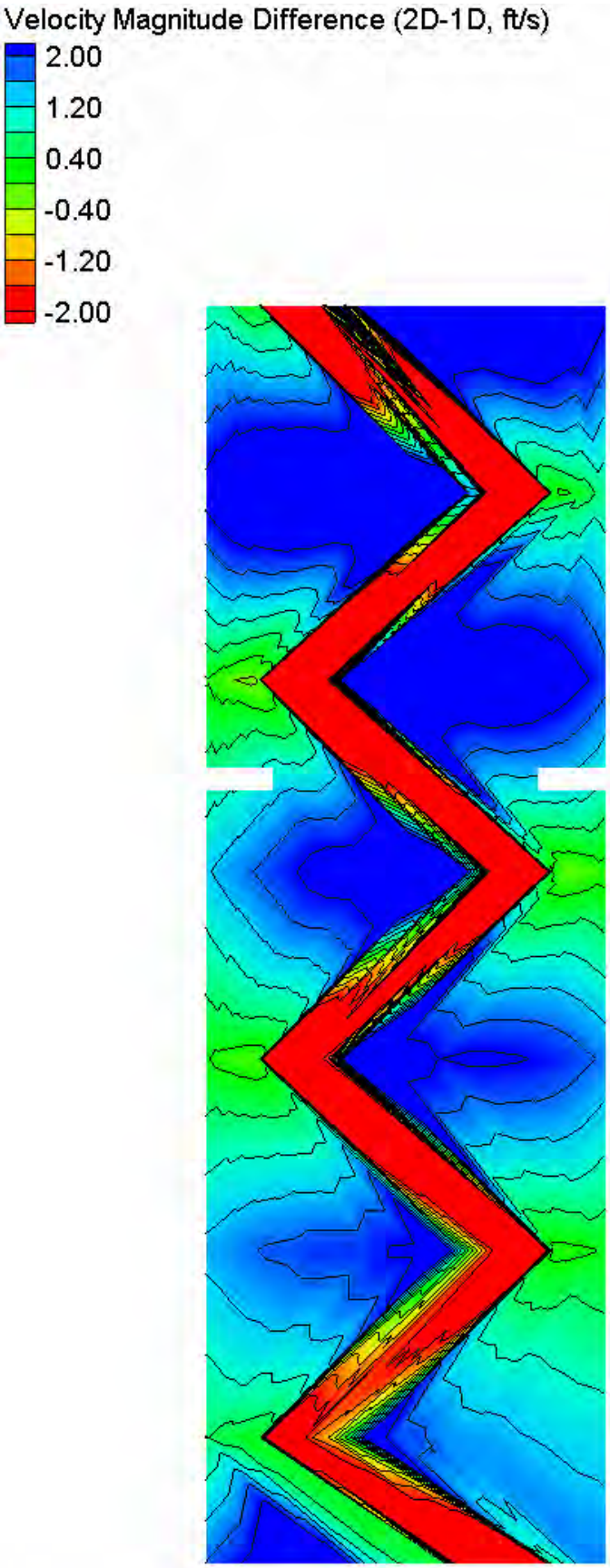

Velocity Magnitude Difference Contours – Large Channel – Meandering (1.5 sinuosity)

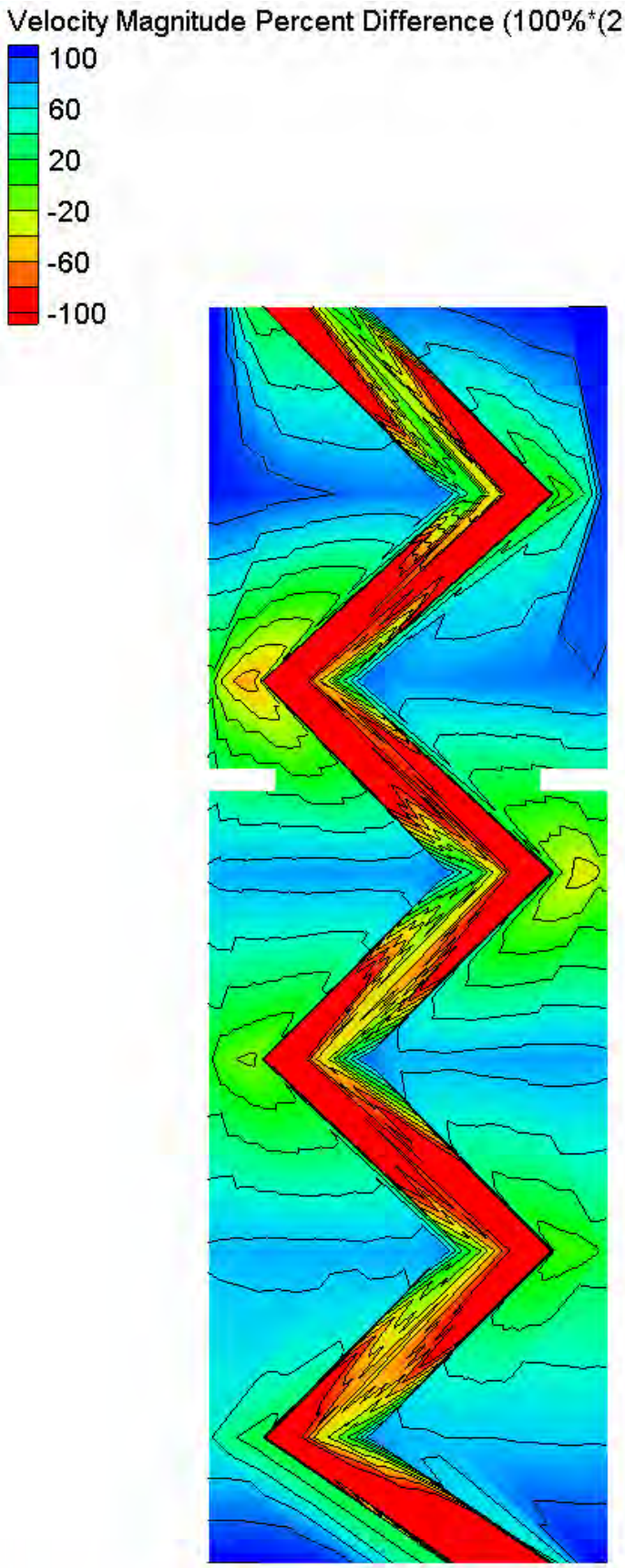

Velocity Magnitude Percent Difference Contours – Large Channel – Meandering (1.5 sinuosity)

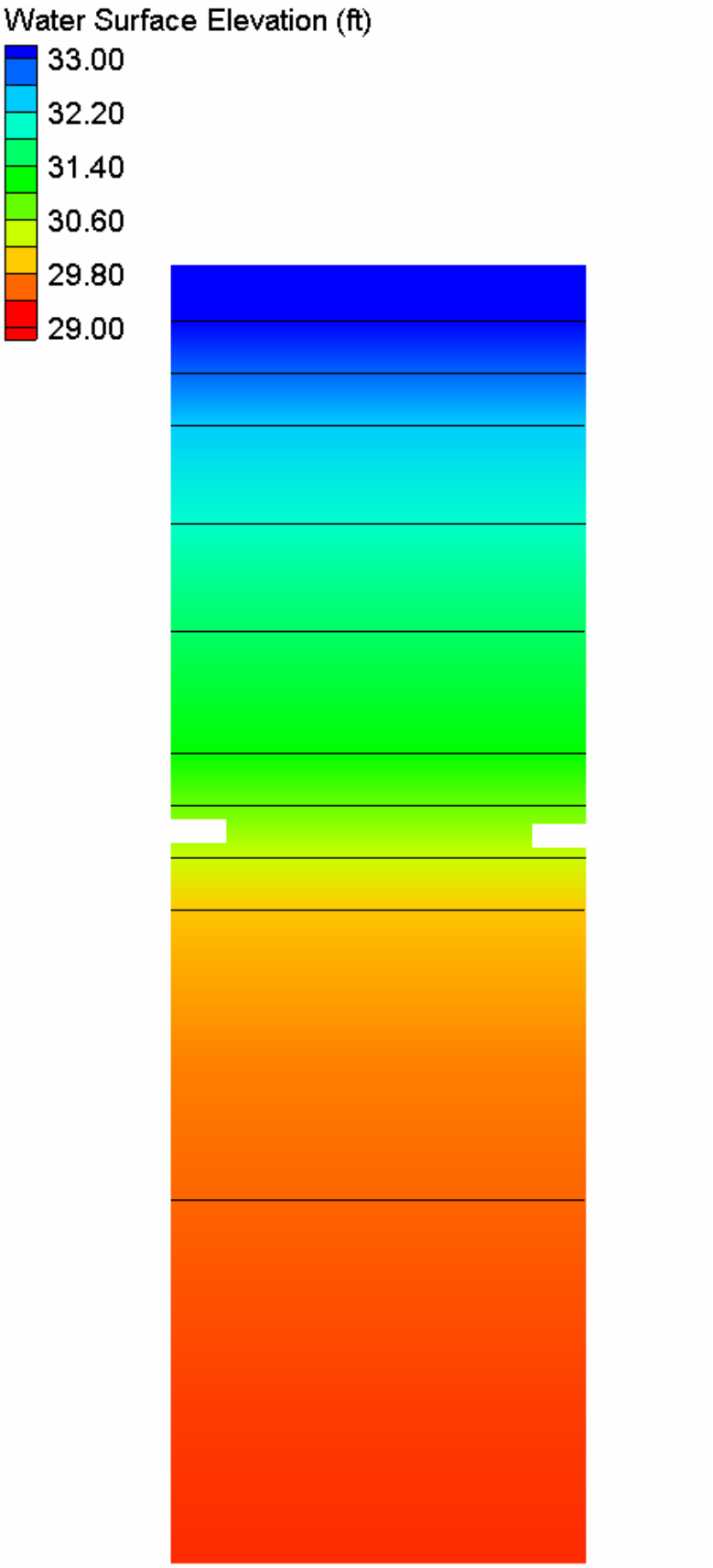

HEC-RAS Water Surface Elevation Contours – Large Channel – Meandering (1.75 sinuosity)

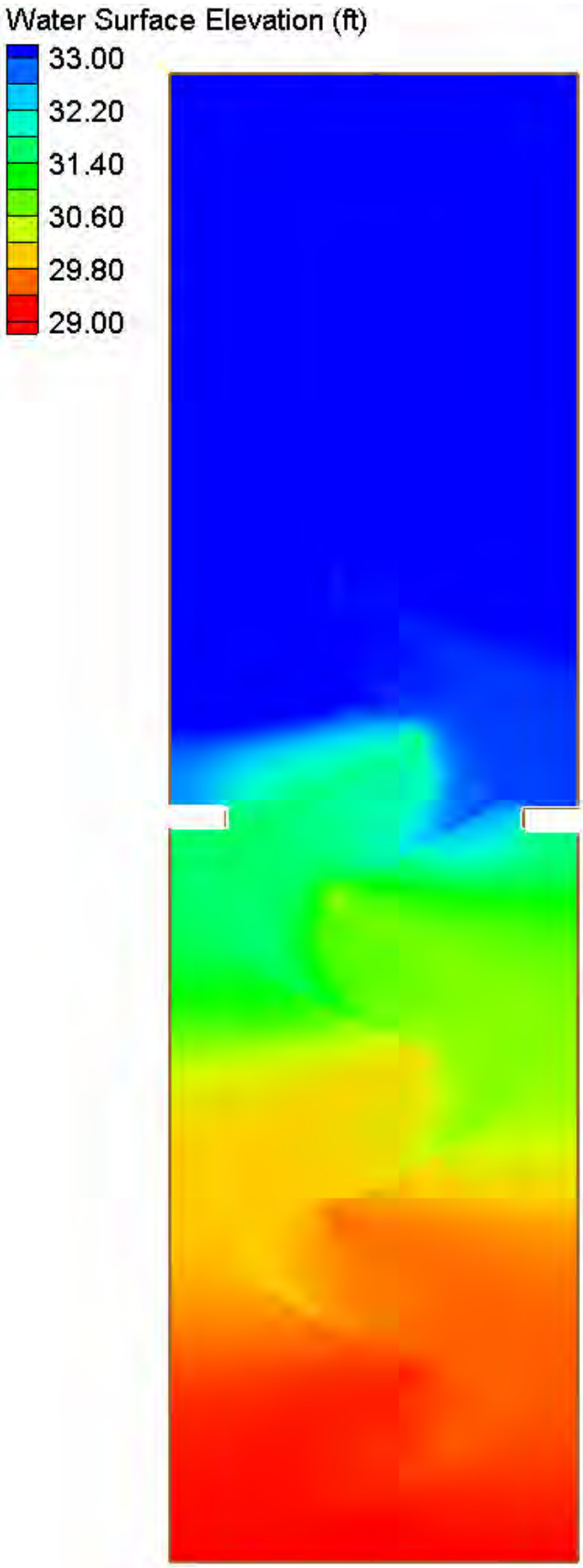

FESWMS Water Surface Elevation Contours – Large Channel – Meandering (1.75 sinuosity)

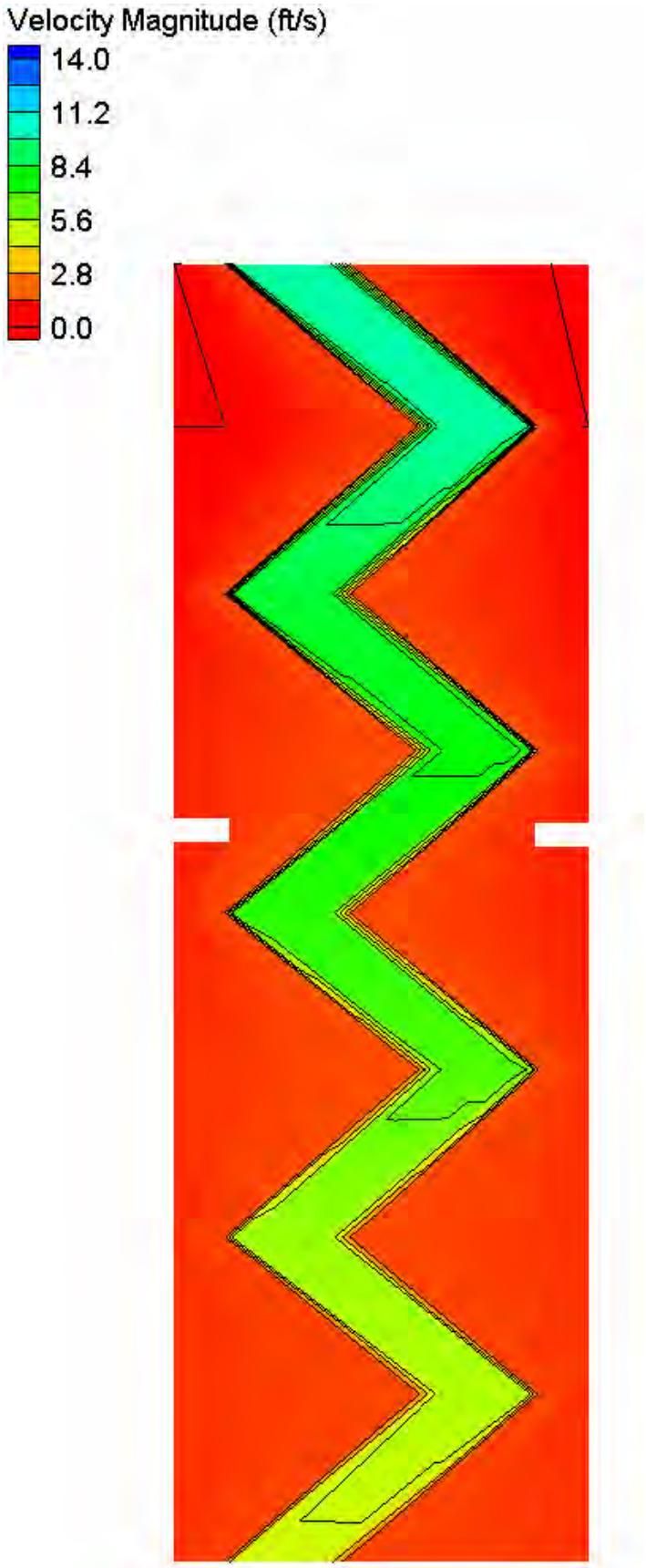

HEC-RAS Velocity Magnitude Contours – Large Channel – Meandering (1.75 sinuosity)

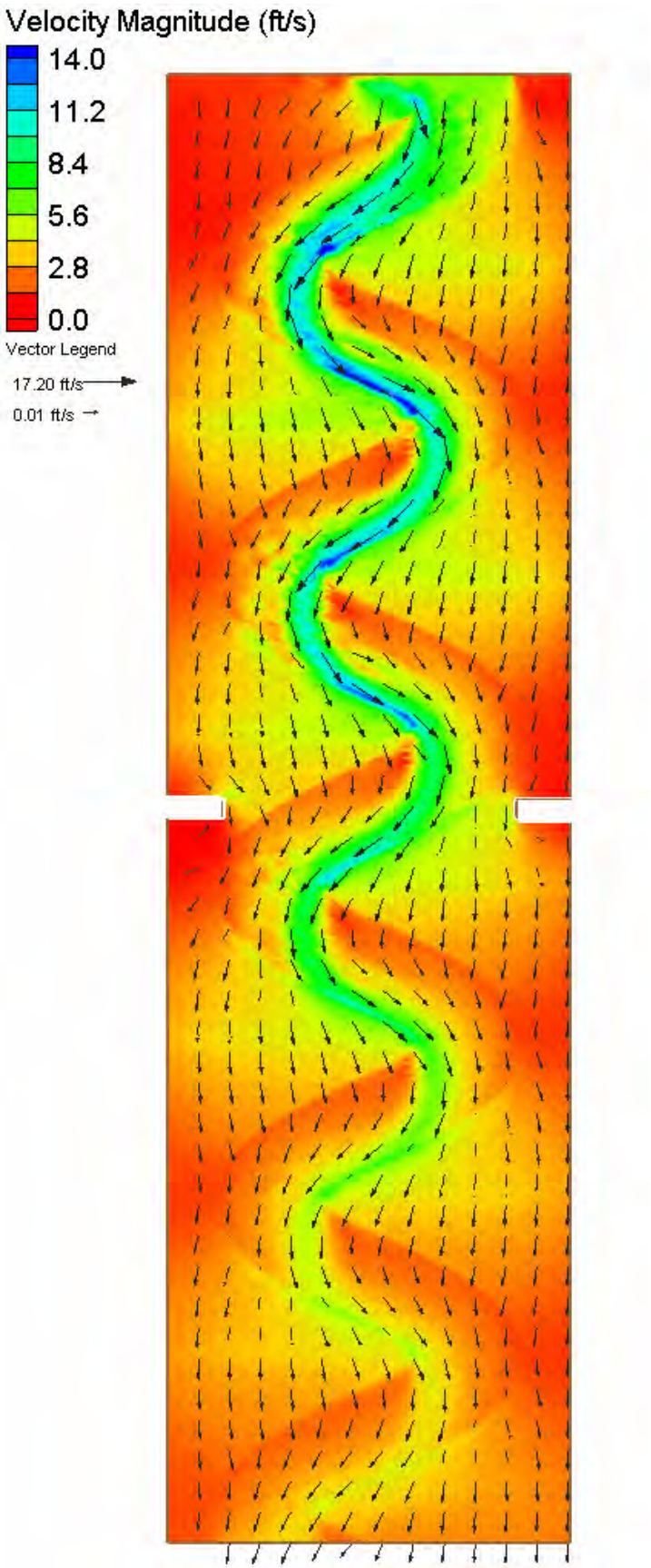

FESWMS Velocity Magnitude Contours – Large Channel – Meandering (1.75 sinuosity)

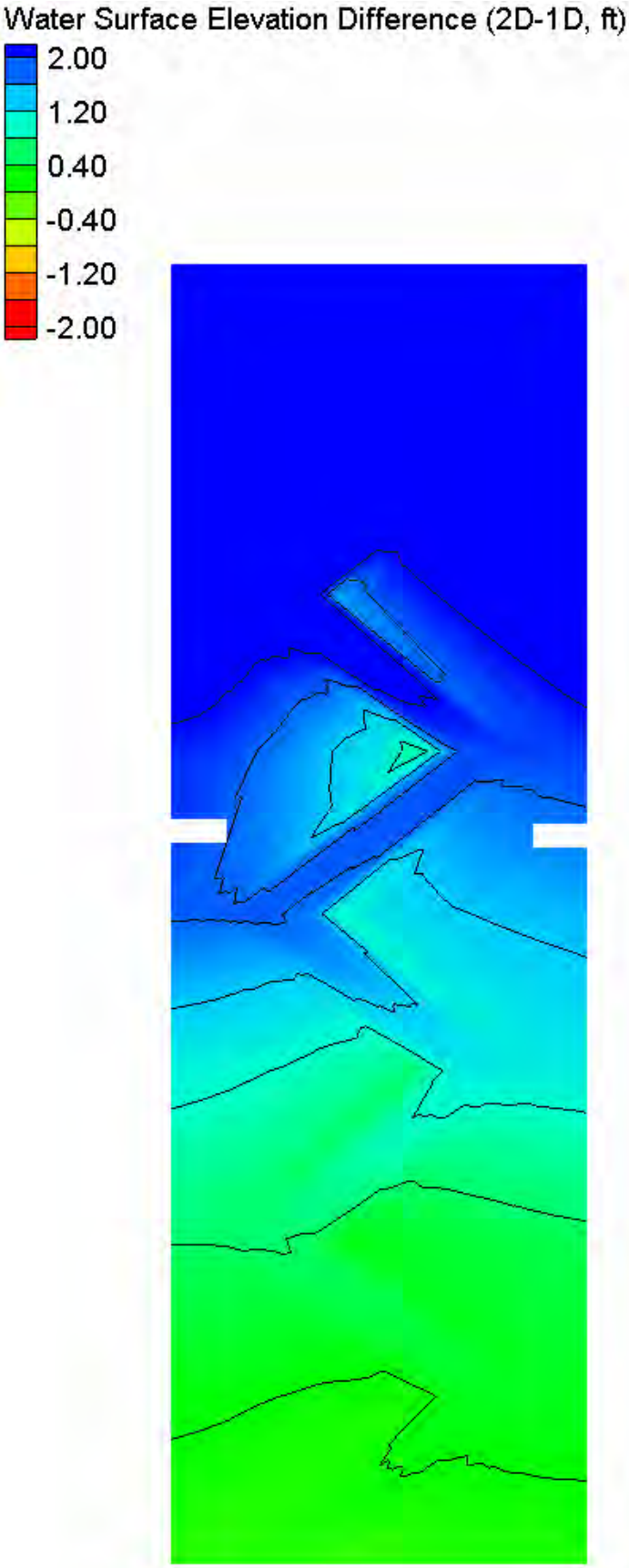

Water Surface Elevation Difference Contours – Large Channel – Meandering (1.75 sinuosity)

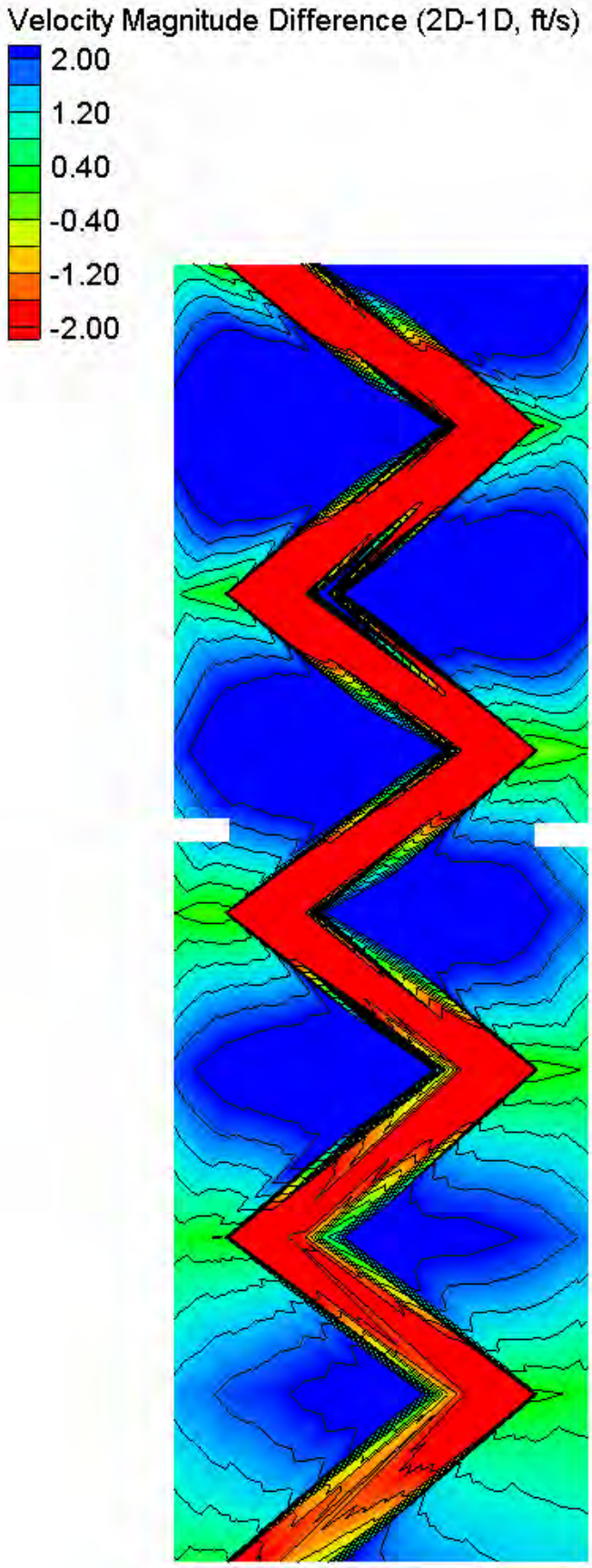

Velocity Magnitude Difference Contours – Large Channel – Meandering (1.75 sinuosity)

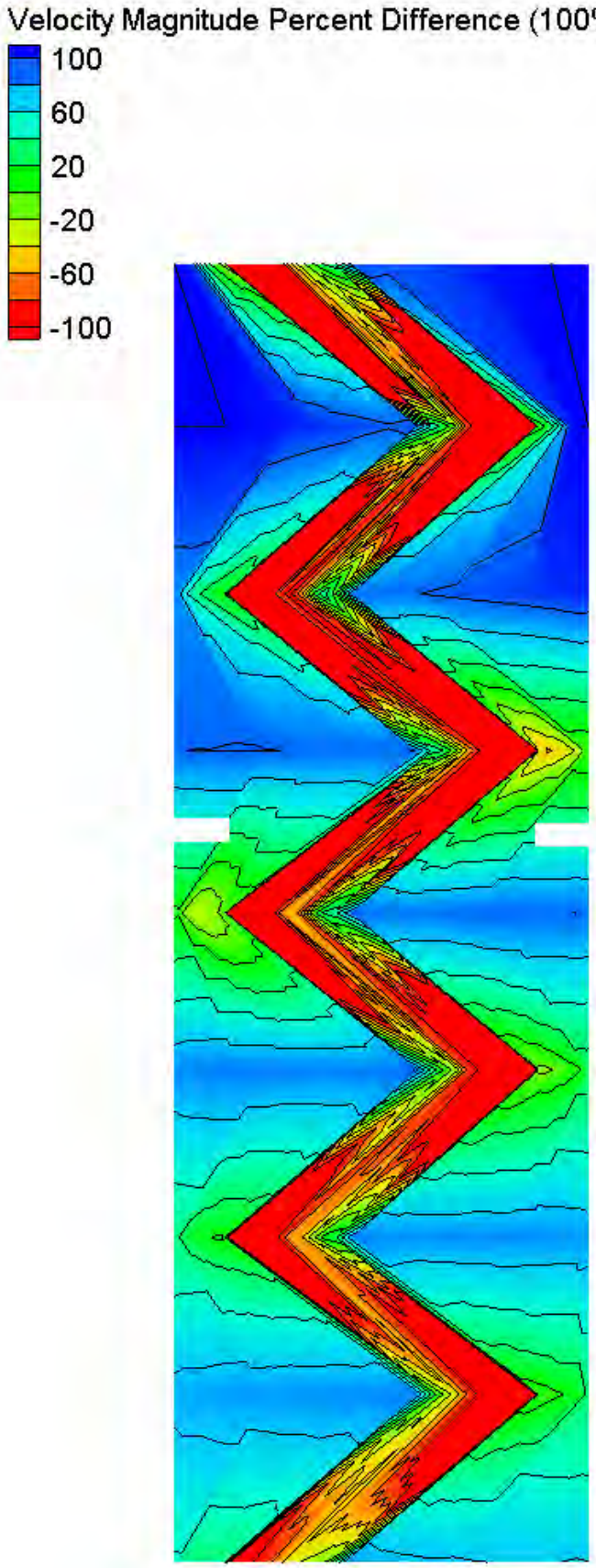

Velocity Magnitude Percent Difference Contours – Large Channel – Meandering (1.75 sinuosity)

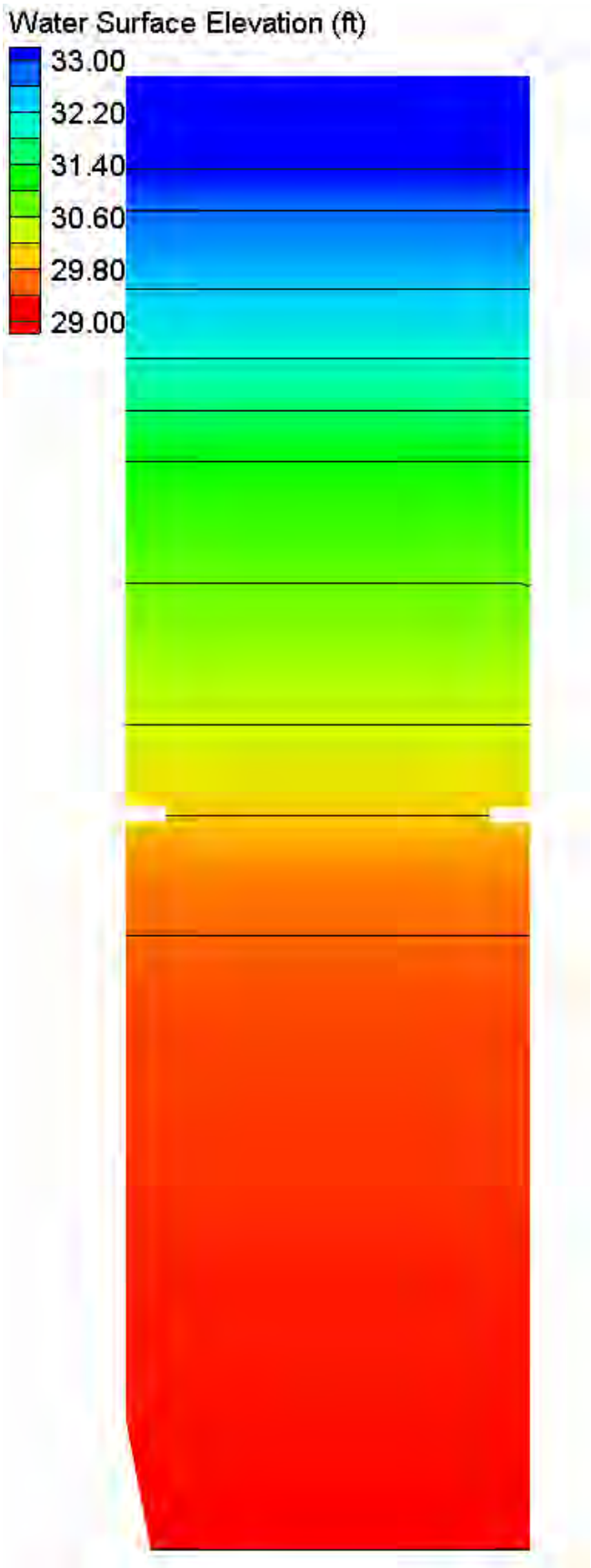

HEC-RAS Water Surface Elevation Contours – Large Channel – Meandering (2.0 sinuosity)

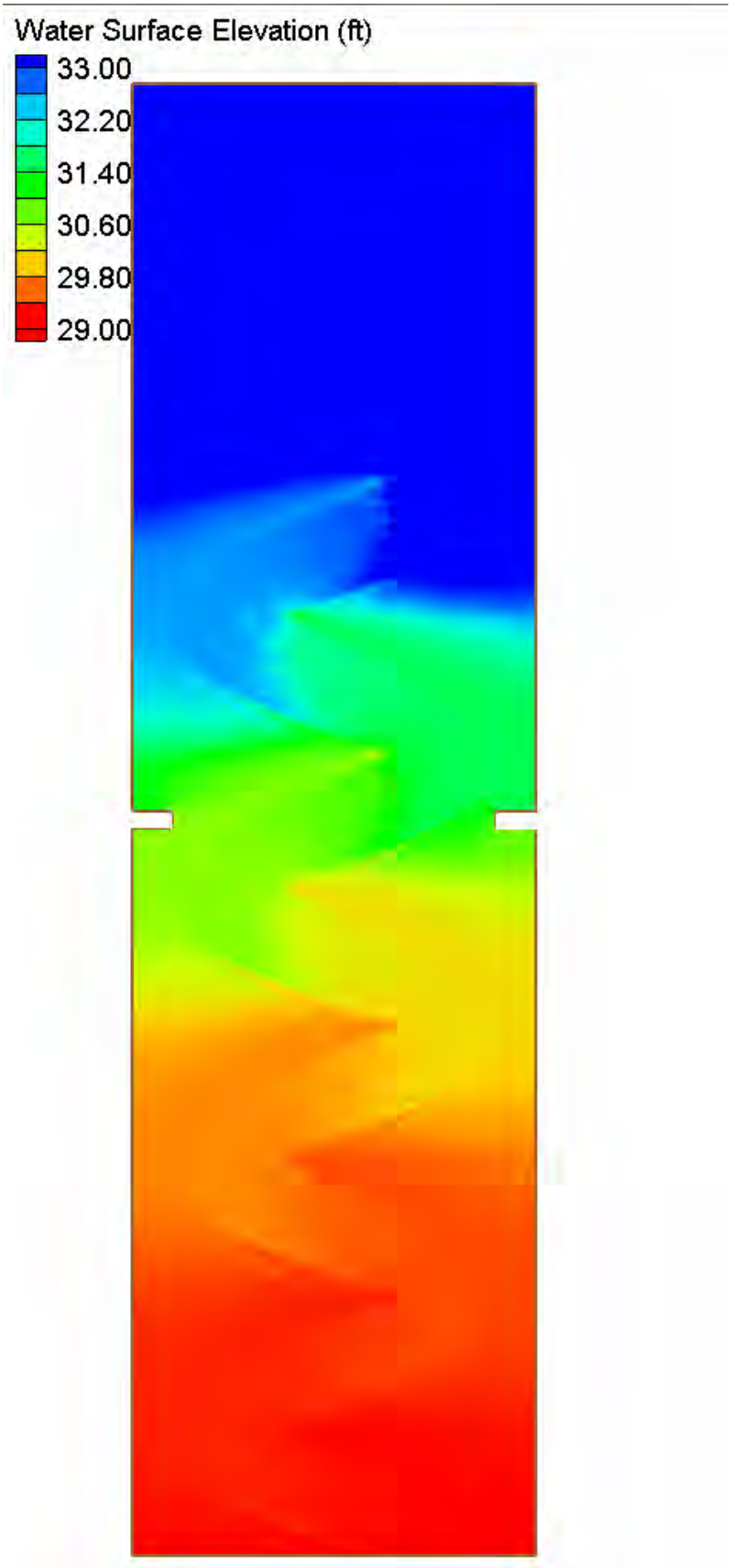

FESWMS Water Surface Elevation Contours – Large Channel – Meandering (2.0 sinuosity)

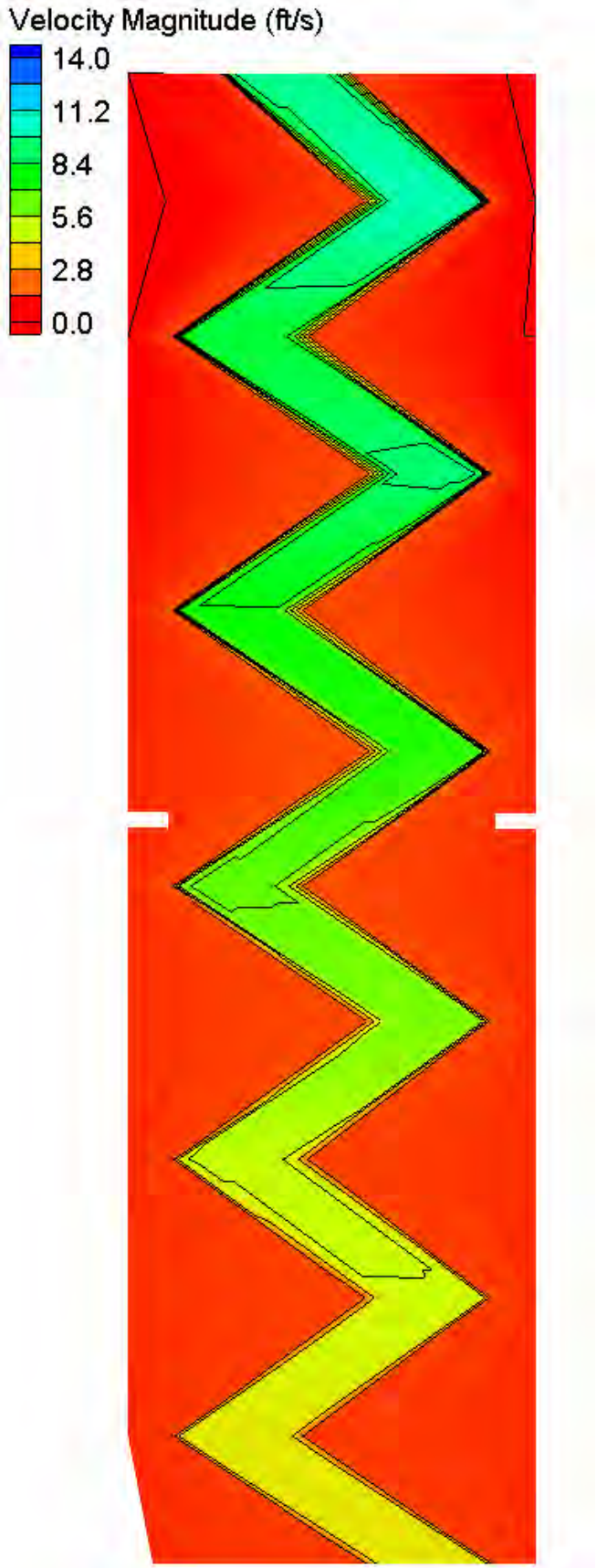

HEC-RAS Velocity Magnitude Contours – Large Channel – Meandering (2.0 sinuosity)

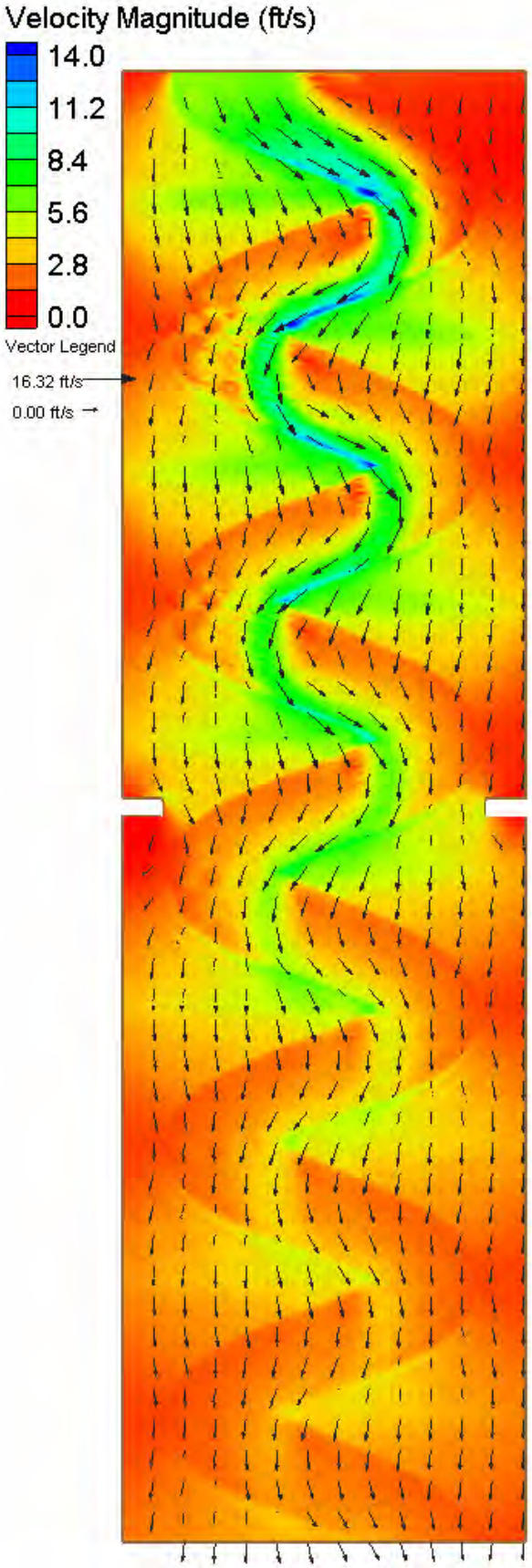

FESWMS Velocity Magnitude Contours – Large Channel – Meandering (2.0 sinuosity)

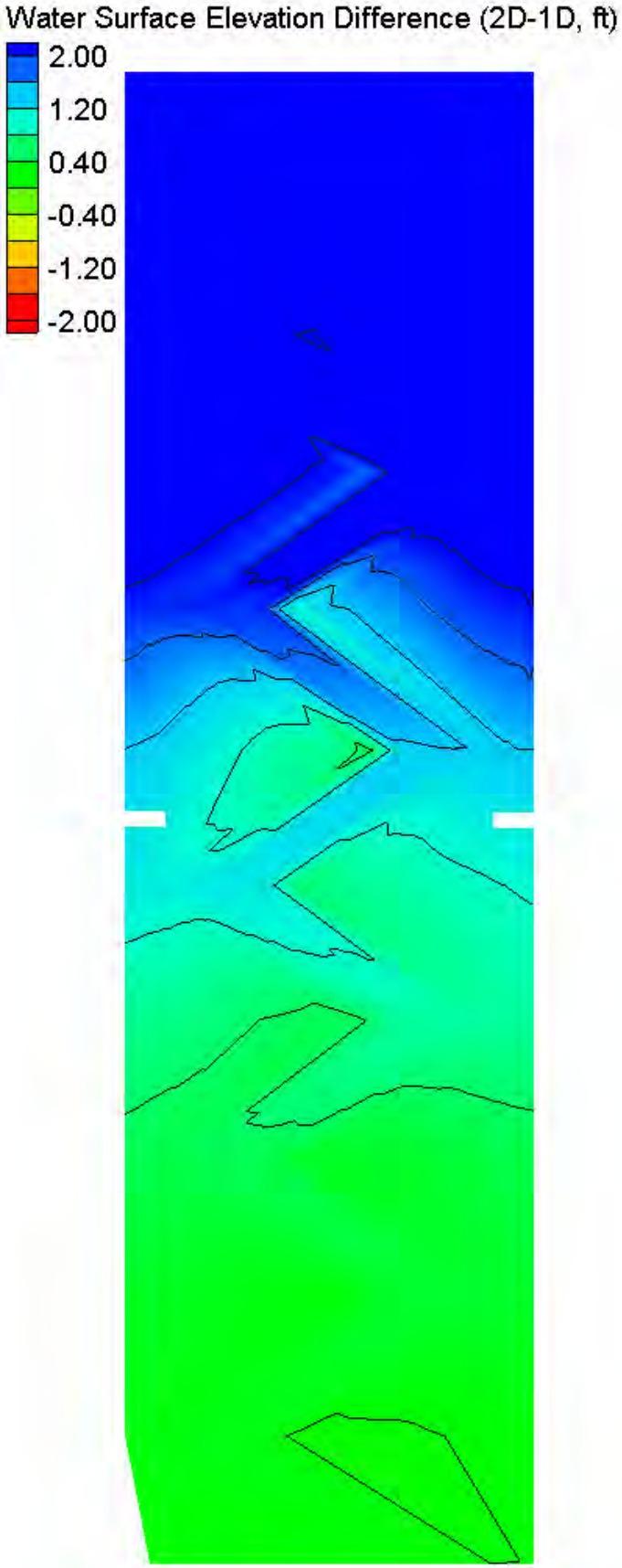

Water Surface Elevation Difference Contours – Large Channel – Meandering (2.0 sinuosity)

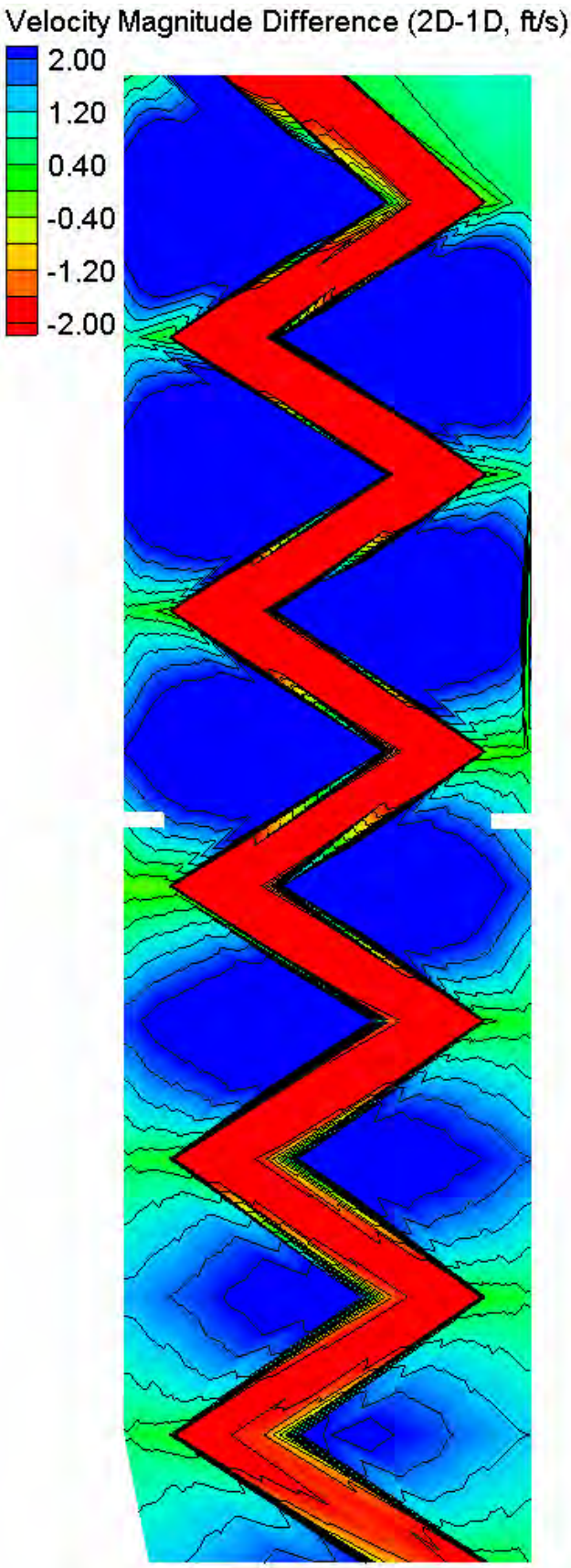

Velocity Magnitude Difference Contours – Large Channel – Meandering (2.0 sinuosity)

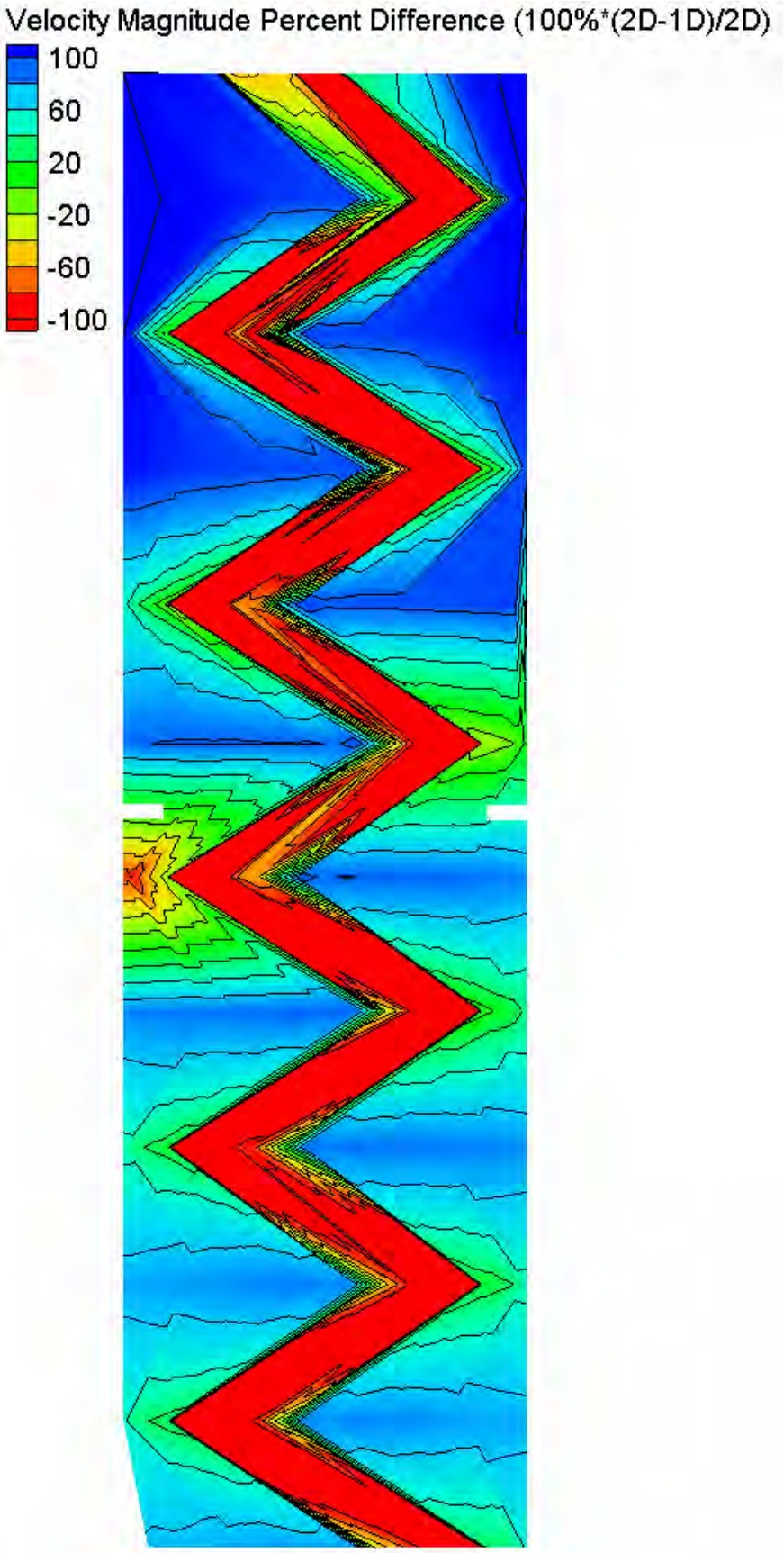

Velocity Magnitude Percent Difference Contours – Large Channel – Meandering (2.0 sinuosity)

Asymmetric Floodplains

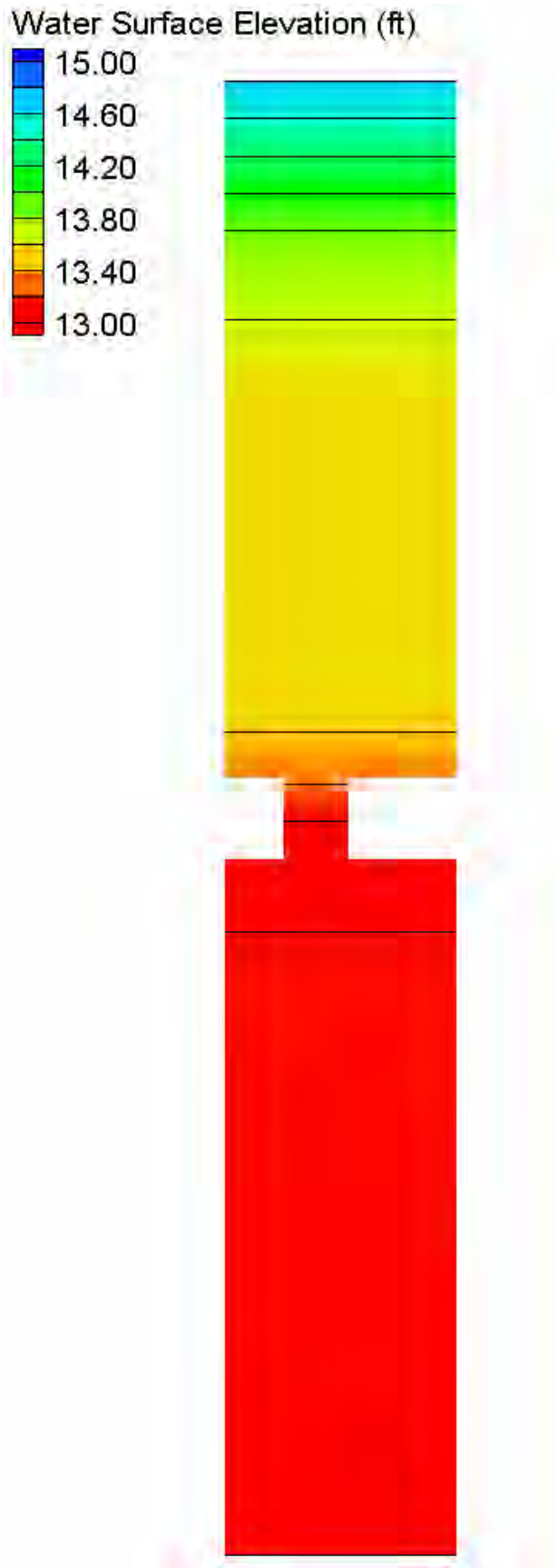

HEC-RAS Water Surface Elevation Contours – Small Channel – Asymmetric (25% reduction)

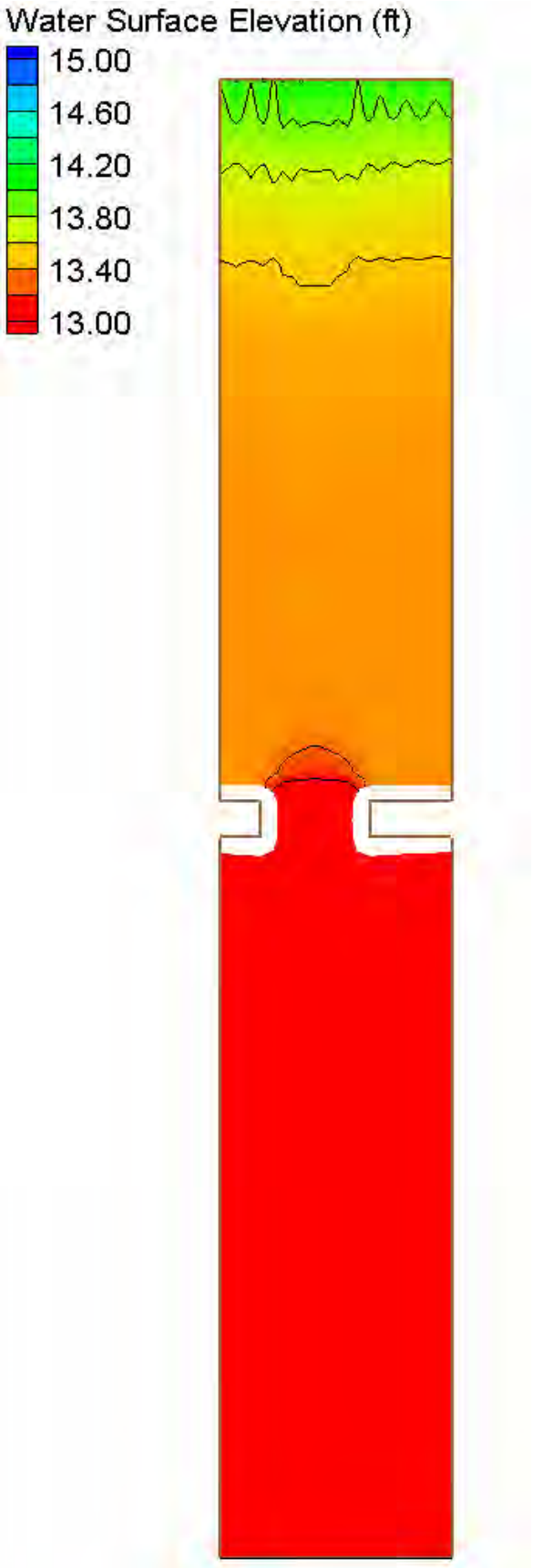

FESWMS Water Surface Elevation Contours – Small Channel – Asymmetric (25% reduction)

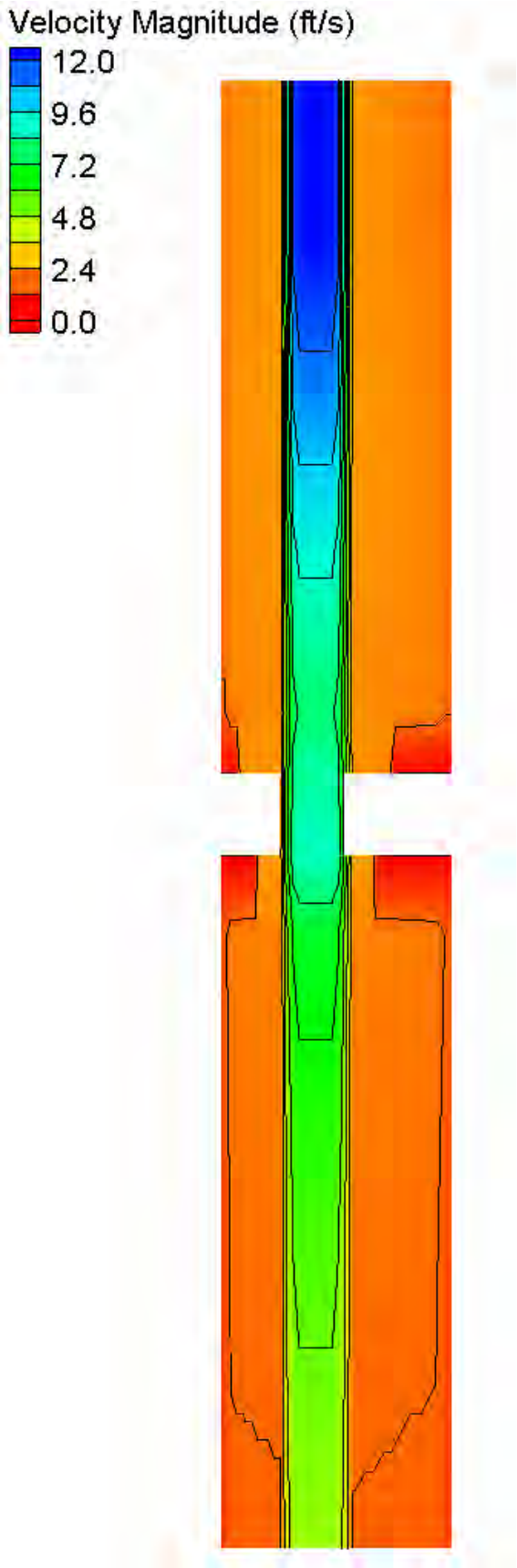

HEC-RAS Velocity Magnitude Contours – Small Channel – Asymmetric (25% reduction)

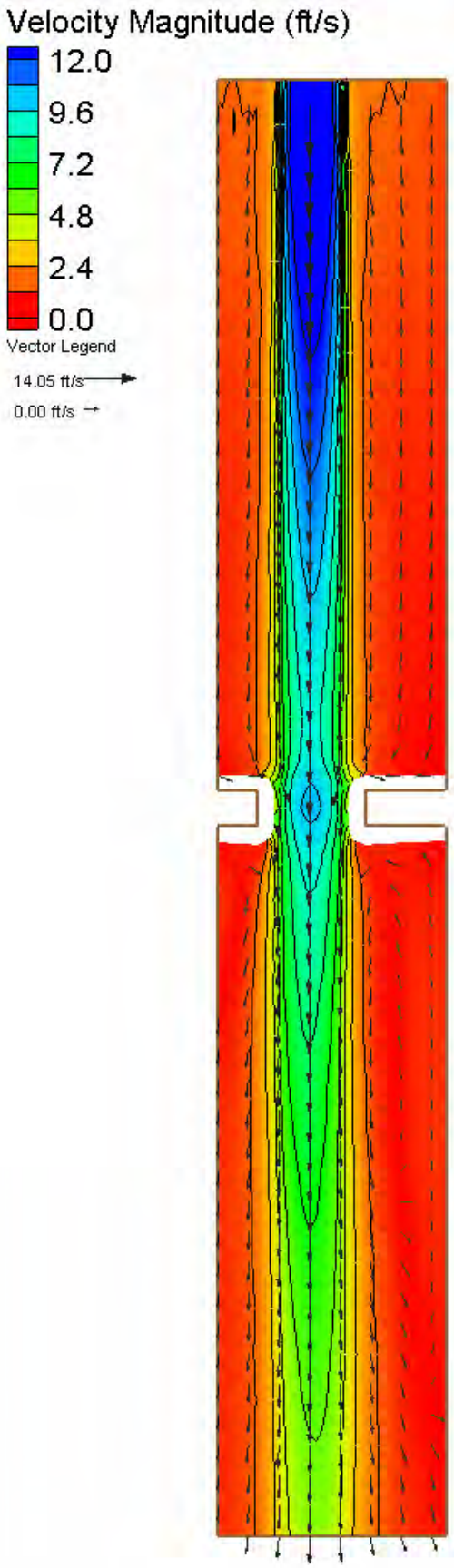

FESWMS Velocity Magnitude Contours – Small Channel – Asymmetric (25% reduction)

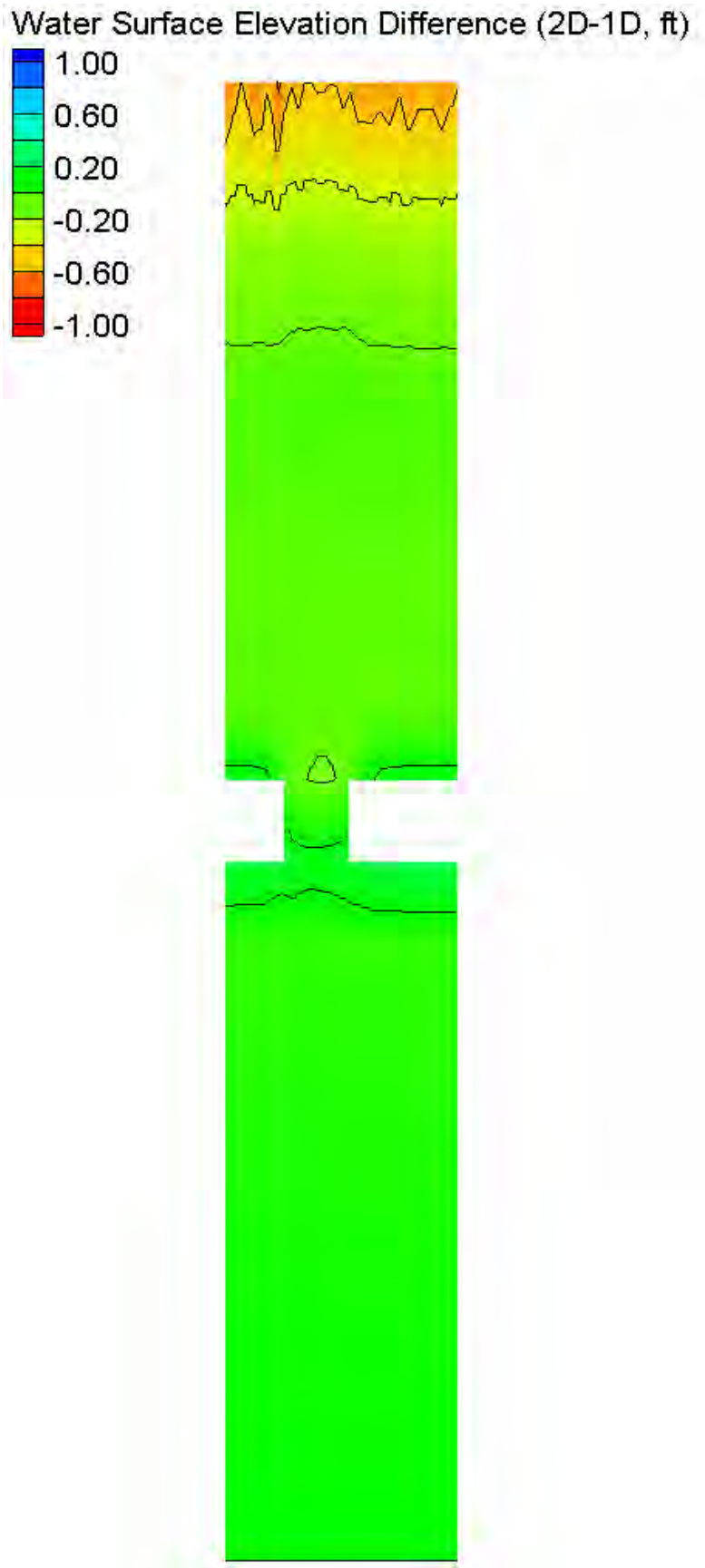

Water Surface Elevation Difference Contours – Small Channel – Asymmetric (25% reduction)

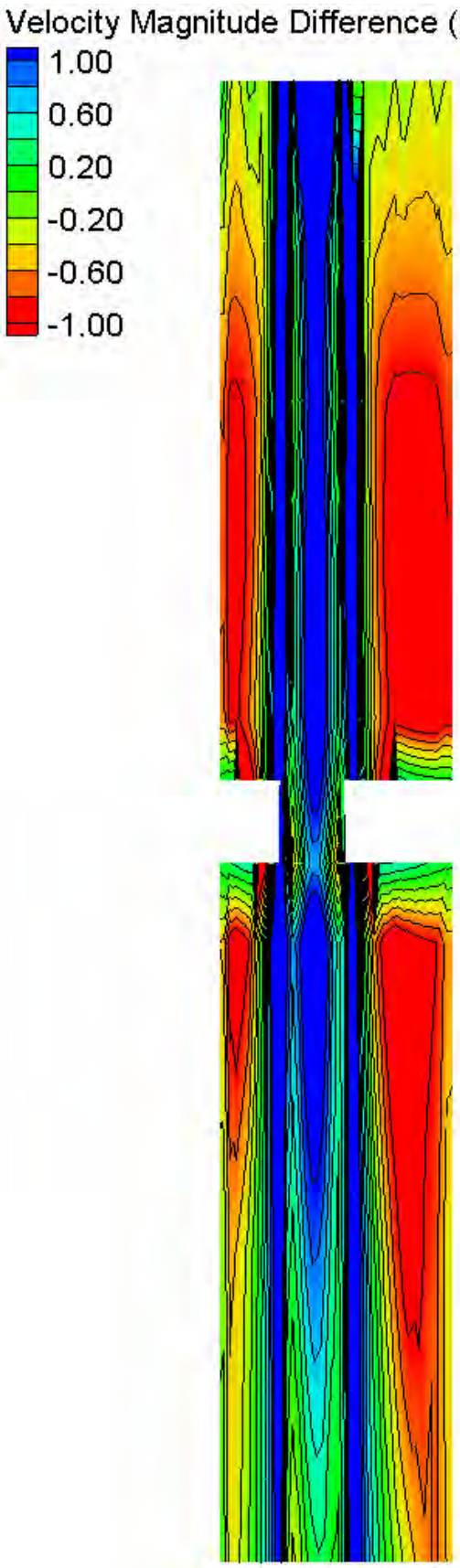

Velocity Magnitude Difference Contours – Small Channel – Asymmetric (25% reduction)

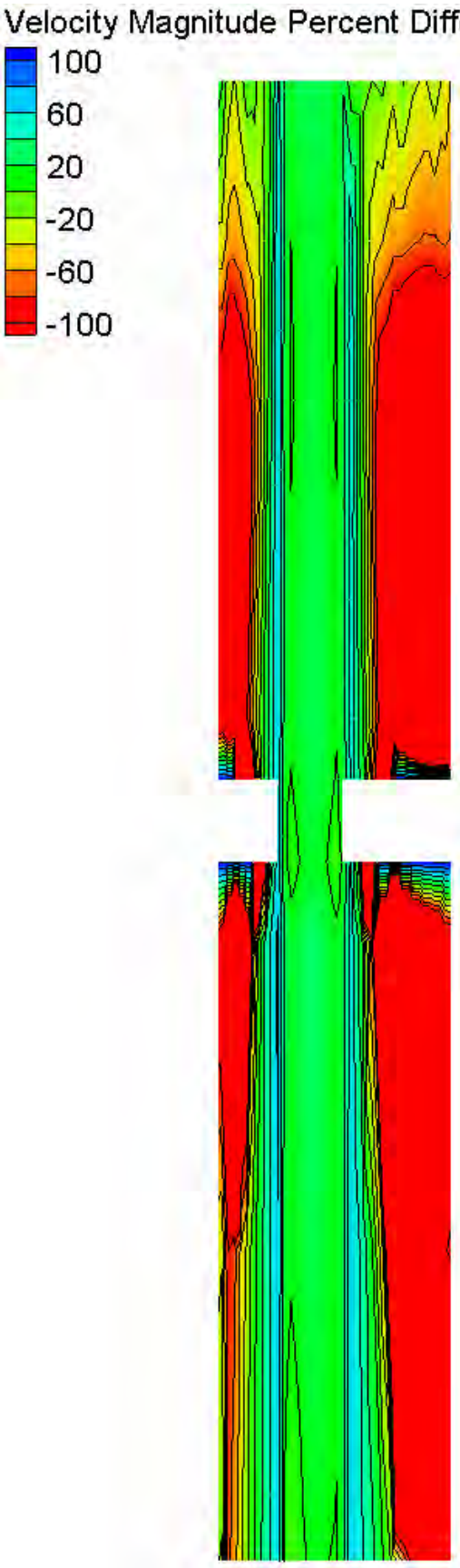

Velocity Magnitude Percent Difference Contours – Small Channel – Asymmetric (25% reduction)

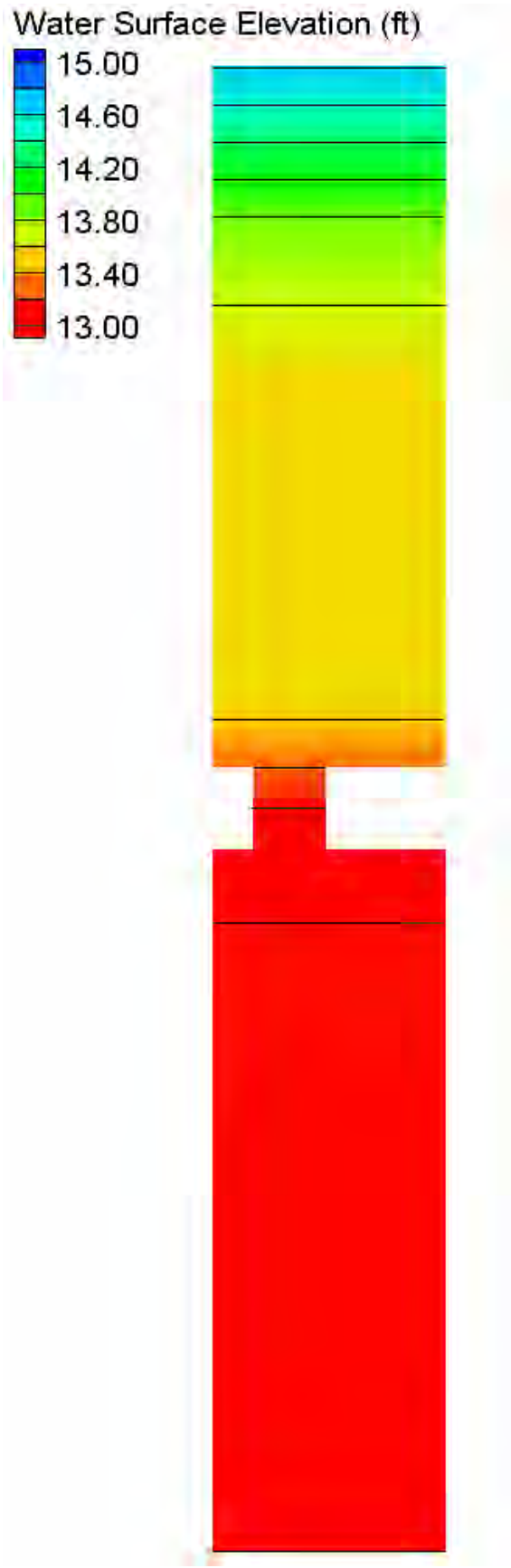

HEC-RAS Water Surface Elevation Contours – Small Channel – Asymmetric (50% reduction)

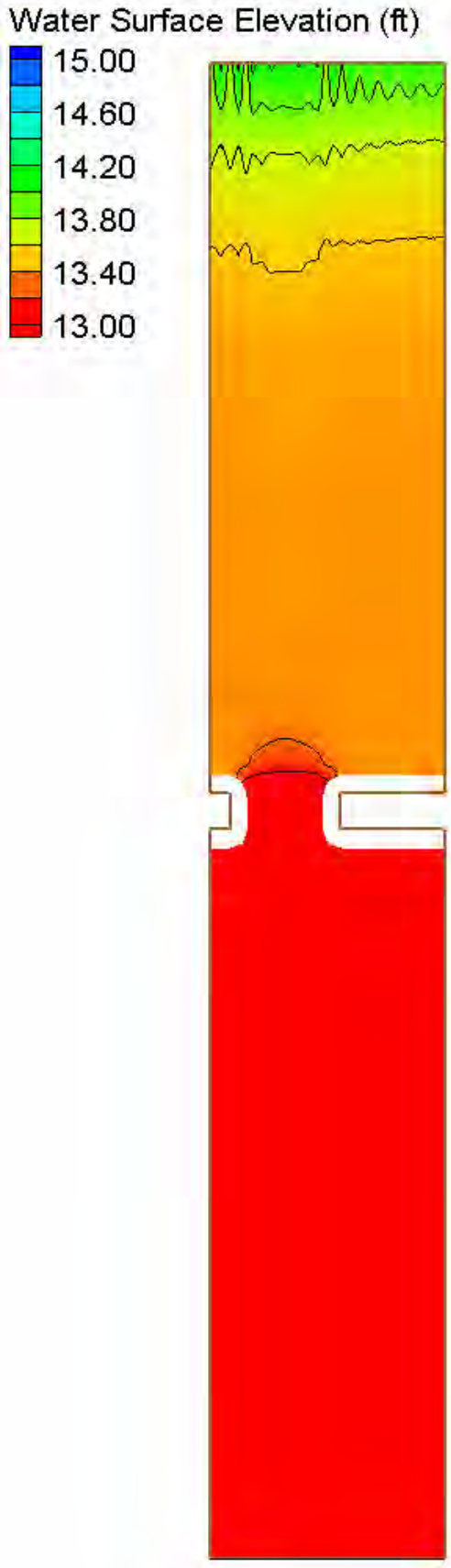

FESWMS Water Surface Elevation Contours – Small Channel – Asymmetric (50% reduction)

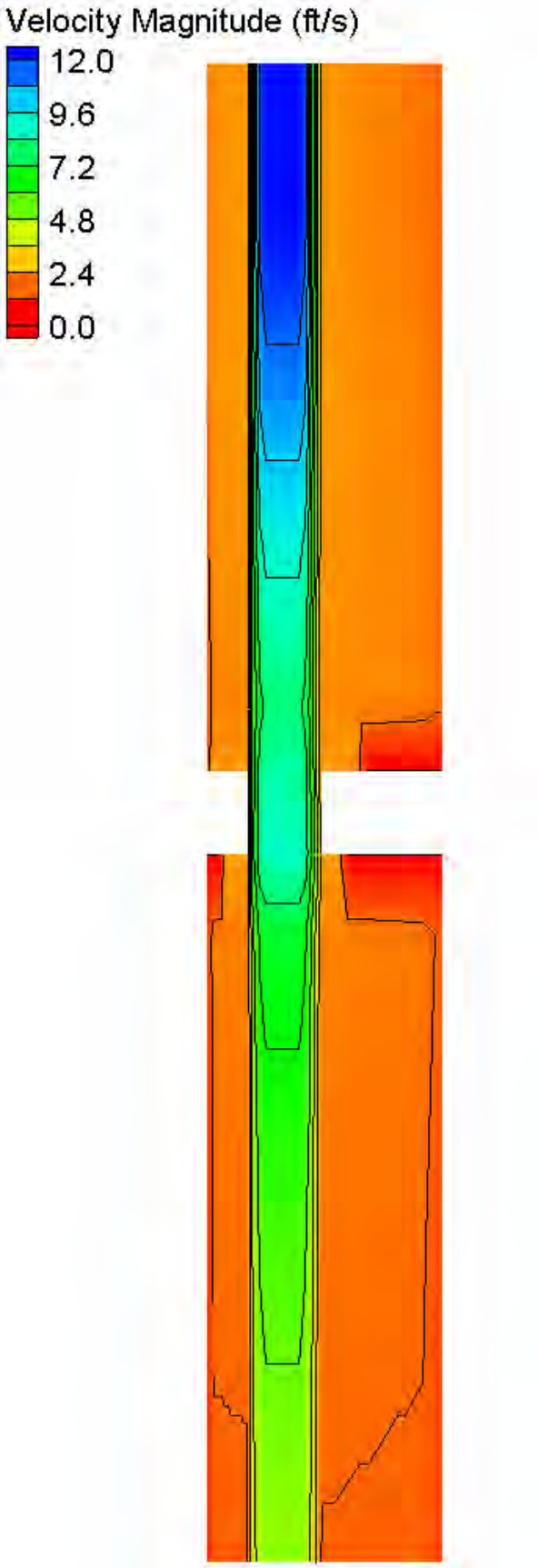

HEC-RAS Velocity Magnitude Contours – Small Channel – Asymmetric (50% reduction)

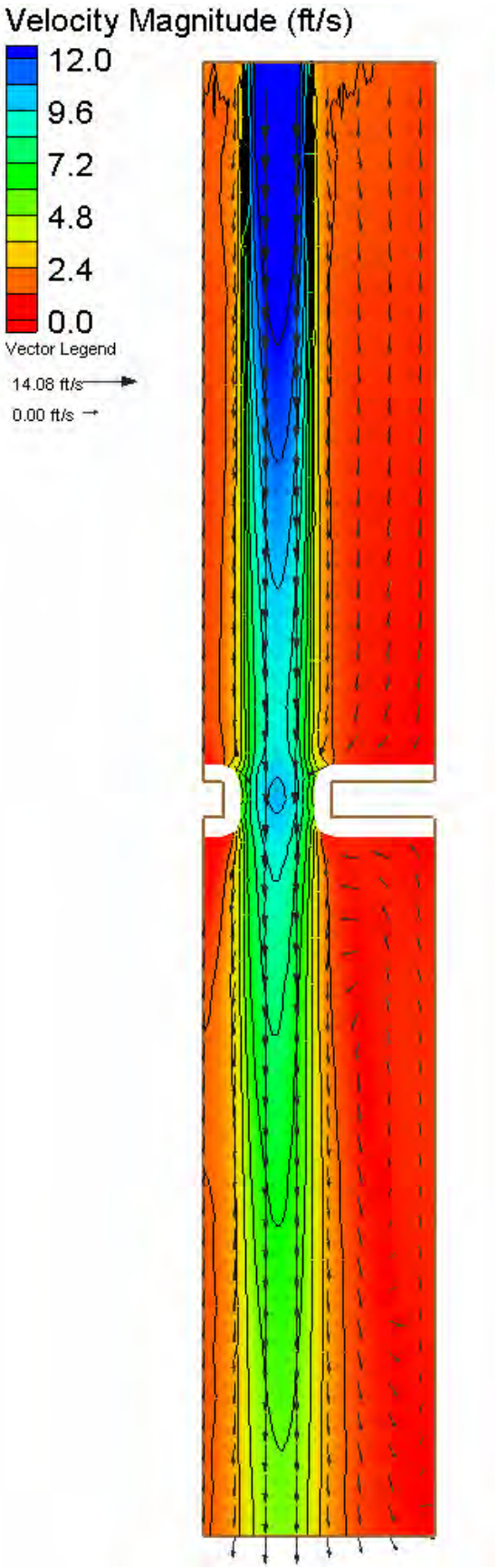

FESWMS Velocity Magnitude Contours – Small Channel – Asymmetric (50% reduction)

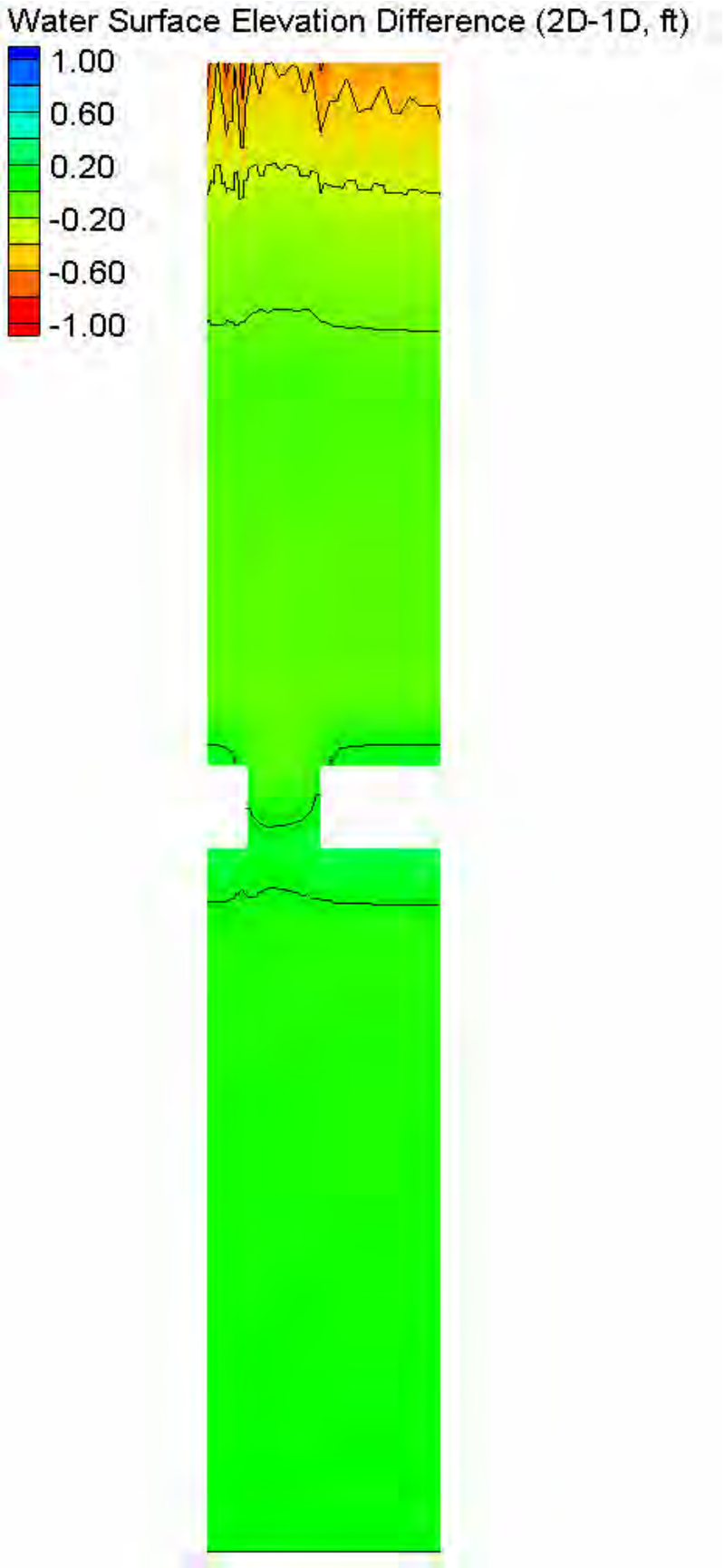

Water Surface Elevation Difference Contours – Small Channel – Asymmetric (50% reduction)

Velocity Magnitude Difference Contours – Small Channel – Asymmetric (50% reduction)

Velocity Magnitude Percent Difference Contours – Small Channel – Asymmetric (50% reduction)

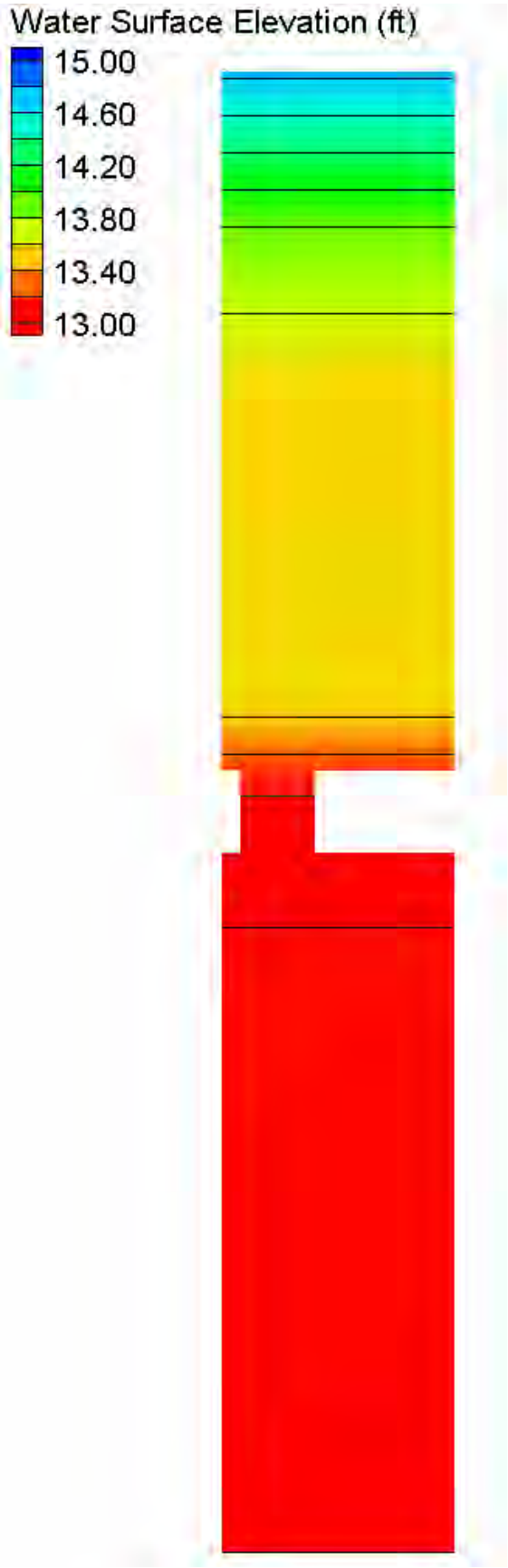

HEC-RAS Water Surface Elevation Contours – Small Channel – Asymmetric (75% reduction)

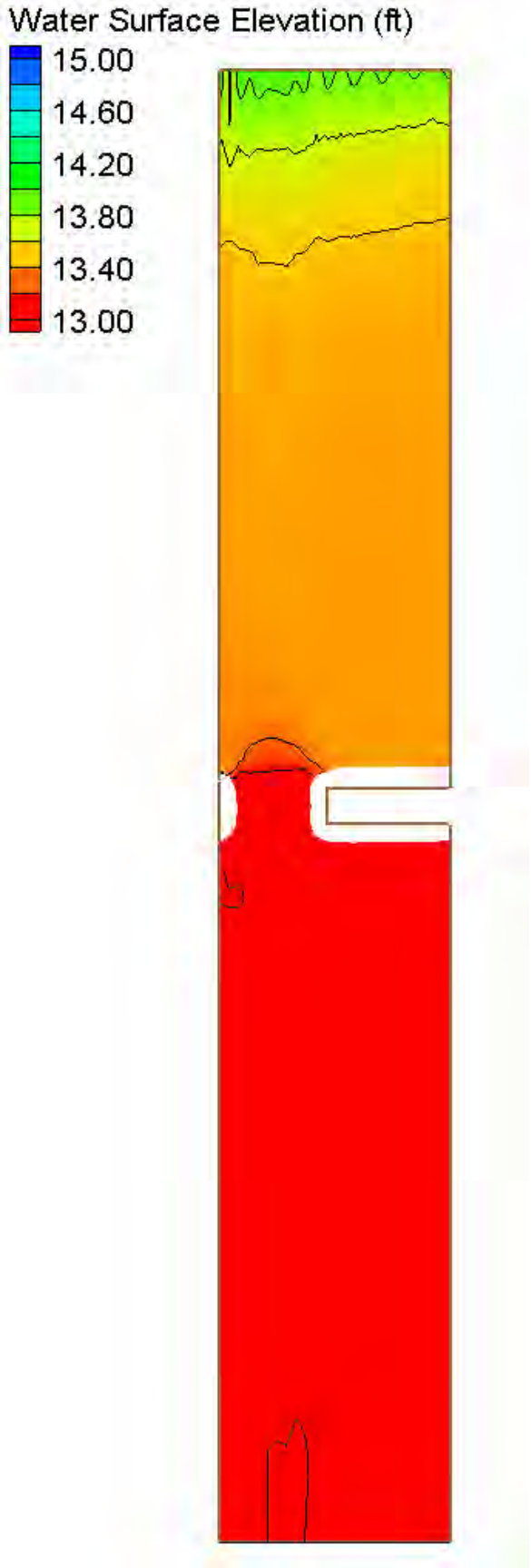

FESWMS Water Surface Elevation Contours – Small Channel – Asymmetric (75% reduction)

HEC-RAS Velocity Magnitude Contours – Small Channel – Asymmetric (75% reduction)

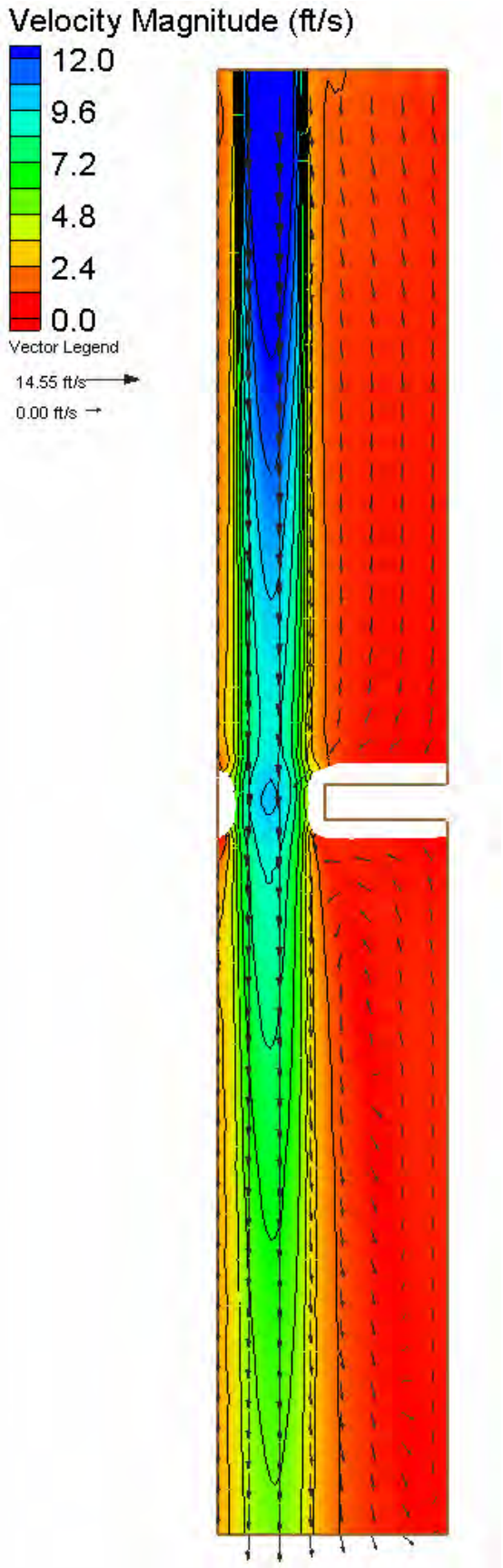

FESWMS Velocity Magnitude Contours – Small Channel – Asymmetric (75% reduction)

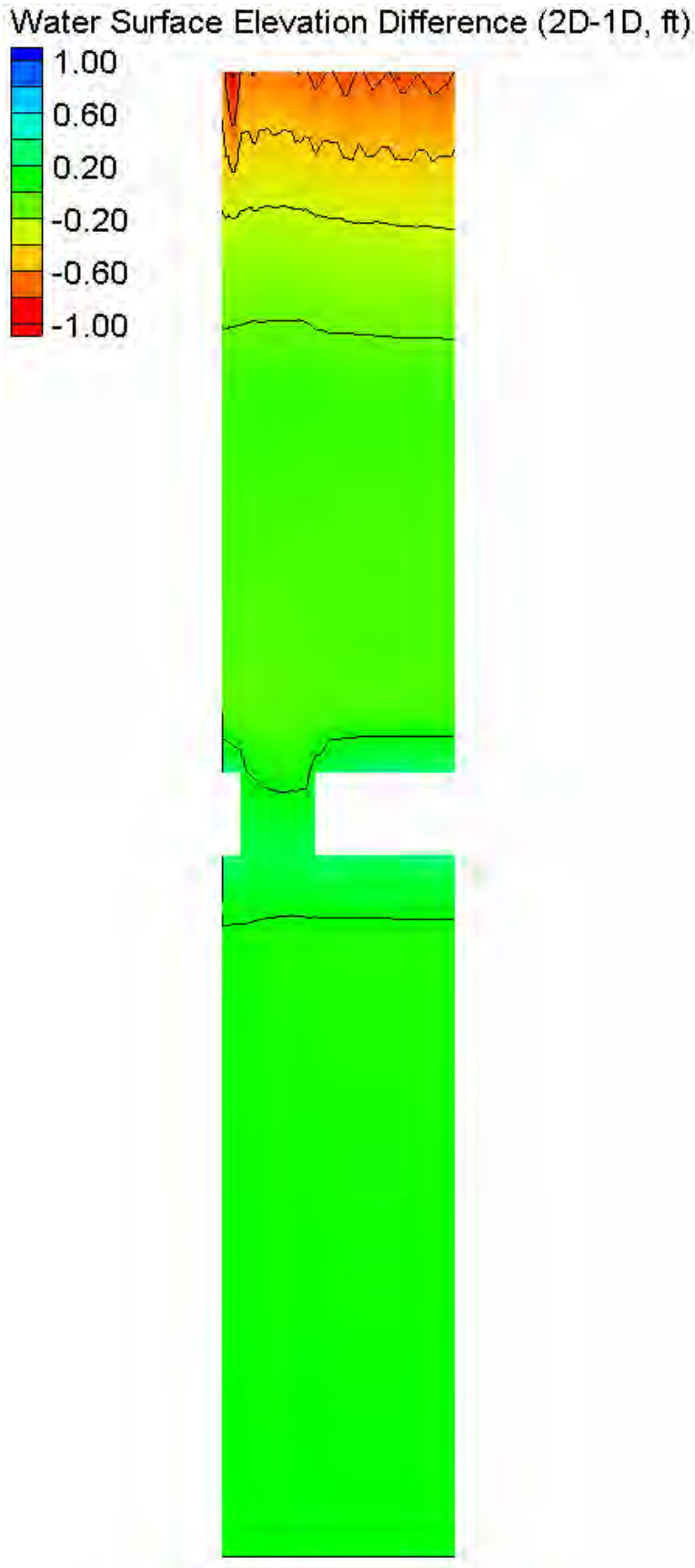

Water Surface Elevation Difference Contours – Small Channel – Asymmetric (75% reduction)

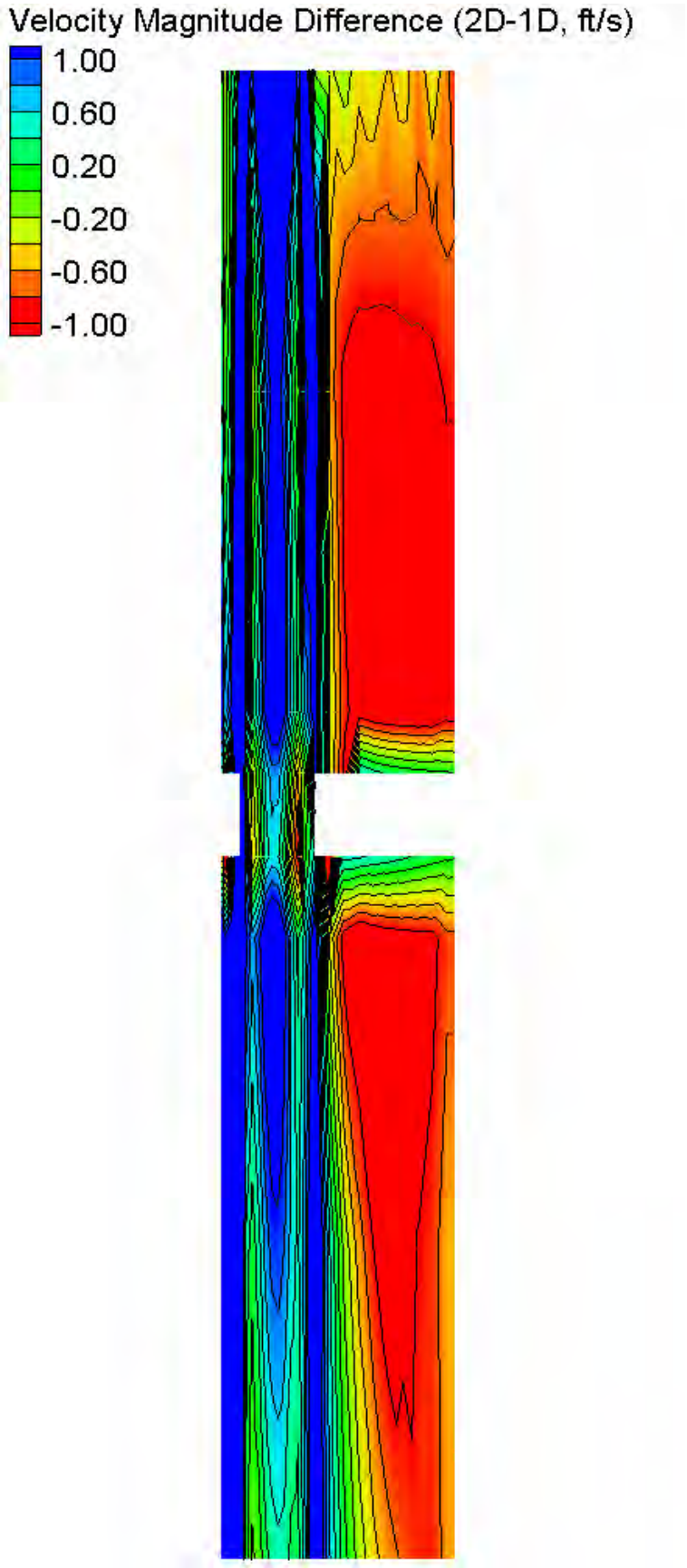

Velocity Magnitude Difference Contours – Small Channel – Asymmetric (75% reduction)

Velocity Magnitude Percent Difference Contours – Small Channel – Asymmetric (75% reduction)

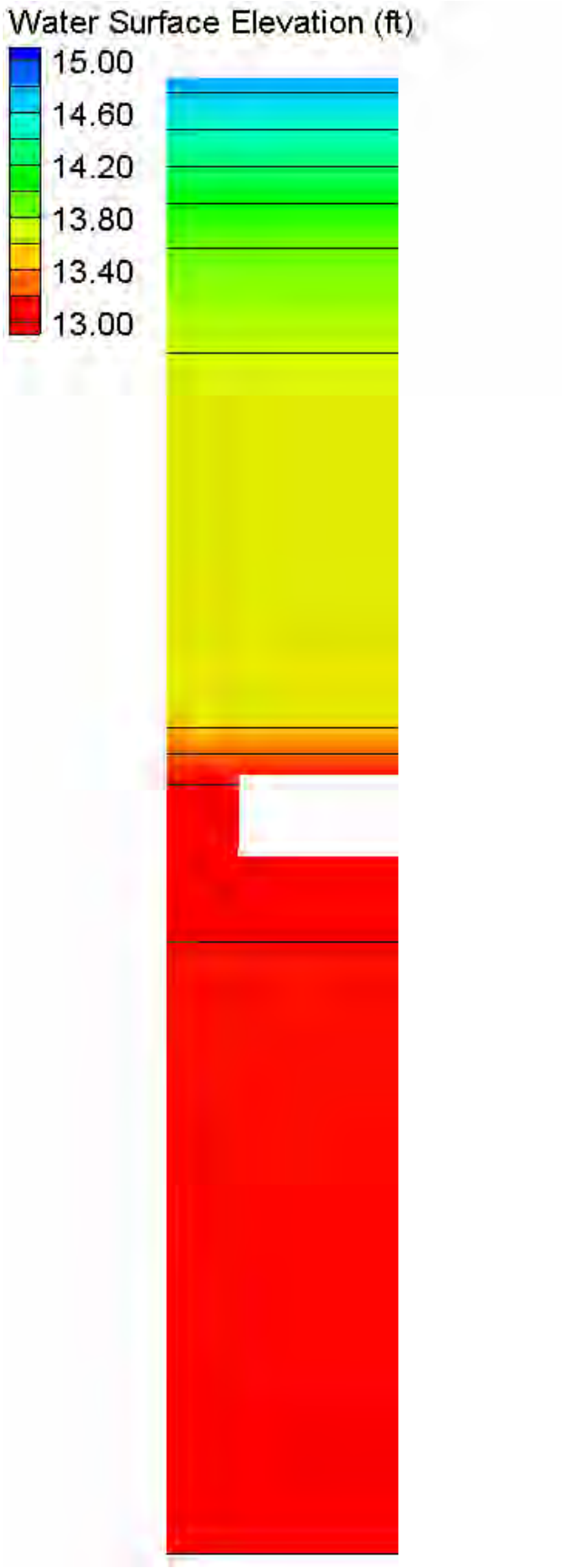

HEC-RAS Water Surface Elevation Contours – Small Channel – Asymmetric (100% reduction)

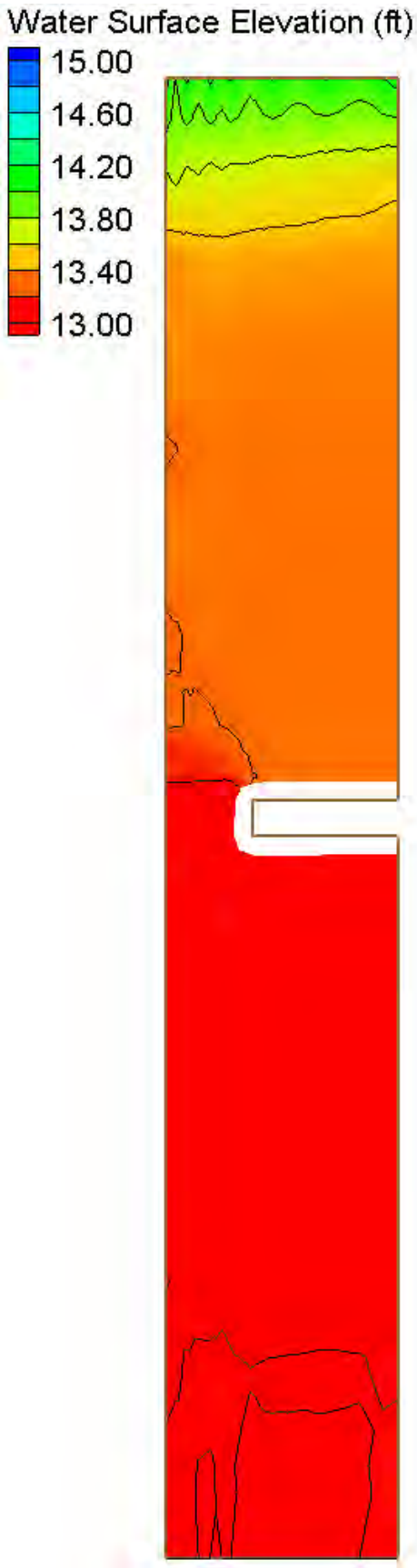

FESWMS Water Surface Elevation Contours – Small Channel – Asymmetric (100% reduction)

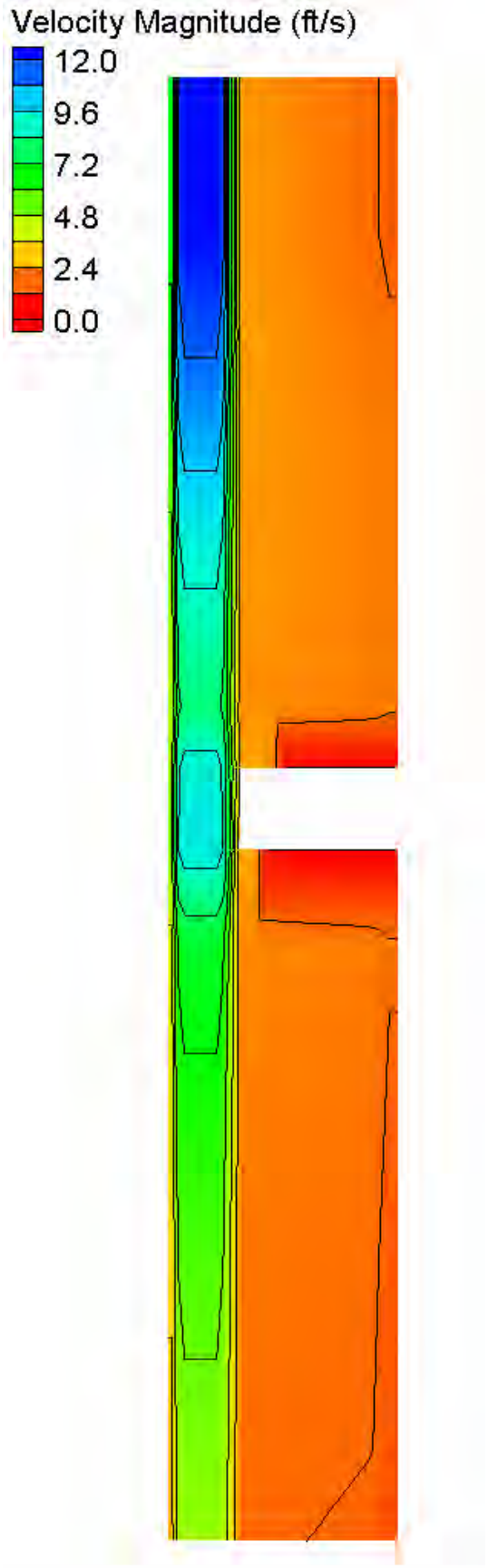

HEC-RAS Velocity Magnitude Contours – Small Channel – Asymmetric (100% reduction)

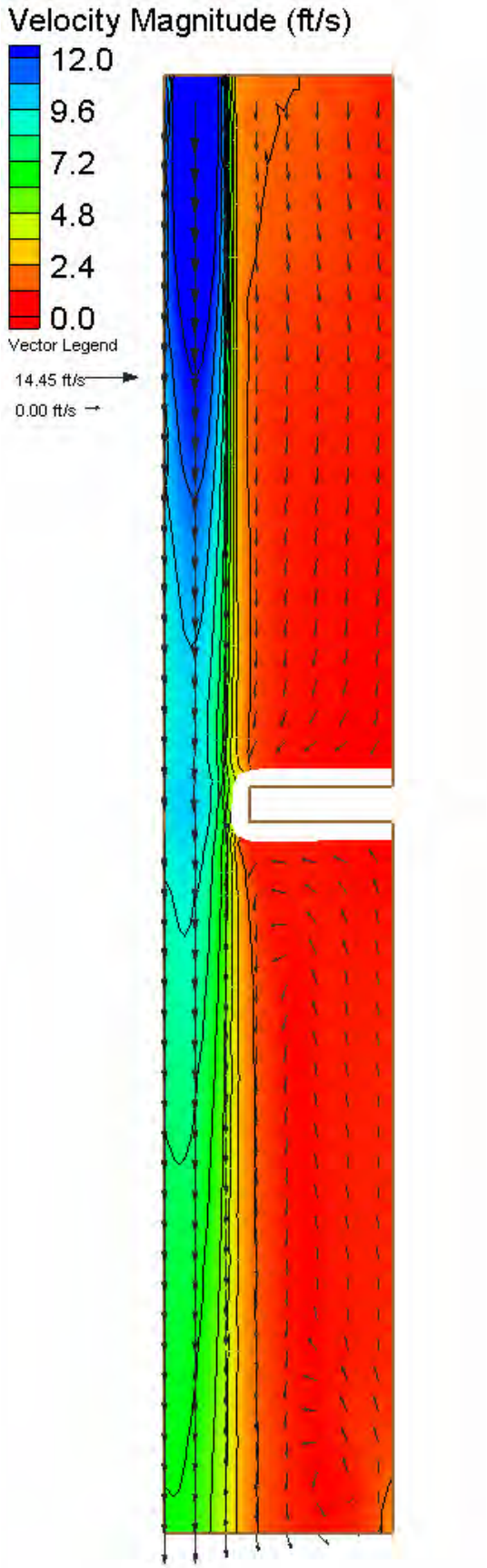

FESWMS Velocity Magnitude Contours – Small Channel – Asymmetric (100% reduction)

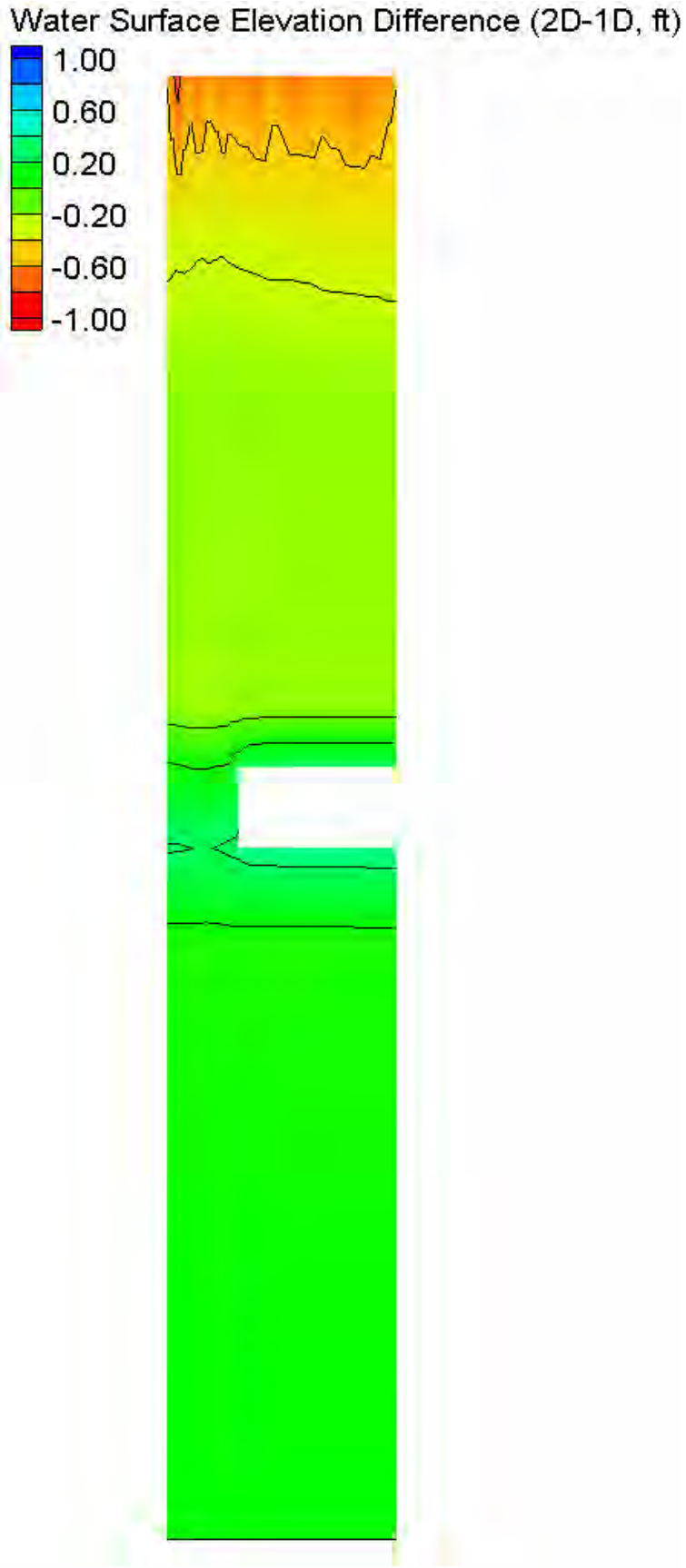

Water Surface Elevation Difference Contours – Small Channel – Asymmetric (100% reduction)

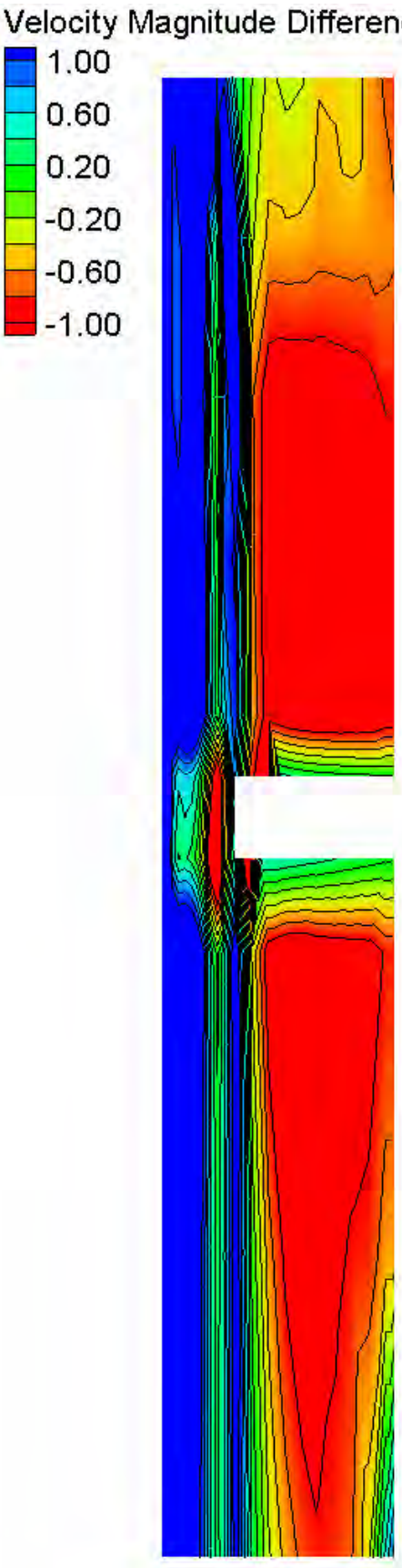

Velocity Magnitude Difference Contours – Small Channel – Asymmetric (100% reduction)

Velocity Magnitude Percent Difference Contours – Small Channel – Asymmetric (100% reduction)

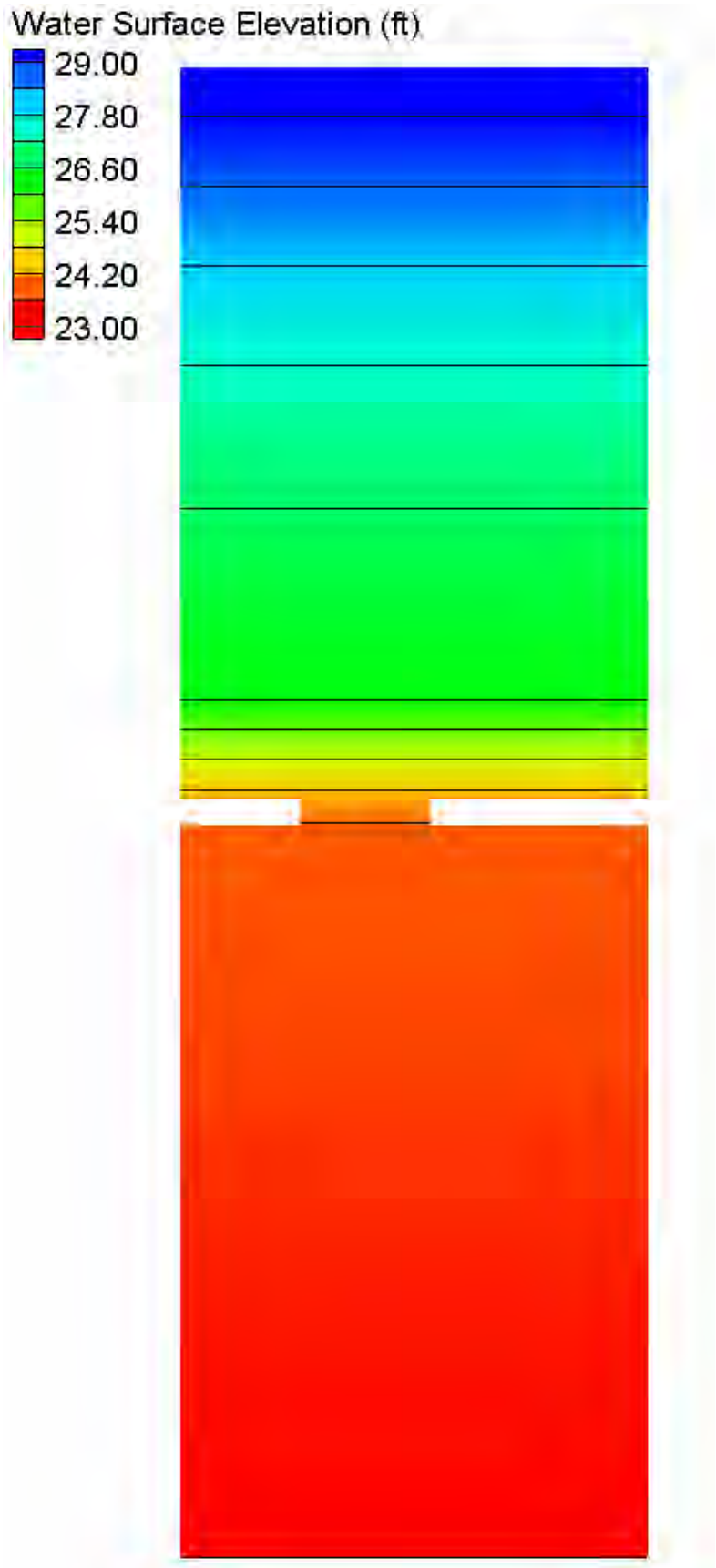

HEC-RAS Water Surface Elevation Contours – Large Channel – Asymmetric (25% reduction)

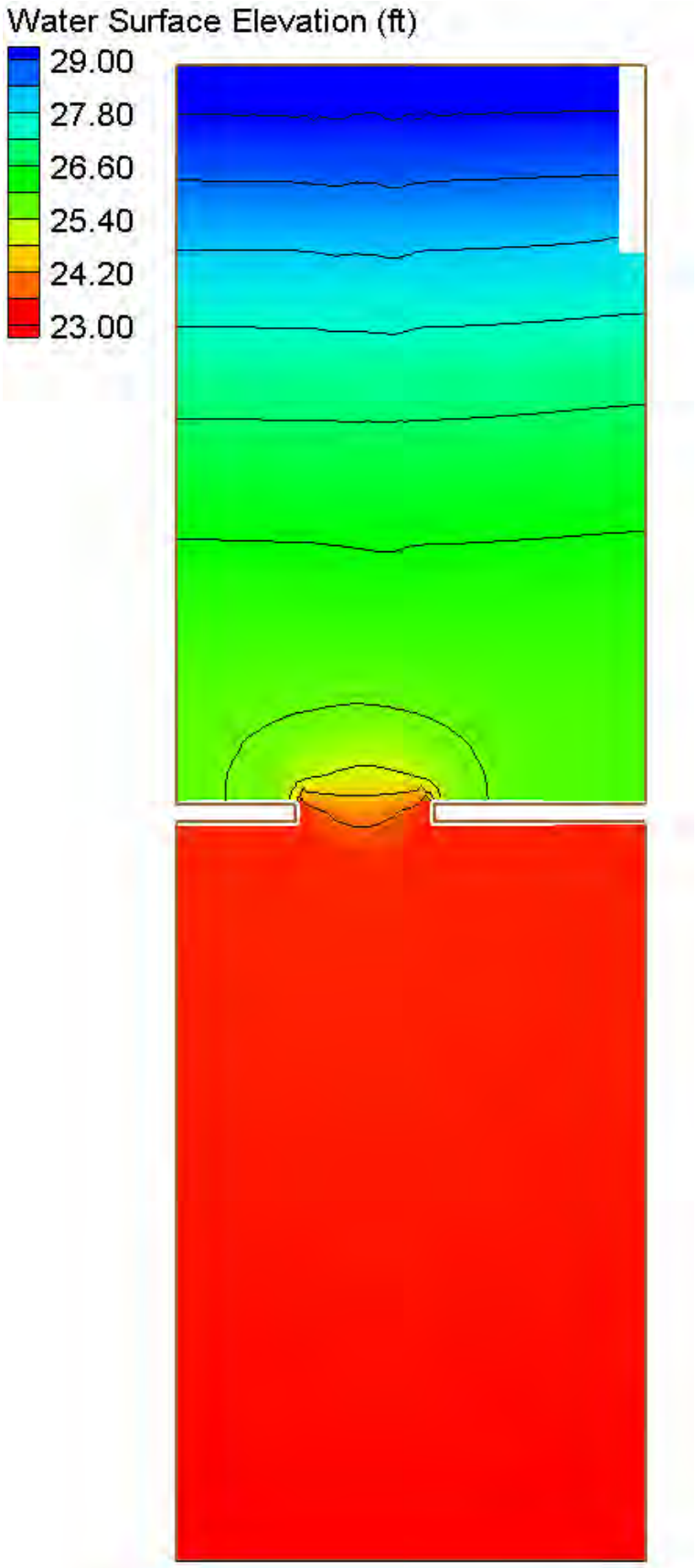

FESWMS Water Surface Elevation Contours – Large Channel – Asymmetric (25% reduction)

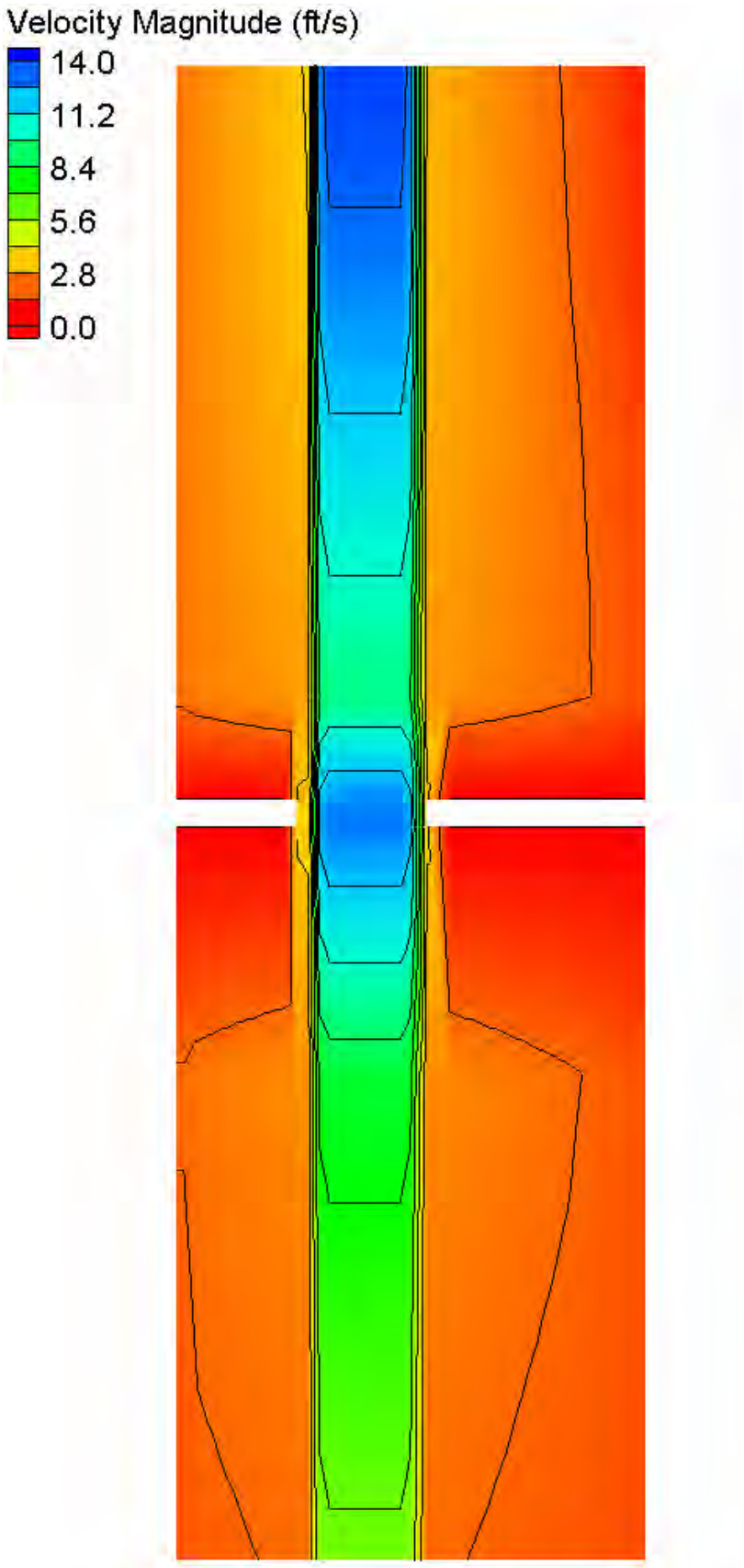

HEC-RAS Velocity Magnitude Contours – Large Channel – Asymmetric (25% reduction)

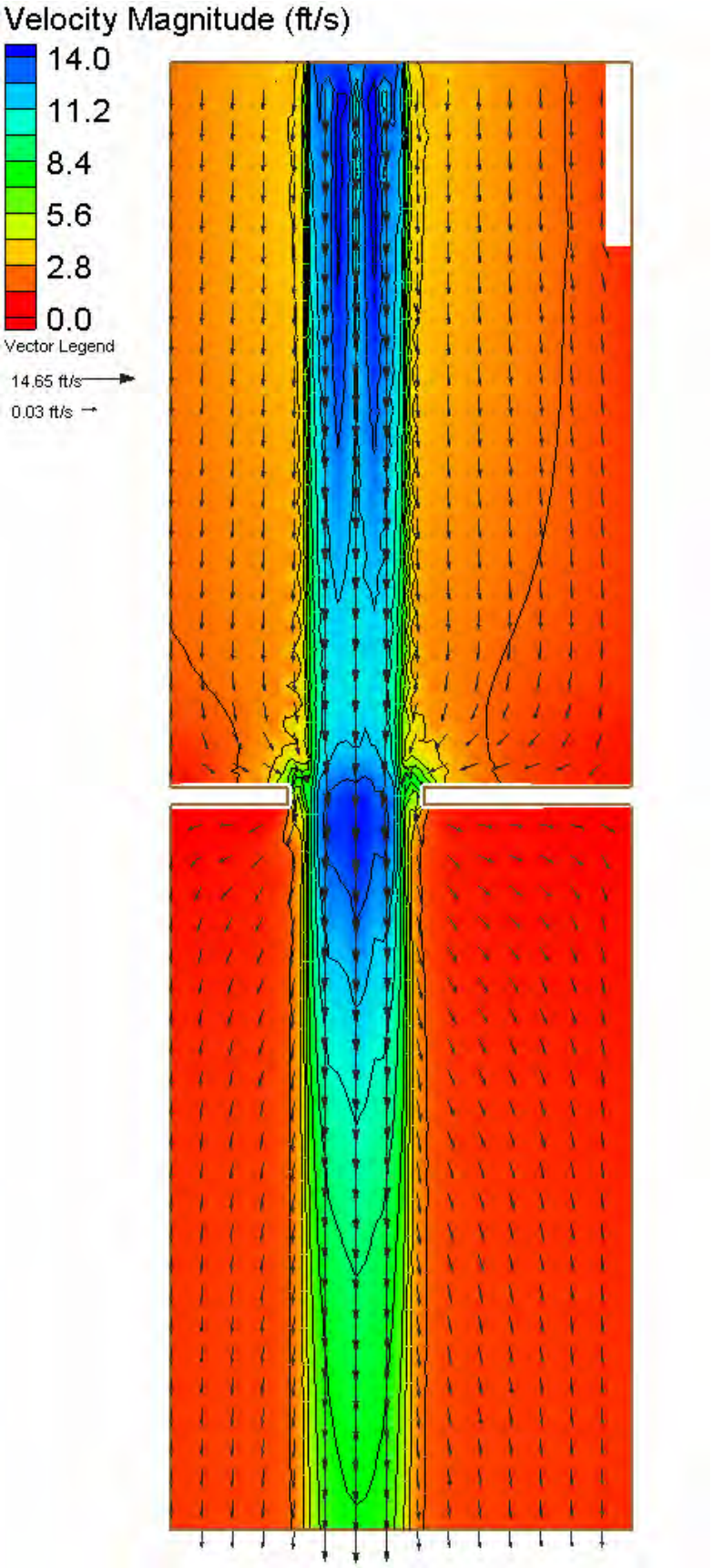

FESWMS Velocity Magnitude Contours – Large Channel – Asymmetric (25% reduction)

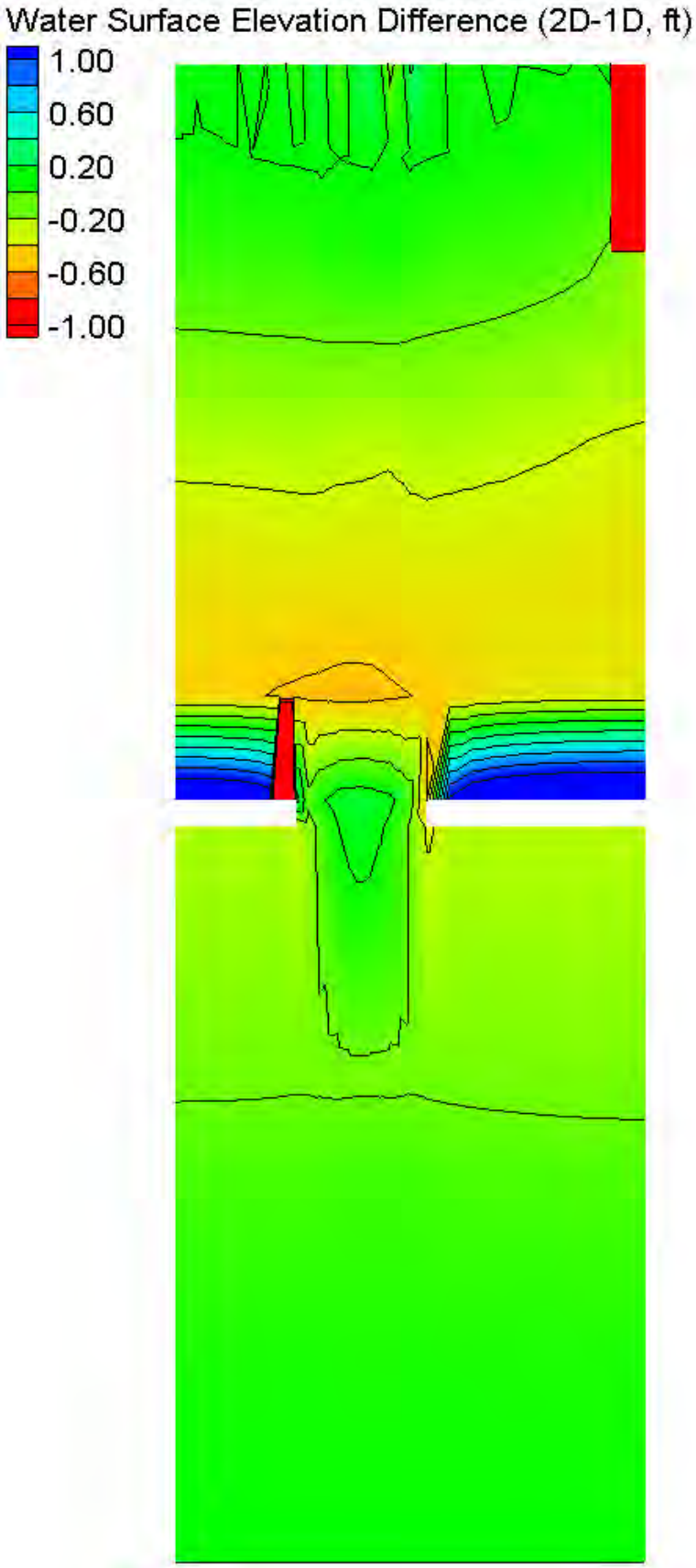

Water Surface Elevation Difference Contours – Large Channel – Asymmetric (25% reduction)

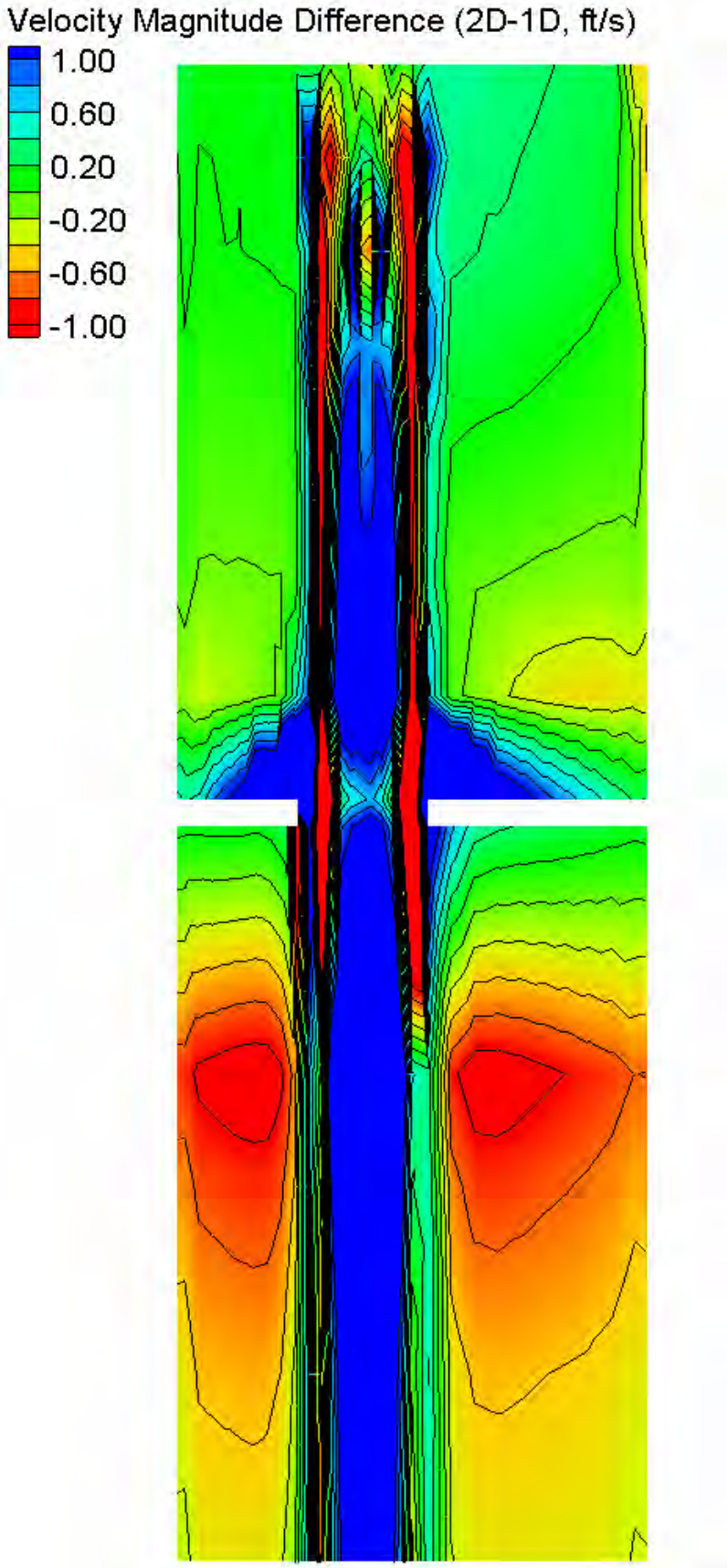

Velocity Magnitude Difference Contours – Large Channel – Asymmetric (25% reduction)

Velocity Magnitude Percent Difference Contours – Large Channel – Asymmetric (25% reduction)

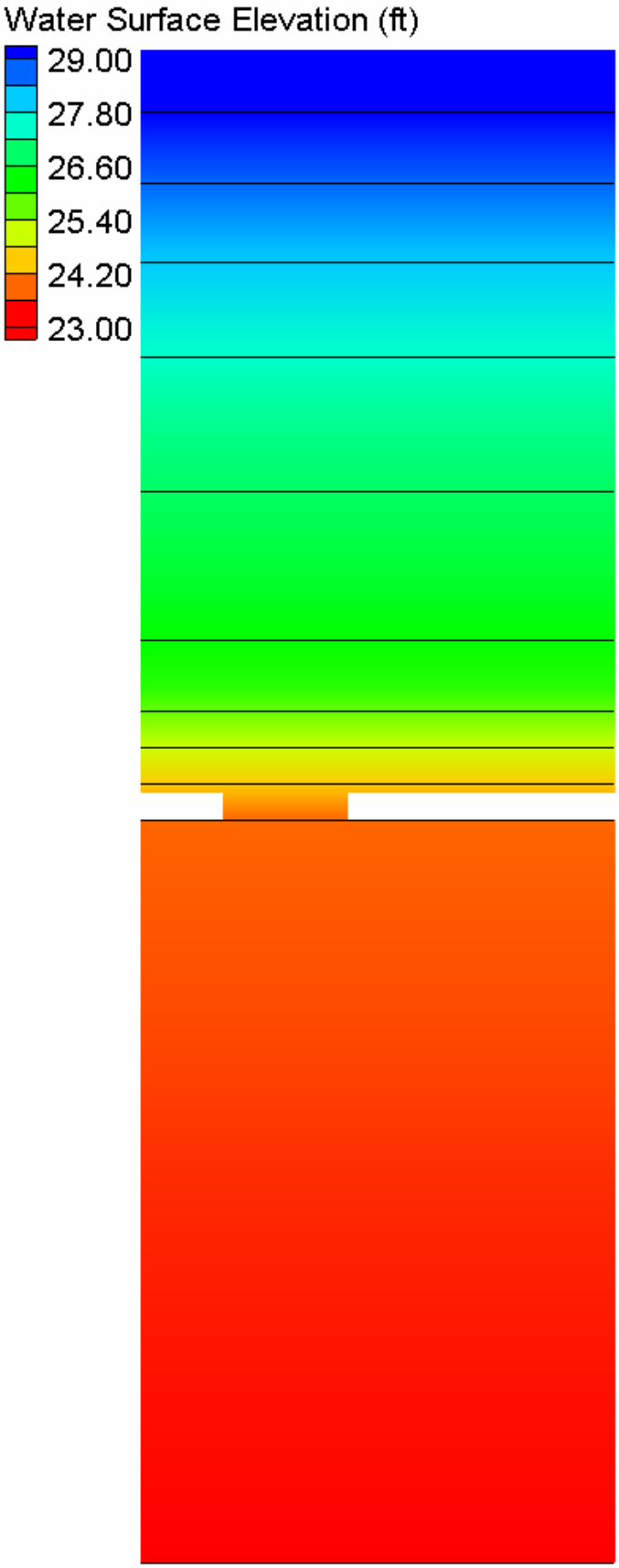

HEC-RAS Water Surface Elevation Contours – Large Channel – Asymmetric (50% reduction)

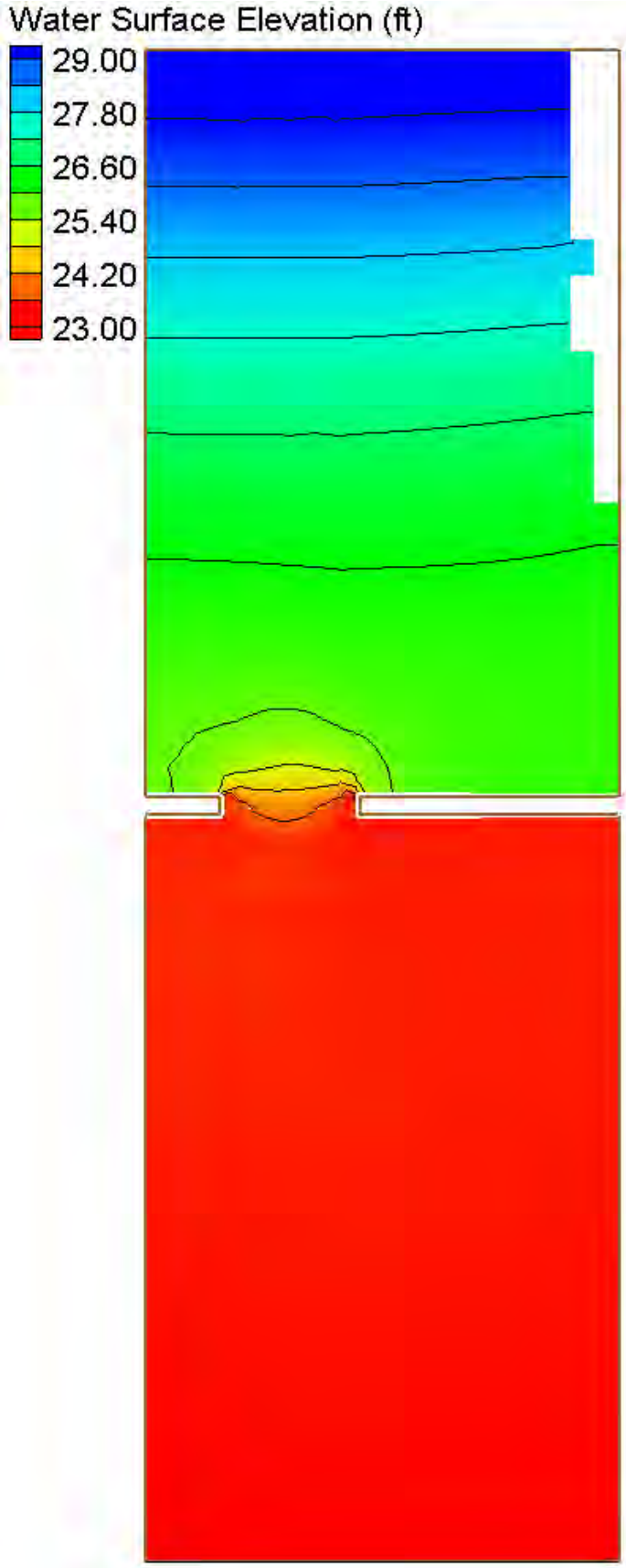

FESWMS Water Surface Elevation Contours – Large Channel – Asymmetric (50% reduction)

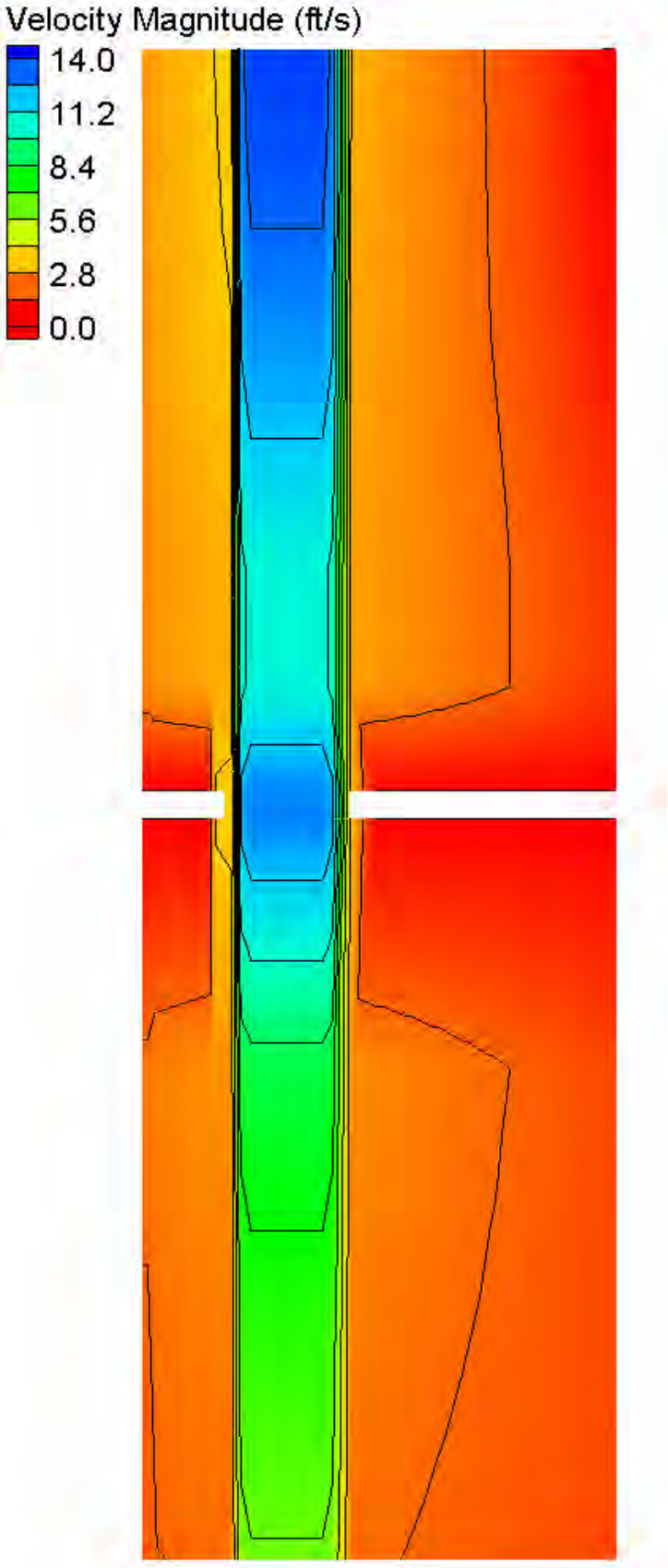

HEC-RAS Velocity Magnitude Contours – Large Channel – Asymmetric (50% reduction)

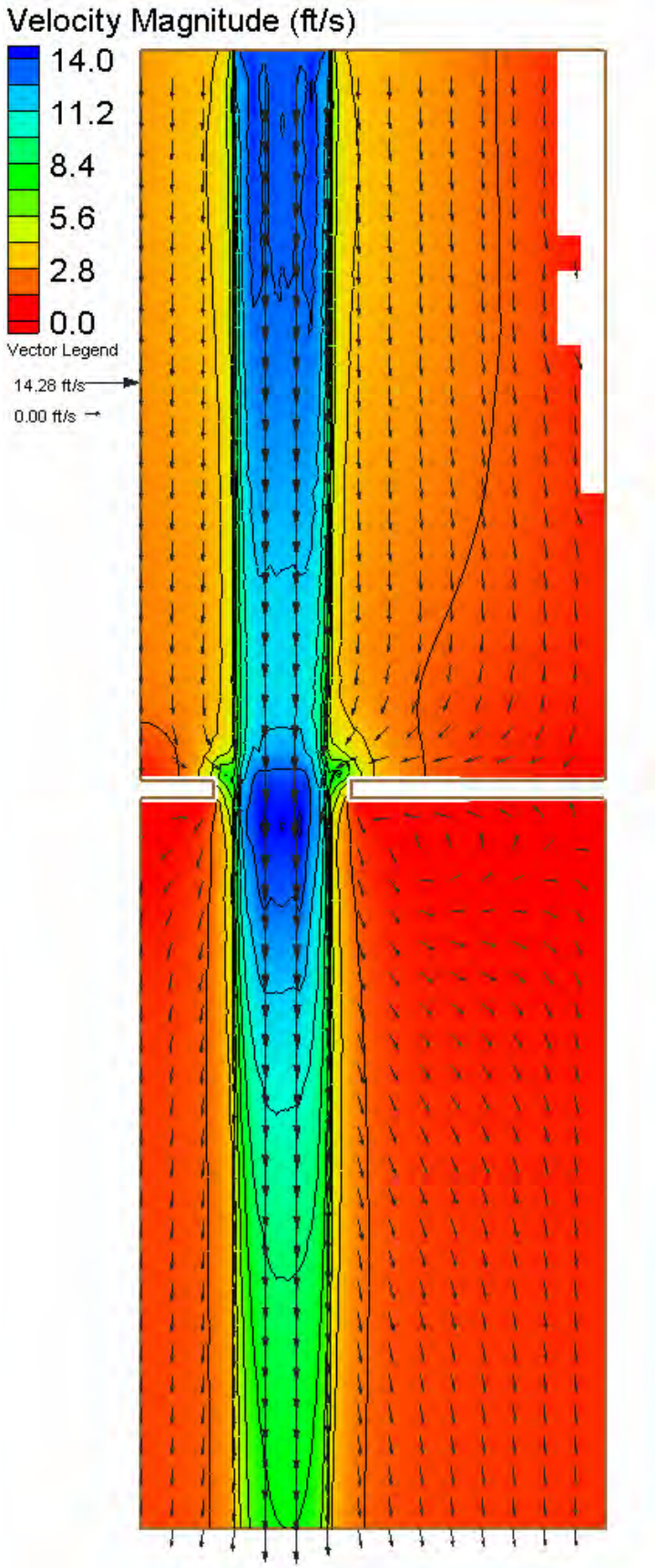

FESWMS Velocity Magnitude Contours – Large Channel – Asymmetric (50% reduction)

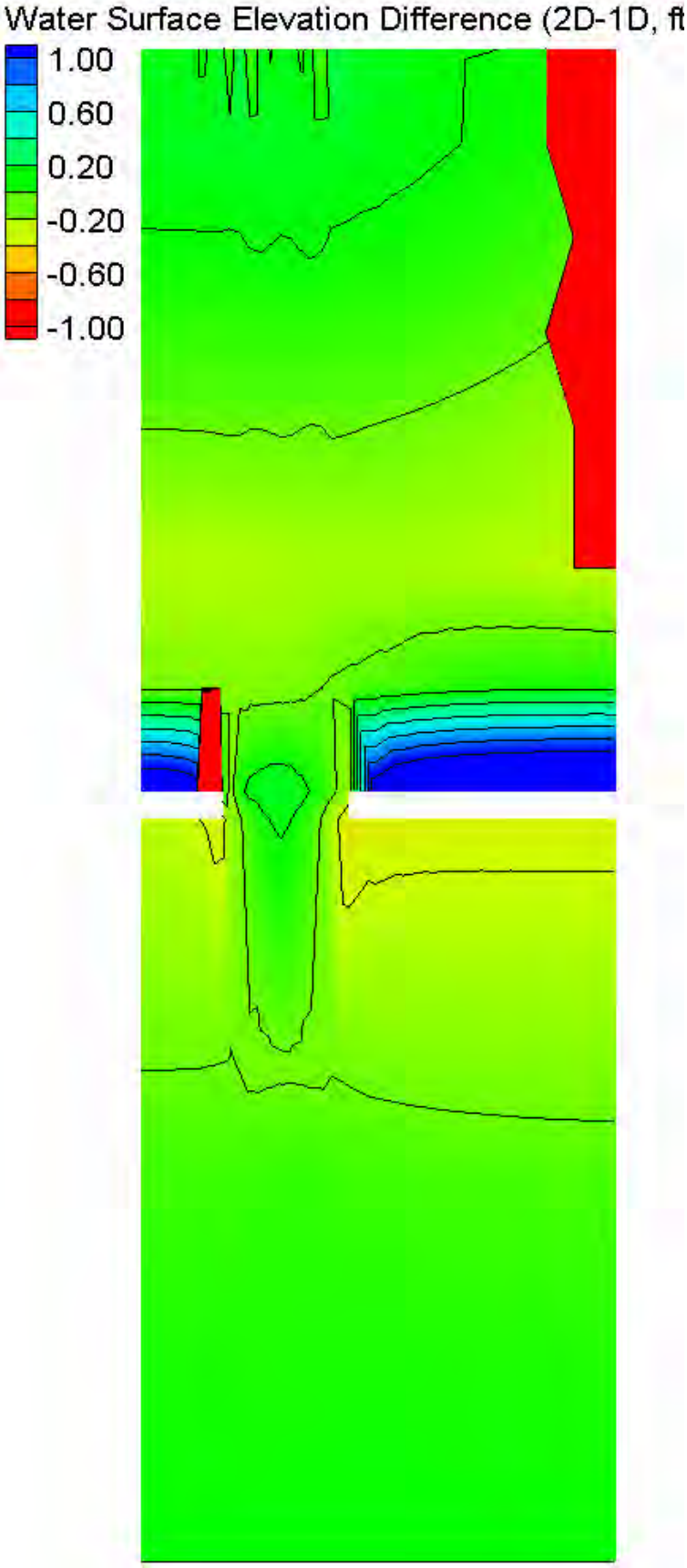

Water Surface Elevation Difference Contours – Large Channel – Asymmetric (50% reduction)

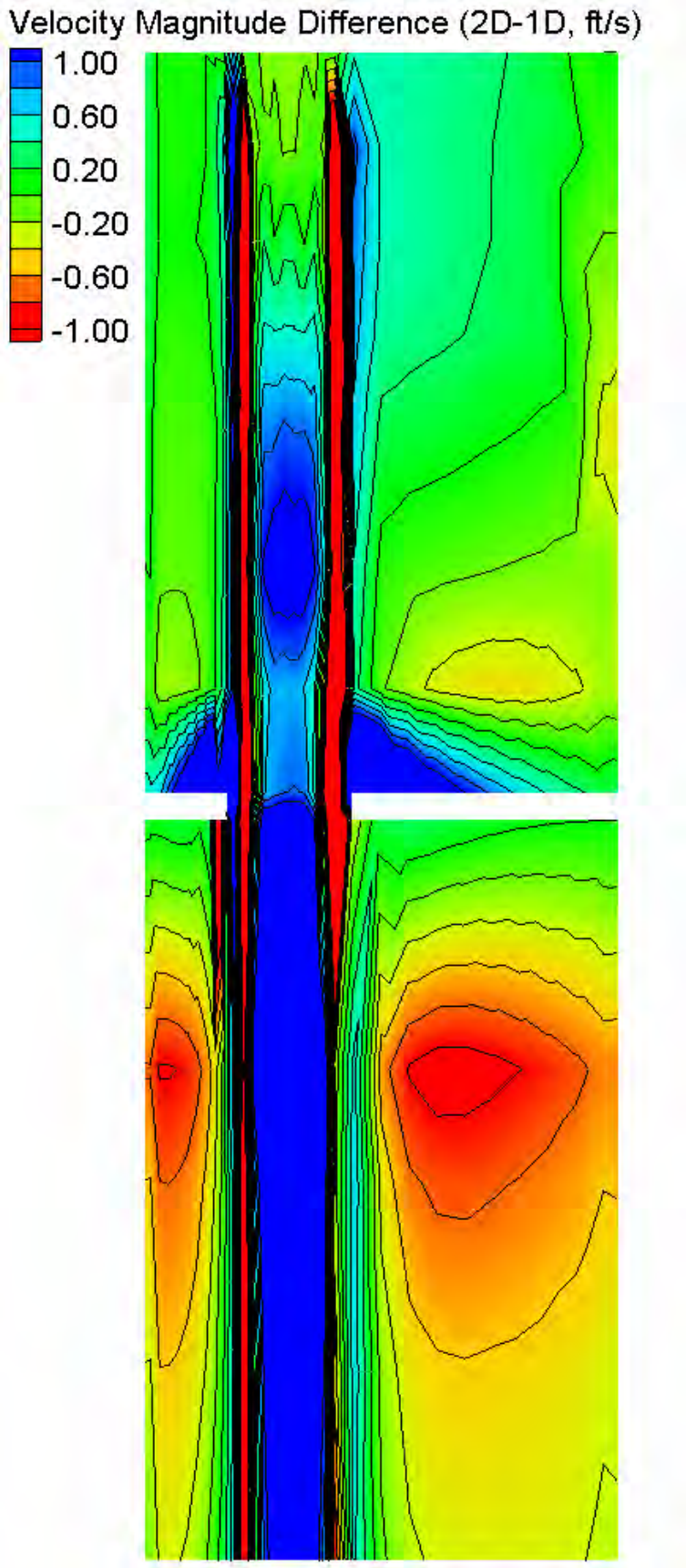

Velocity Magnitude Difference Contours – Large Channel – Asymmetric (50% reduction)

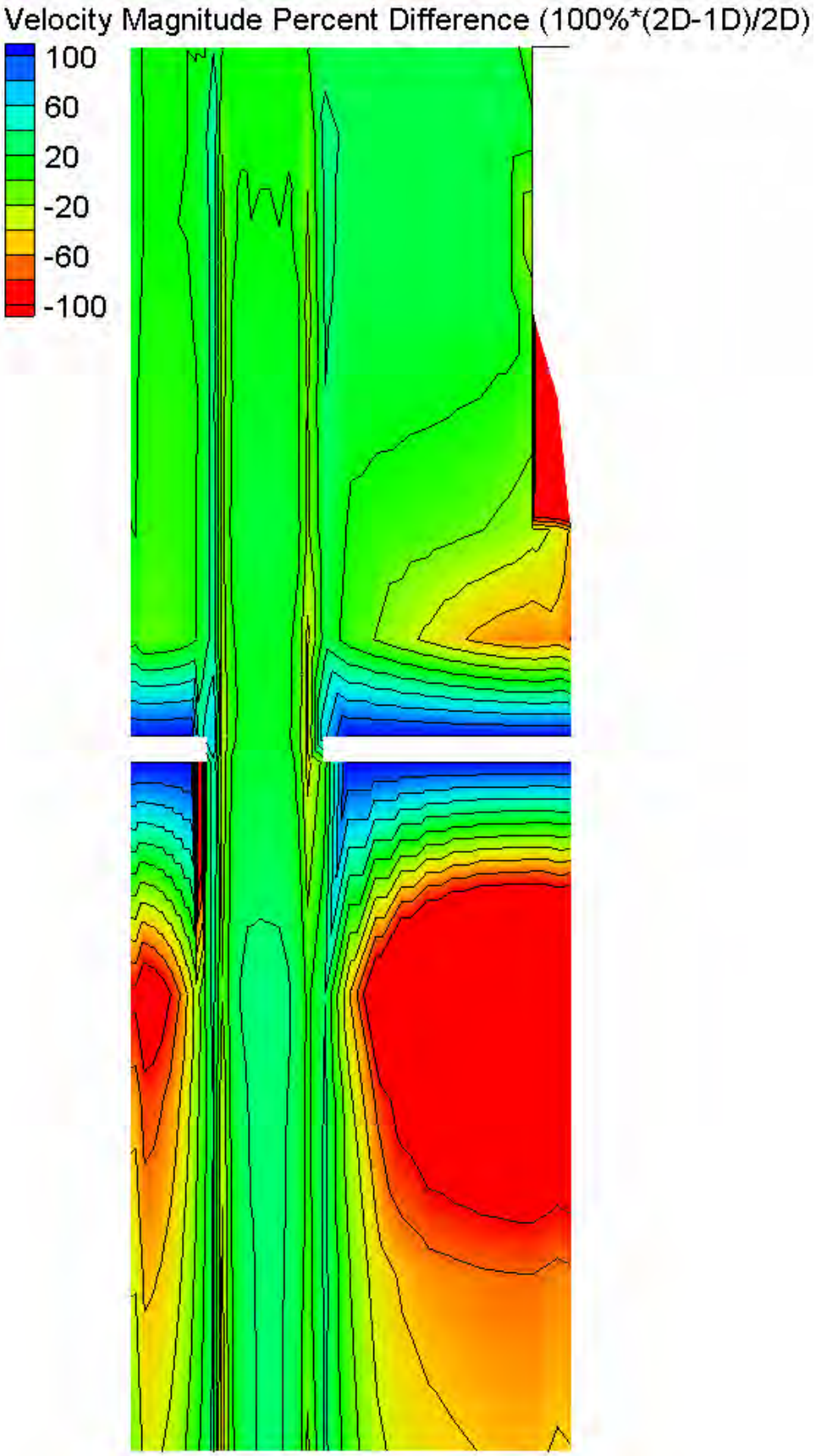

Velocity Magnitude Percent Difference Contours – Large Channel – Asymmetric (50% reduction)

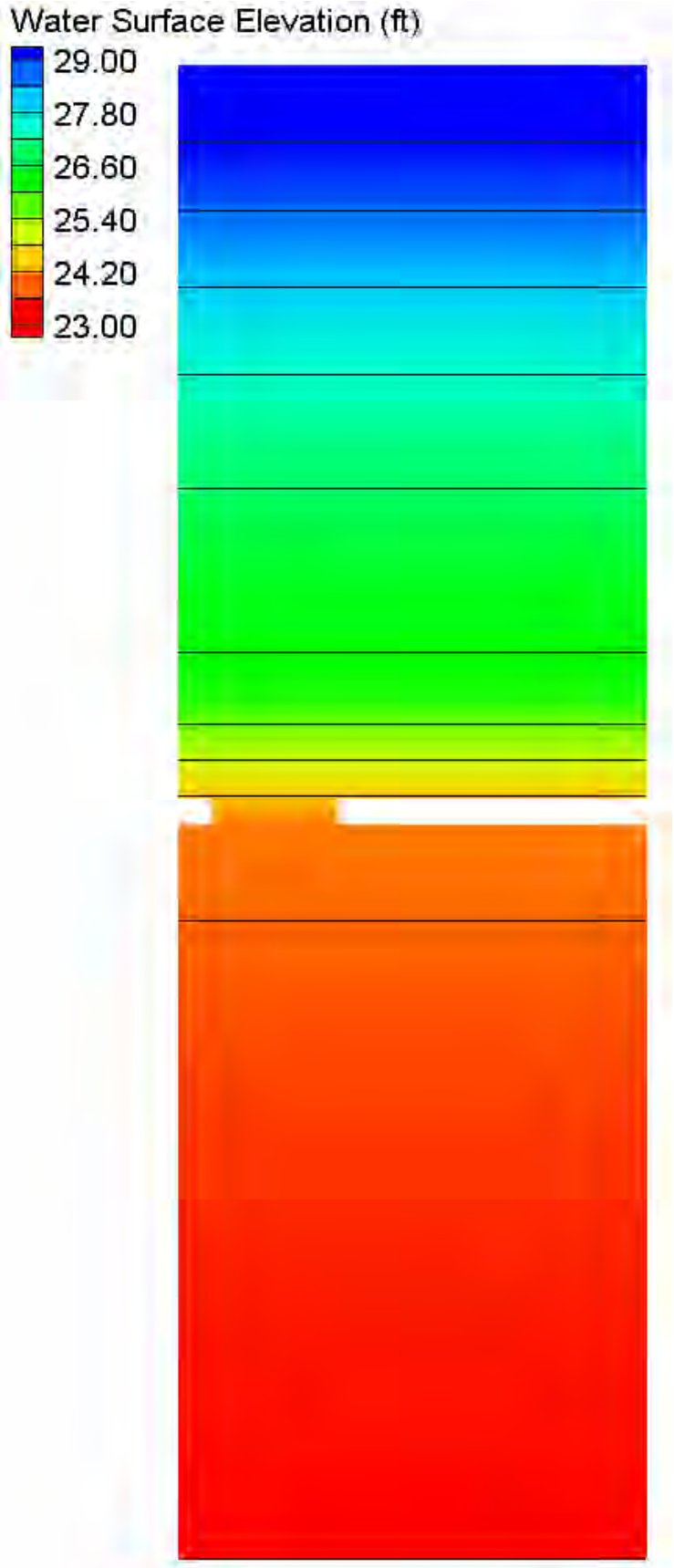

HEC-RAS Water Surface Elevation Contours – Large Channel – Asymmetric (75% reduction)

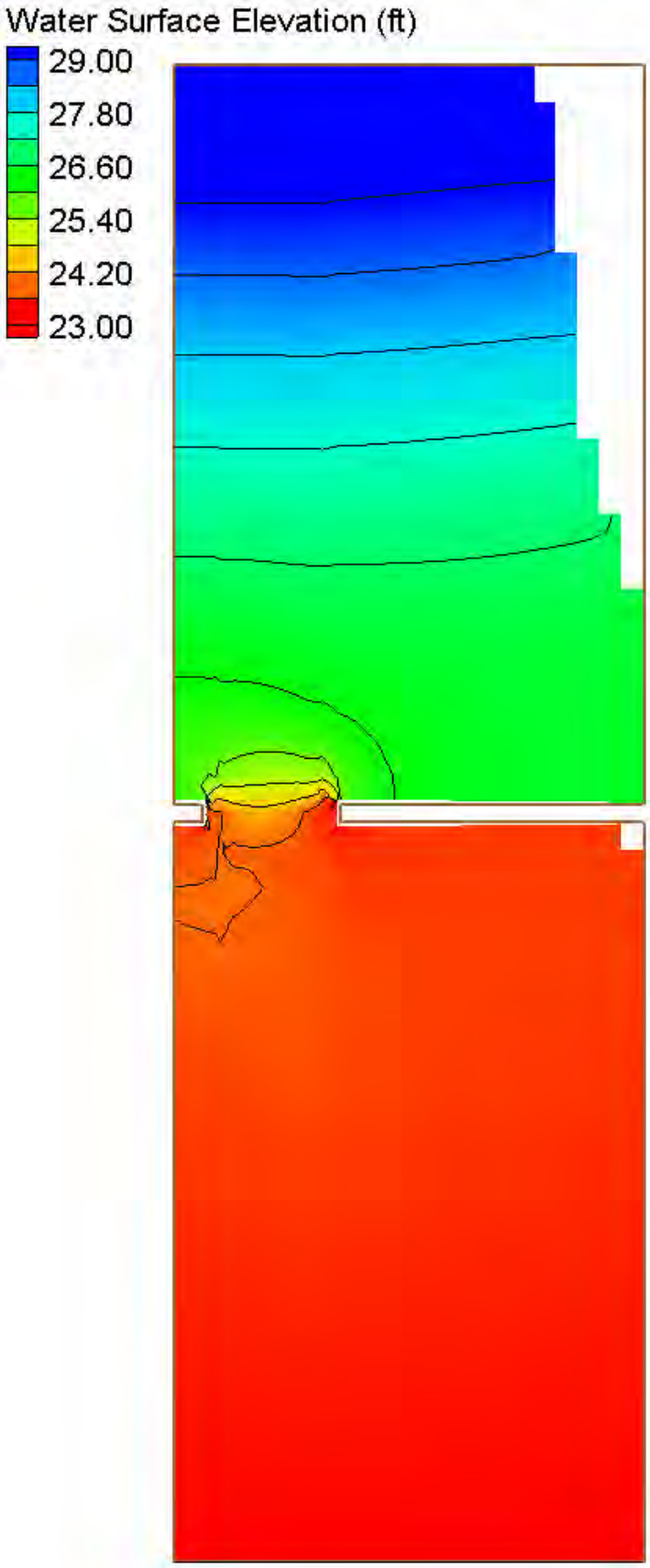

FESWMS Water Surface Elevation Contours – Large Channel – Asymmetric (75% reduction)

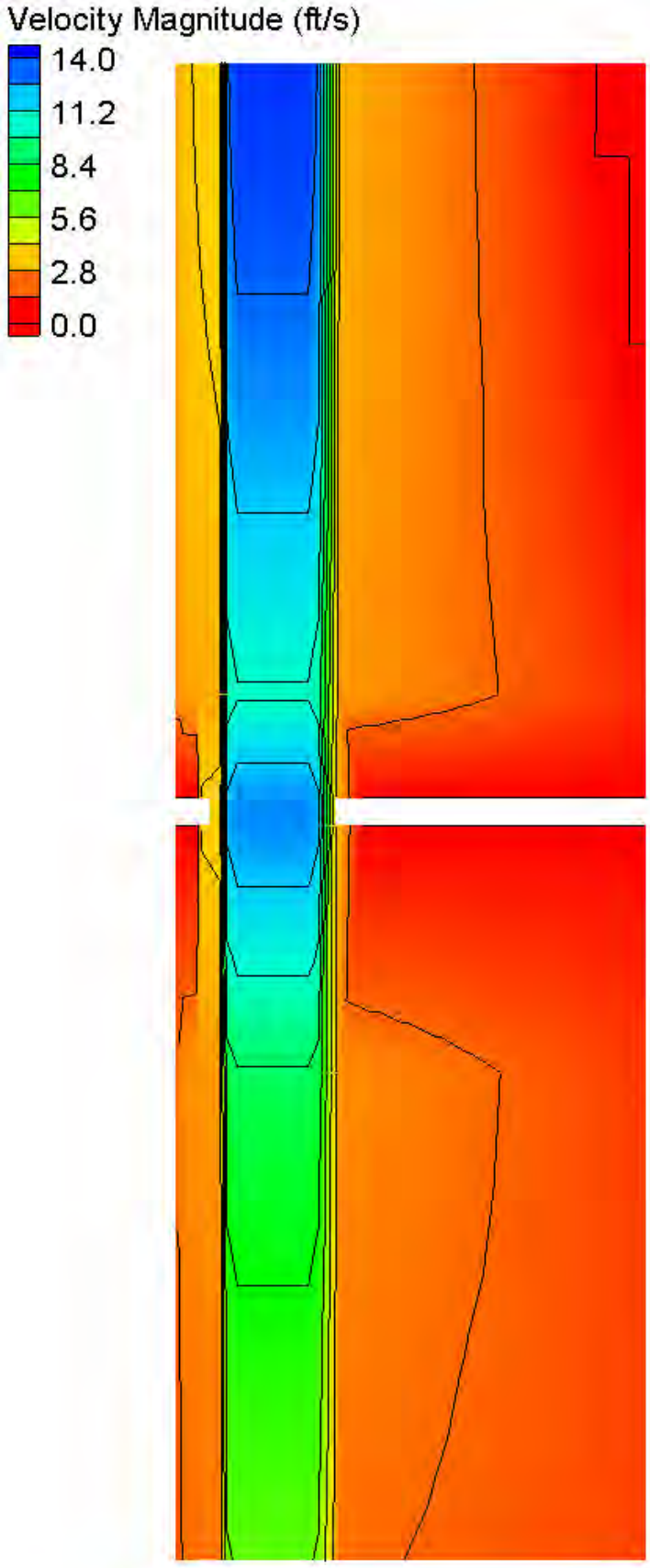

HEC-RAS Velocity Magnitude Contours – Large Channel – Asymmetric (75% reduction)

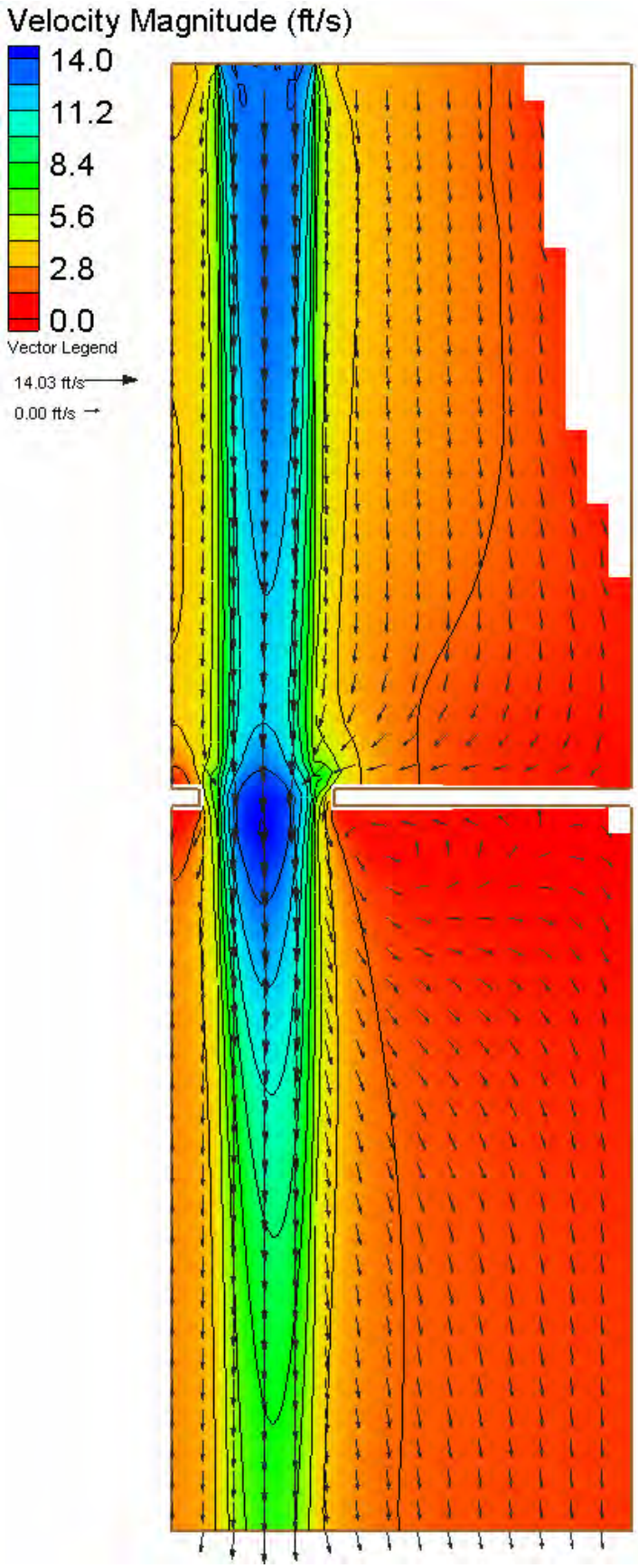

FESWMS Velocity Magnitude Contours – Large Channel – Asymmetric (75% reduction)

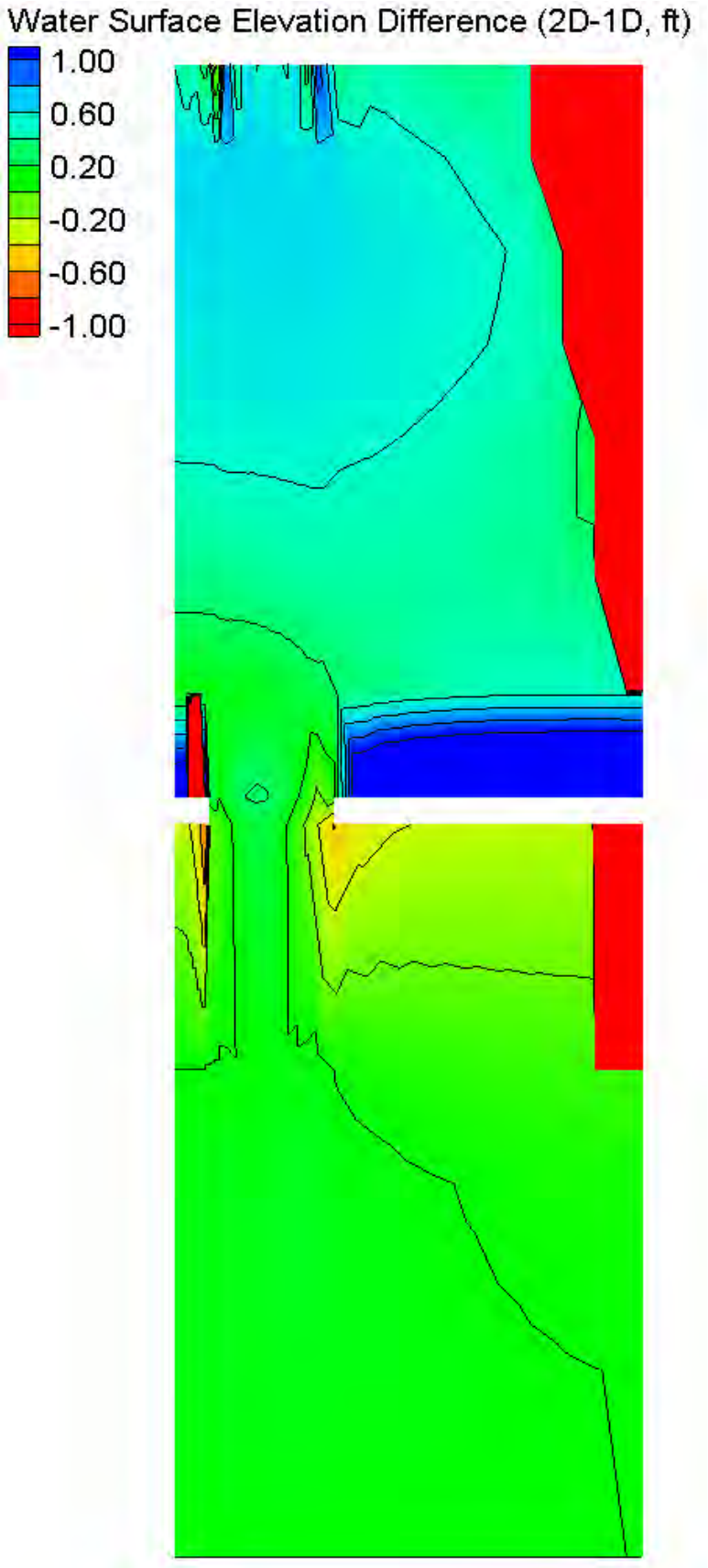

Water Surface Elevation Difference Contours – Large Channel – Asymmetric (75% reduction)

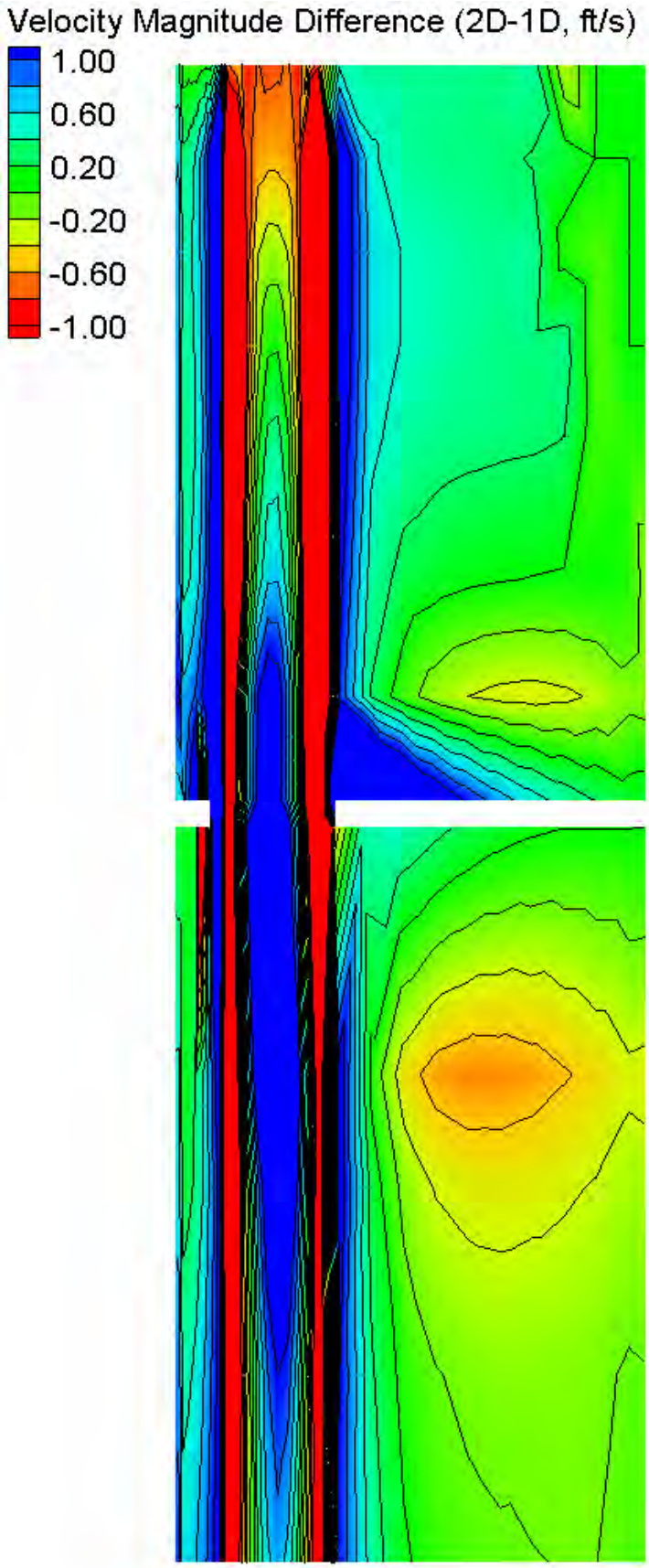

Velocity Magnitude Difference Contours – Large Channel – Asymmetric (75% reduction)

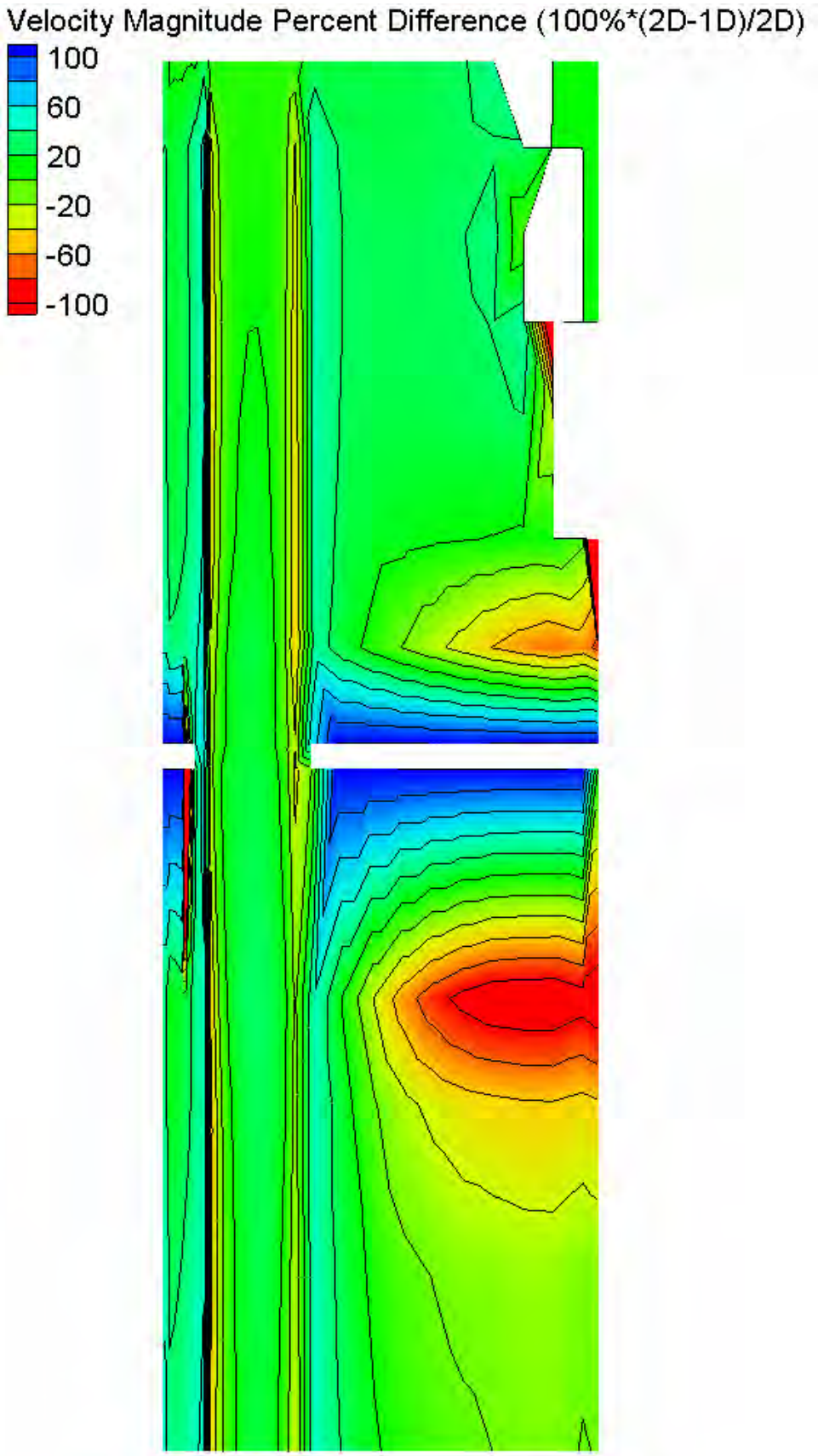

Velocity Magnitude Percent Difference Contours – Large Channel – Asymmetric (75% reduction)

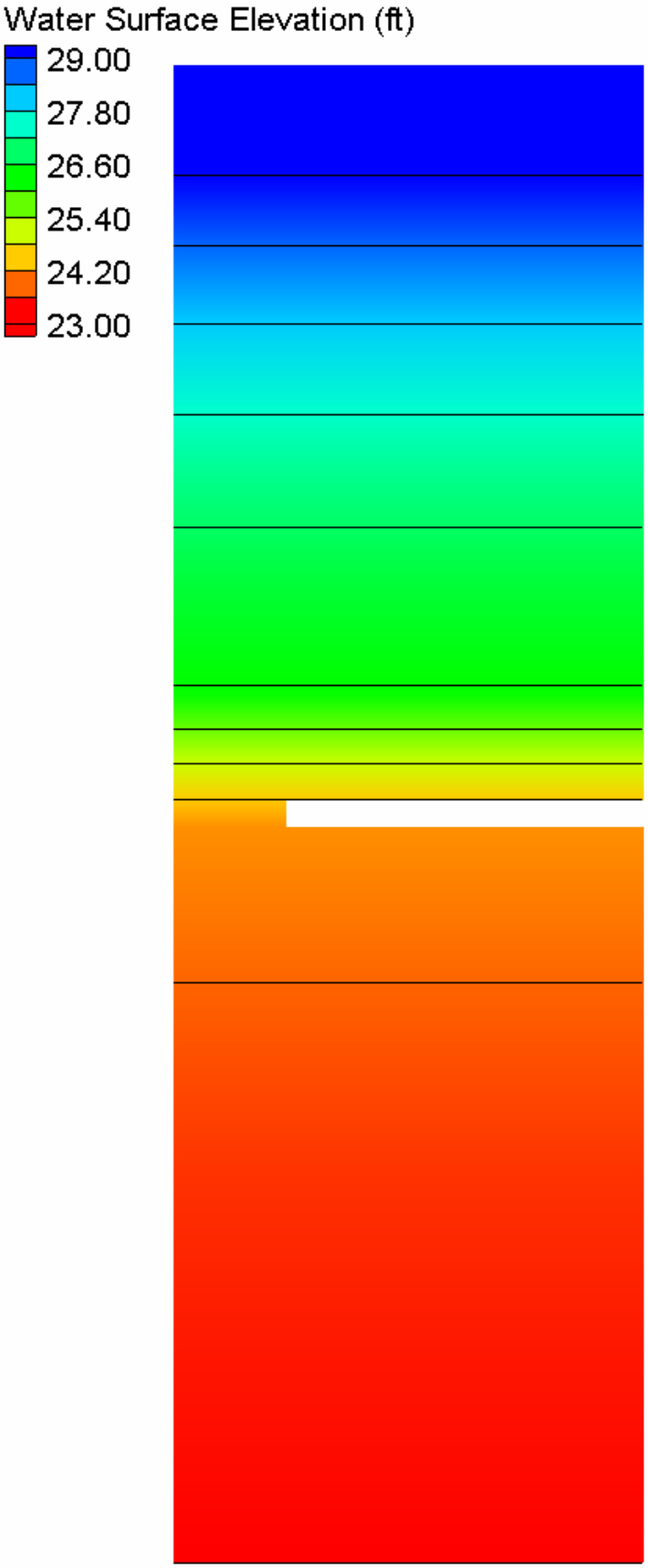

HEC-RAS Water Surface Elevation Contours – Large Channel – Asymmetric (100% reduction)

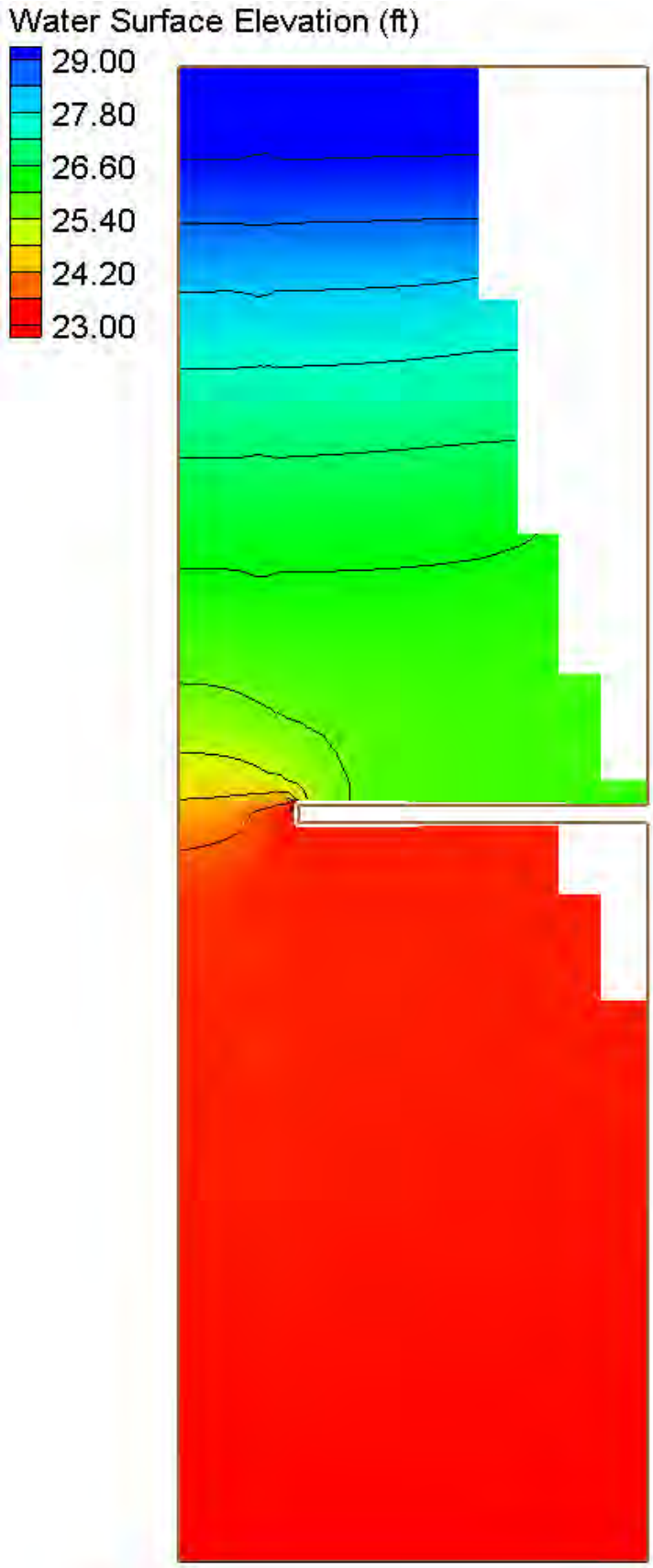

FESWMS Water Surface Elevation Contours – Large Channel – Asymmetric (100% reduction)

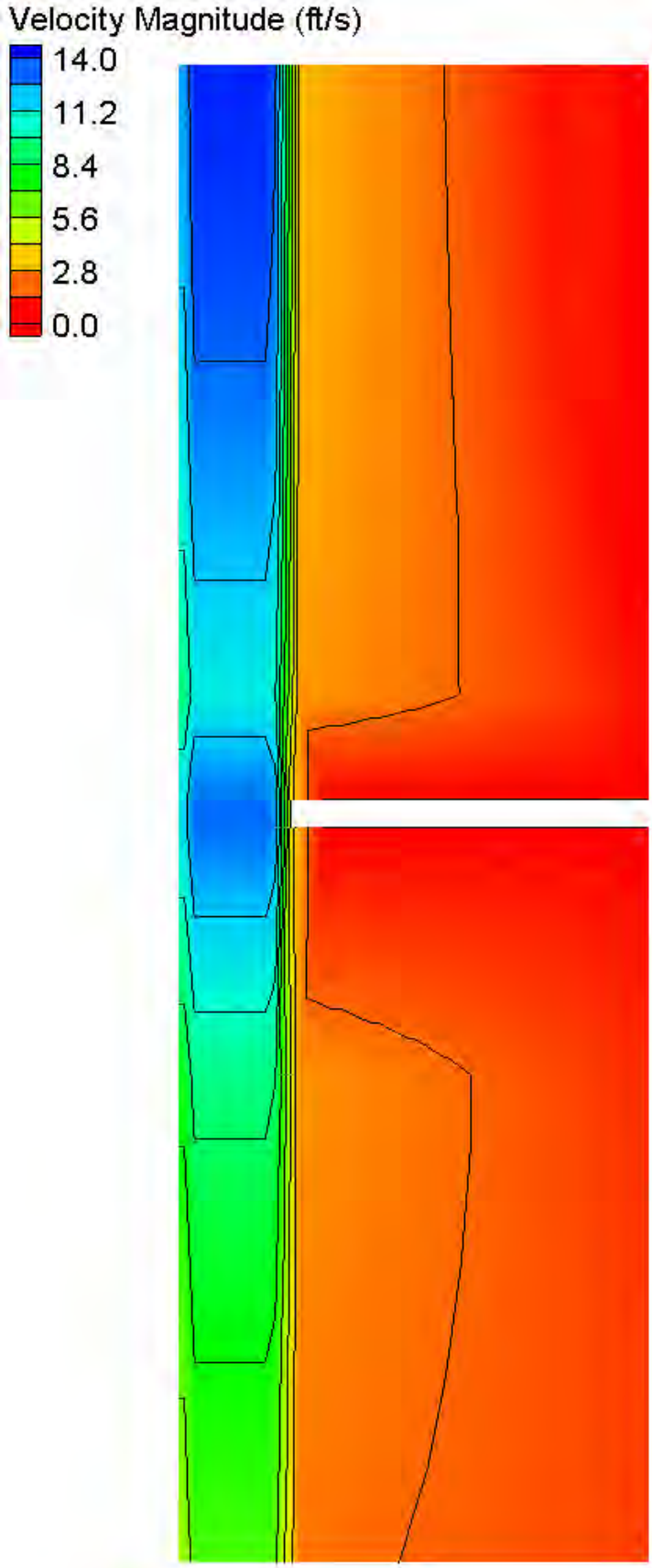

HEC-RAS Velocity Magnitude Contours – Large Channel – Asymmetric (100% reduction)

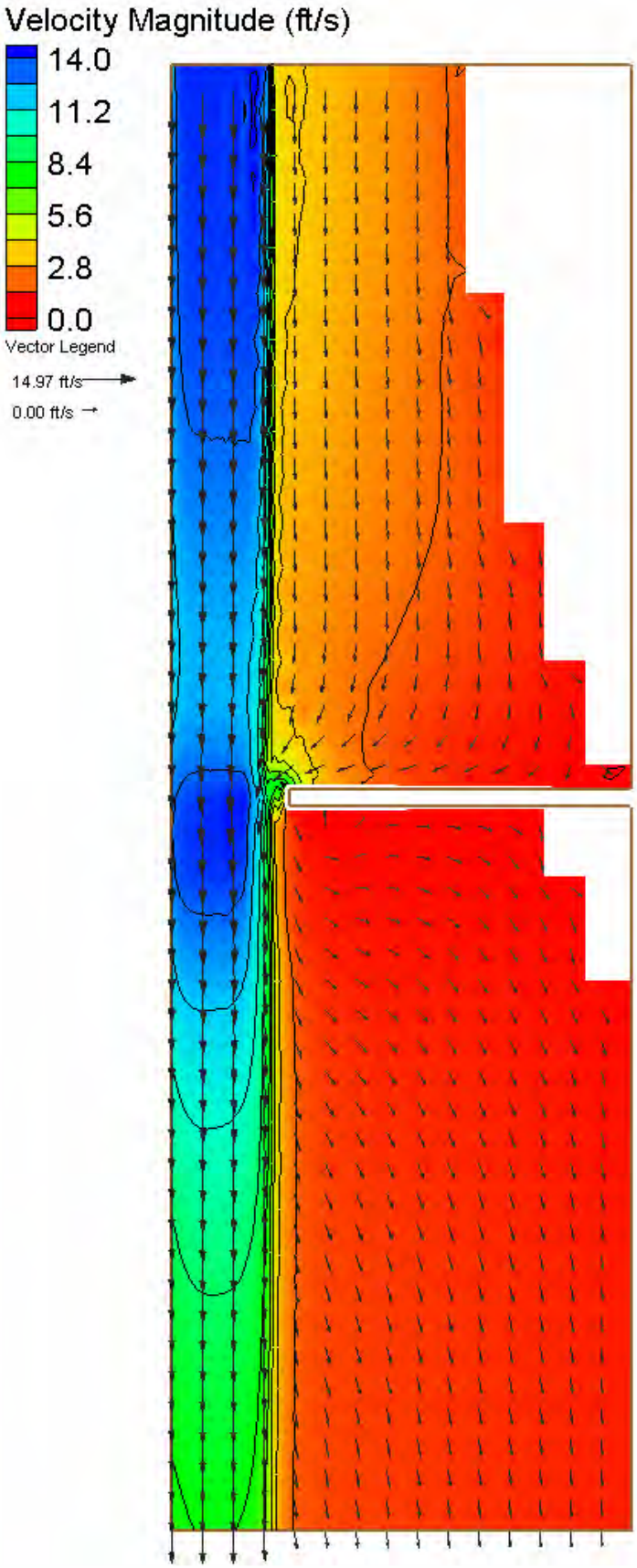

FESWMS Velocity Magnitude Contours – Large Channel – Asymmetric (100% reduction)

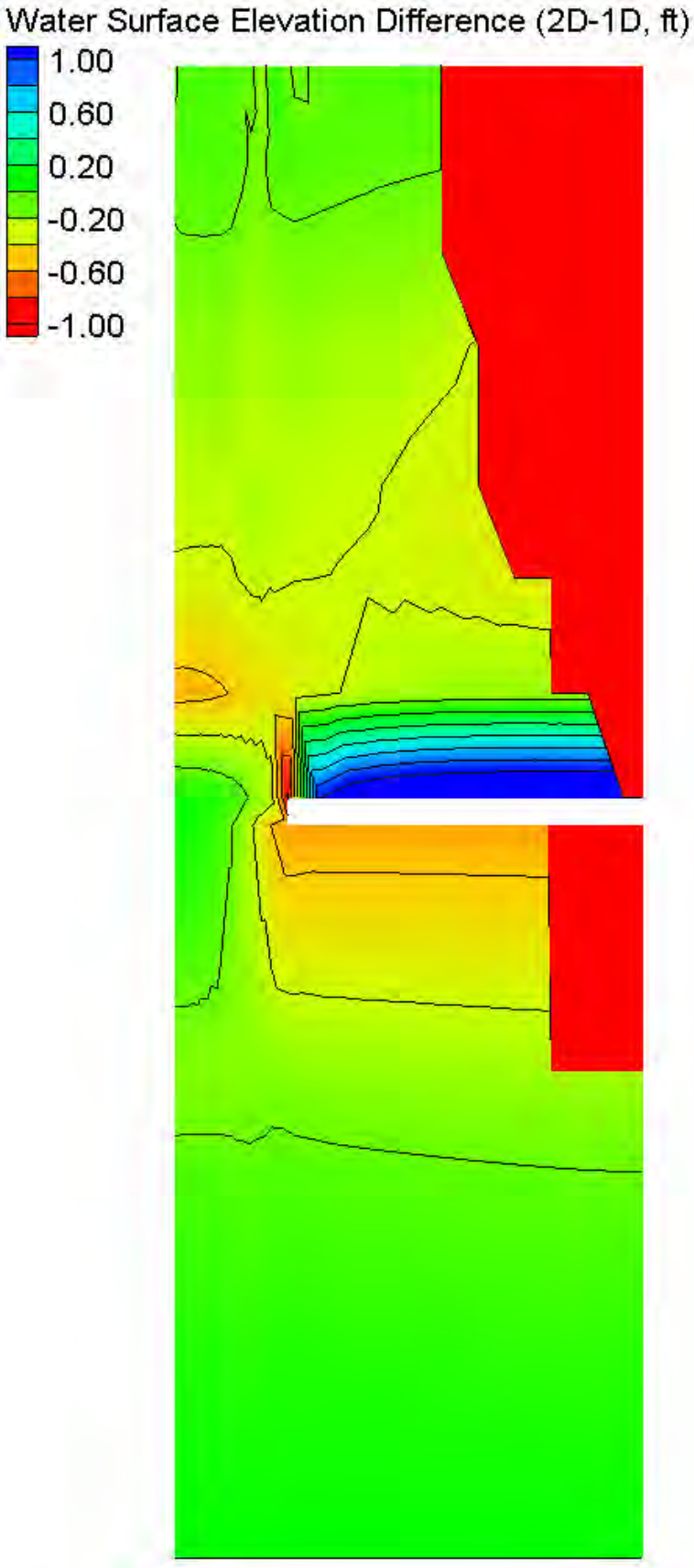

Water Surface Elevation Difference Contours – Large Channel – Asymmetric (100% reduction)

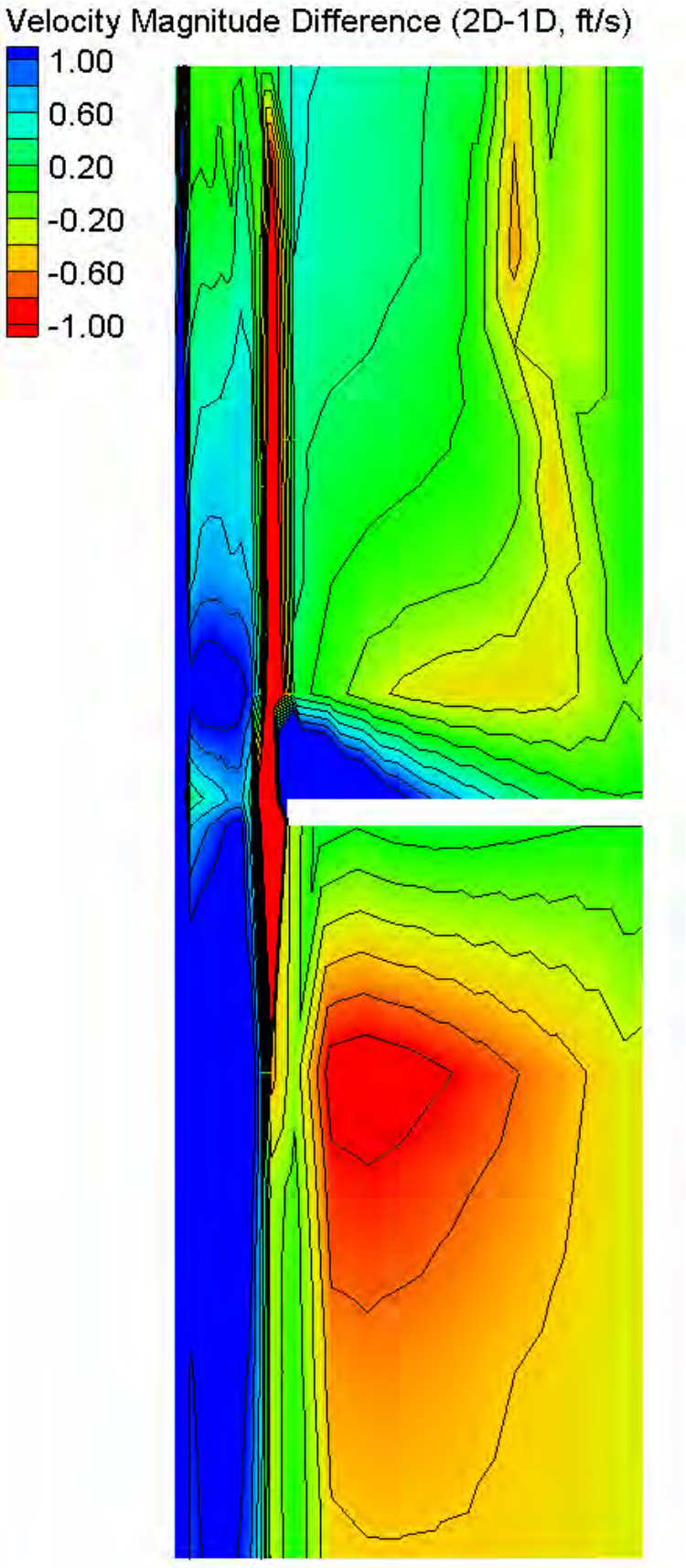

Velocity Magnitude Difference Contours – Large Channel – Asymmetric (100% reduction)

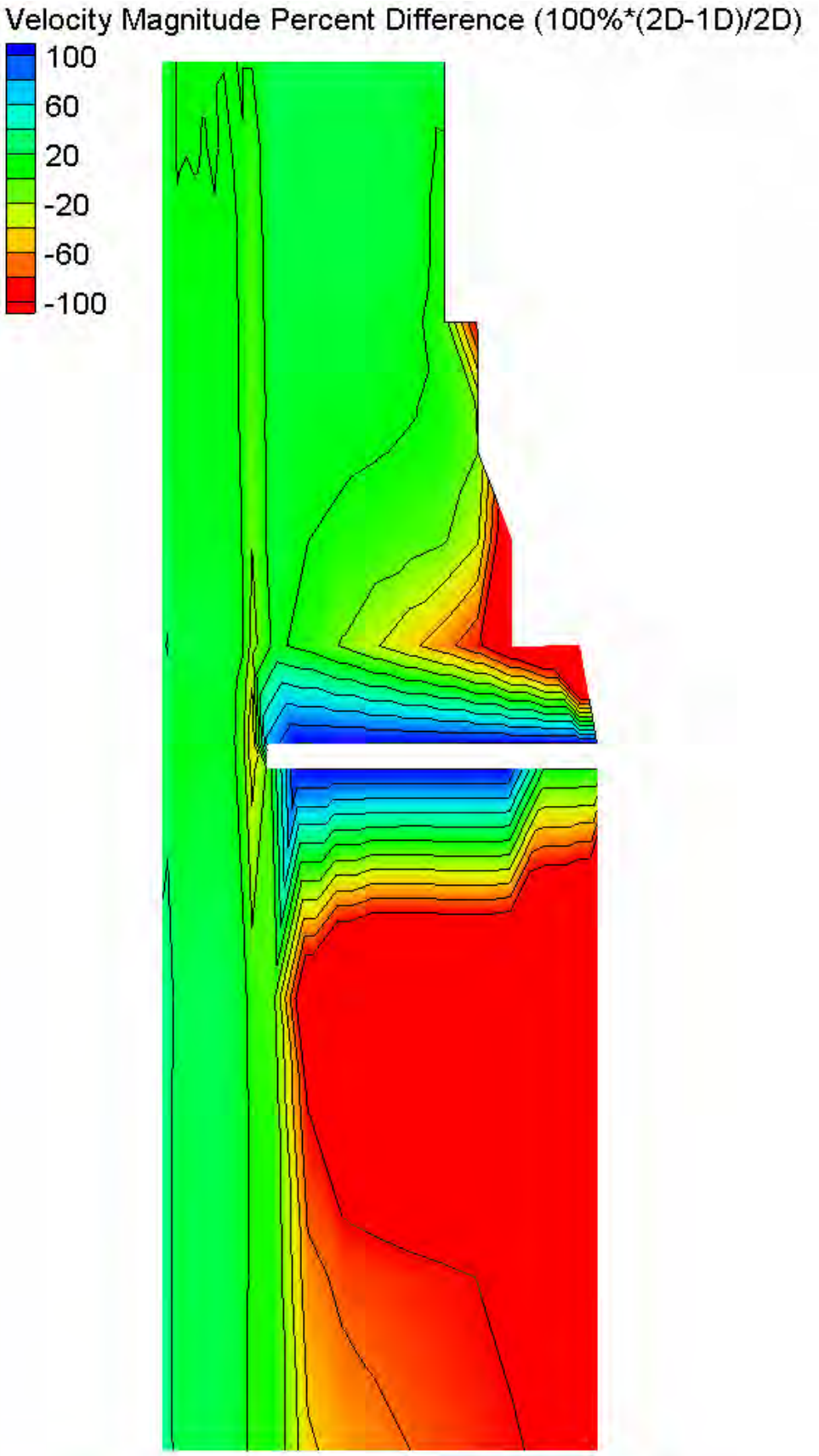

Velocity Magnitude Percent Difference Contours – Large Channel – Asymmetric (100% reduction)

Bridges with Large Piers/High Blockage

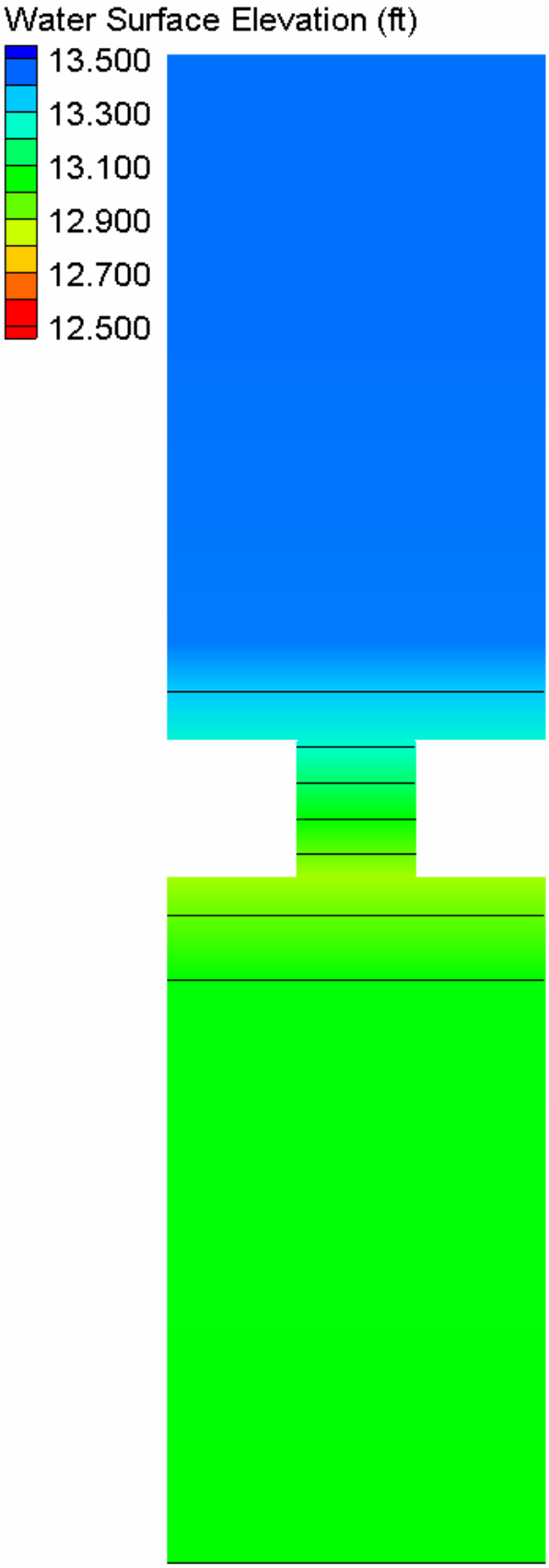

HEC-RAS Water Surface Elevation Contours – Small Channel – Large Pier Blockage (5%)

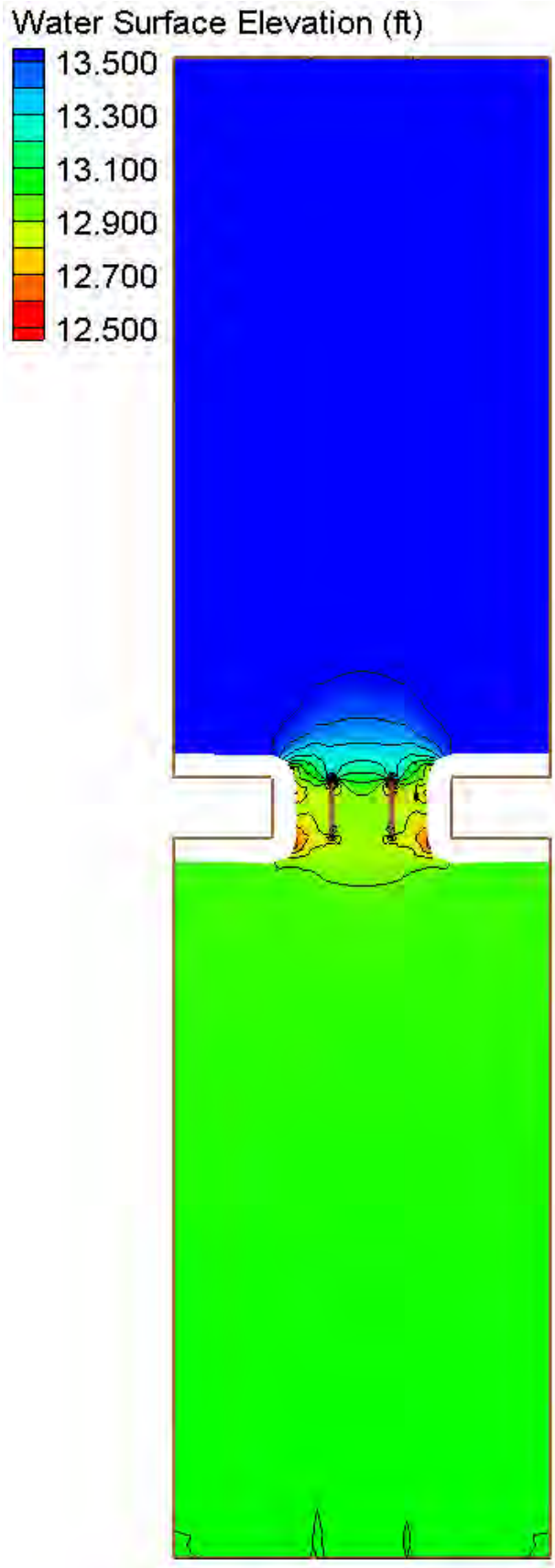

FESWMS Water Surface Elevation Contours – Small Channel – Large Pier Blockage (5%)

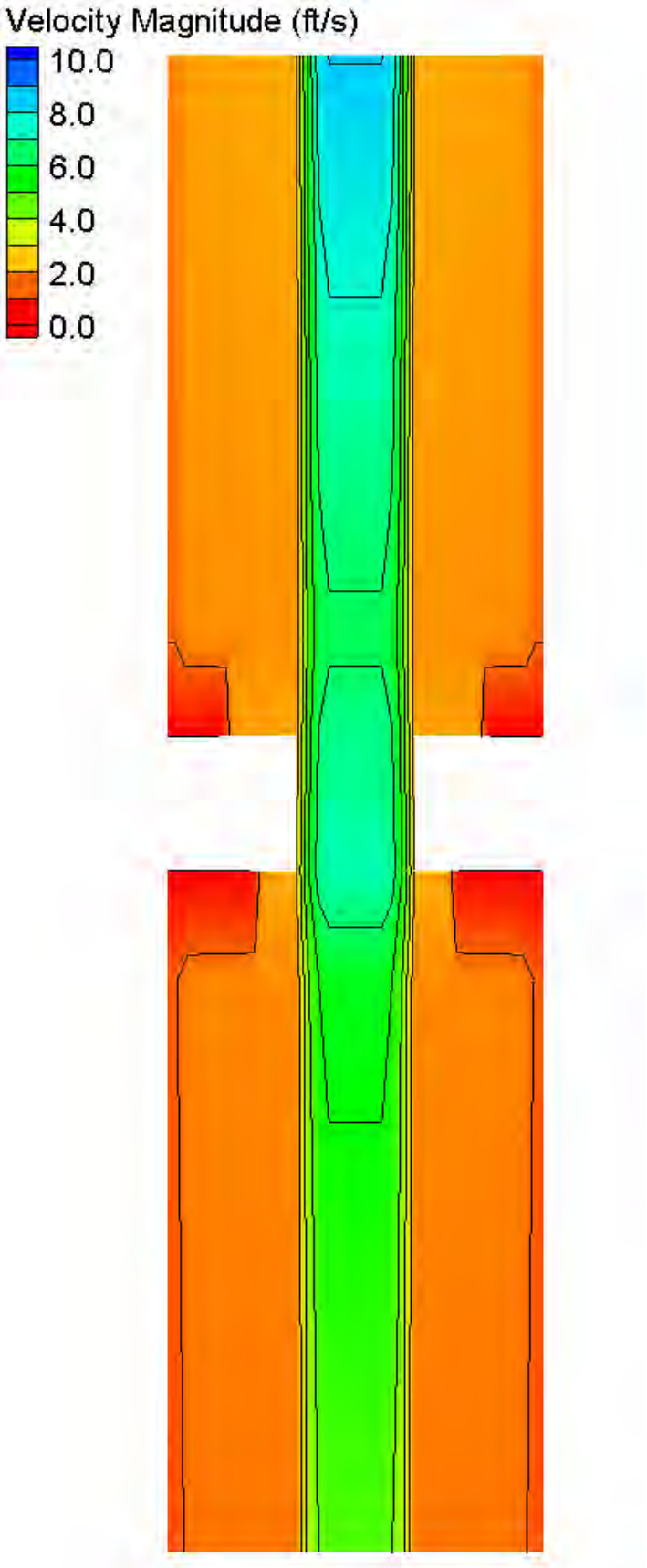

HEC-RAS Velocity Magnitude Contours – Small Channel – Large Pier Blockage (5%)

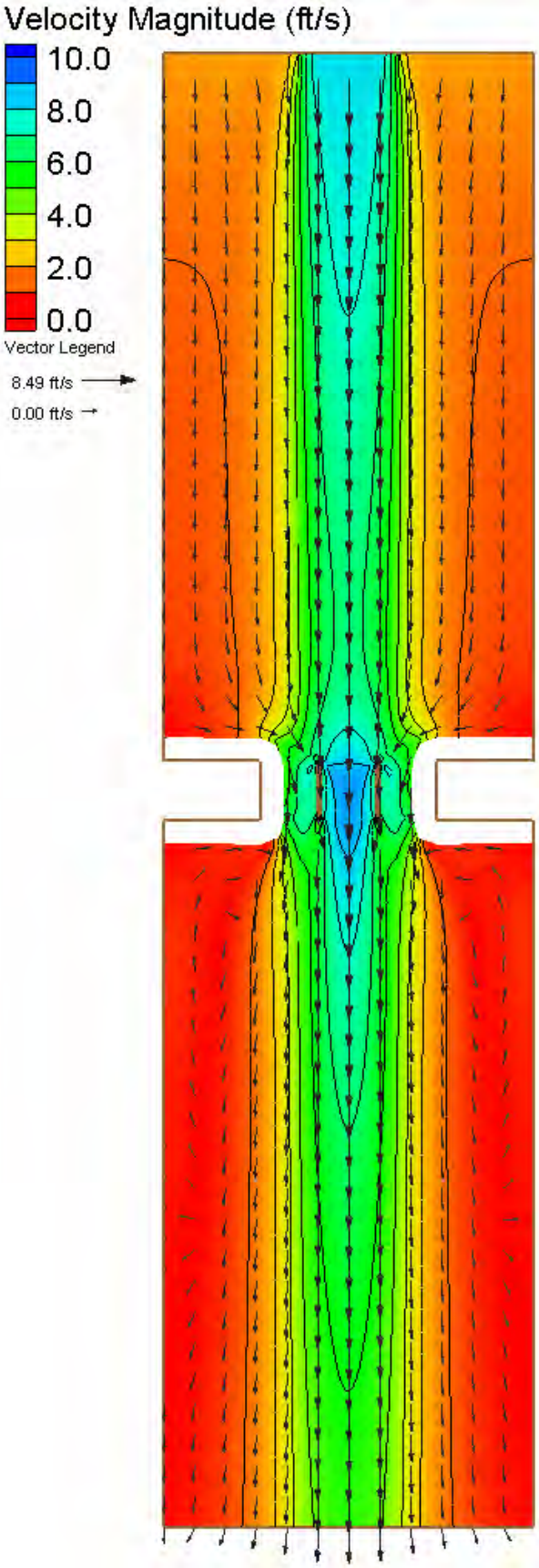

FESWMS Velocity Magnitude Contours – Small Channel – Large Pier Blockage (5%)

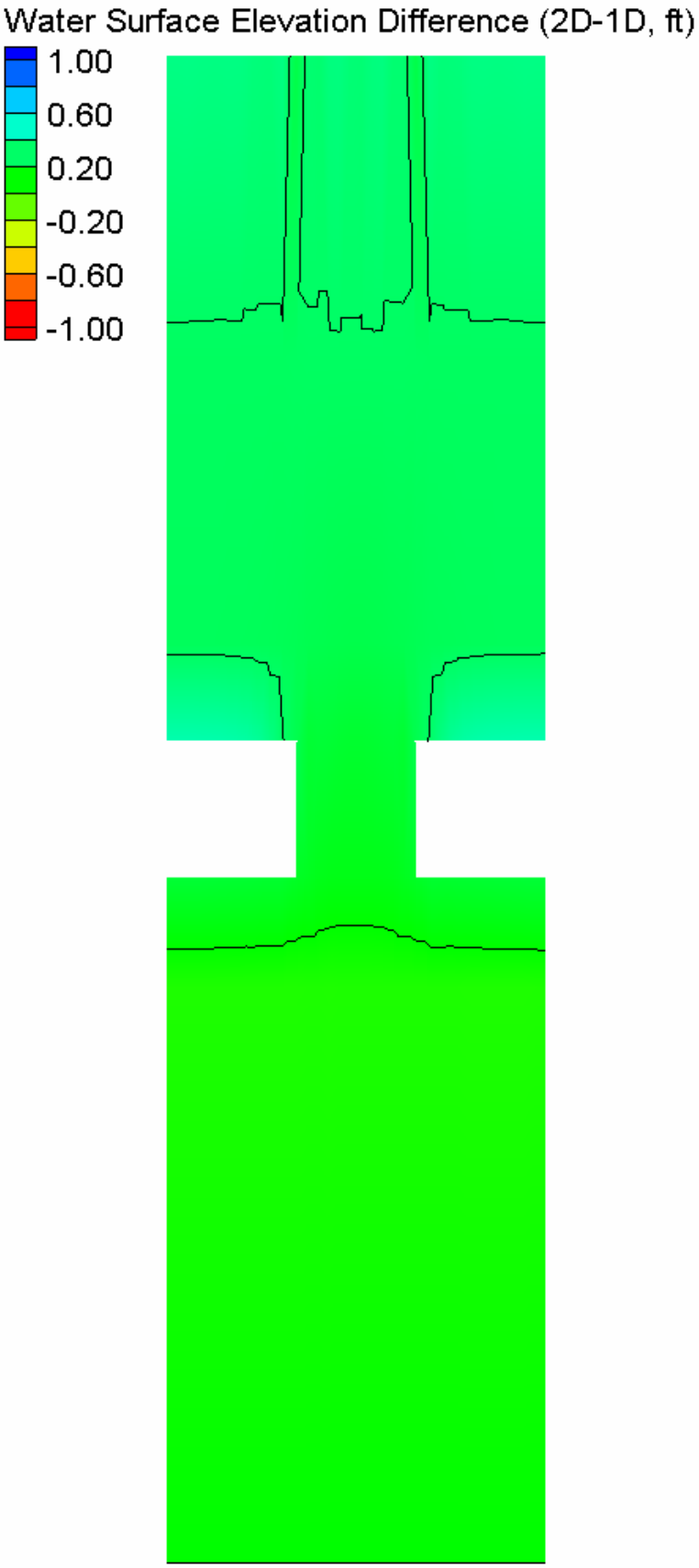

Water Surface Elevation Difference Contours – Small Channel – Large Pier Blockage (5%)

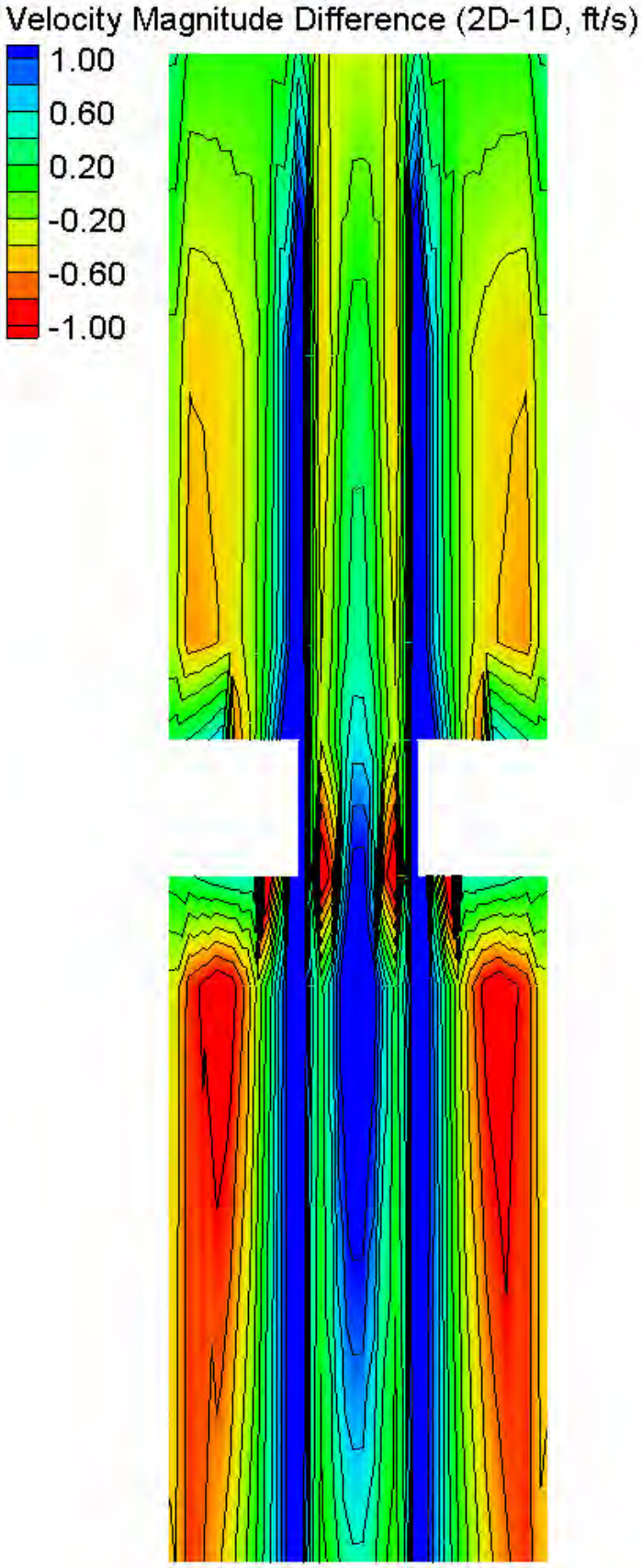

Velocity Magnitude Difference Contours – Small Channel – Large Pier Blockage (5%)

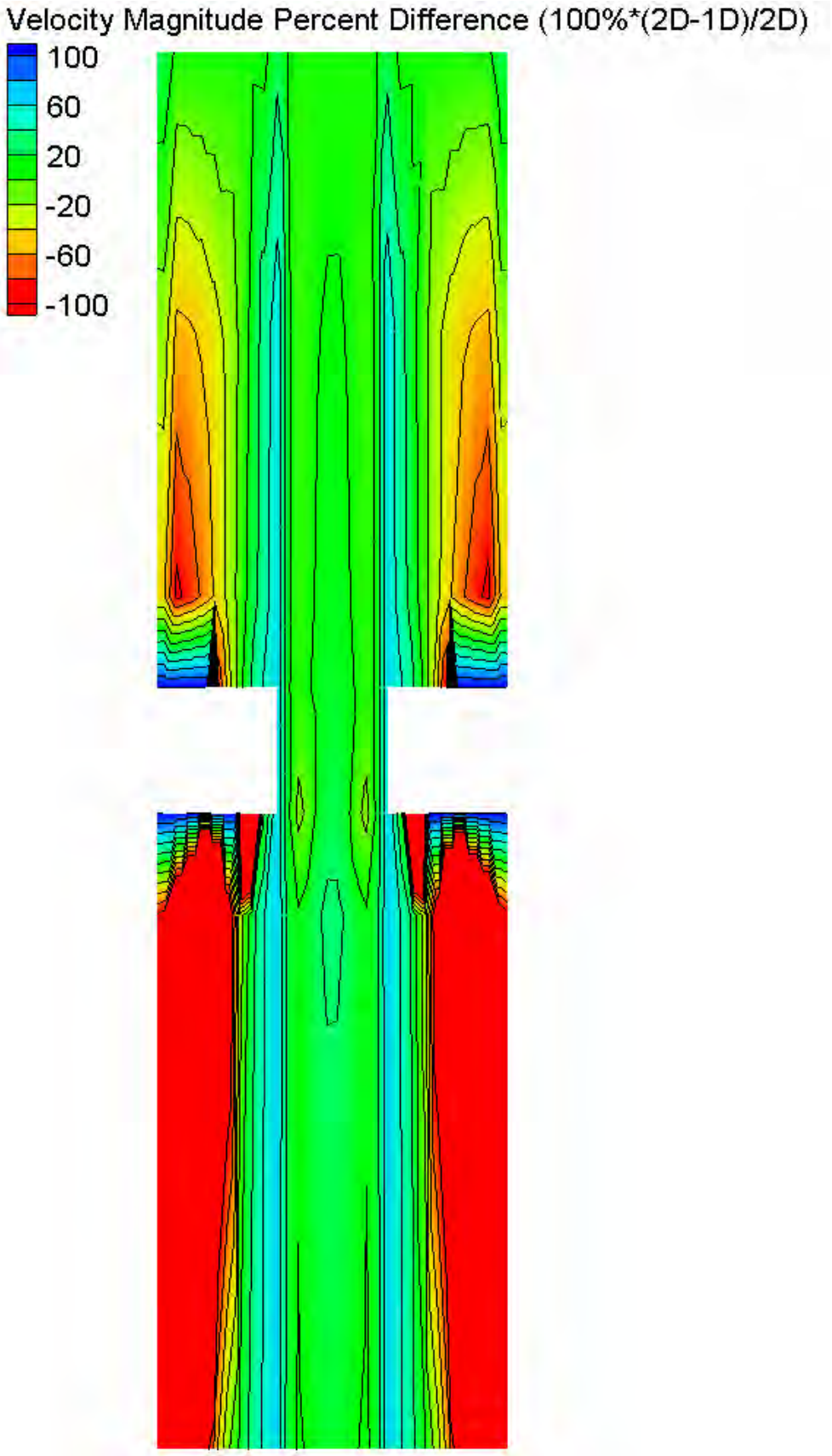

Velocity Magnitude Percent Difference Contours – Small Channel – Large Pier Blockage (5%)

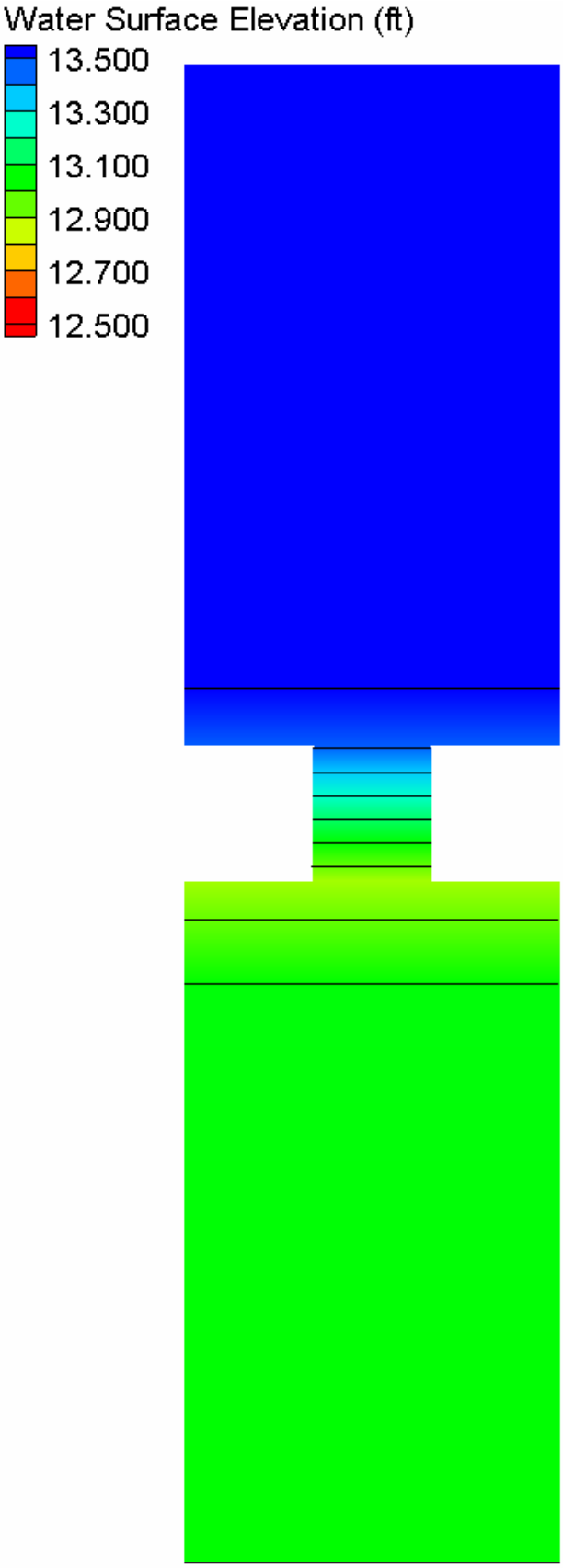

HEC-RAS Water Surface Elevation Contours – Small Channel – Large Pier Blockage (15%)

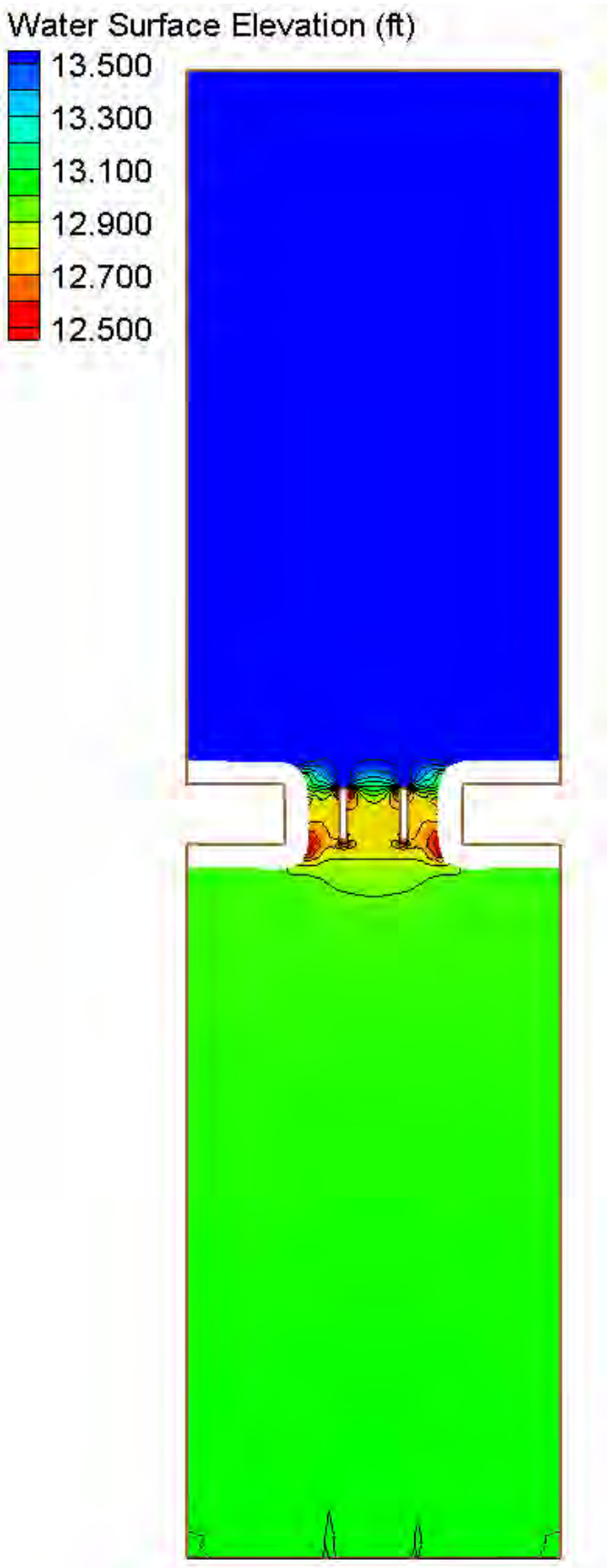

FESWMS Water Surface Elevation Contours – Small Channel – Large Pier Blockage (15%)

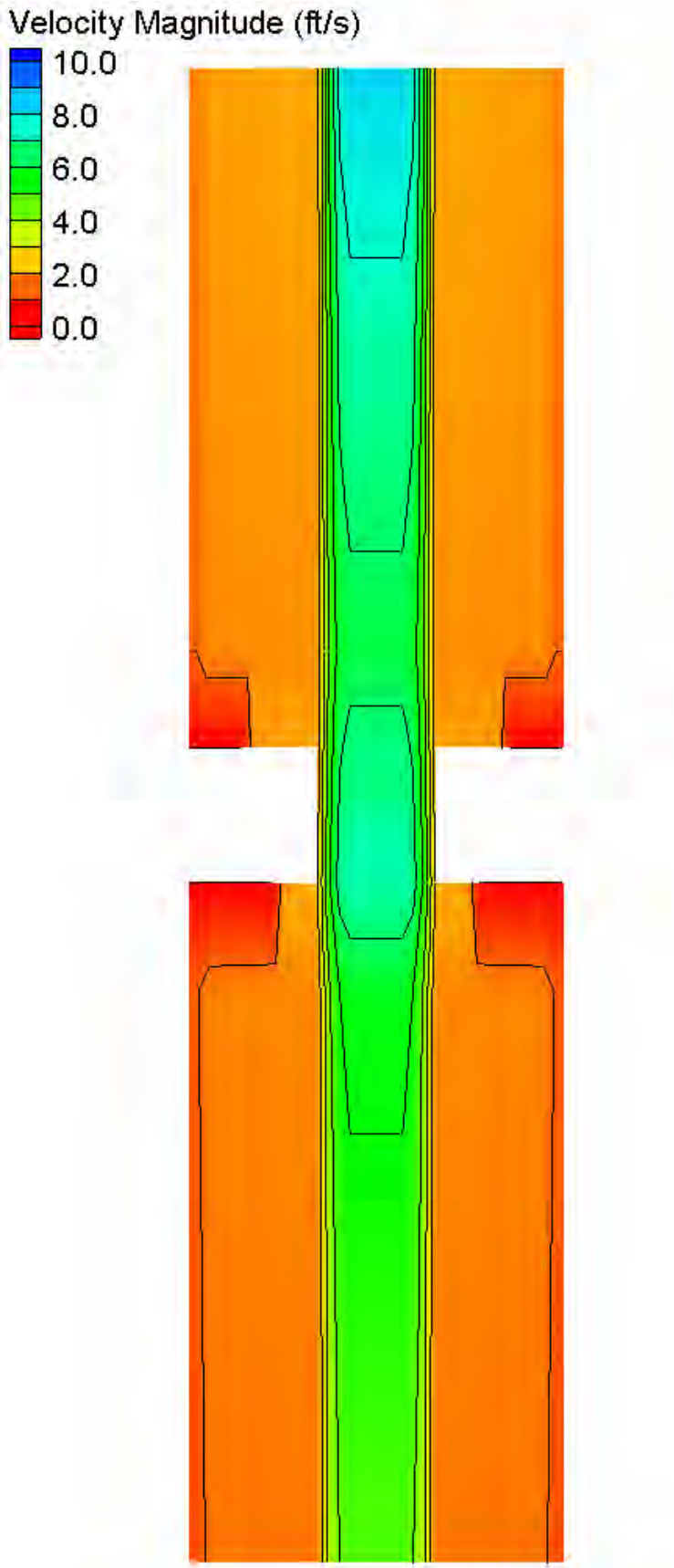

HEC-RAS Velocity Magnitude Contours – Small Channel – Large Pier Blockage (15%)

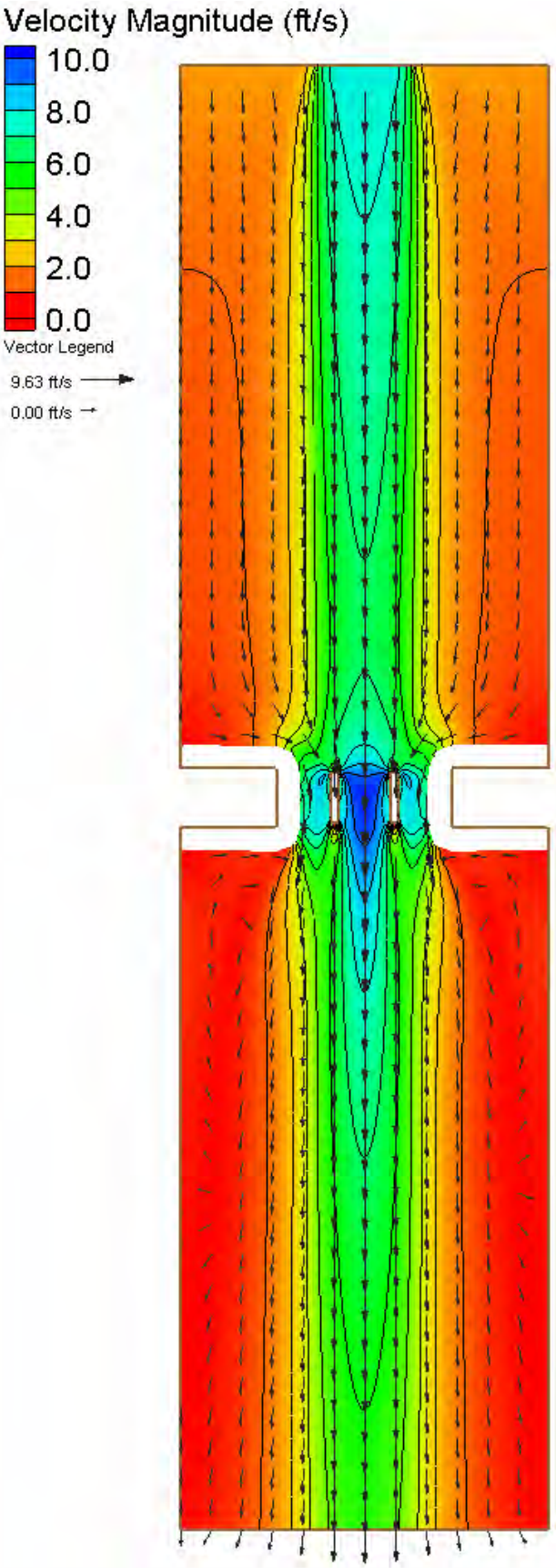

FESWMS Velocity Magnitude Contours – Small Channel – Large Pier Blockage (15%)

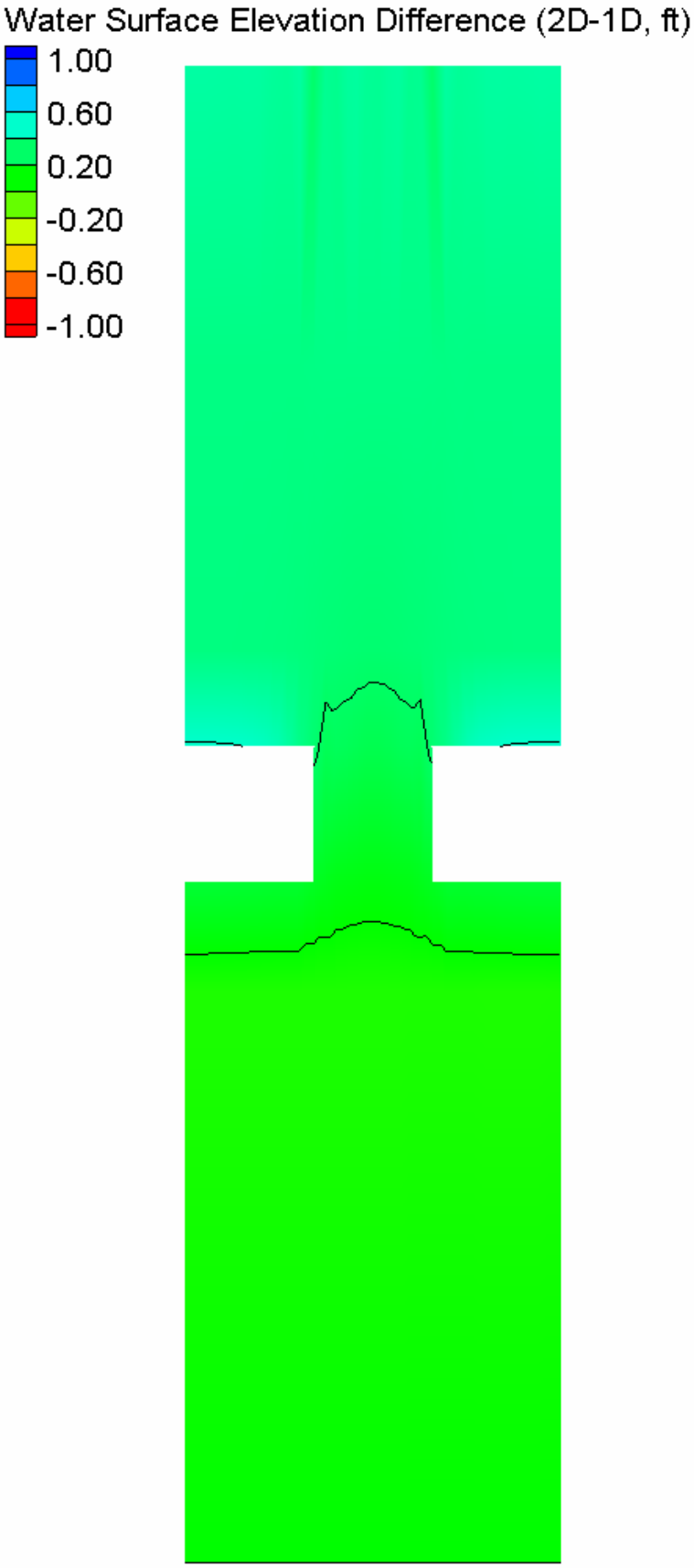

Water Surface Elevation Difference Contours – Small Channel – Large Pier Blockage (15%)

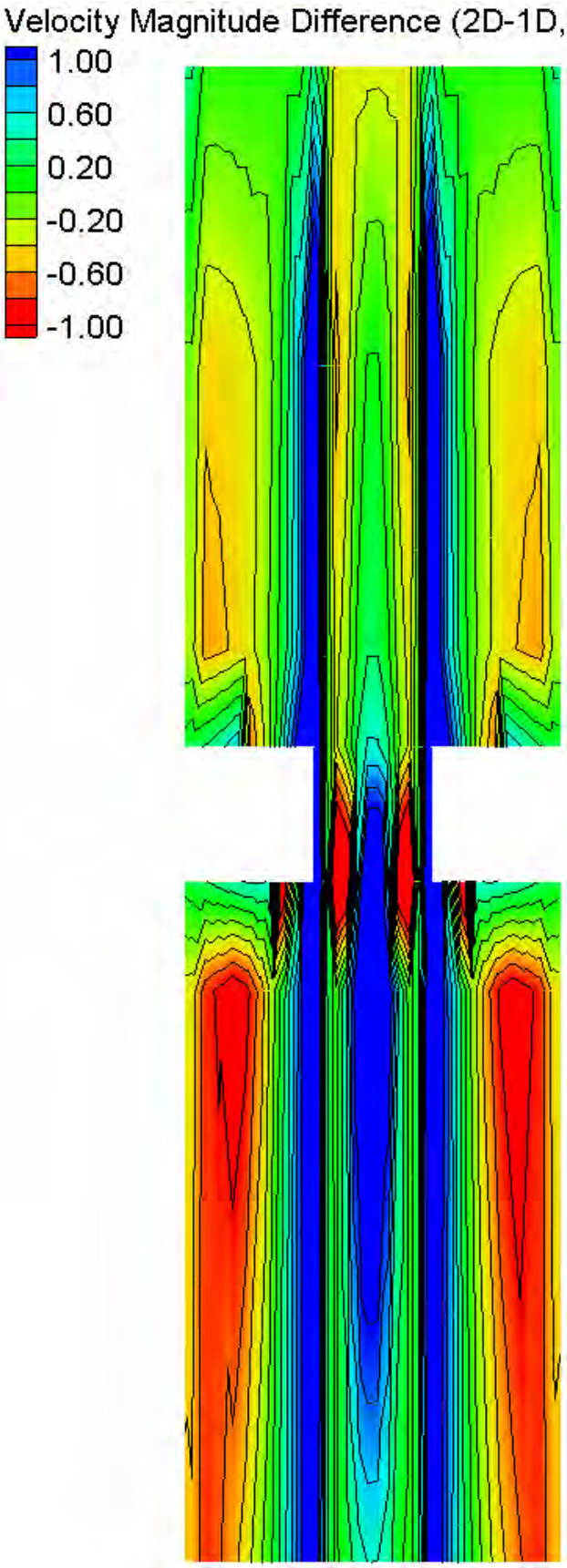

Velocity Magnitude Difference Contours – Small Channel – Large Pier Blockage (15%)

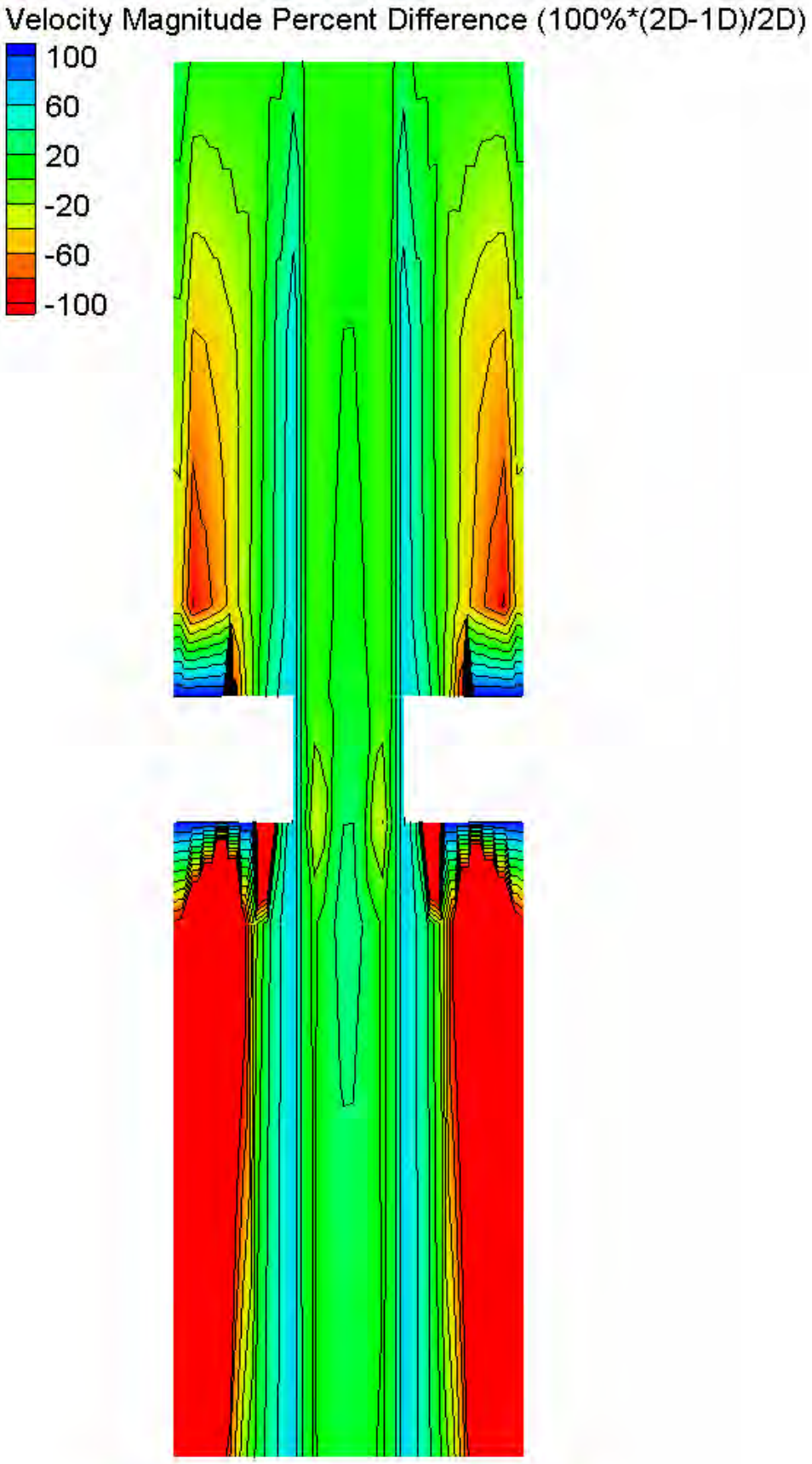

Velocity Magnitude Percent Difference Contours – Small Channel – Large Pier Blockage (15%)

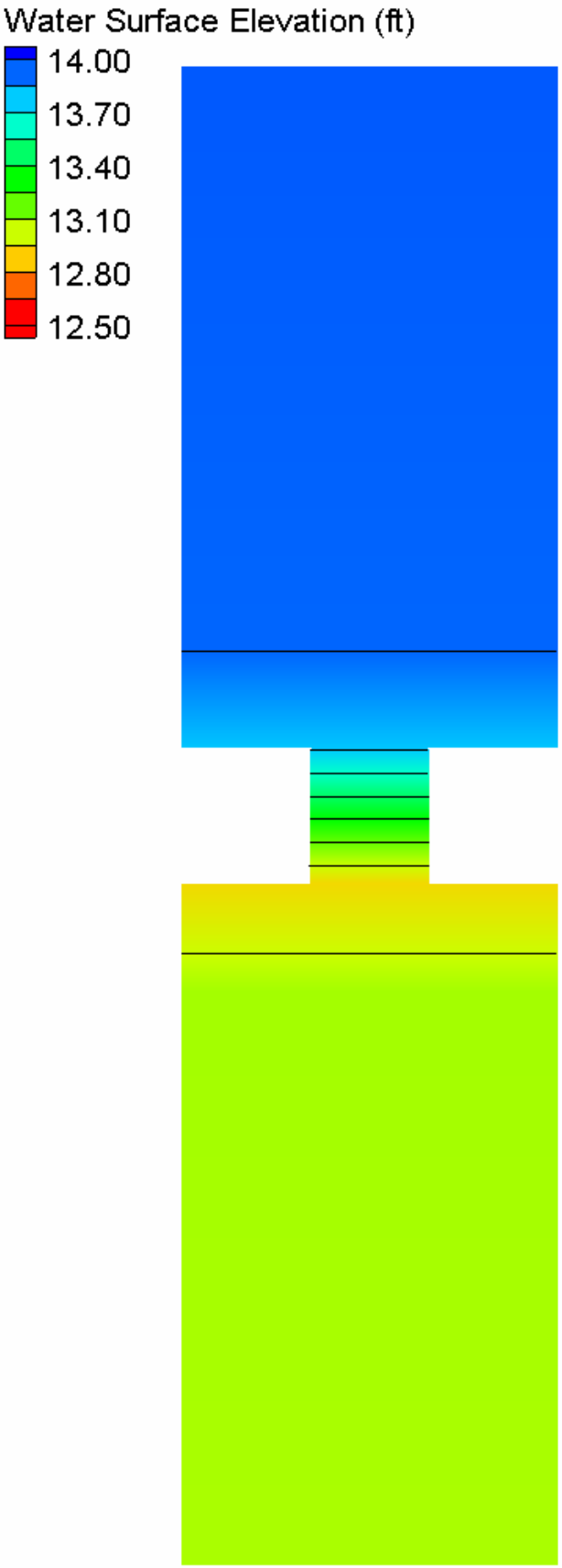

HEC-RAS Water Surface Elevation Contours – Small Channel – Large Pier Blockage (25%)

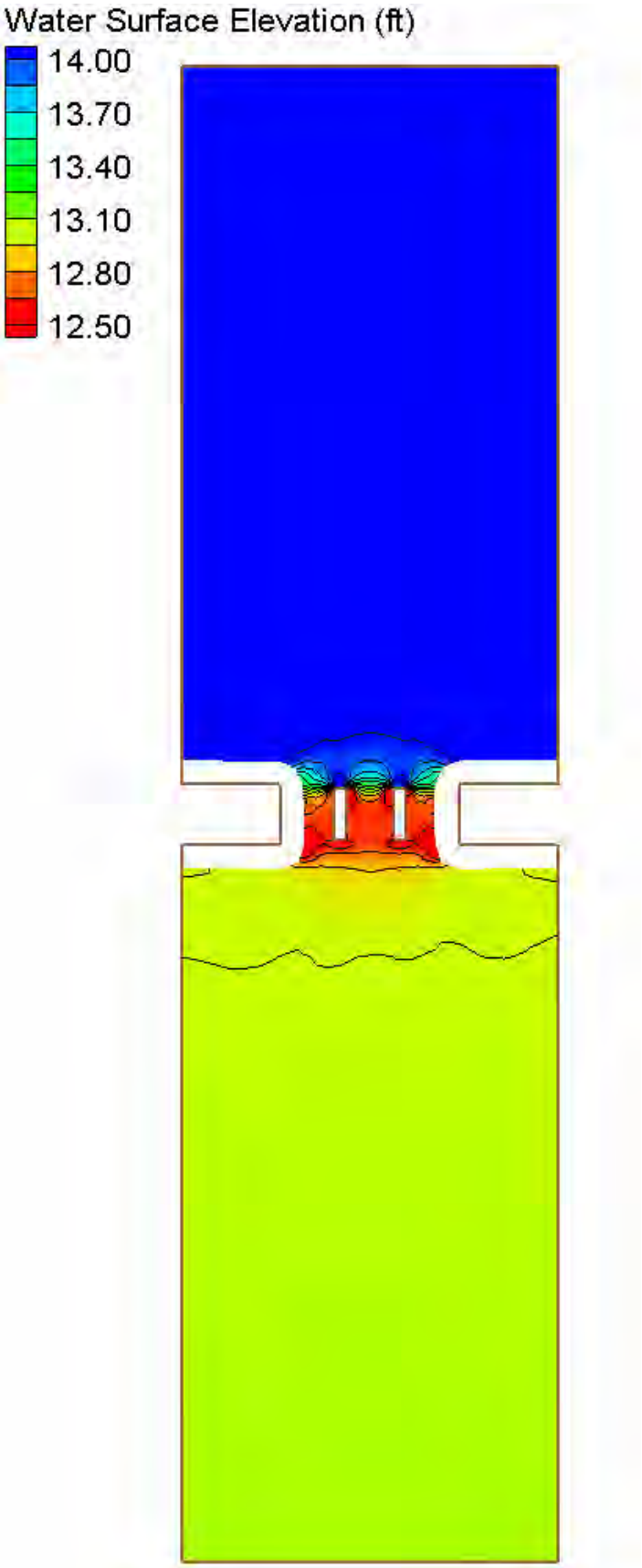

FESWMS Water Surface Elevation Contours – Small Channel – Large Pier Blockage (25%)

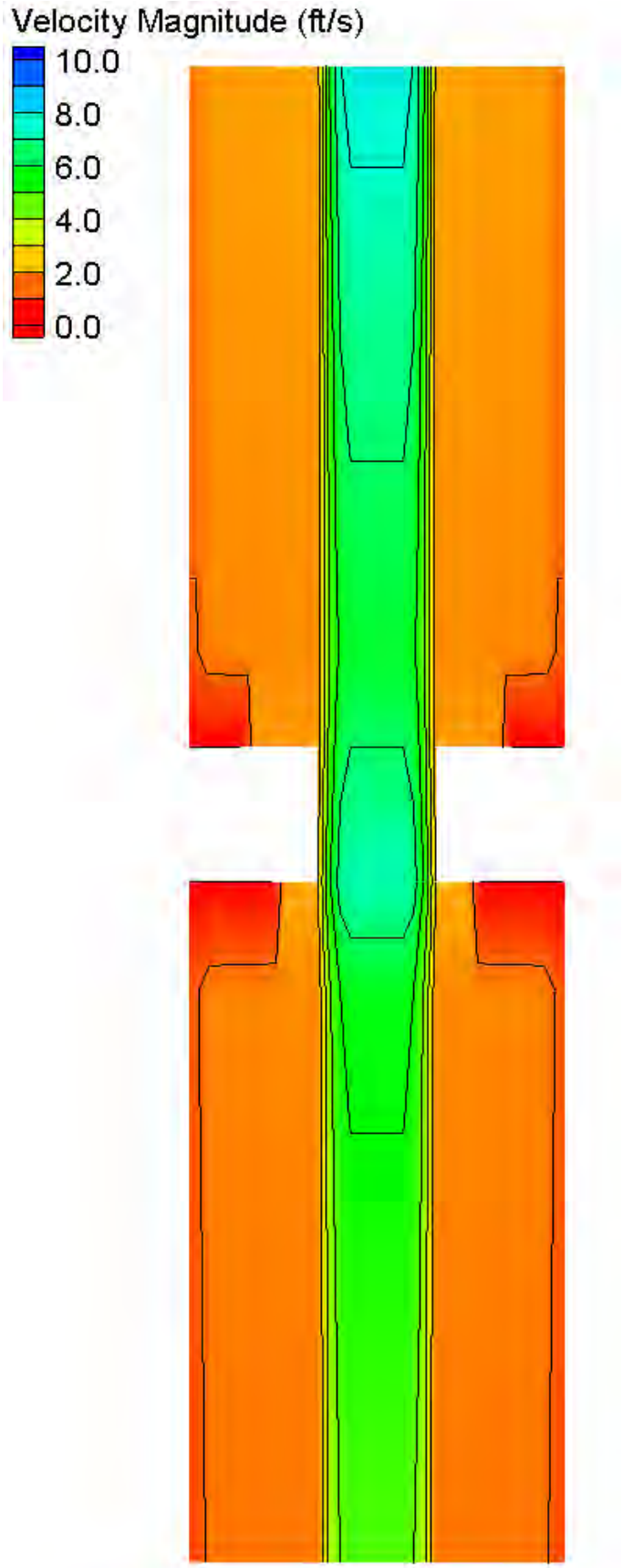

HEC-RAS Velocity Magnitude Contours – Small Channel – Large Pier Blockage (25%)

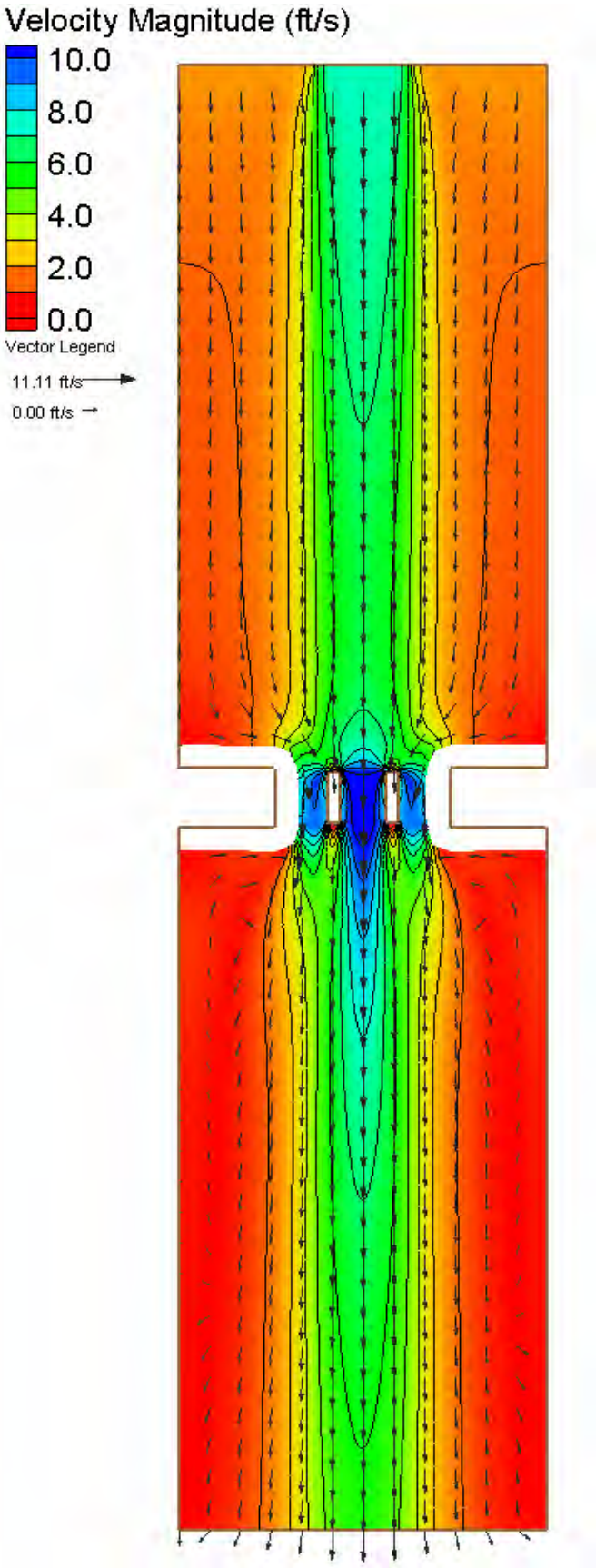

FESWMS Velocity Magnitude Contours – Small Channel – Large Pier Blockage (25%)

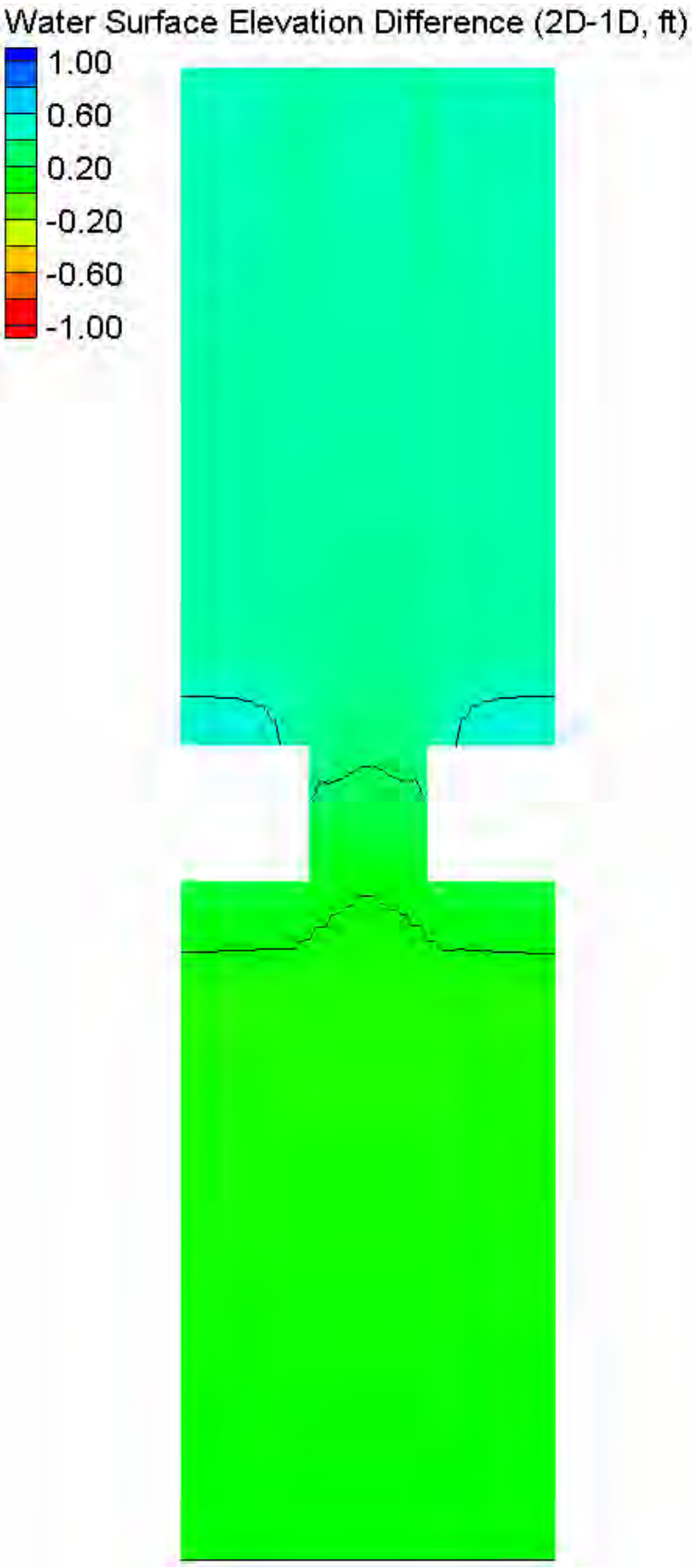

Water Surface Elevation Difference Contours – Small Channel – Large Pier Blockage (25%)

Velocity Magnitude Difference Contours – Small Channel – Large Pier Blockage (25%)

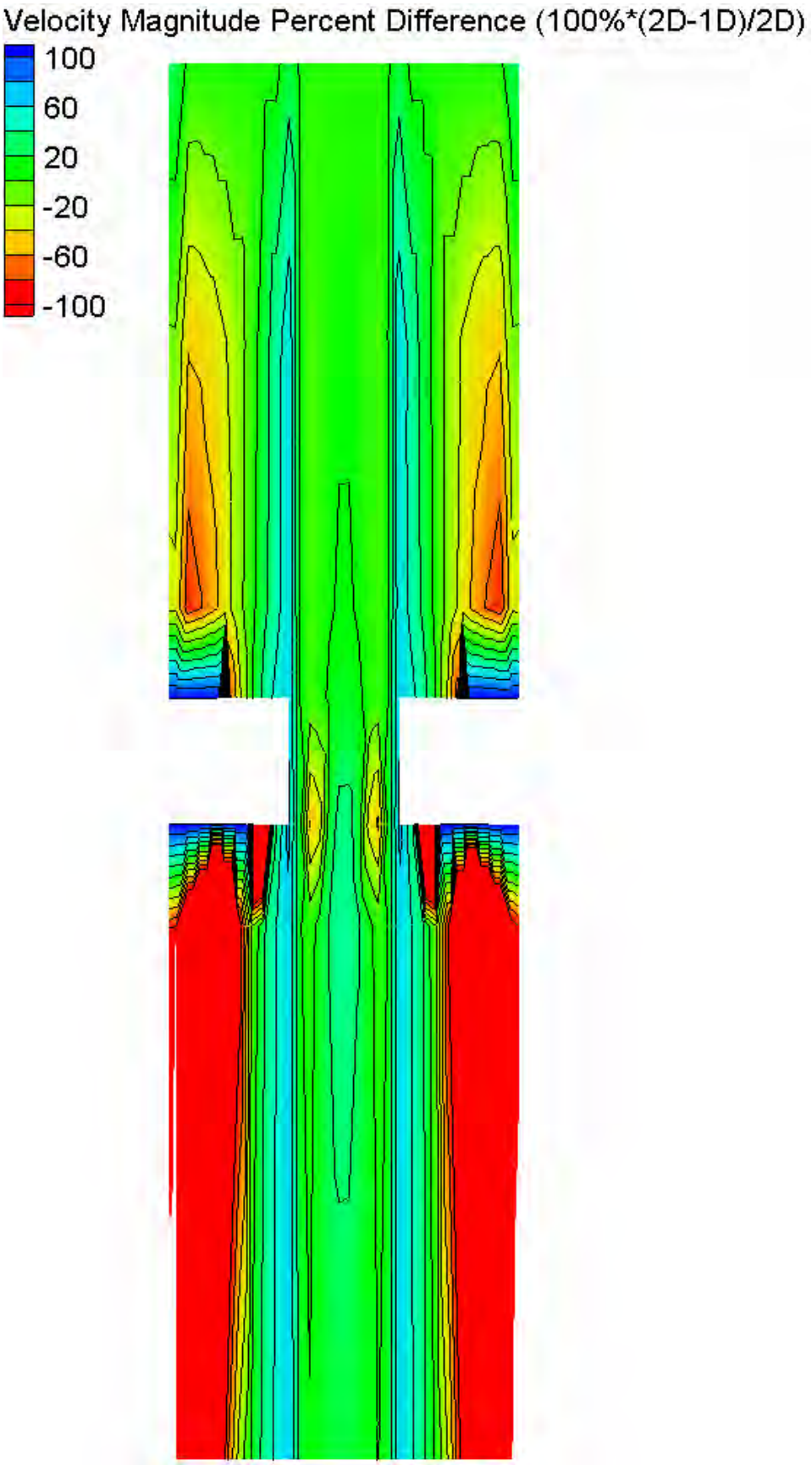

Velocity Magnitude Percent Difference Contours – Small Channel – Large Pier Blockage (25%)

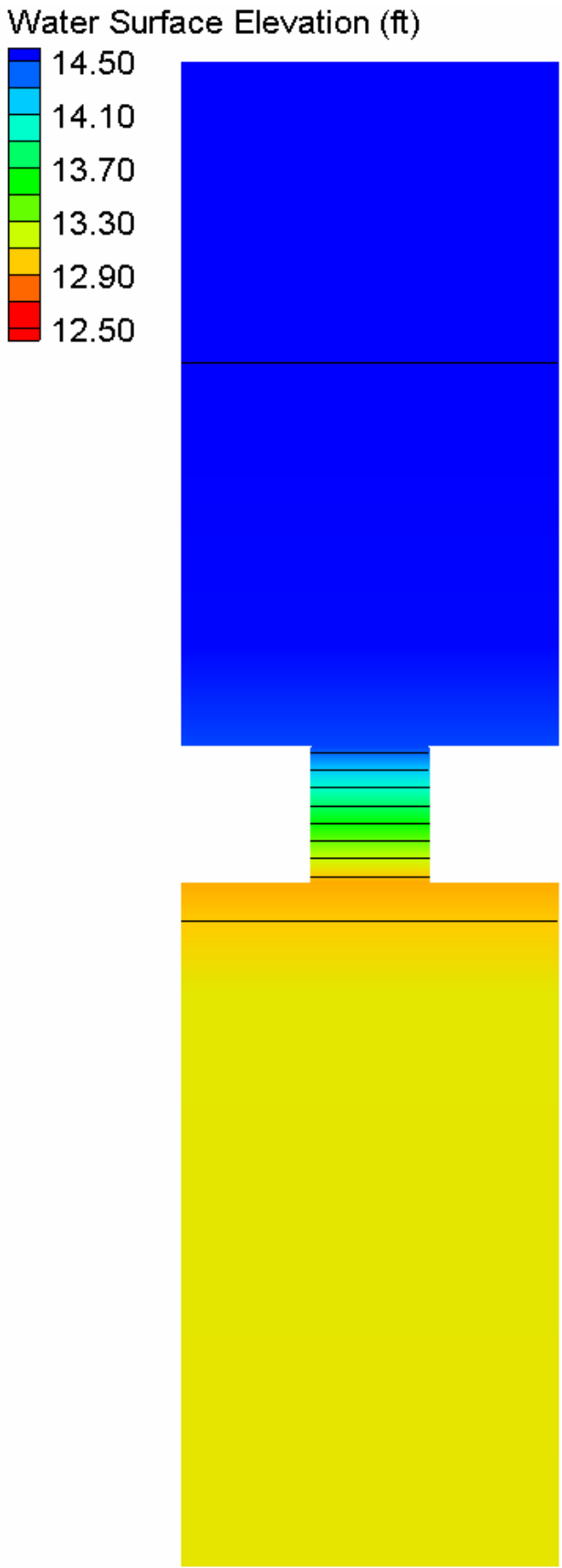

HEC-RAS Water Surface Elevation Contours – Small Channel – Large Pier Blockage (35%)

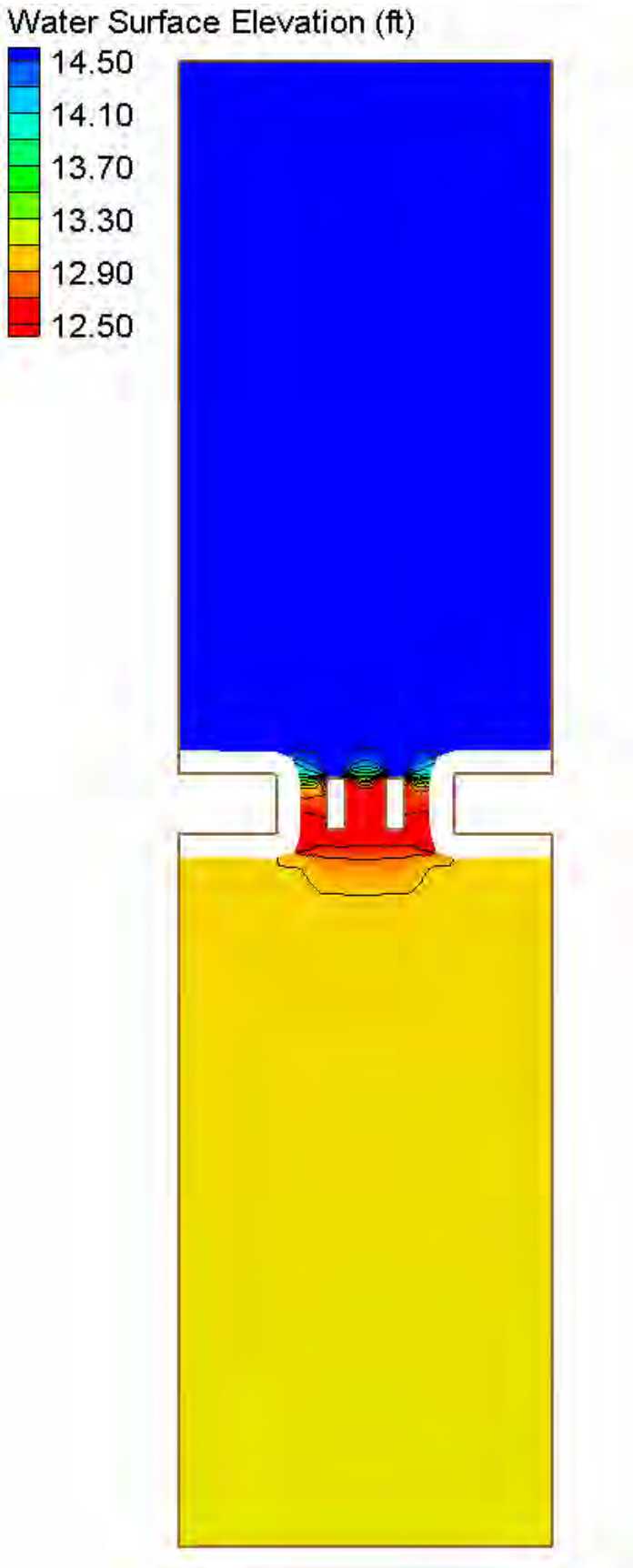

FESWMS Water Surface Elevation Contours – Small Channel – Large Pier Blockage (35%)

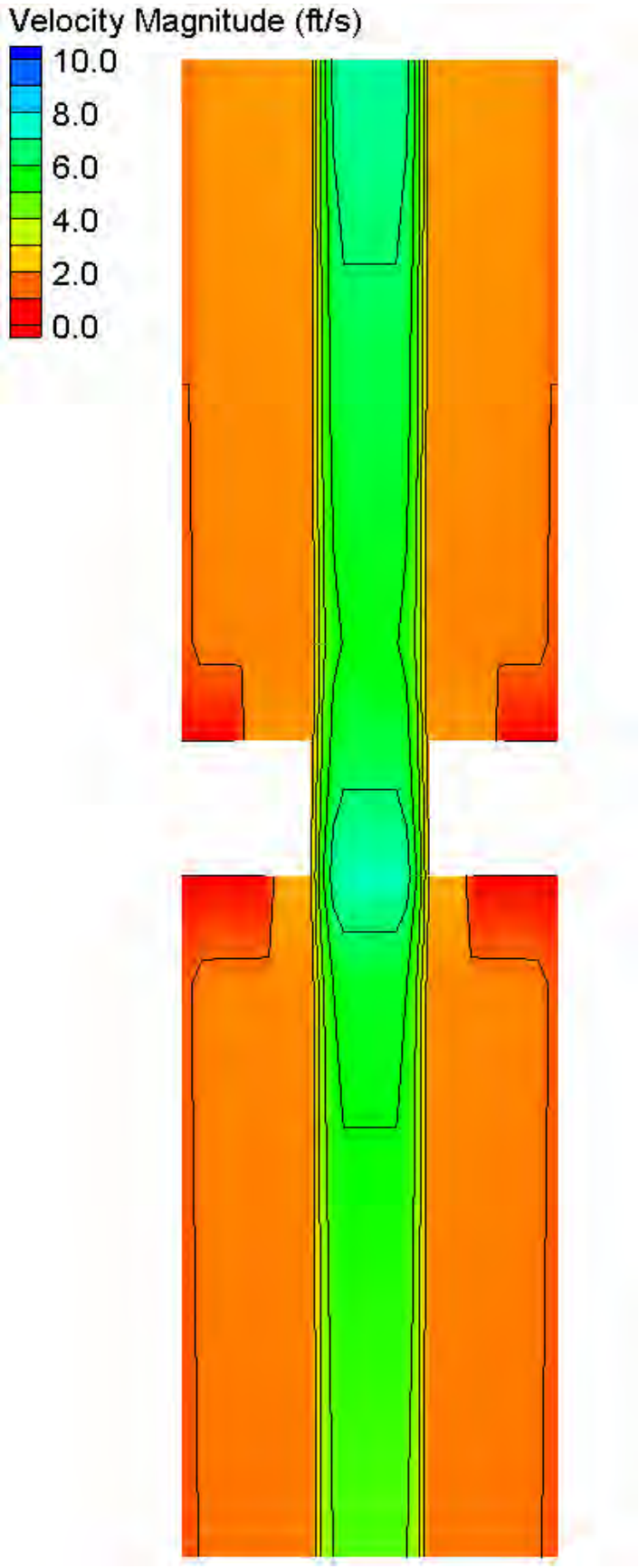

HEC-RAS Velocity Magnitude Contours – Small Channel – Large Pier Blockage (35%)

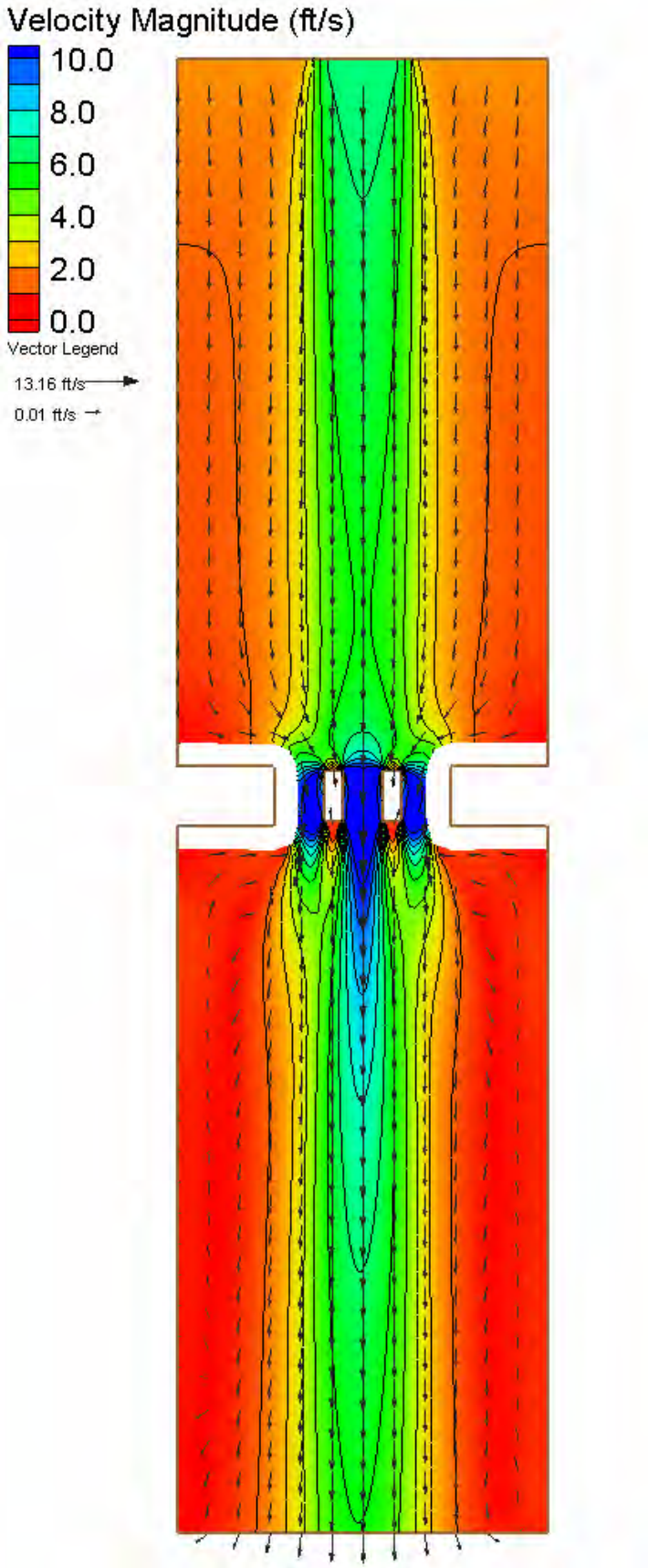

FESWMS Velocity Magnitude Contours – Small Channel – Large Pier Blockage (35%)

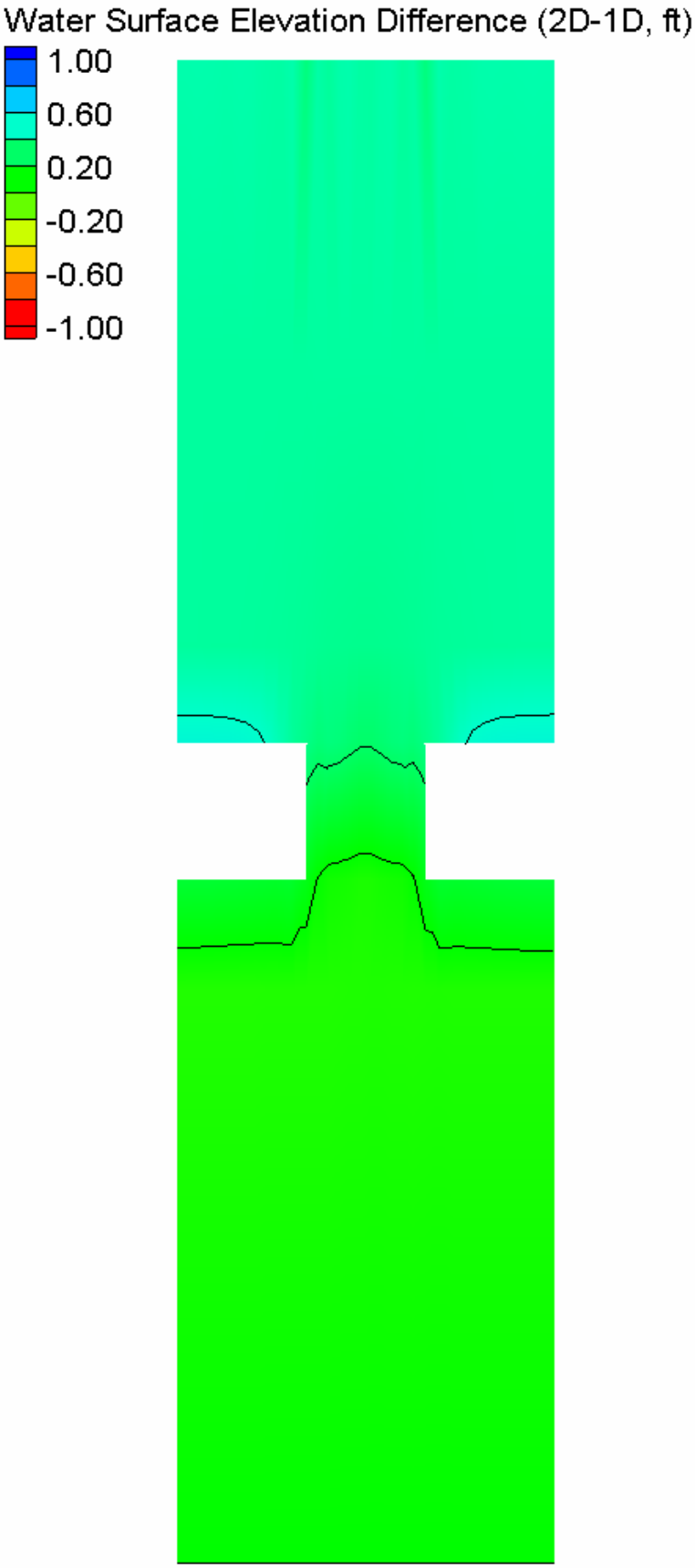

Water Surface Elevation Difference Contours – Small Channel – Large Pier Blockage (35%)

Velocity Magnitude Difference Contours – Small Channel – Large Pier Blockage (35%)

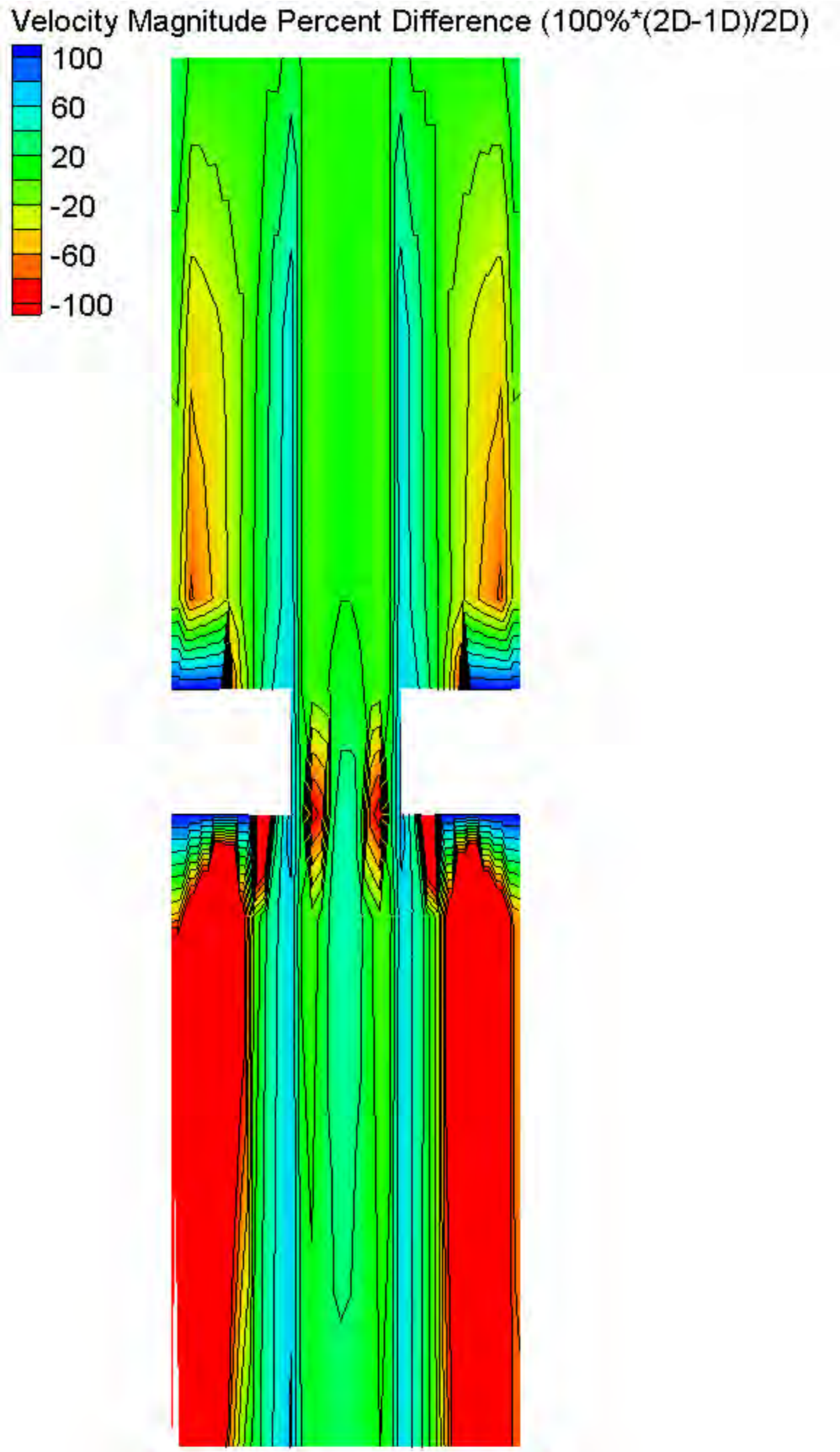

Velocity Magnitude Percent Difference Contours – Small Channel – Large Pier Blockage (35%)

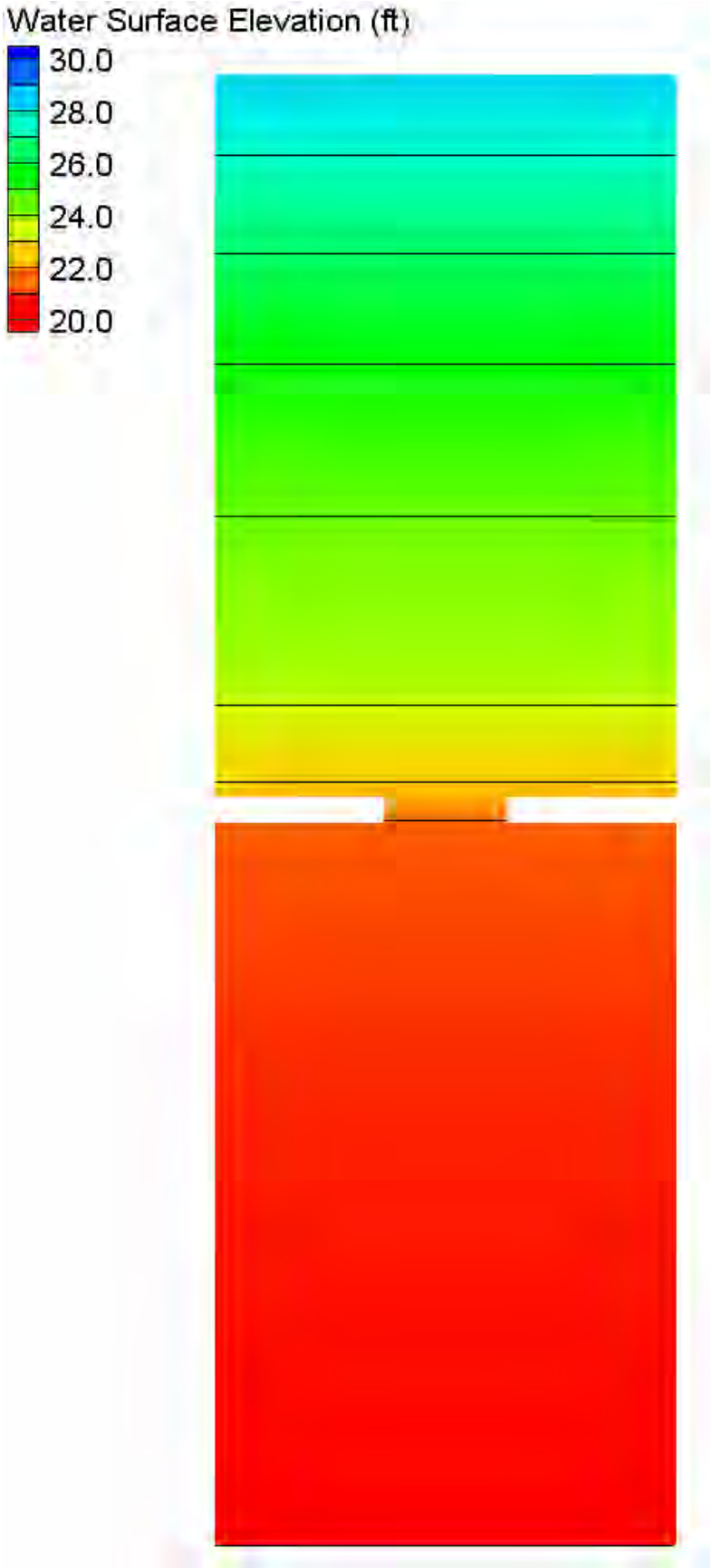

HEC-RAS Water Surface Elevation Contours – Large Channel – Large Pier Blockage (5%)

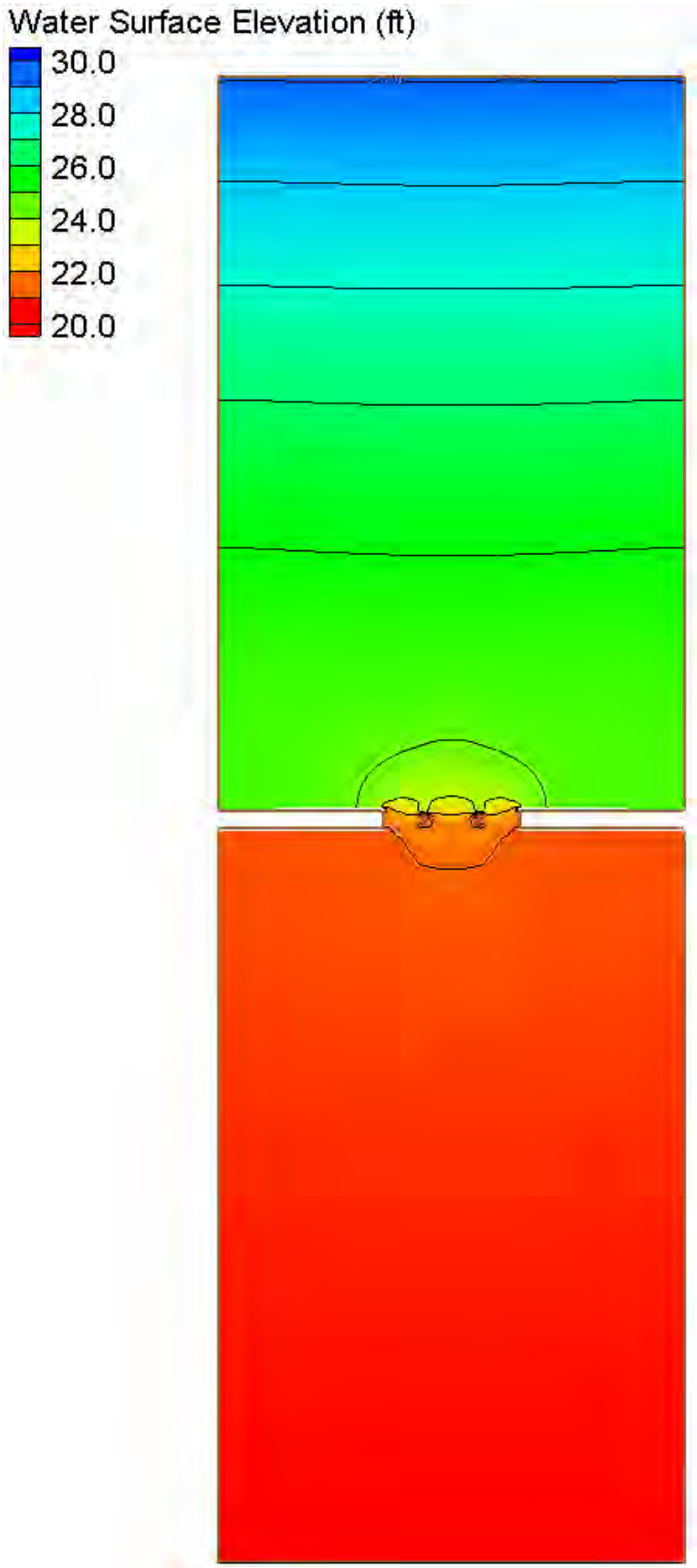

FESWMS Water Surface Elevation Contours – Large Channel – Large Pier Blockage (5%)

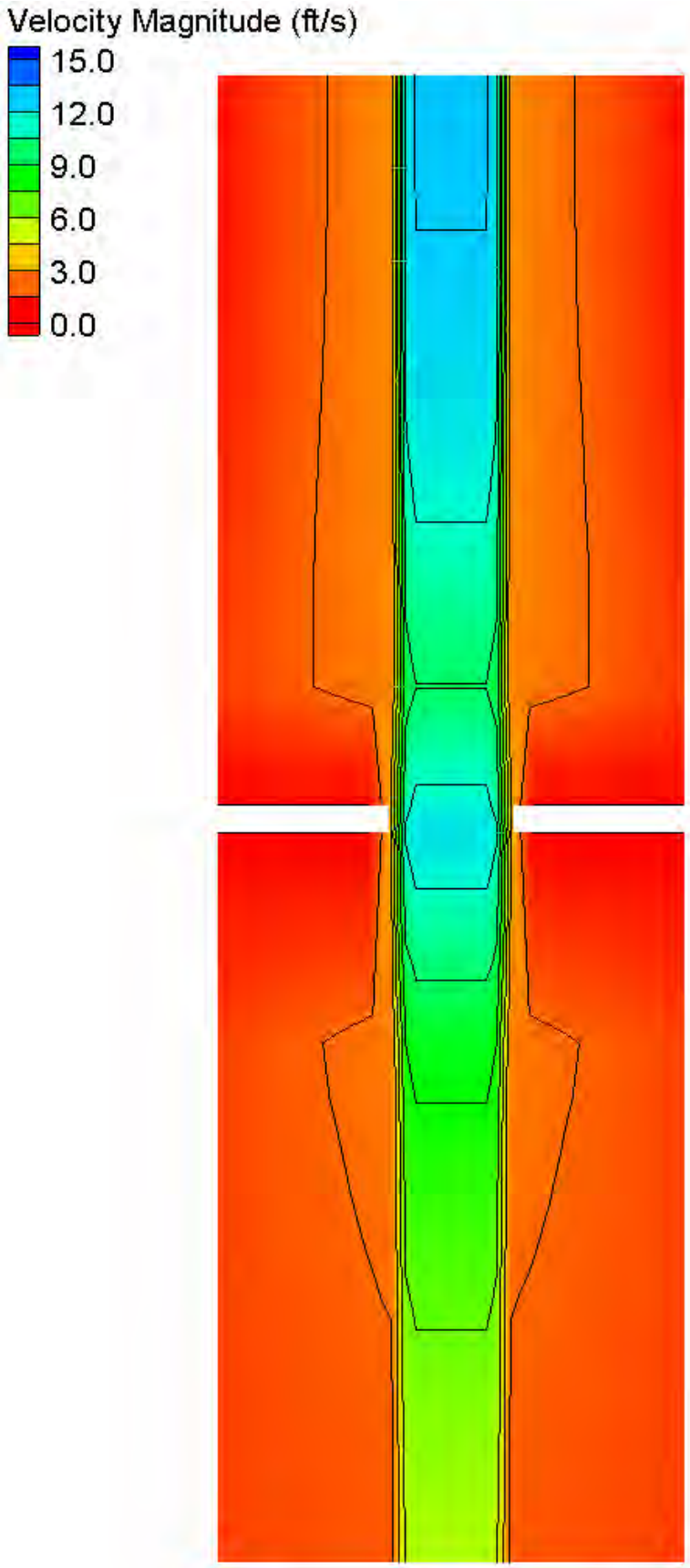

HEC-RAS Velocity Magnitude Contours – Large Channel – Large Pier Blockage (5%)

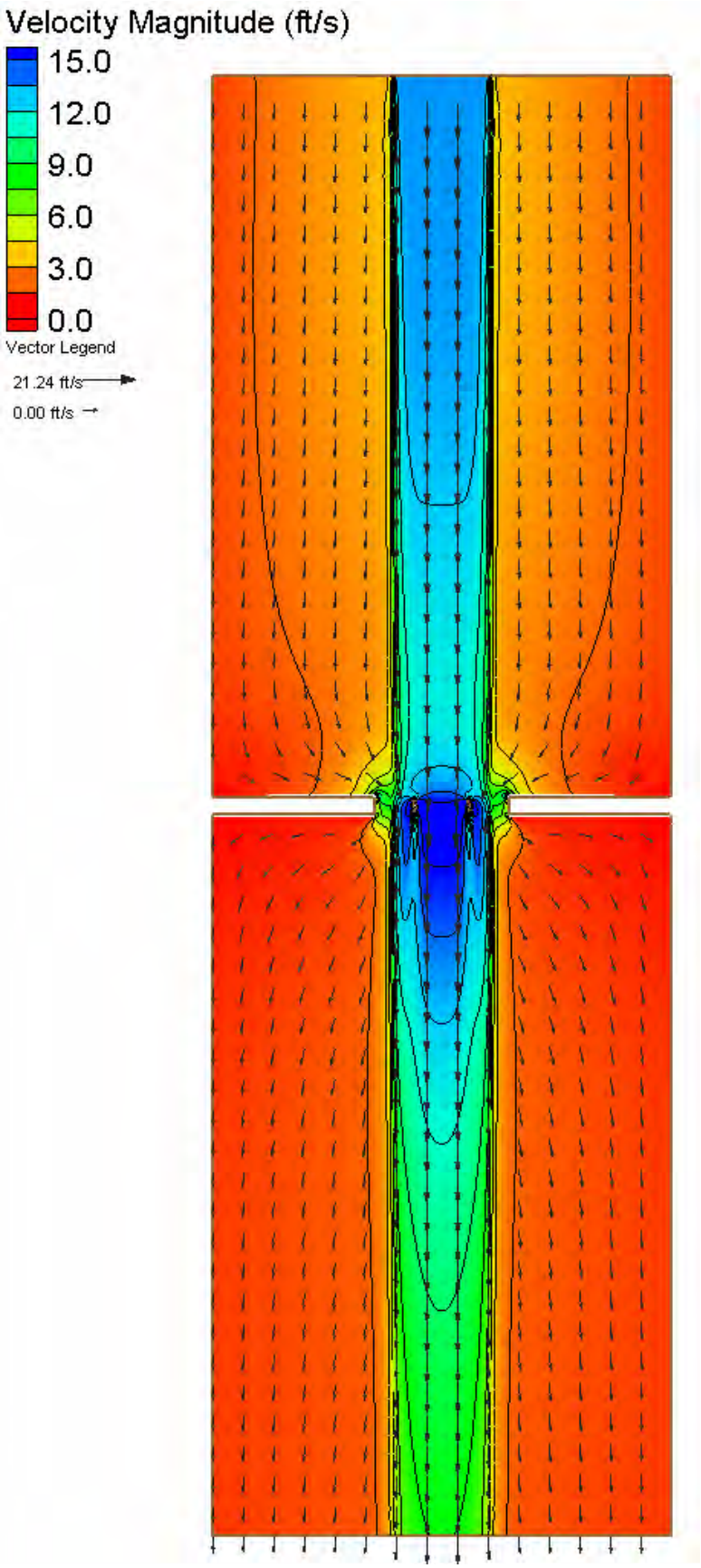

FESWMS Velocity Magnitude Contours – Large Channel – Large Pier Blockage (5%)

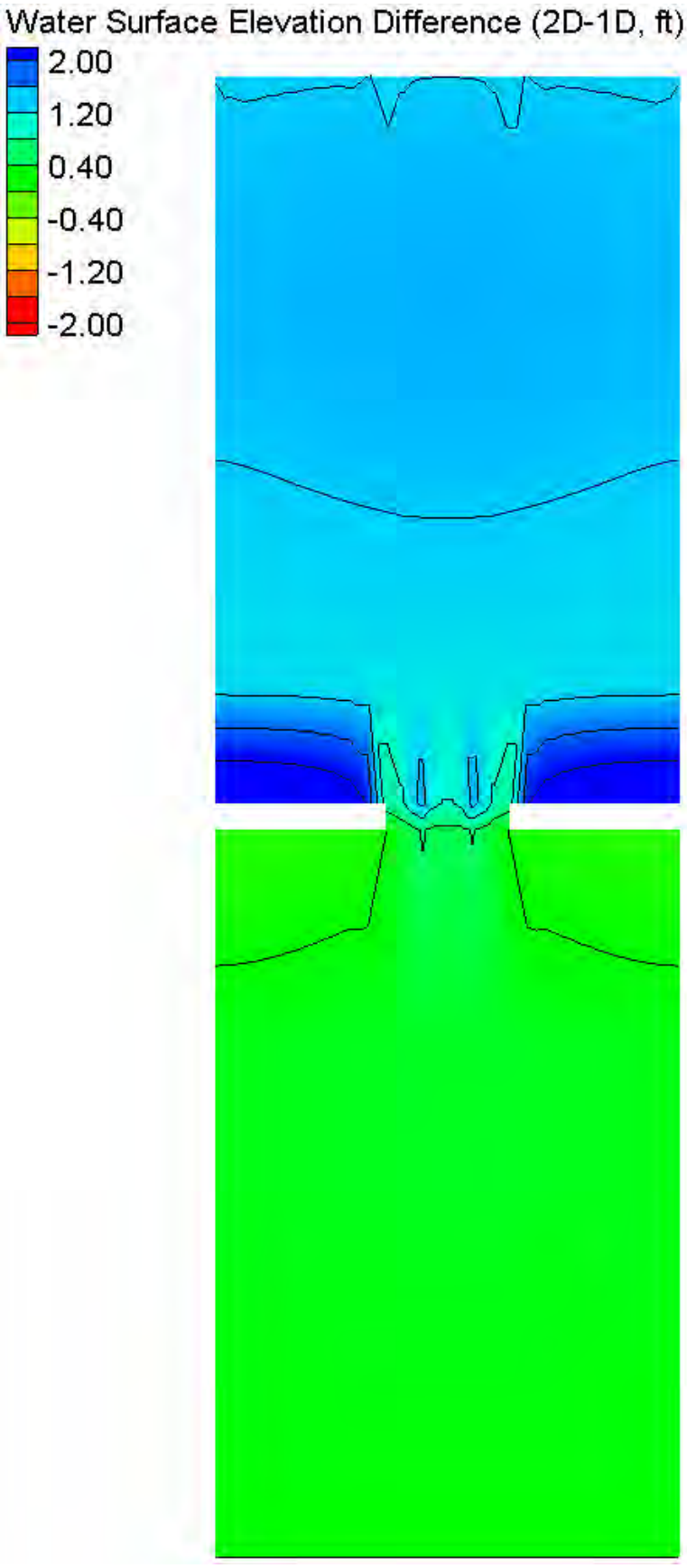

Water Surface Elevation Difference Contours – Large Channel – Large Pier Blockage (5%)

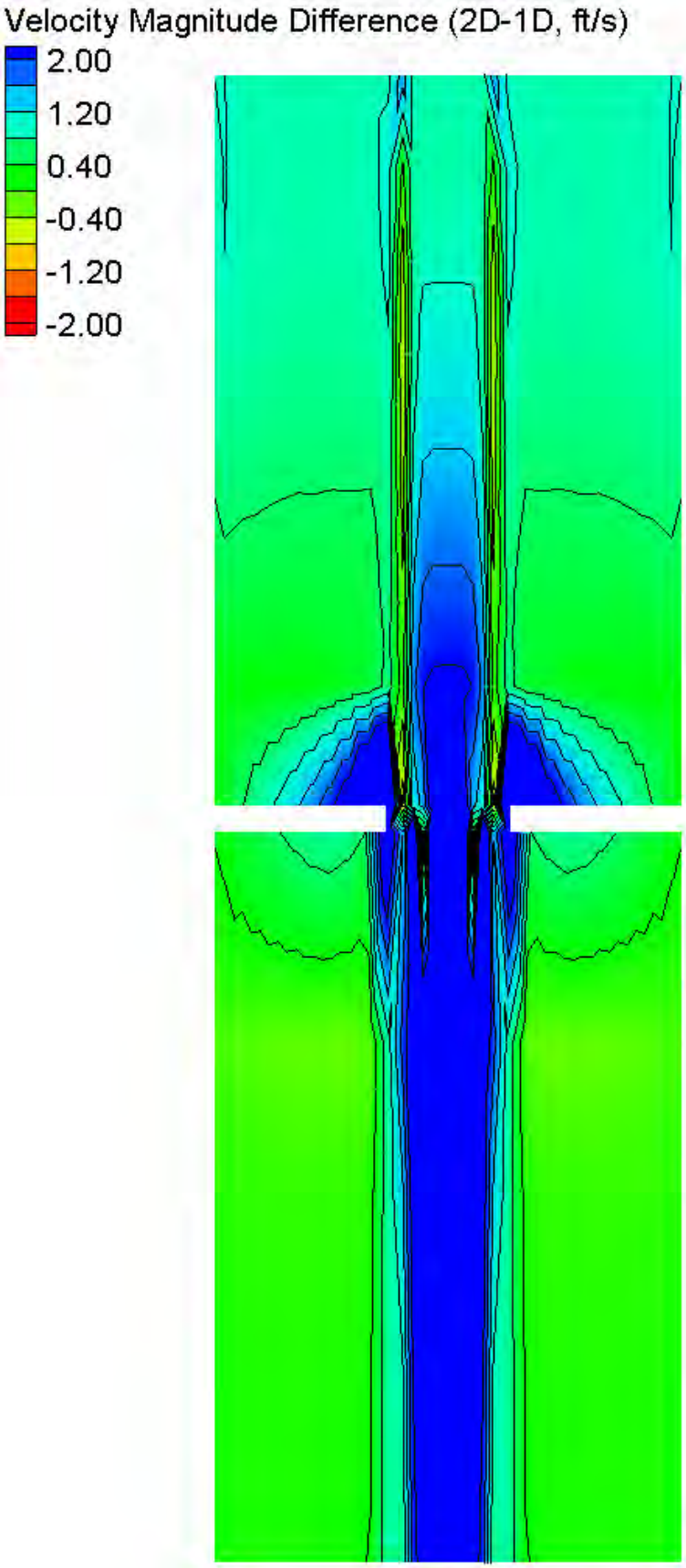

Velocity Magnitude Difference Contours – Large Channel – Large Pier Blockage (5%)

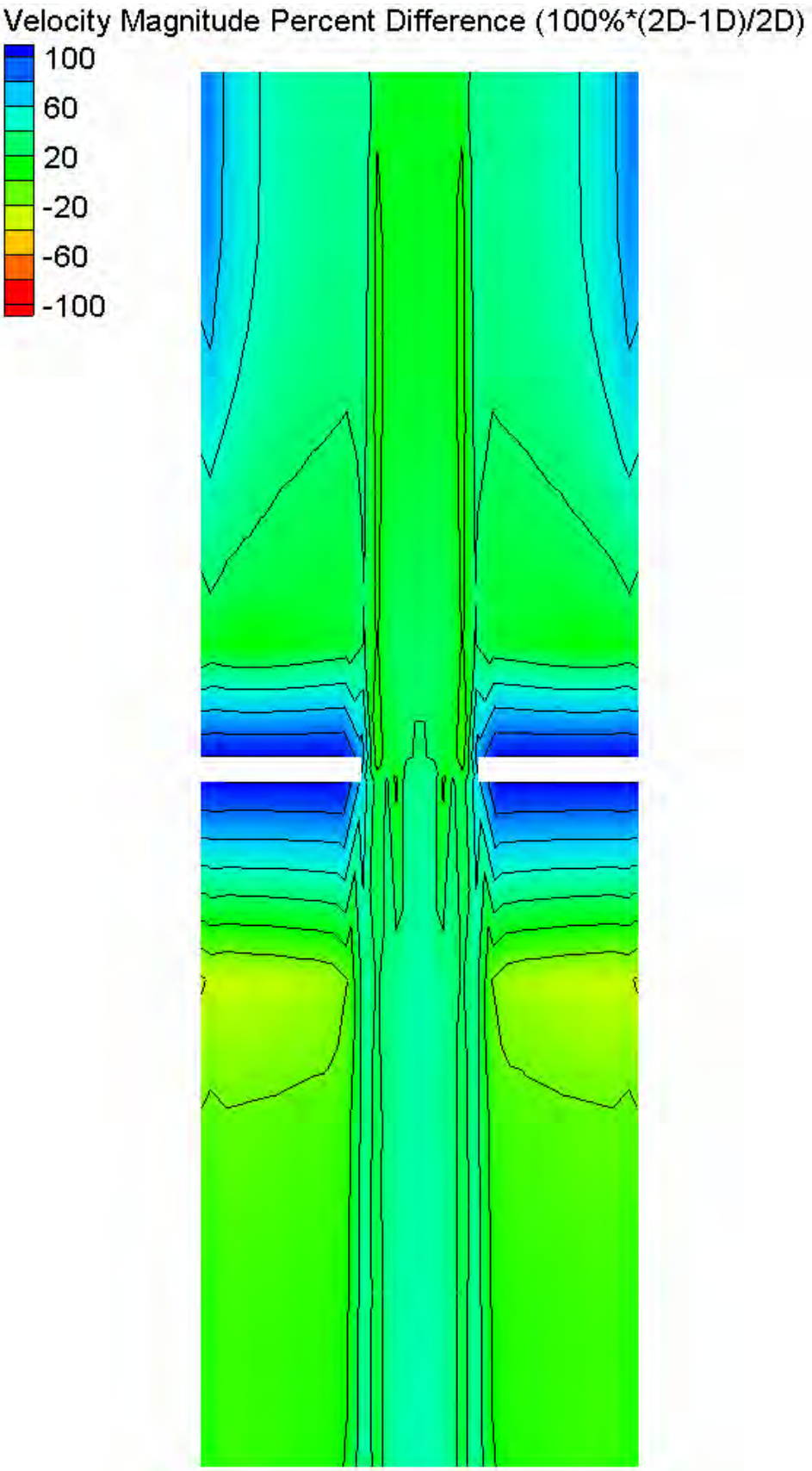

Velocity Magnitude Percent Difference Contours – Large Channel – Large Pier Blockage (5%)

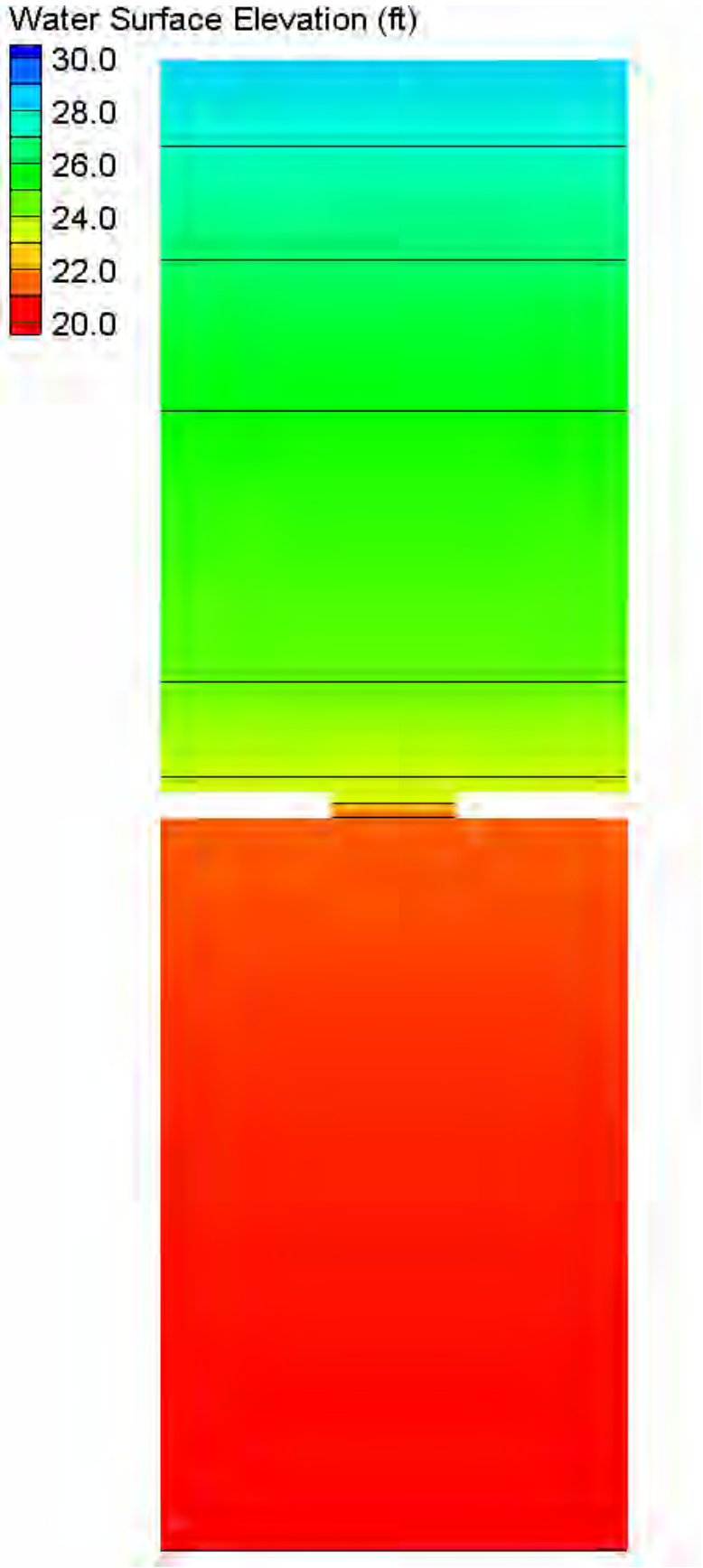

HEC-RAS Water Surface Elevation Contours – Large Channel – Large Pier Blockage (15%)

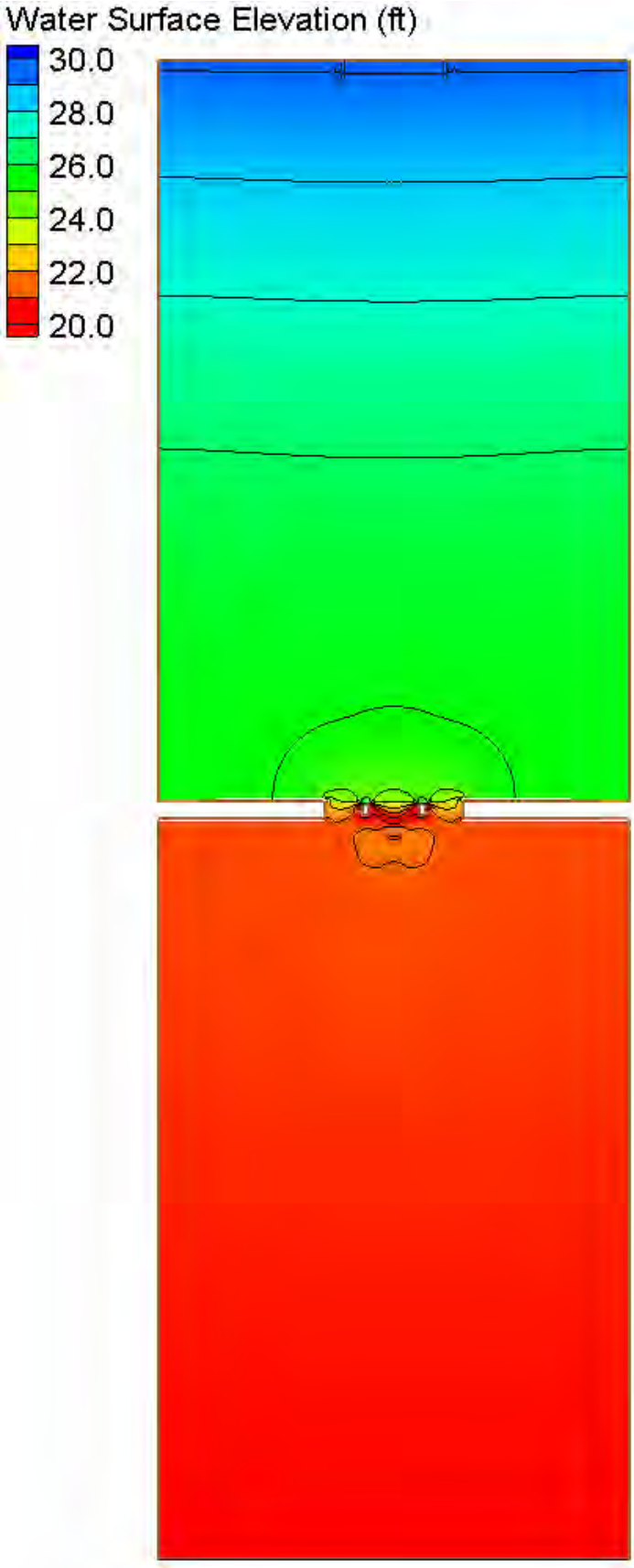

FESWMS Water Surface Elevation Contours – Large Channel – Large Pier Blockage (15%)

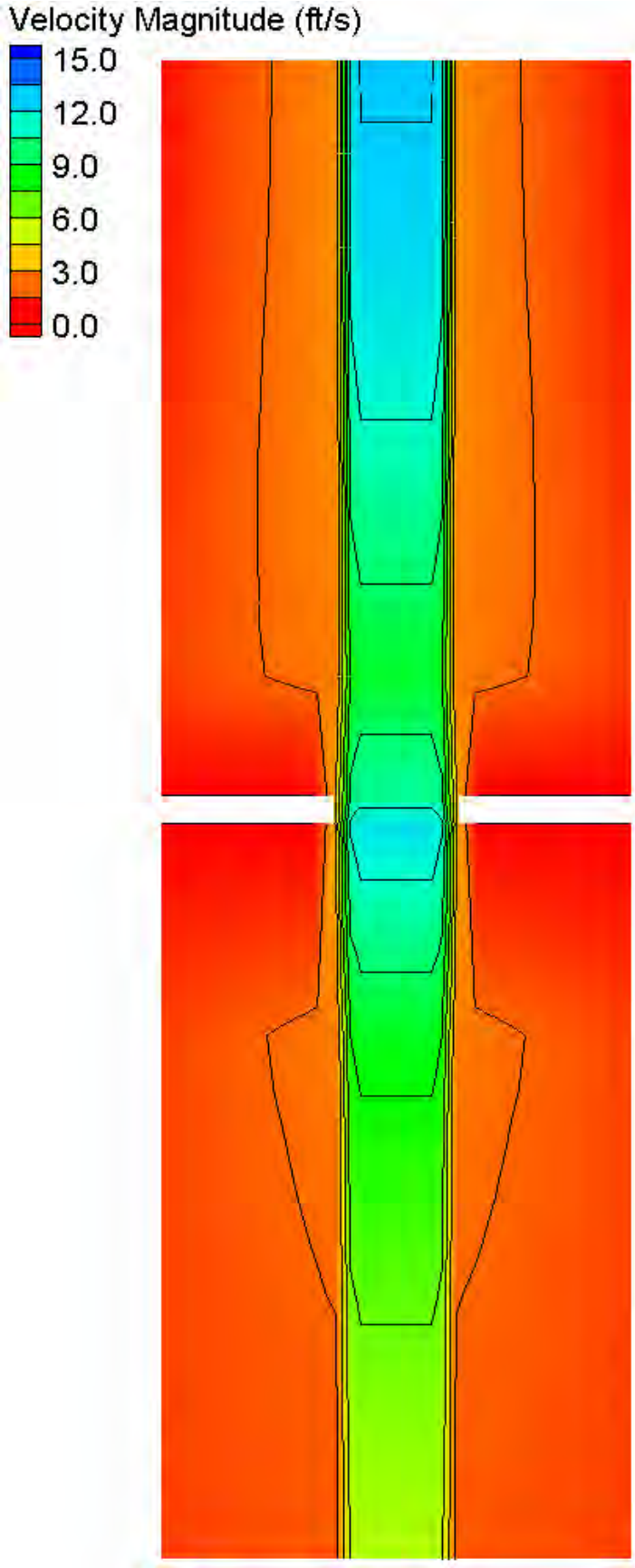

HEC-RAS Velocity Magnitude Contours – Large Channel – Large Pier Blockage (15%)

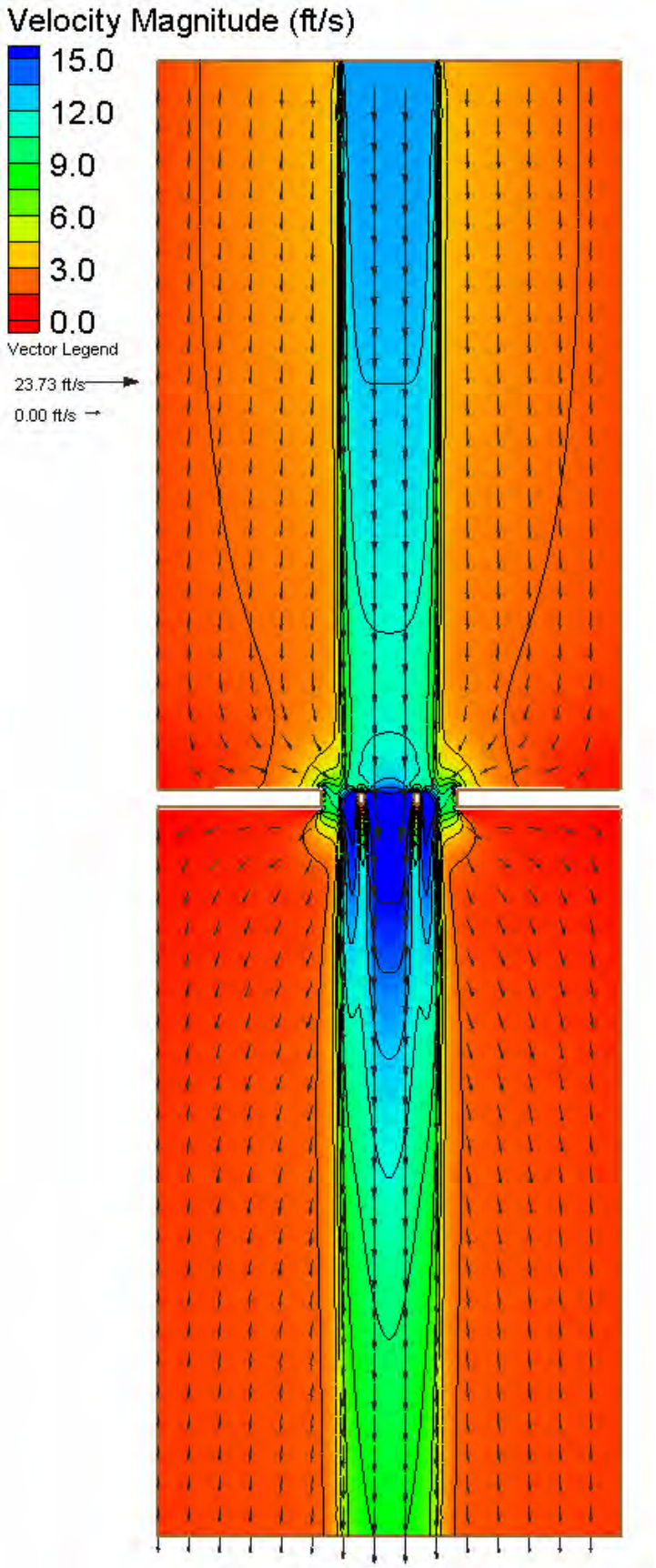

FESWMS Velocity Magnitude Contours – Large Channel – Large Pier Blockage (15%)

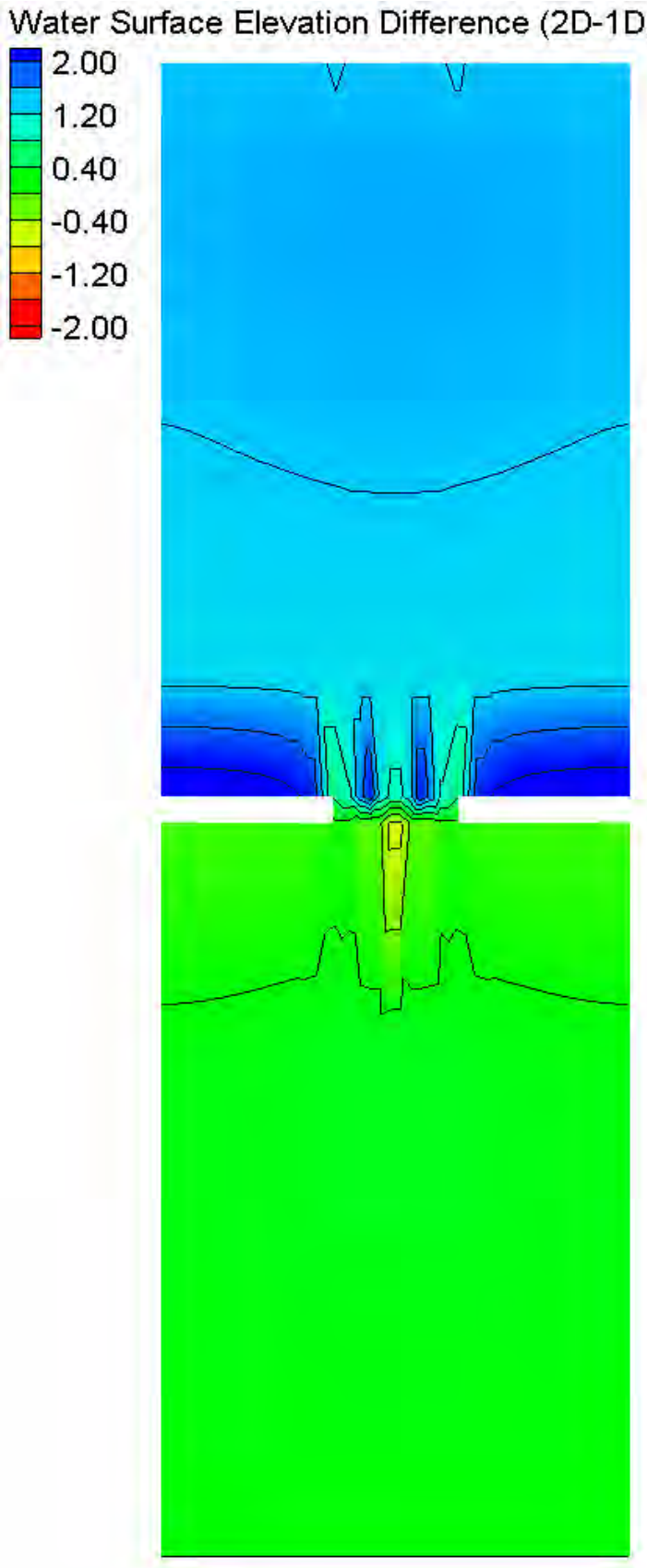

Water Surface Elevation Difference Contours – Large Channel – Large Pier Blockage (15%)

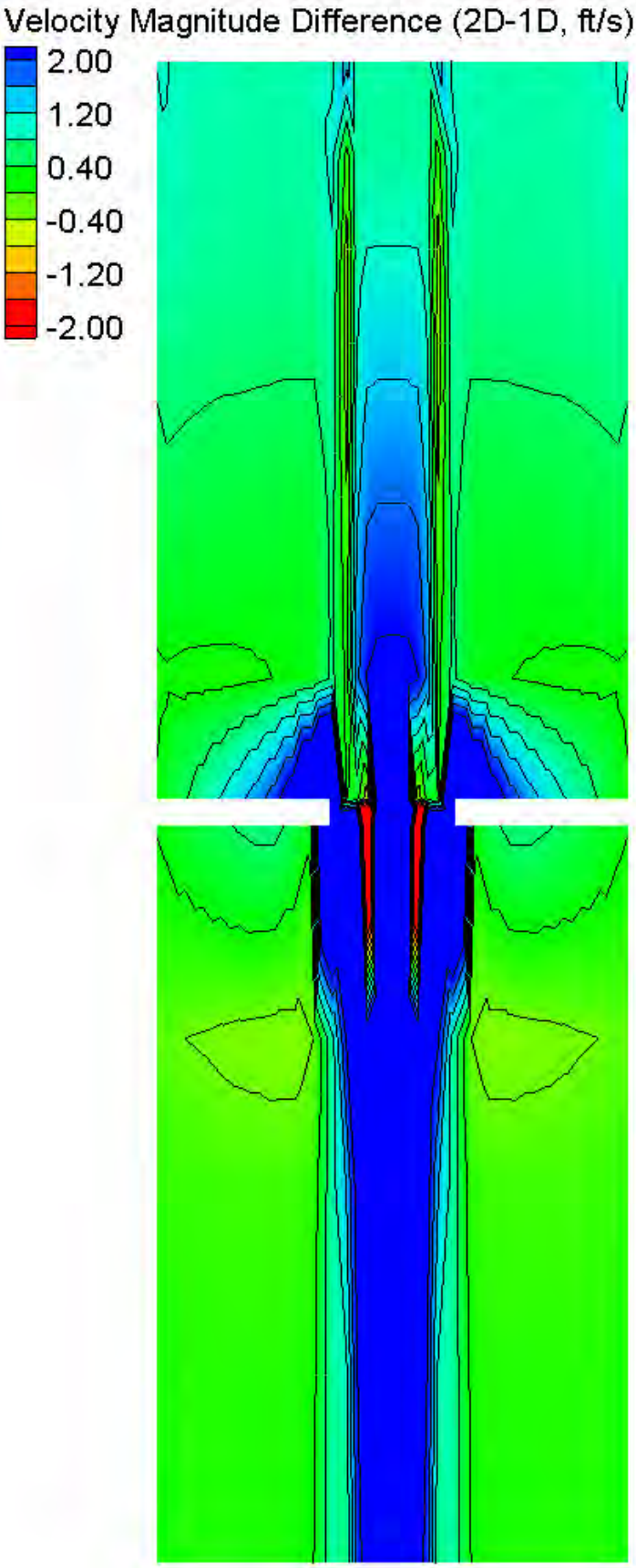

Velocity Magnitude Difference Contours – Large Channel – Large Pier Blockage (15%)

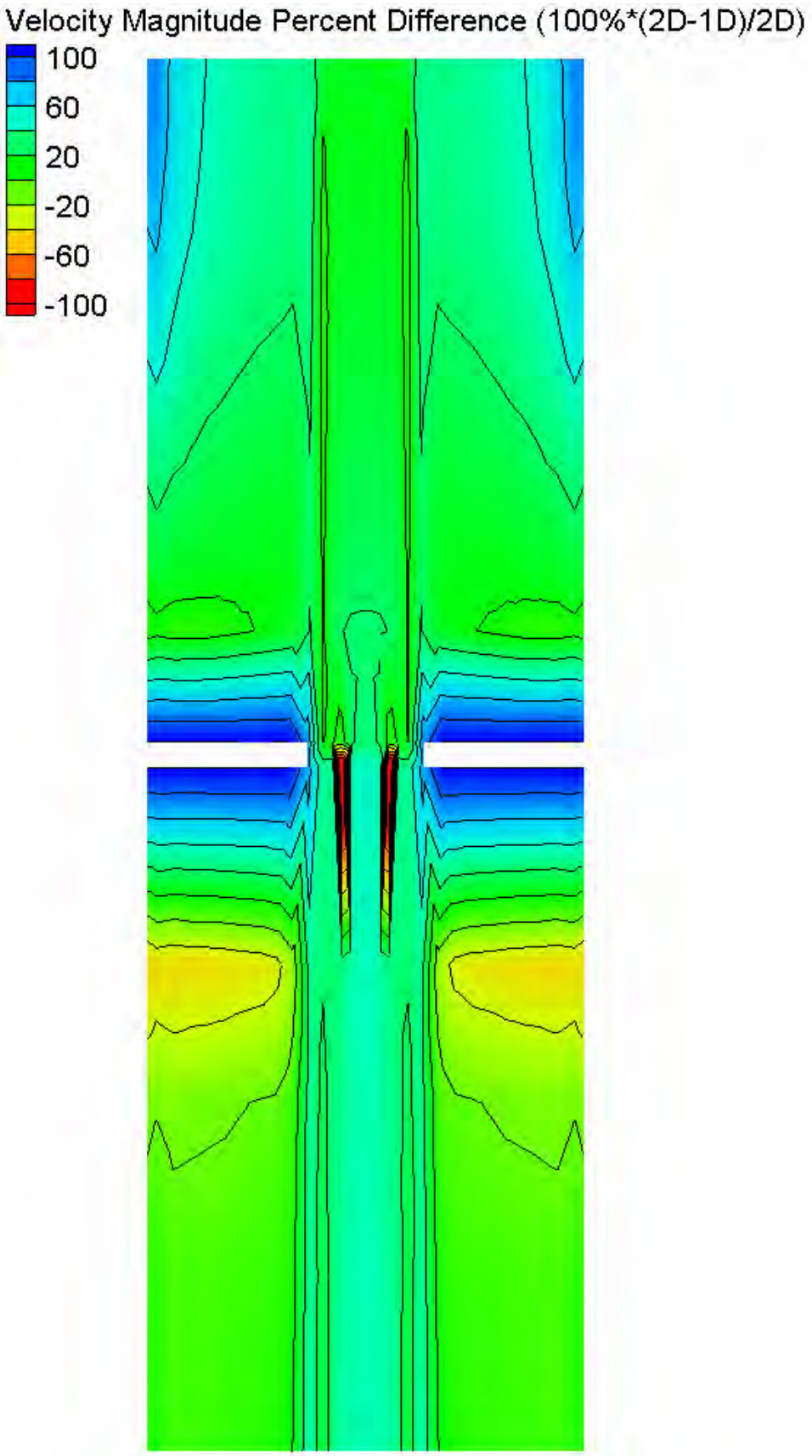

Velocity Magnitude Percent Difference Contours – Large Channel – Large Pier Blockage (15%)

HEC-RAS Water Surface Elevation Contours – Large Channel – Large Pier Blockage (25%)

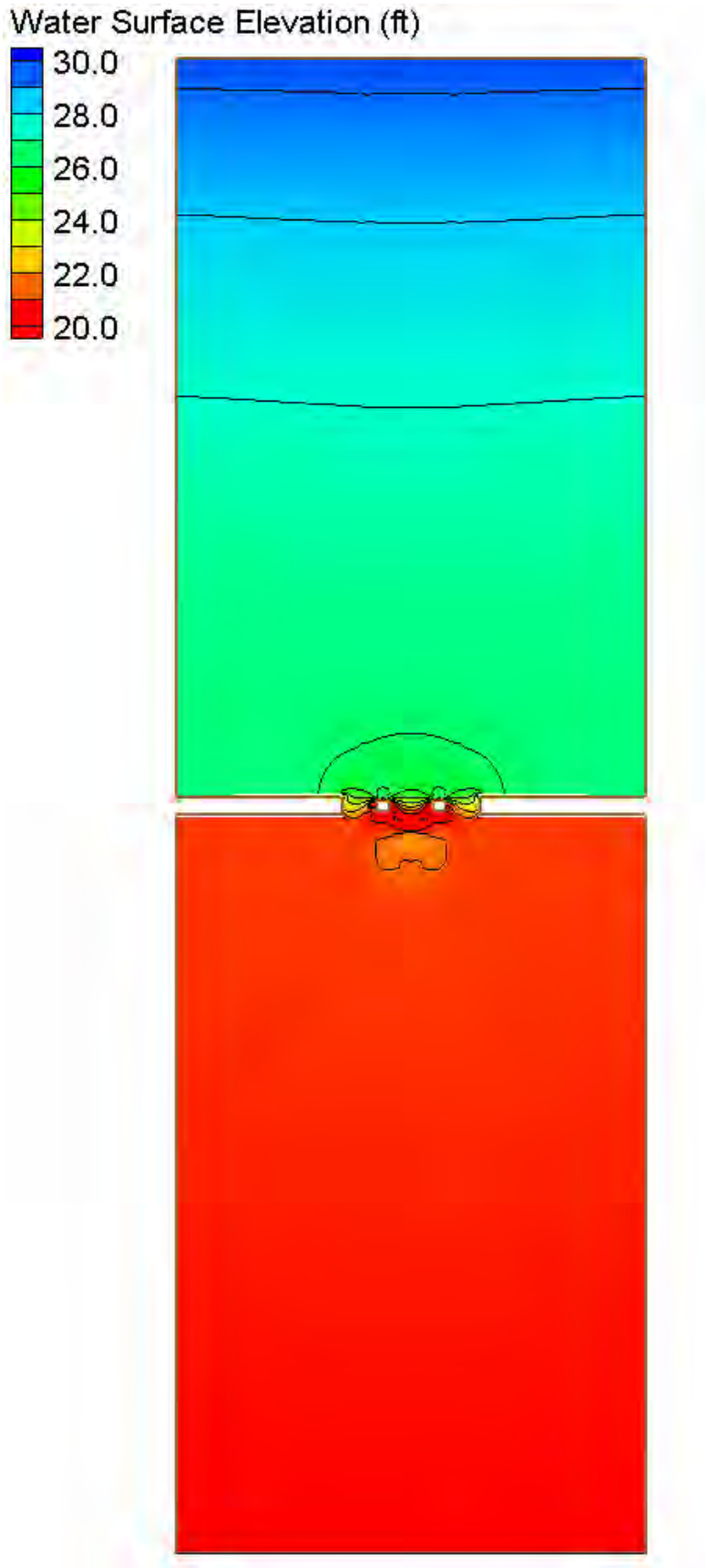

FESWMS Water Surface Elevation Contours – Large Channel – Large Pier Blockage (25%)

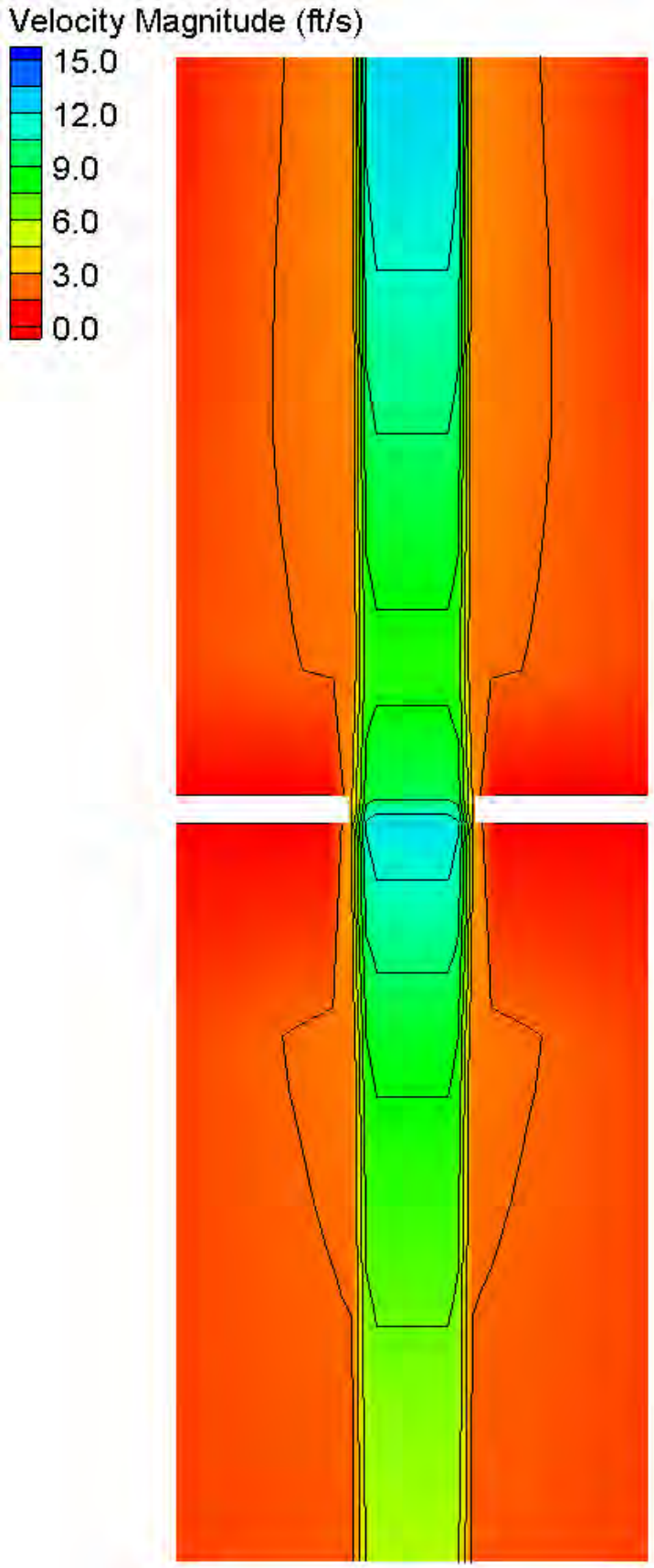

HEC-RAS Velocity Magnitude Contours – Large Channel – Large Pier Blockage (25%)

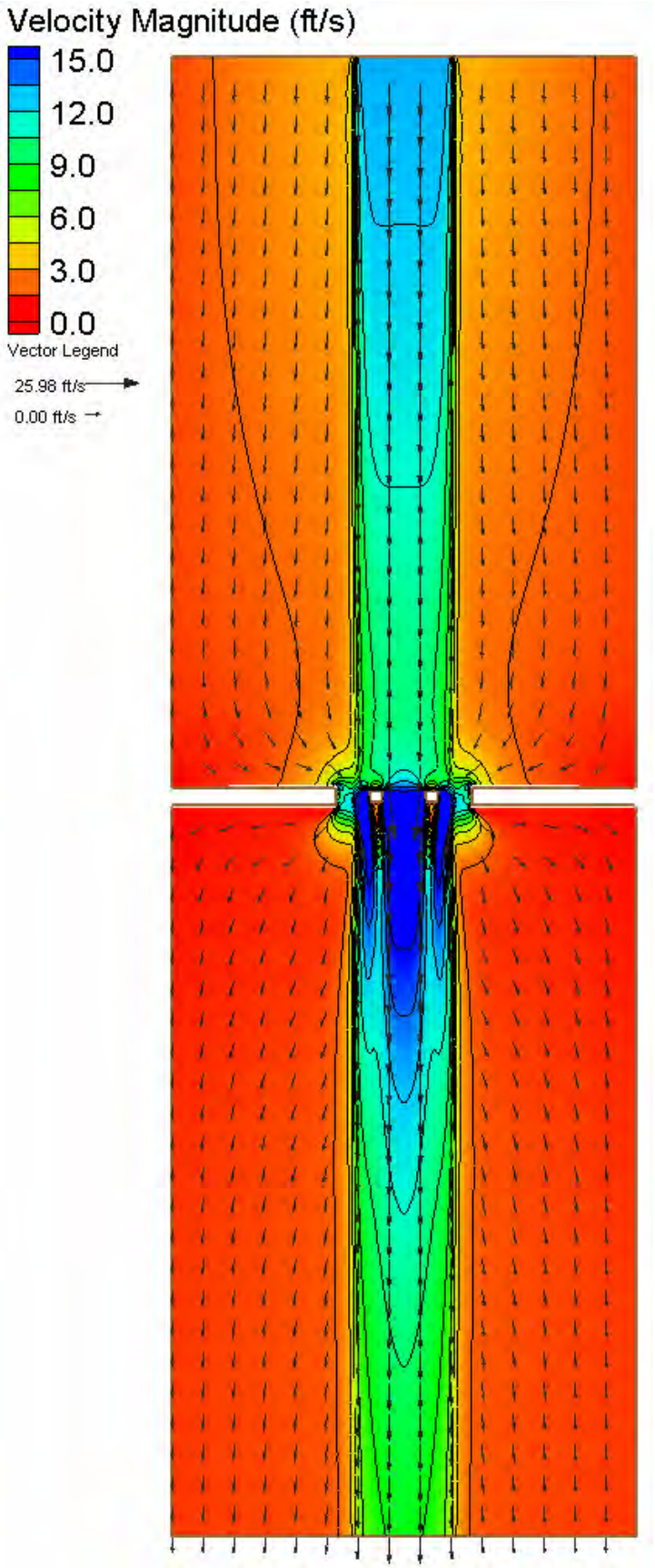

FESWMS Velocity Magnitude Contours – Large Channel – Large Pier Blockage (25%)

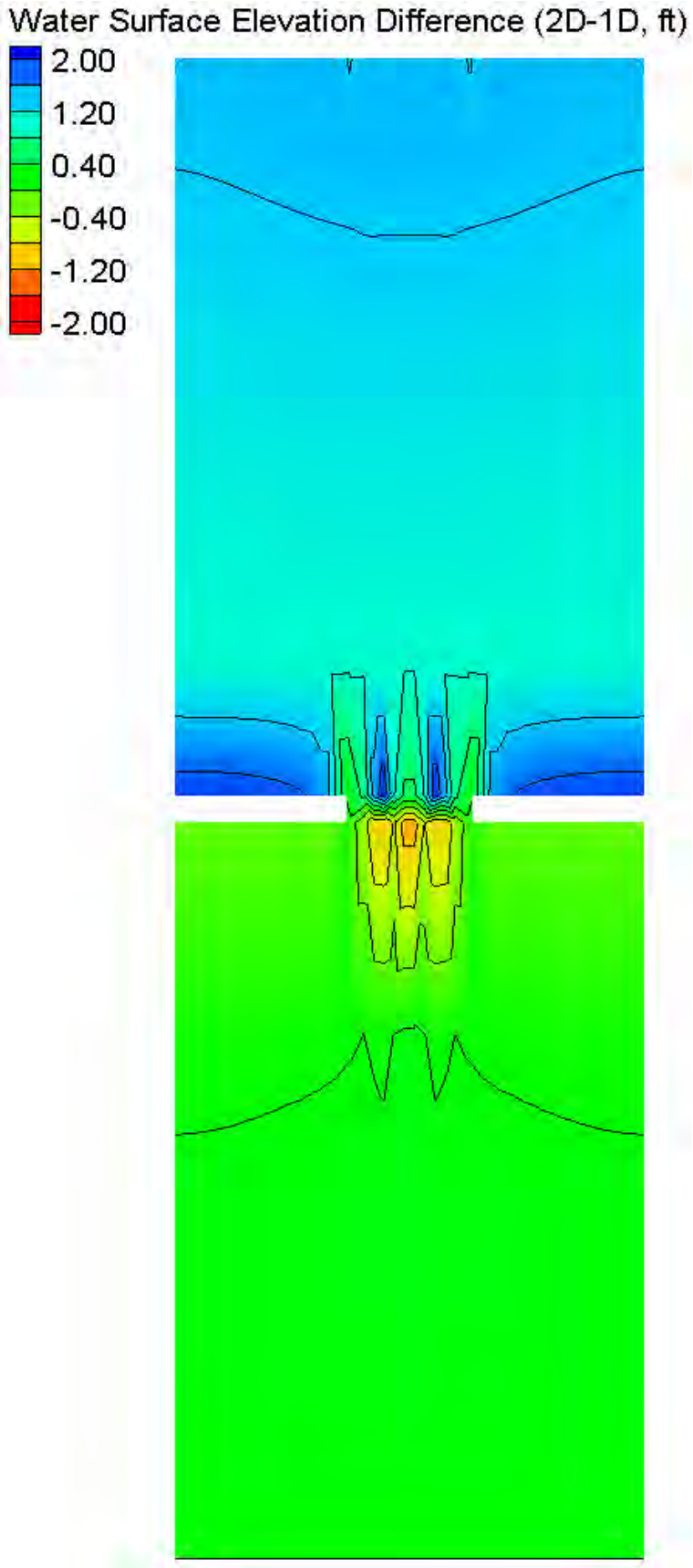

Water Surface Elevation Difference Contours – Large Channel – Large Pier Blockage (25%)

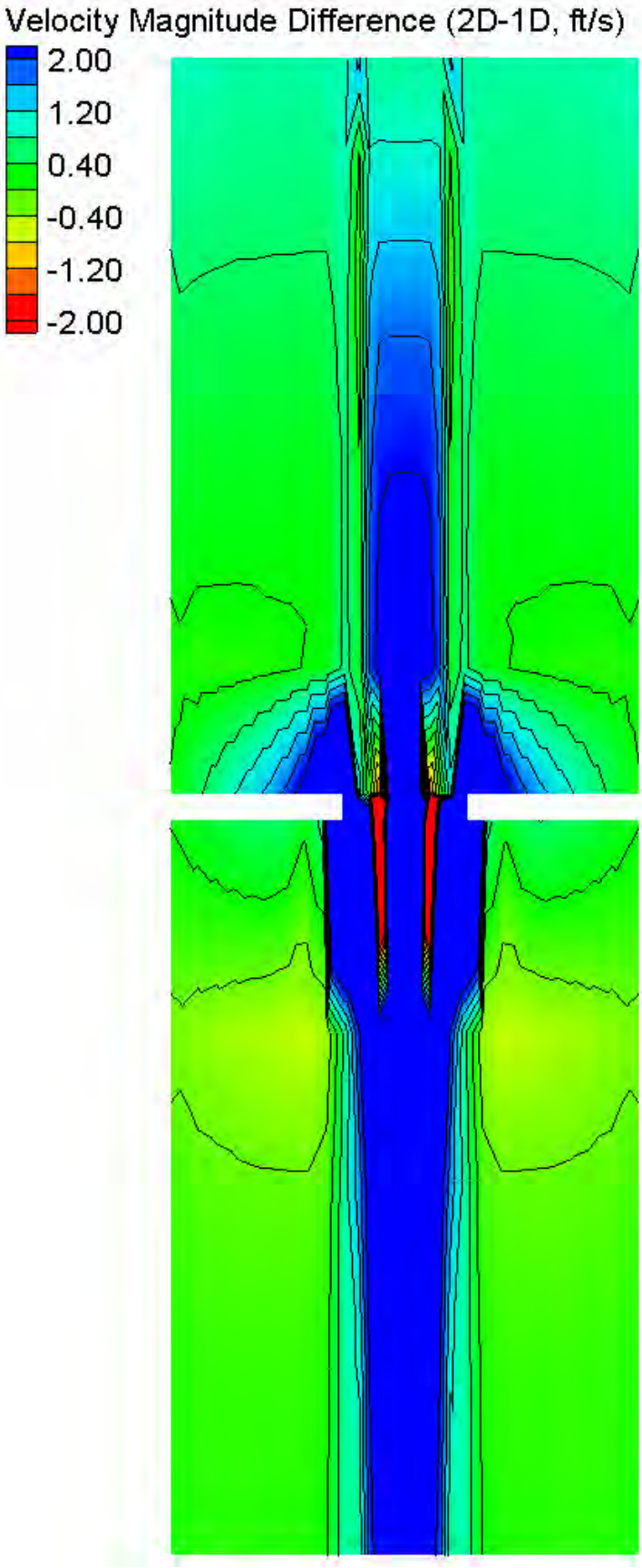

Velocity Magnitude Difference Contours – Large Channel – Large Pier Blockage (25%)

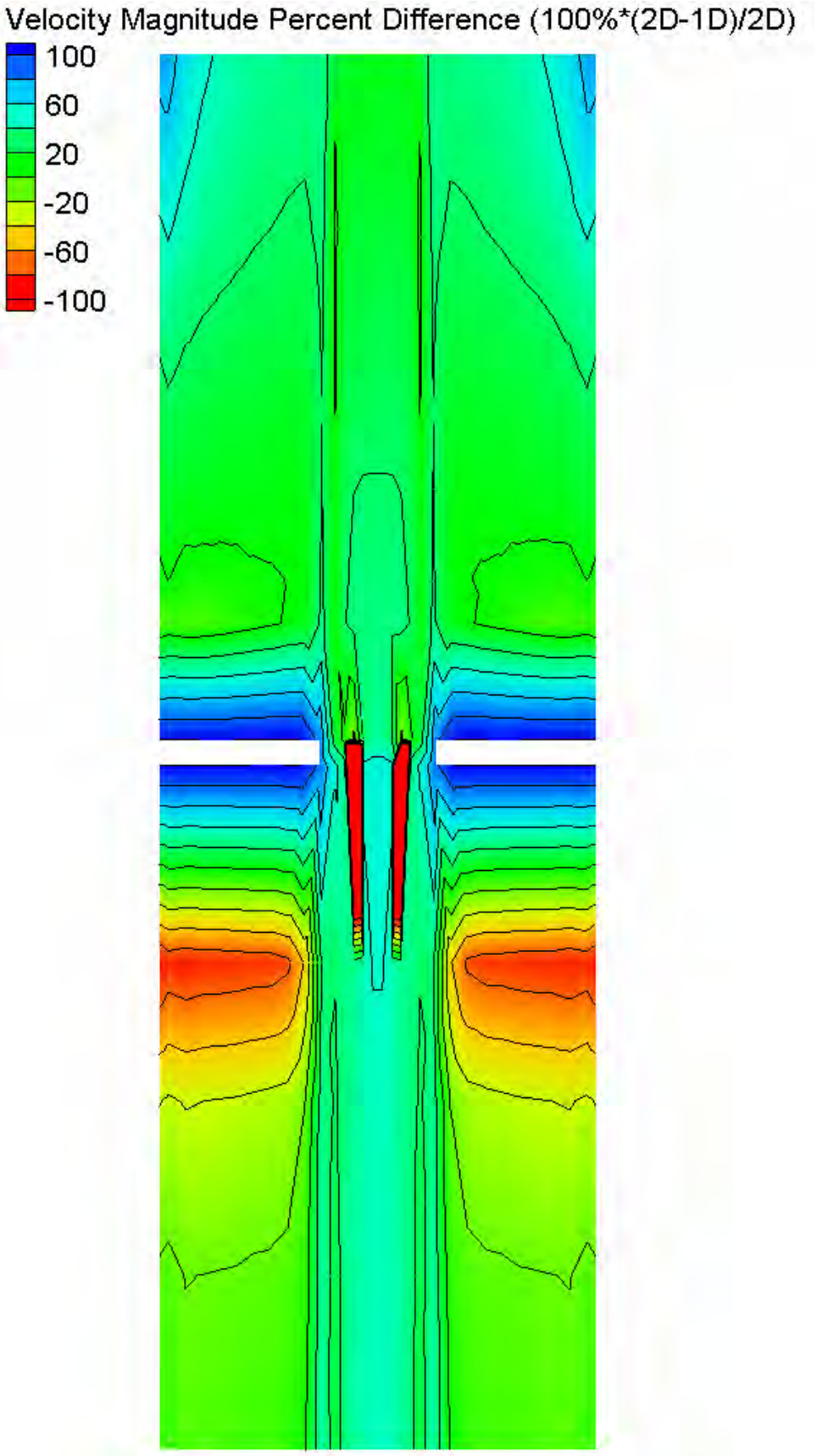

Velocity Magnitude Percent Difference Contours – Large Channel – Large Pier Blockage (25%)

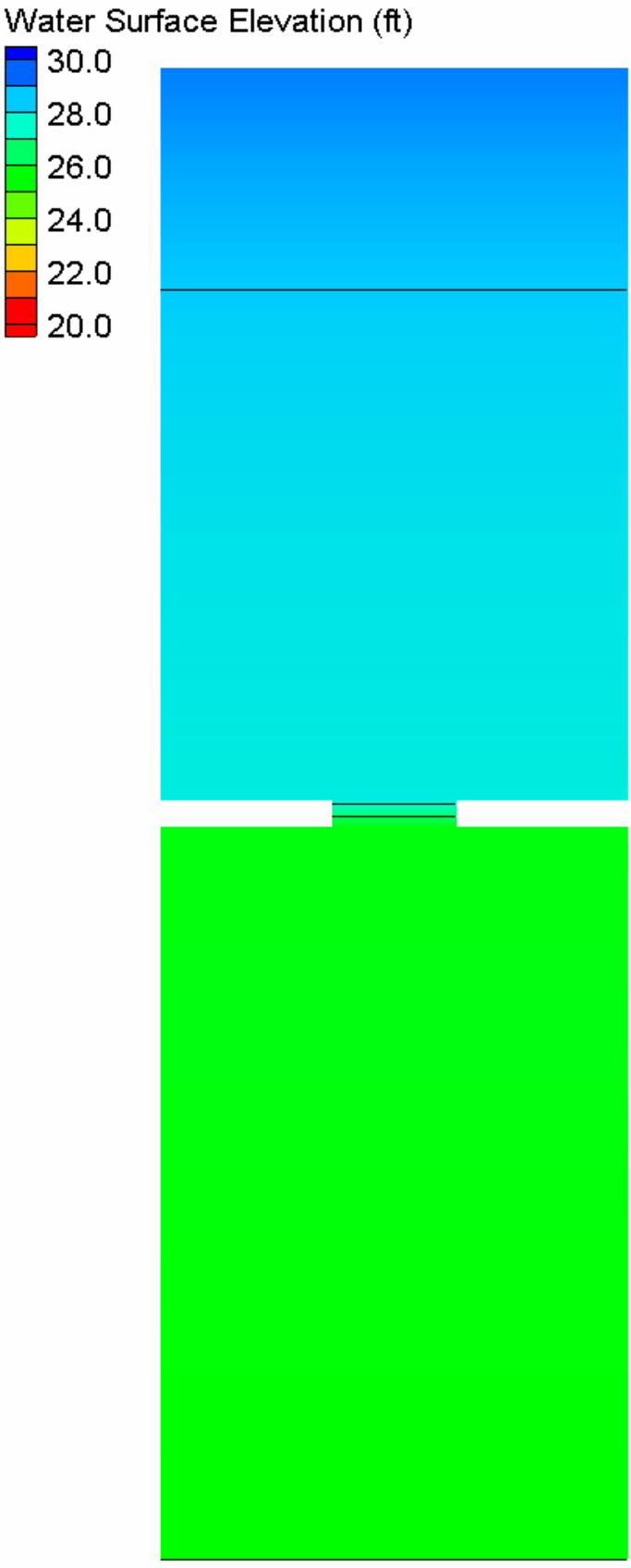

HEC-RAS Water Surface Elevation Contours – Large Channel – Large Pier Blockage (35%)

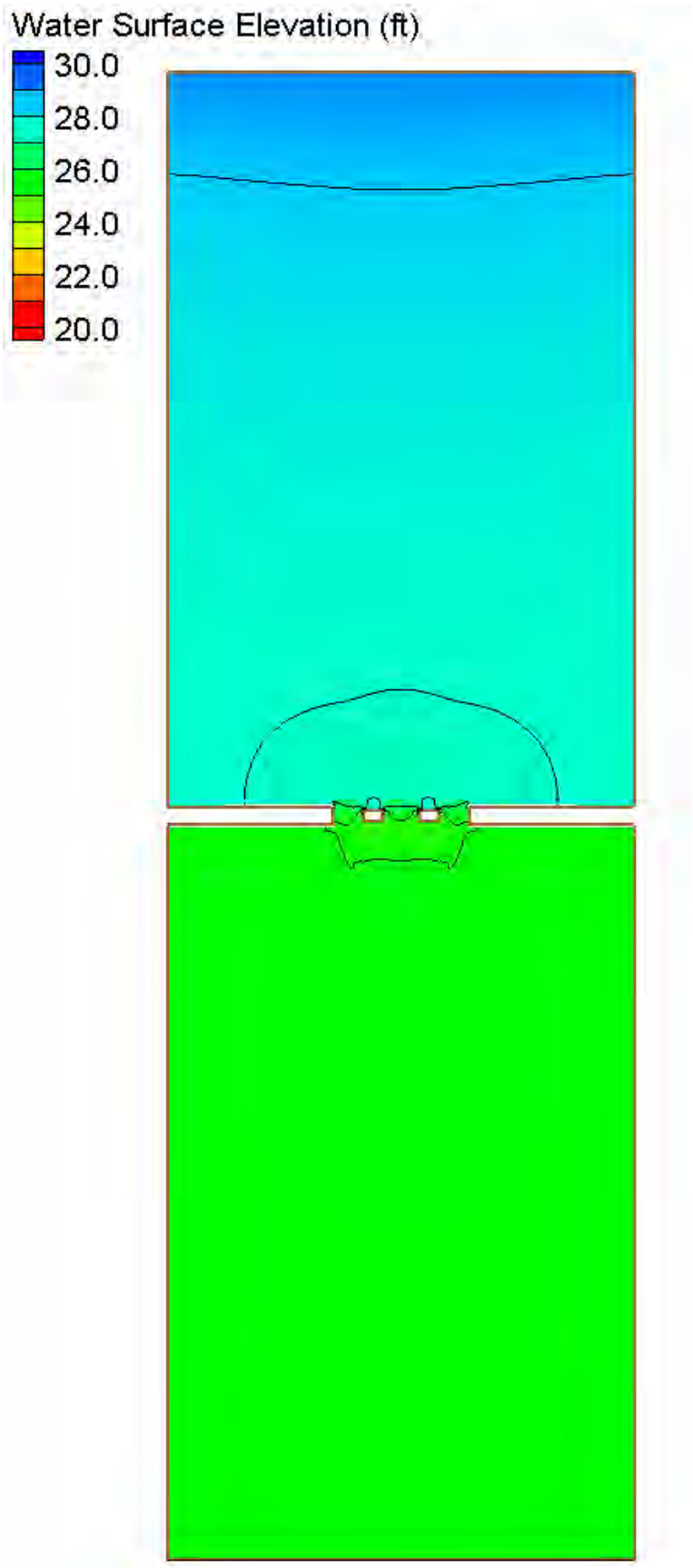

FESWMS Water Surface Elevation Contours – Large Channel – Large Pier Blockage (35%)

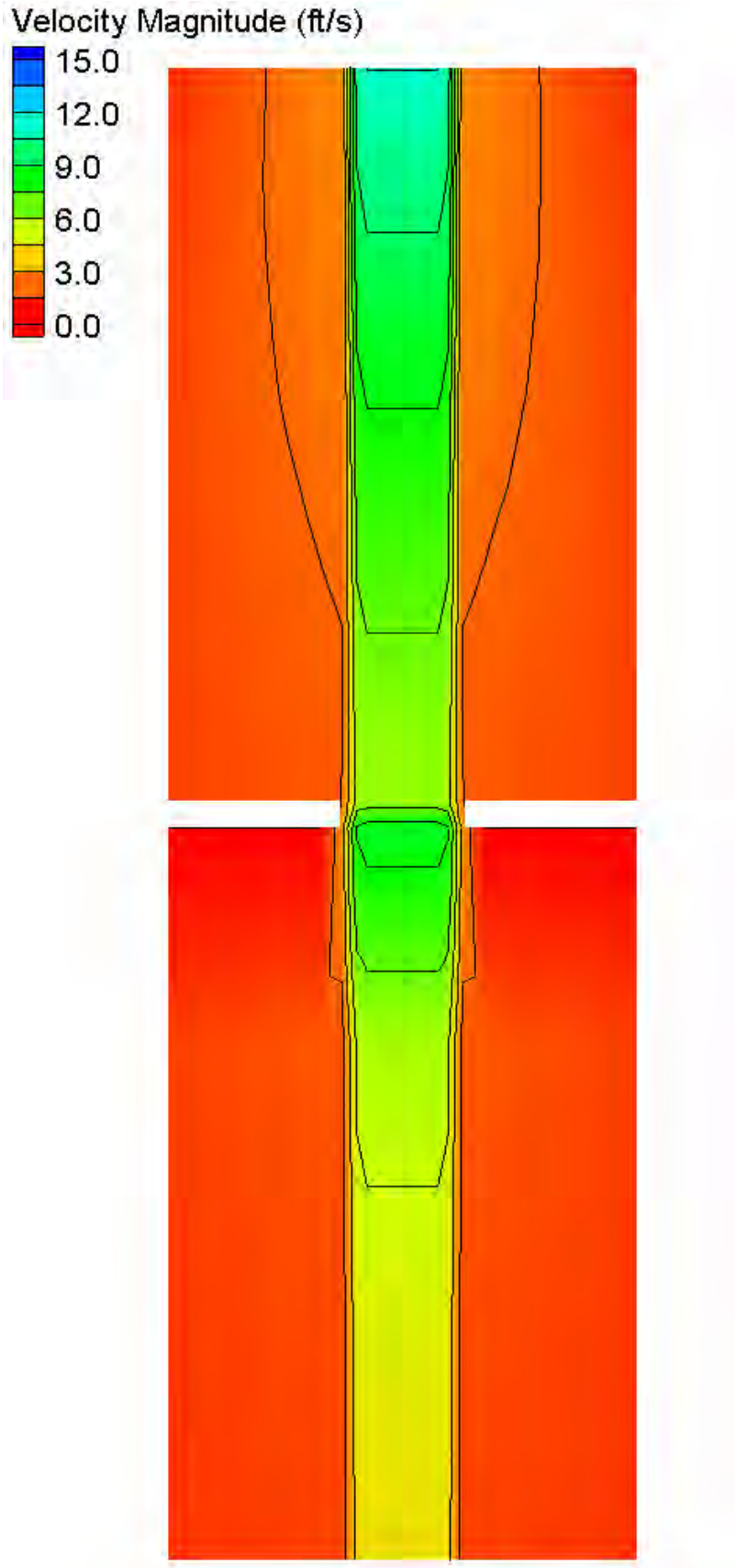

HEC-RAS Velocity Magnitude Contours – Large Channel – Large Pier Blockage (35%)

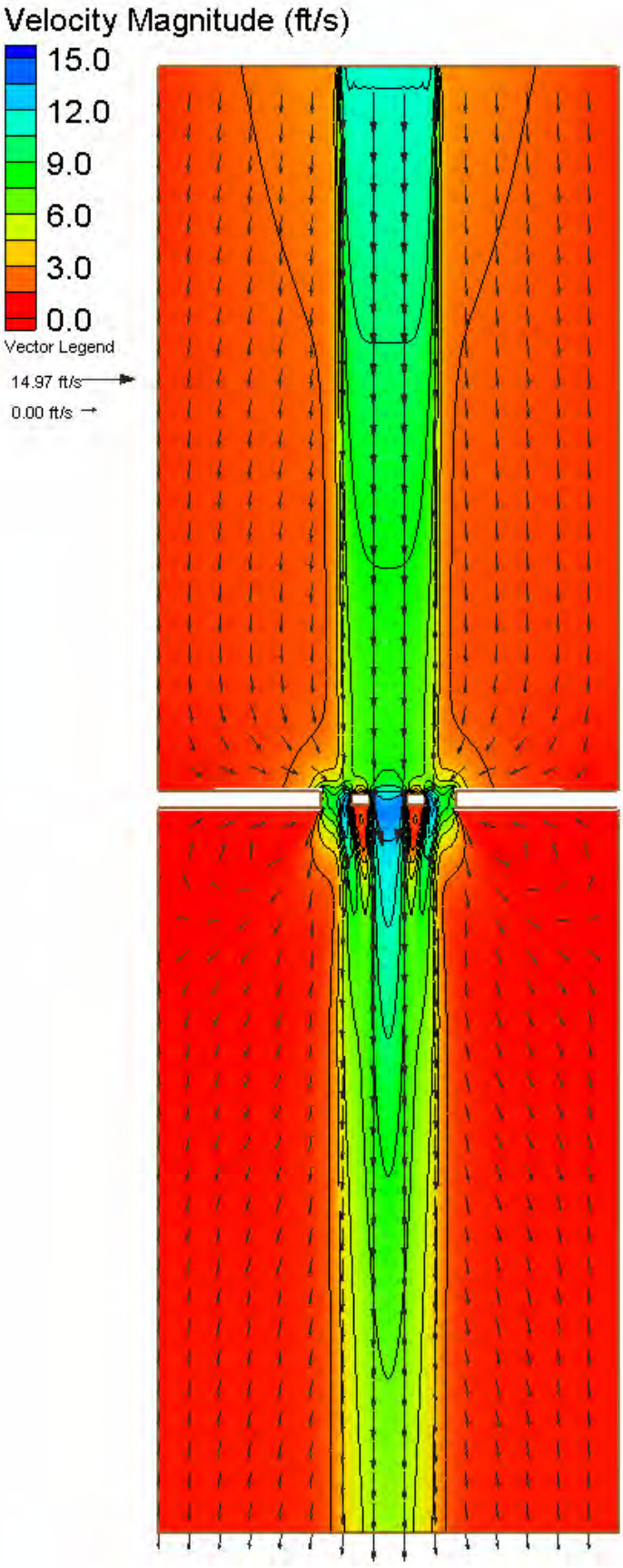

FESWMS Velocity Magnitude Contours – Large Channel – Large Pier Blockage (35%)

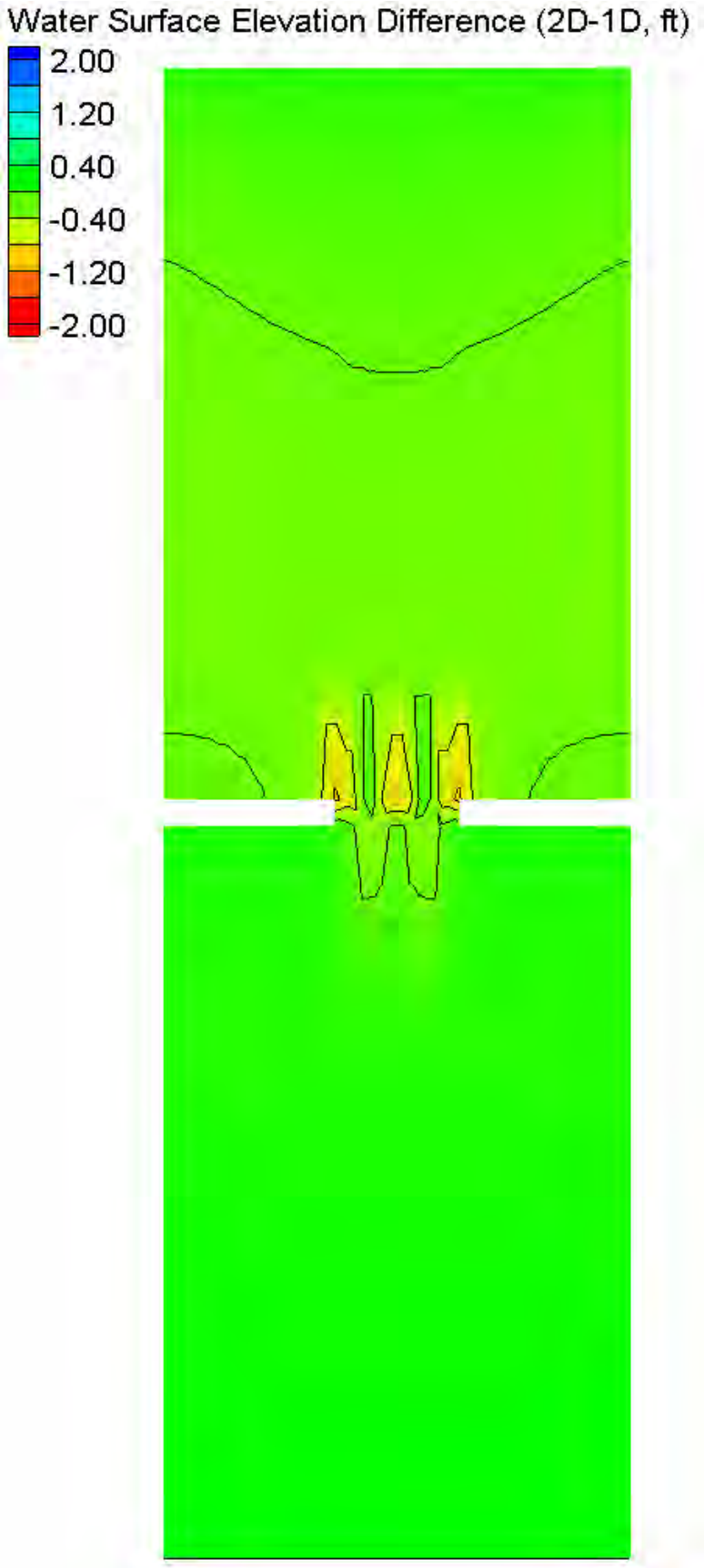

Water Surface Elevation Difference Contours – Large Channel – Large Pier Blockage (35%)

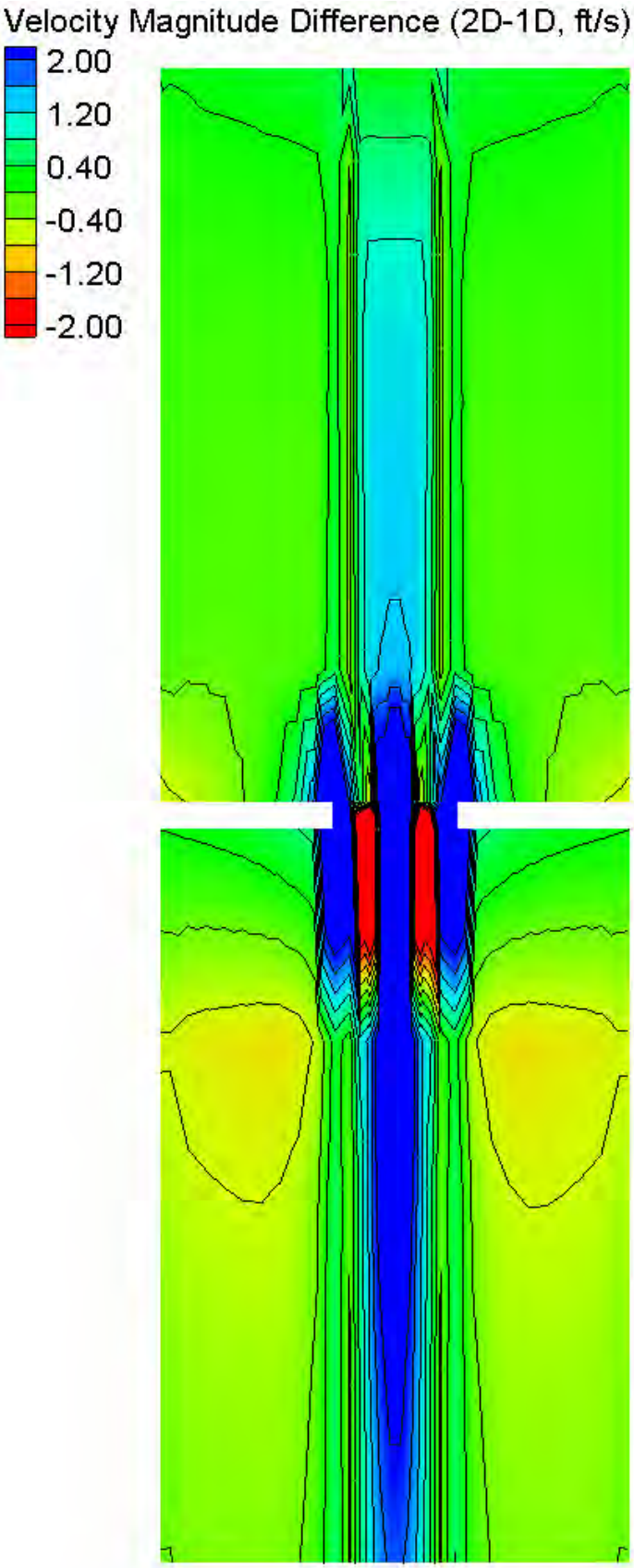

Velocity Magnitude Difference Contours – Large Channel – Large Pier Blockage (35%)

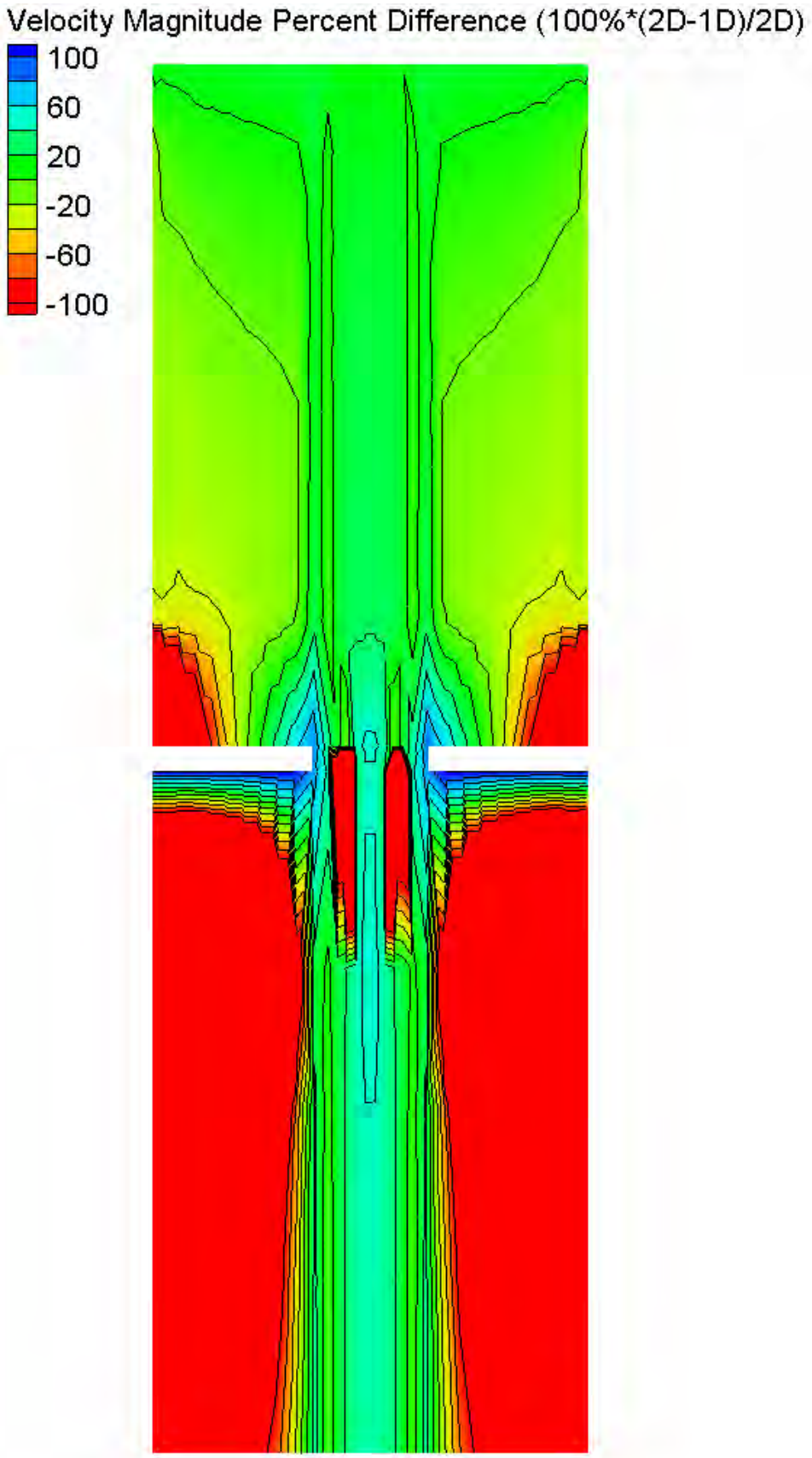

Velocity Magnitude Percent Difference Contours – Large Channel – Large Pier Blockage (35%)

Tidal Hydraulics

Rma2 Simulations Only

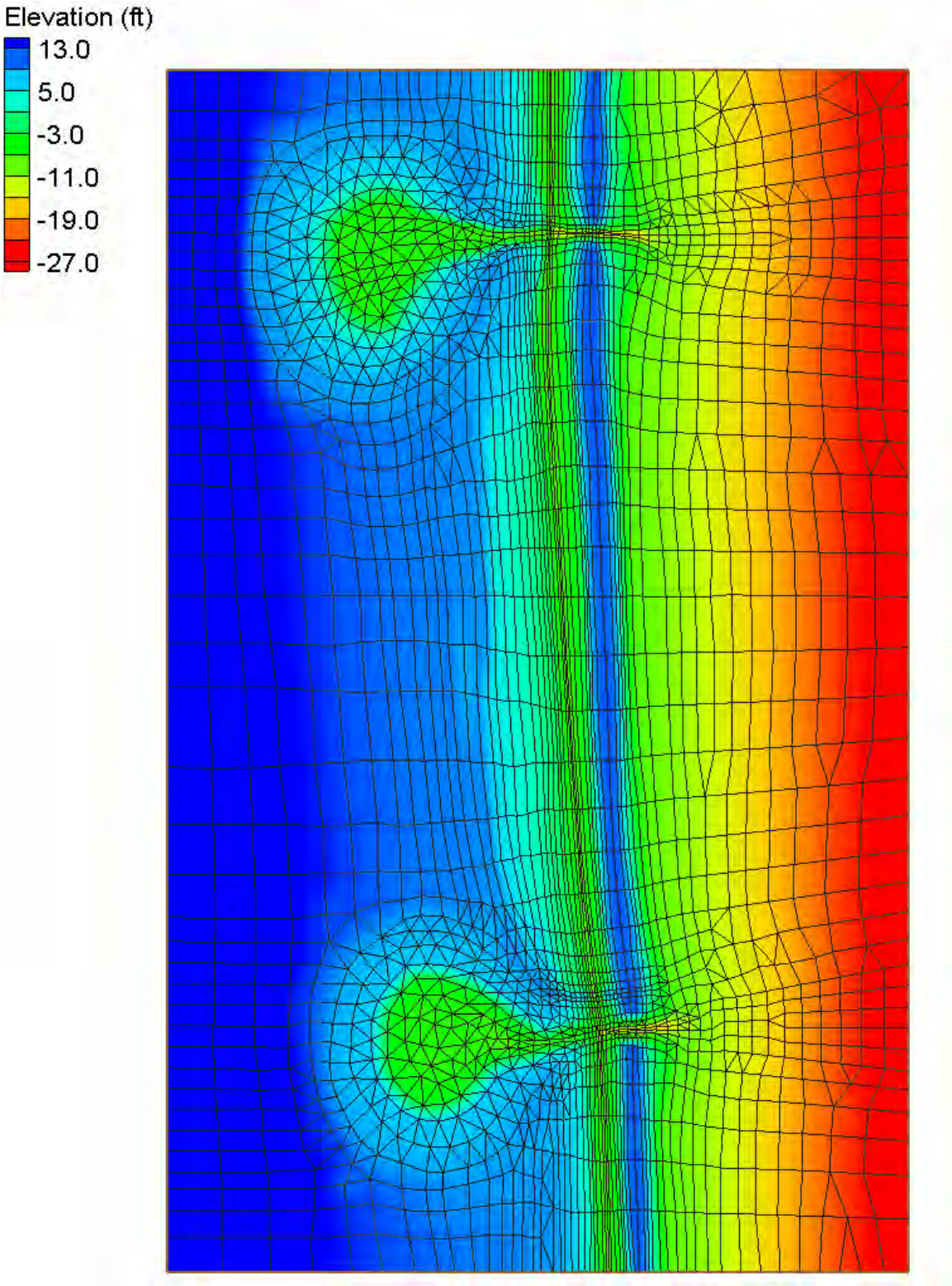

Simple Case RMA2 Model Mesh

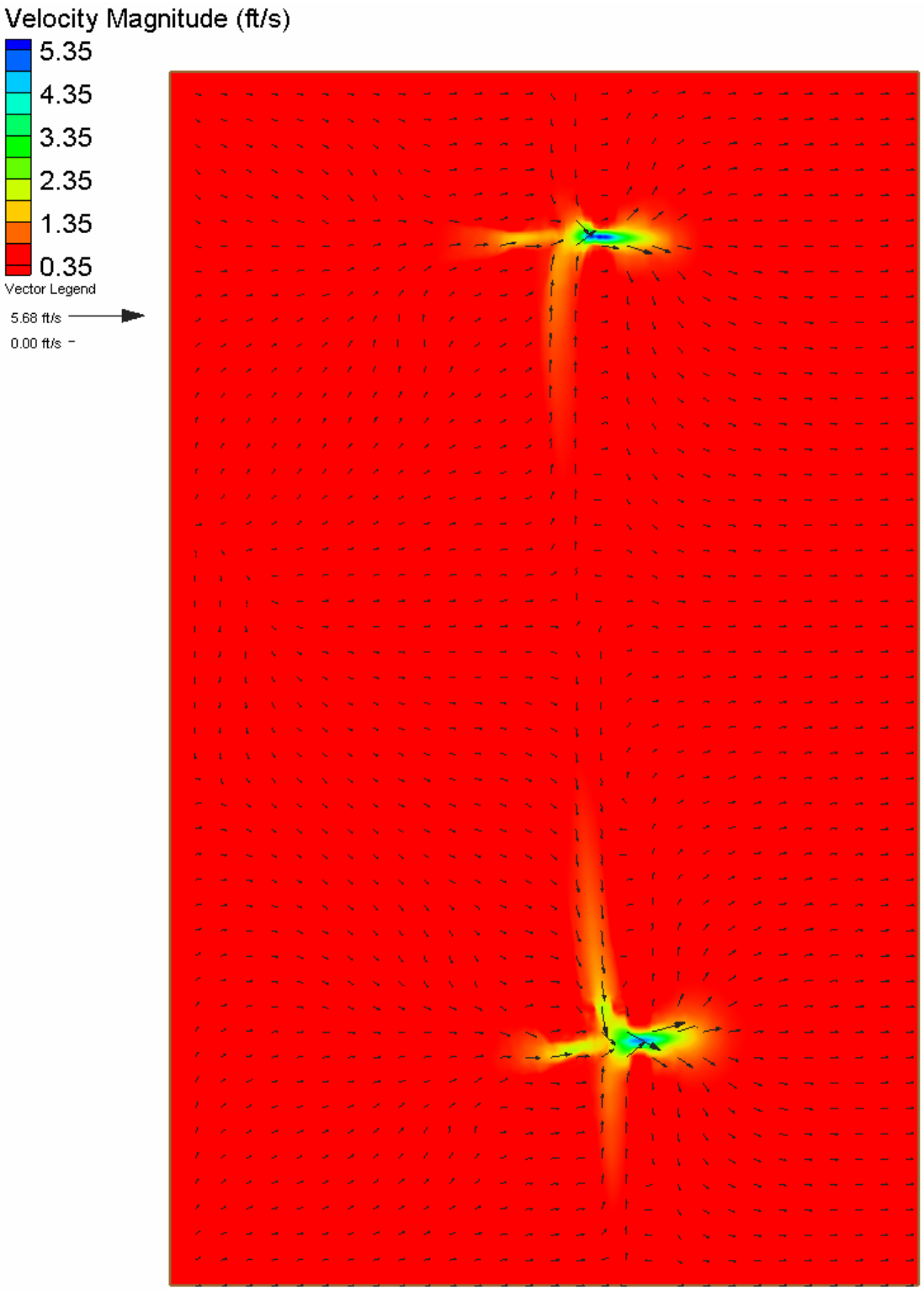

Simple Case Velocity Magnitude Contours at Time of Maximum Velocities

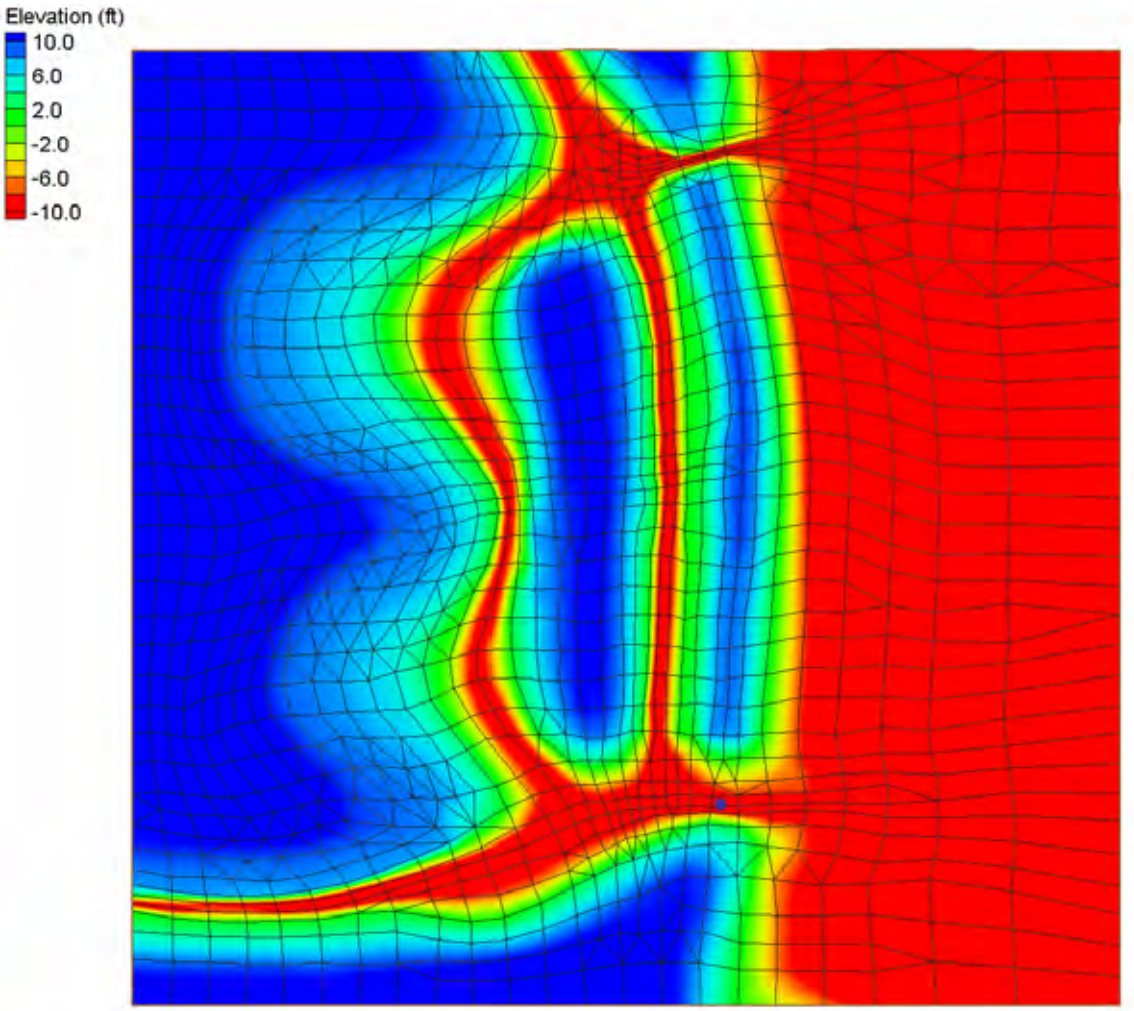

Complex Case Model Mesh

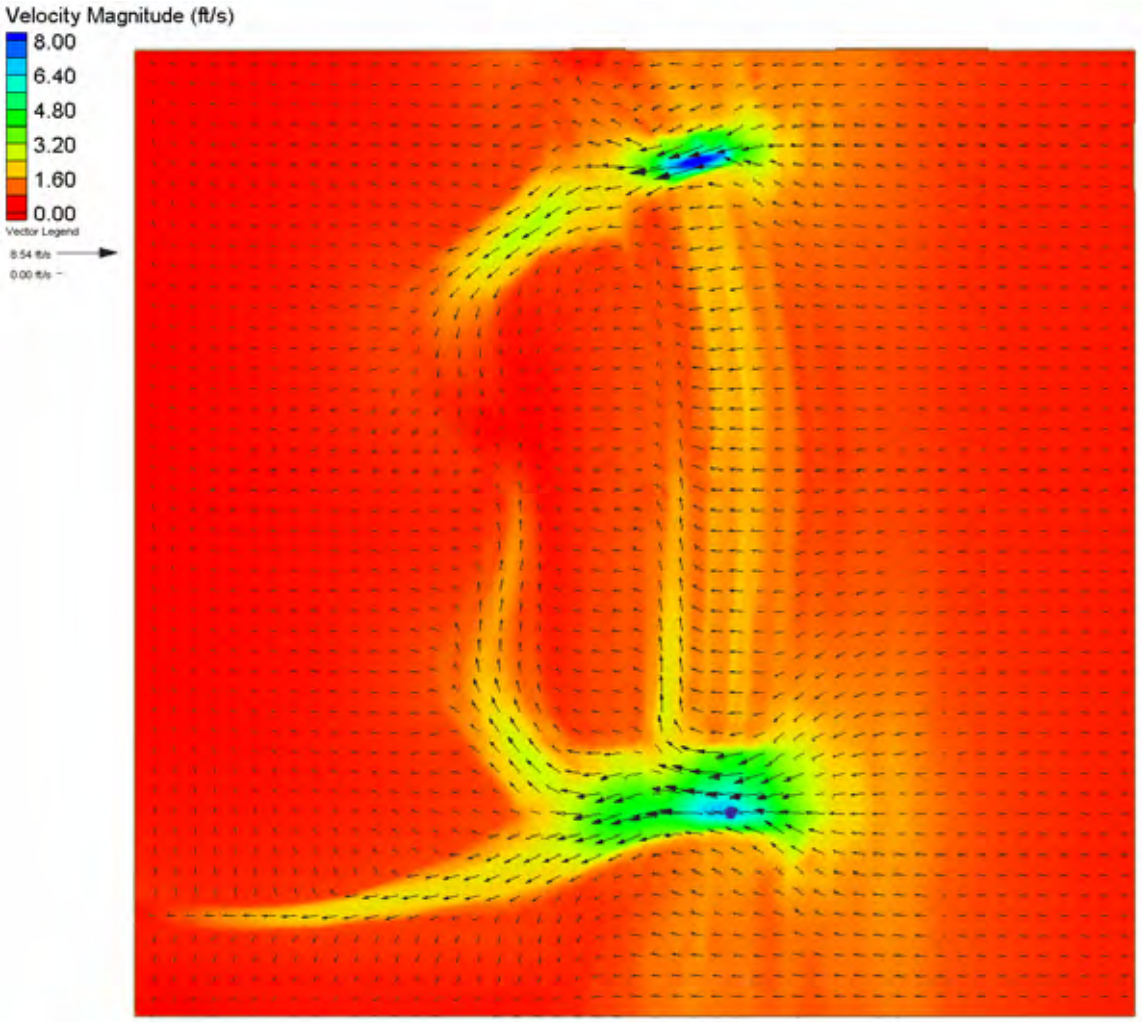

Complex Case Velocity Magnitude Contours at Time of Maximum Velocities